Animal Models and Human Reproduction

Animal Models and Human Reproduction

Edited by

Heide Schatten
Department of Veterinary Pathobiology
University of Missouri-Columbia, Columbia, USA

and

Gheorghe M. Constantinescu
Department of Biomedical Sciences
College of Veterinary Medicine
University of Missouri-Columbia, Columbia, USA

WILEY Blackwell

Copyright © 2017 by John Wiley & Sons, Inc. All rights reserved 2017

Published by John Wiley & Sons, Inc., Hoboken, New Jersey
Published simultaneously in Canada

No part of this publication may be reproduced, stored in a retrieval system, or transmitted in any form or by any means, electronic, mechanical, photocopying, recording, scanning, or otherwise, except as permitted under Section 107 or 108 of the 1976 United States Copyright Act, without either the prior written permission of the Publisher, or authorization through payment of the appropriate per-copy fee to the Copyright Clearance Center, Inc., 222 Rosewood Drive, Danvers, MA 01923, (978) 750-8400, fax (978) 750-4470, or on the web at www.copyright.com. Requests to the Publisher for permission should be addressed to the Permissions Department, John Wiley & Sons, Inc., 111 River Street, Hoboken, NJ 07030, (201) 748-6011, fax (201) 748-6008, or online at http://www.wiley.com/go/permission.

Limit of Liability/Disclaimer of Warranty: While the publisher and authors have used their best efforts in preparing this book, they make no representations or warranties with respect to the accuracy or completeness of the contents of this book and specifically disclaim any implied warranties of merchantability or fitness for a particular purpose. No warranty may be created or extended by sales representatives or written sales materials. The advice and strategies contained herein may not be suitable for your situation. You should consult with a professional where appropriate. Neither the publisher nor authors shall be liable for any loss of profit or any other commercial damages, including but not limited to special, incidental, consequential, or other damages.

For general information on our other products and services or for technical support, please contact our Customer Care Department within the United States at (800) 762-2974, outside the United States at (317) 572-3993 or fax (317) 572-4002.

Wiley also publishes its books in a variety of electronic formats. Some content that appears in print may not be available in electronic formats. For more information about Wiley products, visit our website at www.wiley.com.

Library of Congress Cataloging-in-Publication Data:

Names: Schatten, Heide, editor. | Constantinescu, Gheorghe M., 1932- editor.
Title: Animal models and human reproduction / edited by Heide Schatten, Gheorghe M. Constantinescu.
Description: Hoboken, New Jersey : John Wiley & Sons Inc., [2017] | Includes bibliographical references and index.
Identifiers: LCCN 2016045187| ISBN 9781118881606 (cloth) | ISBN 9781118881422 (Adobe PDF) | ISBN 9781118881347 (epub)
Subjects: | MESH: Reproduction | Models, Animal | Reproductive Physiological Phenomena | Reproductive Techniques
Classification: LCC QH481 | NLM QH 481 | DDC 571.8/4--dc23
LC record available at https://lccn.loc.gov/2016045187

Set in 10/12 pt WarnockPro-Regular by Thomson Digital, Noida, India

Printed and bound in Singapore by C. O. S. Printers Pte Ltd

10 9 8 7 6 5 4 3 2 1

Contents

List of Contributors *xv*

1 Anatomy of the Reproductive System *1*
Gheorghe M. Constantinescu
1.1 Male Genital Organs in Domestic Mammals *1*
1.1.1 The Testicle *1*
1.1.2 The Epididymis, Ductus Deferens, and Spermatic Cord *2*
1.1.3 The Descent of the Testicle *3*
1.1.4 The Tunics of the Spermatic Cord and the Testicle *4*
1.1.5 The Accessory Genital Glands *4*
1.1.6 The Penis and the Prepuce *4*
1.2 Female Genital Organs in Domestic Mammals *5*
1.2.1 The Ovary *5*
1.2.2 The Uterine Tube: Salpinx, Fallopian Tube *7*
1.2.3 The Uterus *7*
1.2.4 The Vagina and the Vestibule *8*
1.2.5 The Vulva and the Clitoris *8*
1.2.6 The Mammary Gland *9*
1.3 The Genital System in Domestic Mammals Species by Species *9*
1.3.1 The Genital System in the Carnivores: Cat and Dog *9*
1.3.2 The Genital System in the Pig *15*
1.3.3 The Genital System in the Ruminants *20*
1.3.4 The Genital System in the Horse *30*
1.4 Genital Organs in Laboratory Mammals *35*
1.4.1 The Genital System in the Rabbit *38*
1.4.2 The Genital System in the Mouse *42*
1.4.3 The Genital System in the Rat *47*
1.4.4 The Mammary Glands in Laboratory Animals *50*
1.4.5 The Genital System in the Xenopus laevis: African Clawed Frog *51*
1.4.6 The Genital System in the Brachidanio rerio (Zebrafish) *56*
References *56*

2 Anatomy of Mammalian (Endocrine) Glands Controlling the Reproduction *59*
Gheorghe M. Constantinescu
2.1 The Hypothalamus Including the Hypophysis *59*

Downloaded From Vet-eBooks.com

2.2 The Cerebral Epiphysis *61*
2.3 The Thyroid Gland *61*
2.4 The Adrenal Glands *62*
2.5 The Sexual Glands *63*
2.6 The Liver *63*
References *63*

3 Models for Investigating Placental Biology *65*
Laramie Pence and Bhanu P. Telugu
3.1 Introduction *65*
3.2 Classification of Placenta *66*
3.3 Development of Human Placenta *69*
3.3.1 Trophoblast Subtypes and Development of Functional Placenta *69*
3.3.2 Placental Development *71*
3.3.3 Development of Fetal Membranes *71*
3.4 Modeling Placental Development and Diseases of Placental Origin *73*
3.4.1 In Vitro Cell Models *73*
3.4.2 Animal Models *76*
3.4.3 Alternative Animal Models *79*
3.5 Summary *82*
References *82*

4 Early Developmental Programming of the Ovarian Reserve, Ovarian Function, and Fertility *91*
Francesca Mossa, Siobhàn W. Walsh, Alex C.O. Evans, Fermin Jimenez-Krassel, and James J. Ireland
4.1 Introduction *91*
4.2 Impact of Prenatal Environmental Challenges on Fetal Oogonia (Germ Cells) *92*
4.2.1 Farm Animal Models *92*
4.3 Impact of Prenatal Environmental Challenges on Fetal Follicle/Oocyte Numbers (Healthy versus Atretic) and Oocyte Quality *94*
4.3.1 Farm Animal Models *94*
4.3.2 Humans/Primates *94*
4.4 Impact of Prenatal Environmental Challenges on the Ovarian Reserve (Total Number of Morphologically Healthy Follicles/Oocytes in Ovaries) in Offspring *95*
4.4.1 Farm Animal Models *95*
4.4.2 Rodent Models *97*
4.4.3 Humans/Primates *97*
4.5 Impact of Prenatal Environmental Challenges on Ovarian Function (e.g., Pituitary Gonadotropin Secretion, Ovarian Hormone/Growth Factor Production, Response to Gonadotropins, Follicle Development, Irregular Reproductive Cycles, and Ovulation Rate) in Offspring *98*
4.5.1 Farm Animal Models *98*
4.5.2 Rodent Models *99*
4.5.3 Humans/Primates *99*
4.6 Impact of Prenatal Environmental Challenges on Fertility (as Measured by Conception Rates, Fecundity, or Age at Puberty or Menopause) in Offspring *100*
4.6.1 Farm Animal Models *100*
4.6.2 Rodent Models *100*

Downloaded From Vet-eBooks.com

4.6.3 Humans/Primates *101*
4.7 Summary and Conclusion *101*
References *102*

5 Small Non-Coding RNAS in Gametogenesis *109*
Lukasz Smorag and D. V. Krishna Pantakani
5.1 Small Non-Coding RNAs *109*
5.2 Function of sncRNAs in Gametogenesis *109*
5.2.1 miRNAs Biogenesis *110*
5.2.2 Function of miRNAs in the Process of Spermatogenesis *112*
5.2.3 *endo*-siRNAs Biogenesis *115*
5.2.4 *endo*-siRNAs in the Process of Spermatogenesis *115*
5.2.5 pi-RNAs Biogenesis *117*
5.2.6 Role of piRNAs in Male Germ Cell Development *117*
Acknowledgment *119*
References *119*

6 The Ovarian Follicle of Cows as a Model for Human *127*
Marc-André Sirard
6.1 Introduction *127*
6.1.1 Why We Know More About Cow Than Human Reproduction *127*
6.2 A Similar Physiology of Folliculogenesis *128*
6.2.1 Basic Physiology of Reproduction *128*
6.2.2 Time from Primordial Follicle to Ovulation *129*
6.2.3 Follicular Waves *130*
6.2.4 Characteristics of the Dominant Follicle *131*
6.3 Assisted Reproduction *131*
6.3.1 Response to Ovarian Stimulation *132*
6.3.2 Response to FSH Coasting *133*
6.3.3 Response to IVM *134*
6.3.4 Biomarker Analysis *134*
6.4 Testing the Competence Hypothesis *136*
6.5 Conclusion *136*
References *136*

7 Production of Energy and Determination of Competence: Past Knowledge, Present Research, and Future Opportunities in Oocyte and Embryo Metabolism *145*
Jason R. Herrick, Elena Silva, and Rebecca L. Krisher
7.1 Introduction *145*
7.2 Measuring Metabolism *145*
7.2.1 Approaches *145*
7.2.2 Limitations *147*
7.3 The Relationship Between Oocyte Metabolism and Quality *148*
7.3.1 Energy Substrates During Oocyte Maturation *148*
7.3.2 Oocyte Metabolic Pathways *149*
7.3.3 Oocyte Metabolism of Fatty Acids *151*
7.4 Embryo Metabolism *152*
7.4.1 Precompaction: More Than Just Pyruvate *153*

Downloaded From Vet-eBooks.com

7.4.2 Postcompaction: More Than Just Glucose *154*
7.4.3 Lactate: The Other Carbohydrate *155*
7.4.4 Noncarbohydrates *156*
7.5 Metabolic Biomarkers *157*
7.5.1 The Oocyte *157*
7.5.2 The Embryo *158*
7.6 Toward Personalized Culture Media: Formulating Media for Specific Maternal Conditions *158*
7.6.1 Maternal Impact on Embryo Development *158*
7.6.2 Impaired Embryo Metabolism *159*
7.6.3 Mitochondrial Dysfunction *159*
7.6.4 Endoplasmic Reticulum Stress *160*
7.7 Summary *161*
References *162*

8 Signal Transduction Pathways in Oocyte Maturation *177*
François J. Richard, Nicolas Santiquet, Annick Bergeron, and Daulat Raheem Khan
8.1 Introduction *177*
8.1.1 Oocyte Maturation *178*
8.1.2 Oocyte Nuclear Maturation *178*
8.1.3 Cumulus Cell Expansion *179*
8.1.4 The Impact of FSH During *In Vitro* Maturation *179*
8.2 Phosphodiesterase *181*
8.2.1 Overview *181*
8.2.2 Cyclic Nucleotide Signaling *182*
8.2.3 Phosphodiesterase Superfamily *182*
8.2.4 Oocyte Meiosis and cAMP *183*
8.2.5 PDE3A *184*
8.2.6 PDE8A *186*
8.2.7 Cyclic GMP and PDE5/6 *187*
8.2.8 Cellular Compartmentalization of Cyclic Nucleotide Signaling *188*
8.2.9 C-Type Natriuretic Peptide (CNP) and cGMP *189*
8.3 Gap Junction Communications *192*
8.3.1 Connexin, Connexon, and Gap Junctions *192*
8.3.2 Gap Junction Communications and Oocyte Maturation *193*
8.4 Metabolic Switch (AMPK) *193*
8.4.1 Overview *193*
8.4.2 Structure and Regulation of AMPK *194*
8.4.3 Activators of AMPK *194*
8.4.4 Downstream Targets of AMPK *195*
8.4.5 AMPK in Reproductive Function *195*
8.4.6 AMPK in Oocyte Function *196*
8.5 Conclusion *198*
References *198*

9 Pig Models of Reproduction *213*
B.R. Mordhorst and R.S. Prather
9.1 Introduction *213*

Downloaded From Vet-eBooks.com

9.2 Early Embryonic Development *213*
9.3 Oocyte Maturation *215*
9.4 Fertilization *216*
9.5 Tubouterine Contractility *216*
9.6 Development to the Blastocyst Stage *216*
9.7 Pregnancy and Developmental Programming *217*
9.8 Puberty *222*
9.9 Reproductive Disease *223*
9.10 Summary *223*
Acknowledgments *223*
References *223*

10 The Mare as an Animal Model for Reproductive Aging in the Woman *235*
Elaine M. Carnevale
10.1 Introduction *235*
10.2 Ovarian Activity and Reproductive Cycles *236*
10.2.1 Ovarian Reserve *236*
10.2.2 Assessment of Antral Follicles *236*
10.2.3 Reproductive Cycles *237*
10.2.4 Reproductive Senescence *238*
10.3 The Follicle *238*
10.3.1 Follicle Growth and Selection *238*
10.3.2 Follicular Environment *238*
10.4 Fertility *239*
10.4.1 Natural Decline in Fertility with Aging *239*
10.4.2 Assisted Reproductive Procedures *239*
10.4.3 Maternal Age and Pregnancy Failure *240*
10.5 The Oocyte *240*
10.5.1 Oocyte Donation *240*
10.5.2 Oocyte Morphology and Viability *241*
10.6 Conclusions *242*
References *242*

11 Spotlight on Reproduction in Domestic Dogs as a Model for Human Reproduction *247*
Shirley J. Wright
11.1 Introduction *247*
11.1.1 Scope of the Chapter *247*
11.1.2 Dog's Importance to Modern Human Society *247*
11.1.3 Dog Taxonomy *248*
11.1.4 Dog Origin *248*
11.1.5 Dog Breeds *250*
11.1.6 Dog Genome *251*
11.1.7 Dog as a Model for Human Genetic Disorders *254*
11.1.8 Dog Life span *255*
11.2 Dog Reproduction *255*
11.2.1 Dog Onset of Puberty *255*
11.2.2 Dog Fertility *256*
11.2.3 Reproductive Anatomy of the Male Dog *256*

Downloaded From Vet-eBooks.com

11.2.4 Reproductive Physiology of the Male Dog *260*
11.2.5 Reproductive Anatomy of the Female Dog *280*
11.2.6 Reproductive Physiology of the Female Dog *287*
11.2.7 Dog Fertilization *298*
11.2.8 Dog Pregnancy, Development and Birth *318*
11.3 Dog-Assisted Reproductive Technology *321*
11.3.1 Artificial Insemination *321*
11.3.2 Superovulation *322*
11.3.3 Oocyte *In Vitro* Maturation *322*
11.3.4 *In Vitro* Fertilization *323*
11.3.5 Intracytoplasmic Sperm Injection *324*
11.3.6 Embryo Transfer *325*
11.3.7 Cryopreservation *325*
11.3.8 Sperm Sexing *326*
11.3.9 Somatic Cell Nuclear Transfer in Dogs *327*
11.3.10 Dog Embryonic Stem Cells and Induced Pluripotent Stem Cells *327*
11.3.11 Genetically Modified Dogs *328*
11.4 Dog Contraception *328*
11.5 The Dog as a Model for Human Reproduction *328*
11.5.1 Disorders of Sexual Development *329*
11.5.2 Cancer *330*
11.5.3 Obesity *331*
11.5.4 Dog Infertility *331*
11.5.5 Aneuploidy *331*
11.6 Concluding Statements *332*
Acknowledgments *333*
References *333*

12 Animal Models of Inflammation During Pregnancy *359*
Karen E. Racicot and Keith E. Latham
12.1 Introduction *359*
12.2 Local Inflammation of the Pregnant Female Reproductive Tract *360*
12.2.1 Introduction *360*
12.2.2 *In Utero* Inflammation and Adverse Pregnancy Outcomes *360*
12.2.3 Ascending Infections and Adverse Pregnancy Outcomes *361*
12.3 Systemic Inflammation During Pregnancy *361*
12.3.1 Introduction *361*
12.3.2 Systemic Viral or Bacterial Infection *363*
12.3.3 Maternal Stress: Chronic Sterile Inflammation *364*
12.3.4 Preeclampsia-Related Inflammation Models *364*
12.3.5 Models of Antiphospholipid Antibody Syndrome (APS) *365*
12.4 Genetic Models and Cellular Manipulation to Study Inflammation During Pregnancy *365*
12.4.1 Introduction *365*
12.4.2 Breeding Cross Models of Induced Inflammation *365*
12.4.3 Genetically Modified Models of Inflammation and Pregnancy *367*
12.4.4 Immune Cell Manipulation to Study Inflammation *367*
12.5 Inflammation During Pregnancy and Offspring Disease *370*
12.5.1 Introduction *370*

Downloaded From Vet-eBooks.com

12.5.2 Models of Inflammation During Pregnancy Resulting in Offspring Disease *371*
12.6 Perspectives and Conclusions *372*
Acknowledgments *373*
References *373*

13 Practical Approaches, Achievements, and Perspectives in the Study on Signal Transduction in Oocyte Maturation and Fertilization: Focusing on the African Clawed Frog *Xenopus laevis*as an Animal Model *383*
Ken-ichi Sato
13.1 Introduction to Reproductive Biology of Frog Oocytes and Eggs *383*
13.2 Practical Approaches *383*
13.2.1 Maintenance of Adult Frogs *383*
13.2.2 Collection of Immature Oocytes and Unfertilized Eggs *384*
13.2.3 Preparation of Sperm *385*
13.2.4 In Vitro Oocyte Maturation and Fertilization *386*
13.2.5 Microinjection and Other Pharmacological Treatments *386*
13.2.6 Biochemical Fractionations of Oocytes and Eggs *390*
13.2.7 Biochemical and Cell Biological Assays *391*
13.2.8 Indirect Immunofluorescent Study *393*
13.2.9 Protein Identification by Mass Spectrometry Analysis *394*
13.2.10 Emerging Approaches: Live-Cell Imaging and Genome Manipulations *394*
13.3 Achievements and Perspectives *395*
Acknowledgments *396*
Appendix *396*
References *399*

14 Prezygotic Chromosomal Examination of Mouse Spermatozoa *401*
Hiroyuki Watanabe and Hiroyuki Tateno
14.1 Introduction *401*
14.2 Procedure of Sperm Chromosome Screening *402*
14.2.1 Sperm Genome Cloning Using an Androgenic Embryo (Step (a)) *402*
14.2.2 Induction of PCC for Rapid Chromosome Visualization (Step (b)) *403*
14.2.3 Production of Diploid Embryos by Fusion of Blastomere with MII Oocytes (Step (c)) *403*
14.3 Practical Use of SCS Before Fertilization *404*
14.4 Conclusion *406*
Acknowledgments *406*
Addendum *406*
References *406*

15 Molecular and Cellular Aspects of Mammalian Sperm Acrosomal Exocytosis *409*
Florenza A. La Spina, Cintia Stival, Dario Krapf, and Mariano G. Buffone
15.1 Introduction *409*
15.2 Structure of the Acrosome *409*
15.3 Intermediate Stages of Exocytosis *412*
15.4 Sperm Capacitation Prepare the Sperm to Undergo Acrosomal Exocytosis *412*
15.5 Physiological Site for the Occurrence of Acrosomal Exocytosis *414*
15.6 SNARES and Other Proteins from the Fusion Machinery *416*

Downloaded From Vet-eBooks.com

15.7 Hyperpolarization *417*
15.8 Actin Cytoskeleton *417*
15.9 Calcium *418*
References *419*

16 Sperm Chromatin Dynamics Associated with Male Fertility in Mammals *427*
Naseer A. Kutchy, Sule Dogan, Abdullah Kaya, Arlindo Moura, and Erdogan Memili
16.1 Introduction *427*
16.2 Sperm Chromatin Structure Modulates Sperm Nuclear Shape and Function *429*
16.3 The Bull Is a Suitable Model for the Study of Male Fertility in Humans *430*
16.4 Conclusions and Prospects *430*
Acknowledgments *431*
References *431*

17 Epigenome Modification and Ubiquitin-Dependent Proteolysis During Pronuclear Development of the Mammalian Zygote: Animal Models to Study Pronuclear Development *435*
Jan Nevoral and Peter Sutovsky
17.1 Introduction *435*
17.2 Milestones of Pronuclear Development *436*
17.3 Nuclear Envelope, Nuclear Pore Complexes, and Nuclear Lamina Changes During Pronuclear Development *438*
17.4 Molecular Mechanism of Paternal and Maternal Pronucleus Biogenesis *440*
17.5 Role of UPS in Pronuclear Biogenesis *442*
17.6 Posttranslational Modifications of Pronuclear Histones *443*
17.7 Sirtuin Family Histone Deacetylases in Gametogenesis and Development *446*
17.8 Clinical and Technological Considerations *447*
17.9 Conclusions *450*
Acknowledgments *450*
References *450*

18 Alterations of the Epigenome Induced by the Environment in Reproduction *467*
Zhao-Jia Ge, Shen Yin, and Heide Schatten
18.1 Introduction *467*
18.2 Epigenetic Reprogramming *467*
18.2.1 The Epigenetic Reprogramming in Germ Lines *469*
18.2.2 The Epigenetic Reprogramming in Early Embryo *470*
18.3 Environment and Epigenetic Alterations *470*
18.4 Animal Models Used in Reproduction to Research Epigenetic Alterations Induced by the Environment *472*
18.4.1 Viable Yellow (A^{vy}) Mouse Model *472*
18.4.2 Axin 1 Mouse (Fu) Model *472*
18.4.3 Micronutrient Animal Models *472*
18.4.4 The Protein-Restricted Diet Model *473*
18.4.5 The Caloric Restriction Model *473*
18.4.6 The Animal Model of Zinc Deficiency *473*
18.4.7 Undernutrition Models *473*
18.4.8 The Obese Model *473*
18.4.9 The Diabetes Mellitus Model *474*

Downloaded From Vet-eBooks.com

18.4.10 Polycystic Ovary Syndrome (PCOS) *474*
18.4.11 The Aging Model *474*
18.4.12 Other Models *474*
18.5 Effects of Environment on Epigenetic Modifications in Humans *475*
18.6 Epigenetics and Assisted Reproductive Technology (ART) *475*
18.7 Priorities for the Future *476*
Acknowledgments *476*
References *476*

19 Toward Development of Pluripotent Porcine Stem Cells by Road Mapping Early Embryonic Development *485*
Stoyan Petkov, Kristine Freude, Kaveh Mashayekhi, Poul Hyttel, and Vanessa Hall
19.1 Introduction *485*
19.2 Current Status on the Pluripotent State in the Pig Embryo *489*
19.3 Current Status of the Establishment of Porcine Embryonic Stem Cells (pESCs) *491*
19.4 Current Status in Establishment of Porcine-Induced Pluripotent Stem Cells *494*
19.5 Future Perspectives: Use of Global Profiling on Pluripotent Cells from Pig Embryo and Pluripotent Stem Cells *499*
19.6 Discussion and Conclusions *501*
Acknowledgments *502*
References *502*

20 Applications of Metabolomics in Reproductive Biology *509*
Ana Luiza Cazaux Velho, Rodrigo Oliveira, Thu Dinh, Arlindo Moura, Abdullah Kaya, and Erdogan Memili
20.1 Introduction *509*
20.2 Metabolomics and Reproductive Biology *510*
20.3 Metabolomics Studies in Large Animals as Models for Humans *513*
20.4 Conclusions and Future Prospects *513*
Acknowledgments *514*
Conflict of Interest *514*
References *514*

21 Cryopreservation of Mammalian Oocytes *519*
Muhammad Anzar
21.1 Principles of Cryopreservation *519*
21.1.1 Water and Cell Cryopreservation *519*
21.1.2 Cryoprotectants *520*
21.1.3 Cooling Rate *522*
21.2 Cryopreservation of Mammalian Oocytes *522*
21.2.1 History *522*
21.2.2 Mammalian Oocyte *529*
21.2.3 Cryopreservation Methods *530*
Acknowledgments *542*
Abbreviations *543*
References *543*

Index *557*

Downloaded From Vet-eBooks.com

Downloaded From Vet-eBooks.com

List of Contributors

Muhammad Anzar
Agriculture and Agri-Food Canada
Saskatoon Research and Development Center
Saskatoon, Canada

Annick Bergeron
Centre de Recherche en Biologie de la Reproduction
Département des Sciences Animales
Faculté des sciences de l'agriculture et de l'alimentation
Université Laval
Québec, Canada

Mariano G. Buffone
Instituto de Biología y Medicina Experimental (IBYME)
National Research Council of Argentina (CONICET)
Buenos Aires, Argentina

Elaine M. Carnevale
Equine Reproduction Laboratory
Department of Biomedical Sciences
Colorado State University
CO, USA

Gheorghe M. Constantinescu
Department of Biomedical Sciences
College of Veterinary Medicine
University of Missouri-Columbia
Columbia, USA

Thu Dinh
Department of Animal and Dairy Sciences
Mississippi State University
MS, USA

Sule Dogan
IVF Michigan P.C.
MI, USA

Alex C.O. Evans
School of Agriculture and Food Science
University College Dublin
Dublin, Ireland

Kristine Freude
Faculty of Health and Medical Sciences
Department of Veterinary Clinical and Animal Sciences
University of Copenhagen, Denmark

Zhao-Jia Ge
College of Animal Science and Veterinary Medicine
Qingdao Agricultural University
Qingdao, China

Vanessa Hall
Faculty of Health and Medical Sciences
Department of Veterinary Clinical and Animal Sciences
University of Copenhagen
Denmark

Downloaded From Vet-eBooks.com

Jason R. Herrick
Colorado Center for Reproductive Medicine
CO, USA

Poul Hyttel
Faculty of Health and Medical Sciences
Department of Veterinary Clinical and Animal Sciences
University of Copenhagen
Denmark

James J. Ireland
Michigan State University
MI, USA

Fermin Jimenez-Krassel
Michigan State University
MI, USA

Abdullah Kaya
Department of Animal Reproduction and Artificial Insemination
Selcuk University
Konya, Turkey

Daulat Raheem Khan
Centre de Recherche en Biologie de la Reproduction
Département des Sciences Animales
Faculté des sciences de l'agriculture et de l'alimentation
Université Laval
Québec, Canada

Dario Krapf
Institute of Molecular and Cell Biology of Rosario (CONICET-UNR) and
Área Biología
Facultad de Ciencias Biológicas y Farmacéuticas
UNR
Rosario, Argentina

Rebecca L. Krisher
Colorado Center for Reproductive Medicine
CO, USA

Naseer A. Kutchy
Department of Animal and Dairy Sciences
Mississippi State University
MS, USA

Keith E. Latham
Department of Animal Science
Reproductive and Developmental Science Program
Michigan State University
MI, USA

Kaveh Mashayekhi
Faculty of Health and Medical Sciences
Department of Veterinary Clinical and Animal Sciences
University of Copenhagen
Denmark

and

BioTalentum Ltd.
Aulich Lajos str. 26. 2100
Gödöllő, Hungary

and

Sandor Life Sciences
Sandor Medicaids Group Pvt. Ltd.
Hyderabad, 500043 India

Erdogan Memili
Department of Animal and Dairy Sciences
Mississippi State University
MS, USA

B.R. Mordhorst
Division of Animal Science
University of Missouri-Columbia
Columbia, USA

Francesca Mossa
Dipartimento di Medicina Veterinaria
Università degli Studi di Sassari
Sassari, Italy

Arlindo Moura
Department of Animal Sciences
Federal University of Ceara
Fortaleza, Brazil

Downloaded From Vet-eBooks.com

Jan Nevoral
Department of Veterinary Sciences
Czech University of Life Sciences
Prague, Czech Republic

and

Division of Animal Science
University of Missouri-Columbia
Columbia, USA

Rodrigo Oliveira
Department of Animal Production
Federal Rural University of Rio de Janeiro
Rio de Janeiro, Brazil

D. V. Krishna Pantakani
Department of Clinical Chemistry
University of Göttingen
Göttingen, Germany

Laramie Pence
Animal Bioscience and Biotechnology Laboratory
USDA Agricultural Research Science
MD, USA

and

Department of Animal and Avian Sciences
University of Maryland
MD, USA

Stoyan Petkov
Institute for Farm Animal Genetics
Friedrich-Loeffler-Institute
Neustadt, Germany

R.S. Prather
Division of Animal Science
University of Missouri-Columbia
Columbia, USA

and

National Swine Resource and Research Center
University of Missouri-Columbia
Columbia, USA

Karen E. Racicot
Department of Obstetrics
Gynecology and Reproductive Biology
Reproductive and Development Science Program
Van Andel Institute
Michigan State University
MI, USA

François J. Richard
Centre de Recherche en Biologie de la Reproduction
Département des Sciences Animales
Faculté des sciences de l'agriculture et de l'alimentation
Université Laval
Québec, Canada

Nicolas Santiquet
National Foundation for Fertility Research
Lone Tree
CO, USA

Ken-ichi Sato
Laboratory of Cell Signaling and Development
Department of Molecular Biosciences
Faculty of Life Sciences
Kyoto Sangyo University
Kyoto, Japan

Heide Schatten
Department of Veterinary Pathobiology
University of Missouri-Columbia
Columbia, USA

Elena Silva
Colorado Center for Reproductive Medicine
CO, USA

Marc-André Sirard
Département des Sciences Animales
Pavillon des services
Chaire de Recherche du Canada en Génomique Animale, Canada

Downloaded From Vet-eBooks.com

Lukasz Smorag
Institute of Human Genetics
University of Göttingen
Göttingen, Germany

Florenza A. La Spina
Instituto de Biología y Medicina Experimental (IBYME)
National Research Council of Argentina (CONICET)
Buenos Aires, Argentina

Cintia Stival
Institute of Molecular and Cell Biology of Rosario (CONICET-UNR) and
Área Biología
Facultad de Ciencias Biológicas y Farmacéuticas
UNR
Rosario, Argentina

Peter Sutovsky
Division of Animal Science
University of Missouri-Columbia
Columbia, USA

and

Department of Obstetrics
Gynecology and Women's Health
University of Missouri-Columbia
Columbia, USA

Hiroyuki Tateno
Department of Biological Sciences
Asahikawa Medical University
Asahikawa, Japan

Bhanu P. Telugu
Animal Bioscience and Biotechnology Laboratory
USDA Agricultural Research Science
MD, USA

and

Department of Animal and Avian Sciences
University of Maryland
MD, USA

Ana Luiza Cazaux Velho
Department of Animal and Dairy Sciences
Mississippi State University
MS, USA

and

Department of Animal Science
Federal University of Ceara
Fortaleza, Brazil

Siobhàn W. Walsh
Department of Chemical and Life Sciences
Waterford Institute of Technology
Waterford, Ireland

Hiroyuki Watanabe
Department of Biological Sciences
Asahikawa Medical University
Asahikawa, Japan

Shirley J. Wright
Department of Biology
University of Dayton
OH, USA

Shen Yin
Key Laboratory of Animal Reproduction and Germplasm Enhancement in Universities of Shandong
College of Animal Science and Technology
Institute of Reproductive Sciences
Qingdao Agricultural University
Qingdao, China

Downloaded From Vet-eBooks.com

1

Anatomy of the Reproductive System

Gheorghe M. Constantinescu

Department of Biomedical Sciences, College of Veterinary Medicine, University of Missouri-Columbia, Columbia, USA

The complexity of the organs that the mammalian reproductive system consists of, necessitates a general view of the systematization and short description of each structure involved. The following domestic mammals are subject of this chapter: cat (*Felis catus*), dog (*Canis familiaris*), pig (*Sus scrofa domestica*), large ruminant (*Bos Taurus*), sheep (*Ovis aries*), goat (*Capra hircus*), and horse (*Equus caballus*).

The anatomy of the reproductive system of laboratory animals and the nonmammalian animal models follow the description of domestic mammals' anatomy (König and Liebich, 2004; Nickel *et al.*, 1984). The laboratory animals are the rabbit (*Oryctolagus cuniculus*), the mouse (*Mus musculus*), and the rat (*Rattus norvegicus*). The nonmammalian animal models are the African clawed frog (*Xenopus laevis L.*) and the zebrafish (*Brachidanio/Danio rerio*).

The English anatomical terms are translated from *Nomina Anatomica Veterinaria* (NAV) (2012, *op. cit.* as ICVGAN) and from Gheorghe M. Constantinescu and Oskar Schaller, *Illustrated Veterinary Anatomical Nomenclature* 4th edn, Thieme (2012, *op. cit.*). For the corresponding terms in humans, the following reference is suggested: Heinz Feneis and Wolfgang Dauber, *Pocket Atlas of Human Anatomy Based on the International Nomenclature* (2000, *op. cit.*).

1.1 Male Genital Organs in Domestic Mammals

The male reproductive system of all mammalian species, including the laboratory animals, consists of the paired testicle, epididymis, ductus deferens, spermatic cord, accompanying tunics, accessory genital glands (single structures or pairs), the male urethra, the penis, and the prepuce.

Details of all components of the male reproductive system can be found in Schatten and Constantinescu (2007), Blackwell (*op. cit.*), Constantinescu and Constantinescu (2010), Omphaloskepsis (*op. cit.*), deLahunta and Habel (1986), Saunders (*op. cit.*), and Dyce (2010), 4th edn, Elsevier (*op. cit.*). For the laboratory animals except the rabbit, the details can be found in Constantinescu (2011) (a Color (water color) Atlas and Text, AALAS (*op. cit.*)). For the rabbit the details can be found in Barone (1973) Masson (*op. cit.*), and Barone (1978) École Nationale Vétérinaire Lyon (*op. cit.*).

1.1.1 The Testicle

The male gonad, with endocrine and exocrine functions, the *testicle*, is the essential organ of the male reproductive system, producing *testosterone* and *spermatozoa*, respectively. It has an ovoid

Animal Models and Human Reproduction, First Edition. Edited by Heide Schatten and Gheorghe M. Constantinescu.
© 2017 John Wiley & Sons, Inc. Published 2017 by John Wiley & Sons, Inc.

Downloaded From Vet-eBooks.com

shape, with the long axis species-specific oriented, a lateral and a medial surfaces, a free and an epididymal border, a head end, where the head of the epididymis is attached, and a tail end, where the tail of the epididymis is attached. (The body of the epididymis is not attached to the testicle.)

The testicle is intimately covered by a white and inextensible fibrous capsule called *Tunica albuginea*, which runs inside of the testicle walls, called *Septa* or *Septula*, which separate the testicular tissue into lobes (see Figure 1.1). Within the lobes, the *testicular parenchyma*, which is the functional tissue of the testis, consists of *seminiferous tubules, Leydig cells,* and *Sertoli cells.* The seminiferous tubules start as convoluted, and end as straight tubules that build up the *rete testis* within the *mediastinum testis*. The septa/septula converge into a structure called mediastinum testis.

1.1.2 The Epididymis, Ductus Deferens, and Spermatic Cord

The *epididymis* is the first excretory organ of the male reproductive system. It presents a head, a body, and a tail, all surrounded by the continuation of the testicular albuginea. The epididymis consists of *ductuli efferentes*—the continuation of the rete testis, and the *ductus epididymidis.*

The *ductus deferens* is the continuation of the ductus epididymidis and opens on the roof of the prostatic urethra at the level of colliculus seminalis. Within the spermatic cord it is connected to the *mesorchium* by the *mesoductus deferens*, whereas within the peritoneal cavity it is connected with the symmetrical duct and the paired ureter by the *genital fold.* An embryonic remnant of the fetal uterus (*uterus masculinus*) can be seen in some species within the genital fold.

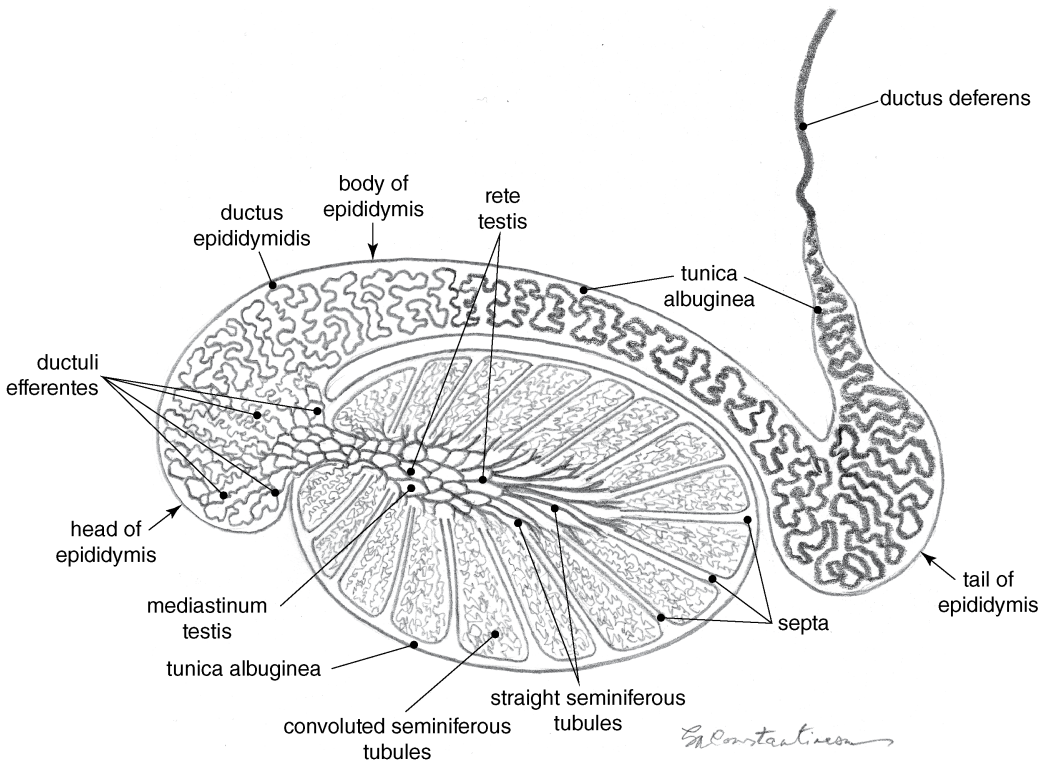

Figure 1.1 Internal organization of testicle and epididymis.

Downloaded from Vet-eBooks.com

The *spermatic cord* (Funiculus spermaticus) (see Figure 1.2) consists of the following:

- The ductus deferens with its blood and nerve supply surrounded and attached to the *mesorchium* by the *mesoductus deferens*
- The blood and lymphatic vessels and nerves supplying the testicle and the epididymis and smooth muscle fibers, all surrounded by the *visceral lamina of the vaginal tunic* and collectively called mesorchium.

The spermatic cord is connected to the *parietal lamina of the vaginal tunic* by the *mesofuniculus.*

1.1.3 The Descent of the Testicle

Starting its development on the roof of the abdominal cavity, the testicle with the epididymis is connected to the skin by a long mesenchymal tract (ligament) called *gubernaculum testis*, which runs within the inguinal canal. (The inguinal canal is outlined by the superficial and deep inguinal rings, the arcus inguinalis, and the internal abdominal oblique M. For details, see any veterinary anatomy book.) Pushing the transverse fascia and the parietal peritoneum through the deep inguinal ring, it will appear lined by the peritoneum under the name of *vaginal ring.* The space between the parietal and the visceral laminae of the *vaginal tunic* (continuation of peritoneum) within the inguinal canal is called *vaginal canal*, and that surrounding the testicle is

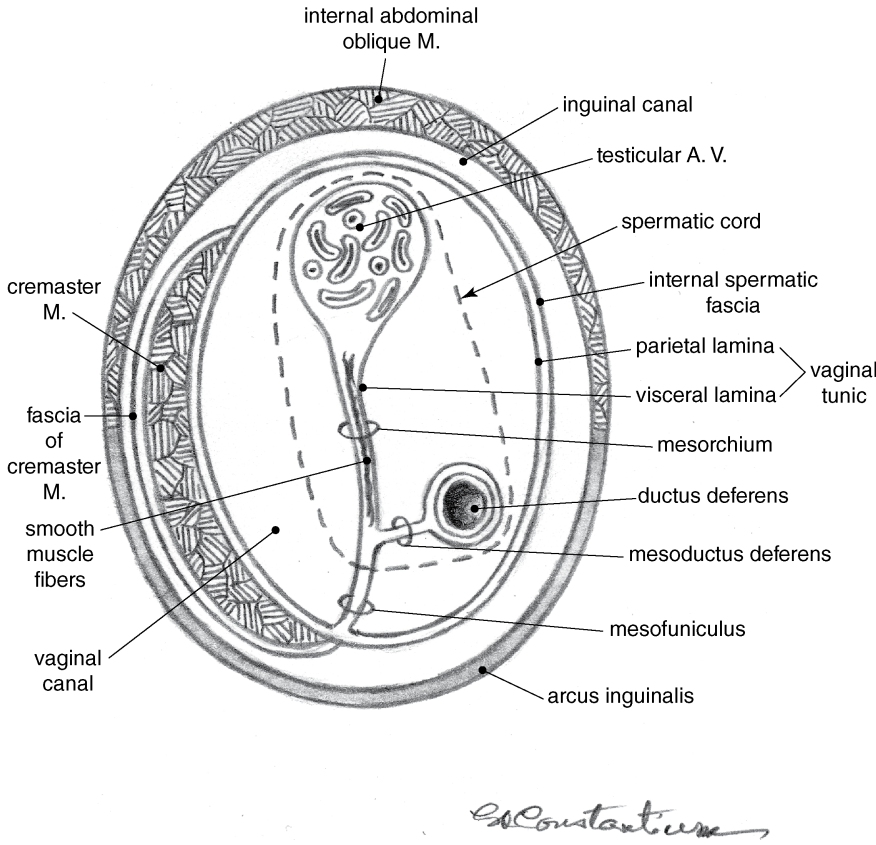

Figure 1.2 Transverse section through the spermatic cord (outlined by the broken line).

Downloaded from Vet-eBooks.com

called *vaginal cavity*. Before the testicle passes through the inguinal canal surrounded by the intraabdominal tunics (see below), these tunics enclosing the gubernaculum testis protrude through the inguinal canal under the embryological term of *vaginal process*. By the retraction of gubernaculum testis, the testicle passes through the inguinal canal and establishes finally within the *scrotum* (see below). After birth, the gubernaculum testis is represented by three ligaments: *proper ligament of testicle* (between the tail head of the testicle and the tail of the epididymis), the *ligament of the tail of the epididymis* (between the tail of epididymis and the external spermatic fascia), and the *scrotal ligament* (between the external spermatic fascia and dartos).

1.1.4 The Tunics of the Spermatic Cord and the Testicle

The systematization of these tunics in *intraabdominal* and *extraabdominal* eases their comprehension.

1.1.4.1 The Intraabdominal Tunics

These are the structures that are brought by the testicle from the abdominal cavity during its descent. The *internal spermatic fascia* is the continuation of the transverse fascia. The *vaginal tunic* is the continuation of the peritoneum (see above). The *cremaster M*. protected by the *cremasteric fascia* is intimately attached to the internal spermatic fascia, as a bundle of fibers from the internal abdominal oblique M.

1.1.4.2 The Extraabdominal Tunics

These are structures outside of the *inguinal canal.* They consist of the *external spermatic fascia*, which continues the superficial fascia of the abdomen and the loose subcutaneous connective tissue, and the skin which in the testicular area duplicates in a skin layer, the *scrotal skin*, and a layer of smooth muscle fibers called *Tunica dartos*. Together the scrotal skin and the tunica dartos are called *Scrotum*. The symmetrical external spermatic fascia surrounds the penis as the *superficial fascia of penis*, and continues in the perineal region as the *deep perineal fascia*. Tunica dartos surrounds the penis as the *deep fascia of penis* and continues as the *superficial perineal fascia.*

1.1.5 The Accessory Genital Glands

The glands of the ampullae of the ductus deferens, the vesicular glands/seminal vesicles, the prostate, and the bulbourethral glands differ from species to species in number and aspect, and from intact male to a sexually immature or an orchiectomized male.

There are no *ampullae of the ductus deferens* in the cat and in the pig. The *vesicular glands* are present in ungulates, but in the horse they are called *seminal vesicles.* The carnivores lack the vesicular glands. The *prostate* is the only accessory gland in the dog. In all species it consists of a body (surrounding the prostatic urethra) and a disseminate part (within the walls of the urethra). The latter is found in the pig, ox, and goat, is deficient ventrally in the sheep, and represented by a few lobules in carnivores. No disseminate part of prostate is found in the horse. The *bulbourethral glands,* absent only in the dog, are located symmetrically at the level of the curvature made by the urethral isthmus, between the pelvic and the penile parts of urethra.

1.1.6 The Penis and the Prepuce

The *penis* is an external genital, and the male organ of copulation. It consists of a root, a body, and a free part surrounded and protected by the prepuce, and the glans penis.

Downloaded From Vet-eBooks.com

The *root* of the penis consists of two crura and the bulbus penis. The paired *crus penis* is the origin (proximal end) of corpus cavernosum penis. They are attached to the ischiatic arch covered by the ischiocavernosus muscles and join with each other in a "V"-shaped fashion to build up the corpus cavernosum penis. Between the two crura the *bulbus penis* is located. The latter is a proximal enlargement (at the origin) of spongy tissue that surrounds the penile urethra, spongy tissue called *corpus spongiosum penis.*

The *body of the penis* is represented by the continuation of the two crura, distally, and is called *corpus cavernosum penis*. The penile urethra surrounded by the corpus spongiosum penis runs on the ventral side of it.

The *free part of the penis* includes the glans penis, distal to the attachment of the prepuce. The *glans penis* is the head of the penis, containing the *corpus spongiosum glandis*. In the tomcat a *cartilage*, and in the dog, mouse, and rat an *os penis* is included. Species-specific characteristics will be detailed later on.

The *prepuce* is the skin surrounding and protecting the free part of the penis in the resting position. It is a fold of skin consisting of an external and an internal laminae, continuous at the *preputial ostium.* The internal lamina attaches to the origin (proximal end, or base) of the free part of the penis, where it continues with the skin of the free part of the penis, visible when the penis is fully erect.

1.2 Female Genital Organs in Domestic Mammals

The female reproductive system of all mammalian species consists of the paired ovary, uterine, or fallopian tube (salpinx), and the uterus, the vagina, the vestibule, vulva, and clitoris. The mammary glands are associated with the female genital organs, and will be described in general terms.

Details of all components of the female reproductive system can be found in Schatten and Constantinescu (2007, *op. cit.*)

1.2.1 The Ovary

Similar to the male, the female gonad is a mixed gland with endocrine and exocrine functions. The *ovary* is the essential organ of the female genital system, producing *progesterone,* and *estradiol,* also *oxytocin, relaxin, inhibin,* and *activin*. As the exocrine function the ovary produces *ovules* (ovocytes, oocytes). Ovoid in shape, with a medial and a lateral surface, a free and mesovarian borders, tubal and uterine extremities, the ovary is provided with a hilus.

Notice that the mesovarium is attached to the mesovarian border, opposite to the free border, and the uterine extremity (toward the tip of the uterine horn) is opposite to the tubal extremity, in close proximity to the infundibulum of the uterine tube. Also, the hilus is the area of attachment of the mesovarium, and entrance of ovarian vessels.

A *tunica albuginea* intimately covers the ovary, similar to that of the testicle. In all species the *stroma* is the framework of the ovary (see Figures 1.3 and 1.4), consisting of fibrous tissue and smooth muscle, whereas the *parenchyma* is the functional tissue of the ovary. Except in the horse, the ovary consists of a peripheral cortex and a central medulla. In the mare the cortex is central, and the medulla is peripheral.

The *cortex* of the most mammals except the mare, which is also called the parenchymal zone, contains all categories of follicles: primary, secondary, tertiary (vesicular ovarian follicles), the

Downloaded From Vet-eBooks.com

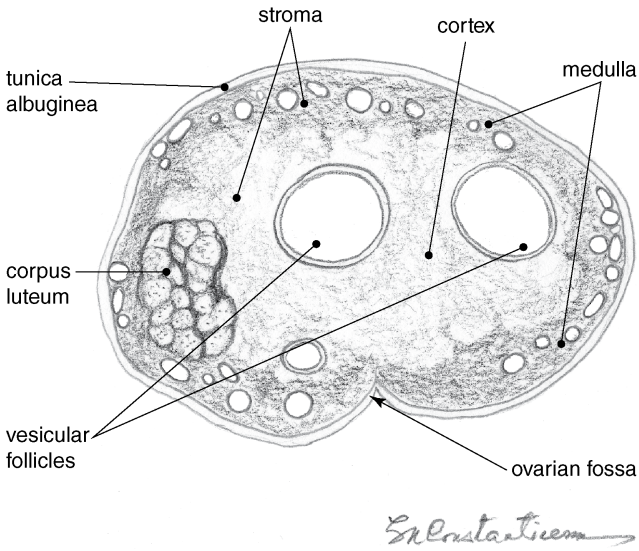

Figure 1.3 Internal organization of the mare's ovary.

corpus luteum, the corpus albicans, and atretic ovarian follicles. A mature follicle eliberates the ovule, which leaves the ovary through the cortex.

The *medulla*, also called the vascular zone, consists of vessels and nerves nourishing the ovary and is located in all species except the mare, after entering the *hilus*. In the mare, the free border of the ovary has an indentation/depression called the *ovarian fossa*, where the mature ovule leaves the ovary (the ovulation occurs), reason that some clinician call the ovarian fossa *ovulation fossa*.

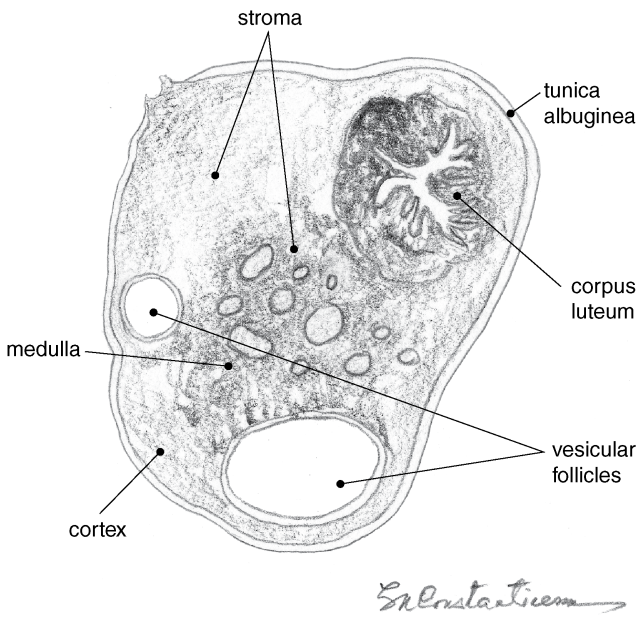

Figure 1.4 Internal organization of the cow's ovary.

Downloaded from Vet-eBooks.com

The ovary is connected to the surrounding structures by the *suspensory ligament* (to the diaphragm), the *proper ligament* (to the apex of the uterine horn), and the *mesovarium* (which is the most cranial segment of the *broad ligament*). In a similar manner in which the mesepididymis separates the mesorchium in a proximal and a distal segment, the mesosalpinx separates the mesovarium into a proximal and distal segment.

Two groups of vestigial structures from the developmental life called epoöphoron and paroöphoron may be associated with the ovary after birth.

1.2.2 The Uterine Tube: Salpinx, Fallopian Tube

The *uterine tube* extends from the apex of the uterine horn (where it is attached to), and this is called the uterine end, to the vicinity of the ovary (and this is called the ovarian end) on the lateral side of the broad ligament. It is flexuous and has an uneven size, basically being divided into two distinct portions, the ampulla and the isthmus. We can distinguish two openings or ostia, the infundibulum, and the fimbriae, and in some species (carnivores, horse) the uterine part of the uterine tube, provided with a papilla.

The closest opening to the ovary is the *abdominal ostium* within the *infundibulum*. The latter is the funnel-shaped ovarian end of the tube. The infundibulum is provided with a fringe of processes called *fimbriae*, around the opening of the infundibulum. The fimbria, which is intimately attached to the ovary, is called *ovarian fimbria*. It is important to mention that the abdominal opening of the uterine tube corresponds to the peritoneal cavity, allowing the connection between the external environment (through the vagina) and the peritoneal cavity. The *ampulla* is the widest part of the tube, between the abdominal ostium and the isthmus. The *isthmus* is the narrow part of the salpinx, continuing with the uterine part of the tube. The *uterine part of the salpinx* is the shortest segment of the tube. It passes through the wall of the apex of the uterine horn and in some species (see above) ends on a papilla, whereas in the other species the salpinx gradually continues with the uterine horn. At this level, the salpinx opens into the uterus through the *uterine ostium of the uterine tube.*

As a part of the broad ligament, the *mesosalpinx* holds in place the uterine tube. The *ovarian bursa* is outlined by the distal mesovarium, the mesosalpinx, and the ovary. The entrance into the ovarian bursa is medially oriented.

1.2.3 The Uterus

The *uterus* is the organ of pregnancy, or gestation. In most mammals it consists of three major components: two horns, one body, and one cervix or neck, and it is called *uterus bicornis.* In the rabbit and the rat, the horns and cervix are paired, this type of uterus being called *uterus duplex*. In these two species the uterine horns run together side by side for a short distance caudally, and end by their own cervices. Therefore, there is no body of uterus in these two species. In primates, including humans, the uterus has only one body and the cervix, which is a characteristic of the *uterus simplex*. Nevertheless, Feneis and Dauber (2000) 5th edn Thieme (*op. cit.*) listed on p. 168.9 right and left uterine horns as "pointed extensions of the uterus at the entrance of the uterine tubes owing to the incomplete union of both paramesonephric ducts" (from the intrauterine development).

The uterine horns of the uterus bicornis and duplex expose mesometrial and free borders, and corresponding cavities. The uterine body and the cervix of the uterus bicornis have a right and a left mesometrial border, a dorsal and a ventral surface, and a cavity (for the cervix the cavity is called cervical canal). The cervices of the uterus duplex expose short right and left mesometrial

Downloaded From Vet-eBooks.com

borders, dorsal and ventral surfaces, and their own, totally separated from each other, cervical canals. In all species the cervix has two openings: the internal uterine orifice opening toward the uterus and an external uterine orifice, between the cervix and the vagina.

The *uterine horns* vary from species to species in shape, size, and location. Each uterine horn has two openings: at the *apex* (tip) it communicates with the uterine tube through the uterine orifice of the tube, whereas caudally it opens into the body of the uterus. Here they are separated by a fold of mucosa called *uterine velum*, except in the mare. The mesometrial borders serve for the attachment of the *mesometrium*, the last component of the broad ligament.

The *body of uterus* is a unique compartment, where the embryo and the fetus develop before birth. In the mare, because of the lack of uterine velum, the caudal extent of the uterine body is called *fundus*. The mesometrium is provided with the *round ligament of the uterus*, which may extend from the apex of the uterine horn or uterine body to the deep inguinal ring enclosed in a lateral fold of the broad ligament. The round ligament of the uterus in carnivores will be described later.

The *cervix* has thick muscular walls and a narrow canal through which the fetus will exit the uterus. It has different species-specific structures, which make easy or complicate the birth and the artificial insemination (A.I.). It is important to note that the cervix has two distinct parts: a *prevaginal* and a *vaginal part*. The former is the part of the cervix cranial to the vagina, and the latter is the part that protrudes into the vagina. The more the cervix projects into the vagina, the deeper the *vaginal fornix*, the cranial blind pouch of the vagina surrounding the vaginal part of the cervix. Both vaginal part of the cervix and the fornix are very important structures in the mare and the female dog.

1.2.4 The Vagina and the Vestibule

The *vagina* is the canal located between the cervix and the external urethral orifice, or the hymen. The vaginal fornix has already been described. The *hymen* is a poorly developed transverse fold of the floor of the vagina just cranial to the external urethral ostium. The vagina opens into the vestibule through the *vaginal ostium.* Remnants of embryological structures can be seen on the floor of the vagina, on both sides of the external urethral orifice in the cow.

The last compartment of the female genital organs, the *vestibule,* communicates cranially with the vagina and caudally with one of the external parts of the female genital organ, the vulva. It is a very long canal in the domestic mammals in comparison to humans, and with the exception of the cat, shorter than the vagina. In the domestic mammals it is not considered an external organ, as it is considered in humans. On the lateral walls and the floor of the vestibule, an erectile tissue (*the vestibular bulb*) and several glands can be seen. The constrictor muscle of the vestibule and vagina is well developed in the female dog and the mare. A *suburethral diverticulum* is shown in the sow and the ruminants. In the female dog a *urethral tubercle* is seen at the vastibulovaginal junction.

1.2.5 The Vulva and the Clitoris

In the domestic mammals the vulva and the clitoris are considered the female external genital parts.

The *vulva* is located in a subanal position and is provided by two pairs of *labia, major and minor*, not easily distinguishable in the domestic mammals, as in humans, with some exceptions. Usually the vulva consists of two symmetrical labiae. The labiae meet in a dorsal and a ventral *commissures*, differently shaped in the domestic mammals. The contact borders of the two

Downloaded From Vet-eBooks.com

labiae between the two commissures outline the *pudendal fissure,* the external urogenital opening.

Rudimentary partial homologue of the penis, the *clitoris* is located on the floor of the vestibule (some exceptions in laboratory animals). The only notable difference between the penis and the clitoris consists of the lack of urethra in the clitoris. The two *crura* and the *body with the corpus cavernosum*, the *glans with the corpus spongiosum,* and the *fascia of the clitoris* are the major components of this organ. The glans is protected within the *fossa of the clitoris*. The *prepuce* and the *frenulum* are also associated with the clitoris.

1.2.6 The Mammary Gland

The mammary gland(s) are associated with the female genital system. A detailed description for all species of domestic mammals with the blood supply, lymph drainage, and nerve supply is available in Schatten and Constantinescu (2007, *op. cit.*).

1.3 The Genital System in Domestic Mammals Species by Species

The male and the female genital systems in all species will follow the same step-by-step description as it was chosen for the general description, single or several structures under the same section.

In Section 1.3.1.1, the first section describes the testicle, epididymis, ductus deferens, spermatic cord, and investing tunics in the male. The second section describes the accessory genital glands, the third section describes the penis and the prepuce, and the fourth section describes the male urethra.

Section 1.3.1.2 consists of five sections providing a general description on female reproductive organs. No mammary glands will be described as a separate section. Illustrations are provided for the domestic mammals in Schatten and Constantinescu (2007, *op. cit.*), and for the laboratory animals (see Figures 1.68–1.70).

1.3.1 The Genital System in the Carnivores: Cat and Dog (Constantinescu, 2002)

1.3.1.1 Male Genitalia

The Testicle, Epididymis, Ductus Deferens, Spermatic Cord, Tunics

The descent of the testicles occurs very late during the development (around the second week after birth). They reach the scrotum at the end of the third week.

The *testicles* are located just under the anus in the cat, and in the lower perineal region in the dog (between the two thighs). Globular in shape, the testicles of the cats and dogs are oblique, with the long axis cranioventrally oriented. The testicular artery running deep to the albuginea makes a species-specific characteristic design (see Figures 1.5 and 1.6). The average weight of testicles in the cat is 1.3 g, whereas in the dog it varies with the breeds between 7 and 20 g.

The *epididymis* is similar in cats and dogs, and it follows the general description. The ductus epididymidis is as long as 1.5–3 mm in the cat, and 5–8 mm in the dog.

The *ductus deferens* lack the ampulla in the cat, and in the dog is less distinct. Since there are no vesicular glands in both species, there is no ejaculatory duct.

The *spermatic cord* is the longest in the cat, because of the location of the testicles, and runs horizontally. In the dog it is slightly obliquely oriented in a dorsocranial direction.

Downloaded From Vet-eBooks.com

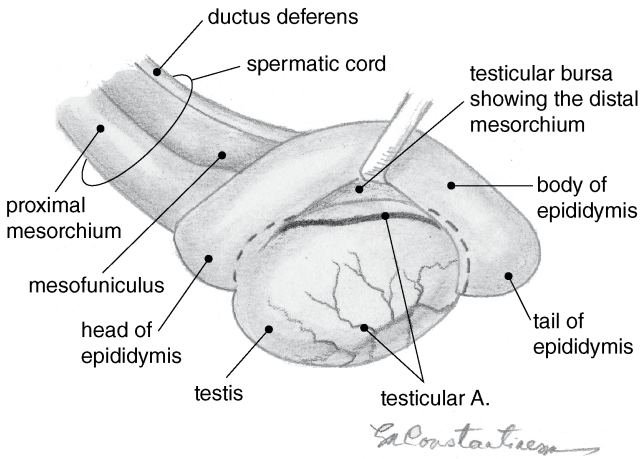

Figure 1.5 Testicle of the dog: lateral aspect.

The *testicular tunics* are similar to the general description, but the characteristic for both species is the fact that there is no ligament of the tail of the epididymis. The parietal lamina of the vaginal tunic and the internal spermatic fascia are adherent to the tail of the epididymis, which does not leave any space for the ligament of the tail of the epididymis. Instead, the scrotal ligament connects the tail of the epididymis directly to the tunica dartos.

Accessory Genital Glands

No *ampullae of the ductus deferentes*, no *vesicular glands* are present in both species.

The *prostate* (see Figure 1.7) is common to both species. In the cat the body of the prostate is bilobed, with a slightly lobulated surface, and does not completely surround the urethra, leaving ventrally a free space. The disseminate part is limited to the dorsal wall of the intrapelvic urethra. In the dog the body of the prostate is voluminous, bilobed, with a lobulated surface, and surrounds the urethra completely. The disseminate part is located similar to that of the cat.

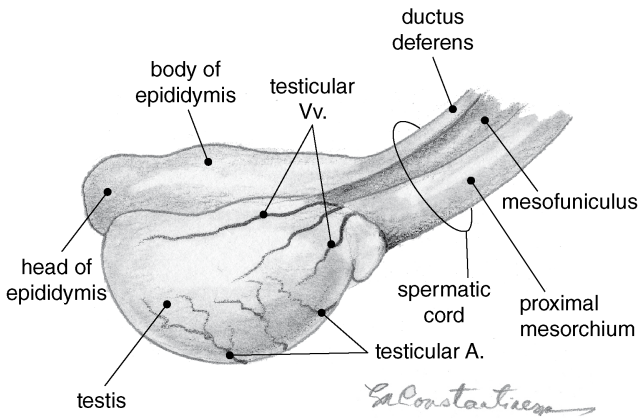

Figure 1.6 Testicle of the dog: medial aspect.

Downloaded from Vet-eBooks.com

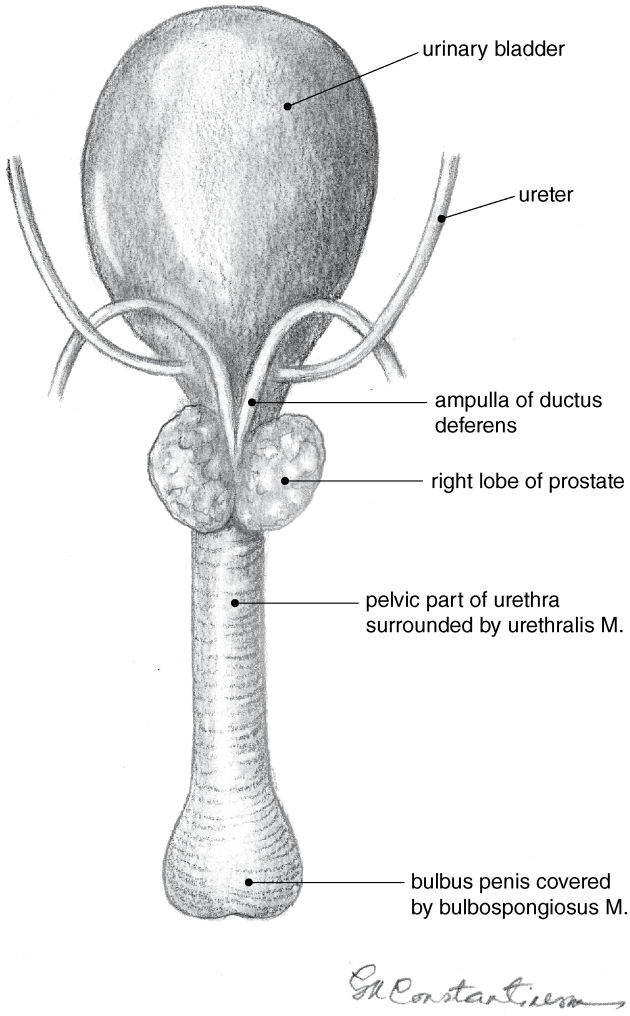

Figure 1.7 Accessory genital glands in the male dog: dorsal view.

The *bulbourethral glands* are present in the cat only. They are located dorsolateral to the urethral isthmus, spheroidal in shape, and pretty voluminous (5–6 mm in diameter).

The Penis and the Prepuce

The main characteristic of the carnivores *penis* is the fact that a *cartilage* in the cat, and a *bone* in the dog (*Os penis*) are found within the glans penis. The cartilage of the cat may ossify. The os penis of the dog is triangularly shaped on a transverse section and presents a ventral groove that protects the urethra and the corpus spiongiosum glandis.

In the cat the location of the penis is just ventral to the testicles, and obliquely oriented in a ventrocaudal direction, with the urethral aspect in a dorsal position. During the erection it changes to a ventrocranial oblique position, with the urethral side ventral. The penis is provided with more erectile tissues than the penis of the dog. The glans penis is short and conique, and provided with numerous *keratinized papillae* oriented toward the base of the penis.

Downloaded from Vet-eBooks.com

In the dog the penis is located in a subabdominal position, parallel to the ventral contour of the abdominal wall. The crura of the corpus cavernosum are long and covered by strong and voluminous ischiocavernosus muscles. They connect with one another in the corpus cavernosum penis, which distinctly shows the separation between the two halves; even though they are fused, a thick septum separates the two halves. The corpus spongiosum penis, which continues with the corpus spongiosum glandis, is poorly developed in comparison to the cat. The former begins with the bulbus penis, which in the dog is paired and covered by the bulbospongiosus muscle. It is big, originates close to the ischial arch, and extends close to the scrotum. The corpus spongiosum glandis surrounds the penile urethra.

The body of the penis is short. Instead, the *glans penis* is voluminous and long, and consists of a bulb and a *long part*. The bulbus penis, which covers dorsally the proximal part of the os penis, is 2.5 cm in diameter in the resting functional status, whereas during the copulation it can reach 8 cm in diameter. With the help of the symmetrical constrictor muscle of bulbus vestibuli (of the female), and the slow engorgement of the bulb, the penis is "locked" and allows the male to perform the second time of copulation, which lasts approximately 20 min. For details, see Evans (1993), Saunders (*op. cit.*), and Evans and deLahunta (2013), Elsevier (*op. cit.*). The long part of the glans penis surrounds the "V"-shaped part of the os penis. A corona glandis is present in the dog (see Figure 1.8).

The *prepuce* of the cat is detached and placed under the scrotum. It is short and opens in a caudal direction The preputial orifice is directed caudoventrally. In the dog the prepuce is long and in its cranial portion is attached to the ventral wall of the abdomen only by a fold of skin. The internal lamina is attached to the middle of bulbus glandis and covers the rest of the gland as the penis skin. The preputial cavity is wide. A pair of cranial preputial muscles is attached to the prepuce.

The Male Urethra

In the cat the *preprostatic part of the pelvic urethra* is much longer than that of the dog. In both species the prostatic part is associated with the prostate gland. The *urethral crest* and the *colliculus seminalis* are prominent in both species. There are only two symmetrical openings on both sides of colliculus seminalis for the ductus deferentes (no vesicular glands in carnivores). A spongy layer (cavernous tissue) surrounds the pelvic urethra and continues with the corpus spongiosum penis. The urethralis muscle surrounds the pelvic urethra, and continues as the bulbospongiosus muscle, which surrounds the *penile urethra* and the bulbus penis. The urethra opens distally by the external urethral orifice. The bulboglandularis muscles are present only in the cat.

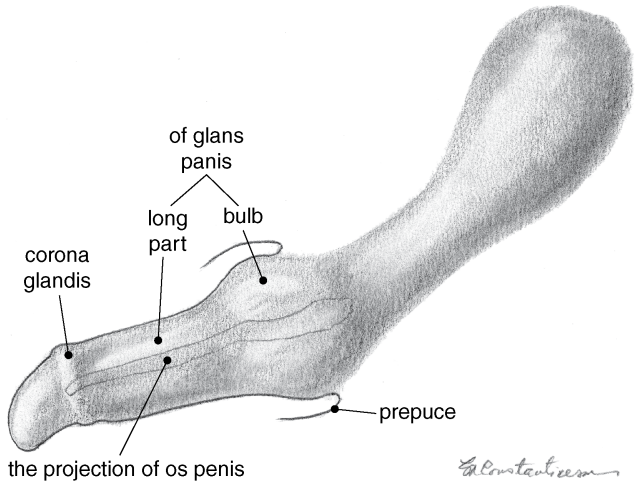

Figure 1.8 Penis of the dog.

Downloaded from Vet-eBooks.com

1.3.1.2 Female Genitalia (see Figure 1.9)

The Ovary

Bean shaped and flat, the *ovaries* are protected within the ovarian bursae. The entrance into the *ovarian bursa* of the dog is very narrow. The *suspensory ligament* is very long, while the *proper ligament of the ovary* is much shorter.

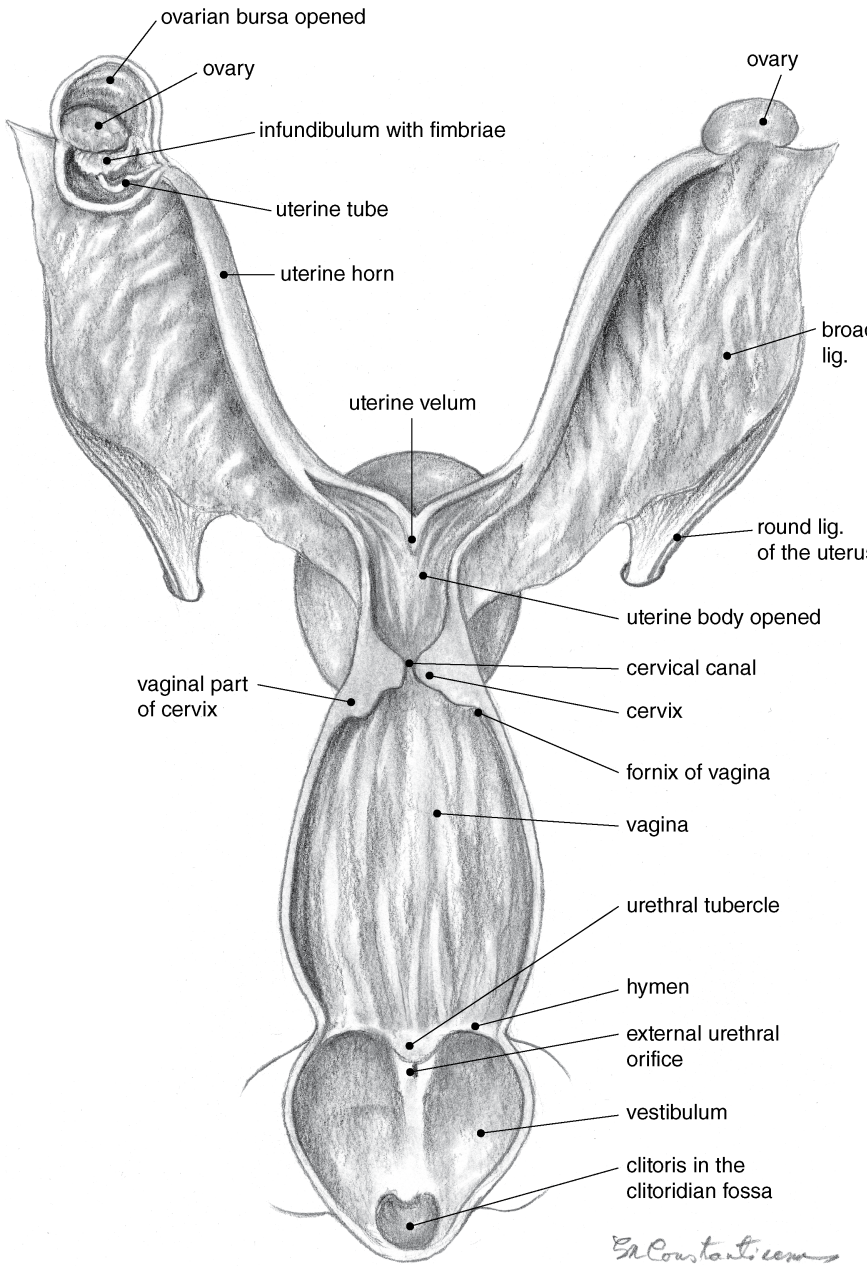

Figure 1.9 Genital apparatus of the female dog: dorsal aspect.

Downloaded from Vet-eBooks.com

The Salpinx

Twice as long in the dog as in the cat, the *uterine tubes* are very narrow and each ends on a small *uterine papilla*. The flexuosity shown in the large mammals is almost absent.

The Uterus

Twice as long and wide in the dog as in the cat, the *uterine horns* have rounded cranial ends and they meet with each other to form the body of the uterus caudally.

The *uterine body* is also twice as long and wide in the dog as in the cat. Inside, it is provided with a *uterine velum* starting from the junction of the two horns, and which incompletely separates the uterine cavity.

The *cervix* in carnivores (see Figure 1.10) has unique characteristics, very important during the performing of the A.I. (see McCarthy (2005), p. 414, Elsevier *op. cit.*). The *cervical canal* is short, and communicates with the uterine body by the internal uterine orifice. The vaginal part of cervix protrudes into the vagina on the roof as a rounded *cervical tubercle*, which continues as a very developed dorsal median fold. Thus, the external uterine orifice opens on the ventral aspect of the cervical tubercle, and is directed toward the vaginal floor. The *vaginal fornix* is located only on the ventral side of the tubercle—the external uterine orifice is not surrounded by the fornix as it is in the large mammals. In the cat the cervical tubercle has fine folds.

The *broad ligament* consists of the mesovarium, mesosalpinx, and mesometrium. The *round ligament* of the uterus originates from the lateral surface of mesometrium and in the dog it is enclosed in a fold of the broad ligament and passes through the inguinal canal accompanied by the transverse fascia and the parietal peritoneum collectively known as the *vaginal process*. The round ligament of the uterus concealed within the vaginal process exits the inguinal canal and can be felt under the skin as far as close to the vulva. In the cat the round ligament of the uterus is not accompanied by the vaginal process (see Watson, 2009, *op. cit.*).

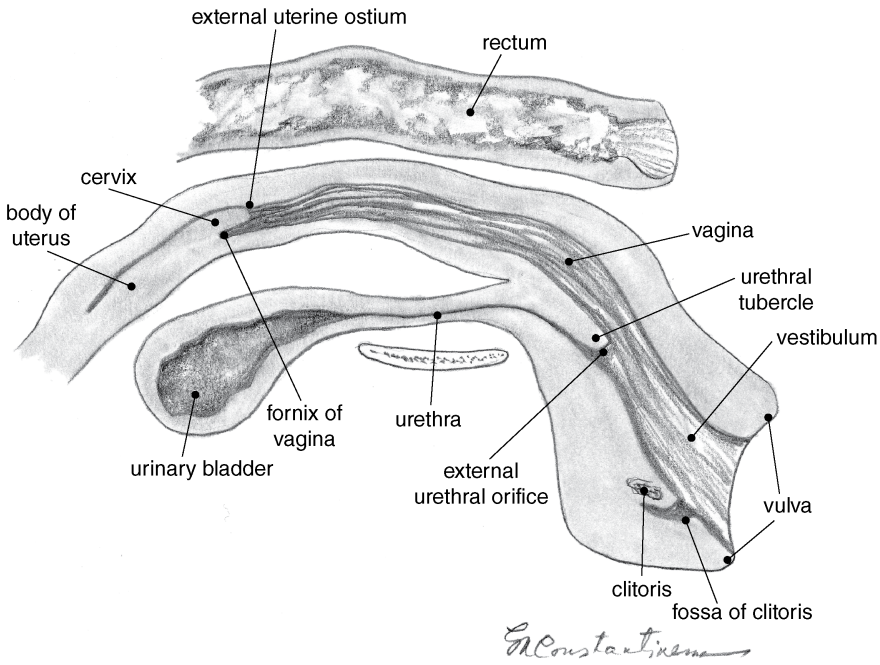

Figure 1.10 Sagittal section through the uterus and vagina of the dog. (Modified and redrawn from Evans (1993).)

Downloaded from Vet-eBooks.com

The Vagina and the Vestibule

The *vagina* is a very long canal in the dog as against that in the cat, and lasts from the external uterine ostium to the external urethral ostium, located on the floor between the vagina and the vestibule. The most important structures of the mucosa are the *cervical tubercle* and the *dorsal median fold*. Along with the other smaller longitudinal mucosal folds, the urethral tubercle (in the dog only), and the shallow transversal ridge of the mucosa (the potential hymen) cranial to the external urethral orifice, these are the most relevant structures of the vagina in both species.

The last of the internal genital organs, the *vestibule*, has a very peculiar position—it is caudoventrally obliquely oriented, which makes the A.I. technique difficult, especially for the beginners. In length the vestibule of the cat is proportionately much longer than that of the dog, and seems to have the same length as the vagina. The external urethral orifice opens in a deep mucosal groove—there is no urethral tubercle. The *vestibular bulb*, involved in the mating process, is present only in the dog, surrounded by a rich venous plexus. In the cat only the venous plexus persists, richer and denser than in the dog. The minor vestibular glands are present in both species, whereas the major glands are present only in the cat.

The Vulva and the Clitoris

Together with the clitoris, the *vulva* is a part of the external genital organs. The *vulvar labiae* are thick in both species, and sometimes the major labiae can be differentiated from the minor labiae, especially in the dog. The dorsal commissure of the vulva is rounded in the dog and pointed in the cat, whereas the ventral commissure is pointed in the dog and rounded in the cat.

Very large in both species especially in the dog, the *clitoris* consists of two crura (2–3 cm in the dog), a body (4 cm in the dog), and the glans. The *crura* and the *body* lie on the floor of the vestibule, whereas the *glans* (less visible in the cat than in the dog) lies on the floor of the *clitoral fossa*. The cat *clitoral glans* includes a small cartilage that resembles the os penis of the male. In the resting position the clitoris of the dog lies in the clitoral fossa with the glans down as shown on page 428, Fig. 13-6 in McCarthy (2005, *op. cit.*). During copulation, the clitoris becomes erect and takes a considerable role in the process.

1.3.2 The Genital System in the Pig

1.3.2.1 Male Genitalia

The Testicle, Epididymis, Ductus Deferens, Spermatic Cord, and Tunics

In the pig the descent of the testicles occurs several days before birth (around the 110th day of gestation). The cryptorchidism is relatively frequent in this species.

The long and eliptical *testicles* are very large in the boar. They are located in a subanal position, close to the anus, with the tail ends oriented dorsocaudally. The location of the testicles pulls the spermatic cords far caudally. They are very long, and the inguinal canal is very much obliquely oriented, which causes frequent inguinal herniae. The species-specific design of the testicular artery is shown in Figures 1.11 and 1.12.

The *epididymis* is voluminous. Its tail is so much detached that it looks like an appendix to the testicle. The *epididymal duct* is long and tortuous. The *proper ligament of the testicle* and the *ligament of the tail of the epididymis* are strong.

The *ductus deferens* is as long as the spermatic cord. It is not provided with an ampulla. After exiting the vaginal canal it changes the direction in a sharp caudal angle, crosses the direction of the corresponding ureter and ventral to it in its way to the prostatic urethra, covered by the vesicular gland. In castrated males the entire abdominal route of the ductus deferent is exposed. The genital fold binds down the paired ureters, the ductus deferentes, and the cranial extents of

Downloaded From Vet-eBooks.com

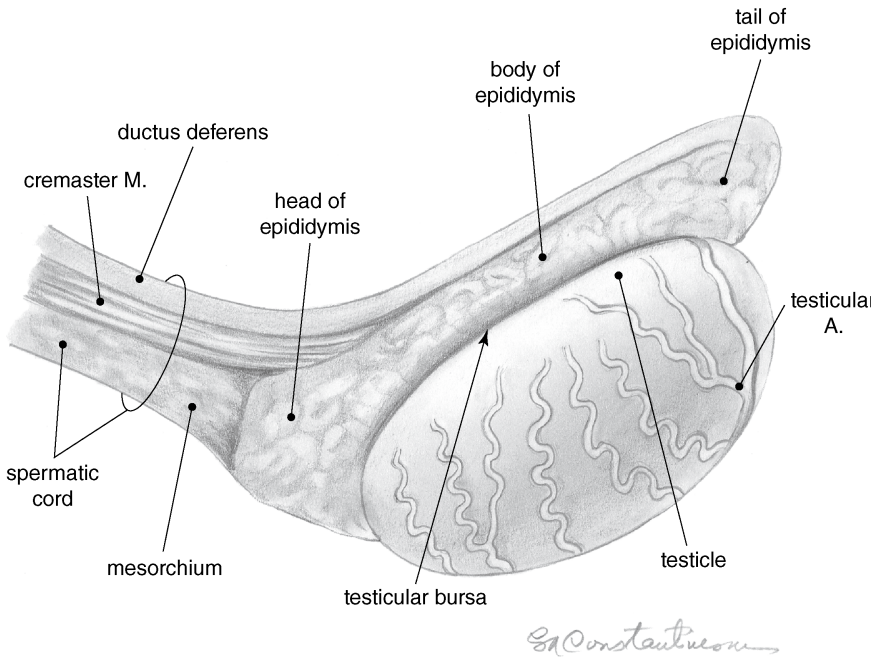

Figure 1.11 Testicle, epididymis, and spermatic cord of the boar: lateral aspect.

the vesicular glands. In the final leg of its journey, the ductus deferens passes through the prostate gland and opens on the corresponding side of the *colliculus seminalis*.

The *spermatic cord* is slightly different from the other species in that the *mesofuniculus* is in a vertical position and attached to the dorsal wall of the vaginal canal.

The *testicular tunics* are thicker than in the carnivores, especially the extraabdominal tunics, as follows: The *scrotum* is divided into two halves by a deep *scrotal raphe*. The *scrotal ligament* is strong to maintain the testicle suspended within the scrotum. The *external spermatic fascia* is thick.

Accessory Genital Glands (see Figure 1.13)

The *ampulla* of the ductus deferens is provided with glands.

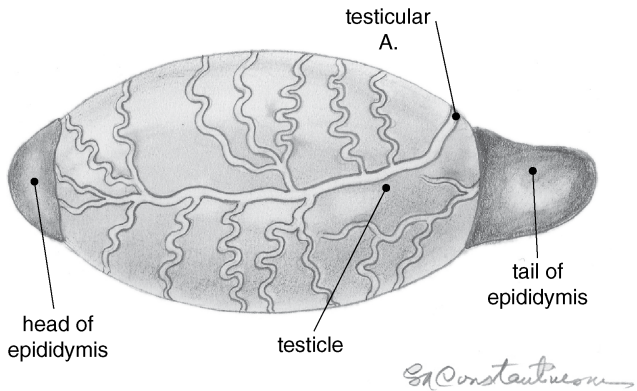

Figure 1.12 Testicle of the boar: the free border.

Downloaded from Vet-eBooks.com

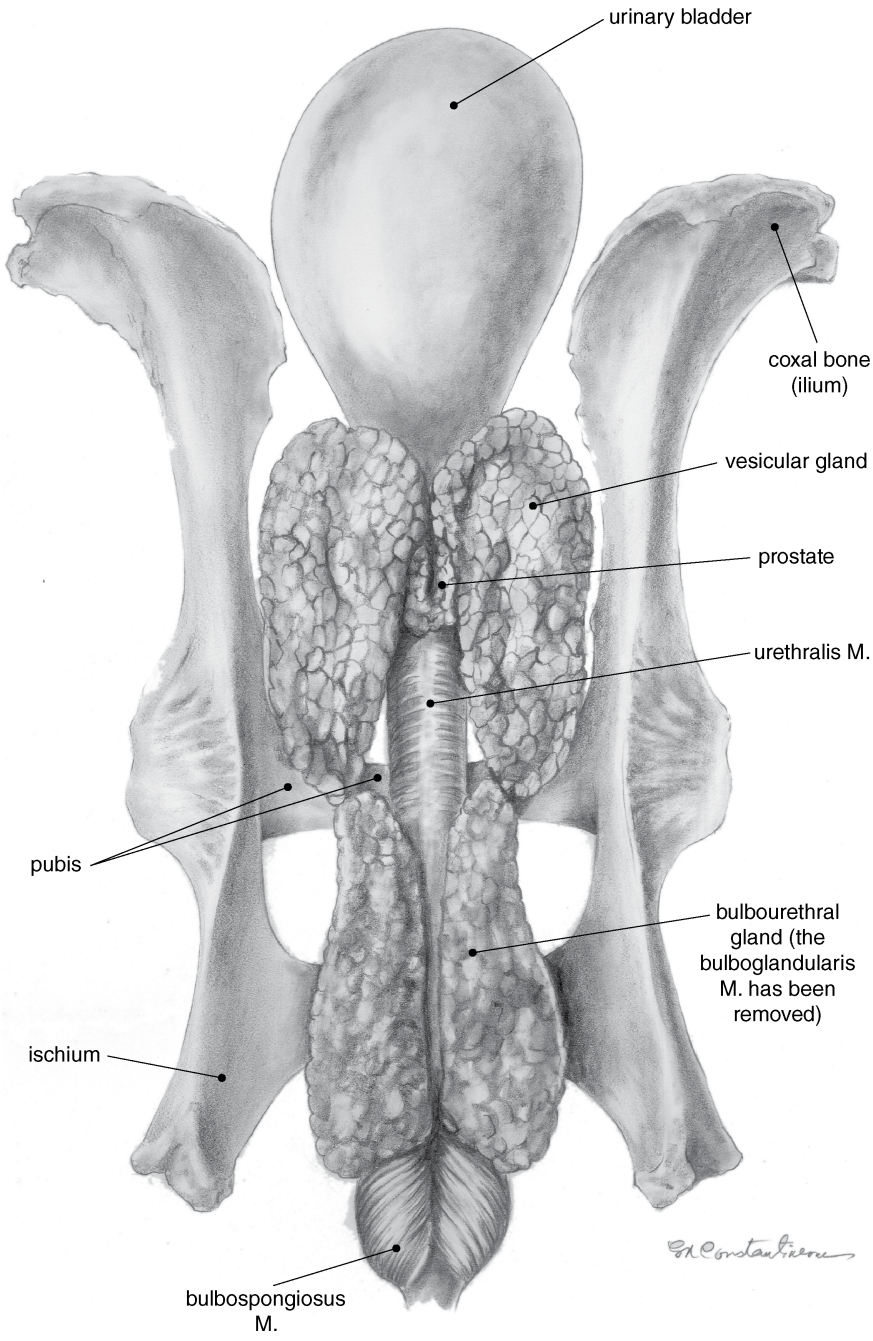

Figure 1.13 Accessory genital glands of a mature boar: dorsal aspect.

The *vesicular gland* is enormous in the boar, and gradually regresses after castration. It is pyramidally shaped, with the base of the pyramid cranially oriented and dropped into the abdominal cavity over the neck of the urinary bladder. The symmetrical glands touch each other in the median plane, covering and hiding the small prostate gland. The surface of the vesicular

Downloaded from Vet-eBooks.com

gland is lobulated. The unique excretory canal of each gland opens on the ipsilateral side of the ductus deferens, lateral to the *colliculus seminalis*.

The *prostate gland* has a very small compact part, and a widely disseminated part. The former consists of two symmetrical lobes and is overlapped by the vesicular glands, whereas the latter completely surrounds the urethra.

The *bulbourethral glands* are very large and cover almost completely the pelvic urethra from the cranial extent of the pelvic floor to the bulbus penis. Completely surrounded by the bulboglandularis muscles, the glands touch each other by the medial borders. One excretory canal of each gland opens into the penile urethra ventral to the *urethral recess* (specific to the pig and ruminants only) (see Constantinescu and Schaller, 2007, pp. 210–211, *op. cit.*; Garrett, 1987, *op. cit.*).

The Penis and the Prepuce (see Figure 1.14)

A fibroelastic type, the *penis* of the pig is very long, with a wide and thick root (the bulbus penis is voluminous). Its body is provided with a *sigmoid flexure*, starting after the two crura form the corpus cavernosum penis. The corpus spongiosum penis and the bulbus spongiosus muscle are limited to the bulbus penis. The ischiocavernosus muscles are attached to the proximal curve of the sigmoid flexure. The retractor penis muscles extend cranial to the distal flexure of the sigmoid flexure. The *glans penis* is very reduced, and the apex of penis is cylindrical and spiraled first to the right, then dorsally, and finally to the left. This shape is due to the asymmetry of the corpora cavernosa before fusing with each other, and to the albuginea. A *raphe penis* joins the glans to the free part of the penis (see Figure 1.14).

The *prepuce* is divided into two uneven compartments by a circular fold of the internal lamina, which separates the *preputial cavity* into a very long caudal compartment (20–25 cm) and a very short cranial compartment. The latter is provided with a *preputial diverticulum,* a large dorsal bilobed sac, specific to the pig, with approximately 135 ml capacity. The two symmetrical halves of the diverticulum are separated by a median fold of the roof. The strong *cranial preputial muscles* cover the preputial diverticulum helping to empty it, and fuse with each other on the ventral aspect of the prepuce. The *caudal preputial muscles* are thin and extend from the superficial inguinal ring to the lateral borders of the prepuce. They do not reach the preputial orifice.

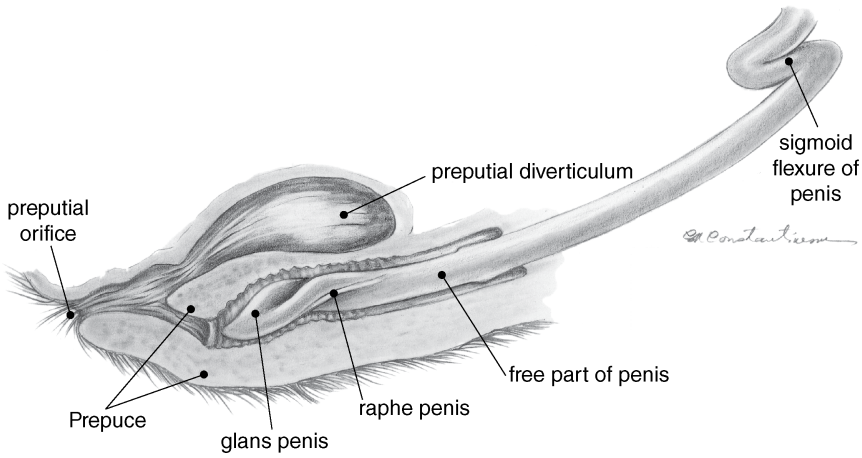

Figure 1.14 The pig's penis within the prepuce: lateral view.

Downloaded from Vet-eBooks.com

The Male Urethra

The *male urethra* in the pig (and in the ruminants) is unique in terms of the presence of a urethral recess. This structure is described in Section 1.3.3 (see Figure 1.22).

1.3.2.2 Female Genitalia

The Ovary, Salpinx, Uterus, Vagina, Vestibule, Vulva, and Clitoris (Figures 1.15 and 1.16)

In the sow the *ovaries* are berry shaped, each *follicle* or *corpus luteum* being exposed on the ovarian surface, separated from each other by deep grooves. The *ovarian hilus* is easily depicted on the mesovarian border. The uterus is as long in this species as the ovaries are hanging inside of the abdominal cavity mingled with the intestinal loops. The ovary is totally enveloped in the infundibulum of the salpinx. The *ovarian bursa* is very large and wide.

Suspended by a short mesosalpinx, the *uterine tube* opens on the inner side of the mesosalpinx facing the ovary. The *infundibulum* completely surrounds the ovary. The uterine ostium is surrounded by numerous little endometrial tubercles disposed in a double/triple rosette.

The *uterine horns* are extremely long and flexuous, intermingling with the jejunal loops. They open separately into the *body*, which is short. The *cervix* is proportionately long and is provided with endometrial cushion-like prominences called *pulvini,* which interdigitate with each other occluding the cervical canal.

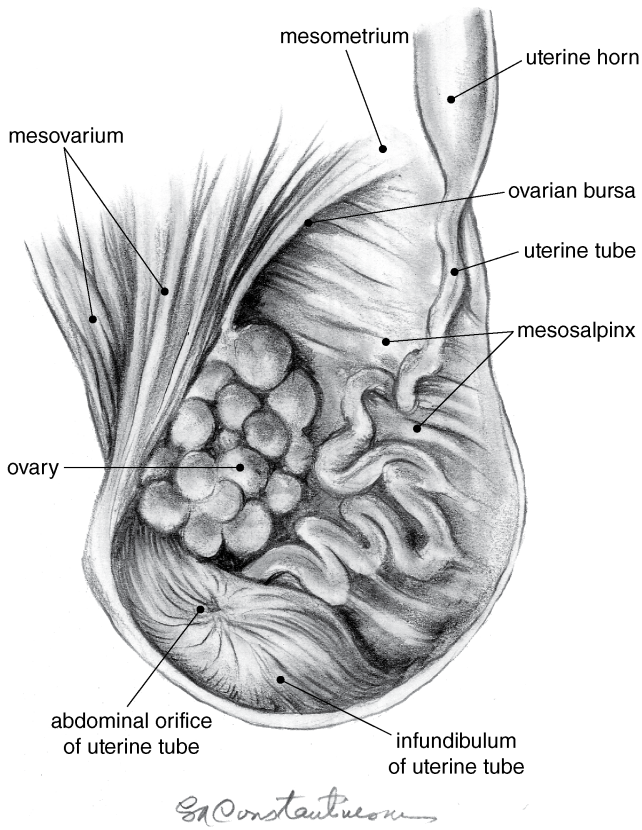

Figure 1.15 The ovary of the sow.

Downloaded from Vet-eBooks.com

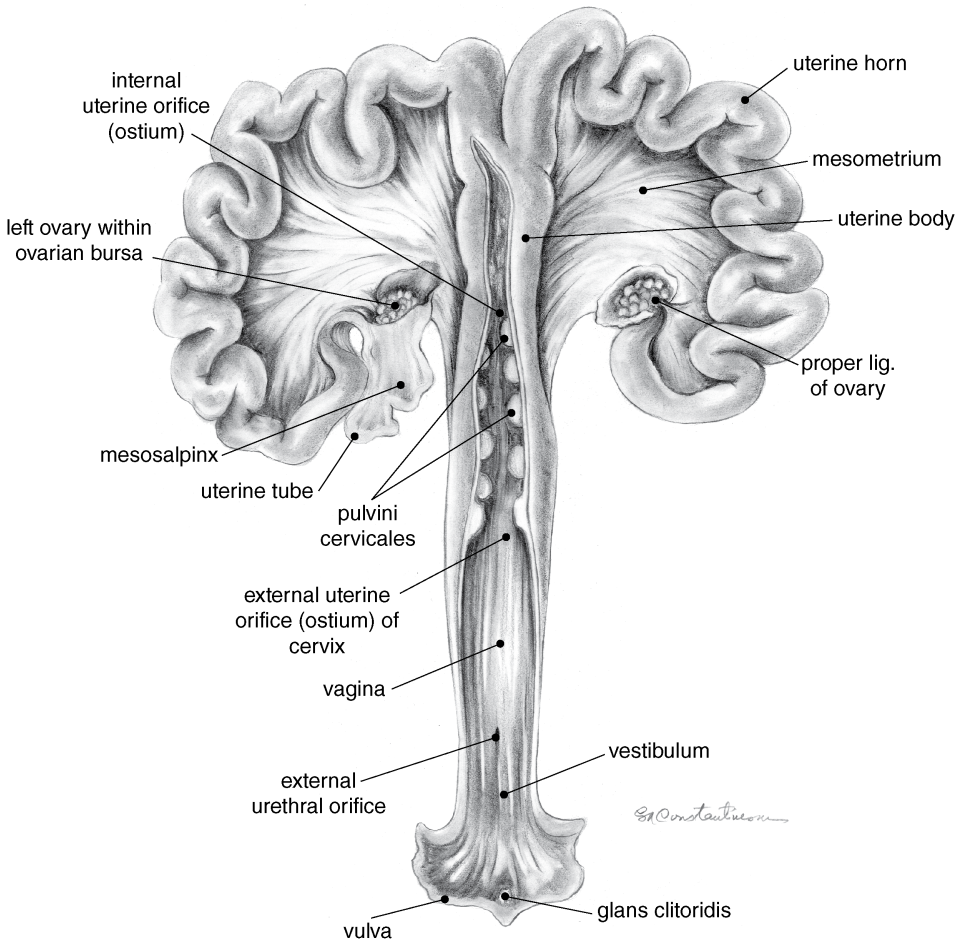

Figure 1.16 The uterus of the sow: dorsal view.

There is no fornix in the sow. The *vagina* is almost as long as the cervix, and is provided with prominent longitudinal folds and a hymen in very young animals.

Shorter than the vagina, the *vestibule* is provided with a reduced *suburethral diverticulum*, *minor vestibular glands*, and a *vestibular bulb*.

The two labiae of the *vulva* are thick, and the ventral commissure is pointed. The *clitoris* is very long and flexuous, and the *preputial cavity (fossa of the clitoris)* is shallow.

1.3.3 The Genital System in the Ruminants (Constantinescu, 2001, 2004a)

1.3.3.1 Male Genitalia

For details of the male urethra, major muscles, blood supply, lymph drainage, and nerve supply to the male genital system, see Schatten and Constantinescu (2007, *op. cit.*).

The Testicle, Epididymis, Ductus Deferens, Spermatic Cord, and Tunics (See Figures 1.17–1.20)

In the ruminants, the *testicles* are ovoid shaped, and in a vertical position, with the head of the *epididymis* proximal, and the tail distal. The epididymal canal is as long as 40–60 m, and the *ductus deferens* is provided with an *ampulla*. With species-specific design of the testicular artery and the

Downloaded From Vet-eBooks.com

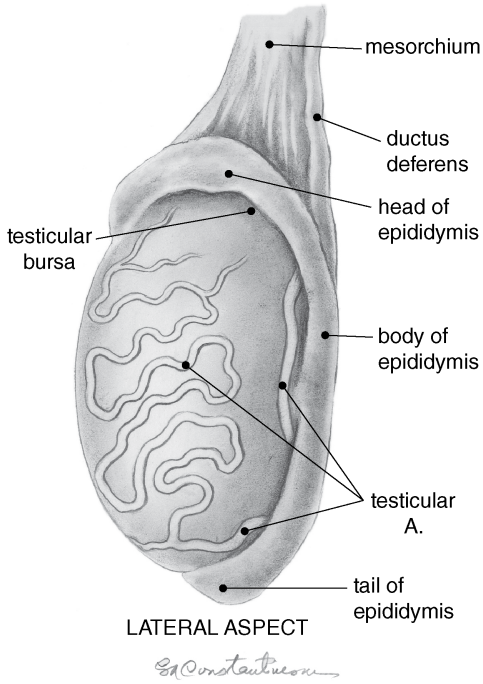

Figure 1.17 The left testicle and epididymis of the bull: lateral aspect.

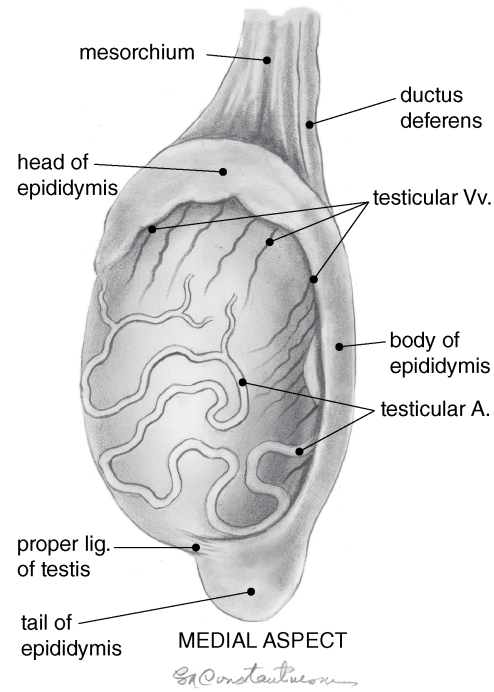

Figure 1.18 The left testicle and epididymis of the bull: medial aspect.

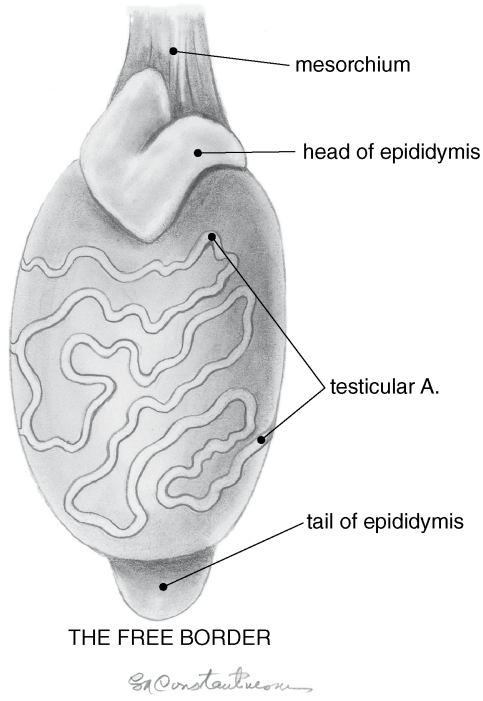

Figure 1.19 The left testicle and epididymis of the bull: the free border.

Downloaded From Vet-eBooks.com

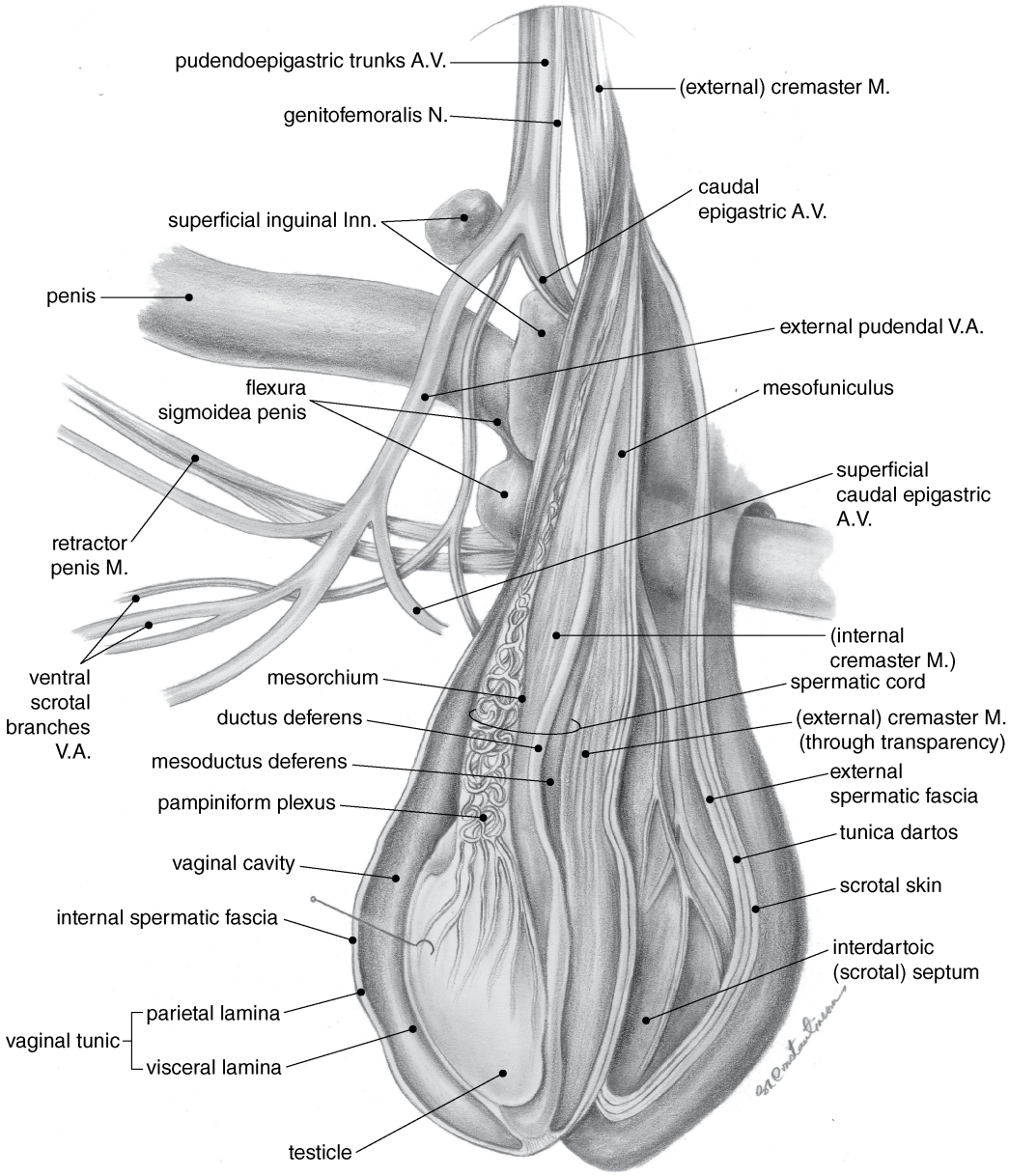

Figure 1.20 The testicle and the spermatic cord of the bull.

presence of the *ligament of the tail of the epididymis* in addition to the *proper ligament of the testicle* and the *scrotal ligament*, there are no notable differences from the general description of structures listed above. There is a short *ejaculatory duct* in ruminants. A reduced *uterus masculinus* can be seen in the bull. The *spermatic cord* and the *tunics* do not differ from the other species.

The Accessory Genital Glands (Figures 1.21 and 1.22)

The *vesicular glands* are elongated and large in the bull, rounded and much smaller in the buck and the ram. The surface of the glands is uneven and lobulated. The common excretory duct joins the ductus deferens in a short *ejaculatory duct* before opening into the urethra.

Downloaded From Vet-eBooks.com

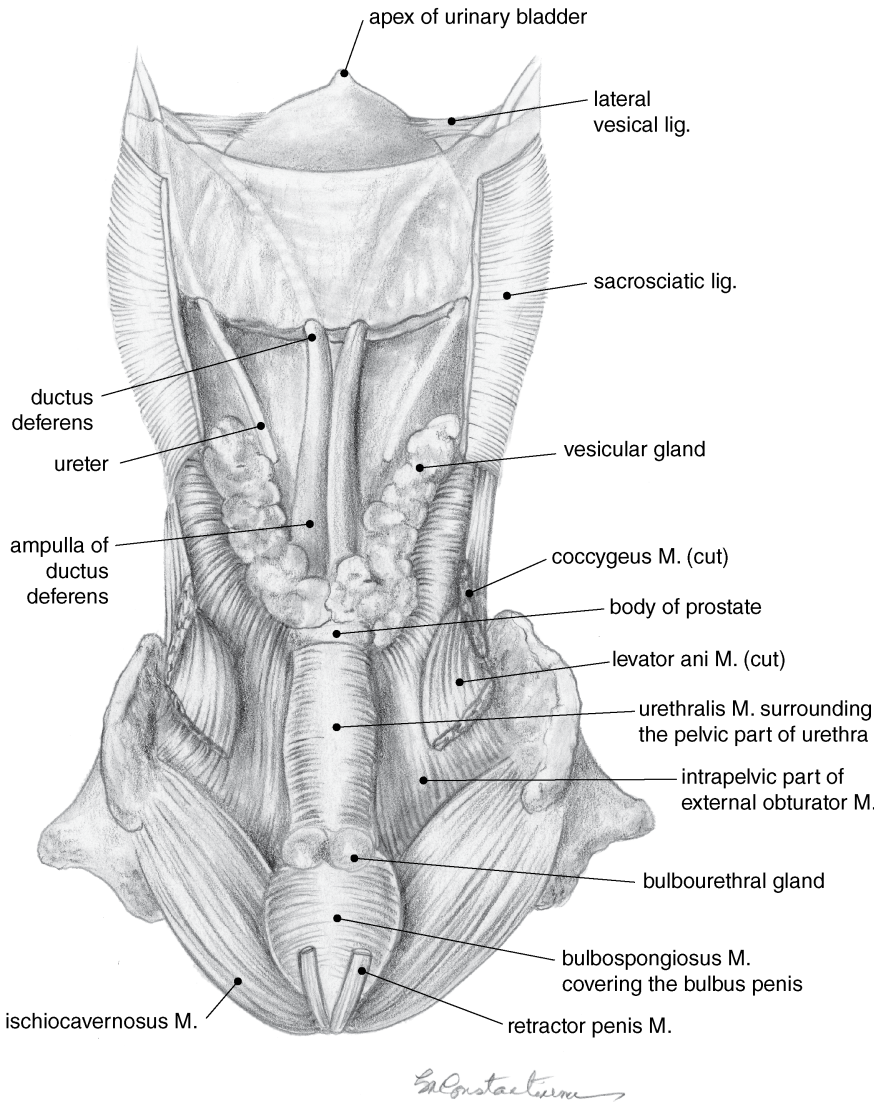

Figure 1.21 Genital apparatus in the bull: dorsal view. (Modified and redrawn from Barone (1978), Nickel *et al.* (1984), and Sack (1991).)

Only in the bull, the *prostate* has a reduced *body* on the dorsal aspect of the urethra. The body lacks in the small ruminants. The *disseminated part* is present in all ruminants, fully extended in the bull and the buck, and only on the dorsal wall of the urethra in the ram.

The *bulbourethral glands*, elliptical in the bull and spherical in the ram and buck, are located symmetrically on both sides of the urethral isthmus. They are covered by the *bulboglandularis muscles*. The excretory canal opens into the urethra via the *urethral recess*, common to the pig and all ruminants (see Figure 1.22).

The Penis and the Prepuce (Figures 1.23–1.25)

The *penis* in ruminants is fibroelastic, very long, but with a reduced diameter. The tunica albuginea is very thick. The body of the penis is provided with a *sigmoid flexure*, similar to that of

Downloaded from Vet-eBooks.com

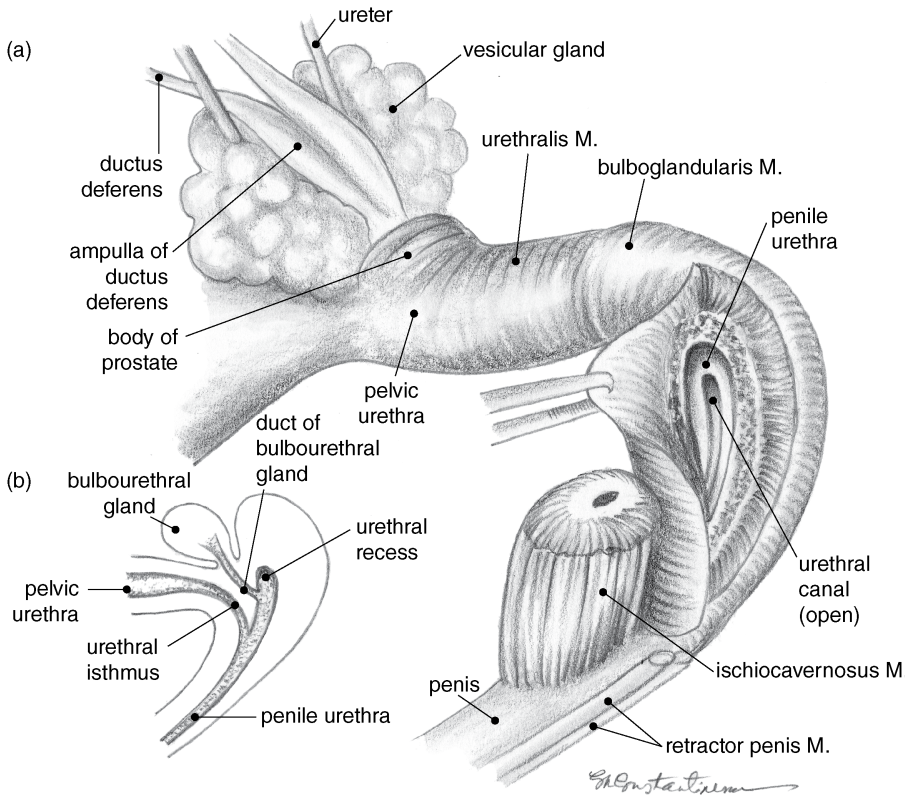

Figure 1.22 The urethral recess in the bull. (Redrawn from Garrett (1987).) (a) Topography of urethral recess. (b) Schematic representation of a median section.

the pig, but relative to its position it is located caudal to the testicles. The free part of the penis differs within these three species (see Figures 1.23–1.25). For details, see Schatten and Constantinescu (2007, *op. cit.*).

The *prepuce* is long and narrow, as the preputial orifice is (see Figure 1.25). Both cranial and caudal preputial muscles are present in ruminants.

Blocking the nerve supply to some of the most clinically important male (and female) genital organs, the easiest method is suggested and illustrated in Schatten and Constantinescu (2007, *op. cit.*), pp. 39–41, Figure 1.54.

1.3.3.2 Female Genitalia (Constantinescu et al., 1969, 1977; Constantinescu and Theodorescu, 1977)

The Ovary, Salpinx, Uterus, Vagina, Vestibule, Vulva, and Clitoris (Figures 1.26–1.31)

The *ovary* is relatively small in comparison to the size of the species. Ovoidal and flattened, the ovary looks like an almond. Most of the surface is uneven, as a result of numerous *follicles* and *corpora lutea* in various stages of development. These structures are as big as to be easily palpable by rectal palpation. The *ovarian hilus* is distinct and located on the mesovarian border. In nulliparous and primiparous individuals, the ovaries can be palpated within the pelvic inlet. The more pregnancies the animal has had, the more cranially the ovaries are located. They drop within the abdominal cavity pulled by the increasingly larger pregnant uterus, and in the cow they are more and more difficult to be palpated by rectal exploration.

Downloaded From Vet-eBooks.com

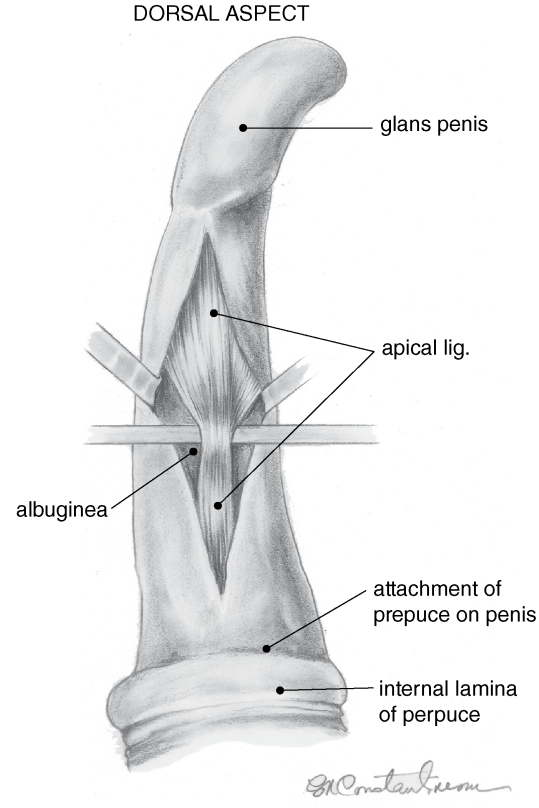

Figure 1.23 The bull's penis: dorsal aspect.

The *salpinx* or *uterine tube* is flexuous, mobile, and twice as long in the cow as in the small ruminants (20–28 versus 10–16 cm). The *infundibulum* surrounds and covers the ovary, outlining a wide *ovarian bursa*.

The *uterus* is a classical type of uterus bicornis. The *uterine horns* are three times longer in the cow (35–45 cm) versus 12–15 cm in the small ruminants. The tips of the horns are progressively increased in volume and take a spiral shape, similar to the ram's horns. Before they approach to each other to continue as the uterine body, the two horns are attached by the *intercornual ligament*, double in the cow. This is a clinically important structure for establishing the age of

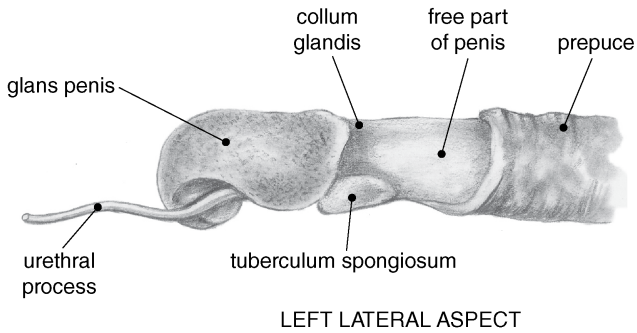

Figure 1.24 The ram's penis: left lateral aspect.

Downloaded From Vet-eBooks.com

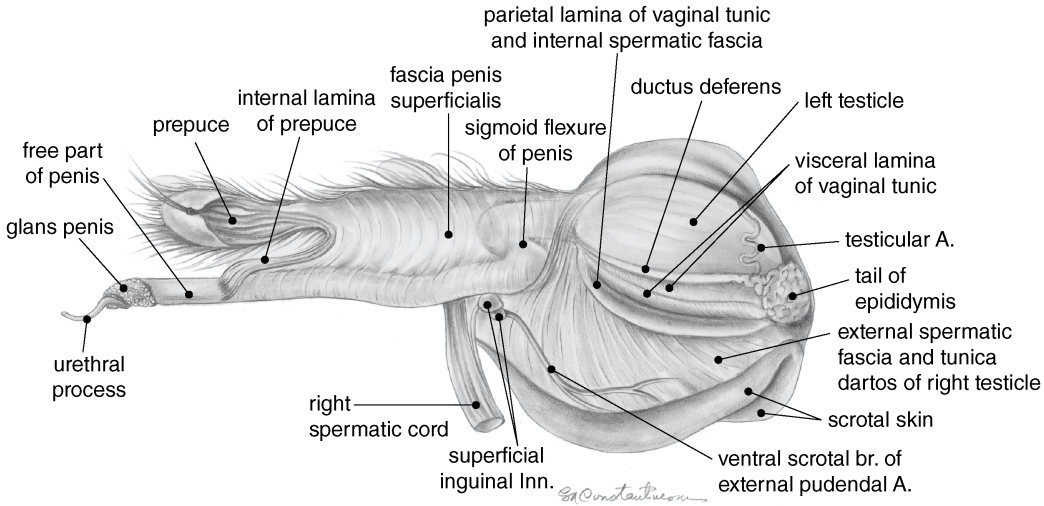

Figure 1.25 The penis and the left testicle—left lateral aspect—of the buck.

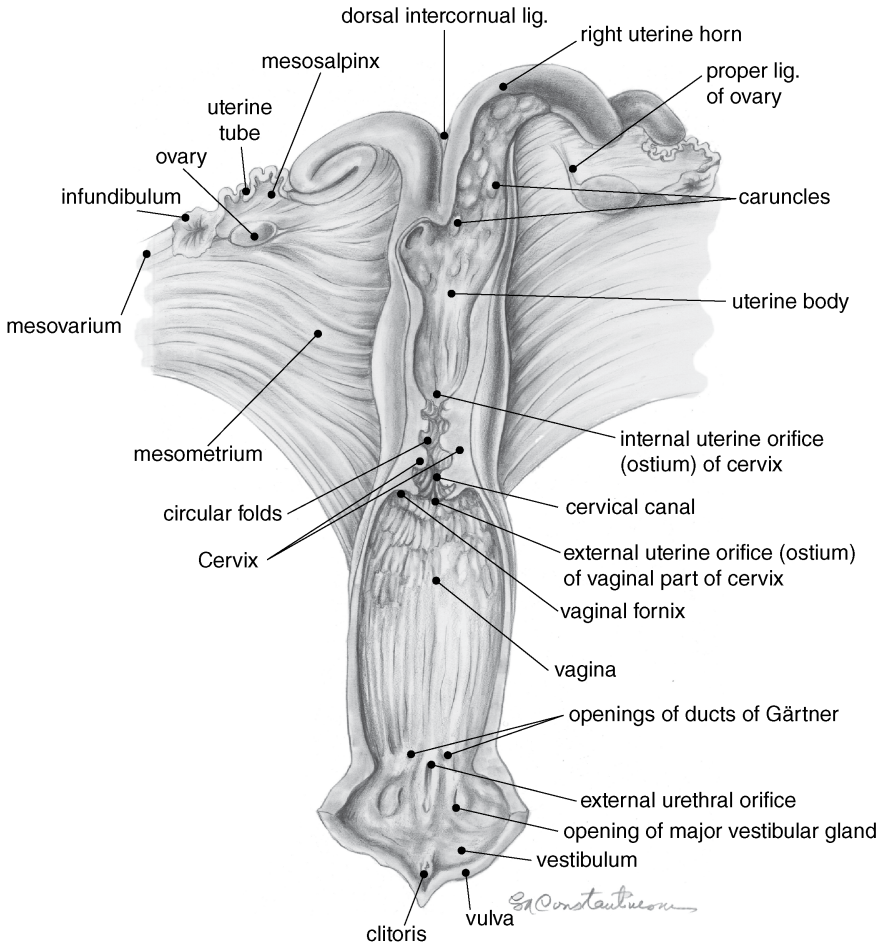

Figure 1.26 The uterus, vagina, and vestibulum of the cow: dorsal view.

Downloaded From Vet-eBooks.com

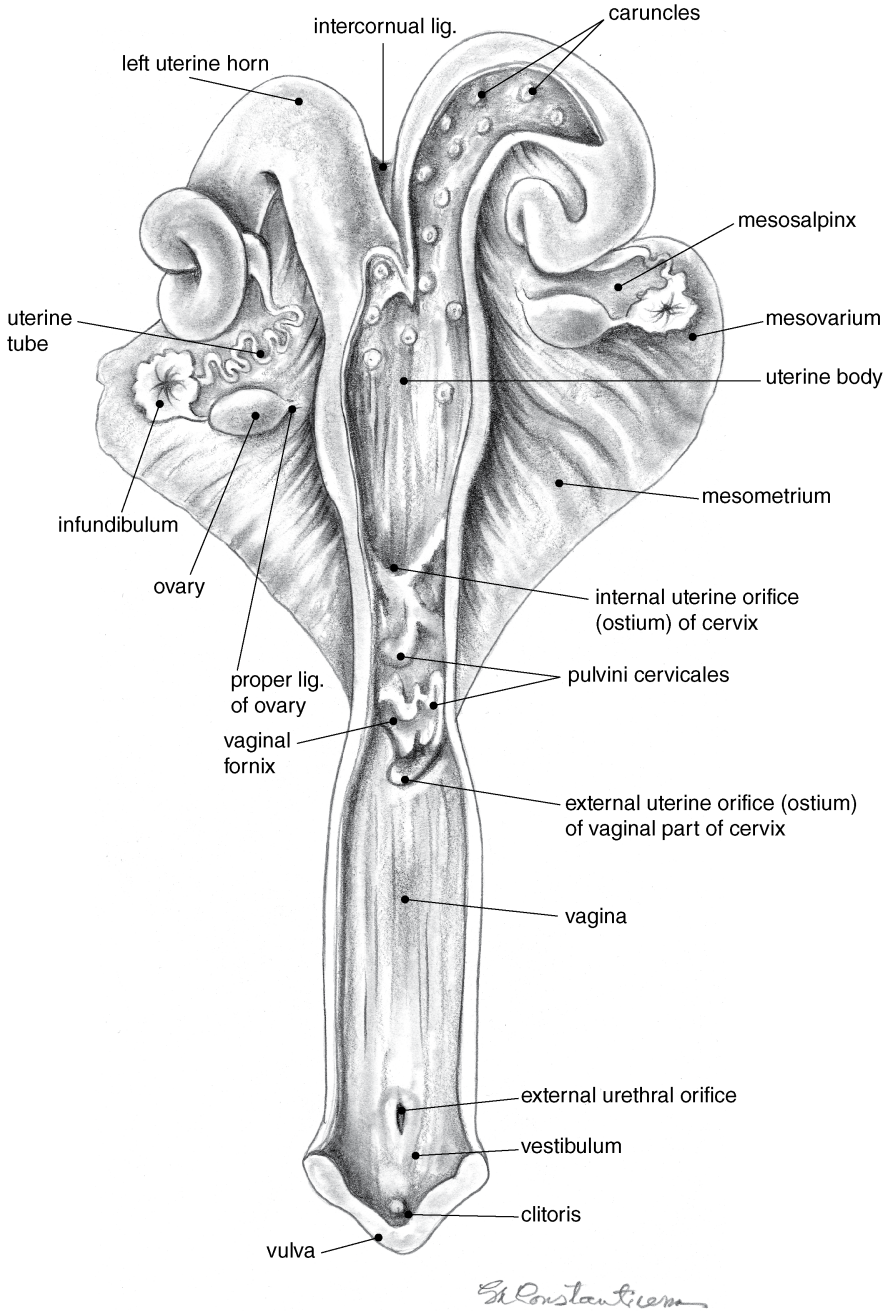

Figure 1.27 The genital tract of the ewe: dorsal view.

gestation, or any anomalies of the ovaries by rectal palpation, pulling the entire uterus from the abdominal cavity into the pelvic cavity to ease the investigation. The uterine horns are separated inside of the uterus by the uterine velum, similar to the carnivores and the sow; therefore, they open inside of the body independent from each other. The *body of the uterus* is short, and provided with a very large mesometrium. The *round ligament of the uterus* is small. The

Downloaded from Vet-eBooks.com

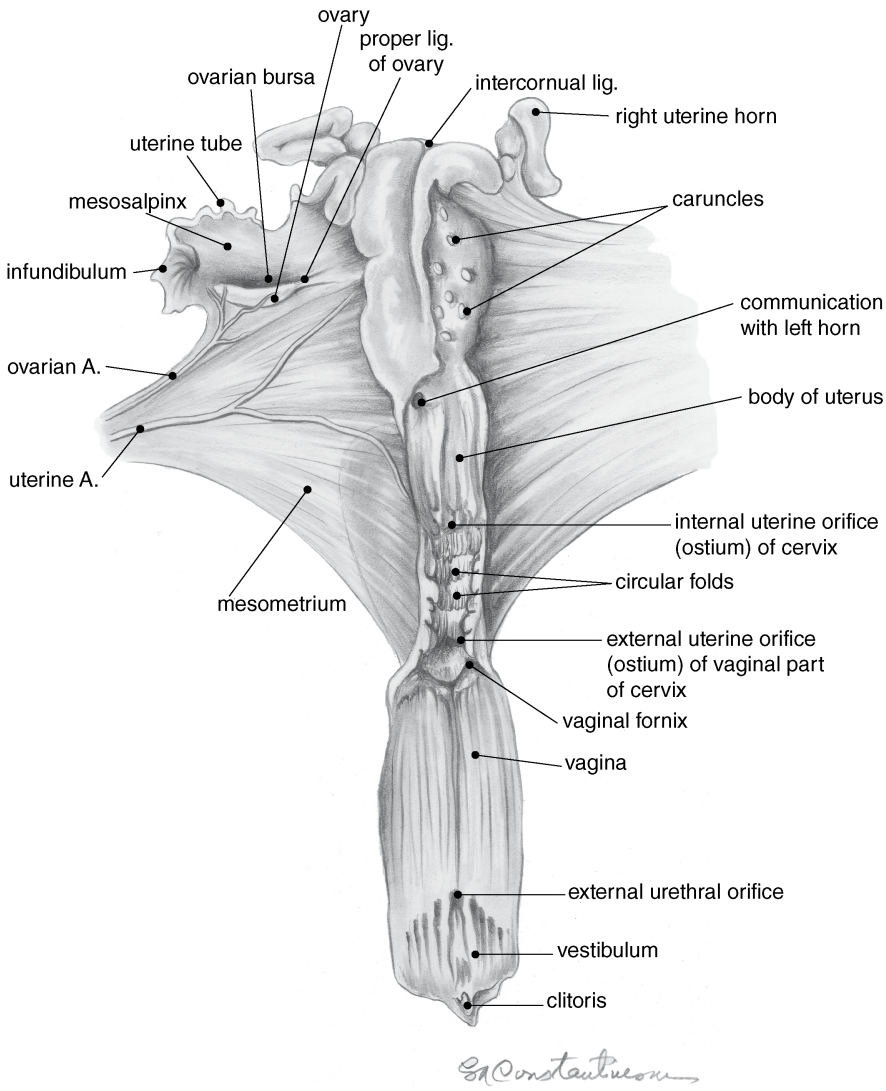

Figure 1.28 The genital tract of the female goat: dorsal aspect.

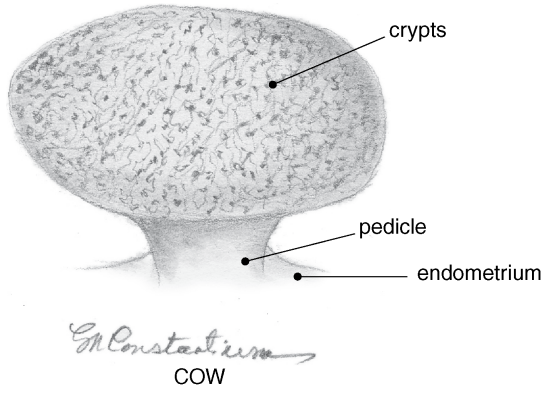

Figure 1.29 Uterine caruncles in ruminants: cow.

Downloaded from Vet-eBooks.com

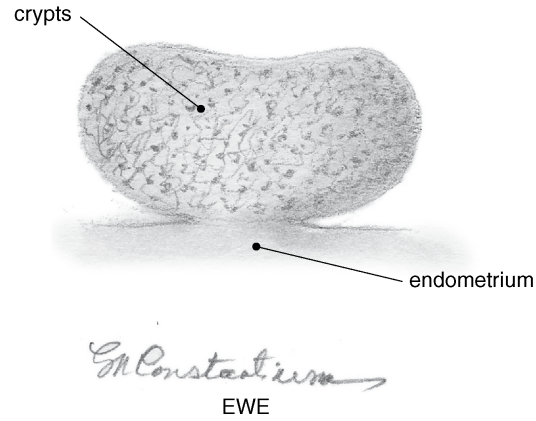

Figure 1.30 Uterine caruncles in ruminants: ewe.

endometrium is provided with elevations of the mucosa of different size and shape called *caruncles*, all pediculated. The shape of the caruncles differs slightly among ruminants, but the surface has a spongy aspect, with crypts in which the villi of the *cotyledons* of the placenta implant. Each caruncle and the corresponding cotyledon make a *placentome*. The *cervix* is as long as 10 cm in the cow, and 4 cm in small ruminants. It is rigid and easy to identify by rectal palpation in the cow. The cervical canal is irregular, with four circular folds that interdigitate with each other. The last fold protrudes within the vagina, and is provided with additional longitudinal folds, giving to the vaginal part of the cervix the aspect of an open flower.

The *vagina* in the cow is long (~30 cm) and wide, whereas in the small ruminants it measures only 10 cm. Folds of the mucosa as annular ridges are prominent. The *fornix* is deeper dorsally (see Figures 1.26–1.28). A small *hymen* may be observed in some cows.

The *vestibule* continues the vagina caudal to the external urethral ostium. It is caudoventrally oriented, hanging over the ischial arch. A *suburethral diverticulum* (present only in the sow and the ruminants) opens into the *external urethral orifice*. *Minor and major vestibular glands*, as well as two symmetrical *Gärtner's ducts,* are observed on the floor of the vestibule. No major or minor vestibular glands are present in the goat, occasionally they are present in the ewe (see Figures 1.26–1.28).

The *vulva* is similar in all three species. The *clitoris* is located in a shallow *fossa*, is flexuous, provided with a very small *glans* or no glans, with the *prepuce* less evident.

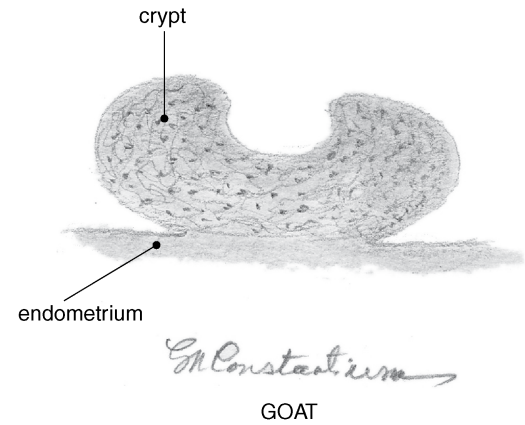

Figure 1.31 Uterine caruncles in ruminants: goat.

Downloaded From Vet-eBooks.com

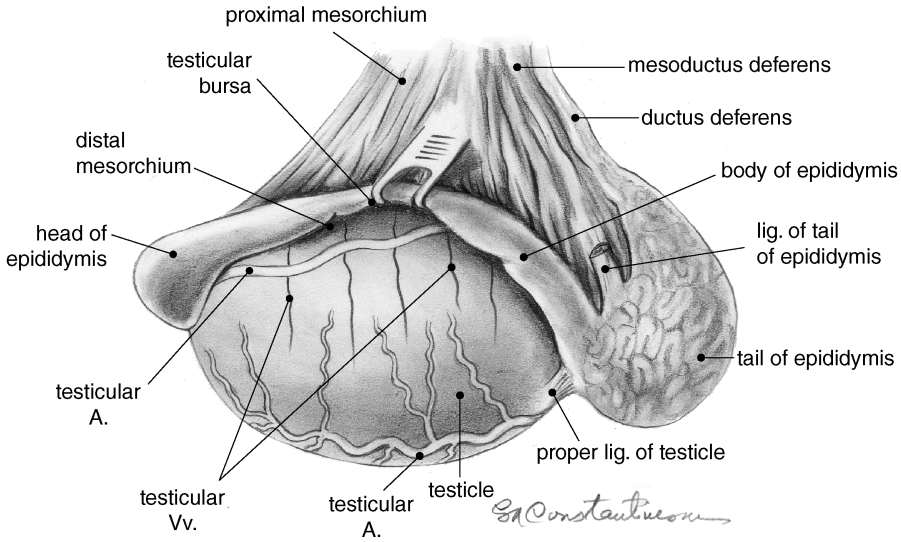

Figure 1.32 The left testicle of the stallion: lateral aspect.

1.3.4 The Genital System in the Horse

1.3.4.1 Male Genitalia

For details of the male urethra, major muscles, blood supply, lymph drainage, and nerve supply to the male genital system, see Schatten and Constantinescu (2007, *op. cit.*).

The Testicle, Epididymis, Ductus Deferens, Spermatic Cord, and Tunics (Figures 1.32–1.35)

Ovoidal shaped, the *testicle* of the horse is horizontally positioned, with the head cranially, and the tail caudally. The mediastinum testis is small and pushed to the periphery of the testicle.

The *epididymis* covers the dorsal border of the testicle; the head of it does not exceed the head of the testicle, whereas the tail of the epididymis is very detached. The *epididymal canal* (85 m)

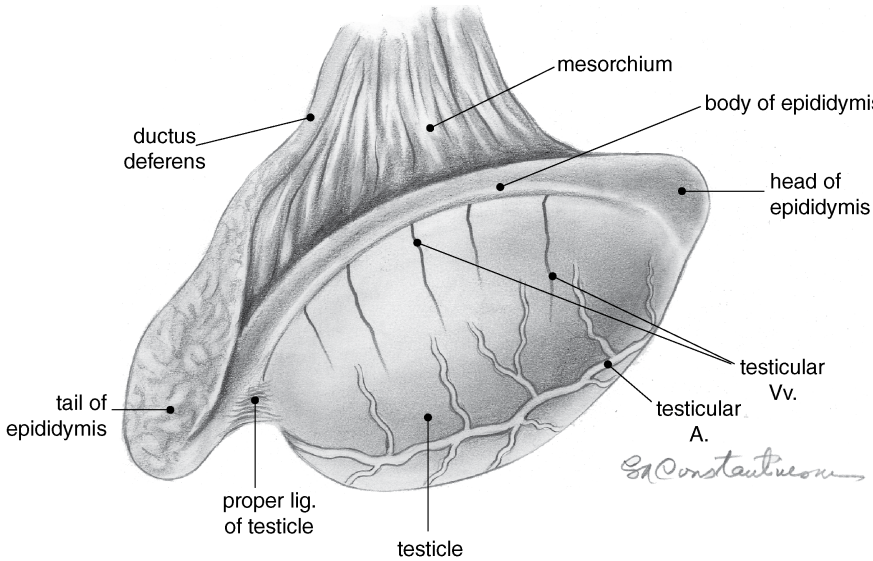

Figure 1.33 The left testicle of the stallion: medial aspect.

Downloaded From Vet-eBooks.com

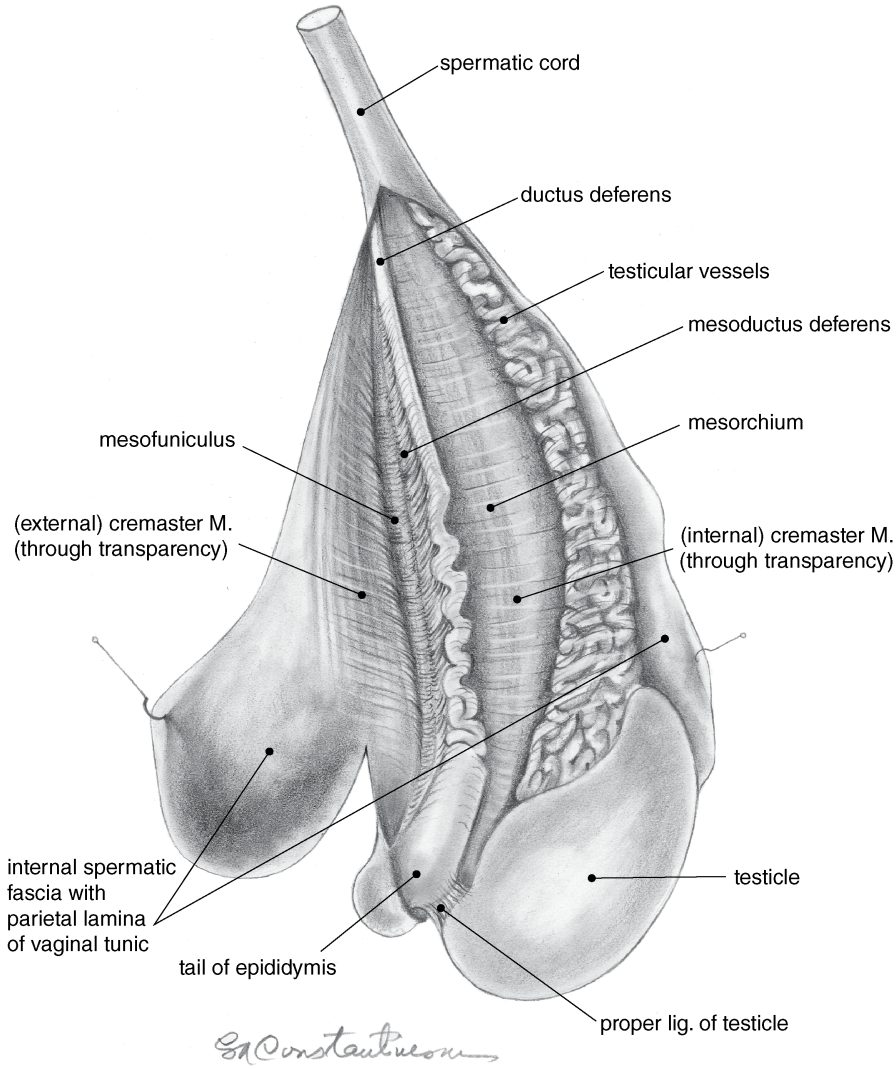

Figure 1.34 The testicle, spermatic cord, and testicular tunics of the stallion.

is the longest in the domestic species. The *testicular bursa*, the *proper ligament of the testicle*, the *ligament of the tail of the epididymis*, and the *scrotal ligament* are all well defined.

Each *ductus deferens* is provided with an *ampulla*. The ampullae, the seminal vesicles, and the two ureters are all together connected by the *genital fold*, in the middle of which the *uterus masculinus* is visible.

The *spermatic cord* is short but voluminous, and in a vertical position.

The *tunics* and the *cremaster muscle* are strong, some tunics very thick, but similar to those of the other species.

The Accessory Genital Glands (see Figure 1.35)

The *vesicular glands* called in the horse also *seminal vesicles* because they look like small bladders join their excretory ducts with the ampullae of the ductus deferentes in the *ejaculatory ducts*.

The *prostate* shows only the compact part, with two lobes connected by an isthmus, and located on the dorsal side of the urethra.

Downloaded from Vet-eBooks.com

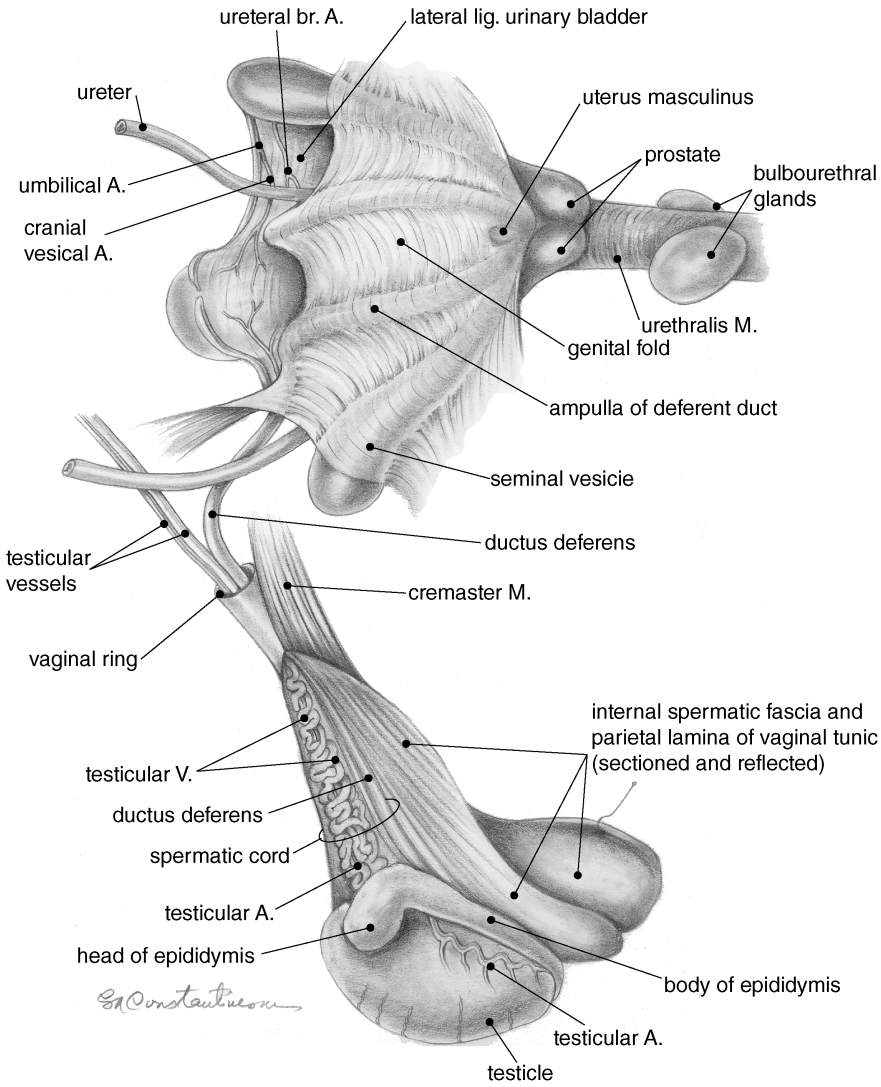

Figure 1.35 The genital apparatus, except the penis, of the stallion.

The *bulbourethral glands* are ovoidal in shape, located on the dorsal aspect of the urethral isthmus, covered by the *bulboglandularis muscles* and each gland provided with several (6–8) excretory ducts.

The Penis and the Prepuce (Figures 1.36 and 1.37)

The musculocavernous type of the horse *penis* (see Figure 1.36) is provided with numerous cavernous spaces and less trabeculae. During the erection its length increases by 60% and is fully used in the long-lasting mating process. The *root of the penis* is well represented, and the *crura* are covered by strong *ischiocavernosus muscles*. The *body of the penis* is suspended to the pelvic symphysis by a ligament. The urethral groove is wide and protects the urethra surrounded by the *corpus spongiosum penis*. The *glans penis* contains the *corpus spongiosum penis*, is voluminous, and during the erection the *corona glandis* can reach 13–16 cm in diameter. The glans penis is,

Downloaded From Vet-eBooks.com

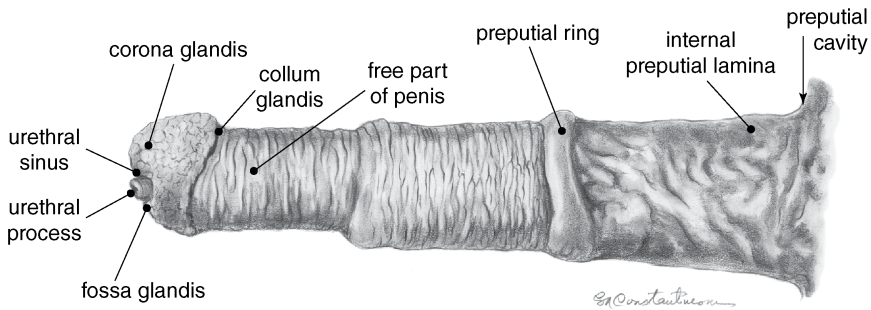

Figure 1.36 The penis of the horse.

in the horse, a very complex and unique structure, with its corona glandis, *collum glandis, fossa glandis, the urethral sinus,* and the *septum glandis.*
The *prepuce* is also unique in the horse, with the *external* and *internal laminae,* the *preputial fold* and *ring*, the corresponding cavities and orifices (see Figure 1.37).

1.3.4.2 Female Genitalia

The Ovary, Salpinx, Uterus, Vagina, Vestibule, Vulva, and Clitoris (Figure 1.38)
The *ovary* of the mare is a unique structure. The uniqueness comes from the fact that the cortex and the medulla of the other species are, in the mare, reversed. Thus, the cortex with the follicles is central, and the vascular medulla is peripheral. Consequently, there is *one ovarian fossa* located on the free border of each ovary, close to the abdominal ostium of the uterine tube (salpinx). The opposite border of the ovary is connected to the mesovarium. The ovaries are located caudal to the kidney and are palpable by rectum.

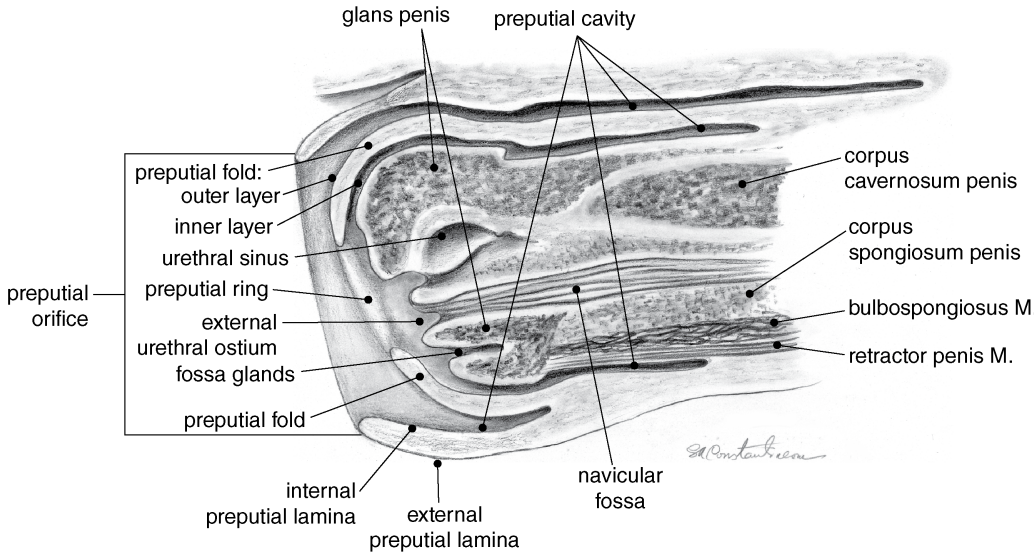

Figure 1.37 Median section through the free part of the penis and of the prepuce in the horse.

Downloaded From Vet-eBooks.com

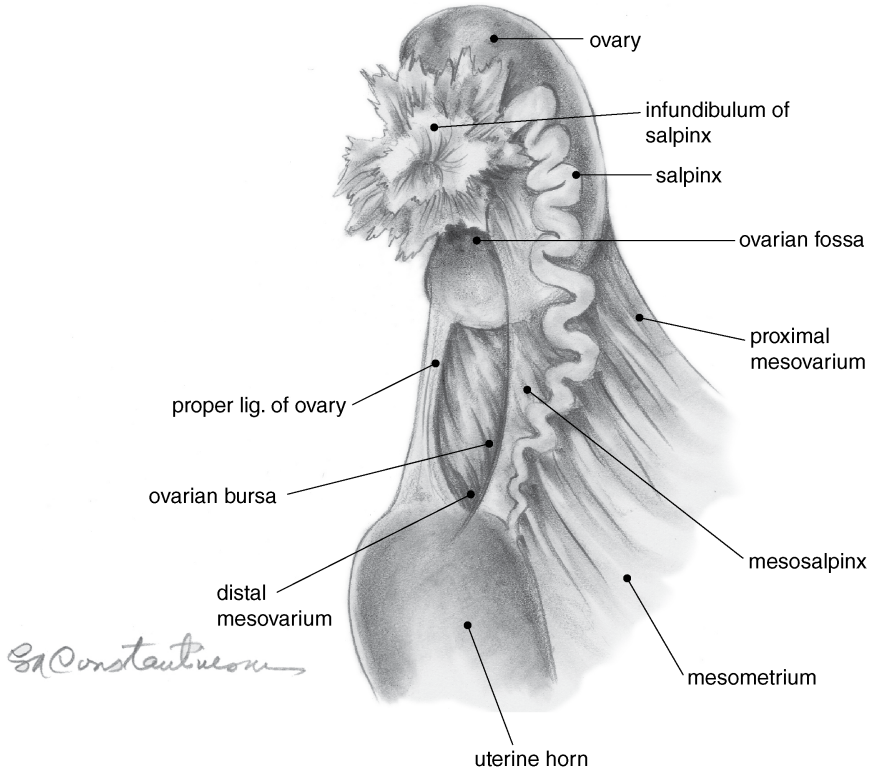

Figure 1.38 The ovary and uterine tube of the mare: ventral aspect.

The *salpinx* (see Figure 1.38) is very flexuous, with abundant *fimbriae* surrounding the *infundibulum,* with the abdominal ostium in the center of it. In the mare only, the uterine tube opens into the uterine horn in the center of a *small papilla provided with a sphincter*.

The *uterus* (see Figure 1.39) has a relatively short, but large *body*. Not being divided as in the other species by the uterine velum, the cranial end of the body is called *uterine fundus*. The two *uterine horns* are slightly curved ventrally. Centered by a straight *cervical canal*, the *cervix* opens into the vagina by a very prominent and plicated portion. This *vaginal portion* of the cervix is anchored to the walls of the vagina by vertical folds called *frenula* (singular frenulum). During diestrus, estrus, and pregnancy, the vaginal part of the cervix and its relationships with the vagina are different from each other as they are shown in Figures 1.40–1.45. The broad ligaments are strong, and as long as from near the tip of the uterine horns to the deep inguinal rings; each ligament is provided with a short round ligament.

The *vagina* is long and wide, to accommodate the impressive size of the penis. Just in front of the large external urethral orifice, on the floor of the vagina a sort of transversal fold of the mucosa can be seen, similar to the *hymen*.

The *vestibule* and the vulva hung over the ischial arch. Only the *minor vestibular glands* are present. The *vestibular bulb* is very developed, playing an essential role in copulation.

The *vulva* and the *clitoris* are strongly connected (see Figure 1.39). The vulva has two pigmented *labiae*, whose ventral commissure is rounded ventrally and pointed dorsally. The 7–9 cm long clitoris exposes a very voluminous *glans* located within the *clitoral fossa*. The *frenulum of the clitoris*, the *recesses*, and the *sinuses* are shown in Figures 1.46 and 1.47 and

Downloaded From Vet-eBooks.com

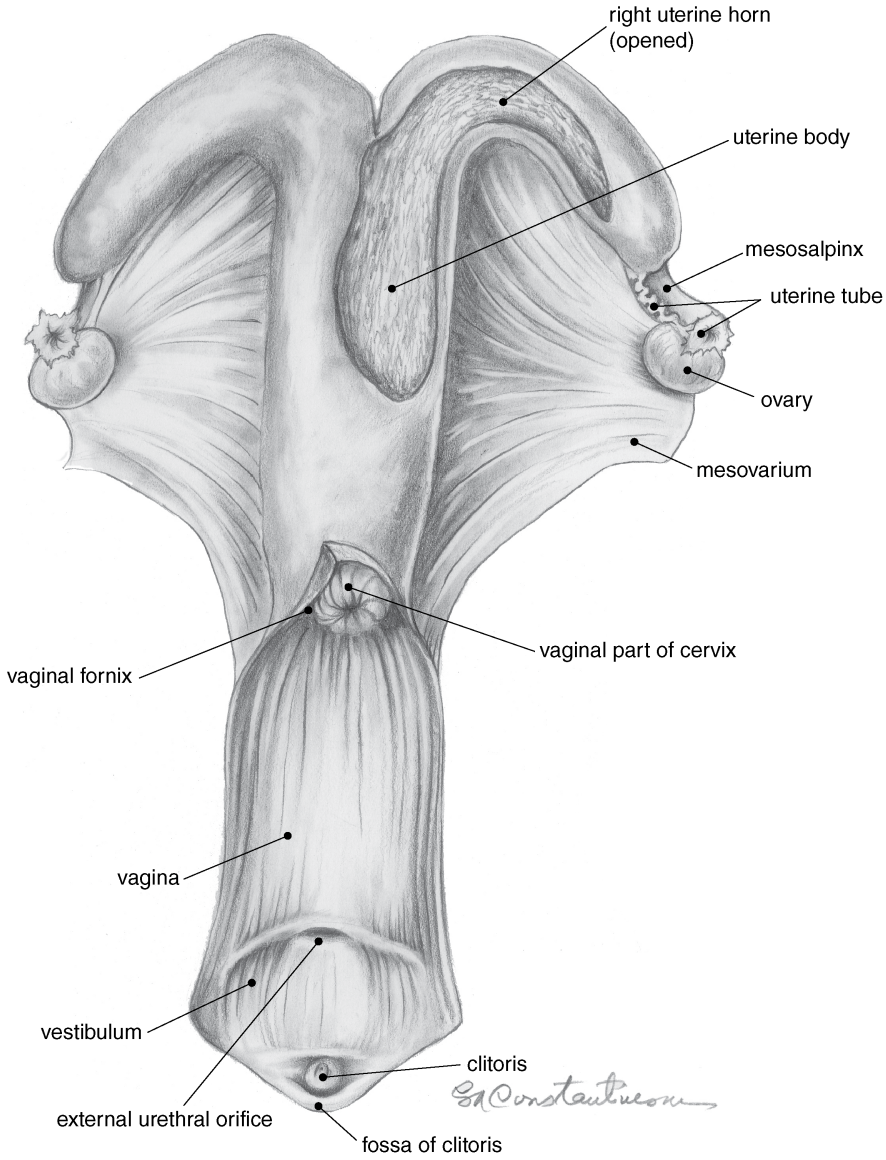

Figure 1.39 The genital tract of the mare: dorsal aspect.

are of an extremely high importance in the mare theriogenology (Youngquist and Threffall, 2007).

1.4 Genital Organs in Laboratory Mammals

(See text and figures in Constantinescu (2011).)

The genital organs in laboratory animals will be described species by species, both male and female. At the end, the mammary glands of all of the three mammalian species (rabbit, mouse, and rat) will be described in separate sections.

Downloaded from Vet-eBooks.com

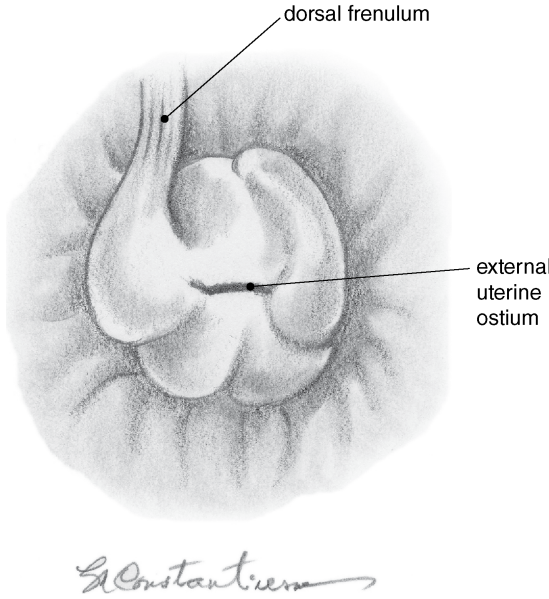

Figure 1.40 The vaginal part of the cervix in the mare during diestrus, estrus, and pregnancy (also see Figure 1.41–1.45). Diestrus: the cervix—caudal view.

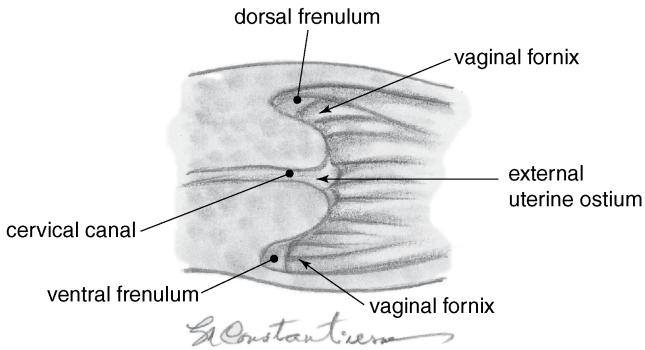

Figure 1.41 Diestrus: the vaginal portion of the cervix—median section.

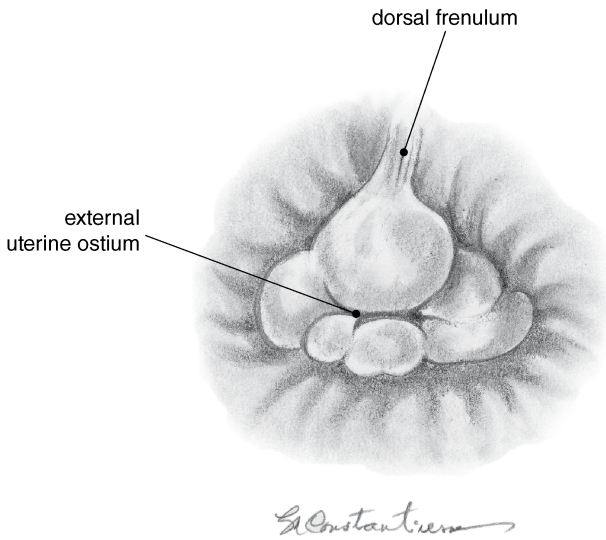

Figure 1.42 Estrus: the cervix—caudal view.

Downloaded From Vet-eBooks.com

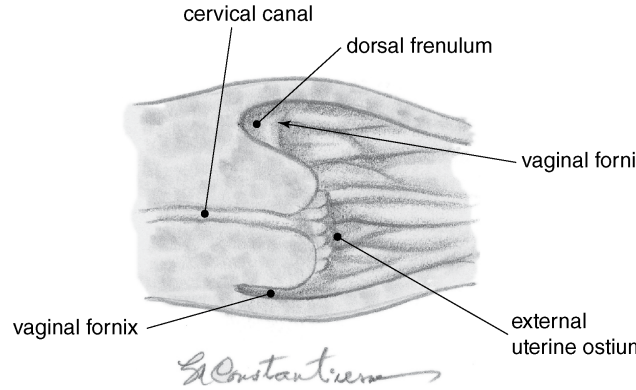

Figure 1.43 Estrus: the vaginal portion of the cervix—median section.

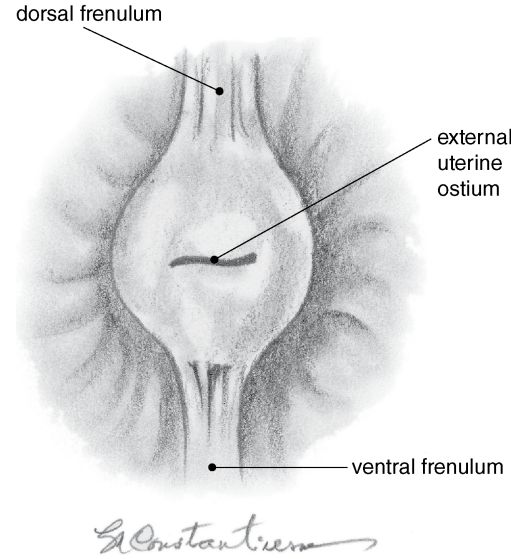

Figure 1.44 Pregnancy: the cervix—caudal view.

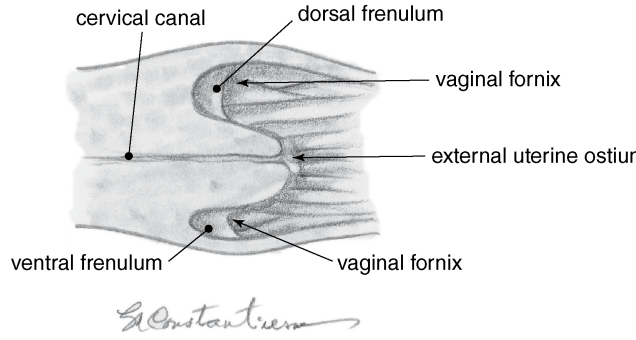

Figure 1.45 Pregnancy: the vaginal portion of the cervix: median section.

Downloaded from Vet-eBooks.com

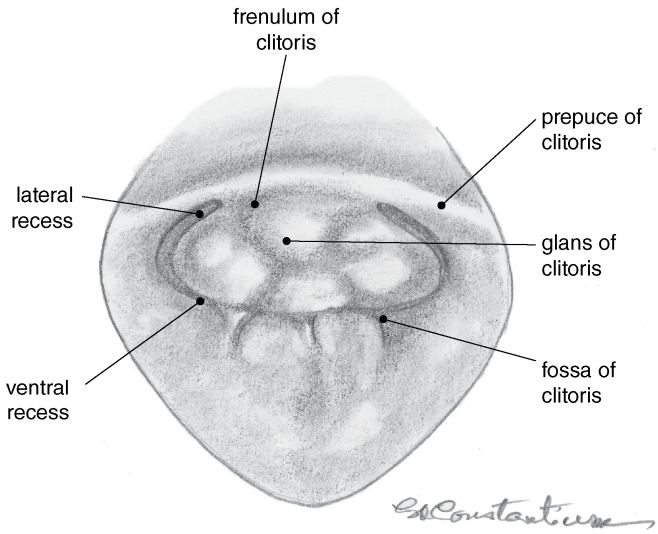

Figure 1.46 The clitoris of the mare (also see Figure 1.47). The clitoris *in situ*.

1.4.1 The Genital System in the Rabbit (Barone et al., 1973; Barone, 1978; Constantinescu, 2004b)

1.4.1.1 Male Genitalia (Figures 1.48–1.51)

The Testicle, Epididymis, Ductus Deferens, Spermatic Cord, and Tunics

The *testicle* (see Figures 1.48 and 1.49) is small, oval shaped and elongated, 3–3.5 cm long and 1–1.5 cm wide, located almost in a horizontal position in the scrotum, with the head cranially oriented and abundantly covered by the head of the epididymis. The location of the scrotum is ventral to the prepuce and the anus. Remember in the tomcat the scrotum is located between the prepuce (ventrally) and the anus (dorsally).

The *epididymis* has a voluminous *head* that covers almost completely the head of the testicle, a slender *body*, and a round, long, and mobile *tail*. The *proper ligament of the testicle* and the *ligament of the tail of the epididymis* are present as common to all species except the carnivores

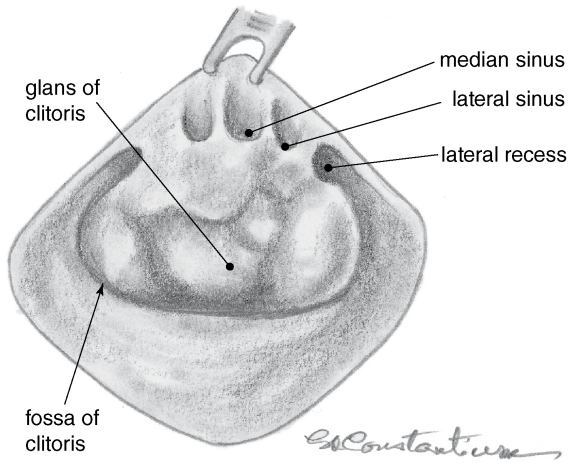

Figure 1.47 The prepuce of clitoris reflected.

Downloaded from Vet-eBooks.com

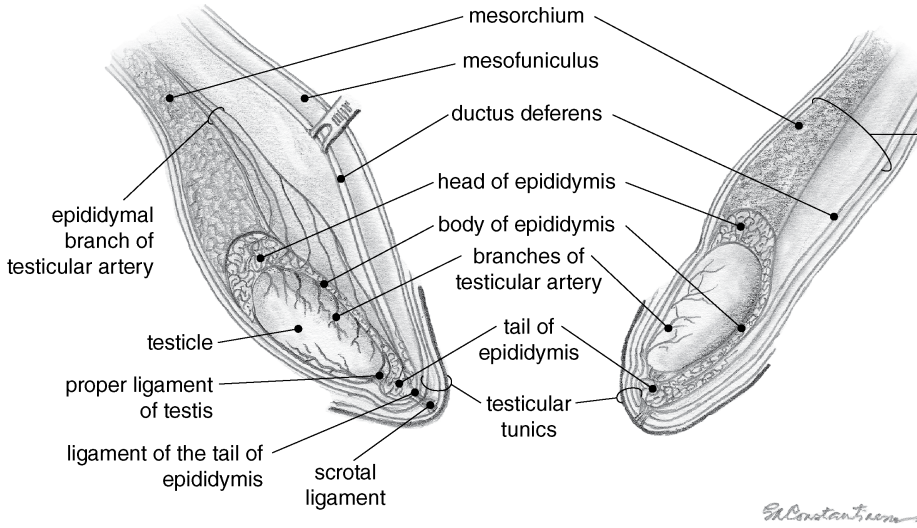

Figure 1.48 Testicle of the rabbit: medial aspect.

Figure 1.49 Testicle of the rabbit: lateral aspect.

(remember the latter are not provided with the ligament of the tail of the epididymis). In addition, there is a *scrotal ligament* in the rabbit.

The *ductus deferens* is flexuous, runs within the spermatic cord very similar to the other species, and ends with an *ampulla*. The ampulla insinuates under the seminal vesicle and the vesicular gland and joins the ducts of the latter before opening together in the corresponding *colliculus seminalis*. Though very short, the joined ducts can be considered as the *ejaculatory ducts*.

The *spermatic cord* is long and voluminous. The *internal spermatic fascia* is completely surrounded by a strong and thick *cremaster muscle*, which is able to retract the testicle within the peritoneal cavity completely. This happens during the fights among males to dominate the females in heat. The fights of the males target the testicles of the opponent, trying to castrate, therefore eliminate him from the competition. The retraction of the testicles within the peritoneal cavity is possible because the spermatic cord is horizontally positioned, and the deep inguinal ring is very large, particularities of the rabbit.

The *testicular tunics* are similar to the other species.

Accessory Genital Glands (Figures 1.50 and 1.51)

The accessory genital glands in the male rabbit are different from any other species, yet controversial by different anatomists. We can distinguish an impair seminal vesicle, an impair vesicular gland, an impair (dorsal) prostate, a pair of paraprostatic glands ventral to the latter, and a pair of bulbourethral glands.

The *seminal vesicle*, impair and bilobed, called by Popesko *et al.* (2002, *op. cit.*) as the vesicular part of the vesicular gland, located at the level of the neck of the urinary bladder covers the ampullae of the ductus deferentes and the ureters. The *vesicular gland,* called by Popesko *et al.* (2002, *op. cit.*) as the compact part of the vesicular gland, partially covers the seminal vesicle and the ampullae of the ductus deferentes. According to Barone *et al.* (1973, *op. cit.*), the *prostate* consists of three glands: the *cranial prostate,* which is the vesicular gland, the *prostate* (the dorsal or caudal prostate), and a paired *paraprostatic glands* (the ventral prostate) located ventral to the previous gland. The true (caudal or dorsal) prostate, called also by Popesko *et al.* (2002) as impair, is located caudal to the vesicular gland. The paraprostatic glands are very small, rounded, and located ventral to the dorsal prostate. The *bulbourethral glands* located at the

Downloaded From Vet-eBooks.com

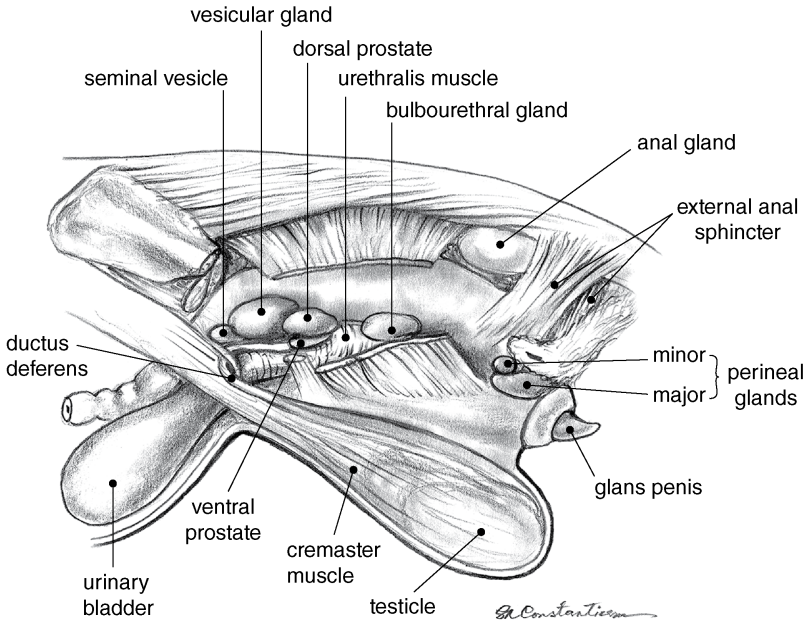

Figure 1.50 Male genital apparatus in the rabbit: left lateral view. (Redrawn and modified from Barone *et al.* (1973).)

isthmus of the urethra and separated from the prostate are connected by a bridge that gives the glands the appearance of a voluminous bilobed mass.

The Penis and the Prepuce (See Figure 1.50)

The *penis* is as long as 8 cm and oriented caudally, similar to that of the tomcat. The free part is not provided with spicules, like that of the tomcat, but there is a longitudinal raphe visible. The glans penis is small. The ischiocavernosus muscles are strong. There is no retractor penis muscle, but a symmetrical subischiocavernosus muscle instead, a characteristic of this species.

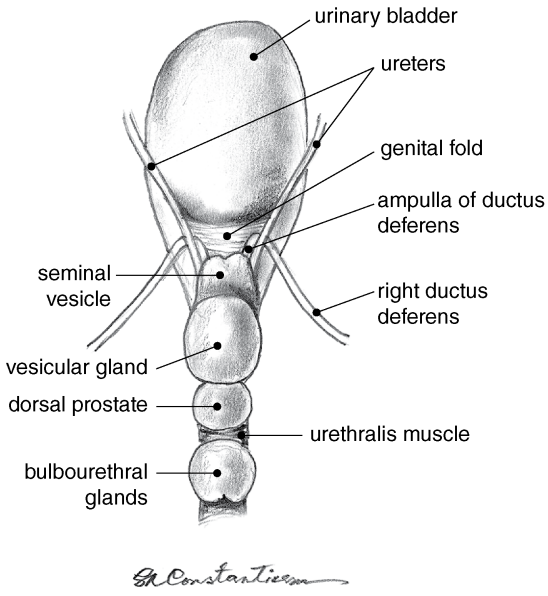

Figure 1.51 Accessory genital glands in the male rabbit: dorsal aspect. (Adapted from Barone *et al.* (1973), and redrawn from Constantinescu (2004b).)

Downloaded from Vet-eBooks.com

The *prepuce* consists of the *internal lamina*—without preputial glands—and the *external lamina* provided with long hairs. Between the prepuce and the anus a symmetrical *perineal sinus* is present. Two pairs of *major and minor perineal glands* located caudal to the ischiocavernosus muscles open into the perineal sinuses.

1.4.1.2 Female Genitalia (Figures 1.52 and 1.53)

The Ovary, Salpinx, Uterus, Vagina, Vestibule, Vulva, and Clitoris

The *ovary* is long, thin, and flat, with an uneven surface due to the follicles. The cranial pole is surrounded by an adipose body. Topographically, they are far caudal from the kidneys, at the level of the fifth lumbar vertebra. The *proper ligaments of the ovaries* are very long, thus the ovaries are not as close to the tips of the uterine horns as in the other species. The *ovarian bursa* is deep and wide.

The *uterine tube* is relatively long, with the *ampulla* three times wider than the *isthmus.* The *infundibulum* is provided with a multitude of small *fimbriae*. The *uterine ostium* of the salpinx is surrounded by small *caruncles of the uterine mucosa*, which are disposed in four divergent directions (Barone *et al.*, 1973, *op. cit.*; Barone, 1978, *op. cit.*)

The *uterus* is a duplex type of uterus. This means that the *two horns* come close to each other at the caudal end, but they do not open into a uterine body. Instead, they open separately into the vagina by two distinct *side by side cervices* (sing. cervix), similar to the rat. There is no body of uterus in the rabbit (and the rat). The uterine horns are flexuous and attached to long *broad ligaments*. The *round ligament of the uterus* is as long as it penetrates within the inguinal canal accompanied by the vaginal process, similar to the female dog. The *cervix* protrudes into the

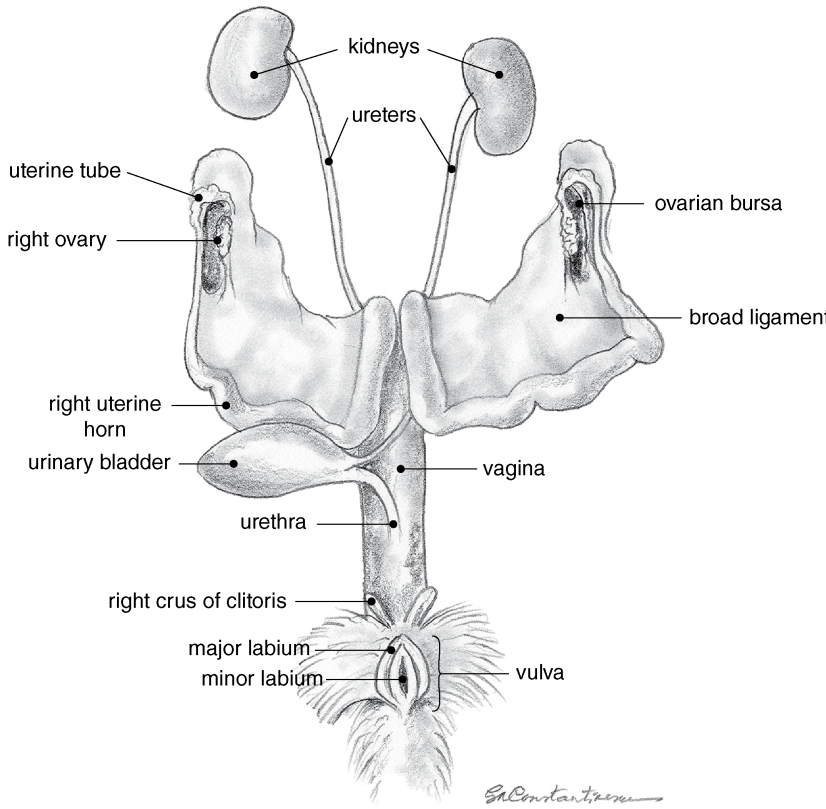

Figure 1.52 Genital apparatus in the female rabbit: ventral aspect. (Redrawn and modified from Barone *et al.* (1973), and redrawn from Constantinescu (2004b).)

Downloaded from Vet-eBooks.com

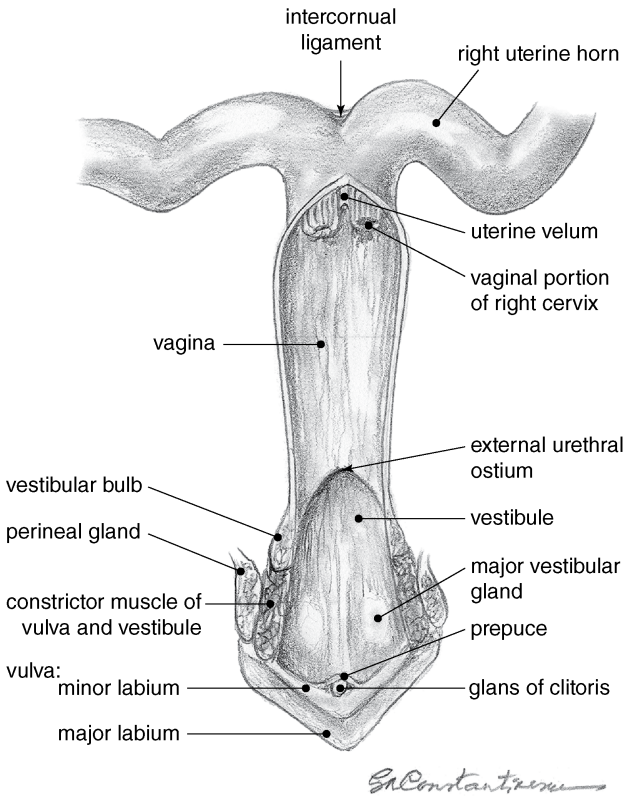

Figure 1.53 Uterus, vagina, and volva in the female rabbit: dorsal aspect, opened. (Redrawn and modified from Barone *et al.* (1973), and redrawn from Constantinescu (2004b).)

vagina with its *vaginal portion*, provided with involute folds of the mucosa resembling a flower in full bloom. There is a *uterine velum* between the vaginal portions of the cervices.

The *vagina* is very long, filling almost the entire pelvic canal. The *vaginal fornix* is very deep, and surrounds both vaginal portions of the two cervices. The *hymen* is rudimentary.

The *vestibule* is topographically located caudal to the ischial arch, on the ventral aspect of the rectum. The *external urethral ostium* is very wide. *Major vestibular glands* are present on the floor, lateral to the projection of the body of clitoris. The *vestibular bulb* and the *constrictor muscle of the vestibule and vagina* are well represented.

The *vulva* is provided with *major and minor symmetrical labiae*. The *clitoris* is strong, and long up to 4 cm. It shows a small *glans* and is located in a deep *clitoral fossa*, protected by the *clitoral prepuce*. As in the male, the *subischiocavernosus muscle* is also present in the female rabbit. Within the clitoral fossa, very well-developed *preputial glands* can be observed. *Major and minor perineal glands* are lining the symmetrical *perineal sinus*.

1.4.2 The Genital System in the Mouse (Constantinescu, 2006)

1.4.2.1 Male Genitalia

The Testicle, Epididymis, Ductus Deferens, Spermatic Cord, and Tunics (Figures 1.54 and 1.55)

The *testicle* is round, and covered on both head and tail by the epididymis. It is located similar to the rabbit, between the anus and the prepuce, with the long axis parallel to the rectum. The *proper ligament of the testis* is well represented.

Downloaded from Vet-eBooks.com

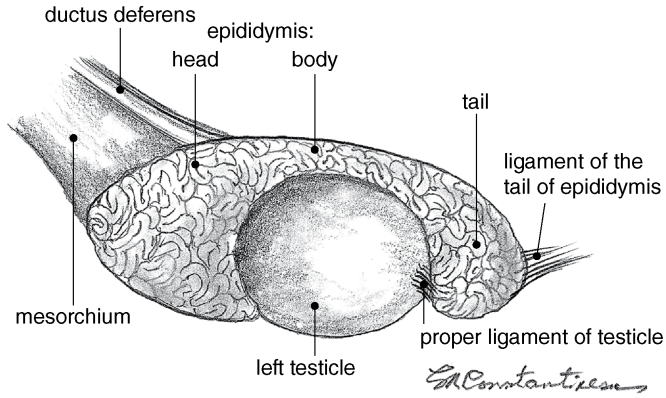

Figure 1.54 Testicle of the mouse: left, lateral aspect. (Redrawn and adapted from Constantinescu (2011) with permission from the American Association for Laboratory Animal Science (AALAS).)

The *epididymis* is enormous, especially its head. With the *head, body, and tail*, the entire epididymis covers intimately the testicle. The *ligament of the tail of the epididymis* is short and covered by the tail of the epididymis.

The *ductus deferens* is very long, and together with the rest of the *spermatic cord* and the *endoabdominal testicular tunics* are enclosed in an abundant amount of fat. The *ampullae of the ductus deferentes* are very well developed, connected by the *genital fold*, and provided with an unpaired *ampullary gland*. The *extraabdominal testicular tunics* are not different from those of the rabbit or the domestic mammals. The *scrotal ligament* is present. The *cremaster muscle* is not as well developed as in the rabbit, but still strong.

The *spermatic cord* and the *tunics* do not show anything in particular.

Accessory Genital Glands (Figure 1.56)

The accessory genital glands of the mouse and the rat have particularities that put them in a different category.

The *ampullary gland* is small, elongated, and located between the ducts of the vesicular glands and fully shown on the dorsal aspect. Its caudal extent is covered by the dorsal prostate gland. The entire surface is slightly lobulated.

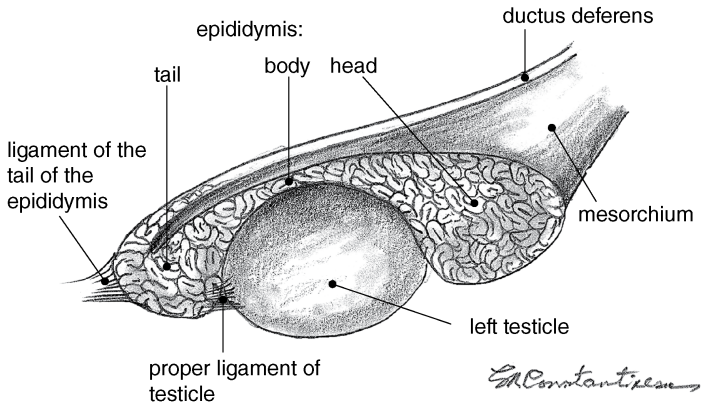

Figure 1.55 Testicle of the mouse: left, medial aspect. (Redrawn and adapted from Constantinescu (2011) with permission from the American Association for Laboratory Animal Science (AALAS).)

Downloaded from Vet-eBooks.com

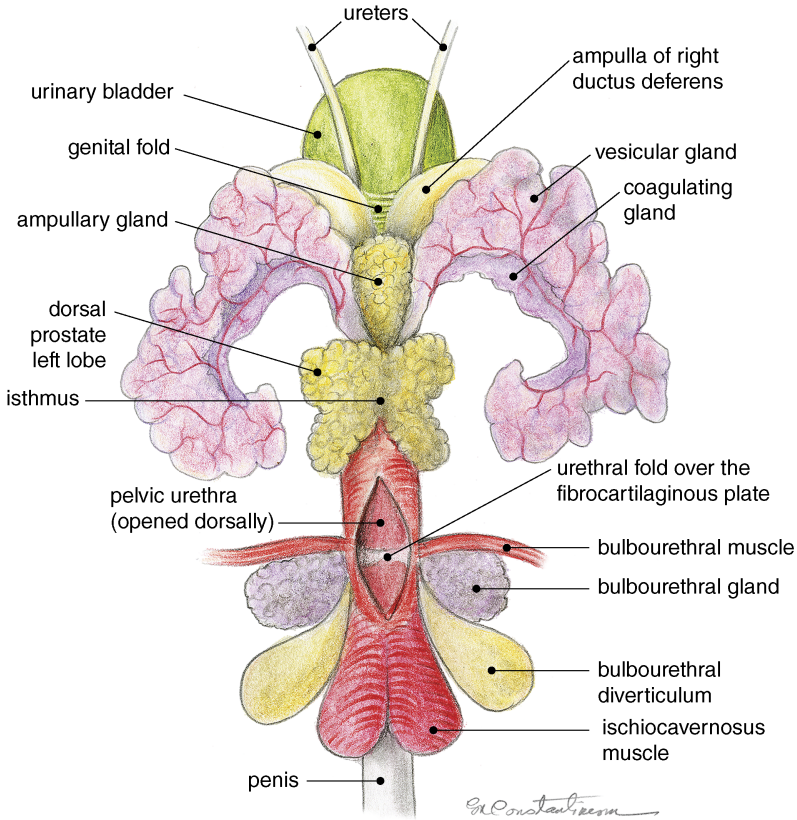

Figure 1.56 Accessory gantal glands in the male mouse: dorsal aspect. (Redrawn and adapted from Constantinescu (2011) with permission from the American Association for Laboratory Animal Science (AALAS).)

The *vesicular glands* are enormous, mostly located within the peritoneal cavity, in a shape resembling the ram's horns. With the surface lobulated and very well supplied by blood, they parallel the curvature of the ampullae of the ductus deferentes in their way to the prostatic urethra, running on both sides of the ampullary gland. The ducts enter under the dorsal prostate before reaching the urethra.

The *coagulating glands* common to the mouse and the rat are much smaller than the vesicular glands, still with an uneven surface, and are located and protected in the lesser curvature of the vesicular glands.

The *prostate* consists of two separate glands: a dorsal, and a ventral prostate. The *dorsal prostate* is the largest, resembling a butterfly, having *two symmetrical lobes connected by an isthmus*, and with an uneven surface. The *ventral prostate* is much smaller, consisting of *two lobes* and is provided with an even surface.

The *bulbourethral glands* are big, rounded, and with a lobulated surface. They are covered by the respective *bulboglandularis muscles*, and their ducts are running in front of the ducts of two symmetrical *bulbourethral diverticula.* The latter are specific to the mouse, have a smooth surface, and have the role of temporary deposit of the glands' secretion. However, their ducts do not communicate with each other and open separately into the *urethral recess,* specific to the mouse, rat, pig, and ruminants. The cast of the pelvic urethra clearly shows separate ducts of the bulbourethral diverticula and of the bulbourethral glands. The urethral isthmus is shown in the

Downloaded from Vet-eBooks.com

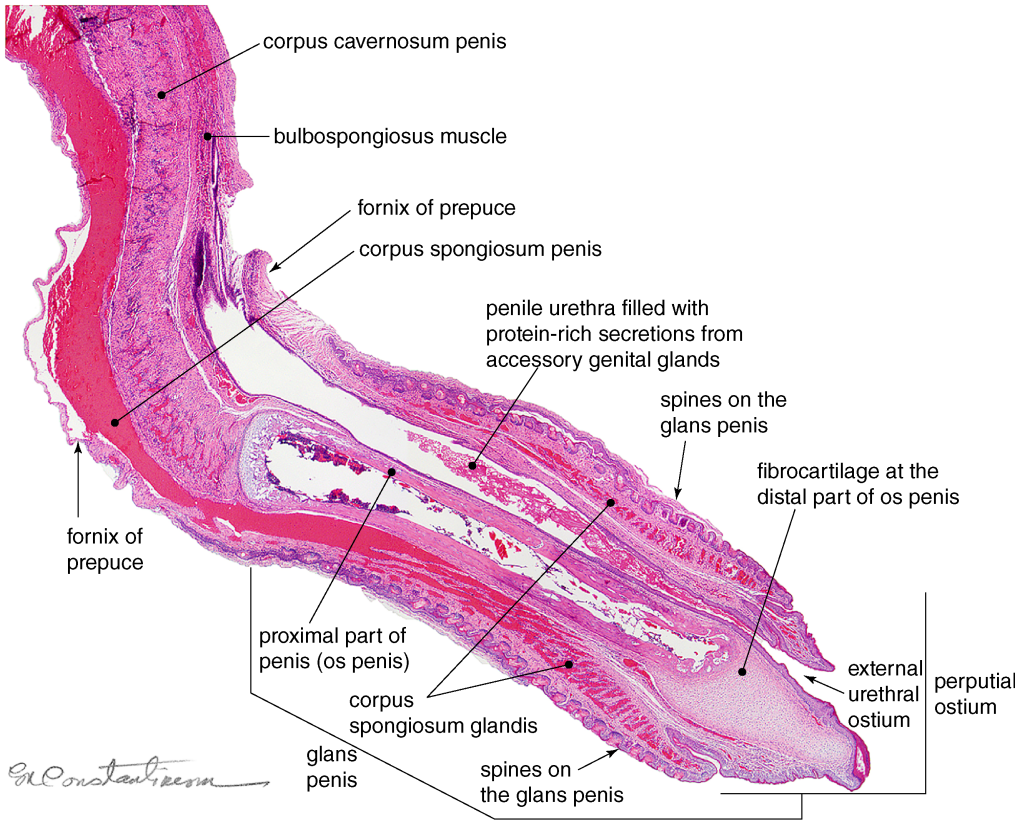

Figure 1.57 Mouse. Penis (median section) stained by hematoxylin and eosin. (Redrawn and adapted from Constantinescu (2011) with permission from the American Association for Laboratory Animal Science (AALAS).)

cast between the ducts of the bulbourethral diverticula and the urethral recess, where inside of the urethra a fibrocartilaginous plate can be seen.

The Penis and the Prepuce (Figure 1.57)

The *penis* of the mouse is ventrally oriented, and slightly bent horizontally. Thus, it is caudally oriented at the level of the *glans penis/os penis*, in continuation to the strong *corpus cavernosum penis*. A median section through the penis shows, in addition, the conical-shaped *cartilage,* which covers the distal end of the os penis; the *urethra,* which is positioned dorsally in the resting sexual activity, and the *external urethral ostium*; the *corpus spongiosum penis,* and the *corpus spongiosum glandis*. Note that the glans penis is provided with *small spines*. The cartilage on the tip of the os penis will ossify and fuse with the os penis. The *prepuce* with the *ostium* and the *fornices* are also shown in this median section.

1.4.2.2 Female Genitalia

The Ovary, Salpinx, Uterus, Vagina, Vestibule, Vulva, and Clitoris (Figures 1.58 and 1.59)

The *ovary* is small, elliptically shaped, smooth, and located in the proximity of the corresponding kidney, anchored by a long *suspensory ligament* and a fairly long *mesovarium*.

The *salpinx* is very flexuous and short, and the *ampulla* and the *infundibulum* surround the ovary from the caudal to the cranial pole. It is suspended by a short *mesosalpinx*.

Downloaded From Vet-eBooks.com

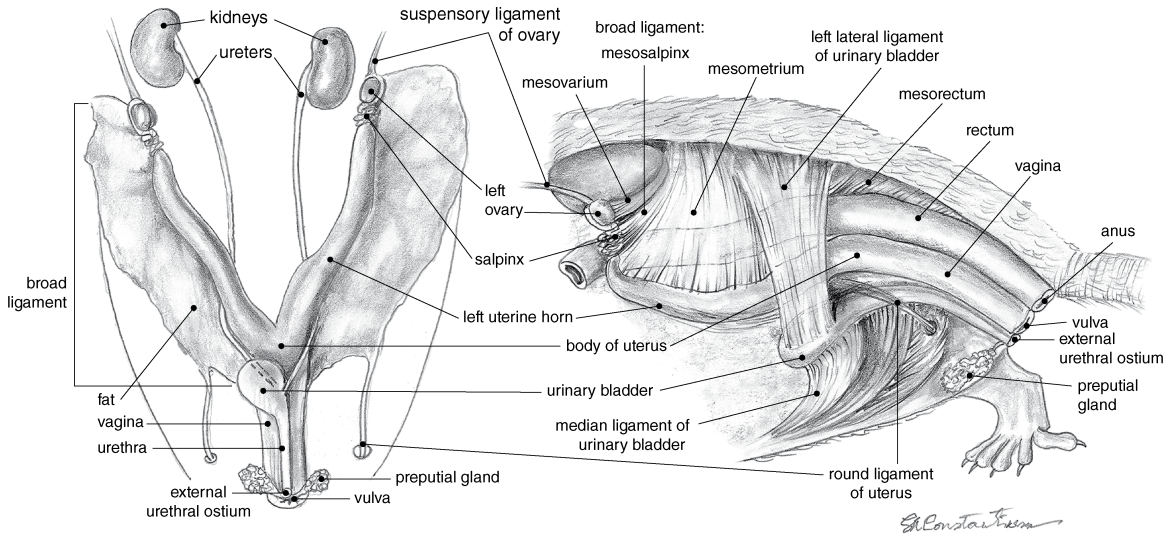

Figure 1.58 Genital apparatus in the female mouse: ventral aspect.

Figure 1.59 Genital apparatus in the female mouse *in situ*: left lateral aspect. (Redrawn and adapted from Constantinescu (2011) with permission from the American Association for Laboratory Animal Science (AALAS).)

Downloaded From Vet-eBooks.com

The *uterus* has two long *horns* bent ventrally, flexuous, and suspended by a long *meometrium* embedded in a large amount of fat. The *round ligament of the uterus* accompanied by the mesometrium penetrates the vaginal ring and passes through the inguinal canal, accompanied by the external pudendal artery and vein. The *body of uterus* is short, and the mouse is provided by *one cervical canal and uterine ostium*. The *vaginal part of the cervix* protrudes significantly into the vagina and has longitudinal striations.

The *vagina* is long, uniform as lumen, with longitudinal folds and very deep *fornices* around the vaginal part of the cervix. There is a *hymen* at the end of the vagina, at the transition to the vestibule, but no external urethral ostium is present in the vagina. Instead, the urethra is as long as paralleling the vagina, vestibule, and vulva, and opening by the external urethral orifice immediately ventral to the vulva.

The *vestibule* is very short and provides support for the *vulva.*

The *clitoris* is *not* associated with the vestibulum or the vulva, but with the *external urethral ostium*. The urethra passes through the *corpus cavernosum clitoridis* before opening through the external urethral ostium. We can say that the vulva consists of the *vaginal orifice*, and the external urethral orifice, to which the clitoris is associated (the latter is located at the base of the clitoris). There is a pair of *preputial glands* symmetrically located ventral to the external urethral ostium.

1.4.3 The Genital System in the Rat (Constantinescu, 2007)

(See text and figures in Constantinescu (2011).)

1.4.3.1 Male Genitalia

The Testicle, Epididymis, Ductus Deferens, Spermatic Cord, and Tunics (Figures 1.60 and 1.61)

The *testicle* is similar to that of the mouse, the only noticeable difference being that the tail of the epididymis is very long, detached from the caudal pole of the testicle, and separated from the latter by a big amount of fat. The scrotum extends caudally between the anus and the prepuce, so that it is very apparent and rounded.

The *epididymis* doesn't surround the testicle as that of the mouse. The *ligament of the tail of the epididymis* is very long.

The *ductus deferens* is proportionally longer than that of the mouse, and together with the intraabdominal testicular tunics is surrounded by a less abundant amount of fat. The *ampullae* are less developed as in the mouse.

The *spermatic cord* and the *tunics* are similar to those of the mouse.

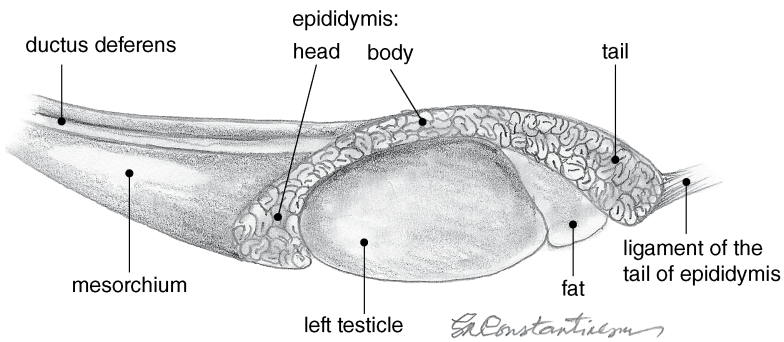

Figure 1.60 Testicle of the rat: left, lateral aspect. (Redrawn and adapted from Constantinescu (2011) with permission from the American Association for Laboratory Animal Science (AALAS).)

Downloaded from Vet-eBooks.com

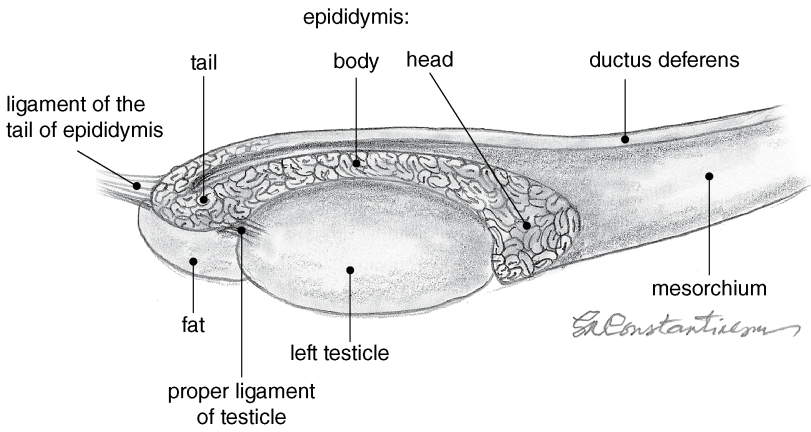

Figure 1.61 Testicle of the rat: left, medial aspect. (Redrawn and adapted from Constantinescu (2011) with permission from the American Association for Laboratory Animal Science (AALAS).)

Accessory Genital Glands (Figures 1.62 and 1.63)

The *ampullary gland* located on the dorsal aspect is flat, rectangular, with irregular borders, and covers the last segments of ductus deferentes and vesicular glands.

The *vesicular glands* are very large, but not as big as those of the mouse. Their curvature may be inward oriented. They are also lobulated and well supplied by blood. The *genital fold* is present.

The *coagulating glands* are located in the same place, and larger than in the mouse. Their surface is between smooth and slightly lobulated.

The *dorsal prostate* consists of two symmetrical spheroidal-shaped, smooth lobes, which originate from the ventral aspect, just caudal to the ventral prostate (see Figure 1.62). The *ventral prostate* consists of two symmetrical elongated, slightly lobulated sacs that drop within the peritoneal cavity, just caudal to the urinary bladder (see Figure 1.63). They can be seen also on the dorsal aspect (see Figure 1.62). The genital fold interconnect the two ventral lobes, leaving a triangular space in between.

The *bulbourethral glands* are spheroidal shaped, smooth, and covered by the *bulboglandularis muscles* (see Figure 1.62). There are *no* bulbourethral diverticula, as in the mouse. The *urethral recess* is present (Figure 1.64).

The Penis and the Prepuce (Figure 1.65)

The *penis* of the rat has many similarities with the penis of the mouse. It is bent at 90° angle, with the proximal (longer part) vertical, and the distal (shorter part) horizontal. The latter contains the *os penis*. A median section through the penis shows the *cartilage* fused with the distal end of the os penis, the *corpus cavernosum penis, corpus spongiosum penis, corpus spongiosum glandis,* the *urethra* with the *external urethral ostium,* and the *glans penis* with the *spines*. The cartilage on the distal end of the os penis will ossify later. The *prepuce* exposes the *external* and *internal laminae,* the *fornix,* and the *preputial ostium*. The *preputial glands* are present, as in the mouse.

1.4.3.2 Female Genitalia

The Ovary, Salpinx, Uterus, Vagina, Vestibule, Vulva, and Clitoris (Figures 1.66 and 1.67)

The *ovaries* are small and similar to those of the mouse.

The *salpinx* is also similar to that of the mouse.

Downloaded From Vet-eBooks.com

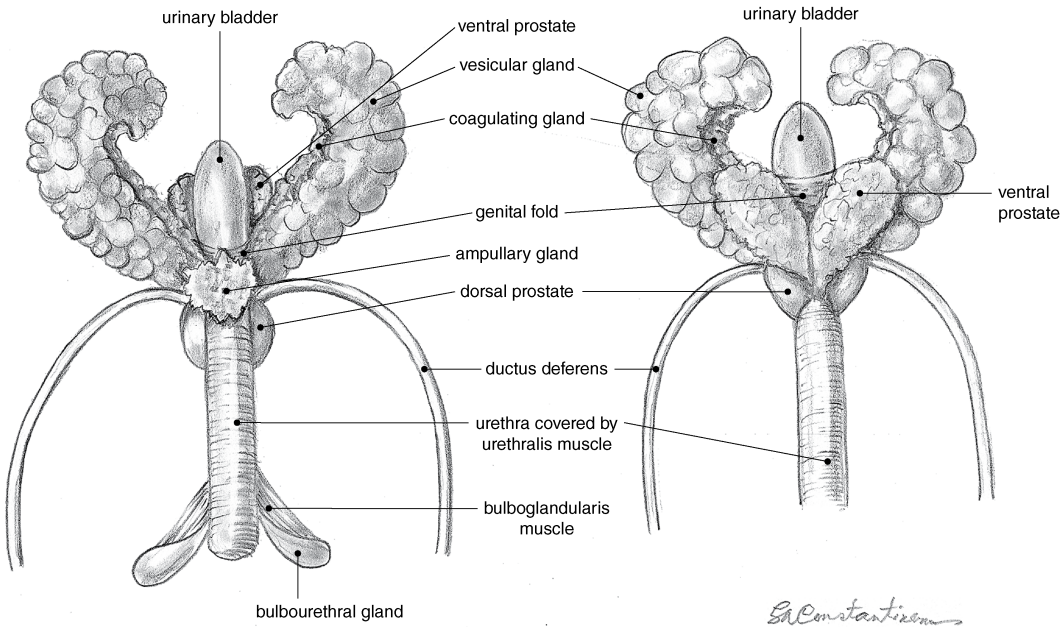

Figure 1.62 Accessory genital glands in the male rat: dorsal aspect.

Figure 1.63 Accessory genital glands in the male rat: ventral aspect.

Downloaded From Vet-eBooks.com

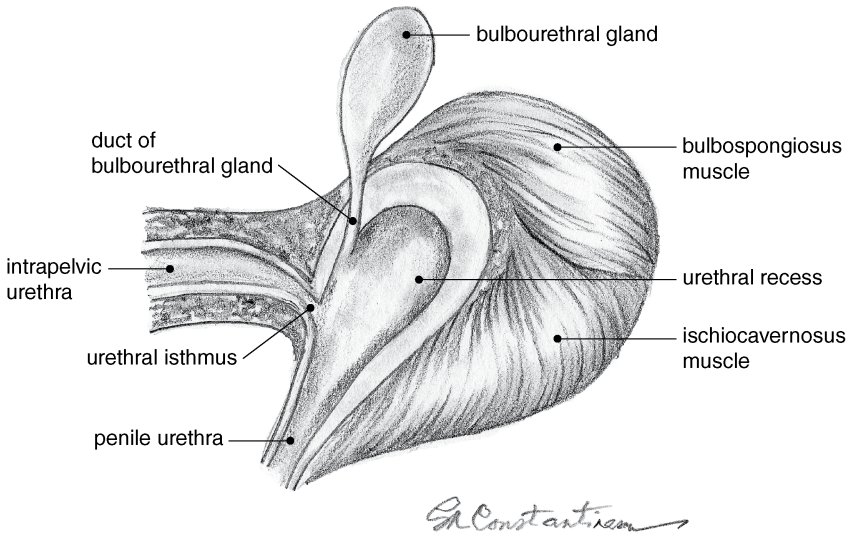

Figure 1.64 The urethral recess in the male rat: median section. (Redrawn and adapted from Constantinescu (2007 and 2011) with permission from the American Association for Laboratory Animal Science (AALAS).)

The *uterus duplex* of the rat (similar to that of the rabbit) has in general a reduced volume. The *uterine horns* are not flexuous like in the mouse; they connect to each other to continue with their own *cervix*; therefore, apparently *there is no uterine body* in the rat. However, the body of uterus is listed on Fig. 1.66 and 1.67. The two cervices open separate from each other into the vagina—the *vaginal parts* of the *two cervices* have two *external uterine ostia*. The *broad ligament* and the *round ligament of the uterus* are similar to those of the mouse.

The *vagina* is similar to that of the mouse, except that there are two external uterine openings surrounded by a deep *vaginal fornix*.

The *vestibule*, the *vulva*, the *clitoris*, the *urethra* and external urethral orifice, and the *preputial glands* are similar to those of the mouse.

1.4.4 The Mammary Glands in Laboratory Animals (Figures 1.68–1.70)

There are four or five pairs of mammary glands in the female *rabbit* (*one axillary* and *one thoracique*, or *two thoracique*—cranial and caudal, *one* or *two abdominal*—cranial and caudal, and *one inguinal*). The papillae are visible and their tips are provided with 8–10 papillary openings versus 5–7 in the cat, 8–14 in the dog, 2–3 in the sow, 1 in all ruminants, and 2 in the mare. The openings correspond to the number of glandular complexes.

There are five pairs of mammary glands in the mouse (*axillary, cranial and caudal thoracic, abdominal,* and *inguinal)* and six pairs in the rat (*one more abdominal pair*).

In the *mouse* the axillary glands are separated from the thoracic glands (both cranial and caudal) on the lateral and ventral aspects of the body, whereas on the dorsal aspect all these symmetrical glands are fused by a median bridge. The abdominal and inguinal glands extend to the dorsum. The inguinal glands extend laterally from the perineal area and completely encircle the external genitalia ventrally, but they do not extend dorsally.

In the *rat* none of the mammary glands reaches the dorsum. The axillary and the thoracic glands are fused ventrally ipsilaterally, whereas the axillary and the cranial thoracic glands are shown as a unique structure on the lateral side. The caudal thoracic and the cranial abdominal glands are connected laterally by a narrow glandular bridge. The symmetrical inguinal mammary glands surround, but do not reach, the external genitalia.

Downloaded From Vet-eBooks.com

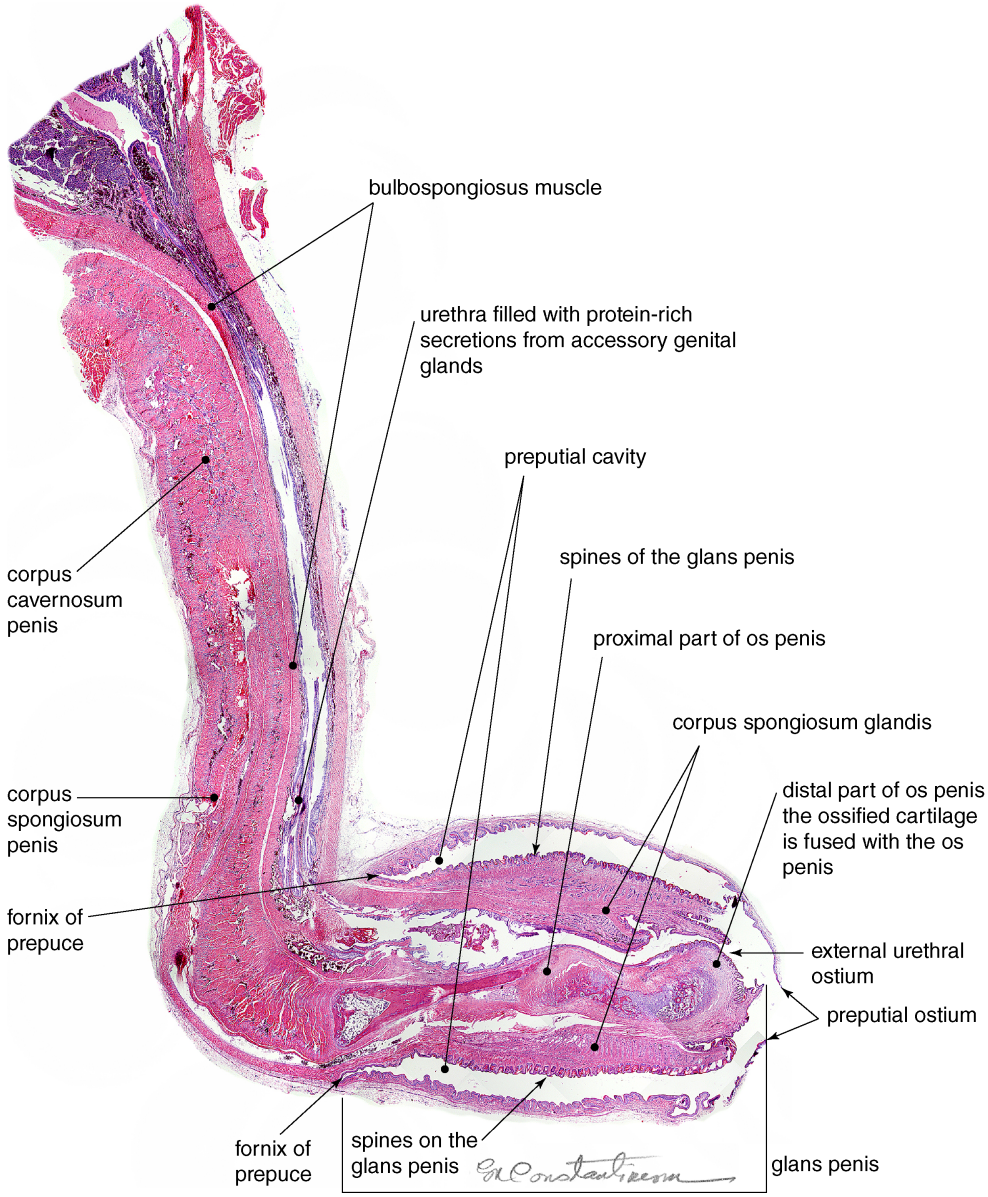

Figure 1.65 Rat. Penis (median section), stained by hematoxylin eosin. (Redrawn and adapted from Constantinescu (2011) with permission from the American Association for Laboratory Animal Science (AALAS).)

1.4.5 The Genital System in the Xenopus laevis: African Clawed Frog (Constantinescu, 2005a)

1.4.5.1 Male Genitalia (Figure 1.71)

The male reproductive organs of this frog consist of two intraabdominal *testicles* with the pair mesorchium and efferent vessels, attached to the kidneys, in the cranial proximity to the adrenal glands (see Figure 1.71). The semen passes into the kidneys through these fine efferent ducts. From here, the semen passes with the urine through the urogenital ducts into the cloaca. There

Downloaded From Vet-eBooks.com

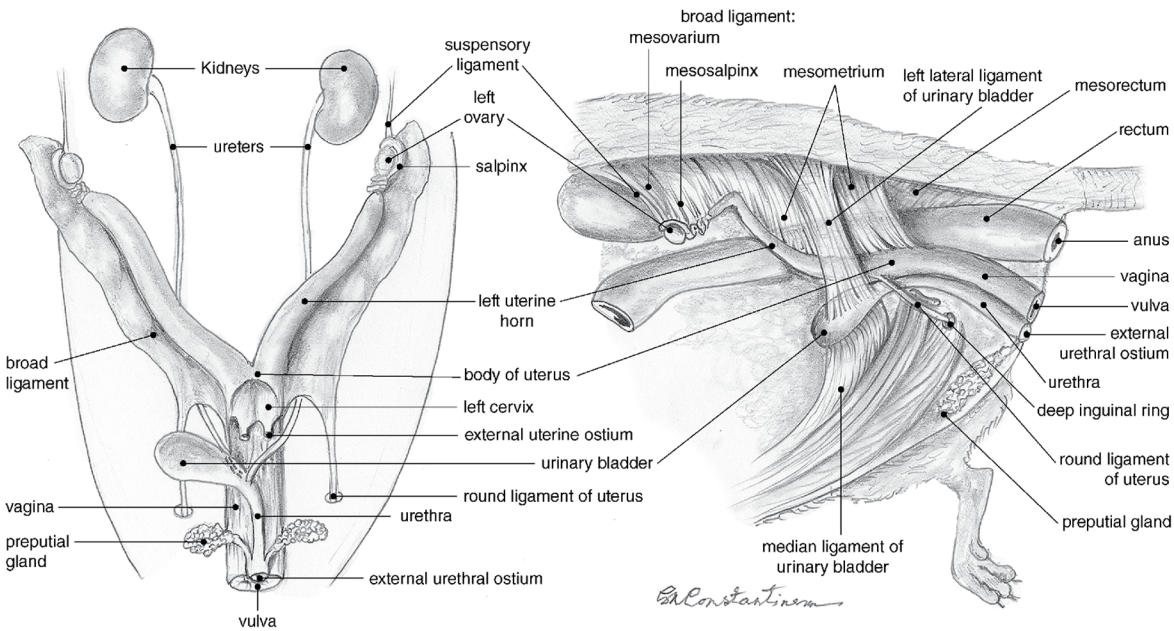

Figure 1.66 Genital apparatus in the female rat: ventral aspect. (Redrawn and adapted from Constantinescu (2007 and 2011) with permission from the American Association for Laboratory Animal Science (AALAS).)

Figure 1.67 Genital apparatus in the female rat: left lateral aspect. (Redrawn and adapted from Constantinescu (2011) with permission from the American Association for Laboratory Animal Science (AALAS).)

Downloaded from Vet-eBooks.com

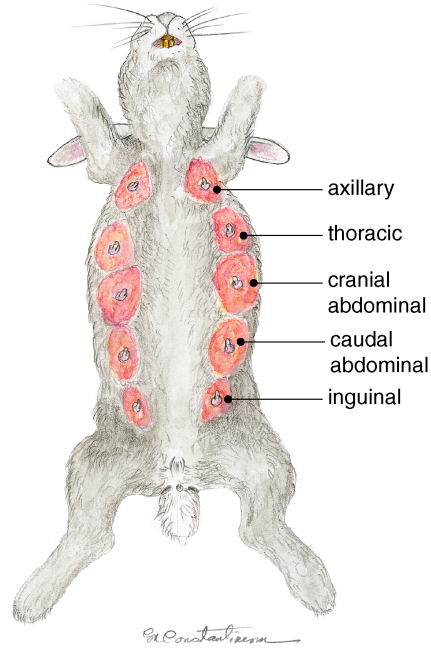

Figure 1.68 Rabbit. Mammary glands: ventral aspect. (Redrawn and modified from Barone (1978).)

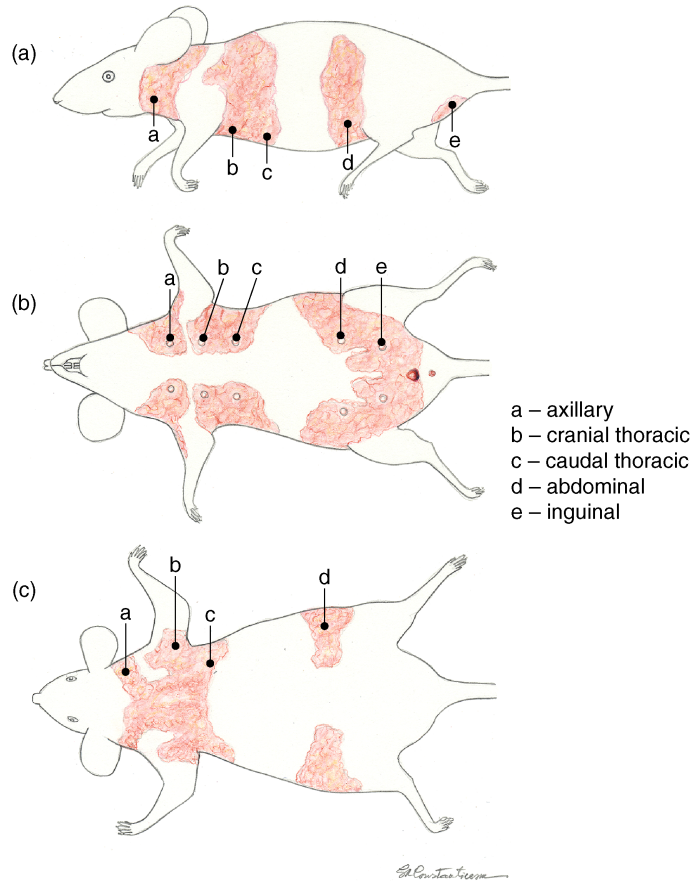

Figure 1.69 Mouse. Mammary glands in lateral (a), ventral (b), and dorsal (c) aspects. (Redrawn and adapted from Constantinescu (2006 and 2011) with permission from the American Association for Laboratory Animal Science (AALAS).)

Downloaded from Vet-eBooks.com

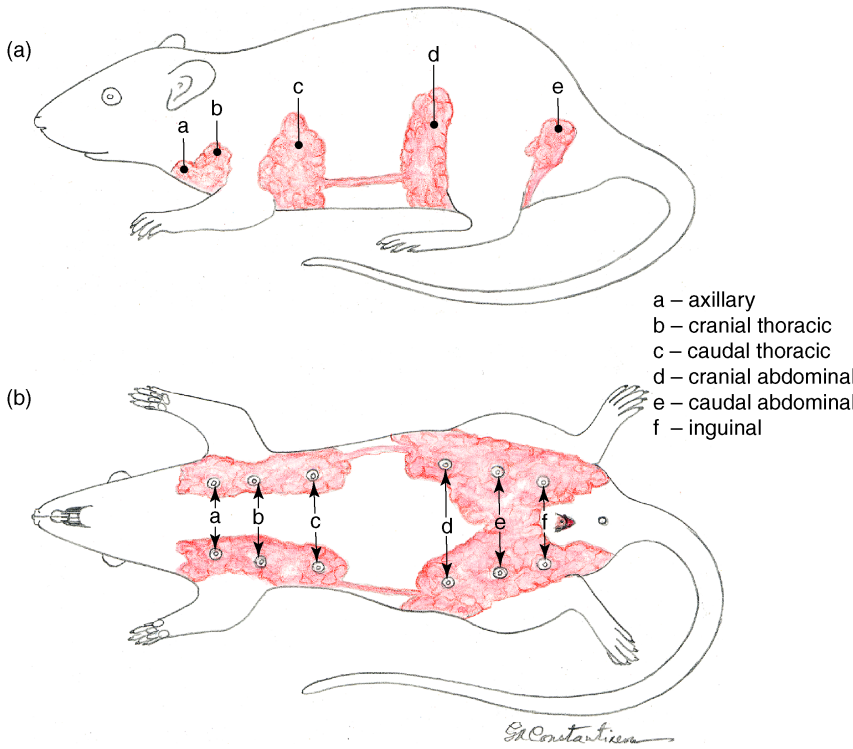

Figure 1.70 Rat. Mammary glands in left lateral (a) and ventra (b) aspects. (Redrawn and adapted from Constantinescu (2007 and 2011) with permission from the American Association for Laboratory Animal Science (AALAS).)

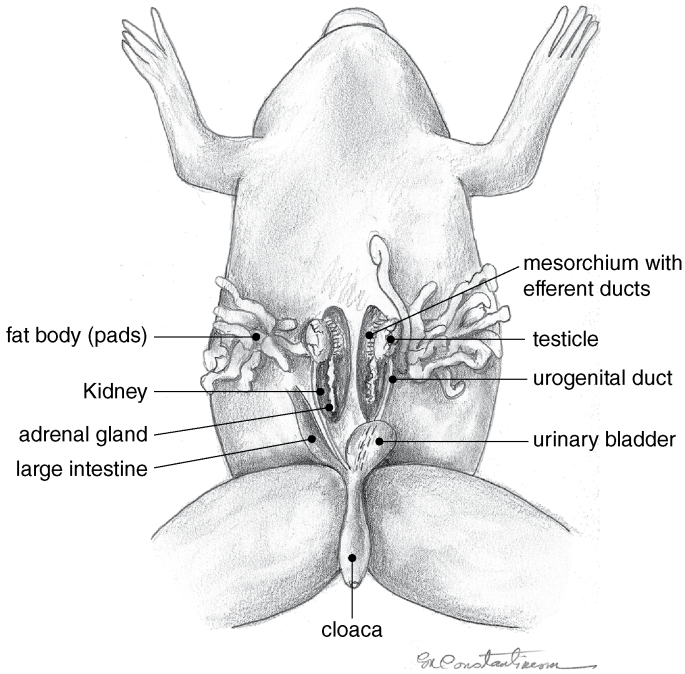

Figure 1.71 Male genital apparatus in the *Xenopus laevis in situ*: ventral aspect. (Redrawn and adapted from Constantinescu (2005a) with permission from the American Association for Laboratory Animal Science (AALAS).)

Downloaded from Vet-eBooks.com

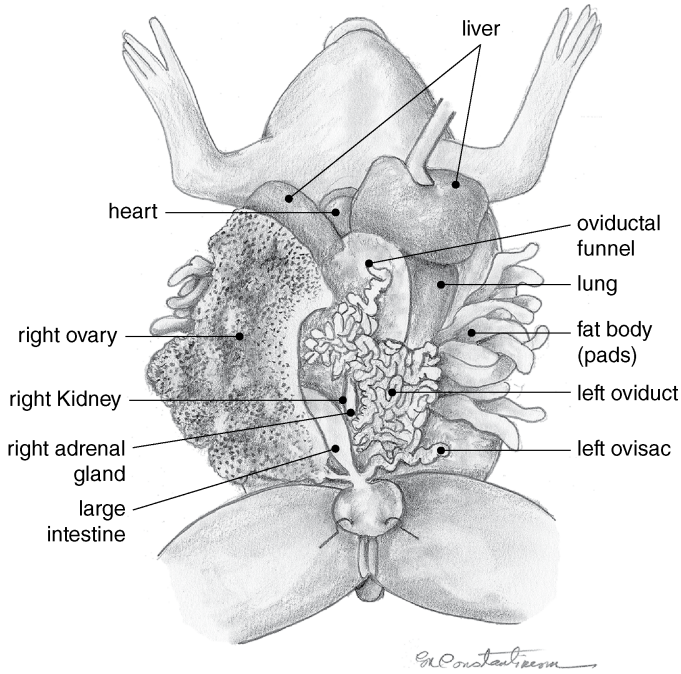

Figure 1.72 Female genital apparatus in the *Xenopus laevis in situ*: ventral aspect. (Redrawn and adapted from Constantinescu (2005a) with permission from the American Association for Laboratory Animal Science (AALAS).)

is no penis in the *Xenopus laevis*. Instead, during the mating process (embracement/amplexus), which may last several days, the grip of the male stimulates the releasing of eggs wrapped in a jelly substance looking like a spawn. The sperm fertilizes the eggs outside the body.

1.4.5.2 Female Genitalia

The female reproductive organs consist of two *ovaries,* two *oviducts*, and two *ovisacs*. The ovisacs open into the cloaca, common to the urinary system (see Figure 1.72).

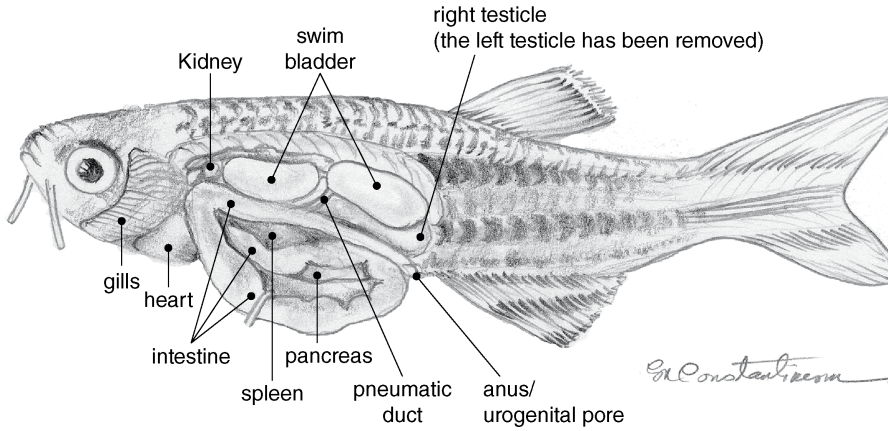

Figure 1.73 Male genital apparatus in the Zebrafish *in situ*: left lateral aspect. (Redrawn and adapted from Constantinescu (2005b) with permission from the American Association for Laboratory Animal Science (AALAS).)

Downloaded from Vet-eBooks.com

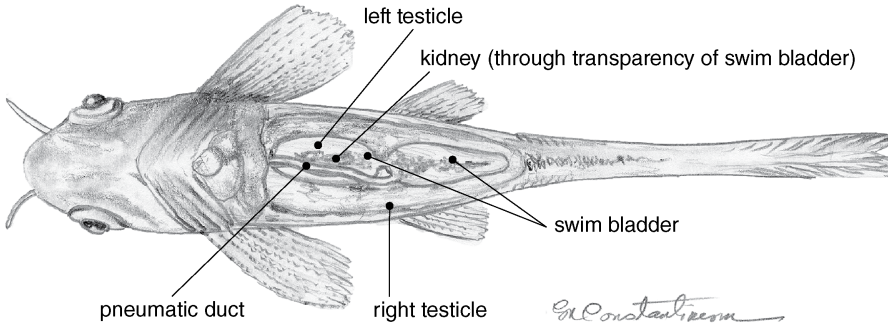

Figure 1.74 Male genital apparatus in zebrafish *in situ*: ventral aspect. (Redrawn and adapted from Constantinescu (2005b) with permission from the American Association for Laboratory Animal Science (AALAS).)

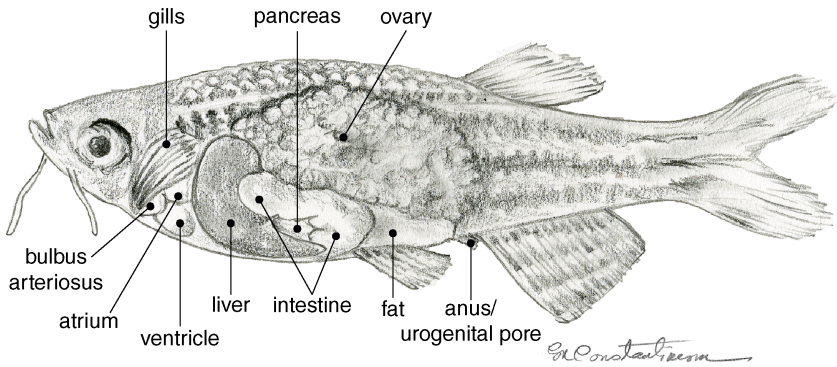

Figure 1.75 Female genital apparatus in zebrafish *in situ*: left lateral aspect. (Redrawn and adapted from Constantinescu (2005b) with permission from the American Association for Laboratory Animal Science (AALAS).)

1.4.6 The Genital System in the Brachidanio rerio (Zebrafish) (Constantinescu, 2005b)

1.4.6.1 Male Genitalia

The male reproductive organs in zebrafish consist of two intraabdominal *testicles* located in close proximity to the swim bladder, the intestine, and the kidneys (see Figures 1.73 and 1.74). The sperm is ejected through the cloaca.

1.4.6.2 Female Genitalia

The female reproductive organs consist of two large *ovaries.* The eggs are expelled through the urogenital/anal pore (see Figure 1.75).

References

Barone, R. (1978) *Anatomie Comparée des Mammifères Domestiques, tome troisième, fascicule II, Appareil Uro-génital*, Laboratoire d'Anatomie École Nationale Vétérinaire, Lyon, France.

Barone, R., Pavaux, C., Blin, P.C., and Cuq, P. (1973) *Atlas d'anatomie du lapin* (*Atlas of Rabbit Anatomy*), Masson, Paris.

Constantinescu, G.M. (2001) *Guide to Regional Ruminant Anatomy Based on the Dissection of the Goat*, Iowa State University Press, Ames.

Constantinescu, G.M. (2002) *Clinical Anatomy for Small Animal Practitioners*, Iowa State University Press, Ames.

Downloaded From Vet-eBooks.com

Constantinescu, G.M. (2004a) Teaching clinical anatomy of genital organs in the large animals, The XXVth Congress of the European Association of Veterinary Anatomists, Oslo, Norway.
Constantinescu, G.M. (2004b) Rabbit Anatomy, poster for AALAS (American Association of Laboratory Animal Science).
Constantinescu, G.M. (2005a) The Anatomy of *Xenopus laevis*, poster for AALAS.
Constantinescu, G.M. (2005b) The Anatomy of Zebrafish, poster for AALAS.
Constantinescu, G.M. (2006) The Anatomy of the Mouse, poster for AALAS.
Constantinescu, G.M. (2007) The Anatomy of the Rat, poster for AALAS.
Constantinescu, G.M. (2011) *Comparative Anatomy of the Mouse and the Rat: A Color Atlas and Text*, AALAS.
Constantinescu, G.M., and Constantinescu, I.A. (2010) *Clinical Dissection Guide for Large Animals; Horse and Large Ruminants*, 2nd edn., Omphaloskepsis Books.
Constantinescu, G.M., and Schaller, O. (2007) *Illustrated Veterinary Anatomical Nomenclature*, 3rd revised edn, Enke, Stuttgart.
Constantinescu, G.M., and Theodorescu, D. (1977) *Aspecte practice privind topografia şi ramurile pre- şi post-ganglionare ale plexului pelviperineal la vacă*, Symposium, Timişoara, Romania.
Constantinescu, G.M., Cosoroabă, I., and Constantinescu, D.M. (1969) *Micul bazin la vacă*, Symposium, Timişoara, Romania.
Constantinescu, G.M., Theodorescu, D., and Fuciu, O. (1977) L'anatomie clinique du plexus pelvi-périnéal chez la vache et le mouton. *Zbl.für Vet. Med. C*, **G**, 367.
deLahunta, A., and Habel, R.E. (1986) *Applied Veterinary Anatomy*, Saunders, Philadelphia.
Dyce, K.M., Sack, W.O., and Wensing, C.J.G. (2010) *Textbook of Veterinary Anatomy*, 4th edn, Elsevier, St. Louis, MO.
Evans, H.E (1993) *Miller's Anatomy of the Dog*, 3rd edn, Saunders, Philadelphia, PA.
Evans, H.E, and deLahunta, A. (2013) *Miller's Anatomy of the Dog*, 4th edn, Elsevier, pp. 382–384.
Feneis, H., and Dauber, W. (2000) *Pocket Atlas of Human Anatomy Based on the International Nomenclature*, 4th edn, Thieme.
Garrett, P.D. (1987) Urethral recess in male goats, sheep, cattle, and swine. *J. Am. Vet. Med. Assoc.*, **191**, 689.
ICVGAN (International Committee on Veterinary Gross Anatomical Nomenclature) (2012) *Nomina Anatomica Veterinaria*, 5th edn (revised version), published on the website of the World Association of Veterinary Anatomists (http://www.wava=amav.org), the Editorial Committee, Hannover (Germany), Columbia, MO (USA), Ghent (Belgium), Sapporo (Japan).
König, H.E. and Liebich, H.-G. (2004) *Veterinary Anatomy of Domestic Mammals: Textbook and Colour Atlas*, Schattauer, Stuttgart.
McCarthy, T.O. (2005) *Veterinary Endoscopy for the Small Animal Practitioner*, Elsevier, pp. 414, 428.
Nickel, R., Schummer, A., and Seiferle, E. (1984) *Lehrbuch der Anatomie der Haustiere, Bd. IV*, Paul Parey.
Popesko, P., Rajtová, V., and Horák, J. (2002) *A Colour Atlas of the Anatomy of Small Laboratory Animals*, vol. 1, Saunders.
Sack, W.O. (1991) *Rooney's Guide to the Dissection of the Horse*, 6th edn, Veterinary Textbooks, Ithaca, NY.
Schatten, H., and Constantinescu, G.M. (2007) *Comparative Reproductive Biology*, Blackwell Publishing, Ames, IA.
Watson, A. (2009) Vaginal ring and round ligament of the uterus in the female cat. *Anat. Hist. Embryol.*, **38**, 319–320.
Youngquist, R.S. and Threffall, W.K. (2007) *Current Therapy in Large Animal Theriogenology*, 2nd edn, Elsevier.

Downloaded From Vet-eBooks.com

2

Anatomy of Mammalian (Endocrine) Glands Controlling the Reproduction

Gheorghe M. Constantinescu

Department of Biomedical Sciences, College of Veterinary Medicine, University of Missouri-Columbia, Columbia, USA

The (endocrine) glands of mammals controlling the reproduction consist of the following glands (Constantinescu, 2002, 2011, *op. cit.*; König and Liebig, 2004, *op. cit.*; Evans and deLahunta, 2013, *op. cit.*): hypophysis (pituitary gland), cerebral epiphysis (pineal body), adrenal glands, sexual glands (endocrine testicle, accessory genital glands, endocrine ovary, and uterine endometrium), the liver, and the placenta. All these glands contribute to sustain and regulate the physiological reproductive activity. All endocrine glands empty their secretion (hormones) into the blood stream. Except the accessory genital glands and the liver, all of the above are endocrine glands, and this is the reason why "endocrine" is within parentheses. The hormones and growth factors will be detailed in a separate chapter.

The international terminology is used throughout this chapter, based on the Nomina Anatomica Veterinaria 5th edn (2012, op. cit.) International Committee on Veterinary Gross Anatomical Nomenclature (ICVGAN) on the website of the World Association of Veterinary Anatomists (http://www.wava=amav.org).

2.1 The Hypothalamus Including the Hypophysis (Figures 2.1 and 2.2)

The *hypothalamus* is the most ventral component of the diencephalon, and consists of several structures that release hormones and other substances involved in the reproduction. Among them is the *hypophysis* or pituitary gland, which is located in all species on the ventral aspect of the diencephalon (see Figure 2.1). It consists of two parts or lobes: glandular—adenohypophysis and neural—neurohypophysis, and the cavity of the hypophysis, as major parts. The relationship to the brain is made by a very fine funnel-shaped stalk called infundibulum, which communicates with the neurohypophyseal recess of the third ventricle.

The adenohypophysis consists of the following parts: tuberal, intermediate, distal, and pharyngeal. The tuberal part covers the infundibulum; the intermediate part lies between the distal part and the neural lobe of the hypophysis; the distal part is the largest part of the glandular lobe; the pharyngeal part is a remnant of the hypophyseal sac (Rathke's pouch), synonymous with the cavity of hypophysis.

The neurohypophysis consists of the infundibulum and the neural lobe. The infundibulum is a funnel-shaped stalk, and has three parts: the root, where the nerve fibers of the infundibulum join the tuber cinereum, the hollow part, which continues the neurohypophyseal recess of the third ventricle, and the solid part.

Animal Models and Human Reproduction, First Edition. Edited by Heide Schatten and Gheorghe M. Constantinescu.
© 2017 John Wiley & Sons, Inc. Published 2017 by John Wiley & Sons, Inc.

Downloaded From Vet-eBooks.com

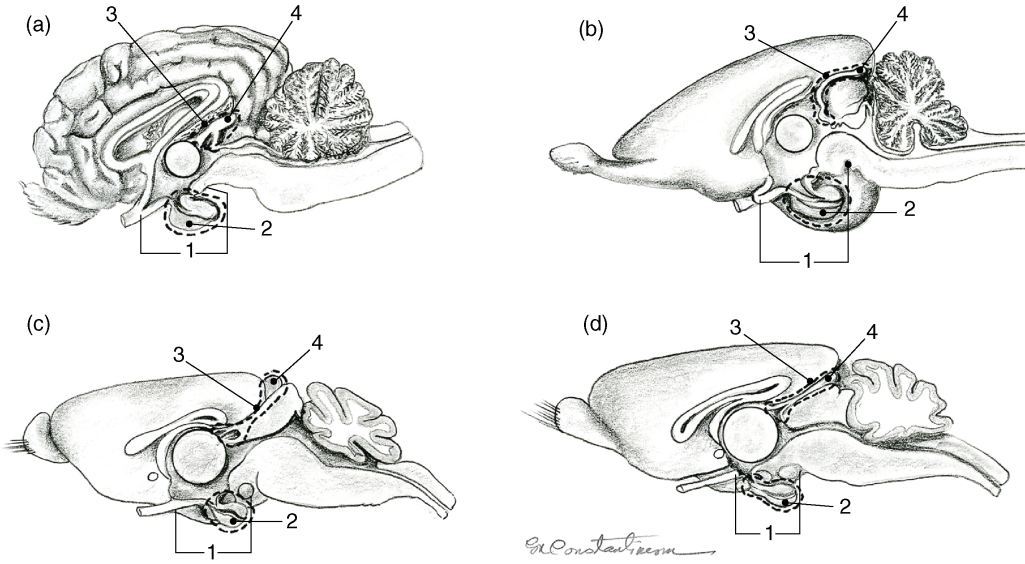

Figure 2.1 Hypothalamus and epithalamus (median section, right half of brain). (a) Horse. (b) Rabbit. (Redrawn and modified from Popesko *et al.* (2002a, 2002b), *op. cit.*). (c) Mouse. (d) Rat. (Parts (c) and (d) redrawn and modified with permission from American Association for Laboratory Animal Science (AALAS)). 1: hypothalamus; 2: hypophysis; 3: epithalamus (partially covered by the mesencephalic tectum in the mouse); 4: cerebral epiphysis.

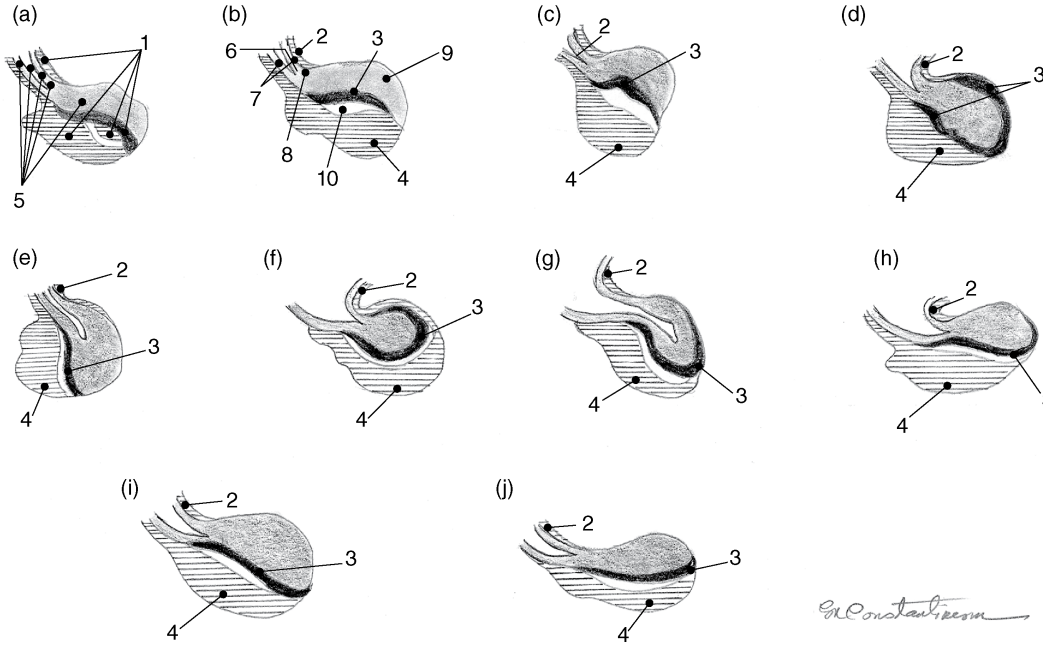

Figure 2.2 Hypophysis (median section, right half). (a) Ox. (b) Sheep. (c) Goat. (d) Horse. (e) Pig. (f) Dog. (g) Cat. (h) Rabbit. (i) Mouse. (j) Rat. 1: adenohypophysis, consisting of 2–4; 2: tuberal part; 3: intermediate part; 4: distal part; 5: neurohypophysis, consisting of 6–9; 6: infundibulum, consisting of a hollow part (7) and solid part (8); 9: neural lobe; 10: cavity of hypophysis. (Redrawn and modified from Nickel *et al.* (1984), *op. cit.* for the ox, goat, horse, pig, dog, and cat; Barone and Simmoens (2010), *op. cit.* for the sheep; Atwell, *op. cit.* and Campbell (1966), *op. cit.* for the rabbit; Sano and Sasaki (1969), *op. cit.*, and Hashimoto *et al.* (1998), *op. cit.* for the mouse; Popesko *et al.* (2002a, 2002b), *op. cit.*, for the rat.)

Downloaded from Vet-eBooks.com

The cavity of the hypophysis, located between the intermediate and distal parts of the adenohypophysis, is synonymous with the pharyngeal part of the adenohypophysis, or the Rathke's pouch.

The entire gland exposes differences among species, illustrated in the Figure 2.2.

2.2 The Cerebral Epiphysis (see Figure 2.1)

The *cerebral epiphysis*, or the pineal gland, belongs to the epithalamus, the most dorsal component of the diencephalon. It is located on the dorsocaudal aspect of the diencephalon, and provides the peduncle (the rostral part), connected with the right and left habenula. The latter anchors the cerebral epiphysis to the thalamus (the middle component of the diencephalon).

2.3 The Thyroid Gland (Figure 2.3)

The *thyroid gland* is located in all mammalian species on the lateral aspects of the first tracheal rings, even on the thyroid cartilage, exceeding the trachea cranially. It consists of two lobes, right and left, and in some species an isthmus connecting the lobes ventrally. The development of hypophysis in the rabbit is described by Wayne (1918, *op. cit.*), and the development of the same gland in the Albino rat is described by Schwind (1928, *op. cit.*). The isthmus is glandular in the large ruminants pig, rabbit, rat, and the carnivores—in which it may be absent—and fibrous in the small ruminants (sheep and goats) and horse, and may be absent in all these last three species. In the large ruminants, pig, dog, and rabbit, the anterior poles of the lobes extend to the cricoid cartilage of the larynx, whereas in the mouse the lobes extend further cranially, to the

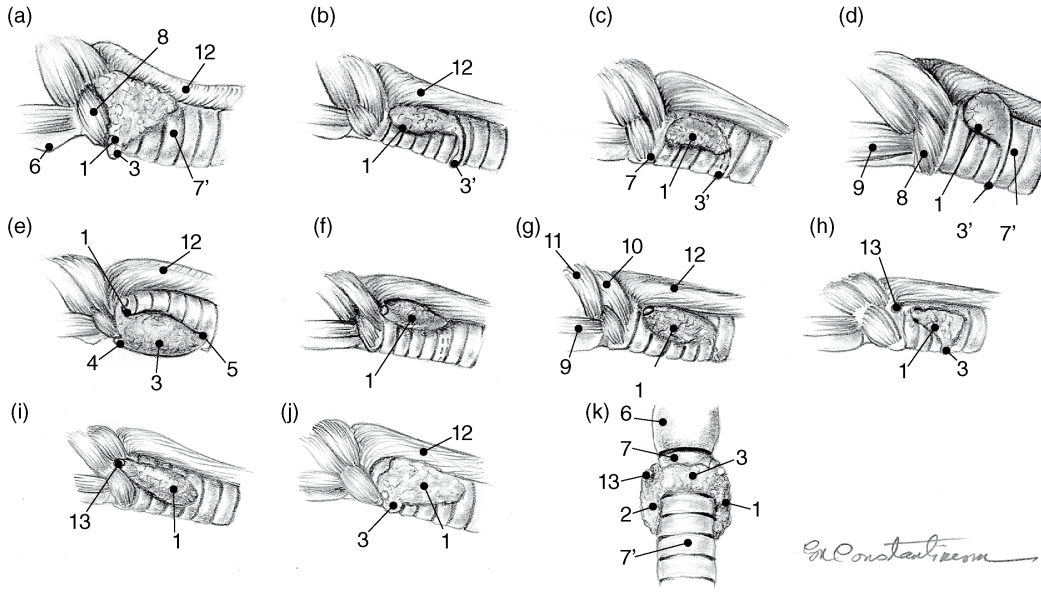

Figure 2.3 Thyroid gland (left lateral aspect). (a) Ox. (b) Sheep. (c) Goat. (d) Horse. (e) Pig. (f) Dog. (g) Cat. (h) Rabbit. (i) Mouse. (j) Rat. (k) Rat ventral aspect.1: left lobe of thyroid gland; 2: right lobe; 3: glandular isthmus; 3′: fibrous isthmus; 4: pyramidal lobe; 5: caudal lobe; 6: thyroid cartilage; 7: cricoid cartilage; 7′: tracheal rings; 8: cricothyroideus; 9: thyrohyoideus; 10: cricopharyngeus; 11: thyropharyngeus; 12: esophagus; 13: external parathyroid gland. (Redrawn and modified from Barone and Simmoens (2010), *op. cit.* for the ox, sheep, pig, and dog; Constantinescu (2001), *op. cit.* for the goat; Nickel *et al.* (1984), *op. cit.* for the horse and pig; Popesko *et al.* (2002a), *op. cit.* for the rabbit; Popesko *et al.* (2002b), *op. cit.* for the mouse and rat; Hudson and Hamilton (2010), *op. cit.* for the cat.)

Downloaded From Vet-eBooks.com

thyroid cartilage. In the pig, the two lobes of the thyroid gland show cranially a small pyramidal lobe, and caudally a small so-called caudal lobe. There are also *accessory thyroid glands*, small nodules of thyroid tissue anywhere between tongue and heart.

With a smooth or finely granulated/lobulated surface, and of various species-specific shapes and colors, the thyroid gland is in some species in intimate or close relationships with the *parathyroid glands*. (The parathyroid glands do *not* contribute to the physiology of reproduction; they are only topographically associated with the thyroid gland in some species.) Those parathyroid glands that can be seen on the surface of the thyroid gland or are independent of the thyroid gland are called external, whereas those incorporated into the thyroid gland are called internal. The external parathyroid glands are located on the cranial pole of each lobe of the thyroid gland in carnivores, mouse, and rat; on the cricoid cartilage in front of the cranial pole of each lobe of the thyroid gland in the rabbit; near the end of the external carotid A. in the pig and ruminants; and far caudally, near the thoracic inlet, in the horse.

The location, shape, and size of all of the characteristics of the thyroid glands with or without an isthmus are shown in Figure 2.3.

2.4 The Adrenal Glands (Figure 2.4)

Also known as the suprarenal glands (the term fits the human anatomy), the *adrenal glands* are located close to the kidneys, in different position, shape, color, and volume for each species. The most unusual location is shown in the ruminants, in which, due to the enormous development of the rumen, the kidneys are pushed toward the midline. Therefore, the relationship between the adrenal glands and the corresponding kidneys is as peculiar as it is shown in Figure 2.4.

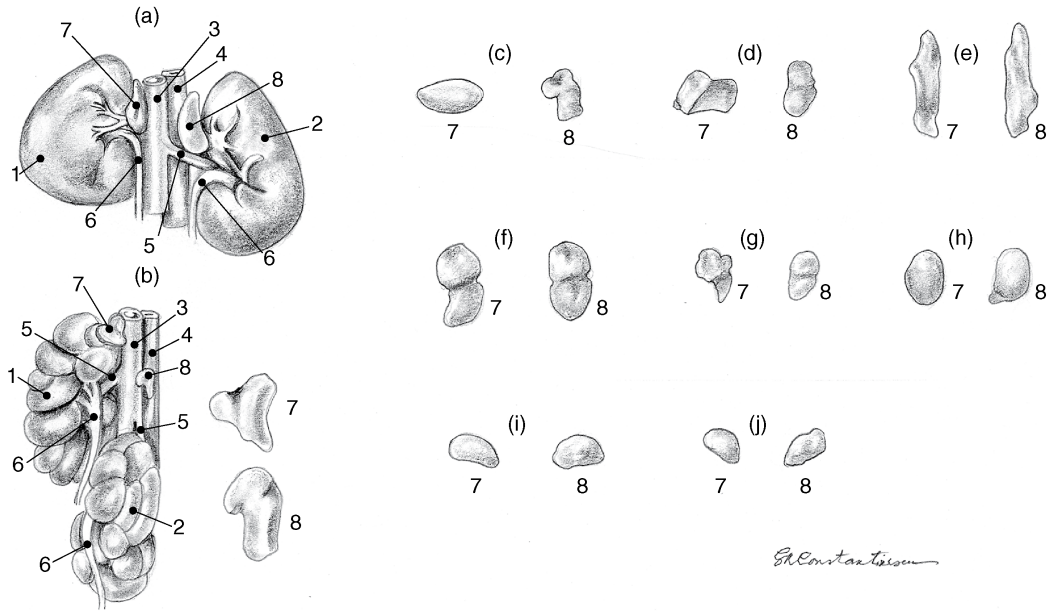

Figure 2.4 Adrenal glands (ventral aspect). (a) Horse. (b) Ox. (c) Sheep. (d) Goat. (e) Pig. (f) Dog. (g) Cat. (h) Rabbit. (i) Mouse. (j) Rat. 1: right kidney; 2: left kidney; 3: abdominal aorta; 4: caudal vena cava; 5: renal arteries; 6: ureters; 7: right adrenal gland; 8: left adrenal gland. (Redrawn and modified from Constantinescu and Constantinescu (2010), *op. cit.* for the horse and ox; Nickel *et al.* (1984), *op. cit.* for the sheep, goat, pig, and cat; Barone and Simmoens (2010) for the dog; Popesko *et al.* (2002a), *op. cit.* for the rabbit; Popesko *et al.* (2002b), *op. cit.* for the mouse and rat.)

Downloaded from Vet-eBooks.com

2.5 The Sexual Glands

The *endocrine testicle* is represented by the interstitial (Leydig) cells and the sustentacular (Sertoli) cells. The Leydig cells are located between the seminiferous tubules (the reason why they are called "interstitial" cells), whereas the Sertoli cells are found within the seminiferous tubules (all of them visible under the microscope—see Histology books).

The *male accessory genital glands* are the prostate, the vesicular glands, and the coagulating and ampullary glands (in the mouse and rat), and the bulbourethral glands. All of them are described and illustrated in the Chapter 1. These glands contribute with their secretion to the formation of the seminal plasma, and to the sperm transport during ejaculation. They are *not* endocrine glands.

The *endocrine ovary* is represented by the ripening follicles and the corpora lutea (see Figures 1.3 and 1.4).

The *uterine endometrium* is the mucous membrane lying the uterine cavity. It has a thick lamina propria and is covered by columnar epithelium (Constantinescu and Schaller (2012), *op. cit.*). It differs from species to species, from the nonpregnant to the various stages of the pregnant uterus. (For details, see books on histology and physiology of reproduction.). The uterine endometrium secretes the prostaglandin F2α (PGF2α), a hormone.

During the development of the embryo/fetus, the fetal membranes concur with the endometrium in the formation of the *placenta*, an organ that may be defined as an apposition or fusion of fetal and maternal tissue for the purposes of physiological exchange and hormone production (Dyce *et al*., 2010). There are several types of chorioallantoic group, which include the diffuse placenta (in mare and sow), cotyledonary placenta (in ruminants), zonary placenta (in carnivores), and discoidal placenta (in rodents and humans). They are described in Chapters 11 and 12 in Schatten and Constantinescu (2007, *op. cit.*).

2.6 The Liver

The *liver* controls the reproduction by insulin-like growth factors, stimulating steroidogenesis, mammary growth, and fetal development. It is *not* an endocrine gland, it does *not* release any hormone.

References

Barone, R. and Simmoens, P. (2010) *Anatomie Comparée des Mammifères Domestiques, tome septième, Neurologie II*, Vigot Frères, Paris.

Campbell, H.J. (1966) The development of the primary portal plexus in the median eminence of the rabbit. *J. Anat.*, **100**, 2, 381–387.

Constantinescu, G.M. (2001) *Guide to Regional Ruminant Anatomy Based on the Dissection of the Goat*, Iowa State University Press, Ames, IA.

Constantinescu, G.M. (2002) *Clinical Anatomy for Small Animal Practitioners*, Iowa State University Press, Ames, IA.

Constantinescu, G.M. (2011) *Comparative Anatomy of the Mouse and the Rat: A Color Atlas and Text*. American Association for Laboratory Animal Science (AALAS).

Constantinescu, G.M. and Constantinescu, I.A. (2010) *Clinical Dissection Guide for Large Animals, Horse and Large Ruminants*, 2nd edn, Omphaloskepsis Books.

Downloaded From Vet-e-Books.com

Constantinescu, G.M. and Schaller, O. (2012) *Illustrated Veterinary Anatomical Nomenclature*, 3rd revised edn, Enke, Stuttgart, Germany.

Dyce, K.M., Sack, W.O., and Wensing, C.J.G. (2010) *Textbook of Veterinary Anatomy*, 4th edn, Saunders, St. Louis, MO.

Evans, H. and deLahunta, A. (2013) *Miller's Anatomy of the Dog*, 4th edn, Saunders, pp. 382–384.

Hashimoto, H., Ishikawa, H., and Kusakabe, M. (1998) Three-dimensional analysis of the developing pituitary gland in the mouse. *Dev. Dyn.*, **212**, 157–166.

Hudson, L.C. and Hamilton, W.P. (2010) *Atlas of Feline Anatomy for Veterinarians*, 2nd edn, Teton New Media.

ICVGAN (International Committee on Veterinary Gross Anatomical Nomenclature) (2012) *Nomina Anatomica Veterinaria*, 5th edn (revised version), published on the website of the World Association of Veterinary Anatomists (http://www.wava=amav.org). The Editorial Committee, Hannover (Germany), Columbia, MO (USA), Ghent (Belgium), Sapporo (Japan).

König, H.E. and Liebich, H.-G. (2004) *Veterinary Anatomy of Domestic Mammals: Textbook and Colour Atlas*, Schattauer, Stuttgart, Germany.

Nickel, R., Schummer, A., and Seiferle, E. (1984) *Lehrbuch der Anatomie der Haustiere, Bd. IV*, Paul Parey.

Popesko, P., Rajtová, V., and Horák, J. (2002a) *A Colour Atlas of the Anatomy of Small Laboratory Animals: Volume 1: Rabbit, Guinea Pig*, Saunders.

Popesko, P., Rajtová, V., and Horák, J. (2002b) *A Colour Atlas of the Anatomy of Small Laboratory Animals: Volume 2: Rat, Mouse, Hamster*, Saunders.

Sano, M. and Sasaki, F. (1969) Embryonic development of the mouse anterior pituitary studied by light and electron microscopy. *Z. Anat. Entwickl. Gesch.*, **129**, 195–222.

Schatten, H. and Constantinescu, G.M. (2007) *Comparative Reproductive Biology*, Blackwell.

Schwind, J.L. (1928) The development of the hypophysis cerebri of the albino rat. *Am. J. Anat.*, **41**, 295–320.

Wayne, A.J. (1918) The development of *Hypophysis cerebri* of the rabbit (*Lepus cuniculus L.*). *Am. J. Anat.*, **24** (3), 271–337.

Downloaded From Vet-eBooks.com

3

Models for Investigating Placental Biology

Laramie Pence[1,2] *and Bhanu P. Telugu*[1,2]

[1]*Animal Bioscience and Biotechnology Laboratory, USDA Agricultural Research Science, MD, USA*
[2]*Department of Animal and Avian Sciences, University of Maryland, MD, USA*

3.1 Introduction

Viviparity and reproductive success in mammals is dependent on the establishment and maintenance of a functional placenta. The placenta is a distinguishing feature of all eutherian mammals, and its role during pregnancy is essential and conserved across species. During pregnancy, the placenta performs several essential functions, including providing a medium for nutrient, gas, and waste exchange between the fetus and mother; protecting the semiallogeneic fetus from immunological and physical assaults; diverting a share of maternal nutrients toward the growth of fetus during pregnancy and postnatally during lactation; influencing maternal behavior to care for the new born; among others. In order to accomplish this gamut of functions, the placental trophoblast cells resort to a combination of disguise (or mimicry), manipulation of maternal physiology, and genetic arms race with the mother. In humans, for example, semi-allogeneic placental cells "disguise" and evade attack from NK cells in decidua by expressing nonclassical HLA molecules, HLA-E, and HLA-G that lack antigen presentation but are recognized as self. Likewise, extravillous trophoblast cells invading the maternal deciduum "mimic" endothelial-like cells (endovascular mimicry) by switching surface integrins, replacing the existing endothelial cells in blood vessels, and consequently providing unrestricted blood flow to the placenta and the growing fetus. Manipulation of maternal physiology to bias allocation of nutrients to the growing fetus is achieved by producing hormones such as human placental lactogen. Human placental lactogen acts on maternal prolactin receptors to increase resistance to insulin, causing circulating blood sugar to remain elevated following a meal in order to facilitate uptake by the fetus. Finally, an evolving genetic arms race between mother and fetus is evident from clad- and placental-specific expansion of gene families in various species (prolactin-like genes in the mouse, pregnancy-associated glycoproteins in the ungulates, etc.), emergence of novel placental cell types (bi- and trinucleate cells of ruminant ungulates, polyploidy giant cells of rodents, chorionic girdle cells of equids, extravillous cytotrophoblasts of humans, etc.), epigenetic silencing of genes in the placenta, unique adaptation of endometrium such as decidualization, among others. Needless to mention, dysequilibrium of this highly regulated process results in pregnancy disorders of placental origin.

The eutherian placenta is also an organ of several paradoxes. For an organ that essentially performs the same basic functions across various species, it is arguably one of the most diverse organs. Placentas differ in distribution, density, and shape of chorionic villi; extent of invasion

Animal Models and Human Reproduction, First Edition. Edited by Heide Schatten and Gheorghe M. Constantinescu.
© 2017 John Wiley & Sons, Inc. Published 2017 by John Wiley & Sons, Inc.

Downloaded From Vet-eBooks.com

into maternal endometrium; and the number of placental membranes separating the maternal and fetal circulation (interhemal membranes). Following fertilization, initial development of the embryo follows a series of predicted events in all animal species. The zygote first undergoes a series of orchestrated reductive cleavage events, where every cleavage division leads to a progressively smaller totipotent blastomere cell, ultimately leading to the formation of a ball of cells called morula. Following this stage, the cells on the outside develop tight junctions, acquire sodium and water transporters that pump sodium ions and water into the embryo, respectively, and create a fluid-filled embryo called as blastocyst. Formation of the blastocyst marks the first visual cell fate decision, with trophectoderm cells on the outside committed to the placental development, and the cells on the inside (inner cell mass or ICM) committed to the development of fetus and some components of extraembryonic membranes. However, the similarities between different eutherians end here. In humans and rodents that have a highly invasive blastocyst, the embryo implants immediately following escape from the zona pellucida, invades into the uterus, and starts developing placenta. Whereas in pigs, ruminants, and other ungulate species with a shallow placenta, there is a commitment to placenta development and expansion before implantation, with no invasion or an invasion limited to superficial uterine epithelial cells. Species such as felids and canids show a placenta that is intermediate between these two types.

These differences in anatomy and histology of placenta, types of placenta, degrees of invasion, and associated diversity in the endocrinological, immunological, and metabolic exchange between fetus and mother make finding a suitable animal model for studying diseases of placental origin in humans problematic and a source of intense debate. Experimental hysterectomies in the first trimester of pregnancy are not practical in humans. Consequently, primary and immortalized human placental cells from pathological pregnancies or term pregnancies have been used as a proxy. However, *in vitro* culture systems cannot replicate the complex interactions between placental and endometrial cells. On the other hand, using primate models that have a placenta closely related to human have not been practical due to the high costs of maintenance. This chapter highlights the key differences in placentas, discusses the development and unique aspects of the human placenta, and outlines the advantages and disadvantages of existing *in vitro* cell culture and *in vivo* animal models. It also provides the reader with an appreciation of the complexity of placental biology and an array of options to better guide selection of a model for investigation.

3.2 Classification of Placenta

Similarities in placenta structure can be a way to establish phylogenetic relationships (Luckett, 1993) and has been used successfully by grouping rodents with lagomorphs and tenrecs with elephant shrews (Mossman, 1991). However, some have concluded that identifying phylogenetic relationships on these criteria is not consistent with morphological or molecular data (Mossman, 1987; D'Erchia *et al.*, 1996). Placentas have been classified in several different ways. The majority of classification systems categorize different placenta types based on morphological characteristics. These characteristics include the gross shape and distribution of the chorionic tissues interacting with the uterus, and the number of cell types separating the maternal and fetal circulations (Leiser and Kaufmann, 1994; Carter and Enders, 2004). Here we outline the two major classification systems, the first based on organ shape and the second based on the interhemal distance between fetal and maternal blood circulations.

There are four basic placental shapes that have been established: diffuse, cotyledonary, zonary, and discoid. Examples of diffuse placenta can be observed in swine and horse (King, 1993).

Downloaded From Vet-eBooks.com

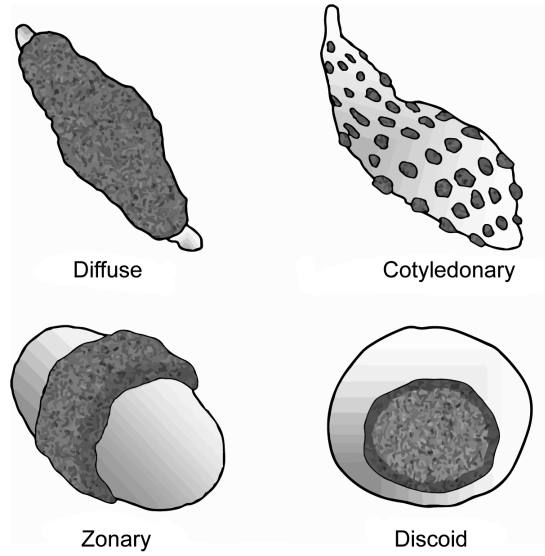

Figure 3.1 Classification of placenta based on shape. (Adapted from Furukawa *et al.* (2014).)

These placentas have chorionic villi distributed over the entire surface of the uterine lumen and, in the case of swine, are noninvasive. The chorionic villi of diffuse placentas are closely packed and convoluted, which creates an extensive surface area. This facilitates movement of diffusible molecules between the maternal and fetal circulation and also participates in the uptake of nutritional secretions from uterine glands. Ruminant ungulates (cattle, sheep, goats, and deer) possess a cotyledonary placenta. These placentas are characterized by numerous small placental cotyledons that are dense in chorionic villi and interact with uterine caruncles forming a feto-maternal exchange unit called the "placentome" (Steven and Morris, 1975). The fetal cotyledons begin to associate with maternal caruncles early in gestation and connections between these two structures are established by day 35 in ewes and day 45 in cattle. A variety of species, including carnivores, have a zonary placenta, which is named after the zone of chorion surrounding the middle of the fetus that is intimately in contact with the maternal uterus. Finally, the discoid placenta can be found in higher primates and rodents. In these animals the placenta resembles a disc with specific regions of chorion that interact with the maternal uterus and have varying degrees of invasiveness (Figure 3.1).

A second system of classification categorizes placentas based on the number of intact cell layers between fetal and maternal circulatory systems. This system was first proposed by Grosser in 1909 and 1927 (Grosser, 1909, 1927), and is described by Mossman (1987), Steven and Morris (1975), and Amoroso (1952). This classification system is generally considered more informative when considering functional differences among placental types. For example, a major role of the placenta is to maintain nutrition for the fetus and secrete factors to maintain pregnancy in the mother. The number of cell layers between maternal and fetal circulatory systems influences the diffusion rate of molecules crossing the placenta, and therefore is an important characteristic in defining placenta types (Pere, 2003; Mihaly and Morgan, 1983; Furukawa *et al.*, 2014). The four main categories in this system are epitheliochorial, synepitheliochorial, endotheliochorial, and hemochorial. The epitheliochorial placenta is the least invasive type, with both the luminal epithelium of the uterine endometrium and the epithelium of the chorionic villi of the placenta remain intact. Swine show no erosion of the luminal epithelium, whereas horse have moderate and transient invasion (e.g., chorionic girdle cells). Six cell layers

Downloaded From Vet-eBooks.com

separate the maternal and fetal circulations in epitheliochorial placentas. Ruminant ungulates possess synepitheliochorial placentas. This placenta is derived from the epitheliochorial type, with 5–6-cell types remaining intact between fetal and maternal circulatory systems. However, synepitheliochorial placentas are characterized by fusion events between trophoblast cells and uterine epithelium, which results in binucleated or trinucleated trophoblast cells. A variety of species possess the third type called endotheliochorial placenta. These species include carnivores, insectivores, some bats, and others (Carter and Enders, 2004; Mess and Carter, 2006). In this type, invading trophoblasts breach the uterine epithelium and underlying connective tissue (stroma), however trophoblasts do not directly contact maternal blood. Instead, these trophoblasts become associated with the endothelium of the maternal capillary network, which results in four cell layers between the fetal and maternal circulations. Finally, the placenta of rodents, lagomorphs, and higher primates can be categorized as hemochorial. These placentas are characterized by highly invasive trophoblasts that penetrate the maternal uterine epithelium, the stroma, and the endothelial vessels of the maternal circulatory system. All maternal tissues are eroded, which results in fetal chorion in direct contact with maternal blood. Three cell types separate the fetal and maternal blood: fetal trophoblast, fetal connective tissue (interstitium), and the fetal endothelial cells comprising the fetal capillaries. The hemochorial placenta can be further designated based on how many layers of trophoblast are present between fetal and maternal blood: hemomonochorial (primates), hemodichorial (rabbits), and hemotrichorial (mice and rats) (Figure 3.2) (Enders, 1965; Enders and Welsh, 1993; Enders and Blankenship, 1999).

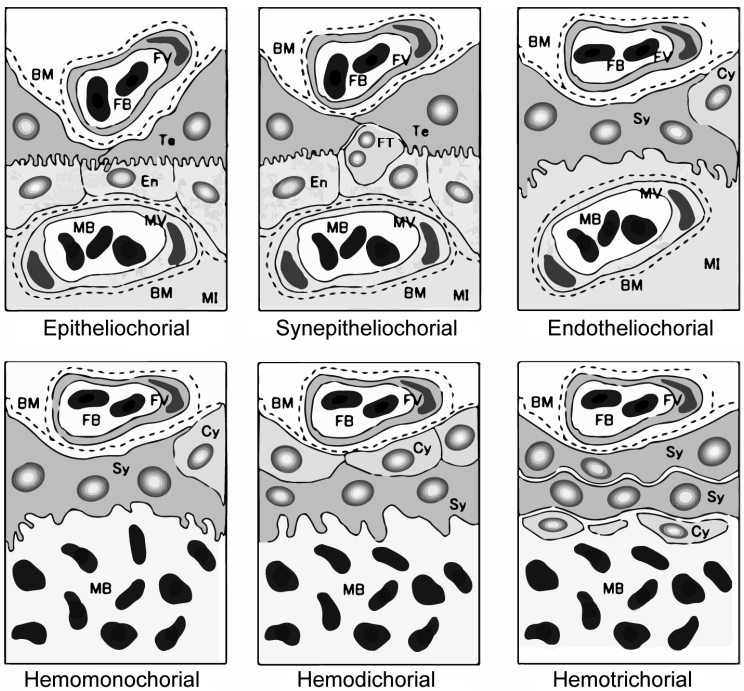

Figure 3.2 Classification of placenta type based on the number of intact cell layers between fetal and maternal circulatory systems. BM: basement membrane; Te: trophectoderm; Cy: cytotrophoblast; En: endometrium; FB: fetal blood; FV: fetal vessel; MB: maternal blood; MI: maternal interstitium; MV: maternal vessel; FT: fused trophoblast; Sy: syncytiotrophoblast. (Adapted from Furukawa *et al.* (2014).)

Downloaded From Vet-eBooks.com

3.3 Development of Human Placenta

3.3.1 Trophoblast Subtypes and Development of Functional Placenta

Many trophoblast subtypes, listed in the following sections, differentiate from the initial trophectoderm of the blastocyst. These subtypes specialize in a variety of functions, including mediating implantation, promotion of blood supply, exchange of nutrients and gases between mother and fetus, and stimulating changes in maternal physiology (Hamilton and Boyd, 1960; Cross *et al.*, 1994). Ultimately, trophoblasts give rise to the fetal portion of the placenta. Much of what is known about trophoblast cell lineage has been a result of studying murine mutants and trophoblast stem cell lines, as well as morphological study of different stages of human placentas and a limited availability of trophoblast cells derived from human term placentas.

3.3.1.1 Syncytiotrophoblast

In humans, during the very early stages of implantation (approximately by 9 days post coitum), trophoblast subtypes emerge via proliferation from the initial trophectoderm stem cell population of the blastocyst. First, the primitive syncytiotrophoblast forms around the blastocyst and invades into the maternal endometrium to form blood-filled lacunae (later intervillous spaces). These multinucleated syncytiotrophoblasts invade the luminal epithelia and underlying stroma to become completely embedded within the endometrial stroma by 7–8 days post coitum (dpc) (Enders *et al.*, 1983). Syncytiotrophoblasts grow by fusion of cytotrophoblast cells rather than nuclear division, and soon encapsulate the embryo. The primitive syncytium represents the first invasive trophoblast cell type (Knöfler and Pollheimer, 2013). Within the syncytiotrophoblast layer, intercellular spaces or lacunae begin to appear by 11 days post coitum. This stage is referred to as "lacunar stage" (Enders, 1989). Syncytiotrophoblasts invade and rupture the maternal endothelial cells comprising the endometrial capillaries, and cause the lacunae to become filled with maternal blood (Enders and King, 1991; Knoth and Larsen, 1972). Once lacunae are formed by invasive syncytiotrophoblasts, primitive cytotrophoblasts, also from the trophectoderm, proliferate, invade, and fuse with overlying syncytiotrophoblast cells to form primary villi that contact the functional maternal decidua, called the *decidua basalis*, to form anchoring villi (Castellucci *et al.*, 1990). The primitive cytotrophoblasts undergo asymmetric cell division; one daughter cell remains undifferentiated to maintain the progenitor cell pool and the other daughter cell is an intermediate between cyto- and syncytiotrophoblast (Aplin, 2010). Cytotrophoblasts that fuse to form the outermost syncytiotrophoblast layer are known as villous (nonmigratory) cytotrophoblast cells (Gude *et al.*, 2004). The cytotrophoblast cells that reach the decidual plate (contribution of the uterine decidua to the placenta) join laterally with adjacent cytotrophoblasts to create the cytotrophoblast shell. This shell attaches the embryo firmly to the maternal deciduum, and the decidual and trophoblast cells blend to form the junctional zone (Aplin, 1991). Maternal tissue that remains adhered to the placenta after delivery forms the bottom of the intervillous space and is called the basal plate, while parts of the junctional zone that remain adhered to the uterine wall after delivery constitute the placental bed (Kaufmann *et al.*, 2003).

3.3.1.2 Extravillous Cytotrophoblasts

Villous cytotrophoblasts (trophoblasts residing outside the placental villi) that come in contact with maternal decidua also differentiate into extravillous cytotrophoblasts, a distinct endocrine population. Extravillous cells that are in contact with the villous basement membrane continue to proliferate and grow into villi, while those that lose contact with the stroma undergo an epithelial-mesenchymal transition, become invasive, and are called column cytotrophoblast

Downloaded From Vet-eBooks.com

cells (Aplin, 2010; Cross *et al.*, 2003). This differentiation represents a change from proliferative to an invasive phenotype that also secretes cytokines (Wallace *et al.*, 2012). Column cytotrophoblast cells that penetrate the decidua (or placental bed) through maternal blood vessels are called endovascular trophoblasts, and eventually replace the vascular endothelium of these arteries. Early in pregnancy endovascular trophoblasts create plugs in blood vessels, resulting in a temporary hypoxic environment that is thought to influence further differentiation of extravillous trophoblasts (James *et al.*, 2006). Replacement of maternal endothelial cells and pericytes of the maternal arteries produces vascular beds that are nonresponsive to vasoactive mediators (Pijnenborg *et al.*, 1981; Lim *et al.*, 1997; Kaufmann *et al.*, 2003). The end result is a permanent widening of the endometrial arterioles, ensuring unabated supply of maternal blood to the fetus. A second set of column cytotrophoblast cells, called interstitial trophoblasts, penetrate the decidua through the uterine stroma and recruit maternal arterioles to facilitate expansion of the villi. As interstitial trophoblasts infiltrate deeper into maternal decidua, they terminally differentiate into the multinucleated placental bed giant cells (Gude *et al.*, 2004).

It is critically important for normal fetal development that maternal uterine spiral arteries are correctly remodeled. Incomplete artery remodeling by invasive trophoblasts is thought to result in an underperfused placenta, resulting in diseases such as intrauterine growth restriction and preeclampsia. The first step to maternal spiral artery invasion is induced by maternal activation of local renin-angiotensin systems, which results in lumen dilation and disorganized vascular smooth muscle. Next, endovascular trophoblasts invade arterial walls and replace maternal endothelial cells, which causes the maternal spiral arteries to undergo further dilation (Brosens *et al.*, 1967; Craven *et al.*, 1998; Hirano *et al.*, 2002; Kaufmann *et al.*, 2003). The maternal uterine arteries are adapted into large low-resistant vessels that are independent of maternal vasoconstriction and are capable of delivering an increased blood supply that is required during the second and third trimester (Figure 3.3) (Robertson *et al.*, 1967; Zhou *et al.*, 1997; James *et al.*, 2006).

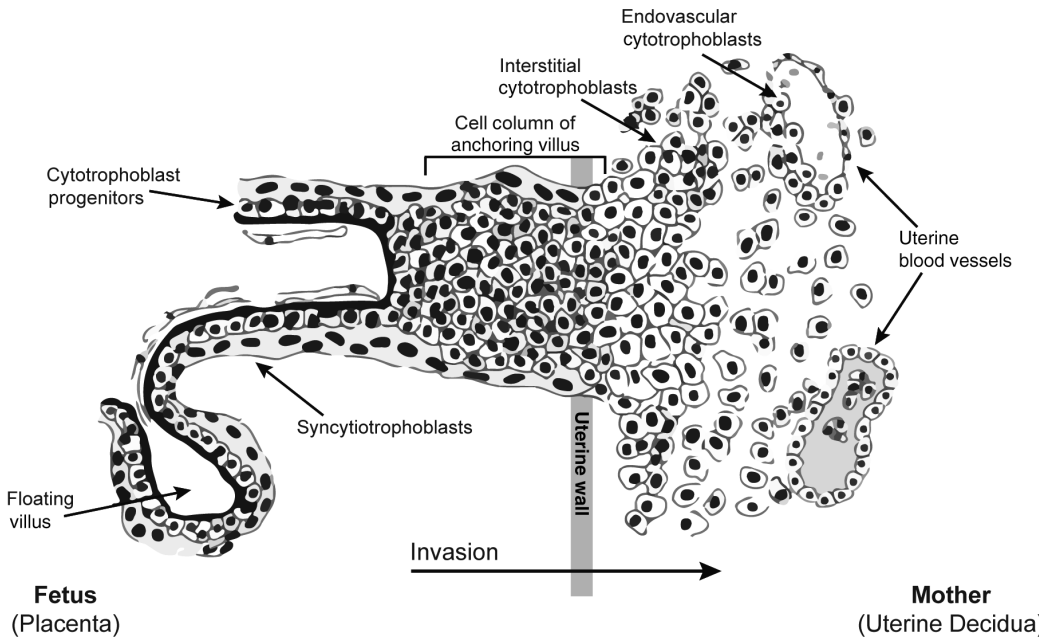

Figure 3.3 Illustration of the human fetal–maternal interface at 10–12 weeks gestation. (Adapted from Weier *et al.* (2010).).

Downloaded From Vet-eBooks.com

3.3.2 Placental Development

The villi are seen in various stages of transitional morphogenesis beginning in the third week. Primary villi consist of a core of cytotrophoblast surrounded by syncytiotrophoblast. Primary villi develop into secondary and tertiary villi throughout gestation as the villous cytotrophoblasts continue to produce daughter cells that differentiate and fuse with the overlying multinucleated syncytiotrophoblasts. Secondary villi are characterized by the invasion of mesenchymal cells from the extraembryonic primitive mesoderm that arises from the primitive streak and a vascular network ensues thereafter (Jones and Fox, 1991). This penetration of mesoderm enlarges the secondary villus, which grows toward the decidua. By the end of the third week, angiogenesis and vasculogenesis begins in core mesodermal cells of the secondary villi, transforming them into tertiary villi (Kaufmann, 1985; Castellucci *et al.*, 1990). Terminal villi, called chorionic villi, form areas of vasculosyncytial membrane that bring the fetal and maternal blood circulations in close proximity (1–2 μm barrier) to each other, which enables oxygen exchange (Burton and Tham, 1992).

With the completion of development of terminal villi and the establishment of a functional vascular network by the second month, the interhemal membrane consists of a continuous layer of syncytiotrophoblast and an underlying single layer of cytotrophoblast cells overlying the endothelial cells of fetal blood vessels. The placenta at this stage can therefore be called a hemodichorial-type placenta. By the fourth month, however, the cytotrophoblast cells become dissociated from each other and leave the syncytiotrophoblast layer as the only barrier between the maternal blood and the endothelial cells of the fetal vessels. The placenta at this stage is referred to as hemomonochorial type. The syncytial trophoblast layer becomes progressively thin as pregnancy advances further. The syncytiotrophoblast overlying the villi frequently break off, forming multinucleate syncytial knots, and can enter the maternal circulation through the intervillous space (Covone *et al.*, 1984).

The developed human placenta is composed of three major layers; the extravillous cytotrophoblasts make up the outermost layer, then column cytotrophoblasts, and finally the innermost layer consists of the chorionic villi. In the early weeks of development, the chorionic villi are distributed throughout the entire surface of the chorion. Later, they become confined to the region of greatest blood supply in the embryonic pole or antimesometrial area, thereby forming a discoid-shaped placenta. Expanding villi in the embryonic pole are referred to as *chorion frondsum* or bushy chorion. By the third month, the villi on the rest of the chorionic surface degenerate, forming a smooth chorion or *chorion leave*.

3.3.3 Development of Fetal Membranes

Following blastocyst formation, endoderm cells arising from the ICM spread along the inner surface of the trophectoderm, eventually lining the blastocoelic cavity. This creates a bilaminar structure, which results in the formation of the yolk sac cavity that is bound by extraembryonic endoderm and trophoblast. In week 2, mesodermal tissue arising from embryonic ectoderm creates a mesoderm trophoblast combination outside the embryonic disc called the chorion, and a mesoderm extraembryonic endoderm combination called the yolk sac. A blood supply soon develops in the mesoderm tissue associated with the yolk sac. This so-called yolk sac placenta is the first exchange system between the mother and the fetus. Initially the yolk sac placenta is in contact with the trophectoderm and forms a trilaminar membrane, later in development the yolk sac is displaced by the growing allantois, which projects into a space between called the exocoelom. The allantois comes into contact with the chorion, becomes vascularized, and creates the umbilical vessels. This results in the establishment of the chorioallantoic placenta.

Downloaded From Vet-eBooks.com

In humans, the yolk sac placenta, as it is known in other species, is never completely formed and instead a secondary yolk sac is formed due to the collapse of the bilaminar yolk sac. This results in a small portion of the original yolk sac continuing as a free yolk sac but begins to degenerate around 9 weeks gestation (Freyer and Renfree, 2009). This series of events results in four extraembryonic membranes found in eutherian embryos, namely, the chorion, amnion, yolk sac, and allantois.

The chorion becomes the outermost tissue, and consists of the trophoblast cell layer associated with maternal decidua and underlying mesenchyme. This tissue is in direct contact with maternal tissues and is the primary membrane involved in nutrient, gas, and waste exchange between the fetus and the mother. It is also involved in maternal immune suppression and hormone synthesis and secretion. The amnion is derived from the folding of chorion tissue and is the innermost membrane, initially in direct contact with the embryo. In humans, after 4–5 weeks of gestation, amniotic fluid accumulates within the membrane and creates the amniotic sac. The amniotic fluid plays a vital role in the homeostasis of the embryo; it provides nutrients, physical protection by cushioning the embryo from sudden movements, and allowing space to grow, as well as maintaining temperature. The yolk sac is attached to the ventral side of the embryo and is a derivative of endoderm. In macrolecithal embryos, the yolk sac is the main source of nutrition but in mammals the yolk sac is transitory. In humans, the yolk sac is incorporated into the primordial gut during the fourth week of gestation and is replaced by a definitive chorioallantoic membrane. In other mammals, such as rodents, the yolk sac persists alongside a chorioallantoic placenta. Despite its transient nature, the yolk sac is a critical part of the development of the mammalian embryo. In most eutherians, during early pregnancy the yolk sac is the sole provider of blood cells to the embryo. Precursors of blood cells are produced elsewhere but undergo differentiation in the yolk sac (Palis and Yoder, 2001). The first establishment of maternal–fetal

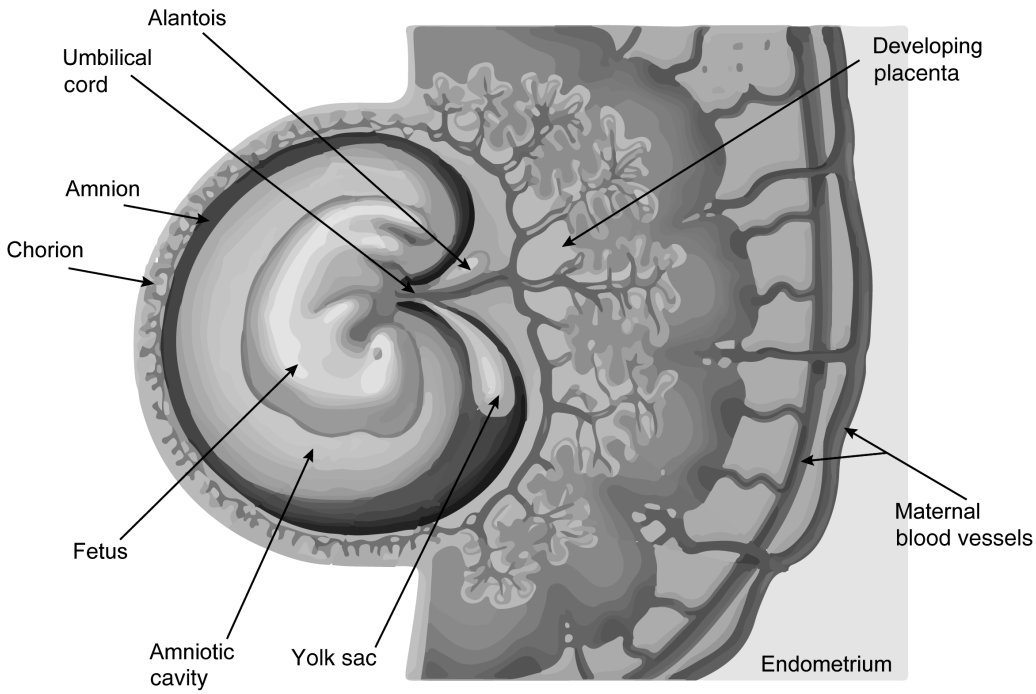

Figure 3.4 Early human conceptus.

Downloaded From Vet-eBooks.com

nutrient and gas exchange depends on the vasculogenesis and angiogenesis initiated by the yolk sac. Even in humans, where the yolk sac degenerates early and does not connect to the uterus, the yolk sac provides the only source of blood cells in the first couple weeks of gestation and is the main site of erythropoiesis from weeks 3–6 (Palis and Yoder, 2001; Tavian and Peault, 2005). The human yolk sac appears to have an important role in the transfer of substances such as iron and folic acid in the early weeks of embryo development (Gulbis *et al.*, 1998; Jauniaux *et al.*, 2007). The fourth fetal membrane, the allantois, begins as an endodermally derived vascular evagination from the ventral surface of the hindgut and contributes to the vascular mesenchyme of the chorioallantoic placenta. It is critical for fetal–maternal exchange that the blood vessels of the allantois become the umbilical arteries and vein (Figure 3.4).

3.4 Modeling Placental Development and Diseases of Placental Origin

3.4.1 In Vitro Cell Models

Experimental embryology and discovery of novel culture methods have advanced our ability to understand the development of placenta and disease pathways. *In vitro* systems that can mimic early pregnancy events in human can be useful tools for studying placental development. However, there has been limited success in establishing reliable human placenta cell lines. As an alternative, immortal lines from placental trophoblast-derived tumors have been used and although limited, trophoblast subtype cell lines from human term placentas and some earlier term placentas have also been used. Additionally, the establishment of human embryonic stem cell lines derived from blastocysts has produced a variety of techniques used to induce differentiation to trophoblast lineage from these lines. Each of these *in vitro* systems has inherent advantages and disadvantages but ultimately give a closer look at how human trophoblasts most likely develop *in vivo* and develop into a functioning placenta.

3.4.1.1 Choriocarcinoma-Derived Trophoblast Cell Lines

Human choriocarcinoma-derived trophoblast cell lines, such as BeWo, Jar, and JEG3M, and primary trophoblast culture mostly derived from term pregnancies have been used with some success to study trophoblast lineage development. A major disadvantage of these cell lines is that they can only be used to tell a small part of the story. They are composed of already committed trophoblast cells, and consequently lineage decisions cannot be observed. Due to their tumor cell origins, choriocarcinoma-derived trophoblast cell lines behave differently than primary trophoblasts by proliferating and invading at an increased rate. Their exact place in the trophoblast lineage is also unclear. However, they do share some useful characteristics with primary trophoblast lines. They can fuse to produce syncytial cells, and can invade through artificial connective tissue matrix. In a comparative study it was found that BeWo cells resemble normal trophoblasts more closely than do Jar and JEG3M cells due to the inverse relationship between invasiveness and differentiation it shares with primary trophoblasts (Hohn *et al.*, 1998). BeWo cells were established from choriocarcinoma specimens cultured on human decidual tissue from the endometrium of a normal pregnancy. Cells displaying characteristics of trophoblast tissue culture emerged from these specimens, including characteristic hormone chorionic gonadotropin production, which is indicative of undifferentiated trophoblast cells (Pattillo *et al.*, 1968). BeWo cells have been used to study the role of VEGF in cytotrophoblast differentiation (Charnock-Jones *et al.*, 1994), IgG transport across the placenta (Ellinger *et al.*,

Downloaded From Vet-eBooks.com

1999), and syncytiotrophoblast formation in different oxygen environments (Kudo *et al.*, 2003). Primary trophoblast cell culture and cultured explants from term placenta have been used to study cytotrophoblast differentiation (Genbacev and Miller, 2000), and trophoblast invasion (Aplin, 2006). Despite successful establishment of permanent trophoblast stem cell lines in the mouse, trophoblast stem cells from humans have yet to be isolated and cultured (Tanaka *et al.*, 1998; Roberts and Fisher, 2011). Primate trophoblast stem cells have been generated from outgrowths of Rhesus monkey blastocysts, but due to the expression of chorionic gonadotropin and concomitant absence of CDX2 expression, these cells may not actually be trophoblast stem cells, but instead represent a differentiated state (Vandevoort *et al.*, 2007; Roberts and Fisher, 2011).

3.4.1.2 Trophoblast Cells Derived from Human Embryonic Stem Cells

Recently, human embryonic stem cells (hESC) have shown potential as an alternative *in vitro* model to study early trophoblast differentiation events (Thomson *et al.*, 1998; Schulz *et al.*, 2008). hESC in culture can proliferate without a known limit and can differentiate into all three embryonic germ layers as well as extraembryonic tissues. This is especially valuable in the study of human trophoblast lineage development and function. hESCs cultured in unconditioned media will spontaneously differentiate and result in a mixed population of cells of mesoderm and trophectoderm lineage (Thomson *et al.*, 1998). These stem cells can also be stimulated to differentiate into the trophoblast lineage by knocking down pluripotency genes, by culturing into embryoid bodies to promote spontaneous differentiation to trophoblast (Harun *et al.*, 2006), or by culturing the stem cells on an attachment substrate and treating with BMP4 (Schulz *et al.*, 2008; Xu *et al.*, 2002).

Knockdown of POU5F1 and NANOG Expression

Knockdown of expression of pluripotency transcriptional regulators, *POU5F1* and *NANOG*, using various approaches, has revealed their potential roles in trophectoderm differentiation and provided a route to establishing putative trophoblast cell lines. Knockdown of *POU5F1* expression via RNAi followed by culturing in the absence of FGF2 leads to trophectoderm differentiation (Matin *et al.*, 2004; Hay *et al.*, 2004). Alternatively, transfection of double-stranded RNAs targeting *NANOG* results in significant downregulation of *NANOG* and *POU5F1*, and ultimately trophectoderm specification (Hyslop *et al.*, 2005). Gene knockdown via *POU5F1* and *NANOG* RNAi lentiviral vectors have also been used successfully in hESCs to stimulate differentiation resulting in cells that have upregulation of trophoblast markers and trophoblast morphology (Zaehres *et al.*, 2005). However, purification of these putative trophoblast cells and characterization has not been fully accomplished and therefore may not be useful for all types of studies.

Trophoblasts Derived from hESC Embryoid Bodies

A second approach to stimulate differentiation to the trophoblast lineage is by culturing hESC-derived embryoid bodies (EB). hES cells cultured in suspension and in the absence of FGF2 and feeder cells are capable of forming spherical aggregates called embryoid bodies. These hESC-derived embryoid bodies form all three embryonic germ layers and can form a central cavity (Itskovitz-Eldor *et al.*, 2000). Additionally, transplanting embryoid bodies to matrigel drops, which mimic extracellular matrix, causes outgrowths of trophoblast-like cells that secrete hCG (Gerami-Naini *et al.*, 2004). Furthermore, mononulcear suspension of the trophoblast-like outgrowths respond to 8-bromo-cAMP treatment with an increase in hCG production, another hallmark characteristic of trophoblast cells (Strauss *et al.*, 1992). These methods have been used to derive cytotrophoblast cell lines that have the capacity to differentiate into various trophoblast cell types, including syncytiotrophoblast and extravillous cytotrophoblast (Harun *et al.*,

Downloaded From Vet-eBooks.com

2006). EBs containing trophoblast cells were selected based on high concentrations of hCG production. They were disaggregated and then reaggregated in trophoblast stem cell medium, and cytotrophoblasts populations were determined via immunostaining for cytokeratin and hCG (Harun *et al.*, 2006). Another approach based on cell adherence has also been used to derive trophoblast lines from hESC embryoid bodies. In this approach, hES cell colony fragments were cultured in feeder-free semisolid methylcellulose medium, which caused spontaneous formation of cystic EBs after 5–7 days. After 2 weeks, an adherent cell layer formed on the surface of the culture dish, which showed expression of endothelial markers, PECAM-1 and VE-cadherin, suggesting formation of a trophoblast layer with an endothelial network at the surface (Peiffer *et al.*, 2007).

BMP-Treatment of hESCs

Finally, BMP4 treatment of hESCs appears to be the most promising method to derive trophoblast cells but remains poorly understood. When treated with BMP4, hESCs will differentiate to trophoblast derivatives as evidenced by morphology, expression of trophoblast markers, and the presence of high concentrations of placental hormones (Xu *et al.*, 2002). After five days of treatment, hESC colonies express trophectoderm genes such as *KRT7*, *CGA*, *CGB*, and *IGFBP3* (Schulz *et al.*, 2008). When colonies are dissociated and plated at low density, treatment of BMP4 results in cells fusing to form multinucleated cells that resemble syncytiotrophoblast (Xu *et al.*, 2002). There has been some controversy as to whether treating hESCs with BMP4 really does stimulate differentiation into trophoblast only. Some have argued that differentiation promoted by BMP4 treatment results in mostly mesoderm (i.e., primitive streak) cell lineage (Amita *et al.*, 2013; Roberts *et al.*, 2014). It has been shown that along with the presence of BMPs, the absence of FGF2 is required for differentiation to trophoblast. In the presence of both FGF2 and BMP4, FGF2 acts through the MEK-ERK pathway to maintain *NANOG* levels and induces differentiation to mesendoderm (Yu *et al.*, 2011). Additionally, it has been reported that BMP treatment only infrequently induces trophoblast differentiation, instead results in extraembryonic endoderm formation (Pera *et al.*, 2004) and expression of select mesodermal genes (Bernardo *et al.*, 2011; Drukker *et al.*, 2012). However, the variability in the results from these studies may reflect the diversity in hESC lines used, culture conditions, and analytical approaches (Golos *et al.*, 2013). A recent breakthrough has revealed that hESC differentiation to mesoderm and trophoblast lineages is actually controlled by the induction of endogenous WNT expression stimulated by BMP4 treatment. The use of WNT3A alone is sufficient to induce mesoderm differentiation, and BMP4 treatment along with a WNT inhibitor limits differentiation to trophoblast only (Kurek *et al.*, 2015). This suggests that using a combination of BMP4 and WNT inhibitor will result in a homogenous population of trophoblast progenitors, which can be used for *in vitro* studies that rely on a purified trophoblast cell population. Using hESCs is a particularly valuable tool for understanding early pregnancy events in humans, but due to ethical boundaries confirming *in vitro* results *in vivo* is impossible. For example, BMP4 can induce differentiation to trophoblast *in vitro* but this has not been demonstrated *in vivo* in any mammal (Xu *et al.*, 2002).

3.4.1.3 Placental Explant Culture

Although primary cytotrophoblast cultures from term placenta are used for routine investigation and yield important insights into differentiation into syncytiotrophoblast cells and studying affects of environmental factors, purity of the isolates from placental preparations cannot always be guaranteed, and the resulting cells have limited life span in culture. Additionally, there are concerns that the pathological cells revert to their "normal" status when cultured and when removed from *in vivo* stressors, limiting their value. Finally, the cells isolated from their native

Downloaded From Vet-eBooks.com

environment lack the complex interactions and feedback from the decidual cells, the latter of which is expected to influence their physiology. For these reasons, explant cultures of the whole placenta or primary villi from term placenta have been widely used to replicate native interactions of the maternal–fetal interface, and to study placental transport, metabolism, and endocrine function. Several adaptations of placental explant culture have been described, including perfusion of the whole organ or a single cotyledon, co-culture of villi with decidual implants, culture of placental slices on artificial substratum, to name a few. Arguably, perfusion of the whole placenta closely mimics the *in vivo* system, as it retains complexity of the organ in its native form (Schneider, 1991; Bajoria *et al.*, 1997). However, the limitation here is that whole placenta from first trimester pregnancies is rarely available, and those from pathological specimens, such as from systemic lupus, are less than ideal for investigation. As a proxy, explant cultures of primary villi and decidual tissue have been used to replicate the interaction of primary trophoblast cells with decidual cells and their differentiation *in vitro*. Earliest studies have been used successfully to measure oxygen consumption (Villee, 1953; Hellman *et al.*, 1950), transport of amino acids (Tremblay *et al.*, 1965; Sybulski and Tremblay, 1967; Litonjua *et al.*, 1967), and cytotrophoblast differentiation (Fox, 1970; Genbacev *et al.*, 1992). Subsequently, enzymatic function, xenobiotic metabolism, and molecule transport have been evaluated in human explants (Barnea *et al.*, 1993; Kay *et al.*, 1997). The system, however, has found greater utility in investigating mechanisms associated with postimplantation events such as proliferation and differentiation of extravillous cytotrophoblast, reconstitution of cell columns and interactions with the extracellular matrix, and invasion into decidual tissue (Genbacev *et al.*, 1992; Vicovac *et al.*, 1995; Dunk *et al.*, 2003). The main advantage of this system is that trophoblasts are co-cultured with cell types from their natural environment; however, this also limits ability to monitor the function and activities of individual cell types. Needless to say, the explant culture continues to be a useful tool for investigating villous trophoblast proliferation, differentiation, and invasion, and for investigating interactions with decidual and environmental factors. One caution is to infer results to age-matched placentas, as explants from different stages of pregnancies are expected to be heterogeneous.

3.4.2 Animal Models

3.4.2.1 Mouse

Extensive genetic and morphological details of trophoblast lineage specification have been discovered in the mouse, using trophoblast stem cell lines, as well as gene knockout studies that have revealed specific phenotypes associated with placental pathologies. There is an obvious advantage to using rodents as animal models due to their small size, short generation time, and extensive genetic engineering resources. From a phylogenetic view point, rodents and lagomorphs are a sister group to primates and both belong to the same superorder, suggesting a possibly strong evolutionary relationship (Mess, 2014). There is a wealth of knowledge about the development and function of the mouse placenta from both genetic and physiological perspectives. Studying the mouse and other small mammals does not have the same limitations as those found in using nonhuman primates or human tissue, and as such the mouse is one of the best studied animal models for placentation.

Comparative Anatomy

The placentas of both mouse and human are discoid in shape and are categorized as hemochorial type. The fetal–maternal interaction facilitated by the placenta is similar between the mouse and humans. There are three distinct features that emerge in the definitive placentas of both mouse and human, and despite having different names, there is evidence that these three

Downloaded From Vet-eBooks.com

features have analogous functions (Georgiades *et al.*, 2002). The first region: the fetal placenta in humans and labyrinth in mouse is characterized by the presence of both maternal and fetal blood channels that allow for nutrient and gas exchange. In this region, the trophoblasts of the chorionic villi are directly bathed in maternal blood (therefore, hemochorial), a characteristic found in both the human fetal placenta and the mouse labyrinthine zone. However, in mouse the trophoblast portion of the labyrinthine interface consists of three layers (hence, hemotrichorial), while in human the fetal placenta interface consists of only one layer of trophoblast (hence, hemomonochorial). This difference may affect fetomaternal exchange processes. Second, the basal plate/cytotrophoblastic shell in humans and junctional zone/spongiotrophoblast zone in mice is a region that neighbors the maternal surface of the fetal placenta/labyrinth and exclusively contains maternal blood vessels. The third region that has analogous function is the uterine tissue of the mother that surrounds the basal plate/junctional zone. Trophoblasts derived from embryo tissue invade the maternal uterine tissue, with the depth of invasion being much shallower in mice as compared to humans. Trophoblast cells of the human placenta invade the decidualized maternal endometrium and further into the underlying myometrium to completely remodel maternal spiral arteries, whereas mouse trophoblasts invade only into the decidua (Pijnenborg *et al.*, 1981; Georgiades *et al.*, 2002). These differences make the mouse model less desirable for specific studies of trophoblast invasion and vascular remodeling. Additionally, unlike in humans, the rodent yolk sac placenta persists for the full length of gestation and plays a crucial role alongside the chorioallantoic placenta. In addition to the structural and functional differences, it has been argued that the brief gestation period of murine rodents is not conducive to studying events needed to sustain a 9-month pregnancy as in humans (Mess, 2014). Instead, murine rodent models may be best suited for studying early molecular events in placentation and not later events in human pregnancy such as placental pathologies that develop over time.

3.4.2.2 Placenta-Specific Gene Manipulation Tools in Mouse

In order to understand the molecular function behind placenta specific developmental processes as well as placental pathologies, certain gene manipulation methods can be performed in mice that limit confounding effects from embryonic gene functions. Although the current methods have limitations, the use of chimeras and transgenics has opened up a lot of possibilities in how placenta biology can be investigated.

Chimeras

Early embryonic cells are not restricted in their lineage contribution. Therefore, it is possible to create chimeras by combining blastomeres from cleavage stage embryos (2–8-cell stage). At this stage, blastomeres from both contributing embryos have the potential to contribute to both embryonic and extraembryonic lineages. Chimeras can also be created by aggregating embryonic stem cells with early embryonic blastomeres. In this case, ES cells are more constricted in their lineage contribution and will not contribute to the primitive endoderm or trophectoderm. Using this approach one can determine the lineage-specific affects of a mutation by combining a mutant embryo with wild-type ES cells (the trophectoderm will be mutant) or a wild-type embryo with mutant ES cells (the trophectoderm will be wild type) (Tam and Rossant, 2003). A drawback to this method, however, is that in each case the embryo will still be a mixture of mutant and wild-type cells, a result that would not be useful in many cases. A variation of this can be performed by combining tetraploid embryos with diploid ES cells. In this case the tetraploid embryo will mainly give rise to the extraembryonic primitive endoderm and trophectoderm, and the ES cells to the embryo. This method has been used with some success, but restriction of tetraploid cells from the fetus is not always complete, which may lead to

Downloaded From Vet-eBooks.com

inconclusive or false results. Eakin *et al.* (2005) found that tetraploid cells contribute consistently to embryonic ectoderm and the tetraploid cells may persist into midgestation (Chu *et al.*, 2011). This result suggests that using tetraploid embryos is not a reliable way to show rescue of an embryonic lethal phenotype. Finally, chimeras can also be created by injecting trophectoderm stem cells into blastocysts (Takahashi *et al.*, 2006). The TS cells will contribute exclusively to the trophoblastic lineage and not the primitive endodermal lineage. Mutant TS cells can be combined with wild-type embryos to discern the origin of complex phenotypes that may or may not be the result of dysfunction in the extraembryonic tissues.

Placenta-Specific Promoters for Transgene Expression

Placenta-specific gene manipulation can also be achieved by producing transgenic mice that use trophoblast specific promoters to drive expression of a transgene construct. Several placenta-specific promoters have been identified that are active in various trophoblast subtypes and at various developmental time points. For example, the *Tpbpa* promoter has been used to drive expression of GFP (Simmons *et al.*, 2007). This gene is expressed at E7.5 in mice exclusively in the ectoplacental cone and later in the junctional zone (Calzonetti *et al.*, 1995). This promoter was also used to ablate all *Tpbpa*-positive cells, which include certain trophoblast giant cells and glycogen trophoblast cells, by driving expression of Cre recombinase to activate expression of a cytotoxin (Hu and Cross, 2011).

Despite the lack of a rodent orthologue, the upstream locus control region of the human gene *human chorionic somatomammotrophin* (*hCS*) has been successfully used to drive transgene expression exclusively in rodent syncytiotrophoblast (Jin *et al.*, 2009; Su *et al.*, 2000). Another gene that encodes the purine-catabolizing enzyme adenine deaminase (ADA) is active in all trophoblast subtypes and a 770-bp region upstream of the gene is able to drive expression of a reporter construct in all cell types in the placenta (Winston *et al.*, 1992; Shi *et al.*, 1997). For a complete review, refer to Renaud *et al.* (2011).

Lentiviral Transduction of the Trophectoderm

Lentiviruses are a subset of retroviruses that are able to transduce both dividing and nondividing cells and deliver RNA that is subsequently transcribed to complementary DNA and stably integrated into the genome of the host cell and transmitted to the host cells progeny. Lentiviral gene transfer can be successfully performed in murine ES cells and into preimplantation mouse embryos (Pfeifer *et al.*, 2002; Ikawa *et al.*, 2003). Lentiviral gene transfer can also be specified to the placental lineage by simply immersing a zona-free blastocyst into a solution containing lentivirus. The lentivirus is only able to penetrate the outer-most cell layer, the trophectoderm, which shields the ICM from being transduced (Okada *et al.*, 2007; Georgiades *et al.*, 2007). Okada *et al.* (2007) were able to use this method to rescue previously embryonic lethal phenotypes by causing ectopic expression of the deficient gene in the placenta. This lentiviral transduction system has also been used to deliver short hairpin-RNA (shRNA) to target and silence genes in the trophectoderm, which shows there is the potential to create loss-of-function phenotypes specific to the placenta (Georgiades *et al.*, 2007; Lee *et al.*, 2009). Additionally, trophectoderm lentiviral transduction has been used to deliver Cre recombinase transgenes to embryos that already contain floxed genes (Georgiades *et al.*, 2007; Morioka *et al.*, 2009). This method has proved to be a robust way to create placenta-specific knockouts, with the only limitation being the availability of a transgenic mouse containing loxp sites around the gene of interest. Furthermore, Fan *et al.* (2011) demonstrated that the lentivirus can be used to deliver a firefly luciferase transgene to the trophectoderm. Once the embryos are transferred into surrogate females, bioluminescent imaging can be used to noninvasively track the placenta-specific gene expression as the embryos develop.

Downloaded From Vet-eBooks.com

3.4.3 Alternative Animal Models

3.4.3.1 Guinea Pig

The guinea pig, in some respects, may actually be a better non-rodent model for the study of human placentation. First, the gestation in guinea pig is relatively long and produces precocial young, in contrast to short gestation periods and altricial young in mice. This means the hemochorial placenta found in guinea pigs must sustain the embryo through more advanced developmental stages, a process that is more analogous to human pregnancy. This could lend to more reliable studies of late stage pregnancy events due to the requirement of the placenta to maintain fetal–maternal exchange over a longer period of time and the potential for pathologies to develop. Second, both the guinea pig placenta and human placenta are categorized as hemomonochorial, meaning that there is only one layer of trophoblast (to be specific, syncytiotrophoblast in both) that separates maternal blood from fetal blood in the fetal placenta/labyrinth zone. The basal plate in humans is analogous to the junctional zone in guinea pigs, and both human and guinea pig trophoblasts invade through the decidua and into myometrium of the uterus. Likewise, the fetal placenta in humans is analogous in function to the labyrinth in guinea pig. In both species, maternal blood-filled spaces are lined with embryo-derived syncytial trophoblasts called intervillous spaces in humans, and maternal blood channels or lacunae in guinea pigs. In contrast to humans, guinea pig placentas possess a unique structure called the subplacenta, which consists of extravillous trophoblasts that invade deep into the decidua and transform maternal arteries. This feature can be compared with the cytotrophoblasts columns of the human placenta, which are also the source of extravillous trophoblasts (Mess, 2014; Mess *et al.*, 2007). However, unlike humans but similar to other rodents, the guinea pig has a yolk sac placenta that persists and functions alongside the chorioallantoic placenta until term (Perry, 1981; Jollie, 1990).

The guinea pig is an established model for studying placental transfer. Since the guinea pig placenta is hemomonochorial like the human placenta, the fetal–maternal transport barrier is very similar. The guinea pig model has been used for investigating nutrient and hormone transfer, parasite and bacterial transfer, as well as transfer of radioisotopes, to name a few (Levack *et al.*, 2002; Jansson and Persson, 1990; Flori *et al.*, 2003). Fetal growth restriction models have also been created in guinea pig via uterine artery ligation and maternal nutrient restriction (Lingas *et al.*, 1999; Lafeber *et al.*, 1984). The guinea pig genome has been sequenced, but unfortunately there is still a lack of genetic tools in this species.

3.4.3.2 Rabbit

The rabbit is one of the most widely used experimental mammals after mice and rat. The rabbit has a hemodichorial placenta, that is, there are two layers of trophoblast cells between the maternal and fetal blood. Since the human placenta has more/variable trophoblastic epithelial layers early in pregnancy, this may be useful for placenta studies investigating early human pregnancy events. A distinguishing feature of rabbit placentation is the development of a thin lamina of uninucleated decidual cells adjacent to the myometrium in the decidua basalis at term (Mossman, 1987). Due to its relatively large size as compared to other rodents, fetal and placental growth can be monitored in the rabbit using ultrasound equipment (Chavatte-Palmer *et al.*, 2008; Polisca *et al.*, 2010). Blood flow has been monitored this way in an induced intrauterine growth restriction model in the rabbit (Eixarch *et al.*, 2009) and in the vascularization of rabbit placenta (Fischer *et al.*, 2012). Intrauterine growth restriction can be induced via uterine artery ligation, but is also naturally occurring in rabbits. Rabbits have large litters, which invariably causes growth restriction in pups that are in the middle of the uterine horn. These runts are further away from the blood supply coming from the ovarian and cervical ends leading to a natural occurrence of growth restriction (Swanson and David, 2015).

Downloaded From Vet-eBooks.com

3.4.3.3 Sheep

The sheep has been a popular animal model for the study of maternal–fetal interactions. Sheep are amenable to invasive procedures, and are able to maintain surgically placed catheters in both the maternal and the fetal vasculature. This allows for multiple samplings from both the maternal and fetal side of the placenta (Meschia *et al.*, 1965; Battaglia *et al.*, 1968). This makes the sheep an attractive alternative to rodent models for the investigation of placental and fetal physiology *in vivo* over a length of time (Barry and Anthony, 2008). However, the sheep placenta is quite different in structure to the human placenta. The sheep placenta is classified as synepitheliochorial, which signifies the presence of a feto–maternal syncytium and the persistence of a maternal epithelium at the fetal–maternal interface (Wooding, 1992). It is also a polycotyledonary placenta with 70–100 concave cotyledons. Cotyledons are the fetal portion of the placentomes; the maternal portions are called caruncles. In these placentomes, fetal trophoblast cells intertwine with the uterine endometrium. Furthermore, unique binucleated trophoblast cells fuse with uterine epithelial cells in the caruncle space, which represents the extent of invasive implantation in ruminant ungulates. Sheep also possess multiple-branched villi that may be analogous to the branched villi in the human placenta in that they branch into intermediate and terminal villi (Barry and Anthony, 2008).

3.4.3.4 Nonhuman Primates

Nonhuman primates are the closest relative to humans, so it is not surprising that much of the placental morphology, function, and development resemble human placenta biology. However, there are still significant differences and limitations to consider. The great apes (which include gorillas, orangutans, and chimpanzees) and Old World monkeys (which include baboons and rhesus macaques) are more similar in placentation to humans than are New World monkeys. The implantation of all great ape placentas occurs interstitially as in humans. This results in a single discoid-shaped placenta and is categorized as hemomonochorial. Old World monkeys, which are more commonly used for placentation studies, also have hemomonochorial placentas with similar villous structure as compared to humans. A key similarity in both orders is that extravillous trophoblasts remodel maternal spiral arteries (Enders, 1997; Blankenship and Enders, 2003). However, important differences emerge; extravillous trophoblasts in Old World monkeys do not invade interstitially as they do in humans and invasiveness is much shallower, only reaching to the decidua. This difference is important when studying placenta disorders because when there is shallow trophoblast invasion in humans this leads to conditions such as preeclampsia and fetal growth restriction, however this shallow invasiveness is normal in Old World monkeys and does not cause these conditions. In opposition to this, there have been reports of the natural occurrence of preeclampsia in both Old World Monkeys and great apes, which is sometimes seen as a disease unique to humans (Palmer *et al.*, 1979; Stout and Lemmon, 1969). Furthermore, a model in which uteroplacental ischemia was induced via uterine artery ligation in baboons resulted in preeclamptic-like symptoms, which included similar renal pathology, and elevated levels of soluble FLT-1 (Makris *et al.*, 2007). Additionally, the differences in implantation between human and Old World Monkeys result in differing endometrial reactions. The superficial implantation in the rhesus macaque results in proliferation of surface uterine epithelium, which forms an epithelial plaque (Enders *et al.*, 1985). This feature is not seen in human placentation, instead interstitial implantation leads to the formation of a pronounced decidua, which is defined as endometrial stromal cell differentiation. Ultimately however, these two implantation strategies both allow for early and direct access to the maternal circulation, which provides critical feto–maternal exchange (Wooding and Burton, 2008). Unfortunately, there are practical limitations to using these models as well, including long gestational periods and high cost of maintenance (Table 3.1).

Downloaded From Vet-eBooks.com

Table 3.1 Comparison of animal models for the study of placentation MSA: maternal spiral arteries.

	Human *(Homo sapien)*	Mouse *(Mus musculus)*	Guinea Pig *(Cavia porcellus)*	Rabbit *(Oryctolagus cuniculus)*	Sheep *(Ovis aries)*	Rhesus Macaque *(Macaca mulatta)*
Implantation type	Interstitial	Eccentric	Interstitial	Fusion	Centric	Interstitial
Implantation time (post coitum)	9 days	4 days	5–6 days	6–7 days	17–18 days	8–9 days
Placental shape	Discoid	Discoid	Discoid	Discoid	Cotyledonary	Bidiscoid
Interhaemal barrier	Hemomonochorial	Hemotrichorial	Hemomonochorial	Hemodichorial	Synepitheliochorial	Hemomonochorial
Gestation	280 days	20 days	65 days	31 days	152 days	164 days
Trophoblast invasion of MSA	Deep, reach myometrial vessels	Shallow, limited to proximal decidua	Extensive, reach the perimetrial surface of the uterine wall	Deep, reach myometrial vessels	None, trophoblasts fuse with uterine cells in the caruncle space	Shallow-deep, reach maternal decidua
Feto–maternal exchange site	Villi	Labyrinth	Labyrinth	Labyrinth	Villi	Villi
Advantages	• The best model to study human placentation is the human, but with few exceptions human tissue cannot be used	• Many genetic tools • Amenable to embryonic manipulations • Early trophoblast development is similar to human	• Placentation is very similar to humans • Gestation time is relatively long and pups are born precocial as in humans	• Natural IUGR model	• Amenable to invasive procedures	• Closest relative to humans evolutionarily, and very similar placentation and pregnancy
Disadvantages	• Little to no available tissue • Tissue that is available is of suboptimal quality or of pathological origins	• Placental structures and function differ from human • Gestation is much shorter and pups are born altricial	• Little to no genetic tools available, however the genome has been sequenced and annotated	• Little to no genetic tools available, however the genome has been sequenced and annotated	• Very different placentation as compared to humans	• Shallow trophoblast invasion • Practical limitations such as long gestation time and high cost of maintenance
Recommendation for use	• Human study is limited to human-derived cell lines and limited term placental tissue	• Preimplantation embryo events including trophoblast differentiation	• Trophoblast invasion and maternal artery remodeling studies • Study of late pregnancy events	• IUGR studies • Study of early human placentation events	• Maternal–fetal interaction studies	• Comparative genomics • Evaluation of assisted reproduction technologies

Downloaded From Vet-eBooks.com

3.5 Summary

Placenta or afterbirth is often an afterthought, being shed unceremoniously following the birth of the offspring. However, with mounting evidence for *in utero* origins of adult diseases, placenta is now considered a key link to wellness in embryonic and adult life. As discussed in this chapter, every species has a unique placenta, and while there are parallels, there are also unique and important differences. As argued by Schmidt A *et al.* (2015), "only humans have human placenta" and any attempt to use nonhuman animal models for investigating human placenta-specific diseases requires extreme caution and restraint from drawing direct parallels to human conditions, and in extrapolation of the results. In the absence of experimental hysterectomies that can be performed in the first trimester of human pregnancies, a comprehensive approach employing multiple model systems is key to unraveling the mysteries, and investigating the pathologies of this complex organ.

References

Amita, M., Andrei, P., Adachi, K., Alexenko, A.P., Sinha, S., Schust, D.J., Schulz, L.C., Roberts, R.M., and Ezashi, T. (2013) Complete and unidirectional conversion of human embryonic stem cells to trophoblast by BMP4. *Proc. Natl. Acad. Sci.*, **110** (13), E1212–E1221.

Amoroso E.C. (1952) Placentation. *Marshall's Physiology of Reproduction*, vol. 2, Longmans, Green & Co, London.

Aplin J.D. (1991) Implantation, trophoblast differentiation and haemochorial placentation: mechanistic evidence *in vivo* and *in vitro*. *J. Cell Sci.*, **99** (Part 4), 681–692.

Aplin J.D. (2006) *In vitro* analysis of trophoblast invasion. *Methods Mol. Med.*, **122**, 45–57.

Aplin J.D. (2010) Developmental cell biology of human villous trophoblast: current research problems. *Int. J. Dev. Biol.*, **54** (2–3), 323–329.

Bajoria, R., Sooranna, S.R., and Contractor, S.F. (1997) Endocytotic uptake of small unilamellar liposomes by human trophoblast cells in culture. *Hum. Reprod.*, **12** (6), 1343–1348.

Barnea, E.R., Neubrun, D., and Shurtz-Swirski, R. (1993) Effect of insulin on human chorionic gonadotrophin secretion by placental explants. *Hum. Reprod.*, **8** (6), 858–862.

Barry, J.S. and Anthony, R.V. (2008) The pregnant sheep as a model for human pregnancy. *Theriogenology*, **69** (1), 55–67.

Battaglia, F.C., Meschia, G., Makowski, E.L., and Bowes, W. (1968) The effect of maternal oxygen inhalation upon fetal oxygenation. *J. Clin. Investig.*, **47** (3), 548–555.

Bernardo, A.S., Faial, T., Gardern, L., Niakan, K.K., Ortmann, D., Senner, C.E., Callery, E.M., Trotter, M.W., Hemberger, M., Smith, J.C., Bardwell, L., Moffett, A., and Pdersen, R.A. (2011) BRACHYURY and CDX2 mediate BMP-induced differentiation of human and mouse pluripotent stem cells into embryonic and extraembryonic lineages. *Cell Stem Cell*, **9** (2), 144–155.

Blankenship, T.N. and Enders, A.C. (2003) Modification of uterine vasculature during pregnancy in macaques. *Microsc. Res. Technol.*, **60** (4), 390–401.

Brosens, I., Robertson, W.B., and Dixon, H.G. (1967) The physiological response of the vessels of the placental bed to normal pregnancy. *J. Pathol. Bacteriol.*, **93** (2), 569–579.

Burton, G.J. and Tham, S.W. (1992) Formation of vasculo-syncytial membranes in the human placenta. *J. Dev. Physiol.*, **18** (1), 43–47.

Calzonetti, T., Stevenson, L., and Rossant, J. (1995) A novel regulatory region is required for trophoblast-specific transcription in transgenic mice. *Dev. Biol.*, **171** (2), 615–626.

Downloaded From Vet-eBooks.com

Carter, A.M. and Enders, A.C. (2004) Comparative aspects of trophoblast development and placentation. *Reprod. Biol. Endocrinol.*, **2**, 46.

Castellucci, M., Scheper, M., Scheffen, I., Celona, A., and Kaufmann, P. (1990) The development of the human placental villous tree. *Anat. Embryol.*, **181** (2), 117–128.

Charnock-Jones, D.S., Sharkey, A.M., Boocock, C.A., Ahmed, A., Plevin, R., Ferrara, N., and Smith, S.K. (1994) Vascular endothelial growth factor receptor localization and activation in human trophoblast and choriocarcinoma cells. *Biol. Reprod.*, **51** (3), 524–530.

Chavatte-Palmer, P., Laigre, P., Simonoff, E., Chesné, P., Challah-Jacques, M., and Renard, J.P. (2008) *In utero* characterisation of fetal growth by ultrasound scanning in the rabbit. *Theriogenology*, **69** (7), 859–869.

Chu, C., Qu, K., Zhong, F., Artandi, S.E., and Chang, H.Y. (2011) Genomic maps of lincRNA occupancy reveal principles of RNA–chromatin interactions. *Mol. Cell*, **44** (4), 667–678.

Covone, A.E., Mutton, D., Johnson, P.M., and Adinolfi, M. (1984) Trophoblast cells in peripheral blood from pregnant women. *Lancet*, **2** (8407), 841–843.

Craven, C.M., Morgan, T., and Ward, K. (1998) Decidual spiral artery remodelling begins before cellular interaction with cytotrophoblasts. *Placenta*, **19** (4), 241–252.

Cross, J.C., Werb, Z., and Fisher, S.J. (1994) Implantation and the placenta: key pieces of the development puzzle. *Science*, **266** (5190), 1508–1518.

Cross, J.C., Baczyk, D., Dobric, N., Hemberger, M., Hughes, M., Simmons, D.G., Yamamoto, H., and Kingdom, J.C. (2003) Genes, development and evolution of the placenta. *Placenta*, **24** (2–3), 123–130.

D'Erchia, A.M., Gissi, C., Pesole, G., Saccone, C., and Arnason, U. (1996) The guinea-pig is not a rodent. *Nature*, **381** (6583), 597–600.

Drukker, M., Tang, C., Ardehali, R., Rinkevich, Y., Seita, J., Lee, A.S., Mosley, A.R., Weissman, I.L., and Soen, Y. (2012) Isolation of primitive endoderm, mesoderm, vascular endothelial and trophoblast progenitors from human pluripotent stem cells. *Nat. Biotechnol.*, **30** (6), 531–542.

Dunk, C., Petkovic, L., Baczyk, D., Rossant, J., Winterhager, E., and Lye, S. (2003) A novel *in vitro* model of trophoblast-mediated decidual blood vessel remodeling. *Lab. Invest.*, **83** (12), 1821–1828.

Eakin, G.S., Hadjantonakis, A.K., Papaioannou, V.E., and Behringer, R.R. Developmental potential and behavior of tetraploid cells in the mouse embryo. (2005) Developmental Biology **288**, 150–159.

Eixarch, E., Figueras, F., Hernández-Andrade, E., Crispi, F., Nadal, A., Torre, I., Oliveira, S., and Gratacós, E. (2009) An experimental model of fetal growth restriction based on selective ligature of uteroplacental vessels in the pregnant rabbit. *Fetal Diagn. Ther.*, **26** (4), 203–211.

Ellinger, I., Schwab, M., Stefanescu, A., Hunziker, W., Fuchs, R., and Stefanescu, W. (1999) IgG transport across trophoblast-derived BeWo cells: a model system to study IgG transport in the placenta. *Eur. J. Immunol.*, **29** (3), 733–744.

Enders A.C. (1965) A comparative study of the fine structure of the trophoblast in several hemochorial placentas. *Am. J. Anat.*, **116**, 29–67.

Enders A.C. (1989) Trophoblast differentiation during the transition from trophoblastic plate to lacunar stage of implantation in the rhesus monkey and human. *Am. J. Anat.*, **186** (1), 85–98.

Enders, A.C. and Blankenship, T.N. (1999) Comparative placental structure. *Adv. Drug Deliv. Rev.*, **38** (1), 3–15.

Enders, A.C. and King, B.F. (1991) Early stages of trophoblastic invasion of the maternal vascular system during implantation in the macaque and baboon. *Am. J. Anat.*, **192** (4), 329–346.

Enders, A.C. and Welsh, A.O. (1993) Structural interactions of trophoblast and uterus during hemochorial placenta formation. *J. Exp. Zool.*, **266** (6), 578–587.

Downloaded From Vet-eBooks.com

Enders, A.C., Hendricks, A.G., and Schlafke, S. (1983) Implantation in the rhesus monkey: initial penetration of endometrium. *Am. J. Anat.*, **167** (3), 275–298.

Enders, A.C., Welsh, A.O., and Sclafke, S. (1985) Implantation in the rhesus monkey: endometrial responses. *Am. J. Anat.*, **173** (3), 147–169.

Enders A.C. (1997) Cytotrophoblast invasion of the endometrium in the human and macaque early villous stage of implantation. *Placenta*, **18** (Suppl. 2), 83–95.

Fan, X., Ren, P., Dhal, S., Bejerano, G., Goodman, S.B., Druzin, M.L., Gambhir, S.S., and Nayak, N.R. (2011) Noninvasive monitoring of placenta-specific transgene expression by bioluminescence imaging. *PLoS One*, **6** (1), e16348.

Fischer, B., Chavatte-Palmer, P., Viebahn, C., Santos, A.N., and Duranthon, V. (2012) Rabbit as a reproductive model for human health. *Reproduction*, **144** (1), 1–10.

Flori, P., Hafid, J., Thonier, V., Bellete, B., Raberin, H., and Tran Manh Sung, R. (2003) Parasite load in guinea pig foetus with real time PCR after maternofoetal transmission of *Toxoplasma gondii*. *Parasite*, **10** (2), 133–140.

Fox H. (1970) Effect of hypoxia on trophoblast in organ culture: a morphologic and autoradiographic study. *Am. J. Obstet. Gynecol.*, **107** (7), 1058–1064.

Freyer, C. and Renfree, M.B. (2009) The mammalian yolk sac placenta. *J. Exp. Zool. B Mol. Dev. Evol.*, **312** (6), 545–554.

Furukawa, S., Kuroda, Y., and Sugiyama, A. (2014) A comparison of the histological structure of the placenta in experimental animals. *J. Toxicol. Pathol.*, **27** (1), 11–18.

Genbacev, O. and Miller, R.K. (2000) Post-implantation differentiation and proliferation of cytotrophoblast cells: *in vitro* models—a review. *Placenta*, **21** (Suppl. A), S45–S49.

Genbacev, O., Schubach, S.A., and Miller, R.K. (1992) Villous culture of first trimester human placenta: model to study extravillous trophoblast (EVT) differentiation. *Placenta*, **13** (5), 439–461.

Georgiades, P., Ferguson-Smith, A.C., and Burton, G.J. (2002) Comparative developmental anatomy of the murine and human definitive placentae. *Placenta*, **23** (1), 3–19.

Georgiades, P., Cox, B., Gertsenstein, M., Chawengsaksophak, K., and Rossant, J. (2007) Trophoblast-specific gene manipulation using lentivirus-based vectors. *Biotechniques*, **42** (3), 317–318.

Gerami-Naini, B., Dovzhenko, O.V., Durning, M., Wegner, F.H., Thomson, J.A., and Golos, T.G. (2004) Trophoblast differentiation in embryoid bodies derived from human embryonic stem cells. *Endocrinology*, **145** (4), 1517–1524.

Golos, T.G., Giakoumopoulos, M., and Gerami-Naini, B. (2013) Review: trophoblast differentiation from human embryonic stem cells. *Placenta*, **34**, S56–S61.

Grosser O. (1909) Vergleichende Antomie und Entwicklunsgeschchte der Eihaute und der Placenta, Braumuller, Wien und Leipzig.

Grosser O. (1927) Fruhentwicklung, Eihautbidung und Placentation des Menschen und der Saugetiere.

Gude, N.M., Roberts, C.T., Kalionis, B., and King, R.G. (2004) Growth and function of the normal human placenta. *Thromb. Res.*, **114** (5–6), 397–407.

Gulbis, B., Jauniaux, E., Cotton, F., and Stordeur, P. (1998) Protein and enzyme patterns in the fluid cavities of the first trimester gestational sac: relevance to the absorptive role of secondary yolk sac. *Mol. Hum. Reprod.*, **4** (9), 857–862.

Hamilton, W.J. and Boyd, J.D. (1960) Development of the human placenta in the first three months of gestation. *J. Anat.*, **94** (Part 3), 297–328.

Harun, R.M., Ruban, L., Matin, M., Draper, J., Jenkins, N.M., Liew, G.C., Andrews, P.W., Li, T.C., Lair, S.M., and Moore, H.D. (2006) Cytotrophoblast stem cell lines derived from human embryonic stem cells and their capacity to mimic invasive implantation events. *Hum. Reprod.*, **21** (6), 1349–1358.

Downloaded From Vet-eBooks.com

Hay, D.C., Sutherland, L., Clark, J., and Burdon, T. (2004) Oct-4 knockdown induces similar patterns of endoderm and trophoblast differentiation markers in human and mouse embryonic stem cells. *Stem Cells*, **22**, 225–235.

Hellman, L.M., Harris, Jr., B.A., and Andrews, M.C. (1950) Studies of the metabolism of the human placenta: oxygen consumption and anaerobic glyolysis in relation to aging and severe toxemia. *Bull. Johns Hopkins Hosp.*, **87** (3), 203–214.

Hirano, H., Imai, Y., and Ito, H. (2002) Spiral artery of placenta: development and pathology-immunohistochemical, microscopical, and electron-microscopic study. *Kobe J. Med. Sci.*, **48** (1–2), 13–23.

Hohn, H.P., Linke, M., Ugele, B., and Denker, H.W. (1998) Differentiation markers and invasiveness: discordant regulation in normal trophoblast and choriocarcinoma cells. *Exp. Cell Res.*, **244** (1), 249–258.

Hu, Dong and Cross, J.C. (2011) Ablation of Tpbpa-positive trophoblast precursors leads to defects in maternal spiral artery remodeling in the mouse placenta. *Dev. Biol.*, **358** (1), 231–239.

Hyslop, L., Stojkovic, M., and Armstrong, L. (2005) Downregulation of NANOG induces differentiation of human embryonic stem cells to extraembryonic lineages. *Stem Cells*, **23**, 1035–1043.

Ikawa, M., Tanaka, N., Kao, W., and Verma, I.M. (2003) Generation of transgenic mice using lentiviral vectors: a novel preclinical assessment of lentiviral vectors for gene therapy. *Mol. Ther.*, **8** (4), 666–673.

Itskovitz-Eldor, J., Schuldiner, M., Karsenti, D., Eden, A., Yanuka, O., Amit, M., Soreq, H., and Benvenisty, N. (2000) Differentiation of human embryonic stem cells into embryoid bodies compromising the three embryonic germ layers. *Mol. Med.*, **6** (2), 88–95.

James, J.L., Stone, P.R., and CHamley, L.W. (2006) The regulation of trophoblast differentiation by oxygen in the first trimester of pregnancy. *Hum. Reprod. Update*, **12** (2), 137–144.

Jansson, T. and Persson, E. (1990) Placental transfer of glucose and amino acids in intrauterine growth retardation: studies with substrate analogs in the Awake guinea pig. *Pediatr. Res.*, **28** (3), 203–208.

Jauniaux, E., Johns, J., Gulbis, B., Spasic-Boskovic, O., and Burton, G.J. (2007) Transfer of folic acid inside the first-trimester gestational sac and the effect of maternal smoking. *Am. J. Obstet. Gynecol.*, **197** (1), 58.

Jin, Y., Lu, S.Y., Fresnoza, A., Detillieux, K.A., Duckworth, M.L., and Cattini, P.A. (2009) Differential placental hormone gene expression during pregnancy in a transgenic mouse containing the human growth hormone/chorionic somatomammotropin locus. *Placenta*, **30** (3), 226–235.

Jollie W.P. (1990) Development, morphology, and function of the yolk-sac placenta of laboratory rodents. *Teratology*, **41** (4), 361–381.

Jones, C.J. and Fox, H. (1991) Ultrastructure of the normal human placenta. *Electorn Microsc. Rev.*, **4** (1), 129–178.

Kaufmann P. (1985) Basic morphology of the fetal and maternal circuits in the human placenta. *Contrib. Gynecol. Obstet.*, **13**, 5–17.

Kaufmann, P., Black, S., and Huppertz, B. (2003) Endovascular trophoblast invasion: implications for the pathogenesis of intrauterine growth retardation and preeclampsia. *Biol. Reprod.*, **69** (1), 1–7.

Kay, H.H., Robinette, B., Shin, Y.Y., Siew, P., Shellhaas, C.S., and Tyrey, L. (1997) Placental villous glucose metabolism and hormone release respond to varying oxygen tensions. *J. Soc. Gynecol. Investig.*, **4** (5), 241–246.

King G.J. (1993) Comparative placentation in ungulates. *J. Exp. Zool.*, **266** (6), 588–602.

Knöfler, M. and Pollheimer, J. (2013) Human placental trophoblast invasion and differentiation: a particular focus on Wnt signaling. *Front. Genet.*, **4**, 190.

Downloaded From Vet-eBooks.com

Knoth, M. and Larsen, J.F. (1972) Ultrastructure of a human implantation site. *Acta Obstet. Gynecol. Scand.*, **51** (4), 385–393.

Kudo, Y., Boyd, C.A., Sargent, I.L., and Reman, C.W. (2003) Hypoxia alters expression and function of syncytin and its receptor during trophoblast cell fusion of human placental BeWo cells: implications for impaired trophoblast syncytialisation in pre-eclampsia. *Biochim. Biophys. Acta*, **1638** (1), 63–71.

Kurek, D., Neagu, A., Tastemel, M., Tüysüz, N., Lehmann, J., van de Werken, H., Philipsen, S., van der Linden, R., Maas, A., van Ijcken, W., Drukker, M., and ten Berge, D. (2015) Endogenous WNT signals mediate BMP-induced and spontaneous differentiation of epiblast stem cells and human embryonic stem cells. *Stem Cell Rep.*, **4** (1), 114–128.

Lafeber, H.N., Roph, T.P., and Jones, C.T. (1984) Studies on the growth of the fetal guinea pig: the effects of ligation of the uterine artery on organ growth and development. *J. Dev. Physiol.*, **6** (6), 441–459.

Lee, D., Karim Rumi, M.A., Konno, T., and Soares, M.J. (2009) *In vivo* genetic manipulation of the rat trophoblast cell lineage using lentiviral vector delivery. *Genesis*, **47** (7), 433–439.

Leiser, R. and Kaufmann, P. (1994) Placental structure: in a comparative aspect. *Exp. Clin. Endocrinol.*, **102** (3), 122–134.

Levack, V., Hone, P.A., Phipps, A.W., and Harrison, J.D. (2002) The placental transfer of cerium: experimental studies and estimates of doses to the human fetus from 141Ce and 144Ce. *Int. J. Radiat. Biol.*, **78** (3), 227–235.

Lim, K.H., Zhou, Y., Janatpour, M., McMaster, M., Bass, K., Chun, S.H., and Fisher, S.J. (1997) Human cytotrophoblast differentiation/invasion is abnormal in pre-eclampsia. *Am. J. Pathol.*, **151** (6), 1809–1818.

Lingas, R., Dean, F., and Matthews, S.G. (1999) Maternal nutrient restriction (48 h) modifies brain corticosteroid receptor expression and endocrine function in the fetal guinea pig. *Brain Res.*, **846** (2), 236–242.

Litonjua, A.D., Canlas, M., Soliman, J., and Paulino, D.Q. (1967) Uptake of alpha-aminoisobutyric acid in placental slices at term. *Am. J. Obstet. Gynecol.*, **99** (2), 242–246.

Luckett W.P. (1993) Uses and limitations of mammalian fetal membranes and placenta for phylogenetic reconstruction. *J. Exp. Zool.*, **266** (6), 514–527.

Makris, A., Thornton, C., Thompson, J., Thomson, S., Martin, R., Ogle, R., Waugh, R., McKenzie, P., Kirwan, P., and Hennessy, A. (2007) Uteroplacental ischemia results in proteinuric hypertension and elevated sFLT-1. *Kidney Int.*, **71** (10), 977–984.

Matin, M.M., Walsh, J.R., and Gokhale, P.J. (2004) Specific knockdown of Oct4 and beta2-microglobulin expression by RNA interference in human embryonic stem cells and embryonic carcinoma cells. *Stem Cells*, **22**, 659–668.

Meschia, G., Cotter, J.R., Breathnach, C.S., and Barron, D.H. (1965) The diffusibility of oxygen across the sheep placenta. *Q. J. Exp. Physiol. Cognate Med. Sci.*, **50** (4), 466–480.

Mess A. (2014) Placental evolution within the supraordinal clades of eutheria with the perspective of alternative animal models for human placentation. *Adv. Biol.*, **2014**, 21.

Mess, A. and Carter, A.M. (2006) Evolutionary transformations of fetal membrane characters in Eutheria with special reference to Afrotheria. *J. Exp. Zool. B Mol. Dev. Evol.*, **306** (2), 140–163.

Mess, A., Zaki, N., Kadyrov, M., Korr, H., and Kaufmann, P. (2007) Caviomorph placentation as a model for trophoblast invasion. *Placenta*, **28** (11–12), 1234–1238.

Mihaly, G.W. and Morgan, D.J. (1983) Placental drug transfer: effects of gestational age and species. *Pharmacol. Ther.*, **23** (2), 253–266.

Morioka, Y., Isotani, A., Oshima, R.G., Okabe, M., and Ikawa, M. (2009) Placenta-specific gene activation and inactivation using integrase-defective lentiviral vectors with the Cre/LoxP system. *Genesis*, **47** (12), 793–798.

Downloaded From Vet-eBooks.com

Mossman H.W. (1987) *Vertebrate Fetal Membranes: Comparative Ontogeny and Morphology; Evolution; Phylogenetic Significance; Basic Functions; Research Opportunities*, Macmillan, Houndmills, UK.

Mossman H.W. (1991) Classics revisited: comparative morphogenesis of the fetal membranes and accessory uterine structures. *Placenta*, **12** (1), 1–5.

Okada, Y., Ueshin, Y., Isotani, A., Saito-Fujita, T., Nakashima, H., Kimura, K., Mizoguchi, A., Oh-Hora, M., Mori, Y., Ogata, M., Oshima, R.G., Okabe, M., and Ikawa, M. (2007) Complementation of placental defects and embryonic lethality by trophoblast-specific lentiviral gene transfer. *Nat. Biotechnol.*, **25** (2), 233–237.

Palis, J. and Yoder, M.C. (2001) Yolk-sac hematopoiesis: the first blood cells of mouse and man. *Exp. Hematol.*, **29** (8), 927–936.

Palmer, A.E., London, W.T., Sly, D.L., and Rice, J.M. (1979) Spontaneous preeclamptic toxemia of pregnancy in the patas monkey (*Erythrocebus patas*). *Lab. Anim. Sci.*, **29** (1), 102–106.

Pattillo, R.A., Gey, G.O., Deifs, E., and Mattingly, R.F. (1968) *In vitro* identification of the trophoblastic stem cell of the human villous placenta. *Am. J. Obstet. Gynecol.*, **100** (4), 582–528.

Peiffer, I., Belhomme, D., Barbet, R., Haydont, V., Zhou, Y.P., Fortunel, N.O., Li, M., Hatzfeld, A., Fabiani, J.N., and Hatzfeld, J.A. (2007) Simultaneous differentiation of endothelial and trophoblastic cells derived from human embryonic stem cells. *Stem Cell Dev.*, **16** (3), 393–402.

Pera, M.F., Andrade, J., Houssami, S., Reubinoff, B., Trounson, A., Stanley, E.G., Ward-van Oostwaard, D., and Mummery, C. (2004) Regulation of human embryonic stem cell differentiation by BMP-2 and its antagonist noggin. *J. Cell Sci.*, **117** (Part 7), 1269–1280.

Pere M.C. (2003) Materno-foetal exchanges and utilisation of nutrients by the foetus: comparison between species. *Reprod. Nutr. Dev.*, **43** (1), 1–15.

Perry J.S. (1981) The mammalian fetal membranes. *J. Reprod. Fertil.*, **62** (2), 321–335.

Pfeifer, A., Ikawa, M., Dayn, Y., and Verma, I.M. (2002) Transgenesis by lentiviral vectors: lack of gene silencing in mammalian embryonic stem cells and preimplantation embryos. *Proc. Natl. Acad. Sci. USA*, **99** (4), 2140–2145.

Pijnenborg, R., Robertson, W.B., Brosens, I., and Dixon, G. (1981) Review article: trophoblast invasion and the establishment of haemochorial placentation in man and laboratory animals. *Placenta*, **2** (1), 71–91.

Polisca, A., Scotti, L., Orlandi, R., Brecchia, G., and Boiti, C. (2010) Doppler evaluation of maternal and fetal vessels during normal gestation in rabbits. *Theriogenology*, **73** (3), 358–366.

Renaud, S.J., Karim Rumi, M.A., and Soares, M.J. (2011) Review: genetic manipulation of the rodent placenta. *Placenta*, **32** (Suppl. 2), S130–S135.

Roberts, R.M. and Fisher, S.J. (2011) Trophoblast stem cells. *Biol. Reprod.*, **84** (3), 412–421.

Roberts, R.M., Loh, K.M., Amita, M., Bernardo, A.S., Adachi, K., Alexenko, A.P., Schust, D.J., Schulz, L.C., Telugu, B.P., Ezashi, T., and Pedersen, R.A. (2014) Differentiation of trophoblast cells from human embryonic stem cells: to be or not to be? *Reproduction*, **147** (5), D1–D12.

Robertson, W.B., Brosens, I., and Dixon, H.G. (1967) The pathological response of the vessels of the placental bed to hypertensive pregnancy. *J. Pathol. Bacteriol.*, **93** (2), 581–592.

Schmidt, A., Morales-Prieto, D.M., Pastuschek, J., Frohlich, K., and Markert, U.R. (2015) Only humans have human placentas: molecular differences between mice and humans. *J. Reprod. Immunol.*, **108**, 65–71.

Schneider H. (1991) The role of the placenta in nutrition of the human fetus. *Am. J. Obstet. Gynecol.*, **164** (4), 967–973.

Downloaded From Vet-eBooks.com

Schulz, L.C., Ezashi, T., Das, P., Westfall, S.D., Livingston, K.A., and Roberts, R.M. (2008) Human embryonic stem cells as models for trophoblast differentiation. *Placenta*, **29** (Suppl. A), S10–S16.

Shi, D., Winston, J.H., Blackburn, M.R., Datta, S.K., Hanten, G., and Kellems, R.E. (1997) Diverse genetic regulatory motifs required for murine adenosine deaminase gene expression in the placenta. *J. Biol. Chem.*, **272** (4), 2334–2341.

Simmons, D.G., Fortier, A.L., and Cross, J.C. (2007) Diverse subtypes and developmental origins of trophoblast giant cells in the mouse placenta. *Dev. Biol.*, **304** (2), 567–578.

Steven, D.H. and Morris, G. (1975) *Comparative Placentation: Development of the Foetal Membranes*, Academic Press, New York.

Stout, C. and Lemmon, W.B. (1969) Glomerular capillary endothelial swelling in a pregnant chimpanzee. *Am. J. Obstet. Gynecol.*, **105** (2), 212–215.

Strauss, J.F., Kido S., Sayegh R., Sakuragi N., and Gafvels M.E. (1992) The cAMP signalling system and human trophoblast function. *Placenta*, **13** (5), 389–403.

Su, Y., Liebhaber, S.A., and Cooke, N.E. (2000) The human growth hormone gene cluster locus control region supports position-independent pituitary- and placenta-specific expression in the transgenic mouse. *J. Biol. Chem.*, **275** (11), 7902–7909.

Swanson, A.M. and David, A.L. (2015) Animal models of fetal growth restriction: considerations for translational medicine. *Placenta*, **36** (6), 623–630.

Sybulski, S. and Tremblay, P.C. (1967) Uptake and incorporation into protein of radioactive glycine by human placentas *in vitro*. *Am. J. Obstet. Gynecol.*, **97** (8), 1111–1118.

Takahashi, Y., Dominici, M., Swift, J., Nagy, C., and Ihle, J.N. (2006) Trophoblast stem cells rescue placental defect in SOCS3-deficient mice. *J. Biol. Chem.*, **281** (17), 11444–11445.

Tam, P.P. and Rossant, J. (2003) Mouse embryonic chimeras: tools for studying mammalian development. *Development*, **130** (25), 6155–6163.

Tanaka, S., Kunath, T., Hadjantonakis, A., Nagy, A., and Rossant, J. (1998) Promotion of trophoblast stem cell proliferation by FGF4. *Science*, **282** (5396), 2072–2075.

Tavian, M. and Peault, B. (2005) Embryonic development of the human hematopoietic system. *Int. J. Dev. Biol.*, **49** (2–3), 243–250.

Thomson, J.A., Itskovits-Eldo, J., Shapiro, S.S., Waknitz, M.A., Swiergiel, J.J., Marshall, V.S., and Jones, J.M. (1998) Embryonic stem cell lines derived from human blastocysts. *Science*, **282** (5391), 1145–1147.

Tremblay, P.C., Sybulski, S., and Maughan, G.B. (1965) Role of the placenta in fetal malnutrition. *Am. J. Obstet. Gynecol.*, **91**, 597–605.

Vandevoort, C.A., Thirkill, T.L., and Douglas, G.C. (2007) Blastocyst-derived trophoblast stem cells from the rhesus monkey. *Stem Cells Dev.*, **16** (5), 779–788.

Vicovac, L., Jones, C.J., and Aplin, J.D. (1995) Trophoblast differentiation during formation of anchoring villi in a model of the early human placenta *in vitro*. *Placenta*, **16** (1), 41–56.

Villee C.A. (1953) The metabolism of human placenta *in vitro*. *J. Biol. Chem.*, **205** (1), 113–123.

Wallaces, A.E., Fraser, R., and Cartwright, J.E. (2012) Extravillous trophoblast and decidual natural killer cells: a remodelling partnership. *Hum. Reprod. Update*, **18** (4), 458–471.

Weier, J.F. *et al.* (2010) Somatic genomic variations in extra-embryonic tissues. *Curr. Genomics*, **11**, 402–408.

Winston, J.H., Hanten, G.R., Overbeek, P.A., and Kellems, R.E. (1992) 5′ Flanking sequences of the murine adenosine deaminase gene direct expression of a reporter gene to specific prenatal and postnatal tissues in transgenic mice. *J. Biol. Chem.*, **267** (19), 13472–13479.

Wooding F.B. (1992) Current topic: the synepitheliochorial placenta of ruminants: binucleate cell fusions and hormone production. *Placenta*, **13** (2), 101–113.

Downloaded From Vet-eBooks.com

Wooding, F.B. and Burton, G.J. (2008) *Comparative Placentation: Structures, Functions, and Evolution*, Springer, Berlin.

Xu, R.H., Chen, X., Li, D.S., Li, R., Addicks, G.C., Glennon, C., Zwaka, T.P., and Thomson, J.A. (2002) BMP4 initiates human embryonic stem cell differentiation to trophoblast. *Nat. Biotechnol.*, **20** (12), 1261–1264.

Yu, P., Pan, G., Yu, J., and Thomson, J.A. (2011) FGF2 sustains NANOG and switches the outcome of BMP4-induced human embryonic stem cell differentiation. *Cell Stem Cell*, **8** (3), 326–334.

Zaehres, H., Lensch, M.W. Daheron, L. Sewart, S.A. Itskovitz-Eldor, J. and Daley, G.Q. (2005) High-efficiency RNA interference in human embryonic stem cells. *Stem Cells*, **23**, 299–305.

Zhou, Y., Fisher, S.J., Janatpour, M., Genbacev, O., Dejana, E., Wheelock, M., and Damsky, C.H. (1997) Human cytotrophoblasts adopt a vascular phenotype as they differentiate: a strategy for successful endovascular invasion? *J. Clin. Invest.*, **99** (9), 2139–2151.

Downloaded From Vet-eBooks.com

4

Early Developmental Programming of the Ovarian Reserve, Ovarian Function, and Fertility

Francesca Mossa,[1] Siobhàn W. Walsh,[2] Alex C.O. Evans,[3] Fermin Jimenez-Krassel,[4] and James J. Ireland[4]

[1]*Dipartimento di Medicina Veterinaria, Università degli Studi di Sassari, Sassari, Italy*
[2]*Department of Chemical and Life Sciences, Waterford Institute of Technology, Waterford, Ireland*
[3]*School of Agriculture and Food Science, University College Dublin, Dublin, Ireland*
[4]*Michigan State University, MI, USA*

4.1 Introduction

The environment encountered during fetal life exerts a profound influence on development, physiological function, and risk of disease in adult life in mammals (Barker, 2007; Langley-Evans and McMullen, 2010). Development is a plastic process since the fetus has the ability to change its structure and/or function in response to physiological cues from the mother, and as such a range of different phenotypes can be expressed from a given genotype. The developing conceptus responds to hormonal, nutritional, and metabolic conditions during sensitive periods of cellular proliferation, differentiation, and maturation, resulting in structural and/or functional changes in cells, tissues, and organ systems. It is assumed that the developing fetus interprets these stimuli as being reflective of what it will experience during post natal life and therefore it adapts accordingly. These changes may have short-term and/or long-term consequences for health and disease susceptibility. Hence, the term "programming" has been adopted to describe the process whereby a stimulus or an insult at a sensitive period of fetal or perinatal life has permanent effects on the structure, physiology, and metabolism of different organs and systems.

The primary prenatal environmental factors investigated thus far are under- and over-nutrition and endocrine-disrupting compounds (EDC). Undernutrition and malnutrition during gestation in women may be the result of severe nausea and vomiting, dieting and pregnancy in adolescent girls, or may occur in low- to middle-income economic conditions (Black *et al.*, 2013). Poor maternal nutrition, including micronutrient deficiencies, contributes to at least 20% of maternal deaths and it increases the probability of poor pregnancy outcomes such as intrauterine growth restriction, resulting in low birth weight, stunting, wasting, and mortality (Salam *et al.*, 2014). However, few studies have examined the effects of maternal undernutrition on ovarian function and fertility in offspring. On the other hand, it is estimated that 3.3 billon people globally will become overweight or obese by 2030 (Kelly *et al.*, 2008) and many studies have reported a negative effect of obesity on fertility (Sinclair and Watkins, 2013), yet the possible link between maternal overnutrition and fertility in offspring remains largely uninvestigated.

Finally, natural and artificial dietary components, as well as environmental chemicals, may interfere with the physiological action of hormones and many of these EDC act as steroid

Animal Models and Human Reproduction, First Edition. Edited by Heide Schatten and Gheorghe M. Constantinescu.
© 2017 John Wiley & Sons, Inc. Published 2017 by John Wiley & Sons, Inc.

Downloaded From Vet-eBooks.com

Table 4.1 Length of gestation, placentation type, litter size, and age at puberty in humans, farm animals, and women (Senger, 2003; Cupps, 1991).

Species	Gestation length (days)	Placenta	Litter size	Age at puberty in females
Human	271–289	Discoid, hemochorial	1	11–12 years
Sheep	144–152	Cotiledonary, syndesmochorial	1–2	7 months
Cattle	277–290	Cotiledonary, syndesmochorial	1–2	11 months
Pig	112–115	Diffuse, epitheliochorial	8–12	6 months
Rat	22	Discoid, hemochorial	6–9	50 days
Mouse	19–20	Discoid, hemochorial	6	

receptor agonists and antagonists. Since the fetus is extremely sensitive to steroid hormones, fetal exposure to EDC that can signal via steroid-mediated pathways may have long-term negative consequences on offspring health and reproduction (reviewed by Padmanabhan and Veiga-Lopez (2014) and Richardson *et al.* (2014)).

This chapter focuses on the impact of prenatal environmental challenges, specifically undernutrition, overnutrition, and EDC (excess testosterone, BPA) on fetal oogonia (germ cells), follicle/oocyte numbers and oocyte quality, and on the ovarian reserve, ovarian function, and fertility in offspring of farm animals, rodents, and women (Table 4.1).

4.2 Impact of Prenatal Environmental Challenges on Fetal Oogonia (Germ Cells)

During fetal development, primordial germ cells migrate from the hind gut to the genital ridges and proliferate through mitotic divisions. When primordial gonads begin to differentiate as ovaries, germ cells are called oogonia. Oogonia proliferate and reach a peak number during fetal life, followed by a large-scale cell death. The timing of oogonia development is species specific and is summarized in Table 4.2 (modified from Mossa *et al.* (2015)).

To our knowledge, the impact of maternal undernutrition, overnutrition, excess testosterone, and BPA on oogonia in women and rodent models has not been investigated.

4.2.1 Farm Animal Models

4.2.1.1 Undernutrition

The effect of maternal undernutrition on fetal ovarian development was first investigated in ewes fed either 150% (high energy) or 50% (low energy) of their energy requirements for maintenance (M) during early gestation (Borwick *et al.*, 1997). Gestation in sheep lasts on average 147 days (Table 4.1) and meiosis starts at around day 55 (Table 4.2). Maternal diets low in energy resulted in an increased number of oogonia in their fetuses by days 47 and 62 of gestation compared with fetal ovaries subjected to high-energy maternal diets (Borwick *et al.*, 1997). Results imply that malnutrition impacts oogonia number in fetal ovaries, but control diets (i.e., moderate energy diets) were not tested nor was it established if these maternal diets altered the ovarian reserve (total number of morphologically healthy follicles/oocytes in both ovaries), ovarian function, or fertility in progeny after birth.

Downloaded From Vet-eBooks.com

Table 4.2 Timing of reproductive tract development in laboratory rodents, sheep, cattle, and humans.

	Event (day of gestation/day after birth)			
	Rodents[a)]	**Sheep**	**Cattle**	**Humans**
1st third of gestation	Gonadal differentiation (mice 6)	Müllerian ducts formation (24)	Germ cells visible (35–36)	Müllerian ducts fusion (by 56)
	Germ cells visible (6.5)	Müllerian ducts fusion (34–55)	Start of meiosis (75–80)	Start of meiosis (70–98)
		Start of meiosis (55)	Primordial follicles visible (74–90)	Uterine corpus and cervix differentiation (by 84)
2nd third of gestation	Germ cells migrate toward the genital ridges (8.5–10.5)	Primordial follicles visible (75)	Primary follicles visible (74–140)	Primordial follicles visible (98–105)
	Müllerian ducts formation (11.5)	Aglandular nodules visible in the uterine endometrium (90)	Peak number of germ cells (91–110)	Antral follicles visible (210–245)
	Gonadal differentiation (rat 12.5)	Primary follicles visible (110)	Secondary follicles visible (120–210)	
	Start of meiosis (mice 13, rat 17)			
3rd third of gestation	Müllerian ducts fusion (15–16)	Endometrial gland development first observed (135)		
		Antral follicles visible (135)		
Postnatal life	Development of the uterus (1–15)	Development of the uterus (up to 26)		Development of endometrial glands (birth–puberty)
	Primordial follicles (mice 2–5, rat 1–2)			
	Primary follicles (mice 2–5, rat 2–3)			
	Antral follicles (mice 17, rat 15)			

Gestation has been divided into three parts to better emphasize how the development of the reproductive system may be differentially sensitive during selected windows of gestation (Spencer *et al.*, 2012; Dupont *et al.*, 2012; Rüsse, 1983).
a) Data for rodents are expressed as days post coitum.

When 50% M versus 100% M diets were compared, undernutrition imposed from mating to day 65 of gestation in sheep did not alter number of oogonia. However, fewer oogonia were observed at the resting, diplotene stage of initial meiosis compared to ovaries from control fetuses, indicating a delay in the onset of meiosis in response to undernutrition (Rae *et al.*, 2001). Similarly, underfeeding in sheep (50% M versus 100% M from day 28) did not alter oogonia numbers or rate of apoptosis by day 78, but increased oxidative base lesions within DNA of fetal oogonia (Murdoch *et al.*, 2003). Taken together, results imply that the maturation and quality but not proliferation of fetal oogonia may be negatively impacted by maternal undernutrition.

Downloaded From Vet-eBooks.com

4.3 Impact of Prenatal Environmental Challenges on Fetal Follicle/Oocyte Numbers (Healthy versus Atretic) and Oocyte Quality

Once oogonia enlarge they develop into primary oocytes and enter into the first phase of meiosis. Oocytes become surrounded by a single layer of somatic cells (pre-granulosa) and form primordial follicles that will subsequently grow and form primary, secondary, and antral follicles during fetal life (Table 4.2).

Limited opportunities are available for analysis of human fetal ovaries. Moreover, rodent oocytes are assembled into primordial follicles only after birth (Table 4.2). Thus, studies on the effects of nutrition and excess maternal testosterone or BPA on fetal follicles/oocytes in humans/primates and rodents are limited or lacking.

4.3.1 Farm Animal Models

4.3.1.1 Undernutrition

In ewes, undernutrition (50% M) during different periods of pregnancy did not affect total number of oocytes, but reduced number of follicles beyond the primordial stage in 110-day old fetuses (Rae *et al.*, 2001). This observation suggests that undernutrition may delay fetal ovarian follicular development. In addition, this reduction in nutrition was more severe in fetuses undernourished from mating to day 30 of pregnancy, indicating that undernutrition before gonadal differentiation and during the meiotic proliferation of oogonia compromises subsequent follicular development. It is noteworthy that ovaries were not examined after birth, hence a compensatory effect on rate of ovarian follicular development during the remainder of gestation cannot be excluded.

4.3.1.2 Overnutrition

Fewer follicles were reported in ovaries of ovine fetuses exposed to high compared to moderate levels of a complete diet from day 4 to 130 (Da Silva *et al.*, 2002) or from mating to day 130 of gestation (Da Silva *et al.*, 2003). These studies show that overnutrition, similar to undernutrition, impairs folliculogenesis during fetal life.

4.3.2 Humans/Primates

4.3.2.1 Endocrine Disruptors

Testosterone

Excess maternal testosterone disrupts folliculogenesis and fertility in animal models (Richardson *et al.*, 2014; Padmanabhan *et al.*, 2012). However, the impact of excess maternal testosterone on fetal oogonia has not been evaluated in humans.

BPA

BPA is a component of polycarbonate plastic, which is widely used to manufacture many consumer products, such as linings for most food and beverage cans. BPA has the potential to leach out from these materials during food storage, becoming a dietary contaminant, and its presence has been documented in water, air, and most human fluids (vom Saal and Hughes, 2005; Vandenberg *et al.*, 2009). BPA has both estrogenic and antiandrogenic activity

Downloaded From Vet-eBooks.com

(Quesada *et al.*, 2002) and blood concentrations of BPA are related to ovarian disease in women (Takeuchi *et al.*, 2004). Exposure of pregnant monkeys to BPA during gestation, resulting in circulating levels similar to those in humans exposed to BPA, increased number of multi-oocyte follicles and disrupted oocyte growth/maturation in fetuses, raising reproductive health concerns as in humans (Hunt *et al.*, 2012).

4.4 Impact of Prenatal Environmental Challenges on the Ovarian Reserve (Total Number of Morphologically Healthy Follicles/Oocytes in Ovaries) in Offspring

Most mammals are born with a highly variable but fixed number of morphologically healthy follicles and oocytes that constitute the peak of their ovarian reserve for the remainder of their reproductive life (Monniaux *et al.*, 2014). However, the ovarian reserve diminishes rapidly via atresia (follicle/oocyte death) during aging and is never replenished (Ireland *et al.*, 2011; Kerr *et al.*, 2013). Maternal environmental factors that diminish size of the fetal ovarian reserve would be expected to also impair fertility of offspring.

4.4.1 Farm Animal Models

4.4.1.1 Undernutrition

The number of antral follicles growing during follicular waves (antral follicle count (AFC)) (Burns *et al.*, 2005; Ireland *et al.*, 2008; Jimenez-Krassel *et al.*, 2009; Mossa *et al.*, 2012) and concentrations of anti-Müllerian hormone (AMH) (Ireland *et al.*, 2011; Ribeiro *et al.*, 2014; Souza *et al.*, 2015) and follicle-stimulating hormone (FSH) (Ireland *et al.*, 2007) are markers of size of the ovarian reserve and reproductive potential in cattle. Antral follicle count and AMH are positively associated, whereas circulating FSH concentrations are negatively associated with the size of the ovarian reserve (Burns *et al.*, 2005; Ribeiro *et al.*, 2014; Mossa *et al.*, 2012; Jimenez-Krassel *et al.*, 2015). We used these markers to investigate the effect of maternal nutritional restriction during the first trimester of pregnancy on development of female offspring (Mossa *et al.*, 2013). Female calves born to nutritionally restricted mothers (0.6 M for the first 110 days of gestation) had higher FSH secretion during follicular waves, but lower AFC and AMH concentrations despite similar birth weights, postnatal growth rates (to 95 weeks of age), age at puberty, glucose metabolism, and responses to stress compared to offspring from control mothers (1.2 M) (Mossa *et al.*, 2013). Interestingly, female calves born to nutritionally restricted mothers also had an enlarged aorta and increased arterial blood pressure compared with controls (Mossa *et al.*, 2013). The association between fetal undernutrition/malnutrition and cardiovascular disease during adulthood has been widely documented especially in offspring born small (Barker, 2007; Langley-Evans and McMullen, 2010; Gopalakrishnan *et al.*, 2004). Whether the low AFC and high blood pressure phenotypes were both direct consequences of maternal undernutrition is unknown. This study provides evidence for a negative impact of maternal malnutrition on the ovarian reserve in adult offspring, but it did not investigate the fetal ovarian reserve or mechanisms that mediated the negative effect of maternal undernutrition on the ovarian reserve in offspring. Nevertheless, an increase in maternal testosterone concentration was detected during dietary restriction and growing evidence indicates that fetal exposure to elevated androgen concentration may negatively impact the ovarian reserve (Padmanabhan and Veiga-Lopez, 2014).

Downloaded From Vet-eBooks.com

In a separate study, heifers born to dams that received a low-protein diet during the first trimester followed by a high-protein diet during the second trimester of pregnancy had smaller follicles and fewer primordial and primary follicles and healthy antral follicles as adults (Sullivan *et al.*, 2009). Collectively, these observations in cattle show that maternal undernutrition during the first trimester of gestation is positively linked to several markers of infertility.

Poor maternal nutrition may result in intrauterine growth restriction and low birth weight (Salam *et al.*, 2014). In pigs, growth retardation occurs naturally and comparison with a normally grown littermate makes growth-retarded piglets a useful model to investigate the repercussions of suboptimal growth on reproductive organ development, without the confounding effects of different maternal genotype, nutrition, and husbandry conditions. For example, intrauterine growth-retarded piglets had more primordial follicles, fewer primary and no secondary follicles at birth compared with normally grown piglets originating from the same litter. These observations indicate that intrauterine growth retardation delayed folliculogenesis (Da Silva-Buttkus *et al.*, 2003). A low-protein diet during gestation and lactation in sows caused a reduction in number of antral follicles, coupled with an increase in apoptotic granulosa cells in prepubertal offspring (Sui *et al.*, 2014). Although using a different experimental design, both studies provide evidence for a negative impact of maternal undernutrition, and consequently intrauterine growth restriction, on fetal folliculogenesis in pigs.

4.4.1.2 Overnutrition

To our knowledge, the impact of overnutrition on the ovarian reserve in farm animals has not been examined.

4.4.1.3 Endocrine Disruptors

Testosterone

Extensive research has been conducted to address the effects of excess fetal testosterone exposure using an ovine model (Padmanabhan and Veiga-Lopez, 2013a, 2013b). Two windows of prenatal exogenous testosterone treatment have been investigated: an early and long exposure from the beginning of gonadal differentiation to shortly after the formation of primordial follicles (from day 30 to 90 of gestation; T30–90), and a late but shorter exposure window beginning at the start of meiosis (from day 60 to 90 of gestation; T60–90) (Padmanabhan and Veiga-Lopez, 2014). The reproductive and metabolic phenotypic characteristics of T30–90 sheep are analogous to those of women with polycystic ovarian syndrome (PCOS), perhaps the most important unresolved reproductive disorder in women (Diamanti-Kandarakis and Dunaif, 2012). One of the major phenotypic characteristics of T30–90 ewes is not only a reduced ovarian reserve (Padmanabhan and Veiga-Lopez, 2014) but also the accumulation of antral follicles potentially caused by an increased follicular recruitment (Smith *et al.*, 2009) or by an increased follicular persistence (Manikkam *et al.*, 2006), which is characteristic of women with PCOS (Abbott *et al.*, 2005). Also, T30–90 females showed progressive deterioration of reproductive cyclicity culminating in anovulation during their second breeding season. In contrast, most of the T60–90 cycled. These differences in response to testosterone treatments may be the result of whether fetuses were exposed to excess testosterone during a critical window of susceptibility (Birch *et al.*, 2003).

Collectively, these studies provide evidence for a negative impact of prenatal and neonatal exposure to testosterone on the ovarian reserve and ovarian function in sheep.

Downloaded From Vet-eBooks.com

4.4.2 Rodent Models

4.4.2.1 Undernutrition

In rats, maternal protein restriction decreased the number of preantral and antral follicles and altered expression of key genes involved in follicular development and steroidogenesis in prepubertal female offspring (Guzmán *et al.*, 2014; Bernal *et al.*, 2010). Thus, like farm animal models, undernutrition during pregnancy in rodents diminishes the ovarian reserve in offspring.

4.4.2.2 Overnutrition

Pregnant rabbits exposed to a high-fat diet had offspring with higher numbers of atretic follicles, but similar numbers of healthy primordial, primary, and secondary follicles compared to controls. Reproductive capacity, as assessed by the pregnancy rates and number of offspring per doe, was not altered by prenatal diet (Léveillé *et al.*, 2014). It must be noted that in rabbits the first germ cells are detected 9 days post coitum, but the first signs of meiosis in postnatal life are at approximately 2 weeks after birth and not during fetal life (Gondos, 1969). Hence, this may explain why a high-fat diet during pregnancy in rabbits may not impair the ovarian reserve of offspring.

4.4.2.3 Endocrine Disruptors

BPA

Oocytes from female fetuses exposed to low, environmentally relevant doses of BPA during mid-gestation displayed gross aberrations in meiotic prophase, including synaptic defects and increased levels of recombination (Susiarjo *et al.*, 2007). In the mature female, these aberrations were translated into an increase in aneuploid eggs and embryos (Susiarjo *et al.*, 2007).

Testosterone

In a recent study, pregnant rats were exposed to exogenous testosterone on days 16–19 (group 1) and 20 of gestation (group 2). A significant increase in the number of preantral and antral follicles was observed in ovaries of offspring of group 1 but not group 2 compared to controls (Ramezani Tehrani *et al.*, 2014).

4.4.3 Humans/Primates

4.4.3.1 Undernutrition

Although maternal malnutrition has a well-established negative impact on health of offspring (Barker, 2007; de Boo and Harding, 2006), the impact of undernutrition on the ovarian reserve in human progeny remains largely uninvestigated. A decreased number of primordial follicles was observed in growth-retarded fetuses following placental insufficiency, which can cause severe malnutrition of the fetus (de Bruin *et al.*, 1998).

In contrast, two separate studies that measured serum AMH concentrations, a widely used indicator of the ovarian reserve in humans (Broer *et al.*, 2014), showed no differences in AMH concentrations in both normal and small for gestational age prepubertal girls (Lem *et al.*, 2011) and sexually mature young women (Kerkhof *et al.*, 2010). Such discrepancy between studies may be due to the fact that in the first study placental insufficiency was so severe that fetuses did not survive, whereas in the other two studies girls were born small for gestational age because of different conditions (i.e., preterm birth) that did not impact the ovarian reserve.

Downloaded From Vet-eBooks.com

4.4.3.2 Overnutrition

High maternal pre-pregnancy body mass index (BMI) has been correlated with the high rates of preterm delivery, congenital defects, child morbidity, child respiratory problems (e.g., asthma), and children's mortality (Papachatzi *et al.*, 2013). However, the impact of overnutrition on indicators of the size of the ovarian reserve, such as age at menopause and AMH concentrations, in humans/primates has not been evaluated.

4.4.3.3 Endocrine Disruptors

Impact of maternal exposure to excess testosterone or BPA on the ovarian reserve in humans/primates has not been reported.

4.5 Impact of Prenatal Environmental Challenges on Ovarian Function (e.g., Pituitary Gonadotropin Secretion, Ovarian Hormone/Growth Factor Production, Response to Gonadotropins, Follicle Development, Irregular Reproductive Cycles, and Ovulation Rate) in Offspring

4.5.1 Farm Animal Models

4.5.1.1 Undernutrition

In sheep, maternal undernutrition from mating until day 95 of gestation reduced ovulation rates in adult offspring (Rae *et al.*, 2002). In contrast, maternal undernutrition during the last 100 days of pregnancy in sheep did not impact ovulation rate (Gunn *et al.*, 1995). This indicates that the earliest phases of fetal life and ovarian development, in agreement with other studies (Padmanabhan and Veiga-Lopez, 2014; Richardson *et al.*, 2014; Sloboda *et al.*, 2011; Dupont *et al.*, 2012), are likely more sensitive to maternal nutritional imbalances than later phases of development.

Ten-month-old female lambs undernourished as fetuses during the first month of pregnancy had a higher FSH response to GnRH challenge and higher numbers of small (2–3 mm diameter) follicles. When nutritional restriction was imposed from day 31 to 100 of gestation, a lower number of corpora lutea were observed, indicating a decreased number of ovulations (Kotsampasi *et al.*, 2009). Finally, a low-protein diet during gestation and lactation in sows increased circulating estradiol concentrations in prepubertal offspring (Sui *et al.*, 2014). These results further confirm the relevance of the timing and length of maternal undernutrition on impairment of ovarian function in offspring.

4.5.1.2 Overnutrition

Studies on the association between maternal overnutrition and ovarian function in offspring have not been conducted in farm animals.

4.5.1.3 Endocrine Disruptors

Testosterone

In the above-mentioned T30–90 sheep model, offspring exhibited disrupted cycles, had reduced proportion of ewes with normal cycles, increased rates of ewes with low progesterone production during estrous cycles, decreased proportion of ewes with ovulatory cycles, persistent follicles, and reduced number of corpora lutea in those that cycled (Manikkam *et al.*, 2006;

Downloaded From Vet-eBooks.com

Birch *et al.*, 2003; Clarke *et al.*, 1977). In addition, these ewes had increased preovulatory concentrations of estradiol, delayed and reduced preovulatory LH surges (Veiga-Lopez *et al.*, 2009), and disruption of both the negative and positive feedback systems that regulate GnRH secretion (Veiga-Lopez *et al.*, 2009; Wood and Foster, 1998; Sarma *et al.*, 2005; Sharma *et al.*, 2002; Unsworth *et al.*, 2005; Robinson *et al.*, 1999; Manikkam *et al.*, 2008) compared with control ewes.

BPA

Treatment of pregnant sheep with BPA from day 30 to 90 of gestation resulted in low birth weight, increased LH concentrations, and diminished preovulatory LH surges and cycle disruptions in female offspring (Savabieasfahani *et al.*, 2006), thus supporting a negative impact of maternal BPA exposure on ovarian function in offspring.

4.5.2 Rodent Models

4.5.2.1 Undernutrition

Maternal undernutrition during the last week of gestation in rats increased plasma FSH concentrations and reduced ovarian and uterine weights in offspring at weaning (Léonhardt *et al.*, 2003). Although circulating concentrations of LH, estradiol, and progesterone (indices of pituitary–ovarian function) were not affected in this study (Léonhardt *et al.*, 2003), there was a reduction in percentage of secondary follicles, and a greater number of small, but reduced number of large antral follicles at weaning in offspring. Results implied that maternal food restriction directly altered FSH secretion, thereby disrupting normal folliculogenesis or alternatively that reduced nutrition decreased follicle numbers resulting in less negative feedback and higher FSH secretion. It should be noted that increased FSH secretion is a well-established marker for a diminished ovarian reserve in many species (Burns *et al.*, 2005; Ireland *et al.*, 2007; Iliodromiti and Nelson, 2013; Mossa *et al.*, 2010).

4.5.2.2 Overnutrition

Maternal high-fat diet during gestation resulted in a greater proportion of offspring showing both irregular estrous cycles and prolonged or persistent estrus in rats (Connor *et al.*, 2012).

4.5.2.3 Endocrine Disruptors

Testosterone

Female adult rats exposed as fetuses to exogenous testosterone on day 20 of gestation had higher testosterone and LH concentrations, but lower estrogen and AMH levels compared to controls. However, no effect was detected on offspring ovarian function when testosterone was administered on day 16–19 of gestation (Ramezani Tehrani *et al.*, 2014). These findings suggest the presence of different windows of sensitivity of fetuses to testosterone, similar to nutritional imbalances (Rae *et al.*, 2002a, 2002b; Gunn *et al.*, 1995; Sloboda *et al.*, 2011).

4.5.3 Humans/Primates

4.5.3.1 Undernutrition

Maternal nutrition is recognized as one of the determinants of fetal growth (Knudsen *et al.*, 2008), hence fetal development has often been used as a marker of *in utero* nutrition (Salam *et al.*, 2014). Young women born small for gestational age have reduced ovarian volume, increased FSH secretion, and reduced ovulation rates (Ibáñez *et al.*, 2000, 2002a, 2002b). Results suggest a negative impact of maternal malnutrition on offspring ovarian function in women.

Downloaded From Vet-eBooks.com

Nevertheless, it must be noted that fetal growth is also largely determined by nonnutritional factors, such as genetics, placental function, maternal age, and disease, hence the link between maternal undernutrition and ovarian function is equivocal in women.

4.5.3.2 Overnutrition and Endocrine Disruptors

Growing evidence indicates that implantation and pregnancy rates are lower in obese women than those of normal weight (Gu *et al.*, 2015); however, studies on the impact of overnutrition, as well as excess maternal testosterone or BPA, on ovarian function in the progeny in humans/primates are lacking.

4.6 Impact of Prenatal Environmental Challenges on Fertility (as Measured by Conception Rates, Fecundity, or Age at Puberty or Menopause) in Offspring

4.6.1 Farm Animal Models

4.6.1.1 Undernutrition

The impact of undernutrition on offspring fertility in farm animals has not been directly examined. However, undernutrition at early stages of nutrition reduces AFC (Mossa *et al.*, 2013) and cattle with low AFC have poorer fertility than cows with a higher AFC (Mossa *et al.*, 2012; Jimenez-Krassel *et al.*, 2015). Hence, it is plausible to suggest that undernutrition has negative effects on fertility in cattle.

4.6.1.2 Overnutrition

In seasonal breeding calving systems, it is desirable that cows establish pregnancy following natural mating or service early in their breeding season. This ensures mothers rapidly return to service after calving. A study conducted in beef cattle reports that an increased proportion of heifers born to mothers fed a high- versus low- or moderate-nutrient diet during the third trimester of pregnancy calved in the first 21 days of their first calving season (Cushman *et al.*, 2014). This observation provides evidence for a moderate positive effect of a diet with high nutritional levels during the last third of gestation on reproductive efficiency in female offspring.

4.6.1.3 Endocrine Disruptors

Testosterone

Offspring of T30–90 ewes had lower pregnancy rates compared to controls (Steckler *et al.*, 2007), but further research on the impact of excess testosterone or BPA during gestation on offspring fertility is needed.

4.6.2 Rodent Models

4.6.2.1 Undernutrition

In rats, two separate studies reported different results. In the first one maternal nutrient restriction during pregnancy resulted in an early onset of puberty in female offspring (Sloboda *et al.*, 2009), whereas in the second one maternal food restriction during gestation did not affect the timing of puberty in both male and female pups.(Léonhardt *et al.*, 2003).

Downloaded From Vet-eBooks.com

4.6.2.2 Overnutrition

Similar to maternal undernutrition (Sloboda *et al.*, 2009), maternal consumption of a high-fat diet both prior to and during pregnancy caused an early onset of puberty and determined obesity in female rat offspring (Sloboda *et al.*, 2009).

4.6.2.3 Endocrine Disruptors

Studies on the effects of excess testosterone and BPA exposure during pregnancy on offspring fertility are lacking in both rodents and humans/primates.

4.6.3 Humans/Primates

4.6.3.1 Undernutrition

Associations between prenatal famine and subsequent reproductive performance were conducted for women born in Amsterdam from August 1, 1944, through April 15, 1946, a period encompassing a severe 5-month famine (Lumey and Stein, 1997; Painter *et al.*, 2008; Yarde *et al.*, 2013) and mixed outcomes were produced depending on when measurements were made. No effect of famine exposure was reported on a range of measures of fertility, such as age at menarche, proportion of women having no children, age at first delivery, and family size, in 43-years-old women (Lumey and Stein, 1997). When the same women were examined at 50 years of age, a small but significant decrease in the prevalence of nulliparity was detected for women subjected to famine as fetuses (Painter *et al.*, 2008). Finally, no association between intrauterine famine exposure and reproductive performance was reported on the same women after menopause. However, women born to mothers exposed to the famine were 24% more likely to experience natural menopause at any age compared to controls, suggesting that natural menopause occurred earlier after prenatal famine exposure (Yarde *et al.*, 2013).

Birth weight is considered a proxy for intrauterine nutritional status; the potential association between birth weight and subsequent age at menopause has been investigated. Women born light or heavy for gestational age had increased odds of being postmenopausal by 44–45 years compared to women with normal birth weight per gestational age (Tom *et al.*, 2010). In support of this finding, a weak association existed between birth weight and age at menopause (Painter *et al.*, 2008). In contrast to these studies, however, age at menopause was shown to vary by duration of breastfeeding, weight at 2 years of age, childhood socioeconomic status, but not birth weight (Hardy and Kuh, 2002). In addition, two other studies also failed to show an association between birth weight and age at menopause (Treloar *et al.*, 2000; Cresswell *et al.*, 1997). Taken together, these results imply that maternal factors other than those that impact birth weight may have a critical role in determining age at menopause of progeny.

4.6.3.2 Overnutrition

In women, maternal obesity is associated with younger age at menarche (Keim *et al.*, 2009), but, to our knowledge, the possible link between maternal overnutrition and reproductive capacity in daughters has not been fully unravelled yet.

4.7 Summary and Conclusion

The concept that conditions during fetal and perinatal life can have long-term consequences on our health is now widely accepted, but the effects on the reproductive axis are yet to be fully explored. Evidence indicates that the earliest stages of gestation may be the most sensitive to environmental factors because nutritional imbalances and EDC may reduce number of fetal

Downloaded From Vet-eBooks.com

oogonia and follicles, which in turn permanently impairs the ovarian reserve, ovarian function, and fertility of female offspring. The mechanisms by which environmental factors exert such effects remain unclear. For example, a reduction in oocyte numbers may be the direct result of reduced germ cell proliferation or indirect result of impaired vascularization of the ovary. Understanding these pathways may provide new insights into the factors that cause or contribute to suboptimal fertility in different mammals, including women.

References

Abbott, D.H., Barnett, D.K., Bruns, C.M., and Dumesic, D.A. (2005) Androgen excess fetal programming of female reproduction: a developmental aetiology for polycystic ovary syndrome? *Hum. Reprod. Update*, **11**, 357–374.

Barker, D.J. (2007) The origins of the developmental origins theory. *J. Intern. Med.*, **261**, 412–417.

Bernal, A.B., Vickers, M.H., Hampton, M.B., Poynton, R.A., and Sloboda, D.M. (2010) Maternal undernutrition significantly impacts ovarian follicle number and increases ovarian oxidative stress in adult rat offspring. *PLoS One*, **5**, e15558.

Birch, R.A., Padmanabhan, V., Foster, D.L., Unsworth, W.P., and Robinson, J.E. (2003) Prenatal programming of reproductive neuroendocrine function: fetal androgen exposure produces progressive disruption of reproductive cycles in sheep. *Endocrinology*, **144**, 1426–1434.

Black, R., Victora, C., Walker, S., Bhutta, Z., Christian, P., de Onis, M. *et al.* (2013) Maternal and child undernutrition and overweight in low-income and middle-income countries. *Lancet*, **382**, 427–451.

Borwick, S.C., Rhind, S.M., McMillen, S.R., and Racey, P.A. (1997) Effect of undernutrition of ewes from the time of mating on fetal ovarian development in mid gestation. *Reprod. Fertil. Dev.*, **9**, 711–715.

Broer, S.L., Broekmans, F.J., Laven, J.S., and Fauser, B.C. (2014) Anti-Müllerian hormone: ovarian reserve testing and its potential clinical implications. *Hum. Reprod. Update*, **20**, 688–701.

Burns, D.S., Jimenez-Krassel, F., Ireland, J.L., Knight, P.G., and Ireland, J.J. (2005) Numbers of antral follicles during follicular waves in cattle: evidence for high variation among animals, very high repeatability in individuals, and an inverse association with serum follicle-stimulating hormone concentrations. *Biol. Reprod.*, **73**, 54–62.

Clarke, I.J., Scaramuzzi, R.J., and Short, R.V. (1977) Ovulation in prenatally androgenized ewes. *J. Endocrinol.*, **73**, 385–389.

Connor, K.L., Vickers, M.H., Beltrand, J., Meaney, M.J., and Sloboda, D.M. (2012) Nature, nurture or nutrition? Impact of maternal nutrition on maternal care, offspring development and reproductive function. *J. Physiol.*, **590**, 2167–2180.

Cresswell, J.L., Egger, P., Fall, C.H., Osmond, C., Fraser, R.B., and Barker, D.J. (1997) Is the age of menopause determined *in-utero*? *Early Hum. Dev.*, **49**, 143–148.

Cupps, P. (1991) *Reproduction in Domestic Animals*, 4th edn, Academic Press, Inc., San Diego, CA.

Cushman, R.A., McNeel, A.K., and Freetly, H.C. (2014) The impact of cow nutrient status during the second and third tremesters on age at puberty, antral follicle count, and fertility of daughters. *Livest. Sci.*, **162**, 252–258.

Da Silva, P., Aitken, R.P., Rhind, S.M., Racey, P.A., and Wallace, J.M. (2002) Impact of maternal nutrition during pregnancy on pituitary gonadotrophin gene expression and ovarian development in growth-restricted and normally grown late gestation sheep fetuses. *Reproduction*, **123**, 769–777.

Downloaded From Vet-eBooks.com

Da Silva, P., Aitken, R.P., Rhind, S.M., Racey, P.A., and Wallace, J.M. (2003) Effect of maternal overnutrition during pregnancy on pituitary gonadotrophin gene expression and gonadal morphology in female and male foetal sheep at day 103 of gestation. *Placenta*, **24**, 248–257.

Da Silva-Buttkus, P., van den Hurk, R., te Velde, E.R., and Taverne, M.A. (2003) Ovarian development in intrauterine growth-retarded and normally developed piglets originating from the same litter. *Reproduction*, **126**, 249–258.

de Boo, H.A. and Harding, J.E. (2006) The developmental origins of adult disease (Barker) hypothesis. *Aust. N. Z. J. Obstet. Gynaecol.*, **46**, 4–14.

de Bruin, J.P., Dorland, M., Bruinse, H.W., Spliet, W., Nikkels, P.G., and Te Velde, E.R. (1998) Fetal growth retardation as a cause of impaired ovarian development. *Early Hum. Dev.*, **51**, 39–46.

Diamanti-Kandarakis, E. and Dunaif, A. (2012) Insulin resistance and the polycystic ovary syndrome revisited: an update on mechanisms and implications. *Endocr. Rev.*, **33**, 981–1030.

Dupont, C., Cordier, A.G., Junien, C., Mandon-Pépin, B., Levy, R., and Chavatte-Palmer, P. (2012) Maternal environment and the reproductive function of the offspring. *Theriogenology*, **78**, 1405–1414.

Gondos, B. (1969) Ultrastructure of the germinal epithelium during oogenesis in the rabbit. *J. Exp. Zool.*, **172**, 465–479.

Gopalakrishnan, G.S., Gardner, D.S., Rhind, S.M., Rae, M.T., Kyle, C.E., Brooks, A.N. *et al.* (2004) Programming of adult cardiovascular function after early maternal undernutrition in sheep. *Am. J. Physiol. Regul. Integr. Comp. Physiol.*, **287**, R12–R20.

Gu, L., Liu, H., Gu, X., Boots, C., Moley, K.H., and Wang, Q. (2015) Metabolic control of oocyte development: linking maternal nutrition and reproductive outcomes. *Cell Mol. Life Sci.*, **72**, 251–271.

Gunn, R.G., Sim, D.A., and Hunter, E.A. (1995) Effects of nutrition *in-utero* and in early-life on the subsequent lifetime reproductive performance of Scottish Blackface ewes in 2 management systems. *Anim. Sci.*, **60**, 223–230.

Guzmán, C., García-Becerra, R., Aguilar-Medina, M.A., Méndez, I., Merchant-Larios, H., and Zambrano, E. (2014) Maternal protein restriction during pregnancy and/or lactation negatively affects follicular ovarian development and steroidogenesis in the prepubertal rat offspring. *Arch. Med. Res.*, **45**, 294–300.

Hardy, R. and Kuh, D. (2002) Does early growth influence timing of the menopause? Evidence from a British birth cohort. *Hum. Reprod.*, **17**, 2474–2479.

Hunt, P.A., Lawson, C., Gieske, M., Murdoch, B., Smith, H., Marre, A. *et al.* (2012) Bisphenol A alters early oogenesis and follicle formation in the fetal ovary of the rhesus monkey. *Proc. Natl. Acad. Sci. USA*, **109**, 17525–17530.

Ibáñez, L., Potau, N., Enriquez, G., and de Zegher, F. (2000) Reduced uterine and ovarian size in adolescent girls born small for gestational age. *Pediatr. Res.*, **47**, 575–577.

Ibáñez, L., Valls, C., Cols, M., Ferrer, A., Marcos, M.V., and De Zegher, F. (2002a) Hypersecretion of FSH in infant boys and girls born small for gestational age. *J. Clin. Endocrinol. Metab.*, **87**, 1986–1988.

Ibáñez, L., Potau, N., Ferrer, A., Rodriguez-Hierro, F., Marcos, M.V., and de Zegher, F. (2002b) Reduced ovulation rate in adolescent girls born small for gestational age. *J. Clin. Endocrinol. Metab.*, **87**, 3391–3393.

Iliodromiti, S. and Nelson, S.M. (2013) Biomarkers of ovarian reserve. *Biomark. Med.*, **7**, 147–158.

Ireland, J.J., Ward, F., Jimenez-Krassel, F., Ireland, J.L., Smith, G.W., Lonergan, P. *et al.* (2007) Follicle numbers are highly repeatable within individual animals but are inversely correlated with FSH concentrations and the proportion of good-quality embryos after ovarian stimulation in cattle. *Hum. Reprod.*, **22**, 1687–1695.

Downloaded From Vet-eBooks.com

Ireland, J.L., Scheetz, D., Jimenez-Krassel, F., Themmen, A.P., Ward, F., Lonergan, P. *et al.* (2008) Antral follicle count reliably predicts number of morphologically healthy oocytes and follicles in ovaries of young adult cattle. *Biol. Reprod.*, **79**, 1219–1225.

Ireland, J.J., Smith, G.W., Scheetz, D., Jimenez-Krassel, F., Folger, J.K., Ireland, J.L. *et al.* (2011) Does size matter in females? An overview of the impact of the high variation in the ovarian reserve on ovarian function and fertility, utility of anti-Müllerian hormone as a diagnostic marker for fertility and causes of variation in the ovarian reserve in cattle. *Reprod. Fertil. Dev.*, **23**, 1–14.

Jimenez-Krassel, F., Folger, J.K., Ireland, J.L., Smith, G.W., Hou, X., Davis, J.S. *et al.* (2009) Evidence that high variation in ovarian reserves of healthy young adults has a negative impact on the corpus luteum and endometrium during estrous cycles in cattle. *Biol. Reprod.*, **80**, 1272–1281.

Jimenez-Krassel, F., Scheetz, D., Neuder, L.M., Ireland, J.L.H., Pursley, J.R., Smith, G.W. *et al.* (2015) Anti-Müllerian hormone concentration in dairy heifers is positively associated with productive herd life. *J. Dairy Sci.*, **98** (5), 2355–2361.

Keim, S.A., Branum, A.M., Klebanoff, M.A., and Zemel, B.S. (2009) Maternal body mass index and daughters' age at menarche. *Epidemiology*, **20**, 677–681.

Kelly, T., Yang, W., Chen, C.S., Reynolds, K., and He, J. (2008) Global burden of obesity in 2005 and projections to 2030. *Int. J. Obes. (Lond).*, **32**, 1431–1437.

Kerkhof, G.F., Leunissen, R.W., Willemsen, R.H., de Jong, F.H., Visser, J.A., Laven, J.S. *et al.* (2010) Influence of preterm birth and small birth size on serum anti-Müllerian hormone levels in young adult women. *Eur. J. Endocrinol.*, **163**, 937–944.

Kerr, J.B., Myers, M., and Anderson, R.A. (2013) The dynamics of the primordial follicle reserve. *Reproduction*, **146**, R205–R215.

Knudsen, V.K., Orozova-Bekkevold, I.M., Mikkelsen, T.B., Wolff, S., and Olsen, S.F. (2008) Major dietary patterns in pregnancy and fetal growth. *Eur. J. Clin. Nutr.*, **62**, 463–470.

Kotsampasi, B., Chadio, S., Papadomichelakis, G., Deligeorgis, S., Kalogiannis, D., Menegatos, I. *et al.* (2009) Effects of maternal undernutrition on the hypothalamic–pituitary–gonadal axis function in female sheep offspring. *Reprod. Domest. Anim.*, **44**, 677–684.

Langley-Evans, S.C. and McMullen, S. (2010) Developmental origins of adult disease. *Med. Princ. Pract.*, **19**, 87–98.

Lem, A.J., Boonstra, V.H., Renes, J.S., Breukhoven, P.E., de Jong, F.H., Laven, J.S. *et al.* (2011) Anti-Mullerian hormone in short girls born small for gestational age and the effect of growth hormone treatment. *Hum. Reprod.*, **26**, 898–903.

Léonhardt, M., Lesage, J., Croix, D., Dutriez-Casteloot, I., Beauvillain, J.C., and Dupouy, J.P. (2003) Effects of perinatal maternal food restriction on pituitary–gonadal axis and plasma leptin level in rat pup at birth and weaning and on timing of puberty. *Biol. Reprod.*, **68**, 390–400.

Léveillé, P., Tarrade, A., Dupont, C., Larcher, T., Dahirel, M., Poumerol, E. *et al.* (2014) Maternal high-fat diet induces follicular atresia but does not affect fertility in adult rabbit offspring. *J. Dev. Orig. Health Dis.*, **5**, 88–97.

Lumey, L.H. and Stein, A.D. (1997) *In utero* exposure to famine and subsequent fertility: the Dutch Famine Birth Cohort Study. *Am. J. Public Health*, **87**, 1962–1966.

Manikkam, M., Steckler, T.L., Welch, K.B., Inskeep, E.K., and Padmanabhan, V. (2006) Fetal programming: prenatal testosterone treatment leads to follicular persistence/luteal defects; partial restoration of ovarian function by cyclic progesterone treatment. *Endocrinology*, **147**, 1997–2007.

Manikkam, M., Thompson, R.C., Herkimer, C., Welch, K.B., Flak, J., Karsch, F.J. *et al.* (2008) Developmental programming: impact of prenatal testosterone excess on pre- and postnatal gonadotropin regulation in sheep. *Biol. Reprod.*, **78**, 648–660.

Downloaded From Vet-eBooks.com

Monniaux, D., Clément, F., Dalbiès-Tran, R., Estienne, A., Fabre, S., Mansanet, C. *et al.* (2014) The ovarian reserve of primordial follicles and the dynamic reserve of antral growing follicles: what is the link? *Biol. Reprod.*, **90**, 85.

Mossa, F., Jimenez-Krassel, F., Walsh, S., Berry, D.P., Butler, S.T., Folger, J. *et al.* (2010) Inherent capacity of the pituitary gland to produce gonadotropins is not influenced by the number of ovarian follicles > or = 3 mm in diameter in cattle. *Reprod. Fertil. Dev.*, **22**, 550–557.

Mossa, F., Walsh, S.W., Butler, S.T., Berry, D.P., Carter, F., Lonergan, P. *et al.* (2012) Low numbers of ovarian follicles ≥3 mm in diameter are associated with low fertility in dairy cows. *J. Dairy Sci.*, **95**, 2355–2361.

Mossa, F., Carter, F., Walsh, S.W., Kenny, D.A., Smith, G.W., Ireland, J.L. *et al.* (2013) Maternal undernutrition in cows impairs ovarian and cardiovascular systems in their offspring. *Biol. Reprod.*, **88**, 92.

Mossa, F., Walsh, S.W., Ireland, J.J., and Evans, A.C.O. (2015) Early nutritional programming and progeny performance: is reproductive success already set at birth? *Anim. Front.*, doi: 10.2527/af.2015-0004.

Murdoch, W.J., Van Kirk, E.A., Vonnahme, K.A., and Ford, S.P. (2003) Ovarian responses to undernutrition in pregnant ewes, USA. *Reprod. Biol. Endocrinol.*, **1**, 6.

Padmanabhan, V. and Veiga-Lopez, A. (2013a) Animal models of the polycystic ovary syndrome phenotype. *Steroids*, **78**, 734–740.

Padmanabhan, V. and Veiga-Lopez, A. (2013b) Sheep models of polycystic ovary syndrome phenotype. *Mol. Cell Endocrinol.*, **373**, 8–20.

Padmanabhan, V. and Veiga-Lopez, A. (2014) Reproduction symposium: developmental programming of reproductive and metabolic health. *J. Anim. Sci.*, **92**, 3199–3210.

Padmanabhan, V., Smith, P., and Veiga-Lopez, A. (2012) Developmental programming: impact of prenatal testosterone treatment and postnatal obesity on ovarian follicular dynamics. *J. Dev. Orig. Health Dis.*, **3**, 276–286.

Painter, R.C., Westendorp, R.G., de Rooij, S.R., Osmond, C., Barker, D.J., and Roseboom, T.J. (2008) Increased reproductive success of women after prenatal undernutrition. *Hum. Reprod.*, **23**, 2591–2595.

Papachatzi, E., Dimitriou, G., Dimitropoulos, K., and Vantarakis, A. (2013) Pre-pregnancy obesity: maternal, neonatal and childhood outcomes. *J. Neonatal Perinatal Med.*, **6**, 203–216.

Quesada, I., Fuentes, E., Viso-León, M.C., Soria, B., Ripoll, C., and Nadal, A. (2002) Low doses of the endocrine disruptor bisphenol-A and the native hormone 17beta-estradiol rapidly activate transcription factor CREB. *FASEB J.*, **16**, 1671–1673.

Rae, M.T., Palassio, S., Kyle, C.E., Brooks, A.N., Lea, R.G., Miller, D.W. *et al.* (2001) Effect of maternal undernutrition during pregnancy on early ovarian development and subsequent follicular development in sheep fetuses. *Reproduction*, **122**, 915–922.

Rae, M.T., Kyle, C.E., Miller, D.W., Hammond, A.J., Brooks, A.N., and Rhind, S.M. (2002a) The effects of undernutrition, *in utero*, on reproductive function in adult male and female sheep. *Anim. Reprod. Sci.*, **72**, 63–71.

Rae, M.T., Rhind, S.M., Kyle, C.E., Miller, D.W., and Brooks, A.N. (2002b) Maternal undernutrition alters triiodothyronine concentrations and pituitary response to GnRH in fetal sheep. *J. Endocrinol.*, **173**, 449–455.

Ramezani Tehrani, F., Noroozzadeh, M., Zahediasl, S., Piryaei, A., Hashemi, S., and Azizi, F. (2014) The time of prenatal androgen exposure affects development of polycystic ovary syndrome-like phenotype in adulthood in female rats. *Int. J. Endocrinol. Metab.*, **12**, e16502.

Ribeiro, E.S., Bisinotto, R.S., Lima, F.S., Greco, L.F., Morrison, A., Kumar, A. *et al.* (2014) Plasma anti-Müllerian hormone in adult dairy cows and associations with fertility. *J. Dairy Sci.*, **97** (11), 6888–6900.

Downloaded From Vet-eBooks.com

Richardson, M.C., Guo, M., Fauser, B.C., and Macklon, N.S. (2014) Environmental and developmental origins of ovarian reserve. *Hum. Reprod. Update*, **20**, 353–369.

Robinson, J.E., Forsdike, R.A., and Taylor, J.A. (1999) *In utero* exposure of female lambs to testosterone reduces the sensitivity of the gonadotropin-releasing hormone neuronal network to inhibition by progesterone. *Endocrinology*, **140**, 5797–5805.

Rüsse, I. (1983) Oogenesis in cattle and sheep. *Bibl. Anat.*, **24**, 77–92.

Salam, R.A., Das, J.K., and Bhutta, Z.A. (2014) Multiple micronutrient supplementation during pregnancy and lactation in low-to-middle-income developing country settings: impact on pregnancy outcomes. *Ann. Nutr. Metab.*, **65**, 4–12.

Sarma, H.N., Manikkam, M., Herkimer, C., Dell'Orco, J., Welch, K.B., Foster, D.L. *et al.* (2005) Fetal programming: excess prenatal testosterone reduces postnatal luteinizing hormone, but not follicle-stimulating hormone responsiveness, to estradiol negative feedback in the female. *Endocrinology*, **146**, 4281–4291.

Savabieasfahani, M., Kannan, K., Astapova, O., Evans, N.P., and Padmanabhan, V. (2006) Developmental programming: differential effects of prenatal exposure to bisphenol-A or methoxychlor on reproductive function. *Endocrinology*, **147**, 5956–5966.

Senger, P. (2003) *Pathways to Pregnancy and Parturition*, 2nd edn, Current Conceptions Inc., Pullma, WA.

Sharma, T.P., Herkimer, C., West, C., Ye, W., Birch, R., Robinson, J.E. *et al.* (2002) Fetal programming: prenatal androgen disrupts positive feedback actions of estradiol but does not affect timing of puberty in female sheep. *Biol. Reprod.*, **66**, 924–933.

Sinclair, K.D. and Watkins, A.J. (2013) Parental diet, pregnancy outcomes and offspring health: metabolic determinants in developing oocytes and embryos. *Reprod. Fertil. Dev.*, **26**, 99–114.

Sloboda, D.M., Howie, G.J., Pleasants, A., Gluckman, P.D., and Vickers, M.H. (2009) Pre- and postnatal nutritional histories influence reproductive maturation and ovarian function in the rat. *PLoS One*, **4**, e6744.

Sloboda, D.M., Hickey, M., and Hart, R. (2011) Reproduction in females: the role of the early life environment. *Hum. Reprod. Update*, **17**, 210–227.

Smith, P., Steckler, T.L., Veiga-Lopez, A., and Padmanabhan, V. (2009) Developmental programming: differential effects of prenatal testosterone and dihydrotestosterone on follicular recruitment, depletion of follicular reserve, and ovarian morphology in sheep. *Biol. Reprod.*, **80**, 726–736.

Souza, A.H., Carvalho, P.D., Rozner, A.E., Vieira, L.M., Hackbart, K.S., Bender, R.W. *et al.* (2015) Relationship between circulating anti-Müllerian hormone (AMH) and superovulatory response of high-producing dairy cows. *J. Dairy Sci.*, **98**, 169–178.

Spencer, T.E., Dunlap, K.A., and Filant, J. (2012) Comparative developmental biology of the uterus: insights into mechanisms and developmental disruption. *Mol. Cell Endocrinol.*, **354**, 34–53.

Steckler, T.L., Roberts, E.K., Doop, D.D., Lee, T.M., and Padmanabhan, V. (2007) Developmental programming in sheep: administration of testosterone during 60–90 days of pregnancy reduces breeding success and pregnancy outcome. *Theriogenology*, **67**, 459–467.

Sui, S., He, B., Jia, Y., Li, R., Cai, D., Li, X. *et al.* (2014) Maternal protein restriction during gestation and lactation programs offspring ovarian steroidogenesis and folliculogenesis in the prepubertal gilts. *J. Steroid Biochem. Mol. Biol.*, **143C**, 267–276.

Sullivan, T.M., Micke, G.C., Greer, R.M., Irving-Rodgers, H.F., Rodgers, R.J., and Perry, V.E. (2009) Dietary manipulation of Bos indicus × heifers during gestation affects the reproductive development of their heifer calves. *Reprod. Fertil. Dev.*, **21**, 773–784.

Susiarjo, M., Hassold, T.J., Freeman, E., and Hunt, P.A. (2007) Bisphenol A exposure *in utero* disrupts early oogenesis in the mouse. *PLoS Genet.*, **3**, e5.

Downloaded From Vet-eBooks.com

Takeuchi, T., Tsutsumi, O., Ikezuki, Y., Takai, Y., and Taketani, Y. (2004) Positive relationship between androgen and the endocrine disruptor, bisphenol A, in normal women and women with ovarian dysfunction. *Endocr. J.*, **51**, 165–169.

Tom, S.E., Cooper, R., Kuh, D., Guralnik, J.M., Hardy, R., and Power, C. (2010) Fetal environment and early age at natural menopause in a British birth cohort study. *Hum. Reprod.*, **25**, 791–798.

Treloar, S.A., Sadrzadeh, S., Do, K.A., Martin, N.G., and Lambalk, C.B. (2000) Birth weight and age at menopause in Australian female twin pairs: exploration of the fetal origin hypothesis. *Hum. Reprod.*, **15**, 55–59.

Unsworth, W.P., Taylor, J.A., and Robinson, J.E. (2005) Prenatal programming of reproductive neuroendocrine function: the effect of prenatal androgens on the development of estrogen positive feedback and ovarian cycles in the ewe. *Biol. Reprod.*, **72**, 619–627.

Vandenberg, L.N., Maffini, M.V., Sonnenschein, C., Rubin, B.S., and Soto, A.M. (2009) Bisphenol-A and the great divide: a review of controversies in the field of endocrine disruption. *Endocr. Rev.*, **30**, 75–95.

Veiga-Lopez, A., Astapova, O.I., Aizenberg, E.F., Lee, J.S., and Padmanabhan, V. (2009) Developmental programming: contribution of prenatal androgen and estrogen to estradiol feedback systems and periovulatory hormonal dynamics in sheep. *Biol. Reprod.*, **80**, 718–725.

vom Saal, F.S. and Hughes, C. (2005) An extensive new literature concerning low-dose effects of bisphenol A shows the need for a new risk assessment. *Environ Health Perspect.*, **113**, 926–933.

Wood, R.I. and Foster, D.L. (1998) Sexual differentiation of reproductive neuroendocrine function in sheep. *Rev. Reprod.*, **3**, 130–40.

Yarde, F., Broekmans, F.J., van der Pal-de Bruin, K.M., Schönbeck, Y., te Velde, E.R., Stein, A.D. *et al.* (2013) Prenatal famine, birthweight, reproductive performance and age at menopause: the Dutch hunger winter families study. *Hum. Reprod.*, **28**, 3328–3336.

Downloaded From Vet-eBooks.com

5

Small Non-Coding RNAS in Gametogenesis

Lukasz Smorag[1] *and D. V. Krishna Pantakani*[1,2]

[1]*Institute of Human Genetics, University of Göttingen, Göttingen, Germany*
[2]*Department of Clinical Chemistry, University of Göttingen, Göttingen, Germany*

5.1 Small Non-Coding RNAs

The first endogenous small silencing RNA (RNA interference or RNAi) to be discovered was *lin-4*, which was identified to regulate the protein expression from *lin-14* mRNA (Lee *et al*., 1993; Wightman *et al*., 1993). The recent advances in genomic sequencing technologies together with computational and genetics experimental approaches have revealed the presence of RNAi mechanisms in almost all living organisms (Lagos-Quintana *et al*., 2001; Lau *et al*., 2001; Lee and Ambros, 2001; Shi *et al*., 2013; Wen *et al*., 2014). The functions of RNAi range from heterochromatin formation through mRNA degradation and translation repression (Chu and Rana, 2007). Growing body of evidence suggests that RNAi mechanisms are involved in different aspects of biological processes ranging from regulation of single cell metabolism through controlling of cell fate and development of multicellular organisms. RNAi molecules can be distinguished from other small non-coding RNAs (sncRNAs) such as small nuclear RNAs (snRNAs), small nucleolar RNAs (snoRNAs) or transfer RNAs (tRNAs) by their restricted size (~20–30 nucleotide (nt)) and their association with Argonaute (Ago) family proteins. Argonaute family of proteins from animals can be subdivided into Ago and Piwi subfamilies. Based on the biogenesis mechanisms and type of the Argonaut subfamily that they interact with, RNAi molecules are classified in three groups: microRNAs (miRNAs), endogenous small interfering RNAs (*endo*-siRNAs), and Piwi-interacting RNAs (piRNAs).

5.2 Function of sncRNAs in Gametogenesis

In sexually reproducing organisms, gametes are the only cells capable of transmitting genetic information from one generation to the next. Many transcriptional as well as posttranscriptional mechanisms have been reported to regulate the process of gametogenesis (Pangas and Rajkovic, 2006; Bettegowda and Wilkinson, 2010; Gan *et al*., 2013). One of the recently discovered mechanisms governing gametogenesis includes sncRNAs: miRNAs, *endo*-siRNAs, and piRNAs (Hale *et al*., 2014). By taking advantage of conditional knockout mouse models, many research groups have proven the importance of these sncRNAs in gametogenesis. The loss of total miRNAs caused by depletion of Drosha or Dicer, two enzymes vital for miRNAs biogenesis, specifically in primordial germ cells (PGCs) or spermatogonia, resulted in male infertility

Animal Models and Human Reproduction, First Edition. Edited by Heide Schatten and Gheorghe M. Constantinescu.
© 2017 John Wiley & Sons, Inc. Published 2017 by John Wiley & Sons, Inc.

Downloaded From Vet-eBooks.com

(Hayashi *et al*., 2008; Maatouk *et al*., 2008; Korhonen *et al*., 2011; Wu *et al*., 2012). Similarly, lack of Dicer or Ago2 proteins in mouse oocytes resulted in female infertility (Murchison *et al*., 2007; Kaneda *et al*., 2009).

The function of miRNAs seems to be evolutionary conserved, as Dicer mutation in *Drosophila melanogaster* or in *Caenorhabditis elegans* results in defects in germline formation and sterility (Knight and Bass, 2001; Forstemann *et al*., 2005; Park *et al*., 2007). Surprisingly, depletion of Dgcr8, a cofactor of Drosha, in mouse oocytes did not affect female fertility (Suh *et al*., 2010). Moreover, *Dgcr8*$^{-/-}$ oocytes can be fertilized by wild-type sperm and the resulting zygotes develop and give rise to healthy offspring (Suh *et al*., 2010). These results are in contradiction with previous reports and led to a suggestion that phenotypes observed in *Dicer*$^{-/-}$ females are probably caused by a lack of *endo*-siRNAs, rather than canonical miRNAs (Ma *et al*., 2010). In line with these assumptions, importance of *endo*-siRNAs was reported in the regulation of gene expression in mouse oocytes (Tam *et al*., 2008; Watanabe *et al*., 2008). Similarly, despite its crucial role in mouse spermatogenesis, loss of piRNAs does not have any effect on oocyte maturation or fertilization (Deng and Lin, 2002; Carmell *et al*., 2007; Kuramochi-Miyagawa *et al*., 2008). Taken together, RNAi mechanisms seem to have unequal contribution to gametes formation in male and female mouse models. miRNAs, *endo*-siRNAs, as well as piRNAs contribute to spermatogenesis, while only *endo*-siRNAs and noncanonical miRNAs seem to be crucial for mouse oogenesis. Due to this discrepancy as well as to the fact that scares material from oogenesis, most of the studies focus their investigations only in the process of spermatogenesis to elucidate the function of RNAi mechanisms in gametogenesis.

The following sections will delineate the current knowledge on biogenesis process of sncRNAs—miRNAs, *endo*-siRNAs, and piRNAs—and their function in gametogenesis, particularly in spermatogenesis.

5.2.1 miRNAs Biogenesis

miRNAs are one of the most abundant ncRNA families and best-studied RNAi molecules that regulate gene expression in a posttranscriptional manner. miRNAs are present in almost all living organisms, including plants and animals. The recent miRBase (release 21), the database that coordinate miRNAs naming and cataloging, contains 434 *C. elegans*, 1915 *Mus musculus*, and 2588 *Homo sapiens* miRNAs (Kozomara and Griffiths-Jones, 2014).

The schematic representation of canonical miRNA biosynthesis pathway is illustrated in Figure 5.1. Most of the known miRNAs belong to canonical miRNAs family and only a minor fraction is biosynthesized through noncanonical pathway. miRNAs are single-stranded RNAs (ssRNAs) derived from precursor transcripts called primary miRNAs (pri-miRNAs), which are typically transcribed by RNA polymerase II (RNA Pol II) (Cai *et al*., 2004; Lee *et al*., 2004). Usually, miRNAs are located in genome in close proximity to the other miRNAs (as cluster) and often are transcribed as a single polycistronic pri-miRNA transcript (Lee *et al*., 2002). A typical pri-miRNA spans over several kilobases in length and contains both a 5′ cap and poly(A) tail. It consists of one or more stems of ~33 base pairs (bp) with terminal loop and flanking ssRNA regions. Each single stem-loop structure is then recognized and cleaved in the nucleus by microprocessor complex to yield ~70 nucleotide (nt) hairpin-shaped precursor miRNA (pre-miRNA) (Lee *et al*., 2002). The microprocessor complex consists of ribonuclease III (RNase III), Drosha, and its cofactor DiGeorge syndrome critical region gene 8 (DGCR8) proteins in mammals (Lee *et al*., 2003; Denli *et al*., 2004). DGCR8 interacts with pri-miRNAs through the stem and ssRNA segments and directs Drosha to cleave the substrate (Han *et al*., 2004, 2006).

Following nuclear processing, the nuclear export protein, Exportin 5 together with Ran-GTPase, transports the pre-miRNAs to cytoplasm through nuclear pores (Yi *et al*., 2003).

Downloaded From Vet-eBooks.com

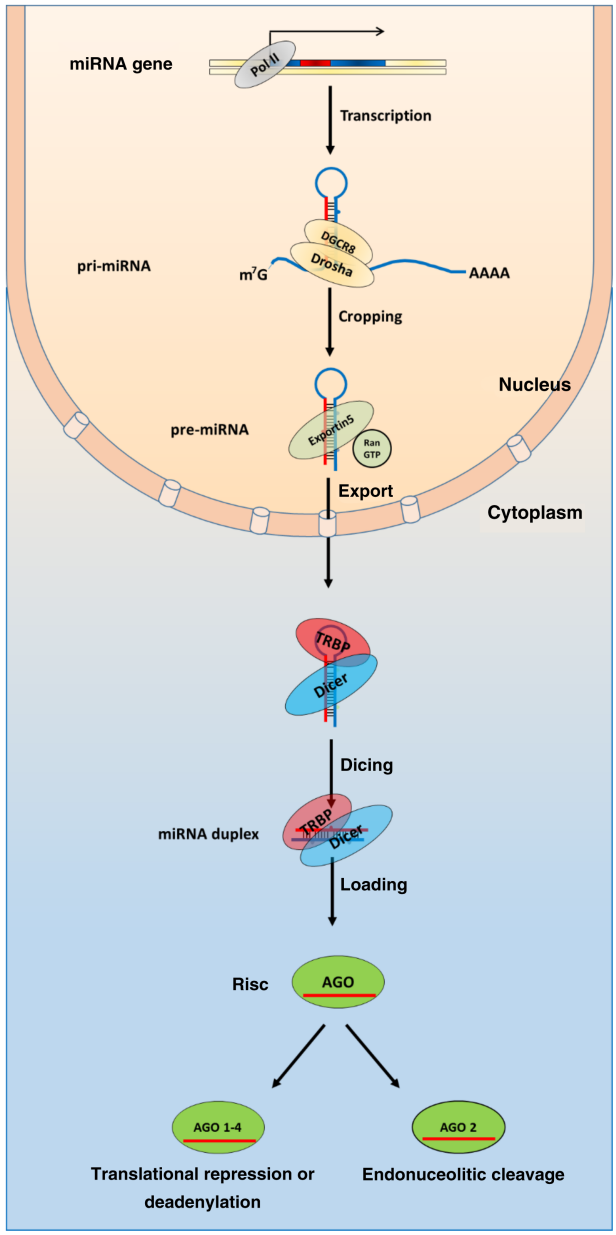

Figure 5.1 Canonical miRNA biosynthesis pathway. Canonical pathway of miRNA processing includes production of primary transcripts (pri-miRNAs) by RNA polymerase II (Pol II). Nascent pri-miRNA transcript is further processed by microprocessor complex (Drosha-Dgcr8) in the nucleus. The resulting precursor miRNAs (pre-miRNAs) are exported from the nucleus to the cytoplasm by Exportin-5-RanGTP complex. In the cytoplasm, pre-miRNAs are cropped further by Dicer to yield miRNA duplex, which is loaded into Ago protein by Dicer TRBP complex. Finally, only one strand from the duplex (termed mature or major) remains in Ago protein forming RISC and regulates the gene expression either by mRNA cleavage or translation repression. The other strand (minor) has no known function and is mostly degraded. (See color plate section.)

Downloaded From Vet-eBooks.com

In cytoplasm, pre-miRNAs undergo further processing catalyzed by other RNase III type protein, Dicer in mammals (Ketting *et al*., 2001). Pre-miRNAs are cleaved near the terminal loop, releasing ~22 nt miRNA duplex (Hutvagner *et al*., 2001). Mammalian Dicer interacts with TAR RNA-binding protein (TRBP). Although, TRBP is not required for processing activity itself, it seems to contribute to the formation of RNA-induced silencing complex (RISC) (Chendrimada *et al*., 2005; Haase *et al*., 2005). The resulting miRNA duplex is subsequently loaded into Ago proteins (Ago 1-4 in mammals) to create effector complex named RISC. Only one strand (major or guide) from miRNA duplex remains in Ago, whereas the other strand (star or passenger miRNA) is degraded. The strand selection and RISC assembly relay on the thermodynamic stabilities of the two miRNA strands in the duplex (Khvorova *et al*., 2003; Schwarz *et al*., 2003).

Mechanism by which major/guide miRNA executes its function depend on the degree of complementarity between miRNA and its target mRNA as well as on specific Ago protein in which the miRNA is loaded (Hutvagner and Zamore, 2002; Meister *et al*., 2004). Full complementarity causes mRNA cleavage and requires Ago2 protein while partial complementarity results in translation repression followed by mRNA deadenylation and engages other members of Ago subfamily (Ma *et al.*, 2010). Direct endonucleolytic cleavage of mRNA target in context of full complementarity is mostly restricted to plants and is a rare event in animals (Llave *et al*., 2002; Rhoades *et al*., 2002; Tang *et al*., 2003; Denli *et al*., 2004; Yekta *et al*., 2004). In animals, miRNAs bind to their target mRNAs through only a limited region called "seed site," leading to translational repression of target mRNAs (Lewis *et al*., 2003, 2005; Lai, 2004; Brennecke *et al*., 2005).

Noncanonical miRNAs bypass the processing by microprocessor complex by using other endonucleases or by direct transcription of a short hairpin-shaped precursor miRNAs. The resulting pre-miRNAs are then exported from the nucleus and are processed by Dicer, as in the canonical pathway (Ruby *et al*., 2007; Babiarz *et al*., 2008).

5.2.2 Function of miRNAs in the Process of Spermatogenesis

Spermatogenesis is a process common for all sexually reproducing animals through mitotic proliferation, meiotic divisions, and maturation phases to finally give rise to functional sperm (Cooke and Saunders, 2002). Since Dicer knockout results in male infertility due to depletion of germ cells, it signifies a need for identification of individual germ cell-specific miRNAs and to elucidate their role in spermatogenesis. In an attempt to identify miRNAs with a function in spermatogenesis, many research groups have characterized miRNA expression profiles of various germ cell populations or testicular cells isolated from prepubertal and adult mice (Yu *et al*., 2005; Ro *et al*., 2007; Yan *et al*., 2007; Song *et al*., 2009). Development of novel, more precise techniques for separation of testicular cells will enable to go even deeper and to identify miRNA profiles of single germ cell populations (Smorag *et al*., 2012). The cataloging of expression profile of germ-cell-specific miRNAs is similar to that of cataloging of coding genes; however, the identification of their function is difficult due to incomplete interaction between miRNA and its target mRNAs in animals, and also single miRNA can regulate several targets.

To recognize the function of selected miRNAs, it is necessary first to identify its targets. This step is mostly performed *in silico*, although additional *in vitro* and *in vivo* experiments are needed to identify the authentic mRNA targets. Until now, only few studies have investigated the function of germ cells specific miRNAs in the process of spermatogenesis and is summarized in Figure 5.2. The first characterized testis-specific miRNA was miR-122a (Yu *et al*., 2005). miR-122a is enriched in postmeiotic cells and regulates chromatin remodeling by targeting *Transition protein 2* (*Tnp2*) gene. In postmeiotic nuclei, histones are replaced by the transition

Downloaded From Vet-e-Books.com

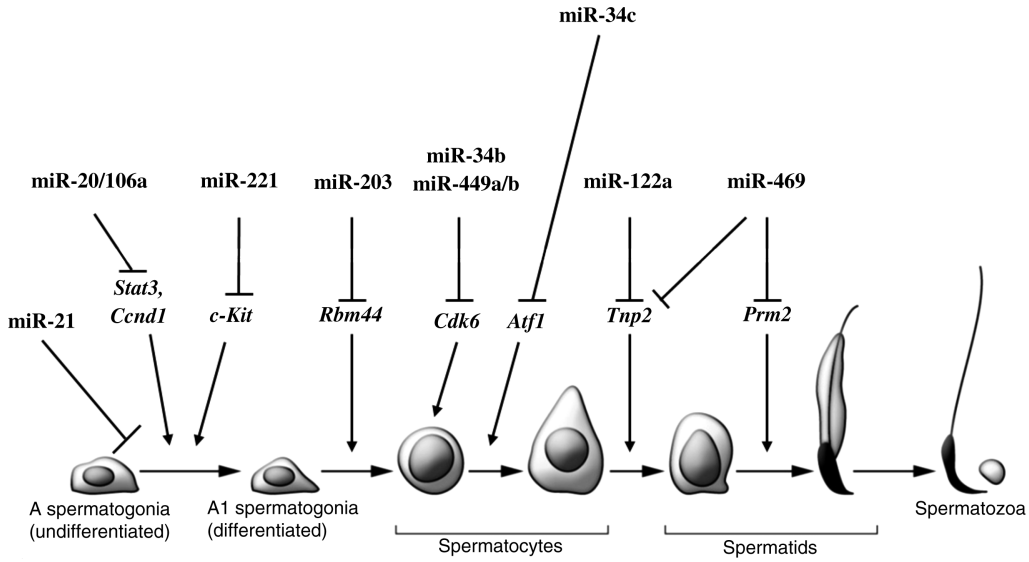

Figure 5.2 Working model for the miRNAs function during spermatogenesis. Spatiotemporal expression of miRNAs regulates sequential steps of male germ cells maturation. (Adapted and modified from Hogarth and Griswold (2010).)

proteins (Tnp1 and Tnp2) which in turn are replaced by the protamine (Prm1 and Prm2). Both Tnp and Prm proteins play an important role in the process of chromatin condensation and depletion of these proteins compromises male fertility (Zhao *et al*., 2004; Kempisty *et al*., 2006). Interestingly, Tnp2 and Prm2 protein expression is also controlled by miR-469 (Dai *et al*., 2011). Silencing of *Tnp2* and *Prm2* in pachytene spermatocytes and round spermatids, respectively, is essential for normal spermatogenesis. Recently, Liang and colleges identified and characterized the function of one more testicular miRNA, miR-34c (Bleckmann *et al*., 2002). miR-34c belongs to larger miR-34 family of miRNAs, which comprises three miRNAs (in mammals) that are encoded by two different genes: miR-34a is encoded by its own transcript, whereas miR-34b and miR-34c share a common primary transcript. In mouse testis, the expression of miR-34c initially appears in pachytene spermatocytes and sharply increases to persist in the round spermatids in adult testis (Bleckmann *et al*., 2002). miR-34c was reported to enhance male germ cell apoptosis through targeting of *Activating transcription factor 1* (*Atf1*) (Liang *et al*., 2012). Atf1 protein has been found specifically in pachytene spermatocytes, however its function is not clear (Bleckmann *et al*., 2002). *In vitro* study has shown that the *Atf1* knockdown has significantly upregulated Bax (an apoptosis promoting protein) expression, while it reduced Bcl-2 (an apoptosis inhibitory protein) expression, resulting in sharp increase in Bax/Bcl-2 ratio in GC-2 cells (Liang *et al*., 2012). As a consequence, increased Bax/Bcl-2 ratio upregulates Caspase-3 and increases the apoptosis (Salakou *et al*., 2007). Apoptosis is required for normal spermatogenesis and is believed to ensure cellular homeostasis and to maintain the balance between germ cells and Sertoli cells (Print and Loveland, 2000).

Soon after that, the function of another member from miR-34 family, miR-34b, in spermatogenesis was demonstrated (Smorag *et al*., 2012). miR-34b is enriched in primary spermatocytes and was shown to inhibit their proliferation by targeting *Cyclin depend kinase 6* (*Cdk6*) (Smorag *et al*., 2012). Cdk6 may regulate the G_1 cell cycle progression in spermatogonia in postnatal testis and the suppression of Cdk6 by miR-34b may inhibit proliferation, thereby, may allow

Downloaded From Vet-eBooks.com

initiation of meiosis and further differentiation (Zindy *et al*., 2001). The observed apoptosis and cell cycle regulation functions of miR-34 family led to propose them as potential tumor suppressor molecules (Lee *et al.*, 2011; Misso *et al.*, 2014). To test this hypothesis, mouse model carrying the targeted deletion of all three members of miR-34 family was generated (Concepcion *et al.*, 2012). However, the complete depletion of miR-34 family expression resulted only in slight increase in cell proliferation *in vitro*, and showed no gross effects *in vivo* as the miR-34-deficient male mice developed normally and exhibited normal spermatogenesis and fertility (Concepcion *et al.*, 2012).

Previous studies have revealed that several miRNAs may regulate the same mRNA target, thus the lack of a single miRNA may not result in phenotype manifestation in nonstress condition. A recent study by Bao and colleagues identified that the expression pattern of miR-449 cluster resembled that of miR-34 and share a cohort of common target genes (Bao *et al*., 2012). The miR-449 cluster consists of three members: miR-449a, miR-449b, and miR-449c—and the genetic ablation of miR-449 cluster do not result in any gross abnormalities (similar to depletion of miR-34 cluster). The first evidence for existence of redundant functions between miR-34 and miR-449 clusters comes from studies by Yang *et al.* and Smorag *et al.*, in which the authors have identified *Cdk6* gene as the target of miR-449a/b and miR-34b, respectively (Yang *et al*., 2009; Smorag *et al*., 2012). In support of the redundant function of miR-34 and miR-449, two researcher groups have shown that double knockout of miR-34 and miR-449 clusters in mice leads to infertility due to impaired gametes formation (Song *et al*., 2014; Wu *et al*., 2014).

Apart from miR-34 and miR-449 clusters, the function of testis-specific miRNAs: miR-21, miR-20/106a, and miR-221—have been related to self-renewal and stemness maintenance of spermatogonial stem cells (SSCs) (Niu *et al*., 2011; Smorag *et al*., 2012; He *et al*., 2013; Yang *et al*., 2013). Although the downstream target genes are yet to be identified, the inhibition of miR-21 in SSC-enriched population increases the number of germ cells undergoing apoptosis, indicating that it is important in maintaining SSC population (Niu *et al*., 2011). On the other hand, miR-20 and miR-106a, the members of miR-17-92 cluster or its paralogs, regulate SSC renewal via targeting *Signal transducer and activator of transcription 3* (*Stat3*) and *Cyclin D1* (*Ccnd1*) genes (He *et al*., 2013). Stat3 regulates the expression of *Neurogenin3* (*Neurog3*) to drive the differentiation of SSC and progenitor spermatogonia in the mammalian germline (Kaucher *et al*., 2012). On the other hand, SSCs overexpressing *Ccnd1* failed to recolonize seminiferous tubules after transplantation, indicating that regulation of *Ccnd1* expression is an important determinant of long-term SSC function (Lee *et al*., 2009). Similar to the function of miR-21 and miR-20/106a, the miR-221 has been shown to regulate SSCs differentiation by suppression of c-Kit protein expression (Zhang *et al*., 2011; Smorag *et al*., 2012; Yang *et al*., 2013). The study by Smorag *et al.* has identified miR-203 expression as being specific for premeiotic cells and their further *in silico* studies have identified *RNA binding motif 44* (*Rbm44*) gene as the potential target of miR-203 (Smorag *et al*., 2012). The expression of Rbm44 is enriched in primary and secondary spermatocytes and may regulate morphological and structural maturation of premeiotic cells (Smorag *et al*., 2012). These observations led to a suggestion that the miR-203-mediated regulation of *Rbm44* might be important for the maturation of premeiotic cells (Smorag *et al.*, 2012).

On the basis of the above observations, we suggest that the spatiotemporal expression of miRNAs is crucial for the process of spermatogenesis (Figure 5.2). SSC-specific miRNAs regulate the expression of the genes controlling SSC proliferation and differentiation, while premeiotic cells-specific miRNAs may regulate the entry into meiosis, and finally, miRNAs expressed in meiotic cells may aid in inhibition of cell proliferation and promote further differentiation toward spermatozoa.

Downloaded From Vet-eBooks.com

5.2.3 *endo*-siRNAs Biogenesis

endo-siRNAs are slightly shorter (~21nt) than miRNAs and seem to be ubiquitous among higher eukaryotes. Till now, *endo*-siRNAs have been identified in worms, flies, mouse, and human (Babiarz *et al*., 2008; Ghildiyal *et al*., 2008; Tam *et al*., 2008; Han *et al*., 2009; Chen *et al*., 2012). These RNAs are derived from repetitive sequences, sense–antisense transcript pairs, or long stem-loop structures and they are dependent only on Dicer, but not Drosha. Similar to miRNAs, *endo*-siRNAs form the complex with Ago subfamily proteins and function as posttranscriptional regulator that target RNAs including mRNAs, transcripts of pseudo-genes, retrotransposons, and ncRNAs.

By contrast to miRNAs biosynthesis, *endo*-siRNAs are derived from long double-stranded RNAs (dsRNAs). In worms, they are synthesized by RNA-dependent RNA polymerase (RdRP) that canalizes the formation of dsRNAs (Pak and Fire, 2007). In flies and mammals, whose genome do not encode such RdRP proteins, the precursors of *endo*-siRNAs are derived either from single-stranded, self-hybridizing transcripts that form a long stem-loop structure (inverted repeats) or from dsRNAs, resulting from sense–antisense transcription (Chung *et al*., 2008; Czech *et al*., 2008; Ghildiyal *et al*., 2008; Kawamura *et al*., 2008). Some of these sense–antisense pairs (*cis-endo*-siRNAs) are transcribed from convergent transcription of the same loci, whereas others (*trans-endo*-siRNAs) are derived from similar but separate loci. In the cytoplasm, precursors of *endo*-siRNAs are processed in analogous way to pre-miRNAs. They are then cleaved by Dicer (mammals) or Dicer2 (flies) and loaded into Argonaut protein, forming RISC complex. Comparable with miRNAs, also in this case strand selection depend on the thermodynamic stabilities of the two siRNAs, although only flies require partner protein, LOQS. In mammals it has not been determined whether TRBP is involved in this pathway. By association with Ago2 proteins, siRNAs form RISC and negatively regulate the expression of targeting gene by inducing mRNA cleavage (Czech *et al*., 2008; Watanabe *et al*., 2008). The current knowledge concerning *endo*-siRNAs synthesis is illustrated in Figure 5.3.

5.2.4 *endo*-siRNAs in the Process of Spermatogenesis

Although *endo*-siRNAs have been described in many species, still little is known about their function. In the context of gametogenesis, *endo*-siRNAs were first described in *C. elegans* (Han *et al*., 2009). Due to the size differences, worms' *endo*-siRNAs were divided into two groups: 21nt and 26nt in length. The shorter form seems to be ubiquitously expressed, while longer one is germ cell specific (Han *et al*., 2009). Further, 26nt *endo*-siRNAs are subdivided into two distinct classes: Class I is presented in sperm, whereas class II is highly enriched in oocyte and embryos (Han *et al*., 2009). Computational analysis has revealed that 26nt *endo*-siRNAs have perfect complementarity to their predicted target genes, suggesting that they may function as canonical siRNAs to direct the cleavage of mRNA targets (Han *et al*., 2009). In agreement with *endo*-siRNA expression profiles, target genes for class I *endo*-siRNAs were highly enriched in sperm (Han *et al*., 2009). According the model proposed by Han *et al.* (2009), class I *endo*-siRNAs repress their target genes during spermatogenesis and mutation(s) that abolish their repression by *endo*-siRNAs leads to male infertility (Han *et al*., 2009). Although, *in silico* study has revealed the correlation between expression profiles of *endo*-siRNAs and their potential targets, further experimental work is necessary to validate *in vivo* function of *endo*-siRNAs in worm gametogenesis.

Recent studies on the expression of *endo*-siRNAs in murine spermatogenic cells unveiled yet another layer of gene regulation during mammalian male germ cells development (Song *et al*., 2011). A total of 73 testicular *endo*-siRNAs are identified till date and can be classified into:

Downloaded From Vet-eBooks.com

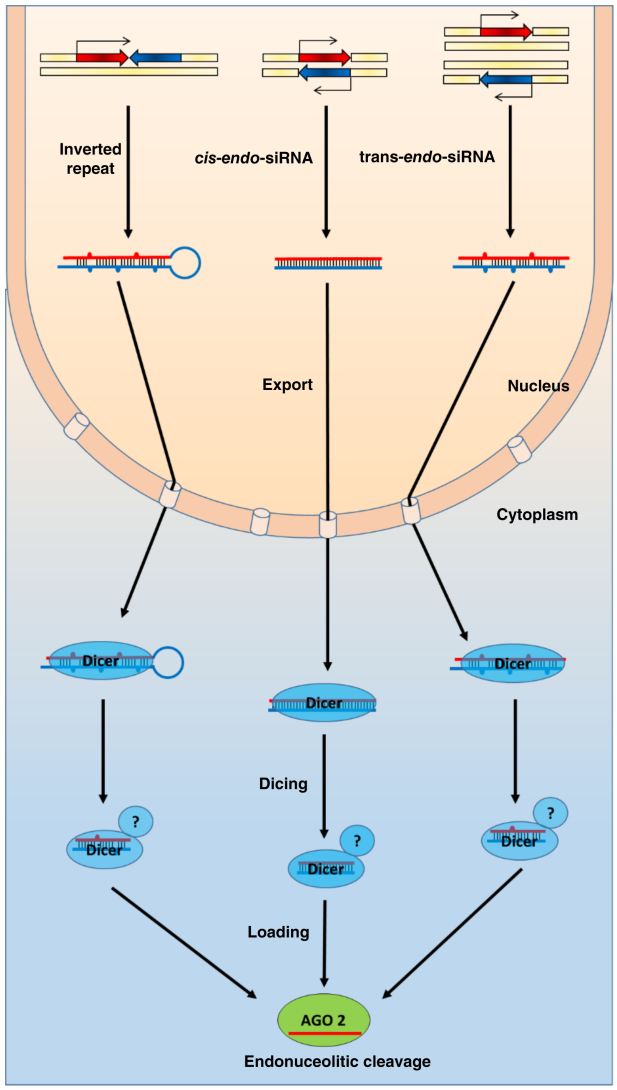

Figure 5.3 Biogenesis pathway of endogenous small interfering RNAs (*endo*-siRNAs). Precursors of *endo*-siRNAs are derived from double-stranded precursors, including long stem-loop structures (inverted repeats), bidirectional strands transcription (*cis-endo*-siRNAs), or repetitive sequence pairs (*trans-endo*-siRNA). Further *endo*-siRNA precursors are transported to cytoplasm and further processed by Dicer to produce double-stranded RNAs of ~21 nt, which is then loaded into Ago2 protein and forms RISC. Unlike miRNAs, the export of *endo*-siRNA precursors from the nucleus to cytoplasm as well as assembly of the effector complexes (RISC) is poorly understood. (For color detail, please see color plate section.)

premeiotic specific, postmeiotic specific, and ubiquitously expressed *endo*-siRNAs. Although selected siRNAs were able to reduce the expression of targets genes *in vitro*, further studies are necessary to demonstrate their *in vivo* function (Song *et al*., 2011). The first functional study on role of *endo*-siRNAs in spermatogenesis was performed in *D. melanogaster* (Wen *et al*., 2015). This study showed that the knockout of hpRNA1 (the name comes from hairpin RNAs, a subtype of fly *endo*-siRNAs) results in derepression of its target, *ATP synthaseβ*, in testis and leads to impaired spermatogenesis and male fertility. Further studies aimed at identifying novel

Downloaded From Vet-eBooks.com

endo-siRNAs and their functional characterization is imperative to understand the role these sncRNAs in development and gametogenesis.

5.2.5 pi-RNAs Biogenesis

piRNAs have a longer size ranging 24–31 nt in length and their expression is mostly restricted to germ cells and some of them are known to regulate silencing of transposon elements (Aravin *et al*., 2006; Girard *et al*., 2006; Brennecke *et al*., 2007). The piRNAs differ from miRNAs and *endo*-siRNAs in that they originate from ssRNAs, do not require Dicer for their processing, and form the RISC together with Piwi clade of Argonaut protein (Vagin *et al*., 2006; Houwing *et al*., 2007). The precise mechanisms of piRNAs biogenesis remain poorly characterized. Study in *D. melanogaster* suggests that piRNAs correspond to intergenic repetitive elements and might be involved in silencing of transposon elements. The potential mechanism of piRNAs synthesis includes ping-pong cycle (Gunawardane *et al*., 2007). In this cycle, Piwi and Aubergine (AUB), the members of fly Piwi clade of Argonaut proteins, associate with piRNAs derived mainly from antisense transcripts of retrotransposons. At the same time, Ago3, the other member of fly Piwi clade, interacts with piRNAs that arise mostly from sense transcripts (Brennecke *et al*., 2007). Since there are no evidences for the activity of other enzymes, it is believed that Piwi proteins process piRNA precursors and generate mature piRNAs. Finally, Piwi proteins cleave target RNAs relative to associated small RNAs (Saito *et al*., 2006). The scheme of hypothetical mechanism regulating piRNAs biogenesis in flies is illustrated in part A in Figure 5.4.

In contrast to flies, there are two distinct piRNA subpopulations observed in mammals during gametogenesis: prepachytene and pachytene piRNAs. They share molecular characteristics but differ in genome origin, Piwi binding partners, expression time, and function. Prepachytene piRNAs interact with MILI and MIWI2 (members of mouse Piwi clade of Argonaut proteins) and participate in silencing of transposon elements, and hence are equivalent to fly piRNAs (part A in Figure 5.4) (Aravin *et al*., 2007, 2008; Carmell *et al*., 2007; Kuramochi-Miyagawa *et al*., 2008). The ping-pong mechanism originally proposed in *D. melanogaster* might also apply to mouse prepachytene piRNAs (Aravin *et al*., 2008). The pachytene piRNAs associate with MILI and MIWI (part B in Figure 5.4), but their function has not yet been identified (Aravin *et al*., 2006, 2007; Girard *et al*., 2006; Grivna *et al*., 2006).

5.2.6 Role of piRNAs in Male Germ Cell Development

The piRNAs are known to play crucial role in the fertility of diverse species as evidenced by the fertility defects observed in mutants lacking piRNA processing Piwi proteins (Cox *et al*., 1998; Carmell *et al*., 2007; Batista *et al*., 2008; Zheng and Wang, 2012; Saxe *et al*., 2013). The well-known function of piRNAs is to protect germline cells from transposons and others non-self elements, thereby ensuring genome integrity (Aravin *et al*., 2003, 2007). In flies and in mouse prepachytene stage cells, piRNAs are mostly derived from transposons and were identified to target transposons themselves to keep them silence. In contrast, worm piRNAs protect the genome against non-self DNA, but they seem to have limited role in transposon silencing (Das *et al*., 2008). Until now, Tc3 is the only transposon family known to be silenced by piRNAs (Das *et al*., 2008). Worms developed the mechanism consisting of piRNAs and *endo*-siRNAs, including 21U-RNAs (21nt in length with 5′-uridine) and 22G-RNAs (22nt in length with 5′-guanine), respectively. On the one hand, 21U-RNAs are loaded into PRG-1 (one of the *C. elegans* Piwi proteins) and are able to recognize and cleave virtually any sequence. On the other hand, 22G-RNAs is loaded into CRS1 (member of *C. elegans* Argonaut protein),

Downloaded From Vet-eBooks.com

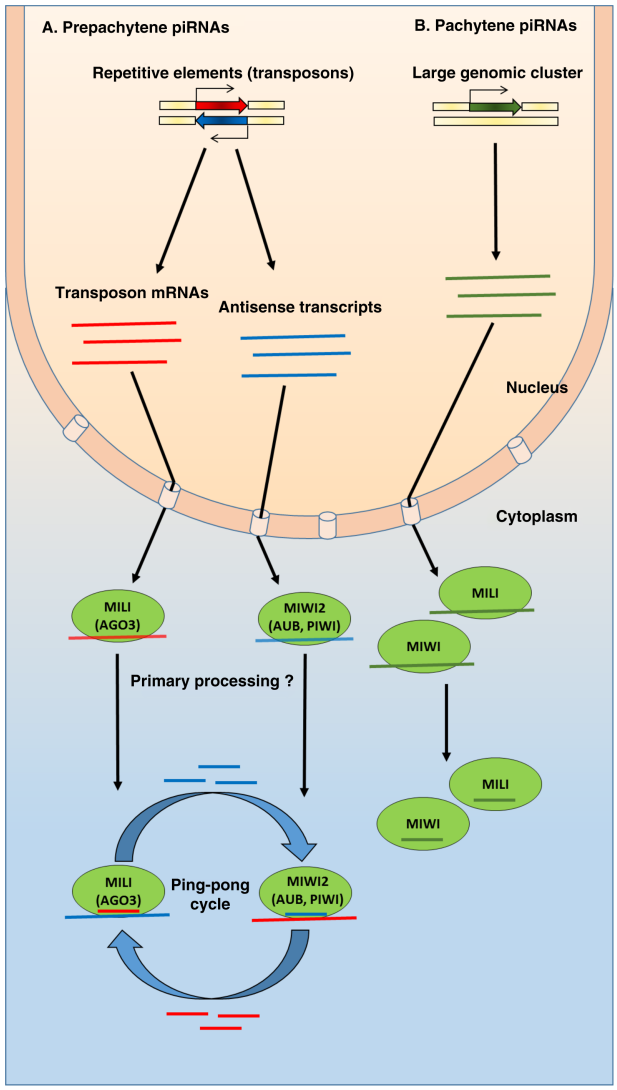

Figure 5.4 piRNAs biosynthesis pathway. Precursors of piRNAs are derived from single-stranded RNAs that are transcribed from repetitive elements, transposons, or large genomic piRNAs cluster. piRNAs are not dependent on either Drosha or Dicer but rather use the nuclease activity of Piwi proteins for their processing. In mouse, two classes of piRNAs have been identified: prepachytene piRNAs and pachytene piRNAs. Prepachytene piRNAs are equivalent to fly piRNAs and the fly ping-pong model explains their synthesis. In this model, MIWI2 (AUB and PIWI in flies) associate with piRNAs derived mainly from antisense transcripts of the retrotransposons, whereas MILI (flies AGO3) associates with piRNAs arising mostly from transposon mRNA. Briefly, MIWI2 associates with antisense piRNAs and cleaves transposon mRNAs. Resulting sense piRNAs in turn associates with MILI and subsequently cleaves antisense transcript to produce antisense piRNA that subsequently bind to MIWI2. This reciprocal reaction known as the ping-pong cycle provides continuous generation of piRNAs required for silencing of transposable elements. Pachytene piRNAs are unique for mammals and their function and mechanism of biosynthesis are unknown. It is hypothesized that MILI and MIWI proteins drive primary processing of piRNAs form ribonucleoprotein complex called Piwi-interacting RNA complex (piRC).

Downloaded From Vet-eBooks.com

recognizes genes expressed in germ cells, and acts to protect them from PRG1-mediated silencing. Unlike in lower organisms, mammalian piRNAs seems to play additional role during spermatogenesis. In their study, Gan *et al*. (2011) have characterized piRNA profile during specific stage of mouse spermatogenesis. Authors identified that piRNAs could derive not only from repetitive sequence but also from coding sequence, thus regulating expression of protein-coding genes. Growing body of evidences suggests that piRNAs can serve as additional level of gene expression control in germ cell.

Acknowledgment

This work was partly supported by the University Medical Center Göttingen (Forschungsförderungsprogramm) grant to D.V. Krishna Pantakani.

References

Aravin, A.A., Lagos-Quintana, M., Yalcin, A., Zavolan, M., Marks, D., Snyder, B., Gaasterland, T., Meyer, J., and Tuschl, T. (2003) The small RNA profile during *Drosophila melanogaster* development. *Dev. Cell*, **5**, 337–350.

Aravin, A., Gaidatzis, D., Pfeffer, S., Lagos-Quintana, M., Landgraf, P., Iovino, N., Morris, P., Brownstein, M.J., Kuramochi-Miyagawa, S., Nakano, T., Chien, M., Russo, J.J., Ju, J., Sheridan, R., Sander, C., Zavolan, M., and Tuschl, T. (2006) A novel class of small RNAs bind to MILI protein in mouse testes. *Nature*, **442**, 203–207.

Aravin, A.A., Sachidanandam, R., Girard, A., Fejes-Toth, K., and Hannon, G.J. (2007) Developmentally regulated piRNA clusters implicate MILI in transposon control. *Science*, **316**, 744–747.

Aravin, A.A., Sachidanandam, R., Bourc'his, D., Schaefer, C., Pezic, D., Toth, K.F., Bestor, T., and Hannon, G.J. (2008) A piRNA pathway primed by individual transposons is linked to *de novo* DNA methylation in mice. *Mol. Cell*, **31**, 785–799.

Babiarz, J.E., Ruby, J.G., Wang, Y., Bartel, D.P., and Blelloch, R. (2008) Mouse ES cells express endogenous shRNAs, siRNAs, and other Microprocessor-independent, Dicer-dependent small RNAs. *Genes Dev.*, **22**, 2773–2785.

Bao, J., Li, D., Wang, L., Wu, J., Hu, Y., Wang, Z., Chen, Y., Cao, X., Jiang, C., Yan, W., and Xu, C. (2012) MicroRNA-449 and microRNA-34b/c function redundantly in murine testes by targeting E2F transcription factor-retinoblastoma protein (E2F-pRb) pathway. *J. Biol. Chem.*, **287**, 21686–21698.

Batista, P.J., Ruby, J.G., Claycomb, J.M., Chiang, R., Fahlgren, N., Kasschau, K.D., Chaves, D.A., Gu, W., Vasale, J.J., Duan, S., Conte, D., Jr. Luo, S., Schroth, G.P., Carrington, J.C., Bartel, D.P., and Mello, C.C. (2008) PRG-1 and 21U-RNAs interact to form the piRNA complex required for fertility in *C. elegans*. *Mol. Cell*, **31**, 67–78.

Bettegowda, A. and Wilkinson, M.F. (2010) Transcription and post-transcriptional regulation of spermatogenesis. *Philos Trans. R. Soc. Lond. B*, **365**, 1637–1651.

Bleckmann, S.C., Blendy, J.A., Rudolph, D., Monaghan, A.P., Schmid, W., and Schutz, G. (2002) Activating transcription factor 1 and CREB are important for cell survival during early mouse development. *Mol. Cell. Biol.*, **22**, 1919–1925.

Brennecke, J., Stark, A., Russell, R.B., and Cohen, S.M. (2005) Principles of microRNA-target recognition. *PLoS Biol.*, **3**, e85.

Downloaded From Vet-eBooks.com

Brennecke, J., Aravin, A.A., Stark, A., Dus, M., Kellis, M., Sachidanandam, R., and Hannon, G.J. (2007) Discrete small RNA-generating loci as master regulators of transposon activity in *Drosophila*. *Cell*, **128**, 1089–1103.

Cai, X., Hagedorn, C.H., and Cullen, B.R. (2004) Human microRNAs are processed from capped, polyadenylated transcripts that can also function as mRNAs. *RNA*, **10**, 1957–1966.

Carmell, M.A., Girard, A., van de Kant, H.J., Bourc'his, D., Bestor, T.H., de Rooij, D.G., and Hannon, G.J. (2007) MIWI2 is essential for spermatogenesis and repression of transposons in the mouse male germline. *Dev. Cell*, **12**, 503–514.

Chen, L., Dahlstrom, J.E., Lee, S.H., and Rangasamy, D. (2012) Naturally occurring *endo*-siRNA silences LINE-1 retrotransposons in human cells through DNA methylation. *Epigenetics*, **7**, 758–771.

Chendrimada, T.P., Gregory, R.I., Kumaraswamy, E., Norman, J., Cooch, N., Nishikura, K., and Shiekhattar, R. (2005) TRBP recruits the Dicer complex to Ago2 for microRNA processing and gene silencing. *Nature*, **436**, 740–744.

Chu, C.Y. and Rana, T.M. (2007) Small RNAs: regulators and guardians of the genome. *J. Cell. Physiol.*, **213**, 412–419.

Chung, W.J., Okamura, K., Martin, R., and Lai, E.C. (2008) Endogenous RNA interference provides a somatic defense against Drosophila transposons. *Curr. Biol.*, **18**, 795–802.

Concepcion, C.P., Han, Y.C., Mu, P., Bonetti, C., Yao, E., D'Andrea, A., Vidigal, J.A., Maughan, W.P., Ogrodowski, P., and Ventura, A. (2012) Intact p53-dependent responses in miR-34-deficient mice. *PLoS Genet.*, **8**, e1002797.

Cooke, H.J. and Saunders, P.T. (2002) Mouse models of male infertility. *Nat. Rev. Genet.*, **3**, 790–801.

Cox, D.N., Chao, A., Baker, J., Chang, L., Qiao, D., and Lin, H. (1998) A novel class of evolutionarily conserved genes defined by piwi are essential for stem cell self-renewal. *Genes Dev.*, **12**, 3715–3727.

Czech, B., Malone, C.D., Zhou, R., Stark, A., Schlingeheyde, C., Dus, M., Perrimon, N., Kellis, M., Wohlschlegel, J.A., Sachidanandam, R., Hannon, G.J., and Brennecke, J. (2008) An endogenous small interfering RNA pathway in *Drosophila*. *Nature*, **453**, 798–802.

Dai, L., Tsai-Morris, C.H., Sato, H., Villar, J., Kang, J.H., Zhang, J., and Dufau, M.L. (2011) Testis-specific miRNA-469 upregulated in gonadotropin-regulated testicular RNA helicase (GRTH/DDX25)-null mice silences transition protein 2 and protamine 2 messages at sites within coding region: implications of its role in germ cell development. *J. Biol. Chem.*, **286**, 44306–44318.

Das, P.P., Bagijn, M.P., Goldstein, L.D., Woolford, J.R., Lehrbach, N.J., Sapetschnig, A., Buhecha, H.R., Gilchrist, M.J., Howe, K.L., Stark, R., Matthews, N., Berezikov, E., Ketting, R.F., Tavare, S., and Miska, E.A. (2008) Piwi and piRNAs act upstream of an endogenous siRNA pathway to suppress Tc3 transposon mobility in the *Caenorhabditis elegans* germline. *Mol. Cell*, **31**, 79–90.

Deng, W. and Lin, H. (2002) miwi, a murine homolog of piwi, encodes a cytoplasmic protein essential for spermatogenesis. *Dev. Cell*, **2**, 819–830.

Denli, A.M., Tops, B.B., Plasterk, R.H., Ketting, R.F., and Hannon, G.J. (2004) Processing of primary microRNAs by the Microprocessor complex. *Nature*, **432**, 231–235.

Forstemann, K., Tomari, Y., Du, T., Vagin, V.V., Denli, A.M., Bratu, D.P., Klattenhoff, C., Theurkauf, W.E., and Zamore, P.D. (2005) Normal microRNA maturation and germ-line stem cell maintenance requires Loquacious, a double-stranded RNA-binding domain protein. *PLoS Biol.*, **3**, e236.

Gan, H., Lin, X., Zhang, Z., Zhang, W., Liao, S., Wang, L., and Han, C. (2011) piRNA profiling during specific stages of mouse spermatogenesis. *RNA*, **17**, 1191–1203.

Downloaded From Vet-eBooks.com

Gan, H., Cai, T., Lin, X., Wu, Y., Wang, X., Yang, F., and Han, C. (2013) Integrative proteomic and transcriptomic analyses reveal multiple post-transcriptional regulatory mechanisms of mouse spermatogenesis. *Mol. Cell. Proteomics*, **12**, 1144–1157.

Ghildiyal, M., Seitz, H., Horwich, M.D., Li, C., Du, T., Lee, S., Xu, J., Kittler, E.L., Zapp, M.L., Weng, Z., and Zamore, P.D. (2008) Endogenous siRNAs derived from transposons and mRNAs in *Drosophila* somatic cells. *Science*, **320**, 1077–1081.

Girard, A., Sachidanandam, R., Hannon, G.J., and Carmell, M.A. (2006) A germline-specific class of small RNAs binds mammalian Piwi proteins. *Nature*, **442**, 199–202.

Grivna, S.T., Beyret, E., Wang, Z., and Lin, H. (2006) A novel class of small RNAs in mouse spermatogenic cells. *Genes Dev.*, **20**, 1709–1714.

Gunawardane, L.S., Saito, K., Nishida, K.M., Miyoshi, K., Kawamura, Y., Nagami, T., Siomi, H., and Siomi, M.C. (2007) A slicer-mediated mechanism for repeat-associated siRNA 5′ end formation in *Drosophila*. *Science*, **315**, 1587–1590.

Haase, A.D., Jaskiewicz, L., Zhang, H., Laine, S., Sack, R., Gatignol, A., and Filipowicz, W. (2005) TRBP, a regulator of cellular PKR and HIV-1 virus expression, interacts with Dicer and functions in RNA silencing. *EMBO Rep.*, **6**, 961–967.

Hale, B.J., Yang, C.X., and Ross, J.W. (2014) Small RNA regulation of reproductive function. *Mol. Reprod. Dev.*, **81**, 148–159.

Han, J., Lee, Y., Yeom, K.H., Kim, Y.K., Jin, H., and Kim, V.N. (2004) The Drosha-DGCR8 complex in primary microRNA processing. *Genes Dev.*, **18**, 3016–3027.

Han, J., Lee, Y., Yeom, K.H., Nam, J.W., Heo, I., Rhee, J.K., Sohn, S.Y., Cho, Y., Zhang, B.T., and Kim, V.N. (2006) Molecular basis for the recognition of primary microRNAs by the Drosha-DGCR8 complex. *Cell*, **125**, 887–901.

Han, T., Manoharan, A.P., Harkins, T.T., Bouffard, P., Fitzpatrick, C., Chu, D.S., Thierry-Mieg, D., Thierry-Mieg, J., and Kim, J.K. (2009) 26G *endo*-siRNAs regulate spermatogenic and zygotic gene expression in *Caenorhabditis elegans*. *Proc. Natl. Acad. Sci. USA*, **106**, 18674–18679.

Hayashi, K., Chuva de Sousa Lopes, S.M., Kaneda, M., Tang, F., Hajkova, P., Lao, K., O'Carroll, D., Das, P.P., Tarakhovsky, A., Miska, E.A., and Surani, M.A. (2008) MicroRNA biogenesis is required for mouse primordial germ cell development and spermatogenesis. *PLoS One*, **3**, e1738.

He, Z., Jiang, J., Kokkinaki, M., Tang, L., Zeng, W., Gallicano, I., Dobrinski, I., and Dym, M. (2013) MiRNA-20 and mirna-106a regulate spermatogonial stem cell renewal at the post-transcriptional level via targeting STAT3 and Ccnd1. *Stem Cells*, **31**, 2205–2217.

Hogarth, C.A. and Griswold, M.D. (2010) The key role of vitamin A in spermatogenesis. *J. Clin. Invest.*, **120**, 956–962.

Houwing, S., Kamminga, L.M., Berezikov, E., Cronembold, D., Girard, A., van den Elst, H., Filippov, D.V., Blaser, H., Raz, E., Moens, C.B., Plasterk, R.H., Hannon, G.J., Draper, B.W., and Ketting, R.F. (2007) A role for Piwi and piRNAs in germ cell maintenance and transposon silencing in Zebrafish. *Cell*, **129**, 69–82.

Hutvagner, G. and Zamore, P.D. (2002) A microRNA in a multiple-turnover RNAi enzyme complex. *Science*, **297**, 2056–2060.

Hutvagner, G., McLachlan, J., Pasquinelli, A.E., Balint, E., Tuschl, T., and Zamore, P.D. (2001) A cellular function for the RNA-interference enzyme Dicer in the maturation of the let-7 small temporal RNA. *Science*, **293**, 834–838.

Kaneda, M., Tang, F., O'Carroll, D., Lao, K., and Surani, M.A. (2009) Essential role for Argonaute2 protein in mouse oogenesis. *Epigenetics Chromatin*, **2**, 9.

Kaucher, A.V., Oatley, M.J., and Oatley, J.M. (2012) NEUROG3 is a critical downstream effector for STAT3-regulated differentiation of mammalian stem and progenitor spermatogonia. *Biol. Reprod.*, **86** 164.

Downloaded From Vet-eBooks.com

Kawamura, Y., Saito, K., Kin, T., Ono, Y., Asai, K., Sunohara, T., Okada, T.N., Siomi, M.C., and Siomi, H. (2008) *Drosophila* endogenous small RNAs bind to Argonaute 2 in somatic cells. *Nature*, **453**, 793–797.

Kempisty, B., Jedrzejczak, P., and Jagodzinski, P.P. (2006) [Structure and role of protamines 1 and 2 in spermatogenesis and male infertility]. *Ginekol. Pol.*, **77**, 238–245.

Ketting, R.F., Fischer, S.E., Bernstein, E., Sijen, T., Hannon, G.J., and Plasterk, R.H. (2001) Dicer functions in RNA interference and in synthesis of small RNA involved in developmental timing in *C. elegans*. *Genes Dev.*, **15**, 2654–2659.

Khvorova, A., Reynolds, A., and Jayasena, S.D. (2003) Functional siRNAs and miRNAs exhibit strand bias. *Cell*, **115**, 209–216.

Knight, S.W. and Bass, B.L. (2001) A role for the RNase III enzyme DCR-1 in RNA interference and germ line development in *Caenorhabditis elegans*. *Science*, **293**, 2269–2271.

Korhonen, H.M., Meikar, O., Yadav, R.P., Papaioannou, M.D., Romero, Y., Da Ros, M., Herrera, P.L., Toppari, J., Nef, S., and Kotaja, N. (2011) Dicer is required for haploid male germ cell differentiation in mice. *PLoS One*, **6**, e24821.

Kozomara, A. and Griffiths-Jones, S. (2014) miRBase: annotating high confidence microRNAs using deep sequencing data. *Nucleic Acids Res.*, **42**, D68–D73.

Kuramochi-Miyagawa, S., Watanabe, T., Gotoh, K., Totoki, Y., Toyoda, A., Ikawa, M., Asada, N., Kojima, K., Yamaguchi, Y., Ijiri, T.W., Hata, K., Li, E., Matsuda, Y., Kimura, T., Okabe, M., Sakaki, Y., Sasaki, H., and Nakano, T. (2008) DNA methylation of retrotransposon genes is regulated by Piwi family members MILI and MIWI2 in murine fetal testes. *Genes Dev.*, **22**, 908–917.

Lagos-Quintana, M., Rauhut, R., Lendeckel, W., and Tuschl, T. (2001) Identification of novel genes coding for small expressed RNAs. *Science*, **294**, 853–858.

Lai, E.C. (2004) Predicting and validating microRNA targets. *Genome Biol.*, **5**, 115.

Lau, N.C., Lim, L.P., Weinstein, E.G., and Bartel, D.P. (2001) An abundant class of tiny RNAs with probable regulatory roles in *Caenorhabditis elegans*. *Science*, **294**, 858–862.

Lee, R.C. and Ambros, V. (2001) An extensive class of small RNAs in *Caenorhabditis elegans*. *Science*, **294**, 862–864.

Lee, R.C., Feinbaum, R.L., and Ambros, V. (1993) The *C. elegans* heterochronic gene lin-4 encodes small RNAs with antisense complementarity to lin-14. *Cell*, **75**, 843–854.

Lee, Y., Jeon, K., Lee, J.T., Kim, S., and Kim, V.N. (2002) MicroRNA maturation: stepwise processing and subcellular localization. *EMBO J.* **21**, 4663–4670.

Lee, Y., Ahn, C., Han, J., Choi, H., Kim, J., Yim, J., Lee, J., Provost, P., Radmark, O., Kim, S., and Kim, V.N. (2003) The nuclear RNase III Drosha initiates microRNA processing. *Nature*, **425**, 415–419.

Lee, Y., Kim, M., Han, J., Yeom, K.H., Lee, S., Baek, S.H., and Kim, V.N. (2004) MicroRNA genes are transcribed by RNA polymerase II. *EMBO J.*, **23**, 4051–4060.

Lee, J., Kanatsu-Shinohara, M., Morimoto, H., Kazuki, Y., Takashima, S., Oshimura, M., Toyokuni, S., and Shinohara, T. (2009) Genetic reconstruction of mouse spermatogonial stem cell self-renewal *in vitro* by Ras-cyclin D2 activation. *Cell Stem Cell*, **5**, 76–86.

Lee, Y.M., Lee, J.Y., Ho, C.C., Hong, Q.S., Yu, S.L, Tzeng, C.R. Yang, P.C., and Chen, H.W. (2011) miRNA-34b as a tumor suppressor in estrogen-dependent growth of breast cancer cells. *Cancer Res.*, **13**, R116.

Lewis, B.P., Shih, I.H., Jones-Rhoades, M.W., Bartel, D.P., and Burge, C.B. (2003) Prediction of mammalian microRNA targets. *Cell*, **115**, 787–798.

Lewis, B.P., Burge, C.B., and Bartel, D.P. (2005) Conserved seed pairing, often flanked by adenosines, indicates that thousands of human genes are microRNA targets. *Cell*, **120**, 15–20.

Downloaded From Vet-eBooks.com

Liang, X., Zhou, D., Wei, C., Luo, H., Liu, J., Fu, R., and Cui, S. (2012) MicroRNA-34c enhances murine male germ cell apoptosis through targeting ATF1. *PLoS One*, **7**, e33861.

Llave, C., Kasschau, K.D., Rector, M.A., and Carrington, J.C. (2002) Endogenous and silencing-associated small RNAs in plants. *Plant Cell*, **14**, 1605–1619.

Ma, J., Flemr, M., Stein, P., Berninger, P., Malik, R., Zavolan, M., Svoboda, P., and Schultz, R.M. (2010) MicroRNA activity is suppressed in mouse oocytes. *Curr. Biol.*, **20**, 265–270.

Maatouk, D.M., Loveland, K.L., McManus, M.T., Moore, K., and Harfe, B.D. (2008) Dicer1 is required for differentiation of the mouse male germline. *Biol. Reprod.*, **79**, 696–703.

Meister, G., Landthaler, M., Patkaniowska, A., Dorsett, Y., Teng, G., and Tuschl, T. (2004) Human Argonaute2 mediates RNA cleavage targeted by miRNAs and siRNAs. *Mol. Cell*, **15**, 185–197.

Misso, G., Di Martino, M.T., De Rosa, G., Farooqi, A.A., Lombardi, A., Campani, V., Zarone, M.R., Gulla, A., Tagliaferri, P., Tassone, P., and Caraglia, M. (2014) mir-34: a new weapon against cancer? *Mol. Ther. Nucleic Acids* **3**, e194.

Murchison, E.P., Stein, P., Xuan, Z., Pan, H., Zhang, M.Q., Schultz, R.M., and Hannon, G.J. (2007) Critical roles for Dicer in the female germline. *Genes Dev.*, **21**, 682–693.

Niu, Z., Goodyear, S.M., Rao, S., Wu, X., Tobias, J.W., Avarbock, M.R., and Brinster, R.L. (2011) MicroRNA-21 regulates the self-renewal of mouse spermatogonial stem cells. *Proc. Natl. Acad. Sci. USA*, **108**, 12740–12745.

Pak, J. and Fire, A. (2007) Distinct populations of primary and secondary effectors during RNAi in *C. elegans*. *Science*, **315**, 241–244.

Pangas, S.A. and Rajkovic, A. (2006) Transcriptional regulation of early oogenesis: in search of masters. *Hum. Reprod. Update*, **12**, 65–76.

Park, J.K., Liu, X., Strauss, T.J., McKearin, D.M., and Liu, Q. (2007) The miRNA pathway intrinsically controls self-renewal of *Drosophila* germline stem cells. *Curr. Biol.*, **17**, 533–538.

Print, C.G. and Loveland, K.L. (2000) Germ cell suicide: new insights into apoptosis during spermatogenesis. *Bioessays*, **22**, 423–430.

Rhoades, M.W., Reinhart, B.J., Lim, L.P., Burge, C.B., Bartel, B., and Bartel, D.P. (2002) Prediction of plant microRNA targets. *Cell*, **110**, 513–520.

Ro, S., Park, C., Sanders, K.M., McCarrey, J.R., and Yan, W. (2007) Cloning and expression profiling of testis-expressed microRNAs. *Dev. Biol.*, **311**, 592–602.

Ruby, J.G., Jan, C.H., and Bartel, D.P. (2007) Intronic microRNA precursors that bypass Drosha processing. *Nature*, **448**, 83–86.

Saito, K., Nishida, K.M., Mori, T., Kawamura, Y., Miyoshi, K., Nagami, T., Siomi, H., and Siomi, M.C. (2006) Specific association of Piwi with rasiRNAs derived from retrotransposon and heterochromatic regions in the Drosophila genome. *Genes Dev.*, **20**, 2214–2222.

Salakou, S., Kardamakis, D., Tsamandas, A.C., Zolota, V., Apostolakis, E., Tzelepi, V., Papathanasopoulos, P., Bonikos, D.S., Papapetropoulos, T., Petsas, T., and Dougenis, D. (2007) Increased Bax/Bcl-2 ratio up-regulates caspase-3 and increases apoptosis in the thymus of patients with myasthenia gravis. *In Vivo*, **21**, 123–132.

Saxe, J.P., Chen, M., Zhao, H., and Lin, H. (2013) Tdrkh is essential for spermatogenesis and participates in primary piRNA biogenesis in the germline. *EMBO J.*, **32**, 1869–1885.

Schwarz, D.S., Hutvagner, G., Du, T., Xu, Z., Aronin, N., and Zamore, P.D. (2003) Asymmetry in the assembly of the RNAi enzyme complex. *Cell*, **115**, 199–208.

Shi, Z., Montgomery, T.A., Qi, Y., and Ruvkun, G. (2013) High-throughput sequencing reveals extraordinary fluidity of miRNA, piRNA, and siRNA pathways in nematodes. *Genome Res.*, **23**, 497–508.

Smorag, L., Zheng, Y., Nolte, J., Zechner, U., Engel, W., and Pantakani, D.V. (2012) MicroRNA signature in various cell types of mouse spermatogenesis: evidence for stage-specifically

Downloaded From Vet-eBooks.com

expressed miRNA-221, -203 and -34b-5p mediated spermatogenesis regulation. *Biol. Cell*, **104**, 677–692.

Song, R., Ro, S., Michaels, J.D., Park, C., McCarrey, J.R., and Yan, W. (2009) Many X-linked microRNAs escape meiotic sex chromosome inactivation. *Nat. Genet.*, **41**, 488–493.

Song, R., Hennig, G.W., Wu, Q., Jose, C., Zheng, H., and Yan, W. (2011) Male germ cells express abundant endogenous siRNAs. *Proc. Natl. Acad. Sci. USA*, **108**, 13159–13164.

Song, R., Walentek, P., Sponer, N., Klimke, A., Lee, J.S., Dixon, G., Harland, R., Wan, Y., Lishko, P., Lize, M., Kessel, M., and He, L. (2014) miR-34/449 miRNAs are required for motile ciliogenesis by repressing cp110. *Nature*, **510**, 115–120.

Suh, N., Baehner, L., Moltzahn, F., Melton, C., Shenoy, A., Chen, J., and Blelloch, R. (2010) MicroRNA function is globally suppressed in mouse oocytes and early embryos. *Curr. Biol.*, **20**, 271–277.

Tam, O.H., Aravin, A.A., Stein, P., Girard, A., Murchison, E.P., Cheloufi, S., Hodges, E., Anger, M., Sachidanandam, R., Schultz, R.M., and Hannon, G.J. (2008) Pseudogene-derived small interfering RNAs regulate gene expression in mouse oocytes. *Nature*, **453**, 534–538.

Tang, G., Reinhart, B.J., Bartel, D.P., and Zamore, P.D. (2003) A biochemical framework for RNA silencing in plants. *Genes Dev.*, **17**, 49–63.

Vagin, V.V., Sigova, A., Li, C., Seitz, H., Gvozdev, V., and Zamore, P.D. (2006) A distinct small RNA pathway silences selfish genetic elements in the germline. *Science*, **313**, 320–324.

Watanabe, T., Totoki, Y., Toyoda, A., Kaneda, M., Kuramochi-Miyagawa, S., Obata, Y., Chiba, H., Kohara, Y., Kono, T., Nakano, T., Surani, M.A., Sakaki, Y., and Sasaki, H. (2008) Endogenous siRNAs from naturally formed dsRNAs regulate transcripts in mouse oocytes. *Nature*, **453**, 539–543.

Wen, J., Mohammed, J., Bortolamiol-Becet, D., Tsai, H., Robine, N., Westholm, J.O., Ladewig, E., Dai, Q., Okamura, K., Flynt, A.S., Zhang, D., Andrews, J., Cherbas, L., Kaufman, T.C., Cherbas, P., Siepel, A., and Lai, E.C. (2014) Diversity of miRNAs, siRNAs, and piRNAs across 25 *Drosophila* cell lines. *Genome Res.*, **24**, 1236–1250.

Wen, J., Duan, H., Bejarano, F., Okamura, K., Fabian, L., Brill, J.A., Bortolamiol-Becet, D., Martin, R., Ruby, J.G., and Lai, E.C. (2015) Adaptive regulation of testis gene expression and control of male fertility by the *Drosophila* hairpin RNA pathway. *Mol. Cell*, **57**, 165–178.

Wightman, B., Ha, I., and Ruvkun, G. (1993) Posttranscriptional regulation of the heterochronic gene lin-14 by lin-4 mediates temporal pattern formation in *C. elegans*. *Cell*, **75**, 855–862.

Wu, Q., Song, R., Ortogero, N., Zheng, H., Evanoff, R., Small, C.L., Griswold, M.D., Namekawa, S.H., Royo, H., Turner, J.M., and Yan, W. (2012) The RNase III enzyme DROSHA is essential for microRNA production and spermatogenesis. *J. Biol. Chem.*, **287**, 25173–25190.

Wu, J., Bao, J., Kim, M., Yuan, S., Tang, C., Zheng, H., Mastick, G.S., Xu, C., and Yan, W. (2014) Two miRNA clusters, miR-34b/c and miR-449, are essential for normal brain development, motile ciliogenesis, and spermatogenesis. *Proc. Natl. Acad. Sci. USA*, **111**, E2851–E2857.

Yan, N., Lu, Y., Sun, H., Tao, D., Zhang, S., Liu, W., and Ma, Y. (2007) A microarray for microRNA profiling in mouse testis tissues. *Reproduction*, **134**, 73–79.

Yang, X., Feng, M., Jiang, X., Wu, Z., Li, Z., Aau, M., and Yu, Q. (2009) miR-449a and miR-449b are direct transcriptional targets of E2F1 and negatively regulate pRb-E2F1 activity through a feedback loop by targeting CDK6 and CDC25A. *Genes Dev.*, **23**, 2388–2393.

Yang, Q.E., Racicot, K.E., Kaucher, A.V., Oatley, M.J., and Oatley, J.M. (2013) MicroRNAs 221 and 222 regulate the undifferentiated state in mammalian male germ cells. *Development*, **140**, 280–290.

Yekta, S., Shih, I.H., and Bartel, D.P. (2004) MicroRNA-directed cleavage of HOXB8 mRNA. *Science*, **304**, 594–596.

Downloaded From Vet-eBooks.com

Yi, R., Qin, Y., Macara, I.G., and Cullen, B.R. (2003) Exportin-5 mediates the nuclear export of pre-microRNAs and short hairpin RNAs. *Genes Dev.*, **17**, 3011–3016.

Yu, Z., Raabe, T., and Hecht, N.B. (2005) MicroRNA Mirn122a reduces expression of the posttranscriptionally regulated germ cell transition protein 2 (Tnp2) messenger RNA (mRNA) by mRNA cleavage. *Biol. Reprod.*, **73**, 427–433.

Zhang, L., Tang, J., Haines, C.J., Feng, H.L., Lai, L., Teng, X., and Han, Y. (2011) c-kit and its related genes in spermatogonial differentiation. *Spermatogenesis*, **1**, 186–194.

Zhao, M., Shirley, C.R., Hayashi, S., Marcon, L., Mohapatra, B., Suganuma, R., Behringer, R.R., Boissonneault, G., Yanagimachi, R., and Meistrich, M.L. (2004) Transition nuclear proteins are required for normal chromatin condensation and functional sperm development. *Genesis*, **38**, 200–213.

Zheng, K. and Wang, P.J. (2012) Blockade of pachytene piRNA biogenesis reveals a novel requirement for maintaining post-meiotic germline genome integrity. *PLoS Genet.*, **8**, e1003038.

Zindy, F., den Besten, W., Chen, B., Rehg, J.E., Latres, E., Barbacid, M., Pollard, J.W., Sherr, C.J., Cohen, P.E., and Roussel, M.F. (2001) Control of spermatogenesis in mice by the cyclin D-dependent kinase inhibitors p18(Ink4c) and p19(Ink4d). *Mol. Cell. Biol.*, **21**, 3244–3255.

Downloaded From Vet-eBooks.com

6

The Ovarian Follicle of Cows as a Model for Human

Marc-André Sirard

Département des Sciences Animales Pavillon des services, Chaire de Recherche du Canada en Génomique Animale, Canada

6.1 Introduction

Infertility, which is generally defined as the inability to get pregnant after 1 year of unprotected sex, is a relatively common problem. In the United States, about 12% of women of childbearing age have received infertility services at some point in their lives (Center for Disease Control and Prevention, 2014). Assisted reproductive technology (ART), which includes hormonal stimulation, artificial insemination, *in vitro* fertilization (IVF), and surrogacy, plays an important role in helping these women become pregnant. Since the 1978 birth of Louise Brown, the first baby born following conception by IVF, techniques have greatly improved. However, the pregnancy rate per cycle is only around 30% in women using ART (Center for Disease Control and Prevention, 2014). Besides individual variability linked to genetics and negative environmental factors, one of the main issues behind this low success is low oocyte quality, a consequence of our lack of knowledge of ovarian physiology and oocyte competence. Our understanding of the precisely regulated process of folliculogenesis grows every year, but the complexity of the very dynamic transformation of ovarian tissues throughout the menstrual cycle is incredible. These unknown elements hamper the work that is being done to overcome infertility, as it is sometimes impossible to comprehend the causes of the problems, or the reasons behind successful procedures. Adding to the challenge is the fact that the opportunities to study women ovarian physiology directly are scarce. Normal ovarian tissue from women of reproductive age are not readily available (Campbell *et al.*, 2003), and ethical concerns forbid experimentations that could affect the future fertility of women. Additionally, logistical limitations when working with human subjects also limit potential experiments with frequent sampling or observations.

6.1.1 Why We Know More About Cow Than Human Reproduction

The dairy industry is already using all the possible tools for herd reproductive management. Synchronization protocols are used extensively, along with artificial insemination (AI), sperm sexing, superovulation, IVF, and embryo transfer. All these techniques were adopted quickly by producers, as they help to maximize the genetic improvement of cattle breeds. These techniques have been tested and optimized in order to take full advantage of reproductive management. The ovarian physiology of the cow is one of the best understood, and numerous research laboratories already use it as a model for the study of reproductive biology. Moreover, cattle and large farm animals in general have several advantages that make them good subjects for

Animal Models and Human Reproduction, First Edition. Edited by Heide Schatten and Gheorghe M. Constantinescu.
© 2017 John Wiley & Sons, Inc. Published 2017 by John Wiley & Sons, Inc.

Downloaded From Vet-eBooks.com

research: They are easily available, relatively cheap to buy, easier to handle than nondomestic animals, and big enough to allow detailed endocrinological and morphological studies (Campbell *et al.*, 2003). The world cattle population size is considerable, and most of them are intended for slaughter, which will make their tissues eventually available for experimentation. In general, the use of farm animals as experimental subjects lowers the number of laboratory animals needed. Additionally, minimally invasive procedures such as ultrasound and embryo transfer can be used on animals kept in different environments or subject to different treatments.

Comparative research between species allows the study of biological mechanisms by using an animal model with certain research advantages to obtain preliminary knowledge for other species, especially for those in which research may be difficult, impractical, or unethical (Ginther, 2012). Bovine and human reproductive biology share numerous characteristics: cows and women are monovular, cycle continuously while not pregnant, have a gestation period of approximately 9 months, and their ovaries are similar in size (approximately 3 cm × 2 cm × 1.5 cm) and morphology (Adams and Pierson, 1995). The cow has been suggested as a good animal model to study human ovarian function (Adams and Pierson, 1995; Campbell *et al.*, 2003; Yapura *et al.*, 2011), and has been used successfully to explore certain aspects of human follicular physiology (Baerwald *et al.*, 2003a, 2003b; Ginther *et al.*, 2001; Malhi *et al.*, 2005, 2006, 2007; Mihm and Evans, 2008; Yapura *et al.*, 2011). Moreover, techniques such as ultrasound monitoring of individual follicles and ovulation induction were initially developed in cattle (Adams and Pierson, 1995; Dowling, 1954).

The mare has also been suggested as a good model to study human ovarian function because the two species share numerous characteristics (as reviewed in Ginther, 2012), especially concerning ovarian ageing (Carnevale, 2008). Indeed, unlike most other domestic farm animals, working or pet mares are often kept until an old age (>20 years), and contain a valuable population of oocytes that have been kept in meiotic arrest for decades (Carnevale, 2008). However, the seasonality of equine reproduction is an important difference; cows may therefore be more appropriate for comparative studies. Furthermore, horses do not respond to superovulation due to the lack of effective gonadotropins and the anatomy of their ovaries. Finally, the amount of equine ovarian tissues available is very limited as horse slaughter is currently banned in the United States, and in the countries that allow it, the number of animals slaughtered is largely inferior to the number of cattle slaughtered.

This chapter will highlight the similarities and differences between bovine and human female reproduction, in order to justify the use of the cow as a model to study ovarian physiology, folliculogenesis, and oocyte development.

6.2 A Similar Physiology of Folliculogenesis

6.2.1 Basic Physiology of Reproduction

Cows and women share numerous characteristics in regard to folliculogenesis. The estrous cycle of the cow lasts about 21 days, and the human menstrual cycle is slightly longer, lasting 28 days on average. As already mentioned, both species are monovular, which means that a process allows the selection of a dominant follicle, and ultimately leads to the ovulation of only one oocyte per cycle. In cows, there is great variability between animals for the size of the ovarian reserve of preantral follicles (Silva-Santos *et al.*, 2011), and the number of antral follicles recruited during each follicular wave (Burns *et al.*, 2005). However, the number of antral follicles is highly similar between waves for the same animal (Burns *et al.*, 2005). This

Downloaded From Vet-eBooks.com

extreme variation between individuals of the same species can also be observed in humans; the mean maximum number of follicles recruited each month is 880, but can vary from 100 to 7500 (Wallace and Kelsey, 2010). In most mammals, the ovarian reserve of primordial follicles is fully established before birth, and the recruitment of follicles into a growing pool of primary follicles starts during fetal life (Oktem and Oktay, 2008). This process of recruitment is continuous, even before puberty and through pregnancy, and is gonadotropin independent (Hunter *et al.*, 2004).

In women, the store of primordial follicles shrinks with age until it is unable to provide enough follicles to sustain menstrual cyclicity. This end of reproductive ability, called menopause, occurs at a mean age of 51 years, when the ovarian reserve drops to approximately 1000 follicles (Faddy and Gosden, 1996). Cows do not undergo menopause, but their fertility decreases gradually as they get older, and they may eventually become infertile (Erickson *et al.*, 1976; Erickson, 1966; Malhi *et al.*, 2007). Old cows (13–16 years old) with decreased fertility, but that can still reproduce, present hormonal changes that are consistent with those reported for women approaching the menopause transition (Malhi *et al.*, 2005, 2007). The effect of a prolonged meiotic arrest lasting for years, or even decades in women, on oocyte competence is difficult to study with most of the usual animal models as their reproductive life span is too short. Given the long reproductive life span of cattle, cows represent a good model for this aspect of reproduction as their primordial follicles can remain dormant in the ovary for more than a decade.

The ovulatory follicle diameter varies from 14 to 19 mm in cattle (Echternkamp *et al.*, 2009; Souza *et al.*, 2007), and from 19 to 25 mm in humans (Ben-Nun *et al.*, 1986; Hata *et al.*, 1983). The corpus luteum has a similar life span in both species, and several studies shed light on the crucial role that the immune system plays in the physiology of this structure in cows (Pate *et al.*, 2010). The mature corpus luteum is composed of luteal cells that secrete progesterone, and is ~2.5–3.0 cm in diameter in human and bovine species. However, while the human corpus luteum retains the ability to secrete estradiol and inhibin (Devoto *et al.*, 2009; Illingworth *et al.*, 1991), the bovine corpus luteum does not (Henderson and Franchimont, 1981; Schams and Berisha, 2004). The equine corpus luteum also does not produce inhibin (Ginther, 1992). Figure 6.1 shows a comparison between human and bovine follicular growth.

6.2.2 Time from Primordial Follicle to Ovulation

During the first stages of follicle development, the increase in follicular diameter is mostly caused by granulosa cell proliferation. As the primordial follicle is surrounded by few granulosa cells, growth starts extremely slowly. In rats, whose ovarian cycles last 4–5 days (Nequin *et al.*, 1979), some very small follicles with less than four granulosa cells would have grown of only one cell after 7 days (Hirshfield, 1989). In bovine and ovine, the time between primordial follicle activation and ovulation was estimated to be 6 months (Cahill and Mauleon, 1980; Lussier *et al.*, 1987). Therefore, it takes a period equivalent to approximately two estrous cycles for a cow follicle to grow through the antral stage and reach preovulatory size (Lussier *et al.*, 1987). In women, the time for early growing follicles to reach the preantral stage was suggested to be about 6 months, or even close to a year (Campbell *et al.*, 2003; Gougeon, 1986, 1996; Trounson *et al.*, 2013). More studies are needed to confirm the estimations for cattle and humans; current knowledge on the time from primordial follicle to ovulation in these species is summarized in Figure 6.1. Experiments in sheep suggested that the rate of primordial follicle activation is not regulated by gonadotropins, but instead by an intraovarian anti-Müllerian hormone (AMH) feedback loop (Campbell *et al.*, 2000, 2003; Dufour *et al.*, 1979).

Downloaded From Vet-eBooks.com

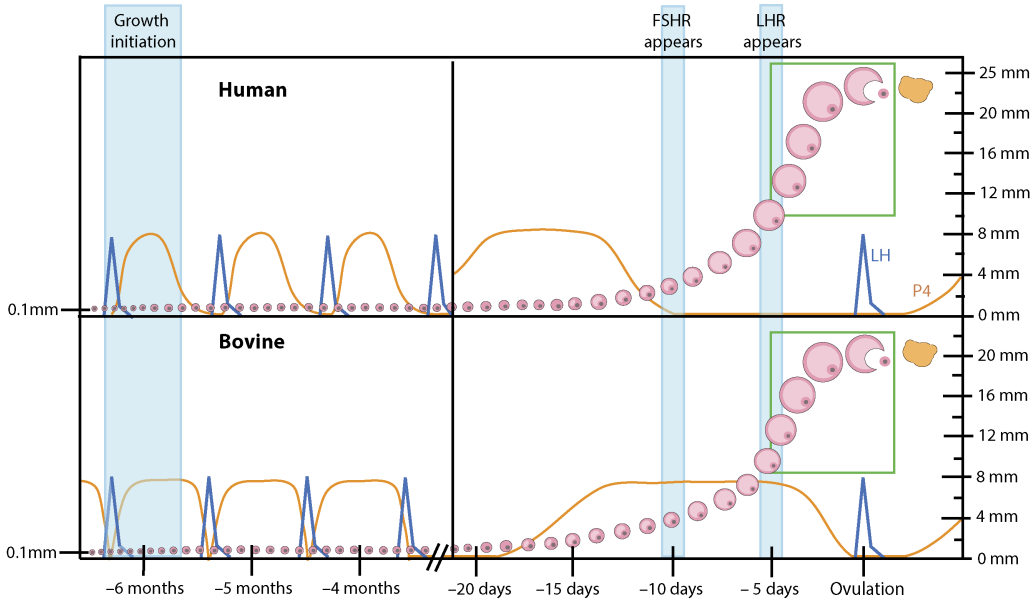

Figure 6.1 Development of the ovulatory follicle in human (top) and bovine (bottom). Progesterone profiles and LH surges are shown in orange and blue, respectively. Key elements of the dominant follicle's development are presented. The green box shows the window for competence acquisition. (See color plate section.)

6.2.3 Follicular Waves

The wave-like pattern of antral follicular development in cattle has been known for more than 50 years (Rajakoski, 1960). To understand the dynamics of the whole cycle, a number of healthy heifers were slaughtered so that each day of the estrous cycle was represented. As such an experiment cannot be performed on women, characterization of the human follicular wave pattern came much later. Based on the study of ovaries collected from laparotomy patients, it was initially thought that antral follicles continuously grew from primordial ones without a clear pattern (Gougeon, 1979). Several years later, evidence from animal models brought a new understanding of follicular dynamics, and revealed the presence of follicular waves in women ovaries, where two or three follicular waves can be observed during a cycle, the last being the ovulatory one (Baerwald *et al.*, 2003a; Ginther *et al.*, 2004; Gougeon, 1986). The anovulatory waves can be either major (the dominant follicle reaches >10 mm) or minor (all follicles <10 mm) (Baerwald *et al.*, 2003b). The follicles from the ovulatory wave reach similar diameters, whether they originate from a cycle with two or three waves (Baerwald *et al.*, 2003b). Cows have a similar wave pattern with two or three waves (Ginther *et al.*, 1989a), but only major anovulatory waves are present. The dominant follicle of nonovulatory waves reaches a diameter similar or larger than the diameter of the ovulatory follicle, and follicles ovulated from three-wave cycles are slightly smaller than those from two-wave cycles (Ginther *et al.*, 1989b).

In both cattle and humans, the recruitment of follicles for a follicular wave is controlled by a rise of FSH levels above a biological threshold (Adams *et al.*, 1992; Baerwald, 2009; Brown, 1978). The number of follicles in a wave seems to be regulated by the duration of the FSH surge, as an artificial prolongation of this increased level of hormone can raise the number of follicles recruited (Gibbons *et al.*, 1997; Lolis *et al.*, 1995).

Downloaded From Vet-eBooks.com

In cows, follicular waves can be observed long before puberty, as early as 2 weeks of age (Adams *et al.*, 1994; Evans *et al.*, 1994). They continue to occur in the usual fashion during pregnancy, with the exception of the absence of the selective growth and ovulation of the ovulatory follicle (Pierson and Ginther, 1986). Follicular waves take place until depletion of the ovarian reserve. The occurrence of follicular waves during pregnancy has not yet been documented in women, and for obvious ethical reasons, follicular dynamics in prepubertal girls remain poorly understood (Baerwald *et al.*, 2012). However, it is known that follicles develop to the preantral and early antral stages during childhood (Peters *et al.*, 1978).

6.2.4 Characteristics of the Dominant Follicle

Deviation occurs in cattle around 2.5 days after the beginning of the wave, when the largest follicles reach a diameter of 8.5 mm (Ginther *et al.*, 1997). Follicular growth switches from FHS- to LH-dependence, a transition that plays an important role to select the dominant follicle. Dominance lasts approximately 5 days in the cow (Stock and Fortune, 1993), and the dominant follicle starts to grow before his subordinates, approximately 6 and 10 h before the second and third largest, respectively (Ginther *et al.*, 1997). This was not confirmed in women by Baerwald *et al.* (2003b); however, the team suggested that this discrepancy was caused by the ultrasound imaging techniques used. It seems that in the cow every follicle has the ability to achieve dominance, as upon the removal of dominant follicles the subordinates become dominant (Gibbons *et al.*, 1997). The follicular phase is longer in women (14 days) than in cows (3 days), mainly because the human corpus luteum secretes estradiol and inhibin A, which inhibit FSH secretion. Progesterone secretion is different in cows and women, as shown in Figure 6.1. However, as described in Campbell *et al.* (2003), hormonal treatment can be used in cows to mimic the length of the human follicular phase.

The ovulatory LH surge stimulates the final oocyte maturation, and initiates the ovulation process, which will ultimately lead to the formation of the corpus luteum through a major reorganization of follicular cells. In bovine granulosa cells, the LH surge modifies the expression of numerous genes (Gilbert *et al.*, 2011). The expression of the LH receptor (LHR) is dynamic during the ovulation process: In human and primate, it is high in preovulatory mural granulosa cells, increases rapidly in cumulus cells of post-LH follicles, and then decreases with ovulation to rise again in the newly formed corpus luteum (Jeppesen *et al.*, 2012; Xu *et al.*, 2011). In women, the FSH receptor (FSHR) is downregulated in preovulatory follicles after the LH surge (Grøndahl *et al.*, 2011), and does not reappear (Xu *et al.*, 2011). Interestingly, the expression patterns of several genes, including LHR, are different in GnRHa-triggered human follicles compared to hCG-triggered ones (Borgbo *et al.*, 2013). Such comparative studies of gene expression have not been made in cows, but information is available about the effects of GnRH-triggered (Assidi *et al.*, 2008; Gilbert *et al.*, 2011) and hCG-triggered (Ndiaye *et al.*, 2005) LH surges. In human granulosa cells the expression of genes related to cell cycle and proliferation decreased after hCG stimulation, while the expression of genes related to inflammation, angiogenesis, extracellular matrix, and growth factors increased (Wissing *et al.*, 2014).

6.3 Assisted Reproduction

Nowadays, ART is routinely used in humans and cattle. Using these techniques, the pregnancy rate per cycle is approximately 30% in women (Center for Disease Control and Prevention, 2014), while embryo transfer in cattle is associated with pregnancy rates of approximately 60%

Downloaded From Vet-eBooks.com

(Mapletoft, 2012). However, as pointed out by de Mello Bianchi *et al.* (2010), there is a critical difference between routine ART in humans and cattle: In humans, the embryos are transferred back into the same patient the eggs originated from, while in cattle they are transferred to several fertile and healthy recipients. This capacity, in bovine, to distinguish between an ovarian or fertilization effect versus a uterine effect is very powerful. Although surrogate mothers are often used in humans, experiments such as the manipulation of oocyte quality, which are regularly performed in cows, cannot be performed in women. The most important techniques and their outcomes in each species will be discussed in the following sections.

6.3.1 Response to Ovarian Stimulation

Ovarian stimulation is a key aspect of reproductive management. With an artificial increase of the FSH concentration, the development of several follicles toward ovulation is stimulated. The oocytes may be collected from the resulting follicles and used for IVM and IVF, or the follicles may be given time to reach ovulation. When the follicles are left to ovulate, the number of ovulated oocytes is greater than without stimulation, and the process is called superovulation. The ovulated oocytes can be fertilized *in vivo* using artificial insemination (AI). In the dairy industry, superovulation followed by AI is used frequently to obtain a greater number of offspring from valuable cows, whose embryos are collected before implantation and then transferred to healthy recipients. In women, oocytes are usually collected just before ovulation, and uterine flushing is never performed as the embryos implant very rapidly once in the uterus. The ovarian response may vary greatly between individuals; in cows and women, superovulation can produce from 0 to more than 50 oocytes, and in human IVF treatment, the median number of collected eggs is nine (Seidel *et al.*, 2003; Sunkara *et al.*, 2011).

Ovarian stimulation induces the development of several follicles that evade the selection mechanisms, and it is unsure if this has an impact on oocyte quality. A recent study found that there are transcriptional differences between superovulated and naturally ovulated cattle oocytes (Chu *et al.*, 2012). In cows, individuals with consistently high numbers of follicles during follicular waves produce more oocytes following superovulation, but the proportion of good oocytes leading to transferable embryos is greater in individuals with normal range follicle numbers (Ireland *et al.*, 2007; Shaw *et al.*, 1995). However, this difference does not seem to be linked to some underlying lower oocyte quality in animals with more follicles, as IVM of oocytes from antral follicles provided similar outcomes for cows with high and low follicle numbers (Ireland *et al.*, 2007). Similar observations have been made in humans, as the proportion of good embryos decreased with the rise of the number of retrieved oocytes above a certain level (Meniru and Craft, 1997). These results suggest that ovarian stimulation may impact the development of follicles, leading to reduced oocyte quality.

In addition to the variability between individuals, the ovarian response to stimulation may also be affected by ovarian ageing. The prevalence of poor ovarian response in women, which is defined as the retrieval of less than four oocytes, increases with age to reach more than 50% in women over 40 years of age (Ferraretti *et al.*, 2011). Markers of ovarian reserve, such as antral follicle counts and AMH levels, can be used successfully to predict the ovarian response (La Marca and Sunkara, 2014), and to plan the IVF treatment accordingly. The ovarian response is also reduced in superovulated mature cows compared to heifers (Desaulniers *et al.*, 1995).

Ovarian stimulation may have negative effects on the patient. In women, one of the main concerns is the ovarian hyperstimulation syndrome (OHSS), a serious condition that may lead to severe complications and even death (Cluroe and Synek, 1995; Delvigne and Rozenberg, 2003). The overall incidence is estimated to be <5% (Delvigne and Rozenberg, 2002), but women with polycystic ovaries (PCO) are 10 times more likely to develop the symptoms (MacDougall

Downloaded From Vet-eBooks.com

et al., 1993). Because of the possible life-threatening complications, efforts are being made to reduce the occurrence of OHSS in women. Strategies to lower the amount of fertility drugs are used, and personalization of treatments to accommodate individual characteristics is explored. While ovarian cysts are a relatively common problem in cattle (Vanholder *et al.*, 2006), cows do not face such severe complications following ovarian stimulation, and this allows experimentation not possible in humans.

6.3.2 Response to FSH Coasting

Coasting (or FSH withdrawal) is a procedure that is used following ovarian stimulation in cows and women, but for different reasons. In cows, a coasting period without any FSH stimulation was introduced several years ago as a reproductive management technique to improve oocyte competence, while fertility clinics use it as a first choice treatment to prevent severe OHSS (Delvigne and Rozenberg, 2001). The artificial withdrawal of FSH during a prolonged period mimics the single follicle dominance and prevents recruitment of new follicles (Nivet *et al.*, 2012). In natural cycles, a decrease in FSH levels for several days is observed in women and cows before ovulation (Cooke *et al.*, 1997; Stricker *et al.*, 2006). It is during this period of follicular dominance, after the FSH surge and before the preovulatory LH surge, that oocyte competence acquisition occurs in large mammals (Sirard *et al.*, 2006). Therefore, using an artificial coasting period would be closer to normal ovarian physiology, and should produce more competent oocytes. In cattle, the first studies on this aspect of follicular maturation indicated that a bolus injection of FSH, followed by ovarian aspiration 48 h later, produced the highest blastocyst rates (Sirard *et al.*, 1999). A more recent study in bovine identified a specific coasting time window, from 44 to 68 h post FSH, that led to improved success rates (Nivet *et al.*, 2012). While follicles continue to grow after this period, the enclosed oocytes are significantly less competent; follicular size is not correlated with oocyte competence in larger bovine follicles (Nivet *et al.*, 2012). During FSH coasting in cattle, basal LH also seems to be an important factor for follicle development and oocyte quality, even if its suppression did not impact blastocyst rates (Labrecque *et al.*, 2014; Nivet *et al.* submitted).

In women, the wave of the dominant follicle is exposed to a LH surge before collection. However, a clear demonstration has been made that replacing FSH with a basal LH level allows similar or even superior results. Low-dose hCG was successfully used alone to complete controlled ovarian stimulation in GnRH agonist and antagonist protocols (Blockeel *et al.*, 2009; Filicori *et al.*, 2005). In addition to a reduction of the costs, low-hCG protocols were associated with a reduced number of small preovulatory follicles, a more estrogenic intrafollicular environment, and better fertilization rates (Filicori *et al.*, 2005). The use of GnRH agonists or antagonists is a fundamental difference between human and bovine IVF, and it results in a decreased basal LH, thereby preventing follicular growth. As the goal of coasting protocols in fertility clinics is to prevent OHSS, several studies focused on this particular aspect. One of the largest studies on coasting in women (Mansour *et al.*, 2005) supports the value of this technique for OHSS prevention. Unlike what had been done in cattle, they did not use an arbitrary time as a coasting period: FSH support was withdrawn when the dominant follicle reached 15–16 mm in diameter and until estradiol levels dropped below 3000 pg/ml, resulting in a coasting period of 2–7 days. In other studies, coasting for more than 3–4 days negatively impacted the number of oocytes retrieved (Owj *et al.*, 2007), implantation rates (Moreno *et al.*, 2004; Nardo *et al.*, 2006; Ulug *et al.*, 2004), and pregnancy rates (Corbett *et al.*, 2014; Mansour *et al.*, 2005). Others observed that coasting up to 4 days neither improved nor impaired IVF outcomes and pregnancy rates (Lukaszuk *et al.*, 2011; Moon *et al.*, 2008; Owj *et al.*, 2007; Talebi Chahvar *et al.*, 2014; Ulug *et al.*, 2004; Yilmaz *et al.*, 2010). In other studies, longer coasting periods (up to

Downloaded From Vet-eBooks.com

8 days) did not impact live birth rates (Abdalla and Nicopoullos, 2010), and it has been suggested that coasting is not effective at all to prevent OHSS (D'Angelo *et al.*, 2011). These human studies confirmed that women and cows share a similar time window of required FSH support beyond which the oocyte or the follicle can no longer be rescued.

6.3.3 Response to IVM

In most mammalian species studied, removal of oocytes from antral follicles causes spontaneous resumption of meiosis and completion of nuclear maturation (Edwards, 1965). This pseudo-maturation is believed to be linked to the removal of an inhibitory factor when the oocyte is physically taken out of the follicular environment (Tsafriri and Pomerantz, 1986). This characteristic of oocyte development makes IVM possible. The technique was developed in cattle during the 1980s with oocytes retrieved from ovaries collected at slaughterhouses (Sirard and First, 1988), and was improved when the utilization of FSH coasting was introduced (Blondin *et al.*, 2002). In bovine, IVM without coasting results in blastocyst rates around 30% (Rizos *et al.*, 2002).

In vitro maturation has several advantages for women, as it allows the reduction or elimination of the use of stimulatory gonadotropin hormones during fertility treatment. Aside from reducing the costs of the treatment and the unpleasant side effects of gonadotropins, IVM can reduce the risk of OHSS. However, pregnancy and live birth rates in women are considerably lower with IVM compared to conventional IVF (Gremeau *et al.*, 2012), and clinicians are reluctant to adopt it more widely for this reason. Oocytes used for human IVM originate from rapidly growing follicles recruited continuously by repetitive FSH treatment, and the bovine model suggests that while they may be meiotically competent, these oocytes have limited capacity to develop further (Blondin and Sirard, 1995; Sirard, 2011). In cattle, IVM results can be improved with adequate management of the chromatin status at retrieval (Sirard, 2011). The low pregnancy rates achieved with IVM in women led a team to develop a new system: simulated physiological oocyte maturation (SPOM) (Albuz *et al.*, 2010). They substantially improved bovine and mouse oocyte development outcomes by mimicking the physiological steps that they undergo during natural maturation inside a follicle. Cumulus–oocyte complexes were cultured in the presence of cAMP modulators for the first 1–2 h pre-IVM to increase cAMP levels, then a phosphodiesterase inhibitor was added to prevent precocious maturation, and finally FSH was used to induce oocyte maturation. A similar system was tested with sheep oocytes: the cleavage rates were not affected, but embryos from SPOM oocytes had approximately 1.6-fold more cells than control embryos (Rose *et al.*, 2013). While these results were promising, recent studies did not confirm the beneficial impact of SPOM, and even reported adverse effects (Guimaraes *et al.*, 2015). Some preliminary experiments were performed with human oocytes but the heparin in the recovery media interacted negatively with cAMP modulators to produce an adverse effect on oocyte developmental competence (Zeng *et al.*, 2013).

6.3.4 Biomarker Analysis

The study of oogenesis and folliculogenesis with genomic tools brings new insights to our understanding of reproductive biology (Bonnet *et al.*, 2008; Labrecque and Sirard, 2014). It allows the identification of genes and pathways that are involved in the precisely regulated development of the follicle, and provides clues to understand the impact of various factors affecting it. The combination of transcriptomic analyses brings us closer to build the whole bovine folliculome (Sirard, 2014). In addition to this valuable knowledge, genomic tools allow

Downloaded From Vet-eBooks.com

the identification of biomarkers, which are useful in research and can also be applied in clinics. Small differences at the level of follicular physiology or oocyte development may have a big impact on IVM or IVF outcomes, but current methods are unable to identify these differences. Follicular fluid was investigated as a potential source of biochemical predictors of oocyte quality in humans, but nothing truly reliable has been found yet (Revelli *et al.*, 2009). In cattle and humans, follicular size has been used as a criterion for selection of oocytes, but it was recently proven not to be a good indicator of competence for oocytes from large follicles (Nivet *et al.*, 2012). Morphological characteristics of bovine and human follicles and oocytes are still used to predict competence, but they are not always effective (Blondin and Sirard, 1995; Rienzi *et al.*, 2011; Vassena *et al.*, 2003).

The close relationship between the follicular cells and the oocyte allows bidirectional communication, which is essential to follicular development and oocyte competence. Therefore, differences in gene expression in follicular cells may be linked to specific characteristics of the oocyte. During IVF treatments, these cells are collected along with the oocytes but are usually discarded shortly after. However, they represent a valuable resource, since their analysis can provide information about the oocyte in a noninvasive way, and they are already available. Previous studies in our laboratory linked several biomarkers with various follicular characteristics in cattle and humans. The following table highlights the main aspects of follicular development for which biomarkers are currently available in granulosa cells (Table 6.1).

The greatest value of the cow model is its capacity to provide explanations for phenotypes observed at ovulation. In humans, most tissues (granulosa and cumulus cells), follicular fluid, and exosome metabolites are collected roughly 34 h post hCG, just prior to ovulation. Although data obtained at this time can be used to find biomarkers associated with outcomes, they do not provide explanations for the quality of the oocytes. In bovine, corresponding data can be collected 24 h post LH. Since collection can be made at any time during the stimulation process in bovine, post LH data and data from earlier events can be compared. We now have transcriptome analysis of granulosa cells at 6 and 22 h post LH, which have been compared to samples collected just before the LH surge (Gilbert *et al.*, 2012), at the end of the dominant phase with early, mid, or late coasting (Nivet *et al.*, 2012), and at the growth-plateau phase in early dominant, and predominant follicles (5–9 mm). Since we also have the average oocyte quality data for all these stages, it becomes possible to work toward finding a cause, or a series of events leading to competent oocytes. Since the cumulative changes should be present in the oocyte before IVF, the bovine model can provide the molecular explanation for the progressive acquisition of competence in human oocytes (which are available for marker validation at that time).

Table 6.1 Main aspects of follicular development for which granulosa cells' biomarkers are available.

	Bovine	**Human**
Follicular growth stages (medium-sized)	Douville and Sirard, 2014	
Follicular growth stages (dominant)	Girard *et al.*, 2015	
Response to LH surge	Gilbert *et al.*, 2011; Gilbert *et al.*, 2012	Wissing *et al.*, 2014
Coasting	Nivet *et al.*, 2012	
IVF outcome		Hamel *et al.*, 2008; Hamel *et al.*, 2010a, 2010b
Follicle differentiation	Evans *et al.*, 2004; Hayashi *et al.*, 2010	

Downloaded From Vet-eBooks.com

6.4 Testing the Competence Hypothesis

Oocyte competence is a concept that includes five key steps: the ability to resume meiosis, to cleave following fertilization, to develop to the blastocyst stage, to induce a pregnancy resulting in a live birth, and in good health (Sirard *et al.*, 2006). There is a need to gather knowledge about ovarian physiology and the various elements of oocyte competence in order to improve current fertility treatments. As ethical concerns forbid direct experimentations with humans, the best option is to use an animal model whose ovarian physiology is similar to ours. While the mouse is the best known mammalian model, it is not a relevant model to study human reproduction failure (Neuber and Powers, 2000). Moreover, in this species, oocyte competence is gained more abruptly and rapidly at the end of oocyte growth. As detailed earlier, humans and cattle share numerous characteristics regarding ovarian physiology and follicular development; however, one final characteristic makes the cow the best model to study oocyte competence: The first stages of embryogenesis are quite similar in bovines and humans (Anderiesz *et al.*, 2000; Navara *et al.*, 1995). This aspect is of utmost importance to test the follicle competence hypothesis, as several levels of oocyte competence are related to embryo development. Therefore, the modulations of follicular development in cows can be used as a model to investigate the different levels of oocyte competence.

The bovine ovarian follicle was suggested as the best *in vitro* model to study reproductive toxicology (Petro *et al.*, 2010, 2012). It has already contributed to research on the mechanisms of action of specific drugs on ovarian cells (Tosca *et al.*, 2010), to explore nonclassical mechanisms of steroid sensing in the ovary (Ivell *et al.*, 2014), to study the impact of hyperlipidaemia or elevated concentrations of serum NEFAs on fertility (Leroy *et al.*, 2010; Van Hoeck *et al.*, 2011), to investigate uterine infections and immunity (Herath *et al.*, 2006), and to study reproductive aging (Malhi *et al.*, 2005, 2007). The bovine model was also successfully used as a screening tool to investigate the effects of human preovulatory follicular fluid on oocyte and embryo quality (Valckx *et al.*, 2015).

6.5 Conclusion

In conclusion, the bovine model is best for investigating late folliculogenesis events that are linked to oocyte competence, and can be used as both *in vivo* and *in vitro* models. Cattle have four main advantages as a model for the study of human reproduction failure: (i) similar follicular dynamics; (ii) similar pattern of progressive oocyte competence acquisition before ovulation; (iii) similar timing of embryonic genome activation associated with oocyte programming; and (iv) the possibility to disconnect the donor from the recipient allows a more accurate evaluation of oocyte quality.

References

Abdalla, H. and Nicopoullos, J.D. (2010) The effect of duration of coasting and estradiol drop on the outcome of assisted reproduction: 13 years of experience in 1,068 coasted cycles to prevent ovarian hyperstimulation. *Fertil. Steril.*, **94** (5), 1757–1763.

Adams, G. and Pierson, R. (1995) Bovine model for study of ovarian follicular dynamics in humans. *Theriogenology*, **43** (1), 113–120.

Downloaded From Vet-eBooks.com

Adams, G.P., Matteri, R., Kastelic, J., Ko, J., and Ginther, O. (1992) Association between surges of follicle-stimulating hormone and the emergence of follicular waves in heifers. *J. Reprod. Fertil.*, **94** (1), 177–188.

Adams, G.P., Evans, A.C., and Rawlings, N.C. (1994) Follicular waves and circulating gonadotrophins in 8-month-old prepubertal heifers. *J. Reprod. Fertil.*, **100** (1), 27–33.

Albuz, F.K., Sasseville, M., Lane, M., Armstrong, D.T., Thompson, J.G., and Gilchrist, R.B. (2010) Simulated physiological oocyte maturation (SPOM): a novel *in vitro* maturation system that substantially improves embryo yield and pregnancy outcomes. *Hum. Reprod.*, **25** (12), 2999–3011.

Anderiesz, C., Ferraretti, A.P., Magli, C., Fiorentino, A., Fortini, D., Gianaroli, L., Jones, G., and Trounson, A. (2000) Effect of recombinant human gonadotrophins on human, bovine and murine oocyte meiosis, fertilization and embryonic development *in vitro*. *Hum. Reprod.*, **15** (5), 1140–1148.

Assidi, M., Dufort, I., Ali, A., Hamel, M., Algriany, O., Dielemann, S., and Sirard, M.A. (2008) Identification of potential markers of oocyte competence expressed in bovine cumulus cells matured with follicle-stimulating hormone and/or phorbol myristate acetate *in vitro*. *Biol. Reprod.*, **79** (2), 209–222.

Baerwald, A. (2009) Human antral folliculogenesis: what we have learned from the bovine and equine models. *Anim. Reprod.*, **6**, 20–29.

Baerwald, A.R., Adams, G.P., and Pierson, R.A. (2003a) A new model for ovarian follicular development during the human menstrual cycle. *Fertil. Steril.*, **80** (1), 116–122.

Baerwald, A.R., Adams, G.P., and Pierson, R.A. (2003b) Characterization of ovarian follicular wave dynamics in women. *Biol. Reprod.*, **69** (3), 1023–1031.

Baerwald, A.R., Adams, G.P., and Pierson, R.A. (2012) Ovarian antral folliculogenesis during the human menstrual cycle: a review. *Hum. Reprod. Update*, **18** (1), 73–91.

Ben-Nun, I., Gruber, A., Abramowicz, J., Fejgin, M., and Ben-Aderet, N. (1986) Management of gonadotrophin-induced cycles characterized by a significant discrepancy between oestrogen levels and dominant follicle size. *Hum. Reprod.*, **1** (6), 365–368.

Blockeel, C., De Vos, M., Verpoest, W., Stoop, D., Haentjens, P., and Devroey, P. (2009) Can 200 IU of hCG replace recombinant FSH in the late follicular phase in a GnRH-antagonist cycle? A pilot study. *Hum. Reprod.*, **24** (11), 2910–2916.

Blondin, P. and Sirard, M.A. (1995) Oocyte and follicular morphology as determining characteristics for developmental competence in bovine oocytes. *Mol. Reprod. Dev.*, **41** (1), 54–62.

Blondin, P., Bousquet, D., Twagiramungu, H., Barnes, F., and Sirard, M.A. (2002) Manipulation of follicular development to produce developmentally competent bovine oocytes. *Biol. Reprod.*, **66** (1), 38–43.

Bonnet, A., Dalbiès-Tran, R., and Sirard, M.A. (2008) Opportunities and challenges in applying genomics to the study of oogenesis and folliculogenesis in farm animals. *Reproduction*, **135** (2), 119–128.

Borgbo, T., Povlsen, B.B., Andersen, C.Y., Borup, R., Humaidan, P., and Grondahl, M.L. (2013) Comparison of gene expression profiles in granulosa and cumulus cells after ovulation induction with either human chorionic gonadotropin or a gonadotropin-releasing hormone agonist trigger. *Fertil. Steril.*, **100** (4), 994–1001.

Brown, J. (1978) Pituitary control of ovarian function: concepts derived from gonadotrophin therapy. *Aust. N. Z. J. Obstet. Gynaecol.*, **18** (1), 47–54.

Burns, D.S., Jimenez-Krassel, F., Ireland, J.L.H., Knight, P.G., and Ireland, J.J. (2005) Numbers of antral follicles during follicular waves in cattle: evidence for high variation among animals, very

Downloaded From Vet-e-Books.com

high repeatability in individuals and an inverse association with serum follicle-stimulating hormone concentrations. *Biol. Reprod.*, **73** (1), 54–62.

Cahill, L. and Mauleon, P. (1980) Influences of season, cycle and breed on follicular growth rates in sheep. *J. Reprod. Fertil.*, **58** (2), 321–328.

Campbell, B.K., Telfer, E.E., Webb, R., and Baird, D.T. (2000) Ovarian autografts in sheep as a model for studying folliculogenesis. *Mol. Cell. Endocrinol.*, **163** (1–2), 131–139.

Campbell, B.K., Souza, C., Gong, J., Webb, R., Kendall, N., Marsters, P., Robinson, G., Mitchell, A., Telfer, E.E., and Baird, D.T. (2003) Domestic ruminants as models for the elucidation of the mechanisms controlling ovarian follicle development in humans. *Reprod. Suppl.*, **61**, 429–443.

Carnevale, E. (2008) The mare model for follicular maturation and reproductive aging in the woman. *Theriogenology*, **69** (1), 23–30.

Center for Disease Control and Prevention . (2014) Assisted Reproductive Technology: Fertility Clinic Success Rates Report, U.S. Department of Health and Human Services, CDC, National Center for Chronic Disease Prevention and Health Promotion, Division of Reproductive Health, Atlanta, 567 pp.

Chu, T., Dufort, I., and Sirard, M.A. (2012) Effect of ovarian stimulation on oocyte gene expression in cattle. *Theriogenology*, **77** (9), 1928–1938.

Cluroe, A.D. and Synek, B.J. (1995) A fatal case of ovarian hyperstimulation syndrome with cerebral infarction. *Pathology*, **27** (4), 344–346.

Cooke, D., Crowe, M., and Roche, J. (1997) Circulating FSH isoform patterns during recurrent increases in FSH throughout the oestrous cycle of heifers. *J. Reprod. Fertil.*, **110** (2), 339–345.

Corbett, S., Shmorgun, D., Claman, P., Healey, S., and Gysler, M. (2014) The prevention of ovarian hyperstimulation syndrome. *J. Obstet. Gynaecol. Can.*, **36** (11), 1024–1036.

D'Angelo, A., Brown, J., and Amso, N.N. (2011) Coasting (withholding gonadotrophins) for preventing ovarian hyperstimulation syndrome. *Cochrane Database Syst. Rev.*, **6**, 1–40.

de Mello Bianchi, P.H., Serafini, P., da Rocha, A.M., Hassun, P.A., da Motta, E.L.A., Baruselli, P.S., and Baracat, E.C. (2010) Review: follicular waves in the human ovary: a new physiological paradigm for novel ovarian stimulation protocols. *Reprod. Sci.*, **17** (12), 1067–1076.

Delvigne, A. and Rozenberg, S. (2001) Preventive attitude of physicians to avoid OHSS in IVF patients. *Hum. Reprod.*, **16** (12), 2491–2495.

Delvigne, A. and Rozenberg, S. (2002) Epidemiology and prevention of ovarian hyperstimulation syndrome (OHSS): a review. *Hum. Reprod. Update*, **8** (6), 559–577.

Delvigne, A. and Rozenberg, S. (2003) Review of clinical course and treatment of ovarian hyperstimulation syndrome (OHSS). *Hum. Reprod. Update*, **9** (1), 77–96.

Desaulniers, D.M., Lussier, J.G., Goff, A.K., Bousquet, D., and Guilbault, L.A. (1995) Follicular development and reproductive endocrinology during and after superovulation in heifers and mature cows displaying contrasting superovulatory responses. *Theriogenology*, **44** (4), 479–497.

Devoto, L., Fuentes, A., Kohen, P., Céspedes, P., Palomino, A., Pommer, R., Muñoz, A., and Strauss, J.F. (2009) The human corpus luteum: life cycle and function in natural cycles. *Fertil. Steril.*, **92** (3), 1067–1079.

Douville, G. and Sirard, M.A. (2014) Changes in granulosa cells gene expression associated with growth, plateau and atretic phases in medium bovine follicles. *J. Ovarian Res.*, **7**, 1–16.

Dowling, D. (1954) The induction of ovulation in cattle. *Aust. Vet. J.*, **30** (8), 240–244.

Dufour, J., Cahill, L.P., and Mauleon, P. (1979) Short- and long-term effects of hypophysectomy and unilateral ovariectomy on ovarian follicular populations in sheep. *J. Reprod. Fertil.*, **57** (2), 301–309.

Echternkamp, S.E., Cushman, R.A., and Allan, M.F. (2009) Size of ovulatory follicles in cattle expressing multiple ovulations naturally and its influence on corpus luteum development and fertility. *J. Anim. Sci.*, **87** (11), 3556–3568.

Downloaded From Vet-eBooks.com

Edwards, R. (1965) Maturation *in vitro* of mouse, sheep, cow, pig, rhesus monkey and human ovarian oocytes. *Nature*, **208** (5008), 349–351.

Erickson, B.H. (1966) Development and senescence of the postnatal bovine ovary. *J. Anim. Sci.*, **25** (3), 800–805.

Erickson, B., Reynolds, R., and Murphree, R. (1976) Ovarian characteristics and reproductive performance of the aged cow. *Biol. Reprod.*, **15** (4), 555–560.

Evans, A.C., Adams, G.P., and Rawlings, N.C. (1994) Follicular and hormonal development in prepubertal heifers from 2 to 36 weeks of age. *J. Reprod. Fertil.*, **102** (2), 463–470.

Evans, A.C., Ireland, J.L., Winn, M.E., Lonergan, P., Smith, G.W., Coussens, P.M., and Ireland, J.J. (2004) Identification of genes involved in apoptosis and dominant follicle development during follicular waves in cattle. *Biol. Reprod.*, **70** (5), 1475–1484.

Faddy, M.J. and Gosden, R.G. (1996) A model conforming the decline in follicle numbers to the age of menopause in women. *Hum. Reprod.*, **11** (7), 1484–1486.

Ferraretti, A.P., La Marca, A., Fauser, B.C., Tarlatzis, B., Nargund, G., and Gianaroli, L. (2011) ESHRE consensus on the definition of 'poor response' to ovarian stimulation for *in vitro* fertilization: the Bologna criteria. *Hum. Reprod.*, **26** (7), 1616–1624.

Filicori, M., Cognigni, G.E., Gamberini, E., Parmegiani, L., Troilo, E., and Roset, B. (2005) Efficacy of low-dose human chorionic gonadotropin alone to complete controlled ovarian stimulation. *Fertil. Steril.*, **84** (2), 394–401.

Gibbons, J.R., Wiltbank, M.C., and Ginther, O.J. (1997) Functional interrelationships between follicles greater than 4 mm and the follicle-stimulating hormone surge in heifers. *Biol. Reprod.*, **57** (5), 1066–1073.

Gilbert, I., Robert, C., Dieleman, S., Blondin, P., and Sirard, M.A. (2011) Transcriptional effect of the LH surge in bovine granulosa cells during the peri-ovulation period. *Reproduction*, **141** (2), 193–205.

Gilbert, I., Robert, C., Vigneault, C., Blondin, P., and Sirard, M.A. (2012) Impact of the LH surge on granulosa cell transcript levels as markers of oocyt developmental competence in cattle. *Reproduction*, **143**, 735–747.

Ginther, O. (1992) *Reproductive Biology of the Mare: Basic and Applied Aspects*, 2nd edn, Equiservices Publishing, pp. 141–151.

Ginther, O.J. (2012) The mare: a 1000-pound guinea pig for study of the ovulatory follicular wave in women. *Theriogenology*, **77** (5), 818–828.

Ginther, O., Kastelic, J., and Knopf, L. (1989a) Composition and characteristics of follicular waves during the bovine estrous cycle. *Anim. Reprod. Sci.*, **20** (3), 187–200.

Ginther, O.J., Knopf, L., and Kastelic, J.P. (1989) Temporal associations among ovarian events in cattle during oestrous cycles with two and three follicular waves. *J. Reprod. Fertil.*, **87** (1), 223–230.

Ginther, O.J., Kot, K., Kulick, L.J., and Wiltbank, M.C. (1997) Emergence and deviation of follicles during the development of follicular waves in cattle. *Theriogenology*, **48** (1), 75–87.

Ginther, O.J., Beg, M.A., Bergfelt, D.R., Donadeu, F.X., and Kot, K. (2001) Follicle selection in monovular species. *Biol. Reprod.*, **65** (3), 638–647.

Ginther, O.J., Gastal, E.L., Gastal, M.O., Bergfelt, D.R., Baerwald, A.R., and Pierson, R.A. (2004) Comparative study of the dynamics of follicular waves in mares and women. *Biol. Reprod.*, **71** (4), 1195–1201.

Girard, A., Dufort, I., Douville, G., and Sirard, M.A., and (2015) Global gene expression in granulosa cells of growing, plateau and atretic dominant follicles in cattle. *Reprod. Biol. Endocrinol.*, **13**, 17.

Gougeon, A. (1979) Qualitative changes in medium and large antral follicles in the human ovary during the menstrual cycle. *Ann. Biol. Anim. Biochem. Biophys.*, **19**, 1461–1468.

Downloaded From Vet-eBooks.com

Gougeon, A. (1986) Dynamics of follicular growth in the human: a model from preliminary results. *Hum. Reprod.*, **1** (2), 81–87.

Gougeon, A. (1996) Regulation of ovarian follicular development in primates: facts and hypotheses. *Endocr. Rev.*, **17** (2), 121–155.

Gremeau, A.S., Andreadis, N., Fatum, M., Craig, J., Turner, K., McVeigh, E., and Child, T. (2012) *In vitro* maturation or *in vitro* fertilization for women with polycystic ovaries? A case–control study of 194 treatment cycles. *Fertil. Steril.*, **98** (2), 355–360.

Grøndahl, M.L., Nielsen, M.E., Dal Canto, M., Fadini, R., Rasmussen, I., Westergaard, L., Kristensen, S., and Andersen, C.Y. (2011) Anti-Müllerian hormone remains highly expressed in human cumulus cells during the final stages of folliculogenesis. *Reprod. Biomed. Online*, **22** (4), 389–398.

Guimaraes, A.L., Pereira, S.A., Leme, L.O., and Dode, M.A. (2015) Evaluation of the simulated physiological oocyte maturation system for improving bovine *in vitro* embryo production. *Theriogenology*, **83** (1), 52–57.

Hamel, M., Dufort, I., Robert, C., Gravel, C., Leveille, M.C., Leader, A., and Sirard, M.A. (2008) Identification of differentially expressed markers in human follicular cells associated with competent oocytes. *Hum. Reprod.*, **23**, 1118–1127.

Hamel, M., Dufort, I., Robert, C., Leveille, M.C., Leader, A., and Sirard, M.A. (2010a) Genomic assessment of follicular marker genes as pregnancy predictors for human IVF. *Mol. Hum. Reprod.* **16**, 87–96.

Hamel, M., Dufort, I., Robert, C., Leveille, M.C., Leader, A., and Sirard, M.A. (2010b) Identification of follicular marker genes as pregnancy predictors for human IVF: new evidence for the involvement of luteinization process. *Mol. Hum. Reprod.*, **16** (8), 548–556.

Hata, T., Yoshino, K., Nagahara, Y., Matsunaga, I., and Kitao, M. (1983) Precise day of ovulation determined by real-time ultrasound evidence of graafian follicular development. *Int. J. Gynaecol. Obstet.*, **21** (6), 435–438.

Hayashi, K.G., Ushizawa, K., Hosoe, M., and Takahashi, T. (2010) Differential genome-wide gene expression profiling of bovine largest and second-largest follicles: identification of genes associated with growth of dominant follicles. *Reprod. Biol. Endocrinol.*, **8**, 11.

Henderson, K.M. and Franchimont, P. (1981) Regulation of inhibin production by bovine ovarian cells *in vitro*. *J. Reprod. Fertil.*, **63** (2), 431–442.

Herath, S., Dobson, H., Bryant, C.E., and Sheldon, I.M. (2006) Use of the cow as a large animal model of uterine infection and immunity. *J. Reprod. Immunol.*, **69** (1), 13–22.

Hirshfield, A.N. (1989) Granulosa cell proliferation in very small follicles of cycling rats studied by long-term continuous tritiated-thymidine infusion. *Biol. Reprod.*, **41** (2), 309–316.

Hunter, M.G., Robinson, R.S., Mann, G.E., and Webb, R. (2004) Endocrine and paracrine control of follicular development and ovulation rate in farm species. *Anim. Reprod. Sci.*, **82–83**, 461–477.

Illingworth, P.J., Reddi, K., Smith, K.B., and Baird, D.T. (1991) The source of inhibin secretion during the human menstrual cycle. *J. Clin. Endocrinol. Metab.*, **73** (3), 667–673.

Ireland, J.J., Ward, F., Jimenez-Krassel, F., Ireland, J.L., Smith, G.W., Lonergan, P., and Evans, A.C. (2007) Follicle numbers are highly repeatable within individual animals but are inversely correlated with FSH concentrations and the proportion of good-quality embryos after ovarian stimulation in cattle. *Hum. Reprod.*, **22** (6), 1687–1695.

Ivell, R., Dai, Y., Mann, N., and Anand-Ivell, R. (2014) Non-classical mechanisms of steroid sensing in the ovary: lessons from the bovine oxytocin model. *Mol. Cell. Endocrinol.*, **382** (1), 466–471.

Jeppesen, J.V., Kristensen, S.G., Nielsen, M.E., Humaidan, P., Dal Canto, M., Fadini, R., Schmidt, K.T., Ernst, E., and Yding Andersen, C. (2012) LH-receptor gene expression in human granulosa and cumulus cells from antral and preovulatory follicles. *J. Clin. Endocrinol. Metab.*, **97** (8), 1524–1531.

Downloaded From Vet-eBooks.com

La Marca, A. and Sunkara, S.K. (2014) Individualization of controlled ovarian stimulation in IVF using ovarian reserve markers: from theory to practice. *Hum. Reprod. Update*, **20** (1), 124–140.
Labrecque, R. and Sirard, M.A. (2014) The study of mammalian oocyte competence by transcriptome analysis: progress and challenges. *Mol. Hum. Reprod.*, **20** (2), 103–116.
Labrecque, R., Vigneault, C., Blondin, P., and Sirard, M.A. (2014) Gene expression analysis of bovine oocytes at optimal coasting time combined with GnRH antagonist during the no-FSH period. *Theriogenology*, **81** (8), 1092–1100.
Leroy, J.L., Van Hoeck, V., Clemente, M., Rizos, D., Gutierrez-Adan, A., Van Soom, A., Uytterhoeven, M., and Bols, P.E. (2010) The effect of nutritionally induced hyperlipidaemia on *in vitro* bovine embryo quality. *Hum. Reprod.*, **25** (3), 768–778.
Lolis, D., Tsolas, O., and Messinis, I. (1995) The follicle-stimulating hormone threshold level for follicle maturation in superovulated cycles. *Fertil. Steril.*, **63** (6), 1272–1277.
Lukaszuk, K., Liss, J., and Jakiel, G. (2011) "Internal coasting" for prevention of ovarian hyperstimulation syndrome (OHSS) in IVF/ICSI. *Ginekol. Pol.*, **82** (11), 812–816.
Lussier, J.G., Matton, P., and Dufour, J.J. (1987) Growth rates of follicles in the ovary of the cow. *J. Reprod. Fertil.*, **81** (2), 301–307.
MacDougall, M.J., Tan, S.L., Balen, A., and Jacobs, H.S. (1993) A controlled study comparing patients with and without polycystic ovaries undergoing *in-vitro* fertilization. *Hum. Reprod.*, **8** (2), 233–237.
Malhi, P.S., Adams, G.P., and Singh, J. (2005) Bovine model for the study of reproductive aging in women: follicular, luteal and endocrine characteristics. *Biol. Reprod.*, **73** (1), 45–53.
Malhi, P.S., Adams, G.P., Pierson, R.A., and Singh, J. (2006) Bovine model of reproductive aging: response to ovarian synchronization and superstimulation. *Theriogenology*, **66** (5), 1257–1266.
Malhi, P.S., Adams, G.P., Mapletoft, R.J., and Singh, J. (2007) Oocyte developmental competence in a bovine model of reproductive aging. *Reproduction*, **134** (2), 233–239.
Mansour, R., Aboulghar, M., Serour, G., Amin, Y., and Abou-Setta, A.M. (2005) Criteria of a successful coasting protocol for the prevention of severe ovarian hyperstimulation syndrome. *Hum. Reprod.*, **20** (11), 3167–3172.
Mapletoft, R.J. (2012) Perspectives on bovine embryo transfer. *Adv. Dairy Technol.*, **24**, 83–93.
Meniru, G.I. and Craft, I.L. (1997) Utilization of retrieved oocytes as an index of the efficiency of superovulation strategies for *in-vitro* fertilization treatment. *Hum. Reprod.*, **12** (10), 2129–2132.
Mihm, M. and Evans, A. (2008) Mechanisms for dominant follicle selection in monovulatory species: a comparison of morphological, endocrine and intraovarian events in cows, mares and women. *Reprod. Domest. Anim.*, **43** (s2), 48–56.
Moon, H.S., Joo, B.S., Moon, S.E., Lee, S.K., Kim, K.S., and Koo, J.S. (2008) Short coasting of 1 or 2 days by withholding both gonadotropins and gonadotropin-releasing hormone agonist prevents ovarian hyperstimulation syndrome without compromising the outcome. *Fertil. Steril.*, **90** (6), 2172–2178.
Moreno, L., Diaz, I., Pacheco, A., Zuniga, A., Requena, A., and Garcia-Velasco, J.A. (2004) Extended coasting duration exerts a negative impact on IVF cycle outcome due to premature luteinization. *Reprod. Biomed. Online*, **9** (5), 500–504.
Nardo, L.G., Cheema, P., Gelbaya, T.A., Horne, G., Fitzgerald, C.T., Pease, E.H., Brison, D.R., and Lieberman, B.A. (2006) The optimal length of 'coasting protocol' in women at risk of ovarian hyperstimulation syndrome undergoing *in vitro* fertilization. *Hum. Fertil.*, **9** (3), 175–180.
Navara, C., Simerly, C., and Schatten, G. (1995) Imaging motility during fertilization. *Theriogenology*, **44** (8), 1099–1114.
Ndiaye, K., Fayad, T., Silversides, D.W., Sirois, J., and Lussier, J.G. (2005) Identification of downregulated messenger RNAs in bovine granulosa cells of dominant follicles following stimulation with human chorionic gonadotropin. *Biol. Reprod.*, **73** (2), 324–333.

Downloaded From Vet-eBooks.com

Nequin, L.G., Alvarez, J., and Schwartz, N.B. (1979) Measurement of serum steroid and gonadotropin levels and uterine and ovarian variables throughout 4 day and 5 day estrous cycles in the rat. *Biol. Reprod.*, **20** (3), 659–670.

Neuber, E., and Powers, R.D. (2000) Is the mouse a clinically relevant model for human fertilization failures? *Hum. Reprod.*, **15** (1), 171–174.

Nivet, A.L., Bunel, A., Labrecque, R., Belanger, J., Vigneault, C., Blondin, P., and Sirard, M.A. (2012) FSH withdrawal improves developmental competence of oocytes in the bovine model. *Reproduction*, **143** (2), 165–171.

Oktem, O. and Oktay, K. (2008) The ovary. *Ann. N. Y. Acad. Sci.*, **1127** (1), 1–9.

Owj, M., Tehrani Nejad, E., Amirchaghmaghi, E., Ezabadi, Z., and Baghestani, A.R. (2007) The effect of withholding gonadotropin (a coasting period) on the outcome of *in vitro* fertilization cycles. *Eur. J. Obstet. Gynecol. Reprod. Biol.*, **133** (1), 81–85.

Pate, J.L., Toyokawa, K., Walusimbi, S., and Brzezicka, E. (2010) The interface of the immune and reproductive systems in the ovary: lessons learned from the corpus luteum of domestic animal models. *Am. J. Reprod. Immunol.*, **64** (4), 275–286.

Peters, H., Byskov, A.G., and Grinsted, J. (1978) Follicular growth in fetal and prepubertal ovaries of humans and other primates. *Clin. Endocrinol. Metab.*, **7** (3), 469–485.

Petro, E.M., Covaci, A., Leroy, J.L., Dirtu, A.C., De Coen, W., and Bols, P.E. (2010) Occurrence of endocrine disrupting compounds in tissues and body fluids of Belgian dairy cows and its implications for the use of the cow as a model to study endocrine disruption. *Sci. Total Environ.*, **408** (22), 5423–5428.

Petro, E., Leroy, J., Van Cruchten, S., Covaci, A., Jorssen, E., and Bols, P. (2012) Endocrine disruptors and female fertility: focus on (bovine) ovarian follicular physiology. *Theriogenology*, **78** (9), 1887–1900.

Pierson, R. and Ginther, O. (1986) Ovarian follicular populations during early pregnancy in heifers. *Theriogenology*, **26** (5), 649–659.

Rajakoski, E. (1960) The ovarian follicular system in sexually mature heifers with special reference to seasonal, cyclical and left–right variations. *Acta Endocrinol. Suppl.*, **(52)**, 1–68.

Revelli, A., Delle Piane, L., Casano, S., Molinari, E., Massobrio, M., and Rinaudo, P. (2009) Follicular fluid content and oocyte quality: from single biochemical markers to metabolomics. *Reprod. Biol. Endocrinol.*, **7** (40), 4330–4337.

Rienzi, L., Vajta, G., and Ubaldi, F. (2011) Predictive value of oocyte morphology in human IVF: a systematic review of the literature. *Hum. Reprod. Update*, **17** (1), 34–45.

Rizos, D., Fair, T., Papadopoulos, S., Boland, M.P., and Lonergan, P. (2002) Developmental, qualitative and ultrastructural differences between ovine and bovine embryos produced *in vivo* or *in vitro*. *Mol. Reprod. Dev.*, **62** (3), 320–327.

Rose, R.D., Gilchrist, R.B., Kelly, J.M., Thompson, J.G., and Sutton-McDowall, M.L. (2013) Regulation of sheep oocyte maturation using cAMP modulators. *Theriogenology*, **79** (1), 142–148.

Schams, D. and Berisha, B. (2004) Regulation of corpus luteum function in cattle: an overview. *Reprod. Domest. Anim.*, **39** (4), 241–251.

Seidel, G.E., Elsden, R.P., and Hasler, J.F. (2003) Embryo transfer in dairy cattle. Hoard's Dairyman Books. 96 pp.

Shaw, D., Farin, P., Washburn, S., and Britt, J. (1995) Effect of retinol palmitate on ovulation rate and embryo quality in superovulated cattle. *Theriogenology*, **44** (1), 51–58.

Silva-Santos, K.C., Santos, G.M.G., Siloto, L.S., Hertel, M.F., Andrade, E.R., Rubin, M.I.B., Sturion, L., Melo-Sterza, F.A., and Seneda, M.M. (2011) Estimate of the population of preantral follicles in the ovaries of Bos taurus indicus and Bos taurus taurus cattle. *Theriogenology*, **76** (6), 1051–1057.

Downloaded From Vet-eBooks.com

Sirard, M.A. (2011) Follicle environment and quality of *in vitro* matured oocytes. *J. Assist. Reprod. Genet.*, **28** (6), 483–488.

Sirard, M.A. (2014) Toward building the cow folliculome. *Anim. Reprod. Sci.*, **149** (1–2), 90–97.

Sirard, M.A. and First, N.L. (1988) *In vitro* inhibition of oocyte nuclear maturation in the bovine. *Biol. Reprod.*, **39** (2), 229–234.

Sirard, M.A., Picard, L., Dery, M., Coenen, K., and Blondin, P. (1999) The time interval between FSH administration and ovarian aspiration influences the development of cattle oocytes. *Theriogenology*, **51** (4), 699–708.

Sirard, M.A., Richard, F., Blondin, P., and Robert, C. (2006) Contribution of the oocyte to embryo quality. *Theriogenology*, **65** (1), 126–136.

Souza, A.H., Gumen, A., Silva, E.P., Cunha, A.P., Guenther, J.N., Peto, C.M., Caraviello, D.Z., and Wiltbank, M.C. (2007) Supplementation with estradiol-17beta before the last gonadotropin-releasing hormone injection of the Ovsynch protocol in lactating dairy cows. *J. Dairy Sci.*, **90** (10), 4623–4634.

Stock, A.E. and Fortune, J.E. (1993) Ovarian follicular dominance in cattle: relationship between prolonged growth of the ovulatory follicle and endocrine parameters. *Endocrinology*, **132** (3), 1108–1114.

Stricker, R., Eberhart, R., Chevailler, M.C., Quinn, F.A., and Bischof, P. (2006) Establishment of detailed reference values for luteinizing hormone, follicle stimulating hormone, estradiol and progesterone during different phases of the menstrual cycle on the Abbott ARCHITECT analyzer. *Clin. Chem. Lab. Med.*, **44** (7), 883–887.

Sunkara, S.K., Rittenberg, V., Raine-Fenning, N., Bhattacharya, S., Zamora, J., and Coomarasamy, A. (2011) Association between the number of eggs and live birth in IVF treatment: an analysis of 400 135 treatment cycles. *Hum. Reprod.*, **26** (7), 1768–1774.

Talebi Chahvar, S., Zosmer, A., Caragia, A., Balestrini, S., Sabatini, L., Tranquilli, A.L., and Al-Shawaf, T. (2014) Coasting, embryo development and outcomes of blastocyst transfer: a case–control study. *Reprod. Biomed. Online*, **29** (2), 231–238.

Tosca, L., Rame, C., Chabrolle, C., Tesseraud, S., and Dupont, J. (2010) Metformin decreases IGF1-induced cell proliferation and protein synthesis through AMP-activated protein kinase in cultured bovine granulosa cells. *Reproduction*, **139** (2), 409–418.

Trounson, A., Gosden, R., and Eichenlaub-Ritter, U. (2013) *Biology and Pathology of the Oocyte: Role in Fertility, Medicine and Nuclear Reprogramming*, 2nd edn, Cambridge University Press, p. 466.

Tsafriri, A. and Pomerantz, S.H. (1986) Oocyte maturation inhibitor. *Clin. Endocrinol. Metab.*, **15** (1), 157–170.

Ulug, U., Ben-Shlomo, I., and Bahceci, M. (2004) Predictors of success during the coasting period in high-responder patients undergoing controlled ovarian stimulation for assisted conception. *Fertil. Steril.*, **82** (2), 338–342.

Valckx, S.D., De Bie, J., Michiels, E.D., Goovaerts, I.G., Punjabi, U., Ramos-Ibeas, P., Gutierrez-Adan, A., Bols, P.E., and Leroy, J.L. (2015) The effect of human follicular fluid on bovine oocyte developmental competence and embryo quality. *Reprod. Biomed. Online*, **30** (2), 203–207.

Van Hoeck, V., Sturmey, R.G., Bermejo-Alvarez, P., Rizos, D., Gutierrez-Adan, A., Leese, H.J., Bols, P.E., and Leroy, J.L. (2011) Elevated non-esterified fatty acid concentrations during bovine oocyte maturation compromise early embryo physiology. *PLoS One*, **6** (8), 1–8.

Vanholder, T., Opsomer, G., and De Kruif, A. (2006) Aetiology and pathogenesis of cystic ovarian follicles in dairy cattle: a review. *Reprod. Nutr. Dev.*, **46** (2), 105–119.

Vassena, R., Mapletoft, R.J., Allodi, S., Singh, J., and Adams, G.P. (2003) Morphology and developmental competence of bovine oocytes relative to follicular status. *Theriogenology*, **60** (5), 923–932.

Downloaded From Vet-eBooks.com

Wallace, W.H.B. and Kelsey, T.W. (2010) Human ovarian reserve from conception to the menopause. *PloS One*, **5** (1), 1–9.

Wissing, M.L., Kristensen, S.G., Andersen, C.Y., Mikkelsen, A.L., Host, T., Borup, R., and Grondahl, M.L. (2014) Identification of new ovulation-related genes in humans by comparing the transcriptome of granulosa cells before and after ovulation triggering in the same controlled ovarian stimulation cycle. *Hum. Reprod.*, **29** (5), 997–1010.

Xu, F., Stouffer, R.L., Müller, J., Hennebold, J.D., Wright, J.W., Bahar, A., Leder, G., Peters, M., Thorne, M., and Sims, M. (2011) Dynamics of the transcriptome in the primate ovulatory follicle. *Mol. Hum. Reprod.*, **17** (3), 152–165.

Yapura, J., Mapletoft, R.J., Pierson, R., Singh, J., Naile, J., Giesy, J.P., and Adams, G.P. (2011) A bovine model for examining the effects of an aromatase inhibitor on ovarian function in women. *Fertil. Steril.*, **96** (2), 434–438.

Yilmaz, N., Uygur, D., Ozgu, E., and Batioglu, S. (2010) Does coasting, a procedure to avoid ovarian hyperstimulation syndrome, affect assisted reproduction cycle outcome? *Fertil. Steril.*, **94** (1), 189–193.

Zeng, H.T., Ren, Z., Guzman, L., Wang, X., Sutton-McDowall, M.L., Ritter, L.J., De Vos, M., Smitz, J., Thompson, J.G., and Gilchrist, R.B. (2013) Heparin and cAMP modulators interact during pre-*in vitro* maturation to affect mouse and human oocyte meiosis and developmental competence. *Hum. Reprod.*, **28** (6), 1536–1545.

Downloaded From Vet-eBooks.com

7

Production of Energy and Determination of Competence: Past Knowledge, Present Research, and Future Opportunities in Oocyte and Embryo Metabolism

Jason R. Herrick, Elena Silva, and Rebecca L. Krisher

Colorado Center for Reproductive Medicine, CO, USA

7.1 Introduction

Oocytes and embryos undergo multiple physiological changes (completion of meiosis, fertilization, activation of the embryonic genomes, etc.) in three very different environments (the follicle, the oviduct, and the uterus) as they progress from the immature (germinal vesicle) oocyte to the hatched blastocyst. During this time, oocytes and embryos exhibit a unique combination of metabolic plasticity and sensitivity. Cumulus oocyte complexes and embryos are able to use a variety of metabolic substrates via multiple pathways during development, including glycolysis, the pentose phosphate pathway, the polyol pathway, the hexosamine biosynthesis pathway, and the tricarboxylic acid cycle (Figure 7.1). Although these cells are capable of adapting their metabolic activity to utilize a variety of nutrients in their environment, such adaptation often comes at the cost of reduced viability. This relationship between metabolic activity and viability is central to the successful application of assisted reproductive technologies for treatment of infertility. Only by understanding the metabolic requirements of the oocyte and embryo can we design culture systems that support the development of viable embryos with the best chance of resulting in healthy offspring. In this chapter we describe the current understanding of metabolism in the oocytes and embryos from a variety of species. A number of similarities and differences between species are highlighted to illustrate the complex nature of metabolic activity during development and the difficulty in selecting a single model species for translational research.

7.2 Measuring Metabolism

7.2.1 Approaches

Before we examine oocyte and embryo metabolism, it is worthwhile to understand the techniques used to measure metabolism, as well as the shortcomings of these approaches. Two techniques have been widely used: radiolabeled substrates and microfluorescence. Radiolabeled substrates provide information about specific pathways, depending on the location of the label on the original substrate and the end metabolite. Microfluorescence is based upon enzymatically coupled reactions associated with changing ratios of $NAD(P)^+$:NAD(P)H. Although both result in precise quantitation of substrate metabolism, these techniques have some inherent advantages and disadvantages. For example, the medium used during the

Animal Models and Human Reproduction, First Edition. Edited by Heide Schatten and Gheorghe M. Constantinescu.
© 2017 John Wiley & Sons, Inc. Published 2017 by John Wiley & Sons, Inc.

Downloaded From Vet-eBooks.com

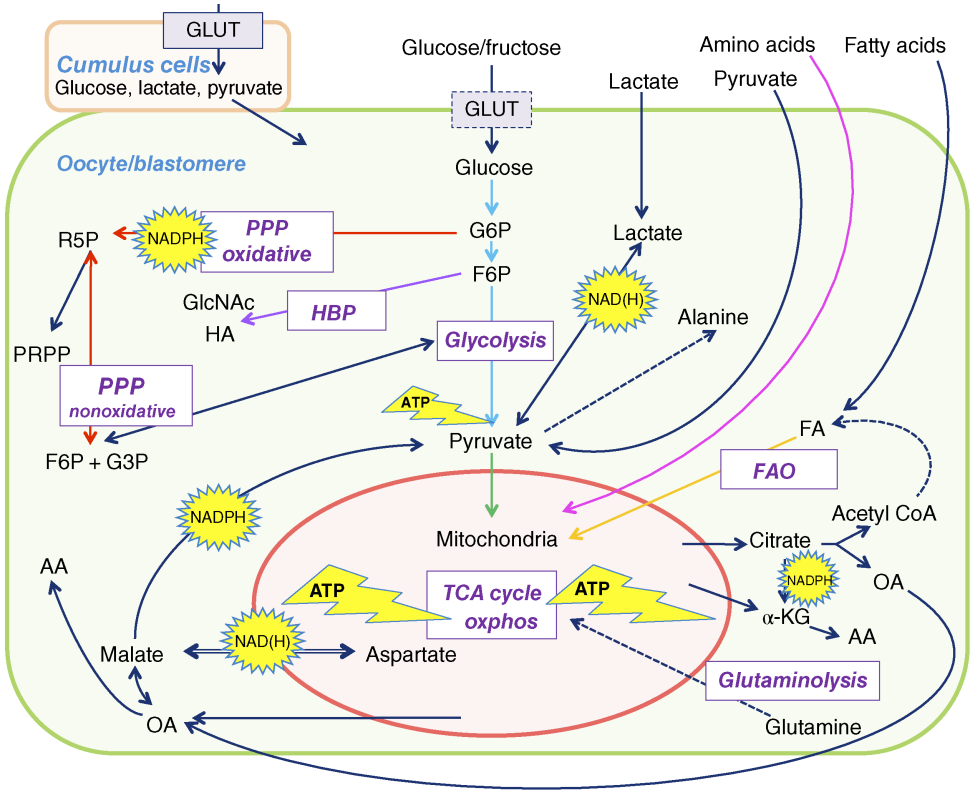

Figure 7.1 An overview of the interrelated metabolic pathways that may function in mammalian oocytes and early embryos. Multiple energy substrates can be both taken up and produced by the oocyte or embryo to meet metabolic needs via multiple pathways, maintain redox and osmotic balance, and modify the external culture environment. The oocyte receives significant metabolic substrates via gap junction communication with cumulus cells (depicted in the upper left corner), while the embryo may take up a variety of substrates directly from the culture media. Dashed lines represent pathways that have only been hypothesized. Pathways names are shown in white boxes, and important end products in yellow. *Abbreviations:* α-KG, alpha ketoglutarate; AA, amino acids; ATP; adenosine triphosphate; F6P, fructose 6 phosphate; FA, fatty acids; FAO, fatty acid β-oxidation; FAS, fatty acid synthase; G3P, glyceraldehyde 3 phosphate; G6P, glucose-6-phosphate; GlcNAc, *N*-acetylglucosamine; GLUT, glucose transporters; HA, hyaluronic acid; HBP, hexosamine biosynthetic pathway; OA, oxaloacetate; Oxphos, oxidative phosphorylation; PRPP, phosphoribosyl pyrophosphate; R5P, ribose-5-phosphate; TCA, tricarboxylic acid. (Reproduced from Krisher (2013b) with permission from Wiley.) (See color plate section.)

measurement period is often modified so that the sensitivity of the assay for a particular substrate of interest is increased. Thus, the oocyte or embryo is adapting to a different, less favorable condition during the measurement period, and any subsequent culture of that oocyte is negatively affected. Another drawback to metabolic measurement is that we do not know what metabolic pathways are used by oocytes or embryos *in vivo*, as this cannot be measured with our *in vitro* assays. Of course, we can compare the metabolism of *in vivo*-derived oocytes or embryos with that of *in vitro*-matured oocytes or *in vitro*-cultured embryos, but we must keep in mind that there will likely be some sort of adaptation to the *in vitro* environment (Lane and Gardner, 1998). Although the measurement techniques available for use come with caveats, they have provided us with significant information regarding oocyte or embryo metabolism.

A more recent addition to the technologies that can be employed to measure oocyte metabolism is metabolomics (Hollywood *et al.*, 2006; Brison *et al.*, 2007; Seli *et al.*, 2007;

Downloaded From Vet-eBooks.com

Krisher *et al.*, 2015a). Metabolomics has the advantage of being able to measure multiple substrates simultaneously in an optimized culture environment. Several platforms can be adapted for metabolomics, although mass spectrometry-based approaches are ideally suited for the sensitivity, complex composition, and low sample volume inherent in analyses of culture media. Typically, medium is analyzed following *in vitro* culture, after the oocyte or embryo has been removed, and compared with medium without an oocyte or embryo to ascertain how the composition of the culture medium was altered by the oocyte or embryo. Although an indirect measurement, it provides specific information about what substrates the oocyte or embryo is taking up and producing, providing clues as to the pathways in operation. Importantly, it permits culture in optimized culture conditions that support oocyte maturation or embryo development, which improves the relevance of the measurements. Another advantage of metabolomics is that it can provide information about both expected and unknown metabolites, depending upon the type of analysis selected. In this way, novel metabolic mechanisms may be revealed. One disadvantage of a metabolomics approach is that for most analyses, quantitation is relative such that use/production of a metabolite is based upon comparisons between media with and without an oocyte or embryo rather than direct measurement of the metabolite. Metabolomics analysis of culture media is also noninvasive, which allows the oocyte or embryo to be used for other manipulations, including transfer, after measurements. This approach could potentially be used to define a metabolic signature characteristic of high-quality oocytes or embryos that could be used to select embryos for transfer (Singh and Sinclair, 2007).

7.2.2 Limitations

Analyzing the metabolism of oocytes and/or COC has inherent complicating factors, regardless of the approach used. First, metabolic activity changes during maturation from the germinal vesicle (GV) to metaphase II (MII) stage (Rieger and Loskutoff, 1994; Steeves and Gardner, 1999a; Spindler *et al.*, 2000; Songsasen *et al.*, 2007) and during development from the zygote to the blastocyst (Flood and Wiebold, 1988; Thompson *et al.*, 1996; Lane and Gardner, 2000; Herrick *et al.*, 2007). Therefore, measuring metabolic activity during any given period of development includes not only baseline metabolism for an oocyte or embryo at a given stage of development but also the metabolic changes associated with progressing to the next developmental stage. Second, all metabolic measurements, unless conducted in follicular, oviductal, or uterine fluids, are essentially done in abnormal *in vitro* conditions, which may alter the results. Last, metabolism results may be affected by the medium used for the assessment, so that results can be difficult to compare between studies. For example, different pyruvate, glucose, and/or lactate concentrations in the measurement medium alter glucose metabolism in oocytes (Krisher and Bavister, 1999; Brad *et al.*, 2003b; Krisher *et al.*, 2007). Ultimately, oocyte and embryo metabolism are influenced by the environment both before and during metabolic assessment, as well as inherent differences in oocyte or embryo physiology. (Gardner and Leese, 1990; Thompson *et al.*, 1991; Lane and Gardner, 1998; Khurana and Niemann, 2000; Spindler *et al.*, 2000; Swain *et al.*, 2002).

Another major complication when evaluating oocyte metabolism is the presence (or absence) of cumulus cells. There is a dynamic and complex interaction between the oocyte and its surrounding cumulus cells throughout the growth of the follicle and maturation of the oocyte (Downs *et al.*, 2002), such that they function as a metabolic unit. These two cell types have different metabolic profiles, highlighting the interrelationships between cell types and the complexities of metabolic control mechanisms within the cumulus–oocyte complex (COC) (Zuelke and Brackett, 1992; Downs and Utecht, 1999; Downs *et al.*, 2002; Sutton *et al.*, 2003a). Metabolic enzyme activities differ between the two cell types, as do pyruvate oxidation, lactate

Downloaded From Vet-eBooks.com

production, and oxygen consumption (Cetica *et al.*, 1999, 2002; Downs *et al.*, 2002; Sutton *et al.*, 2003a; Clark *et al.*, 2006; Thompson *et al.*, 2007). The cumulus cells actively transfer a variety of metabolites to the oocytes via gap junctions (Biggers *et al.*, 1967; Leese and Barton, 1985; Downs *et al.*, 1986, 2002; Gardner and Leese, 1990; Saito *et al.*, 1994; Downs, 1995; Sutton *et al.*, 2003a). This functional interaction is critical for the maintenance of oocyte developmental competence (Heller *et al.*, 1981; Eppig, 1991). The decision to examine the intact COC versus the denuded oocyte must be made carefully, and based upon the hypothesis to be tested. Removal of the cumulus cells almost certainly alters oocyte metabolism dramatically, particularly at stages prior to MII (Heller *et al.*, 1981; Eppig, 1991; Saito *et al.*, 1994; Downs, 1995). For example, oocyte dependence on pyruvate is specific to the denuded oocyte, as oocytes can utilize a number of substrates during maturation and fertilization if the cumulus cells are intact (Biggers *et al.*, 1967; Johnson *et al.*, 2007).

7.3 The Relationship Between Oocyte Metabolism and Quality

Oocyte quality, or competence, sets the stage for all further developmental events. Initially, the oocyte must not only undergo nuclear maturation (resumption of meiosis and progression and arrest at metaphase II) but also coordinate a complex array of cytoplasmic events that allow the oocyte to support subsequent embryonic development (Eppig, 1996; Eppig *et al.*, 1996). Importantly, these two components of oocyte maturation are not linked; nuclear maturation frequently occurs in the absence of correct cytoplasmic maturation. Multiple aspects of cytoplasmic maturation have been proposed, including carbohydrate and lipid metabolism, mitochondrial function and location, reduction of oxygen radicals, accumulation of maternal mRNAs and proteins, epigenetic programming, communication between cumulus cells and the oocyte, and secretion of oocyte-derived growth factors, although this is certainly an incomplete list. Our understanding of oocyte physiology is now at crossroads, in which we have come to appreciate all of these components as interacting cellular pathways necessary for successful embryo development. However, our limited understanding of these cytoplasmic events is evident when we compare the competence of oocytes matured *in vivo* and *in vitro*. Although many offspring have been produced from *in vitro*-matured oocytes, particularly in domestic species, the percentage of the original pool of immature oocytes that is capable of producing a pregnancy is small (Singh *et al.*, 1997). We simply cannot, at this point, correctly replicate the processes of oocyte maturation *in vitro*. In this section, we will focus on what is understood about oocyte metabolism, and the critical relationship between metabolism and oocyte quality (Krisher, 2004; Krisher *et al.*, 2007).

7.3.1 Energy Substrates During Oocyte Maturation

Due to the known importance of metabolism to oocyte quality, it is not terribly surprising that energy substrates provided to the COC during maturation have an impact on subsequent oocyte competence. Importantly, the cumulus cells and oocyte have different requirements during this period, and both must be accounted for. As a unit, the COC requires a range of substrates, including carbohydrates, amino acids, and fatty acids. The milieu created by interactions between theca, granulosa, cumulus cells, and oocyte supports the coordinated development of the entire follicle, as well as oocyte competence. An obvious approach to designing medium to support *in vitro* oocyte maturation is to mimic follicular fluid substrate concentrations (Leese and Barton, 1985; Gardner and Leese, 1990; Nichol *et al.*, 1992; Brad *et al.*, 2003b; Iwata *et al.*, 2004, 2006; Leroy *et al.*, 2004; Harris *et al.*, 2005; Orsi *et al.*, 2005; Herrick *et al.*,

Downloaded From Vet-eBooks.com

2006b). In fact, substrate analysis of follicular fluid has been explored as a way to predict oocyte competence. Concentrations of both carbohydrates and amino acids in follicular fluid may discriminate between good and poor quality oocytes (Sinclair *et al.*, 2008; Pacella *et al.*, 2012; Wallace *et al.*, 2012; Matoba *et al.*, 2014). Control of ammonium, a by-product of amino acid metabolism, may also be important *in vivo*, since follicles containing good quality oocytes have reduced urea concentrations (Matoba *et al.*, 2014). Reduced palmitic and elevated linolenic, stearic, and arachodonic acids, as well as lower total saturated fatty acids and a lower *n*-6:*n*-3 PUFA ratio, are associated with good oocyte quality (O'Gorman *et al.*, 2013; Matoba *et al.*, 2014). Using follicular fluid metabolic substrates to create a model for prediction of oocyte quality has been attempted, with encouraging results (O'Gorman *et al.*, 2013).

Conversely, metabolic activity of the intact COC can affect the concentrations of energy substrates in the environment (Leese and Lenton, 1990; Herrick *et al.*, 2006b; Sutton-McDowall *et al.*, 2010). This is particularly true in the small volumes of medium used for *in vitro* maturation, which complicates translation of follicular fluid values to *in vitro* maturation medium. For example, bovine COC metabolism in microdrop culture accounts for a decrease of 3–4 mM glucose during IVM, with a corresponding increase in lactate concentration (Sutton-McDowall *et al.*, 2004). Although bovine follicular fluid contains only ~2 mM glucose, bovine COC were better supported *in vitro* in elevated glucose concentrations. This could indicate that, at physiological concentrations, glucose was depleted from the medium before maturation was complete (Sutton-McDowall *et al.*, 2004, 2010).

7.3.2 Oocyte Metabolic Pathways

In the intact COC, glucose is typically metabolized by cumulus cells, with the resulting pyruvate and lactate being delivered to the oocyte via gap junctions (Saito *et al.*, 1994; Downs and Utecht, 1999). However, metabolism of glucose via glycolysis, the pentose phosphate pathway (PPP), and the tricarboxylic acid (TCA) cycle play a variety of roles during oocyte maturation (mice (Downs and Utecht, 1999), cats (Spindler *et al.*, 2000), cattle (Rieger and Loskutoff, 1994; Krisher and Bavister, 1999), sheep (O'Brien *et al.*, 1996), and pigs (Krisher *et al.*, 2007)). Metabolism of glucose, regardless of its relative contribution, may be a critical factor in determining oocyte competence (Krisher and Bavister, 1999; Sutton-McDowall *et al.*, 2004). Glucose metabolism mediates nuclear maturation and redox balance via the PPP activity in the oocyte, cumulus expansion and glycosylation via the hexosamine biosynthetic pathway (HBP) in the cumulus cells, and energy production via glycolysis in both cell types (Downs *et al.*, 1998; Herrick *et al.*, 2006a; Sutton-McDowall *et al.*, 2010). The HBP converts glucose to glucosamine, which is then used to produce extracellular matrix (hyaluronic acid) in expanding cumulus cells (Sutton-McDowall *et al.*, 2006). Glycolysis and PPP activity are both involved in the resumption and progression of meiosis (Tsutsumi *et al.*, 1992; Zuelke and Brackett, 1992; Rieger and Loskutoff, 1994; Downs *et al.*, 1996, 1998; Downs and Utecht, 1999; Steeves and Gardner, 1999a; Cetica *et al.*, 2002; Herrick *et al.*, 2006a). Glycolysis, in addition to contributing to ATP production, works to maintain redox potential in the oocyte (Hashimoto *et al.*, 2000a). The PPP, while not directly involved in energy production, also contributes to oocyte quality by providing reducing power (NADPH), ribose for DNA and RNA synthesis, and building blocks for purine synthesis (Krisher, 1999). ATP produced from pyruvate and amino acid metabolism in the TCA cycle provides energy for maturation (Quinn and Wales, 1973; Bae and Foote, 1975; Rieger and Loskutoff, 1994; Van Blerkom *et al.*, 1995; O'Brien *et al.*, 1996; Steeves and Gardner, 1999a; Spindler *et al.*, 2000; Hemmings *et al.*, 2012), but the quantity of intracellular ATP is not directly related to oocyte competence (Brad *et al.*, 2003a; Herrick *et al.*, 2003; Krisher *et al.*, 2007). Both glycolysis and mitochondrial oxidation are essential metabolic components of oocyte

Downloaded From Vet-eBooks.com

maturation, and may be predictive of quality (Krisher and Bavister, 1999; Spindler *et al.*, 2000; Banwell and Thompson, 2008; Scott *et al.*, 2008; Tejera *et al.*, 2011; Martino *et al.*, 2012; Sugimura *et al.*, 2012; Ruvolo *et al.*, 2013; Zeng *et al.*, 2014).

Oxygen is an important factor regulating COC metabolism that affects both ATP production and the proportion of oocytes reaching MII (20% > 5%). Interestingly, elevated glucose concentrations in low O_2 conditions can rescue meiotic maturation via glycolytic ATP production (Hashimoto *et al.*, 2000a). In the mouse, oocytes matured in low oxygen are energetically much more similar to *in vivo*-matured oocytes and produce higher quality embryos after IVF than those matured in high oxygen (Preis *et al.*, 2007). In contrast, most bovine IVM uses high oxygen to support oocyte competence, although modifications to the maturation medium that are conducive to a low oxygen environment can be made (Oyamada and Fukui, 2004; Bermejo-Alvarez *et al.*, 2010).

7.3.2.1 Murine Oocyte Metabolism

Mouse oocytes prefer pyruvate as an energy source, since this substrate alone is able to support nuclear maturation, viability, and early development in the absence of cumulus cells (Biggers *et al.*, 1967; Leese and Barton, 1984; Fagbohun and Downs, 1992; Downs and Mastropolo, 1994; Downs and Hudson, 2000). Pyruvate metabolism via oxidative phosphorylation is highest during meiotic maturation (Downs *et al.*, 2002). Cumulus cells transfer not only pyruvate and lactate but also glucose into the mouse oocyte via gap junctions (Saito *et al.*, 1994; Downs and Utecht, 1999). Glucose can also enter the oocyte through the cumulus cells or directly into the oocyte (Saito *et al*., 1994; Downs and Utecht, 1999; Wang *et al*., 2012). During the first hour of maturation, glucose is necessary and sufficient to support oocyte competence (Frank *et al.*, 2013). Consumption of glucose and pyruvate are interrelated in the mouse COC (Downs *et al.*, 1997, 2002; Downs and Utecht, 1999). Despite the primary role of pyruvate in mouse oocyte metabolism, metabolism of glucose via the PPP has been associated with both nuclear maturation and increased competence (Downs *et al.*, 1998; Downs, 2015). As in other species, communication between the oocyte and cumulus cells is important in the control of metabolism. It was in the mouse that the mechanism of this regulation was first described as involving the oocyte-secreted factors BMP15 and GDF9 (Su *et al.*, 2008). The granulosa cells in turn produce EGF-like peptides near the time of oocyte maturation (Conti *et al.*, 2006). These EGF-like peptides promote oxidative phosphorylation in the oocyte and HBP activity in the cumulus cells (Richani *et al.*, 2014).

7.3.2.2 Bovine Oocyte Metabolism

Among domestic species, oocyte metabolism has been most extensively studied in the bovine. Glycolysis is the primary metabolic pathway in cumulus cells, which then delivers pyruvate and lactate to the oocyte for metabolism; alanine and aspartate are also metabolized by the oocyte (Cetica *et al.*, 2003; Sutton-McDowall *et al.*, 2010). Metabolism is regulated via bidirectional communication between the cumulus cells and oocyte (Sutton *et al.*, 2003a; Sutton-McDowall *et al.*, 2010). In fact, cumulus cell glycolysis and oocyte oxidative phosphorylation are linked (Gutnisky *et al.*, 2013). The oocyte uses oxidative metabolism considerably more than its surrounding cumulus cells, while the cumulus cells consume many times more glucose (Thompson, 2006). Interestingly, FSH and EGF-like peptides stimulate glycolysis in cumulus cells, while BMP15 regulates oocyte oxidative metabolism via the cumulus cells (Sutton-McDowall *et al.*, 2012b, 2015; Sugimura *et al.*, 2014). In addition, BMP15 directs glucose metabolism to the HBP in cumulus cells, promoting expansion of the cumulus cells (Caixeta *et al.*, 2013). BMP15 also helps to maintain cumulus cell–oocyte gap junctions, facilitating the transfer of metabolic substrates (Sugimura *et al.*, 2014). Metabolism of glucose increases

Downloaded From Vet-eBooks.com

throughout meiotic maturation in both cell types, without an increase in lactate production (Sutton *et al.*, 2003a). Oocyte metabolism of pyruvate through the TCA cycle peaks at 12 h of IVM (Rieger and Loskutoff, 1994; Steeves and Gardner, 1999a). Two-thirds of the mitochondrial respiration is coupled to ATP synthesis (Sugimura *et al.*, 2012). The concentration of glucose in maturation medium *in vitro* is important for both nuclear and cytoplasmic maturation; some is required to complete the maturation process, although high concentrations can result in oxidative stress and reduced oocyte competence (Hashimoto *et al.*, 2000b; Sutton *et al.*, 2003b; Sutton-McDowall *et al.*, 2010).

In addition to glycolysis, glucose is also metabolized via the PPP (Rieger and Loskutoff, 1994) and the HBP in bovine COC (Sutton-McDowall *et al.*, 2004; Thompson, 2006). Inclusion of glucosamine decreases glucose consumption in bovine COC by providing an alternative source of substrate for HA production (Sutton-McDowall *et al.*, 2004). However, glucosamine in maturation medium can decrease oocyte competence, potentially by increasing *O*-linked glycosylation of signaling proteins (Thompson, 2006; Frank *et al.*, 2013). Glutamine also plays a significant role in bovine oocyte metabolism, and unlike carbohydrates is able to support nuclear maturation in basal media (Bilodeau-Goeseels, 2006). The metabolism of glutamine through the TCA cycle also increases throughout nuclear maturation in both COC and oocytes, although oocyte glutamine metabolism depends on the presence of cumulus cells (Zuelke and Brackett, 1993; Rieger and Loskutoff, 1994; Steeves and Gardner, 1999a). Changes in metabolic enzyme activity in the COC and the oocyte reflect metabolism in each cell type. Activities of phosphofructokinase, glucose-6-phosphate dehydrogenase, and lipase increase in the oocyte but decrease in the cumulus cells during maturation (Cetica *et al.*, 2002). The activities of phosphofructokinase, glucose-6-phosphate dehydrogenase, and lactate dehydrogenase were higher in COC than in oocytes, while lipase activity was higher in oocytes than in COC (Cetica *et al.*, 1999, 2002).

7.3.2.3 Porcine Oocyte Metabolism

Work from our laboratory suggests that glucose is the primary energy substrate for pig oocytes (Krisher *et al.*, 2007), which differs from other species. *In vitro*-matured porcine oocytes metabolize more glucose via the glycolytic pathway than glucose via PPP, pyruvate via the TCA cycle, or glutamine via the TCA cycle. However, this may not be entirely optimal as *in vivo*-matured oocytes metabolized equivalent amounts of glucose via glycolysis and the PPP (Krisher *et al.*, 2007). These two pathways appear to be regulated by ATP and NADPH, respectively (Alvarez *et al.*, 2013). The importance of the PPP in porcine oocytes in our study and others suggests that this pathway is particularly important in this species (Flood and Wiebold, 1988; Sato *et al.*, 2007). Pyruvate metabolism was also reduced in *in vitro*-matured porcine oocytes compared with those matured *in vivo* (Krisher *et al.*, 2007). Cumulus cell metabolism provides pyruvate during oocyte maturation (Sutton-McDowall *et al.*, 2004; Herrick *et al.*, 2006a), so the noted decrease is unlikely to be due to pyruvate shortage but rather due to metabolic anomalies as a result of the *in vitro* environment. The oocyte may use pyruvate in pathways other than the TCA cycle, such as amino acid synthesis. In feline oocytes for example, the majority of pyruvate taken up by the oocyte is not metabolized by the TCA cycle (Spindler *et al.*, 2000). Alternatively, key regulatory enzymes for pyruvate metabolism may not be present or active.

7.3.3 Oocyte Metabolism of Fatty Acids

The study of carbohydrate metabolism has overshadowed the contribution of fatty acid β-oxidation (FAO) until relatively recently, when we have started to appreciate the importance of FAO in the maturing oocyte (Downs *et al.*, 2009; Dunning *et al.*, 2010). Cow, pig, and cat oocytes have large stores of intracellular lipids, while the mouse has fewer lipid stores, a fact

Downloaded From Vet-eBooks.com

reflected by the color of the cytoplasm (McEvoy *et al.*, 2000; Leroy *et al.*, 2005a). In humans and domestic ruminants, palmitic, stearic, and oleic are the most abundant fatty acids in oocytes, while pig oocytes contain greater polyunsaturated fatty acids, particularly linoleic acid (Homa *et al.*, 1986; Matorras *et al.*, 1998; McEvoy *et al.*, 2000; Kim *et al.*, 2001). The type of fatty acids present may also reflect oocyte quality (Kim *et al.*, 2001; Zeron *et al.*, 2001).

FAO machinery is present and active in the oocytes of domestic and laboratory species (Cetica *et al.*, 2002; Gentile *et al.*, 2004; Cerri *et al.*, 2009; Dunning *et al.*, 2010). Evidence now clearly points to the role of FAO during meiotic maturation in oocyte competence in mouse, cat, cow, and pig (Ferguson and Leese, 1999, 2006; Spindler *et al.*, 2000; Sturmey and Leese, 2003; Sturmey *et al.*, 2006, 2009; Dunning *et al.*, 2010, 2014; Paczkowski *et al.*, 2013). Bovine oocytes can develop after maturation without exogenous energy substrates only if fatty acid metabolism is active, although mouse oocytes cannot, thus suggesting that FAO may be more important in species with increased intracellular lipid (Ferguson and Leese, 1999, 2006). Oocytes are capable of taking up exogenous fatty acids from the culture environment (Ferguson and Leese, 1999). The addition of fatty acids (FA), or carnitine to stimulate FAO, to oocyte maturation medium has largely resulted in better progression to MII and increased developmental competence in mouse, cow, and pig (Leroy *et al.*, 2005b; Downs *et al.*, 2009; Dunning *et al.*, 2010, 2011; Marei *et al.*, 2010; Somfai *et al.*, 2011; Van Hoeck *et al.*, 2011; Wu *et al.*, 2011; You *et al.*, 2012). However, an overabundance of fatty acids can be detrimental to both nuclear and cytoplasmic maturation (Van Hoeck *et al.*, 2011; Homa and Brown, 1992; Leroy *et al.*, 2005b; Marei *et al.*, 2010; Jungheim *et al.*, 2011), although cumulus cells do offer some degree of protection (Lolicato *et al.*, 2015). Fatty acid metabolism may play a particularly important role in the pig oocyte, with its large endogenous stores of lipids (McEvoy *et al.*, 2000; Sturmey *et al.*, 2009). Triglycerides decrease during maturation in pigs, suggesting that they are metabolized (Sturmey and Leese, 2003). Mitochondria and lipid droplets colocalize near the periphery in the pig oocyte, possibly to gain easier access to oxygen for FAO, suggesting a metabolic role during oocyte maturation (Sturmey *et al.*, 2006, 2009).

7.4 Embryo Metabolism

Early studies of embryonic metabolism involved recovering murine embryos from the female reproductive tract and culturing them in media with various substrates to determine which nutrients were "required" for the embryo to progress to subsequent developmental stages. Mouse zygotes can cleave to the 2-cell stage in a simple medium with BSA if pyruvate or oxaloacetate are included, but not if glucose, lactate, or phosphoenolpyruvate were the only energy sources (Biggers *et al.*, 1967). However, 2-cell embryos can develop to the blastocyst stage with lactate (50.0 mM), pyruvate (0.3 mM), oxaloacetate (0.3 mM), or phosphoenolpyruvate (10.0 mM) as the sole energy substrate other than BSA (Brinster, 1965a). Glucose does not support the development of embryos at these early stages unless lactate is also included in the medium (Brinster, 1965b).

These pioneering studies of Biggers and Brinster led to a model in which early embryos utilize pyruvate, or other citric acid cycle intermediates, for ATP production, with an increased ability to utilize glucose as development proceeds. Sixty years later, this model is still surprisingly accurate and widely cited as the generalized pattern of metabolic activity in the mammalian embryo. However, these studies were conducted in simple media (salts, carbohydrates, and protein) that do not support optimal development. Analysis of fluids from the oviduct and the uterus have indicated that lactate is usually the most abundant carbohydrate (1–10.5 mM) in the female reproductive tract, followed by glucose (0.2–4.5 mM) and pyruvate (0.1–0.4 mM)

Downloaded From Vet-eBooks.com

(Gardner and Leese, 1990; Nichol *et al.*, 1992; Gardner *et al.*, 1996; Harris *et al.*, 2005; Hugentobler *et al.*, 2008). Similarly, oviductal and uterine fluids contain all 20 of the basic amino acids (Harris *et al.*, 2005; Hugentobler *et al.*, 2007; Li *et al.*, 2007). This is in stark contrast to early culture medium formulations in which glucose (5.5 mM) and lactate (≥21 mM) were present in supraphysiological concentrations and no amino acids were present (Brinster, 1965a; Whitten and Biggers, 1968).

The first generation of studies on embryo metabolism also focused on the culture requirements of the mouse embryo. Although the mouse is still widely used for studies of embryo physiology, its utility as a research model has more to do with the size and availability of mice rather than similarities between the physiology of murine embryos and the embryos of other species. Murine embryos differ from other taxa in several important ways that could affect their metabolic activity, including the rate of cell division and the amount of time the embryo spends in the uterus before attaching to the uterus. Since cell divisions require ATP, embryos that undergo more cell division are likely to require more ATP and have different metabolic profiles. Similarly, the embryo is dependent on endogenous energy stores and nutrients in the oviductal and uterine fluids between ovulation and implantation. Therefore, the metabolic profiles of species with a large amount of endogenous energy stores (pigs and carnivores) or species that spend a considerable amount of time in the uterus before implantation (ruminants and horses) are different from that of the mouse (limited energy reserves and implantation only 4.5 days after ovulation).

7.4.1 Precompaction: More Than Just Pyruvate

In the murine embryo between the zygote and 8-cell stages, pyruvate uptake is higher than that of glucose (Leese and Barton, 1984; Gardner and Leese, 1986; Houghton *et al.*, 1996). Early murine embryos also take up and metabolize glutamine, with increased utilization in the absence of pyruvate and lactate (Gardner *et al.*, 1989; Chatot *et al.*, 1990; Du and Wales, 1993). In ruminants, pyruvate uptake also exceeds that of glucose at the early cleavage stages (Rieger *et al.*, 1992b) (Gardner *et al.*, 1993; Thompson *et al.*, 1996). Similarly, ~90% of ATP is derived from oxidative metabolism prior to compaction, with pyruvate and glutamine being the preferred substrates (Thompson *et al.*, 1991, 1996; Rieger *et al.*, 1992b; Gardner *et al.*, 1993).

Even though glucose is not the "preferred substrate," early embryos do utilize glucose with significant increases in glucose uptake, glycolysis, and glucose oxidation in the mouse and increases in PPP and glycolysis in the cow occurring at the time of fertilization (Wales and Brinster, 1968; Leese and Barton, 1984; Pantaleon *et al.*, 2001; Comizzoli *et al.*, 2003). Glucose consumption, hexokinase activity, and lactate production also increase between the zygote and morula stages (Wales and Brinster, 1968; Leese and Barton, 1984; Gardner and Leese, 1986, 1988; O'Fallon and Wright, 1986; Saito *et al.*, 1994; Houghton *et al.*, 1996).

In ruminants, embryos actively take up glucose for metabolism through glycolysis and the PPP, with increased activity between the 2-cell and morula stages (Thompson *et al.*, 1991, 1996; Rieger *et al.*, 1992a, 1992b; Gardner *et al.*, 1993; Krisher *et al.*, 1999; Steeves *et al.*, 1999). However, oxidation of glucose was low at all stages, representing less than ~10% of total glucose uptake (Thompson *et al.*, 1991; Rieger *et al.*, 1992b). Therefore, glucose is important for embryonic development, but not necessarily for ATP production.

In the mouse, glucose uptake is similar between the 2- and 8-cell stages, but more glucose is converted to lactate at the 8-cell stage (40%) than at the 2-cell stage (25%), indicating a block to glycolysis in the early embryo (Barbehenn *et al.*, 1974, 1978; Gardner and Leese, 1988). This block may be mediated by the inhibition of phosphofructokinase in the early embryo by high concentrations of citrate and a high ATP:ADP ratio (Barbehenn *et al.*, 1974, 1978). As the

Downloaded From Vet-eBooks.com

embryo develops, the ATP:ADP ratio decreases, removing the inhibition of phosphofructokinase and allowing the embryo to begin to utilize glucose (Leese *et al.*, 1984; Rozell *et al.*, 1992; Gardner, 1998). In addition, inclusion of EDTA, which inhibits 3-phosphoglycerate kinase and maintains a high ATP:ADP ratio in mouse embryos, also inhibits glycolysis and stimulates development of early stage embryos by (Gardner and Lane, 1996; Lane and Gardner, 2001).

In contrast to murine and ruminant embryos, glucose may be the most important substrate for the development of porcine embryos. Porcine embryos do consume a significant amount of pyruvate and pyruvate oxidation increases steadily throughout development, but the majority of the pyruvate taken up by the embryo is not oxidized (Gandhi *et al.*, 2001; Swain *et al.*, 2002). Glycolysis is the most active metabolic pathway throughout development, with significant amounts of glucose and glutamine oxidation as well (Flood and Wiebold, 1988; Swain *et al.*, 2002; Sturmey and Leese, 2003). In fact, porcine embryos can be cultured from the 1-cell to blastocyst stage in the presence of only glucose or glutamine (Petters *et al.*, 1990). However, the porcine embryo exhibits an extreme degree of plasticity when it comes to the nutrients required for development. Although glucose may be the preferred substrate, porcine blastocysts are routinely produced in media containing only pyruvate, lactate, and glutamine (Yoshioka *et al.*, 2008).

Although there has been only one study of metabolism in feline embryos, they appear to be more similar to porcine embryos than they are to rodents of ruminants. Embryos recovered from the oviducts at the 16-cell stage metabolized about twice as much glucose through glycolysis (0.84 pmol/embryo/3 h) as they did pyruvate through the TCA cycle (0.38 pmol/embryo/3 h) (Herrick *et al.*, 2007). However, similar to porcine embryos, feline embryos can be cultured to the blastocyst stage in the absence of glucose (Freistedt *et al.*, 2001; Murakami *et al.*, 2011). Interestingly, both porcine and feline embryos have a large amount of lipid, which might serve as an important energy source in the absence of carbohydrates.

7.4.2 Postcompaction: More Than Just Glucose

Early studies indicate that after the 4-cell stage, murine embryos were able to develop to the blastocyst stage with glucose as the only substrate (Brinster, 1965b). Similarly, early studies of glucose and pyruvate consumption found a decrease in pyruvate uptake and an increase in glucose uptake at the morula stage, which was interpreted as a switch in nutrient preferences (Leese and Barton, 1984; Houghton *et al.*, 1996). Although consumption of glucose, glycolytic activity, and/or lactate production are higher at blastocyst stages than at early cleavage stages in most species (pig, mouse, cow, sheep, cat), consumption of pyruvate does not always decline during this same period. Even in the mouse, studies have shown that the decrease in pyruvate consumption originally viewed as a change in "preference" was in fact dependent on the concentration of glucose and lactate present in the medium (Gardner and Leese, 1988; Lane and Gardner, 2000). If glucose is not provided to the embryo, the embryo can continue to utilize pyruvate at the blastocyst stage (Gardner and Leese, 1988). Similarly, in the presence of physiological concentrations of lactate ($\leq$5 mM), blastocysts will continue to oxidize a significant amount of pyruvate even in the presence of glucose (Houghton *et al.*, 1996; Lane and Gardner, 2000). Oxygen consumption also increased at the blastocyst stage, indicative of increased activity of Na^+/K^+-ATPase protein synthesis during this period (Houghton *et al.*, 1996). Interestingly, the ICM cells appear to metabolize more glucose and convert more glucose to lactate than TE cells (Hewitson and Leese, 1993).

A similar metabolic profile is observed in ruminant embryos. Postcompaction there is an increase in glucose uptake, lactate production, glycolytic activity, and the proportion of ATP produced via glycolysis (Thompson *et al.*, 1991, 1996; Rieger *et al.*, 1992b; Gardner *et al.*, 1993).

Downloaded From Vet-eBooks.com

Pyruvate uptake and oxidation also increase during blastocyst development (Rieger *et al.*, 1992b; Gardner *et al.*, 1993; Thompson *et al.*, 1993, 1996; Krisher *et al.*, 1999; Khurana and Niemann, 2000). Isolated TE cells from bovine blastocysts consumed less glucose and more pyruvate, and produced more lactate than ICM cells (Gopichandran and Leese, 2003). The TE also exhibited a higher rate of amino acid turnover than the ICM, with amino acids produced by one cell type being the same as those consumed by the other (Gopichandran and Leese, 2003). In addition, the composition of the blastocoel fluid was found to have a different carbohydrate and amino acid content than the surrounding medium, indicating that the environment of the ICM is actively regulated (Gopichandran and Leese, 2003).

In pigs, glycolysis remains the most active pathway in blastocysts (Gandhi *et al.*, 2001; Swain *et al.*, 2002). Pyruvate uptake and oxidation are increased in the blastocysts compared to previous stages, but oxidation of glucose and glutamine seem to be responsible for the majority of oxygen consumption and ATP production (Flood and Wiebold, 1988; Swain *et al.*, 2002; Sturmey and Leese, 2003).

Glycolysis and pyruvate oxidation are both higher in feline blastocysts (pmol metabolized/embryo) than in 16-cell feline embryos, with about five times more glucose being metabolized through glycolysis (9.46 pmol/embryo/3 h) than pyruvate being oxidized in the TCA cycle (1.80 pmol/embryo/3 h) in blastocysts (Herrick *et al.*, 2007). This is slightly higher than reports for bovine blastocysts (approximately two to three times more glucose than pyruvate), but much lower than reports for porcine blastocysts (~20–27 times more glucose than pyruvate), in which the same methods were used to measure glycolysis and pyruvate oxidation (Rieger and Guay, 1988; Rieger *et al.*, 1992b; Krisher *et al.*, 1999; Swain *et al.*, 2002).

7.4.3 Lactate: The Other Carbohydrate

Although pyruvate and glucose seem to be the main carbohydrates used by the embryo to produce ATP, analysis of oviductal and uterine fluids have indicated that lactate is the most abundant carbohydrate in the embryo's environment during development (Gardner and Leese, 1990; Harris *et al.*, 2005). Although lactate can be converted to pyruvate and metabolized (Khurana and Niemann, 2000; Lane and Gardner, 2000), its most important role may be in controlling the activity of other metabolic pathways. Glucose uptake is not affected by the concentrations of lactate present at any stage of development, but the effect of lactate on the proportion of glucose metabolized via glycolysis is stage dependent (Edwards *et al.*, 1998; Lane and Gardner, 2000). In the zygote, increasing concentrations of lactate within the physiological range (≤10 mM) increases the glycolytic activity. In contrast, glycolytic activity in the morula is not affected by lactate (Edwards *et al.*, 1998). Physiological concentrations of lactate do not affect pyruvate uptake in 1-, 2-, or 8-cell embryos, but pyruvate uptake by the blastocysts is decreased by 5 or 10 mM lactate (Lane and Gardner, 2000). Data from other species on metabolic control by lactate are more limiting. In cattle, oxidation of lactate and pyruvate appear to be inversely related, with inclusion of one substrate in the medium inhibiting metabolism of the other during precompaction development (Khurana and Niemann, 2000). In cats, high concentrations (>6 mM) of lactate inhibit glycolytic activity in day 3 embryos (~16 cells), but stimulate glycolysis in blastocysts (Herrick *et al.*, 2007). Pyruvate oxidation was not affected by lactate (3, 6, or 12 mM) in cat embryos on day 3 or at the blastocyst stage.

Many of these effects may be mediated by interactions between lactate, the activity of lactate dehydrogenase (LDH), and the cytoplasmic ratio of NAD^+:NADH within the embryo (Lane and Gardner, 2000; Lane and Gardner, 2005). Glycolysis (glyceraldehydes-3-phosphate to 1,2 bisphosphoglycerate by glyceraldehyde phosphate dehydrogenase) and the conversion of lactate to pyruvate by LDH both consume NAD^+ and produce NADH. In order for continued activity

Downloaded From Vet-eBooks.com

of these NAD^+-dependent reactions, the embryo must regenerate NAD^+ within the cytoplasm. One way the embryo can do this is by converting pyruvate to lactate, which consumes NADH and produces NAD^+. However, high concentrations of lactate inhibit LDH and make it difficult for the embryo to regenerate NAD^+ using this mechanism. Alternatively, embryos can generate NAD^+ from a series of coupled reactions, known as the malate and aspartate shuttle, in which NAD^+ is produced in the cytoplasm during the conversion of oxaloacetate to malate (Lane and Gardner, 2005). Malate is transported into the mitochondria where it is converted back to oxaloacetate, which produces NADH that can be used in oxidative phosphorylation. Oxaloacetate and glutamate are transaminated to α-ketoglutarate and aspartate, respectively, which are transported back into the cytoplasm and converted back to oxaloacetate and glutamate. All enzymes of this system were present and active at the 1- and 2-cell stages, but proper functioning of this shuttle is dependent on the presence of sufficient aspartate in the medium (Lane and Gardner, 2005).

7.4.4 Noncarbohydrates

7.4.4.1 Amino Acids

With the exception of glutamine, the majority of metabolic studies have focused on carbohydrates. However, several early studies provided evidence for important roles of amino acids during development. Biggers *et al.* (1967) found that 1-cell murine embryos would not progress to the 2-cell stage in a simple salt solution containing BSA (a potential source of amino acids). In contrast, Kane (1987) reported that rabbit zygotes could complete four to five cell divisions (~25 cells) within 48 h of culture in the presence of BSA, similar to the conditions tested by Biggers. If both amino acids and BSA were present, 80% of rabbit zygotes could develop to the hatched blastocyst stage (Kane, 1972). These results suggest that mouse zygotes are unable to utilize amino acids (derived from the BSA) or endogenous lipids for even a single cell cycle. However, rabbit embryos can use endogenous lipids to a limited extent, but can meet most of their metabolic needs with amino acids. Subsequent studies have indicated that porcine, bovine, and ovine embryos will also develop to the morula or blastocyst stages with protein and/or AA as the only exogenous nutrient sources (Petters *et al.*, 1990; Thompson *et al.*, 1992; Sutton-McDowall *et al.*, 2012a). Dunning *et al.* (2010) even demonstrated limited cleavage (10–15%) of 1-cell murine embryos in the presence of glutamine and the nonessential amino acids, contradicting the long-standing "requirement" for pyruvate 9 Biggers *et al.*, 1967).

Numerous studies have shown that amino acids have beneficial effects on the development of embryos from multiple species when added to the culture medium (Liu and Foote, 1995; McKiernan *et al.*, 1995; Lane and Gardner, 1997; Steeves and Gardner, 1999b; Biggers *et al.*, 2000; Lane *et al.*, 2001; Suzuki and Yoshioka, 2006). More recent studies have shown that specific amino acids are consumed (depleted from the medium) and produced (secreted into the medium) by embryos from mice, pigs, cattle, and humans (Houghton *et al.*, 2002; Orsi and Leese, 2004; Humpherson *et al.*, 2005; Wale and Gardner, 2012). Presumably, some of the consumed amino acids are used for protein synthesis, but other possible fates for the amino acids are not clear. Amino acids can act as osmotic buffers, helping the embryo to maintain cellular homeostasis (Baltz and Zhou, 2012). Ammonium production by embryos cultured with amino acids also indicates that some amino acids are being converted to TCA cycle intermediates for generation of ATP (Gardner *et al.*, 2001; Lane *et al.*, 2001). Since ammonium can be inhibitory to development, embryos have mechanism to detoxify ammonium and prevent its buildup in the cytoplasm or the culture medium. Murine and bovine embryos are capable of producing glutamine from ammonium and glutamate and/or producing alanine from

Downloaded From Vet-eBooks.com

glutamate, pyruvate, and ammonium (Orsi and Leese, 2004; Wale and Gardner, 2013). The resulting alanine and glutamine are secreted into the medium, which has been observed in a number of studies (Houghton *et al.*, 2002; Orsi and Leese, 2004; Humpherson *et al.*, 2005; Wale and Gardner, 2013; Krisher *et al.*, 2015a).

7.4.4.2 Lipids

Again, the studies of Biggers and Kane were the first evidence of a role for lipids. The inability of the 1-cell mouse embryo to cleave to the 2-cell stage in the presence of BSA was indicative of its inability to use endogenous lipid stores (the only other nutrients present other than the BSA (Biggers *et al.*, 1967)). In contrast, rabbit zygotes were able to complete three to four cell divisions (~10 cells within 48 h) in the absence of any exogenous nutrients (Kane, 1987). Unfortunately, there have been few other studies like that of Kane (1987) investigating the ability of embryos from other species to develop in the absence of exogenous carbohydrates, amino acids, or lipids. However, analysis of oocytes from multiple species has found significant amounts of intracellular lipids (Matorras *et al.*, 1998; McEvoy *et al.*, 2000; Paczkowski *et al.*, 2014), especially in oocytes from pigs and carnivores (Guraya, 1965; Homa *et al.*, 1986; Apparicio *et al.*, 2012). In addition, even those species with a relatively low concentration of lipids, such as mice, rabbits, and humans, have been shown to actively metabolize this nutrient source (Khandoker and Tsujii, 1998; Haggarty *et al.*, 2006; Dunning *et al.*, 2010; Paczkowski *et al.*, 2014). Finally, inhibition of fatty acid oxidation decreases embryonic development in both mice and cattle (Hewitson *et al.*, 1996; Ferguson and Leese, 2006). Interestingly, Dunning *et al.* (2010) found that supplementing a simple medium lacking carbohydrates or protein (containing glutamine and nonessential amino acids) with carnitine increased the proportion of murine zygotes cleaving from ~15 to ~30%. Since carnitine is a cofactor necessary for entry of lipid into the mitochondria, this finding suggests that the inability of the mouse embryo to utilize intracellular lipids was largely due to the absence of carnitine, which can partially negate the "requirement" for pyruvate.

7.5 Metabolic Biomarkers

7.5.1 The Oocyte

Now that we know oocyte metabolism is intimately associated with oocyte quality, the obvious question is whether we can use metabolic biomarkers to predict the ability of an oocyte to develop successfully. It may be possible to analyze the follicular environment using metabolomics to generate a fingerprint of a healthy metabolic environment (Singh and Sinclair, 2007; Nel-Themaat and Nagy, 2011; Wallace *et al.*, 2012; O'Gorman *et al.*, 2013). We could also measure metabolism *in vitro*, and build a metabolic profile indicative of high-quality oocytes. Consumption or production of several amino acids, including arginine, glutamate, glutamine, isoleucine, and valine, appears to be a signature of developmentally competent human oocytes (Hemmings *et al.*, 2013). Similarly, the consumption and production of glutamine and alanine, respectively, as well as utilization of a panel of amino acids including alanine, arginine, glutamine, leucine, and tryptophan, were associated with the developmental ability of bovine oocytes (Hemmings *et al.*, 2012). Oocyte oxygen consumption has also been associated with oocyte quality (Ruvolo *et al.*, 2013). Although the oocyte presents particular challenges in this regard due to its intimate association with cumulus cells during maturation, metabolic biomarkers hold promise for the identification and selection of high-quality oocytes.

Downloaded From Vet-eBooks.com

7.5.2 The Embryo

Morphology is the most widely used method to identify viable embryos. However, it is widely accepted that this parameter provides only limited information about an embryo's ability to implant and support a viable pregnancy. In human ART, other parameters are becoming more widely used to assist in this regard, including chromosomal analysis and morphokinetics. Given that embryo metabolism is so closely linked to viability, a metabolic biomarker is of great interest (Nel-Themaat and Nagy, 2011; Gardner and Wale, 2013). Metabolomics platforms are an excellent method to noninvasively analyze multiple metabolites across groups of substrates simultaneously, which could lead to the identification of an accurate, multicomponent metabolic biomarker of embryo viability. Initial reports suggested that metabolomic analyses may provide a better predictive tool for embryo selection compared to morphology alone (Nagy *et al.*, 2008; Cortezzi *et al.*, 2013). Amino acid turnover is suggested to be predictive of embryo quality in several species (Houghton *et al.*, 2002; Brison *et al.*, 2004; Sturmey *et al.*, 2008, 2010; Hemmings *et al.*, 2012). Retrospective studies defined associations between spent media profiles and the potential for successful implantation, developing a viability index rather than identifying specific metabolites (Nagy *et al.*, 2008; Sakkas *et al.*, 2008; Scott *et al.*, 2008; Seli *et al.*, 2010; Marhuenda-Egea *et al.*, 2011; Pudakalakatti *et al.*, 2013; Zivi *et al.*, 2014). Unfortunately, randomized controlled trials using selection on days 2, 3, and 5 of culture based upon this metabolomics viability index did not increase pregnancy rate (Hardarson *et al.*, 2012; Vergouw *et al.*, 2012; Uyar and Seli, 2014). Despite this setback, many groups are still working to better profile metabolism in embryos, and use this information to develop metabolic biomarkers.

7.6 Toward Personalized Culture Media: Formulating Media for Specific Maternal Conditions

7.6.1 Maternal Impact on Embryo Development

Advanced maternal age and increased body mass index (BMI) are common sources of female infertility and both conditions are linked with altered embryo metabolism (Picton *et al.*, 2010; Purcell and Moley, 2011). Advanced maternal age (AMA) is associated with decreased numbers of oocytes retrieved after ovarian stimulation and increased numbers of abnormal oocytes (Eppig and O'Brien, 1995; Lim and Tsakok, 1997). In addition, there is a significant increase in the numbers of aneuploid embryos with an increase in maternal age, resulting in a higher risk of miscarriage (Munné *et al.* 1995; Kushnir and Frattarelli, 2009). Similarly, overweight and obese women have lower numbers of oocytes retrieved, reduced oocyte quality, and increased risk of gestational diabetes, miscarriages, and childhood metabolic disorders (Jungheim and Moley, 2010; Cardozo *et al.*, 2011; Purcell and Moley, 2011; Lane *et al.*, 2015).

Current metabolomics studies using experimental animal models have shown that the period in which the oocyte is exposed to the maternal environment affects subsequent embryo metabolism and is a key factor that impacts a successful pregnancy (Krisher, 2013a; Krisher *et al.*, 2015b). For example, amino acid metabolism in early embryos from women 37 years or older differs significantly from those of embryos from younger women (Picton *et al.*, 2010). Since amino acids are critical for embryo development (Bavister and Arlotto, 1990; Lane *et al.*, 2001), the appropriate type and concentration of amino acids for inclusion in culture media may depend on the age of the oocyte donor. In the future, metabolomics studies will be a powerful tool to characterize metabolic disorders in oocytes and embryos from distinct patient groups

Downloaded From Vet-eBooks.com

with the aim to develop more appropriate *in vitro* culture systems. Current knowledge about the impact of maternal status on oocytes and embryos and potential therapeutic approaches will be discussed in this section.

7.6.2 Impaired Embryo Metabolism

The oocyte plays a major role in determining pregnancy success and offspring health. Some components of oocyte quality are widely recognized, including mitochondrial integrity and redox balance. In addition, novel pathways have been revealed in recent years such as sirtuin's role in mitochondria function and metabolism regulation. Most of these physiological pathways are interconnected and their activity affects oocyte quality and subsequent embryonic development.

7.6.3 Mitochondrial Dysfunction

Even though there are likely multiple contributory factors to poor oocyte quality, a common characteristic of compromised oocytes in both AMA and obesity is mitochondria status (Chappel, 2013; Wu *et al.*, 2015). Production of ATP via oxidative phosphorylation in the mitochondria is a critical component of oocyte maturation and influences its quality (Van Blerkom *et al.*, 1995; Wilding *et al.*, 2005). After fertilization, the early embryo has a low metabolic rate (Leese, 1991) and a reduced ability to manage cellular stress (Baltz *et al.*, 1991). Increased mitochondrial membrane potential during the 1- to 2-cell stage is important for the development of early mouse preimplantation embryos and is associated with better blastocyst quality (Komatsu *et al.*, 2014). In addition, enzymatic inhibition of mitochondrial membrane potential in the 8-cell embryo reduces the birth weight of female offspring and increases adiposity at 4 weeks (Zander-Fox *et al.*, 2015), demonstrating the importance of mitochondria function for the production of a healthy offspring.

In addition to ATP production, reducing equivalents and metabolic intermediates that are part of the antioxidant defense are also formed in the mitochondria (Dumollard *et al.*, 2009). With aging, there is a decline in molecules responsible for antioxidant defense, leading to increased mitochondrial DNA mutations, reduced mitochondrial function, increased ROS levels, and increased cell damage (Bentov *et al.*, 2010). Mitochondrial impairment leading to a reduced capability to scavenge ROS in oocytes from older women has been proposed as a contributor to increased chromosomal errors and reduced embryonic development (Wilding *et al.*, 2001; Bartmann *et al.*, 2004). Therefore, mitochondrial activity associated with ATP production and antioxidative defense is linked with oocyte competence, blastocyst development, and offspring health. Deficiencies in oxidative phosphorylation and increased levels of ROS in the long term compromise oocyte quality and impair fertility (Wilding *et al.*, 2009).

7.6.3.1 Reduced Sirtuin Activity

Sirtuins (silent information regulator 2 (Sir2) proteins) are a family of metabolic modulators with NAD^+-dependent deacetylase activity. These proteins have emerged as sensors of the energetic status of the cells because of their regulation by the NAD^+/NADH ratio (Yang *et al.*, 2007), in addition to the regulation of oxidative status in the oocyte (Kawamura *et al.*, 2010; Di Emidio *et al.*, 2014). Seven members of the sirtuin family have been identified in mammals (SIRT1-7). Multiple studies have focused on the role of SIRT1-3 in the oocyte and embryo. SIRT1 is considered a sensor of oxidative status; it is located in the nucleus and migrates to cytoplasm under oxidative stress; SIRT1 influences oocyte maturation by regulating the redox state and spindle assembly (Di Emidio *et al.*, 2014). SIRT2 is also localized in the nucleus and

Downloaded From Vet-eBooks.com

cytoplasm and has been studied as a regulator of spindle assembly and chromosome alignment in mouse oocytes (Zhang *et al.*, 2014). The mitochondrial SIRT3 regulates the oxidative response and has a protective function *in vitro*; IVF and *in vitro*-cultured embryos originated from induced SIRT3 knockdown embryos present defective postimplantation development (Kawamura *et al.*, 2010). Activation of this family of deacetylases is known to be beneficial to the oocyte and improves embryo development in mice, suggesting that the age-related decline in sirtuin activity may contribute to the decline in oocyte quality with age (Kawamura *et al.*, 2010; Zhang *et al.*, 2014). Also, rats fed a high-fat diet display inhibited sirtuin signaling pathway with increased follicle loss (Wang *et al.*, 2014b), supporting that sirtuin activity is critical for fertility.

7.6.4 Endoplasmic Reticulum Stress

Similar to the effect of maternal BMI on mitochondria, it is well recognized that a high extracellular lipid environment caused by maternal overnutrition damages the endoplasmic reticulum (ER) causing ER stress (Borradaile *et al.*, 2006). There is a close relation between ER and mitochondria. In somatic cells, ER stress impairs mitochondrial function through the disruption of mitochondrial membrane potential and further increases in oxidative stress (Vannuvel *et al.*, 2013).

The disruption of the oocyte organelles by ER stress affects oocyte development and embryo metabolism (Wu *et al.*, 2010, 2015). Oocytes from mice fed a high-fat diet have increased markers of ER stress and reduced mitochondria membrane potential (Wu *et al.*, 2015). Treatment of the obese female mice with the ER stress inhibitor salubrinal successfully restored oocyte mitochondria membrane potential and embryo development, confirming that regulation of ER function and, consequently, mitochondria activity has beneficial effects on female fertility.

7.6.4.1 Stimulation of Mitochondrial Function and Control of Oxidative Stress

Due to the large impact of mitochondria status on embryo metabolism, current research focuses on the control of oxidative stress and/or stimulation of mitochondrial function. One approach to overcoming mitochondrial dysfunction is to enzymatically stimulate mitochondrial activity. The addition of dichloroacetic acid, an indirect stimulator of the enzyme complex pyruvate dehydrogenase, had a positive effect on ATP production and embryo cell number (McPherson *et al.*, 2014), supporting the hypothesis that stimulation of mitochondria activity is a feasible method to optimize embryo function during *in vitro* culture. Even though the impact of this pharmacological component was significant, its use in a clinical setting remains problematic.

There is significant evidence to support the idea that constituent antioxidants and the maintenance of an oxidative balance influence pregnancy (Ruder *et al.*, 2008). Therefore, the addition of antioxidants to the culture medium is a physiological approach that has positive effects on mitochondrial function, regulation of ROS levels, and embryo development (Olson and Seidel, 2000; Hosseini *et al.*, 2009; Yuan *et al.*, 2012). The addition of alpha tocopherol (a form of vitamin E) and vitamin C (Olson and Seidel, 2000; Wang *et al.*, 2002; Natarajan *et al.*, 2010), *N*-acetylcysteine (Liu *et al.*, 2012), α-lipoic acid (Talebi *et al.*, 2012), and glutathione (Luvoni *et al.*, 1996; Ozawa *et al.*, 2006) have beneficial effects on embryo development and a reduction of oxidative stress. However, few studies have analyzed the impact of these components specifically in embryos from females with reduced fertility. Recent data have shown that a combination of antioxidants is necessary to specifically address the deficiencies in embryos from reproductively aged mice during culture (Silva *et al.*, 2015). Interestingly, a combination of four antioxidants was necessary to improve blastocyst development and mitochondria function in

Downloaded From Vet-eBooks.com

embryos from aged mice, whereas the addition of only two antioxidants was sufficient to improve embryo development from young females. These findings support the hypothesis that embryos from different maternal age groups have different requirements and highlight the necessity of correct regulation of the culture medium based on maternal status. In addition, it demonstrates that development of embryos originating from reproductively aged females can be improved in a culture medium with complex antioxidant supplementation.

Because the sirtuin family has been considered a major regulator of metabolism, stimulation of this pathway could be a target for medium formulation. The use of resveratrol, a stimulator of SIRT1, during embryo or oocyte culture has produced beneficial effects in different species (Giaretta *et al.*, 2013; Liu *et al.*, 2013; Salzano *et al.*, 2014; Wang *et al.*, 2014a). These studies have shown that targeted stimulation of sirtuin proteins is an efficient method to overcome the process of oxidative stress and increase ATP production. Since sirtuins are NAD^+ dependent, another therapeutic method is the supplementation of culture media with NAD^+ precursors, such as nicotinamide riboside (Canto *et al.*, 2012). These precursors play a major role in regulating metabolic/mitochondrial diseases in other cell types, but there is limited information on how they may work in oocytes or embryos (Houtkooper and Auwerx, 2012; Houtkooper *et al.*, 2012). In a mouse model for polycystic ovarian syndrome, which is associated with obesity in women, the addition of nicotinic acid, a NAD^+ precursor, was beneficial to oocyte metabolism (Jimenez *et al.*, 2013). Although the impact of the NAD^+–sirtuin pathway on cell metabolism and mitochondria function is promising, further studies are necessary to establish how to stimulate this pathway in oocytes and embryos originated from patients with compromised sirtuin function as in AMA or obesity.

Ultimately, the aim of individualized culture medium formulations for these specific disease states is to activate mitochondrial activity, improve oxidative balance, and minimize damage caused by ROS. Because the oocyte is more susceptible to environmental insults, early treatment could have greater therapeutic benefits. If medium supplementation starts during oocyte maturation, the optimal control of mitochondrial function, ATP production, and redox balance could potentially reduce chromosomal errors. Currently, the use of oocyte *in vitro* maturation (IVM) to treat human infertility is limited, making treatment during embryo culture the most feasible approach. Determination of metabolic parameters of embryos from distinct patient groups will allow for improved supplementation to medium for optimal blastocyst development and minimized metabolic perturbations.

7.7 Summary

It is clear that metabolic activity is a critical indicator of oocyte and embryo viability. The success of assisted reproductive technologies involving even a small amount of time in culture is dependent on providing the oocyte or embryo with an appropriate combination of substrates that will support normal metabolic activity and minimize cellular stress. Although our understanding of oocyte and embryo metabolism has improved greatly since the early work of Biggers and Brinster, there is still much work to be done. We do not know what substrates and pathways oocytes and embryos utilize *in vivo*, so we still do not have a good definition of "normal" oocyte or embryo metabolism. Our understanding of the mechanisms controlling metabolic activity is also lacking. Although we may know that the activity of a given pathway is too high or too low, we do not know how to alter the composition of culture media to induce specific changes in the metabolic activity of the oocyte or embryo. Finally, we are just starting to realize the diversity of metabolic mechanisms present among the oocytes and embryo from different species. Since human oocytes and embryos are not available for detailed, hypothesis-driven studies, research

Downloaded From Vet-eBooks.com

must be conducted on animal models. However, interpretation of the results of those studies and extrapolation to clinical practice must be done with careful consideration of the similarities and differences between human oocytes and embryos and those of the model species.

References

Alvarez, G.M., Ferretti, E.L., Gutnisky, C., Dalvit, G.C., and Cetica, P.D. (2013) Modulation of glycolysis and the pentose phosphate pathway influences porcine oocyte *in vitro* maturation. *Reprod. Domest. Anim.*, **48**, 545–553.

Apparicio, M., Ferreira, C.R., Tata, A., Santos, V.G., Alves, A.E., Mostachio, G.Q., Pires-Butler, E.A., Motheo, T.F., Padilha, L.C., Pilau, E.J., Gozzo, F.C., Eberlin, M.N., Lo Turco, E.G., Luvoni, G.C., and Vicente, W.R. (2012) Chemical composition of lipids present in cat and dog oocyte by matrix-assisted desorption ionization mass spectrometry (MALDI- MS). *Reprod. Domest. Anim.*, **47** (Suppl. 6), 113–117.

Bae, I.H. and Foote, R.H. (1975) Carbohydrate and amino acid requirements and ammonia production of rabbit follicular oocytes matured *in vitro*. *Exp. Cell Res.*, **91**, 113–118.

Baltz, J.M. and Zhou, C. (2012) Cell volume regulation in mammalian oocytes and preimplantation embryos. *Mol. Reprod. Dev.*, **79**, 821–831.

Baltz, J.M., Biggers, J.D., and Lechene, C. (1991) Two-cell stage mouse embryos appear to lack mechanisms for alleviating intracellular acid loads. *J. Biol. Chem.*, **266**, 6052–6057.

Banwell, K.M. and Thompson, J.G. (2008) *In vitro* maturation of mammalian oocytes: outcomes and consequences. *Semin. Reprod. Med.*, **26**, 162–174.

Barbehenn, E.K., Wales, R.G., and Lowry, O.H. (1974) The explanation for the blockade of glycolysis in early mouse embryos. *Proc. Natl. Acad. Sci. USA*, **71**, 1056–1060.

Barbehenn, E.K., Wales, R.G., and Lowry, O.H. (1978) Measurement of metabolites in single preimplantation embryos: a new means to study metabolic control in early embryos. *J. Embryol. Exp. Morphol.*, **43**, 29–46.

Bartmann, A.K., Romao, G.S., Ramos Eda, S., and Ferriani, R.A. (2004) Why do older women have poor implantation rates? A possible role of the mitochondria. *J. Assist. Reprod. Genet.*, **21**, 79–83.

Bavister, B.D. and Arlotto, T. (1990) Influence of single amino acids on the development of hamster one-cell embryos *in vitro*. *Mol. Reprod. Dev.*, **25**, 45–51.

Bentov, Y., Esfandiari, N., Burstein, E., and Casper, R.F. (2010) The use of mitochondrial nutrients to improve the outcome of infertility treatment in older patients. *Fertil. Steril.*, **93**, 272–275.

Bermejo-Alvarez, P., Lonergan, P., Rizos, D., and Gutierrez-Adan, A. (2010) Low oxygen tension during IVM improves bovine oocyte competence and enhances anaerobic glycolysis. *Reprod. BioMed. Online*, **20**, 341–349.

Biggers, J.D., Whittingham, D.G., and Donahue, R.P. (1967) The pattern of energy metabolism in the mouse oocyte and zygote. *Proc. Natl. Acad. Sci. USA*, **58**, 560–567.

Biggers, J.D., McGinnis, L.K., and Raffin, M. (2000) Amino acids and preimplantation development of the mouse in protein-free potassium simplex optimized medium. *Biol. Reprod.*, **63**, 281–293.

Bilodeau-Goeseels, S. (2006) Effects of culture media and energy sources on the inhibition of nuclear maturation in bovine oocytes. *Theriogenology*, **66**, 297–306.

Borradaile, N.M., Han, X., Harp, J.D., Gale, S.E., Ory, D.S., and Schaffer, J.E. (2006) Disruption of endoplasmic reticulum structure and integrity in lipotoxic cell death. *J. Lipid Res.*, **47**, 2726–2737.

Brad, A.M., Bormann, C.L., Swain, J.E., Durkin, R.E., Johnson, A.E., Clifford, A.L., and Krisher, R.L. (2003a) Glutathione and adenosine triphosphate content of *in vivo* and *in vitro* matured porcine oocytes. *Mol. Reprod. Dev.*, **64**, 492–498.

Downloaded From Vet-eBooks.com

Brad, A.M., Herrick, J.R., Lane, M., Gardner, D.K., and Krisher, R.L. (2003b) Glucose and lactate concentrations affect the metabolism of *in vitro* matured porcine oocytes. *Biol. Reprod.*, **68** (Suppl. 1), 356.

Brinster, R.L. (1965a) Studies on the development of mouse embryos *in vitro*. II: the effect of energy source. *J. Exp. Zool.*, **158**, 59–68.

Brinster, R.L. (1965b) Studies on the development of mouse embryos *in vitro*: IV. Interaction of energy sources. *J. Reprod. Fertil.*, **10**, 227–240.

Brison, D.R., Houghton, F.D., Falconer, D., Roberts, S.A., Hawkhead, J., Humpherson, P.G., Lieberman, B.A., and Leese, H.J. (2004) Identification of viable embryos in IVF by non-invasive measurement of amino acid turnover. *Hum. Reprod.*, **19**, 2319–2324.

Brison, D.R., Hollywood, K., Arnesen, R., and Goodacre, R. (2007) Predicting human embryo viability: the road to non-invasive analysis of the secretome using metabolic footprinting. *Reprod. BioMed. Online*, **15**, 296–302.

Caixeta, E.S., Sutton-McDowall, M.L., Gilchrist, R.B., Thompson, J.G., Price, C.A., Machado, M.F., Lima, P.F., and Buratini, J. (2013) Bone morphogenetic protein 15 and fibroblast growth factor 10 enhance cumulus expansion, glucose uptake, and expression of genes in the ovulatory cascade during *in vitro* maturation of bovine cumulus–oocyte complexes. *Reproduction*, **146**, 27–35.

Canto, C., Houtkooper, R.H., Pirinen, E., Youn, D.Y., Oosterveer, M.H., Cen, Y., Fernandez-Marcos, P.J., Yamamoto, H., Andreux, P.A., Cettour-Rose, P., Gademann, K., Rinsch, C., Schoonjans, K., Sauve, A.A., and Auwerx, J. (2012) The NAD(+) precursor nicotinamide riboside enhances oxidative metabolism and protects against high-fat diet-induced obesity. *Cell Metabol.*, **15**, 838–847.

Cardozo, E., Pavone, M.E., and Hirshfeld-Cytron, J.E. (2011) Metabolic syndrome and oocyte quality. *Trends Endocrinol. Metabol.*, **22**, 103–109.

Cerri, R.L.A., Juchem, S.O., Chebel, R.C., Rutigliano, H.M., Bruno, R.G.S., Galvao, K.N., Thatcher, W.W., and Santos, J.E.P. (2009) Effect of fat source differing in fatty acid profile on metabolic parameters, fertilization, and embryo quality in high-producing dairy cows. *J. Dairy Sci.*, **92**, 1520–1531.

Cetica, P., Pintos, L.N., Dalvit, G.C., and Beconi, M.T. (1999) Effect of lactate dehydrogenase activity and isoenzyme localization in bovine oocytes and utilization of oxidative substrates on *in vitro* maturation. *Theriogenology*, **51**, 541–550.

Cetica, P., Pintos, L., Dalvit, G., and Beconi, M. (2002) Activity of key enzymes involved in glucose and triglyceride catabolism during bovine oocyte maturation *in vitro*. *Reproduction*, **124**, 675–681.

Cetica, P., Pintos, L., Dalvit, G., and Beconi, M. (2003) Involvement of enzymes of amino acid metabolism and tricarboxylic acid cycle in bovine oocyte maturation *in vitro*. *Reproduction*, **126**, 753–763.

Chappel, S. (2013) The role of mitochondria from mature oocyte to viable blastocyst. *Obstet. Gynecol. Int.*, **2013**, 183024.

Chatot, C.L., Tasca, R.J., and Ziomek, C.A. (1990) Glutamine uptake and utilization by preimplantation mouse embryos in CZB medium. *J. Reprod. Fertil.*, **89**, 335–346.

Clark, A.R., Stokes, Y.M., Lane, M., and Thompson, J.G. (2006) Mathematical modelling of oxygen concentration in bovine and murine cumulus–oocyte complexes. *Reproduction*, **131**, 999–1006.

Comizzoli, P., Urner, F., Sakkas, D., and Renard, J.P. (2003) Up-regulation of glucose metabolism during male pronucleus formation determines the early onset of the s phase in bovine zygotes. *Biol. Reprod.*, **68**, 1934–1940.

Conti, M., Hsieh, M., Park, J.Y., and Su, Y.Q. (2006) Role of the epidermal growth factor network in ovarian follicles. *Mol. Endocrinol.*, **20**, 715–723.

Downloaded From Vet-eBooks.com

Cortezzi, S.S., Cabral, E.C., Trevisan, M.G., Ferreira, C.R., Setti, A.S., Braga, D.P., Figueira Rde, C., Iaconelli, A. Jr., Eberlin, M.N., and Borges, E. Jr. (2013) Prediction of embryo implantation potential by mass spectrometry fingerprinting of the culture medium. *Reproduction*, **145**, 453–462.

Di Emidio, G., Falone, S., Vitti, M., D'Alessandro, A.M., Vento, M., Di Pietro, C., Amicarelli, F., and Tatone, C. (2014) SIRT1 signalling protects mouse oocytes against oxidative stress and is deregulated during aging. *Hum. Reprod.*, **29**, 2006–2017.

Downs, S.M. (1995) The influence of glucose, cumulus cells, and metabolic coupling on ATP levels and meiotic control in the isolated mouse oocyte. *Dev. Biol.*, **167**, 502–512.

Downs, S.M. (2015) Nutrient pathways regulating the nuclear maturation of mammalian oocytes. *Reprod. Fertil. Dev.*, **27**, 572–582.

Downs, S.M. and Hudson, E.D. (2000) Energy substrates and the completion of spontaneous meiotic maturation. *Zygote*, **8**, 339–351.

Downs, S.M. and Mastropolo, A.M. (1994) The participation of energy substrates in the control of meiotic maturation in murine oocytes. *Dev. Biol.*, **162**, 154–168.

Downs, S.M. and Utecht, A.M. (1999) Metabolism of radiolabeled glucose by mouse oocytes and oocyte–cumulus cell complexes. *Biol. Reprod.*, **60**, 1446–1452.

Downs, S.M., Coleman, D.L., and Eppig, J.J. (1986) Maintenance of murine oocyte meiotic arrest: uptake and metabolism of hypoxanthine and adenosine by cumulus cell-enclosed and denuded oocytes. *Dev. Biol.*, **117**, 174–183.

Downs, S.M., Humpherson, P.G., Martin, K.L., and Leese, H.J. (1996) Glucose utilization during gonadotropin-induced meiotic maturation in cumulus cell-enclosed mouse oocytes. *Mol. Reprod. Dev.*, **44**, 121–131.

Downs, S.M., Houghton, F.D., Humpherson, P.G., and Leese, H.J. (1997) Substrate utilization and maturation of cumulus cell-enclosed mouse oocytes: evidence that pyruvate oxidation does not mediate meiotic induction. *J. Reprod. Fertil.*, **110**, 1–10.

Downs, S.M., Humpherson, P.G., and Leese, H.J. (1998) Meiotic induction in cumulus cell-enclosed mouse oocytes: involvement of the pentose phosphate pathway. *Biol. Reprod.*, **58**, 1084–1094.

Downs, S.M., Humpherson, P.G., and Leese, H.J. (2002) Pyruvate utilization by mouse oocytes is influenced by meiotic status and the cumulus oophorus. *Mol. Reprod. Dev.*, **62**, 113–123.

Downs, S.M., Mosey, J.L., and Klinger, J. (2009) Fatty acid oxidation and meiotic resumption in mouse oocytes. *Mol. Reprod. Dev.*, **76**, 844–853.

Du, Z.F. and Wales, R.G. (1993) Effect of culture from the zygote stage on the metabolism of glucose and glutamine by 2-cell embryos and blastocysts recovered from outbred or F1 hybrid female mice. *Reprod. Fertil. Dev.*, **5**, 555–565.

Dumollard, R., Carroll, J., Duchen, M.R., Campbell, K., and Swann, K. (2009) Mitochondrial function and redox state in mammalian embryos. *Semin. Cell Dev. Biol.*, **20**, 346–353.

Dunning, K.R., Cashman, K., Russell, D.L., Thompson, J.G., Norman, R.J., and Robker, R.L. (2010) Beta-oxidation is essential for mouse oocyte developmental competence and early embryo development. *Biol. Reprod.*, **83**, 909–918.

Dunning, K.R., Akison, L.K., Russell, D.L., Norman, R.J., and Robker, R.L. (2011) Increased beta-oxidation and improved oocyte developmental competence in response to l-carnitine during ovarian *in vitro* follicle development in mice. *Biol. Reprod.*, **85**, 548–555.

Dunning, K.R., Russell, D.L., and Robker, R.L. (2014) Lipids and oocyte developmental competence: the role of fatty acids and β-oxidation. *Reproduction*, **148**, R15–R27.

Edwards, L.J., Williams, D.A., and Gardner, D.K. (1998) Intracellular pH of the preimplantation mouse embryo: effects of extracellular pH and weak acids. *Mol. Reprod. Dev.*, **50**, 434–442.

Downloaded From Vet-eBooks.com

Eppig, J.J. (1991) Intercommunication between mammalian oocytes and companion somatic cells. *Bioessays*, **13**, 569–574.
Eppig, J.J. (1996) Coordination of nuclear and cytoplasmic oocyte maturation in eutherian mammals. *Reprod. Fertil. Dev.*, **8**, 485–489.
Eppig, J.J. and O'Brien, M. (1995) *In vitro* maturation and fertilization of oocytes isolated from aged mice: a strategy to rescue valuable genetic resources. *J. Assist. Reprod. Genet.*, **12**, 269–273.
Eppig, J.J., O'Brien, M., and Wigglesworth, K. (1996) Mammalian oocyte growth and development *in vitro*. *Mol. Reprod. Dev.*, **44**, 260–273.
Fagbohun, C.F. and Downs, S.M. (1992) Requirement for glucose in ligand-stimulated meiotic maturation of cumulus cell-enclosed mouse oocytes. *J. Reprod. Fertil.*, **96**, 681–697.
Ferguson, E.M. and Leese, H.J. (1999) Triglyceride content of bovine oocytes and early embryos. *J. Reprod. Fertil.*, **116**, 373–378.
Ferguson, E.M. and Leese, H.J. (2006) A potential role for triglyceride as an energy source during bovine oocyte maturation and early embryo development. *Mol. Reprod. Dev.*, **73**, 1195–1201.
Flood, M.R. and Wiebold, J.L. (1988) Glucose metabolism by preimplantation pig embryos. *J. Reprod. Fertil.*, **84**, 7–12.
Frank, L.A., Sutton-McDowall, M.L., Russell, D.L., Wang, X., Feil, D.K., Gilchrist, R.B., and Thompson, J.G. (2013) Effect of varying glucose and glucosamine concentration *in vitro* on mouse oocyte maturation and developmental competence. *Reprod. Fertil. Dev.*, **25**, 1095–1104.
Freistedt, P., Stojkovic, M., and Wolf, E. (2001) Efficient *in vitro* production of cat embryos in modified synthetic oviduct fluid medium: effects of season and ovarian status. *Biol. Reprod.*, **65**, 9–13.
Gandhi, A.P., Lane, M., Gardner, D.K., and Krisher, R.L. (2001) Substrate utilization in porcine embryos cultured in NCSU23 and G1.2/G2.2 sequential culture media. *Mol. Reprod. Dev.*, **58**, 269–275.
Gardner, D.K. (1998) Changes in requirements and utilization of nutrients during mammalian preimplantation embryo development and their significance in embryo culture. *Theriogenology*, **49**, 83–102.
Gardner, D.K. and Lane, M. (1996) Alleviation of the "2-cell block" and development to the blastocyst of CF1 mouse embryos: role of amino acids, EDTA and physical parameters. *Hum. Reprod.*, **11**, 2703–2712.
Gardner, D.K. and Leese, H.J. (1986) Non-invasive measurement of nutrient uptake by single cultured pre-implantation mouse embryos. *Hum. Reprod.*, **1**, 25–27.
Gardner, D.K. and Leese, H.J. (1988) The role of glucose and pyruvate transport in regulating nutrient utilization by preimplantation mouse embryos. *Development*, **104**, 423–429.
Gardner, D.K. and Leese, H.J. (1990) Concentrations of nutrients in mouse oviduct fluid and their effects on embryo development and metabolism *in vitro*. *J. Reprod. Fertil.*, **88**, 361–368.
Gardner, D.K. and Wale, P.L. (2013) Analysis of metabolism to select viable human embryos for transfer. *Fertil. Steril.*, **99**, 1062–1072.
Gardner, D.K., Clarke, R.N., Lechene, C.P., and Biggers, J.D. (1989) Development of a noninvasive ultramicrofluorometric method for measuring net uptake of glutamine by single preimplantation mouse embryos. *Gamete Res.*, **24**, 427–438.
Gardner, D.K., Lane, M., and Batt, P. (1993) Uptake and metabolism of pyruvate and glucose by individual sheep preattachment embryos developed *in vivo*. *Mol. Reprod. Dev.*, **36**, 313–319.
Gardner, D.K., Lane, M., Calderon, I., and Leeton, J. (1996) Environment of the preimplantation human embryo *in vivo*: metabolite analysis of oviduct and uterine fluids and metabolism of cumulus cells. *Fertil. Steril.*, **65**, 349–353.
Gardner, D.K., Lane, M., Stevens, J., and Schoolcraft, W.B. (2001) Noninvasive assessment of human embryo nutrient consumption as a measure of developmental potential. *Fertil. Steril.*, **76**, 1175–1180.

Downloaded From Vet-eBooks.com

Gentile, L., Monti, M., Sebastiano, V., Merico, V., Nicolai, R., Calvani, M., Garagna, S., Redi, C.A., and Zuccotti, M. (2004) Single-cell quantitative RT-PCR analysis of Cpt1b and Cpt2 gene expression in mouse antral oocytes and in preimplantation embryos. *Cytogenet. Genome Res.*, **105**, 215–221.

Giaretta, E., Spinaci, M., Bucci, D., Tamanini, C., and Galeati, G. (2013) Effects of resveratrol on vitrified porcine oocytes. *Oxid. Med. Cell. Longev.*, **2013**, 920257.

Gopichandran, N. and Leese, H.J. (2003) Metabolic characterization of the bovine blastocyst, inner cell mass, trophectoderm and blastocoel fluid. *Reproduction*, **126**, 299–308.

Guraya, S.S. (1965) A histochemical analysis of lipid yolk deposition in the oocytes of cat and dog. *J. Exp. Zool.*, **160**, 123–135.

Gutnisky, C., Morado, S., Dalvit, G.C., Thompson, J.G., and Cetica, P.D. (2013) Glycolytic pathway activity: effect on IVM and oxidative metabolism of bovine oocytes. *Reprod. Fertil. Dev.*, **25**, 1026–1035.

Haggarty, P., Wood, M., Ferguson, E., Hoad, G., Srikantharajah, A., Milne, E., Hamilton, M., and Bhattacharya, S. (2006) Fatty acid metabolism in human preimplantation embryos. *Hum. Reprod.*, **21**, 766–773.

Hardarson, T., Ahlstrom, A., Rogberg, L., Botros, L., Hillensjo, T., Westlander, G., Sakkas, D., and Wikland, M. (2012) Non-invasive metabolomic profiling of day 2 and 5 embryo culture medium: a prospective randomized trial. *Hum. Reprod.*, **27**, 89–96.

Harris, S.E., Gopichandran, N., Picton, H.M., Leese, H.J., and Orsi, N.M. (2005) Nutrient concentrations in murine follicular fluid and the female reproductive tract. *Theriogenology*, **64**, 992–1006.

Hashimoto, S., Minami, N., Takakura, R., Yamada, M., Imai, H., and Kashima, N. (2000a) Low oxygen tension during *in vitro* maturation is beneficial for supporting the subsequent development of bovine cumulus oocyte complexes. *Mol. Reprod. Dev.*, **57**, 353–360.

Hashimoto, S., Minami, N., Yamada, M., and Imai, H. (2000b) Excessive concentration of glucose during *in vitro* maturation impairs developmental competence of bovine oocytes after *in vitro* fertilization: relevance to intracellular reactive oxygen species and glutathione contents. *Mol. Reprod. Dev.*, **56**, 520–526.

Heller, D.T., Cahill, D.M., and Schultz, R.M. (1981) Biochemical studies of mammalian oogenesis: metabolic cooperativity between granulosa cells and growing mouse oocytes. *Dev. Biol.*, **84**, 455–464.

Hemmings, K.E., Leese, H.J., and Picton, H.M. (2012) Amino acid turnover by bovine oocytes provides an index of oocyte developmental competence *in vitro*. *Biol. Reprod.*, **86**, 165, 161–112.

Hemmings, K.E., Maruthini, D., Vyjayanthi, S., Hogg, J.E., Balen, A.H., Campbell, B.K., Leese, H.J., and Picton, H.M. (2013) Amino acid turnover by human oocytes is influenced by gamete developmental competence, patient characteristics and gonadotrophin treatment. *Hum. Reprod.*, **28**, 1031–1044.

Herrick, J.R., Brad, A.M., Krisher, R.L., and Pope, W.F. (2003) Relationship between intracellular adenosine triphosphate or glutathione concentration and *in vivo* developmental potential of porcine oocytes. *Anim. Reprod. Sci.*, **78**, 123–131.

Herrick, J.R., Brad, A.M., and Krisher, R.L. (2006a) Chemical manipulation of glucose metabolism in porcine oocytes: effects on nuclear and cytoplasmic maturation *in vitro*. *Reproduction*, **131**, 289–298.

Herrick, J.R., Lane, M., Gardner, D.K., Behboodi, E., Memili, E., Blash, S., Echelard, Y., and Krisher, R.L. (2006b) Metabolism, protein content, and *in vitro* embryonic development of goat cumulus–oocyte complexes matured with physiological concentrations of glucose and L-lactate. *Mol. Reprod. Dev.*, **73**, 256–266.

Herrick, J.R., Bond, J.B., Magarey, G.M., Bateman, H.L., Krisher, R.L., Dunford, S.A., and Swanson, W.F. (2007) Toward a feline-optimized culture medium: impact of ions, carbohydrates, essential

Downloaded From Vet-eBooks.com

amino acids, vitamins, and serum on development and metabolism of *in vitro* fertilization-derived feline embryos relative to embryos grown *in vivo*. *Biol. Reprod.*, **76**, 858–870.
Hewitson, L.C. and Leese, H.J. (1993) Energy metabolism of the trophectoderm and inner cell mass of the mouse blastocyst. *J. Exp. Zool.*, **267**, 337–343.
Hewitson, L.C., Martin, K.L., and Leese, H.J. (1996) Effects of metabolic inhibitors on mouse preimplantation embryo development and the energy metabolism of isolated inner cell masses. *Mol. Reprod. Dev.*, **43**, 323–330.
Hollywood, K., Brison, D.R., and Goodacre, R. (2006) Metabolomics: current technologies and future trends. *Proteomics*, **6**, 4716–4723.
Homa, S.T. and Brown, C.A. (1992) Changes in linoleic acid during follicular development and inhibition of spontaneous breakdown of germinal vesicles in cumulus-free bovine oocytes. *J. Reprod. Fertil.*, **94**, 153–160.
Homa, S.T., Racowsky, C., and McGaughey, R.W. (1986) Lipid analysis of immature pig oocytes. *J. Reprod. Fertil.*, **77**, 425–434.
Hosseini, S.M., Forouzanfar, M., Hajian, M., Asgari, V., Abedi, P., Hosseini, L., Ostadhosseini, S., Moulavi, F., Safahani Langrroodi, M., Sadeghi, H., Bahramian, H., Eghbalsaied, S., and Nasr-Esfahani, M.H. (2009) Antioxidant supplementation of culture medium during embryo development and/or after vitrification-warming: which is the most important? *J. Assist. Reprod. Genet.*, **26**, 355–364.
Houghton, F.D., Thompson, J.G., Kennedy, C.J., and Leese, H.J. (1996) Oxygen consumption and energy metabolism of the early mouse embryo. *Mol. Reprod. Dev.*, **44**, 476–485.
Houghton, F.D., Hawkhead, J.A., Humpherson, P.G., Hogg, J.E., Balen, A.H., Rutherford, A.J., and Leese, H.J. (2002) Non-invasive amino acid turnover predicts human embryo developmental capacity. *Hum. Reprod.*, **17**, 999–1005.
Houtkooper, R.H. and Auwerx, J. (2012) Exploring the therapeutic space around NAD+. *J. Cell Biol.*, **199**, 205–209.
Houtkooper, R.H., Pirinen, E., and Auwerx, J. (2012) Sirtuins as regulators of metabolism and healthspan. *Nat. Rev. Mol. Cell Biol.*, **13**, 225–238.
Hugentobler, S.A., Diskin, M.G., Leese, H.J., Humpherson, P.G., Watson, T., Sreenan, J.M., and Morris, D.G. (2007) Amino acids in oviduct and uterine fluid and blood plasma during the estrous cycle in the bovine. *Mol. Reprod. Dev.*, **74**, 445–454.
Hugentobler, S.A., Humpherson, P.G., Leese, H.J., Sreenan, J.M., and Morris, D.G. (2008) Energy substrates in bovine oviduct and uterine fluid and blood plasma during the oestrous cycle. *Mol. Reprod. Dev.*, **75**, 496–503.
Humpherson, P.G., Leese, H.J., and Sturmey, R.G. (2005) Amino acid metabolism of the porcine blastocyst. *Theriogenology*, **64**, 1852–1866.
Iwata, H., Hashimoto, S., Ohota, M., Kimura, K., Shibano, K., and Miyake, M. (2004) Effects of follicle size and electrolytes and glucose in maturation medium on nuclear maturation and developmental competence of bovine oocytes. *Reproduction*, **127**, 159–164.
Iwata, H., Inoue, J., Kimura, K., Kuge, T., Kuwayama, T., and Monji, Y. (2006) Comparison between the characteristics of follicular fluid and the developmental competence of bovine oocytes. *Anim. Reprod. Sci.*, **91**, 215–223.
Jimenez, P.T., Frolova, A.I., Chi, M.M., Grindler, N.M., Willcockson, A.R., Reynolds, K.A., Zhao, Q., and Moley, K.H. (2013) DHEA-mediated inhibition of the pentose phosphate pathway alters oocyte lipid metabolism in mice. *Endocrinology*, **154**, 4835–4844.
Johnson, M.T., Freeman, E.A., Gardner, D.K., and Hunt, P.A. (2007) Oxidative metabolism of pyruvate is required for meiotic maturation of murine oocytes *in vivo*. *Biol. Reprod.*, **77**, 2–8.
Jungheim, E.S. and Moley, K.H. (2010) Current knowledge of obesity's effects in the pre- and periconceptional periods and avenues for future research. *Am. J. Obstet. Gynecol.*, **203**, 525–530.

Downloaded From Vet-eBooks.com

Jungheim, E.S., Macones, G.A., Odem, R.R., Patterson, B.W., Lanzendorf, S.E., Ratts, V.S., and Moley, K.H. (2011) Associations between free fatty acids, cumulus oocyte complex morphology and ovarian function during *in vitro* fertilization. *Fertil. Steril.*, **95**, 1970–1974.

Kane, M.T. (1972) Energy substrates and culture of single cell rabbit ova to blastocysts. *Nature*, **238**, 468–469.

Kane, M.T. (1987) Minimal nutrient requirements for culture of one-cell rabbit embryos. *Biol. Reprod.*, **37**, 775–778.

Kawamura, Y., Uchijima, Y., Horike, N., Tonami, K., Nishiyama, K., Amano, T., Asano, T., Kurihara, Y., and Kurihara, H. (2010) Sirt3 protects *in vitro*-fertilized mouse preimplantation embryos against oxidative stress-induced p53-mediated developmental arrest. *J. Clin. Investig.*, **120**, 2817–2828.

Khandoker, M. and Tsujii, H. (1998) Metabolism of exogenous fatty acids by preimplantation rabbit embryos. *Jpn. J. Fertil. Steril.*, **43**, 195–201.

Khurana, N.K. and Niemann, H. (2000) Energy metabolism in preimplantation bovine embryos derived *in vitro* or *in vivo*. *Biol. Reprod.*, **62**, 847–856.

Kim, J.Y., Kinoshita, M., Ohnishi, M., and Fukui, Y. (2001) Lipid and fatty acid analysis of fresh and frozen-thawed immature and *in vitro* matured bovine oocytes. *Reproduction*, **122**, 131–138.

Komatsu, K., Iwase, A., Mawatari, M., Wang, J., Yamashita, M., and Kikkawa, F. (2014) Mitochondrial membrane potential in 2-cell stage embryos correlates with the success of preimplantation development. *Reproduction*, **147**, 627–638.

Krisher, R. (1999) Exposure of bovine oocytes to perturbants of the pentose phosphate pathway affects subsequent embryonic development. *Biol. Reprod.*, **60** (Suppl. 1), 390.

Krisher, R.L. (2004) The effect of oocyte quality on development. *J. Anim. Sci.*, **82** (E-Suppl.), E14–E23.

Krisher, R.L. (2013a) *In vivo* and *in vitro* environmental effects on mammalian oocyte quality. *Annu. Rev. Anim. Biosci.*, **1**, 393–417.

Krisher, R.L. (2013b) Oocyte and embryo metabolomics, in *Control of Pig Reproduction IX*, (eds H. Rodriguez-Martinez, N.M. Soede, and W.L. Flowers), Society of Reproduction and Fertility, vol. 68, pp. 1–18.

Krisher R.L. and Bavister, B.D. (1999) Enhanced glycolysis after maturation of bovine oocytes *in vitro* is associated with increased developmental competence. *Mol. Reprod. Dev.*, **53**, 19–26.

Krisher, R.L., Lane, M., and Bavister, B.D. (1999) Developmental competence and metabolism of bovine embryos cultured in semi-defined and defined culture media. *Biol. Reprod.*, **60**, 1345–1352.

Krisher, R.L., Brad, A.M., Herrick, J.R., Sparman, M.L., and Swain, J.E. (2007) A comparative analysis of metabolism and viability in porcine oocytes during *in vitro* maturation. *Anim. Reprod. Sci.*, **98**, 72–96.

Krisher, R.L., Heuberger, A.L., Paczkowski, M., Stevens, J., Pospisil, C., Prather, R.S., Sturmey, R.G., Herrick, J.R., and Schoolcraft, W.B. (2015a) Applying metabolomic analyses to the practice of embryology: physiology, development and assisted reproductive technology. *Reprod. Fertil. Dev.*, **27**, 602–620.

Krisher, R.L., Schoolcraft, W.B., and Katz-Jaffe, M.G. (2015b) Omics as a window to view embryo viability. *Fertil. Steril.*, **103**, 333–341.

Kushnir, V.A. and Frattarelli, J.L. (2009) Aneuploidy in abortuses following IVF and ICSI. *J. Assist. Reprod. Genet.*, **26**, 93–97.

Lane, M. and Gardner, D.K. (1997) Differential regulation of mouse embryo development and viability by amino acids. *J. Reprod. Fertil.*, **109**, 153–164.

Lane, M. and Gardner, D.K. (1998) Amino acids and vitamins prevent culture-induced metabolic perturbations and associated loss of viability of mouse blastocysts. *Hum. Reprod.*, **13**, 991–997.

Downloaded From Vet-eBooks.com

Lane, M. and Gardner, D.K. (2000) Lactate regulates pyruvate uptake and metabolism in the preimplantation mouse embryo. *Biol. Reprod.*, **62**, 16–22.
Lane, M. and Gardner, D.K. (2001) Inhibiting 3-phosphoglycerate kinase by EDTA stimulates the development of the cleavage stage mouse embryo. *Mol. Reprod. Dev.*, **60**, 233–240.
Lane, M. and Gardner, D.K. (2005) Mitochondrial malate–aspartate shuttle regulates mouse embryo nutrient consumption. *J. Biol. Chem.*, **280**, 18361–18367.
Lane, M., Hooper, K., and Gardner, D.K. (2001) Effect of essential amino acids on mouse embryo viability and ammonium production. *J. Assist. Reprod. Genet.*, **18**, 519–525.
Lane, M., Zander-Fox, D.L., Robker, R.L., and McPherson, N.O. (2015) Peri-conception parental obesity, reproductive health, and transgenerational impacts. *Trends Endocrinol. Metabol.*, **26**, 84–90.
Leese, H.J. (1991) Metabolism of the preimplantation mammalian embryo. *Oxf. Rev. Reprod. Biol.*, **13**, 35–72.
Leese, H.J. and Barton, A.M. (1984) Pyruvate and glucose uptake by mouse ova and preimplantation embryos. *J. Reprod. Fertil.*, **72**, 9–13.
Leese, H.J. and Barton, A.M. (1985) Production of pyruvate by isolated mouse cumulus cells. *J. Exp. Zool.*, **234**, 231–236.
Leese, H.J. and Lenton, E.A. (1990) Glucose and lactate in human follicular fluid: concentrations and interrelationships. *Hum. Reprod.*, **5**, 915–919.
Leese, H.J., Biggers, J.D., Mroz, E.A., and Lechene, C. (1984) Nucleotides in a single mammalian ovum or preimplantation embryo. *Anal. Biochem.*, **140**, 443–448.
Leroy, J.L.M.R., Vanholder, T., Delanghe, J.R., Opsomer, G., Van Soom, A., Bols, P.E.J., and de Kruif, A. (2004) Metabolite and ionic composition of follicular fluid from different-sized follicles and their relationship to serum concentrations in dairy cows. *Anim. Reprod. Sci.*, **80**, 201–211.
Leroy, J.L.M.R., Genicot, G., Donnay, I., and Van Soom, A. (2005a) Evaluation of the lipid content in bovine oocytes and embryos with nile red: a practical approach. *Reprod. Domest. Anim.*, **40**, 76–78.
Leroy, J.L.M.R., Vanholder, T., Mateusen, B., Christophe, A., Opsomer, G., de Kruif, A., Genicot, G., and Van Soom, A. (2005b) Non-esterified fatty acids in follicular fluid of dairy cows and their effect on developmental capacity of bovine oocytes *in vitro*. *Reproduction*, **130**, 485–495.
Li, R., Whitworth, K., Lai, L., Wax, D., Spate, L., Murphy, C.N., Rieke, A., Isom, C., Hao, Y., Zhong, Z., Katayama, M., Schatten, H., and Prather, R.S. (2007) Concentration and composition of free amino acids and osmolalities of porcine oviductal and uterine fluid and their effects on development of porcine IVF embryos. *Mol. Reprod. Dev.*, **74**, 1228–1235.
Lim, A.S. and Tsakok, M.F. (1997) Age-related decline in fertility: a link to degenerative oocytes? *Fertil. Steril.*, **68**, 265–271.
Liu, Z. and Foote, R.H. (1995) Effects of amino acids on the development of *in-vitro* matured/*in-vitro* fertilization bovine embryos in a simple protein-free medium. *Hum. Reprod.*, **10**, 2985–2991.
Liu, J., Liu, M., Ye, X., Liu, K., Huang, J., Wang, L., Ji, G., Liu, N., Tang, X., Baltz, J.M., Keefe, D.L., and Liu, L. (2012) Delay in oocyte aging in mice by the antioxidant *N*-acetyl-L-cysteine (NAC). *Hum. Reprod.*, **27**, 1411–1420.
Liu, M., Yin, Y., Ye, X., Zeng, M., Zhao, Q., Keefe, D.L., and Liu, L. (2013) Resveratrol protects against age-associated infertility in mice. *Hum. Reprod.*, **28**, 707–717.
Lolicato, F., Brouwers, J.F., de Lest, C.H., Wubbolts, R., Aardema, H., Priore, P., Roelen, B.A., Helms, J.B., and Gadella, B.M. (2015) The cumulus cell layer protects the bovine maturing oocyte against fatty acid-induced lipotoxicity. *Biol. Reprod.*, **92**, 16.
Luvoni, G.C., Keskintepe, L., and Brackett, B.G. (1996) Improvement in bovine embryo production *in vitro* by glutathione-containing culture media. *Mol. Reprod. Dev.*, **43**, 437–443.

Downloaded From Vet-eBooks.com

Marei, W.F., Wathes, D.C., and Fouladi-Nashta, A.A. (2010) Impact of linoleic acid on bovine oocyte maturation and embryo development. *Reproduction*, **139**, 979–988.

Marhuenda-Egea, F., Gonsálvez-Álvarez, R., Martínez-Sabater, E., Lledó, B., Ten, J., and Bernabeu, R. (2011) Improving human embryos selection in IVF: non-invasive metabolomic and chemometric approach. *Metabolomics*, **7**, 247–256.

Martino, N.A., Lacalandra, G.M., Filioli Uranio, M., Ambruosi, B., Caira, M., Silvestre, F., Pizzi, F., Desantis, S., Accogli, G., and Dell'Aquila, M.E. (2012) Oocyte mitochondrial bioenergy potential and oxidative stress: within-/between-subject, *in vivo* versus *in vitro* maturation, and age-related variations in a sheep model. *Fertil. Steril.*, **97**, 720–728.

Matoba, S., Bender, K., Fahey, A.G., Mamo, S., Brennan, L., Lonergan, P., and Fair, T. (2014) Predictive value of bovine follicular components as markers of oocyte developmental potential. *Reprod. Fertil. Dev.*, **26**, 337–345.

Matorras, R., Ruiz, J.I., Mendoza, R., Ruiz, N., Sanjurjo, P., and Rodriguez-Escudero, F.J. (1998) Fatty acid composition of fertilization-failed human oocytes. *Hum. Reprod.*, **13**, 2227–2230.

McEvoy, T.G., Coull, G.D., Broadbent, P.J., Hutchinson, J.S., and Speake, B.K. (2000) Fatty acid composition of lipids in immature cattle, pig and sheep oocytes with intact zona pellucida. *J. Reprod. Fertil.*, **118**, 163–170.

McKiernan, S.H., Clayton, M.K., and Bavister, B.D. (1995) Analysis of stimulatory and inhibitory amino acids for development of hamster one-cell embryos *in vitro*. *Mol. Reprod. Dev.*, **42**, 188–199.

McPherson, N.O., Zander-Fox, D., and Lane, M. (2014) Stimulation of mitochondrial embryo metabolism by dichloroacetic acid in an aged mouse model improves embryo development and viability. *Fertil. Steril.*, **101**, 1458–1466.

Munné, S., Alikani, M., Tomkin, G., Grifo, J., and Cohen, J. (1995) Embryo morphology, developmental rates, and maternal age are correlated with chromosome abnormalities. *Fertil. Steril.*, **64**, 382–391.

Murakami, M., Dong, Y.J., Suzuki, T., Taniguchi, M., Kaedei, Y., Sato, Y., Tanihara, F., and Otoi, T. (2011) Development and subsequent cryotolerance of domestic cat embryos cultured in serum-free and serum-containing media. *Cryobiology*, **63**, 170–174.

Nagy, Z.P., Sakkas, D., and Behr, B. (2008) Symposium: innovative techniques in human embryo viability assessment. Non-invasive assessment of embryo viability by metabolomic profiling of culture media ('metabolomics'). *Reprod. BioMed. Online*, **17**, 502–507.

Natarajan, R., Shankar, M.B., and Munuswamy, D. (2010) Effect of alpha-tocopherol supplementation on *in vitro* maturation of sheep oocytes and *in vitro* development of preimplantation sheep embryos to the blastocyst stage. *J. Assist. Reprod. Genet.*, **27**, 483–490.

Nel-Themaat, L. and Nagy, Z.P. (2011) A review of the promises and pitfalls of oocyte and embryo metabolomics. *Placenta*, **32**, 23.

Nichol, R., Hunter, R.H., Gardner, D.K., Leese, H.J., and Cooke, G.M. (1992) Concentrations of energy substrates in oviductal fluid and blood plasma of pigs during the peri-ovulatory period. *J. Reprod. Fertil.*, **96**, 699–707.

O'Brien, J.K., Dwarte, D., Ryan, J.P., Maxwell, W.M.C., and Evans, G. (1996) Developmental capacity, energy metabolism and ultrastructure of mature oocytes from prepubertal and adult sheep. *Reprod. Fertil. Dev.*, **8**, 1029–1037.

O'Fallon, J.V. and Wright, R.W. Jr. (1986) Quantitative determination of the pentose phosphate pathway in preimplantation mouse embryos. *Biol. Reprod.*, **34**, 58–64.

O'Gorman, A., Wallace, M., Cottell, E., Gibney, M.J., McAuliffe, F.M., Wingfield, M., and Brennan, L. (2013) Metabolic profiling of human follicular fluid identifies potential biomarkers of oocyte developmental competence. *Reproduction*, **146**, 389–395.

Downloaded From Vet-eBooks.com

Olson, S.E. and Seidel, G.E. Jr. (2000) Culture of *in vitro*-produced bovine embryos with vitamin E improves development *in vitro* and after transfer to recipients. *Biol. Reprod.*, **62**, 248–252.

Orsi, N.M. and Leese, H.J. (2004) Amino acid metabolism of preimplantation bovine embryos cultured with bovine serum albumin or polyvinyl alcohol. *Theriogenology*, **61**, 561–572.

Orsi, N.M., Gopichandran, N., Leese, H.J., Picton, H.M., and Harris, S.E. (2005) Fluctuations in bovine ovarian follicular fluid composition throughout the oestrous cycle. *Reproduction*, **129**, 219–228.

Oyamada, T. and Fukui, Y. (2004) Oxygen tension and medium supplements for *in vitro* maturation of bovine oocytes cultured individually in a chemically defined medium. *J. Reprod. Dev.*, **50**, 107–117.

Ozawa, M., Nagai, T., Fahrudin, M., Karja, N.W., Kaneko, H., Noguchi, J., Ohnuma, K., and Kikuchi, K. (2006) Addition of glutathione or thioredoxin to culture medium reduces intracellular redox status of porcine IVM/IVF embryos, resulting in improved development to the blastocyst stage. *Mol. Reprod. Dev.*, **73**, 998–1007.

Pacella, L., Zander-Fox, D.L., Armstrong, D.T., and Lane, M. (2012) Women with reduced ovarian reserve or advanced maternal age have an altered follicular environment. *Fertil. Steril.*, **98**, 986–994.

Paczkowski, M., Silva, E., Schoolcraft, W., and Krisher, R. (2013) Comparative importance of fatty acid beta-oxidation to nuclear maturation, gene expression, and glucose metabolism in mouse, bovine, and porcine cumulus oocyte complexes. *Biol. Reprod.*, **88**, 111.

Paczkowski, M., Schoolcraft, W.B., and Krisher, R.L. (2014) Fatty acid metabolism during maturation affects glucose uptake and is essential to oocyte competence. *Reproduction*, **148**, 429–439.

Pantaleon, M., Ryan, J.P., Gil, M., and Kaye, P.L. (2001) An unusual subcellular localization of GLUT1 and link with metabolism in oocytes and preimplantation mouse embryos. *Biol. Reprod.*, **64**, 1247–1254.

Petters, R.M., Johnson, B.H., Reed, M.L., and Archibong, A.E. (1990) Glucose, glutamine and inorganic phosphate in early development of the pig embryo *in vitro*. *J. Reprod. Fertil.*, **89**, 269–275.

Picton, H.M., Elder, K., Houghton, F.D., Hawkhead, J.A., Rutherford, A.J., Hogg, J.E., Leese, H.J., and Harris, S.E. (2010) Association between amino acid turnover and chromosome aneuploidy during human preimplantation embryo development *in vitro*. *Mol. Hum. Reprod.*, **16**, 557–569.

Preis, K.A., Seidel, G.E. Jr., and Gardner, D.K. (2007) Reduced oxygen concentration improves the developmental competence of mouse oocytes following *in vitro* maturation. *Mol. Reprod. Dev.*, **74**, 893–903.

Pudakalakatti, S.M., Uppangala, S., D'Souza, F., Kalthur, G., Kumar, P., Adiga, S.K., and Atreya, H.S. (2013) NMR studies of preimplantation embryo metabolism in human assisted reproductive techniques: a new biomarker for assessment of embryo implantation potential. *NMR Biomed.*, **26**, 20–27.

Purcell, S.H. and Moley, K.H. (2011) The impact of obesity on egg quality. *J. Assist. Reprod. Genet.*, **28**, 517–524.

Quinn, P. and Wales, R.G. (1973) The relationships between the ATP content of preimplantation mouse embryos and their development *in vitro* during culture. *J. Reprod. Fertil.*, **35**, 301–309.

Richani, D., Sutton-McDowall, M.L., Frank, L.A., Gilchrist, R.B., and Thompson, J.G. (2014) Effect of epidermal growth factor-like peptides on the metabolism of *in vitro*-matured mouse oocytes and cumulus cells. *Biol. Reprod.*, **90**, 49.

Rieger, D. and Guay, P. (1988) Measurement of the metabolism of energy substrates in individual bovine blastocysts. *J. Reprod. Fertil.*, **83**, 585–591.

Downloaded From Vet-eBooks.com

Rieger, D. and Loskutoff, N.M. (1994) Changes in the metabolism of glucose, pyruvate, glutamine and glycine during maturation of cattle oocytes *in vitro*. *J. Reprod. Fertil.*, **100**, 257–262.

Rieger, D., Loskutoff, N.M., and Betteridge, K.J. (1992a) Developmentally related changes in the metabolism of glucose and glutamine by cattle embryos produced and co-cultured *in vitro*. *J. Reprod. Fertil.*, **95**, 585–595.

Rieger, D., Loskutoff, N.M., and Betteridge, K.J. (1992b) Developmentally related changes in the uptake and metabolism of glucose, glutamine and pyruvate by cattle embryos produced *in vitro*. *Reprod. Fertil. Dev.*, **4**, 547–557.

Rozell, M.D., Williams, J.E., and Butler, J.E. (1992) Changes in concentration of adenosine triphosphate and adenosine diphosphate in individual preimplantation sheep embryos. *Biol. Reprod.*, **47**, 866–870.

Ruder, E.H., Hartman, T.J., Blumberg, J., and Goldman, M.B. (2008) Oxidative stress and antioxidants: exposure and impact on female fertility. *Hum. Reprod. Update*, **14**, 345–357.

Ruvolo, G., Fattouh, R.R., Bosco, L., Brucculeri, A.M., and Cittadini, E. (2013) New molecular markers for the evaluation of gamete quality. *J. Assist. Reprod. Genet.*, **30**, 207–212.

Saito, T., Hiroi, M., and Kato, T. (1994) Development of glucose utilization studied in single oocytes and preimplantation embryos from mice. *Biol. Reprod.*, **50**, 266–270.

Sakkas, D., Morita, H., Yamashita, N., Kato, O., Botros, L., Roos, P., and Seli, E. (2008) Evaluation of embryo quality by metabolomics: a new strategy to aid single embryo transfer. *J. Mamm. Ova Res.*, **25**, 26–31.

Salzano, A., Albero, G., Zullo, G., Neglia, G., Abdel-Wahab, A., Bifulco, G., Zicarelli, L., and Gasparrini, B. (2014) Effect of resveratrol supplementation during culture on the quality and cryotolerance of bovine *in vitro* produced embryos. *Anim. Reprod. Sci.*, **151**, 91–96.

Sato, H., Iwata, H., Hayashi, T., Kimura, K., Kuwayama, T., and Monji, Y. (2007) The effect of glucose on the progression of the nuclear maturation of pig oocytes. *Anim. Reprod. Sci.*, **99**, 299–305.

Scott, R., Seli, E., Miller, K., Sakkas, D., Scott, K., and Burns, D.H. (2008) Noninvasive metabolomic profiling of human embryo culture media using Raman spectroscopy predicts embryonic reproductive potential: a prospective blinded pilot study. *Fertil. Steril.*, **90**, 77–83.

Seli, E., Sakkas, D., Scott, R., Kwok, S.C., Rosendahl, S.M., and Burns, D.H. (2007) Noninvasive metabolomic profiling of embryo culture media using Raman and near-infrared spectroscopy correlates with reproductive potential of embryos in women undergoing *in vitro* fertilization. *Fertil. Steril.*, **88**, 1350–1357.

Seli, E., Vergouw, C.G., Morita, H., Botros, L., Roos, P., Lambalk, C.B., Yamashita, N., Kato, O., and Sakkas, D. (2010) Noninvasive metabolomic profiling as an adjunct to morphology for noninvasive embryo assessment in women undergoing single embryo transfer. *Fertil. Steril.*, **94**, 535–542.

Silva, E., Greene, A.F., Strauss, K., Herrick, J.R., Schoolcraft, W.B., and Krisher, R.L. (2015) Antioxidant supplementation during *in vitro* culture improves mitochondrial function and development of embryos from aged female mice. *Reprod. Fertil. Dev.*, **27**, 975–983.

Sinclair, K.D., Lunn, L.A., Kwong, W.Y., Wonnacott, K., Linforth, R.S.T., and Craigon, J. (2008) Amino acid and fatty acid composition of follicular fluid as predictors of *in-vitro* embryo development. *Reprod. BioMed. Online*, **16**, 859–868.

Singh, R. and Sinclair, K.D. (2007) Metabolomics: approaches to assessing oocyte and embryo quality. *Theriogenology*, **68** (Suppl. 1), S56–S62.

Singh, B., Meng, L., Rutledge, J.M., and Armstrong, D.T. (1997) Effects of epidermal growth factor and follicle stimulating hormone during *in vitro* maturation on cytoplasmic maturation of porcine oocytes. *Mol. Reprod. Dev.*, **46**, 401–407.

Downloaded From Vet-eBooks.com

Somfai, T., Kaneda, M., Akagi, S., Watanabe, S., Haraguchi, S., Mizutani, E., Dang-Nguyen, T.Q., Geshi, M., Kikuchi, K., and Nagai, T. (2011) Enhancement of lipid metabolism with L-carnitine during *in vitro* maturation improves nuclear maturation and cleavage ability of follicular porcine oocytes. *Reprod. Fertil. Dev.*, **23**, 912–920.

Songsasen, N., Spindler, R.E., and Wildt, D.E. (2007) Requirement for, and patterns of, pyruvate and glutamine metabolism in the domestic dog oocyte *in vitro*. *Mol. Reprod. Dev.*, **74**, 870–877.

Spindler, R.E., Pukazhenthi, B.S., and Wildt, D.E. (2000) Oocyte metabolism predicts the development of cat embryos to blastocyst *in vitro*. *Mol. Reprod. Dev.*, **56**, 163–171.

Steeves, T.E. and Gardner, D.K. (1999a) Metabolism of glucose, pyruvate, and glutamine during the maturation of oocytes derived from pre-pubertal and adult cows. *Mol. Reprod. Dev.*, **54**, 92–101.

Steeves, T.E. and Gardner, D.K. (1999b) Temporal and differential effects of amino acids on bovine embryo development in culture. *Biol. Reprod.*, **61**, 731–740.

Steeves, T.E., Gardner, D.K., Zuelke, K.A., Squires, T.S., and Fry, R.C. (1999) *In vitro* development and nutrient uptake by embryos derived from oocytes of pre-pubertal and adult cows. *Mol. Reprod. Dev.*, **54**, 49–56.

Sturmey, R.G. and Leese, H.J. (2003) Energy metabolism in pig oocytes and early embryos. *Reproduction*, **126**, 197–204.

Sturmey, R.G., O'Toole, P.J., and Leese, H.J. (2006) Fluorescence resonance energy transfer analysis of mitochondrial:lipid association in the porcine oocyte. *Reproduction*, **132**, 829–837.

Sturmey, R.G., Brison, D.R., and Leese, H.J. (2008) Symposium: innovative techniques in human embryo viability assessment. Assessing embryo viability by measurement of amino acid turnover. *Reprod. BioMed. Online*, **17**, 486–496.

Sturmey, R.G., Reis, A., Leese, H.J., and McEvoy, T.G. (2009) Role of fatty acids in energy provision during oocyte maturation and early embryo development. *Reprod. Domest. Anim.*, **44** (Suppl. 3), 50–58.

Sturmey, R.G., Bermejo-Alvarez, P., Gutierrez-Adan, A., Rizos, D., Leese, H.J., and Lonergan, P. (2010) Amino acid metabolism of bovine blastocysts: a biomarker of sex and viability (erratum appears in *Mol. Reprod. Dev.*, 2010, 77 (5), 472). *Mol. Reprod. Dev.*, **77**, 285–296.

Su, Y.-Q., Sugiura, K., Wigglesworth, K., O'Brien, M.J., Affourtit, J.P., Pangas, S.A., Matzuk, M.M., and Eppig, J.J. (2008) Oocyte regulation of metabolic cooperativity between mouse cumulus cells and oocytes: BMP15 and GDF9 control cholesterol biosynthesis in cumulus cells. *Development*, **135**, 111–121.

Sugimura, S., Matoba, S., Hashiyada, Y., Aikawa, Y., Ohtake, M., Matsuda, H., Kobayashi, S., Konishi, K., and Imai, K. (2012) Oxidative phosphorylation-linked respiration in individual bovine oocytes. *J. Reprod. Dev.*, **58**, 636–641.

Sugimura, S., Ritter, L.J., Sutton-McDowall, M.L., Mottershead, D.G., Thompson, J.G., and Gilchrist, R.B. (2014) Amphiregulin co-operates with bone morphogenetic protein 15 to increase bovine oocyte developmental competence: effects on gap junction-mediated metabolite supply. *Mol. Hum. Reprod.*, **20**, 499–513.

Sutton, M.L., Cetica, P.D., Beconi, M.T., Kind, K.L., Gilchrist, R.B., and Thompson, J.G. (2003a) Influence of oocyte-secreted factors and culture duration on the metabolic activity of bovine cumulus cell complexes. *Reproduction*, **126**, 27–34.

Sutton, M.L., Gilchrist, R.B., and Thompson, J.G. (2003b) Effects of *in-vivo* and *in-vitro* environments on the metabolism of the cumulus–oocyte complex and its influence on oocyte developmental capacity. *Hum. Reprod. Update*, **9**, 35–48.

Sutton-McDowall, M.L., Gilchrist, R.B., and Thompson, J.G. (2004) Cumulus expansion and glucose utilisation by bovine cumulus–oocyte complexes during *in vitro* maturation: the influence of glucosamine and follicle-stimulating hormone. *Reproduction*, **128**, 313–319.

Downloaded From Vet-eBooks.com

Sutton-McDowall, M.L., Mitchell, M., Cetica, P., Dalvit, G., Pantaleon, M., Lane, M., Gilchrist, R.B., and Thompson, J.G. (2006) Glucosamine supplementation during *in vitro* maturation inhibits subsequent embryo development: possible role of the hexosamine pathway as a regulator of developmental competence. *Biol. Reprod.*, **74**, 881–888.

Sutton-McDowall, M.L., Gilchrist, R.B., and Thompson, J.G. (2010) The pivotal role of glucose metabolism in determining oocyte developmental competence. *Reproduction*, **139**, 685–695.

Sutton-McDowall, M.L., Feil, D., Robker, R.L., Thompson, J.G., and Dunning, K.R. (2012a) Utilization of endogenous fatty acid stores for energy production in bovine preimplantation embryos. *Theriogenology*, **77**, 1632–1641.

Sutton-McDowall, M.L., Mottershead, D.G., Gardner, D.K., Gilchrist, R.B., and Thompson, J.G. (2012b) Metabolic differences in bovine cumulus–oocyte complexes matured *in vitro* in the presence or absence of follicle-stimulating hormone and bone morphogenetic protein 15. *Biol. Reprod.*, **87**, 87.

Sutton-McDowall, M.L., Purdey, M., Brown, H.M., Abell, A.D., Mottershead, D.G., Cetica, P.D., Dalvit, G.C., Goldys, E.M., Gilchrist, R.B., Gardner, D.K., and Thompson, J.G. (2015) Redox and anti-oxidant state within cattle oocytes following *in vitro* maturation with bone morphogenetic protein 15 and follicle stimulating hormone. *Mol. Reprod. Dev.*, **82**, 281–888.

Suzuki, C. and Yoshioka, K. (2006) Effects of amino acid supplements and replacement of polyvinyl alcohol with bovine serum albumin in porcine zygote medium. *Reprod. Fertil. Dev.*, **18**, 789–795.

Swain, J.E., Bormann, C.L., Clark, S.G., Walters, E.M., Wheeler, M.B., and Krisher, R.L. (2002) Use of energy substrates by various stage preimplantation pig embryos produced *in vivo* and *in vitro*. *Reproduction*, **123**, 253–260.

Talebi, A., Zavareh, S., Kashani, M.H., Lashgarbluki, T., and Karimi, I. (2012) The effect of alpha lipoic acid on the developmental competence of mouse isolated preantral follicles. *J. Assist. Reprod. Genet.*, **29**, 175–183.

Tejera, A., Herrero, J., de Los Santos, M.J., Garrido, N., Ramsing, N., and Meseguer, M. (2011) Oxygen consumption is a quality marker for human oocyte competence conditioned by ovarian stimulation regimens. *Fertil. Steril.*, **96**, 618–623.

Thompson, J.G. (2006) The impact of nutrition of the cumulus oocyte complex and embryo on subsequent development in ruminants. *J. Reprod. Dev.*, **52**, 169–175.

Thompson, J.G., Simpson, A.C., Pugh, P.A., Wright, R.W. Jr., and Tervit, H.R. (1991) Glucose utilization by sheep embryos derived *in vivo* and *in vitro*. *Reprod. Fertil. Dev.*, **3**, 571–576.

Thompson, J.G., Simpson, A.C., Pugh, P.A., and Tervit, H.R. (1992) Requirement for glucose during *in vitro* culture of sheep preimplantation embryos. *Mol. Reprod. Dev.*, **31**, 253–257.

Thompson, J.G., Bell, A.C., Pugh, P.A., and Tervit, H.R. (1993) Metabolism of pyruvate by pre-elongation sheep embryos and effect of pyruvate and lactate concentrations during culture *in vitro*. *Reprod. Fertil. Dev.*, **5**, 417–423.

Thompson, J.G., Partridge, R.J., Houghton, F.D., Cox, C.I., and Leese, H.J. (1996) Oxygen uptake and carbohydrate metabolism by *in vitro* derived bovine embryos. *J. Reprod. Fertil.*, **106**, 299–306.

Thompson, J.G., Lane, M., and Gilchrist, R.B. (2007) Metabolism of the bovine cumulus–oocyte complex and influence on subsequent developmental competence. *Soc. Reprod. Fertil. Suppl.*, **64**, 179–190.

Tsutsumi, O., Satoh, K., Taketani, Y., and Kato, T. (1992) Determination of enzyme activities of energy metabolism in the maturing rat oocyte. *Mol. Reprod. Dev.*, **33**, 333–337.

Uyar, A. and Seli, E. (2014) Metabolomic assessment of embryo viability. *Semin. Reprod. Med.*, **32**, 141–152.

Van Blerkom, J., Davis, P.W., and Lee, J. (1995) ATP content of human oocytes and developmental potential and outcome after *in-vitro* fertilization and embryo transfer. *Hum. Reprod.*, **10**, 415–424.

Downloaded From Vet-eBooks.com

Van Hoeck, V., Sturmey, R.G., Bermejo-Alvarez, P., Rizos, D., Gutierrez-Adan, A., Leese, H.J., Bols, P.E.J., and Leroy, J. (2011) Elevated non-esterified fatty acid concentrations during bovine oocyte maturation compromise early embryo physiology. *PLoS One*, **6**, e23183.

Vannuvel, K., Renard, P., Raes, M., and Arnould, T. (2013) Functional and morphological impact of ER stress on mitochondria. *J. Cell. Physiol.*, **228**, 1802–1818.

Vergouw, C.G., Kieslinger, D.C., Kostelijk, E.H., Botros, L.L., Schats, R., Hompes, P.G., Sakkas, D., and Lambalk, C.B. (2012) Day 3 embryo selection by metabolomic profiling of culture medium with near-infrared spectroscopy as an adjunct to morphology: a randomized controlled trial. *Hum. Reprod.*, **27**, 2304–2311.

Wale, P.L. and Gardner, D.K. (2012) Oxygen regulates amino acid turnover and carbohydrate uptake during the preimplantation period of mouse embryo development. *Biol. Reprod.*, **87**, 24.

Wale, P.L. and Gardner, D.K. (2013) Oxygen affects the ability of mouse blastocysts to regulate ammonium. *Biol. Reprod.*, **89**, 75.

Wales, R.G. and Brinster, R.L. (1968) The uptake of hexoses by pre-implantation mouse embryos *in vitro*. *J. Reprod. Fertil.*, **15**, 415–422.

Wallace, M., Cottell, E., Gibney, M.J., McAuliffe, F.M., Wingfield, M., and Brennan, L. (2012) An investigation into the relationship between the metabolic profile of follicular fluid, oocyte developmental potential, and implantation outcome. *Fertil. Steril.*, **97**, 1078–1084.

Wang, X., Falcone, T., Attaran, M., Goldberg, J.M., Agarwal, A., and Sharma, R.K. (2002) Vitamin C and vitamin E supplementation reduce oxidative stress-induced embryo toxicity and improve the blastocyst development rate. *Fertil. Steril.*, **78**, 1272–1277.

Wang, Q., Chi, M.M., Schedl, T., and Moley, K.H. (2012) An intercellular pathway for glucose transport into mouse oocytes. *Am. J. Physiol. Endocrinol. Metabol.*, **302**, E1511–E1518.

Wang, F., Tian, X., Zhang, L., He, C., Ji, P., Li, Y., Tan, D., and Liu, G. (2014a) Beneficial effect of resveratrol on bovine oocyte maturation and subsequent embryonic development after *in vitro* fertilization. *Fertil. Steril.*, **101**, 577–586.

Wang, N., Luo, L.L., Xu, J.J., Xu, M.Y., Zhang, X.M., Zhou, X.L., Liu, W.J., and Fu, Y.C. (2014b) Obesity accelerates ovarian follicle development and follicle loss in rats. *Metabol. Clin. Exp.*, **63**, 94–103.

Whitten, W.K. and Biggers, J.D. (1968) Complete development *in vitro* of the pre-implantation stages of the mouse in a simple chemically defined medium. *J. Reprod. Fertil.*, **17**, 399–401.

Wilding, M., Dale, B., Marino, M., di Matteo, L., Alviggi, C., Pisaturo, M.L., Lombardi, L., and De Placido, G. (2001) Mitochondrial aggregation patterns and activity in human oocytes and preimplantation embryos. *Hum. Reprod.*, **16**, 909–917.

Wilding, M., Di Matteo, L., and Dale, B. (2005) The maternal age effect: a hypothesis based on oxidative phosphorylation. *Zygote*, **13**, 317–323.

Wilding, M., Coppola, G., Dale, B., and Di Matteo, L. (2009) Mitochondria and human preimplantation embryo development. *Reproduction*, **137**, 619–624.

Wu, L.L., Dunning, K.R., Yang, X., Russell, D.L., Lane, M., Norman, R.J., and Robker, R.L. (2010) High-fat diet causes lipotoxicity responses in cumulus–oocyte complexes and decreased fertilization rates. *Endocrinology*, **151**, 5438–5445.

Wu, G.Q., Jia, B.Y., Li, J.J., Fu, X.W., Zhou, G.B., Hou, Y.P., and Zhu, S.E. (2011) L-Carnitine enhances oocyte maturation and development of parthenogenetic embryos in pigs. *Theriogenology*, **76**, 785–793.

Wu, L.L., Russell, D.L., Wong, S.L., Chen, M., Tsai, T.S., St John, J.C., Norman, R.J., Febbraio, M.A., Carroll, J., and Robker, R.L. (2015) Mitochondrial dysfunction in oocytes of obese mothers: transmission to offspring and reversal by pharmacological endoplasmic reticulum stress inhibitors. *Development*, **142**, 681–691.

Downloaded From Vet-eBooks.com

Yang, H., Yang, T., Baur, J.A., Perez, E., Matsui, T., Carmona, J.J., Lamming, D.W., Souza-Pinto, N.C., Bohr, V.A., Rosenzweig, A., de Cabo, R., Sauve, A.A., and Sinclair, D.A. (2007) Nutrient-sensitive mitochondrial NAD+ levels dictate cell survival. *Cell*, **130**, 1095–1107.

Yoshioka, K., Suzuki, C., and Onishi, A. (2008) Defined system for *in vitro* production of porcine embryos using a single basic medium. *J. Reprod. Dev.*, **54**, 208–213.

You, J., Lee, J., Hyun, S.-H., and Lee, E. (2012) L-Carnitine treatment during oocyte maturation improves *in vitro* development of cloned pig embryos by influencing intracellular glutathione synthesis and embryonic gene expression. *Theriogenology*, **78**, 235–243.

Yuan, Y., Wheeler, M.B., and Krisher, R.L. (2012) Disrupted redox homeostasis and aberrant redox gene expression in porcine oocytes contribute to decreased developmental competence. *Biol. Reprod.*, **87**, 78.

Zander-Fox, D.L., Fullston, T., McPherson, N.O., Sandeman, L., Kang, W.X., Good, S.B., Spillane, M., and Lane, M. (2015) Reduction of mitochondrial function by FCCP during mouse cleavage stage embryo culture reduces birth weight and impairs the metabolic health of offspring. *Biol. Reprod.*, **92**, 124.

Zeng, H.T., Richani, D., Sutton-McDowall, M.L., Ren, Z., Smitz, J.E., Stokes, Y., Gilchrist, R.B., and Thompson, J.G. (2014) Prematuration with cyclic adenosine monophosphate modulators alters cumulus cell and oocyte metabolism and enhances developmental competence of *in vitro*-matured mouse oocytes. *Biol. Reprod.*, **91**, 47.

Zeron, Y., Ocheretny, A., Kedar, O., Borochov, A., Sklan, D., and Arav, A. (2001) Seasonal changes in bovine fertility: relation to developmental competence of oocytes, membrane properties and fatty acid composition of follicles. *Reproduction*, **121**, 447–454.

Zhang, L., Hou, X., Ma, R., Moley, K., Schedl, T., and Wang, Q. (2014) Sirt2 functions in spindle organization and chromosome alignment in mouse oocyte meiosis. *FASEB J.*, **28**, 1435–1445.

Zivi, E., Barash, D., Aizenman, E., Gibson, D., and Shufaro, Y. (2014) Zygote serine decreased uptake from the fertilization medium is associated with implantation and pregnancy. *J. Assist. Reprod. Genet.*, **31**, 889–897.

Zuelke, K.A. and Brackett, B.G. (1992) Effects of luteinizing hormone on glucose metabolism in cumulus-enclosed bovine oocytes matured *in vitro*. *Endocrinology*, **131**, 2690–2696.

Zuelke, K.A. and Brackett, B.G. (1993) Increased glutamine metabolism in bovine cumulus cell-enclosed and denuded oocytes after *in vitro* maturation with luteinizing hormone. *Biol. Reprod.*, **48**, 815–820.

Downloaded From Vet-eBooks.com

8

Signal Transduction Pathways in Oocyte Maturation*

François J. Richard,[1] Nicolas Santiquet,[2] Annick Bergeron,[1] and Daulat Raheem Khan[1]

[1]*Centre de Recherche en Biologie de la Reproduction, Département des Sciences Animales, Faculté des sciences de l'agriculture et de l'alimentation, Université Laval, Québec, Canada*
[2]*National Foundation for Fertility Research, Lone Tree, CO, USA*

8.1 Introduction

The ovary is the female's reservoir of germ cells. With the exception of a few species, the female reproductive organs contain a limited number of gametes required for the purpose of perpetuating the species. This number is reached prior to birth. Female gametes are produced in the ovary during fetal life and the ovary remains mostly dormant until puberty. The onset of the ovulation cycles determines fertility. The oocyte is located in a "niche" called the ovarian follicle. Each ovarian follicle comprises an oocyte surrounded by somatic cells called cumulus cells, granulosa cells, which form an internal pseudo-stratified epithelium that has a steroidogenic function important for female reproduction, and theca cells, which form fibroblastic tissue that has a steroidogenic function that differs from that of granulosa cells. These follicular somatic cells sustain the growth of the oocyte and facilitate ovulation as an egg. Exchanges between the oocyte and the somatic cells occur in both directions (Eppig, 1991; Matzuk and Burns, 2012).

Meiosis begins at the time of ovarian follicle establishment. The oocytes initiate their first meiotic division and stop at the dictyate stage of prophase I during which the nucleus forms a germinal vesicle (GV stage), the hallmark of meiotic arrest (Figure 8.1c). The encapsulation of the oocyte by somatic cells forms the primordial follicles and allows an extensive network of gap junctions to be established creating an electrophysiological syncytium between the oocyte and the surrounding cumulus and granulosa cells. The development of primordial follicles into preovulatory follicles takes approximately 6 months in swine, during which the somatic cells of the follicles proliferate and differentiate while the oocyte grows. The length of this period is species-specific. The meiotic competence of oocytes, defined as the ability to resume meiosis (germinal vesicle breakdown, GVBD), is not acquired until late during oocyte growth. In swine, this occurs when the oocyte reaches 115 μm in diameter (Motlik and Fulka, 1986), whereas in cattle full ability to progress to metaphase I occurs at 110 μm (Fair, 1995). Oocyte maturation is a critical step with respect to female fertility since it includes all the final preparation for fertilization of the oocyte by the spermatozoon. The egg becomes a zygote once fertilized. The competence of the oocyte to develop into an embryo is progressively acquired during the final stage of oocyte growth during follicular development.

*__Disclosure:__ Authors declare no potential conflicts of interest.

Animal Models and Human Reproduction, First Edition. Edited by Heide Schatten and Gheorghe M. Constantinescu.
© 2017 John Wiley & Sons, Inc. Published 2017 by John Wiley & Sons, Inc.

Downloaded From Vet-eBooks.com

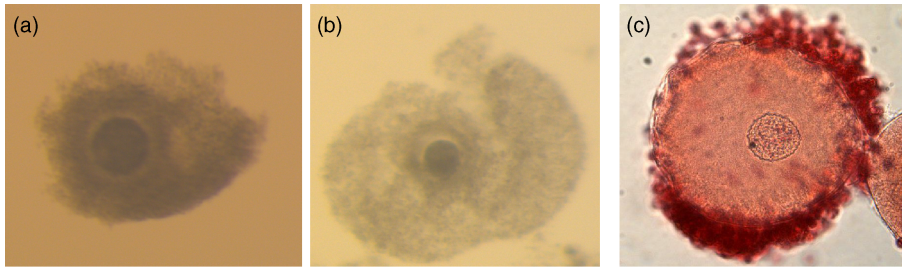

Figure 8.1 Micrograph of a bovine cumulus–oocyte complex before (a) and after (b) *in vitro* maturation (IVM) for 24 h in the presence of FSH, LH, and estradiol. Bovine oocyte at the GV stage, the hallmark of oocyte meiotic arrest is validated by the presence of the entire nuclear membrane surrounding the nuclear material (c). The oocyte has been denuded of cumulus cells before fixation and staining with orcein.

8.1.1 Oocyte Maturation

Oocyte maturation is fundamental to successful fertilization and embryonic development, and allows the female gamete to acquire all the competences required to give rise to a new and healthy individual (Sirard *et al.*, 2006). It is divided into two main processes: (i) nuclear maturation, which includes the resumption of the first meiotic division and is visualized histologically by the rupture of the germinal vesicle followed by a second block at metaphase-II; and (ii) cumulus expansion (Figure 8.1), which is the result of extracellular matrix secretion by the cumulus cells that enables fertilization of the egg and subsequent development into an embryo.

8.1.2 Oocyte Nuclear Maturation

In vivo, numerous cascades of events are spatiotemporally regulated in the preovulatory follicle by the two pituitary gonadotropins that drive ovulation, namely, follicle-stimulating hormone (FSH) and luteinizing hormone (LH). In the preovulatory follicle, the oocyte is released from meiotic arrest upon the LH surge. However, once oocyte meiotic competence is acquired in antral follicles (as occurs in 2-mm-diameter follicles in cattle and swine), meiosis may resume spontaneously *in vitro* (Edwards, 1965; Motlik *et al.*, 1984; Pincus and Enzmann, 1935). This chapter is primarily concerned with the latter population of oocytes.

Nuclear maturation is the continuity of oocyte meiosis from the G2/M phase transition to metaphase II. Several cell cycle kinases are reportedly involved in this G2/M-phase transition. In large animals, the synthesis of cyclin B is a limiting step (Lévesque and Sirard, 1996) in the activation of M-phase promoting factor (MPF), the key detector that integrates cell cycle signaling. Formed by cyclin B and Cdk1, MPF is a cyclin-dependent kinase inhibited by phosphorylation. The link between cyclic AMP-dependent protein kinase (PKA) and MPF inhibition is still not fully understood, but Wee1, a kinase that specifically inhibits MPF activation, has been proposed to be activated by cyclic adenosine monophosphate (cAMP) in murine oocytes (Han and Conti, 2006). Cyclic AMP-dependent protein kinase (PKA) is proposed to phosphorylate Wee1, which maintains inactive MPF by phosphorylating Cdc2 on Tyr15. Alternatively, a recent study supports the inactivation of Cdc25b phosphatase activity through PKA phosphorylation as a mechanism for the maintenance of meiotic arrest (Pirino *et al.*, 2009). The effect of a gene null mutation of Cdc25b by homologous recombination in embryonic stem cells manifests a female infertility phenotype (Lincoln *et al.*, 2002). Oocytes are blocked at the GV stage because of the inability of Cdc25b to activate MPF. Although PKA may

Downloaded From Vet-eBooks.com

appear to be a key regulator of MPF, other results also suggest that the v-akt murine thymoma viral oncogene (AKT) is a regulator of the G2/M phase transition (Okumura *et al.*, 2002).

8.1.3 Cumulus Cell Expansion

The granulosa/cumulus cells receive the induction signal(s) of oocyte maturation. Luteinizing hormone is the most well-known induction factor of oocyte maturation *in vivo*. The preovulatory LH surge induces oocyte nuclear maturation, sets the appropriate spatiotemporal gene expression pattern in granulosa/cumulus cells, and stimulates cumulus cell expansion and ovulation. Epidermal growth factor (EGF) is also a well-accepted induction factor that stimulates oocyte maturation in addition to cumulus expansion (Dekel and Sherizly, 1985). Recently, EGF-like factors such as epiregulin, amphiregulin, and beta-celluline were described as being involved in the induction of murine oocyte nuclear maturation (Park *et al.*, 2004). The EGF-like factors are actively regulated following the LH surge (Hsieh *et al.*, 2007; Panigone *et al.*, 2008) and are expressed in cumulus cells both *in vitro* and *in vivo* (Shimada *et al.*, 2006). However, culture conditions that support the complete efficacy of these factors have still to be fully determined (Romero and Smitz, 2009) and may show interspecies variation.

Cumulus expansion is observed in response to these induction signals, and refers to the ability of cumulus cells to synthesize an extracellular matrix that is essential for fertilization (Figure 8.1a and b). Cumulus cell expansion *in vitro* is stimulated by FSH (Eppig, 1980a, 1980b). Cumulus cells secrete glycosaminoglycans, primarily hyaluronic acid, which forms the backbone of the extracellular matrix. The synthesis of hyaluronic acid is dependent on HAS-2 gene regulation and requires glucose (Fagbohun and Downs, 1992; Thompson, 2006). Organization of the extracellular matrix is essential for oocyte fertilization and requires secreted proteins such as TSG-6 (Kahmann *et al.*, 2000), versican (Camaioni *et al.*, 1996; Russell *et al.*, 2003), the heavy chain of inter-alpha-inhibitor (Chen *et al.*, 1992), and PTX-3 (Salustri *et al.*, 2004), which interacts with the latter (Scarchilli *et al.*, 2007; Suzuki *et al.*, 2004).

In the following sections, we will address the role and the contribution of several enzymes and molecules to the process of oocyte maturation, including oocyte nuclear maturation and cumulus cell expansion. We will first review the impact of FSH during *in vitro* maturation (IVM). Next, we will discuss the role of cAMP and the contribution of phosphodiesterase (PDE) to the promotion of intracellular cAMP action into the cells. The following section will focus on the recently proposed inhibitory role of natriuretic peptides. Finally, the contribution of gap junction communication (GJC) and the involvement of the metabolic switch, adenosine 5′-monophosphate-activated protein kinase (AMPK) in oocyte maturation will be discussed.

8.1.4 The Impact of FSH During *In Vitro* Maturation

Follicular development is regulated by gonadotropins and involves proliferation of follicular somatic cells (granulosa and cumulus). Pituitary gonadotropins have been implicated in oocyte maturation and the acquisition of developmental competence (Gilbert *et al.*, 2012; Nivet *et al.*, 2013). In fact, granulosa and cumulus cells communicate through autocrine/paracrine mechanisms to coordinate follicular development under the influence of gonadotropins. These hormones confer follicular cell-specific gene expression patterns through activation of their downstream intracellular pathways and impart peculiar functional properties that ultimately determine oocyte quality.

During follicular development, granulosa and cumulus cell activities such as proliferation, differentiation, metabolism, and steroidogenesis are regulated by FSH. Although preantral follicular development has been demonstrated independent of FSH (Abel *et al.*, 2000), various

Downloaded From Vet-eBooks.com

studies indicate that the growth of preantral follicles could be enhanced by FSH treatment (Cortvrindt *et al.*, 1997). Moreover, FSH has been widely used in *in vitro* oocyte maturation (Ali and Sirard, 2005; Meinecke and Meinecke-Tillmann, 1979; Silvestre *et al.*, 2007) because cumulus cells lack functional LH receptors at this stage (Peng *et al.*, 1991). In fact, follicular somatic cell properties are modulated by the binding of FSH to its cognate receptors. These receptors are expressed in granulosa cells from the primary to preovulatory stages, and in cumulus cells during the periovulatory period (Oktay *et al.*, 1997). This suggests that FSH is a requisite for antral follicular development that influences preantral growth in addition to oocyte maturation.

Follicle-stimulating hormone influences multiple intracellular networks. A well-characterized signaling cascade is the activation of adenylyl cyclase (AC) and subsequent synthesis of cAMP (Means *et al.*, 1974). The formation of cAMP prompts activation of PKA, which in turn activates key transcription factors such as SP1/SP3 and CREB, and eventually regulates transcription of downstream genes in cumulus and granulosa cells (Gloaguen *et al.*, 2011). Nevertheless, the growing complexity associated with FSH signaling asserts that AC/cAMP/PKA is not the only pathway activated by FSH (Figure 8.2). There are several other molecular events that occur independent of the cAMP/PKA pathway (Gloaguen *et al.*, 2011). In particular, activation of AKT follows FSH stimulation, which suggests the role of exchange protein activated by cAMP (EPAC) in this process (Wayne *et al.*, 2007). In addition, FSH has also been reported to promote phosphatidylinositol 3-kinase (PI3K) activity (Zeleznik *et al.*, 2003), which results in activation of transcription factor FOXO1 (Wayne *et al.*, 2007). At the receptor level, FSH has been shown to interact with G protein-coupled receptor kinases (GRKs) and beta-arrestins (Reiter and Lefkowitz, 2006), which result in internalization and recycling of the FSH receptors (Kara *et al.*, 2006).

In parallel, there is convincing evidence that the EGF pathway is also activated by FSH in cumulus and granulosa cells. Interestingly, FSH induces amphiregulin (AREG) in different species (Caixeta *et al.*, 2013; Prochazka *et al.*, 2011; Shimada *et al.*, 2006), which results in oocyte maturation by acting on the EGF receptor (Downs and Chen, 2008). The mechanism by which FSH contributes to EGF receptor activation is intriguing. It has been suggested that metalloprotease ADAM17 is phosphorylated in response to FSH stimulation, which splits a

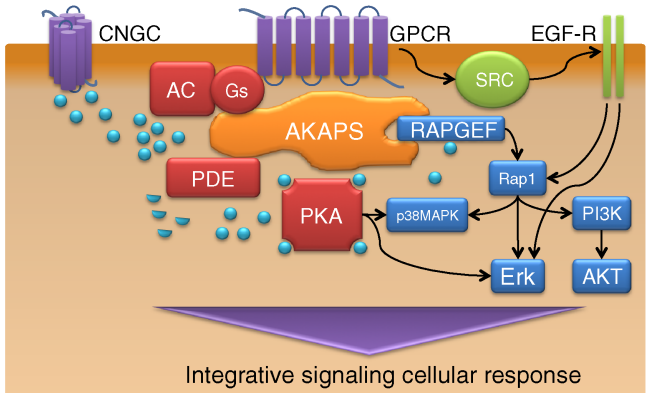

Figure 8.2 Schematic representation of the cAMP signaling cascade following the binding of a specific ligand to the specific G protein-coupled receptor (GPCR). This binding induces Gs protein translocation to activate adenylyl cyclase, which synthesizes cAMP (black dot) from ATP. Different targets are known for cAMP: cyclic nucleotide-gated channels (CNGC); protein kinase A (PKA); Rap guanine nucleotide exchange factor (RAPGEF), which activates ERK. Phosphodiesterase (PDE) hydrolyzes cAMP to inactive 5′-AMP. All of these molecules can be segregated by anchoring proteins such as A-kinase anchor proteins (AKAPs). (See color plate section.)

Downloaded From Vet-eBooks.com

pro-EGF-like protein, releasing an EGF-like ligand that subsequently activates the EGF receptor (Yamashita *et al.*, 2010; Yamashita *et al.*, 2007). The alternative route is by transactivation of the EGF receptor by the FSH receptor through Src recruitment since FSH effects in cumulus cells are sensitive to SRC inhibition (Cottom *et al.*, 2003; Wayne *et al.*, 2007) implying a role in FSH signaling. Although ADAM17 has been implicated in this process (Yamashita *et al.*, 2014), protein kinase C (PKC) is shown to be involved in EGF receptor transactivation by FSH to induce porcine oocyte maturation (Chen *et al.*, 2008, 2014). More recently, it has been shown that FSH-deficient mice were unable to express EGF receptors (El-Hayek *et al.*, 2014). This indicates that FSH not only transactivates the EGF receptor, but also controls its expression.

Activation of ERK1/2 is central for induction of oocyte maturation by the EGF pathway since inhibition of the EGF receptor abrogates cumulus expansion, oocyte maturation, and ovulation (Shimada *et al.*, 2006; Shupe *et al.*, 2011). Follicle-stimulating hormone-induced EGF receptor transactivation triggers Ras, which in turn activates the Raf1/MEK/ERK pathway inducing ERK phosphorylation (Cottom *et al.*, 2003; Shupe *et al.*, 2011; Wayne *et al.*, 2007). In addition, the effects of FSH in murine cumulus cells require p38 activation, which precedes an autocrine activation of the EGF receptor in cumulus cells (Shimada *et al.*, 2006). Of interest is the indication from our recent study in bovine cumulus cells of opposing regulation of FSH-stimulated ERK1/2 phosphorylation by the PKA and EGF pathways. Indeed, FSH seemed to increase ERK1/2 phosphorylation by stimulating the EGF pathway with a simultaneous stimulation of dual specific phosphatase1 (DUSP1) in a PKA-dependent fashion that maintained ERK1/2 phosphorylation at a specific level (Khan *et al.*, submitted). This is significant with respect to oocyte maturation because of the adverse effects of reduced or elevated levels of ERK1/2 phosphorylation (Fan *et al.*, 2009).

Follicle-stimulating hormone has been implicated in the acquisition of oocyte competence both *in vivo* and *in vitro* (Ali and Sirard, 2005; Nivet *et al.*, 2013) and transactivation of the EGF receptor by FSH is apparently involved in this process. It has been shown that cumulus cells derived under IVM conditions were deficient in EGF-like peptides (Richani *et al.*, 2013). Moreover, supplementation of IVM culture systems with exogenous EGF-like peptides improves oocyte developmental competence (Prochazka *et al.*, 2011; Richani *et al.*, 2013). A recent study shows that cumulus cell-derived AREG regulates translation of a subset of transcripts within the murine oocyte during maturation, and perturbation of this factor impacts oocyte quality (Chen *et al.*, 2013). Furthermore, it has been suggested that cumulus cells respond differently to oocyte-derived paracrine factors than granulosa cells, which is a reflection of the distinct properties of these cell types (Wigglesworth *et al.*, 2014). Therefore, it is suggested that FSH elicits various signaling pathways and probably improves oocyte quality through transactivation of the EGF pathway, which controls protein translation in oocytes.

8.2 Phosphodiesterase

8.2.1 Overview

The importance attributed to the role of PDEs in cell signaling has increased over the years. Recent studies have shown that PDEs are involved in numerous biological functions including reproduction. The treatment of erectile dysfunction using family-5-specific PDE inhibitors such as Viagra®, Cialis®, and Levitra® serves as a good example. The tremendous pharmaceutical success of specific PDE inhibitors illustrates the physiological importance of PDE in cellular signaling. Phosphodiesterases are organized into 11 families and hydrolyze cyclic nucleotides. In

Downloaded From Vet-eBooks.com

the ovary, the best-known mediators of signaling associated with gonadotropins such as FSH and LH are cyclic nucleotides via their G protein-coupled receptors (GPCRs).

8.2.2 Cyclic Nucleotide Signaling

Ovarian physiology is primarily based on the response to the gonadotropins, FSH and LH, which underlie fertility. The gonadotropin response is predominantly mediated through cyclic nucleotides (Figure 8.2). The FSH and LH receptors are members of the G protein-coupled, seven transmembrane domain receptor family. This class of receptor stimulates the synthesis of cAMP from ATP by AC. This cyclic nucleotide is known to act on three distinct targets: (i) PKA, with its two cAMP-binding regulatory subunits allowing activation of two catalytic subunits; (ii) cyclic nucleotide-gated channels (CNGC) regulating the transport of ions and small molecules; and (iii) exchange protein directly activated by cAMP (EPAC or RAPGEF), which can activate the Raf, ERK, and AKT signaling pathways. In addition, as previously described, FSH may transactivate the EGF receptor and downstream kinases such as ERK (Khan *et al.*, submitted; Gloaguen *et al.*, 2011). This stimulation induces cell-specific responses depending on the stimulus, dose, and targeted cell type.

This description of the cellular response to gonadotropin is incomplete without the PDE enzyme, which hydrolyzes cAMP and cyclic guanosine monophosphate (cGMP) to their inactive forms, 5′-AMP and 5′-GMP, respectively, thereby terminating cyclic nucleotide-mediated signaling such as gonadotropin response. Once the intracellular concentration of cyclic nucleotides has returned to the basal level, the cell is ready to respond to a new stimulus. This responsiveness to the extracellular environment allows cells to synchronize their responses to the gonadotropin signal sent by the pituitary gland. The enzymes of the PDE family not only terminate cyclic nucleotide signaling, but also have a significant modulatory influence. The schematic illustration of the cAMP response to a stimulus following activation of GPCRs (Figure 8.3) shows a rapid increase in the intracellular concentration of cAMP, followed by a momentary "plateau," and then a decrease to the basal intracellular level at a particular rate. In simple terms, the increase in intracellular concentration of cAMP is the result of cyclase activation, whereas the decrease is attributed to PDE. However, it should be understood that cAMP synthesis and cAMP degradation do not proceed at the same rate. Hydrolysis can be an order of magnitude faster than synthesis (Beavo and Brunton, 2002). Given this differential, it can be appreciated that early activation of PDE will modify not only the profile of the decreasing portion of the cAMP curve but also the "plateau" reached, and even the kinetics of the initial increase. These profound effects on the cAMP curve profile translate to different cellular responses. A delay in the activation of PDE will also have a major impact on all sections of the cAMP curve and hence on the cellular response. These considerations have aroused the interest of the scientific community concerned with PDEs and their impact on cellular physiology.

8.2.3 Phosphodiesterase Superfamily

The PDE superfamily is organized into 11 different families, numbered from 1 to 11. Each family comprises isoenzymes of various genes, identified by a letter and a numeral. For example, PDE4D2 is isoenzyme 2 of gene D of family PDE4. The family classification is based on biochemical properties such as specificity for cyclic nucleotides, enzyme kinetics, K_m and V_{max} values, and the response to specific PDE inhibitors (Table 8.1). The enzymes PDE4, PDE7, and PDE8 specifically hydrolyze cAMP, whereas PDE5, PDE6, and PDE9 are specific for cGMP. Both cyclic nucleotides are hydrolyzed by PDE1, PDE2, PDE3, PDE10, and PDE11, subject to biochemical characteristics unique to each family. In general, it can be claimed that PDE1

Downloaded From Vet-eBooks.com

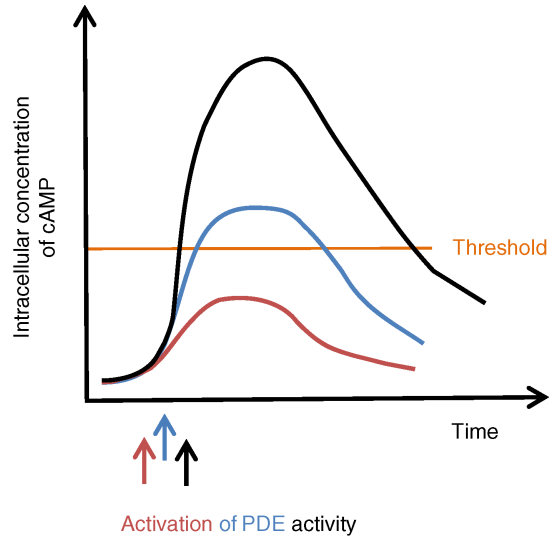

Figure 8.3 Schematic representation of a theoretical intracellular cAMP accumulation after an extracellular stimulus. Cyclic AMP concentration changes over time, illustrating the global response due to cyclase and PDE activities. The curves represent activation of PDE at different time points (↑). Blue represents a "normal" response. Early PDE activation is represented in red, whereas a late activation is shown in black. Based on a threshold of physiological consequence, the cell activates the appropriate cAMP-dependent signaling pathway. The threshold is thus surpassed for about 40% of the total time (in the "normal" situation), not reached at all, or surpassed to a large degree for more than half of the total time. This illustrates the marked impact that PDE activation may have on cAMP accumulation and hence on the cell response.

to PDE4 are expressed in a broad range of tissues, whereas the PDE5 to PDE11 families are much less abundant. Table 8.1 lists the main characteristic of each PDE family, the number of genes currently identified and a nonexhaustive list of specific PDE inhibitors. Based on sequence alignment, the catalytic domains are very similar to each other, whereas the regulatory N-terminal regions differ, imparting specific biochemical properties to each PDE family. For example, PDE3 seems to be the only PDE bearing putative transmembrane domain, suggesting membrane anchorage and hence possible membrane-based segregation of this family. The cellular compartmentalization of this family of PDE provides a good example of the dynamics of microdomain signaling (Neves *et al.*, 2008). By regulating the duration, amplitude, and segregation of intracellular cyclic nucleotide concentration, PDE plays a critical role in a large variety of signaling pathways.

8.2.4 Oocyte Meiosis and cAMP

Pincus and Enzmann (1935) were the first to report that mammalian oocytes in culture spontaneously resume meiosis and then become ready for fertilization. A key role for cAMP in the control of spontaneous meiotic resumption in oocytes *in vitro* was first proposed in the 1970s (Cho *et al.*, 1974). This study showed that a cAMP derivative, not hydrolyzable by PDE and capable of crossing the cellular membrane, inhibited spontaneous meiotic resumption. Cyclic AMP may be synthesized in the female gamete in conjunction with activation of GPCR, as shown with GPR3 and GPR12 (Hinckley *et al.*, 2005; Mehlmann *et al.*, 2004), or may enter via gap junctions existing between granulosa cells, cumulus cells, and the oocyte (Dekel, 1988).

The contribution of PDE to the control of spontaneous meiotic resumption has been studied using nonspecific PDE inhibitors such as 3-isobutyl-1-methylxanthine, also known as IBMX (Magnusson and Hillensjo, 1977), which block spontaneous meiotic resumption, suggesting that active PDE must be involved (Vivarelli *et al.*, 1983). Researchers next characterized calcium–calmodulin-sensitive PDE in rodent oocytes (Bornslaeger *et al.*, 1984), although there was no clear involvement of this PDE family in the oocyte meiotic process. It was not until the mid-1990s that the first studies were published, showing that PDE3A expressed in the oocyte (Reinhardt *et al.*, 1995) played a crucial role in meiotic resumption (Tsafriri *et al.*, 1996).

Downloaded From Vet-eBooks.com

Table 8.1 Characteristics of the phosphodiesterase superfamily.

Family	Genes	Characteristic	N-terminal domains	Specific inhibitor
PDE1	3	Ca-CaM-activated	Calmodulin, PKA	Nimodipine, Vinpocetine, zaprinast, SCH51866
PDE2	1	cGMP activated	GAF-A, GAF-B	EHNA
PDE3	2	cGMP inhibited, cAMP selective	6 Transmembrane domains, PKA, AKT	Cilostamide, milrinone, amrinone, enoximone
PDE4	4	cAMP-specific	Anchoring, PKA, UCR1, UCR2	Rolipram, RO 20-1724, denbufylline, zadarverine
PDE5	1	cGMP-specific	PKG, GAF-A, GAF-B	Sildenafil, zaprinast, DMPPO, E4021, SCH51866, GF248
PDE6	3	cGMP-specific	GAF-A, GAF-B	Sildenafil, zaprinast, DMPPO, E4021, GF248
PDE7	2	cAMP-specific, Rolipram insensitive	Anchoring	BMS-586353, benzothieno- and benzothiadiazine dioxides, BRL-50481
PDE8	2	cAMP-selective IBMX-insensitive	PAS	Dipyridamole, (IBMX-insensitive), PF-04957325
PDE9	1	cGMP-specific IBMX-insensitive		Zaprinast (IBMX-insensitive)
PDE10	1	cAMP/cGMP	PKA, GAF-A, GAF-B	Papaverine, TP-10
PDE11	1	cAMP/cGMP	GAF-A, GAF-B	Dipyridamole, zaprinast

Ca-CaM: Calcium calmodulin kinase; cGMP: cyclic guanosine monophosphate; cAMP: cyclic adenosine monophosphate; IBMX: 3-isobutyl-1-methylxanthine; GAF domain: cGMP-specific and cGMP-stimulated phosphodiesterases, *Anabaena* adenylate cyclases, and *Escherichia coli* FhlA; PAS: Per-Arnt-Sim; UCR: upstream conserved region.

8.2.5 PDE3A

The PDE3 family includes two genes: A and B. In general, PDE3A is expressed in many different cell types, unlike PDE3B, which is predominantly expressed in cell types involved in glucose and lipid metabolism for the maintenance of energy homeostasis (Choi *et al.*, 2006). Although there are three described isoforms of PDE3A (Shitsukawa *et al.*, 2001), it is still not clearly established how these are regulated (alternative sites of transcription initiation, splicing, or posttranslational modification). The human PDE3A gene is located on chromosome 12, spans a region of 314 kb, and is encoded by 16 exons. Phosphodiesterase 3 has a high affinity for both cyclic nucleotides, with K_m values between 0.1 and 0.8 μM. This family is characterized as a cGMP-inhibited PDE (Manganiello *et al.*, 1990), since the endogenous biological effect of cGMP mediated by PDE3 appears to be an increase in cAMP concentration, as observed in vascular smooth muscle cells (Maurice and Haslam, 1990) and other tissues. Although this family may hydrolyze cGMP, the presence of endogenous cGMP inhibits cAMP hydrolysis, a biochemical characteristic that has relevance in the signaling pathway involved in the maintenance of meiotic arrest (Figure 8.4).

The study of PDE3 involvement in the process of oocyte meiotic resumption began in the mid-1990s using two different approaches. First, *in situ* hybridization was used to validate the presence of PDE3A mRNA in rat oocytes (Reinhardt *et al.*, 1995).[1] Application of the PDE3

1 It should be noted that PDE3A and PDE3B designations were inverted in this chapter.

Downloaded From Vet-eBooks.com

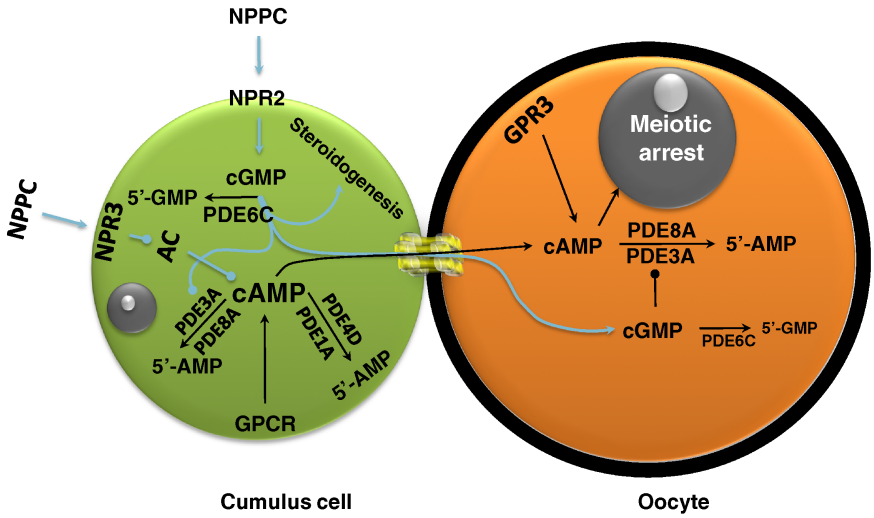

Figure 8.4 Schematic showing the signaling pathways involved during the maintenance of oocytes in meiotic arrest. See the text for details. Blue lines are the proposed NPPC signaling pathway. The white lines and characters represent the newly proposed pathways and molecules involved in the maintenance of oocyte meiotic arrest. A line ending with a dot indicates inhibition, whereas a line ending with an arrowhead represents activation. (See color plate section.)

family-specific inhibitors, cilostamide and milrinone, showed that both independently inhibited the meiotic resumption normally observed *in vitro* (Tsafriri *et al.*, 1996), suggesting the important contribution of this family of enzymes to the management of intracellular cAMP. The effect of PDE3 inhibitors on meiotic resumption *in vitro* has also been demonstrated in mice (Wiersma *et al.*, 1998), cattle (Mayes and Sirard, 2002; Thomas *et al.*, 2002), swine (Laforest *et al.*, 2005; Sasseville *et al.*, 2006, 2007), monkeys (Jensen *et al.*, 2002), and humans (Nogueira *et al.*, 2003). This inhibition is reversible and effective at different levels. Thus, these results support the potential for a novel contraceptive strategy for humans (Conti *et al.*, 1998; Wiersma *et al.*, 1998). *In vivo* trials with mice and rats have shown the efficacy of specific PDE3 inhibitors for preventing pregnancy by stopping oocyte maturation without interfering with the ovulation cycle, that is, maintenance of the oocyte in meiotic arrest in a state that is not ready to be fertilized (Wiersma *et al.*, 1998). Cardiac rhythm was also monitored as PDE3 is also expressed in heart tissue and a marked increase was observed. No specific inhibitor of oocyte PDE3A has been reported to date.

The PDE3A gene has been cloned from mice using a cDNA library prepared from mature oocytes, meaning those that have reached metaphase II (Shitsukawa *et al.*, 2001). Analysis of the cloned PDE3A sequence revealed six putative transmembrane domains, several phosphorylation sites for PKA and AKT, and potentially three active isoforms. Kinetic analysis of PDE activity in mice suggests the presence of a functional truncated PDE3 isoform found mainly in the supernatant fraction, thereby suggesting the presence of a soluble form in mouse oocytes (Richard *et al.*, 2001; Shitsukawa *et al.*, 2001). More interesting is the significant increase in PDE activity observed minutes before the beginning of meiotic resumption during the first hours of COC-IVM (Richard *et al.*, 2001). These data provide further support for the importance of the contribution of PDE3A to the decrease in intracellular cAMP concentrations and induction of the kinase-mediated cascade of events in meiotic resumption.

Female mice bearing a PDE3A-null mutation are sterile (Masciarelli *et al.*, 2004), whereas those with the PDE3B-null mutation are fertile (Choi *et al.*, 2006). The infertility of the former is

Downloaded From Vet-eBooks.com

a result of ovulation occurring while the oocytes are still in meiotic arrest, that is, not ready to be fertilized. Meiotic resumption can be induced in oocytes from PDE3A-null mice by inhibiting PKA while microinjecting protein kinase inhibitor peptide (Masciarelli *et al.*, 2004), suggesting a role for PDE3A in the inhibition of meiotic resumption in mammals by maintaining a high intracellular concentration of cAMP.

Despite the absence of functional PDE3A in rodent cumulus cells (Richard *et al.*, 2001), it is actively regulated during IVM in swine cumulus cells. Almost inactive at the time of COC collection from ovaries, cilostamide-sensitive (PDE3) activity has been shown to reach a maximum after 19 h of IVM. The increase was attributed to gonadotropin-dependent transcriptional regulation of PDE3A (Sasseville *et al.*, 2007). Although there are no reports of cilostamide-sensitive PDE activity in human cumulus cells, this does not mean that it is absent. While the vast majority of cilostamide-sensitive PDE activity in cattle is present in the oocyte, 15% of the total cAMP-PDE activity in cumulus cells has been found responsive to cilostamide and therefore attributable to PDE3. Inhibition of PDE3 activity in cumulus cells *in vitro* should conceivably influence not only oocyte nuclear maturation, but also oocyte developmental competence. For example, it should highlight that an increased intracellular concentration of cAMP will result in a potential activation of the cAMP response-gene and thus may influence cytoplasmic maturation, which may have an impact on oocyte quality and consequently oocyte developmental competence.

Investigations on the effects of pharmaceutical compounds that maintain a high intracellular concentration of cAMP have been carried out during bovine IVM. These compounds delayed the onset of meiotic resumption, although when using a specific sequence of pharmacological compounds, the yield of blastocyst embryos in a standard IVF culture system was significantly increased without delaying oocyte nuclear maturation. These results were reproduced in mice (Albuz *et al.*, 2010) and with decreased efficiency in sheep (Rose *et al.*, 2013). Other teams have also assessed the effects of PDE3 inhibitors on embryo yield in culture without improvement (Guimarães *et al.*, 2014). The embryo yield in mice was increased (Nogueira *et al.*, 2003), and in humans, the COC culture period was prolonged with no decrease in fertilization or developmental potential (Nogueira *et al.*, 2006). The quality of meiosis observed subsequent to temporary nuclear arrest by PDE3 inhibition is reportedly satisfactory, based on spindle formation and chromosome configuration (Vanhoutte *et al.*, 2007). In addition, GJC, and hence the electrophysiological syncytium, are maintained open in COC during exposure to the inhibitor (Shu *et al.*, 2008; Vanhoutte *et al.*, 2009). Thus, postponing spontaneous meiotic resumption *in vitro* by inhibiting cAMP hydrolysis in cumulus cells appears to be an effective strategy that does not compromise the ability of the oocyte to develop into an embryo. Most of the strategies for maintaining the oocyte in meiotic arrest *in vitro* use pharmacological compounds that act on the cAMP signaling pathway. Since these strategies resulted in a supra-physiological concentration of cAMP that may impact other signaling pathways, expression of different cAMP-responsive genes in cumulus cells may be hypothesized. Thus, transcriptomic studies in cumulus cells should address this hypothesis. The side effects of these strategies on the embryos and live births subsequently obtained are not yet known, and require investigation. The role of other PDE enzyme families must also be clarified.

8.2.6 PDE8A

The maintenance of oocytes in meiotic arrest by inhibition of PDE activity is not as effective in cattle as it is in swine and mice (Bilodeau-Goeseels, 2011). The use of nonspecific PDE inhibitors such as IBMX or hypoxanthine was found to be very effective for maintaining murine oocytes in meiotic arrest (Downs *et al.*, 1985). However, only a small proportion of bovine oocytes were

Downloaded From Vet-eBooks.com

maintained in meiotic arrest in the presence of these compounds (Sirard and First, 1988). These results suggest that the intraoocyte cAMP levels in cattle must be maintained at an elevated level and/or actively regulated. Close analysis of the results obtained in cattle using PDE3 inhibitors leads to the conclusion that the efficacy of PDE3 inhibitors is mitigated and short-lived (Mayes and Sirard, 2002; Thomas *et al.*, 2002). Their efficacy is increased when used in combination with a cyclase activator such as forskolin (Thomas *et al.*, 2002). These results suggest the involvement of another PDE family. Since IBMX is known to be ineffective as an inhibitor of the PDE8 family, the presence of functional PDE8 in bovine COC was investigated in a recent study (Sasseville *et al.*, 2009a, 2009b).

PDE8 is a recently discovered PDE family and is one of the least studied. Its involvement in steroidogenesis was discovered in Leydig cells (Shimizu-Albergine *et al.*, 2012; Vasta *et al.*, 2006). This family comprises two isozymes, represented by genes A and B. Their affinity for cAMP is very high, with a K_m value of 0.15 μM, and both are insensitive to IBMX. They may be inhibited by high concentrations of dipyridamole (Soderling *et al.*, 1998). However, the regulation of this family of PDE enzymes has not been well studied in any cell types.

3-Isobutyl-1-methylxanthine-insensitive PDE activity is low in rat COC (Richard *et al.*, 2001). Consistent with the low PDE8 activity measured in the murine ovary, PDE8A-null female mice display no abnormal reproductive phenotype (Dr. Joseph Beavo, personal communication). Before proposing any ovarian role for PDE8 in female reproductive physiology, we must determine the reproductive phenotypes of PDE8B-null and double PDE8A and PDE8B-knockout mice. Interestingly, a recent publication identified PDE7B as an upregulated transcript in mouse cumulus cells when COCs were cultured *in vitro* as opposed to *in vivo* (Kind *et al.*, 2013).

Whereas the role of gonadotropin in steroid synthesis during folliculogenesis is well described, almost nothing is known about the contribution of PDE8 as a cAMP-degrading enzyme. A study conducted in cattle describes the presence of PDE8 transcripts in granulosa cells, cumulus cells, and the oocyte (Sasseville *et al.*, 2009a). 3-Isobutyl-1-methylxanthine-insensitive PDE activity increased during folliculogenesis, particularly in granulosa cells, which may place PDE8 at the crossroads of the signaling pathway that responds to FSH and LH. Since functional PDE8 was also present in cumulus cells and the oocyte, it may be presumed to have a role in oocyte meiotic resumption (Sasseville *et al.*, 2009a). Our attempts to show a significant contribution of PDE8 to the latter and to the improvement of oocyte quality have so far fallen short of expectations. New specific PDE8 inhibitors such as Pfizer compound PF-04957325 will be among the new investigative tools used during the next few years.

8.2.7 Cyclic GMP and PDE5/6

There is no current consensus in the scientific community regarding the role of cGMP in oocyte physiology. Experiments in rats using a cGMP analogue suggest a role for cGMP in meiotic resumption (Tornell *et al.*, 1984, 1990a, 1990b). However, cGMP-PDE activity measured in porcine COCs during IVM is significantly increased, particularly after 24 h of IVM (Sasseville *et al.*, 2008). Although the presence of PDE5 can be demonstrated by Western blotting, PDE6D is specifically regulated during IVM. The role of these PDE families does not appear to be associated with oocyte meiotic resumption, since upregulation of PDE5 and PDE6 appears to occur afterward, mostly in association with progesterone secretion by COCs (Sasseville *et al.*, 2008).

However, a cGMP-PDE might not be sufficiently active during the first hour of IVM to prevent an increase in intracellular cGMP that is capable of producing a decrease in PDE3 activity. Short of decreasing this cAMP-hydrolyzing activity, cAMP might reach a concentration high enough to delay oocyte maturation. An approach to test this hypothesis would be to

Downloaded From Vet-eBooks.com

microinject active cGMP-PDE into the oocyte to determine whether it can promote meiotic resumption. Active PDE5 has been shown to do so in murine oocytes (Vaccari *et al.*, 2009). In addition, cAMP-PDE3 activity is inhibited by cGMP (Bornslaeger *et al.*, 1984; Vaccari *et al.*, 2009). These experiments demonstrate the efficacy of cGMP to decrease PDE3 cAMP-PDE activity and thus maintain oocytes in meiotic arrest by increasing the intracellular concentration of cAMP (Figure 8.4).

8.2.8 Cellular Compartmentalization of Cyclic Nucleotide Signaling

The fundamental roles of both cAMP and cGMP in the process of oocyte meiotic resumption in mammals raise several new prospects for the use of specific PDE inhibitors as an approach to contraception. Although initial results show that control of oocyte nuclear maturation holds great promise, the systemic effects of these compounds are major (Wiersma *et al.*, 1998) and much work will be necessary before commercial applications and large-scale strategies can be envisaged.

Although we are beginning to understand the functional expression of PDE3A in the mammalian oocyte and its mode of regulation, the localization of this enzyme remains unknown. The latest developments in the world of PDE suggest that the intracellular localization of PDE enzymes might be the master key in the fine-tuning of our understanding of cyclic-nucleotide-mediated regulation (Baillie *et al.*, 2005; Calaghan *et al.*, 2008; Castro *et al.*, 2006). As illustrated in Figure 8.2, interactions with binding proteins such as A-kinase anchor proteins (AKAPs) allow molecular segregation of key molecules involved in signal transduction. This organization would make the signal transduction system very efficient and consequently able to influence the mode of response according to the maturation state of cells such as the oocyte. Because PDE3A possesses transmembrane domains, it has the potential for integration into the cell membrane (Shitsukawa *et al.*, 2001). However, only the full-length protein would have this transmembrane domain, which could provide a specific mode of regulation based on the isoform present.

Membrane compartmentalization may be an important aspect of oocyte physiology; the volume of the human female gamete, with a diameter of 100 μm, is nearly 2000 times that of cumulus cells and other somatic cells with diameters averaging 8 μm. Therefore, the oocyte must organize its signal transduction machinery if signals are to reach their destination and be effective rather than lost as a result of diffusion. Studies of *Drosophila* have shown specific transcript localization inside the female gamete (Cooperstock and Lipshitz, 2001; Whittaker *et al.*, 1999). Studies of murine oocytes have demonstrated microdomain organization of the plasma membrane involving the ganglioside GM1 (Comiskey and Warner, 2007). The presence of GM1 revealed by cholera toxin beta staining (Figure 8.5a and b) also suggests microdomain organization of the plasma membrane of cumulus cells and the oocyte as already suggested (Sasseville *et al.*, 2009a, 2009b). In addition, the presence of caveolae in amphibian oocytes (Buschiazzo *et al.*, 2011; Sadler, 2001) also illustrates compartmentalization at the membrane level. Whereas a recent study has shown compartmentalization of PDE6C in porcine COCs during IVM (Sasseville *et al.*, 2008), studies of signal transduction compartmentalization in mammalian oocytes remain scant. Nothing has been reported about compartmentalization of PDE3A in mammalian oocytes. Here, we report preliminary data supporting the presence of lipid raft microdomains in porcine COCs in association with GM1 and Cav-1. Phosphodiesterase 3A does not show appreciable segregation to the triton-insoluble fraction at the time of complex collection (Figure 8.5c). However, the detergent-resistant membrane fraction corresponding to lipid raft microdomains from granulosa cells shows a signal corresponding to PDE3A (Figure 8.5). Studies of other PDEs suggest that PDE3A might be found in lipid raft

Downloaded From Vet-eBooks.com

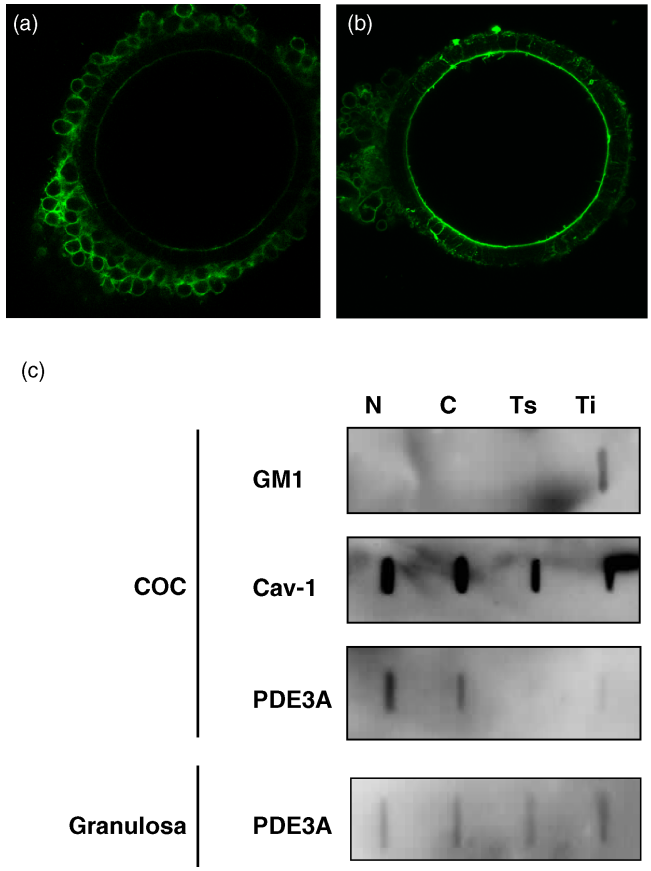

Figure 8.5 Porcine cumulus–oocyte complex (a) and partially denuded oocyte (b) were incubated with Alexa Fluor 488 coupled with cholera toxin beta for 30 min at room temperature, washed three times, and observed under a confocal microscope. Cholera toxin beta specifically labels ganglioside GM1 lipid raft microdomains (1:15,000 dilution; Sigma-Aldrich, C3741). The signal is apparent on the surface of cumulus cells and in the oocyte membrane. (c) Porcine cumulus–oocyte complexes (COC) were processed as described (Adam *et al.*, 2008) to isolate nuclei (N), cytosol (C), and Triton X-100 soluble (Ts) and insoluble (Ti) fractions. Ti is lipid-raft enriched. Caveolin-1 (Cav-1; 1:500; BD Transduction Laboratories, 610059) is present in all fractions. PDE3A (1:500; Santa Cruz Biotechnology, Inc., SC-11828) is predominantly present in the nuclei and cytosol, but a weak signal is detected in Ti. In granulosa cells, PDE3A is associated with Ti, suggesting PDE3A segregation in porcine granulosa/cumulus cells.

microdomains of the COC. It has also been published that PDE3B is associated with adipocyte caveolae (Nilsson *et al.*, 2006). Therefore, it is to be expected that the mode of regulation of PDE3A is not restricted to enzymatic activation, but also involves intracellular localization of the enzyme, which adds a whole new perspective to the regulation of this physiological target and the regulation of oocyte nuclear maturation.

8.2.9 C-Type Natriuretic Peptide (CNP) and cGMP

Recently, an alternative signaling pathway has been proposed for the maintenance of a high concentration of cAMP in the oocyte. Indeed, as already mentioned, PDE can regulate the amount of cAMP by promoting its degradation into 5′-AMP. Furthermore, cGMP is able to

Downloaded From Vet-eBooks.com

inhibit PDE3 activity and maintain the oocyte in meiotic arrest. In the rat oocyte, the cGMP concentration decreases in parallel with the cAMP concentration (Tornell *et al.*, 1990a, 1990b). Microinjection of specific cGMP-PDE into the oocyte promotes resumption of meiosis in mice (Norris *et al.*, 2009; Vaccari *et al.*, 2009). A pharmacological analogue of cGMP and stimulation of cGMP production by nitric oxide can also inhibit meiotic resumption (Sela-Abramovich *et al.*, 2008; Tornell *et al.*, 1984). Cyclic GMP is believed to flow from the somatic cells to the oocyte through GJC as closure of gap junctions in intact follicles decreases the cGMP concentration in the oocyte and stimulates meiotic resumption (Norris *et al.*, 2009; Sela-Abramovich *et al.*, 2006). Moreover, the LH surge allows the closure of GJCs (Norris *et al.*, 2009, 2010; Vaccari *et al.*, 2009). However, interspecies variations and contradictions exist in the literature concerning the exact role of cGMP in the regulation of meiotic arrest. Indeed, use of the cGMP analogue 8-bromo-cGMP during IVM maintains meiotic arrest in hamster COCs, but has no effect on oocytes denuded of their cumulus cells (DO) demonstrating that cGMP signaling might require cumulus cells (Hubbard and Terranova, 1982). Of interest is that in mice, 8-bromo-cGMP inhibits meiotic resumption in both COCs and DOs during IVM (Bu *et al.*, 2004). Moreover, COCs and DOs cultured in the presence of sildenafil (a specific inhibitor of PDE5 that degrades cGMP) resume meiosis suggesting that cGMP degradation is not involved in the mode of regulation of meiotic arrest (Vaccari *et al.*, 2009). On the other hand, another study demonstrated that Sildenafil can inhibit meiotic resumption and that this effect was reversible (Wang *et al.*, 2008). Despite interspecies specificity and contradictions in the literature, cGMP has recently been considered as a major player in the regulation of meiotic resumption. More recently, the efforts of several research teams investigating cGMP signaling have greatly improved our knowledge of cGMP signaling during the maintenance of meiotic arrest. Indeed, the mechanisms of cGMP generation in somatic cells and transfer to the oocyte have been deciphered. The atrial (ANP), brain (BNP), and C-type (CNP) natriuretic peptides have been identified as fundamental to the maintenance of meiotic arrest both *in vitro* and *in vivo* in many different species (Franciosi *et al.*, 2014; Santiquet *et al.*, 2014a; Zhang *et al.*, 2010, 2015). Natriuretic peptides bind to their natriuretic receptors, which are members of the guanylyl cyclase (GC), receptor family (Suga *et al.*, 1992). Thus, binding of the natriuretic peptide to its receptor induces the production of cGMP in the cell. Although the natriuretic peptide family is composed of these major types (Potter *et al.*, 2009) other natriuretic peptides have been identified in nature such as, Dendroaspis natriuretic peptide, urodilatin (an alternative splice variant of pro-ANP), and other natriuretic-like peptides extracted from snake venom (Fry *et al.*, 2005; Schirger *et al.*, 1999; Schulz-Knappe *et al.*, 1988; Schweitz *et al.*, 1992; Zhang *et al.*, 2011). Both ANP and BNP bind with high affinity to the guanylyl cyclase-A receptor (NPR-A), whereas CNP binds to the guanylyl cyclase-B receptor (NPR-B) (Suga *et al.*, 1992).

In mice, NPR-B mRNA is expressed in both granulosa and cumulus cells with expression being higher in the latter (Zhang *et al.*, 2010). Moreover, NPR-B mRNA has been shown to be expressed more abundantly in granulosa cells than any other transmembrane or soluble GC (Robinson *et al.*, 2012). In swine, NPR-B is expressed in cumulus cells but not in the oocyte (Hiradate *et al.*, 2014), whereas in mice, the NPR-B ligand (CNP) transcript is expressed in both granulosa and cumulus cells with higher expression in the former (Zhang *et al.*, 2010). C-type natriuretic peptide activity *in vitro* is promoted by 17β-estradiol and oocyte-derived paracrine factors, whereas FSH has no effect. Indeed, 17β-estradiol, GDF9, and BMP15 promote NPR-B expression in cumulus cells (Zhang *et al.*, 2010, 2011). The level of CNP transcripts, but not that of NPR-B, increases in the presence of FSH (Sato *et al.*, 2012). Thus, the constant dialogue between the oocyte, somatic cells, and the pituitary–gonadal axis can regulate natriuretic peptide signaling and thereby meiotic resumption. The importance of CNP/NPR-B signaling in fertility and meiotic resumption has been demonstrated using

Downloaded From Vet-eBooks.com

NPR-B or CNP mutant mice. In both mutants, the oocytes resume meiosis prematurely resulting in premature ovarian failure (Zhang *et al.*, 2010). In humans, NPR-B has been shown to be fundamental to female fertility. Indeed, a mutation in the Npr-B gene causes severe disproportionate dwarfism and female infertility. The primary effects of the Npr-B mutation in female infertility are premature oocyte meiotic resumption and subsequent premature ovarian failure (Geister *et al.*, 2013).

Atrial natriuretic peptide (ANP) that binds preferentially to NPR-A can inhibit meiotic resumption in many species. Indeed, in rat and swine, the presence of ANP inhibits meiotic resumption (Tornell *et al.*, 1990a, 1990b; Zhang *et al.*, 2005). In mice, intraperitoneal injection of ANP inhibits follicular growth, ovulation, and steroidogenesis (Tsai *et al.*, 2005). However, ANP mutant mice have no fertility issues (John *et al.*, 1995). Atrial natriuretic peptide is present in the follicular fluid of human preovulatory follicles and its presence has been shown to be positively associated with fertilization success *in vitro*. In addition, ANP has an anti-apoptotic effect on human granulosa cells (Dineva *et al.*, 2011). However, the inhibition of meiotic resumption has not yet been tested in humans.

Brain natriuretic peptide (BNP), which also binds preferentially to NPR-A, is present in the ovaries of goat and pigs (Peng *et al.*, 2013; Zhang *et al.*, 2014a, 2014b). Similar to the other two natriuretic peptides, BNP can inhibit meiotic resumption in pigs (Zhang *et al.*, 2015). However, null BNP mice are fertile (Tamura *et al.*, 2000). To date, no information is available on BNP involvement in human fertility.

As already mentioned, ANP and BNP mutant mice are fertile, which is consistent with the fact that NPR-A receptor-mutant mice are also fertile (Zhang *et al.*, 2014a, 2014b). In addition, BNP can inhibit meiotic resumption. This effect is also reproduced in NPR-A knockout mice, suggesting that BNP can not only interact with NPR-A to maintain meiotic arrest but can also interact with NPR-B (Zhang *et al.*, 2014b). Indeed, although ANP and BNP have a higher affinity for NPR-A, they can still bind to NPR-B and NPR-C (Suga *et al.*, 1992). Knockdown of Npr-A increased Npr-C expression and signaling in vascular smooth muscle cells (Li *et al.*, 2012).

The NPR-C receptor is able to bind all three major natriuretic peptides (ANP, BNP, and CNP). It is called the clearance receptor as it can internalize natriuretic peptides for intracellular degradation and thereby regulate their extracellular levels (Potter, 2011). Interestingly, binding of natriuretic peptides to this receptor has also been shown to promote signaling pathways. Indeed, NPR-C can regulate many physiological processes via coupling to inhibitory G proteins that cause the inhibition of AC and activation of phospholipase-C (Anand-Srivastava, 2005; Berl *et al.*, 1991; Costa *et al.*, 2006, 2007; Murthy *et al.*, 2000; Resink *et al.*, 1988; Rose and Giles, 2008). Oocytes and embryos matured *in vitro* from NPR-C mutant mice develop normally (Lee *et al.*, 2013). Moreover, it has been shown that human chorionic gonadotropin induces a decrease in ovarian CNP, a phenomenon that still occurs in NPR-C mutant mice, suggesting that NPR-C does not regulate the availability of extracellular CNP (Lee *et al.*, 2013). However, the expression of NPR-C is highly regulated in the murine ovary in response to gonadotropin stimulation even if it does not have any impact on oocyte maturation. Recently, it has been proposed that NPR-C could have a signaling function during porcine IVM. Indeed, stimulation of NPR-C does not inhibit meiotic resumption. However, meiotic resumption is inhibited when NPR-C is stimulated in addition to suboptimal stimulation of NPR-B in the presence of CNP (Santiquet *et al.*, 2014a).

These data support the involvement of CNP signaling through cGMP to inhibit PDE3 in the oocyte. However, fine-tuning of this signaling may differ among species. For example, ANP and NPR-C may be involved in maintaining the porcine oocyte in meiotic arrest *in vitro*. More experiments are required to further understand the contribution of natriuretic peptide and cGMP in the maintenance of oocyte meiotic arrest.

Downloaded From Vet-eBooks.com

8.3 Gap Junction Communications

Gap junctions are channels that connect the growing oocyte and its surrounding somatic cells to form an electrophysiological syncytium allowing communications. In this section, we will summarize what is currently known about the composition, the regulation, and the role of GJC during oocyte maturation.

8.3.1 Connexin, Connexon, and Gap Junctions

Gap junctions are intercellular channels that allow the passage of ions, amino acids, nucleotides, metabolites, and secondary messengers (e.g., calcium, glucose, cAMP, cGMP, IP3, and small RNAs) between adjacent cells (Harris, 2007). They directly connect the cytoplasm of two neighboring cells. This singular means of communication plays a key role in ovarian follicle physiology. Gap junctions are composed of transmembrane connexin proteins. These connexins contain four transmembrane domains linked by one cytoplasmic and two extracellular loops. The N- and C-termini are both located on the cytoplasmic side. The cytoplasmic loops and the C-terminal region vary most among connexins and are subject to posttranslational modification such as phosphorylation (Laird, 2005; Solan and Lampe, 2005). Twenty connexin genes have been identified in mice, whereas 21 are known in humans (Sohl and Willecke, 2003).

Gap junctions are ubiquitously expressed in mammalian cells. During murine development, the transfer of molecules through gap junctions starts as early as the 8-cell stage embryo (McLachlin and Kidder, 1986). In the developing murine ovary, gap junctions can be detected between granulosa cells, and between granulosa/cumulus cells and the oocyte as early as 12.5 days of gestation (Mitchell and Burghardt, 1986; Perez-Armendariz *et al.*, 2003). After birth, when primordial follicles are predominantly formed, gap junctions are largely present in granulosa cells (Juneja *et al.*, 1999). Thereafter, gap junctions couple the oocyte and the surrounding cumulus/granulosa cells into a functional electrophysiological syncytium during follicular development.

In the mouse, connexin 43 (C×43) is the predominant connexin expressed in cumulus/granulosa cells, and connexin 37 (C×37) is the major connexin expressed in the oocyte. Other connexins, for example, C×32, C×37, and C×45, are also expressed in rodent follicles (Simon *et al.*, 1997; Valdimarsson *et al.*, 1993; Wright *et al.*, 2001). Fifteen different connexin mRNAs have been detected in human cumulus cells (Wang *et al.*, 2009). The predominant connexins expressed in porcine COCs are C×43, C×45, and C×60 (Santiquet *et al.*, 2013). Gap junctions can be composed of one or more types of connexin, which interact with each other to form homomeric, heteromeric, or heterotypic channels (Mese *et al.*, 2007). The ability of the cell to mix gap junction connexin content in this manner increases permeability regulation for GJC (Cottrell and Burt, 2005; Weber *et al.*, 2004).

The expression of multiple connexins in follicles reflects the important role of GJC during folliculogenesis. Evidence for the primordial role of GJC in follicular and oocyte growth and maturation has been revealed by generating knockout mice lacking different connexins. Indeed, C×37-deficient mice exhibited folliculogenesis arrest at the early antral stage; the oocyte failed to reach meiotic and cytoplasmic competence, and females were infertile (Carabatsos *et al.*, 2000; Simon *et al.*, 1997). Mice lacking C×43 die as neonates as a result of cardiac dysfunction (Reaume *et al.*, 1995). However, to circumvent this early mortality, prenatal C×43 knockout ovaries have been grafted under the kidney capsule of adult mice to study further development. Under these conditions, folliculogenesis did not proceed beyond the primary follicular stage, and oocyte growth was delayed. Furthermore, oocytes recovered from the grafts did not complete meiosis and could not be fertilized (Ackert *et al.*, 2001; Juneja *et al.*, 1999), supporting the crucial supportive role of C×43 in GJC of the electrophysiological syncytium.

Downloaded From Vet-eBooks.com

8.3.2 Gap Junction Communications and Oocyte Maturation

Intercellular GJC have been shown to play a crucial role in ovarian physiology, and particularly in the process of oocyte meiotic resumption by controlling the flow of meiotic inhibitors and allowing the oocyte to maintain meiotic arrest. Indeed, resumption of meiosis in oocytes has been found to coincide with a progressive interruption of cell-to-cell coupling following the LH surge *in vivo* (Bornslaeger and Schultz, 1985; Dekel *et al.*, 1981; Racowsky, 1984). *In vitro*, the loss of GJC between the oocyte and cumulus cells is accompanied by meiotic resumption and subsequent maturation in rat and murine follicles (Larsen *et al.*, 1987; Racowsky *et al.*, 1989). Until recently, cAMP was the only consensus meiotic inhibitory molecule known to pass through GJC to inhibit meiotic resumption (Bornslaeger and Schultz, 1985); however, a role for cGMP has also been proposed. Moreover, GJC are involved in the regulation of chromatin remodeling and transcription during the first steps of bovine IVM (Luciano *et al.*, 2011). Indeed, the disruption of GJC correlates with rapid chromatin condensation and RNA synthesis arrest.

The regulation of GJC by transcription, translation, posttranslational modification, transport, formation of gap junction plaques at the plasma membrane, and degradation are extremely complex and modify the permeability of gap junctions. In the preovulatory murine follicle, LH signaling induces a decrease in GJC permeability (Norris *et al.*, 2008). Luteinizing hormone has been shown to increase the phosphorylation of C×43 on specific serine residues through a MAPK-dependent pathway (Norris *et al.*, 2008). Posttranslational modification of connexin, for example, by phosphorylation, can modify the permeability of GJC (Laird, 2005; Solan and Lampe, 2005). In the follicle, LH triggers the phosphorylation of C×43 and consequently the closure of GJC, which in turn induces meiotic resumption of the oocyte (Norris *et al.*, 2008). The closure of GJC is believed to block the flow of inhibitory molecules (cAMP and cGMP) from the somatic cells to the oocyte. Phosphorylation of C×43 and the closure of GJC in the follicle are triggered by EGF signaling. Indeed, mural granulosa cells secrete EGF-like factor into the follicular fluid in response to LHR activation, which results in EGFR activation and signaling in cumulus cells. Activation of EGFR stimulates the phosphorylation of C×43, resulting in the closure of GJC. Therefore, it blocks the flow of inhibitory molecules from the cumulus cells to the oocyte and meiosis resumes (Norris *et al.*, 2009, 2010). Moreover, inactivation of EGFR blocks LH-induced C×43 phosphorylation (Andric *et al.*, 2010; Hsieh *et al.*, 2011).

Interestingly, GJCs have been shown to allow the passage of small/micro RNAs in multiple cell types. These RNAs are able to regulate gene expression in neighboring cells (Katakowski *et al.*, 2010; Kizana *et al.*, 2009; Lim *et al.*, 2011; Wolvetang *et al.*, 2007). Recently, the transfer of large mRNAs by vesicular exo/endocytosis between cumulus cells and the oocyte has been identified as a possible means of regulating bovine oocyte nuclear maturation, demonstrating that RNA transfer may be another way for cumulus cells to influence the fate of the oocyte (Macaulay *et al.*, 2014). Moreover, it has been shown that murine somatic cells can regulate the translation of crucial mRNAs in oocytes (Chen *et al.*, 2013). Thus, small/micro RNA transfer through GJC may impact oocyte maturation, and may also influence oocyte developmental competence.

8.4 Metabolic Switch (AMPK)

8.4.1 Overview

Adenosine 5′-monophosphate-activated protein kinase (AMPK) is a sensor of cellular energy. This kinase is activated either by stress-depleting intracellular ATP or by intense ATP consumption, as occurs in response to exercise. Adenosine 5′-monophosphate-activated

Downloaded From Vet-eBooks.com

protein kinase is involved in the regulation of whole body energy balance as well as that of a single cell. This section aims to describe the role of the metabolic switch, AMPK, in the process of oocyte maturation. Depending on the species, AMPK activation has different physiological effects. These effects highlight the importance of COC energy metabolism in the physiology of oocyte maturation.

8.4.2 Structure and Regulation of AMPK

Adenosine 5′-monophosphate-activated protein kinase is a serine/threonine kinase known as a metabolic switch because of its sensitivity to the cellular AMP:ATP ratio. It is a heterotrimeric enzyme with a catalytic α-subunit and two regulatory subunits, β and γ. Two isoforms of the α-subunit, two isoforms of the β-subunit, and three isoforms of the γ subunits are encoded in both humans and rodents. (Kahn *et al.*, 2005). Adenosine monophosphate allosterically activates AMPK, promoting Thr172 phosphorylation of AMPK (Sanders *et al.*, 2007). Two kinases have been described as being responsible for Thr172 phosphorylation: the serine/threonine-protein kinase LKB1 (Woods *et al.*, 2003) and the calmodulin-dependent protein kinase kinase (CaMKK) (Hurley *et al.*, 2005). The identity of the phosphatase involved is still unknown despite evidence implicating protein phosphatase 2C (Sanders *et al.*, 2007).

8.4.3 Activators of AMPK

Adenosine 5′-monophosphate-activated protein kinase activation may occur in different ways. Reports from the literature suggest that metabolic stress is probably the most common form of AMPK activation, and numerous cellular stresses lead to depletion of ATP content. A brief description of the most reported types of AMPK activation follows.

Arsenite is a metabolic poison. Sodium arsenite has been shown to activate AMPK in a dose-dependent manner *in vitro* (Lochhead *et al.*, 2000). Furthermore, arsenite was reported as a carcinogenic metal that induces AMPK (Lee *et al.*, 2006).

Different pathological conditions such as hypoxia, ischemia, and glucose deprivation are known to activate AMPK (Kahn *et al.*, 2005). When exposed to hypoxia, cells acquire adaptive strategies to maintain an optimal intracellular ATP level (Hochachka *et al.*, 1996). This is well demonstrated in alveolar epithelia cells. Adenosine 5′-monophosphate-activated protein kinase regulates hypoxia-induced sodium-potassium ATPase endocytosis through PKC phosphorylation (Gusarova *et al.*, 2009). In cardiac muscle cells, hypoxia increases glycolysis to generate an increased level of ATP, and AMPK activation is clearly involved (Marsin *et al.*, 2000).

Recent evidence has suggested the involvement of AMPK in type 2 diabetes. This pathological condition is primarily caused by insulin resistance and is characterized by an elevated glucose level in blood plasma. In point of fact, AMPK is most probably one of the major targets for antidiabetic drugs. Metformin and thiazolidinediones are administered in type 2 diabetes. Both are reported to affect AMPK activation (Fryer *et al.*, 2002; Zhou *et al.*, 2001), which in turn has the potential to decrease plasma glucose by increasing glucose uptake in muscle and other tissues, and by repressing the expression of gluconeogenesis enzymes in the liver (Hardie, 2008).

Adenosine 5′-monophosphate-activated protein kinase is also activated by exercise and contraction of skeletal muscles (Winder and Hardie, 1996). The level of AMPK activation in response to the latter depends on the intensity of exercise (Aschenbach *et al.*, 2004). A key target of AMPK is glucose uptake. Glycolysis is triggered by increased expression of glucose transporter GLUT4 following AMPK activation (Zheng *et al.*, 2001). In cardiac cells, AMPK activation also stimulates glycolysis by specific phosphorylation of 6-phosphofructo-2-kinase (PFK2), a key glycolytic enzyme (Marsin *et al.*, 2000).

Downloaded From Vet-eBooks.com

Cytokines released by adipocytes (termed adipokines) are known to regulate whole-body energy balance. Leptin and adiponectin both activate AMPK, whereas AMPK is inhibited by resistin (Hardie, 2007).

Activation of AMPK has been achieved by pharmacological targeting in different cell types such as hepatocytes, adipocytes, and muscle: the most commonly used compounds are AICAR (5-aminoimidazole-4-carboxamide-1-*b*-D-ribofuranoside), ZMP (5-aminoimidazole-4-carboxamide-1-*b*-D-ribofuranosyl 5′-monophosphate), metformin, and rosiglitazone (a thiazolidinedione). Activation of AMPK by AICAR, an adenosine analogue, results from cellular uptake via adenosine transporters and conversion to ZMP by adenosine kinase. These pharmacological compounds are useful tools for assessing the physiological role of AMPK activation.

8.4.4 Downstream Targets of AMPK

Once activated, AMPK phosphorylates multiple targets result in their respective activation or inhibition. More specifically, AMPK activates elongation factor-2 kinase (EF2K) to inhibit protein synthesis; PGC1α (PPARγ coactivator-1α) to increase mitochondria biogenesis; PFK2 to elevate glycogenesis; and AS160 (AKT substrate of 160 kDa) to increase glucose uptake. Activated AMPK also inhibits other kinases such as mammalian target of rapamycin (mTOR) resulting in decreased protein synthesis; HMGR (3-hydroxy-3-methlyglutaryl coenzyme A reductase) involved in sterol synthesis; ACC1 (acetyl-CoA carboxylase-1) implicated in fatty acid synthesis; ACC2 (acetyl-CoA carboxylase-2) implicated in fatty acid oxidation; and finally decreased glycogen synthesis by inhibiting glycogen synthase. The majority of these responses have been described in muscle cells and liver (Hardie, 2007; Kahn *et al.*, 2005).

8.4.5 AMPK in Reproductive Function

Female fertility is highly influenced by metabolic conditions. Diabetes, obesity, insulin resistance, and metabolic syndrome all impair reproductive functions. A prime example is presented by polycystic ovarian syndrome (PCOS) diagnosed in women with insulin resistance (Gruzman *et al.*, 2009). A negative metabolic status occurs after calving in dairy cows and persists until the end of the lactation peak. This period of negative energy balance covers the expected fertilization window. Thus, reproductive functions are often impaired in high-producing dairy cows as a consequence of the important negative metabolic status of the animal (Chagas *et al.*, 2007). In swine, increasing evidence supports that nutrition and changes in metabolic status influence reproductive function through variations in metabolites and associated reproductive hormones such as insulin, FSH, and LH (Prunier and Quesnel, 2000; Schams *et al.*, 1999).

As already mentioned, AMPK is involved in different physiological processes such as metabolic regulation of lipids, proteins, and glucose, cellular proliferation and survival, and reproductive function. First described in 1957 (Ungar *et al.*, 1957), metformin has been used in French clinics for the last 30 years. Among the most well-known effects of metformin are the return to regular menstrual cycles, ovulation, and a reduction in insulin and androgens levels in women with PCOS (De Leo *et al.*, 1999; Glueck *et al.*, 1999; Pirwany *et al.*, 1999; Velazquez *et al.*, 1994). The effect of metformin could be explained either by its central effects on the hypothalamus and pituitary, or the increased sensitivity of peripheral tissue to insulin/IGF1, which has a specific effect on the ovary. Metformin is also described as an AMPK activator (Zhou *et al.*, 2001).

Recent publications have described the effect of AMPK activation on ovarian function (Bilodeau-Goeseels *et al.*, 2007; Downs *et al.*, 2002; Kola *et al.*, 2006; Mayes *et al.*, 2007;

Downloaded From Vet-eBooks.com

Tosca *et al.*, 2005). Species-specific responses have been observed following administration of pharmacological compounds. Despite the observed differences, AMPK activation produced physiological ovarian responses. This recently described role of AMPK in ovarian physiology has garnered attention and the species-specific effects of AMPK activation in COC will be discussed.

8.4.6 AMPK in Oocyte Function

A decade ago, Melk, a member of Snf1/AMPK kinase family, was described as being expressed in the murine oocyte and preimplantation embryo (Heyer *et al.*, 1997). A few years later, the functionality of AMPK was investigated in murine oocytes. Mammalian oocytes spontaneously resume meiosis when cultured *in vitro* (Pincus and Enzmann, 1935). In the presence of dbcAMP, a permeable and nonhydrolyzable cAMP analogue, murine oocytes are maintained in meiotic arrest, that is, they do not resume meiosis. In combination with dbcAMP, pharmacological activators of AMPK reversed meiotic arrest allowing meiotic resumption to occur. These effects of AMPK activators were dose-dependent and efficient in both DOs and COCs (Downs *et al.*, 2002). Alpha-1 and alpha-2 subunits of AMPK are expressed in murine DOs and COCs (Downs *et al.*, 2002). In addition to reversing dbcAMP inhibition, administration of AMPK activators also reversed the effects of the nonspecific PDE inhibitor IBMX, and the specific PDE3 inhibitor, milrinone (Downs *et al.*, 2002). The effect of AMPK activation on oocyte nuclear maturation was validated by microinjection of constitutively active AMPK into the oocyte, which showed the same ability to reverse dbcAMP-arrested mouse oocytes (Chen *et al.*, 2006). A construct containing inactive AMPK was inefficient at reversing meiotic arrest suggesting a specific role for AMPK. As reported in several other cell types, AICAR phosphorylated acetyl CoA carboxylase (ACC) and decreased its activity. The ACC enzyme is involved in fatty acid synthesis, which lends further support to the role of AMPK as a metabolic hub. Both compound C, a potent AMPK inhibitor (Zhou *et al.*, 2001), and adenine 9-β-D-arabinofuranoside (araA), a competitive AMPK inhibitor (Henin *et al.*, 1996), reversed the effect of AICAR (Chen *et al.*, 2006). These data support the unique efficacy of AMPK activation in reversing nuclear maturation of dbcAMP-arrested mouse oocytes.

As mentioned earlier, AMPK is activated during cell poisoning by compounds such as arsenite (Kahn *et al.*, 2005), and by cellular deprivation of ATP. Exposure of murine oocytes to arsenite reversed the nuclear maturation of dbcAMP-arrested DOs and COCs (LaRosa and Downs, 2006) and this effect was inhibited by the AMPK inhibitors, compound C and araA (LaRosa and Downs, 2006). These results further suggest that the role played by AMPK is specific and of physiological relevance and is not an artifact of the *in vitro* culture system.

When murine COCs were cultured *in vitro* in the presence of dbcAMP, the number of oocytes maintained in meiotic arrest was decreased by the addition of FSH (Chen and Downs, 2008). This effect was reversed by both compound C and araA, suggesting the involvement of AMPK in the FSH signaling pathway in murine COCs. Oocyte metabolism in the murine model of streptozotocin-induced diabetes was altered with a significantly decreased level of ATP and a 20% increase in the AMP:ATP ratio (Ratchford *et al.*, 2007). However, contrary to the acceleration observed *in vitro*, nuclear maturation was delayed in diabetic mice (Ratchford *et al.*, 2007). The activity of AMPK measured by the phosphorylated form of AMPK was decreased in oocytes from diabetic animals (Ratchford *et al.*, 2007), suggesting that diabetes did not produce the expected stimulation of AMPK. Interestingly, diabetic oocytes matured *in vitro* in the presence of the AMPK activator, AICAR, showed elevated AMPK activity, and an increased percentage of oocyte nuclear maturation (Ratchford *et al.*, 2007). These results support the key role of AMPK in the physiology of oocyte cellular energy balance.

Downloaded From Vet-e-Books.com

The observed effect of AMPK activators on murine oocytes is unique and has not been reported in any other species. In large species such as swine and cattle, the addition of AMPK activators during IVM resulted in inhibition of nuclear maturation (Bilodeau-Goeseels *et al.*, 2007; Mayes *et al.*, 2007; Santiquet *et al.*, 2014a; Tosca *et al.*, 2007). However, the inhibitory effect of AMPK activators was transient (Mayes *et al.*, 2007). Oocyte nuclear maturation was inhibited in the presence of a specific PDE3 inhibitor, cilostamide (Laforest *et al.*, 2005), whereas the AMPK activator, ZMP, neither reversed nor increased the effect of cilostamide (Mayes *et al.*, 2007). However, in the mouse, AMPK activators reversed the inhibitory effect of a PDE3 inhibitor (Downs *et al.*, 2002). An additional major difference in the response to AMPK activators between mice and large animals is the requirement for cumulus cells. In mice, AMPK activators are efficient in COCs as well as in DOs. However, in large animals, the efficacy of AMPK activators requires the presence of cumulus cells, suggesting that the physiological relevance of AMPK in oocyte maturation is different between species. The observed effect in large animals leads us to hypothesize that cell-specific site activation of AMPK results in a different physiological response. This physiological difference joins others that have previously been reported: (i) murine oocytes show a rapid resumption of meiosis compared with large animal species, (ii) protein synthesis is not required in murine oocytes, whereas it is necessary for large animal species (Fulka *et al.*, 1986), (iii) cumulus cells actively modulate meiotic resumption in large animal species (Byskov *et al.*, 1997; Macaulay *et al.*, 2014; Sasseville *et al.*, 2009b; Shimada and Terada, 2002), and (iv) RNA transcription is required in porcine cumulus cells (Meinecke and Meinecke-Tillmann, 1993). Moreover, different responses to the activation of AMPK further highlight the distinct physiological processes of oocyte maturation among species. A functional link has been established between glucose bioavailability and oocyte nuclear maturation (Funahashi *et al.*, 2008; Herrick *et al.*, 2006; Rose-Hellekant *et al.*, 1998; Sutton-McDowall *et al.*, 2005) and this relationship was also established in mice (Fagbohun and Downs, 1992). Cumulus cells use glucose to supply the oocyte with pyruvate (Biggers *et al.*, 1967; Eppig *et al.*, 2000), and COC increase energy substrate uptake in response to FSH (Sutton-McDowall *et al.*, 2004, 2005). Modification of energy substrate bioavailability modulates oocyte meiotic progression (Sutton-McDowall *et al.*, 2004, 2005). Recently, the effect of glucose metabolism was proposed to be associated with cytoplasmic maturation and developmental competence (Sutton-McDowall *et al.*, 2006). Following the same line of evidence, the use of metformin during IVM and culture *in vitro* improved the blastocyst yield when used in combination with insulin (Lee *et al.*, 2005). These results support the role of energy metabolism in COCs for oocyte maturation, cytoplasmic maturation, and developmental competence.

Maturation of bovine COCs in glucose-free medium perturbed oocyte maturation and cumulus expansion (Rose-Hellekant *et al.*, 1998). Nuclear maturation of bovine oocytes is inhibited in the presence of AMPK activators, AICAR and metformin. This is a short-term effect in DOs (Bilodeau-Goeseels *et al.*, 2007) since no effect was observed after 22 h of culture (Tosca *et al.*, 2007). Metformin increased Thr172 phosphorylation of AMPK (Santiquet *et al.*, 2014b; Tosca *et al.*, 2007), but did not affect cAMP content (Bilodeau-Goeseels *et al.*, 2007). Glucose influences nuclear maturation since a low concentration in the culture medium decreased the number of oocytes reaching metaphase II (Sutton-McDowall *et al.*, 2005). The effect of the metabolic switch on oocyte nuclear maturation is well supported by the differential expression *in vivo* of the AMPK gamma-1 subunit transcript in oocytes exposed to LH for 6 h (close to meiotic resumption) when compared with the 2-h timepoint (Algriany, 2007). Once again, these data support the view that energy metabolism is of primary importance for oocyte maturation and will influence oocyte developmental competence.

A possible direct impact of exposing COCs to AMPK activators could be the perturbation of GJC between cumulus cells and the oocyte. In a recent study, a marked decrease in GJC was observed in

Downloaded From Vet-eBooks.com

a murine model of type 1 diabetes (Ratchford *et al.*, 2008). This effect was supported by decreased C×37 transcript and protein levels (Ratchford *et al.*, 2008). In the mouse, gonadotropins induced meiotic resumption via GJCs (Downs, 2001), but only in the presence of glucose (Downs and Mastropolo, 1994). In cattle, GJCs are downregulated during IVM (Sutovsky *et al.*, 1993), but can be modulated through the cAMP pathway (Thomas *et al.*, 2004a, 2004b). In swine, GJCs are significantly upregulated during the first hours of IVM and significantly downregulated concomitantly with nuclear maturation (Santiquet *et al.*, 2012, 2013; Sasseville *et al.*, 2009a, 2009b). Culturing porcine oocytes with cumulus cells (COC) for 4 h is sufficient to optimize the timing for GVBD; this supports the idea that cumulus cells make an important contribution during the first hours of IVM while the gap junctions are fully functional (Sasseville *et al.*, 2009b), for example, by delivering energy molecules such as pyruvate to the oocyte. Exposure of porcine COCs to the AMPK activator, AICAR, resulted in a significant decrease in GJC that was explained by decreased protein synthesis (Santiquet *et al.*, 2014b).

In conclusion, PCOS is the most common cause of infertility in women of reproductive age. This is a metabolic syndrome predominantly characterized by hyperandrogenism and anovulation (Franks, 1995). The use of metformin as a biguanide insulin-sensitive pharmacological compound inhibits insulin secretion (Edgerton *et al.*, 2009). Metformin is used for the treatment of PCOS patients (Velazquez *et al.*, 1994) and improved efficacy is observed in combination with clomiphene citrate, a selective estrogen receptor modulator (Nestler *et al.*, 1998). Metformin is probably the most well-known drug administered to PCOS patients (Radosh, 2009). The effect of metformin is systemic, but some studies report a clear ovarian effect such as steroidogenesis, cell viability in granulosa cells (Mansfield *et al.*, 2003; Sonntag *et al.*, 2005), and increased lactate production (Richardson *et al.*, 2009). Finally, an improved IVM outcome has recently been reported in response to pretreatment with metformin (Wei *et al.*, 2008). This supports a clear ovarian cellular response to metformin, and sensitivity to energy metabolism that influences gamete quality and viability.

8.5 Conclusion

Oocyte maturation is a physiological event important to the female gamete. It permits meiotic resumption; progression from the GV stage to reach the metaphase-II stage in order for fertilization to occur. At the same time, cumulus cells start to secrete an extracellular matrix that provides the required stimuli to spermatozoa to facilitate fertilization of the oocyte. In this chapter we have presented various elements of the signaling occurring during oocyte maturation. From FSH stimulation through cyclic nucleotides and phosphodiesterases, we discussed the role of natriuretic factors, GJCs, and the metabolic switch, AMPK.

More work is required to elucidate the signaling cascades occurring during oocyte maturation. Transcriptomic studies suggest a plethora of new pathways and many of these new upcoming interactions will require further validation. Because oocyte competency for embryo production begins with oocyte maturation, many more studies are necessary to elucidate the cascade of events occurring during oocyte maturation.

References

Abel, M.H., Wootton, A.N., Wilkins, V., Huhtaniemi, I., Knight, P.G., and Charlton, H.M. (2000) The effect of a null mutation in the follicle-stimulating hormone receptor gene on mouse reproduction. *Endocrinology*, **141**, 1795–1803.

Downloaded From Vet-eBooks.com

Ackert, C.L., Gittens, J.E., O'Brien M.J., Eppig, J.J., and Kidder, G.M. (2001) Intercellular communication via connexin43 gap junctions is required for ovarian folliculogenesis in the mouse. *Dev. Biol.*, **233**, 258–270.

Adam, R.M., Yang, W., Di Vizio, D., Mukhopadhyay, N.K., and Steen, H. (2008) Rapid preparation of nuclei-depleted detergent-resistant membrane fractions suitable for proteomics analysis. *BMC Cell Biol.*, **9**, 30.

Albuz, F.K., Sasseville, M., Lane, M., Armstrong, D.T., Thompson, J.G., and Gilchrist, R.B. (2010) Simulated physiological oocyte maturation (SPOM): a novel *in vitro* maturation system that substantially improves embryo yield and pregnancy outcomes. *Hum. Reprod.*, **25**, 2999–3011.

Algriany, O. (2007) Expression analysis of genes implicated in meiotic resumption *in vivo* and developmental competence of bovine oocytes, in *Department of Farm Animals Health*, Utrecht University, Utrecht, p. 172.

Ali, A., and Sirard, M.A. (2005) Protein kinases influence bovine oocyte competence during short-term treatment with recombinant human follicle stimulating hormone. *Reproduction*, **130**, 303–310.

Anand-Srivastava, M.B. (2005) Natriuretic peptide receptor-C signaling and regulation. *Peptides*, **26**, 1044–1059.

Andric, N., Thomas, M., and Ascoli, M. (2010) Transactivation of the epidermal growth factor receptor is involved in the lutropin receptor-mediated down-regulation of ovarian aromatase expression *in vivo*. *Mol. Endocrinol.*, **24**, 552–560.

Aschenbach, W.G., Sakamoto, K., and Goodyear, L.J. (2004) 5′ Adenosine monophosphate-activated protein kinase, metabolism and exercise. *Sports Med.*, **34**, 91–103.

Baillie, G.S., Scott, J.D., and Houslay, M.D. (2005) Compartmentalisation of phosphodiesterases and protein kinase A: opposites attract. *FEBS Lett.*, **579**, 3264–3270.

Beavo, J.A. and Brunton, L.L. (2002) Cyclic nucleotide research: still expanding after half a century. *Nat. Rev. Mol. Cell Biol.*, **3**, 710–718.

Berl, T., Mansour, J., and Teitelbaum, I. (1991) ANP stimulates phospholipase C in cultured RIMCT cells: roles of protein kinases and G protein. *Am. J. Physiol.*, **260**, F590–F595.

Biggers, J.D., Whittingham, D.G., and Donahue, R.P. (1967) The pattern of energy metabolism in the mouse oocyte and zygote. *Proc. Natl. Acad. Sci. USA*, **58**, 560–567.

Bilodeau-Goeseels, S. (2011) Cows are not mice: the role of cyclic AMP, phosphodiesterases, and adenosine monophosphate-activated protein kinase in the maintenance of meiotic arrest in bovine oocytes. *Mol. Reprod. Dev.*, **78**, 734–743.

Bilodeau-Goeseels, S., Sasseville, M., Guillemette, C., and Richard, F.J. (2007) Effects of adenosine monophosphate-activated kinase activators on bovine oocyte nuclear maturation *in vitro*. *Mol. Reprod. Dev.*, **74**, 1021–1034.

Bornslaeger, E.A. and Schultz, R.M. (1985) Regulation of mouse oocyte maturation: effect of elevating cumulus cell cAMP on oocyte cAMP levels. *Biol. Reprod.*, **33**, 698–704.

Bornslaeger, E.A., Wilde, M.W., and Schultz, R.M. (1984) Regulation of mouse oocyte maturation: involvement of cyclic AMP phosphodiesterase and calmodulin. *Dev. Biol.*, **105**, 488–499.

Bu, S., Xie, H., Tao, Y., Wang, J., and Xia, G. (2004) Nitric oxide influences the maturation of cumulus cell-enclosed mouse oocytes cultured in spontaneous maturation medium and hypoxanthine-supplemented medium through different signaling pathways. *Mol. Cell. Endocrinol.*, **223**, 85–93.

Buschiazzo, J., Alonso, T.S., Biscoglio, M., Antollini, S.S., and Bonini, I.C. (2011) Nongenomic steroid- and ceramide-induced maturation in amphibian oocytes involves functional caveolae-like microdomains associated with a cytoskeletal environment. *Biol. Reprod.*, **85**, 808–822.

Byskov, A.G., Andersen, C.Y., Hossaini, A., and Guoliang, X. (1997) Cumulus cells of oocyte–cumulus complexes secrete a meiosis-activating substance when stimulated with FSH. *Mol. Reprod. Dev.*, **46**, 296–305.

Downloaded From Vet-eBooks.com

Caixeta, E.S., Machado, M.F., Ripamonte, P., Price, C., and Buratini, J. (2013) Effects of FSH on the expression of receptors for oocyte-secreted factors and members of the EGF-like family during *in vitro* maturation in cattle. *Reprod. Fertil. Dev.*, **25**, 890–899.

Calaghan, S., Kozera, L., and White, E. (2008) Compartmentalisation of cAMP-dependent signalling by caveolae in the adult cardiac myocyte. *J. Mol. Cell. Cardiol.*, **45**, 88–92.

Camaioni, A., Salustri, A., Yanagishita, M., and Hascall, V.C. (1996) Proteoglycans and proteins in the extracellular matrix of mouse cumulus cell–oocyte complexes. *Arch. Biochem. Biophys.*, **325**, 190–198.

Carabatsos, M.J., Sellitto, C., Goodenough, D.A., and Albertini, D.F. (2000) Oocyte–granulosa cell heterologous gap junctions are required for the coordination of nuclear and cytoplasmic meiotic competence. *Dev. Biol.*, **226**, 167–179.

Castro, L.R., Verde, I., Cooper, D.M., and Fischmeister, R. (2006) Cyclic guanosine monophosphate compartmentation in rat cardiac myocytes. *Circulation*, **113**, 2221–2228.

Chagas, L.M., Bass, J.J., Blache, D., Burke, C.R., Kay, J.K., Lindsay, D.R., Lucy, M.C., Martin, G.B., Meier, S., Rhodes, F.M. *et al.* (2007) Invited review: new perspectives on the roles of nutrition and metabolic priorities in the subfertility of high-producing dairy cows. *J. Dairy Sci.*, **90**, 4022–4032.

Chen, J. and Downs, S.M. (2008) AMP-activated protein kinase is involved in hormone-induced mouse oocyte meiotic maturation *in vitro*. *Dev. Biol.*, **313**, 47–57.

Chen, L., Mao, S.J., and Larsen, W.J. (1992) Identification of a factor in fetal bovine serum that stabilizes the cumulus extracellular matrix: a role for a member of the inter-alpha-trypsin inhibitor family. *J. Biol. Chem.*, **267**, 12380–12386.

Chen, J., Hudson, E., Chi, M.M., Chang, A.S., Moley, K.H., Hardie, D.G., and Downs, S.M. (2006) AMPK regulation of mouse oocyte meiotic resumption *in vitro*. *Dev. Biol.*, **291**, 227–238.

Chen, X., Zhou, B., Yan, J., Xu, B., Tai, P., Li, J., Peng, S., Zhang, M., and Xia, G. (2008) Epidermal growth factor receptor activation by protein kinase C is necessary for FSH-induced meiotic resumption in porcine cumulus–oocyte complexes. *J. Endocrinol.*, **197**, 409–419.

Chen, J., Torcia, S., Xie, F., Lin, C.J., Cakmak, H., Franciosi, F., Horner, K., Onodera, C., Song, J.S., Cedars, M.I. *et al.* (2013) Somatic cells regulate maternal mRNA translation and developmental competence of mouse oocytes. *Nat. Cell. Biol.*, **15**, 1415–1423.

Chen, Q., Zhang, W., Ran, H., Feng, L., Yan, H., Mu, X., Han, Y., Liu, W., Xia, G., and Wang, C. (2014) PKCδ and θ possibly mediate FSH-induced mouse oocyte maturation via NOX-ROS-TACE cascade signaling pathway. *PLoS One*, **9**, e111423.

Cho, W.K., Stern, S., and Biggers, J.D. (1974) Inhibition effect of dibutyryl cAMP on mouse oocyte maturation *in vitro*. *J. Exp. Zool.*, **187**, 383–386.

Choi, Y.H., Park, S., Hockman, S., Zmuda-Trzebiatowska, E., Svennelid, F., Haluzik, M., Gavrilova, O., Ahmad, F., Pepin, L., Napolitano, M. *et al.* (2006) Alterations in regulation of energy homeostasis in cyclic nucleotide phosphodiesterase 3B-null mice. *J. Clin. Invest.*, **116**, 3240–3251.

Comiskey, M. and Warner, C.M. (2007) Spatio-temporal localization of membrane lipid rafts in mouse oocytes and cleaving preimplantation embryos. *Dev. Biol.*, **303**, 727–739.

Conti, M., Andersen, C.B., Richard, F.J., Shitsukawa, K., and Tsafriri, A. (1998) Role of cyclic nucleotide phosphodiesterases in resumption of meiosis. *Mol. Cell. Endocrinol.*, **145**, 9–14.

Cooperstock, R.L. and Lipshitz, H.D. (2001) RNA localization and translational regulation during axis specification in the *Drosophila* oocyte. *Int. Rev. Cytol.*, **203**, 541–566.

Cortvrindt, R., Smitz, J., and Van Steirteghem, A.C. (1997) Assessment of the need for follicle stimulating hormone in early preantral mouse follicle culture *in vitro*. *Hum. Reprod.*, **12**, 759–768.

Costa, M.A., Elesgaray, R., Balaszczuk, A.M., and Arranz, C. (2006) Role of NPR-C natriuretic receptor in nitric oxide system activation induced by atrial natriuretic peptide. *Regul. Pept.*, **135**, 63–68.

Costa, M.A., Elesgaray, R., Caniffi, C., Fellet, A., and Arranz, C. (2007) Role of cardiovascular nitric oxide system in C-type natriuretic peptide effects. *Biochem. Biophys. Res. Commun.*, **359**, 180–186.

Downloaded From Vet-eBooks.com

Cottom, J., Salvador, L.M., Maizels, E.T., Reierstad, S., Park, Y., Carr, D.W., Davare, M.A., Hell, J.W., Palmer, S.S., Dent, P. *et al.* (2003) Follicle-stimulating hormone activates extracellular signal-regulated kinase but not extracellular signal-regulated kinase kinase through a 100-kDa phosphotyrosine phosphatase. *J. Biol. Chem.*, **278**, 7167–7179.

Cottrell, G.T. and Burt, J.M. (2005) Functional consequences of heterogeneous gap junction channel formation and its influence in health and disease. *Biochim. Biophys. Acta*, **1711**, 126–141.

De Leo, V., la Marca, A., Ditto, A., Morgante, G., and Cianci, A. (1999) Effects of metformin on gonadotropin-induced ovulation in women with polycystic ovary syndrome. *Fertil. Steril.*, **72**, 282–285.

Dekel, N. (1988) Regulation of oocyte maturation: the role of cAMP. *Ann. N. Y. Acad. Sci.*, **541**, 211–216.

Dekel, N. and Sherizly, I. (1985) Epidermal growth factor induces maturation of rat follicle-enclosed oocytes. *Endocrinology*, **116**, 406–409.

Dekel, N., Lawrence, T.S., Gilula, N.B., and Beers, W.H. (1981) Modulation of cell-to-cell communication in the cumulus–oocyte complex and the regulation of oocyte maturation by LH. *Dev. Biol.*, **86**, 356–362.

Dineva, J., Vangelov, I., Nikolov, G., Gulenova, D., and Ivanova, M. (2011) Atrial natriuretic peptide is an antiapoptotic factor for human granulosa luteinized cells with impact on the results of COH/IVF in women undergoing IVF program. *J. Obstet. Gynaecol. Res.*, **37**, 511–519.

Downs, S.M. (2001) A gap-junction-mediated signal, rather than an external paracrine factor, predominates during meiotic induction in isolated mouse oocytes. *Zygote*, **9**, 71–82.

Downs, S.M. and Chen, J. (2008) EGF-like peptides mediate FSH-induced maturation of cumulus cell-enclosed mouse oocytes. *Mol. Reprod. Dev.*, **75**, 105–114.

Downs, S.M. and Mastropolo, A.M. (1994) The participation of energy substrates in the control of meiotic maturation in murine oocytes. *Dev. Biol.*, **162**, 154–168.

Downs, S.M., Coleman, D.L., Ward-Bailey, P.F., and Eppig, J.J. (1985) Hypoxanthine is the principal inhibitor of murine oocyte maturation in a low molecular weight fraction of porcine follicular fluid. *Proc. Natl. Acad. Sci. USA*, **82**, 454–458.

Downs, S.M., Hudson, E.R., and Hardie, D.G. (2002) A potential role for AMP-activated protein kinase in meiotic induction in mouse oocytes. *Dev. Biol.*, **245**, 200–212.

Edgerton, D.S., Johnson, K.M., and Cherrington, A.D. (2009) Current strategies for the inhibition of hepatic glucose production in type 2 diabetes. *Front. Biosci.*, **14**, 1169–1181.

Edwards, R.G. (1965) Maturation *in vitro* of mouse, sheep, cow, pig, rhesus monkey and human ovarian oocytes. *Nature*, **208**, 349–351.

El-Hayek, S., Demeestere, I., and Clarke, H.J. (2014) Follicle-stimulating hormone regulates expression and activity of epidermal growth factor receptor in the murine ovarian follicle. *Proc. Natl. Acad. Sci. USA*, **111**, 16778–16783.

Eppig, J.J. (1980a) Regulation of cumulus oophorus expansion by gonadotropins *in vivo* and *in vitro*. *Biol. Reprod.*, **23**, 545–552.

Eppig, J.J. (1980b) Role of serum in FSH stimulated cumulus expansion by mouse oocyte–cumulus cell complexes *in vitro*. *Biol. Reprod.*, **22**, 629–633.

Eppig, J.J. (1991) Intercommunication between mammalian oocytes and companion somatic cells. *Bioessays*, **13**, 569–574.

Eppig, J.J., Hosoe, M., O'Brien, M.J., Pendola, F.M., Requena, A., and Watanabe, S. (2000) Conditions that affect acquisition of developmental competence by mouse oocytes *in vitro*: FSH, insulin, glucose and ascorbic acid. *Mol. Cell. Endocrinol.*, **163**, 109–116.

Fagbohun, C.F. and Downs, S.M. (1992) Requirement for glucose in ligand-stimulated meiotic maturation of cumulus cell-enclosed mouse oocytes. *J. Reprod. Fertil.*, **96**, 681–697.

Fair, T. (1995) Oocyte growth in cattle: ultrastructure, transcription and developmental competence, in *Department of Animal Science and Production*, University College Dublin, Dublin, p. 140.

Downloaded From Vet-eBooks.com

Fan, H.Y., Liu, Z., Shimada, M., Sterneck, E., Johnson, P.F., Hedrick, S.M., and Richards, J.S. (2009) MAPK3/1 (ERK1/2) in ovarian granulosa cells are essential for female fertility. *Science*, **324**, 938–941.

Franciosi, F., Coticchio, G., Lodde, V., Tessaro, I., Modina, S.C., Fadini, R., Dal Canto, M., Renzini, M.M., Albertini, D.F., and Luciano, A.M. (2014) Natriuretic peptide precursor C delays meiotic resumption and sustains gap junction-mediated communication in bovine cumulus-enclosed oocytes. *Biol. Reprod.*, **91**, 61.

Franks, S. (1995) Polycystic ovary syndrome. *N. Engl. J. Med.*, **333**, 853–861.

Fry, B.G., Wickramaratana, J.C., Lemme, S., Beuve, A., Garbers, D., Hodgson, W.C., and Alewood, P. (2005) Novel natriuretic peptides from the venom of the inland taipan (Oxyuranus microlepidotus): isolation, chemical and biological characterisation. *Biochem. Biophys. Res. Commun.*, **327**, 1011–1015.

Fryer, L.G., Parbu-Patel, A., and Carling, D. (2002) The anti-diabetic drugs rosiglitazone and metformin stimulate AMP-activated protein kinase through distinct signaling pathways. *J. Biol. Chem.*, **277**, 25226–25232.

Fulka, J. Jr., Motlik, J., Fulka, J., and Jilek, F. (1986) Effect of cycloheximide on nuclear maturation of pig and mouse oocytes. *J. Reprod. Fertil.*, **77**, 281–285.

Funahashi, H., Koike, T., and Sakai, R. (2008) Effect of glucose and pyruvate on nuclear and cytoplasmic maturation of porcine oocytes in a chemically defined medium. *Theriogenology*, **70**, 1041–1047.

Geister, K.A., Brinkmeier, M.L., Hsieh, M., Faust, S.M., Karolyi, I.J., Perosky, J.E., Kozloff, K.M., Conti, M., and Camper, S.A. (2013) A novel loss-of-function mutation in Npr2 clarifies primary role in female reproduction and reveals a potential therapy for acromesomelic dysplasia, Maroteaux type. *Hum. Mol. Genet.*, **22**, 345–357.

Gilbert, I., Robert, C., Vigneault, C., Blondin, P., and Sirard, M.A. (2012) Impact of the LH surge on granulosa cell transcript levels as markers of oocyte developmental competence in cattle. *Reproduction*, **143**, 735–747.

Gloaguen, P., Crepieux, P., Heitzler, D., Poupon, A., and Reiter, E. (2011) Mapping the follicle-stimulating hormone-induced signaling networks. *Front. Endocrinol.*, **2**, 45.

Glueck, C.J., Wang, P., Fontaine, R., Tracy, T., and Sieve-Smith, L. (1999) Metformin-induced resumption of normal menses in 39 of 43 (91%) previously amenorrheic women with the polycystic ovary syndrome. *Metabolism*, **48**, 511–519.

Gruzman, A., Babai, G., and Sasson, S. (2009) Adenosine monophosphate-activated protein kinase (AMPK) as a new target for antidiabetic drugs: a review on metabolic, pharmacological and chemical considerations. *Rev. Diabet. Stud.*, **6**, 13–36.

Guimarães, A.L.S., Pereira, S.A., Leme, L.O., and Dode, M.A.N. (2014) Evaluation of the simulated physiological oocyte maturation system for improving bovine *in vitro* embryo production. *Theriogenology*, **83** (1), 52–57.

Gusarova, G.A., Dada, L.A., Kelly, A.M., Brodie, C., Witters, L.A., Chandel, N.S., and Sznajder, J.I. (2009) Alpha1-AMP-activated protein kinase regulates hypoxia-induced Na,K-ATPase endocytosis via direct phosphorylation of protein kinase C zeta. *Mol. Cell. Biol.*, **29**, 3455–3464.

Han, S.J. and Conti, M. (2006) New pathways from PKA to the Cdc2/cyclin B complex in oocytes: Wee1B as a potential PKA substrate. *Cell Cycle*, **5**, 227–231.

Hardie, D.G. (2007) AMP-activated/SNF1 protein kinases: conserved guardians of cellular energy. *Nat. Rev. Mol. Cell Biol.*, **8**, 774–785.

Hardie, D.G. (2008) AMPK: a key regulator of energy balance in the single cell and the whole organism. *Int. J. Obes.*, **32** (Suppl. 4), S7–S12.

Harris, A.L. (2007) Connexin channel permeability to cytoplasmic molecules. *Prog. Biophys. Mol. Biol.*, **94**, 120–143.

Henin, N., Vincent, M.F., and van den Berghe, G. (1996) Stimulation of rat liver AMP-activated protein kinase by AMP analogues. *Biochim. Biophys. Acta*, **1290**, 197–203.

Downloaded From Vet-eBooks.com

Herrick, J.R., Brad, A.M., and Krisher, R.L. (2006) Chemical manipulation of glucose metabolism in porcine oocytes: effects on nuclear and cytoplasmic maturation *in vitro*. *Reproduction*, **131**, 289–298.

Heyer, B.S., Warsowe, J., Solter, D., Knowles, B.B., and Ackerman, S.L. (1997) New member of the Snf1/AMPK kinase family, Melk, is expressed in the mouse egg and preimplantation embryo. *Mol. Reprod. Dev.*, **47**, 148–156.

Hinckley, M., Vaccari, S., Horner, K., Chen, R., and Conti, M. (2005) The G-protein-coupled receptors GPR3 and GPR12 are involved in cAMP signaling and maintenance of meiotic arrest in rodent oocytes. *Dev. Biol.*, **287**, 249–261.

Hiradate, Y., Hoshino, Y., Tanemura, K., and Sato, E. (2014) C-type natriuretic peptide inhibits porcine oocyte meiotic resumption. *Zygote*, **22**, 372–377.

Hochachka, P.W., Buck, L.T., Doll, C.J., and Land, S.C. (1996) Unifying theory of hypoxia tolerance: molecular/metabolic defense and rescue mechanisms for surviving oxygen lack. *Proc. Natl. Acad. Sci. USA*, **93**, 9493–9498.

Hsieh, M., Lee, D., Panigone, S., Horner, K., Chen, R., Theologis, A., Lee, D.C., Threadgill, D.W., and Conti, M. (2007) Luteinizing hormone-dependent activation of the epidermal growth factor network is essential for ovulation. *Mol. Cell. Biol.*, **27**, 1914–1924.

Hsieh, M., Thao, K., and Conti, M. (2011) Genetic dissection of epidermal growth factor receptor signaling during luteinizing hormone-induced oocyte maturation. *PLoS One*, **6**, e21574.

Hubbard, C.J. and Terranova, P.F. (1982) Inhibitory action of cyclic guanosine 5′-phosphoric acid (GMP) on oocyte maturation: dependence on an intact cumulus. *Biol. Reprod.*, **26**, 628–632.

Hurley, R.L., Anderson, K.A., Franzone, J.M., Kemp, B.E., Means, A.R., and Witters, L.A. (2005) The Ca2+/calmodulin-dependent protein kinase kinases are AMP-activated protein kinase kinases. *J. Biol. Chem.*, **280**, 29060–29066.

Jensen, J.T., Schwinof, K.M., Zelinski-Wooten, M.B., Conti, M., DePaolo, L.V., and Stouffer, R.L. (2002) Phosphodiesterase 3 inhibitors selectively block the spontaneous resumption of meiosis by macaque oocytes *in vitro*. *Hum. Reprod.*, **17**, 2079–2084.

John, S.W., Krege, J.H., Oliver, P.M., Hagaman, J.R., Hodgin, J.B., Pang, S.C., Flynn, T.G., and Smithies, O. (1995) Genetic decreases in atrial natriuretic peptide and salt-sensitive hypertension. *Science*, **267**, 679–681.

Juneja, S.C., Barr, K.J., Enders, G.C., and Kidder, G.M. (1999) Defects in the germ line and gonads of mice lacking connexin43. *Biol. Reprod.*, **60**, 1263–1270.

Kahmann, J.D., O'Brien R., Werner, J.M., Heinegard, D., Ladbury, J.E., Campbell, I.D., Day, A.J. (2000) Localization and characterization of the hyaluronan-binding site on the link module from human TSG-6. *Structure*, **8**, 763–774.

Kahn, B.B., Alquier, T., Carling, D., and Hardie, D.G. (2005) AMP-activated protein kinase: ancient energy gauge provides clues to modern understanding of metabolism. *Cell Metab.*, **1**, 15–25.

Kara, E., Crepieux, P., Gauthier, C., Martinat, N., Piketty, V., Guillou, F., and Reiter, E. (2006) A phosphorylation cluster of five serine and threonine residues in the C-terminus of the follicle-stimulating hormone receptor is important for desensitization but not for beta-arrestin-mediated ERK activation. *Mol. Endocrinol.*, **20**, 3014–3026.

Katakowski, M., Buller, B., Wang, X., Rogers, T., and Chopp, M. (2010) Functional microRNA is transferred between glioma cells. *Cancer Res.*, **70**, 8259–8263.

Kind, K.L., Banwell, K.M., Gebhardt, K.M., Macpherson, A., Gauld, A., Russell, D.L., and Thompson, J.G. (2013) Microarray analysis of mRNA from cumulus cells following *in vivo* or *in vitro* maturation of mouse cumulus–oocyte complexes. *Reprod. Fertil. Dev.*, **25**, 426–438.

Kizana, E., Cingolani, E., and Marban, E. (2009) Non-cell-autonomous effects of vector-expressed regulatory RNAs in mammalian heart cells. *Gene Ther.*, **16**, 1163–1168.

Kola, B., Boscaro, M., Rutter, G.A., Grossman, A.B., and Korbonits, M. (2006) Expanding role of AMPK in endocrinology. *Trends Endocrinol. Metab.*, **17**, 205–215.

Downloaded From Vet-eBooks.com

Laforest, M.F., Pouliot, E., Gueguen, L., and Richard, F.J. (2005) Fundamental significance of specific phosphodiesterases in the control of spontaneous meiotic resumption in porcine oocytes. *Mol. Reprod. Dev.*, **70**, 361–372.

Laird, D.W. (2005) Connexin phosphorylation as a regulatory event linked to gap junction internalization and degradation. *Biochim. Biophys. Acta*, **1711**, 172–182.

LaRosa, C. and Downs, S.M. (2006) Stress stimulates AMP-activated protein kinase and meiotic resumption in mouse oocytes. *Biol. Reprod.*, **74**, 585–592.

Larsen, W.J., Wert, S.E., and Brunner, G.D. (1987) Differential modulation of rat follicle cell gap junction populations at ovulation. *Dev. Biol.*, **122**, 61–71.

Lee, M.S., Kang, S.K., Lee, B.C., and Hwang, W.S. (2005) The beneficial effects of insulin and metformin on *in vitro* developmental potential of porcine oocytes and embryos. *Biol. Reprod.*, **73**, 1264–1268.

Lee, M., Hwang, J.T., Yun, H., Kim, E.J., Kim, M.J., Kim, S.S., and Ha, J. (2006) Critical roles of AMP-activated protein kinase in the carcinogenic metal-induced expression of VEGF and HIF-1 proteins in DU145 prostate carcinoma. *Biochem. Pharmacol.*, **72**, 91–103.

Lee, K.B., Zhang, M., Sugiura, K., Wigglesworth, K., Uliasz, T., Jaffe, L.A., and Eppig, J.J. (2013) Hormonal coordination of natriuretic peptide type C and natriuretic peptide receptor 3 expression in mouse granulosa cells. *Biol. Reprod.*, **88**, 42.

Lévesque, J.T. and Sirard, M.A. (1996) Resumption of meiosis is initiated by the accumulation of cyclin B in bovine oocytes. *Biol. Reprod.*, **55**, 1427–1436.

Li, Y., Madiraju, P., and Anand-Srivastava, M.B. (2012) Knockdown of natriuretic peptide receptor-A enhances receptor C expression and signalling in vascular smooth muscle cells. *Cardiovasc. Res.*, **93**, 350–359.

Lim, P.K., Bliss, S.A., Patel, S.A., Taborga, M., Dave, M.A., Gregory, L.A., Greco, S.J., Bryan, M., Patel, P.S., and Rameshwar, P. (2011) Gap junction-mediated import of microRNA from bone marrow stromal cells can elicit cell cycle quiescence in breast cancer cells. *Cancer Res*, **71**, 1550–1560.

Lincoln, A.J., Wickramasinghe, D., Stein, P., Schultz, R.M., Palko, M.E., De Miguel, M.P., Tessarollo, L., and Donovan, P.J. (2002) Cdc25b phosphatase is required for resumption of meiosis during oocyte maturation. *Nat. Genet.*, **30**, 446–449.

Lochhead, P.A., Salt, I.P., Walker, K.S., Hardie, D.G., and Sutherland, C. (2000) 5-Aminoimidazole-4-carboxamide riboside mimics the effects of insulin on the expression of the 2 key gluconeogenic genes PEPCK and glucose-6-phosphatase. *Diabetes*, **49**, 896–903.

Luciano, A.M., Franciosi, F., Modina, S.C., and Lodde, V. (2011) Gap junction-mediated communications regulate chromatin remodeling during bovine oocyte growth and differentiation through cAMP-dependent mechanism(s). *Biol. Reprod.*, **85**, 1252–1259.

Macaulay, A.D., Gilbert, I., Caballero, J., Barreto, R., Fournier, E., Tossou, P., Sirard, M.A., Clarke, H.J., Khandjian, E.W., Richard, F.J. *et al.* (2014) The gametic synapse: RNA transfer to the bovine oocyte. *Biol. Reprod.*, **91**, 90.

Magnusson, C. and Hillensjo, T. (1977) Inhibition of maturation and metabolism in rat oocytes by cyclic AMP. *J. Exp. Zool.*, **201**, 139–147.

Manganiello, V.C., Smith, C.J., Degereman, E., and Belfrage, P. (1990) Cyclic GMP-inhibited cyclic nucleotide phosphodiesterase, in *Cyclic Nucleotide Phosphodiesterases: Structure, Regulation, and Drug Action* (eds J. Beavo and M.D. Houslay), vol. 2, John Wiley & Sons, Inc., Chichester, 87–116.

Mansfield, R., Galea, R., Brincat, M., Hole, D., and Mason, H. (2003) Metformin has direct effects on human ovarian steroidogenesis. *Fertil. Steril.*, **79**, 956–962.

Marsin, A.S., Bertrand, L., Rider, M.H., Deprez, J., Beauloye, C., Vincent, M.F., Van den Berghe, G., Carling, D., and Hue, L. (2000) Phosphorylation and activation of heart PFK-2 by AMPK has a role in the stimulation of glycolysis during ischaemia. *Curr. Biol.*, **10**, 1247–1255.

Downloaded From Vet-eBooks.com

Masciarelli, S., Horner, K., Liu, C., Park, S.H., Hinckley, M., Hockman, S., Nedachi, T., Jin, C., Conti, M., and Manganiello, V. (2004) Cyclic nucleotide phosphodiesterase 3A-deficient mice as a model of female infertility. *J. Clin. Invest.*, **114**, 196–205.

Matzuk, M.M. and Burns, K.H. (2012) Genetics of mammalian reproduction: modeling the end of the germline. *Annu. Rev. Physiol.*, **74**, 503–528.

Maurice, D.H. and Haslam, R.J. (1990) Nitroprusside enhances isoprenaline-induced increases in cAMP in rat aortic smooth muscle. *Eur. J. Pharmacol.*, **191**, 471–475.

Mayes, M.A. and Sirard, M.A. (2002) Effect of type 3 and type 4 phosphodiesterase inhibitors on the maintenance of bovine oocytes in meiotic arrest. *Biol. Reprod.*, **66**, 180–184.

Mayes, M.A., Laforest, M.F., Guillemette, C., Gilchrist, R.B., and Richard, F.J. (2007) Adenosine 5′-monophosphate kinase-activated protein kinase (PRKA) activators delay meiotic resumption in porcine oocytes. *Biol. Reprod.*, **76**, 589–597.

McLachlin, J.R. and Kidder, G.M. (1986) Intercellular junctional coupling in preimplantation mouse embryos: effect of blocking transcription or translation. *Dev. Biol.*, **117**, 146–155.

Means, A.R., MacDougall, E., Soderling, T.R., and Corbin, J.D. (1974) Testicular adenosine 3′:5′-monophosphate-dependent protein kinase: regulation by follicle-stimulating hormone. *J. Biol. Chem.*, **249**, 1231–1238.

Mehlmann, L.M., Saeki, Y., Tanaka, S., Brennan, T.J., Evsikov, A.V., Pendola, F.L., Knowles, B.B., Eppig, J.J., and Jaffe, L.A. (2004) The Gs-linked receptor GPR3 maintains meiotic arrest in mammalian oocytes. *Science*, **306**, 1947–1950.

Meinecke, B. and Meinecke-Tillmann, S. (1979) Effects of gonadotropins on oocyte maturation and progesterone production by porcine ovarian follicles cultured *in vitro*. *Theriogenology*, **11**, 351–365.

Meinecke, B. and Meinecke-Tillmann, S. (1993) Effects of A-amanitin on nuclear maturation of porcine oocytes *in vitro*. *J. Reprod. Fertil.*, **98**, 195–201.

Mese, G., Richard, G., and White, T.W. (2007) Gap junctions: basic structure and function. *J. Invest. Dermatol.*, **127**, 2516–2524.

Mitchell, P.A. and Burghardt, R.C. (1986) The ontogeny of nexuses (gap junctions) in the ovary of the fetal mouse. *Anat. Rec.*, **214**, 283–288.

Motlik, J. and Fulka, J. (1986) Factors affecting meiotic competence in pig oocytes. *Theriogenology*, **25**, 87–96.

Motlik, J., Crozet, N., and Fulka, J. (1984) Meiotic competence *in vitro* of pig oocytes isolated from early antral follicles. *J. Reprod. Fertil.*, **72**, 323–328.

Murthy, K.S., Teng, B.Q., Zhou, H., Jin, J.G., Grider, J.R., and Makhlouf, G.M. (2000) G(i-1)/G(i-2)-dependent signaling by single-transmembrane natriuretic peptide clearance receptor. *Am. J. Physiol. Gastrointest. Liver Physiol.*, **278**, G974–G980.

Nestler, J.E., Jakubowicz, D.J., Evans, W.S., and Pasquali, R. (1998) Effects of metformin on spontaneous and clomiphene-induced ovulation in the polycystic ovary syndrome. *N. Engl. J. Med.*, **338**, 1876–1880.

Neves, S.R., Tsokas, P., Sarkar, A., Grace, E.A., Rangamani, P., Taubenfeld, S.M., Alberini, C.M., Schaff, J.C., Blitzer, R.D., Moraru, I.I. *et al.* (2008) Cell shape and negative links in regulatory motifs together control spatial information flow in signaling networks. *Cell*, **133**, 666–680.

Nilsson, R., Ahmad, F., Sward, K., Andersson, U., Weston, M., Manganiello, V., and Degerman, E. (2006) Plasma membrane cyclic nucleotide phosphodiesterase 3B (PDE3B) is associated with caveolae in primary adipocytes. *Cell Signal.*, **18**, 1713–1721.

Nivet, A.L., Vigneault, C., Blondin, P., and Sirard, M.A. (2013) Changes in granulosa cells' gene expression associated with increased oocyte competence in bovine. *Reproduction*, **145**, 555–565.

Nogueira, D., Albano, C., Adriaenssens, T., Cortvrindt, R., Bourgain, C., Devroey, P., and Smitz, J. (2003) Human oocytes reversibly arrested in prophase I by phosphodiesterase type 3 inhibitor *in vitro*. *Biol. Reprod.*, **69**, 1042–1052.

Downloaded From Vet-eBooks.com

Nogueira, D., Ron-El, R., Friedler, S., Schachter, M., Raziel, A., Cortvrindt, R., and Smitz, J. (2006) Meiotic arrest *in vitro* by phosphodiesterase 3-inhibitor enhances maturation capacity of human oocytes and allows subsequent embryonic development. *Biol. Reprod.*, **74**, 177–184.

Norris, R.P., Freudzon, M., Mehlmann, L.M., Cowan, A.E., Simon, A.M., Paul, D.L., Lampe, P.D., and Jaffe, L.A. (2008) Luteinizing hormone causes MAP kinase-dependent phosphorylation and closure of connexin 43 gap junctions in mouse ovarian follicles: one of two paths to meiotic resumption. *Development*, **135**, 3229–3238.

Norris, R.P., Ratzan, W.J., Freudzon, M., Mehlmann, L.M., Krall, J., Movsesian, M.A., Wang, H., Ke, H., Nikolaev, V.O., and Jaffe, L.A. (2009) Cyclic GMP from the surrounding somatic cells regulates cyclic AMP and meiosis in the mouse oocyte. *Development*, **136**, 1869–1878.

Norris, R.P., Freudzon, M., Nikolaev, V.O., and Jaffe, L.A. (2010) Epidermal growth factor receptor kinase activity is required for gap junction closure and for part of the decrease in ovarian follicle cGMP in response to LH. *Reproduction*, **140**, 655–662.

Oktay, K., Briggs, D., and Gosden, R.G. (1997) Ontogeny of follicle-stimulating hormone receptor gene expression in isolated human ovarian follicles. *J. Clin. Endocrinol. Metab.*, **82**, 3748–3751.

Okumura, E., Fukuhara, T., Yoshida, H., Hanada Si, S., Kozutsumi, R., Mori, M., Tachibana, K., and Kishimoto, T. (2002) Akt inhibits Myt1 in the signalling pathway that leads to meiotic G2/M-phase transition. *Nat. Cell. Biol.*, **4**, 111–116.

Panigone, S., Hsieh, M., Fu, M., Persani, L., and Conti, M. (2008) Luteinizing hormone signaling in preovulatory follicles involves early activation of the epidermal growth factor receptor pathway. *Mol. Endocrinol.* **22**, 924–936.

Park, J.Y., Su, Y.Q., Ariga, M., Law, E., Jin, S.L., and Conti, M. (2004) EGF-like growth factors as mediators of LH action in the ovulatory follicle. *Science*, **303**, 682–684.

Peng, X.R., Hsueh, A.J., LaPolt, P.S., Bjersing, L., and Ny, T. (1991) Localization of luteinizing hormone receptor messenger ribonucleic acid expression in ovarian cell types during follicle development and ovulation. *Endocrinology*, **129**, 3200–3207.

Peng, J.Y., Xin, H.Y., Han, P., Zhao, H.B., Bai, L., An, X.P., and Cao, B.Y. (2013) Identification and gene expression analyses of natriuretic peptide system in the ovary of goat (Capra hircus) *Gene*, **524**, 105–113.

Perez-Armendariz, E.M., Saez, J.C., Bravo-Moreno, J.F., Lopez-Olmos, V., Enders, G.C., and Villalpando, I. (2003) Connexin43 is expressed in mouse fetal ovary. *Anat. Rec. A Discov. Mol. Cell. Evol. Biol.*, **271**, 360–367.

Pincus, G. and Enzmann, E.V. (1935) The comparative behavior of mammalian eggs *in vivo* and *in vitro*: I. The activation of ovarian eggs. *J. Exp. Med.*, **62**, 665–675.

Pirino, G., Wescott, M.P., and Donovan, P.J. (2009) Protein kinase A regulates resumption of meiosis by phosphorylation of Cdc25B in mammalian oocytes. *Cell Cycle*, **8**, 665–670.

Pirwany, I.R., Yates, R.W., Cameron, I.T., and Fleming, R. (1999) Effects of the insulin sensitizing drug metformin on ovarian function, follicular growth and ovulation rate in obese women with oligomenorrhoea. *Hum. Reprod.*, **14**, 2963–2968.

Potter, L.R. (2011) Natriuretic peptide metabolism, clearance and degradation. *FEBS J*, **278**, 1808–1817.

Potter, L.R., Yoder, A.R., Flora, D.R., Antos, L.K., and Dickey, D.M. Natriuretic peptides: their structures, receptors, physiologic functions and therapeutic applications. *Handb. Exp. Pharmacol.*, **2009**, 341–366.

Prochazka, R., Petlach, M., Nagyova, E., and Nemcova, L. (2011) Effect of epidermal growth factor-like peptides on pig cumulus cell expansion, oocyte maturation, and acquisition of developmental competence *in vitro*: comparison with gonadotropins. *Reproduction*, **141**, 425–435.

Prunier, A. and Quesnel, H. (2000) Nutritional influences on the hormonal control of reproduction in female pigs. *Livest. Prod. Sci.*, **63**, 1–16.

Downloaded From Vet-eBooks.com

Racowsky, C. (1984) Effect of forskolin on the spontaneous maturation and cyclic AMP content of rat oocyte–cumulus complexes. *J. Reprod. Fertil.*, **72**, 107–116.

Racowsky, C., Baldwin, K.V., Larabell, C.A., DeMarais, A.A., and Kazilek, C.J. (1989) Down-regulation of membrana granulosa cell gap junctions is correlated with irreversible commitment to resume meiosis in golden Syrian hamster oocytes. *Eur. J. Cell Biol.*, **49**, 244–251.

Radosh, L. (2009) Drug treatments for polycystic ovary syndrome. *Am. Fam. Physician*, **79**, 671–676.

Ratchford, A.M., Chang, A.S., Chi, M.M., Sheridan, R., and Moley, K.H. (2007) Maternal diabetes adversely affects AMP-activated protein kinase activity and cellular metabolism in murine oocytes. *Am. J. Physiol. Endocrinol. Metab.*, **293**, E1198–E1206.

Ratchford, A.M., Esguerra, C.R., and Moley, K.H. (2008) Decreased oocyte–granulosa cell gap junction communication and connexin expression in a type 1 diabetic mouse model. *Mol. Endocrinol.*, **22**, 2643–2654.

Reaume, A.G., de Sousa, P.A., Kulkarni, S., Langille, B.L., Zhu, D., Davies, T.C., Juneja, S.C., Kidder, G.M., and Rossant, J. (1995) Cardiac malformation in neonatal mice lacking connexin43. *Science*, **267**, 1831–1834.

Reinhardt, R.R., Chin, E., Zhou, J., Taira, M., Murata, T., Manganiello, V.C., and Bondy, C.A. (1995) Distinctive anatomical patterns of gene expression for cGMP-inhibited cyclic nucleotide phosphodiesterases. *J. Clin. Invest.*, **95**, 1528–1538.

Reiter, E. and Lefkowitz, R.J. (2006) GRKs and beta-arrestins: roles in receptor silencing, trafficking and signaling. *Trends Endocrinol. Metab.*, **17**, 159–165.

Resink, T.J., Scott-Burden, T., Baur, U., Jones, C.R., and Buhler, F.R. (1988) Atrial natriuretic peptide induces breakdown of phosphatidylinositol phosphates in cultured vascular smooth-muscle cells. *Eur. J. Biochem.*, **172**, 499–505.

Richani, D., Ritter, L.J., Thompson, J.G., and Gilchrist, R.B. (2013) Mode of oocyte maturation affects EGF-like peptide function and oocyte competence. *Mol. Hum. Reprod.*, **19**, 500–509.

Richard, F.J., Tsafriri, A., and Conti, M. (2001) Role of phosphodiesterase type 3A in rat oocyte maturation. *Biol. Reprod.*, **65**, 1444–1451.

Richardson, M.C., Ingamells, S., Simonis, C.D., Cameron, I.T., Sreekumar, R., Vijendren, A., Sellahewa, L., Coakley, S., and Byrne, C.D. (2009) Stimulation of lactate production in human granulosa cells by metformin and potential involvement of adenosine 5′ monophosphate-activated protein kinase. *J. Clin. Endocrinol. Metab.*, **94**, 670–677.

Robinson, J.W., Zhang, M., Shuhaibar, L.C., Norris, R.P., Geerts, A., Wunder, F., Eppig, J.J., Potter, L.R., and Jaffe, L.A. (2012) Luteinizing hormone reduces the activity of the NPR2 guanylyl cyclase in mouse ovarian follicles, contributing to the cyclic GMP decrease that promotes resumption of meiosis in oocytes. *Dev. Biol.*, **366**, 308–316.

Romero, S. and Smitz, J. (2009) Epiregulin can effectively mature isolated cumulus–oocyte complexes, but fails as a substitute for the hCG/epidermal growth factor stimulus on cultured follicles. *Reproduction*, **137**, 997–1005.

Rose-Hellekant, T.A., Libersky-Williamson, E.A., and Bavister, B.D. (1998) Energy substrates and amino acids provided during *in vitro* maturation of bovine oocytes alter acquisition of developmental competence. *Zygote*, **6**, 285–294.

Rose, R.A. and Giles, W.R. (2008) Natriuretic peptide C receptor signalling in the heart and vasculature. *J. Physiol.*, **586**, 353–366.

Rose, R.D., Gilchrist, R.B., Kelly, J.M., Thompson, J.G., and Sutton-McDowall, M.L. (2013) Regulation of sheep oocyte maturation using cAMP modulators. *Theriogenology*, **79**, 142–148.

Russell, D.L., Ochsner, S.A., Hsieh, M., Mulders, S., and Richards, J.S. (2003) Hormone-regulated expression and localization of versican in the rodent ovary. *Endocrinology*, **144**, 1020–1031.

Sadler, S.E. (2001) Low-density caveolae-like membrane from *Xenopus laevis* oocytes is enriched in Ras. *J. Cell. Biochem.*, **83**, 21–32.

Downloaded From Vet-eBooks.com

Salustri, A., Garlanda, C., Hirsch, E., De Acetis, M., Maccagno, A., Bottazzi, B., Doni, A., Bastone, A., Mantovani, G., Beck Peccoz, P. *et al.* (2004) PTX3 plays a key role in the organization of the cumulus oophorus extracellular matrix and in *in vivo* fertilization. *Development*, **131**, 1577–1586.

Sanders, M.J., Grondin, P.O., Hegarty, B.D., Snowden, M.A., and Carling, D. (2007) Investigating the mechanism for AMP activation of the AMP-activated protein kinase cascade. *Biochem. J.*, **403**, 139–148.

Santiquet, N.W., Develle, Y., Laroche, A., Robert, C., and Richard, F.J. (2012) Regulation of gap junctional communication between cumulus cells during *in vitro* maturation in swine, a gap-FRAP study. *Biol. Reprod.*, **87**, 1–8.

Santiquet, N., Robert, C., and Richard, F.J. (2013) The dynamics of connexin expression, degradation and localisation are regulated by gonadotropins during the early stages of *in vitro* maturation of swine oocytes. *PLoS One*, **8**, e68456.

Santiquet, N., Papillon-Dion, E., Djender, N., Guillemette, C., and Richard, F.J. (2014a) New elements in the C-type natriuretic peptide signaling pathway inhibiting swine *in vitro* oocyte meiotic resumption. *Biol. Reprod.*, **91**, 16.

Santiquet, N., Sasseville, M., Laforest, M., Guillemette, C., Gilchrist, R.B., and Richard, F.J. (2014b) Activation of 5′ adenosine monophosphate-activated protein kinase blocks cumulus cell expansion through inhibition of protein synthesis during *in vitro* maturation in swine. *Biol. Reprod.*, **91**, 51.

Sasseville, M., Cote, N., Guillemette, C., and Richard, F.J. (2006) New insight into the role of phosphodiesterase 3A in porcine oocyte maturation. *BMC Dev. Biol.*, **6**, 47.

Sasseville, M., Cote, N., Vigneault, C., Guillemette, C., and Richard, F.J. (2007) 3′5′-Cyclic adenosine monophosphate-dependent upregulation of phosphodiesterase type 3A in porcine cumulus cells. *Endocrinology*, **148**, 1858–1867.

Sasseville, M., Cote, N., Gagnon, M.C., and Richard, F.J. (2008) Up-regulation of 3′5′-cyclic guanosine monophosphate-specific phosphodiesterase in the porcine cumulus–oocyte complex affects steroidogenesis during *in vitro* maturation. *Endocrinology*, **149**, 5568–5576.

Sasseville, M., Albuz, F.K., Cote, N., Guillemette, C., Gilchrist, R.B., and Richard, F.J. (2009a) Characterization of novel phosphodiesterases in the bovine ovarian follicle. *Biol. Reprod.*, **81**, 415–425.

Sasseville, M., Gagnon, M.C., Guillemette, C., Sullivan, R., Gilchrist, R.B., and Richard, F.J. (2009b) Regulation of gap junctions in porcine cumulus–oocyte complexes: contributions of granulosa cell contact, gonadotropins, and lipid rafts. *Mol. Endocrinol.*, **23**, 700–710.

Sato, Y., Cheng, Y., Kawamura, K., Takae, S., and Hsueh, A.J. (2012) C-type natriuretic peptide stimulates ovarian follicle development. *Mol. Endocrinol.*, **26**, 1158–1166.

Scarchilli, L., Camaioni, A., Bottazzi, B., Negri, V., Doni, A., Deban, L., Bastone, A., Salvatori, G., Mantovani, A., Siracusa, G. *et al.* (2007) PTX3 interacts with inter-alpha-trypsin inhibitor: implications for hyaluronan organization and cumulus oophorus expansion. *J. Biol. Chem.*, **282**, 30161–30170.

Schams, D., Berisha, B., Kosmann, M., Einspanier, R., and Amselgruber, W.M. (1999) Possible role of growth hormone, IGFs, and IGF-binding proteins in the regulation of ovarian function in large farm animals. *Domest. Anim. Endocrinol.*, **17**, 279–285.

Schirger, J.A., Heublein, D.M., Chen, H.H., Lisy, O., Jougasaki, M., Wennberg, P.W., and Burnett, J.C. Jr. (1999) Presence of Dendroaspis natriuretic peptide-like immunoreactivity in human plasma and its increase during human heart failure. *Mayo Clin. Proc.*, **74**, 126–130.

Schulz-Knappe, P., Forssmann, K., Herbst, F., Hock, D., Pipkorn, R., and Forssmann, W.G. (1988) Isolation and structural analysis of "urodilatin," a new peptide of the cardiodilatin-(ANP)-family, extracted from human urine. *Klin. Wochenschr.*, **66**, 752–759.

Schweitz, H., Vigne, P., Moinier, D., Frelin, C., and Lazdunski, M. (1992) A new member of the natriuretic peptide family is present in the venom of the green mamba (Dendroaspis angusticeps) *J. Biol. Chem.*, **267**, 13928–13932.

Downloaded From Vet-eBooks.com

Sela-Abramovich, S., Edry, I., Galiani, D., Nevo, N., and Dekel, N. (2006) Disruption of gap junctional communication within the ovarian follicle induces oocyte maturation. *Endocrinology*, **147**, 2280–2286.

Sela-Abramovich, S., Galiani, D., Nevo, N., and Dekel, N. (2008) Inhibition of rat oocyte maturation and ovulation by nitric oxide: mechanism of action. *Biol. Reprod.*, **78**, 1111–1118.

Shimada, M. and Terada, T. (2002) FSH and LH induce progesterone production and progesterone receptor synthesis in cumulus cells: a requirement for meiotic resumption in porcine oocytes. *Mol. Hum. Reprod.*, **8**, 612–618.

Shimada, M., Hernandez-Gonzalez, I., Gonzalez-Robayna, I., and Richards, J.S. (2006) Paracrine and autocrine regulation of epidermal growth factor-like factors in cumulus oocyte complexes and granulosa cells: key roles for prostaglandin synthase 2 and progesterone receptor. *Mol. Endocrinol.*, **20**, 1352–1365.

Shimizu-Albergine, M., Tsai, L.C., Patrucco, E., and Beavo, J.A. (2012) cAMP-specific phosphodiesterases 8A and 8B, essential regulators of Leydig cell steroidogenesis. *Mol. Pharmacol.*, **81**, 556–566.

Shitsukawa, K., Andersen, C.B., Richard, F.J., Horner, A.K., Wiersma, A., van Duin, M., and Conti, M. (2001) Cloning and characterization of the cyclic guanosine monophosphate-inhibited phosphodiesterase PDE3A expressed in mouse oocyte. *Biol. Reprod.*, **65**, 188–196.

Shu, Y.M., Zeng, H.T., Ren, Z., Zhuang, G.L., Liang, X.Y., Shen, H.W., Yao, S.Z., Ke, P.Q., and Wang, N.N. (2008) Effects of cilostamide and forskolin on the meiotic resumption and embryonic development of immature human oocytes. *Hum. Reprod.*, **23**, 504–513.

Shupe, J., Cheng, J., Puri, P., Kostereva, N., and Walker, W.H. (2011) Regulation of Sertoli-germ cell adhesion and sperm release by FSH and nonclassical testosterone signaling. *Mol. Endocrinol.*, **25**, 238–252.

Silvestre, M.A., Alfonso, J., Garcia-Mengual, E., Salvador, I., Duque, C.C., and Molina, I. (2007) Effect of recombinant human follicle-stimulating hormone and luteinizing hormone on *in vitro* maturation of porcine oocytes evaluated by the subsequent *in vitro* development of embryos obtained by *in vitro* fertilization, intracytoplasmic sperm injection, or parthenogenetic activation. *J. Anim. Sci.*, **85**, 1156–1160.

Simon, A.M., Goodenough, D.A., Li, E., and Paul, D.L. (1997) Female infertility in mice lacking connexin 37. *Nature*, **385**, 525–529.

Sirard, M.A. and First, N.L. (1988) *In vitro* inhibition of oocytes nuclear maturation in the bovine. *Biol. Reprod.*, **39**, 229–234.

Sirard, M.A., Richard, F., Blondin, P., and Robert, C. (2006) Contribution of the oocyte to embryo quality. *Theriogenology*, **65**, 126–136.

Soderling, S.H., Bayuga, S.J., and Beavo, J.A. (1998) Cloning and characterization of a cAMP-specific cyclic nucleotide phosphodiesterase. *Proc. Natl. Acad. Sci. USA*, **95**, 8991–8996.

Sohl, G. and Willecke, K. (2003) An update on connexin genes and their nomenclature in mouse and man. *Cell Commun. Adhes.*, **10**, 173–180.

Solan, J.L. and Lampe, P.D. (2005) Connexin phosphorylation as a regulatory event linked to gap junction channel assembly. *Biochim. Biophys. Acta*, **1711**, 154–163.

Sonntag, B., Gotte, M., Wulfing, P., Schuring, A.N., Kiesel, L., and Greb, R.R. (2005) Metformin alters insulin signaling and viability of human granulosa cells. *Fertil. Steril.*, **84** (Suppl. 2), 1173–1179.

Suga, S., Nakao, K., Hosoda, K., Mukoyama, M., Ogawa, Y., Shirakami, G., Arai, H., Saito, Y., Kambayashi, Y., Inouye, K. *et al.* (1992) Receptor selectivity of natriuretic peptide family, atrial natriuretic peptide, brain natriuretic peptide, and C-type natriuretic peptide. *Endocrinology*, **130**, 229–239.

Sutovsky, P., Flechon, J.E., Flechon, B., Motlik, J., Peynot, N., Chesne, P., and Heyman, Y. (1993) Dynamic changes of gap junctions and cytoskeleton during *in vitro* culture of cattle oocyte cumulus complexes. *Biol. Reprod.*, **49**, 1277–1287.

Downloaded From Vet-eBooks.com

Sutton-McDowall, M.L., Gilchrist, R.B., and Thompson, J.G. (2004) Cumulus expansion and glucose utilisation by bovine cumulus–oocyte complexes during *in vitro* maturation: the influence of glucosamine and follicle-stimulating hormone. *Reproduction*, **128**, 313–319.

Sutton-McDowall, M.L., Gilchrist, R.B., and Thompson, J.G. (2005) Effect of hexoses and gonadotrophin supplementation on bovine oocyte nuclear maturation during *in vitro* maturation in a synthetic follicle fluid medium. *Reprod. Fertil. Dev.*, **17**, 407–415.

Sutton-McDowall, M.L., Mitchell, M., Cetica, P., Dalvit, G., Pantaleon, M., Lane, M., Gilchrist, R.B., and Thompson, J.G. (2006) Glucosamine supplementation during *in vitro* maturation inhibits subsequent embryo development: possible role of the hexosamine pathway as a regulator of developmental competence. *Biol. Reprod.*, **74**, 881–888.

Suzuki, M., Kobayashi, H., Tanaka, Y., Kanayama, N., and Terao, T. (2004) Reproductive failure in mice lacking inter-alpha-trypsin inhibitor (ITI): ITI target genes in mouse ovary identified by microarray analysis. *J. Endocrinol.*, **183**, 29–38.

Tamura, N., Ogawa, Y., Chusho, H., Nakamura, K., Nakao, K., Suda, M., Kasahara, M., Hashimoto, R., Katsuura, G., Mukoyama, M. *et al.* (2000) Cardiac fibrosis in mice lacking brain natriuretic peptide. *Proc. Natl. Acad. Sci. USA*, **97**, 4239–4244.

Thomas, R.E., Armstrong, D.T., and Gilchrist, R.B. (2002) Differential effects of specific phosphodiesterase isoenzyme inhibitors on bovine oocyte meiotic maturation. *Dev. Biol.*, **244**, 215–225.

Thomas, R.E., Armstrong, D.T., and Gilchrist, R.B. (2004a) Bovine cumulus cell–oocyte gap junctional communication during *in vitro* maturation in response to manipulation of cell-specific cyclic adenosine 3′,5′-monophosphate levels. *Biol. Reprod.*, **70**, 548–556.

Thomas, R.E., Thompson, J.G., Armstrong, D.T., and Gilchrist, R.B. (2004b) Effect of specific phosphodiesterase isoenzyme inhibitors during *in vitro* maturation of bovine oocytes on meiotic and developmental capacity. *Biol. Reprod.*, **71**, 1142–1149.

Thompson, J.G. (2006) The impact of nutrition of the cumulus oocyte complex and embryo on subsequent development in ruminants. *J. Reprod. Dev.*, **52**, 169–175.

Tornell, J., Brannstrom, M., and Hillensjo, T. (1984) Different effects of cyclic nucleotide derivatives upon the rat oocyte–cumulus complex *in vitro*. *Acta Physiol. Scand.*, **122**, 507–513.

Tornell, J., Billig, H., and Hillensjo, T. (1990a) Resumption of rat oocyte meiosis is paralleled by a decrease in guanosine 3′,5′-cyclic monophosphate (cGMP) and is inhibited by microinjection of cGMP. *Acta Physiol. Scand.*, **139**, 511–517.

Tornell, J., Carlsson, B., and Billig, H. (1990b) Atrial natriuretic peptide inhibits spontaneous rat oocyte maturation. *Endocrinology*, **126**, 1504–1508.

Tosca, L., Froment, P., Solnais, P., Ferre, P., Foufelle, F., and Dupont, J. (2005) Adenosine 5′-monophosphate-activated protein kinase regulates progesterone secretion in rat granulosa cells. *Endocrinology*, **146**, 4500–4513.

Tosca, L., Uzbekova, S., Chabrolle, C., and Dupont, J. (2007) Possible role of 5′AMP-activated protein kinase in the metformin-mediated arrest of bovine oocytes at the germinal vesicle stage during *in vitro* maturation. *Biol. Reprod.*, **77**, 452–465.

Tsafriri, A., Chun, S.Y., Zhang, R., Hsueh, A.J., and Conti, M. (1996) Oocyte maturation involves compartmentalization and opposing changes of cAMP levels in follicular somatic and germ cells: studies using selective phosphodiesterase inhibitors. *Dev. Biol.*, **178**, 393–402.

Tsai, E.M., Yang, Y.Y., Lee, T.T., Chang, Y., Li, S., and Lee, J.N. (2005) Atrial natriuretic peptide inhibits ovarian functions in female mice. *Eur. J. Obstet. Gynecol. Reprod. Biol.*, **119**, 215–218.

Ungar, G., Freedman, L., and Shapiro, S.L. (1957) Pharmacological studies of a new oral hypoglycemic drug. *Proc. Soc. Exp. Biol. Med.* **95**, 190–192.

Downloaded From Vet-eBooks.com

Vaccari, S., Weeks, J.L. 2nd, Hsieh, M., Menniti, F.S., and Conti, M. (2009) Cyclic GMP signaling is involved in the luteinizing hormone-dependent meiotic maturation of mouse oocytes. *Biol. Reprod.*, **81**, 595–604.

Valdimarsson, G., De Sousa, P.A., and Kidder, G.M. (1993) Coexpression of gap junction proteins in the cumulus–oocyte complex. *Mol. Reprod. Dev.*, **36**, 7–15.

Vanhoutte, L., De Sutter, P., Nogueira, D., Gerris, J., Dhont, M., and van der Elst, J. (2007) Nuclear and cytoplasmic maturation of *in vitro* matured human oocytes after temporary nuclear arrest by phosphodiesterase 3-inhibitor. *Hum. Reprod.*, **22**, 1239–1246.

Vanhoutte, L., Nogueira, D., Dumortier, F., and De Sutter, P. (2009) Assessment of a new *in vitro* maturation system for mouse and human cumulus-enclosed oocytes: three-dimensional prematuration culture in the presence of a phosphodiesterase 3-inhibitor. *Hum. Reprod.*, **24**, 1946–1959.

Vasta, V., Shimizu-Albergine, M., and Beavo, J.A. (2006) Modulation of Leydig cell function by cyclic nucleotide phosphodiesterase 8A. *Proc. Natl. Acad. Sci. USA*, **103**, 19925–19930.

Velazquez, E.M., Mendoza, S., Hamer, T., Sosa, F., and Glueck, C.J. (1994) Metformin therapy in polycystic ovary syndrome reduces hyperinsulinemia, insulin resistance, hyperandrogenemia, and systolic blood pressure, while facilitating normal menses and pregnancy. *Metabolism*, **43**, 647–654.

Vivarelli, E., Conti, M., De Felici, M., and Siracusa, G. (1983) Meiotic resumption and intracellular cAMP levels in mouse oocytes treated with compounds which act on cAMP metabolism. *Cell Differ.*, **12**, 271–276.

Wang, S., Ning, G., Chen, X., Yang, J., Ouyang, H., Zhang, H., Tai, P., Mu, X., Zhou, B., Zhang, M. *et al.* (2008) PDE5 modulates oocyte spontaneous maturation via cGMP–cAMP but not cGMP–PKG signaling. *Front. Biosci.*, **13**, 7087–7095.

Wang, H.X., Tong, D., El-Gehani, F., Tekpetey, F.R., and Kidder, G.M. (2009) Connexin expression and gap junctional coupling in human cumulus cells: contribution to embryo quality. *J. Cell. Mol. Med.*, **13**, 972–984.

Wayne, C.M., Fan, H.Y., Cheng, X., and Richards, J.S. (2007) Follicle-stimulating hormone induces multiple signaling cascades: evidence that activation of Rous sarcoma oncogene, RAS, and the epidermal growth factor receptor are critical for granulosa cell differentiation. *Mol. Endocrinol.*, **21**, 1940–1957.

Weber, P.A., Chang, H.C., Spaeth, K.E., Nitsche, J.M., and Nicholson, B.J. (2004) The permeability of gap junction channels to probes of different size is dependent on connexin composition and permeant-pore affinities. *Biophys. J.*, **87**, 958–973.

Wei, Z., Cao, Y., Cong, L., Zhou, P., Zhang, Z., and Li, J. (2008) Effect of metformin pretreatment on pregnancy outcome of *in vitro* matured oocytes retrieved from women with polycystic ovary syndrome. *Fertil. Steril.*, **90**, 1149–1154.

Whittaker, K.L., Ding, D., Fisher, W.W., and Lipshitz, H.D. (1999) Different 3′ untranslated regions target alternatively processed hu-li tai shao (hts) transcripts to distinct cytoplasmic locations during Drosophila oogenesis. *J. Cell Sci.*, **112** (Part 19), 3385–3398.

Wiersma, A., Hirsch, B., Tsafriri, A., Hanssen, R.G., van de Kant, M., Kloosterboer, H.J., Conti, M., and Hsueh, A.J. (1998) Phosphodiesterase 3 inhibitors suppress oocyte maturation and consequent pregnancy without affecting ovulation and cyclicity in rodents. *J. Clin. Invest.*, **102**, 532–537.

Wigglesworth, K., Lee, K.B., Emori, C., Sugiura, K., and Eppig, J.J. (2014) Transcriptomic diversification of developing cumulus and mural granulosa cells in mouse ovarian follicles. *Biol. Reprod.*, **5**, 121756.

Winder, W.W. and Hardie, D.G. (1996) Inactivation of acetyl-CoA carboxylase and activation of AMP-activated protein kinase in muscle during exercise. *Am. J. Physiol.*, **270**, E299–E304.

Downloaded From Vet-eBooks.com

Wolvetang, E.J., Pera, M.F., and Zuckerman, K.S. (2007) Gap junction mediated transport of shRNA between human embryonic stem cells. *Biochem. Biophys. Res. Commun.*, **363**, 610–615.

Woods, A., Johnstone, S.R., Dickerson, K., Leiper, F.C., Fryer, L.G., Neumann, D., Schlattner, U., Wallimann, T., Carlson, M., and Carling, D. (2003) LKB1 is the upstream kinase in the AMP-activated protein kinase cascade. *Curr. Biol.*, **13**, 2004–2008.

Wright, C.S., Becker, D.L., Lin, J.S., Warner, A.E., and Hardy, K. (2001) Stage-specific and differential expression of gap junctions in the mouse ovary: connexin-specific roles in follicular regulation. *Reproduction*, **121**, 77–88.

Yamashita, Y., Kawashima, I., Yanai, Y., Nishibori, M., Richards, J.S., and Shimada, M. (2007) Hormone-induced expression of tumor necrosis factor alpha-converting enzyme/A disintegrin and metalloprotease-17 impacts porcine cumulus cell oocyte complex expansion and meiotic maturation via ligand activation of the epidermal growth factor receptor. *Endocrinology*, **148**, 6164–6175.

Yamashita, Y., Kawashima, I., Gunji, Y., Hishinuma, M., and Shimada, M. (2010) Progesterone is essential for maintenance of Tace/Adam17 mRNA expression, but not EGF-like factor, in cumulus cells, which enhances the EGF receptor signaling pathway during *in vitro* maturation of porcine COCs. *J. Reprod. Dev.*, **56**, 315–323.

Yamashita, Y., Okamoto, M., Ikeda, M., Okamoto, A., Sakai, M., Gunji, Y., Nishimura, R., Hishinuma, M., and Shimada, M. (2014) Protein kinase C (PKC) increases TACE/ADAM17 enzyme activity in porcine ovarian somatic cells, which is essential for granulosa cell luteinization and oocyte maturation. *Endocrinology*, **155**, 1080–1090.

Zeleznik, A.J., Saxena, D., and Little-Ihrig, L. (2003) Protein kinase B is obligatory for follicle-stimulating hormone-induced granulosa cell differentiation. *Endocrinology*, **144**, 3985–3994.

Zhang, M., Tao, Y., Zhou, B., Xie, H., Wang, F., Lei, L., Huo, L., Sun, Q., and Xia, G. (2005) Atrial natriuretic peptide inhibits the actions of FSH and forskolin in meiotic maturation of pig oocytes via different signalling pathways. *J. Mol. Endocrinol.*, **34**, 459–472.

Zhang, M., Su, Y.Q., Sugiura, K., Xia, G., and Eppig, J.J. (2010) Granulosa cell ligand NPPC and its receptor NPR2 maintain meiotic arrest in mouse oocytes. *Science*, **330**, 366–369.

Zhang, M., Su, Y.Q., Sugiura, K., Wigglesworth, K., Xia, G., and Eppig, J.J. (2011a) Estradiol promotes and maintains cumulus cell expression of natriuretic peptide receptor 2 (NPR2) and meiotic arrest in mouse oocytes *in vitro*. *Endocrinology*, **152**, 4377–4385.

Zhang, Y., Wu, J., Yu, G., Chen, Z., Zhou, X., Zhu, S., Li, R., and Lu, Q. (2011b) A novel natriuretic peptide from the cobra venom. *Toxicon*, **57**, 134–140.

Zhang, W., Chen, Q., Yang, Y., Liu, W., Zhang, M., Xia, G., and Wang, C. (2014a) Epidermal growth factor-network signaling mediates luteinizing hormone regulation of BNP and CNP and their receptor NPR2 during porcine oocyte meiotic resumption. *Mol. Reprod. Dev.*, **81**, 1030–1041.

Zhang, Y., Hao, X., Xiang, X., Wei, K., Xia, G., and Zhang, M. (2014b) Porcine natriuretic peptide type B (pNPPB) maintains mouse oocyte meiotic arrest via natriuretic peptide receptor 2 (NPR2) in cumulus cells. *Mol. Reprod. Dev.*, **81**, 462–469.

Zhang, W., Yang, Y., Liu, W., Chen, Q., Wang, H., Wang, X., Zhang, Y., Zhang, M., and Xia, G. (2015) Brain natriuretic peptide and C-type natriuretic peptide maintain porcine oocyte meiotic arrest. *J. Cell Physiol.*, **230**, 71–81.

Zheng, D., MacLean, P.S., Pohnert, S.C., Knight, J.B., Olson, A.L., Winder, W.W., and Dohm, G.L. (2001) Regulation of muscle GLUT-4 transcription by AMP-activated protein kinase. *J. Appl. Physiol.*, **91**, 1073–1083.

Zhou, G., Myers, R., Li, Y., Chen, Y., Shen, X., Fenyk-Melody, J., Wu, M., Ventre, J., Doebber, T., Fujii, N. *et al.* (2001) Role of AMP-activated protein kinase in mechanism of metformin action. *J. Clin. Invest.*, **108**, 1167–1174.

Downloaded From Vet-eBooks.com

9

Pig Models of Reproduction

B.R. Mordhorst[1] *and R.S. Prather*[1,2]

[1]*Division of Animal Science, University of Missouri-Columbia, Columbia, USA*
[2]*National Swine Resource and Research Center, University of Missouri-Columbia, Columbia, USA*

9.1 Introduction

Genetically modified swine serve as recognized models in agriculture and biomedicine (Forabosco *et al*., 2013; Li and Li, 2012; Luo *et al*., 2012b; Meurens *et al*., 2012; Petters and Sommer, 2000; Prather *et al*., 2003, 2008, 2013; Prather, 2013; Whyte and Prather, 2011). Generation of swine biomedical models is in part largely due to insufficiency or inadequacy of other models to exhibit the complete pathological condition experienced in humans (Prather *et al*., 2013). Even before the advent of new innovations in gene modification, pigs were appreciated for their physiological similarity to humans in surgical and toxicology testing (Bode *et al*., 2010; Swindle *et al*., 1994, 2012). While existing pig models have been developed for many pathological conditions, including cardiovascular diseases, cystic fibrosis, various cancers, degenerative eye diseases, dermatological conditions, metabolic diseases, muscular atrophies, neurodegenerative disease, osteoporosis, and organ failure—reviewed in Fan and Lai (2013), Luo *et al*. (2012b), Petters and Sommer (2000), and Prather *et al*. (2013)—pigs are also useful models for human reproduction. This chapter will highlight literature evidencing the benefits and use of pigs in areas of human reproduction.

9.2 Early Embryonic Development

Rodents have long prevailed as translational models. A significant portion of our founding reproductive knowledge is based on mouse, rat, guinea pig, and hamster research. Early mouse embryo culture work by Brinster (1965a, 1965b) established many fundamental requirements of culture media for all mammalian species. Nevertheless, there is evidence that in certain areas of human reproduction, the pig may be a worthy alternative to rodents. A field of study where swine may be the most suitable model is embryo development to the blastocyst stage. In the United States, there is a growing trend of couples seeking assisted reproductive therapies (ART). Each year more children are conceived *in vitro*, further illustrating the importance of optimizing culture conditions for embryonic metabolism and proper epigenetic programming. The Centers for Disease Control and Prevention report that over 1% of all infants born every year are conceived using ART in the United States (CDC, 2014). Hoffman *et al*. (2003) estimated that there were nearly 400,000 embryos cryogenically stored in reporting U.S. clinics (almost 80%),

Animal Models and Human Reproduction, First Edition. Edited by Heide Schatten and Gheorghe M. Constantinescu.
© 2017 John Wiley & Sons, Inc. Published 2017 by John Wiley & Sons, Inc.

Downloaded From Vet-eBooks.com

only 2.8% were donated for research; however, many of these were of lesser quality and unable to grow at normal rates rendering them less than optimal for research. In addition to the quality and number of available human embryos, Niakan *et al.* (2012) noted that the main hurdles to obtaining reliable human embryo gene expression data are the challenges of obtaining and analyzing gene expression in single oocytes, embryos, or blastomeres. Porcine ovaries can overcome this challenge as they typically can be easily obtained from slaughter facilities in large quantities, and each ovary has several follicles that can be aspirated for use in *in vitro* maturation (IVM) and *in vitro* fertilization (IVF).

Numbers of embryos are not limited in porcine culture as thousands of oocytes can easily be processed each week. These oocytes are relatively inexpensive, and the oocytes and embryos are larger than those of mouse (60 versus 120 μm diameter, thus ~10× the volume) and have almost twice the RNA (Olszanska and Borgul, 1993) and more protein, making it easier to isolate enough material for analysis, and easier to inject with reagents. Incidentally, the reagents that are developed for humans generally work for pigs, as there is more amino acid conservation in proteins between humans and pigs compared to humans and mice. The swine genome is also very similar to the human, as a phylogenetic approach shows that the swine genome is three times closer to the human than to the mouse, and on average the synteny blocks of swine–human are further down the phylogenetic tree than the mouse or dog (Wernersson *et al.*, 2005). Moreover, the pig embryo may arguably be the large domestic species that has been most rigorously studied *in vitro* partly due to its importance as in biomedicine, but also for its accessibility for use in culture (Sun and Nagai, 2003). This is evidenced by a number of reviews documenting the extensive research of porcine IVF and IVM (Abeydeera, 2001, 2002; Bauer *et al.*, 2010; Coy and Romar, 2002; Kątska-Książkiewicz, 2006a, 2006b; Long *et al.*, 1999; Machaty *et al.*, 1998; Nagai, 2001; Nagai *et al.*, 2006; Prather and Day, 1998; Sun and Nagai, 2003). A comparison of many of the similar parameters discussed in the following sections is provided in Table 9.1.

Table 9.1 Comparison of pig, human, and mouse embryogenesis.

	Pig	Human	Mouse
Days viable in culture postfertilization	7	7	4
Cell stage at embryonic genome activation	4	4	2
Germinal vesicle breakdown (h)[a)]	20	20	2–5
Germline competent ESCs available[b)]	No	No	Yes
Cytoskeletal dynamics			
Meiotic spindle number	2	2	1
Microtubule organization	Sperm aster extends through oocyte cytoplasm	Sperm aster extends through oocyte cytoplasm	Cytoplasmic asters within mature oocytes
Microtubule polarity	Not observed	Not observed	Highly polar
Centrosome inheritance	Paternal	Paternal	Maternal
Oxidative phosphorylation dependence[c)]	No	No	Yes

a) Hours post luteinizing hormone surge.
b) ESCs = Embryonic stem cells.
c) Dependent on oxidative phosphorylation prior to implantation.

Downloaded From Vet-eBooks.com

9.3 Oocyte Maturation

Several have noted that "porcine oocytes are closely related to human oocytes in terms of morphology and timing of meiotic maturation" (Ellederova *et al*., 2004; Ješeta and Bodart, 2012; Vodicka *et al*., 2005). In swine and human oocytes, germinal vesicle breakdown occurs after about 20 h (Edwards, 1965); however, in mice this occurs within a few hours (Wassarman *et al*., 1976). In mice the average timing to metaphase II is strain dependent, but is on average 7–13 h post luteinizing hormone surge, whereas in humans and swine this occurs after about 40 h (Ješeta and Bodart, 2012; Niakan *et al*., 2012).

While there is parallelism of meiotic stages between porcine and human oocytes, they also share an increase in meiotic abnormalities. Aneuploidy is characteristically a dire condition where via meiotic nondisjunction an abnormal number of chromosomes (monosomy or trisomy) are segregated to the oocyte. Most aneuploid pregnancies result in fetal death and those surviving to term commonly have mental retardation (i.e., the condition of Down syndrome, trisomy of chromosome 21). In humans, aneuploidy is a leading cause of miscarriage, congenital birth defects, and mental retardation (Hassold and Hunt, 2001). While further research is warranted, a review by Nagaoka *et al*. (2012) estimates the aneuploidy incidence at conception in humans to be at least 10%; although it may be possibly as high as 50%. Hornak *et al*. (2012) reported 4.7% of *in vivo* porcine morulas and blastocysts carry a chromosome abnormality, 1.6% of which was true polyploidy and 46.8% mixoploidy. In any event, this is a much higher than incidence in other mammals; for example, in mice aneuploidy frequency within fertilized eggs is 1–2% (Bond and Chandley, 1983). There is a significant need for a better model of aneuploidy, and some researchers have attempted to cause abnormalities by mating closely related species of mice, thereby causing mutations in genes regulating meiotic synapsis (reviewed in Hassold *et al*. (2007)). In swine, aneuploidy naturally occurs at a rate similar to humans and is estimated to be 11.9–21.6% (Koenig and Stormshak, 1993). Inglot *et al*. (2012) used a wild boar–domestic pig cross as a model for Robertsonian translocation, a whole-arm acrocentric chromosome translocation resulting in loss of short arms. In humans, Robertsonian translocation occurs at a frequency of 1/1000 people, the most regular occurring chromosomal rearrangement in our species (Therman *et al*., 1989).

There is some evidence that the effect of age on aneuploidy appears to be inverse between species: in pigs, young gilts have a higher frequency of aneuploidy (Lechniak *et al*., 2007); however, in humans, aged oocytes have a much higher incidence of aneuploidy and strong evidence (regarding maternal age and frequency of Down syndrome) of this has been long realized (Penrose, 2009). Thus, prepubertal pig ovaries may be a good model for aged oocytes in humans. It has already been suggested that the miniature pig may be an excellent model for human aneuploidy (Vodicka *et al*., 2005). Several studies have demonstrated the value of pigs for evaluation of aneuploidy via different methods: selection by brilliant cresyl blue test (Pawlak *et al*., 2011), *in situ* hybridization (Vozdova *et al*., 2001; Zudova *et al*., 2003), and genomic hybridization (Hornak *et al*., 2011, 2012). The frequency of aneuploidy as measured by genomic hybridization was 12.1 versus 8.7% in young versus older miniature pigs (Hornak *et al*., 2011); however, further verification with larger numbers of more genetically variable swine is warranted. Other pig experiments have provided useful culture advice regarding techniques that can increase the incidence of aneuploidy and include extended interval between electrofusion and activation in somatic cell nuclear transfer (You *et al*., 2010), maturation exceeding 40 h (Sosnowski *et al*., 2003), and that use of caffeine can help prevent or restore centrosome and spindle abnormality (Miao *et al*., 2009). Recent examination of swine aneuploidy has also provided insight into regulation of spindle assembly checkpoints (Brevini *et al*., 2012; Wei *et al*., 2014).

Downloaded From Vet-eBooks.com

9.4 Fertilization

In mouse oocytes, the main cause of fertilization failure is unsuccessful spermatozoa penetration, while the majority of fertilization failure in human and pig oocytes is a consequence of oocyte cytoplasm insufficiency to support pronuclear formation (Lee *et al*., 2003; Neuber and Powers, 2000). Additionally, human and swine zygotes have similar centriole inheritance where one centriole of paternal (proximal centriole of spermatozoon) origin is incorporated into the oocyte cytoplasm after fertilization (Sathananthan *et al*., 1996; Sutovsky and Schatten, 1999). Conversely, mice have only maternal inheritance of centrioles (Schatten *et al*., 1986). Swine also subsist in the literature as a valuable live animal model for assessing effects of toxicity on male fertility, including exposure to electromagnetic fields (Bernabò *et al*., 2007, 2010; Li *et al*., 2010) and the efficacy of spermicides (as well as irritability within the female tract) (D'cruz *et al*., 2005; D'Cruz and Uckun, 2007). Furthermore, pigs have been meticulously investigated for design of a zona pellucida immununocontraceptive vaccine, including the identification of epitopes for antibodies and interspecies testing (Afzalpurkar and Gupta, 1997; Afzalpurkar *et al*., 1997; Bartol *et al*., 2015; Gupta *et al*., 1995, 1996; Hasegawa *et al*., 1992, 1994, 1995, 2002; Kaul *et al*., 1996; Koyama *et al*., 1991, 1996; Samoylova *et al*., 2012; Shigeta *et al*., 2000).

9.5 Tubouterine Contractility

For conception, high levels of contractility and peristalsis are needed to transport sperm in natural or artificial insemination; in contrast, lower levels of activity may be required for implantation after IVF embryos are transferred; therefore, knowledge of controlling uterine activity and cyclicity is important for ART success. Insufficient levels of uterine activity can lead to ectopic pregnancy, abortion, endometriosis, and retrograde bleeding (Bulletti and De Ziegler, 2005; Kissler *et al*., 2005; Leyendecker *et al*., 2004). To further complicate matters, a shift in the balance of different prostaglandins likely has a causative role in preeclampsia (Friedman, 1988). Perfused swine uteri can remain physiologically active for up to 7 h post mortem and serve as a popular model for investigating uterine activity after pharmacological or hormonal treatment. Studies have investigated effects of various pharmacologic treatments on uterine contractility and peristalsis in swine uteri via oxytocic drugs (Dittrich *et al*., 2003, 2009; Muller *et al*., 2006), tocolytic drugs (Maltaris *et al*., 2006b), spasmolytic drugs (Kunzel *et al*., 2011, 2014), prostaglandins (Dittrich *et al*., 2009; Mueller *et al*., 2006a), estrogen (Maltaris *et al*., 2006a) and progesterone (Mueller *et al*., 2006b), muscarinic-receptor agonists (Dittrich *et al*., 2009), lysophosphatidic acid (Markiewicz *et al*., 2012), a vasoconstrictor (endothelin-1), and serum from pre-eclamptic women (Maltaris *et al*., 2005; Ducolomb *et al*., 2009).

9.6 Development to the Blastocyst Stage

Of the domestic livestock species, the pig has the most similar timing of development to the blastocyst stage compared to humans (Krisher, 2012). The pig embryo also mimics some of the temporal events of development as observed in human embryos; for example, the pig, human, and rat are the only known species that make the major transition from maternal control of development to zygotic control of development during the 4-cell stage (Braude *et al*., 1988; Prather, 1993). Some may argue that the human embryo begins transcription at the 8-cell stage, but Braude *et al*. (1988) showed (i) qualitative changes in protein synthesis between the 2-cell

Downloaded From Vet-eBooks.com

and 4-cell stages, (ii) α-amanitin treatment blocked development at the 4-cell stage (since α-amanitin blocks polymerase II-dependent RNA synthesis, it was concluded that transcription is necessary for cleavage to the 8-cell stage), and (iii) the change in the pattern of protein synthesis that occurs between the 2-cell and the 4-cell stages is α-amanitin sensitive. Clearly, significant transcription occurs during the 4-cell stage.

While the mouse has been used for a number of excellent studies in previous research, it has also been recognized that the mouse differs in a number of aspects from nonrodent mammals, which has resulted in increased research using the porcine system as representative for humans (reviewed in Schatten and Sun (2009, 2010, 2011a, 2011b, 2011c)); this is especially true for the early embryo stages in which cytoskeletal and mitochondrial dynamics are different in the mouse compared to nonrodent mammalian species. Also, in contrast to the mouse, where preimplantation development depends upon oxidative phosphorylation (Leese, 1991), human (Gott *et al*., 1990) and pig (Machaty *et al*., 2001) embryos do not have this dependency. The shift in mitochondrial morphology from immature to mature between the oocyte and blastocyst stages is also similar in human and pig embryos (Krisher and Prather, 2012).

9.7 Pregnancy and Developmental Programming

The pig placenta is an epitheliochorial diffuse type being less invasive of the maternal system than the hemochorial discoid-type placenta of humans that deeply decidualizes the uterus. While there may be six cellular layers between the piglet and its maternal blood supply, this difference actually has been useful in immunological studies because large macromolecules and maternally derived antibodies are not transferred across the placenta. However, the interhaemal distance (diffusion distance between maternal and fetal arterial supply) is not comparatively different among any of the placental types (Wooding and Flint, 1994). In the pig, the short distance is attributed to interdigitating microvilli as well as indentation of epithelia from both uterine and trophoblast layers (reviewed in Enders and Blankenship (1999) and (Enders and Carter, 2004)). In human, there is a pathological condition that occurs in instances where fetal spiral artery invasion (as well as other factors that are not known) is not deep enough into the maternal endometrial tissue; this condition is known as pre-eclampsia or a more serious complication eclampsia. Worldwide, preeclampsia or eclampsia is a leading cause of maternal and fetal mortality (MacKay *et al*., 2001; Roberts and Cooper, 2001). Preeclampsia typically leads to cases where infants are born premature (small for gestational age) and many of which experience intrauterine growth restriction (IUGR). These neonates typically have increased health impairments and morbidity. In both livestock species and humans, the intrauterine environment experienced by the neonate can affect programming of health and development postnataly (Barker, 1990, 1995; Godfrey and Barker, 2000; Murphy *et al*., 2006; Wu *et al*., 2006). Adequate fetal growth is supported by the placenta that itself must grow and acquire proper vascularity and function to support fetal growth. Reduced fetal and placental growth are characteristics of IUGR across a number of species (Wu *et al*., 2006), and pigs have been used for many of these studies (Table 9.2). Placental vascularity and growth is largely regulated by angiogenic factors, such as vascular endothelial growth factor (VEGF), produced in fetal and maternal tissues. Interestingly, in pigs the Meishan breed has increased VEGF expression, placental vascularity, and overall placental efficiency compared to common breeds such as Yorkshire (Biensen *et al*., 1998; Vonnahme and Ford, 2004; Wilson *et al*., 1998). The Meishan has been useful in studying placental control of fetal growth and the limiting factor of uterine capacity among breeds. Wu *et al*. (2006) noted: "Among

Downloaded From Vet-eBooks.com

Table 9.2 Impact of postnatal treatments after experiencing intrauterine growth restriction.

Reference	Treatment	Findings suggest
Che *et al.* (2015)[a)]	Global nutrient restriction	Nutrient restriction from 7 to 21 days of age after experiencing IUGR can potentially aid the IUGR piglet's susceptibility to oxidative stress and their reduced antioxidant defense
Krueger *et al.* (2014)	*Ad libitum* feeding after restriction	IUGR piglets nutrient restricted (57% energy intake of control) from 80 to 100 days of age then allowed *ad libitum* access had lighter final body weight at 131 days of age. During restrictive period, low birth weight restricted pigs had levels of 50% fat oxidation compared to pigs with normal birth weights
Han *et al.* (2013)[a)]	High global nutrition	Immune function impairment with increased nutrition (higher nutrient formulated milk from 7 to 21 days of age) in IUGR piglets
Liu *et al.* (2012a, 2014)[a)]	High fat	IUGR pigs fed high-fat diet (10% lard) after 5 months of age may increase probability of mitochondrial dysfunction. Second study demonstrates that the high-fat diet induces inflammatory response system
Morise *et al.* (2009)[a)]	Excess protein	High protein intake from 7 to 28 days of age reduced adiposity in both control and IUGR birth weight groups
Schoknecht *et al.* (1997)	Exogenous IGF-1	In IUGR piglets, exogenous IGF-1 delivery via osmotic minipump at the rate of 4 μg/h for 7 days restored body weight and composition to that of normal piglets within 7 days (10 days of age). IGF-1 infusion led to a slight increase in weight gain in both control and IUGR neonates
Attig *et al.* (2008)[a)]; Attig *et al.* (2013)[a)]	Leptin supply	In female piglets leptin injections (0.5 mg/kg) from 2–10 days of age increased weight and growth of organs involved in metabolic regulation, and restored normal levels of adiposity IUGR piglets. Morphological and functional maturation changes in several organs of IUGR piglets receiving leptin compared with controls indicating enhanced ovarian and immune maturity and digestive function

a) In studies, piglets were designated intrauterine growth restricted (IUGR) on the basis of weight difference from litter averages.

domestic animals, pigs exhibit the most severe, naturally occurring IUGR." In most pig breeds (excluding prolific and ancient breeds such as Meishans), fetuses distribute evenly within the uterus, and fetal development of each piglet is dependent on the limited uterine capacity and position of other fetuses (Anderson and Parker, 1976; Knight *et al.*, 1977). Due to this spacing and capacity, piglets near the uterotubal junction and the cervix are typically largest and there are usually some piglets within the litter that will be much smaller 'runts' and are growth restricted if they had limited placental surface area for nutrient exchange within the uterus (Perry and Rowell, 1969).

Somatic cell nuclear transfer (SCNT), a process for reprogramming cells, is comparatively more popular in swine than in human and mouse due to the lack of readily available porcine embryonic stem cells (pESCs). Availability of pESCs is impeded by several factors: (i) challenges of culturing the cells, (ii) achieving pluripotency in the cells, and (iii) few validated successful pESC protocols (Brevini *et al.*, 2007; Hall, 2008; Piedrahita *et al.*, 1990). Piglets derived from SCNT are recounted to have common developmental abnormalities such

Downloaded From Vet-eBooks.com

as macroglossia, muscle weakness, poor abdominal muscle development near the umbilicus (exophalos), high as well as low birth weights, and increased mortality (reviewed in (Estrada *et al.* (2007); Li *et al.* (2014a), and Piedrahita *et al.* (1990)). Many of these characteristics at birth are not dissimilar to the human condition Beckwith–Wiedemann syndrome, notorious as large offspring syndrome in domestic ruminants. Developmental incompetency associated with this condition is believed to be largely due to loss of parental imprinting and epigenetic modification occurring with assisted reproduction. A number of studies demonstrate alterations in DNA methylation and differences in gene expression to have long-term underlying roles in developmental programming, including multigenerational impacts (Li *et al.*, 2014b; Wei *et al.*, 2010).

Our laboratory has investigated and optimized techniques for detection of methylation differences between muscle tissue of cloned and *in vitro* produced piglets (Li *et al.*, 2014a), donor and embryo cells in nuclear transfer (Bonk *et al.*, 2007), as well as between blastocysts produced via SCNT, parthenogenetically, and *in vitro* (Bonk *et al.*, 2008). Additionally, we also examined ways to correct aberrant expression *in vitro* by use of the histone deacetylase inhibitors scriptaid and oxamflatin (Mao *et al.*, 2014; Whitworth *et al.*, 2011; Zhao *et al.*, 2010) as have other laboratories (Hou *et al.*, 2014). Moreover, we have explored programming impacts of nuclear remodeling (reviewed in Prather *et al.* (2004) as well as using deep sequencing techniques to reveal transcripts indicative of what *in vitro* embryos may be "asking for" (Bauer *et al.*, 2010; Prather *et al.*, 2014).

A phenotype of SCNT piglets that is not common in Beckwith–Wiedemann syndrome, but that is common with IUGR, is low birth weight. While cattle and sheep clones are commonly born oversized, Estrada *et al.* (2007) have indicated increased numbers of low-birth-weight or IUGR piglets compared to AI controls; however, there does not seem to be an effect between transgenic and nontransgenic clones (Kurome *et al.*, 2008). Several have observed structural deformity, aberrations in protein and gene expression, and changes in methylation in the placentas of pigs cloned by nuclear transfer (Cao *et al.*, 2014; Chae *et al.*, 2006; Lee *et al.*, 2007; Tian *et al.*, 2008; Wei *et al.*, 2010; Zhang *et al.*, 2014). Placental deficit due to these abnormalities restricts normal embryonic growth of tissues contributing to the SCNT phenotypes by limiting nutrient uptake and exchange with the maternal system.

Experimental models with reduced rates of placental blood flow and nutrient transfer include but are not limited to maternal nutrition (deficiency and excess), genotype, environmental stress, and disease (for reviews, see Reynolds *et al.* (2006) and Wu *et al.* (2006)). Examples of many IUGR conditions have been evaluated in pigs in the area of maternal nutrient status. Maternal nutrient restrictions, including nutrient restriction in obese dams (Ovilo *et al.*, 2014) and protein and energy restrictions (Atinmo *et al.*, 1974a, 1974b, 1976; Pond, 1973; Pond *et al.*, 1968, 1969; Schoknecht *et al.*, 1997; Wu *et al.*, 1998), have been studied in the pig (Table 9.3). Examples of nutritional supplementation in gestating pigs include arginine (reviewed in Wu *et al.* (2010, 2013)), L-glutamine (reviewed in Wu *et al.* (2010)), folic acid (Liu *et al.*, 2011, 2012b), and omega fatty acids (reviewed in (Kim *et al.* (2007)). Brief summaries of effects observed as a result of maternal gestational supplementation are listed in Table 9.4. Additionally, there are several investigations of treatment of piglets in postnatal life after having experienced IUGR *in utero*, and include effects-restricted intake (Che *et al.*, 2015), *ad libitum* feeding after restriction (Krueger *et al.*, 2014), high global nutrient intake (Han *et al.*, 2013), high fat intake (Liu *et al.*, 2012a, 2014), excess protein intake (Morise *et al.*, 2009), exogenous insulin-like growth factor-1 (Schoknecht *et al.*, 1997), and leptin supply (Attig *et al.*, 2008, 2013). There are advantages to using swine as models to examine effects of developmental programming. In addition to the obvious similarities in physiology, pigs are monogastric omnivores, have similar protein and lipid metabolism, and consume many foods and supplements within human diets

Downloaded From Vet-eBooks.com

Table 9.3 Effects of maternal nutrient restriction on piglet parameters.

Reference	Restriction	Effects compared to controls
Ovilo *et al.* (2014)	Global	Nutrient restriction (50% control diet) during last two-thirds of gestation in obese dams led to lower birth weights, plasma triglyceride concentrations, and expression of *HSD11B1*. Females from nutrient restricted dams presented elevated cortisol concentrations, decreased expression of two anorexic peptides, and continued to be heavier and fatter at 7 months of age
Pond *et al.* (1968)[a)]	Protein	No differences in birth weight, live pigs/litter, or serum protein level from 2 to 3 days of age compared with controls litters with restriction for last three-fourths of gestation
Pond *et al.* (1969)	Protein	At birth piglets from dams not receiving protein restriction until day 24 and those from control dams were similar in weight, whereas those whose dams were protein restricted until day 16 and then after day 20 were significantly lighter. Piglets from protein-restricted dams throughout gestation were lighter at birth than all other treatments
Atinmo *et al.* (1974a, 1974b)	Protein	Piglets from dams protein restricted throughout gestation had significantly reduced body, brain, and liver weights at birth. Blood hemoglobin, serum albumin, and brain RNA content at birth compared to piglets of control and energy-restricted dams. At 20 weeks of age, pigs from protein-restricted dams had lower body weight, backfat, and carcass length
Atinmo *et al.* (1976)	Protein	Piglets most restricted (0.5%) throughout pregnancy had elevated levels of growth hormone at 12 weeks of age even though fostered to control dams
Schoknecht *et al.* (1997)	Protein	At 3 days of age, piglets experiencing maternal restriction from day 63 of pregnancy to parturition were lighter, had lower levels of circulating IGF-1, and less total protein mass in their bodies
Wu *et al.* (1998)	Protein	Placental and endometrial tissue from protein-restricted dams at days 40 and 60 had decreased nitric oxide and polyamine synthesis (arginine and ornithine) implicated in vascular growth of the placenta and endometrium
Atinmo *et al.* (1974a, 1974b)	Energy	Piglets from energy-restricted dams (50% control diet intake) throughout gestation had similar birth weights, weaning weight, average daily gain, carcass parameters, and other growth measures compared with controls. Energy restriction during gestation decreased blood hemoglobin and serum albumin at birth

a) Experiment number 2 data reported.

compared to other ungulates. Additionally, pigs have a short generation interval, so the effects of programming, which may be multigenerational, can be observed in a shorter period of time. Concerns with effects of environmental toxins, hormones, antioxidants, and the possibility for preventative/therapeutic treatments have led to an increase in investigations of placental transfer. The ewe is an established translational model for pregnancy and has been used to study the impact of hormonal and environmental insults across the fetal–maternal placental interface (Corbel *et al.*, 2013; Dominguez *et al.*, 2013; Herreros *et al.*, 2010; Morel *et al.*, 2009; Morrison, 2008; Sheppard *et al.*, 2011; Wester-Rosenlof *et al.*, 2014). Investigators have tested efficacy and risk of late gestational treatment of allopurinol, a drug with antioxidant properties, in sows to reduce effects of birth asphyxia, and as a preventative therapy for placental insufficiency in low-birth-weight pregnancies (Gieling *et al.*, 2014; Prickaerts *et al.*, 2014; van Dijk *et al.*, 2008). These groups tested placental transfer of the drug as well as its effects on

Downloaded From Vet-eBooks.com

Table 9.4 Effects of maternal supplementation during gestation on piglet parameters.

Reference	Supplementation	Findings suggest
Reviewed in Wu *et al.* (2010, 2013)	Arginine	Supplementation with 0.80% L-arginine to dams consuming a typical gestation diet between days 14 and 28 or with 0.83% L-arginine in addition to a typical gestation diet between days 30 and 114 of pregnancy increases litter numbers and birth weights. Supplementation of 0.80% but not 0.40% L-arginine in gilts consuming a typical gestation diet from day 0 to 25 of gestation postbreeding reduced numbers of corpora lutea and progesterone concentrations perhaps explaining the reduction in litter size
Reviewed in Wu *et al.* (2010)	Glutamine and arginine	Supplementing the gestation diet with 0.4% L-arginine plus 0.6% L-glutamine is proposed to increase nutrient utilization, increase birth weights, and reduce variation of birth weight
Liu *et al.* (2011, 2012b)	Folic acid	Gene expression and one-carbon metabolism of hepatic tissue were augmented by maternal supplementation (30 mg/kg folic acid throughout gestation) indicating folic acid supplementation can help deter affects of IUGR. Several measures of gene expression and mitochondrial function were normalized to levels of non-IUGR piglets with folic acid supplementation
Reviewed in Kim *et al.* (2007)	Omega fatty acids	Supplementation of sows with omega fatty acids shows increases in omega-3 and omega -6 fatty acids in sow milk. Some studies have also indicated increases of these fatty acids in the piglet plasma, some tissues, growing conceptuses, and endometrium. There are also reports for improved postnatal growth, decreased preweaning mortality, and decreased birth weight, with mixed results on effect of litter size

markers of brain plasticity, field behavior, learning ability, and brain, hippocampus, and spleen weights. Results from these investigators indicate that late gestational treatment of allopurinol caused no adverse effects on measured parameters and may be a viable therapy for reducing effects of placental insufficiency in low-birth-weight pregnancies.

Notwithstanding, studies of transplacental transfer of antiarrhythmics in pig demonstrated that the pig has closer transplacental transfer to humans than that of the pregnant ewe model (Bode *et al.*, 2010; Wiest *et al.*, 1996). Measurement of blood flow in larger livestock species is easier than within small common laboratory species and can be done with ultrasound equipment that is used in human medicine. Umbilical and uterine blood flow in pigs can be measured as easily as other previously investigated species such as horse, cattle, and sheep. Effects of ovarian steroid hormones and the conceptus on uterine blood flow in swine have been elucidated as well as within other domestic livestock species (Ford, 1995; Ford and Christenson, 1979; Ford *et al.*, 1982a, 1982b, 1984a, 1984b; Ford and Stice, 1985; Reynolds *et al.*, 1985; Stice *et al.*, 1987). A study by Harris *et al.* (2013) measured umbilical blood flow to fetuses of sows that were lightly exercised three times a week to evaluate effects of maternal activity level on maternal behavior, maternal body condition, umbilical blood flow, *in utero* fetal growth, parturition characteristics, and fetal serum lactate levels at birth. Umbilical blood flow was increased by approximately 100 ml/min by day 84 of gestation in lightly exercised pigs; however, the exercise did not affect maternal weight, back fat, loin muscle area, or any measured fetal or placental parameters of size.

Downloaded From Vet-eBooks.com

9.8 Puberty

In addition to concerns regarding developmental programming and postnatal life, there has been a growing concern with early attainment of puberty. Precocious puberty has been on the rise in the United States and occurs in 1 in 5000 children (Cesario and Hughes, 2007). It has even been suggested (Kaplowitz and Oberfield, 1999) that the age of puberty should be lower (as low as 6 years of age in females). This proposal is refuted by many endocrinology societies deeming that this may lead to too many cases of abnormal puberty going undetected. Timing of puberty is affected by genetics, nutrition, and environment. Factors such as gender, race, and obesity are known to have an effect on timing of puberty (Kaplowitz *et al*., 2001). Work has focused on more recent concerns growing in the United States such as early puberty as a result of IUGR and/or low birth weight, environmental exposure to endocrine disrupting signals, and medical conditions such as congenital adrenal hyperplasia (reviews by Cesario and Hughes (2007), Dunger *et al*. (2006), Ong *et al*. (2004), Parker (1991), and Roy *et al*. (2009)).

It has long been recognized that infants whom experienced intrauterine growth restriction have rapid post-natal weight gain after alimentation to higher nutrition; indeed they are programmed to have a "thrifty phenotype". David Barker and coworkers recognized a suite of late-onset metabolic and cardiovascular complications associated with nutrient restriction in pregnancy (Barker, 1990; Barker, 1995, 1998; Godfrey and Barker, 2000). There is some evidence that calorie restriction without malnutrition can have long term positive effects on health (Omodei and Fontana, 2011; Speakman and Mitchell, 2011). Studies investigating the question as to whether caloric restriction after IUGR could reduce the chances of developing late-onset metabolic disorders are for many reasons not feasible in human experimentation. A study in swine by Nebendahl *et al*. (2013) evaluated the effect of low birth weight and subsequent caloric restriction on gene expression and lipid droplet number in juvenile gilt livers. This group demonstrated that a 3-week postnatal feed restriction of 60% control diet led to reduced lipid droplet area in gilts of low and normal birth weights (58.3 and 72%). Furthermore, low birth weight gilts had 3.7 times higher lipid droplet number, 4.6 times greater droplet area, as well as 194 differentially expressed genes in the liver compared to gilts with normal birth weight. In underfed pigs, an additional 5-week period of realimented feeding at control levels still did not augment expression levels of four genes involved in metabolism.

The timing of puberty after exposure to endocrine disrupting signals from environmental and dietary toxins was also previously modeled in swine. Studies in prepubertal boars focused on reproductive effects after exposure to di(2-ethylhexyl) phthalate (DEHP), a compound commonly found in plastics. Oral biweekly low dosage for a period of 6 weeks can cause changes in peripheral plasma-luteinizing hormone concentration (a critical hormone in the hypothalamic pituitary adrenal axis of puberty) and can cause precocious development of the bulbourethral glands (Ljungvall *et al*., 2006, 2008). An earlier experiment from this group examined intramuscular injection of DEHP and estradiol benzoate concentrations in hormone concentrations within plasma as well as testicular development. While estradiol benzoate decreased testicular body weight after 5 weeks of treatment, it also had long-term (7.5 months after exposure) effects on the weight of seminal vesicles. Exposure to DEHP increased testosterone concentration and Leydig cell area at 7.5 months of age (Ljungvall *et al*., 2005). Magolski *et al*. (2014) concluded that precocious puberty is not observed in gilts consuming either beef that was treated with growth implants (100 mg trenbolone acetate and 14 mg estradiol benzoate) or tofu; however, with the tofu diet, estrogen equivalents were 570 times the control and approximately 170 times the implanted supplements. These studies have important implications for American diets and considerations of the increasing numbers of adolescents experiencing precocious puberty.

Downloaded From Vet-eBooks.com

9.9 Reproductive Disease

Pigs are employed as models for aberrant ovarian situations such as polycystic syndrome and cancer. To achieve a polycystic condition, sows and gilts can be treated with dexamethasone mid estrous cycle; studies have investigated steroidogenic activity and innervation (Dzienis *et al*., 2004; Kozlowska *et al*., 2009, 2011, 2013). Polycystic ovary syndrome affects 5% of women within reproductive age (Solomon, 1999). This condition occurs in swine and some studies have used these noninduced ovaries in experimentation (Salih *et al*., 2008; Szulanczyk, 2009). However, some researchers have taken advantage of the frequent naturally occurring polycystic ovary syndrome in the Ossabaw Island pig that has been characterized to have very suitable endocrine and follicular parameters for studying this syndrome (Aye *et al*., 2014; Krisher *et al*., 2006, 2008; Lowe *et al*., 2007; Newell-Fugate, 2013; Newell-Fugate *et al*., 2010, 2011). The Ossabaw Island pig also serves a beneficial role in diabetes and obesity research and is a fitting model for maternal and childhood obesity (Fisher, 2011; Martin *et al*., 1973; Newell-Fugate *et al*., 2014; Ovilo *et al*., 2014; Padilla *et al*., 2013; Spurlock and Gabler, 2008; Toedebusch *et al*., 2014). As our technology and costs for creating genetically engineered pigs improve, more genetically modified models may be created for use in modeling human reproduction and pathologies. For example, there are pigs expressing the *BRCA1* transgene, a gene highly correlated with breast and ovarian cancer development (Luo *et al*., 2011, 2012a, 2012b), that can be used to mimic the development, progression of these cancers, and test potential therapies. Another transgenic model that could be useful for studies of reproductive vascular pathological conditions such as preeclampsia is a pig model that has overexpression of human catalase, an enzyme involved in the regulation of vascular tone, specific to vascular endothelial cells (Whyte *et al*., 2011). The valued comparable size, physiology, and genetics of the pig will lead to future production of new models for use in biomedicine.

9.10 Summary

In many aspects, the physiology, developmental timing, and genetics of pigs are similar to that of humans rendering them a useful translational model for human reproduction, including the areas of fertilization, *in vitro* development to the blastocyst stage, pregnancy, puberty, and disease. Much is yet to be learned from pigs; with the advent of new technologies in gene, modification pigs may be even more advantageous to previously existing and new models.

Acknowledgments

The authors would like to acknowledge funding from Food for the 21st Century, the University of Missouri Predoctoral Molecular Life Sciences Fellowship, and the NIH via U42 OD011140.

References

Abeydeera, L.R. (2001) *In vitro* fertilization and embryo development in pigs. *Reprod. Suppl.*, **58**, 159–173.

Abeydeera, L.R. (2002) *In vitro* production of embryos in swine. *Theriogenology*, **57**, 257–273.

Downloaded From Vet-eBooks.com

Afzalpurkar, A. and Gupta, S.K. (1997) Identification of epitopes of monoclonal antibodies to porcine zona pellucida 3 beta glycoprotein, a homologue of the mouse/human sperm receptor. *Am. J. Reprod. Immunol.*, **38**, 26–32.

Afzalpurkar, A., Sacco, A.G., Yurewicz, E.C., and Gupta, S.K. (1997) Induction of native protein reactive antibodies by immunization with peptides containing linear B-cell epitopes defined by anti-porcine ZP3 beta monoclonal antibodies. *J. Reprod. Immunol.*, **33**, 113–125.

Anderson, L.L. and Parker, R.O. (1976) Distribution and development of embryos in the pig. *J. Reprod. Fertil.*, **46**, 363–368.

Atinmo, T., Pond, W., and Barnes, R. (1974a) Effect of dietary energy vs. protein restriction on blood constituents and reproductive performance in swine. *J. Nutr.*, **104**, 1033–1040.

Atinmo, T., Pond, W., and Barnes, R. (1974b) Effect of maternal energy vs. protein restriction on growth and development of progeny in swine. *J. Anim. Sci.*, **39**, 703–711.

Atinmo, T., Baldijrao, C., Pond, W.G., and Barnes, R.H. (1976) Decreased dietary protein or energy intake and plasma growth hormone levels of the pregnant pig, its fetuses and developing progeny. *J. Nutr.*, **106**, 940–946.

Attig, L. *et al.* (2008) Study of hypothalamic leptin receptor expression in low-birth-weight piglets and effects of leptin supplementation on neonatal growth and development. *Am. J. Physiol. Endocrinol. Metab.*, **295**, E1117–E1125.

Attig, L. *et al.* (2013) Postnatal leptin promotes organ maturation and development in IUGR piglets. *PloS One*, **8**, e64616.

Aye, M.M. *et al.* (2014) Acute hypertriglyceridemia induces platelet hyperactivity that is not attenuated by insulin in polycystic ovary syndrome. *J. Am. Heart Assoc.*, **3**, e000706.

Barker, D.J. (1990) The fetal and infant origins of adult disease. *BMJ*, **301**, 1111.

Barker, D.J. (1995) Fetal origins of coronary heart disease. *BMJ*, **311**, 171–174.

Barker, D.J. (1998) *In utero* programming of chronic disease. *Clin. Sci.*, **95**, 115–128.

Bartol, F.F., Spate, L., Samoylov, A., Cochran, A., Petrenko, V., Prather, R.S., and Samoylova, T. (2015) Phage-peptide constructs for immunocontraception of wild pigs: effects on events associated with fertilization *in vitro*. Society for the Study of Reproduction Annual Meeting, No. 443. Available at http://www.ssr.org/sites/ssr.org/files/uploads/attachments/node/315/2015_ssr_abstracts.pdf.

Bauer, B.K. *et al.* (2010) Transcriptional profiling by deep sequencing identifies differences in mRNA transcript abundance in *in vivo*-derived versus *in vitro*-cultured porcine blastocyst stage embryos. *Biol. Reprod.*, **83**, 791–798.

Bernabò, N. *et al.* (2007) Effects of 50 Hz extremely low frequency magnetic field on the morphology and function of boar spermatozoa capacitated *in vitro*. *Theriogenology*, **67**, 801–815.

Bernabò, N. *et al.* (2010) Extremely low frequency electromagnetic field exposure affects fertilization outcome in swine animal model. *Theriogenology*, **73**, 1293–1305.

Biensen, N.J., Wilson, M.E., and Ford, S.P. (1998) The impact of either a Meishan or Yorkshire uterus on Meishan or Yorkshire fetal and placental development to days 70, 90, and 110 of gestation. *J. Anim. Sci.*, **76**, 2169–2176.

Bode, G. *et al.* (2010) The utility of the minipig as an animal model in regulatory toxicology. *J. Pharmacol. Toxicol. Methods*, **62**, 196–220.

Bond, D. and Chandley, A.C. (1983) *Aneuploidy*, Oxford University Press, Oxford.

Bonk, A.J. *et al.* (2007) Correlation of developmental differences of nuclear transfer embryo cells to the methylation profiles of nuclear transfer donor cells in swine. *Epigenetics*, **2**, 179–186.

Bonk, A.J. *et al.* (2008) Aberrant DNA methylation in porcine *in vitro*-, parthenogenetic-, and somatic cell nuclear transfer-produced blastocysts. *Mol. Reprod. Dev.*, **75**, 250–264.

Braude, P., Bolton, V., and Moore, S. (1988) Human gene expression first occurs between the four- and eight-cell stages of preimplantation development. *Nature*, **332**, 459–461.

Downloaded From Vet-eBooks.com

Brevini, T.A.L., Antonini, S., Cillo, F., Crestan, M., and Gandolfi, F. (2007) Porcine embryonic stem cells: facts, challenges and hopes. *Theriogenology*, **68** (Suppl. 1), S206–S213.

Brevini, T.A. *et al.* (2012) Centrosome amplification and chromosomal instability in human and animal parthenogenetic cell lines. *Stem Cell Rev.*, **8**, 1076–1087.

Brinster, R.L. (1965a) Studies on the development of mouse embryos *in vitro*. *J. Reprod. Fertil.*, **10**, 227–240.

Brinster, R.L. (1965b) Studies on the development of mouse embryos *in vitro*. II. The effect of energy source. *J. Exp. Zool.*, **158**, 59–68.

Bulletti, C. and De Ziegler, D. (2005) Uterine contractility and embryo implantation. *Curr. Opin. Obstet. Gynecol.*, **17**, 265–276.

Cao, Z. *et al.* (2014) Dynamic reprogramming of 5-hydroxymethylcytosine during early porcine embryogenesis. *Theriogenology*, **81**, 496–508.

CDC (Center for Disease Control and Prevention) (2014) Fertility clinic success rates report: Clinic tables and data dictionary. Public-use data file and documentation. Available at http://www.cdc.gov/art/artdata/index.html.

Cesario, S.K. and Hughes, L.A. (2007) Precocious puberty: a comprehensive review of literature. *J. Obstet. Gynecol. Neonatal Nurs.*, **36**, 263–274.

Chae, J.-I. *et al.* (2006) Proteomic analysis of the extraembryonic tissue from cloned porcine embryos. *Mol. Cell. Proteomics*, **5**, 1559–1566.

Che, L. *et al.* (2015) Effect of postnatal nutrition restriction on the oxidative status of neonates with intrauterine growth restriction in a pig model. *Neonatology*, **107**, 93–99.

Corbel, T. *et al.* (2013) Bisphenol A disposition in the sheep maternal-placental-fetal unit: mechanisms determining fetal internal exposure. *Biol. Reprod.*, **89**, 11.

Coy, P. and Romar, R. (2002) *In vitro* production of pig embryos: a point of view. *Reprod. Fertil. Dev.*, **14**, 275–286.

D'Cruz, O.J. and Uckun, F.M. (2007) Preclinical evaluation of a dual-acting microbicidal prodrug WHI-07 in combination with vanadocene dithiocarbamate in the female reproductive tract of rabbit, pig, and cat. *Toxicol. Pathol.*, **35**, 910–927.

D'cruz, O.J., Erbeck, D., and Uckun, F.M. (2005) A study of the potential of the pig as a model for the vaginal irritancy of benzalkonium chloride in comparison to the nonirritant microbicide PHI-443 and the spermicide vanadocene dithiocarbamate. *Toxicol. Pathol.*, **33**, 465–476.

Dittrich, R. *et al.* (2003) The extracorporeal perfusion of swine uterus as an experimental model: the effect of oxytocic drugs. *Horm. Metab. Res.*, **35**, 517–522.

Dittrich, R. *et al.* (2009) Differences in muscarinic-receptor agonist-, oxytocin-, and prostaglandin-induced uterine contractions. *Fertil. Steril.*, **92**, 1694–1700.

Dominguez, E. *et al.* (2013) Doppler evaluation of the effects of propofol, etomidate and alphaxalone on fetoplacental circulation hemodynamics in the pregnant ewe. *Placenta*, **34**, 738–744.

Ducolomb, Y. *et al.* (2009) *In vitro* effect of malathion and diazinon on oocytes fertilization and embryo development in porcine. *Cell Biol. Toxicol.*, **25**, 623–633.

Dunger, D.B., Ahmed, M.L., and Ong, K.K. (2006) Early and late weight gain and the timing of puberty. *Mol. Cell. Endocrinol.*, **254–255**, 140–145.

Dzienis, A., Majewski, M., Wojtkiewicz, J., Piskula, M., and Jana, B. (2004) Adrenergic innervation and steroidogenic activity of cystic porcine ovaries. *Rocz. Akad. Med. Bialymst.*, **49** (Suppl. 1), 114–116.

Edwards, R. (1965) Maturation *in vitro* of mouse, sheep, cow, pig, rhesus monkey and human ovarian oocytes. *Nature*, **208**, 349–351.

Ellederova, Z. *et al.* (2004) Protein patterns of pig oocytes during *in vitro* maturation. *Biol. Reprod.*, **71**, 1533–1539.

Downloaded From Vet-eBooks.com

Enders, A.C. and Blankenship, T.N. (1999) Comparative placental structure. *Adv. Drug Deliv. Rev.*, **38**, 3–15.

Enders, A.C. and Carter, A.M. (2004) What can comparative studies of placental structure tell us?: A review. *Placenta*, **25** (Suppl.), S3–S9.

Estrada, J. *et al.* (2007) Swine generated by somatic cell nuclear transfer have increased incidence of intrauterine growth restriction (IUGR). *Cloning Stem Cells*, **9**, 229–236.

Fan, N. and Lai, L. (2013) Genetically modified pig models for human diseases. *J. Genet. Genom.*, **40**, 67–73.

Fisher, K.D. (2011) Dietary manipulation causes childhood obesity-like characteristics in pigs. Thesis, Virginia Polytechnic Institute and State University.

Forabosco, F., Löhmus, M., Rydhmer, L., and Sundström, L.F. (2013) Genetically modified farm animals and fish in agriculture: a review. *Livest. Sci.*, **153**, 1–9.

Ford, S.P. (1995) Control of blood flow to the gravid uterus of domestic livestock species. *J. Anim. Sci.*, **73**, 1852–1860.

Ford, S.P. and Christenson, R.K. (1979) Blood flow to uteri of sows during the estrous cycle and early pregnancy: local effect of the conceptus on the uterine blood supply. *Biol. Reprod.*, **21**, 617–624.

Ford, S.P. and Stice, S.L. (1985) Effects of the ovary and conceptus on uterine blood flow in the pig. *J. Reprod. Fertil. Suppl.*, **33**, 83–90.

Ford, S.P., Christenson, R.K., and Ford, J.J. (1982a) Uterine blood flow and uterine arterial, venous and luminal concentrations of oestrogens on days 11, 13 and 15 after oestrus in pregnant and non-pregnant sows. *J. Reprod. Fertil.*, **64**, 185–190.

Ford, S.P., Reynolds, L.P., and Magness, R.R. (1982b) Blood flow to the uterine and ovarian vascular beds of gilts during the estrous cycle or early pregnancy. *Biol. Reprod.*, **27**, 878–885.

Ford, S.P., Reynolds, L.P., Farley, D.B., Bhatnagar, R.K., and Van Orden, D.E. (1984a) Interaction of ovarian steroids and periarterial alpha 1-adrenergic receptors in altering uterine blood flow during the estrous cycle of gilts. *Am. J. Obstet. Gynecol.*, **150**, 480–484.

Ford, S.P., Reynolds, L.P., and Ferrell, C.L. (1984b) Blood flow, steroid secretion and nutrient uptake of the gravid uterus during the periparturient period in sows. *J. Anim. Sci.*, **59**, 1085–1091.

Friedman, S.A. (1988) Preeclampsia: a review of the role of prostaglandins. *Obstet. Gynecol.*, **71**, 122–137.

Gieling, E.T. *et al.* (2014) Chronic allopurinol treatment during the last trimester of pregnancy in sows: effects on low and normal birth weight offspring. *PloS One*, **9**, e86396.

Godfrey, K.M. and Barker, D.J. (2000) Fetal nutrition and adult disease. *Am. J. Clin. Nutr.*, **71**, 1344s–1352s.

Gott, A.L., Hardy, K., Winston, R.M., and Leese, H.J. (1990) Non-invasive measurement of pyruvate and glucose uptake and lactate production by single human preimplantation embryos. *Hum. Reprod.*, **5**, 104–108.

Gupta, S.K. *et al.* (1995) Localization of epitopes for monoclonal antibodies at the N-terminus of the porcine zona pellucida glycoprotein pZPC. *Mol. Reprod. Dev.*, **42**, 220–225.

Gupta, S.K. *et al.* (1996) Mapping of epitopes on porcine zona pellucida-3 alpha by monoclonal antibodies inhibiting oocyte–sperm interaction. *Biol. Reprod.*, **55**, 410–415.

Hall, V. (2008) Porcine embryonic stem cells: a possible source for cell replacement therapy. *Stem Cell Rev.*, **4**, 275–282.

Han, F. *et al.* (2013) Effects of high nutrient intake on the growth performance, intestinal morphology and immune function of neonatal intra-uterine growth-retarded pigs. *Br. J. Nutr.*, **110**, 1819–1827.

Downloaded From Vet-eBooks.com

Harris, E.K., Berg, E.P., Berg, E.L., and Vonnahme, K.A. (2013) Effect of maternal activity during gestation on maternal behavior, fetal growth, umbilical blood flow, and farrowing characteristics in pigs. *J. Anim. Sci.*, **91**, 734–744.

Hasegawa, A., Koyama, K., Inoue, M., Takemura, T., and Isojima, S. (1992) Antifertility effect of active immunization with ZP4 glycoprotein family of porcine zona pellucida in hamsters. *J. Reprod. Immunol.*, **22**, 197–210.

Hasegawa, A., Koyama, K., Okazaki, Y., Sugimoto, M., and Isojima, S. (1994) Amino acid sequence of a porcine zona pellucida glycoprotein ZP4 determined by peptide mapping and cDNA cloning. *J. Reprod. Fertil.*, **100**, 245–255.

Hasegawa, A., Yamasaki, N., Inoue, M., Koyama, K., and Isojima, S. (1995) Analysis of an epitope sequence recognized by a monoclonal antibody MAb-5H4 against a porcine zona pellucida glycoprotein (pZP4) that blocks fertilization. *J. Reprod. Fertil.*, **105**, 295–302.

Hasegawa, A., Hamada, Y., Shigeta, M., and Koyama, K. (2002) Contraceptive potential of synthetic peptides of zona pellucida protein (ZPA). *J. Reprod. Immunol.*, **53**, 91–98.

Hassold, T. and Hunt, P. (2001) To err (meiotically) is human: the genesis of human aneuploidy. *Nat. Rev. Genet.*, **2**, 280–291.

Hassold, T., Hall, H., and Hunt, P. (2007) The origin of human aneuploidy: where we have been, where we are going. *Hum. Mol. Genet.*, **16**, R203–R208.

Herreros, M.A. *et al.* (2010) Pregnancy-associated changes in plasma concentration of the endocrine disruptor di(2-ethylhexyl) phthalate in a sheep model. *Theriogenology*, **73**, 141–146.

Hoffman, D.I. *et al.* (2003) Cryopreserved embryos in the United States and their availability for research. *Fertil. Steril.*, **79**, 1063–1069.

Hornak, M. *et al.* (2011) Frequency of aneuploidy related to age in porcine oocytes. *PloS One*, **6**, e18892.

Hornak, M., Oracova, E., Hulinska, P., Urbankova, L., and Rubes, J. (2012) Aneuploidy detection in pigs using comparative genomic hybridization: from the oocytes to blastocysts. *PloS One*, **7**, e30335.

Hou, L. *et al.* (2014) Effects of histone deacetylase inhibitor oxamflatin on *in vitro* porcine somatic cell nuclear transfer embryos. *Cell Reprogram.*, **16**, 253–265.

Inglot, P. *et al.* (2012) Cadmium-induced changes in genomic DNA-methylation status increase aneuploidy events in a pig Robertsonian translocation model. *Mutat. Res.*, **747**, 182–189.

Ješeta, M. and Bodart, J.-F.L. (2012) Comparing pig and amphibian oocytes: methodologies for aneuploidy detection and complementary lessons for MAPK involvement in meiotic spindle morphogenesis. *Aneuploidy in Health and Disease*, InTech, pp. 193–216.

Kaplowitz, P.B. and Oberfield, S.E. (1999) Reexamination of the age limit for defining when puberty is precocious in girls in the United States: implications for evaluation and treatment. Drug and Therapeutics and Executive Committees of the Lawson Wilkins Pediatric Endocrine Society. *Pediatrics*, **104**, 936–941.

Kaplowitz, P.B., Slora, E.J., Wasserman, R.C., Pedlow, S.E., and Herman-Giddens, M.E. (2001) Earlier onset of puberty in girls: relation to increased body mass index and race. *Pediatrics*, **108**, 347–353.

Kątska-Książkiewicz, K. (2006a) Recent achievements in *in vitro* culture and preservation of ovarian follicles in mammals. *Reprod. Biol.*, **6**, 3–16.

Kątska-Książkiewicz, L. (2006b) Pig embryo production by *in vitro* maturation and fertilization of ovarian oocytes: a review. *J. Anim. Feed Sci.*, **15**, 525–542.

Kaul, R., Afzalpurkar, A., and Gupta, S.K. (1996) Strategies for designing an immunocontraceptive vaccine based on zona pellucida synthetic peptides and recombinant antigen. *J. Reprod. Fertil.. Suppl.*, **50**, 127–134.

Downloaded From Vet-eBooks.com

Kim, S.W., Mateo, R.D., Yin, Y., and Wu, G. (2007) Functional amino acids and fatty acids for enhancing production performance of sows and piglets. *Asian Australas. J. Anim. Sci.*, **20**, 295.

Kissler, S. *et al.* (2005) Diminished pregnancy rates in endometriosis due to impaired uterotubal transport assessed by hysterosalpingoscintigraphy. *BJOG*, **112**, 1391–1396.

Knight, J.W., Bazer, F.W., Thatcher, W.W., Franke, D.E., and Wallace, H.D. (1977) Conceptus development in intact and unilaterally hysterectomized-ovariectomized gilts: interrelations among hormonal status, placental development, fetal fluids and fetal growth. *J. Anim. Sci.*, **44**, 620–637.

Koenig, J.L. and Stormshak, F. (1993) Cytogenetic evaluation of ova from pubertal and third-estrous gilts. *Biol. Reprod.*, **49**, 1158–1162.

Koyama, K., Hasegawa, A., Inoue, M., and Isojima, S. (1991) Blocking of human sperm-zona interaction by monoclonal antibodies to a glycoprotein family (ZP4) of porcine zona pellucida. *Biol. Reprod.*, **45**, 727–735.

Koyama, K. *et al.* (1996) Studies on the epitope of pig zona pellucida recognized by a fertilization-blocking monoclonal antibody. *J. Reprod. Fertil. Suppl.*, **50**, 135–142.

Kozlowska, A., Majewski, M., and Jana, B. (2009) Expression of steroidogenic enzymes in porcine polycystic ovaries. *Folia Histochem. Cytobiol.*, **47**, 257–264.

Kozlowska, A., Wojtkiewicz, J., Majewski, M., and Jana, B. (2011) Localization of substance P, calcitonin gene related peptide and galanin in the nerve fibers of porcine cystic ovaries. *Folia Histochem. Cytobiol.*, **49**, 622–630.

Kozlowska, A., Wojtkiewicz, J., Majewski, M., and Jana, B. (2013) The noradrenergic innervation and steroidogenic activity of porcine cystic ovaries. *Physiol. Res.*, **62**, 421–433.

Krisher, R. (2012) Utility of animal models for human embryo culture development: domestic species. *Methods Mol. Biol.* **912**, 27–37.

Krisher, R.L. and Prather, R.S. (2012) A role for the Warburg effect in preimplantation embryo development: metabolic modification to support rapid cell proliferation. *Mol. Reprod. Dev.*, **79**, 311–320.

Krisher, R.L., Wulster-Radcliffe, M.C., Spurlock, M.E., and Sturek, M.S. (2006) The Ossabaw pig as a model of polycystic ovary syndrome. *FASEB J.*, **20**, A825.

Krisher, R.L., Lowe, J., Bailey, A., and Sturek, M. (2008) Endocrine parameters and ovarian dynamics in Ossabaw miniature swine with metabolic syndrome suggest a model for polycystic ovary syndrome. *FASEB J.*, **22**, 757–824.

Krueger, R. *et al.* (2014) Higher body fatness in intrauterine growth retarded juvenile pigs is associated with lower fat and higher carbohydrate oxidation during ad libitum and restricted feeding. *Eur. J. Nutr.*, **53**, 583–597.

Kunzel, J. *et al.* (2011) Myometrial response to neurotropic and musculotropic spasmolytic drugs in an extracorporeal perfusion model of swine uteri. *Reprod. Biomed. Online*, **23**, 132–140.

Kunzel, J. *et al.* (2014) Effects of interactions between progesterone and prostaglandin on uterine contractility in a perfused swine uterus model. *In Vivo*, **28**, 467–475.

Kurome, M. *et al.* (2008) Production of transgenic and non-transgenic clones in miniature pigs by somatic cell nuclear transfer. *J. Reprod. Dev.*, **54**, 156–163.

Lechniak, D. *et al.* (2007) Gilts and sows produce similar rate of diploid oocytes *in vitro* whereas the incidence of aneuploidy differs significantly. *Theriogenology*, **68**, 755–762.

Lee, J.-W., Tian, X.C., and Yang, X. (2003) Failure of male pronucleus formation is the major cause of lack of fertilization and embryo development in pig oocytes subjected to intracytoplasmic sperm injection. *Biol. Reprod.*, **68**, 1341–1347.

Lee, S.-Y. *et al.* (2007) Comparative proteomic analysis associated with term placental insufficiency in cloned pig. *Proteomics*, **7**, 1303–1315.

Downloaded From Vet-eBooks.com

Leese, H.J. (1991) Metabolism of the preimplantation mammalian embryo. *Oxf. Rev. Reprod. Biol.*, **13**, 35–72.

Leyendecker, G. *et al.* (2004) Uterine peristaltic activity and the development of endometriosis. *Annals N. Y. Acad. Sci.*, **1034**, 338–355.

Li, X.J. and Li, W. (2012) Beyond mice: genetically modifying larger animals to model human diseases. *J. Genet. Genom.*, **39**, 237–238.

Li, D.-K. *et al.* (2010) Exposure to magnetic fields and the risk of poor sperm quality. *Reprod. Toxicol.*, **29**, 86–92.

Li, G. *et al.* (2014a) Dysregulation of genome-wide gene expression and DNA methylation in abnormal cloned piglets. *BMC Genomics*, **15**, 811.

Li, G. *et al.* (2014b) Dysregulation of genome-wide gene expression and DNA methylation in abnormal cloned piglets. *BMC Genomics*, **15**, 811.

Liu, J.B., Chen, D.W., Yu, B., and Mao, X.B. (2011) Effect of maternal folic acid supplementation on hepatic one-carbon unit associated gene expressions in newborn piglets. *Mol. Biol. Rep.*, **38**, 3849–3856.

Liu, J. *et al.* (2012a) Intrauterine growth retardation increases the susceptibility of pigs to high-fat diet-induced mitochondrial dysfunction in skeletal muscle. *PloS One*, **7**, e34835.

Liu, J. *et al.* (2012b) Effects of intrauterine growth retardation and maternal folic acid supplementation on hepatic mitochondrial function and gene expression in piglets. *Arch. Anim. Nutr.*, **66**, 357–371.

Liu, J. *et al.* (2014) Effects of intrauterine growth retardation and postnatal high-fat diet on hepatic inflammatory response in pigs. *Arch. Anim. Nutr.*, **68**, 111–125.

Ljungvall, K. *et al.* (2005) Delayed effects on plasma concentration of testosterone and testicular morphology by intramuscular low-dose di(2-ethylhexyl)phthalate or oestradiol benzoate in the prepubertal boar. *Theriogenology*, **64**, 1170–1184.

Ljungvall, K. *et al.* (2006) Early post-natal exposure to low dose oral di(2ethylhexyl) phthalate affects the peripheral LH-concentration in plasma, but does not affect mating behavior in the post-pubertal boar. *Reprod. Toxicol.*, **21**, 160–166.

Ljungvall, K., Veeramachaneni, D.N., Hou, M., Hulten, F., and Magnusson, U. (2008) Morphology and morphometry of the reproductive organs in prepubertal and postpubertal male pigs exposed to di(2-ethylhexyl) phthalate before puberty: precocious development of bulbourethral glands. *Theriogenology*, **70**, 984–991.

Long, C.R., Dobrinsky, J.R., and Johnson, L.A. (1999) *In vitro* production of pig embryos: comparisons of culture media and boars. *Theriogenology*, **51**, 1375–1390.

Lowe, J., Sturek, M., and Krisher, R. (2007) Characterizing the Ossabaw minipig as an animal model for polycystic ovary syndrome. *Biol. Reprod.* **77**, 210–211.

Luo, Y. *et al.* (2011) High efficiency of BRCA1 knockout using rAAV-mediated gene targeting: developing a pig model for breast cancer. *Transgenic Res.*, **20**, 975–988.

Luo, Y., Bolund, L., and Sørensen, C.B. (2012a) Pig gene knockout by rAAV-mediated homologous recombination: comparison of BRCA1 gene knockout efficiency in Yucatan and Göttingen fibroblasts with slightly different target sequences. *Transgenic Res.*, **21**, 671–676.

Luo, Y., Lin, L., Bolund, L., Jensen, T., and Sørensen, C. (2012b) Genetically modified pigs for biomedical research. *J. Inherit. Metab. Dis.*, **35**, 695–713.

Machaty, Z., Day, B.N., and Prather, R.S. (1998) Development of early porcine embryos *in vitro* and *in vivo*. *Biol. Reprod.*, **59**, 451–455.

Machaty, Z., Thompson, J.G., Abeydeera, L.R., Day, B.N., and Prather, R.S. (2001) Inhibitors of mitochondrial ATP production at the time of compaction improve development of *in vitro* produced porcine embryos. *Mol. Reprod. Dev.*, **58**, 39–44.

Downloaded From Vet-eBooks.com

MacKay, A.P., Berg, C.J., and Atrash, H.K. (2001) Pregnancy-related mortality from preeclampsia and eclampsia. *Obstet. Gynecol.*, **97**, 533–538.

Magolski, J.D. *et al.* (2014) Consumption of ground beef obtained from cattle that had received steroidal growth promotants does not trigger early onset of estrus in prepubertal pigs. *J. Nutr.*, **144**, 1718–1724.

Maltaris, T. *et al.* (2005) Increased uterine arterial pressure and contractility of perfused swine uterus after treatment with serum from pre-eclamptic women and endothelin-1. *Clin. Sci.*, **109**, 209–215.

Maltaris, T. *et al.* (2006a) The role of oestradiol in the uterine peristalsis in the perfused swine uterus. *Reprod. Domes. Anim.*, **41**, 522–526.

Maltaris, T. *et al.* (2006b) The extracorporeal perfusion of the swine uterus as an experimental model: the effect of tocolytic drugs. *Eur. J. Obstet. Gynecol. Reprod. Biol.*, **126**, 56–62.

Mao, J. *et al.* (2014) Oxamflatin treatment enhances cloned porcine embryo development and nuclear reprogramming. *Cell Reprogram.*, **17**, 28–40.

Markiewicz, W., Kaminska, K., Bogacki, M., Maslanka, T., and Jaroszewski, J. (2012) Participation of analogues of lysophosphatidic acid (LPA): oleoyl-*sn*-glycero-3-phosphate (L-alpha-LPA) and 1-oleoyl-2-*O*-methyl-rac-glycerophosphothionate (OMPT) in uterine smooth muscle contractility of the pregnant pigs. *Pol. J. Vet. Sci.*, **15**, 635–643.

Martin, R., Gobble, J., Hartsock, T., Graves, H., and Ziegler, J. (1973) Characterization of an obese syndrome in the pig. *Exp. Biol. Med.*, **143**, 198–203.

Meurens, F., Summerfield, A., Nauwynck, H., Saif, L., and Gerdts, V. (2012) The pig: a model for human infectious diseases. *Trends Microbiol.*, **20**, 50–57.

Miao, Y.L. *et al.* (2009) Centrosome abnormalities during porcine oocyte aging. *Environ. Mol. Mutagen.*, **50**, 666–671.

Morel, O. *et al.* (2009) Radiofrequency ablation of retained placenta accreta after conservative management: preliminary evaluation in the pregnant ewe and in normal human placenta *in vitro*. *BJOG*, **116**, 915–922.

Morise, A. *et al.* (2009) Impact of intrauterine growth retardation and early protein intake on growth, adipose tissue, and the insulin-like growth factor system in piglets. *Pediatr. Res.*, **65**, 45–50.

Morrison, J.L. (2008) Sheep models of intrauterine growth restriction: fetal adaptations and consequences. *Clin. Exp. Pharmacol. Physiol.*, **35**, 730–743.

Mueller, A. *et al.* (2006a) Uterine contractility in response to different prostaglandins: results from extracorporeally perfused non-pregnant swine uteri. *Hum. Reprod.*, **21**, 2000–2005.

Mueller, A. *et al.* (2006b) Role of estrogen and progesterone in the regulation of uterine peristalsis: results from perfused non-pregnant swine uteri. *Hum. Reprod.*, **21**, 1863–1868.

Muller, A. *et al.* (2006) Modulation of uterine contractility and peristalsis by oxytocin in estrogen-primed non-pregnant swine uteri. *Eur. J. Med. Res.*, **11**, 157.

Murphy, V.E., Smith, R., Giles, W.B., and Clifton, V.L. (2006) Endocrine regulation of human fetal growth: the role of the mother, placenta, and fetus. *Endocr. Rev.*, **27**, 141–169.

Nagai, T. (2001) The improvement of *in vitro* maturation systems for bovine and porcine oocytes. *Theriogenology*, **55**, 1291–1301.

Nagai, T., Funahashi, H., Yoshioka, K., and Kikuchi, K. (2006) Update of *in vitro* production of porcine embryos. *Front. Biosci.*, **11**, 2565–2573.

Nagaoka, S.I., Hassold, T.J., and Hunt. P.A. (2012) Human aneuploidy: mechanisms and new insights into an age-old problem. *Nat. Rev. Genet.*, **13**, 493–504.

Nebendahl, C. *et al.* (2013) Effects on transcriptional regulation and lipid droplet characteristics in the liver of female juvenile pigs after early postnatal feed restriction and refeeding are dependent on birth weight. *PloS One*, **8**, e76705.

Downloaded From Vet-eBooks.com

Neuber, E. and Powers, R. (2000) Is the mouse a clinically relevant model for human fertilization failures? *Hum. Reprod.*, **15**, 171–174.
Newell-Fugate, A. (2013) Validation of the obese Ossabaw miniature pig as a model of the obese polycystic ovary syndrome phenotype with concomitant metabolic syndrome: exploration of polycystic ovary syndrome pathophysiology using *in vivo* and *in vitro*. Thesis, University of Illinois at Urbana-Champaign.
Newell-Fugate, A. *et al.* (2010) 320 Baseline and superovulation hyperandrogenism and follicular dynamics in the Ossabaw pig suggest an animal model for polycystic ovary syndrome. *Reprod. Fertil. Dev.*, **23**, 256–257.
Newell-Fugate, A.E. *et al.* (2011) Follicular Dynamics and Estrous Cycle Features of the Ossabaw Pig Model of Polycystic Ovary Syndrome (PCOS). *Biol. Reprod.* **85**, 818.
Newell-Fugate, A.E. *et al.* (2014) Effects of diet-induced obesity on metabolic parameters and reproductive function in female Ossabaw minipigs. *Comp. Med.*, **64**, 44–49.
Niakan, K.K., Han, J., Pedersen, R.A., Simon, C., and Pera, R.A.R. (2012) Human pre-implantation embryo development. *Development*, **139**, 829–841.
Olszanska, B. and Borgul, A. (1993) Maternal RNA content in oocytes of several mammalian and avian species. *J. Exp. Zool.*, **265**, 317–320.
Omodei, D. and Fontana, L. (2011) Calorie restriction and prevention of age-associated chronic disease. *FEBS Lett.*, **585**, 1537–1542.
Ong, K.K. *et al.* (2004) Opposing influences of prenatal and postnatal weight gain on adrenarche in normal boys and girls. *J. Clin. Endocrinol. Metab.*, **89**, 2647–2651.
Ovilo, C. *et al.* (2014) Prenatal programming in an obese swine model: sex-related effects of maternal energy restriction on morphology, metabolism and hypothalamic gene expression. *Br. J. Nutr.*, **111**, 735–746.
Padilla, J. *et al.* (2013) Vascular transcriptional alterations produced by juvenile obesity in Ossabaw swine. *Physiol. Genomics*, **45**, 434–446.
Parker, L.N. (1991) Adrenarche. *Endocrinol. Metab. Clin. North Am.*, **20**, 71–83.
Pawlak, P., Pers-Kamczyc, E., Renska, N., Kubickova, S., and Lechniak, D. (2011) Disturbances of nuclear maturation in BCB positive oocytes collected from peri-pubertal gilts. *Theriogenology*, **75**, 832–840.
Penrose, L.S. (2009) The relative effects of paternal and maternal age in mongolism. 1933. *J. Genetics*, **88**, 9–14.
Perry, J.S. and Rowell, J.G. (1969) Variations in foetal weight and vascular supply along the uterine horn of the pig. *J. Reprod. Fertil.*, **19**, 527–534.
Petters, R.M. and Sommer, J.R. (2000) Transgenic animals as models for human disease. *Transgenic Res.*, **9**, 347–351.
Piedrahita, J.A., Anderson, G.B., and BonDurant, R.H. (1990) On the isolation of embryonic stem cells: comparative behavior of murine, porcine and ovine embryos. *Theriogenology*, **34**, 879–901.
Pond, W. (1973) Influence of maternal protein and energy nutrition during gestation on progeny performance in swine. *J. Anim. Sci.*, **36**, 175–182.
Pond, W.G., Wagner, W.C., Dunn, J.A., and Walker, E.F. (1968) Reproduction and early postnatal growth of progeny in swine fed a protein-free diet during gestation. *J. Nutr.*, **94**, 309–316.
Pond, W.G. *et al.* (1969) Effect of protein deprivation of swine during all or part of gestation on birth weight, postnatal growth rate and nucleic acid content of brain and muscle of progeny. *J. Nutr.*, **99**, 61–67.
Prather, R.S. (1993) Nuclear control of early embryonic development in domestic pigs. *J. Reprod. Fertil. Suppl.*, **48**, 17–29.
Prather, R.S. (2013) Pig genomics for biomedicine. *Nat. Biotechnol.*, **31**, 122–124.

Downloaded From Vet-eBooks.com

Prather, R.S. and Day, B.N. (1998) Practical considerations for the *in vitro* production of pig embryos. *Theriogenology*, **49**, 23–32.

Prather, R., Hawley, R., Carter, D., Lai, L., and Greenstein, J. (2003) Transgenic swine for biomedicine and agriculture. *Theriogenology*, **59**, 115–123.

Prather, R.S., Sutovsky, P., and Green, J.A. (2004) Nuclear remodeling and reprogramming in transgenic pig production. *Exp. Biol. Med.*, **229**, 1120–1126.

Prather, R.S., Shen, M., and Dai, Y. (2008) Genetically modified pigs for medicine and agriculture. *Biotechnol. Genet. Eng. Rev.*, **25**, 245–266.

Prather, R.S., Lorson, M., Ross, J.W., Whyte, J.J., and Walters, E. (2013) Genetically engineered pig models for human diseases. *Annu. Rev. Anim. Biosci.*, **1**, 203–219.

Prather, R.S., Redel, B.K. Whitworth, K.M., and Zhao, M.-T. (2014) Genomic profiling to improve embryogenesis in the pig. *Anim. Reprod. Sci.*, **149**, 39–45.

Prickaerts, J., Gieling, E.T., Bruder, A.K., van der Staay, F.J., and Vanmierlo, T. (2014) Long-term effects of prenatal allopurinol treatment on brain plasticity markers in low and normal birth weight piglets. *Int. J. Dev. Neurosci.*, **33**, 29–32.

Reynolds, L.P., Ford, S.P., and Ferrell, C.L. (1985) Blood flow and steroid and nutrient uptake of the gravid uterus and fetus of sows. *J. Anim. Sci.*, **61**, 968–974.

Reynolds, L.P. *et al.* (2006) Evidence for altered placental blood flow and vascularity in compromised pregnancies. *J. Physiol.*, **572**, 51–58.

Roberts, J.M. and Cooper, D.W. (2001) Pathogenesis and genetics of pre-eclampsia. *Lancet*, **357**, 53–56.

Roy, J.R., Chakraborty, S., and Chakraborty, T.R. (2009) Estrogen-like endocrine disrupting chemicals affecting puberty in humans: a review. *Med. Sci. Monit.*, **15**, 137–145.

Salih, S.M. *et al.* (2008) Regulation of catechol *O*-methyltransferase expression in granulosa cells: a potential role for follicular arrest in polycystic ovary syndrome. *Fertil. Steril.*, **89**, 1414–1421.

Samoylova, T.I. *et al.* (2012) Phage display allows identification of zona pellucida-binding peptides with species-specific properties: novel approach for development of contraceptive vaccines for wildlife. *J. Biotechnol.*, **162**, 311–318.

Sathananthan, A. *et al.* (1996) The sperm centriole: its inheritance, replication and perpetuation in early human embryos. *Hum. Reprod.*, **11**, 345–356.

Schatten, H. and Sun, Q.Y. (2009) The functional significance of centrosomes in mammalian meiosis, fertilization, development, nuclear transfer, and stem cell differentiation. *Environ. Mol. Mutagen.*, **50**, 620–636.

Schatten, H. and Sun, Q.Y. (2010) The role of centrosomes in fertilization, cell division and establishment of asymmetry during embryo development. *Semin. Cell Dev. Biol.*, **21**, 174–184.

Schatten, H. and Sun, Q.Y. (2011a) Centrosome dynamics during mammalian oocyte maturation with a focus on meiotic spindle formation. *Mol. Reprod. Dev.*, **78**, 757–768.

Schatten, H. and Sun, Q.Y. (2011b) New insights into the role of centrosomes in mammalian fertilization and implications for ART. *Reproduction*, **142**, 793–801.

Schatten, H. and Sun, Q.Y. (2011c) The significant role of centrosomes in stem cell division and differentiation. *Microsc. Microanal.*, **17**, 506–512.

Schatten, H., Schatten, G., Mazia, D., Balczon, R., and Simerly, C. (1986) Behavior of centrosomes during fertilization and cell division in mouse oocytes and in sea urchin eggs. *Proc. Natl. Acad. Sci. USA*, **83**, 105–109.

Schoknecht, P.A. *et al.* (1997) Exogenous insulin-like growth factor-I increases weight gain in intrauterine growth-retarded neonatal pigs. *Pediatr. Res.*, **42**, 201–207.

Sheppard, K.M., Padmanabhan, V., Coolen, L.M., and Lehman, M.N. (2011) Prenatal programming by testosterone of hypothalamic metabolic control neurones in the ewe. *J. Neuroendocrinol.*, **23**, 401–411.

Downloaded From Vet-eBooks.com

Shigeta, M., Hasegawa, A., Hamada, Y., and Koyama, K. (2000) Analysis of B cell epitopes of a glycoprotein porcine zona pellucida (pZP1). *J. Reprod. Immunol.*, **47**, 159–168.
Solomon, C.G. (1999) The epidemiology of polycystic ovary syndrome: prevalence and associated disease risks. *Endocrinol. Metab. Clin. North Am.*, **28**, 247–263.
Sosnowski, J., Waroczyk, M., and Switonski, M. (2003) Chromosome abnormalities in secondary pig oocytes matured *in vitro*. *Theriogenology*, **60**, 571–581.
Speakman, J.R. and Mitchell, S.E. (2011) Caloric restriction. *Mol. Aspects Med.*, **32**, 159–221.
Spurlock, M.E. and Gabler, N.K. (2008) The development of porcine models of obesity and the metabolic syndrome. *J. Nutr.*, **138**, 397–402.
Stice, S.L., Ford, S.P., Rosazza, J.P., and Van Orden, D.E. (1987) Interaction of 4-hydroxylated estradiol and potential-sensitive Ca2+ channels in altering uterine blood flow during the estrous cycle and early pregnancy in gilts. *Biol. Reprod.*, **36**, 369–375.
Sun, Q.-Y. and Nagai, T. (2003) Molecular mechanisms underlying pig oocyte maturation and fertilization. *J. Reprod. Dev.*, **49**, 347–359.
Sutovsky, P. and Schatten, G. (1999) Paternal contributions to the mammalian zygote: fertilization after sperm–egg fusion. *Int. Rev. Cytol.*, **195**, 1–65.
Swindle, M.M., Smith, A.C., Laber-Laird, K., and Dungan, L. (1994) Swine in biomedical research: management and models. *ILAR J.*, **36**, 1–5.
Swindle, M.M., Makin, A., Herron, A.J., Clubb, F.J., and Frazier, K.S. (2012) Swine as models in biomedical research and toxicology testing. *Vet. Pathol. Online*, **49**, 344–356.
Szulanczyk, K. (2009) Histological changes within ovarian cortex, oviductal and uterine mucosa in case of ovarian cysts presence in sows. *Folia Histochem. Cytobiol*, **47**, 99–103.
Therman, E., Susman, B., and Denniston, C. (1989) The nonrandom participation of human acrocentric chromosomes in Robertsonian translocations. *Annals Hum. Genet.*, **53**, 49–65.
Tian, X.C. *et al.* (2008) Altered gene expression in cloned piglets. *Reprod. Fertil. Dev.*, **21**, 60–66.
Toedebusch, R.G. *et al.* (2014) Unique transcriptomic signature of omental adipose tissue in Ossabaw swine: a model of childhood obesity. *Physiol. Genomics*, **46**, 362–375.
van Dijk, A.J., Parvizi, N., Taverne, M.A., and Fink-Gremmels, J. (2008) Placental transfer and pharmacokinetics of allopurinol in late pregnant sows and their fetuses. *J. Vet. Pharmacol. Ther.*, **31**, 489–495.
Vodicka, P. *et al.* (2005) The miniature pig as an animal model in biomedical research. *Annals N. Y. Acad. Sci.*, **1049**, 161–171.
Vonnahme, K.A. and Ford, S.P. (2004) Differential expression of the vascular endothelial growth factor-receptor system in the gravid uterus of Yorkshire and Meishan pigs. *Biol. Reprod.*, **71**, 163–169.
Vozdova, M. *et al.* (2001) Frequency of aneuploidy in pig oocytes matured *in vitro* and of the corresponding first polar bodies detected by fluorescent *in situ* hybridization. *Theriogenology*, **56**, 771–776.
Wassarman, P., Josefowicz, W., and Letourneau, G. (1976) Meiotic maturation of mouse oocytes *in vitro*: inhibition of maturation at specific stages of nuclear progression. *J. Cell Sci.*, **22**, 531–545.
Wei, Y. *et al.* (2010) Aberrant expression and methylation status of putatively imprinted genes in placenta of cloned piglets. *Cell. Reprogram.*, **12**, 213–222.
Wei, X. *et al.* (2014) Hec1 inhibition alters spindle morphology and chromosome alignment in porcine oocytes. *Mol. Biol. Rep.*, **41**, 5089–5095.
Wernersson, R. *et al.* (2005) Pigs in sequence space: a 0.66X coverage pig genome survey based on shotgun sequencing. *BMC Genomics*, **6**, 70–87.
Wester-Rosenlof, L. *et al.* (2014) A1M/alpha1-microglobulin protects from heme-induced placental and renal damage in a pregnant sheep model of preeclampsia. *PloS One*, **9**, e86353.

Downloaded From Vet-eBooks.com

Whitworth, K.M., Zhao, J., Spate, L.D., Li, R., and Prather, R.S. (2011) Scriptaid corrects gene expression of a few aberrantly reprogrammed transcripts in nuclear transfer pig blastocyst stage embryos. *Cell Reprogram.*, **13**, 191–204.

Whyte, J.J. and Prather, R.S. (2011) Genetic modifications of pigs for medicine and agriculture. *Mol. Reprod. Dev.*, **78**, 879–891.

Whyte, J.J. *et al.* (2011) Vascular endothelium-specific overexpression of human catalase in cloned pigs. *Transgenic Res*, **20**, 989–1001.

Wiest, D., Swindle, M.M., Garner, S., Smith, A., and Gillette, P. (1996) Pregnant Yucatan miniature swine as a model for investigating fetal drug therapy, in *Advances in Swine in Biomedical Research* (eds M. Tumbleson and L. Schook), Springer, pp. 629–635.

Wilson, M.E., Biensen, N.J., Youngs, C.R., and Ford, S.P. (1998) Development of Meishan and Yorkshire littermate conceptuses in either a Meishan or Yorkshire uterine environment to day 90 of gestation and to term. *Biol. Reprod.*, **58**, 905–910.

Wooding, F. and Flint, A. (1994) Placentation, in *Marshall's Physiology of Reproduction, vol. 3, Part 1* (ed. G.E. Lamming), Chapman & Hall, London, pp. 233–460.

Wu, G., Pond, W.G., Flynn, S.P., Ott, T.L., and Bazer, F.W. (1998) Maternal dietary protein deficiency decreases nitric oxide synthase and ornithine decarboxylase activities in placenta and endometrium of pigs during early gestation. *J. Nutr.*, **128**, 2395–2402.

Wu, G., Bazer, F.W., Wallace, J.M., and Spencer, T.E. (2006) Board-invited review: intrauterine growth retardation—implications for the animal sciences. *J. Anim. Sci.*, **84**, 2316–2337.

Wu, G. *et al.* (2010) Impacts of amino acid nutrition on pregnancy outcome in pigs: mechanisms and implications for swine production. *J. Anim. Sci.*, **88**, E195–E204.

Wu, G. *et al.* (2013) Impacts of arginine nutrition on embryonic and fetal development in mammals. *Amino Acids*, **45**, 241–256.

You, J., Song, K., and Lee, E. (2010) Prolonged interval between fusion and activation impairs embryonic development by inducing chromosome scattering and nuclear aneuploidy in pig somatic cell nuclear transfer. *Reprod. Fertil. Dev.*, **22**, 977–986.

Zhang, X. *et al.* (2014) Altered imprinted gene expression and methylation patterns in mid-gestation aborted cloned porcine fetuses and placentas. *J. Assist. Reprod. Genetics*, **31**, 1511–1517.

Zhao, J. *et al.* (2010) Histone deacetylase inhibitors improve *in vitro* and *in vivo* developmental competence of somatic cell nuclear transfer porcine embryos. *Cell Reprogram.*, **12**, 75–83.

Zudova, D., Rezacova, O., Kubickova, S., and Rubes, J. (2003) Aneuploidy detection in porcine embryos using fluorescence *in situ* hybridization. *Cytogenet. Genome Res.*, **102**, 179–183.

Downloaded From Vet-eBooks.com

10

The Mare as an Animal Model for Reproductive Aging in the Woman

Elaine M. Carnevale

Equine Reproduction Laboratory, Department of Biomedical Sciences, Colorado State University, CO, USA

10.1 Introduction

The impact of maternal aging on fertility is well documented in the woman, although causes and solutions for the age-related decline in fertility are complex and elusive. One complicating factor is the lack of applicable animal models to study reproductive alterations associated with aging. Most research has been conducted on rodents and nonhuman primates. However, the rodent has extensive reproductive variation when compared to women, with an aging process that occurs in intervals of months rather than years and decades. Primate models are the most evolutionarily comparable model for women; but animal availability is limited, and reproductive manipulations are difficult and expensive. Large animal models have been proposed; however, many large animals, especially production species, are not maintained as they age and fertility declines. One exception is the mare. Older horses are often kept as breeding, work, or companion animals. While selection criteria for production species fundamentally include fertility, horses are often valued and selected for performance ability, conformation traits, or success of prodigy. Horses registered with breed or performance associations have recorded linage, and performance ability can often be tracked or indexed. Another differentiating feature for the horse compared to most other species is the use of specific assisted reproductive technologies, such as intracytoplasmic sperm injection (ICSI), for the production of offspring from subfertile mares or stallions in a manner that mirrors human reproductive medicine. The mare's reproductive tract is large and easily imaged or manipulated with minimal discomfort, allowing many reproductive procedures to be performed without harm or distress to the animal. However, the most impactful factors in supporting the equine model for the human are similarities in follicular dynamics and age-associated changes in reproduction.

In this chapter, reproductive aging in the mare and woman will be compared, with a focus on unique possibilities to use the mare in a research capacity. The mare could represent the best large animal model in this area, with availability of older animals, a long reproductive life span, and the potential to naturally develop the multifactorial and complex changes associated with reproductive aging. In general, when young mares are discussed in this chapter, they will be between 2 and 12 years—ages associated with normal cycles and optimal fertility. Mares will be considered middle-aged within their teens, as fertility begins to decline. Old mares will be classified as 20 years of age or older, unless otherwise indicated. The equine population is diverse, and aging is a continuum; therefore, reproductive aging varies among mares in a manner consistent to what is observed for woman.

Animal Models and Human Reproduction, First Edition. Edited by Heide Schatten and Gheorghe M. Constantinescu.
© 2017 John Wiley & Sons, Inc. Published 2017 by John Wiley & Sons, Inc.

Downloaded From Vet-eBooks.com

10.2 Ovarian Activity and Reproductive Cycles

10.2.1 Ovarian Reserve

The ovarian depletion of follicles is considered the primary cause of reproductive failure in women and mares. In both species, the full complement of oocytes is present before birth, and the eventual depletion of oocytes from the ovary is the probable cause of reproductive cessation. Female puberty will occur prior to, broadly, 15 and 1.5 years in the human and equine, respectively, and reproductive cessation will occur at approximately 50 and 25 years. Consequently, in the woman versus the mare, the interval of meiotic arrest of oocytes in primordial follicles prior to puberty is approximately 10 times longer, although the time from birth to cessation of reproductive activity is only approximately twice as long. The length of reproductive activity from puberty until menopause or cessation of reproduction is nearly 1.5 times longer in the woman than mare, with the lengths measured in decades (approximately 3.5 decades in woman and 2.5 decades in mare).

Individual duration of reproductive activity has been related to the number of oocytes remaining in the ovaries. The number of normal primordial germ cells present at 7 years in the girl has been estimated at 300,000 (Baker 1963). In contrast, the mean number of primordial follicles in women at 45–55 years is markedly reduced and varies with menstrual activity (regular menses, 1392 follicles; irregular menses, 142 follicles) with a relatively complete loss of follicles postmenopause (Richardson *et al*., 1987). The population of ovarian follicles is less defined in mares. However, numbers of primordial follicles in mares at 2–4 years were limited and variable (mean of 35,950 and range of 5600–75,000 primordial follicles) (Driancourt *et al*., 1982). Approximately, 238,000 nongrowing follicles were present in the ovaries of women at a similar stage of their reproductive life span (16–20 years, as projected from Hansen *et al*. (2008)), suggesting the woman has more primordial follicles in the early stages of reproductive activity.

The rate of depletion of oocytes from the ovaries has received more attention in the woman than mare. Ginther (1992) estimated that if a mare used 100 follicles per cycle and cycled continuously, the ovarian reserve of approximately 40,000 follicles would be depleted in 25 years. However, no model to explain loss of the ovarian reserve has been developed for the mare. Complex models have been constructed for women to determine the rate of follicle loss and cessation of reproduction. Follicle loss in the woman has been proposed to be doubled after follicle counts fall to 25,000 at approximately 37.5 years (Faddy *et al*., 1992) or to occur at a constantly increasing rate with age (Hansen *et al*., 2008). The depletion of nongrowing follicles was determined to be from atresia in younger women and from entrance into the pool of growing follicles in older women (Gougeon *et al*., 1994). Although the ovarian reserve is less defined in the mare than woman, methods to repeatedly obtain ovarian biopsies have been developed for the mare (Haag *et al*., 2013a, 2013b), providing potential future opportunities to assess ovarian changes over time for individual animals.

10.2.2 Assessment of Antral Follicles

Although limited information is available on primordial follicle counts in mares, the assessment of antral follicles is easily accomplished with the potential for daily or repeated ultrasound imaging. In contrast to the woman, the mare is seasonally polyestrus with regular reproductive cycles during periods of long daylight and a winter period of anestrus. During the vernal transition from winter anestrus to spring cyclicity, follicle-stimulating hormone (FSH) promotes waves of follicular growth before levels of luteinizing hormone (LH) are sufficient to induce ovulation (reproductive seasonality reviewed in Ginther (1992)). While the transitional period is

Downloaded From Vet-eBooks.com

a marked difference from women, it presents a unique opportunity to study ovarian activity and follicular reserves during a natural interval of elevated FSH. When compared among pony mares considered young, middle-aged, or old, the number of follicles at least 10 mm in diameter differed significantly among the groups with a progressive decline in follicle numbers with age during the spring transition (Carnevale *et al*., 1997). Middle-aged and old mares had 36 and 70% fewer antral follicles, respectively, when compared to young mares. One-third of the old mares had only one follicle at least 20 mm in diameter prior to the first ovulation of the year (Carnevale *et al*., 1997). Although unique to the mare, the ovarian response during the vernal transition appears to reflect the ovarian reserve, with fewer follicles available to respond to FSH stimuli with progressive age.

10.2.3 Reproductive Cycles

During the natural breeding season, equine reproductive cycles and ovarian activity reflect similar age-associated changes as observed in women. In general, the mare will go through the following cyclic changes after puberty: (i) normal cycles, (ii) shortened cycles, (iii) elongated cycles, (iv) intermittent cycles, and (v) reproductive senescence. The progression of these stages and age of reproductive cessation is dependent on the individual mare with a potential genetic component.

The first cycle alteration associated with aging in the woman and mare is a shortening of the interval between cycles. In both species, the luteal phase is of normal length; but the follicular phase is shortened by approximately 15% of the length observed in younger females, and earlier and higher elevations of FSH occur within the cycle (Carnevale *et al*., 1993a; Klein *et al*., 2002). In the mare this is associated with a larger mean follicle diameter at the end of the luteal phase, slower growth rate of the dominant follicle, and ovulation of a smaller follicle than observed in young mares (Carnevale *et al*., 1993a). Similar findings were observed when women at least 45 years of age were compared with women 22–34 years of age, with the older group having larger follicles at early stages of development, a slower follicle growth rate, and ovulation of smaller follicles (Santoro *et al*., 2003). Clinically, at this stage many mares have extensive follicular activity on their ovaries with numerous medium or large follicles and a propensity for multiple ovulations (Carnevale, unpublished observations). Significantly, more multiple ovulations occur in Thoroughbred mares aged 17–19 years than 2–4 years (Morel *et al*., 2005), and the propensity toward multiple ovulations and potential twinning in women at this reproductive stage is thought to be associated with the alterations in FSH (Lambalk *et al*., 1998a, 1998b). Although follicular activity is pronounced at this time in the mare, observations during the spring transition suggest that this is because of increased growth or maintenance of antral follicles while the reserve pool of follicles is declining.

With aging, women's cycles will eventually elongate with intermittent cycles and at least one interval of 60 days or longer between menstrual cycles (Soules *et al*., 2001). In the mare, this stage of reproductive activity is associated with a normal luteal phase and a significant increase in the length of the follicular phase (Carnevale *et al*., 1993a). The lengthened follicular phase is associated with a delayed recruitment of follicles into the ovulatory wave, probably caused by insufficient follicle numbers (Ginther *et al*., 1993). Intervals with no luteal tissue or follicular growth are associated with elevations in FSH and LH (Carnevale *et al*., 1994). The lapses in cyclicity in the old mare are associated with minimal or no follicular growth. When a follicle is recruited and begins to grow, concentrations of gonadotropins will decrease. In most cases, a single follicle is observed on the ovaries. Intermittent or occasional cycles will be followed by a complete failure of ovarian follicular growth (Carnevale *et al*., 1994), with the cessation of reproductive activity similar to menopause in the woman.

Downloaded From Vet-eBooks.com

10.2.4 Reproductive Senescence

Reproductive cessation is associated with elevated gonadotropins, and no follicle growth in women and mares (Chakravarti *et al*., 1976; Carnevale *et al*., 1994). The timing of ovarian failure varies, but the average age at menopause for women is approximately 51 years, although the age has varied from 40 to 60 years (te Velde *et al*., 1998). Many mares will cease to cycle in their twenties (Carnevale *et al*., 1994; Vanderwall and Woods, 1990; Wesson and Ginther, 1981), although this can rarely occur in their teens, and some mares will still have follicular growth as they approach 30 years (Carnevale, personal observations). The depletion of the ovarian reserve of primordial follicles appears to be the underlying cause of reproductive cessation in the mare and woman. The longer interval of reproductive quiescence prior to puberty in the woman is probably offset by fewer primordial follicles in the mares' ovarian reserve. The similar progression toward reproductive senescence suggests similar ovarian mechanisms are occurring in both species.

10.3 The Follicle

10.3.1 Follicle Growth and Selection

The dynamics of follicular development are similar in the mare and woman with predominantly single ovulations, long follicular phases, and notable similarities in selection of the dominant follicle and follicle wave patterns (Ginther *et al*., 2004; Ginther, 2012). The follicles in mares are larger than in women, approximately double in diameter prior to ovulation (44.8 and 21.8 mm, respectively) (Ginther *et al*., 2004). The large size of the equine follicle and ease of assess allow unique possibilities, such as repeated follicular fluid collections and injections (da Silveira *et al*., 2012). Substantial volumes of follicular fluid and numerous granulosa cells can be obtained for experimental purposes from equine follicles. The unique aspects of the equine ovary and species similarities provide opportunities to study follicle dynamics and age-associated changes in ovarian activity.

10.3.2 Follicular Environment

The follicle and oocyte are interdependent during growth and maturation. Although a single oocyte is present, the follicle also contains follicular fluid, granulosa cells, and cumulus cells that could impact oocyte developmental potential and serve as fertility markers (review of oocyte environment by Dumesic *et al*. (2015)). Gross age-associated differences in equine follicles are evident, including a slower growth rate during the follicular phase and a higher incidence of ovulatory failure (Carnevale *et al*., 1994). Age-associated differences have also been described in equine follicle cell gene expression (Cox *et al*., 2015; da Silveira *et al*., 2015; Sessions-Bresnahan and Carnevale, 2015) and miRNAs (da Silviera *et al*., 2015). The complexity of the follicular environment and experimental variations make an overview of findings in these areas difficult between the mares and women; however, this will likely change as more information is obtained.

The mare model does provide a unique opportunity to study the process of oocyte and follicle maturation prior to ovulation. In mares and women, ovulation occurs at approximately the same interval of 36–39 h after administration of human chorionic gonadotropin, suggesting similar timing of follicle and oocyte maturation (Edwards and Steptoe, 1975; Ginther, 1992). In one

Downloaded From Vet-eBooks.com

study designed to compare the expression of key genes associated with maturation of the equine follicle and oocyte (Campos-Chillon *et al*., 2015), follicular cells and oocytes were collected at timed intervals (0, 6, 9, and 12 h) after administration of a recombinant equine LH. Findings of the study suggest that quantitative and temporal alterations occur in signaling for oocyte and follicle maturation with aging. Gene expression for the LH receptor did not have the expected profile over time in old mares. Although a similar temporal pattern of expression was observed, amphiregulin and epiregulin mRNAs were significantly elevated in the granulosa cells of old mares compared to young mares. Phosphodiesterase profiles (PDE4D in cumulus cells and PDE3A in oocytes) differed in young and old mares. Although protein concentrations were not analyzed, gene expression suggested an accelerated or asynchronous maturation of the oocyte and follicle in old mares (Campos-Chillon *et al*., 2015).

The equine model has some distinct advantages when studying follicle development and maturation. Development can be tracked using ultrasonography starting at deviation of the dominant from subordinate follicles and continuing until ovulation. The ovaries can be easily and repeatedly imaged using transrectal ultrasonography, and transvaginal procedures have been developed for ovarian manipulations, including follicle injections or recovery of follicular contents. Follicles are large (approximately 22 mm at deviation and 45 mm prior to ovulation), and the follicles contain an abundant volume of follicular fluid and large numbers of cumulus and granulosa cells. Timing and induction of follicle and oocyte maturation can be easily achieved, and the maturation process occurs over a similar time interval as for women. In addition, extensive research has been done on the equine follicle, age-associated changes have been observed, and similarities with follicular function in women have been documented (see reviews Carnevale (2008) and Ginther (2012)).

10.4 Fertility

10.4.1 Natural Decline in Fertility with Aging

The deleterious impact of reproductive aging on fertility is notable in both the mare and woman. In the woman, peak fertility occurs in the twenties, and a substantial decline in fertility is observed after 35 years of age with a progressive decrease until menopause (Soules *et al*., 2001). In women, child bearing typically ends 10 years before menopause, and on average most women deliver their last child by 41 years (reviewed in Liu and Case (2011)). Fertility in the mare begins to decline as they enter their teen years, with a pronounced loss in fertility after 20 years (reviewed in Ginther (1992), Madill (2002), and Scoggin (2015)). In a general comparison, infertility rates of mares in their teens are similar to women in their thirties, and infertility rates are similar for mares approximately 20 years and women 40 years of age. When woman and mares reach 45 and 25 years, respectively, reproductive success is very limited. Therefore, the interval within the reproductive life span associated with a precipitous loss of fertility occurs with an approximate ratio of 1 human to 1.5 mare years, and for both species approximately 40% of their reproductive life span is associated with suboptimal fertility.

10.4.2 Assisted Reproductive Procedures

Assisted reproductive techniques have been used to help augment the age-associated decline in fertility for women and mares, although success is still diminished for older individuals. Maternal age in women is negatively associated with pregnancy after *in vitro* fertilization

Downloaded From Vet-eBooks.com

(van Loendersloot *et al*., 2010). When equine oocytes were fertilized *in vitro* using ICSI, cleavage rates were similar for oocytes from young, middle-aged, and old mares; however, pregnancy loss rates in surrogate mares had a linear increase with donor age, with loss rates around 10% for oocytes from young mares and over 70% for the oldest group of donors (Frank-Guest *et al*., 2010). After *in vitro* fertilization in women, a similar concept was observed with zygote production to the pronuclear stage not affected by age of the oocyte donor; however, pregnancy rates decreased and miscarriage rates increased with increasing maternal age (Yan *et al*., 2012). One differing aspect of assisted reproductive procedures in the mare is that the older donors' oocytes or embryos are transferred into the reproductive tracts of young, fertile recipients, eliminating potential deleterious impacts from the older animals' reproductive tracts and general health.

10.4.3 Maternal Age and Pregnancy Failure

Maternal age in woman is associated with miscarriage, stillbirth, and chromosomal abnormalities at birth (Heffner 2004). The risk of spontaneous abortion increases (20–24 years, 9% and 45 years and older, 75%) irrespective of a woman's reproductive history (Anderson *et al*., 2000), and the risk of miscarriage is highest when both parents are older. The age-associated effect on fertility in the mare appears to have the most pronounced impact on pregnancy loss, especially at early stages of development. Extrapolations from various studies suggest that fertilization rates *in vivo* are not different for young and old mares, although early embryo loss rates are much higher in older mares (Ball *et al*., 1986, 1989; Carnevale *et al*., 1993b). The equine oviduct provides a protected environment for the early embryo that remains in oviduct for approximately 5.5 days before entry into the uterus. When embryos were removed from oviducts at 1.5 or 3 days after ovulation of inseminated mares, fertilization rates per oocyte were similar for young and old mares; but delayed development and morphologic abnormalities were more prevalent in the early embryos from old than young mares (Carnevale *et al*., 1993b). It is logical to conclude that the age-associated loss of embryo developmental potential is associated with oocyte quality.

10.5 The Oocyte

10.5.1 Oocyte Donation

Ultimately, the cause of fertility decline in the mare and woman has been determined to be oocyte quality. Initial studies in both species involved oocyte donation. Oocytes donated from younger women were used to establish pregnancies in older women (mean ages of 33.4 and 42.7 years) who had failed to conceive with their own oocytes (Navot *et al*., 1991), and donated oocytes were subsequently used to establish pregnancies in women who are no longer fertile using their own oocytes (Sauer *et al*., 1996). A similar concept was used for initial studies in the mare; however, oocytes were collected from the preovulatory follicles of young and old mares and transferred into the oviducts of young, inseminated mares. Embryo development rates were significantly higher in the recipient mares after the transfer of oocytes from young versus old mares (92 and 31%, respectively) (Carnevale and Ginther, 1995). In the study, embryo development was determined at 16 days by ultrasonography of the surrogate mares' uteri. The technique of oocyte transfer was later established as a method to produce offspring from older mares with problems of the reproductive tract or ovulation failure (Carnevale *et al*., 2001).

Downloaded From Vet-eBooks.com

Although oocyte transfer provides a method to bypass various reproductive problems associated with the tubular genitalia, pregnancy rates are still adversely affected by maternal aging (Carnevale *et al*., 2010).

10.5.2 Oocyte Morphology and Viability

The human and equine oocytes are approximately 110–120 μm in diameter (Altermatt *et al*., 2009; Kiessling 2007). The equine oocyte is somewhat unique in that it has a large amount of lipids, defined polarity, and an extensive network of transzonal projections extending from cumulus cells to oolemma. The morphology of equine oocytes has been evaluated prior to ICSI for young and old mares. When compared to oocytes from young mares, oocytes from old mares have a thinner zona pellucida, larger perivitelline space, and a larger space (volume) within the inner zona pellucida; the two latter parameters were associated with developmental competence (Altermatt *et al*., 2009). These differences suggest that oocyte growth is affected during follicle development in older mares, and gene expression for oocyte-specific factors that could influence growth are reduced in oocytes from the dominant follicles of old compared to young mares (Campos-Chillon *et al*., 2015). Whether oocyte quality is being affected by altered ovarian factors during oocyte growth or abnormal oocyte morphologies are a reflection of insufficient follicles to allow an adequate selection process is not known.

Microscopic analyses of oocytes from young and old mares have shown other age-associated differences. Confocal analyses of sperm-injected oocytes that failed to cleave in a clinical assisted reproduction program demonstrate an increase in the intensity and area of cytoplasmic actin vesicles in the potential zygotes of old versus young mares (Ruggeri *et al*., 2015). Results of ongoing research suggest that alterations in the actin cytoskeleton and formation of pronuclei are occurring in sperm-injected oocytes from old mares (Ruggeri and Carnevale, unpublished data), confirming age-associated alterations are present within the ooplasm. The extent that cytoplasmic injections will improve viability of oocytes from old mares is yet to be investigated. However, the mare presents a model to investigate techniques that are controversial in human reproductive medicine, with the potential to determine the extent of cytoplasmic dysfunction.

Electron microscopy has been used to compare the maturing oocytes from young and old mares. The most obvious alteration is the presence of large vesicles (greater than 1% of oocyte volume) within the oocytes of the old animals (Carnevale *et al*., 1999). In the resting pool of follicles (primordial, intermediary, and primary) from women 38–45 years and 25–32 years, oocytes from the older women also had a significantly higher fraction of vacuoles of varying sizes (de Bruin *et al*., 2004). Oocytes from the older women had a lower cytoplasmic fraction of mitochondria. The authors noted changes in mitochondria and dilation of the smooth endoplasmic reticulum and Golgi complex, which suggest a role of oxidative damage (de Bruin *et al*., 2004). The changes in oocyte ultrastructure in both species suggest accumulative damage is occurring in the oocyte with maternal aging.

Altered mitochondrial function has been a primary focus when studying reproductive aging (Bentov and Casper, 2013; Eichenlaub-Ritter *et al*., 2011). Copies of mitochondrial DNA (mtDNA) have been used to infer mitochondrial numbers in oocytes, with one or two copies per organelle (Shoubridge and Wai, 2007). Oocyte mitochondrial number has been postulated to be critical determinant of oocyte developmental quality and to provide sufficient distribution of organelles within the early embryo (Shoubridge and Wai, 2007). Mitochondrial numbers in young and old mares have been compared based on mtDNA. Copy numbers of mtDNA were similar in oocytes collected *in vivo* from young and old mares prior to the initiation of oocyte maturation, and they did not change during the first 12 h of oocyte maturation in young mares; however, a temporal decrease of mtDNA was observed in the oocytes of old mares during

Downloaded From Vet-eBooks.com

maturation (Campos-Chillon *et al*., 2015). A similar finding was observed when oocytes were matured *in vitro*, immature oocytes from young and old mares prior to maturation *in vitro* and oocytes from young mares after maturation had similar copy numbers of mtDNA; however, after *in vitro* maturation of oocytes from old mares, copy numbers of mtDNA were lower, and structural damage was imaged in mitochondria (Rambags *et al*., 2014). The potential loss of mitochondria during oocyte maturation in both species could impact oocyte function and embryo developmental potential. Cytoplasmic transfers of mitochondria have not yet been performed in the mare to determine the effect on fertility.

Confocal evaluations of the metaphase II spindles from old mares' oocytes suggest that chromosome misalignment is probable with aging. The majority of oocytes from old mares (88%) had altered spindle morphologies, which were not observed in oocytes from young mares. Spindle problems included nonaligned chromosomes and spindle disarrangement (Carnevale *et al*., 2012). The extent that aneuploidy occurs in the old mare is not yet known; however, it is likely that aneuploidy is a factor associated with the high embryo and fetal loss rates in older mares. In contrast to humans, aneuploidy is not associated with the birth of offspring with chromosomal abnormalities. The underlying causes of aneuploidy and the potential for other factors to affect oocyte viability are still being studied.

The oocytes of older mares demonstrate age-associated alterations, many of which are similar to those observed in women, allowing the potential to test methods to improve oocyte viability. Because oocyte handling and ICSI are well established for the horse, methods for oocyte microinjections or cytoplasmic transfers should be relatively easy to develop in order to test hypotheses that are currently controversial in human medicine, such as mitochondrial transfers.

10.6 Conclusions

Reproductive aging is a continuum that almost certainly results in complex and multifactorial changes affecting fertility, pregnancy loss, and offspring health. The mare could represent the most available and comparable, nonprimate species to study reproductive aging in the women. The many parallels between the mare and woman suggest that similar age-associated changes are occurring in both species, and our ability to monitor and manipulate the equine reproductive tract allows the potential of unique and extensive studies in reproductive aging.

References

Altermatt, J.L., Suh, T.K., Stokes, J.E., and Carnevale, E.M. (2009) Effects of age and equine follicle-stimulating hormone (eFSH) on collection and viability of equine oocytes assessed by morphology and developmental competency after intracytoplasmic sperm injection (ICSI) *Reprod. Fertil. Dev.*, **21**, 615–623.

Anderson, A.M.N., Wohlfahrt, J., Christens, P., Olsen, J., and Melbye, M. (2000) Maternal age and fetal loss: population based register linkage study. *Br. Med. J.*, **320**, 1708–1712.

Baker T.G. (1963) A quantitative and cytological study of germ cells in human ovaries. *Proc. R. Soc. Lond. B*, **158**, 417–433.

Ball, B.A., Little, T.V., Hillman, R.B., and Woods, G.L. (1986) Pregnancy rates at days 2 and 14 and estimated embryo loss rates prior to day 14 in normal and subfertile mares. *Theriogenology*, **26** (5), 611–619.

Downloaded From Vet-eBooks.com

Ball, B.A., Little, T.V., Weber, J.A., and Woods, G.L. (1989) Survival of day-4 embryos from young, normal mares and aged, subfertile mares after transfer into normal recipient mares. *J. Reprod. Fertil.*, **8**, 187–194.

Bentov, T. and Casper, R.F. (2013) The aging oocyte: can mitochondrial function be improved? *Fertil. Steril.*, **99** (1), 18–22.

Campos-Chillon, F., Farmerie, T.A., Bouma, G.J., Clay, C.M., and Carnevale, E.M. (2015) Effects of aging on gene expression and mitochondrial DNA in the equine oocyte and follicle cells. *Reprod. Fertil. Dev.*, **27**, 925–933.

Carnevale, E.M. (2008) The mare model for follicular maturation and reproductive aging in the woman. *Theriogenology*, **69**, 23–30.

Carnevale, E.M. and Ginther, O.J. (1995) Defective oocytes as a cause of subfertility in old mares. *Biol. Reprod. Monogr.*, **1**, 209–214.

Carnevale, E.M., Bergfelt, D.R., and Ginther, O.J. (1993a) Aging effects on follicular activity and concentrations of FSH, LH, and progesterone in mares. *Anim. Reprod. Sci.*, **31**, 287–299.

Carnevale, E.M., Griffin, P.G., and Ginther, O.J. (1993b) Age-associated subfertility before entry of embryos into the uterus in mares. *Equine Vet. J. Suppl.*, **15**, 31–35.

Carnevale, E.M., Bergfelt, D.R., and Ginther, O.J. (1994) Follicular activity and concentrations of FSH and LH associated with senescence in mares. *Anim. Reprod. Sci.*, **35**, 231–246.

Carnevale, E.M., Hermenet, M.J., and Ginther, O.J. (1997) Age and pasture effects on vernal transition in mares. *Theriogenology*, **47**, 1009–1018.

Carnevale, E.M., Uson, M., Bozzola, J.J., King, S.S., Schmitt, S.J., and Gates, H.D. (1999) Comparison of oocytes from young and old mares with light and electron microscopy. *Theriogenology*, **51** (1), 299.

Carnevale, E.M., Squires, E.L., Maclellan, L.J., Alvarenga, M.A., and Scott, T.J. (2001) Use of oocyte transfer in a commercial breeding program for mares with various abnormalities. *J. Am. Vet. Med. Assoc.*, **218**, 87–91.

Carnevale, E.M., Frank-Guest, B.L., and Stokes, J.E. (2010) Effect of equine oocyte donor age on success of oocyte transfer and intracytoplasmic sperm injection. *Anim. Reprod. Sci.*, **121**, S258–S259.

Carnevale, E.M., Maclellan, L.J., Ruggeri, E., and Albertini, D.F. (2012) Meiotic spindle configurations in metaphase II oocytes from young and old mares. *J. Equine Vet. Sci.*, **32**, 410–411.

Chakravarti, S., Collins, W.P., Forecast, J.D., Newton, J.R., Oram, D.H., and Studd, J.W.W. (1976) Hormone profiles after the menopause. *Br. Med. J.*, **2**, 784–786.

Cox, L., Vanderwall, D.K., Parkinson, K.C., Sweat, A., and Isom, S.C. (2015) Expression profiles of select genes in cumulus–oocyte complexes from young and aged mares. *Reprod. Fertil. Dev.*, **27**, 914–924.

daSilveira, J.C., Veeramachaneni, D.N., Winger, Q.A., Carnevale, E.M., and Bouma, G.J. (2012) Cell-secreted vesicles in equine ovarian follicular fluid contain miRNAs and proteins: a possible new form of communication within the ovarian follicle. *Biol. Reprod.*, **86** 71.

da Silveira, J.C., Winger, Q.A., Bouma, G.J., and Carnevale, E.M. (2015) Effects of age on follicular fluid exosomal microRNAs and granulosa cell transforming growth factor-B signaling during follicle development in the mare. *Reprod. Fertil. Dev.*, **27**, 897–905.

de Bruin, J.P., Dorland, M., Spek, E.R., Posthuma, G., van Haaften, M., Looman, C.W.N., and te Velde, E.R. (2004) Age-related changes in the ultrastructure of the resting follicle pool in human ovaries. *Biol. Reprod.*, **70**, 419–424.

Driancourt, M.A., Paris, A., Roux, C., Mariana, J.C., and Palmer, E. (1982) Ovarian follicular populations in pony and saddle-type mares. *Reprod. Nutr. Dev.*, **22** (6), 1035–1047.

Downloaded From Vet-eBooks.com

Dumesic, D.A., Meldrum, D.R., Katz-Jaffe, M.G., Krisher, R.L., and Schoolcraft, W.B. (2015) Oocyte environment: follicular and cumulus cells are critical for oocyte health. *Fertil. Steril.*, **103** (2), 303–316.

Edwards, R.G. and Steptoe, P.C. (1975) Induction of follicular growth, ovulation and luteinization in the human ovary. *J. Reprod. Fertil.*, **22** (Suppl.), 121–163.

Eichenlaub-Ritter, U., Wieczorek, M., Lüke, S., and Seidel, T. (2011) Age related changes in mitochondrial function and new approaches to study redox regulation in mammalian oocytes in response to age or maturation conditions. *Mitochondrian*, **11**, 783–796.

Faddy, M.J., Gosden, R.G., Gougeon, A., Richardson, S.J., and Nelson, J.F. (1992) Accelerated disappearance of ovarian follicles in mid-life: implications for forecasting menopause. *Hum. Reprod.*, **7** (10), 1342–1346.

Frank-Guest, B.L., Stokes, J.E., and Carnevale, E.M. (2010) Association of oocyte morphology and mare age with pregnancy rates after intracytoplasmic sperm injection. *Anim. Reprod. Sci.*, **121**, S241–S243.

Ginther O.J. (1992) *Reproductive Biology of the Mare: Basic and Applied Aspects*, 2nd edn, Equiservices, Cross Plains, WI.

Ginther O.J. (2012) The mare: a 1000-pound guinea pig for study of the ovulatory follicular wave in women. *Theriogenology*, **77**, 18–828.

Ginther, O.J., Carnevale, E.M., and Bergfelt, D.R. (1993) Delay in emergence of the ovulatory follicular wave in old mares. *J. Equine Vet. Sci.*, **13** (2), 75–79.

Ginther, O.J., Gastal, E.L., Gastal, M.O., Berfgelt, D.R., Baerwald, A.R., and Pierson, R.A. (2004) Comparative study of the dynamics of follicular waves in mare and women. *Biol. Reprod.*, **71**, 1195–1201.

Gougeon, A., Ecochard, R., and Thalabard, J.C. (1994) Age-related changes of the population of human ovarian follicles: increase in the disappearance rate of non-growing and early-growing follicles in aging women. *Biol. Reprod.*, **50**, 653–663.

Haag, K.T., Magalhaes-Padilha, D.M., Fonseca, G.R., Wischral, A., Gastal, M.O., King, S.S., Jones, K.L., Figueiredo, J.R., and Gastal, E.L. (2013a) Quantification, morphology and viability of equine preantral follicles obtained via the Biopsy Pick-Up method. *Theriogenology*, **79**, 599–609.

Haag, K.T., Magalhaes-Padilha, D.M., Gastal, M.O., Figueiredo, J.R., and Gastal, E.L. (2013b) Equine preantral follicle harvesting, processing, and *in vitro* culture: the journey has already started. *Anim. Reprod.*, **10** (3), 187–198.

Hansen, K.R., Knowlton, N.S., Thyer, A.C., Charleston, J.S., Soules, M.R., and Klein, N.A. (2008) A new model of reproductive aging: the decline in ovarian non-growing follicle number from birth to menopause. *Hum. Reprod.*, **23** (3), 699–708.

Heffner, L.J. (2004) Advanced maternal age: how old is too old? *N. Engl. J. Med.*, **351** (19), 1927–1929.

Kiessling, A.A. (2007) Human eggs: the need, the risks, the politics. The Burrill Stem Cell Report, The Bedford Research Foundation, October, 2007, pp. 38–45.

Klein, N.A., Harper, A.J., Houmard, B.S., Sluss, P.M., and Soules, M.R. (2002) Is the short follicular phase in older women secondary to advanced or accelerated dominant follicle development? *J. Clin. Endocrinol. Metab.*, **87**, 5746–5750.

Lambalk, C.B., Boomsma, D.I., De Boer, L., Koning, C.H., Schoute, E., Popp-Snijders, C., and Schoemaker, J. (1998a) Increased levels and pulsatility of follicle-stimulating hormone in mothers of hereditary dizygotic twins. *J. Clin. Endocrinol. Metab.*, **83**, 481–486.

Lambalk, C.B., De Koning, C.H., and Braat, D.D.M. (1998b) The endocrinology of dizygotic twinning in the human. *Mol. Cell. Endocrinol.*, **145**, 97–102.

Liu, K. and Case, A. (2011) Advanced reproductive age and fertility. *J. Obstet. Gynaecol. Canada*, **269**, 1165–1175.

Downloaded From Vet-eBooks.com

Madill, S. (2002) Reproductive considerations: mare and stallion. *Vet. Clin. Equine*, **18**, 591–619.
Morel, M.C.G.D., Newcombe, J.R., and Swindlehurst, J.C. (2005) The effect of age on multiple ovulation rates, multiple pregnancy rates and embryonic vesicle diameter in the mare. *Theriogenology*, **63** (9), 2482–2493.
Navot, D., Bergh, P.A., Williams, M.A., Garrisi, G.J., Guzman, I., Sandler, B., and Grunfeld, L. (1991) Poor oocyte quality rather than implantation failure as a cause of age-related decline in female fertility. *Lancet*, **337**, 1375–1377.
Rambags, B.P.B., van Boxtel, D.C.J., Tharasanit, T., Lenstra, J.A., Colenbrander, B., and Stout, T.A.E. (2014) Advancing maternal age predisposes to mitochondrial damage and loss during maturation of equine oocytes *in vitro*. *Theriogenology*, **81**, 959–965.
Richardson, S.J., Seikas, V., and Nelson, J.F. (1987) Follicular depletion during the menopausal transition: evidence for accelerated loss and ultimate exhaustion. *J. Clin. Endocrinol. Metab.*, **65**, 1231–1237.
Ruggeri, E., DeLuca, K.F., Galli, C., Lazzari, G., DeLuca, J.G., and Carnevale, E.M. (2015) Cytoskeletal alterations associated with donor age and culture interval for equine oocytes and potential zygotes that failed to cleave after intracytoplasmic sperm injection. *Reprod. Fertil. Dev.*, **27**, 944–956.
Santoro, N., Isaac, B., Neal-Perry, G., Adel, T., Weingart, L., Nussbaum, A., Thakur, S., Jinnai, H., Khosla, N., and Barad, D. (2003) Impaired folliculogenesis and ovulation in older reproductive aged women. *J. Clin. Endocrinol. Metab.*, **88** (11), 5502–5509.
Sauer, M.V., Paulson, R.J., and Lobo, R.A. (1996) Oocyte donation to women of advanced reproductive age: pregnancy results and obstetrical outcomes in patients 45 years and older. *Hum. Reprod.*, **11** (11), 2540–2543.
Scoggin C.F. (2015) Not just a number: effect of age on fertility, pregnancy and offspring vigour in thoroughbred brood-mares. *Reprod. Fertil. Dev.*, **27**, 872–879.
Sessions-Bresnahan, D.R. and Carnevale, E.M. (2015) Age-associated changes in granulosa cell transcript abundance in equine preovulatory follicles. *Reprod. Fertil. Dev.*, **27**, 906–913.
Shoubridge, E.A. and Wai, T. (2007) Mitochondrial DNA and the mammalian oocyte. *Curr. Top. Dev. Biol.*, **77**, 87–111.
Soules, M.R., Sherman, S., Parrott, E., Rebar, R., Santoro, N., Utian, W., and Woods, N. (2001) Executive summary: Stages of Reproductive Aging Workshop (STRAW) *Climacteric*, **4**, 267–272.
te Velde, E.R., Scheffer, G.J., Dorland, M., Broekmans, F.J., and Fauser, B.C.J.M. (1998) Developmental and endocrine aspects of normal ovarian aging. *Mol. Cell. Endocrinol.*, **145**, 67–73.
Vanderwall, D.K. and Woods, G.L. (1990) Age-related subfertility in the mare. *Proc. Am. Assoc. Equine Pract.*, **36**, 85–89.
van Loendersloot, L.L., van Wely, M., Limpens, J., Bossuyt, P.M.M., Repping, S., and van der Veen, F. (2010) Predictive factors in *in vitro* fertilization (IVF): a systematic review and meta-analysis. *Hum. Reprod. Update*, **16** (6), 577–589.
Wesson, J.A. and Ginther, O.J. (1981) Influence of season and age on reproductive activity in pony mares on the basis of a slaughterhouse survey. *J. Anim. Sci.*, **52**, 119–129.
Yan, J.H., Wu, K.L., Tang, R., Ding, L.L., and Chen, Z.J. (2012) Effect of maternal age on the outcomes of *in vitro* fertilization and embryo transfer (IVF-ET). *Sci. China Life Sci.*, **55** (8), 694–698.

Downloaded From Vet-eBooks.com

11

Spotlight on Reproduction in Domestic Dogs as a Model for Human Reproduction

Shirley J. Wright

Department of Biology, University of Dayton, OH, USA

11.1 Introduction

11.1.1 Scope of the Chapter

The domestic dog (*Canis lupus familiaris*) is a powerful model for the study of reproduction and development. In addition, the dog model is useful to improve our understanding of human development and disease. The dog has unique anatomy and reproductive physiology. Understanding the dog as a research model organism is central to maximizing its use as a research tool for human reproduction and a means to combat human disease. Dogs are important to human society not only as companion and working animals that have a great impact on our lives, but also as valuable mammals because of their pathological disorders that are similar to human diseases. Recent advances in canine genomics, assisted reproduction in the dog, and the great need for improved models of human disease have generated much renewed interest in the domestic dog. The dog is an excellent experimental model for conserving endangered canid species as well. This chapter presents important aspects of the domestic dog as a valuable research tool for human reproduction with specific focus on canine reproductive biology, and also describes the assisted reproductive technologies available for the dog. First a brief overview will focus on the dog in modern human society, and then dog origins and genome before addressing reproductive biology and assisted reproduction in the dog.

11.1.2 Dog's Importance to Modern Human Society

Domestic dogs are abundant in modern human society. Just how abundant are they? According to the Humane Society of the United States (HSUS), the American Pet Products Association has estimated that in 2012, 83.3 million American households owned a dog (HSUS, 2015). Of these, 47% of households owned at least one dog with 10% owning three or more dogs. An average of 1.47 dogs were owned per household (HSUS, 2015). The American Veterinary Medical Association (AVMA, 2015) estimated that in 2012, 36.5% of American households owned a dog with an average of 1.6 dogs per household representing close to 70 million dogs owned in the United States. In the United Kingdom, 9 million households or 24% of households owned a dog in 2014 according to the Pet Food Manufacturers Association (PFMA, 2015), and 9.4 million companion dogs were estimated to be in the United Kingdom in 2011 (Asher *et al.*, 2011). In 2012, Americans spent an average of $231 on annual routine veterinary visits for their dogs

Animal Models and Human Reproduction, First Edition. Edited by Heide Schatten and Gheorghe M. Constantinescu.
© 2017 John Wiley & Sons, Inc. Published 2017 by John Wiley & Sons, Inc.

Downloaded From Vet-eBooks.com

(HSUS, 2015). More than $49 billion that dog owners spent on routine veterinary care in the United States in 2012 and the multibillion dollar pet food industry are indications of just how important dogs have become in our society. They are our loyal companions, closely sharing our lives.

Dogs have served humans well and are deeply integrated into our society. Besides being our loyal companions, dogs have served several valuable roles and a variety of specific breeds were produced to help with our tasks (Table 11.1). Some work alongside us as laborers carrying heavy loads (working dogs), others hunt or retrieve especially during sporting events (sporting dogs), and they are our pride and joy when we show off their beauty and agility in shows and competitions (show dogs). Dogs also serve a critical role for people with disabilities (service dogs). Service dogs are legally defined by federal law and fall under regulations of the Americans with Disabilities Act of 1990, which was revised in 2010 (ADA, 2010). This Act allows people with disabilities to bring service dogs in public places where they are not normally allowed, such as in restaurants and on public transportation.

Dogs have also served as an important laboratory animal in biomedical research. They are the most widely used nonrodent mammal in the research laboratory (Moody *et al.*, 2006). Dog physiology and anatomy are closer to humans than rodents, and dogs have a longer life span than rodents, which enables long-term evaluation of transplantation research studies (Schneider *et al.*, 2008). The pharmaceutical industry uses dogs to screen potential new therapeutic agents (Moody *et al.*, 2006; Schneider *et al.*, 2008). The dog has been used as a model for stem cell transplantation and regenerative medicine, especially to evaluate clinical therapies (Schneider *et al.*, 2008; Starkey *et al.*, 2005). The forensic community uses dog mitochondrial DNA (mtDNA) analysis to aid in identification of biological traces (Duleba *et al.*, 2015). In addition, the dog is an important model organism for social science and psychology research (*cf.* Moody *et al.*, 2006).

11.1.3 Dog Taxonomy

The domestic dog is a eutherian mammal that is a member of the order Carnivora, family Canidae, and genus *Canis*, which also includes wolves (Evans and De Lahunta, 2013; Vilà and Leonard, 2012; Wozencraft, 2005). The dog is the largest domesticated carnivore. The taxonomic hierarchy of the dog is shown in Table 11.2. Previously, the domestic dog was considered a distinct species, but DNA analysis has proved that the domestic dog is a subspecies of the gray wolf, *C. lupus* (Leonard *et al.*, 2006; Lindblad-Toh *et al.*, 2005; Vilà *et al.*, 1997). Therefore, the domestic dog is now classified as *C. l. familiaris*, a subspecies of the gray wolf instead of a separate species.

11.1.4 Dog Origin

Analysis of mtDNA of ancient dog fossils has revealed that domestic dogs originated from gray wolves (*C. lupus*) about 11,000–32,000 years ago (Boyko, 2011; Freedman *et al.*, 2014; Leonard *et al.*, 2006; Lindblad-Toh *et al.*, 2005; Vilà *et al.*, 1997). Dogs were the first domesticated animal (Larson *et al.*, 2012; Leonard *et al.*, 2006). It has been suggested that they were domesticated before humans began agriculture (Boyko, 2011). How, where, and exactly when dogs became domesticated is debated today (Grimm, 2015a). One idea is that dogs domesticated themselves as humans changed from a nomadic hunter–gatherer society to an agricultural society with dog ancestors taking advantage of a permanent supply of discarded food scraps in village dump sites (Boyko, 2011; Case, 2005; Grimm, 2015a). However, further analysis of two ancient canid skulls (Goyet and Eliseevichi MAE 447/5298) indicates that they were actually wolf skulls instead of

Downloaded From Vet-eBooks.com

Table 11.1 Dogs serve human society in many roles.

Dog group or role	Description	Example
Herding dog	Assists with herding livestock (cattle, sheep, reindeer)	Collie, Samoyed, Sheepdog
Hound group	Assists in hunting, and/or tracking by sight or smell	Hound dogs
Scent hound	Hunts by scent and endurance	Basset Hound, Beagle
Sight hound	Hunts by sight and speed	Greyhound, Whippet
Laboratory research dog	Animal model in biomedical research	Beagle
Show dogs	Entertainment and competition	Any breed
Sporting group (Gun dogs)	Hunts and/or retrieves small game and birds	Pointer, Retriever, Setter, Spaniel
Terrier group	Bred to hunt vermin (rat, fox, badger, otter)	Scottish Terrier
Toy group	Small companion dog or lap dog	Chihuahua, Maltese
Working dog	Performs a specific physical task	Labrador
Service dog	Individually trained to help a person with a disability perform a specific task; legally defined by federal law, not a pet, and falls under regulations of the Americans with Disabilities Act of 2010	Labrador, Retriever
Guide dog	Helps person who is blind or visually impaired	Labrador
Hearing-assistance dog	Alerts person who is deaf or hard-of-hearing	Retriever
Medical-alert dog	Alerts person to take medication before medical issue arises such as an extreme blood sugar level of a diabetic patient	Labrador
Seizure-alert dog	Helps person who has epilepsy during or after a seizure	Labrador
Mobility-assistance dog	Aids person with mobility issue by providing balance or pulling a wheelchair	Labrador
Psychiatric-service dog	Assists to calm person with psychiatric condition such as posttraumatic stress disorder (PTSD) during anxiety attack	Labrador
Autism-assistance dog	Helps and protects person with autism improve independence and social interactions	Labrador
Therapy dog	A pet that provides comfort and emotional support to people; visits hospitals, nursing homes, schools; not legally defined	Most breeds
Search and rescue dog	Assists with a task such as finding disaster victims	German Shepherd
Cadaver dog	Detects human remains	German Shepherd
Detection dog	Sniffs for cancer, explosives, illegal drugs, contraband, invasive species, or accelerants used in arson	German Shepherd, Beagle
Police dog	Assists police to attack and apprehend criminals	German Shepherd, Retriever
Military dog	Assists military as scouts, detects mines, locates soldiers	German Shepherd, Labrador
Guard dog	Guards property or endangered species	Doberman Pinscher
Sled dog	Pulls a load such as a sled	Alaskan Husky
Water dog	Performs a water rescue	Portuguese Water Dog

Sources: ADA (2010), AKC (2015), Case (2005), Moody *et al.* (2006).

Downloaded From Vet-eBooks.com

Table 11.2 Taxonomic hierarchy of the dog.

Kingdom	Animalia
Subkingdom	Bilateria
Infrakingdom	Deuterostomia
Phylum	Chordata
Subphylum	Vertebrata
Infraphylum	Gnathostomata
Superclass	Tetrapoda
Class	Mammalia
Subclass	Theria
Infraclass	Eutheria
Order	Carnivora
Suborder	Caniformia
Family	Canidae
Genus	*Canis*
Species	*C. lupus*
Subspecies	*C. l. familiaris*

Retrieved September 23, 2015, from the Integrated Taxonomic Information System online database, http://www.itis.gov.

dog skulls that shift the timing of dog domestication (Drake *et al.*, 2015). Dogs have been with us since early human history, helping to shape it (Boyko, 2011; Case, 2005; Grimm, 2015a).

11.1.5 Dog Breeds

The dog has a unique population structure with each breed coming from a limited number of founders (Shearin and Ostrander, 2010). According to *Miller's Anatomy of the Dog*, a breed is defined as "any group of animals derived from a common stock and bred for their distinctive features, which are codified as the standard for the breed by those willing to recognize the breed" (Evans and De Lahunta, 2013). Most modern domestic dog breeds are less than 200 years old (Ostrander *et al.*, 2006). They have arisen through selective breeding to meet the needs for certain physical characteristics or desired skills (Bell, 2006; Case, 2005; Schoenebeck and Ostrander, 2014; Simpson and Binns, 2006). Each pedigree dog breed is a genetically closed population with a specific set of recognizable phenotypic characteristics (traits) that define the standard for the breed (Case, 2005; Schoenebeck and Ostrander, 2014). To be a registered pedigree dog means that the dog not only meets the stringent physical characteristics of the breed, but also both of its parents had to be registered as dogs of the same breed that met the high, rigorous pedigree standards for the breed (Ostrander and Wayne, 2005; Ostrander *et al.*, 2006). About 490 pedigree dog breeds are officially recognized globally (Schoenebeck and Ostrander, 2014). In 2015, the American Kennel Club (AKC, 2015) recognized 251 distinct breeds separated into eight groups and each breed is described in detail in *The Complete Dog Book* (American Kennel Club, 2015). The United Kingdom's The Kennel Club (KC, 2015) recognized 215 breeds, and the Federation Cynologique Internationale (FCI, 2015) recognized

Downloaded From Vet-eBooks.com

343 breeds worldwide. The dogs are grouped for show purposes and do not necessarily represent genetic closeness (Evans and De Lahunta, 2013).

The most phenotypically diverse land mammal is the domestic dog (Vilà and Leonard, 2012). Consider the size of the small Chihuahua, Yorkshire Terrier, and Pekinese breeds compared to the large Great Dane, Mastiff, or Newfoundland breeds. Mastiffs can be 50 times heavier than Chihuahuas, and Great Danes can be five times taller than Pekinese (Rimbault *et al.*, 2013). Six variants appear to be responsible for about half of the size variation in dogs (Rimbault *et al.*, 2013). Genetic variation at six loci, some involving genes of the growth hormone and insulin signaling pathways, including growth hormone receptor (*GHR*), insulin-like growth factor 1 (*IGF1*), and insulin-like growth factor 1 receptor (*IGF1R*), are involved with variance in weights of dog breeds (Rimbault *et al.*, 2013).

Dog breeds vary not only in size, but also in other physical features such as shape, head, leg length and hair coat (Young and Bannasch, 2006). For example, there are over 30 terms to describe the shape of a dog's ear, such as bat ear, flying ear, and hooded ear (American Kennel Club, 2015). There is a separate ideal characteristic for each morphological feature for each recognized breed. Dog breeds also vary in behavior, including temperament, energy level, and what they like to do such as hunting or herding. These variations are greater in the dog than any other mammal (Moody *et al.*, 2006; Young and Bannasch, 2006).

11.1.6 Dog Genome

The haploid content of the domestic dog genome is about 2.4 Gb of DNA and is smaller than the human genome, which is about 3.2 Gb of DNA (Lindblad-Toh *et al.*, 2005). Of the carnivores, the domestic dog and gray wolf have one of the highest diploid number of chromosomes among mammals (Basheva *et al.*, 2008; Nie *et al.*, 2012). Like the gray wolf, the domestic dog genome is grouped into 78 chromosomes (diploid number $2n = 78$) that form 39 chromosome pairs: 38 pairs of autosomes and 1 pair of sex chromosomes that includes an X and a Y chromosome (Figure 11.1) (Breen and Thomas, 2006; Case, 2005; Gustavsson, 1963; Lindblad-Toh *et al.*, 2005; Moore and Lambert, 1963). The sex chromosomes in females are XX, and in males are XY (Meyers-Wallen, 2006). The autosomes are acrocentric, meaning their centromere is located close to one end, giving the chromosome a "single-arm" appearance (Breen and Thomas, 2006). Chromosome 1 is the largest of the dog chromosomes and is equivalent in size to human chromosomes 9, 10, 11, and 12 combined (Breen and Thomas, 2006). Other than the four largest dog chromosomes, all of the remaining chromosomes are smaller than human chromosome 19 (Breen and Thomas, 2006).

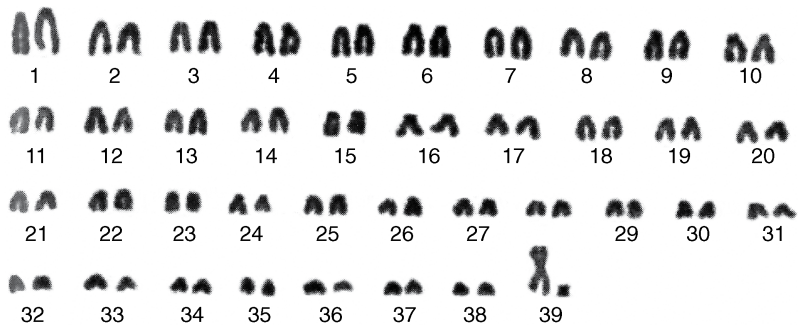

Figure 11.1 Karyotype of a male dog. (Reproduced from Moore W, Lambert PD, The chromosomes of the Beagle dog, *Journal of Heredity*, 1963, **54** (6):273–276, by permission of Oxford University Press.)

Downloaded From Vet-eBooks.com

Various molecular probes and stains are well developed for identifying domestic dog chromosomes (Breen and Thomas, 2006; Thomas *et al.*, 2003). Molecular cytogenetics tools for the dog produce a distinct chromosomal banding pattern with high resolution (Breen and Thomas, 2006; Thomas *et al.*, 2003). It is possible to readily distinguish each dog chromosome for canine cytogenetics and chromosome map production (Breen and Thomas, 2006; Thomas *et al.*, 2003). In addition, the molecular tools are useful to map other species, such as for comparative molecular cytogenetic studies and genome analysis of carnivores (Breen and Thomas, 2006; Nie *et al.*, 2012). High-resolution tools for intra-chromosomal identification and microarray-based genomic profiling analysis have been applied to the dog, especially with dog cancers, which often develop spontaneously as in humans (Figure 11.2) (Thomas *et al.*, 2014). This is very important for melding canine veterinary and human medicine, such as for the new National Cancer Institute comparative brain tumor consortium (LeBlanc *et al.*, 2016).

The sex chromosomes in the dog are metacentric, meaning the centromere is located approximately midway along the chromosome length so that the chromosomes appear "bi-armed" (Figure 11.1). The sex chromosomes are the only metacentric chromosomes of the dog karyotype (Breen and Thomas, 2006; Meyers-Wallen, 2006; Moore and Lambert, 1963). Human sex chromosomes are also metacentric (Federici *et al.*, 2015). In the domestic dog, the X chromosome is over six times longer than the Y chromosome (Figure 11.3). The dog X chromosome is 124 Mb in length, which is shorter than the 156 Mb long human X chromosome or 171 Mb mouse X chromosome (Figure 11.3) (Federici *et al.*, 2015). The Y chromosome is the smallest dog chromosome, being only 20 Mb in length, which is much shorter than the Y chromosome of the human (60 Mb) or mouse (95 Mb) (Figures 11.1–11.3) (Federici *et al.*, 2015; Meyers-Wallen, 2006). The dog X and Y chromosomes share homology at a single pseudoautosomal region (PAR), which is located at the tip of the X and Y chromosomes at the Xp and Yq arms, respectively (Figures 11.3 and 11.4) (Federici *et al.*, 2015). Human sex chromosomes have two PARs located at the tips (one at each end) of the X and Y chromosomes (Xp, Xq, Yp, Yq), with PAR1 (tip of short arm of X and Y) being involved in meiotic recombination (Figure 11.3) (Ross *et al.*, 2005). Mouse PAR regions are located at the tips of the X and Y chromosomes at the Xq and Yq arms (Figure 11.3) (Federici *et al.*, 2015). The PAR length is 6.6 Mb in the dog, which is longer than the human 2.7 Mb length for PAR1 and the mouse 700 kb PAR region (Figure 11.3) (Federici *et al.*, 2015; Ross *et al.*, 2005). Thus, the location and size of the dog PAR region is more similar to the human meiotic recombination PAR1 region than that of the mouse. The dog PAR has 34 annotated genes and transcriptional activity of the dog PAR is low in spermatocytes and spermatids, which are types of immature male reproductive cells (Federici *et al.*, 2015; Lindblad-Toh *et al.*, 2005). During synapsis with the Y chromosome, the dog X chromosome has been reported to self-synapse in pachytene spermatocytes (Figure 11.4) (Federici *et al.*, 2015).

The genome of the domestic dog has been sequenced, including the mitochondrial genome (Hoeppner *et al.*, 2014; Kim *et al.*, 1998; Lindblad-Toh *et al.*, 2005). It was the third fully sequenced mammalian genome (Wade *et al.*, 2006). The dog genome encodes 20,657 protein-encoding genes that is similar to the 21,329 annotated protein coding genes in the human genome (Hoeppner *et al.*, 2014). The dog genome has imprinted genes such as the insulin-like growth factor 2 receptor (*IGF2R*) gene (Nolan *et al.*, 2009). Details of the dog genome sequence have been the subject of several excellent studies and are beyond the scope of this chapter (Hoeppner *et al.*, 2014; Lindblad-Toh *et al.*, 2005; Ostrander *et al.*, 2006; Schoenebeck and Ostrander, 2014). Genome studies have been focused on mapping canine traits and diseases, and comparative genome analysis (Ostrander *et al.*, 2006; Schoenebeck and Ostrander, 2014). Research on the genetic aspects of performance in working dogs is also being addressed (Huson, 2012).

Downloaded From Vet-eBooks.com

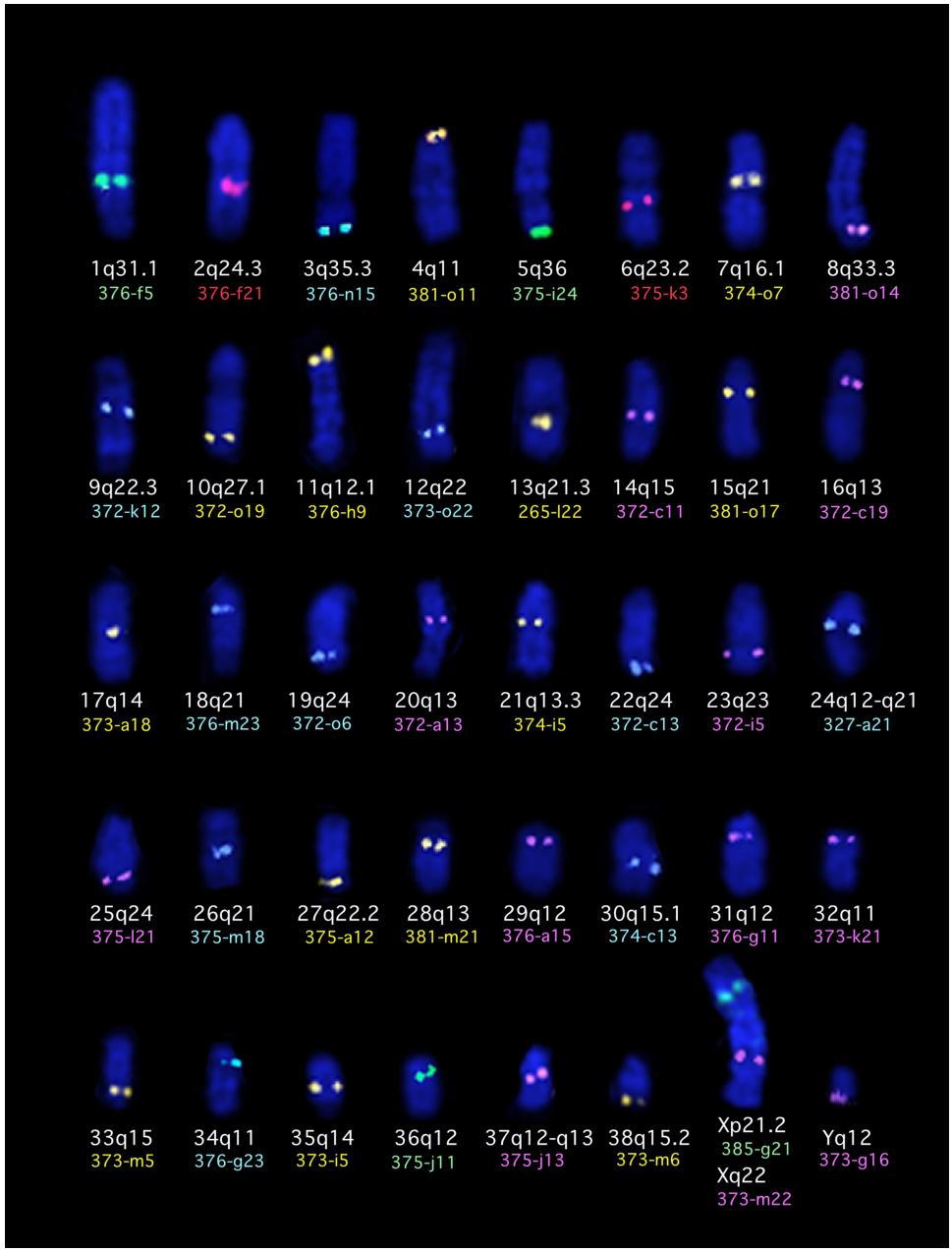

Figure 11.2 Identification of dog chromosomes. Each chromosome was identified using a panel of chromosome-specific single locus fluorescence in situ hybridization (FISH) probes from 41 BAC clones labeled with either DEAC (blue), Spectrum Green (green), Spectrum Gold (yellow), Spectrum Red (red) or biotin-Cy5 (pink), and unequivocally identified based on chromosome size, cytogenetic location of the BAC clone and its fluorochrome label. (Reproduced from Thomas (2003) with permission from Nature Publishing Group.) (See color plate section.)

Downloaded From Vet-eBooks.com

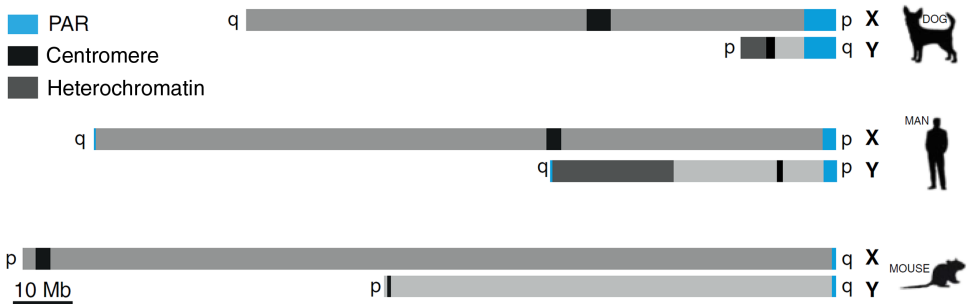

Figure 11.3 PAR regions and centromeres of sex chromosomes. Diagram of dog, human and mouse sex chromosomes showing PAR regions (blue), centromeres (black), heterochromatic regions of the Y chromosomes (dark gray), and p and q arms. (From Federici *et al.* (2015), http://bmcgenomics.biomedcentral.com/articles/10.1186/s12864-015-1501-9. Used under CC BY 4.0 http://creativecommons.org/licenses/by/4.0)

11.1.7 Dog as a Model for Human Genetic Disorders

The long association of dogs with humans has exposed dogs to similar environmental, dietary, and pathological influences as humans have experienced (Breen and Thomas, 2006; Hoeppner *et al.*, 2014). The dog genome may have been similarly affected as that of humans. Dogs have more naturally occurring inherited disorders than other nonhuman species (Starkey *et al.*, 2005). Selective breeding has led to some pedigree dog breeds being prone to certain genetic disorders (Giger *et al.*, 2006; Starkey *et al.*, 2005). Dogs and humans are afflicted with similar genetic disorders many of which are related. It has been reported that the dog has over 450 heritable disorders and approximately 360 are homologous with human conditions (Shearin and Ostrander, 2010; Wilton and Henthorn, 2012). Approximately half of the known canine inherited disorders have a parallel human equivalent (Giger *et al.*, 2006; Starkey *et al.*, 2005). This is almost twice the number of other species (Nagashima *et al.*, 2015). Dogs share

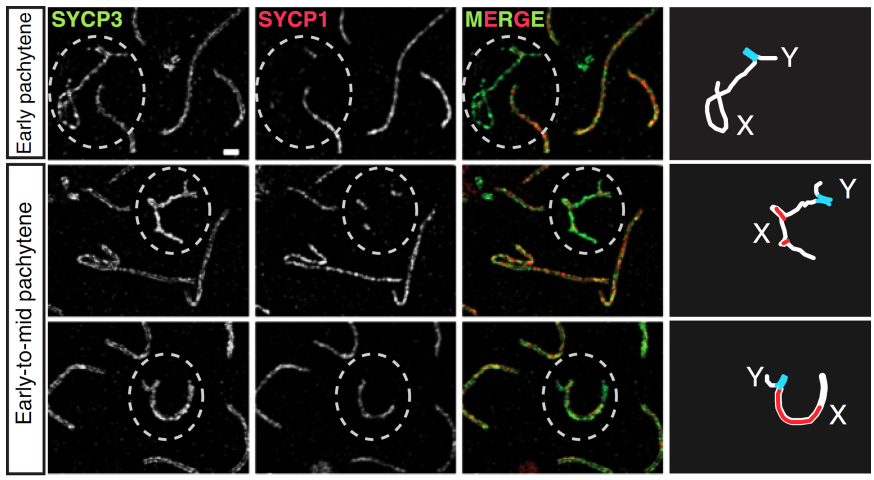

Figure 11.4 Dog sex chromosomes during synapsis. Dog pachytene spermatocyte spread nuclei double-immunostained for SYCP3 (white/green) to resolve lateral elements of the synaptonemal complex, and SYCP1 (red) to identify regions of synapsis. Drawings at right show X-specific and Y-specific regions in white, PAR homologous synapsis (light blue), and X-chromosome heterologous self-synapsis in red. Scale bar, 1 μm. (From Federici *et al.* (2015), http://bmcgenomics.biomedcentral.com/articles/10.1186/s12864-015-1501-9. Used under CC BY 4.0 http://creativecommons.org/licenses/by/4.0)

Downloaded From Vet-eBooks.com

many diseases of humans, including heart disease, muscular dystrophy, cancer (breast cancer, prostate cancer, and osteosarcoma), deafness, blindness (progressive retinal atrophy), and joint disease (Rogers, 2015; Schoenebeck and Ostrander, 2014; Starkey *et al.*, 2005).

Genetic studies have been focusing on comparing the canine genome to the human genome, and more recently, identifying the causes for a specific canine disease condition and finding and correlating that to the human condition. There are many reasons why the dog is an excellent model for enhancing understanding of human inherited disorders (*cf.* Schoenebeck and Ostrander, 2014; Schneider *et al.*, 2008; Starkey *et al.*, 2005). For example, unlike typical laboratory animals such as mice and zebrafish that undergo traditional mutagenesis screens (such as by chemicals or retroviral insertion) to induce mutations, pedigree dogs were selectively bred and their traits and naturally occurring mutations are not biased by genome location (Schoenebeck and Ostrander, 2014). In addition, many canine and human inherited diseases are the result of complex interactions between multiple genes (Schoenebeck and Ostrander, 2014; Starkey *et al.*, 2005). Gene therapy has been successful in dogs for several inherited diseases shared by humans, and has helped provide a foundation for treatment of human patients (Bainbridge *et al.*, 2015; Ellinwood *et al.*, 2006; Switonski, 2014; Tsai *et al.*, 2007). Thus, the dog is a valuable and important model to facilitate understanding of human genetics and genetic diseases.

11.1.8 Dog Life Span

The average life expectancy of the dog is 13 years, and the maximum life span is 29 years (Case, 2005; Grimm, 2015b). Smaller breeds typically have a longer life span than larger breeds (Case, 2005). The medium-sized Australian Cattle dog, Bluey, became the oldest canine on record living 29 years (Grimm, 2015b). In contrast, some large dog breeds such as the Great Dane normally live only 6 or 7 years (Case, 2005). As in humans, aging causes morphological and physiological changes in dogs. In addition, since domestic dogs usually live closely with people, they are exposed to the same environmental conditions as their human caretakers, making the dog an excellent model to study human aging (Grimm, 2015b).

11.2 Dog Reproduction

This section details dog reproduction focusing on reproductive anatomy and physiology, the reproductive cycle and gamete biology. Male and female dogs have both external and internal genital organs, and both will be described in this section. Mature gametes are spermatozoa in males and oocytes in females. Understanding reproductive anatomy of the dog is important for successful breeding, recognizing diseases of the reproductive system and the application of techniques for assisted reproduction. For example, knowing vaginal length and cervical shape are important for artificial insemination procedures. Moreover, understanding uterine anatomical structure is important for success of embryo transfer techniques. Sexual behavior and breeding of dogs is beyond the scope of this chapter and has been reviewed elsewhere (England, 2013; Feldman and Nelson, 2004). In the literature, males are typically referred to as "the dog" or "stud dog" and females are referred to as "the bitch." This chapter will use the terms "male dog" or "male" and "female dog" or "female."

11.2.1 Dog Onset of Puberty

Dogs usually achieve puberty 2–3 months after reaching adult body weight or when they have reached 80–85% of the adult body weight (England, 2013; Forsberg and Reynaud, 2012; Root Kustritz, 2014). Females reach sexual maturity at 6–16 months of age, depending on dog size

Downloaded From Vet-eBooks.com

and breed (Case, 2005; Concannon, 2011; England, 2013). For example, larger female breeds can take 18–24 months to reach puberty (England, 2013; Forsberg and Reynaud, 2012). In male dogs puberty is defined as the time when spermatozoa are first released in the ejaculate (Long, 2006). Normal semen quality and breeding behavior may not necessarily develop at the same time in males (Root Kustritz, 2014). For example, male mounting and thrusting behavior may occur as part of normal play at 4–6 weeks of age, whereas spermatozoa appear in the ejaculate around 10–12 months of age (Case, 2005; England, 2013; Root Kustritz, 2014). Sexual maturity with mature semen quality and normal breeding behavior may not be present until 12–16 months of age (Case, 2005; England, 2013; Long, 2006; Root Kustritz, 2014). Smaller dog breeds reach sexual maturity earlier than larger dog breeds (England, 2013). For example, Toy breeds may reach sexual maturity at 4–6 months of age, whereas large breed males may be sexually mature at 18–24 months of age (Root Kustritz, 2014). In contrast, wolves reach sexual maturity at 2 years of age (Case, 2005).

11.2.2 Dog Fertility

The term "fertility" as used here, refers to the capability of producing offspring. Dogs are highly fertile (Concannon, 2009). After a natural mating, the fertility rate (pregnancy rate) of dogs is about 80% or more, meaning 80% or more of healthy, normal dogs that have mated (without assisted reproduction) produce litters (England and Allen, 1989; England, 2013; England *et al.*, 2009). Commercial kennels can reach a 95% fertility rate of mated females (Concannon, 2009). In humans, the chance of a successful pregnancy during one menstrual cycle (from natural conception, that is, without assisted reproduction) is only 30% (Zinaman *et al.*, 1996). The high fertility rate in dogs is likely because fertile matings can occur up to 5 days before ovulation (release of oocyte from the ovary) and as late as 5–6 days after ovulation (Concannon, 2009; Tsutsui *et al.*, 2009). Another contributing factor to high fertility in dogs is prolonged viability of uterine tubal (oviductal) oocytes (up to 7–8 days after ovulation) and spermatozoa (up to 11 days) (Concannon, 2009; Doak *et al.*, 1967). Although adult females continue the estrous cycle throughout their lives, fertility may decrease with age (Forsberg and Reynaud, 2012). Fertility rates vary with dog breed (Forsberg and Reynaud, 2012). For example, certain breeds such as the Chow Chow have a 53% whelping rate (birth rate) via natural mating (*cf.* Forsberg and Reynaud, 2012).

11.2.3 Reproductive Anatomy of the Male Dog

The male reproductive system consists of individual organs and structures that work together to produce spermatozoa and deliver them to the female reproductive tract (Romano and Brinsko, 2013). The major reproductive organs of the male dog include the testis, system of ducts, prostate gland, and penis (Figure 11.5) (Evans and De Lahunta, 2013). The male reproductive tract includes the testis, epididymis, ductus deferens, urethra, penis, and prostate gland (Figure 11.5) (Constantinescu, 2007). The external genitalia of the dog also include the scrotum. Spermatozoa are released from seminiferous tubules of the testis into straight tubules and then into the rete testis where they drain into efferent ductules and are stored in the epididymis. When needed, spermatozoa exit the epididymis via the ductus deferens where they receive prostatic secretion from the prostate gland before continuing their journey into the urethra and exiting the body via the penis. Reproductive organs and structures in the male dog are comparable to those observed in humans; however, two accessory sex glands, the bulbourethral glands and seminal vesicles characteristic of humans are absent in the dog (Evans and De Lahunta, 2013). Each male reproductive structure of the dog is briefly described in the following sections.

Downloaded From Vet-eBooks.com

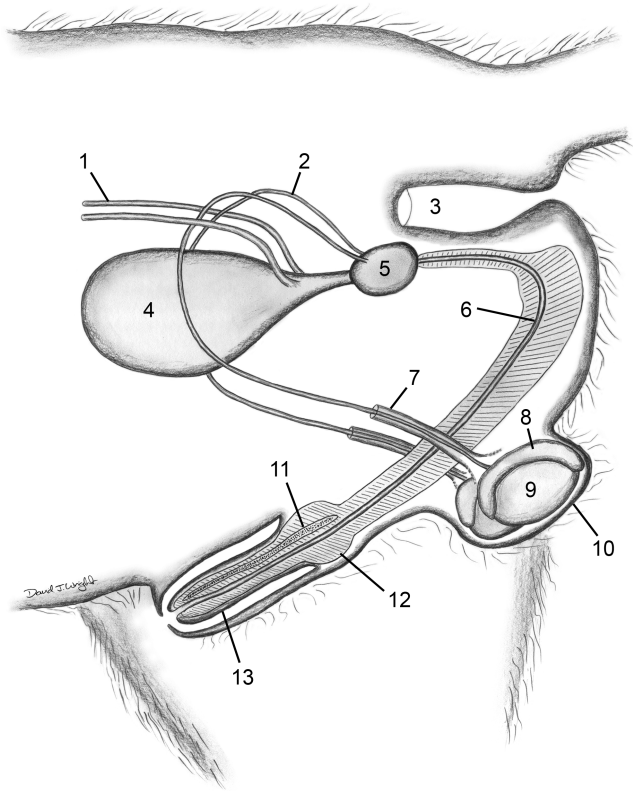

Figure 11.5 Dog male reproductive anatomy. Medial view of right side. 1 = Ureter, 2 = Ductus deferens, 3 = Colon, 4 = Urinary bladder, 5 = Prostate gland, 6 = Penile urethra, 7 = Spermatic cord, 8 = Epididymis, 9 = Testis, 10 = Scrotum, 11 = Os penis, 12 = Bulbus glandis, 13 = Penis. (Courtesy of David J. Wright, Ph.D.)

11.2.3.1 Testis

The dog testis is a paired oval organ that produces spermatozoa during spermatogenesis in seminiferous tubules of the testis (Figure 11.6) (England, 2013; Feldman and Nelson, 2004). The testis also functions as an endocrine organ, producing testosterone (Feldman and Nelson, 2004). In most mammals, the testes migrate from their abdominal position during fetal development to their location outside the body in a sac called the scrotum. In the dog, testicular descent is slower than most mammals and occurs around the time of birth. Dog testes are located halfway between the kidneys and deep inguinal ring of the body wall on the day of birth (Evans and De Lahunta, 2013). Between the second and third weeks after birth, the testes are usually located in the scrotum (Constantinescu, 2007). They have been observed in the scrotum as early as 10 days of age and are palpable by 12–16 weeks of age in most dogs (Root Kustritz, 2014).

Figure 11.6 Dog testis and epididymis. 1 = Spermatic cord, 2 = Ductus deferens, 3 = Vessels and nerves, 4 = Corpus epididymis, 5 = Cauda epididymis, 6 = Caput epididymis, 7 = Testis. (Courtesy of Margaret V. Root Kustritz, D.V.M., Ph.D.)

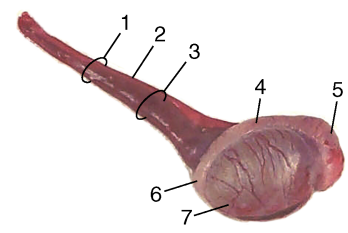

Downloaded From Vet-eBooks.com

Adult dog testes lie obliquely within the scrotum, which is a skin-covered, connective tissue sac located between the hind limbs (Evans and De Lahunta, 2013). Scrotal width is correlated with total body weight (Root Kustritz, 2014). For example, a 10 kg (22 lb) dog has an average total scrotal width of 37 mm (range 31–45 mm), whereas a 20 kg (44 lb) dog has an average total scrotal width of 47 mm (range 38–56 mm) (Root Kustritz, 2014). Skin of the scrotum, muscles of the scrotal wall (cremaster and dartos muscles), and the arrangement of blood vessels in the spermatic cord (described in Section 11.2.3.3) serve to keep the dog testis at 32–36°C, which is a requirement of spermatogenesis (Case, 2005; England, 2013; Plewes and Jennings, 1973; Romano and Brinsko, 2013). This is about 2–6°C lower than the normal body temperature average of 38°C or 101.5°F (range 37.8–39.2°C or 100–102.5°F) (Case, 2005). A median septum divides the scrotum internally into two compartments, each containing one testis and one epididymis (Evans and De Lahunta, 2013). Each testis is surrounded by a double layer of peritoneum with outer tunica vaginalis (composed of parietal and visceral vaginal tunic layers separated by a cavity of the tunica vaginalis) and inner tunica albuginea adhering to the testicular surface.

The testicular surface is smooth (Figure 11.6) (Feldman and Nelson, 2004). Testis size varies markedly with dog breed, and is positively correlated to size of the dog (Feldman and Nelson, 2004; Noakes, 1998). A normal size range for the testis is 1–5 cm in length and 1–3 cm in diameter with an average of 3 cm × 2 cm × 1.5 cm and 11 g in weight (Feldman and Nelson, 2004; Noakes, 1998). Depending on dog size, each testis weighs about 8 g, and can be 19 g (Evans and De Lahunta, 2013; Olar *et al.*, 1983). For example, in an 11 kg (25 pound) dog, the testis averages 3 cm long and 2 cm wide, and weighs 8 g (Evans and De Lahunta, 2013). The dog testis is comparable in size to the adult human testis, which averages 4 cm long, 3 cm from anterior to posterior, and 2.5 cm from left to right (Saladin, 2008). Testis size does not correlate with semen quality (Root Kustritz, 2014). Within the dog testis, U-shaped seminiferous tubules are located in lobules that are separated by connective tissue septae (Constantinescu, 2007; England, 2013). A duct system consisting of straight tubules, centrally located rete testis, and efferent ductules at one pole of the testis gently convey mature spermatozoa from the seminiferous tubules to the epididymis (Constantinescu, 2007).

11.2.3.2 Epididymis

The epididymis is a long, tightly coiled, single convoluted tubule that receives spermatozoa from the testis and stores them within its epididymal duct (Figures 11.6 and 11.7). The epididymal duct is 5–8 mm in length (Constantinescu, 2007). There are a total of two epididymides, each one closely adhering to the dorsolateral surface of the ipsilateral testis (Constantinescu, 2007). The epididymis has a caput (head; which receives spermatozoa from the testis), corpus (body), and cauda (tail) (Figure 11.6). The epididymal caput is located at the cranial end of the testis, and the cauda epididymis is located at the caudal end of the testis (Constantinescu, 2007; Evans and

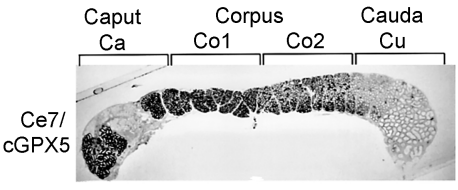

Figure 11.7 Dog epididymis. Expression of Ce7/GPX5 mRNA via *in situ* hybridization in a sagittal-longitudinal section of the dog epididymis with successive regions of tissue indicated (Ca = Caput, Co1 = Proximal corpus, Co2 = Distal corpus, Cu = Cauda). In dogs, both the caput and corpus express Ce7 mRNA, which is caput-restricted in other mammals. (Reproduced from Kirchhoff C, The dog as a model to study human epididymal function at a molecular level, *Molecular Human Reproduction*, 2002, 8(8):695–701, © European Society of Human Reproduction and Embryology, by permission of Oxford University Press.)

Downloaded From Vet-eBooks.com

De Lahunta, 2013). The cauda epididymis eventually straightens out and continues as the ductus deferens (vas deferens). It takes about 14 days for dog spermatozoa to be transported through the epididymis (England, 2013). Spermatozoa are stored in the cauda epididymis, which is plump and pea-sized in thickness in dogs with normal sperm production, but smaller and flaccid in dogs that produce few spermatozoa (England, 2013). The epithelium of the epididymal duct has long stereocilia (Chandler *et al.*, 1981). In the dog, the epididymis secretes alkaline phosphatase, whereas the testis and prostate secrete the enzyme in humans (see Gobello *et al.*, 2002). Canine spermatozoa undergo post-testicular modifications in the epididymis, one of which is the acquisition of progressive motility (Angrimani *et al.*, 2014a, 2014b; Varesi *et al.*, 2013). As spermatozoa of adult male dogs travel through the epididymis, their motility increases from about 0–1% in the caput to 53–63% in the cauda epididymis (Angrimani *et al.*, 2014a, 2014b; Varesi *et al.*, 2013). The epididymis also provides antioxidant activity via glutathione peroxidase and superoxide dismutase that protect epididymal spermatozoa from reactive oxygen species (Angrimani *et al.*, 2014b; Kirchhoff, 2002). Glutathione peroxidase mRNA has been reported to be expressed in the caput and corpus epididymis in the dog with no expression detected in the cauda epididymis (Figure 11.7) (Kirchhoff, 2002). No significant differences, however, were observed in glutathione peroxidase activity or superoxide dismutase activity measured along the length of the dog epididymis (Angrimani *et al.*, 2014b). The pH of dog cauda epididymal fluid is relatively acidic (pH 6.2) and contains 0.6 mM lactate (Carr *et al.*, 1985). The low pH is thought to maintain sperm quiescence and immobility in the epididymis (Carr *et al.*, 1985).

11.2.3.3 Ductus Deferens

The ductus deferens (vas deferens, deferent duct) conveys spermatozoa from the epididymis to the urethra (Figure 11.5). There are a total of two ductus deferentes, each one continuous with the ipsilateral epididymal duct. In an 11 kg (25 pound) dog, the ductus deferens is 17–18 cm long and 1.6–3 mm in diameter (Evans and De Lahunta, 2013). The ductus deferens is joined by the testicular blood vessels, lymph vessels, nerves in the scrotum and connective tissue, and together these structures form a bundle called the spermatic cord (Constantinescu, 2007). In a medium-sized dog, the spermatic cord is 8–10 cm in length (Constantinescu, 2007). The spermatic cord courses upward from the scrotum into the inguinal canal, and passes through the deep inguinal ring in the abdominal wall into the abdomen on its course to the urethra (Constantinescu, 2007).

11.2.3.4 Urethra

The urethra is a hollow tube that conveys urine and semen to the outside of the body (Figure 11.5). In a mature 11 kg (25 lb) dog, the urethra is 25 cm in length (Evans and De Lahunta, 2013). The urethra has three parts, named for their location: pelvic part, prostatic part, and penile part (Evans and De Lahunta, 2013). The urethra begins at the neck of the urinary bladder, pierces through the prostate gland where it receives prostatic secretions, and then courses caudoventrally through the penis ending at the tip of the penis (Figure 11.5).

11.2.3.5 Penis

The penis houses the penile part of the urethra (penile urethra) and conveys urine and sperm-containing semen to outside the body (Figure 11.5). The penis is directed cranially and has three parts: root, body, and glans penis. The nonerectile penis ranges from 6.5 to 24 cm and averages 17.9 cm in the dog (Evans and De Lahunta, 2013). The dog penis has features not found in humans such as a small bone called the os penis that is located in the glans penis (a free region of the penis) dorsal to the penile urethra (Constantinescu, 2007). The os penis is

Downloaded From Vet-eBooks.com

broad proximally and narrow distally and has a ventral groove (7 mm deep and 4 mm wide) for the urethra (Evans and De Lahunta, 2013). In large dogs the os penis is 10 cm long, 1.3 cm wide, and 1 cm thick (Evans and De Lahunta, 2013). The dog penis also has a swelling called the bulbus glandis at the proximal end of the os penis (Case, 2005). The bulbus glandis enlarges to a sphere during early mating and is responsible for the "coital tie" with penile locking that prevents the male and female from separating during copulation, which lasts between 5 and 80 min (Case, 2005). Additional anatomical differences of the dog penis have been described (Constantinescu, 2007).

11.2.3.6 Prostate Gland

The prostate gland is the only accessory sex gland in the dog (Figure 11.5) (Berg, 1958; Constantinescu, 2007; Root Kustritz, 2014). The prostate is yellowish in color, bilobed, and symmetrical or globular (Berg, 1958; Constantinescu, 2007). The gland is located close to the neck of the urinary bladder in the middle of the pelvic inlet where it encircles the cranial part of the urethra (Berg, 1958). The prostate is retroperitoneal (Berg, 1958). Its size varies with the size, breed, and age of the dog. In adults, the prostate is 1.9–2.8 cm long, 1.9–2.7 cm wide, and 1.4–2.5 cm high (Berg, 1958). Its normal weight can be up to 14.5 g, and a good estimate of the prostate gland's weight is 0.21–0.57 g/kg of dog body weight (Berg, 1958; Evans and De Lahunta, 2013). The prostate gland produces prostatic fluid, a watery secretion that is discharged through excretory ducts into the urethra, and this fluid contributes to the first and third fractions of semen of the ejaculate (England, 2013). The prostate contributes to most of the seminal fluid (fluid of semen) in the dog, but only about one-third of the seminal fluid in humans (Ronquist *et al.*, 2013). Seminal fluid provides an optimal environment for sperm survival and motility (Evans and De Lahunta, 2013). Adult dogs secrete 0.5–2.0 ml of prostatic fluid per hour when at rest (Schoonees *et al.*, 1972). Dog prostatic fluid is bacteriocidal and contains bicarbonate, citrate, lactate, glucose, fructose, cholesterol, and enzymes, including acid phosphatase, alkaline phosphatase, amylase, arginine esterase, and coating substances that coat the sperm plasma membrane delaying capacitation of spermatozoa (Brooks, 1990; Carr *et al.*, 1985; England, 2013; Feldman and Nelson, 2004; Schoonees *et al.*, 1972). The dog prostate is under androgenic control (Feldman and Nelson, 2004; Gobello *et al.*, 2002).

11.2.4 Reproductive Physiology of the Male Dog

Adult male dogs are nonseasonal breeders (Case, 2005). They are capable of producing viable gametes throughout the year. The gametes produced in males are called spermatozoa. They are generated via a process called spermatogenesis, which is described in the following section.

11.2.4.1 Dog Spermatogenesis

Spermatogenesis is a dynamic, complex and highly organized process that produces spermatozoa. Spermatogenesis in the dog begins at about 20 weeks (4 months) of development (England, 2013). Spermatozoa are first seen in the ejaculate at 7–9 months depending on dog size (England, 2013). Sperm production is continuous in the adult dog (Forsberg and Reynaud, 2012). Spermatogenesis occurs in the epithelium of the seminiferous tubules of the testis (Leblond and Clermont, 1952; Hess and Renato de Franca, 2008). Residing in the seminiferous epithelium are germ cells that are reproductive cells, and Sertoli cells that are somatic cells that function in nutritive, endocrine, and physical support for the germ cells and their progeny (Amann, 2008; Hess and Renato de Franca, 2008). During spermatogenesis in adult male dogs, spermatogonia that are unspecialized diploid male germ cells (spermatogonial stem cells) located in the cortex of the mature seminiferous epithelium are transformed via mitosis and

Downloaded From Vet-eBooks.com

meiosis into spermatozoa (Amann, 2008; González and Dobrinski, 2015; Hess and Renato de Franca, 2008).

Spermatogenesis is divided into four sequential processes in dogs and other mammals: mitotic, meiotic, postmeiotic, and separation phases (Russell *et al.*, 1990). The *mitotic phase* is also called a proliferative phase because spermatogonia proliferate and differentiate. They undergo mitosis to self-renew, thereby expanding the spermatogonial population, and additionally form primary spermatocytes. The *meiotic phase* involves meiosis of spermatocytes to form round spermatids. Homologous chromosomes of primary spermatocytes pair, become fully synapsed forming a synaptonemal complex, crossover and separate during the meiotic phase (Figure 11.8). About 41 crossover sites were reported per dog spermatocyte: 40 ± 1.4 crossover sites in the autosomes and 1 in the sex chromosomes (Basheva *et al.*, 2008). Crossover sites were closer to the distal chromosome ends (telomeres) than near the centromeres, similar to what has been reported in humans (Basheva *et al.*, 2008). Through two sequential meiotic divisions, primary spermatocytes divide into secondary spermatocytes that in turn divide to become round spermatids. The *postmeiotic phase* is a differentiation phase. During spermiogenesis, round spermatids transform into mature spermatids. Spermiation characterizes the

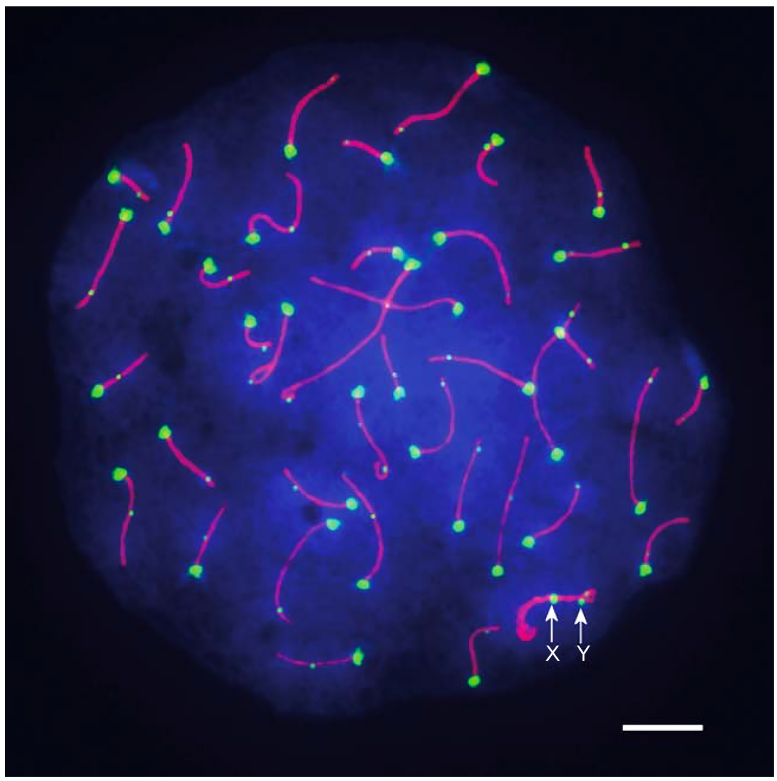

Figure 11.8 Chromosome spread from a dog spermatocyte at pachytene. MLH1 is a mismatch repair protein of mature recombination nodules, and SCP3 is synaptonemal complex protein 3. "Spread from a dog spermatocyte at pachytene, stained with DAPI (blue) and immunolabeled with antibodies to SCP3 (red), MLH1 (green) and centromere proteins (green). Centromeres differ from MLH1 foci by their brighter and more diffuse staining. Arrows indicate centromeres of X and Y chromosomes. Bar represents 5 μm." (Reproduced from *Chromosome Research*, General pattern of meiotic recombination in male dogs estimated by MLH1 and RAD51 immunolocalization, vol. 16, 2008, 709–719, Basheva EA, Bidau CJ, Borodin PM, © Springer 2008. With permission of Springer.) (See color plate section.)

Downloaded From Vet-eBooks.com

separation phase, in which mature spermatids break free from their supporting Sertoli cell and are released into the lumen of the seminiferous tubule as spermatozoa (Amann, 2008; González and Dobrinski, 2015; Hess and Renato de Franca, 2008).

Within the dog seminiferous epithelium, several germ cell generations develop simultaneously (Foote *et al.*, 1972; Muciaccia *et al.*, 2013; Russell *et al.*, 1990). Differentiating spermatogonia are produced at regular intervals (Foote *et al.*, 1972; Muciaccia *et al.*, 2013; Russell *et al.*, 1990). As they develop, germ cells form groupings called *cellular associations* (Hess and Renato de Franca, 2008; Leblond and Clermont, 1952; Muciaccia *et al.*, 2013; Russell *et al.*, 1990). Since the timing of spermatogonial differentiation is consistent in dogs and other mammals, the same combination of cells appear together in layers in recognizable stages (Hess and Renato de Franca, 2008; Leblond and Clermont, 1952; Muciaccia *et al.*, 2013; Russell *et al.*, 1990). This makes it possible to monitor the seminiferous epithelium in testis sections to identify specific stages of spermatogenesis and compare the stages between species. As germ cells differentiate and eventually mature, the process repeats itself. This constitutes the cycle of the seminiferous epithelium, which is an ordered series of the cellular associations in a segment of the seminiferous epithelium over time (Muciaccia *et al.*, 2013; Russell *et al.*, 1990). The average seminiferous epithelium cycle length in the dog has been reported as 13.6 ± 0.7 days (Foote *et al.*, 1972). This was later confirmed at 13.73 ± 0.03 days; however, this value can be shorter (12.55 ± 0.26 days) in the American Pit Bull (Soares *et al.*, 2009). The dog's seminiferous epithelium cycle length is much longer than in the mouse, which is 8.5 days, and closer to the human, which is 16 days (Amann, 2008).

Stages of the cycle of the mammalian seminiferous epithelium have been classified in tissue sections and designated with Roman numerals (Amann, 2008; Clermont, 1963; Hess and Renato de Franca, 2008; Russell *et al.*, 1990). Spermiogenesis occurs in steps with each step given an Arabic numeral in the seminiferous epithelium cycle (Russell *et al.*, 1990). Periodic acid–Schiff (PAS) staining that targets carbohydrate moieties especially in the acrosome, and PAS-hematoxylin (PAS-H) staining have been very useful stains to identify cellular associations in the seminiferous tubule epithelium cycle of mouse and rat testis sections (Muciaccia *et al.*, 2013; Russell *et al.*, 1990). In the dog and human, however, these stains were of marginal value and not recommended to stage spermatogenesis in these species (Russell *et al.*, 1990). Instead, toluidine blue staining of glutaraldehyde fixed sections, and paraffin sections or cryosections stained for immunocytochemistry have yielded excellent results (Federici *et al.*, 2015; Muciaccia *et al.*, 2013; Russell *et al.*, 1990; Soares *et al.*, 2009). By monitoring morphological changes of germ cells and their progeny (such as nuclear appearance and shape especially of the youngest spermatid nucleus, development of the acrosome and flagellum, as well as cell shape and position within the seminiferous epithelium, and cell release into the lumen of the seminiferous tubule), specific stages of the seminiferous epithelium have been established in mammals (Amann, 2008; Clermont, 1963; Hess and Renato de Franca, 2008; Russell *et al.*, 1990).

Dogs have eight distinct seminiferous epithelium cycle stages (cellular associations) designated I–VIII based on shape of the spermatid nucleus, location of spermatids with respect to the basal lamina (basement membrane), presence of meiotic figures, and release of spermatozoa into the tubule lumen (Figure 11.9) (Foote *et al.*, 1972). In the dog seminiferous epithelium cycle, there are 3 major types of spermatogonia (type A, Intermediate and type B) and 12 distinct spermatid steps beginning with the round spermatid (Foote *et al.*, 1972; Ibach *et al.*, 1976; Russell *et al.*, 1990). When a classification system based on the 14-stage rat classification scheme of nuclear morphology was applied to the dog, it was reported to yield 10 stages of the seminiferous epithelium in the dog (Ibach *et al.*, 1976). However, a new classification scheme based on morphogenesis of the acrosome, in addition to the shape of the head of the youngest spermatid generation, confirmed the eight stages of the seminiferous epithelium cycle reported

Downloaded From Vet-eBooks.com

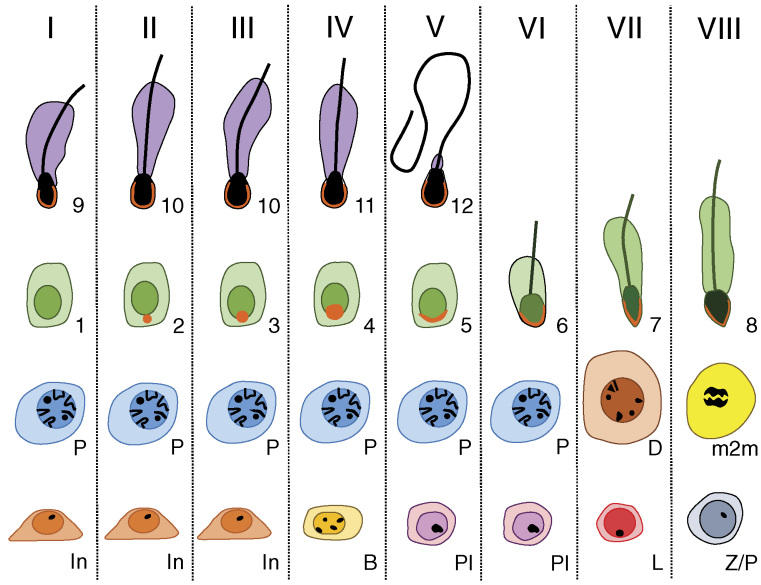

Figure 11.9 Spermatogenic cycle of the dog. Schematic representation of the stages (I to VIII) of the dog seminiferous epithelium cycle based on the acrosome system. The acrosome is shown in bright orange in step 2 to 12 spermatids. Cellular associations at each cycle stage are depicted in each vertical column. Spermatogonia type A (not shown) are present at each cycle stage. For simplicity, flagella of elongating spermatids (step 8 to 11) are drawn short. Cell types include: spermatogonia (B = type B, In = intermediate), spermatocytes (D = diplotene, L = leptotene, m2m = meiotic division, Pl = preleptotene, P = pachytene, and Z/P = zygotene-pachytene), round spermatids (1 to 5) and elongating spermatids (6 to 12). Cells at the bottom of the figure are closest to the basal lamina, and those at the top are closest to the lumen of the seminiferous tubule. (See color plate section.)

earlier by Foote *et al.* (1972) (also see Russell *et al.*, 1990). This new classification scheme was later confirmed by Soares *et al.* (2009) and has been in use since then (Federici *et al.*, 2015). Humans have six cycle stages using nuclear morphology of haploid germ cells as staging criteria, and 12 using acrosomal development detected with immunohistochemistry (Amann, 2008; Clermont, 1963; Federici *et al.*, 2015; Foote *et al.*, 1972; Muciaccia *et al.*, 2013; Russell *et al.*, 1990; Soares *et al.*, 2009). As stated earlier, the seminiferous epithelium cycle has 14 stages in rats and 12 in mice (Russell *et al.*, 1990). Thus, the dog eight-stage seminiferous epithelium cycle is in keeping with that of humans, mice, and rats.

As already stated, one way to classify the stages of the seminiferous epithelium cycle in the dog is to base it on the acrosomal system, which includes the acrosomal membrane and its contents (Figure 11.9) (Russell *et al.*, 1990). The acrosome is a specialized organelle in sperm that is a membranous sac of enzymes and other proteins necessary for fertilization (Russell *et al.*, 1990). Formation of the acrosome is slow in mammals (Russell *et al.*, 1990). The acrosome is absent in the most immature spermatids (round spermatids) and is not complete until late spermiogenesis (Russell *et al.*, 1990). Biogenesis of the acrosome begins with formation of proacrosomal vesicles from the Golgi apparatus, which coalesce to form an acrosomal granule that later touches the nucleus and flattens out over the nuclear surface so that it forms a large acrosomal vesicle or cap that expands to cover roughly the anterior two-thirds of the nuclear surface in mature spermatozoa (Russell *et al.*, 1990). The criteria used to determine the stages of the dog seminiferous epithelium cycle using the progressive changes of the acrosome system are described below (Russell *et al.*, 1990; Soares *et al.*, 2009). Soares *et al.* (2009) reported that type A spermatogonia were present to varying degrees during all eight stages (Soares *et al.*,

Downloaded From Vet-eBooks.com

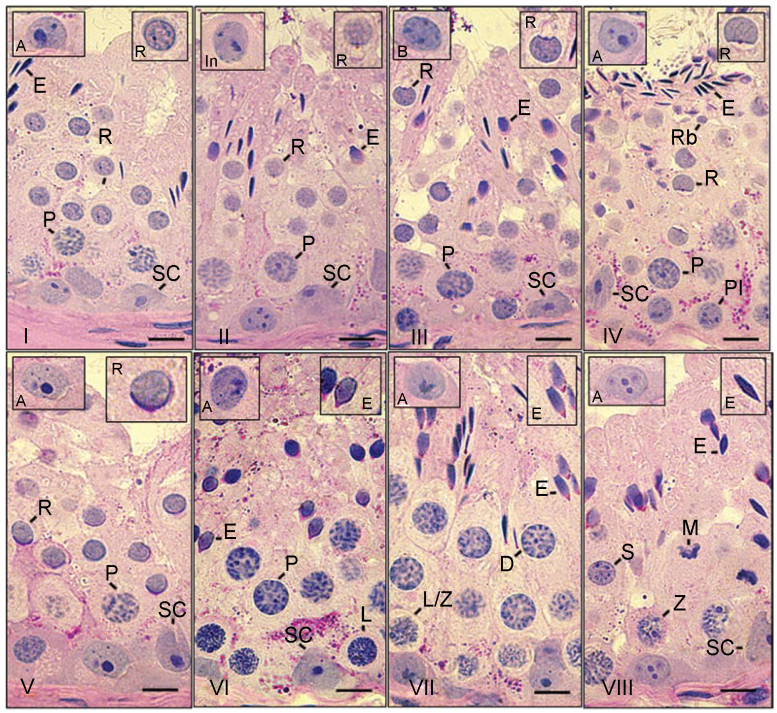

Figure 11.10 Stages of the dog seminiferous epithelium cycle. (Eight different stages based on the acrosome system were identified and the cell types included: A, Type A spermatogonia; In, intermediate spermatogonia; B, Type B spermatogonia; Pl, pre-leptotene; L, leptotene; Z, zygotene; P, pachytene; D, diplotene; M, meiotic division; R, round spermatids; E, elongated spermatids; Rb, residual bodies; SC, Sertoli cell. The figure inserts show a representative spermatogonial cell (upper left) and spermatid step (upper right) for each stage. Bar represents 10 μm. (Reproduced from Soares JM, Avelar GF, França LR, The seminiferous epithelium cycle and its duration in different breeds of dog (*Canis familiaris*), *Journal of Anatomy*, 215(4):462–471, John Wiley & Sons, Inc. © 2009 The Authors, Journal compilation © 2009 Anatomical Society of Great Britain and Ireland, with permission from Wiley.) (See color plate section.)

2009), and Russell *et al.* (1990) calculated the duration of each stage using the 13.6 day cycle length of Foote *et al.* (1972). Testis tissue sections demonstrating each stage of the dog seminiferous epithelium cycle are shown in Figure 11.10, and the stages are described in detail next.

Stage I

The duration of stage I was 27.7 h. During stage I, newly formed early round spermatids (step 1) were present and they lacked distinguishing features with respect to the acrosome system. Step 1 spermatids had a juxtanuclear Golgi apparatus; however, the acrosome system was absent when viewed with light microscopy and transmission electron microscopy. The cells closest to the seminiferous tubule lumen were the elongate spermatids (step 9) that had clear vacuolar spaces within the nucleus where chromatin had not yet fully condensed, and also present was the manchette, which is a transient microtubular-based structure that functions in shaping the spermatid nucleus (Russell *et al.*, 1990; Li *et al.*, 2015). Type A spermatogonia and intermediate spermatogonia (characterized by an intermediate amount of heterochromatin in the ovoid nucleus) were present contacting the basal lamina. Between spermatogonia and spermatids were pachytene spermatocytes containing a large round nucleus with thick chromatin cords.

Downloaded From Vet-eBooks.com

Stage II

The duration of stage II was 23.8 h. Occasional proacrosomal granules were first observed in round spermatids (step 2) during stage II. Elongate spermatids (step 10) were closer to the tubule lumen with their flagella reaching the lumen and their nuclei more condensed than in step 9 spermatids. Mitochondria were not yet aligned along the flagellum of step 10 spermatids. Pachytene spermatocytes were slightly farther away from the basal lamina. Along the basal lamina were intermediate spermatogonia.

Stage III

The duration of stage III was 22.0 h. Stage III was characterized by round spermatids (step 3) that had a round acrosomal vesicle and the acrosome spread slightly over the nucleus. The acrosomal vesicle was somewhat indented along the nuclear surface forming a 70–90° angle. Elongate spermatids (step 10) were even closer to the tubule lumen. Small residual bodies containing excess spermatid cytoplasm were present. Intermediate spermatogonia were adjacent to the tubule lumen and pachytene spermatocytes had more intensely staining nuclei.

Stage IV

The duration of stage IV was 91.2 h. During stage IV, the acrosome indented the nucleus and an extensive acrosomal vesicle was present in round spermatids (step 4). The acrosomal vesicle was flattened along the nucleus so that it formed an angle greater than 90° to about 110° in step 4 spermatids. Type B spermatogonia were observed along the basal lamina, and pachytene spermatocytes with lightly staining chromatin cords and deeply staining nucleoli were present. Also present were elongate spermatids (step 11) that lacked vacuolar structures and thus had more condensed chromatin than step 10 spermatids. In step 11 spermatids, mitochondria were aligned along the flagellum. Large residual bodies containing excess cytoplasm were present as the elongate spermatids underwent spermiation. In addition, emanating usually from the leading edge or acrosomal cap region of the head of late spermatids were tubulobulbar complexes. These complexes are cell surface projections or evaginations of plasma membrane containing cytoplasm and are about 1–2 μm long (Russell and Malone, 1980; Upadhyay *et al.*, 2012). They have three segments, including a proximal tubule with an expanded bulb followed by a distal tubular projection that reaches toward Sertoli cells (Russell and Malone, 1980). Tubulobulbar complexes are thought to function in engulfing unneeded sperm components (Russell and Malone, 1980). Tubulobulbar complexes are also present in human spermatozoa (Russell and Malone, 1980).

Stage V

The duration of stage V was 44.1 h. Spermatid release occurs during stage V. Thus, mainly round spermatids (step 5) were present during Stage V as almost all of the elongate spermatids (step 12) had undergone spermiation into the tubule lumen. Step 5 spermatids had round nuclei and the acrosomal vesicle formed an angle of approximately 120° over the nucleus. Two generations of spermatocytes were present: pachytene spermatocytes and preleptotene spermatocytes.

Stage VI

The duration of stage VI was 27.7 h. During stage VI, spermatid (step 6) nuclei began to elongate and group together. The ratio between the longest nuclear axis (running along nuclear length from tip to caudal end) and shortest nuclear axis (transversely along width of nucleus at equatorial segment) was <1.3 in the elongating spermatids. Preleptotene spermatocytes with speckled chromatin, as well as leptotene spermatocytes were present. Late pachytene spermatocytes that were larger were visible.

Downloaded From Vet-eBooks.com

Stage VII

The duration of stage VII was 35.0 h. Stage VII was characterized by maximal nuclear elongation of spermatids (step 7) in which their longest nuclear axis (running along nuclear length from tip to caudal end) was greater than 1.3 times their width (shortest nuclear axis). The nuclei also appeared more condensed. Primary spermatocytes were in leptotene or zygotene. Diplotene spermatocytes were present.

Stage VIII

The duration of stage VIII was 35.9 h. The elongate spermatids (step 8) of stage VIII were slightly broader and more condensed than step 7 elongating spermatids. Zygotene spermatocytes were present and transitioning into pachytene. Most striking were the many meiotic figures of both meiotic divisions so that secondary spermatocytes and early spermatids were present.

It takes 4–4.5 cycles for dog spermatogenesis to be completed (Russell *et al.*, 1990; Soares *et al.*, 2009). Pulse-labeling with radioactive thymidine as a tracer revealed that the duration of spermatogenesis from spermatogonium to mature spermatozoa is 61.9 ± 0.14 days in several dog breeds, including the Labrador retriever, but can be 10% shorter in the American Pit Bull at 56.5 ± 1.17 days (Soares *et al.*, 2009). The duration of human spermatogenesis is 68–74 days (Amann, 2008; Muciaccia *et al.*, 2013). Thus, the duration of spermatogenesis in the dog is closer to that of humans compared to the mouse that has a 39–40 days duration (Hess and Renato de Franca, 2008). Naturally occurring germ cell loss is observed in dogs as it is in humans, but to a lesser extent (Hess and Renato de Franca, 2008).

Certain proteins key for spermatogenesis in dogs, mice, rats, and humans have specific temporal dynamic expression patterns in the seminiferous tubules (Table 11.3) (Au *et al.*, 2015; Federici *et al.*, 2015; Kuijk *et al.*, 2010). For example, during dog spermatogenesis, NANOG, which functions to establish cell pluripotency, is expressed in nuclei of pachytene spermatocytes and round spermatids, but not in spermatogonia or elongating spermatids (Figure 11.11) (Kuijk *et al.*, 2010). In addition, RAD51 recombinase and γH2AX, which is a phosphorylated form of the histone H2AX variant, were prominent at leptotene when double-strand breaks were present, but decreased as spermatogenesis progressed, being absent by late pachytene and diplotene (Federici *et al.*, 2015). In another example, a matrix metalloproteinase MMP2 (also called gelatinase A), which breaks down the extracellular matrix, was prevalent in the heads of elongate spermatids of stage IV seminiferous epithelium of the dog testis and at the acrosome of ejaculated spermatozoa (Warinrak *et al.*, 2015). Moreover, a metalloproteinase-2 inhibitor, TIMP2 was localized in dog spermatocytes, but not in round spermatids (Warinrak *et al.*, 2015). Matrix metalloproteinases have been found associated with the inner acrosomal membrane in mice, bulls, and humans (Ferrer *et al.*, 2012). They may be involved in sperm penetration of the zona pellucida (extracellular matrix of oocyte) during fertilization, since inhibiting MMP2 significantly blocks fertilization in mice (Ferrer *et al.*, 2012). A final example of a protein with a specific temporal expression pattern in the dog testis is the PIWIL1 protein (Stalker *et al.*, 2016). PIWIL1 is a member of the PIWI family, which is a subgroup of the Argonaute (AGO) family that is expressed in many species, including humans (Russell *et al.*, 2016; Stalker *et al.*, 2016). PIWI proteins are important for fertility of several species, including *Drosophila*, zebrafish, and mice (Russell *et al.*, 2016). In mice, the piwi homologue, miwi, has a critical function in pachytene spermatocytes, since *miwi*-null mice arrest in spermatogenesis at the round spermatid stage (Deng and Lin, 2002). PIWI proteins bind specific small noncoding RNAs (PIWI-interacting RNAs, piRNAs) forming a ribonucleoprotein complex that is guided to retrotransposons that had become expressed during meiosis. The piRNAs direct PIWI1 to silence the retrotransposons via slicer activity or methylation (Russell *et al.*, 2016; Stalker *et al.*, 2016). In the dog, PIWI1 expression

Downloaded From Vet-eBooks.com

Table 11.3 Selected proteins observed during dog spermatogenesis.

Designation	Protein name	Description/location	References
CREST	Centromere protein	Marks centromere location	Federici *et al.* (2015)
γH2AX	Phosphorylated H2AX variant	Marks double-strand breaks and XY body	Federici *et al.* (2015)
H3.1	Histone variant protein	Removed during spermatogenesis	Federici *et al.* (2015)
H3.2	Histone variant protein	Removed during spermatogenesis	Federici *et al.* (2015)
H3.3	Histone variant protein	Removed during spermatogenesis	Federici *et al.* (2015)
HORMAD1	HORMA domain containing 1	Marker of unsynapsed axes	Federici *et al.* (2015)
MLH1	Mismatch repair protein	Shows crossover sites in dog and man	Basheva *et al.* (2008)
MMP2	Matrix metallopeptidase-2 (metalloproteinase-2)	In head of elongate spermatids, and sperm acrosomal region and flagellum	Warinrak *et al.* (2015)
MMP9	Matrix metallopeptidase-9 (metalloproteinase-9)	In spermatocytes, spermatids, and sperm flagellum	Warinrak *et al.* (2015)
NANOG	Homeobox transcription factor	Key regulator of self-renewal and stem-like state	Kuijk *et al.* (2010)
PIWI1	Piwi-like RNA-mediated gene silencing 1	Member of PIWI subfamily of Argonaute proteins; in spermatocytes and spermatids	Stalker *et al.* (2016)
RAD51	RAD51 recombinase	Homologous recombination repair protein	Basheva *et al.* (2008)
		Shows crossover sites	Federici *et al.* (2015)
SYCP1	Synaptonemal complex protein 1	Transverse element protein	Federici *et al.* (2015)
SYCP3	Synaptonemal complex protein 3	Lateral element protein	Basheva *et al.* (2008); Federici *et al.* (2015)
TEX12	Testis expressed 12	Synaptonemal complex central element protein	Federici *et al.* (2015)
TIMP1	TIMP metallopeptidase inhibitor 1 (TIMP metalloproteinase inhibitor-1)	In residual bodies and sperm flagellum	Warinrak *et al.* (2015)
TIMP2	TIMP metallopeptidase inhibitor 2 (TIMP metalloproteinase inhibitor-2)	In spermatocytes and sperm flagellum, but not round spermatids	Warinrak *et al.* (2015)

increased with sexual maturity (Stalker *et al.*, 2016). In addition, PIWI1 was absent from spermatogonia, but became localized to spermatocytes and spermatids of the dog testis (Stalker *et al.*, 2016). Dog *PIWIL1* encodes an 861-amino-acid protein that is 95.9% homologous to human PIWIL1 protein (Stalker *et al.*, 2016). In addition, the canine PIWI1 was reported to bind piRNA-sized small RNAs (Stalker *et al.*, 2016). The PIWI1 size, localization and binding pattern in the dog testis is consistent with a role of PIWI1 protein in spermatogenesis. Members of the PIWI pathway genes have been associated with

Downloaded From Vet-eBooks.com

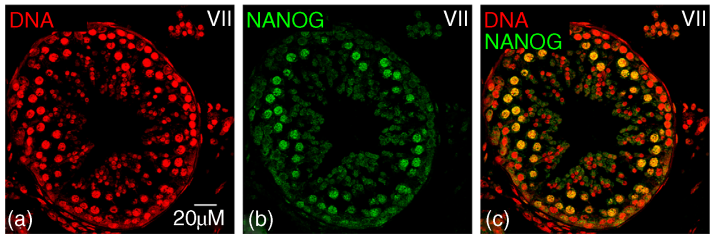

Figure 11.11 NANOG distribution in the dog testis. Confocal fluorescence micrograph of a seminiferous tubule at stage VII stained with: A) TO-PRO®-3 for DNA (red), and B) anti-NANOG antibody (green) with the merged image shown in (C). Nanog staining was present in late pachytene spermatocytes, diplotene spermatocytes and round spermatids, but not in elongating spermatids. (Reproduced from Figure 4A-C of Kuijk EW, de Gier J, Lopes SM, Chambers I, van Pelt AM, Colenbrander B, Roelen BA. (2010) A distinct expression pattern in mammalian testes indicates a conserved role for NANOG in spermatogenesis. *PLoS One* 5(6):e10987. (http://journals.plos.org/plosone/article?id=10.1371%2Fjournal.pone.0010987), © 2010 Kuijk et al. This is an open-access article distributed under the terms of the Creative Commons Attribution License, which permits unrestricted use, distribution, and reproduction in any medium, provided the original author and source are credited, with permission from PLOS.) (See color plate section.)

human spermatogenic disorders (namely, promoter hypermethylation-associated silencing of *PIWIL2* and *TDRD1*) (Heyn *et al.*, 2012). Thus, the dog is an excellent nonrodent model to study the PIWI pathway, and is a resource to generate molecular tools to diagnose human infertility.

MicroRNAs (miRNAs) appear to have an important regulatory role during spermatogenesis in dogs. The miRNAs are endogenous small 19–24 nucleotide long, noncoding, single-stranded RNA sequences that modulate gene expression by posttranscriptional regulation through interaction with mRNA transcripts (Bartel, 2004). Spermatogenic miRNAs have been reported for each stage of spermatogenesis in mice (Kotaja, 2014; Yuan *et al.*, 2015). The miRNAs are differentially expressed during spermatogenesis, and miRNA pathway components are required for normal spermatogenesis and male fertility (Kotaja, 2014; Yuan *et al.*, 2015). Some miRNAs are involved in human infertility (Kotaja, 2014). The canine testis has a repertoire of microRNAs and they have been mapped to the chromosomes from which they are transcribed (Kasimanickam and Kasimanickam, 2015; Kasimanickam *et al.*, 2014). A study examining miRNAs in sexually immature and adult dog testes found that 32 miRNAs were upregulated during spermatogenesis, while 12 were downregulated (Kasimanickam and Kasimanickam, 2015). Dog miRNA expression during spermatogenesis can be disrupted by treatments altering retinoic acid levels (Kasimanickam *et al.*, 2014). Some miRNAs such as miR-141 that were upregulated in the dog via retinoic acid intervention were also significantly increased in human patients with nonobstructive azoospermia (Kasimanickam *et al.*, 2014; Kotaja, 2014). Thus, the dog model is an excellent resource to examine the regulatory role of specific miRNAs during normal spermatogenesis, and to shed light on human male factor infertility in patients with altered miRNA expression profiles that lead to spermatogenic problems.

11.2.4.2 Dog Semen

During ejaculation of the male dog, spermatozoa are mixed with seminal fluid and this mixture is called semen or ejaculate. Dog semen contains spermatozoa from the cauda epididymides and fluid secreted from the prostate gland (England, 2013). Seminal emission occurs over 20–30 min in the dog, unlike humans in which mixing of spermatozoa with accessory gland secretions takes

Downloaded From Vet-e-Books.com

seconds (Cooper, 2011). The volume of dog semen produced is highly variable and depends on dog age, size, and frequency of service, as well as the amount of prostatic fluid produced (Feldman and Nelson, 2004; Olar *et al.*, 1983). Seasons of the year did not influence semen parameters in one study, but did affect seminal testosterone levels and progressive sperm motility in another study (Albrizio *et al.*, 2013; Strzeżek *et al.*, 2015). The total volume of semen per ejaculate is normally 1–40 ml (Feldman and Nelson, 2004).

Dog semen is ejaculated in three continuous fractions (England, 2013; Feldman and Nelson, 2004). The first fraction released is also called the presperm fraction. It has a clear color, relatively small volume (normally 0.5–2 ml), lacks spermatozoa, and is of urethral and prostatic origin (England, 2013). The second fraction is also called the sperm-rich fraction, because it contains spermatozoa, which originate from the epididymis and testis. It has a white or creamy color and small volume (0.5–1 ml) (England, 2013). The third fraction (postsperm fraction, prostatic fluid fraction) originates from the prostate gland and is composed of clear prostatic fluid with few or no spermatozoa. The third fraction is translucent and may have a large volume (up to 40 ml or more) depending on dog characteristics such as breed size (England, 2013; Forsberg and Reynaud, 2012).

The normal spermatozoal concentration of dog semen is between 300×10^6/ml and 800×10^6/ml, and the total number of spermatozoa within each ejaculate ranges from 300×10^6 to 1000×10^6 depending on the dog size (England, 2013). For Toy breeds with small testes, 200 million spermatozoa may be the total sperm count of fertile dogs (Root Kustritz, 2014). The total number of spermatozoa within each ejaculate does not vary with collection technique and is a better parameter for semen evaluation (Root Kustritz, 2014). Daily sperm production averages about $11.7 \pm 0.5 \times 10^6$ to $16.7 \pm 1.4 \times 10^6$ spermatozoa per gram of testicular parenchyma (Olar *et al.*, 1983). The normal percent of spermatozoa that are motile is 80% or more, and 60–70% or more are progressively motile in fresh ejaculate (England, 2013; Root Kustritz, 2014; Strzeżek *et al.*, 2015). Progressively motile spermatozoa swim rapidly in a linear, forward direction and is characteristic of normal, freshly ejaculated spermatozoa. The percentage of progressively motile spermatozoa has been positively correlated with the percentage of morphologically normal spermatozoa (Root Kustritz, 2014). In fertile dogs, the percentage of morphologically normal spermatozoa was reported as 60% or more (Root Kustritz, 2014). Semen may also contain white blood cells and this is normal if the concentration is less than 200 white blood cells/μl of semen (Root Kustritz, 2014).

Dog seminal fluid has low viscosity and does not coagulate as it does in humans (Brewis *et al.*, 2001). The average pH of seminal fluid is 6.2 with a range of 5.5–7.1 (Branam *et al.*, 1984). Dog seminal fluid contains ions (calcium, copper, iron, magnesium, and zinc), cholesterol, and proteins, including glycoproteins and enzymes (Branam *et al.*, 1984). For example, seminal alkaline phosphatase, which is produced by the epididymis is normally found in semen at a concentration of >5000–6800 U/l (England, 2013; Feldman and Nelson, 2004; Root Kustritz, 2014; Strzeżek *et al.*, 2015). Alkaline phosphatase can serve as a marker for epididymal fluid, and is useful to measure in azoospermic semen samples (those lacking spermatozoa) as it can help distinguish between a blockage of the epididymis versus true lack of sperm production (England, 2013; Feldman and Nelson, 2004; Gobello *et al.*, 2002). Seminal carnitine, also secreted by the epididymis in dogs, has the same application as alkaline phosphatase as a marker for secretory versus obstructive azoospermia (Gobello *et al.*, 2002). In addition, the prostate secretes acid phosphatase at a concentration of 800 to >1700 U/l in normal dog semen (Feldman and Nelson, 2004; Strzeżek *et al.*, 2015). Dog seminal fluid also contains antioxidant enzymes, including catalase (0.8–2.9 IU/ml) secreted by the prostate gland, superoxide dismutase (80.0–116.1 IU/ml), and glutathione peroxidase

Downloaded From Vet-eBooks.com

(8.7–45.5 IU/ml) that convey antioxidant protection against reactive oxygen species to spermatozoa that have little cytoplasm (Angrimani *et al.*, 2014b). The concentration of enzyme was reported to vary depending on the dog semen fraction (Angrimani *et al.*, 2014a). The sperm-rich fraction contained the highest amount of superoxide dismutase (116.1 ± 17.0 IU/ml) and glutathione peroxidase (45.5 ± 15.7 IU/ml), and the prostatic fraction contained the highest amount of catalase (2.9 ± 1.8 IU/ml) (Angrimani *et al.*, 2014a). Superoxide dismutase, which is produced by the testis, epididymis, and prostate gland, has been reported as the major antioxidant enzyme in dogs and humans (*cf.* Kawakami *et al.*, 2015). Low seminal plasma concentration of superoxide dismutase has been associated with poor semen quality and with azoospermia (absence of spermatozoa in ejaculate), asthenozoospermia (defective sperm motility), and oligoasthenozoospermia (decreased number of spermatozoa in semen and they have defective motility) in dogs and humans (*cf.* Kawakami *et al.*, 2015).

Compared to other species, dog seminal plasma contains relatively small amounts of monosaccharides (Rigau *et al.*, 2001; Rodríguez-Gil, 2013; Setchell *et al.*, 1994). The highest amount of glucose was reported in the prostatic fraction at 0.04 mM glucose and the other fractions had only 0.01 mM glucose (Rigau *et al.*, 2001). The highest amount of fructose was found in the sperm-rich fraction at 0.06 mM and the other fractions had only 0.1 mM, and 0.1 mM mannose was found in the sperm-rich and prostatic fraction with none detected in the presperm fraction (Rigau *et al.*, 2001). Additional biochemical characteristics of dog seminal plasma have been previously reported (Bartlett, 1962b; Setchell *et al.*, 1994).

Dog seminal fluid also contains small vesicles (exosomes). Prostasomes are small lipid membranous vesicles (exosomes) found in semen of mammals. Dog prostasomes have a mean diameter of 117.6 nm (range 24.4–716.6 nm), which was later confirmed with a mean diameter of 85.5 nm (range 20.3–300.1 nm) (Mogielnicka-Brzozowska *et al.*, 2015; Zelli *et al.*, 2013). As in humans, dog semen contains prostasomes that synthesize ATP and contain many key glycolytic and related enzymes (hexokinase, glucose-6-phosphate isomerase, aldolase, phosphoglycerate kinase, enolase, pyruvate kinase, and glyceraldehyde-3-phosphate dehydrogenase), as well as arginine esterase activity (Mogielnicka-Brzozowska *et al.*, 2015; Ronquist *et al.*, 2013; Zelli *et al.*, 2013). Prostasomes can influence processes related to fertilization such as interacting with spermatozoa to boost sperm motility and have a beneficial effect on cold-stored dog spermatozoa (Mogielnicka-Brzozowska *et al.*, 2015). Another type of exosome in semen of mice, rats, hamsters, bulls, and humans originates from the epididymis and has been named epididymosomes (Sullivan, 2015; Sullivan *et al.*, 2005, 2007). They are involved in important biochemical changes in sperm during transport through the epididymis and act as carriers to transfer specific proteins to epididymal sperm (Sullivan, 2015; Sullivan *et al.*, 2005, 2007). Epididymosomes have not yet been reported in dogs, but small vesicular structures are visible in transmission electron micrographs of the canine epididymis (Chandler *et al.*, 1981). Thus, further investigation of the dog epididymis and exosomes and their possible role in dog reproduction is needed.

11.2.4.3 The Dog Spermatozoon

The first description of dog spermatozoa was by Leeuwenhoek in 1678 (*cf.* Bartlett, 1958). He was able to distinguish their general form and reported a head and motile tail. Modern microscopy has confirmed Leeuwenhoek's findings (Figure 11.12). In addition, much more detail has been revealed with electron microscopy, specialized microscopy techniques, and additional cell and molecular techniques. Specific features of dog spermatozoa are described in the following sections.

Downloaded From Vet-eBooks.com

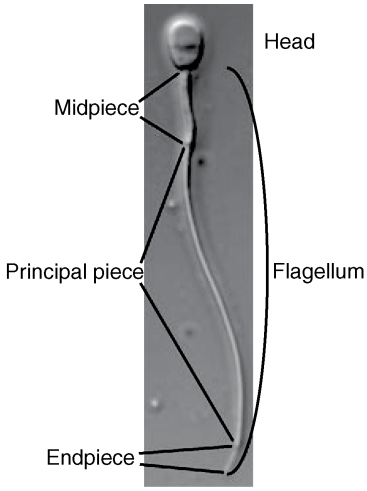

Figure 11.12 Dog spermatozoon. (Reproduced from Mukai C and Travis AJ, What sperm can teach us about energy production, *Reproduction in Domestic Animals*, 47 (Suppl. 4), 164–169, John Wiley & Sons, Inc., © 2012 Blackwell Verlag GmbH, with permission of John Wiley © Sons, Inc.)

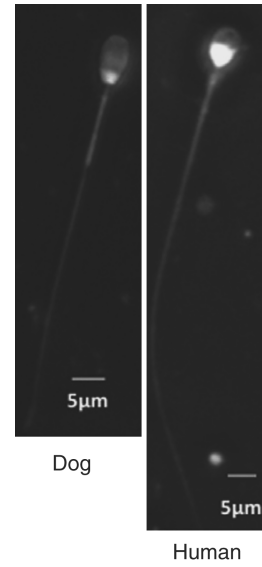

Figure 11.13 Dog and human spermatozoa. Spermatozoa were processed with Trumporph® and observed with a 40× negative phase contrast objective. (Reproduced from *Animal Reproduction Science*, 156, Yániz JL, Soler C, Santolaria P., Computer assisted sperm morphometry in mammals: a review, pages 1–12, 2015, with permission from Elsevier.)

Sperm Shape and Size

Dog spermatozoa are spatulate in shape like a flat wooden spoon or tennis racket (Figure 11.12) (Mukai and Travis, 2012; England, 2013). They are comparable in size and shape to human spermatozoa, which are also spatulate shaped (Figure 11.13; Table 11.4) (Toshimori and Eddy, 2015). Both dog and human spermatozoa have relatively small heads. Their sperm head areas are each $<21\,\mu m^2$ (Table 11.4) (Yániz *et al.*, 2015). In dogs, the sperm midpiece is about 1.5 times longer than the sperm head; whereas in humans it is about the same length as the sperm head (Figure 11.13; Table 11.4). Both dog and human spermatozoa are heteromorphous in shape, meaning they both normally have a high degree of sperm polymorphism within the same ejaculate sample, as well as between individuals (Yániz *et al.*, 2015). In contrast, mouse and rat spermatozoa are falciform-shaped, meaning they have a sickle-shaped head (Setchell, 1982; Toshimori and Eddy, 2015). The total length of rodent spermatozoa is two to three times longer than dog or human spermatozoa (Cummins and Woodall, 1985). In addition, rodent spermatozoa have high homogeneous sperm morphology between and within individuals (Toshimori and Eddy, 2015; Yániz *et al.*, 2015). Thus, dog spermatozoa are more closely matched in shape and size to human spermatozoa. The structural components of dog spermatozoa are described next.

Sperm Organelles

Due to their compact shape and size, dog spermatozoa have few organelles. The membrane-bound organelles present in dog spermatozoon are the sperm nucleus, acrosomal vesicle, and mitochondria (Eddy and O'Brien, 1994). The endoplasmic reticulum, Golgi apparatus, lysosomes, and peroxisomes are absent, being lost during spermiogenesis as is the case for typical mammalian sperm (Flesch and Gadella, 2000). The sperm centriole is located in the sperm neck of the flagellum.

Downloaded From Vet-eBooks.com

Table 11.4 Comparison of morphometric parameters of dog and human spermatozoa.

Sperm parameter[a)]	Dog	References	Human	References
Head length (μm)	7.0 ± 0.0	Bartlett (1962a)	6.11	Cummins and Woodall (1985)
	6.79 ± 0.49	Dahlbom *et al.* (1997)	5.93 ± 0.60	Falzone *et al.* (2011)
	6.61 ± 0.02	Rijsselaere *et al.* (2004)	5.1 ± 0.1	Gergely *et al.* (1999)
	6.1 ± 0.037	Woodall and Johnstone (1988)	4.99	Haifler *et al.* (2015)
	5.9	Cummins and Woodall (1985)	4.98 ± 0.60	Soler *et al.* (2003)
	5.4 ± 0.32	Núñez-Martínez *et al.* (2005)	4.31 ± 0.29	Mossman *et al.* (2013)
Head width (μm)	5.0 ± 0.1	Bartlett (1962a)	4.45 ± 0.23	Falzone *et al.* (2011)
	4.08 ± 0.31	Dahlbom *et al.* (1997)	3.88 ± 0.78	Haifler *et al.* (2015)
	3.9	Cummins and Woodall (1985)	3.45	Cummins and Woodall (1985)
	3.8 ± 0.023	Woodall and Johnstone (1988)	3.1 ± 0.5	Gergely *et al.* (1999)
	3.79 ± 0.03	Rijsselaere *et al.* (2004)	3.04 ± 0.36	Soler *et al.* (2003)
	3.5 ± 0.21	Núñez-Martínez *et al.* (2005)		
Head area (μm^2)	20.57 ± 2.15	Dahlbom *et al.* (1997)	18.83 ± 1.37	Falzone *et al.* (2011)
	20.02 ± 0.62	Rijsselaere *et al.* (2004)	12.27 ± 1.98	Soler *et al.* (2003)
	15.4 ± 1.34	Núñez-Martínez *et al.* (2005)	11.5 ± 0.2	Gergely *et al.* (1999)
Midpiece length (μm)	11.0 ± 0.2	Bartlett (1962a)	6.1 ± 0.1	Gergely *et al.* (1999)
	10.6	Cummins and Woodall (1985)	4.70	Cummins and Woodall (1985)
	10.1 ± 0.074	Woodall and Johnstone (1988)	4.22	Haifler *et al.* (2015)
			2.04 ± 0.19	Mossman *et al.* (2013)
Tail length (μm)	52.23 ± 4.34	Rijsselaere *et al.* (2004)	62.5 ± 0.5	Gergely *et al.* (1999)
	50.0 ± 0.3	Bartlett (1962a)	47.13	Cummins and Woodall (1985)
	45.8	Cummins and Woodall (1985)	43.76 ± 2.66	Mossman *et al.* (2013)
	45.2 ± 0.214	Woodall and Johnstone (1988)		
Total length (μm)	68.0 ± 0.3	Bartlett (1962a)	58.39	Cummins and Woodall (1985)
	62.7	Cummins and Woodall (1985)	48.07 ± 2.68	Mossman *et al.* (2013)
	61.4 ± 0.244	Woodall and Johnstone (1988)		

a) Variations in sperm measurements may be caused by inherent polymorphism within the same ejaculate and between individuals, as well as specimen preparation techniques and viewing methods.

Sperm Head

The head of the spermatozoon is the anterior part of the dog spermatozoon. It functions in sperm–oocyte interactions and contributes the paternal genome to the oocyte. The sperm head is bilaterally flattened and joined to the tail at the connecting piece (Figure 11.14) (Eddy and O'Brien, 1994; England, 2013; Toshimori and Eddy, 2015). The sperm head has two major regions: anterior head also known as acrosomal region, and posterior head also called

Downloaded From Vet-eBooks.com

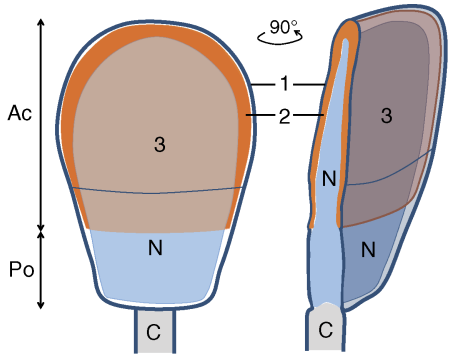

Figure 11.14 Schematic diagram of the regions of a dog sperm head. At right, the sperm has been cut perpendicular to the flat surface of the sperm head (sagittal section). Ac = Acrosomal region, C = Connecting piece of the flagellum, N = Nucleus, Po = Postacrosomal region, 1 = plasma membrane, 2 = acrosome, 3 = portion of acrosome overlying the sperm nucleus.

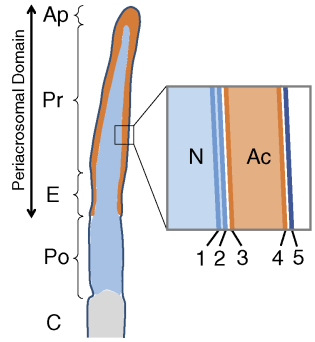

Figure 11.15 Schematic diagram of a dog sperm head depicting membranes and their domains. Sagittal section. Inset shows a magnified area of the sperm head containing the nucleus and acrosome. Ac = Acrosomal contents, Ap = Apical segment domain, C = Connecting piece of the flagellum, E = Equatorial segment domain, N = Nucleus with highly condensed chromatin, Po = Postacrosomal segment domain, Pr = Principal segment domain, 1 = Inner nuclear membrane, 2 = Outer nuclear membrane, 3 = Inner acrosomal membrane, 4 = Outer acrosomal membrane, 5 = Plasma membrane.

postacrosomal region (Figures 11.14 and 11.15) (Fawcett, 1975; Toshimori and Eddy, 2015). The acrosomal region covers about 60% of the sperm head (Feldman and Nelson, 2004; Russell *et al.*, 1990). The postacrosomal region extends from the posterior margin of the acrosomal region to the connecting piece of the flagellum. The head of the spermatozoon contains the haploid sperm nucleus, acrosome, a thin layer of cytoplasm, and the surrounding plasma membrane (Figures 11.14 and 11.15) (Eddy and O'Brien, 1994; Feldman and Nelson, 2004; Toshimori and Eddy, 2015).

Sperm Nucleus

The nucleus of the dog spermatozoon is located in the sperm head (Figures 11.14 and 11.15). The sperm nucleus is surrounded by the sperm nuclear envelope, which is a double membrane consisting of an inner nuclear membrane, which faces the sperm chromatin, and an outer nuclear membrane which is in direct contact with the cytoplasm (Figure 11.15). Sagittal tissue sections of the sperm head (cut perpendicular to the long axis of the dog spermatozoon and viewed with transmission electron microscopy) revealed that the sperm nucleus is flattened bilaterally (Burgess *et al.*, 2001). The dog sperm nucleus is ovoid, long, and broad occupying most of the length and width of the sperm head. It is flat and very thin, with a slightly curved base, and highly curved anterior end (Figures 11.14 and 11.15). The dog sperm nucleus is thicker at the base, slightly narrowed at the region of the equatorial segment, and very thin anteriorly (Bedford, 1982; Burgess *et al.*, 2001). It has been proposed that the equatorial segment region of the plasma membrane rests in the shallow depression created by the contour of the sperm nucleus, which protects the equatorial segment from abrasion by the dense zona pellucida of the oocyte during fertilization (Bedford, 1982).

As a result of meiotic divisions during spermatogenesis, the sperm nucleus contains only one copy of each chromosome (Eddy and O'Brien, 1994). In dogs, the sperm nucleus houses the paternal chromosomes that include one copy each of chromosome 1–38 and either an X or a Y

Downloaded From Vet-eBooks.com

chromosome (Eddy and O'Brien, 1994). The haploid dog sperm nucleus has tightly compacted, highly condensed chromatin, typical of mammalian sperm nuclei. To achieve the highly condensed state of the sperm chromatin, during spermiogenesis chromatin of round spermatids was remodeled so that basic chromosomal proteins replaced the existing histones of chromatin (Table 11.3). Three types of small basic nuclear proteins are involved in repackaging sperm chromatin and condensing it: (i) histones, which have sperm-specific variants called sperm-specific histones, (ii) protamines, which are abundant, short, arginine-rich proteins composed of 27–65 amino acids, and (iii) transition proteins, which are rich in arginine and lysine, related to the histone H1 family, and also assist in repackaging of sperm chromatin (Jodar and Oliva, 2014; Toshimori and Eddy, 2015). During chromatin remodeling, round spermatid histones are replaced by transition proteins 1 and 2 (TNP1, TNP2). Both *TNP1* and *TNP2* genes are expressed in dog and human testes (Kleene and Bagarova, 2008). As chromatin condenses, the transition proteins are replaced by protamines 1 and/or 2 (PRM1, PRM2) (Martin-Coello *et al.*, 2011). Genes encoding protamines are commonly found together in a cluster in mammals (Jodar and Oliva, 2014). The protamine gene cluster members include *PRM1*, *PRM2*, and *TNP2* (transition protamine 2) in the mouse, rat, bull, and human (Jodar and Oliva, 2014). Dogs have one active protamine gene (*PRM2*), and humans have two (*PRM1*, *PRM2*) (Johnson *et al.*, 1988; Kleene and Bagarova, 2008; Lee and Cho, 1999). Protamine genes are expressed as mRNA and protein in testis samples from dogs and humans (Kleene and Bagarova, 2008; Lee and Cho, 1999). The dog *PRM2* gene is located on chromosome 6 along with the *TNP2* transition protein gene, whereas these genes are on chromosome 16 in humans and mice (Jodar and Oliva, 2014; Martin-Coello *et al.*, 2011). Protamine gene mutations have been found in infertile human patients, and protamine knockout mice are infertile (Oliva, 2006; Jodar and Oliva, 2014). Of note is that there is some confusion over a *PRM3* gene found in the protamine gene cluster (Jodar and Oliva, 2014). In the NCBI gene database (accessed November 11, 2015), two protamine genes (*PRM2*, *PRM3*) were listed for dogs and three for humans (*PRM1*, *PRM2*, and *PRM3*). However, the *PRM3* protein is not considered a true protamine and is unrelated to the protamines because it (i) is a very acidic protein with a large proportion of negative residues, (ii) has a low amount of arginine residues, (iii) is localized to the cytoplasm rather than the nucleus, and (iv) is absent from mature spermatozoa, but is present in spermatids in mice (Jodar and Oliva, 2014; Martin-Coello *et al.*, 2011).

Sperm Acrosome

The acrosome is an organelle of the mammalian spermatozoon that is formed from the Golgi complex during spermiogenesis (see Section 11.2.4.1) (Eddy and O'Brien, 1994; Russell *et al.*, 1990; Toshimori and Eddy, 2015). In the dog, the acrosome is located in the anterior of the sperm head between the plasma membrane and sperm nucleus (Figures 11.14 and 11.15) (Burgess *et al.*, 2001; Russell *et al.*, 1990). The acrosome is also called the acrosomal vesicle or acrosomal cap because it is a large membranous, flattened vesicle or cap over the nucleus. In the dog, the acrosome covers about two-thirds of the sperm nuclear surface (Cortes *et al.*, 2006). In sagittal tissue sections, which are cut perpendicular to the broad, flattened aspect of the sperm head (sagittal section) and observed with transmission electron microscopy, the acrosome appears as a thin flattened sac in the shape of a letter "V" with elongated, outstretched arms holding the nucleus (Figures 11.14 and 11.15) (Burgess *et al.*, 2001; Russell *et al.*, 1990). The acrosome has two major segments: anterior acrosome also called acrosomal cap, and posterior acrosome also called equatorial segment that underlie the respective domains of the plasma membrane with the same names (see "Sperm Membranes" section) (Toshimori and Eddy, 2015). The acrosome has an outer acrosomal membrane just underneath the plasma membrane, and an inner acrosomal membrane overlying the outer leaflet of the anterior sperm nuclear envelope

Downloaded From Vet-eBooks.com

(Eddy and O'Brien, 1994; Toshimori and Eddy, 2015). Posteriorly the outer and inner acrosomal membranes are continuous at the equatorial segment (Fawcett, 1975). Many components of the acrosome have been identified in mammalian spermatozoa both within the acrosome and as part of the acrosomal membranes (for a list, see Toshimori and Eddy, 2015). The acrosome contains several hydrolytic enzymes important for fertilization (Flesch and Gadella, 2000; Toshimori and Eddy, 2015). For example, the dog acrosome contains hyaluronidase, *N*-acetylhexosaminidase, and proacrosin (Kawakami *et al.*, 1999a). Proacrosin is in an inactive form within the acrosomal vesicle and is converted to acrosin during the acrosome reaction (Cortes *et al.*, 2006).

Sperm Flagellum

The sperm flagellum (tail) is a very elongated, thin cylindrical structure enclosed by plasma membrane (Figures 11.12 and 11.13). In the dog, the flagellum occupies 90% of the total length of the spermatozoon (Table 11.4). The flagellum functions in sperm motility and the structure of the flagellum reflects this (Fawcett, 1975; Inaba, 2011; Oettlé and Soley, 1985). At the core of the flagellum is the axoneme (axial filament complex, axonemal complex), which runs the full length of the flagellum and generates the flagellum's motive force (Fawcett, 1975; Setchell, 1982; Toshimori and Eddy, 2015). The axoneme consists of two central singlet microtubules surrounded by nine evenly distributed doublet microtubules (Fawcett, 1975; Setchell, 1982; Toshimori and Eddy, 2015). Between the axoneme and plasma membrane is a small amount of cytoplasm, and additional structures depending on the specific region of the sperm flagellum. These additional structures of the flagellum include outer dense fibers, fibrous sheath, and mitochondria (Eddy and O'Brien, 1994; Fawcett, 1975; Setchell, 1982; Toshimori and Eddy, 2015). The sperm flagellum has four distinct segments (listed here from proximal to distal): connecting piece (neck), middle piece (midpiece), principal piece, and endpiece (Figure 11.12) (Fawcett, 1975; Toshimori and Eddy, 2015). The neck of the flagellum connects the proximal part of the midpiece to the sperm head, and contains the sperm centrioles (Fawcett, 1975; Toshimori and Eddy, 2015). The midpiece is a narrow cylindrical section of the flagellum that is about 1.5 times the length of the sperm head (Table 11.4) (Feldman and Nelson, 2004). The midpiece contains the proximal part of the axoneme, outer dense fibers, mitochondria, and plasma membrane (Fawcett, 1975). Nine outer dense fibers surround the axoneme and extend from the sperm neck into the principal piece (Fawcett, 1975; Inaba, 2011; Pesch and Bergmann, 2006; Russell *et al.*, 1990). Dogs express the *Odf1* gene, which encodes one of the major proteins of the outer dense fibers (Kleene and Bagarova, 2008). Mitochondria surround the outer dense fibers in the midpiece (Pesch and Bergmann, 2006). At the distal end of the midpiece is the annulus, which is a fibrous structure that has been proposed to function in preventing caudal displacement of mitochondria (Pesch and Bergmann, 2006). The principal piece connects proximally to the midpiece at the annulus. The principal piece is the longest section of the flagellum (Toshimori and Eddy, 2015). It contains the centrally located axoneme, outer dense fibers, and fibrous sheath lying just underneath the plasma membrane (Fawcett, 1975; Inaba, 2011; Pesch and Bergmann, 2006; Russell *et al.*, 1990). The flagellum terminates in an end piece that contains the axoneme, but lacks the outer dense fibers and fibrous sheath (Pesch and Bergmann, 2006). The description given here is the classical description of the sperm flagellum, and of note is that the scientific literature is sometimes confusing, as the "tail" may or may not include the neck (connecting piece) and midpiece, but usually includes the principal piece and end piece.

Sperm Mitochondria

The mitochondria of the mammalian spermatozoon are located in the midpiece of the flagellum (Figure 11.16) (Fawcett, 1975; Pesch and Bergmann, 2006; Toshimori and Eddy,

Downloaded From Vet-eBooks.com

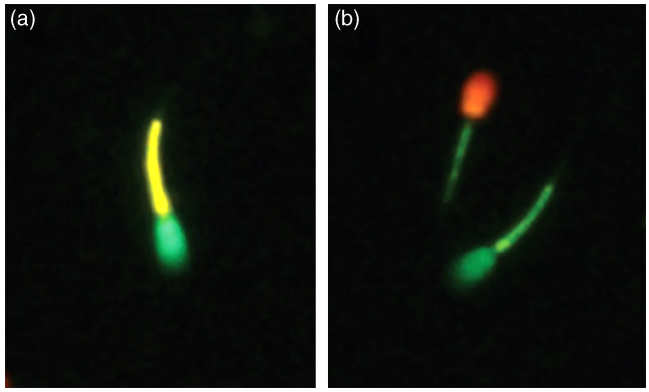

Figure 11.16 Fluorescence micrographs of living dog spermatozoa stained for plasma membrane integrity and inner mitochondrial membrane potential (IMM). Live spermatozoa were triple-stained with propidium iodide (enters cells with damaged membranes only, staining nuclei red), SYBR-14 (becomes deacetylated in living cells, staining their nuclei green), and JC-1 (mitochondria with high IMM fluoresce yellow-orange, and green when IMM is low). (a) Spermatozoon with intact plasma membrane and high IMM. (b) The spermatozoon at left has a damaged plasma membrane and low IMM, while the spermatozoon at right has an intact plasma membrane and low IMM. (Reproduced from Volpe S, Leoci R, Aiudi G, Lacalandra GM. (2009). Relationship between motility and mitochondrial functional status in canine spermatozoa. *Reproduction in Domestic Animals* 44 Suppl 2:275–278, John Wiley & Sons, Inc., © 2009 The Authors. Journal compilation © 2009 Blackwell Verlag GmbH, with permission of John Wiley & Sons, Inc.)

2015). They are positioned in a sheath between the outer dense fibers and plasma membrane in the midpiece (Eddy and O'Brien, 1994; Fawcett, 1975; Pesch and Bergmann, 2006; Toshimori and Eddy, 2015). Mammalian sperm mitochondria are considered more compact and efficient than those of somatic cells or spermatogonia (Amaral *et al.*, 2013). Mitochondria of the dog spermatozoon are elongated and arranged end-to-end forming a helically coiled sheath of 15–17 gyres around the outer dense fibers in the midpiece of the sperm flagellum (*cf.* Fawcett, 1975; Russell *et al.*, 1990). In comparison, mitochondria of human spermatozoa have 10–12 gyres (*cf.* Fawcett, 1975). Mitochondria produce ATP via oxidative phosphorylation that is necessary for flagellar motility of spermatozoa (Amaral *et al.*, 2013). Mitochondrial function has been linked to sperm fertilizing capability in mice and humans (Amaral *et al.*, 2013). Another source of ATP is via glycolysis, which occurs along the length of the dog sperm flagellum (Nascimento *et al.*, 2008).

Mitochondrial health of dog spermatozoa has been monitored using fluorescent indicator dyes (Figure 11.16) (Volpe *et al.*, 2009). For example, the membrane-permeant fluorescent dye, JC-1, is a cationic dye that accumulates in mitochondria with high inner membrane potential (IMM) and coalesces to fluoresce red/orange, characteristic of active, healthy mitochondria (Figure 11.16a) (Volpe *et al.*, 2009). Less of the JC-1 dye enters mitochondria of cells with low IMM, and the dye fluoresces green in dog spermatozoa with less active mitochondria (Figure 11.16b).

Sperm Membranes

The outermost membrane of the dog spermatozoon is the plasma membrane (plasmalemma), which has three major regions: acrosomal region (anterior head), postacrosomal region (posterior head), and flagellar region over the sperm tail (Figure 11.15) (Eddy and O'Brien, 1994; Toshimori and Eddy, 2015). Using a variety of experimental techniques and staining protocols such as immunodetection and lectin staining, researchers discovered that the plasma membrane is heterogeneous and has several domains (Eddy and O'Brien, 1994; Toshimori and Eddy, 2015). The plasma membrane of the sperm head has four major domains: (i) apical

Downloaded From Vet-eBooks.com

segment domain (marginal segment domain, peripheral rim, and anterior band), (ii) principal segment domain (anterior acrosomal domain), (iii) equatorial segment domain (posterior acrosomal domain), and (iv) postacrosomal segment domain (Figure 11.15) (Eddy and O'Brien, 1994; Toshimori and Eddy, 2015). The first three domains are located in the anterior head (acrosome region) and the fourth domain (postacrosomal segment domain) is located in the posterior head (postacrosomal region) (Figure 11.15). Additional membranes of the spermatozoon include the inner and outer acrosomal membranes that surround the acrosome contents, sperm nuclear envelope enclosing the tightly packaged sperm chromatin in the sperm head, and the outer and inner mitochondrial membranes of the flagellum. The plasmalemma is closely juxtaposed to the outer acrosomal membrane in the sperm head (Figure 11.15).

The integrity of the plasma membrane of living dog spermatozoa has been assessed using fluorochromes such as propidium iodide, which does not cross the intact plasma membrane, but can enter cells with damaged membranes (Figure 11.16) (Volpe *et al.*, 2009). Living spermatozoa with intact membranes do not stain with propidium iodide, and appear dark with fluorescence microscopy (propidium iodide-negative). In contrast, the dye enters spermatozoa that had lost their membrane integrity (dead spermatozoa) and stains their nuclei red (propidium iodide-positive).

Plasma membranes of mammalian spermatozoa contain normal amounts of cholesterol and glycolipids, and relatively high amounts of plasmalogens (ether-linked phospholipids) that are glycerophospholipids containing a fatty alcohol with a vinyl-ether bond at the *sn*-1 position and are enriched in polyunsaturated fatty acids at the *sn*-2 position of the glycerol backbone (Braverman and Moser, 2012; Toshimori and Eddy, 2015). Mammalian sperm plasma membranes also contain other ether-linked phospholipids and lipids with long, polyunsaturated aliphatic chains (Toshimori and Eddy, 2015). Membranes of dog spermatozoa have relatively high amounts of phosphatidyl choline, phosphatidyl ethanolamine, sphingomyelin and ethanolamine plasmalogen, and small amounts of choline plasmalogen, phosphatidyl serine, cardiolipin, and phosphatidyl inositol (Table 11.5) (Darin-Bennett *et al.*, 1974). Dog spermatozoa have comparable amounts of phospholipids as human spermatozoa with a difference of more ethanolamine plasmalogen (15.3% dog versus 9.4% human) and slightly less sphingomyelin (18.3% dog versus 21.4% human) (Table 11.5) (Darin-Bennett *et al.*, 1974; Poulos and White, 1973). The major phospholipid-bound fatty acids in dog spermatozoa were palmitic acid (16:0) and docosapentaenoic acid (22:5) (Table 11.6)

Table 11.5 Major phospholipids of dog and human spermatozoa.

Phospholipid[a)]	Dog[b)]	Human[c)]
Phosphatidyl choline	27.5 ± 1.0	28.8
Phosphatidyl ethanolamine	20.1 ± 0.9	21.6
Phosphatidyl inositol	2.7 ± 0.3	1.9
Phosphatidyl serine	3.6 ± 0.3	4.7
Sphingomyelin	18.3 ± 2.0	21.4
Choline plasmalogen	3.6 ± 0.5	2.7
Ethanolamine plasmalogen	15.3 ± 0.9	9.4
Cardiolipin	3.0 ± 0.3	1.6

a) Percent (%) of total lipid phosphorus.
b) From Darin-Bennett *et al.* (1974).
c) From Poulos and White (1973).

Downloaded From Vet-eBooks.com

Table 11.6 Major fatty acids bound to phospholipids of dog and human spermatozoa.

Fatty acid[a]			Dog[b]	Human[c]	
Chemical name	**Common name**	***C:D*** [d]		**Reference 1**	**Reference 2**
Saturated fatty acids (SFAs)					
Tetradecanoic	Myristic	14:0	1.0 ± 0.6	nd[e]	0.92 ± 0.09
Hexadecanoic	Palmitic	16:0	27.2 ± 0.7	33.50 ± 0.7	28.87 ± 0.45
Octadecanoic	Stearic	18:0	13.2 ± 1.4	15.70 ± 0.4	13.35 ± 0.18
Eicosanoic	Arachidic	20:0	<1%	2.60 ± 0.2	1.24 ± 0.09
Docosanoic	Behenic	22:0	nd	3.20 ± 0.2	0.90 ± 0.10
Tetracosanoic	Lignoceric	24:0	nd	2.60 ± 0.3	1.42 ± 0.09
Monounsaturated fatty acids (MUFAs)					
Tetradecenoic	Myristoleic	14:1	nd	nd	0.11 ± 0.03
Hexadecenoic	Palmitoleic	16:1	<0.5%	0.44 ± 0.05	1.27 ± 0.1
Octadecenoic	Oleic	18:1	11.8 ± 0.9	11.60 ± 0.5	11.9[f]
Eicosenoic	Gondoic	20:1	nd	0.65 ± 0.18	0.81 ± 0.05
Docosenoic	Erucic	22:1	nd	0.39 ± 0.05	0.05 ± 0.03
Tetracosenoic	Nervonic	24:1	nd	2.30 ± 0.1	1.01 ± 0.05
Polyunsaturated fatty acids (PUFAs)					
Octadecadienoic	Linoleic	18:2	3.2 ± 0.3	3.20 ± 0.2	6.87[g]
Octadecatrienoic	Linolenic	18:3	1.3 ± 0.3	nd	1.76[h]
Octadecatetraenoic	Stearidonic	18:4	nd	nd	0.30 ± 0.07
Eicosadienoic		20:2	<0.5%	0.48 ± 0.05	1.50 ± 0.07
Eicosatrienoic		20:3	nd	2.50 ± 0.2	3.42 ± 0.08[i]
Eicosatetraenoic	Arachidonic	20:4	6.6 ± 0.7[j]	2.50 ± 0.2	2.73 ± 0.1
Eicosapentaenoic	Timnodonic	20:5	nd	nd	0.43 ± 0.08
Docosadienoic	Brassic	22:2	nd	nd	1.21 ± 0.15
Docosatrienoic		22:3	<1%	nd	0.04 ± 0.01
Docosatetraenoic	DTA	22:4	<1%	0.38 ± 0.04	0 ± 0
Docosapentaenoic	DPA	22:5	28.4 ± 3.0	0.77 ± 0.05	0.84 ± 0.05[k]
Docosahexaenoic	DHA	22:6	3.9 ± 1.8	13.80 ± 0.9	19.01 ± 0.65

a) Fatty acids are expressed as percent (%) of total lipid phosphorus in Darin-Bennett *et al.* (1974); wt% of total in Conquer *et al.* (1999); and mol% in Martinez-Soto *et al.* (2013).
b) From: Darin-Bennett *et al.* (1974).
c) Reference 1: Conquer *et al.* (1999). Reference 2: Martinez-Soto *et al.* (2013).
d) Carbon chain length:number of double bonds.
e) nd: not determined.
f) Value shown is a combined value of vaccenic acid (C18:1n7) 2.57 ± 0.07 plus oleic acid (C18:1n9) 9.33 ± 0.43.
g) Value shown is a combined value of *cis*-linoleic acid (C18:2n6c) 5.67 ± 0.13 plus *trans*-linoleic acid (C18:2n6t) 1.2 ± 0.14.
h) Value shown is a combined value of α-linolenic acid (18:3n3) 0.81 ± 0.10 plus γ-linolenic acid (18:3n6) 0.95 ± 0.11.
i) Value shown is a combined value of eicosatrienoic acid (C20:3n3) 0 ± 0 plus dihomo-γ-linolenic acid (C20:3n6) 3.42 ± 0.08.
j) May also contain 20:3.
k) Value shown is a combined value of DPAn-3 (clupanodonic acid) (C22:5n3) 0.84 ± 0.05 plus DPAn-6 (C22:5n6) 0 ± 0.

Downloaded From Vet-eBooks.com

(Darin-Bennett *et al.*, 1974). High amounts of stearic acid (18:0) and oleic acid (18:1), and moderate levels of arachidonic acid (20:4) were also present in membranes of dog spermatozoa (Table 11.6) (Darin-Bennett *et al.*, 1974). In addition, dog sperm membranes were enriched with long, polyunsaturated aliphatic chains including arachidonic acid (20:4), docosapentaenoic acid (22:5), and docosahexaenoic acid (22:6) (Darin-Bennett *et al.*, 1974). Dog spermatozoa have comparable levels of phospholipid-bound fatty acids as human spermatozoa with the exception that dog spermatozoa have more docosapentaenoic acid (22:5) and less docosahexaenoic acid (22:6) than human spermatozoa (Table 11.6). The large quantities of polyunsaturated fatty acyl residues are important for membrane fluidity of spermatozoa. The concentration of certain phospholipids (phosphatidyl serine, phosphatidyl ethanolamine, cardiolipin, and ethanolamine plasmalogen) has been reported to decrease during capacitation of mammalian spermatozoa (Toshimori and Eddy, 2015).

Sperm Cytoplasm

The mature dog spermatozoon has a small amount of cytoplasm present as a thin layer just underneath its plasma membrane (Russell *et al.*, 1990; Toshimori and Eddy, 2015). This is typical of mammalian spermatozoa. During spermatogenesis, most of the excess spermatid cytoplasm was lost forming residual bodies that were resorbed by Sertoli cells in the testis (Fawcett, 1975). Epididymal spermatozoa in the caput epididymis retain a small cytoplasmic droplet (also called Hermes body) which is a small residue of cytoplasm about 2 μm in diameter located initially at the sperm neck (Angrimani *et al.*, 2014b; Au *et al.*, 2015; Bains *et al.*, 1993; Cooper, 2011). This cytoplasmic droplet migrates along the midpiece of the spermatozoon in a proximal (neck) to distal (annulus) direction during sperm transit in the epididymal duct (Angrimani *et al.*, 2014b; Au *et al.*, 2015; Bains *et al.*, 1993; Cooper, 2011). Cytoplasmic droplets have been reported to contain lipids, lipoproteins, RNAs, carbohydrate moieties, and Golgi-derived vesicles (Bains *et al.*, 1993; Rengan *et al.*, 2012). In addition, cytoplasmic droplets of rat spermatozoa contain a myriad of proteins, including glycolytic enzymes (GLUT-3, hexokinase 1), membrane proteins (aquaporin 7, PH20), membrane traffic proteins such as TMED7/p27, cytoskeletal proteins (actin, tubulin), and proteins of the endoplasmic reticulum such as ribosomal proteins (Au *et al.*, 2015). In the dog, the cytoplasmic droplet is eventually lost in the corpus epididymis or during ejaculation so that mature motile dog spermatozoa lack a cytoplasmic droplet (Figure 11.17) (Angrimani *et al.*, 2014b; Bains *et al.*, 1993). Human spermatozoa also have a cytoplasmic droplet, and it is lost after epididymal transit (Cooper, 2011; Rengan *et al.*, 2012). The cytoplasmic droplet is involved in transitioning a spermatozoon from an immotile infertile cell to a motile fertile spermatozoon (Au *et al.*, 2015). Sperm retention of the cytoplasmic droplet has been associated with infertility in dog and human patients (Au *et al.*, 2015; Cooper, 2011; Cooper and Yeung, 2003; Oettlé, 1993; Peña *et al.*, 2007; Rengan *et al.*, 2012).

Sperm Viability

The viability of dog spermatozoa has been assessed using fluorochromes such as SYBR-14, which becomes deacetylated and then entrapped in living spermatozoa (Volpe *et al.*, 2009). With fluorescence microscopy, the nuclei of SYBR-14-stained viable dog spermatozoa appeared bright green, whereas nuclei of dead sperm cells did not stain (Figure 11.16) (Volpe *et al.*, 2009). In another example (described earlier under "Sperm Membranes" section), propidium iodide, which penetrates damaged cell membranes, stains nuclei of moribund spermatozoa red (Figure 11.16) (Volpe *et al.*, 2009). The viability of dog spermatozoa in the female reproductive tract is up to 11 days (Doak *et al.*, 1967). This is a long duration compared

Downloaded From Vet-eBooks.com

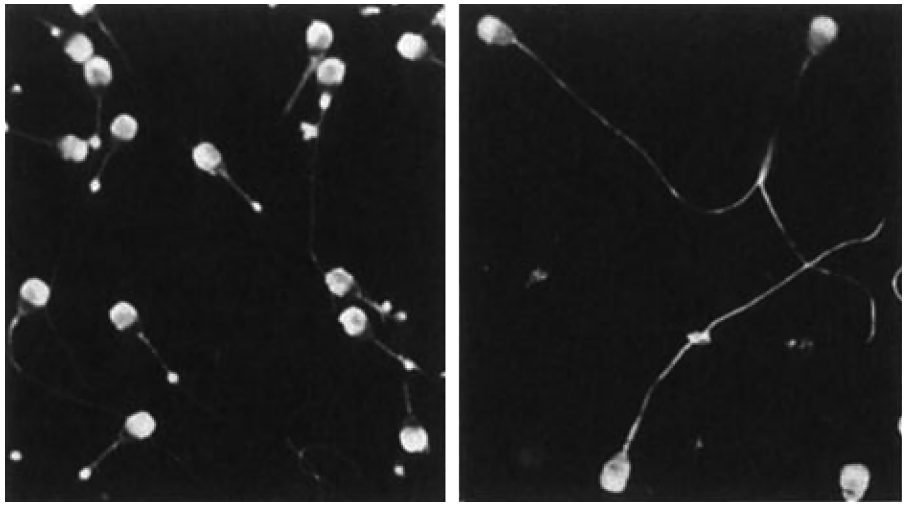

Figure 11.17 Dog spermatozoa stained with lectin revealing the cytoplasmic droplet. Spermatozoa were stained with fluorescein isothiocyanate-conjugated wheat germ agglutinin which intensely stained the cytoplasmic droplet and periacrosomal domain. At left, spermatozoa collected from the ductus deferens (vas deferens) have the cytoplasmic droplet, and at right, ejaculated spermatozoa lack the cytoplasmic droplet, but have additional staining of the postacrosomal segment and flagellum. (Reproduced from Bains HK, Pabst MA, Bawa SR. 1993. Changes in the lectin binding sites on the testicular, epididymal, vas, and ejaculated spermatozoon surface of dog. *Andrologia* 25(1):19–24, John Wiley & Sons, Inc., © 1993 Blackwell Verlag GmbH, with permission of John Wiley & Sons, Inc.)

to other mammals. Prolonged sperm longevity matches the unusual features of female reproduction in dogs (discussed below).

Sperm Motility

During passage through the epididymis and vas deferens, dog spermatozoa become motile (described earlier under "Epididymis"). The pattern of sperm motility changes as sperm travel through the female reproductive tract. This is discussed further in Section 11.2.7.

11.2.5 Reproductive Anatomy of the Female Dog

Dogs are multiparous and multiple litters are possible over the female's lifetime. The anatomy of the female dog supports production of a litter of several fetuses each pregnancy. Reproductive organs in female dogs include several structures comparable to those of the human reproductive system (Figure 11.18). The major female reproductive organs in the dog include the reproductive tract and mammary glands (Evans and De Lahunta, 2013). The female reproductive tract of the dog consists of the ovaries, uterine tubes, uterus, vagina, vestibule, and vulva (Figure 11.18) (Constantinescu, 2007). Draped over the ovaries, uterine tubes, and uterus is the *broad ligament,* which is a double fold of peritoneum (serous membrane) that attaches these organs to the dorsolateral abdominal wall and to the lateral walls of the pelvic cavity. The broad ligament is divided into three regions: the *mesovarium,* which attaches the ovary to the dorsolateral abdominal wall, *mesosalpinx,* which surrounds the ovary attaching it to the medial surface of the broad ligament, and the *mesometrium,* which attaches the uterine horn, uterine body, cervix, and vagina to the abdominal and pelvic walls. The anatomical structure of each female reproductive organ is discussed in the following sections.

Downloaded From Vet-eBooks.com

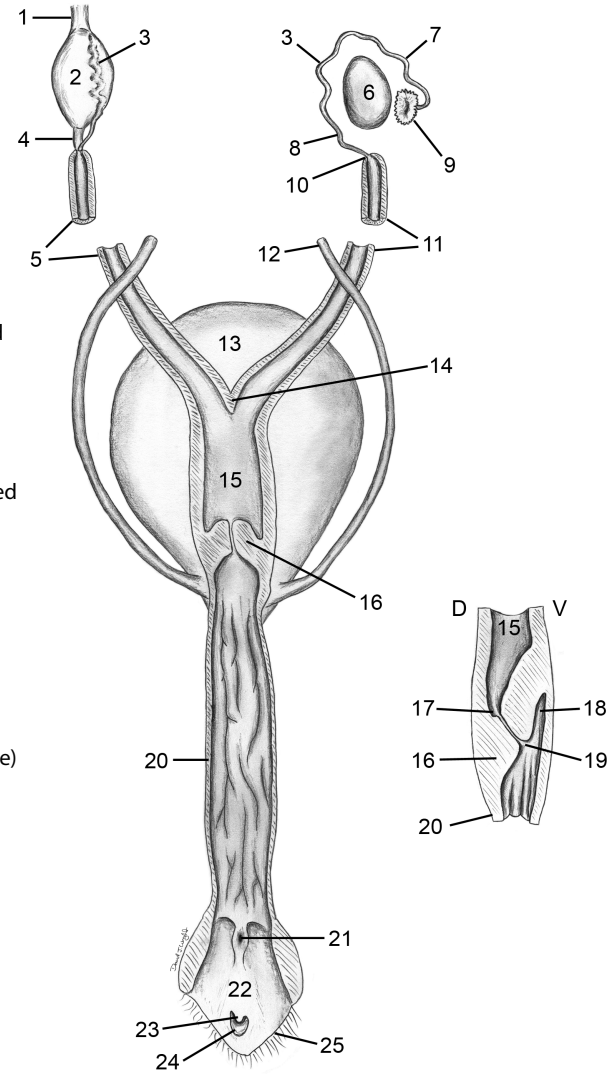

Figure 11.18 Dog female reproductive anatomy. Dorsal view of reproductive tract cut in the dorsal midline along its length to reveal internal morphology. A segment of each uterine horn has been removed. The inset at right is a sagittal section through the uterovaginal junction with dorsal (D) and ventral (V) indicated:
1 = Suspensory ligament of ovary
2 = Ovarian bursa
3 = Uterine tube in/under ovarian bursa
4 = Proper ligament of ovary
5 = Left uterine horn with segment removed
6 = Ovary
7 = Ampulla of uterine tube
8 = Isthmus of uterine tube
9 = Infundibulum of uterine tube
10 = Uterotubal junction
11 = Right uterine horn with segment removed
12 = Ureter
13 = Urinary bladder
14 = Uterine velum
15 = Body of uterus
16 = Cervix
17 = Internal uterine ostium of cervical canal
18 = Fornix
19 = External uterine ostium of cervical canal
20 = Vagina
21 = Urethral opening (external urethral orifice)
22 = Vestibule
23 = Clitoris
24 = Fossa clitoridis
25 = Labium
(Courtesy of David J. Wright, Ph.D.)

11.2.5.1 Ovary

The dog ovary is a paired oval organ located in the abdomen 1–3 cm caudal to the kidneys (Figures 11.18 and 11.19) (Constantinescu, 2007; Evans and De Lahunta, 2013; Fransson, 2012). Each ovary is surrounded by a thick ovarian bursa and is attached to its inner surface (Figure 11.18) (England, 2013; Evans and De Lahunta, 2013; Jones and Joshua, 1988). The ovarian bursa is a small, deep peritoneal pouch formed by the mesosalpinx and mesovarium (Evans and De Lahunta, 2013). The ovarian bursa has a very small slit-like opening on the medial side that is continuous with the peritoneal cavity (Evans and De Lahunta, 2013). The walls of the ovarian bursa are fat-filled and obscure the ovary. This makes observation of the dog ovary via ultrasound difficult, and surgical removal of the ovaries challenging compared to other domestic species (England, 2013; Evans and De Lahunta, 2013). The ovarian bursa is absent in humans.

The ovaries are bilaterally flattened and about 2 cm in length in adult dogs that are in a quiescent phase of the reproductive cycle (Figure 11.19) (Jones and Joshua, 1988). For

Downloaded From Vet-eBooks.com

Figure 11.19 Dog ovary. The ovary was excised from the ovarian bursa of a female in anestrus. Scale bar, 5 mm. (Reproduced from Lunn MO, Wright SJ, 2009, Imaging the zona pellucida of canine and feline oocytes using scanning electron microscopy, *Microscopy and Microanalysis* 15(1), pages 2–14, © 2009 Microscopy Society of America, reproduced with permission of Cambridge University Press.)

example, the ovaries of an 11 kg (25 lb) adult dog are about 15 mm long, 7 mm wide, 5 mm thick, and weigh 300 mg (Evans and De Lahunta, 2013; Fransson, 2012; Jones and Joshua, 1988). Sometimes the left ovary is slightly larger than the right (Fransson, 2012). The quiescent ovary of the sexually mature adult dog is smaller than a human ovary from a premenopausal woman, which measures 42 mm in length (range 30–50 mm), 21 mm in width (range 15–30 mm), is 13 mm thick (range 6–15 mm), and weighs 5–8 g (Clement, 1987; Sadeu and Nogueira, 2011).

The outermost surface of the ovary is a thin superficial layer of epithelial cells called the *surface epithelium of the ovary* (previously called germinal epithelium) (Evans and De Lahunta, 2013). Beneath the surface epithelium of the ovary is a layer of connective tissue that forms a thin capsule called the *tunica albuginea* or *capsule of the ovary* (Evans and De Lahunta, 2013). The dog ovary has subsurface epithelial projections, which are extensions or ingrowths of superficial epithelium that form cortical tubules that invaginate into the tunica albuginea (Figure 11.20) (Barton, 1945; Groppetti *et al.*, 2015).

Like the human ovary, the dog ovary has two regions: an outer *cortex* and an inner *medulla* (Evans and De Lahunta, 2013; Solano-Gallego and Masserdotti, 2016). The ovarian cortex consists of a connective tissue stroma containing follicles that house oocytes. Corpora lutea may also be present in the ovarian cortex depending on the phase of the dog's reproductive cycle. Deep to the ovarian cortex is the medulla that contains blood vessels, nerves, lymphatic vessels, smooth muscle fibers, and loose connective tissue (Evans and De Lahunta, 2013; Solano-Gallego and Masserdotti, 2016).

The dog ovary functions as an endocrine gland producing the steroids, estrogen, and progesterone during the reproductive cycle (Feldman and Nelson, 2004). In addition, both the right and left ovaries function to produce oocytes during oogenesis in ovarian follicles (Constantinescu, 2007). Follicles are located deep to the tunica albuginea (Figure 11.20) (Evans and De Lahunta, 2013). Small primordial follicles are in the ovarian cortex and more advanced follicles occupy the subcortical region (Tesoriero, 1981). The macroscopic appearance of the ovary changes with the reproductive cycle (discussed further under "Stages of the Dog Estrous Cycle") (Evans and De Lahunta, 2013; Groppetti *et al.*, 2015; Reynaud *et al.*, 2006). The external surface of the ovary is smooth during reproductive quiescence (anestrus), and becomes rough and nodular with projecting follicular structures during an active phase (estrus) of the reproductive cycle. This is discussed further in Section 11.2.6.

Downloaded From Vet-eBooks.com

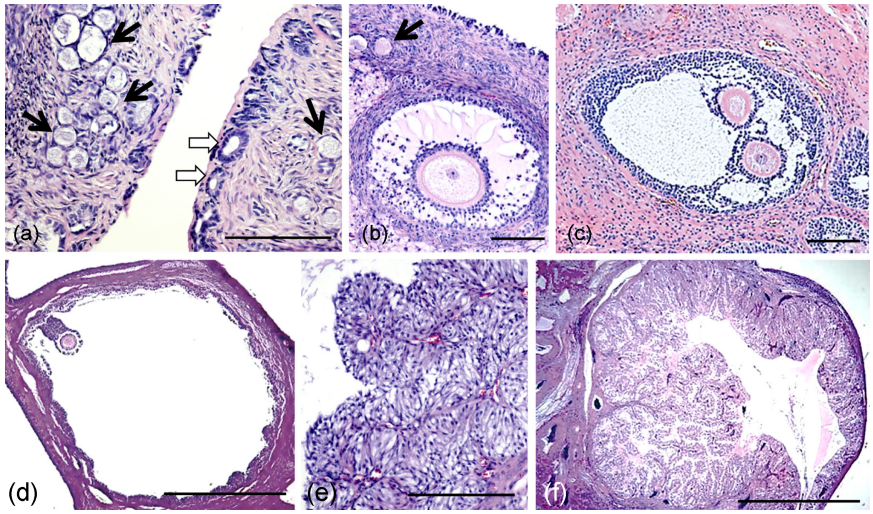

Figure 11.20 Ovarian cortex in the actively cycling dog. (a) Primordial follicles (solid arrows) and cortical tubules (open arrows) are just beneath the capsule of the ovary. (b) A small, multilaminar antral follicle with many layers of granulosa cells and a fully developed thecal layer, and a primary follicle (arrow) in a sub-cortical position. (c) Polyovular antral follicle with two oocytes each surrounded by a zona pellucida. (d) Large tertiary follicle with enormous antrum and cumulus oophorus protruding into the antrum. (e) Granulosa cells of a tertiary follicle showing pre-ovulatory luteinization. (f) Mature preluteinized follicle undergoing ovulation. Scale bars: (a, e) = 200 µm, (b, c) = 500 µm, (d, f) = 1000 µm. (Reproduced from *Animal Reproduction Science*, volume 152, Groppetti D, Aralla M, Bronzo V, Bosi G, Pecile A, Arrighi S., Periovulatory time in the bitch: what's new to know? Comparison between ovarian histology and clinical features, pages 108–116, Copyright 2015, permission from Elsevier.)

11.2.5.2 Uterine Tube

The uterine tube in the dog is a narrow duct 4–10 cm in length and 1–3 mm in diameter (Figure 11.18) (Constantinescu, 2007; Evans and De Lahunta, 2013; Fransson, 2012; Renton *et al.*, 1991). It is similar in length to the human uterine tube that is about 7–11 cm long. The dog has two uterine tubes (oviducts) (Evans and De Lahunta, 2013). Each uterine tube is associated with the ipsilateral ovary and is joined to the uterus (Figure 11.18) (Evans and De Lahunta, 2013). Connecting the peritoneal cavity to the uterine lumen, the uterine tubes function to collect and convey oocytes to the uterus, regulate sperm transport to the oocyte, and transport embryos to the uterine horns (Evans and De Lahunta, 2013; Fransson, 2012). The ovarian bursa covers the uterine tubes, which course around the ovary in the dog (Figure 11.18).

Each uterine tube is divided into four regions from cranial to caudal along its length (Figure 11.18): (i) *infundibulum*, which is the distal end with a distal opening called the abdominal ostium that receives ovulated oocytes from the ovary, (ii) *ampulla*, which is the middle region, (iii) *isthmus*, which is the proximal end, and (iv) *uterotubal junction* (also called tubouterine junction), which contains the uterine ostium, an opening of the uterine tube to the uterine horn (Evans and De Lahunta, 2013; Gelberg and McEntee, 1986). The infundibulum is funnel shaped and has fimbriae on its edges, which swell during ovulation, thus blocking the opening of the ovarian bursa (Figure 11.18) (Evans and De Lahunta, 2013; Renton *et al.*, 1991). The fimbriae are vascular finger-like projections that reveal the junction of the mesosalpinx and mucosal lining of the uterine tube (Fransson, 2012). The fimbriae capture oocytes as they are released from the ovary during ovulation (Evans and De Lahunta, 2013; Fransson, 2012).

Downloaded From Vet-eBooks.com

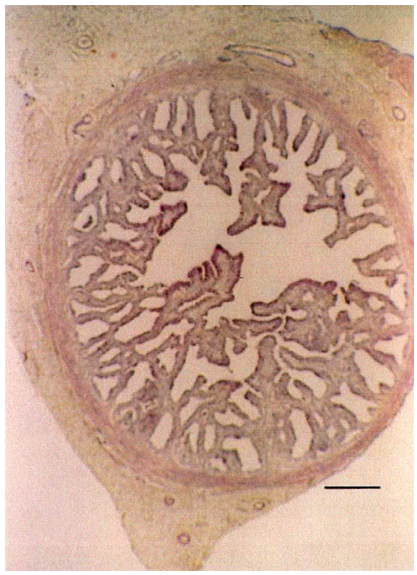

Figure 11.21 Dog uterotubal junction. Hematoxylin-eosin stained section of the distal uterotubal junction of a dog in estrus. Scale bar: 0.25 mm. (Reproduced from Rijsselaere T, England G, Freeman S, Maes D, Van Soom A., 2014, Current knowledge on the transport and fate of spermatozoa in the reproductive tract of the bitch, *Reproduction in Domestic Animals* 49 (Suppl. 2):2–7, © 2014 Blackwell Verlag GmbH, with permission of John Wiley & Sons, Inc.)

The uterine tube consists of a folded inner mucosa (tunica mucosa), muscularis section and outer tunica serosa (Evans and De Lahunta, 2013). The innermost layer of the uterine tube (tunica mucosa) is composed of epithelium (Evans and De Lahunta, 2013). This epithelial lining undergoes cellular changes coupled with the estrous cycle (Evans and De Lahunta, 2013; Reynaud *et al.*, 2012a). During anestrus, there are low cuboidal cells and few ciliated cells; however, during the periovulatory period, elevating progesterone levels trigger these cells to give rise to many ciliated columnar epithelial cells and secretory cells (Evans and De Lahunta, 2013; Reynaud *et al.*, 2012a).

The uterotubal junction is a region in which the lumen of the uterine tube is continuous with the lumen of the uterus (Figure 11.21). The uterotubal junction has a mound-like, round papilla in the dog. In humans, the uterotubal junction is funnel shaped and is not raised as in the dog (Hook and Hafez, 1969; Suarez, 2015). The lumen of the dog uterine tube is narrower at its isthmus (end nearest the uterotubal junction) than at its ampulla (England, 2013). This constriction physically limits passage of spermatozoa into the uterine tube. Spermatozoa must migrate past this junction to reach oocytes for fertilization. The uterotubal junction functions not only to physically restrict sperm passage, but also acts as a "filter" to select against spermatozoa with misfolded proteins or those lacking key proteins in various knockout mice (*Adam1a*$^{-/-}$, *Pdilt*$^{-/-}$, *Tex101*$^{-/-}$, *Ly6k*$^{-/-}$), and this may involve the sperm glycocalyx (Nakanishi *et al.*, 2004; Okabe, 2015; Suarez, 2016; Tecle and Gagneux, 2015).

11.2.5.3 Uterus

The dog uterus is a single organ that is bicornuate in shape (Figure 11.18) (Cochran, 2011; Tsutsui *et al.*, 2002). It has three regions: neck (cervix), body (corpus), and uterine horns (cornua) (Figure 11.18). There are two uterine horns in the dog and they are unfused, muscular, long tubes that are 12–16 cm in length and 5–10 mm in diameter (Figure 11.18) (Fransson, 2012). Each uterine horn is connected to a single, short (3–4 cm long), fused uterine body giving the uterus a Y-shaped appearance (Constantinescu, 2007; England, 2013). Internally, the uterine horns remain separated for a short distance (1 cm) by a small partition (septum) called the uterine velum that partially separates the proximal openings of the uterine horns at the uterine

Downloaded From Vet-eBooks.com

body (Constantinescu, 2007; Evans and De Lahunta, 2013). The most caudal part of the uterus is the cervix, which is a short (1.5–2 cm in length) muscular structure with a narrow lumen (cervical canal) that connects the uterus to the vagina (Figure 11.18) (Constantinescu, 2007; Evans and De Lahunta, 2013). The ventral attachment of the cervix to the uterine wall is cranial to its dorsal attachment so that the cervix and cervical canal lie diagonally (Evans and De Lahunta, 2013). Its external uterine orifice is directed ventrally toward the vagina and its internal uterine orifice faces dorsally (Figure 11.18) (Evans and De Lahunta, 2013). In contrast, humans have a simplex uterus that is a single fused uterus lacking uterine horns (Cochran, 2011).

11.2.5.4 Vagina

The vagina in dogs is a cylindrical structure compressed dorsoventrally by surrounding organs. The vagina extends from the cervix to the vestibule just cranial to the external urethral orifice (Figure 11.18) (Evans and De Lahunta, 2013). The vagina is relatively long in the dog compared to other domestic mammals (Evans and De Lahunta, 2013; Feldman and Nelson, 2004). For example, in an 11 kg (25 pound) adult female dog, the vagina is about 12–16 cm long and 1.5 cm in diameter (Constantinescu, 2007; Evans and De Lahunta, 2013). In large dogs it can be as long as 30 cm (Pineda *et al.*, 1973; Feldman and Nelson, 2004). The vaginal mucosa has large longitudinal folds (rugae) and smaller transverse folds that allow for expansion (Figure 11.18) (Evans and De Lahunta, 2013). For example, the vagina increases in length and diameter during pregnancy and parturition (Evans and De Lahunta, 2013). Lying ventral and cranial to the cervix is the fornix, which is the deepest part of the vagina (Figure 11.18) (Evans and De Lahunta, 2013). The fornix is a slit-like space of the vagina that ends in a blind pouch, and can be easily confused with the external uterine ostium (opening) of the cervix when viewing it from the rear (Feldman and Nelson, 2004; Pineda *et al.*, 1973). The cranial vagina (paracervix) has a dorsal median fold, which is a thickened area that restricts the vaginal lumen near the cervix (Evans and De Lahunta, 2013; Pineda *et al.*, 1973). The dorsal median fold ranges in length from 15 to 42 mm and from 2 to 10 mm in width, and extends about 2–3 cm from the cervix (Pineda *et al.*, 1973). The dorsal median fold prevents visualization of the cervix and is often mistaken for the cervix itself (England, 2013; Feldman and Nelson, 2004; Pineda *et al.*, 1973). These structures have implications for assisted reproductive techniques such as transcervical insemination (Feldman and Nelson, 2004). The vaginal epithelium changes with the estrous cycle and can be monitored by visual inspection, as well as through cytology from gentle scrapings of the vaginal epithelium (vaginal exfoliation cytology) to aid in establishing stages of the estrous cycle (see Section 11.2.6).

11.2.5.5 Vestibule

In the dog, the vestibule is a short (5–6 cm long) chamber that connects the vagina to the vulval opening or cleft of the external genitalia (Figure 11.18) (Constantinescu, 2007; Evans and De Lahunta, 2013). The vestibule extends from the external urethral orifice to the vulvar cleft. The vaginovestibular junction is 1.5–2 cm in diameter (Evans and De Lahunta, 2013). The homologous genital organ in the male is the penile urethra (Evans and De Lahunta, 2013).

11.2.5.6 Vulva

The vulva (external female genitalia) is the external opening of the female reproductive tract (Figure 11.22) (England, 2013; Evans and De Lahunta, 2013). In a nonpregnant 11 kg (25 lb) adult dog, the vulva is 3 cm long (Evans and De Lahunta, 2013). The vulva consists of two parts: vulvar labiae and the vulvar cleft. The vulvar labiae consist of two vertical lips joined dorsally and ventrally, and the slit-like opening between them is the vulvar cleft that is normally closed when the dog is not actively cycling (Figure 11.22). The vulvar labiae correspond to the labia majora in humans (Budras, 2007). The vulvar labiae dramatically change in size and tone with respect to

Downloaded From Vet-eBooks.com

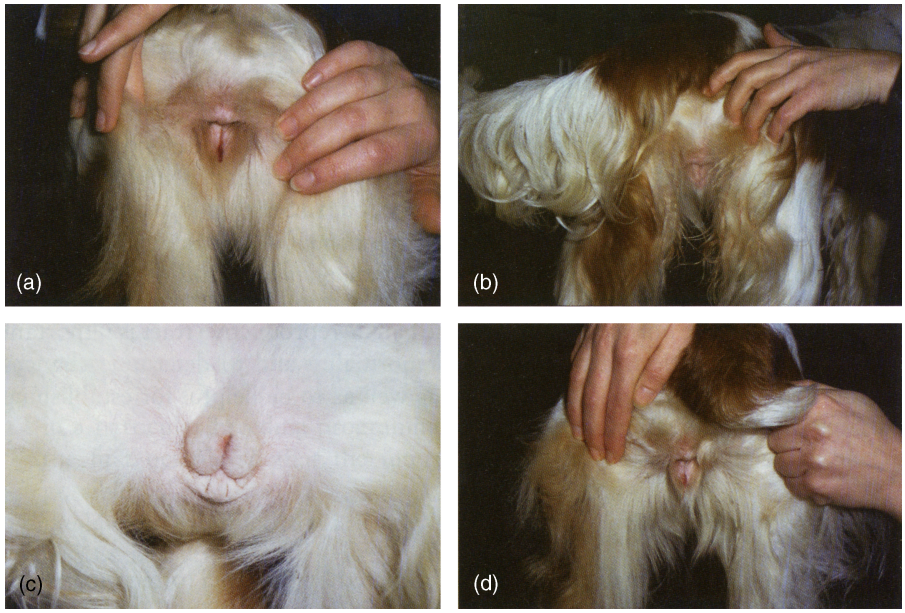

Figure 11.22 Vulval changes during the dog estrous cycle. (a) Proestrus, with discharge at the vulva. (b) Estrus, with tail turned to one side in response to pressure applied to back or perivulval area. (c) Estrus, with swollen vulva. (d) Early diestrus (metestrus), with reduced vulval swelling. (Reproduced from England G, 2013, Dog, *Breeding, Whelping, and Puppy Care*, Fig. 2.1 on page 20, © 2013 by John Wiley & Sons, Ltd, by permission of John Wiley & Sons, Inc.)

the stages of the dog's reproductive cycle. For example, they enlarge dramatically during proestrus and estrus (Figure 11.22). Thus, vulvar labiae are important external landmarks that aid in determining the fertile period in the dog (England, 2013). Additional external genitalia in the dog include the clitoris and urethra.

11.2.5.7 Mammary Glands

Dogs have five pairs of mammary glands (mammae) that are modified sweat glands (compound tubuloalveolar glands) held together with connective tissue (England, 2013; Evans and De Lahunta, 2013). The mammary glands are arranged in two parallel rows lateral to the midline, and extend cranially from the ventral thorax to the inguinal region caudally (Solano-Gallego and Masserdotti, 2016). The number of mammary glands can vary, and four to six pairs are possible (Case, 2005; England, 2013). The mammary glands are numbered from cranial to caudal with the most cranial called M1 (England, 2013). They are also described in relation to general location such as thoracic, abdominal, and inguinal (England, 2013). Mammary glands are relatively small until about 35 days after ovulation when they enlarge, even in females without clinical signs of false pregnancy (England, 2013). The enlargement 35 days after ovulation corresponds to the diestrous/metestrous phase of the reproductive cycle (England, 2013). The mammary glands function to produce milk in response to prolactin, and this occurs not only in pregnant dogs, but also in nonpregnant females (England, 2013). Milk leaves the gland via teats. Each mammary gland has one teat and each teat has 7–14 teat orifices (England, 2013). Breast development of the dog occurs similar to humans, and the mamma of the dog is homologous to the human breast (Peña *et al.*, 2014).

Downloaded From Vet-eBooks.com

11.2.6 Reproductive Physiology of the Female Dog

Adult female dogs are aseasonal, monoestrous breeders meaning they have only one estrus or "heat" in one complete breeding cycle in which they ovulate only once per breeding season (Case, 2005; Concannon, 2009; Jones and Joshua, 1988; Kowalewski, 2014). In addition, sexually mature females can breed year round (Case, 2005; Concannon, 2009; Jones and Joshua, 1988). This is in contrast to many domestic pets such as cats, which are polyestrous in that the estrous cycle repeats many times during the breeding season. In the dog, a period of sexual activity is followed by a long period of obligatory sexual quiescence (Jones and Joshua, 1988; Kowalewski, 2014). Each female breeding cycle lasts about 6–7 months, and is highly variable ranging from 5 to 12 months (Concannon, 2011). This allows the female domestic dog to have two reproductive cycles per year. In a study of 1000 dogs of very different breeds, 92.5% were in heat twice a year and rarely (2.5% of the dogs) did they have one or three cycles in a year (Drier, 1998). Dog breeding cycles are not linked to daylight length except in the Basenji, which cycles in autumn at the Northern and Southern Hemispheres (Case, 2005; Concannon, 2009; Jones and Joshua, 1988). Thus, most sexually mature female dogs are capable of producing viable oocytes twice a year. In addition, reproductive senescence is thought to be absent in the dog, so that females can become pregnant all their lives although fertility declines with age (Forsberg and Reynaud, 2012). While some countries legally allow five or six litters over the female's lifetime, some breeders prefer a maximum of four litters, over concerns for the health of the female and to prevent the cruel practices of puppy mills (puppy farming) (KC, 2015).

11.2.6.1 Dog Oogenesis and Folliculogenesis

Oogenesis is a complex process that begins prenatally with primordial germ cells (PGCs) (Yao and Batchu, 2007). In the dog, PGCs first appear in the embryo's yolk sac endoderm about 17 days post-coitus (Rosenfeld and Schatten, 2007). During sexual differentiation of the dog embryo, the PGCs colonize the genital ridges and give rise to oogonia that proliferate by mitosis within the developing ovary, and eventually grow (increase in size and volume) to develop into primary oocytes (Reynaud *et al.*, 2012a; Sánchez and Smitz, 2012; Yao and Batchu, 2007). Thus, oocytes are derived from PGCs. The PGCs are considered oocytes when they enter prophase of first meiosis (Yao and Batchu, 2007).

Oocytes develop within ovarian follicles during folliculogenesis (Solano-Gallego and Masserdotti, 2016). Folliculogenesis begins when the oocyte leaves pachytene and enters the diplotene phase of meiotic prophase I (Yao and Batchu, 2007). Each follicle contains an oocyte surrounded by follicle cells (somatic cells) arranged either as a single layer of granulosa cells or as multiple granulosa cell layers plus an outer layer of theca cells (Figure 11.20) (Solano-Gallego and Masserdotti, 2016). Folliculogenesis is the process in which a primordial follicle, which is immature, is recruited to grow into a mature preovulatory follicle that contains a viable, mature oocyte (Sadeu and Nogueira, 2011).

Several morphological features characterize follicular growth, including a shape change in granulosa cells from flat to cuboidal, increase in granulosa cell numbers via proliferation, formation of a follicular antrum, increase in oocyte size and follicle size, and presence of a zona pellucida around the oocyte (Figure 11.20). During an active phase of the dog's reproductive cycle, four types of follicles are present in the adult dog ovary, reflecting different stages of folliculogenesis (Figure 11.20). A *primordial follicle* is an inactive follicle containing an immature primary oocyte surrounded by a single layer of flattened granulosa cells. A *primary follicle* is an early growing follicle that contains a primary oocyte surrounded by a single, complete layer of cuboidal or spherical granulosa cells. A *secondary follicle*, also known as a

Downloaded From Vet-eBooks.com

preantral follicle is a midgrowth follicle containing a primary oocyte surrounded by two or more layers of cuboidal granulosa cells, and thecal cell layer. A *tertiary follicle* (also called antral follicle and Graafian follicle) contains an outer thecal layer that is vascularized, and beneath it, multiple layers of granulosa cells that surround a primary oocyte and antrum (Groppetti *et al.*, 2015; Lunardon *et al.*, 2015).

In the dog, folliculogenesis occurs about 2–12 weeks postnatally (Blackmore *et al.* (2004). Thus, the first primordial follicles of the dog ovary are visible 2–3 weeks after birth (Reynaud *et al.*, 2012a). Folliculogenesis has been reported to take 170 days from the primordial follicle stage to ovulation in the dog (*cf.* Chastant-Maillard *et al.*, 2011). The ovaries of prepubertal dogs (12–16 weeks of age) have a full range of follicular structures, from clusters of quiescent primordial follicles to late antral follicles, but lack any corpora lutea since ovulation had not yet occurred (Blackmore *et al.*, 2004). Follicular recruitment begins about 60–100 days before the preovulatory luteinizing hormone (LH) surge in adult female dogs (England *et al.*, 2009). Follicles recruited to grow are either ovulated or degenerate via follicular atresia (England *et al.*, 2009). Several excellent reviews describe folliculogenesis and its endocrine control in the dog (Chastant-Maillard *et al.*, 2011; Concannon, 2009; Concannon *et al.*, 2009; Reynaud *et al.*, 2012a).

Communication between the oocyte and its surrounding granulosa cells is essential for follicle growth and oocyte maturation, as well as formation of a developmentally competent oocyte (Cakmak *et al.*, 2016). This crosstalk is important for formation of the follicular antrum. Secretions from granulosa cells, including hyaluronan and versican (a chondroitin sulfate proteoglycan), generate an osmotic gradient that draws in fluid from the theca cell layer, creating the antrum that is full of follicular fluid characteristic of the tertiary follicle (Rodgers and Irving-Rodgers, 2010). In the adult dog, follicular fluid collected from the antra of follicles >2.5 mm in size was reported to contain steroids, including 17β-estradiol and progesterone (Fahiminiya *et al.*, 2010). These steroids were more concentrated in the follicular fluid than in the blood, and their concentration depended on follicle size (Fahiminiya *et al.*, 2010). The intrafollicular progesterone levels of dog follicles were much higher than those found in follicular fluid of other mammals (Fahiminiya *et al.*, 2010). In addition, canine follicular fluid contained 21 different proteins, including actin-gamma (*ACTG*), albumin, immunoglobulin heavy chains, acute-phase proteins (plasma proteins that alter their concentration during inflammation, such as fibrinogen gamma chain, haptoglobin, complement factor B, apolipoprotein A-I, alpha-2-HS-glycoprotein, transferrin, and retinol-binding protein 4), vitamin D-binding protein, apolipoproteins (*APOA1*, *APOA4*), inhibitor of carbonic anhydrase (*ICA*), two liver proteins (paraoxonase, serotransferrin), gelsolin, and clusterin (Fahiminiya *et al.*, 2010). Many of these proteins have also been detected in human follicular fluid and may play key roles in follicle activity and oocyte maturation (Fahiminiya *et al.*, 2010).

An unusual feature of the dog ovary is multioocyte follicles, also known as polyovular follicles and polyoocytic follicles (Figure 11.20) (Chastant-Maillard *et al.*, 2011; Groppetti *et al.*, 2015; Lunardon *et al.*, 2015; Payan-Carreira and Pires, 2008). Multioocyte follicles have been reported in prepubertal and adult dogs (Figure 11.20) (Chastant-Maillard *et al.*, 2011; Groppetti *et al.*, 2015; Lunardon *et al.*, 2015; Payan-Carreira and Pires, 2008). As many as 2–17 oocytes have been observed in one follicle (Chastant-Maillard *et al.*, 2011; Payan-Carreira and Pires, 2008; Tesoriero, 1981). The incidence of multioocyte follicles was up to 68.4% in prepubertal dogs and declined with age to 30.4% in 7–8-year-old dogs and to 14.3% in dogs aged 10 or more years (Payan-Carreira and Pires, 2008). A similar decline in the incidence of multioocyte follicles was reported with age of the dog (Lunardon *et al.*, 2015). It is unclear whether all of the oocytes of multioocyte follicles are competent to undergo meiosis and are capable of fertilization and supporting development. Interestingly, the oocytes in one follicle can be at various stages of

Downloaded From Vet-eBooks.com

development and the multioocyte follicles may contain viable and atretic oocytes within the same follicle (Blackmore *et al.*, 2004; Chastant-Maillard *et al.*, 2011). In one study, a greater number of conceptuses were detected than there were corpora lutea suggesting the possibility that more than one viable oocyte may be produced from multioocyte follicles, although one may speculate that spontaneous embryo splitting could also account for this (England *et al.*, 2009).

11.2.6.2 Stages of the Dog Estrous Cycle

Dogs inherited the major aspects of their reproductive cycle from wolves (Case, 2005). Like wolves, the reproductive cycle of the domestic female dog is the estrous cycle (Case, 2005; England, 2013; Jones and Joshua, 1988). The dog estrous cycle is divided into four phases: proestrus, estrus, diestrus (also called metestrus), and anestrus (Evans and Cole, 1931). The nonspayed female is in "heat" or "season" during proestrus and estrus (Concannon, 2011). Ovulation and mating occur during the estrous phase (described below).

Several parameters can be used to monitor progression of the reproductive cycle: (i) dog behavior (both females and males), (ii) appearance of female external genitalia and vagina, (iii) reproductive hormone levels such as progesterone and LH, (iv) gross appearance and size of ovaries, (v) ovarian histology, and (vi) vaginal exfoliation cytology, which is sensitive to estrogen levels (Figures 11.22–11.24) (Case, 2005; Concannon *et al.*, 1977; England, 2013). Breeders and veterinarians are interested in the time of ovulation and thus when to breed females. They routinely rely on serum progesterone levels and vaginal cytology in addition to dog behavior to determine when to breed dogs for a successful pregnancy (Case, 2005; England, 2013). Ultrasound may also be used to monitor pregnancy (England, 2013). Unfortunately, serum progesterone cannot be used to confirm pregnancy because of the canine pseudopregnancy period in which serum progesterone levels are high whether the dog is pregnant or not

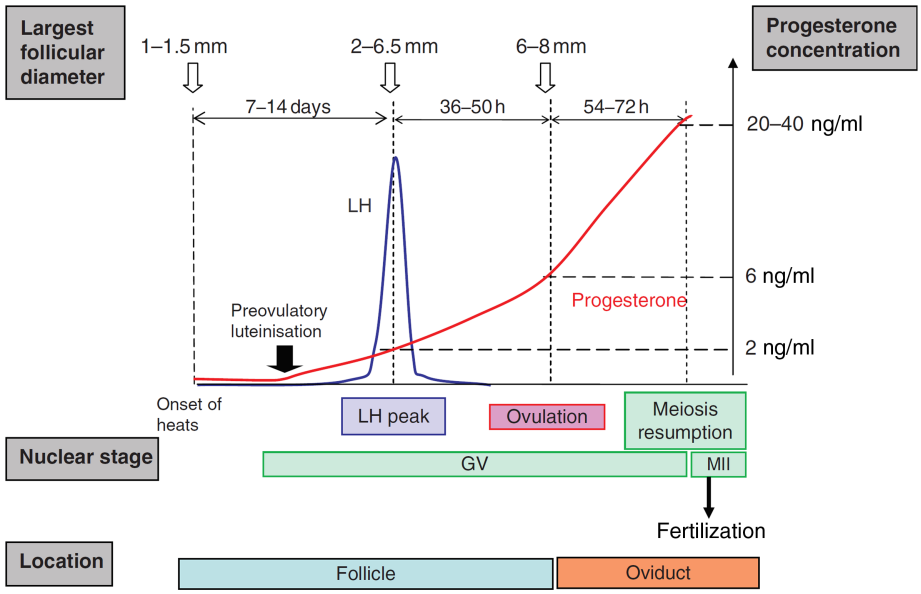

Figure 11.23 Estrous cycle events in the dog. Summary of final follicular growth, endocrine events and meiotic events in the female. (Reproduced from Chastant-Maillard S, Viaris de Lesegno C, Chebrout M, Thoumire S, Meylheuc T, Fontbonne A, Chodkiewicz M, Saint-Dizier M, Reynaud K. 2011. The canine oocyte: uncommon features of *in vivo* and *in vitro* maturation. *Reproduction, Fertility and Development* 23(3):391–402, © CSIRO 2011, reprinted by permission of CSIRO Publishing.) (See color plate section.)

Downloaded From Vet-eBooks.com

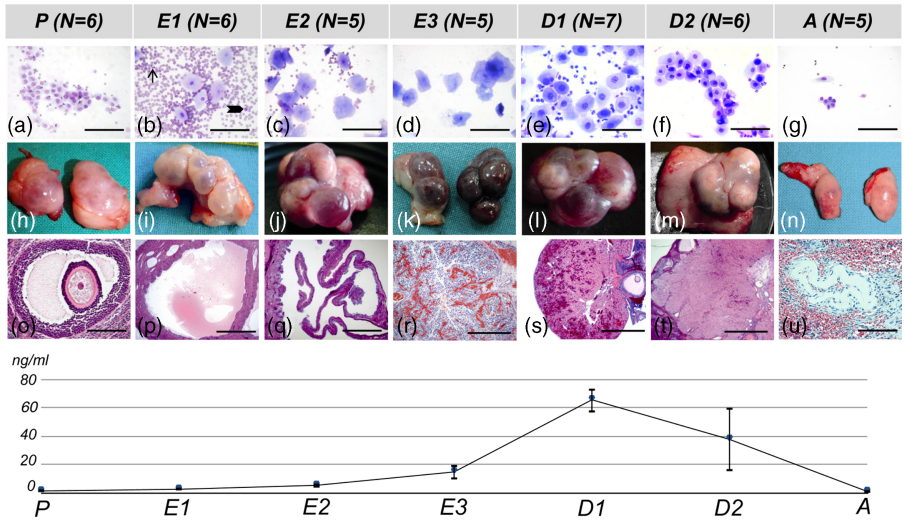

Figure 11.24 Steps of the estrous cycle of the dog. Vaginal cytology (*a-g*), ovarian macroscopic aspects (*h-n*), ovarian histology (*o-u*), and mean blood progesterone levels (graph) in the dog during the estrous cycle. Data were collected during several time points: one in proestrus (*P*), three in estrus (*E1-3*), two in diestrus (*D1*, *D2*) and one in anestrus (*A*). (*a*) Parabasal cells with some erythrocytes, (*b*) intermediate cells, some leukocytes (arrows) and many erythrocytes, (*c*) superficial cells with rare erythrocytes, (*d*) superficial anucleate cells, (*e*) superficial cells, intermediate cells and abundant neutrophils, (*f*) heterogeneous population of epithelial cells with some neutrophils, (*g*) few cells in sample with small groups of parabasal cells, (*h*) translucent, small vesicular structures characterize proestrus, (*i*) vesicular structures increase in diameter during preovulatory estrus, (*j*) large follicles present before ovulation, (*k*) corpora hemorrhagica present after ovulation, (*l*) both corpora hemorrhagica and corpora lutea present at beginning of diestrus, (*m*) mature corpora lutea characterize medium-late diestrus, (*n*) small, inactive ovaries characteristic of anestrus, (*o*) small tertiary follicle, (*p*) large preovulatory follicle, (*q*) ruptured, large follicle just after ovulation, (*r*) collapsed tertiary follicle transforming into a corpus hemorrhagicum, (*s*) corpus hemorrhagicum transforming into corpus luteum, (*t*) mature corpus luteum, and (*u*) involuted corpus luteum (corpus albicans). Scale bars: (*a - g*) = 100 µm, (*o, u*) = 500 µm, (*p, q*) = 700 µm, (*r, s, t*) = 1000 µm. (Reproduced from *Animal Reproduction Science*, volume 152, Groppetti D, Aralla M, Bronzo V, Bosi G, Pecile A, Arrighi S., Periovulatory time in the bitch: whata's new to know? Comparison between ovarian histology and clinical features, pages 108-116, Copyright 2015, with permission from Elsevier.) (See color plate section.)

(Concannon *et al.*, 2009). The physiological pseudopregnancy that follows ovulation in the dog is unlike other domestic animals in which nonpregnant females have a relatively short luteal phase (Concannon, 2009; Kowalewski, 2014). The duration of each phase of the estrous cycle is highly variable between dogs. Details of the phases of the dog's estrous cycle are described in the following sections.

Proestrus

The first phase of the dog estrous cycle is proestrus (proestrous phase). The duration of proestrus varies and lasts from about 6–11 days (range 5–20 days) and averages 9 days (Case, 2005; Concannon, 2011; England, 2013; Jones and Joshua, 1988). Proestrus starts when a bloody vaginal discharge begins (Figure 11.22a). Males are attracted to females during proestrus, but females are unwilling to mate. Low (<2 ng/ml) blood progesterone levels are typical of proestrus (Figure 11.24). Ovaries during proestrus are a little larger and appear smooth with small vesicular surface structures (England, 2013; Groppetti *et al.*, 2015). Small, medium, and large follicles are present with about 44% being medium follicles that are 2–3 mm in diameter (Groppetti *et al.*, 2015). Follicles increase in size during proestrus and accumulate follicular fluid in the follicular

Downloaded From Vet-eBooks.com

antra (England, 2013). Follicles also secrete estradiol, and serum estradiol-17β levels rise during proestrus (Jones and Joshua, 1988; England, 2013). Vaginal bleeding occurs throughout proestrus. Vaginal cytology during proestrus is characterized by parabasal cells, small intermediate cells, erythrocytes, leukocytes, and bacteria (Case, 2005; England, 2013; Groppetti *et al.*, 2015; Jones and Joshua, 1988). The vulva begin to swell during proestrus (Drier, 1998).

Estrus

Estrus (estrous phase) follows proestrus of the dog estrous cycle. Estrus averages 5–9 days, is highly variable, and can last up to almost 3 weeks (Case, 2005; England, 2013). During estrus, the female allows a male to mate with her, oocytes are released from the ovary, and estrus ends when she is no longer receptive to a male. During preovulatory estrus, small (~1.5 mm in diameter), medium (~2.3 mm in diameter), and large (3.8 mm in diameter) follicles are present in the ovary in a proportion of about one-third each (Groppetti *et al.*, 2015). Estrus starts with a surge of LH. Estrus is also characterized by a fall in estradiol levels just prior to the preovulatory LH surge (Case, 2005; Groppetti *et al.*, 2015). The LH surge lasts 24–72 h (Chastant-Maillard *et al.*, 2011). Unlike most mammals, preovulatory luteinization occurs in the dog, and rising blood progesterone levels start at about 2.5 ng/ml (Case, 2005; Groppetti *et al.*, 2015). During preovulatory estrus, the ovarian surface is uneven with large follicles visible on the surface. Ovulation occurs during estrus about 48–72 h (2–3 days) after a plasma peak of LH (LH surge) when the blood progesterone level is between 4 and 10 ng/ml, but has also been reported to be 36–50 h after the LH peak (Chastant-Maillard *et al.*, 2011; Concannon, 2009; Groppetti *et al.*, 2015). The ovaries contain small, medium, and large follicles with about half of the follicles being large (>4 mm in diameter) (Groppetti *et al.*, 2015). Oocytes can be released from anywhere on the ovarian surface (England, 2013). Small breed dogs ovulate 2–10 oocytes per cycle and large breeds can release 5–20 oocytes per cycle (Case, 2005). At the end of estrus, the ovaries contain corpora hemorrhagica (6 mm in diameter) and they comprise about 43% of the ovarian follicular/follicular remnant structures (Groppetti *et al.*, 2015). Vaginal cytology changes during estrus with large nucleated superficial cells present before ovulation, and after ovulation, there are clear anuclear epithelial superficial cells in the absence of red blood cells (Case, 2005; England, 2013; Groppetti *et al.*, 2015; Jones and Joshua, 1988).

Diestrus

Following estrus is diestrus (diestrous phase, also known as metestrus), which lasts about 2 months (60 days) in both the nonpregnant dog and the pregnant dog (Case, 2005; England, 2013). Its duration is variable and ranges 50–80 days (Concannon, 2011). Unlike most mammals, progesterone levels remain high in the nonpregnant dog and she normally undergoes a period of pseudopregnancy (Case, 2005; England, 2013; Kowalewski *et al.*, 2015). During diestrus, the ovary is at its largest size and mature corpora lutea are visible from the ovarian surface (England, 2013; Groppetti *et al.*, 2015). By the end of diestrus, corpora lutea (6 mm in diameter) comprise about 65% of the follicle structure population with the remainder being mostly small follicles (about 1.3 mm in diameter) (Groppetti *et al.*, 2015). Corpora lutea actively secrete progesterone, and blood contains 50–68 ng/ml progesterone depending on the number of corpora lutea present (Groppetti *et al.*, 2015; Kowalewski *et al.*, 2015). By the end of diestrus, progesterone levels return to basal levels (<2 ng/ml) (England, 2013). Vaginal cytology during diestrus abruptly returns to small intermediate cells and parabasal cells with few neutrophils and absence of red blood cells (Case, 2005; England, 2013; Groppetti *et al.*, 2015; Jones and Joshua, 1988). In the pregnant dog, diestrus ends with parturition (birth), and in the nonpregnant female it ends with low (<2 ng/ml) serum progesterone concentration (Case, 2005; Kowalewski *et al.*, 2015).

Downloaded From Vet-eBooks.com

Anestrus

Anestrus (anestrous phase) begins at the end of the diestrous phase of the estrous cycle. Anestrus is an inactive phase of the reproductive cycle. Females are uninterested in mating at this time. The duration of anestrus is highly variable between dogs. Generally anestrus lasts about 4–5.5 months and normally ranges from 2 to 10 months (Case, 2005; England, 2013). The duration of anestrus in dogs has also been reported as 15 weeks (Jones and Joshua, 1988), and 80–240 days (Concannon, 2011). Extreme ranges are 1 month to as long as 2 years (England, 2013). Reproductive hormones are relatively low during anestrus. For example, blood progesterone levels are basal (<2 ng/ml) as are estrogen and LH (Concannon, 2009; Groppetti *et al.*, 2015; Kowalewski *et al.*, 2015). Follicle stimulating hormone (FSH) levels increase somewhat during anestrus (Concannon, 2009). The ovaries during anestrus are ovoid, small, flat, and inactive with small follicles (about 1.3 mm in diameter) and no medium or large follicles (Groppetti *et al.*, 2015). Vaginal cytology during anestrus consists of parabasal cells and small intermediate cells (Case, 2005; Groppetti *et al.*, 2015; Jones and Joshua, 1988). After anestrus the estrous cycle begins again with proestrus.

11.2.6.3 The Dog Oocyte

Karl Ernst von Baer discovered the mammalian oocyte using dog oocytes in 1827 (O'Rahilly and Müller, 2001). Typical of mammalian oocytes, dog oocytes are spherical and surrounded by a zona pellucida (extracellular matrix) (Figure 11.25). The diameter of living oocytes (excluding the zona pellucida) from dogs in anestrus that were preselected from high-quality cumulus–oocyte complexes was reported as 90.7 ± 1.0 μm in diameter (Lunn and Wright, 2013) and 115.3 ± 7.6 μm in diameter (Lee *et al.*, 2008). Fully sized oocytes isolated from 3.5 to 5 mm preovulatory follicles of females with a serum LH concentration <1 ng/ml were 127 ± 2 μm in diameter (range 118–135 μm excluding the zona pellucida), and were 132 ± 2 μm (range 129–144 μm) in diameter when measured within 31 h after the LH surge (De Lesegno *et al.*, 2008; Lee *et al.*, 2008). This is larger in size than freshly aspirated human oocytes at meiotic metaphase II, which are 114.1 ± 0.7 μm in diameter (excluding zona pellucida) and 163.8 ± 1.2 μm in diameter including the zona pellucida (Valeri *et al.*, 2011).

Numerous microvilli characterize the surface of the dog oocyte (De Lesegno *et al.*, 2008; Haenisch-Woehl *et al.*, 2003; Tesoriero, 1981). The microvilli extend toward the zona pellucida, contacting it (De Lesegno *et al.*, 2008; Haenisch-Woehl *et al.*, 2003; Tesoriero, 1981). The dog oocyte contains an abundance of components typical of mammalian oocytes, including cytoplasm, the nucleus, cytoskeleton, endoplasmic reticulum, Golgi, and cortical granules. The general features of these structures are described in the following sections. Changes in their distribution during oocyte meiotic maturation *in vitro* has been addressed previously (see Chastant-Maillard *et al.*, 2011; De Lesegno *et al.*, 2008).

Oocyte Nucleus

The nucleus (also called germinal vesicle) of the dog oocyte is spherical to oval. It is relatively large about 30–40 μm in diameter, typical of mammalian oocytes (De Lesegno *et al.*, 2008). It is spherical and located in a central position in immature dog oocytes and becomes oval and eccentric, with the long axis of the nucleus parallel to the plasma membrane (oolemma) as maturation proceeds (De Lesegno *et al.*, 2008; Jin *et al.*, 2006; Saint-Dizier *et al.*, 2004). Human oocytes also have an eccentric germinal vesicle (Yao and Batchu, 2007). Dog and human germinal vesicles have both heterochromatin and diffuse euchromatin (Jin *et al.*, 2006; Reynaud *et al.*, 2012b; Saint-Dizier *et al.*, 2004). The dog germinal vesicle contains prominent nucleoli that vary in number (usually 1–2) and are about 5–7 μm in diameter (De Lesegno *et al.*, 2008; Saint-Dizier *et al.*, 2004). Nucleolar appearance includes fibrillar, fibrillogranular, and reticulated nucleoli similar to other species (De Lesegno *et al.*, 2008).

Downloaded From Vet-eBooks.com

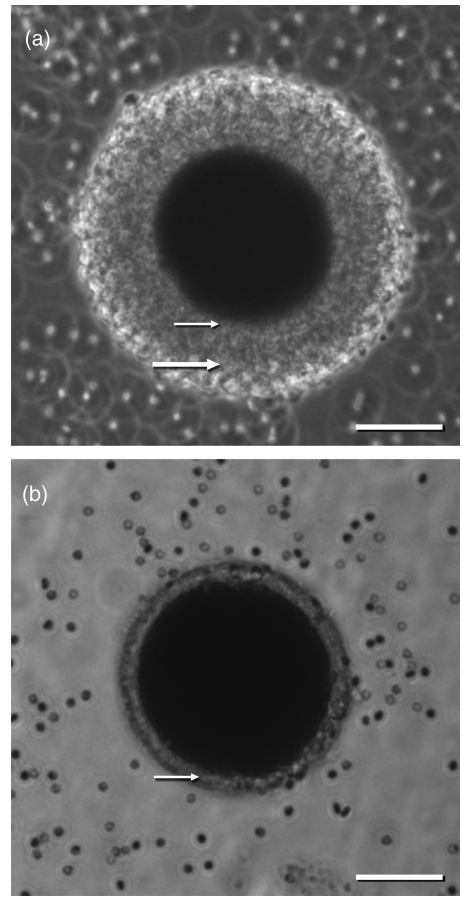

Figure 11.25 Dog oocytes. (a) Cumulus-oocyte complex. (b) Denuded zona-intact oocyte with detached cumulus cells. Small arrow, zona pellucida; large arrow, cumulus cells. Scale bars, 50 μm. (Reproduced from Lunn MO, Wright SJ, 2009, Imaging the zona pellucida of canine and feline oocytes using scanning electron microscopy, *Microscopy and Microanalysis* 15(1), pages 2–14, © 2009 Microscopy Society of America, reproduced with permission of Cambridge University Press.)

Assessment of the germinal vesicle chromatin configuration of the mammalian oocyte focuses especially on the chromatin surrounding the nucleolus (Tan *et al.*, 2009). Typical of mammalian oocytes, the germinal vesicle of the dog oocyte is characterized by a chromatin appearance that changes over time from diffuse to fibrillary, and then condensed and surrounding the nucleolus as the oocyte progresses through maturation (Reynaud *et al.*, 2009; Valentini *et al.*, 2010). Chromatin configuration has been used as a means to assess maturity of the dog oocyte, as in other mammalian species (Chastant-Maillard *et al.*, 2011; Reynaud *et al.*, 2009, 2012b; Tan *et al.*, 2009). The chromatin configuration of the dog germinal vesicle is thought to resemble that of the horse more than the human (Tan *et al.*, 2009). The germinal vesicle chromatin transition is thought to represent different transcription states of the oocyte as it matures (Tan *et al.*, 2009).

Oocyte Cytoplasm

The dog oocyte has a large quantity of cytoplasm called ooplasm. Typical of mammalian oocytes, the ooplasm of the dog oocyte has an accumulation of many organelles important for fertilization such as mitochondria, endoplasmic reticulum, cortical granules, and Golgi complexes. Cytoskeletal components have been identified in dog oocytes and include microfilaments and microtubules (Jin *et al.*, 2006; Kempisty *et al.*, 2015; Saint-Dizier *et al.*, 2004). Microtubules (as detected by anti-α-tubulin antibodies) revealed a subcortical and perinuclear distribution, with asters in germinal vesicle oocytes and a network of microtubules in oocytes

Downloaded From Vet-eBooks.com

undergoing germinal vesicle breakdown (Jin *et al.*, 2006; Kempisty *et al.*, 2015; Saint-Dizier *et al.*, 2004). In meiotic metaphases I and II, oocyte microtubules were restricted to the meiotic spindle, which was located in the oocyte cortex (Saint-Dizier *et al.*, 2004). The meiotic spindle of the dog oocyte was symmetrical, barrel-shaped with wide spindle poles and lacked astral microtubules (Saint-Dizier *et al.*, 2004). The metaphase II spindle was radially oriented as in the human oocyte, and was smaller than the metaphase I spindle of the dog oocyte (Saint-Dizier *et al.*, 2004; Simerly *et al.*, 1995). Microfilaments were observed in the oocyte cortex and also surrounded the germinal vesicle (Chastant-Maillard *et al.*, 2011; Jin *et al.*, 2006; Kempisty *et al.*, 2015). After germinal vesicle breakdown, microfilaments were in the oocyte cortex closely associated with the condensed chromosomes (Chastant-Maillard *et al.*, 2011; Jin *et al.*, 2006; Kempisty *et al.*, 2015).

One of the most striking features of the dog oocyte is its appearance (Figure 11.25). The dog oocyte has abundant, dark lipid contained within round to oval lipid droplets that make the oocyte appear very dark brown-black and opaque (Figure 11.25) (Hewitt and England, 2001; Lunn and Wright, 2009; Reynaud *et al.*, 2005, 2006; Tesoriero, 1981; Turathum *et al.*, 2010). Although dark lipid is characteristic of oocytes of some domestic species such as the pig, horse, and cat, the dog oocyte has a higher abundance of lipid in the cytoplasm than these species (Concannon *et al.*, 2009). The dark opacity of the dog oocyte is unlike human and rodent oocytes that are light in color and transparent (Nagy *et al.*, 2003; Valeri *et al.*, 2011). Lipid analysis of dog oocytes by matrix-assisted laser desorption mass spectrometry (MALDI-MS) revealed that the most abundant lipid was a phosphatidlycholine (34:1) that had 34 carbons and one double bond (Apparicio *et al.*, 2012). This is thought to be the major phospholipid detected in cellular membranes, and was found to be the most abundant lipid of oocytes from humans and other mammals (Apparicio *et al.*, 2012; Ferreira *et al.*, 2010).

Oocyte Mitochondria

Mitochondria of the dog oocyte have been imaged with fluorescence microscopy using potentiometric fluorescent dyes that demonstrate actively functioning mitochondria and by transmission electron microscopy. Mitochondria of dog primary oocytes appeared round or elongated and had transverse cristae in transmission electron micrographs (De Lesegno *et al.*, 2008; Haenisch-Woehl *et al.*, 2003; Tesoriero, 1981). Mitochondria were clustered in the periphery of oocytes collected from prepubertal dogs aged 4–6 months (Haenisch-Woehl *et al.*, 2003). Mitochondrial clouds were also abundant in preovulatory oocytes of sexually mature females (Chastant-Maillard *et al.*, 2011). Upon further examination with fluorescence microscopy, mitochondria of oocytes from sexually mature adult dogs were numerous and distributed heterogeneously when comparing oocytes (De los Reyes *et al.*, 2011; Valentini *et al.*, 2010). The distribution ranged from a fine and even pattern throughout the ooplasm of recently collected oocytes, and was reported to become more clustered, but still evenly distributed during *in vitro* maturation to metaphase II (De los Reyes *et al.*, 2011; Valentini *et al.*, 2010). The pattern of mitochondrial distribution has been reported to be linked to the stage of the estrous cycle of the dog ovary donor (Valentini *et al.*, 2010).

Mitochondria have the important role to produce energy for the energy-consuming processes of oocyte maturation, which involve nuclear, cytoplasmic, and epigenetic changes, including meiotic spindle formation, and also for embryonic development. Mitochondrial dysfunction has been linked to disease and age-related infertility in humans and other mammals (Valentini *et al.*, 2010; Wolf *et al.*, 2015). Mitochondrial replacement therapies such as spindle transfer, pronuclear transfer, and polar body transfer are means to combat mitochondrial dysfunction conditions. While mitochondrial replacement therapies have been performed with human poly-pronuclear oocytes, with limited development to the blastocyst

Downloaded From Vet-eBooks.com

stage, further testing with nonhuman animal models is much needed (Wolf *et al.*, 2015). Thus, the dog with its peripheral mitochondrial clouds in oocytes and prolonged oocyte maturation offers an excellent model to address the efficacy of mitochondrial replacement therapies in oocytes or early embryos for reproductive medicine. In addition, the dog model may be used to address the serious ethical, social, and scientific concerns over mtDNA mismatching in humans as a result of mitochondrial replacement therapies by examining the possible side effects of mtDNA mismatching between the dog and other canid species such as the wolf, coyote, and blue fox.

Oocyte Endoplasmic Reticulum

The dog oocyte contains both smooth and rough endoplasmic reticulum as determined by transmission electron microscopy (Chastant-Maillard *et al.*, 2011; De Lesegno *et al.*, 2008; Tesoriero, 1981). Preovulatory oocytes had large concentric strands of smooth endoplasmic reticulum some of which were perinuclear (Chastant-Maillard *et al.*, 2011; De Lesegno *et al.*, 2008; Tesoriero, 1981). Smooth endoplasmic reticulum surrounded lipid droplets as well as clusters of mitochondria (Chastant-Maillard *et al.*, 2011; De Lesegno *et al.*, 2008). The amount of rough endoplasmic reticulum was low in oocytes from prepubertal dogs (4–6 months old), and highly variable between oocytes collected from sexually mature dogs (Chastant-Maillard *et al.*, 2011; De Lesegno *et al.*, 2008; Haenisch-Woehl *et al.*, 2003). The rough endoplasmic reticulum was organized in parallel strands in preovulatory oocytes (Chastant-Maillard *et al.*, 2011; De Lesegno *et al.*, 2008). Confocal fluorescence microscopy using a fluorescent endoplasmic reticulum-specific probe (ER-Tracker) revealed fluorescent staining only in the oocyte cortex and showed a reticular pattern of cortical endoplasmic reticulum in living zona-intact oocytes isolated from sexually mature dogs at various stages of the estrous cycle (De los Reyes *et al.*, 2012).

Oocyte Cortical Granules

The cortical granules of dog oocytes are located in the oocyte cortex either just under the plasma membrane or about 1 μm deep to the plasma membrane (De Lesegno *et al.*, 2008; Tesoriero, 1981; Turathum *et al.*, 2010). The cortical granules are electron dense and ~0.35–0.4 μm in diameter (De Lesegno *et al.*, 2008; Tesoriero, 1981; Turathum *et al.*, 2010). The cortical granule membrane is separated from the electron dense contents by a small space (De Lesegno *et al.*, 2008; Tesoriero, 1981; Turathum *et al.*, 2010). The diameter of dog cortical granules is comparable to that of human cortical granules, which are 0.35 ± 0.11 μm in diameter in human oocytes at the germinal vesicle stage (Palmerini *et al.*, 2014).

Oocyte Golgi Complex

The Golgi apparatus is known to be involved in synthesis of cortical granules, which are present in the oocyte cortex. When visualized with transmission electron microscopy, the Golgi apparatus structures were very few in oocytes from primordial follicles from prepubertal dogs (Haenisch-Woehl *et al.*, 2003). In later-stage follicles from prepubertal dogs, and during follicular growth in oocytes from sexually mature dogs, Golgi structures became more numerous in oocytes and were distributed in the oocyte cortex (De Lesegno *et al.*, 2008; Haenisch-Woehl *et al.*, 2003; Lopes *et al.*, 2010; Tesoriero, 1981). Preovulatory oocytes (prior to the LH surge) from sexually mature dogs had few and small Golgi structures with a perinuclear and cortical distribution (De los Reyes *et al.*, 2009). In oocytes collected between the LH surge and ovulation, Golgi structures became more numerous and had a cortical distribution (De Lesegno *et al.*, 2008). When Golgi apparatus structures were visualized using immunofluorescence microscopy coupled with antibodies specific to the Golgi apparatus proteins

Downloaded From Vet-eBooks.com

(anti-GM130 and anti-Giantin), the Golgi apparatus was observed homogeneously in the cytoplasm of germinal vesicle stage dog oocytes (De los Reyes *et al.*, 2012). As *in vitro* maturation proceeded, the Golgi apparatus had a subcortical localization at 48 h of culture and this became a cortical distribution by 96 h of culture (De los Reyes *et al.*, 2012). The cortical distribution of the Golgi apparatus in dog oocytes may also reflect the function of the oocyte to synthesize proteins of the zona pellucida that are secreted by the oocyte (as well as cumulus cells) to form the zona pellucida.

Zona Pellucida

Typical of mammalian oocytes, dog oocytes are surrounded by the relatively transparent zona pellucida, which is an acellular, extracellular matrix (Figure 11.25) (Albertini, 2015). The zona pellucida is 15.0 ± 0.4 μm thick (range 10–23 μm thick) in oocytes isolated from ovaries of anestrous dogs (Lee *et al.*, 2008; Lunn and Wright, 2009). The zona pellucida increases in thickness during the estrous cycle so that the zona pellucida of *in vivo* ovulated oocytes was significantly larger at 19.2 ± 2.0 μm thick (Lee *et al.*, 2008). The dog zona pellucida is comparable in appearance and thickness to the human zona that is 17.7 ± 0.3 μm thick in oocytes that have a zona pellucida with high birefringence (Valeri *et al.*, 2011). High birefringence of the human zona pellucida has been associated with higher rates of embryo implantation and successful embryonic development to term compared to zonae with low birefringence that were significantly thinner (16.7 ± 0.3 μm) (Valeri *et al.*, 2011). In humans, zona thickness declines with maternal age (Valeri *et al.*, 2011). In dogs, the thickness of the zona pellucida of oocytes prior to the LH surge was 9.8 ± 0.5 μm (when LH levels were negligible and serum progesterone levels at the time of ovariectomy ranged from 0.32 to 0.84 ng/ml) (De Lesegno *et al.*, 2008). Zona pellucida thickness was reported to increase with *in vivo* meiotic maturation and was thickest at meiotic metaphase II (17 ± 0.3 μm) in oocytes collected about 105 h postovulation or about 5 days after the LH surge (Chastant-Maillard *et al.*, 2011; De Lesegno *et al.*, 2008; Lee *et al.*, 2008). The external surface of the zona pellucida of dog oocytes appears fenestrated and mesh-like when examined with scanning electron microscopy (Figure 11.26) (De los Reyes *et al.*, 2009; Lunn and Wright, 2009, 2013; Palomino and De los Reyes, 2009; Ström-Holst *et al.*, 2000). The external surface of the dog zona pellucida varies in appearance when comparing oocytes, as has been reported for human oocytes (Lunn and Wright, 2009, 2013; Magerkurth *et al.*, 1999).

Transzonal projections, which are cellular processes from the cumulus cells surrounding the zona pellucida, traverse the dog and human zonae pellucidae to touch the oolemma (Chastant-Maillard *et al.*, 2011; De Lesegno *et al.*, 2008; Tesoriero, 1981). Within the transzonal projections of dog oocytes are microfilaments (Chastant-Maillard *et al.*, 2011). These transzonal projections are considered to be important for signaling between the oocyte and surrounding cumulus cells. The transzonal projections decrease in number during meiotic maturation of dog oocytes (Chastant-Maillard *et al.*, 2011; De Lesegno *et al.*, 2008; Tesoriero, 1981). The transzonal projections begin to degenerate about 2 days after ovulation (5 days after the LH peak) and are gone by 3 days after ovulation (Chastant-Maillard *et al.*, 2011; De Lesegno *et al.*, 2008). This is coincident with the resumption of meiotic maturation of the oocyte while it is in the uterine tube (De Lesegno *et al.*, 2008).

In dogs, the zona pellucida is composed of three different glycoproteins, ZPA/ZP2, ZPC/ZP3, and ZPB/ZP4 (Goudet *et al.*, 2008). Similarly, the human zona pellucida is also composed of these proteins plus a ZP1 protein for a total of four different zona pellucida proteins (Goudet *et al.*, 2008). In dogs, the oocyte synthesizes ZPA/ZP2 and the granulosa cells produce ZPC/ZP3 and ZPB/ZP4 (Blackmore *et al.*, 2004). This is thought to prevent premature zona assembly in the cell cytoplasm, and allows assembly to occur outside the oolemma after zona proteins are secreted. Expression of ZP2 and ZP3 genes may be

Downloaded From Vet-eBooks.com

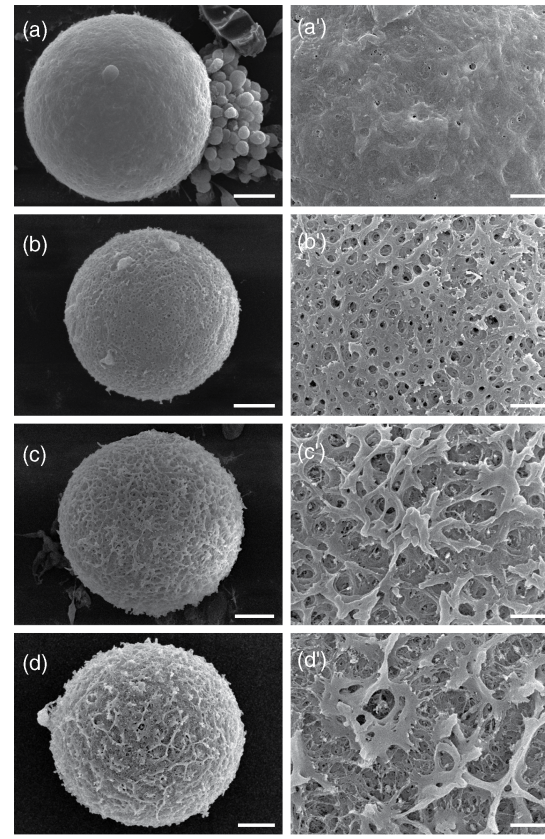

Figure 11.26 Scanning electron micrographs of dog oocytes with zona pellucida. The external surface of the zona pellucida of high-quality oocytes was heterogeneous, ranging from smooth to very rough. Scale bars, 20 μm in A–D, 5 μm in A′–D′. (Reproduced from *Theriogenology*, volume 80, issue 5, Lunn MO, Wright SJ, Distinct subtypes of zona pellucida morphology reflect canine oocyte viability and cumulus-oocyte complex quality, pages 498–506, Copyright 2013, with permission from Elsevier.)

associated with dog oocyte maturation, since ZP2 and ZP3 expressions were upregulated after *in vitro* maturation of dog oocytes for 72 h (Kempisty *et al.*, 2015). During the same period, protein levels for ZP3 and ZP4 were reported to decrease after *in vitro* maturation when compared to freshly collected dog oocytes suggesting a downregulation of these proteins associated with meiotic maturation, which could be linked to infertility (Kempisty *et al.*, 2015). Lack of ZP2 or ZP3 results in infertility in mice (Rankin *et al.*, 2003). Zona pellucida protein, ZP3, has been successfully used as an immune contraceptive target to block fertility in dogs (Shrestha *et al.*, 2014, 2015). Human infertility has been linked to problems with the zona pellucida that involve cross-linking of the zona proteins resulting in zona hardening (Shrestha *et al.*, 2014, 2015). The many characteristics of the dog zona pellucida that are similar to that of the human make the dog a useful model for understanding the human zona pellucida and to address zona-related infertility.

11.2.6.4 Dog Oocyte Maturation and Ovulation

During folliculogenesis, oocytes undergo nuclear and cytoplasmic maturation during growth (Sánchez and Smitz, 2012). They also acquire *meiotic competence,* which is the capacity of the oocyte to resume meiosis and complete nuclear maturation (Sánchez and Smitz, 2012). Meiotic competence in the dog is acquired in oocytes from follicles greater than 2 mm in diameter (Songsasen and Wildt, 2005; Tan *et al.*, 2009). Cytoplasmic maturation of the oocyte involves *developmental competence*, in which a mature oocyte has the capacity to be fertilized and support development to term, producing a viable embryo and eventually a healthy, live birth (Sánchez and Smitz, 2012). *In vitro* studies

Downloaded From Vet-eBooks.com

have shown that although the dog oocyte may have acquired meiotic competence (as it reaches metaphase II), it may not exhibit cytoplasmic maturity (developmental competence) since the *in vitro* matured oocyte is unable to be fertilized (or has a very low rate of fertilization), and does not support development to term (Chastant-Maillard, 2011; Reynaud *et al.*, 2012a; Sánchez and Smitz, 2012).

Dogs are polytocous, that is, they normally have more than one offspring per birth (Concannon, 2011). Thus, multiple oocytes (range 4–12) are recruited and ovulated during one reproductive cycle (Tsutsui *et al.*, 2012; Lee *et al.*, 2005; Reynaud *et al.*, 2006). The ovulation rate in the dog was high and ranged 97–100% of large follicles (England *et al.*, 2009). The number of oocytes that are ovulated depends on breed size of the female with 5.5 ± 0.7 in small breeds less than 10 kg, 7.8 ± 0.7 in medium-sized breeds, and 10.1 ± 1.4 in large breeds greater than 20 kg (Chastant-Maillard *et al.*, 2011; Reynaud *et al.*, 2006).

Dogs are spontaneous ovulators meaning oocytes are released periodically from ovaries in response to changes in hormonal signals within the body (Case, 2005; Concannon, 2009). Ovulation in the dog occurs about 48–72 h (range 1–4 days) after the LH surge (Concannon, 2009; Chastant-Maillard *et al.*, 2011; Groppetti *et al.*, 2015; Rijsselaere *et al.*, 2014). Dogs have one group of follicles that grow and release oocytes per breeding cycle (Case, 2005). Not all oocytes are released from the follicles at the same time during ovulation and oocytes are ovulated over 24–48 h in the dog (Case, 2005; Chastant-Maillard *et al.*, 2010; Groppetti *et al.*, 2015). Ovulation is thought to involve high levels of prostaglandins such as PGE2 and PGF2α (Kowalewski, 2014).

Dogs ovulate a primary oocyte that contains a germinal vesicle (Figure 11.23) (Reynaud *et al.*, 2005). Meiotic maturation of the dog oocyte begins at meiotic prophase I in the ovarian preovulatory follicle prior to the LH surge (Chastant-Maillard *et al.*, 2011). Primary oocytes are ovulated at meiotic prophase I (germinal vesicle stage) and complete meiotic maturation in the uterine tube rather than in the ovarian follicle (Holst and Phemister, 1971). This is unlike oocytes of humans and most mammals that undergo meiotic maturation to metaphase II in the ovary and are ovulated at meiotic metaphase II (Chastant-Maillard *et al.*, 2011; Holst and Phemister, 1971). About 5 days after the LH surge in dogs, the oocyte is in the uterine tube, is at metaphase II, and has a first polar body (De Lesegno *et al.*, 2008; Holst and Phemister, 1971; Sánchez and Smitz, 2012). Recently, ovulated dog oocytes take about 48–72 h to reach metaphase II and become competent to support fertilization (Chastant-Maillard *et al.*, 2010, 2011; Reynaud *et al.*, 2005). The innermost cumulus cells of the cumulus–oocyte complex (oocyte plus surrounding granulosa cells) are unmucified, and form a compact layer of 2–3 cells thick (Reynaud *et al.*, 2006; Valentini *et al.*, 2010). As ovulated dog oocytes are transported in the uterine tube, blood plasma levels of progesterone become increasingly high, since luteinization of preovulatory follicles is a normal feature of dog reproduction (Chastant-Maillard *et al.*, 2011; Concannon, 2011; Kowalewski *et al.*, 2015). Up to 72 h after ovulation and up to 5 days after oocyte maturation to metaphase II, oocytes remain viable and are capable of being fertilized (Case, 2005; Concannon, 2009; Tsutsui *et al.*, 2009). Thus, it is possible for a dog to have puppies from different fathers in one breeding cycle (England, 2013).

11.2.7 Dog Fertilization

Fertilization consists of a complex series of synchronized events that occur over time (Yanagimachi, 1994). During fertilization, haploid gametes (oocyte, spermatozoon) fuse to form a genetically distinct new individual, the embryo. To achieve fertilization in the dog, spermatozoa must be delivered to the female reproductive tract and then travel through it to reach the oocytes, which are located in the uterine tubes (Figure 11.27). Right after ejaculation, spermatozoa are unable to fertilize oocytes and require additional maturational changes that are

Downloaded From Vet-eBooks.com

prerequisite for fertilization. These changes include physiological and morphological alterations of the spermatozoon such as sperm capacitation and the acrosome reaction, which are discussed in the following section, focusing on what is known in the dog.

11.2.7.1 Journey of Spermatozoa in the Female Reproductive Tract

Fertilization is internal in the dog. During natural mating, semen is deposited in the cranial vagina (Figure 11.27) (Feldman and Nelson, 2004). Spermatozoa from the sperm-rich fraction arrive in the uterine tube within 25 s after ejaculation and about 58 s after mounting by the male (Evans, 1933). During coitus, the large volume of seminal prostatic fluid that is ejaculated over a long period (up to 20 min) after the sperm-rich fraction is thought to flush sperm into the uterine lumen (Forsberg and Reynaud, 2012; Rijsselaere *et al.*, 2014). Sperm migration to the uterine tubes may depend on both sperm motility and contractions of the vagina and uterus (Rijsselaere *et al.*, 2014). While up to 63% of epididymal sperm are motile, most develop progressive forward motility upon ejaculation (Angrimani *et al.*, 2014a, 2014b; Varesi *et al.*, 2013).

Natural fertile mating in the dog may occur up to 7 days before ovulation (Doak *et al.*, 1967; Freeman and England, 2013). As a result, spermatozoa need to remain viable even longer until oocytes undergo meiotic maturation prior to fertilization, which is an additional 2–3 days (Chastant-Maillard *et al.*, 2010, 2011; Doak *et al.*, 1967). Dog spermatozoa can maintain their viability for up to 11 days in the female reproductive tract (Doak *et al.*, 1967). Therefore, spermatozoa need a mechanism to remain viable and maintain their other functions such as motility until they are able to fuse with the oocyte. Once in the uterus, dog spermatozoa can bind to the uterine epithelium and are thought to create a sperm storage reservoir within the uterus from which they can be released later when needed (Figure 11.28) (Freeman and England, 2013; Karre *et al.*, 2012; Reynaud *et al.*, 2015; Rijsselaere *et al.*, 2004, 2014). Uterine crypts of the uterine horns and the distal part of the uterotubal junction are considered to serve as the major sperm reservoir in the dog (England *et al.*, 2013; Freeman and England, 2013). Spermatozoa attach to microvilli of uterine epithelial cells by the tip (apical segment domain) of the sperm head (England *et al.*, 2013; Karre *et al.*, 2012). Attachment to the uterine epithelium maintains dog sperm viability and motility, and delays capacitation similar to other species (Pacey *et al.*, 2000; Rijsselaere *et al.*, 2014; Suarez, 2016). In humans and other species, spermatozoa bind the uterine tubal epithelium creating a sperm reservoir there (Suarez, 2016; Vigil *et al.*, 2012). In mice, the lower isthmus of the uterine tube is the major sperm reservoir (La Spina *et al.*, 2016).

Flow of uterine tubal fluid in the female reproductive tract (in the direction from the uterine tube to the uterus), composition of uterine tubal fluid, and the physical surfaces of the tract can act together to guide sperm through regions of the female reproductive tract (Suarez, 2016). The female reproductive tract also functions to maintain sperm viability and motility, and is involved in selecting the best spermatozoa for fertilization (Suarez, 2016). Transport and survival of spermatozoa in the female reproductive tract as well as molecular mechanisms involved have been addressed in depth in excellent reviews (Coy *et al.*, 2012; Gadella and Boerke, 2016; Rijsselaere *et al.*, 2014; Suarez, 2016).

11.2.7.2 Sperm Capacitation

Although ejaculated mammalian spermatozoa have undergone maturational changes in the testis and epididymis, they require additional maturation or "capacitation" in the female reproductive tract before they are competent to fertilize an oocyte (Austin, 1952; Chang, 1951; Cooper and Yeung, 2003; Florman and Fissore, 2015; Yanagimachi, 1994). For example, dog and other mammalian spermatozoa taken directly from the caput epididymis are immotile and unable to fertilize oocytes (Angrimani *et al.*, 2014a, 2014b; Florman and Fissore, 2015;

Downloaded From Vet-eBooks.com

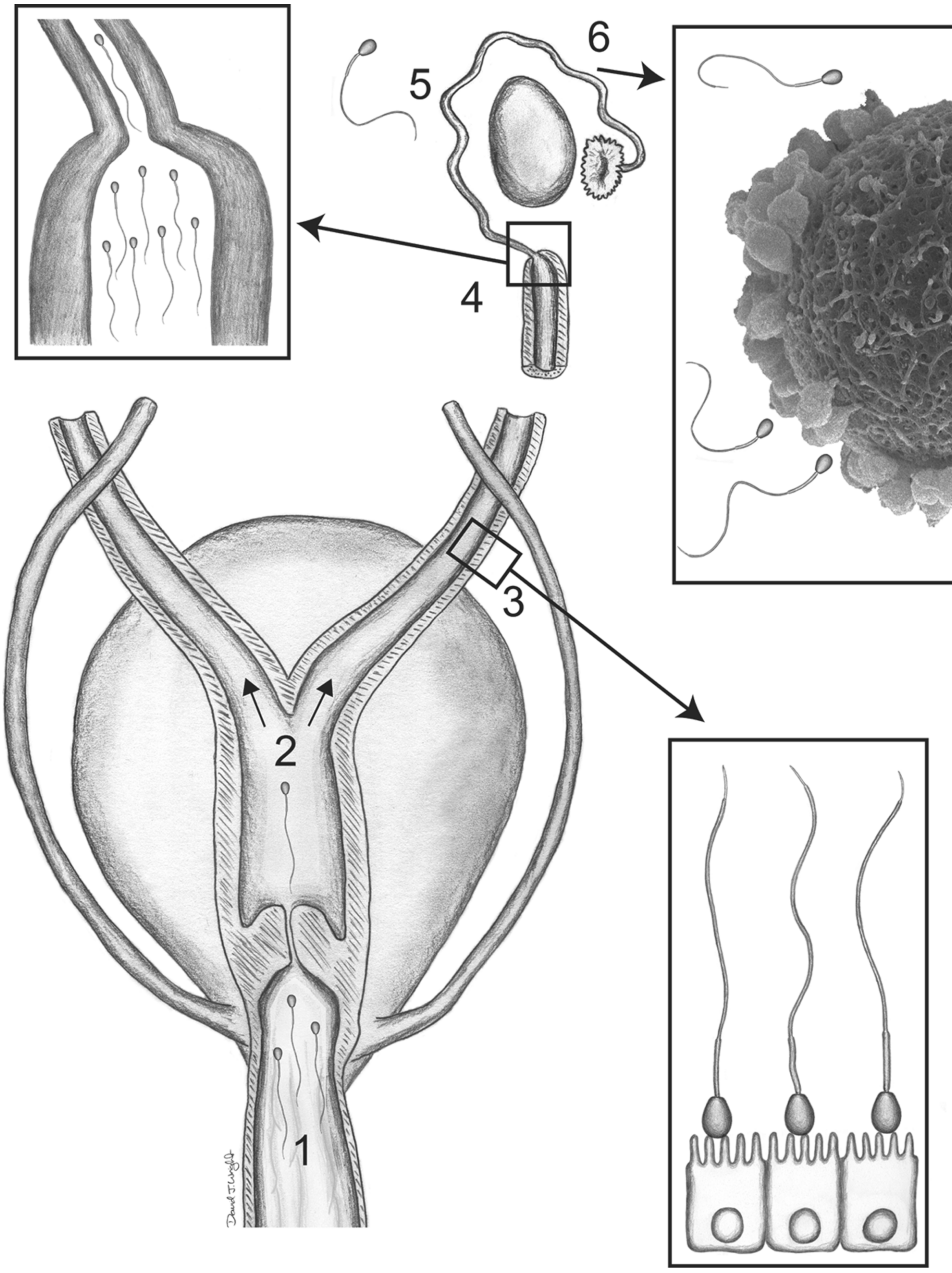

Figure 11.27 Schematic diagram of the steps of sperm capacitation and fertilization *in vivo* in the dog. (1) During ejaculation, millions of spermatozoa are deposited directly into the cranial vagina. They bypass most of the vagina, and are flushed by prostatic fluid through the cervical canal to enter the lumen of the uterine body of the female reproductive tract. These spermatozoa are progressively motile and uncapacitated. (2) As they travel through the uterine lumen, the spermatozoa enter one of the two uterine horns where uterine contractions are thought to equally distribute the spermatozoa throughout the uterine lumen. In addition, the spermatozoa leave the seminal plasma (which consists mostly of prostatic fluid), lose decapitation factors from the sperm surface and begin capacitation. (3) In the first two days after mating, large numbers of spermatozoa bind to the uterine epithelium to form transient reservoirs of quiescent spermatozoa in the uterine crypts and glands, while oocytes are ovulated (if not already present in the uterine tube) and resume meiotic maturation. (4) When spermatozoa reach the utero-

Downloaded From Vet-eBooks.com

Figure 11.28 Scanning electron micrograph of dog spermatozoa (S) in the distal uterotubal junction 12 h after mating. Spermatozoa are bound to the epithelium by their heads. Scale bar = 5 μm. (Reproduced from Rijsselaere T, England G, Freeman S, Maes D, Van Soom A., 2014, Current knowledge on the transport and fate of spermatozoa in the reproductive tract of the bitch, *Reproduction in Domestic Animals* 49 (Suppl. 2):2–7, © 2014 Blackwell Verlag GmbH, with permission of John Wiley & Sons, Inc.)

Varesi *et al.*, 2013). In addition, although freshly ejaculated mammalian spermatozoa are motile, they are still unable to fertilize oocytes until they reside for a period of time in the female reproductive tract or in medium that mimics the female reproductive tract *in vitro* (Florman and Fissore, 2015). In the female reproductive tract, spermatozoa undergo biochemical and physiological changes collectively termed "capacitation" that functionally reprogram the spermatozoon so that it is capable of fertilizing an oocyte (Florman and Fissore, 2015; Yanagimachi, 1994). Capacitation is a complex process that involves many events and pathways in the mammalian spermatozoon over time, with some events concurrent and others sequential (Florman and Fissore, 2015). In dogs and other mammals, spermatozoa undergo capacitation prior to fertilization. Capacitation involves (i) bicarbonate influx and ion fluctuations that alter the sperm membrane potential, (ii) production of reactive oxygen species, (iii) membrane remodeling with enhanced membrane fluidity to redistribute membrane proteins and lipids, (iv) cholesterol efflux from the sperm plasma membrane, (v) intracellular pH increase, (vi) activation of calcium channels leading to an increase in intracellular calcium ions, (vii) modulation of enzyme activities, including activation of adenylyl cyclase resulting in an increase in cyclic adenosine monophosphate (cAMP) levels, (viii) protein kinase A-dependent protein tyrosine phosphorylation, (ix) actin polymerization, and (x) increased energy production,

tubal junction, a very limited number are allowed to pass into the lumen of the uterine tube. The chosen spermatozoa bind to the epithelium of the uterine tube near the uterotubal junction as they complete capacitation, which is characterized by biochemical alterations such as an increase in: reactive oxygen species (ROS), cyclic adenosine monophosphate, intracellular calcium and protein tyrosine phosphorylation. (5) Once capacitated, spermatozoa exhibit hyperactivated motility and detach from the epithelium to migrate through the uterine tube to the cumulus-oocyte complex (spermatozoon shown is highly magnified in the uterine tube). (6) Spermatozoa may acrosome react either close to the cumulus mass or at the surface of the zona pellucida, before binding the zona and penetrating it to fuse with the oocyte. Oocyte is shown with cumulus cells partially removed revealing the zona pellucida. Structures are not drawn to scale. (Courtesy of David J. Wright, Ph.D.)

Downloaded From Vet-eBooks.com

to name a few (Aitken and Nixon, 2013; Breitbart and Finkelstein, 2015; Florman and Fissore, 2015; Hereng *et al.*, 2011; O'Flaherty, 2015). As a result of capacitation, sperm behavior changes. A capacitated spermatozoon is able to (1) exhibit hyperactivated flagellar motility, (2) respond to chemoattractants, (3) undergo the acrosome reaction, and (4) recognize, bind, and fuse to an oocyte (Florman and Fissore, 2015). Capacitation can be mimicked *in vitro* using chemically defined media (Leahy and Gadella, 2015). In the dog, capacitation takes 2–7 h *in vitro* depending on the medium used to induce capacitation (Forsberg and Reynaud, 2012; Mahi and Yanagimachi, 1976). Selected capacitation events are described in the following sections.

Bicarbonate Influx

Bicarbonate (HCO_3^-) initiates sperm capacitation and is essential for sperm motility (Toshimori and Eddy, 2015). Mammalian spermatozoa initiate progressive motility within seconds of exposure to bicarbonate-containing medium (Toshimori and Eddy, 2015). In the dog, bicarbonate activates adenylyl cyclase, which results in stimulation of sperm motility (Okamura *et al.*, 1985). Similar results were reported for human, mouse, rat, boar, bull, and stallion spermatozoa (Okamura *et al.*, 1985; Rathi *et al.*, 2001). Bicarbonate transporters (SLC4, SLC26) in the plasma membrane deliver bicarbonate into the sperm cytoplasm (Lishko *et al.*, 2012; Nishigaki *et al.*, 2014). Bicarbonate activates a soluble adenylyl cyclase (sAC, sACY) that converts ATP to cAMP, thereby elevating cAMP levels in dog and other mammalian spermatozoa (Chen *et al.*, 2000; Lishko *et al.*, 2012). Spermatozoa encounter bicarbonate in seminal fluid and oviductal fluid (Lishko *et al.*, 2012). The bicarbonate concentration in seminal fluid is 2.9 mM in the dog and 8 mM in man (Setchell *et al.*, 1994). Dog prostatic fluid contains bicarbonate at a concentration of 1.7 mEq/kg water or 1.7 mmol/l (Rosenkrantz *et al.*, 1961). Incubating dog spermatozoa in a bicarbonate-free simple medium such as phosphate-buffered saline (PBS) has been reported to delay progression of capacitation; whereas bicarbonate-containing medium (15 mM) induced capacitation (Steckler *et al.*, 2015).

Reactive Oxygen Species Production

Mammalian sperm capacitation is an oxidative event involving reactive oxygen species (ROS) (Aitken and Nixon, 2013; O'Flaherty, 2015). ROS are chemically reactive molecules containing oxygen (Aitken and Nixon, 2013; Chatdarong *et al.*, 2012; O'Flaherty, 2015). They include superoxide radicals ($O_2^{\bullet -}$), hydroxyl radicals ($OH^{\bullet}$), hydrogen peroxide (H_2O_2), and peroxynitrite anions ($ONOO^-$) (Aitken and Nixon, 2013; Chatdarong *et al.*, 2012; O'Flaherty, 2015). In somatic cells ROS are generated as a result of normal metabolic processes such as those that occur in the mitochondrion (Aitken and Nixon, 2013; O'Flaherty, 2015). During capacitation, mammalian spermatozoa generate ROS, which have been detected in freshly ejaculated spermatozoa of dogs, humans, and other mammals (Aitken and Nixon, 2013; Michael *et al.*, 2009; O'Flaherty, 2015). Bicarbonate has been reported to trigger ROS production in mice and pigs (Boerke *et al.*, 2013). Data have suggested the existence of a putative sperm oxidase that generates ROS and has been proposed to be located in the sperm plasma membrane (Aitken and Nixon, 2013; O'Flaherty, 2015). Controlled levels of ROS have been reported to stimulate cholesterol efflux, production of cAMP, and protein tyrosine phosphorylation in mammalian spermatozoa, which are critical events of capacitation (Aitken and Nixon, 2013; Boerke *et al.*, 2013; Gadella and Boerke, 2016; Michael *et al.*, 2009; O'Flaherty, 2015). For example, peroxynitrite is formed by the reaction of superoxide anion and nitric oxide ($NO^{\bullet}$) (Szabo *et al.*, 2007). Nitric oxide is produced via nitric oxide synthase (NOS), which is stimulated by heat shock protein, Hsp90 (Volpe *et al.*, 2008). In dog spermatozoa, Hsp90 has been detected as a strong signal in the neck and proximal midpiece, and weakly in the principal piece of the flagellum, which is similar to the midpiece location of Hsp90 in spermatozoa of other mammals

Downloaded From Vet-eBooks.com

(Volpe *et al.*, 2008). Immunodetection of Hsp90 in human spermatozoa was strong in the neck and midpiece, and weak in the tail (Li *et al.*, 2014). Hsp60 and Hsp70 were also detected in mammalian spermatozoa; in dogs, Hsp60 was reported in the sperm midpiece and Hsp70 in two intensely staining spots in the neck of dog spermatozoa (Volpe *et al.*, 2008). Thus, it is plausible to speculate that one of the roles of the Hsp proteins is to regulate dog sperm motility, although this requires verification. While $O_2^{\bullet -}$ and $NO^{\bullet}$ have been reported to play a role in signaling pathways involving cAMP and protein kinase A, which lead to protein tyrosine phosphorylation, Hsp90 has been shown to regulate sperm motility in the boar (Huang *et al.*, 2000; O'Flaherty, 2015; Volpe *et al.*, 2008). In human spermatozoa, Hsp90 intensity greatly increased during capacitation, and Hsp90 inhibitor studies demonstrated a role of Hsp90 in sperm calcium homeostasis, protein tyrosine phosphorylation, and progesterone-induced sperm function, including hyperactivated motility (Li *et al.*, 2014).

Although low concentrations of ROS have positive effects on sperm function and help induce capacitation, when in excess they cause oxidative stress (Aitken and Nixon, 2013; Amaral *et al.*, 2013; Cassani *et al.*, 2005; Kawakami *et al.*, 2007; Michael *et al.*, 2009; Szabo *et al.*, 2007). In addition, uncontrolled ROS can affect lipid peroxidation due to the high polyunsaturated fatty acid content in the sperm plasma membrane leading to irreversible loss of sperm motility in dogs and other mammals (Tables 11.5 and 11.6) (Aitken and Nixon, 2013; Amaral *et al.*, 2013; Cassani *et al.*, 2005; Kawakami *et al.*, 2007; Michael *et al.*, 2009; Szabo *et al.*, 2007). Seminal plasma and uterine tubal fluid provide protection against ROS damage via antioxidants and antioxidant enzymes such as superoxide dismutase, catalase, and glutathione peroxidase that deactivate ROS (Angrimani *et al.*, 2014a; Cassani *et al.*, 2005; Chatdarong *et al.*, 2012; Gomez *et al.*, 2012; Kobayashi *et al.*, 2014; Neagu *et al.*, 2011). In dog seminal plasma, superoxide dismutase activity was 27.8 ± 10.8 U/ml (43.34 ± 2.47 U/g protein) and catalase activity was 2.2 ± 0.4 U/g protein (Cassani *et al.*, 2005; Kawakami *et al.*, 2007). Asthenozoospermic dogs had significantly lower concentrations of these enzymes in their seminal plasma (Kawakami *et al.*, 2007). In sperm samples from normal dogs, superoxide dismutase activity was 411 ± 152 U/10^{10} spermatozoa, which was lower than in humans, that is, 1470 ± 300 U/10^{10} spermatozoa (*cf.* Cassani *et al.*, 2005). Superoxide dismutase activity has been detected in the dog uterine horn and uterine tubal fluids and fluctuates during the phases of the estrous cycle (Kobayashi *et al.*, 2014). In the nonpregnant female dog, superoxide dismutase activity was highest during diestrus (214.6 ± 18.7 U/ml in uterine horn and 21.3 ± 1.2 U/ml in uterine tube), elevated during estrus (78.2 ± 6.2 U/ml in uterine horn, 29.4 ± 1.6 U/ml in uterine tube) and lowest during anestrus with 10.8 ± 1.0 U/ml in the uterine horn and 18.4 ± 1.0 U/ml in the uterine tube (Kobayashi *et al.*, 2014). Percentages of dog sperm viability, motility, and hyperactivated motility were significantly higher in medium supplemented with superoxide dismutase (Kobayashi *et al.*, 2014).

Membrane Remodeling

During capacitation, sperm membranes remodel their lipid architecture and become more fluid (Yanagimachi, 1994). Spermatozoa that are undergoing capacitation can be revealed by staining with fluorescent dyes such as merocyanine 540, which is a lipophilic, hydrophobic dye that stains cells intensely when their membranes are "destabilized" or in a higher state of disorder such as during capacitation of spermatozoa. In dog spermatozoa stained with merocyanine 540 under capacitating conditions, the sperm membranes exhibited enhanced merocyanine 540 staining, which indicated the membranes destabilized during capacitation (Steckler *et al.*, 2015). In addition, bicarbonate ions were reported to induce this change as was expected since bicarbonate ions are known to induce capacitation in mammalian spermatozoa (Steckler *et al.*, 2015). Similar results were reported for human, boar, bull, and stallion spermatozoa (de Vries *et al.*, 2003; Hallap *et al.*, 2006; Harrison *et al.*, 1996; Rathi *et al.*, 2001).

Downloaded From Vet-eBooks.com

Another critical aspect of mammalian sperm membrane remodeling that occurs during capacitation is removal of coating materials (decapacitation factors) from the surface of the sperm plasma membrane that mask sperm proteins including membrane receptors (Gadella and Boerke, 2016). The decapacitation factors come from the seminal plasma to adhere to the sperm surface, and are thought to be shed by the time the spermatozoa reach the uterine tube (Gadella and Boerke, 2016). Masking of the sperm surface proteins is thought to help maintain the spermatozoa in a quiescent state. In the dog, decapacitation factors in the seminal plasma have been reported to coat the progesterone receptor on the sperm surface (Sirivaidyapong *et al.*, 1999; Wu *et al.*, 2005). For example, progesterone receptor antibodies do not react with uncapacitated dog spermatozoa (Wu *et al.*, 2005). In capacitated spermatozoa, progesterone receptors were located on the apical segment domain and on the principal segment domain of the sperm head (Wu *et al.*, 2005). The progesterone receptors were masked in freshly ejaculated spermatozoa until incubation in capacitation medium gradually exposed the progesterone receptors, allowing the spermatozoa to acrosome react when incubated in the presence of progesterone (P4) (Sirivaidyapong *et al.*, 1999, 2001; Wu *et al.*, 2005).

Cholesterol Efflux

The sterol, cholesterol is involved in maintaining membrane fluidity at lower temperatures. Mammalian spermatozoa lose plasma membrane cholesterol during transport through the epididymis as well as during capacitation in the female reproductive tract (Morales *et al.*, 2012). Cholesterol efflux may depend on production of ROS, which leads to ROS-dependent oxysterol formation allowing reverse sterol transport (cholesterol efflux) from the sperm surface (Aitken and Nixon, 2013; Boerke *et al.*, 2013; Gadella and Boerke, 2016). Sterol depletion is important for tyrosine phosphorylation (Gadella and Boerke, 2016). Transmembrane proteins that are members of the ATP-binding cassette (ABC) transporter superfamily are one of the mediators of cholesterol transport across membranes to apolipoproteins and high-density lipoproteins (HDL) (Leahy and Gadella, 2015). It is thought that HDLs and albumin in uterine tubal fluid (as well as albumin in media for *in vitro* fertilization) are acceptors of sperm cholesterol (Gadella and Boerke, 2016; Leahy and Gadella, 2015). An ABC transporter (ABCA1), which functions in cholesterol efflux across membranes localized to the acrosome, midpiece, and tail of dog spermatozoa in a variable pattern (Palme *et al.*, 2014). After capacitation, ABCA1 localized to the equatorial segment, midpiece, and tail of dog spermatozoa and was absent from the head of acrosome-reacted sperm, but remained on the tail (Palme *et al.*, 2014). Similarly, the ABC transporters ABCA1 and ABCA7 have been detected in the apical head and midpiece of mouse spermatozoa, along with the ABC transporter ABCG1, which localized to the proximal principal piece of mouse spermatozoa (but not the head or midpiece). These ABC transporters were demonstrated to be involved in cholesterol efflux and affected the fertilizing potential of mouse spermatozoa, with $ABCA1^{-/-}$ null mice demonstrating reduced fertility (Morales *et al.*, 2012; Leahy and Gadella, 2015). In addition, the testis-specific ABC transporter ABCA17 was expressed in the apical region of the head and midpiece of mouse spermatozoa, and was involved in cholesterol efflux across the plasma membrane (Morales *et al.*, 2012; Leahy and Gadella, 2015). These results suggest a similar function for the ABC transporters of dog spermatozoa, although this needs to be demonstrated. Disruption of cholesterol efflux has been associated with ineffective capacitation and infertility in mice (*cf.* Whitfield *et al.*, 2015).

Intracellular pH Increase

During capacitation, intracellular pH of the sperm cytoplasm increases as the spermatozoon encounters different environments on its journey to the oocyte (Nishigaki *et al.*, 2014). In the

Downloaded From Vet-eBooks.com

dog, epididymal fluid has a low pH (pH 6.2) as does seminal fluid (pH 6.2, range pH 5.5–7.1) (Branam *et al.*, 1984; Carr *et al.*, 1985). The low pH of epididymal fluid helps maintain spermatozoa in a quiescent state in the epididymis (Nishigaki *et al.*, 2014). The intracellular pH of mammalian epididymal spermatozoa is acidic and helps keep the spermatozoa immotile since the dynein ATPase of the flagellar motile apparatus has been reported to be pH dependent (Nishigaki *et al.*, 2014). The normal location of sperm capacitation *in vivo* is in the female reproductive tract (uterine horn and uterine tube). The pH of uterine tubal fluid at ovulation has been reported to be more alkaline than fluids of the male reproductive tract in mammals (Dale *et al.*, 1998; Nishigaki *et al.*, 2014). For example, human seminal fluid has a pH of 7.5 (normal range pH 7.2–8.0), and human uterine tubal fluid has a comparatively alkaline pH (pH 7.6–7.9) (Banjoko and Adeseolu, 2013; *cf.* Dale *et al.*, 1998). Once deposited in the female reproductive tract, spermatozoa encounter an increase in extracellular pH and bicarbonate ions as well as other components of the uterine horn and uterine tubal environment (Nishigaki *et al.*, 2014). This leads to an intracellular pH increase in the spermatozoon during capacitation, which activates pH-dependent proteins such as CatSper (a calcium ion channel described in the next paragraph), and eventually triggers a calcium influx and sperm activation with hyperactivated motility (Nishigaki *et al.*, 2014). The major transporters involved in pH regulation of mammalian spermatozoa are membrane H^+ transporters, including the Na^+/H^+ antiporters, and bicarbonate (HCO_3^-) transporters (SLC4, SLC26 families) (Nishigaki *et al.*, 2014). Mechanisms regulating dog spermatozoa motility in response to freeze-thawing of spermatozoa have been reported to be sensitive to amiloride, an inhibitor of Na^+/H^+ antiporters (Mogas *et al.*, 2011).

Calcium Influx

Calcium plays an important role during capacitation (Florman and Fissore, 2015; Kawakami *et al.*, 2006). Spermatozoa encounter extracellular calcium in epididymal fluid, seminal fluid, and uterine tubal fluid (Tash and Means, 1983). The calcium concentration is 1.7 mM in epididymal plasma and 1.2 mM in seminal plasma in the dog, whereas human seminal plasma contains 6.3 mM calcium (Tash and Means, 1983). In the dog, intracellular calcium ions increased during capacitation and this correlated with hyperactivated sperm motility (discussed in Section 11.2.7.3) (Kawakami *et al.*, 2004a, 2006). Similar findings have been reported for several mammals, including humans and mice (Florman and Fissore, 2015; Lishko *et al.*, 2012). *Cat*ion channel of *sper*m proteins, CatSper (also called cation channel, sperm associated) are sperm-specific calcium ion channels reported to be the principal ion channel through which mammalian sperm obtain calcium (Chung *et al.*, 2011; Florman and Fissore, 2015; Strünker *et al.*, 2011). CatSper is composed of multiple subunits (*Catsper1-4*, β, γ, and δ), which together form a pore (Florman and Fissore, 2015; Lishko *et al.*, 2012; Strünker *et al.*, 2011). The CatSper genes (*Catsper1-4*, β, γ, and δ) are highly conserved in evolution (Cai and Clapham, 2008). Dogs contain orthologues to several CatSper genes, including *Catsper1-4*, β, γ, and δ according to the NCBI database. In freshly ejaculated, fixed dog spermatozoa, CatSper2 was detected weakly in the acrosome, and midpiece and principal piece of the flagellum (Phillips, 2010). In dog spermatozoa incubated in capacitation medium for 5 h to induce the acrosome reaction and then fixed, staining was strong in the equatorial segment of the sperm head and neck of the flagellum, with occasional weak staining in the postacrosomal region and midpiece (Phillips, 2010). CatSper subunits have been localized to the principal piece of the sperm flagellum in humans and mice (Cheon *et al.*, 2004; Chung *et al.*, 2014; Ren *et al.*, 2001; Tamburrino *et al.*, 2015). Located deep to the plasma membrane, but external to the fibrous sheath, CatSper forms four equidistant linear stripes that run down the length of the principal piece of the mouse sperm flagellum (Chung *et al.*, 2014). The four CatSper "columns" or "domains" appear to structurally organize signaling proteins, including calcineurin,

Downloaded From Vet-eBooks.com

calcium/calmodulin-dependent protein kinase II (CaMKII) and calveolin-1 in the flagellum of mouse spermatozoa (Chung *et al.*, 2014). It is thought that the columnar CatSper domains focus tyrosine phosphorylation in time and space for sperm flagellar function (Chung *et al.*, 2014). Progesterone has been reported to induce calcium ion influx in dog and human spermatozoa (Brewis *et al.*, 2001; Lishko *et al.*, 2011). Progesterone activates CatSper in human spermatozoa (Lishko *et al.*, 2011). Nonfunctional CatSper and loss-of-function CatSper mutations have been reported in infertile human patients (Avenarius *et al.*, 2009; Avidan *et al.*, 2003; Smith *et al.*, 2013; Williams *et al.*, 2015). Suboptimal calcium signaling in spermatozoa has been associated with oligoasthenoteratozoospermia (low sperm numbers and motility, and subnormal sperm morphology) and reduced fertility in human patients (*cf.* Williams *et al.*, 2015). Male mice lacking any of the *CatSper 1-4* or δ genes did not exhibit hyperactivated sperm motility and were infertile, and *CatSper2*$^{-/-}$ null mice lacked calcium ion current (Chung *et al.*, 2011, 2014; Qi *et al.*, 2007; Quill *et al.*, 2003; Ren *et al.*, 2001).

Elevation of cAMP

During capacitation, cAMP levels rise in mammalian spermatozoa (Lishko *et al.*, 2012). In the dog, an increase in cAMP levels was induced by bicarbonate and calcium influx into spermatozoa during capacitation (Kawakami *et al.*, 2006; Okamura *et al.*, 1985). The elevation of cAMP levels stimulated a cAMP-dependent protein kinase that induced sperm tail phosphorylation resulting in an increase in dog sperm motility (Tash and Means, 1983). Disrupting cAMP-dependent protein kinase activity blocked dog sperm motility (Tash *et al.*, 1984, 1986). Additional effects of cAMP and its many targets in mammalian spermatozoa have been previously reviewed in detail (Buffone *et al.*, 2014).

Protein Tyrosine Phosphorylation

Protein tyrosine kinases and phosphatases play an important role in mammalian sperm capacitation (Toshimori and Eddy, 2015). In dogs the amount of tyrosine phosphorylation increased during capacitation (Albarracín *et al.*, 2004a). Uncapacitated dog spermatozoa exhibited phosphotyrosine staining of proteins at the equatorial segment of the sperm head (Petrunkina *et al.*, 2003). During capacitation, protein phosphotyrosine staining progressed distally from the midpiece to the principal piece and then the end piece of dog spermatozoa (Petrunkina *et al.*, 2003). Both glucose and fructose increased overall protein tyrosine phosphorylation in dog spermatozoa (Rigau *et al.*, 2002). Human spermatozoa exhibited a similar protein tyrosine phosphorylation pattern with equatorial segment staining and strong staining in the midpiece and principal piece of the flagellum (Tomes *et al.*, 2004). Human spermatozoa additionally had acrosomal staining (not observed in dog spermatozoa), which was lost after the acrosome reaction (Petrunkina *et al.*, 2003; Tomes *et al.*, 2004). The increased protein tyrosine phosphorylation of the flagellum during capacitation has been correlated with sperm motility in dogs and humans (González-Fernández *et al.*, 2009; Tomes *et al.*, 2004; Toshimori and Eddy, 2015). Moreover, the alterations in the pattern of protein tyrosine phosphorylation during capacitation of dog spermatozoa corresponded to hyperactivated sperm motility (Petrunkina *et al.*, 2003). A cAMP-dependent pathway has been reported to stimulate protein tyrosine phosphorylation in mouse spermatozoa (Buffone *et al.*, 2014). Among proteins that are tyrosine phosphorylated during capacitation of human spermatozoa are those of the fibrous sheath such as calcium binding tyrosine-(Y)-phosphorylation-regulated (CABYR) protein, the axoneme including α-tubulin, and the outer dense fibers such as ODF1 (Toshimori and Eddy, 2015). In mice, a tyrosine phosphoproteome of capacitated mouse spermatozoa has been generated and includes proteins involved in cell metabolism such as hexokinase-1, cell signaling such as calmodulin, and kinases such as cAMP-dependent protein kinase type IIα regulatory subunit

Downloaded From Vet-eBooks.com

(*Prkar2a*), mitochondrial proteins, and structural proteins, including axonemal proteins (Chung *et al.*, 2014). Exposure of dog spermatozoa for 5 min to media supplemented with either 10 mM glucose or 10 mM fructose increased phosphorylation levels of selected proteins involved in cell cycle regulation or general cell function (Fernández-Novell *et al.*, 2011). Glucose stimulated serine phosphorylation of cyclins (cyclin B and E, as well as Cdk2, Cdk6, Cdk4 and Cdc6), protein kinase PYK2/CAK, c-kit, Raf-1, protein phosphatases (PP1, PP2A, PP2B, PPX), the beta-subunit of the insulin receptor, and tyrosine kinases ((TRK) A,B,C), but did not affect tyrosine phosphorylation of these proteins (Fernández-Novell *et al.*, 2011). In contrast, fructose had a different phosphorylation pattern. It increased tyrosine phosphorylation of cyclin A and ERK-1, and serine phosphorylation levels of cyclins B and D3, Cdk1/Cdc2, Cdk2 and Cdk6, while decreasing serine phosphorylation of protein kinases Akt 1, Akt 2, PI3 kinase/p85, ERK-1, protein kinase C, and the beta subunit of the insulin receptor (Fernández-Novell *et al.*, 2011). Thus, dog spermatozoa exhibited a different phosphorylation response depending on the sugar signal it received, suggesting that dog spermatozoa are very versatile in how they obtain energy when encountering different environments on their race to the oocyte.

Mammalian spermatozoa also express protein tyrosine phosphatases (González-Fernández *et al.*, 2009; Tomes *et al.*, 2004). The protein tyrosine phosphatase PTPN11 (but not PTPRB protein tyrosine phosphatase) was reported on the postacrosomal region and midpiece of dog spermatozoa (González-Fernández *et al.*, 2009). In addition, the dual-specificity phosphatases (DUSP3, DUSP4) were also present in dog spermatozoa: DUSP3 was localized to the acrosome and midpiece, and DUSP4 was absent from the head, but present mainly in the connecting piece, midpiece, principal piece, and end piece (González-Fernández *et al.*, 2009). The dual-specificity phosphatases (DUSP3, DUSP4) are a type of phosphatase that can dephosphorylate not only phosphotyrosine residues, but also phosphoserine and phosphothreonine residues as well as nonproteinaceous substrates such as lipids and carbohydrates (González-Fernández *et al.*, 2009). Vanadate-sensitive protein tyrosine phosphatases were reported to regulate dog and human sperm motility (González-Fernández *et al.*, 2009; Tomes *et al.*, 2004). Expression of different tyrosine phosphatases in mammalian spermatozoa was variable and may depend on the species. Although the protein tyrosine phosphatase PTP1B (PTPN1) was absent from dog, boar, and stallion spermatozoa, it was expressed in human and mouse spermatozoa (González-Fernández *et al.*, 2009; Tomes *et al.*, 2004).

Actin Polymerization

The cytoskeletal protein, actin has been detected in uncapacitated mammalian spermatozoa, and actin polymerization has been reported during sperm capacitation (Breitbart and Finkelstein, 2015; Brener *et al.*, 2003; Clarke and Yanagimachi, 1978; Itach *et al.*, 2012; Toshimori and Eddy, 2015). During actin polymerization, globular actin proteins (G-actin), which are unpolymerized, bind together to form filamentous actin (F-actin). In freshly ejaculated, uncapacitated dog spermatozoa, actin was localized mainly to the postacrosomal region with a small amount in the tail (Clarke and Yanagimachi, 1978). Uncapacitated human spermatozoa had a similar actin distribution pattern (Bretibart and Finkelstein, 2015; Brener *et al.*, 2003; Clarke and Yanagimachi, 1978). During capacitation, high concentrations of F-actin were detected in the sperm head and tail of human spermatozoa (Breitbart and Finkelstein, 2015). The actin polymerization step during capacitation is critical for hyperactivated sperm motility and the acrosome reaction in humans and mice (Breitbart and Finkelstein, 2015; Brener *et al.*, 2003; Itach *et al.*, 2012). The molecular mechanism that induces actin polymerization in mammalian spermatozoa has been reported to involve bicarbonate ion-induced activation of the tyrosine kinase Src, which inhibits gelsolin (an active-severing protein detected in the sperm head) and leads to actin polymerization (see Breitbart and Finkelstein, 2015).

Downloaded From Vet-eBooks.com

Increased Energy Requirements

The events of mammalian sperm capacitation consume energy (Bucci *et al.*, 2011; Rogers and Perreault, 1990; Turner, 2006). For example, dynein ATPase of the flagellar motile apparatus requires ATP to generate progressive and hyperactivated sperm motility (Turner, 2006). Moreover, dynein ATPase has been localized to the axoneme throughout the entire length of the mammalian sperm flagellum (Turner, 2006). Mammalian ATP is produced via pathways of oxidative phosphorylation in the mitochondria and glycolysis in the cytoplasm (Bucci *et al.*, 2011; du Plessis *et al.*, 2015; Ruiz-Pesini *et al.*, 2007; Turner, 2006; Volpe *et al.*, 2009). Additional metabolic pathways such as the citric acid cycle in the inner mitochondrial matrix also play a role in metabolism. Mitochondria use oxidizable substrates to produce a proton gradient across the inner mitochondrial membrane (mitochondrial membrane potential), and both the mitochondrial membrane potential and oxygen consumed depend on the activity of the mitochondrial electron transport chain and ATP synthase (Ruiz-Pesini *et al.*, 2007). Oxygen consumption increased when dog spermatozoa were incubated in the presence of either glucose, fructose, lactate, or glycerol, indicating that dog spermatozoa use these as substrates for energy production (Bartlett, 1962b).

While mitochondria of the sperm midpiece generate a large amount of ATP during oxidative phosphorylation, there are conflicting reports on whether the ATP is able to travel down the flagellum fast enough to support all the energy needs for sperm motility (Amaral *et al.*, 2013; du Plessis *et al.*, 2015; Ford, 2006; Nascimento *et al.*, 2008; Ruiz-Pesini *et al.*, 2007). In the dog and human, it has been suggested that sperm motility is independent of mitochondrial respiration, as determined by measuring mitochondrial membrane potential in spermatozoa incubated in the presence of an oxidizable substrate (glucose) in the culture media (Nascimento *et al.*, 2008; Volpe *et al.*, 2009). Both oxidative phosphorylation and glycolysis were reported to generate energy for human sperm motility (Nascimento *et al.*, 2008; Ruiz-Pesini *et al.*, 2007). The glycolytic pathway may play a major role in generating energy for sperm motility when human spermatozoa were cultured in media supplemented with glucose (Nascimento *et al.*, 2008; Ruiz-Pesini *et al.*, 2007).

Another source of energy for sperm motility is via glycolysis, which occurs along the length of the mammalian sperm flagellum (du Plessis *et al.*, 2015; Nascimento *et al.*, 2008; Toshimori and Eddy, 2015). During glycolysis, glucose is broken down to pyruvate in 10 enzymatic steps in the cytosol. Subsequent enzymatic reactions in the mitochondrion oxidize pyruvate to produce the acetyl group of acetyl-coenzyme A, which the citric acid cycle oxidizes to CO_2 in the mitochondrial matrix. The citric acid cycle also generates the electron donors NADH and FADH2, which donate electrons to oxygen via proteins of the electron transport chain in the inner mitochondrial membrane to generate a proton gradient used to produce ATP. Key glycolytic enzymes, including hexokinase type 1, phosphofructokinase, and glyceraldehyde 3-phosphate dehydrogenase-S (GAPDHS), and other metabolic enzymes, including lactate dehydrogenase (LDH), pyruvate dehydrogenase (PDH), and phosphoglucokinase isomerase (also called glucose-6-phosphate isomerase and phosphohexose isomerase), have been detected in the fibrous sheath of the sperm principal piece of several mammals (du Plessis *et al.*, 2015; Toshimori and Eddy, 2015; Turner, 2006; Westhoff and Kamp, 1997). Glycolytic enzymes, including hexokinase, aldolase B (fructose 1,6-bisphosphate aldolase), and pyruvate kinase, and some of their products such as glucose 6-phosphate and fructose 6-phosphate were reported in dog spermatozoa (Albarracín *et al.*, 2004b; Kawakami *et al.*, 1999b; Rigau *et al.*, 2002). Aldolase B was localized to the equatorial segment and midpiece of the dog sperm flagellum (Albarracín *et al.*, 2004b). Fructose kinase and glucose-6-phosphate dehydrogenase activity were also detected in dog spermatozoa (Kawakami *et al.*, 1999b). Fructose kinase is important for fructolysis. Glucose-6-phosphate dehydrogenase catalyzes the first step in the pentose

Downloaded From Vet-eBooks.com

phosphate pathway and generates NADPH that can combat ROS damage in spermatozoa (Kawakami *et al.*, 1999b). The sole glyceraldehyde 3-phosphate dehydrogenase in mouse spermatozoa is Gapds (Miki *et al.*, 2004). Dogs also have a *GAPDHS* orthologue gene (NCBI database), but expression has not yet been reported in dog spermatozoa. Studies with various inhibitors reported that spermatozoa were motile in the presence of mitochondrial oxidative phosphorylation inhibitors, whereas inhibitors of glycolysis reduced sperm motility, but did not affect mitochondrial function (Mukai and Okuno, 2004; Williams and Ford, 2001; du Plessis *et al.*, 2015). Moreover, $Gapds^{-/-}$ null mice were infertile and their spermatozoa lacked progressive forward motility, even though their mitochondrial oxygen consumption was unchanged and the spermatozoa had ATP levels that were 10.4% of wild-type mouse spermatozoa, implying that most of the energy required for mouse sperm motility was generated by glycolysis rather than oxidative phosphorylation (Miki *et al.*, 2004). Human spermatozoa were reported to rely mainly on glycolysis for their energy production, and both oxidative phosphorylation and glycolysis produced energy for human sperm motility (Hereng *et al.*, 2011; Nascimento *et al.*, 2008).

Mammalian spermatozoa acquire the monosaccharide substrates needed for glycolysis from extracellular fluid through two families of glucose transporters (Nomura *et al.*, 2015; Zhao and Keating, 2007): the sodium-dependent glucose transporters (SGLT), which require ATP, and the glucose (hexose) transporters (GLUT), which are ATP- and sodium-independent (Zhao and Keating, 2007). Both transporters have multiple family members: 6 in the SGLT family (SGLT 1-6) and 14 in the GLUT family (GLUT 1-14) (Bucci *et al.*, 2011; Nomura *et al.*, 2015). Dog spermatozoa have several glucose transporters, including SGLT1, GLUT1, GLUT2, GLUT3, and GLUT5, which have been detected with immunofluorescence microscopy and immunoblotting before and after capacitation (Rigau *et al.*, 2002; Bucci *et al.*, 2010). In freshly ejaculated dog spermatozoa, the SGLT1 transporter was located in the acrosomal region (apical segment and principal segment), postacrosomal region, and midpiece with some sperm showing SGLT1 additionally in the equatorial segment (Rigau *et al.*, 2002). During capacitation and the acrosome reaction in dog spermatozoa, the GLUT type of glucose transporters became redistributed (Bucci *et al.*, 2010). In freshly ejaculated dog spermatozoa, GLUT1 was in the apical segment (apical acrosome) of the sperm head and faintly in all sections of the flagellum, and after capacitation had additionally spread to the acrosomal region (principal segment of the anterior sperm head) of capacitated spermatozoa (Bucci *et al.*, 2010). The low-affinity glucose/fructose transporter GLUT2 was reported in the apical segment (apical acrosome) and entire sperm flagellum with intense staining in the connecting piece, and after capacitation GLUT2 expanded to the acrosomal region (principal segment of the anterior sperm head) with loss of the intense connecting piece staining (Bucci *et al.*, 2010). The high-affinity glucose transporter GLUT3 was localized to the principal piece and end piece of the flagellum in fresh spermatozoa, and in capacitated spermatozoa expanded to the acrosomal region (apical and principal segments of the sperm head) and midpiece of the flagellum so that GLUT3 was in the entire flagellum (Bucci *et al.*, 2010). GLUT4, which is the major insulin-stimulated glucose transporter was absent (or below detection levels) from dog spermatozoa similar to other mammals (Bucci *et al.*, 2010; Rigau *et al.*, 2002). GLUT5, which is the only transporter specific to fructose was reported in the acrosome region (apical segment, principal segment), midpiece, and principal piece in fresh dog spermatozoa, and after capacitation acrosomal staining became fainter, whereas the entire flagellum increased staining in capacitated spermatozoa (Bucci *et al.*, 2010; Rigau *et al.*, 2002). In summary, glucose transporters (GLUT1-3 and GLUT5) have been detected in dog spermatozoa and their localization may change during capacitation. Similar to the dog, human spermatozoa have GLUT1, GLUT2, GLUT3, GLUT5, and extremely low levels of GLUT4 (Angulo *et al.*, 1998).

Downloaded From Vet-eBooks.com

To generate energy, mammalian spermatozoa utilize a variety of monosaccharides and other carbon sources, including glucose, fructose, pyruvate, lactate, glycerol, and sorbitol as substrates for ATP generation (du Plessis *et al.*, 2015; Hereng *et al.*, 2011). Dog spermatozoa have been reported to use glucose and fructose to generate ATP (Fernández-Novell *et al.*, 2011). Mammalian seminal plasma contains monosaccharide energy sources to varying degrees depending on the species (Setchell *et al.*, 1994). Dog seminal plasma has very low amounts of hexoses: glucose (0.01 mM in sperm-rich fraction, 0.04 mM in third fraction), fructose (0.06–0.12 mM in sperm-rich fraction, 0–0.17 mM in third fraction), and mannose (0.01 mM in second and third fractions) (Bartlett, 1962b; Rigau *et al.*, 2001; Schoonees *et al.*, 1972; Setchell *et al.*, 1994). These concentrations are very low compared to those of humans, boars, bulls, and rams (Setchell *et al.*, 1994). Dog seminal plasma also contained other metabolizable substrates in low amounts (0.01 mM sorbitol, 0.13 mM citric acid), as well as 1.2–3.3 mM lactic acid, which was comparable to the level in human seminal plasma (Bartlett, 1962b; Schoonees *et al.*, 1972; Setchell *et al.*, 1994). Lactate dehydrogenase activity, which converts lactate to pyruvate, has been reported in dog spermatozoa and its activity increased during capacitation *in vitro* (Kawakami *et al.*, 2006). While the composition of uterine tubal fluid of the dog is not understood, glucose, pyruvate, and lactate have been reported in uterine tubal fluid of all mammals examined thus far (mouse, sow, ewe, cow, mare, and human) with species-specific variations (Aguilar and Reyley, 2005; Hereng *et al.*, 2011; Ruiz-Pesini *et al.*, 2007). Lactate levels were higher than glucose or pyruvate, and these substrates have been utilized as sperm energy sources (Aguilar and Reyley, 2005; Hereng *et al.*, 2011; Ruiz-Pesini *et al.*, 2007). An important consideration is that oviductal fluid composition can change over time and with the region of the uterine tube and stage of the reproductive cycle in humans and pigs, as well as the presence of spermatozoa and oocytes in pigs (Gardner *et al.*, 1996; Quinn, 2003; Romar *et al.*, 2016).

Despite the low levels of fructose and glucose in dog seminal plasma, freshly ejaculated dog spermatozoa were progressively motile and able to maintain their motility for up to 11 days (Doak *et al.*, 1967). In addition, dog spermatozoa undergo capacitation and the acrosome reaction in medium lacking glucose (Albarracín *et al.*, 2004a). Dog spermatozoa were reported to be capable of gluconeogenesis in glucose-free media *in vitro*, which may be essential for maintaining sperm motility for days in the female reproductive tract. It is important to note that gluconeogenesis consumes three times more ATP than the ATP produced via glycolysis, and as a result, gluconeogenesis may be active when energy levels produced via respiration are high after motility needs have been met and the excess glucose could be stored for example as glycogen (Ruiz-Pesini *et al.*, 2007). Both fructose 1,6-bisphosphatase, which is a gluconeogenic enzyme, and aldolase B, which is involved in both gluconeogenesis and glycolysis, were detected in dog spermatozoa (Albarracín *et al.*, 2004b). Fructose 1,6-bisphosphatase was localized to the periacrosomal region of the sperm head, and aldolase B was in the equatorial zone and midpiece of the flagellum (Albarracín *et al.*, 2004b). Inhibition of gluconeogenesis altered aspects of sperm capacitation, including sperm motility, tyrosine phosphorylation, and lectin staining (Albarracín *et al.*, 2004b). Dog spermatozoa were reported to synthesize glucose from lactate, and the glucose was stored as glycogen (Albarracín *et al.*, 2004b). In addition, glycogen, glycogen synthase and glycogen phosphorylase have been detected in freshly ejaculated dog spermatozoa (Albarracín *et al.*, 2004a, 2004b; Ballester *et al.*, 2000; Palomo *et al.*, 2003; Rigau *et al.*, 2002). Glycogen and glycogen synthase were localized to the postacrosomal region and midpiece of freshly obtained dog spermatozoa, and after capacitation were mainly in the midpiece (Albarracín *et al.*, 2004a, 2004b; Palomo *et al.*, 2003). Glycogen accumulated when spermatozoa were in media containing 2 or 10 mM glucose or fructose and the location of glycogen deposition varied according to which hexose the spermatozoa were given (Ballester *et al.*, 2000; Palomo *et al.*, 2003). The glycogen stores in dog spermatozoa may be used to produce

Downloaded From Vet-eBooks.com

energy when levels of external energy-yielding substrates are low. Glycogen was reported to be depleted in dog spermatozoa incubated in substrate-free medium (Ballester *et al.*, 2000; Palomo *et al.*, 2003).

As a result of the events of capacitation, mammalian spermatozoa are able to undergo hyperactivated motility, chemoattraction, the acrosome reaction, and zona binding. These events must occur before the spermatozoon is capable of fertilizing an oocyte *in vivo*. These events are described in the following section.

11.2.7.3 Sperm Motility

In humans and other mammals, spermatozoa acquire motility as they travel through the epididymis and/or as they are released into the female reproductive tract after coitus (Toshimori and Eddy, 2015). Dog spermatozoa acquire motility as they travel through the epididymis (Angrimani *et al.*, 2014a, 2014b; Varesi *et al.*, 2013). For example, only $0.2 \pm 0.1\%$ of spermatozoa derived from the caput epididymis of the dog are motile (mean ± standard error of the mean), $37.0 \pm 4.0\%$ from the corpus epididymis and $63 \pm 5.1\%$ from the cauda epididymis (Angrimani *et al.*, 2014a, 2014b). Varesi *et al.* (2013) reported similar results with epididymal sperm motility in the dog (mean ± standard deviation): $1.3 \pm 2.1\%$ motile spermatozoa in the caput epididymis, $16.2 \pm 11.6\%$ in the corpus epididymis, and $53.1 \pm 25.9\%$ in the cauda epididymis. Healthy mammalian spermatozoa that are motile have three general types of swimming patterns depending on their capacitation status: progressive forward motility, transitional motility, and hyperactivated motility (Figure 11.29) (Kay and Robertson, 1998; Toshimori and Eddy, 2015). Progressive forward motility (also called activated motility, progressive motility), which is characteristic of freshly ejaculated, uncapacitated spermatozoa involves movement in which the sperm flagellum bends slightly in amplitude with uniform, symmetrical waves propagating down the flagellum (proximal to distal) resulting in forward, linear movement (Kay and Robertson, 1998; Toshimori and Eddy, 2015). In contrast, flagella of spermatozoa with hyperactivated motility, which is characteristic of capacitated spermatozoa exhibit exaggerated bends with high amplitude and beat frequency, and asymmetrical waves resulting in circular or helical movement (Figure 11.29) (Kay and Robertson, 1998; Toshimori and Eddy, 2015). When sperm are hyperactivated, they swim with a vigorous whip-like beating, and depending on the species appear to trace a star-spin-like pattern or figure-8 pattern with little progressive movement (Figure 11.29) (Kay and Robertson, 1998; Toshimori and Eddy, 2015; Yanagimachi, 1994). Transitional sperm motility is in between the other two types of swimming pattern in that the sperm flagellum bends with symmetrical, high amplitude and velocity waves, which result in forward movement (Kay and Robertson, 1998). Transitional motility is considered to be a type of progressive forward motility.

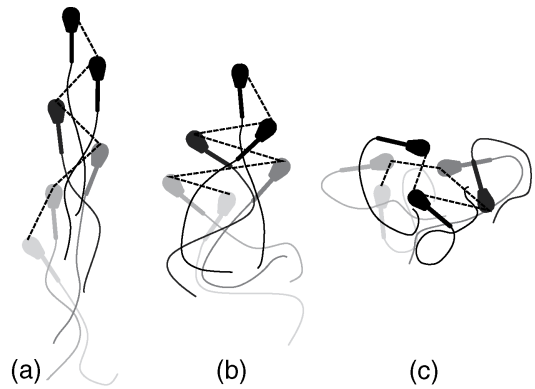

Figure 11.29 Schematic diagram of patterns of dog sperm motility. (a) Progressive forward motility characteristic of freshly ejaculated spermatozoa, (b) transitional motility observed during capacitation, and (c) hyperactivated motility typical of capacitated spermatozoa.

Downloaded From Vet-eBooks.com

Freshly ejaculated dog spermatozoa have been reported to exhibit progressive forward motility prior to capacitation, and during capacitation change their motility pattern to transitional motility followed by hyperactivated motility with the star-spin-like swimming pattern by the time the spermatozoa are capacitated (Figure 11.29) (Freeman and England, 2013; Kawakami *et al.*, 1991). The progressive motility pattern allows spermatozoa to travel from the site of deposition in the female reproductive tract to the uterine tube, whereas the vigorous hyperactivated motility pattern, which provides additional force allows sperm release from the epithelium of the uterine tube sperm reservoirs and subsequent penetration of the oocyte extracellular matrix (Hereng *et al.*, 2011). Freshly ejaculated dog spermatozoa have four motile subpopulations of sperm motility as detected by computer-aided sperm analysis (CASA) and the significance of the different populations is unclear (Mogas *et al.*, 2011; Rigau *et al.*, 2001).

Which receptors on the sperm surface are activated to trigger the changes in sperm motility are not understood, but olfactory receptors on the spermatozoon may be involved in motility, as well as chemotaxis (Toshimori and Eddy, 2015). A critical factor in hyperactivated motility of spermatozoa in mice is calcineurin (Miyata *et al.*, 2015). Calcineurin is a calcium- and calmodulin-dependent serine-threonine phosphatase that is a heterodimer composed of a catalytic subunit with three isoforms (PPP3CA, PPP3CB, and PPP3CC) and a regulatory subunit with two isoforms (PPP3R1 and PPP3R2) with only the *Ppp3cc* and *Ppp3r2* subunits expressed in mouse spermatogenic cells (Miyata *et al.*, 2015). In mouse spermatozoa, calcineurin was localized to the sperm tail, and calcineurin-null mice ($Ppp3cc^{-/-}$) were infertile (Miyata *et al.*, 2015). Although the *Ppp3cc*-null mouse spermatozoa were motile and appeared to exhibit hyperactivated motility, upon closer examination they did not have a flexible midpiece and consequently were unable to penetrate the zona pellucida of the oocyte (Miyata *et al.*, 2015). Dog spermatozoa have been reported to express calcineurin (PPP3C) on the postacrosomal region, midpiece, and rest of the flagellum (Tash *et al.*, 1988). Human spermatozoa have also been reported to express the PPP3CC and PPP3R2 isoforms of calcineurin, and their motility was sensitive to calcineurin inhibition (Miyata *et al.*, 2015). Dog calcineurin (PPP3C) functionally required calcium and calmodulin for its phosphatase activity (Tash *et al.*, 1988). Dog calcineurin may function to remove phosphates from cAMP-dependent protein kinase, which is involved in sperm tail motility (Tash *et al.*, 1986, 1988). The cAMP-dependent protein kinase catalytic subunit localized to the equatorial segment and principal piece of dog spermatozoa (Tash and Means, 1982). Calmodulin localized to the postacrosomal region, midpiece, and principal piece of dog spermatozoa, and a calmodulin inhibitor blocked sperm motility (Tash and Means, 1982).

11.2.7.4 Sperm Chemoattraction

As a result of capacitation, spermatozoa are able to respond to chemoattractants (Florman and Fissore, 2015). During transit in the female reproductive tract, spermatozoa need to distinguish between many different sensory molecules in addition to variations in pH, carbohydrates, and amino acids (Meyer *et al.*, 2012). It is not clear which chemosensory receptor proteins are involved in chemoattraction, but some candidates have been identified. Dog spermatozoa have olfactory receptors (dog testis major olfactory receptor transcript; DTMT) on the midpiece of the flagellum (Vanderhaeghen *et al.*, 1993). Olfactory receptors are G-protein-coupled receptors that are first expressed on late round spermatids and concentrate on the midpiece and cytoplasmic droplet during spermiogenesis in the dog (Parmentier *et al.*, 1992; Vanderhaeghen *et al.*, 1993, 1997). Human and mouse spermatozoa also express olfactory receptors (Fukuda *et al.*, 2004; Parmentier *et al.*, 1992; Vanderhaeghen *et al.*, 1997). Mouse olfactory receptor MOR23 has been reported in mouse spermatogenic cells (round spermatids) and spermatozoa.

Downloaded From Vet-eBooks.com

It regulates sperm motility and chemotaxis via increasing local intracellular Ca^{+2} levels (Fukuda *et al.*, 2004). Human olfactory receptor hOR17-4 also mediates sperm flagellar movement (Spehr *et al.*, 2006). Thus, the olfactory receptor functions as a chemosensor in spermatozoa to affect sperm motility in the mouse and human, suggesting a similar function for olfactory receptors in dog spermatozoa, although this requires functional validation in the dog.

Other chemosensory receptor proteins located in mammalian spermatozoa are members of the Tas1r class of the taste-specific G protein-coupled receptor family (Tas1r taste receptor) (Li *et al.*, 2002; Meyer *et al.*, 2012). The Tas1r taste receptor family forms a heterodimer that detects hydrophilic ligands including sugars and artificial sweeteners, sweet proteins (monellin), and single amino acids (monosodium glutamate), depending on the subunits that comprise the receptor (Li *et al.*, 2002; Meyer *et al.*, 2012). The Tas1r1/Tas1r3 receptor functions to detect glutamate (umami) (Li *et al.*, 2002). The Tas1r3 subunit localized to the acrosomal cap of the sperm head and principal piece of the flagellum of mouse epididymal spermatozoa (Meyer *et al.*, 2012). In freshly ejaculated human spermatozoa, the Tas1r1 subunit was detected in the equatorial segment and postacrosomal region of the sperm head, and midpiece and principal piece of the flagellum (Meyer *et al.*, 2012). The Tas1r3 subunit localized to the acrosomal region, equatorial segment, and flagellum of human spermatozoa (Meyer *et al.*, 2012). In addition, other members of the Tas1r taste receptor signaling pathway are also present in mammalian spermatozoa. For example, both transducin and α-gustducin G-proteins, which are markers for chemosensing cells have been localized to the acrosome (transducin, α-gustducin), midpiece (transducin), and principal piece (α-gustducin) in boar epididymal sperm (Spinaci *et al.*, 2014). The α-gustducin subunit, which is encoded by the *Gnat3* gene, has also been detected in the midpiece and principal piece of the flagellum of mouse, rat, and bull spermatozoa, and in the midpiece of human spermatozoa, as well as the acrosomal region of rat and bull spermatozoa (Fehr *et al.*, 2007). Interestingly, the amount of glutamate has been reported to change along the female reproductive tract, with the concentration of glutamate higher in the fluid of the uterus than in the uterine tube in the mouse (Harris *et al.*, 2005). One could speculate that if the Tas1r1 and Tas1r3 taste receptor subunits dimerize and the receptor functions to detect glutamate in spermatozoa as they travel through the uterine tube, the spermatozoa may use the change in glutamate concentration as a guide to the oocyte. Meyer *et al.* (2012) proposed a model in which the taste receptor activated a G protein that activates phosphodiesterase that converts cAMP to AMP, thereby lowering cAMP levels and preventing cAMP-dependent sperm-activating events such as premature sperm capacitation, hyperactivation, and the acrosome reaction before spermatozoa reach the uterine tube where the ligand for the receptor is at a much lower concentration, and other sperm activation events such as high bicarbonate concentration can override taste receptor signaling. Phenoxy herbicides are potent inhibitors of the Tas1r3 taste receptor, and their effects have been reported: seminomas (germ cell tumors) and testicular dysfunction in military working dogs, testicular dysfunction and impaired spermatogenesis in laboratory animals, and significant decreased sperm quality and fertility in humans (Hayes *et al.*, 1990; Mosinger *et al.*, 2013). In *Tas1r3*$^{-/-}$, *Gnat3*$^{-/-}$ double-null knockout male mice, more than 75% of the spermatozoa had multiple abnormalities, including detached sperm heads, amorphous heads, tails flipped over heads, and looped and kinked sperm flagella (Mosinger *et al.*, 2013). Moreover, in *Tas1r3*$^{-/-}$, *Gnat3*$^{-/-}$ double-null knockout male mice carrying a humanized form of the *TAS1R3* receptor, which is inhibited by phenoxy herbicides, lactisole, and fibrates (clofibrate), clofibrate treatment pharmacologically blocked the humanized TAS1R3 causing inducible male sterility (Mosinger *et al.*, 2013). Taken together, these data suggest that dogs also have a functional Tas1r receptor signaling pathway that is important for sperm function, and that they are an excellent model for understanding the effects of environmental pollutants on human reproduction.

Downloaded From Vet-eBooks.com

It is hypothesized that spermatozoa may be guided to the oocyte by other mechanisms of taxis. In addition to chemotaxis described earlier, thermotaxis, in which spermatozoa are guided by small temperature gradients that are ovulation dependent, may also be involved (Bahat *et al.*, 2003). In rabbits, the uterine tubal temperature has slight variations at ovulation in that the region of the isthmus is about 2 °C warmer than the isthmic–ampullary junction of the uterine tube (Bahat *et al.*, 2003). Rabbit spermatozoa were reported to swim toward the warmer temperature *in vitro* demonstrating a strong thermotactic sperm response in a fraction of the sperm population (Bahat *et al.*, 2003). When tested *in vitro* with mouse spermatozoa, however, it was discovered that temperature gradients created convection currents that influenced the direction in which spermatozoa swam, thus pointing toward rheotaxis (Miki and Clapham, 2013). Sperm positive rheotaxis, in which spermatozoa are guided by a gradient fluid flow and swim against the current has been demonstrated in mice and humans (Miki and Clapham, 2013). Viscosity of uterine tubal fluid is altered during the estrous cycle and also after coitus in response to a rise in prolactin (Miki and Clapham, 2013). Coitus in mice has been reported to induce secretion and fluid flow within the uterine tube, and mouse spermatozoa swam against this flow as they travelled in the uterine tube toward the oocyte (Miki and Clapham, 2013). Under the conditions tested, positive rheotaxis selected for motile spermatozoa in mice and humans (Miki and Clapham, 2013). Whether these other mechanisms of taxis guide spermatozoa in the female reproductive tract have not yet been investigated in the dog.

11.2.7.5 Sperm Acrosome Reaction

At the completion of capacitation, spermatozoa acquire the ability to undergo the acrosome reaction. This occurs in the capacitated spermatozoon prior to fusing with the cumulus–oocyte complex. The acrosome reaction is an exocytotic event in spermatozoa in which the outer membrane of the sperm acrosome fuses with the overlying sperm plasma membrane, releasing acrosomal contents and exposing the inner acrosomal membrane that overlies the sperm nuclear envelope (Yanagimachi, 1994).

The progress of the acrosome reaction can be monitored in dog spermatozoa by examining the distribution of surface membrane glycoconjugates, which changes during mammalian sperm capacitation and the acrosome reaction (Koehler, 1981). Glycoconjugates are molecules with carbohydrate(s) linked via glycosidic bonds such as glycoproteins, glycolipids, oligosaccharides, polysaccharides, and proteoglycans. A variety of lectin proteins (such as wheat germ agglutinin and *Pisum sativum* agglutinin) conjugated to fluorescent dyes have been used to monitor the distribution of glycoconjugates of mammalian spermatozoa during capacitation and the acrosome reaction, with the exact sperm staining pattern depending on the specific lectin used and physiological state of the spermatozoon (Koehler, 1981). For example, when unfixed, live dog spermatozoa with intact acrosomes were exposed to fluorescein isothiocyanate-conjugated *P. sativum* agglutinin, the spermatozoa did not stain; in contrast, dead spermatozoa with a damaged acrosome had bright staining over the periacrosomal region (Peña *et al.*, 2001). When dog spermatozoa were fixed before staining with fluorescein isothiocyanate-conjugated *P. sativum* agglutinin, intense staining was over the periacrosomal region in acrosome-intact spermatozoa before capacitation, and after capacitation became localized to the equatorial segment in acrosome-reacted spermatozoa (Figure 11.30) (Albarracín *et al.*, 2004a; Bains *et al.*, 1993; Kawakami *et al.*, 1993a, 1993b, 2004a, 2004b). In fixed dog spermatozoa, most fluorescently conjugated lectin staining such as from agglutinins of *Arachis hypogea* (peanut), or *Helix pomatia* (snail) was generally over the periacrosomal region of the sperm head of freshly ejaculated spermatozoa, and during capacitation became localized to the sperm equatorial segment in acrosome-reacted spermatozoa (Albarracín *et al.*, 2004a; Bains *et al.*, 1993; Kawakami *et al.*, 1993a, 1993b, 2004a, 2004b; Szász *et al.*, 2000). This general lectin-staining pattern of

Downloaded From Vet-eBooks.com

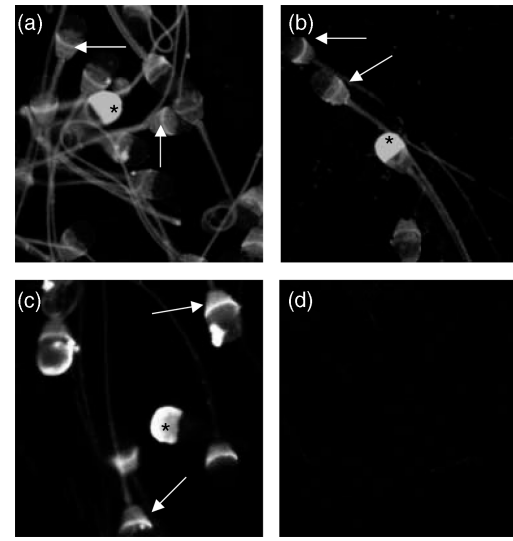

Figure 11.30 Dog spermatozoa stained with lectin revealing acrosomal status. Spermatozoa were stained with lectins from (a) *Arachis hypogaea* (peanut), (b) *Pisum sativum* (pea), (c) *Helix pomatia* (snail), and (d) in the absence of lectins with this image taken under the same conditions of brightness and contrast as the lectin-positive images. Asterisks indicate periacrosomal staining, characteristic of acrosome-intact spermatozoa. Arrows indicate post-acrosomal segment staining, typical of spermatozoa that had been incubated 4 hours in canine capacitation medium, which induces the acrosome reaction. Magnification, ×1000. (Reproduced from Albarracín JL, Mogas T, Palomo MJ, Peña A, Rigau T, Rodríguez-Gil JE, 2004a, In vitro capacitation and acrosome reaction of dog spermatozoa can be feasibly attained in a defined medium without glucose, *Reproduction in Domestic Animals* 39(3):129–135, John Wiley & Sons, Inc., © 2004 Blackwell Verlag, Berlin, with permission of John Wiley & Sons, Inc.

dog spermatozoa is similar to what has been observed in other mammalian spermatozoa (Koehler, 1981).

The acrosome contains many enzymes and proteins important for fertilization that allow the spermatozoon to penetrate through the cumulus cell layer and zona pellucida surrounding the oocyte (Toshimori and Eddy, 2015). The dog acrosome contains enzymes such as proacrosin, which is a serine protease that is cleaved to an active form called acrosin during the acrosome reaction (Cortes *et al.*, 2006; De los Reyes *et al.*, 2011). Dog acrosin has gelatinolytic activity, esterolytic activity, and hydrolyzing activity, which is thought to dissolve the extracellular matrix of the cumulus cells and the zona pellucida during fertilization (Cortes *et al.*, 2006; De los Reyes *et al.*, 2011; Strzeżek *et al.*, 2010). Exocytosis of the acrosomal vesicle is essential for fertilization, as human and mouse spermatozoa lacking an acrosome are sterile (*cf.* La Spina *et al.*, 2016). Interestingly, experiments using knockout mice reported that many of the sperm proteins such as acrosin were not essential for fertilization as null mice lacking these proteins were able to fertilize oocytes (Okabe, 2015). Other enzymes in dog spermatozoa that are released during the acrosome reaction include hyaluronidase and *N*-acetylhexosaminidase (Kawakami *et al.*, 1999a). The acrosome reaction can be mimicked *in vitro* in mammalian spermatozoa, and in the dog it is induced by exposure of spermatozoa to homologous zona pellucida, hyaluronic acid (hyaluronan), calcium ionophore, and progesterone (Brewis *et al.*, 2001; Kawakami *et al.*, 1993b, 2006; Sirivaidyapong *et al.*, 1999, 2001; Szász *et al.*, 2000).

In the dog, the acrosome reaction is thought to occur in the uterine tube. The timing of when the acrosome reaction occurs *in vivo* in the dog has not been observed. In mice, sperm acrosome react *in vivo* in the upper isthmus of the uterine tube, before reaching the zona pellucida of oocytes (La Spina *et al.*, 2016). It has been suggested that the increased levels of hormones in the female reproductive tract, including progesterone, may play a role in human sperm capacitation (López-Torres and Chirinos, 2016). Since there are high levels of progesterone receptors on dog spermatozoa, and progesterone (P4) induces acrosomal exocytosis in dog spermatozoa, it is plausible that by the time the spermatozoa reach the oocyte, they have already acrosome-reacted (Brewis *et al.*, 2001; Sirivaidyapong *et al.*, 1999, 2001; Wu *et al.*, 2005). However, Kawakami *et al.* (2004b) have observed that dog sperm acrosome react upon interaction with the zona pellucida and that the progesterone receptors on the sperm surface were coated. In addition, when spermatozoa attached to uterine tubal epithelial cells, their viability was prolonged and they did

Downloaded From Vet-eBooks.com

not initiate capacitation or the acrosome reaction (Kawakami *et al.*, 1993b, 2004b; Wu *et al.*, 2005). Disruption of progesterone signaling *in vivo* in female dogs given a progesterone antagonist (aglepristone) prevented sperm progression toward the uterine tube and fertilization, but did not block sperm motility into the cranial uterine glands (Reynaud *et al.*, 2015). Spermatozoa in the uterine tips (uterine horns) did not acrosome react in aglepristone-treated dogs, suggesting a role for progesterone in this process (Reynaud *et al.*, 2015).

Aquaporins are a family of intrinsic membrane channel proteins that regulate rapid transport of water across membranes in cells (Kozono *et al.*, 2002). It has not been established whether aquaporins are involved in the acrosome reaction. Dog spermatozoa have low water permeability (Thirumala *et al.*, 2003). Dog spermatozoa express type 1 aquaporin (AQP1) mRNA (Ito *et al.*, 2008). In addition, low levels of AQP1 protein were visualized on immmunoblots, but this protein has not been detected in human and mouse spermatozoa (Ito *et al.*, 2008). Mouse, rat, and human spermatozoa have been reported to express AQP7 and AQP8 protein on the sperm flagellum, and AQP11 protein has been detected on the distal last quarter of the rat epididymal sperm flagellum (*cf.* Yeung, 2010). In addition, siRNA-mediated knockdown of testicular Aqp11 mRNA and protein in hamsters selectively altered the mRNA levels of genes such as *Sept12* that are involved in spermatogenesis (Shannonhouse *et al.*, 2014). AQP1 protein in dog spermatozoa has implications for sperm cryopreservation, as water needs to be transported across the plasma membrane during cryopreservation, and expression levels of aquaporins have been shown to influence cryopreserved mouse embryo survival after thawing (Edashige *et al.*, 2003; Ito *et al.*, 2008). In addition, the functional integrity of the dog sperm plasma membrane can be tested via the hypo-osmotic swelling test in which spermatozoa swell when placed in a hypotonic solution as shown by the curling of the sperm flagellum due to an influx of water (Karger *et al.*, 2014). It has not been investigated whether functional aquaporins aid dog spermatozoa to cope with differing osmolarities of fluid in the male and female reproductive tracts on their path to the oocyte, as has been suggested for other mammalian spermatozoa.

11.2.7.6 Sperm–Oocyte Interaction

A critical function of spermatozoa is to recognize, bind, and fuse to the oocyte during fertilization. Within the uterine tube, the oocyte is surrounded by the zona pellucida and cumulus cells of the cumulus–oocyte complex that the spermatozoon must penetrate to reach the oolemma (Figures 11.25, 11.27 and 11.31). Dog spermatozoa contain the PH20 GPI-anchored sperm membrane protein on the acrosomal region of the sperm head (Sabeur *et al.*, 2002). Dog sperm PH20 has hyaluronidase activity that digests hyaluronic acid of basement membranes enabling the spermatozoon to penetrate through the layers of the cumulus–oocyte complex (Sabeur *et al.*, 2002). It is thought that only acrosome-reacted spermatozoa are able to traverse the zona pellucida in the dog. However, studies using double transgenic mouse spermatozoa and live imaging of spermatozoa in the female reproductive tract *in vitro* revealed that most spermatozoa in the isthmus of the uterine tube had already acrosome reacted before reaching the ampulla, which is the site of fertilization in mice (La Spina *et al.*, 2016). Thus, this process requires further study.

A variety of proteins have been identified to be involved in the events of fertilization. One of the essential proteins for fertilization is IZUMO1 (IZUMO sperm–egg fusion protein 1, encoded by the *IZUMO1* gene), a sperm-specific type 1a transmembrane protein of the IgSF immunoglobulin superfamily named after a Japanese shrine dedicated to marriage (Okabe, 2015; Young *et al.*, 2015). IZUMO1 is required for sperm–oocyte fusion, since gene disruption studies reported that mouse spermatozoa lacking *Izumo1* were unable to fuse with wild-type oocytes (Okabe, 2015; Shrestha *et al.*, 2014; Young *et al.*, 2015). In human and mouse spermatozoa, IZUMO1 is located on the acrosomal cap including the outer and inner acrosomal

Downloaded From Vet-eBooks.com

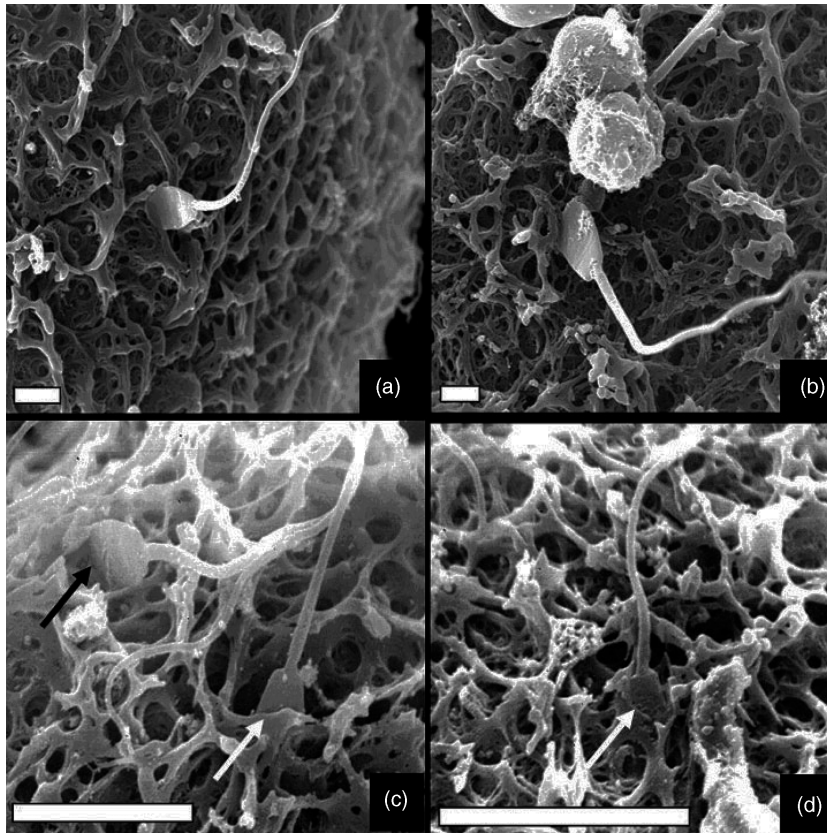

Figure 11.31 Sperm–oocyte interactions in the dog. Scanning electron micrographs of gamete interactions *in vitro*: (a) spermatozoa bound to the zona pellucida, (b) acrosome-reacted spermatozoa at the beginning of zona penetration, (c) spermatozoa penetrating the zona pellucida, and (d) spermatozoa with its head into the zona pellucida. Scale bars: (a) 3 μm, (b) 2 μm, (c and d) 10 μm. (Reproduced from Palomino J, De los Reyes M., A scanning electron microscopy study of frozen/thawed dog sperm during in vitro gamete interaction. *Reproduction in Domestic Animals* 44(2):278–283, © 2008 The Authors. Journal compilation © 2008 Blackwell Verlag, with permission of John Wiley & Sons, Inc.)

membranes and relocates to the plasma membrane and equatorial segment after the acrosome reaction (Inoue *et al.*, 2015; Satouh *et al.*, 2012; Shrestha *et al.*, 2014; Okabe, 2015). In acrosome-reacted dog spermatozoa, IZUMO1 was localized to the anterior of the sperm head similar to mouse and human spermatozoa (Shrestha *et al.*, 2014). Dog IZUMO1 shares approximately 42% amino acid sequence identity with mouse IZUMO1, and antibodies directed against recombinant dog IZUMO1 have been reported to disrupt *in vitro* fertilization of mouse oocytes by mouse spermatozoa (Shrestha *et al.*, 2014). The counterreceptor for IZUMO1 is JUNO (encoded by *IZUMO1R*), which is located on the oocyte surface and is quickly shed from the oocyte after sperm–oocyte fusion in mice (Bianchi *et al.*, 2014). The dog genome has the *IZUMO1R* gene, and thus it is plausible to propose that IZUMO1 and JUNO function in dogs to allow spermatozoa to fuse with oocytes during fertilization. It has been proposed that dipeptidases such as angiotensin-converting enzyme (ACE) may be responsible for degrading IZUMO1 in spermatozoa (Young *et al.*, 2015). ACE has been localized to the periacrosomal region of ejaculated dog spermatozoa and in spermatids in the seminiferous tubules of the dog testis

Downloaded From Vet-eBooks.com

(Sabeur *et al.*, 2001). Additional oocyte receptor molecules not yet identified may be involved in the completion of sperm–oocyte fusion (Inoue *et al.*, 2015).

The dog oocyte is fertilized at meiotic metaphase II (Figure 11.23) (Mahi and Yanagimachi, 1976; Reynaud *et al.*, 2005, 2006). The dog oocyte can be fertilized from about 90 h or more (3.75–5 days) after ovulation, but loses viability at about 6 days after ovulation (England, 2013; Reynaud *et al.*, 2005, 2006). Polyspermy was not observed *in vivo* (Reynaud *et al.*, 2005). Fertilization occurs at the middle and distal portion of the uterine tube (Figure 11.27) (England, 2013; Reynaud *et al.*, 2006). Spermatozoa penetrate the zona pellucida *in vitro* using the anterior tip of the sperm head (Figure 11.31) (Palomino and De los Reyes, 2009). *In vitro* studies have reported that spermatozoa are able to penetrate the zona pellucida by 1 h postinsemination, sperm nuclei decondense in the ooplasm within 3 h postinsemination, a male pronucleus can be detected 8 h postinsemination, and prominent male and female pronuclei are present 12 h after insemination of *in vitro* matured oocytes (Nickson *et al.*, 1993; Yamada *et al.*, 1992).

11.2.8 Dog Pregnancy, Development and Birth

Dog embryos develop within both of the uterine horns, and preimplantation embryos can migrate from one uterine horn to the other in a process called transuterine migration so that the embryos become evenly distributed between the two uterine horns (England, 2013; Shimizu *et al.*, 1990; Tsutsui *et al.*, 2002). Uterine horn migration occurs up to 7–10 days after fertilization (Kowalewski *et al.*, 2015). The duration of pregnancy (gestation) is about 2 months in the dog, and averages 63–65 days, which is much shorter than the 267 days for humans (Case, 2005; Concannon, 2009). If the day of first breeding is used to predict the due date, the range is from 55 to 72 days (Feldman and Nelson, 2004). About 65 ± 1 days after the LH surge of estrus, the dog gives birth (Case, 2005; Concannon *et al.*, 2001; Forsberg and Reynaud, 2012). Because of the long luteal phase during diestrus that occurs in both nonpregnant and pregnant females and the enhanced prolactin levels in pseudopregnant females, neither progesterone (P4) nor prolactin levels can be used as markers to detect pregnancy in the dog (Concannon *et al.*, 2009; Kowalewski *et al.*, 2015). Currently, the only suitable endocrine indicator of pregnancy in the dog is serum levels of placental relaxin, which begins to secrete about 26–30 days after the LH surge (Concannon *et al.*, 2001; Kowalewski *et al.*, 2015). The endocrine events of canine pregnancy have been reviewed in depth elsewhere and will not be addressed here (Concannon *et al.*, 2001; Kowalewski *et al.*, 2015; Verstegen-Onclin and Verstegen, 2008).

An early step of embryonic development is the activation of the embryo's genome, which is referred to as embryonic gene activation (zygotic gene activation, maternal to embryonic gene transition, and maternal to zygotic transition). Prior to embryonic gene activation, the embryo relied on maternal transcripts present in the oocyte. In the dog, a preliminary study reported that very low levels of transcription have been detected in pronuclear stage embryos, and major embryonic gene activation occurs at the 8-cell stage (Chastant-Maillard *et al.*, 2010, 2011; Reynaud *et al.*, 2012a). Thus, there are two waves of embryonic gene activation in the dog: the first, which is very minor, occurs at the pronuclear stage (6 days after LH surge) and the second, which is major, occurs at the 8-cell stage (about 9–10 days after LH surge; about 4–5 days after fertilization). This is comparable to the human in which a minor embryonic gene activation is detected at about the 3-cell stage and the major one at the 4- to 8-cell stage (about 3 days after fertilization) (Niakan *et al.*, 2012).

A major challenge in the analysis of dog embryonic development is the precise and reliable determination of ovulation, fertilization, and beginning of pregnancy (Pieri *et al.*, 2015; Reynaud *et al.*, 2006). Several different methods have been used in the literature resulting in a high variability on the reported timing of developmental events (Pieri *et al.*, 2015; Reynaud *et al.*,

Downloaded From Vet-eBooks.com

Table 11.7 Major developmental milestones in the dog.

Event or stage	Timing (days from LH surge)[a)]	References
Fertilization	5	Concannon *et al.* (2001)
Zygote	6	Concannon *et al.* (2001)
2-Cell embryo	7	Concannon *et al.* (2001)
4-Cell embryo	8	Concannon *et al.* (2001)
8-Cell embryo	9–10	Concannon *et al.* (2001)
16-Cell embryo in oviduct	11	Concannon *et al.* (2001)
Reach uterotubal junction	11–12	Concannon *et al.* (2001)
Morulae 16–32 cell with zona, in uterine horn	12	Concannon *et al.* (2001)
Expanded blastocyst	11–15	Hall *et al.* (2013)
Blastocyst intrauterine migration	13	Concannon *et al.* (2001)
Blastocyst ≥1 mm in thin zona	18	Concannon *et al.* (2001)
Attach to endometrium	18–20	Verstegen-Onclin and Verstegen (2008)
Hatching (zona loss)	19–20	Concannon *et al.* (2001)
Implantation	20–22	Verstegen-Onclin and Verstegen (2008)
Gastrulation begins	20[a)]	Ruvinsky and Hill (2012)
Primitive streak	21[a)]	Ruvinsky and Hill (2012)
Neural tube	22[a)]	Ruvinsky and Hill (2012)
First somite pair	23[a)]	Ruvinsky and Hill (2012)
Heartbeat	25	Concannon *et al.* (2001)
7 mm embryo, C-shaped, limb buds	26–27[a)]	Pieri *et al.* (2015)
10 mm embryo	27–30[a)]	Pieri *et al.* (2015)
18 mm embryo	31–32[a)]	Pieri *et al.* (2015)
Birth	63–66	Concannon *et al.* (2001)

a) Since fertilization occurs 5 days after the preovulatory LH surge (90 h or more after ovulation and 11 days after the onset of proestrus), 5 days were added to data from Ruvinsky and Hill (2012) (reported originally as days after fertilization: >15, 16, 17, 18, and 20 days, respectively), and data from Pieri *et al.* (2015) (crown-rump length reported originally as gestational age, which is days after fertilization: 21–22, 22–25, and 26–27 days).

2006). Selected major developmental milestones using the preovulatory LH surge as the starting point of development are listed in Table 11.7. The data can be converted to days from fertilization to obtain an estimated gestational age by subtracting 5 days from the values shown in Table 11.7, since fertilization occurs 5 days after the LH surge, 90 h or more after ovulation, and 11 days after onset of proestrus (Karre *et al.*, 2012).

The progression of development of the dog embryo proceeds at a comparable rate to other mammals (Table 11.7). *In vitro* studies have reported that the 4-cell stage is reached within 72 h postinsemination of *in vitro* matured oocytes (Yamada *et al.*, 1992). Early cleavages occur in the uterine tube (England, 2013). The dog embryo reaches the morula to blastocyst stage about 8–10 days after fertilization (12 days after LH surge) and exits the uterine tube to enter the uterine horn (Figure 11.32) (Chastant-Maillard *et al.*, 2011; Concannon *et al.*, 2001; England, 2013; Reynaud *et al.*, 2012a). Morulae and early blastocysts (10 days after fertilization) already express transcripts

Downloaded From Vet-eBooks.com

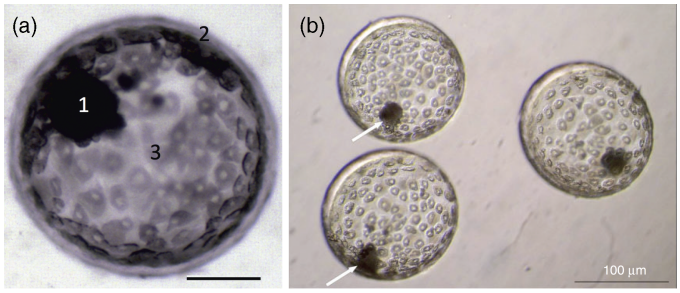

Figure 11.32 Dog blastocyst embryos. (a) Expanded blastocyst derived *in vivo* and retrieved from flushed reproductive tract of inseminated dog at 11 to 15 days following detection of the LH surge. 1, Dark, lipid-rich inner cell mass; 2, zona pellucida; and 3, blastocoel. Scale bar, 100 µm. (b) Three blastocysts collected 11.5 days after ovulation with inner cell mass indicated with arrows. (Reproduced from (a) *The Veterinary Journal*, volume 197, issue 2, Hall V, Hinrichs K, Lazzari G, Betts DH, Hyttel P., Early embryonic development, assisted reproductive technologies, and pluripotent stem cell biology in domestic mammals, pages 128–142, Copyright 2013, with permission from Elsevier. (b) From Chastant-Maillard S, Chastant-Maillard S, Chebrout M, Thoumire S, Saint-Dizier M, Chodkiewicz M, Reynaud K. 2010. Embryo biotechnology in the dog: a review. *Reproduction Fertility and Development* 22(7):1049–1056, © CSIRO 2010, reprinted by permission of CSIRO Publishing.)

for key proteins (Hall *et al.*, 2013; Schäfer-Somi *et al.*, 2008). These include enzymes for prostaglandin synthesis (*COX2*) and matrix-metalloproteinases (*MMP-2*, *MMP-9*), as well as growth factors (*TGF-α*, *IGF-1*, *IGF-2*), cytokines (*IL-1α*, *IL-6*), and immune cell receptors (*CD4*) (Hall *et al.*, 2013; Schäfer-Somi *et al.*, 2008). In addition, like other mammalian embryos, dog morulae and early blastocysts (10 days after fertilization) also express early cell lineage markers for the epiblast (*POU5F1*), hypoblast (*GATA6*), and trophectoderm (*CDX2*) (Hall *et al.*, 2013; Wilcox *et al.*, 2009). Expanded dog blastocysts collected 11–15 days after the LH surge are up to 375 µm in diameter including the zona (340 µm excluding zona) (Figure 11.32) (Hall *et al.*, 2013). The inner cell mass cells of these blastocysts are intensely dark, since they retained the dark lipid of the oocyte; whereas the trophoblast cells are not as dark (Hall *et al.*, 2013). Zona hatching and shedding occur about 14 days after fertilization (19–20 days after LH surge), and embryos implant in the endometrium about 16–18 days after fertilization (21–23 days after LH surge) (Chastant-Maillard *et al.*, 2011; Kowalewski *et al.*, 2015; Reynaud *et al.*, 2012a). It takes about 7–10 days after fertilization (12 days after LH surge) for dog embryos to reach the uterotubal junction and enter the distal end of the uterine horn (uterine tip), which is comparable to humans who take about 7 days after fertilization (Concannon *et al.*, 2001; Kowalewski *et al.*, 2015; Niakan *et al.*, 2012). Additional highlights of developmental milestones of the dog are shown in Table 11.7 and have been described elsewhere in depth (Concannon *et al.*, 2001; Pieri *et al.*, 2015; Pretzer, 2008; Reynaud *et al.*, 2006; Ruvinsky and Hill, 2012; Verstegen-Onclin and Verstegen, 2008).

Parturition (giving birth) is called whelping in the dog (Case, 2005; England, 2013). A good estimate for the whelping date is 56–58 days after the first day of diestrus, or 63–66 days from the LH surge (Case, 2005; Concannon *et al.*, 2001; England, 2013). About 20–30 h prior to the onset of whelping, maternal blood progesterone levels fall (Case, 2005; England, 2013). A study of over 10,000 purebred dogs registered with the Norwegian Kennel Club showed that litter size at birth was 5.4 puppies with a range of 1–18 puppies (Borge *et al.*, 2011). Larger dogs gave birth to more puppies than smaller dogs. For example, certain breeds such as the relatively large, Rhodesian Ridgeback had an average litter size of 8.9 puppies and the relatively small breeds such as the Pomeranian and Toy poodle each had an average litter size of 2.4 puppies. The maximum number of puppies was 22 in a large breed dog (Forsberg and Reynaud, 2012).

Downloaded From Vet-eBooks.com

11.3 Dog-Assisted Reproductive Technology

Assisted reproductive technology (ART) is a procedure used to produce viable gametes and embryos for successful pregnancy without natural mating. In human reproductive medicine, ART is often used to combat infertility. Over 3 million children have been born globally with the assistance of ART (Mainigi *et al.*, 2016). For laboratory rodents and domestic agricultural species, ART has been used to produce viable gametes, embryos and offspring, and is routine in many species. The purpose of ART with domestic mammals is to improve livestock health, and their breeding and production (Hall *et al.*, 2013). In addition, ART is used with domestic mammals to generate animal models of human disease (Hall *et al.*, 2013). Several assisted reproductive technologies are available for the dog and are briefly addressed here. For more in-depth information, several reviews are available (Chastant-Maillard *et al.*, 2010; England, 2013; Forsberg and Reynaud, 2012; Hall *et al.*, 2013).

11.3.1 Artificial Insemination

The breeding of dogs can be achieved naturally or artificially. Artificial insemination (AI) is an ART procedure in which high quality semen is collected from a male and then placed into the female reproductive tract without mating (England, 2013). The first successful AI using canine semen was performed in 1780 by Abbé Lazzaro Spallanzani (Bartlett, 1962a; Forsberg and Reynaud, 2012). Since then, semen for AI has been used fresh, preserved (extended), chilled and warmed to 37 °C, or frozen-thawed, which is semen that was cryopreserved (stored frozen) and subsequently thawed and then warmed before use (England, 2013; Forsberg and Reynaud, 2012). Semen to be shipped is typically extended and chilled (Forsberg and Reynaud, 2012). For long-term storage, semen is placed in an extender and then frozen in straws, which are rapidly thawed when needed (Forsberg and Reynaud, 2012). All of these procedures have been used successfully in dogs (England, 2013; Forsberg and Reynaud, 2012).

Semen can be placed in the dog's vagina, cervix, or directly in the uterine lumen. Techniques to introduce spermatozoa into the uterine lumen include uterine transcervical insemination, which uses a noninvasive instrument for this purpose, and surgery via uterine laparoscopy is used when the other techniques have been unsuccessful (Forsberg and Reynaud, 2012; Romagnoli and Lopate, 2014). It is more challenging to perform uterine transcervical insemination because of the anatomy of the female reproductive tract; namely, the long and narrow vagina with dorsal median fold, small cervical opening, and small cervical canal that is directed at an angle with respect to the vagina (Figure 11.18). Pregnancy rates with vaginal insemination were $80 \pm 16\%$ with fresh semen, $47 \pm 9\%$ with chilled semen, and $45 \pm 24\%$ with frozen-thawed semen, whereas uterine transcervical insemination rates were $95 \pm 4\%$ with fresh semen, $81 \pm 19\%$ with chilled semen, and $70 \pm 11\%$ with frozen-thawed semen (England, 2013). The pregnancy rate with uterine laparoscopy using fresh semen was $95 \pm 4\%$, and with frozen-thawed semen was $95 \pm 7\%$ (England, 2013).

Slightly larger litter sizes were reported for dogs naturally mated rather than artificially inseminated (with fresh or frozen spermatozoa) in a large Norwegian study using 10,256 dogs, 500 of which were artificially inseminated (376 with fresh semen and 124 with frozen semen) (Borge *et al.*, 2011). Litter sizes for dogs artificially inseminated with fresh spermatozoa were reduced by 0.4 puppies per litter, whereas females inseminated with frozen spermatozoa were reduced by 1.3 puppies per litter (Borge *et al.*, 2011). Success with AI depends not only on performing the procedure skillfully, but also ensuring that it is done during the fertile period of the female (England, 2013).

Downloaded From Vet-eBooks.com

11.3.2 Superovulation

Superovulation is an ART procedure involving controlled ovarian hyperstimulation to induce production of a higher than normal number of good quality, mature, ovulated oocytes. It is routine in a variety of animals especially rodents with great success, and is a fundamental step for *in vitro* fertilization procedures with human patients (Mainigi *et al.*, 2016). The technique has been performed with the dog, but it is difficult and intensive, and not all female dogs respond positively to the hormonal regimen of ovarian hyperstimulation (Forsberg and Reynaud, 2012; Reynaud *et al.*, 2004; Yamada *et al.*, 1992, 1993). A successful superovulation procedure involved daily estrone injections of females until a vaginal discharge appeared. Three days later females were injected subcutaneously once with a combination of 400 IU equine chorionic gonadotropin (eCG) and 1000 IU human chorionic gonadotropin (hCG). On the third and fourth day after the gonadotropin (eCG + hCG) injection, females were injected intramuscularly with estradiol. When females were in estrus as determined by vaginal cytology, they were injected intravenously with 1000 IU hCG on the first day of estrus. Ovulation occurred about 72 h after the last intravenous hCG injection (Yamada *et al.*, 1992). Yamada *et al.* (1992, 1993) reported success with the technique, obtaining 18–164 oocytes per Beagle dog within 48–96 h after the hCG injection. Superovulation can be combined with other techniques.

11.3.3 Oocyte *In Vitro* Maturation

Oocyte *in vitro* maturation (IVM) is an ART technique that collects immature oocytes from the ovary and cultures them in the laboratory until they have matured. They can then be used for other ART procedures such as those discussed below. Oocyte IVM has been developed for dog oocytes (Chastant-Maillard *et al.*, 2011; Reynaud *et al.*, 2004). The thick ovarian bursa surrounding the dog ovary prevents laparoscopic aspiration of dog oocytes, even though follicles can be observed via ultrasound. Despite these challenges, oocyte IVM has been established for dog oocytes using ovaries isolated from anestrous females during routine ovariectomy (Chastant-Maillard *et al.*, 2011; England, 2013; Mahi and Yanagimachi, 1976; Reynaud *et al.*, 2004, 2005). For an excellent in-depth description of the protocol and materials needed for IVM, see Reynaud *et al.* (2004). When sliced, the ovary yields immature cumulus–oocyte complexes containing primary oocytes at the germinal vesicle stage (Lunn and Wright, 2009, 2013; Nickson *et al.*, 1993; Reynaud *et al.*, 2004).

The success rate of oocyte IVM in the dog is very low compared to other domestic animals, despite many efforts and modifications to improve it (Chastant-Maillard *et al.*, 2010; Otoi *et al.*, 2000; Yamada *et al.*, 1993). Oocytes collected from anestrous ovaries and cultured 72–96 h *in vitro* have an average 10–20% rate of development to metaphase II (Luvoni *et al.*, 2005; Yamada *et al.*, 1992, 1993), whereas oocytes from preovulatory follicles from superovulated females have a 31.9% success rate (Hall *et al.*, 2013; Yamada *et al.*, 1992, 1993). To observe the nuclear status of the oocytes, the cumulus cells and sometimes the zona pellucida are mechanically stripped from the oocyte after IVM, since the traditional protocol using enzyme treatment with hyaluronidase is unsuccessful with canine oocytes (Lunn and Wright, 2009; Reynaud *et al.*, 2004). A higher percentage of naturally ovulated oocytes progressed to metaphase II *in vitro* than oocytes collected directly from ovaries via the slicing method and then cultured *in vitro* (Lee *et al.*, 2008; Tan *et al.*, 2009). It is thought that this is due to the culture medium lacking a critical component(s) as yet not identified (or tested) that is normally present in the canine cycling ovary and/or uterine tubal fluid. On the other hand, a critical component may need to be actively removed from the cumulus–oocyte complex for meiotic maturation and developmental competence to occur.

Downloaded From Vet-eBooks.com

11.3.4 *In Vitro* Fertilization

In vitro fertilization (IVF) is a technique in which mature oocytes are collected and fertilized with mature, capacitated spermatozoa in the laboratory. Freshly collected spermatozoa isolated from the ejaculate or the cauda epididymis are first capacitated in a special capacitation medium for 2–7 h depending on the species (Gwatkin, 1977; Nagy *et al.*, 2003; Yamada *et al.*, 1992). Capacitated spermatozoa are then transferred to a droplet of fertilizing medium containing oocytes (Gwatkin, 1977; Nagy *et al.*, 2003; Yamada *et al.*, 1992). Greater than 95% IVF success rates have been achieved with rodent models. In the dog, IVF has been conducted using *in vitro*-matured oocytes as well as *in vivo*-matured oocytes.

11.3.4.1 IVF with *In Vitro*-Matured Dog Oocytes

A very low IVF success rate has been reported using *in vitro*-matured dog oocytes from ovaries of unstimulated females in anestrus with only 2–10% of oocytes reaching the pronuclear stage when fertilized with ejaculated dog spermatozoa (De los Reyes *et al.*, 2009; Hall *et al.*, 2013; Mahi and Yanagimachi, 1976; Yamada *et al.*, 1993). Many of the oocytes degenerated and others were of low quality with poor fertilization potential (Hall *et al.*, 2013). Embryos that had formed stopped development at the 4- to 8-cell stage with very few becoming blastocysts, indicating that there is a 4- to 8-cell block under these culture conditions (Chastant-Maillard *et al.*, 2010; Forsberg and Reynaud, 2012; Hall *et al.*, 2013). High rates of polyspermy were also reported with *in vitro*-matured oocytes (Hall *et al.*, 2013; Hatoya *et al.*, 2006; Saint-Dizier *et al.*, 2004). When preovulatory oocytes isolated from 3 to 10 mm follicles from ovaries of superovulated females were used for IVF, 78% of the oocytes were fertilized compared to about 65% of oocytes isolated from ovaries of noninduced females in anestrus (Yamada *et al.*, 1992, 1993). While 37% of the preovulatory oocytes reached the pronuclear stage, only 2% of the fertilized preovulatory oocytes reached the 8-cell stage (Yamada *et al.*, 1992, 1993).

In vitro-matured Beagle oocytes fertilized *in vitro* with freshly ejaculated dog spermatozoa reached the pronuclear stage by 12 h after insemination, 1-cell stage 24 h after insemination, 2-cell stage at 48 h postinsemination, and by 72 h were at the 4-cell stage with the 8-cell stage reached by 96 h after insemination (Yamada *et al.*, 1992). Like human embryos, blastomeres of dog embryos did not divide synchronously as embryos with 3 cells and 5, 6, and 7 cells were observed (Yamada *et al.*, 1993). This is consistent with observations of embryos produced *in vivo* after artificial uterine insemination with fresh semen (Reynaud *et al.*, 2005). The observed developmental heterogeneity has been suggested to relate to the long duration of the ovulation period that occurs over multiple days (Chastant-Maillard *et al.*, 2010). Development to the early morula stage has been reported for *in vitro*-matured oocytes inseminated *in vitro* (Lee *et al.*, 2007). However, to date no live puppy has been born from *in vitro*-matured oocytes that were fertilized *in vitro* (Forsberg and Reynaud, 2012). This is unlike IVF with IVM of oocytes from some domestic animals such as cattle, which is highly successful (Hall *et al.*, 2013). So the current status in the dog is that IVF using oocytes matured *in vitro* produces few early preimplantation embryos that are unable to develop to term, and the cause has not been identified at the writing of this chapter. Thus, this needs further investigation. In contrast, the results are highly successful when IVF is used with *in vivo*-matured oocytes.

11.3.4.2 IVF with *In Vivo*-Matured Dog Oocytes

To overcome the technical difficulties with IVF using *in vitro*-matured oocytes, Nagashima *et al.* (2015) used an improved sperm capacitation protocol, and *in vivo*-matured dog oocytes collected on Day 6 after the preovulatory LH surge (day 4 after ovulation) that were developmentally competent. The capacitation medium used for the study was canine

Downloaded From Vet-eBooks.com

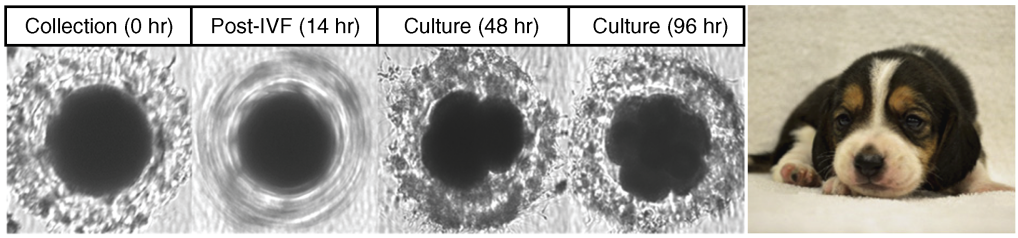

Figure 11.33 Results of *in vitro* fertilization in the dog. An individual dog oocyte imaged in vitro from the time of collection (0 hr) through fertilization (14 hr) to the 4-cell (48 hr) and 8-cell stage (96 hr). At 14 hr post-*in vitro* fertilization, the image is blurred due to motility of attached spermatozoa to the presumptive zygote. At far right, normal developing Beagle puppy (one of seven puppies) at three weeks of age as a result of transfer of in vitro fertilized embryos at the 4-cell stage. (Reproduced from "Figures 2C and 3D" of Nagashima JB, Sylvester SR, Nelson JL, Cheong SH, Mukai C, Lambo C, Flanders JA, Meyers-Wallen VN, Songsasen N, Travis AJ. 2015. Live births from domestic dog (*Canis familiaris*) embryos produced by *in vitro* fertilization. *PLoS One*. 10(12):e0143930. http://journals.plos.org/plosone/article?id=10.1371/journal.pone.0143930. Used under CC0 1.0 Universal https://creativecommons.org/publicdomain/zero/1.0/)

capacitation medium from Mahi and Yanagimachi (1976) modified by the addition of magnesium, which after 2.5–3.5 h enhanced sperm hyperactivation and the physiological progesterone-induced acrosome reaction (Nagashima *et al.*, 2015). The IVF protocol reliably yielded a high percentage (78.8%) of embryos that developed to term when combined with the ART technique of embryo transfer to the uterine tube (Figure 11.33) (Nagashima *et al.*, 2015). When instead Day 5 *in vivo*-matured oocytes were used for IVF, only 29.7% cleaved and they exhibited delayed cleavage (Nagashima *et al.*, 2015). The authors suggested that additional steps beyond nuclear maturation are needed for fertilization in dogs, and previous obstacles for IVF with *in vivo*-matured oocytes centered on a combination of sperm function and oocyte maturation (Nagashima *et al.*, 2015). This breakthrough will greatly expand the use of dog embryos for research and other ART techniques so that important models of human disease and endangered species can be generated.

11.3.5 Intracytoplasmic Sperm Injection

Intracytoplasmic sperm injection (ICSI) is an ART technique in which a single spermatozoon is injected directly into the ooplasm to generate a viable embryo (England, 2013). The technique is used in human infertility cases, for example, when spermatozoa are immotile or few in number, the zona pellucida becomes hardened blocking sperm penetration (with ICSI as an alternative to zona drilling), or to combat polyspermy to ensure delivery of a single spermatozoon (Seidel, 2015). One study used ICSI of dog spermatozoa with 38 homologous oocytes, and reported decondensed sperm nuclei in 16 (42%) injected oocytes and pronuclear stage embryos with two pronuclei in three (7.8%) injected oocytes (Fulton *et al.*, 1998; Forsberg and Reynaud, 2012). ICSI with dog spermatozoa has also been performed on nonhomologous oocytes. Using *in vitro*-matured metaphase II sheep oocytes, Shirazi *et al.* (2014) performed ICSI with testicular, testicular xenographic, and epididymal dog spermatozoa. The epididymal dog sperm nuclei decondensed in about 25% of the injected oocytes. Although male pronuclei formed in only 3.8% (2 out of 52) of the injected oocytes by 12 h after ICSI, the efficiency could increase to 16.7% (18 out of 108 injected oocytes) if the oocytes were activated with ionomycin 1 h after injection (Shirazi *et al.*, 2014). Thus, although ICSI is possible with dog spermatozoa, the efficiency of the technique is limited in dogs at this time most likely due to inappropriate conditions to support oocyte activation for successful

Downloaded From Vet-eBooks.com

embryonic development. Using ICSI with *in vivo*-matured oocytes (collected day 6 after the LH surge using procedures of Nagashima *et al.*, 2015) would be of great interest, since the oocytes have not only meiotic competence, but also developmental competence.

11.3.6 Embryo Transfer

Embryo transfer (ET) is an ART technique in which one or more preimplantation embryos (often produced by IVF) are placed in the uterus of a recipient female who is at a stage of the reproductive cycle that can support embryonic development (England, 2013). The ET technique is successful in dogs. Both fresh and cryopreserved embryos have been transferred with surgical or nonsurgical methods to either the uterine horn or uterine tube with success. In one study, *in vivo*-derived fresh embryos at the zygote, 2-cell and 4-cell stages were transferred to the uterine horn of 8 recipient females, and one dog that had received two zygotes and one 2-cell embryo gave birth to two puppies (Tsutsui *et al.*, 2006). In addition, two dogs that each received four 8-cell embryos gave birth to either one or two puppies (Tsutsui *et al.*, 2006). Thus, embryo transfer is established in the dog and is often combined with other ART procedures such as cryopreservation, and more recently IVF, as well as additional techniques discussed below (Lee *et al.*, 2005; Nagashima *et al.*, 2015).

11.3.7 Cryopreservation

The technique of carefully preserving whole cells or tissues by freezing and storing them at very low temperatures to maintain their viability and function for later use is cryopreservation. Dog gonadal tissue, spermatozoa, oocytes, and embryos have been cryopreserved with various success (Forsberg and Reynaud, 2012). The technique is useful for storage of gametes from all types of dogs, including rare breeds, assistance dogs, dogs with hereditary diseases that are models of human disease, and canids on the verge of extinction. In the case of guide dogs for the visually impaired, dogs are spayed/neutered before it is known that they are suitable for the task, and thus cryopreservation of ovaries or testes is important.

Cryopreservation of dog spermatozoa is successful, and the cryopreserved spermatozoa are routinely used for AI (see England, 1993, 2013; Farstad, 2000; Hori *et al.*, 2011; Pesch and Bergmann, 2006). During semen cryopreservation, spermatozoa are exposed to physical and chemical stresses, such as ice crystal formation and ROS, which reduce their fertilization potential (Martinez-Soto *et al.*, 2013). These stresses damage the spermatozoa by altering their membranes and reducing their motility, acrosomal status and viability (Martinez-Soto *et al.*, 2013). A significant effect on these sperm functional parameters is the lipid composition of the sperm plasma membrane (Martinez-Soto *et al.*, 2013). For example, sperm membrane fluidity is related to the proportion of long-chain polyunsaturated fatty acids to the saturated fatty acids and cholesterol in sperm membranes (Martinez-Soto *et al.*, 2013). In humans, the amount of docosahexaenoic acid (22:6) in sperm membranes correlates with sperm motility (Gulaya *et al.*, 2001). Moreover, spermatozoa from human patients with asthenozoospermia (defective sperm motility) have less docosahexaenoic acid (22:6) in sperm membranes compared to those without the condition (Gulaya *et al.*, 2001). The affected spermatozoa may have less membrane fluidity, which is needed for flagellar movement. In addition, variations in the long-chain poly-unsaturated fatty acids of the sperm membranes result in differences in cryotolerance of spermatozoa (Martinez-Soto *et al.*, 2013). Thus, because of the relatively similar sperm membrane lipid composition (Tables 11.5 and 11.6), ease of sperm collection, published genome, and ability to control the diet of dogs, dog spermatozoa are a useful model for human sperm cryopreservation. After cryopreservation or vitrification (ultra-rapid freezing), dog

Downloaded From Vet-eBooks.com

oocytes have ultrastructural alterations that result in a 58% reduced ability of the oocytes to resume meiosis (93.8% control versus 53.4% vitrified) (Turathum *et al.*, 2010).

Much better success is obtained with embryo cryopreservation. In one study, *in vivo*-derived 8–16-cell embryos that were generated via AI and had been cryopreserved were nonsurgically transferred to four Labrador retriever recipients and seven puppies were born (Abe *et al.*, 2011). In another study, when cryopreserved *in vitro*-derived 4-cell embryos (generated using IVF of *in vivo*-matured oocytes) were placed in the uterine tube, seven healthy puppies were born (Nagashima *et al.*, 2015). For further information on cryopreservation with canine reproductive cells and tissues see Forsberg and Reynaud (2012).

11.3.8 Sperm Sexing

The sex of offspring has been preselected in many species, including livestock and humans (Garner *et al.*, 2013). This involves sperm sexing, a process in which spermatozoa in a semen sample are sorted such that spermatozoa carrying the X chromosome (which have more DNA and are slightly heavier) are identified and separated from those bearing the Y chromosome (Garner *et al.*, 2013). A flow cytometer or cell sorter is used to separate the spermatozoa (Garner *et al.*, 2013; Rodenas *et al.*, 2014). The selected X- or Y-bearing sperm subpopulation is then used to fertilize oocytes so that offspring of the desired sex are generated. For example, in the bovine, female offspring are desired for milk production, whereas males are preferred for meat production (Oi *et al.*, 2013). Dog breeders, trainers, and caretakers also have a specific preference for a dog of a certain sex. For example, females are often preferred for guide dogs for the visually impaired/blind, because they are easier to manage and in some locations, male guide dogs must have additional accoutrements such as street clothes (Oi *et al.*, 2013). In addition, dog breeding with sex-sorted spermatozoa could be used as a model for endangered canids (Rodenas *et al.*, 2014). Fluorescence *in situ* hybridization (FISH) has been used for sperm sexing to identify X- and Y-bearing spermatozoa of many mammals, including dogs and humans (Komaki *et al.*, 2014; Oi *et al.*, 2013). Spermatozoa bearing an X- or Y-chromosome are present in a 50:50 ratio (Komaki *et al.*, 2014; Oi *et al.*, 2013).

Flow cytometric sexing of dog spermatozoa followed by transcervical insemination with nonfrozen X-bearing spermatozoa was reported to yield five puppies with a prevalence of females (three females, two males) (Meyers *et al.*, 2008). This demonstrates that dog spermatozoa remained viable and retained their function during application of these combined ART procedures (Meyers *et al.*, 2008). Coupling sperm sexing and cryopreservation of sexed dog spermatozoa has been reported, but revealed optimization of these methods is needed (Merlo *et al.*, 2015). Some of the challenges included the slow time for sperm sexing, exposure of spermatozoa to long periods at room temperature during sperm sexing, high numbers of spermatozoa required for AI in the dog, and sperm storage issues involving heightened sensitivity of sexed spermatozoa to cryopreservation resulting in relatively more sperm damage than with unsexed, unsorted, live dog spermatozoa (Merlo *et al.*, 2015). Several important changes to the basic cryopreservation protocol were described for use with sex-sorted spermatozoa, including using different sperm extenders (a type of medium used to dilute sperm samples) and different centrifugation parameters (Merlo *et al.*, 2015).

In addition, assessment of semen is useful not only for sperm sexing, but also for dog breeding purposes for diagnosis of sperm quality as this reflects reproductive health of the male. For example, flow cytometry has been successfully used to analyze large numbers of dog spermatozoa stained with a combination of fluorescent dyes to assess the integrity and functionality of dog spermatozoa for breeding and diagnostic purposes (Hossain *et al.*, 2011). Fluorescent dyes

Downloaded From Vet-eBooks.com

target various organelles or functional aspects of the spermatozoa to allow identification of spermatozoa that (i) are viable with intact membranes, for example, using live/dead stains such as SYBR-14/propidium iodide in which live cells fluoresce green and dead cells red, (ii) have destabilized membranes demonstrating an early step in capacitation, as visualized with merocyanine 540, (iii) have nuclei, such as seen with Hoechst dyes, and (iv) are acrosome intact, such as using a plant lectin labeled with a fluorescent dye as a stain (Hossain *et al.*, 2011; Peña *et al.*, 2006). Of value is the determination of fertilizing potential of a sperm population for breeding or AI. Flow cytometry has been used with dog spermatozoa for sorting for sperm selection, sperm sexing, and sperm freezing for cryopreservation (Hossain *et al.*, 2011). Compared to spermatozoa of rodents and domestic mammals, dog spermatozoa are relatively small and similar to the size and shape of human spermatozoa (Table 11.4), and thus dog spermatozoa make a useful model for working out procedures to study human sperm function with flow cytometry.

11.3.9 Somatic Cell Nuclear Transfer in Dogs

Somatic cell nuclear transfer (SCNT) also known as "cloning" is an ART technique to produce a genetic copy of an individual organism. During the procedure, the nucleus of a differentiated somatic cell from an animal to be cloned is transferred to the cytoplasm of an enucleated oocyte, which is an oocyte that had its nucleus removed (Lee *et al.*, 2005). Cloning can be used to restore the genetic potential of a dog that had been spayed or neutered, as well as propagate desirable traits in working dogs and pet dogs (Hall *et al.*, 2013). The first report of a successfully cloned dog was in 2005 using SCNT with *in vivo*-matured enucleated oocytes (Lee *et al.*, 2005). The clone, named Snuppy (for Seoul National University puppy), was cloned from the skin cells of a 3-year-old adult male Afghan hound (Lee *et al.*, 2005). Since then several dogs, including females, of different breeds and ages have been cloned, and even recloned (Jang *et al.*, 2007; Kim *et al.*, 2012; Oh *et al.*, 2011). In addition, pet cloning has been commercialized with the first dog pet clones generated in 2008, three 3 years after the Pit Bull Terrier dog donor had died (Kim *et al.*, 2012). Several reviews have addressed how SCNT is performed and the challenges of dog cloning using SCNT (Chastant-Maillard *et al.*, 2010; Hall *et al.*, 2013; Kim *et al.*, 2012). SCNT is a way to obtain genetically modified dogs as well. Thus, SCNT coupled with other ART techniques is a powerful tool that is very successful with the dog model.

11.3.10 Dog Embryonic Stem Cells and Induced Pluripotent Stem Cells

A stem cell is an undifferentiated cell type that can regenerate itself (self-renew) and has the capability to differentiate into a specialized cell type (Ezashi *et al.*, 2016). This includes *adult stem cells*, which are isolated from adult tissues, *embryonic stem cells* (ESCs), which are collected from blastocyst embryos, and *induced pluripotent stem cells* (iPSCs), which are derived from somatic cells that were genetically reprogrammed to be stem cells (Ezashi *et al.*, 2016). Adult stem cells derived from mesenchymal cells of adult dogs have been used to treat lameness in dogs (Ezashi *et al.*, 2016). Embryonic stem cell lines and iPSCs have been successfully generated by several research groups for the dog (Hayes *et al.*, 2008; *cf.* Ezashi *et al.*, 2016; Hall *et al.*, 2013). Both dog ESCs and iPSCs exhibit many of the expected characteristics of ESCs, such as stem cell and pluripotency cell markers, and ability to form embryoid bodies and teratomas, although germ-line transmission remains to be demonstrated (Ezashi *et al.*, 2016). Although some issues need to be resolved (reviewed in Ezashi *et al.*, 2016; Hall *et al.*, 2013), ESCs and iPSCs have great future utility as a means to understand basic events of cell differentiation, and to generate dog tissues for regenerative medicine and dog models of human disease.

Downloaded From Vet-eBooks.com

11.3.11 Genetically Modified Dogs

11.3.11.1 Transgenic Dogs

Transgenic dogs have been generated using SCNT coupled with embryo transfer (Hong *et al.*, 2009). The first transgenic cloned dogs that carry the red fluorescent protein gene were generated in 2009 from canine fibroblast cells (donor cells) that were manipulated to carry the red fluorescent protein transgene prior to SCNT (Hong *et al.*, 2009). Since then dogs carrying the green fluorescent protein have been produced using SCNT (Kim *et al.*, 2011). Producing transgenic dogs is a route to generating important dog models of human disease (see Hall *et al.*, 2013).

11.3.11.2 Gene-Edited Dogs

The genome-editing tool, clustered regularly interspaced short palindromic repeats (CRISPRs)/CRISPR-associated (Cas)9 system has been successfully used to modify the dog genome in preimplantation embryos (Zou *et al.*, 2015). Spontaneous mutations of the myostatin gene (*MSTN*), which negatively regulates muscle size, had been previously shown to cause muscle hypertrophy in dogs as it does in humans. Using the CRISPR/Cas9 system, Zou *et al.* (2015) targeted the myostatin gene (*MSTN*) by injecting *in vivo*-generated zygotes with a mixture of Cas9 mRNA and MSTN sgRNA to generate *MSTN* gene knockout Beagle dogs (Zou *et al.*, 2015). By performing auto-transplantation (flushing embryos from one uterine tube, performing gene editing, and then transferring the 35 injected zygotes to the remaining uterine tube of 10 dogs), the authors obtained 8 pregnant dogs (80%) that delivered 27 puppies. Of these, two puppies had genetic mutations in the *MSTN* locus: one was a biallelic mutant and the other was a chimera. The *MSTN* knockout dog was a male reaching sexual maturity after birth at 10 months of age, and his spermatozoa were found to have the single mutation, which indicated that the mutation could possibly be transmitted to his offspring (Zou *et al.*, 2015). The CRISPR/Cas9-mediated gene editing tool has also been used in human tri-pronuclear (3PN) zygotes, but the efficiency of the homologous recombination step targeting the β-globin gene was low and the edited embryos were mosaic and mutations were observed at nontarget sites (Liang *et al.*, 2015). The dog offers a valuable model to further understand the molecular mechanism of CRISPR/Cas9-mediated genome editing and to improve the specificity and fidelity of the technique preventing off-target effects using canine preimplantation embryos in place of human embryos.

11.4 Dog Contraception

A variety of techniques have been used to prevent fertility in the dog (England, 2013; Rhodes, 2016). This includes sterilization by spaying or neutering, as well as contraception for intact dogs (England, 2013). One of the contraceptive methods targeted the zona pellucida and/or the Izumo1 sperm protein (Shrestha *et al.*, 2014, 2015). For more information on preventing fertility in both male and female dogs, visit http://www.michelsonprizeandgrants.org/resources/canine-feline-reproduction-contraception/resources#the_female_dog and see also http://www.michelsonprizeand grants.org/michelson-grants/research-findings.

11.5 The Dog as a Model for Human Reproduction

The dog is a remarkable model system to focus on investigations into human reproductive disorders. Advantages of the dog model include its spontaneous pedigree, reproductive anatomy

Downloaded From Vet-eBooks.com

and physiology, genetics and behavior, as well as its relatively long life span and size, which more closely match human parameters than other animal models such as mice. Some of the areas where the dog has served as a model of human reproduction are briefly described in the following section.

11.5.1 Disorders of Sexual Development

Dogs share similar inherited disorders of sexual development (DSD) with humans (Meyers-Wallen, 2012; Poth *et al.*, 2010; Switonski, 2014). This is a heterogeneous group of disorders. In dogs and humans there are three major types of DSD: sex chromosome DSD, XX DSD, and XY DSD. Sex chromosome DSD is due to chromosomal abnormalities, such as sex chromosome aneuploidies (Turner's syndrome, X0, or Klinefelter syndrome, XXY). Other sex chromosome DSD are due to XX/XY chimerisms or mosaicisms. The XX/XY chimerisms occur when two different early embryos—one XX and the other XY—fuse to form one individual. The XX/XY mosaicisms occur due to events such as nondisjunction in the early embryo. Other types of DSD conditions result in sex reversal in which the chromosomal and gonadal sex disagree. These include XX DSD (those with XX chromosomes) and XY DSD (those with XY chromosomes). For example, dogs can be affected by *Sry*-negative XX sex reversal (XX DSD) similar to human patients (Del Carro *et al.*, 2014; Rossi *et al.*, 2014; Marcinkowska-Swojak *et al.*, 2015). In one example of a *Sry*-negative 78,XX testicular DSD dog (XX DSD), the dog's genotype was female (78,XX) and she appeared female at 2 months, but upon closer examination she had an enlarged clitoris with an os penis and uterine horns that followed the path of the ductus deferens and ended in normal scrotal testicles even though she was *Sry* negative (Del Carro *et al.*, 2014). In another example of XX DSD, the *Sry*-negative XX sex reversal condition produced ovotestes and was due to a *Sox9* gene duplication in two dogs (Rossi *et al.*, 2014). In several other dogs with sex reversal due to a 78,XX *Sry*-negative testicular XX DSD, a different mechanism not yet identified was involved (Del Carro *et al.*, 2014; Rossi *et al.*, 2014). In a larger study of 50 dogs with XX DSD, no duplication of SOX9 was found, but instead two highly polymorphic copy number variable regions or CNVRs (one known to be upstream and the other possibly upstream of the SOX9 gene) were implicated in causing XX DSD; however, these regions were also identified in unaffected controls suggesting that within the CNVR there may be mutations that eliminate binding sites for a repressor or enhancer of SOX9 (Marcinkowska-Swojak *et al.*, 2015).

An example of an XY DSD is a genetic disorder of males called canine persistent Müllerian duct syndrome (PMDS) and has been reported in dogs (Meyers-Wallen, 2012; Wu *et al.*, 2009). Male dogs with PMDS have a normal karyotype (78, XY) and develop bilateral testes and appear as males externally (except for about 50% with unilateral or bilateral cryptorchidism) (Wu *et al.*, 2009). However, they also retain their Müllerian ducts, which develop into bilateral uterine tubes, a complete uterus with uterine horns and body, a cervix and the cranial vagina, which enters the dorsal prostate (Wu *et al.*, 2009). Müllerian inhibiting substance (MIS), also known as anti-Müllerian hormone (AMH) is a secreted glycoprotein that normally mediates Müllerian duct regression in males during the sex differentiation phase of embryonic development. A single base pair mutation in exon 3 of the dog MIS receptor II (*MISRII*/*AMHR2*) gene was reported to be caused by a single nucleotide substitution (C241T), which created a premature stop codon instead of an arginine amino acid so that translation stopped at only 80 amino acids (Wu *et al.*, 2009). This resulted in a nonfunctional receptor that was missing most of its extracellular domain, and all of its transmembrane and intracellular domains (Wu *et al.*, 2009). The reproductive tract of dogs with the condition appeared very similar to human patients affected with PMDS (Wu *et al.*, 2009). Thus, the dog is an invaluable model of the human disorder.

Downloaded From Vet-eBooks.com

11.5.2 Cancer

Since dogs live for a relatively long time and often have excellent medical care, the diagnosis of cancer is common in older dogs as they age, similar to humans (Switonski, 2014). Many cancers in dogs are spontaneous, whereas others are due to known mutations and chromosomal translocations (Switonski, 2014). Many cancers in dogs have similar features to human cancers, including genetic background, histology, and response to treatment (Switonski, 2014). Some dog breeds have a predisposition to certain kinds of cancer (Switonski, 2014). Therefore, dogs with cancer are extremely useful models to understand human cancers.

11.5.2.1 Breast Cancer

There is a high incidence of mammary tumors in dogs (Peña *et al.*, 2014). It is one of the most common types of tumor in unspayed female dogs (England, 2013). Spontaneous mammary tumors are the most common type of neoplasm (Peña *et al.*, 2014). Some breeds are at a higher risk for breast cancer than others. Mammary gland lesions/tumors are common in female dogs, but rare in male dogs (Solano-Gallego and Masserdotti, 2016). This has been discussed extensively elsewhere (England, 2013; Peña *et al.*, 2014; Solano-Gallego and Masserdotti, 2016).

11.5.2.2 Testicular Cancer

Testicular tumors are the most common type of male reproductive tract tumor in dogs, representing more than 90% of male genital tract tumors (Hohšteter *et al.*, 2014). They have been ranked as the third most common type of cancer occurrence overall after skin tumors and fibrous tissue tumors (Hohšteter *et al.*, 2014). With aging, male dogs have been reported to have an increase in the prevalence of testicular tumors, with 86% of clinically detected tumors and 57% of nonclinically detected tumors found in older dogs (Hohšteter *et al.*, 2014; Peters *et al.*, 2000). These tumors significantly affected spermatogenesis (Peters *et al.*, 2000). Seminomas (germ cell tumors) and Leydig cell (interstitial cell) tumors were more prevalent than Sertoli cell tumors in the dog (Peters *et al.*, 2000). Male dogs also have another form of testicular tumor found in humans called intratubular germ cell neoplasia of undifferentiated origin (IGCNU) (Hohšteter *et al.*, 2014). Immunohistochemical markers can be used to distinguish these neoplasms in dogs as has been done with human testicular tumor classification (Hohšteter *et al.*, 2014). The dog is an excellent resource for the study of the male reproductive system, especially for testicular tumor formation and treatment, which may help understand and treat human testicular neoplasms.

11.5.2.3 Prostate Cancer

The dog prostate is sensitive to androgens, increasing in size when they are present and shrinking in their absence (Evans and De Lahunta, 2013). As in humans, the dog prostate gland is prone to age-related hypertrophy such as benign prostatic hyperplasia and other pathological changes, and thus makes an excellent model for understanding human prostatic disease (Evans and De Lahunta, 2013; Walsh and Wilson, 1976). A major clinical marker for prostatic secretion in the dog is canine prostate-specific arginine esterase (CPSE), which has trypsin-like activity and is closely related to human prostate specific antigen (PSA), a marker for human prostatic carcinoma (Gobello *et al.*, 2002). The main neoplasia of the prostate in dogs and humans is prostatic adenocarcinoma (Gadelha *et al.*, 2013). Thus, the dog has been used as a model to study the development of prostatic cancer in humans, as it occurs spontaneously in the dog (Gadelha *et al.*, 2013; Gobello *et al.*, 2002).

Downloaded From Vet-eBooks.com

11.5.3 Obesity

Obesity in dogs is becoming a health issue even in purebred dogs (Courcier *et al.*, 2010). Certain dog breeds are more susceptible to obesity than others (Switonski, 2014). Obesity in humans is a major health problem and affects fertility in both women and men. Pregnancy and live birth rate outcomes decline with increasing body mass index in women (Provost *et al.*, 2016). In men, high body mass index has been correlated with low sperm concentration (Alshahrani *et al.*, 2016). Human genetic determinants for at least 52 genetic loci associated with obesity-related traits or obesity susceptibility have been identified (Loos, 2012; Switonski, 2014). Thus, the dog offers an important model to elucidate the mechanisms behind obesity susceptibility and pathogenesis, and its effects on reproductive health.

11.5.4 Dog Infertility

Infertility affects up to 15% of human couples trying to have children and up to 50% of these are due to male fertility problems (see Cassatella *et al.*, 2013). Infertility has been reported in dogs and it results in financial losses for the dog breeding industry (Cassatella *et al.*, 2013; England, 2013). A recent study involving functional and genetic analysis of male infertility reported copy number differences using copy number variation (CNV) analysis when comparing infertile and fertile male dogs for genomic regions that included genes previously reported associated with human infertility (Cassatella *et al.*, 2013). The study found two genomic regions containing two genes *DNM2* and *TEKT1* that are important for spermatogenesis, which had not been identified before and may play a role in human infertility (Cassatella *et al.*, 2013). Thus, genes involved in infertility in the dog can shed light on the same disease in humans.

Infertility in dogs can be related to males and/or females for a variety of reasons/causes. For example, spermatozoa can have defects, which prevent successful fertilization (Pesch and Bergmann, 2006). Morphological abnormalities of dog spermatozoa are found in the head, neck, midpiece, and principal piece of the tail (Bartlett, 1962a; England, 2013; Kawakami *et al.*, 2005). Defective sperm heads can be doubled, misshapen, enlarged, small, bent, detached/free, cratered, and have a knobbed, swollen, or missing acrosome (Bartlett, 1962a, England, 2013). Sperm neck abnormalities include eccentric insertion, cytoplasmic droplets, thickened neck, bent neck, and disintegrated neck (Bartlett, 1962a, England, 2013). Abnormal sperm midpieces can have large cytoplasmic droplets, or be too thick or thin, doubled, coiled, or kinked (Bartlett, 1962a, England, 2013). Defective sperm tails (principal piece) can have cytoplasmic droplets, or are too thin, too thick, doubled, coiled, bent, looped, or missing/detached (Bartlett, 1962a, England, 2013; Kawakami *et al.*, 2005; Oettlé and Soley, 1985; Rota *et al.*, 2008). Dog sperm abnormalities have been correlated with low fertility rates and infertility (Dahlbom *et al.*, 1997; Oettlé and Soley, 1985). These types of sperm abnormalities have been observed in human spermatozoa as well (Rengan *et al.*, 2012). When the cytoplasmic droplet is greater than one-third the size of the sperm head in humans, the droplets are considered sperm defects, as they can harbor higher levels of metabolic enzymes and other constituents leading to an increase in ROS damage, DNA damage, and affect sperm motility (Rengan *et al.*, 2012). Discussion of all of the issues is beyond the scope of this chapter and this has been addressed elsewhere (England, 2013).

11.5.5 Aneuploidy

Aneuploidy (e.g., monosomy and trisomy) is a major cause of congenital birth defects and miscarriage, and is a major impediment to successful pregnancy via ART (Hassold and Hunt, 2001;

Downloaded From Vet-eBooks.com

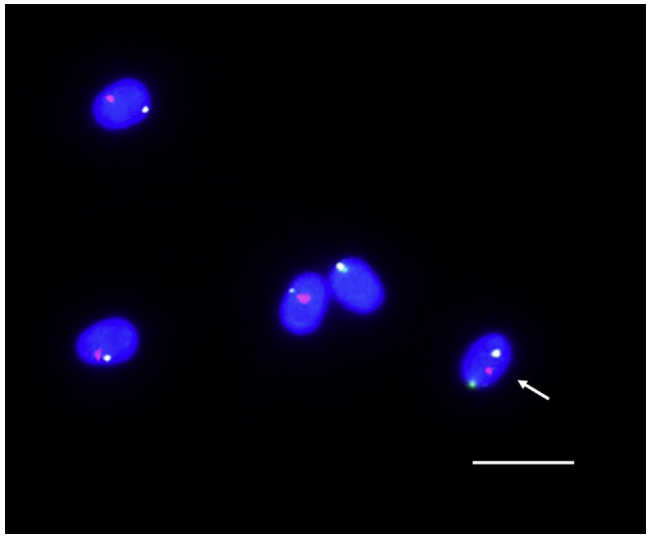

Figure 11.34 Detection of chromosomes X, Y, and 1 in dog spermatozoa by multicolor fluorescence *in situ* hybridization (FISH). Each spermatozoon has one yellow signal for chromosome 1, and either a green signal (X chromosome) or a red signal (Y chromosome). X-bearing spermatozoa have one green and one yellow signal. Y-bearing sperm have one red and one yellow signal. A spermatozoon (arrow) with all three signals (yellow, green and red) was considered to be aneuploid. Bar is 100 µm. (Reproduced from *Theriogenology*, volume 82, number 4, Komaki H, Oi M, Suzuki H., Detection of sex chromosome aneuploidy in dog spermatozoa by triple color fluorescence *in situ* hybridization, pages 652–656, Copyright 2014, with permission from Elsevier.) (See color plate section.)

Nagaoka *et al.*, 2012). Sex chromosome aneuploidy in dog spermatozoa has been detected with the multicolor FISH technique (Figure 11.34) (Komaki *et al.*, 2014). Sex chromosome aneuploidy averaged 0.127% (range 0–0.316%) of the sperm population in a study of eight dogs (Komaki *et al.*, 2014). This is comparable to the aneuploidy frequency reported for humans (0.16–0.96%) (Brahem *et al.*, 2012; Gordeeva *et al.*, 2011; Komaki *et al.*, 2014). The percentage of dog spermatozoa having multiple FISH probe signals, such as one X chromosome, one Y chromosome, and two chromosome 1 signals in one spermatozoon was 0.008%, and 0.08% in spermatozoa containing one chromosome each of the X, Y, and 1 (Komaki *et al.*, 2014), and 0.06–0.37% in humans (Brahem *et al.*, 2012; Gordeeva *et al.*, 2011). Thus, with the detection of sex chromosome aneuploidy in the dog, the dog is a good model to study the causes of aneuploidy.

11.6 Concluding Statements

In summary, this is an exciting time to use the domestic dog model to advance understanding of reproduction and development. Several important breakthroughs have been achieved with the dog, including technologies of assisted reproduction such as IVF, embryo transfer, and SCNT. In addition, using SCNT to generate transgenic dogs has been done, canine stem cells have been produced, and gene editing with the CRISPRs)/CRISPR-associated (Cas)9 system has been achieved. Thus, the dog is an excellent model for endangered canids and human disease. The dog has several advantages compared to the mouse. The dog's relatively long life span, size, genetics, and reproductive anatomy and physiology more closely match human parameters. In addition, dogs live with us and are exposed to the same environmental conditions as humans, and have over 360 heritable diseases that are homologous with human conditions. Funding for

Downloaded From Vet-eBooks.com

dog reproductive research has been limited, which has reduced the number of researchers focusing on canine reproduction (Van Soom *et al.*, 2014). Future researchers will be able to answer many questions in dog and human reproduction to

1) reveal molecular mechanisms controlling dog reproduction, which will greatly facilitate understanding of human reproduction and may lead to new therapies to address reproductive disorders in dogs, agricultural species, and humans;
2) enhance reproductive timing and cryopreservation for dog breeders and veterinarians especially to produce working dogs for human society's many essential needs described in Table 11.1;
3) provide advantages to understand genetic foundations of disease to eradicate deleterious traits from dog breeds (especially pedigree dogs), for example, via gene-editing coupled with IVF and embryo transfer;
4) address overpopulation in dogs especially in countries overwhelmed by stray dogs that carry disease and are a significant threat to inhabitants;
5) aid genome rescue and reproduction in endangered canids by using the dog as a model to work out and establish ART specific for endangered canid species; and finally,
6) advance canine stem cell research and generation of transgenic dogs as important models to understand human diseases.

Thus, the dog model is poised to be more fully utilized as a model of human reproduction, development, and disease and to help in the conservation of endangered canids. Although some challenges remain, we can anticipate many significant discoveries through collaboration and continued hard work using the dog model. It will be exciting to see the new possibilities and achievements the dog model will provide.

Acknowledgments

I thank Drs. Margaret (Peggy) V. Root Kustritz, DVM, Ph.D., and David J. Wright, Ph.D., for the images they provided for this work. I also thank Dr. David Wright for technical help and critical reading of this chapter. Permission to use copyrighted materials is gratefully acknowledged. The sabbatical support of the University of Dayton during my sabbatical is greatly appreciated. I also thank Professor Heide Schatten for her advice and encouragement.

References

Abe, Y., Suwa, Y., Asano, T., Ueta, Y.Y., Kobayashi, N., Ohshima, N., Shirasuna, S., Abdel-Ghani, M.A., Oi, M., Kobayashi, Y., Miyoshi, M., Miyahara, K., and Suzuki, H. (2011) Cryopreservation of canine embryos. *Biol. Reprod.*, **84** (2): 363–368.

Abrishami, M., Abbasi, S., and Honaramooz, A. (2010) The effect of donor age on progression of spermatogenesis in canine testicular tissue after xenografting into immunodeficient mice. *Theriogenology*, **73** (4), 512–522.

ADA (2010) The Americans with Disabilities Act of 1990, U.S. Department of Justice, Civil Rights Division. Retrieved from http://www.ada.gov/service_animals_2010.htm (July 3, 2015).

Aguilar, J. and Reyley, M. (2005) The uterine tubal fluid: secretion, composition and biological effects. *Anim. Reprod. Sci.*, **2** (2), 91–105.

Aitken, R.J. and Nixon, B. (2013) Sperm capacitation: a distant landscape glimpsed but unexplored. *Mol. Hum. Reprod.*, **19** (12), 785–793.

Downloaded From Vet-eBooks.com

AKC (2015) The American Kennel Club. Retrieved from www.akc.org (July 1, 2015).

Albarracín, J.L., Mogas, T., Palomo, M.J., Peña, A., Rigau, T., and Rodríguez-Gil, J.E. (2004a) *In vitro* capacitation and acrosome reaction of dog spermatozoa can be feasibly attained in a defined medium without glucose. *Reprod. Domest. Anim.*, **39** (3), 129–135.

Albarracín, J.L., Fernández-Novell, J.M., Ballester, J., Rauch, M.C., Quintero-Moreno, A., Peña, A., Mogas, T., Rigau, T., Yañez, A., Guinovart, J.J., Slebe, J.C., Concha, I.I., and Rodríguez-Gil, J.E. (2004b) Gluconeogenesis-linked glycogen metabolism is important in the achievement of *in vitro* capacitation of dog spermatozoa in a medium without glucose. *Biol. Reprod.*, **71** (5): 1437–1445.

Albertini, D. (2015) The mammalian oocyte, in *Knobil and Neill's Physiology of Reproduction*, 4th edn (eds T.M. Plant and A.J. Zeleznik), vol. 1, Academic Press, Waltham, MA, pp. 59–98.

Albrizio, M., Siniscalchi, M., Sasso, R., and Quaranta, A. (2013) Effects of the environment on dog semen parameters and testosterone concentration. *Theriogenology*, **80** (7), 800–804.

Alshahrani, S., Ahmed, A.F., Gabr, A.H., Abalhassan, M., and Ahmad, G. (2016) The impact of body mass index on semen parameters in infertile men. *Andrologia*, doi: 10.1111/and.12549.

Amann, R.P. (2008) The cycle of the seminiferous epithelium in humans: a need to revisit? *J. Androl.*, **29** (5), 469–487.

Amaral, A., Lourenço, B., Marques, M., and Ramalho-Santos, J. (2013) Mitochondria functionality and sperm quality. *Reproduction*, **146** (5), R163–R174.

American Kennel Club (2015) *The Complete Dog Book*, 21st edn, American Kennel Club, i-5 Publishing, Irvine, CA, p. 912.

Angrimani, D.S., Lucio, C.F., Veiga, G.A., Silva, L.C., Regazzi, F.M., Nichi, M., and Vannucchi, C.I. (2014a) Sperm maturation in dogs: sperm profile and enzymatic antioxidant status in ejaculated and epididymal spermatozoa. *Andrologia*, **46** (7), 814–819.

Angrimani, D.S., Losano, J.D., Lucio, C.F., Veiga, G.A., Pereda, M.C., Nichi, M., and Vannucchi, C.I. (2014b) Role of residual cytoplasm on oxidative status during sperm maturation in dogs. *Anim. Reprod. Sci.*, **151** (3–4), 256–261.

Angulo, C., Rauch, M.C., Droppelmann, A., Reyes, A.M., Slebe, J.C., Delgado-López, F., Guaiquil, V.H., Vera, J.C., and Concha, I.L. (1998) Hexose transporter expression and function in mammalian spermatozoa: cellular localization and transport of hexoses and vitamin C. *J. Cell Biochem.*, **71** (2), 189–203.

Apparicio, M., Ferreira, C.R., Tata, A., Santos, V.G., Alves, A.E., Mostachio, G.Q., Pires-Butler, E.A., Motheo, T.F., Padilha, L.C., Pilau, E.J., Gozzo, F.C., Eberlin, M.N., Lo Turco, E.G., Luvoni, G.C., and Vicente, W.R. (2012) Chemical composition of lipids present in cat and dog oocyte by matrix-assisted desorption ionization mass spectrometry (MALDI- MS). *Reprod. Domest. Anim.*, **47** (Suppl. 6), 113–117.

Asher, L., Buckland, E.L., Phylactopoulos, C.I., Whiting, M.C., Abeyesinghe, S.M., and Wathes, C.M. (2011) Estimation of the number and demographics of companion dogs in the UK. *BMC Vet. Res.*, **7** (1), 74.

Au, C.E., Hermo, L., Byrne, E., Smirle, J., Fazel, A., Kearney, R.E., Smith, C.E., Vali, H., Fernandez-Rodriguez, J., Simon, P.H., Mandato, C., Nilsson, T., and Bergeron, J.J. (2015) Compartmentalization of membrane trafficking, glucose transport, glycolysis, actin, tubulin and the proteasome in the cytoplasmic droplet/Hermes body of epididymal sperm. *Open. Biol.*, **5** (8), pii: 150080.

Austin, C.R. (1952) The 'capacitation' of the mammalian sperm. *Nature*, **170**, 326.

Austin, C.R. and Short, R.V. (1982) *Reproduction in Mammals. Book 1: Germ Cells and Fertilization*, 2nd edn, Cambridge University Press, Cambridge, 177 pp.

Downloaded From Vet-eBooks.com

Avenarius, M.R., Hildebrand, M.S., Zhang, Y., Meyer, N.C., Smith, L.L., Kahrizi, K., Najmabadi, H., and Smith, R.J. (2009) Human male infertility caused by mutations in the CATSPER1 channel protein. *Am. J. Hum. Genet.*, **84** (4), 505–510.

Avidan, N., Tamary, H., Dgany, O., Cattan, D., Pariente, A., Thulliez, M., Borot, N., Moati, L., Barthelme, A., Shalmon, L., Krasnov, T., Ben-Asher, E., Olender, T., Khen, M., Yaniv, I., Zaizov, R., Shalev, H., Delaunay, J., Fellous, M., Lancet, D., and Beckmann, J.S. (2003) CATSPER2, a human autosomal nonsyndromic male infertility gene. *Eur. J. Hum. Genet.*, **11** (7), 497–502.

The American Veterinary Medical Association (2015) U.S. Pet Ownership and Demographics Sourcebook, AVMA, Schaumberg, IL. Retrieved from https://www.avma.org/KB/Resources/Statistics/Pages/Market-research-statistics-US-pet-ownership.aspx (July 6, 2015).

Bahat, A., Tur-Kaspa, I., Gakamsky, A., Giojalas, L.C., Breitbart, H., and Eisenbach, M. (2003) Thermotaxis of mammalian sperm cells: a potential navigation mechanism in the female genital tract. *Nat. Med.*, **9** (2), 149–150.

Bainbridge, J.W., Mehat, M.S., Sundaram, V., Robbie, S.J., Barker, S.E., Ripamonti, C., Georgiadis, A., Mowat, F.M., Beattie, S.G., Gardner, P.J., Feathers, K.L., Luong, V.A., Yzer, S., Balaggan, K., Viswanathan, A., de Ravel, T.J., Casteels, I., Holder, G.E., Tyler, N., Fitzke, F.W., Weleber, R.G., Nardini, M., Moore, A.T., Thompson, D.A., Petersen-Jones, S.M., Michaelides, M., van den Born, L.I., Stockman, A., Smith, A.J., Rubin, G., and Ali, R.R. (2015) Long-term effect of gene therapy on Leber's congenital amaurosis. *N. Engl. J. Med.*, **372** (20), 1887–1897.

Bains, H.K., Pabst, M.A., and Bawa, S.R. (1993) Changes in the lectin binding sites on the testicular, epididymal, vas, and ejaculated spermatozoon surface of dog. *Andrologia*, **25** (1), 19–24.

Ballester, J., Fernández-Novell, J.M., Rutllant, J., García-Rocha, M., Jesús Palomo, M., Mogas, T., Peña, A., Rigau, T., Guinovart, J.J., and Rodríguez-Gil, J.E. (2000) Evidence for a functional glycogen metabolism in mature mammalian spermatozoa. *Mol. Reprod. Dev.*, **56** (2), 207–219.

Banjoko, S.O. and Adeseolu, F.O. (2013) Seminal plasma pH, inorganic phosphate, total and ionized calcium concentrations in the assessment of human spermatozoa function. *J. Clin. Diagn. Res.*, **7** (11), 2483–2486.

Bartel, D.P. (2004) MicroRNAs: genomics, biogenesis, mechanism, and function. *Cell*, **116** (2), 281–297.

Bartlett, D.J. (1958) Biochemical characteristics of dog semen. *Nature*, **182**, 1605–1606.

Bartlett, D.J. (1962a) Studies on dog semen. I. Morphological characteristics. *J. Reprod. Fertil.*, **3**, 173–189.

Bartlett, D.J. (1962b) Studies on dog semen. II. Biochemical characteristics. *J. Reprod. Fertil.*, **3**, 190–205.

Barton, E.P. (1945) The cyclic changes of epithelial cords in the dog ovary. *J. Morphol.*, **77**, 317–349.

Basheva, E.A., Bidau, C.J., and Borodin, P.M. (2008) General pattern of meiotic recombination in male dogs estimated by MLH1 and RAD51 immunolocalization. *Chromosome Res.*, **16**, 709–719.

Bedford, M.J. (1982) Fertilization, in *Reproduction in Mammals, Book 1: Germ Cells and Fertilization*, 2nd edn (eds C.R. Austin and R.V. Short), Cambridge University Press, Cambridge, pp. 128–163.

Bell, J.S. (2006) American breed clubs and health initiatives, in *The Dog and Its Genome* (eds E.A. Ostrander, U. Giger, and K. Lindblad-Toh), Cold Spring Harbor Press, Cold Spring Harbor, NY, pp. 31–45.

Berg, O.A. (1958) The normal prostate gland of the dog. *Acta Endocrinol*, **27** (2), 129–139.

Bianchi, E., Doe, B., Goulding, D., and Wright, G.J. (2014) Juno is the egg Izumo receptor and is essential for mammalian fertilization. *Nature*, **508** (7497), 483–487.

Blackmore, D.G., Baillie, L.R., Holt, J.E., Dierkx, L., Aitken, R.J., and McLaughlin, E.A. (2004) Biosynthesis of the canine zona pellucida requires the integrated participation of both oocytes and granulosa cells. *Biol. Reprod.*, **71** (2), 661–668.

Downloaded From Vet-eBooks.com

Boerke, A., Brouwers, J.F., Olkkonen, V.M., van de Lest, C.H., Sostaric, E., Schoevers, E.J., Helms, J.B., and Gadella, B.M. (2013) Involvement of bicarbonate-induced radical signaling in oxysterol formation and sterol depletion of capacitating mammalian sperm during *in vitro* fertilization. *Biol. Reprod.*, **88** (1), 21.

Borge, K.S., Tønnessen, R., Nødtvedt, A., and Indrebø, A. (2011) Litter size at birth in purebred dogs: a retrospective study of 224 breeds. *Theriogenology*, **75** (5), 911–919.

Boyko, A.R. (2011) The domestic dog: man's best friend in the genomic era. *Genome Biol*, **12** (2), 216.

Brahem, S., Mehdi, M., Elghezal, H., and Saad, A. (2012) Study of aneuploidy rate and sperm DNA fragmentation in large-headed, multiple-tailed spermatozoa. *Andrologia*, **44** (2), 130–135.

Branam, J.E., Keen, C.L., Ling, G.V., and Franti, C.E. (1984) Selected physical and chemical characteristics of prostatic fluid collected by ejaculation from healthy dogs and from dogs with bacterial prostatitis. *Am. J. Vet. Res.*, **45** (4), 825–829.

Braverman, N.E. and Moser, A.B. (2012) Functions of plasmalogen lipids in health and disease. *Biochim. Biophys. Acta*, **1822** (9), 1442–1452.

Breen, M. and Thomas, R. (2006) Karyotype and chromosomal organization, in *The Dog and Its Genome* (eds E.A. Ostrander, U. Giger, and K. Lindblad-Toh), Cold Spring Harbor Press, Cold Spring Harbor, NY, pp. 159–178.

Breitbart, H. and Finkelstein, M. (2015) Regulation of sperm capacitation and the acrosome reaction by PIP2 and actin modulation. *Asian J. Androl.*, **17** (4), 597–600.

Brener, E., Rubinstein, S., Cohen, G., Shternall, K., Rivlin, J., and Breitbart, H. (2003) Remodeling of the actin cytoskeleton during mammalian sperm capacitation and acrosome reaction. *Biol. Reprod.*, **68** (3), 837–845.

Brewis, I.A., Morton, I.E., Moore, H.D., and England, G.C. (2001) Solubilized zona pellucida proteins and progesterone induce calcium influx and the acrosome reaction in capacitated dog spermatozoa. *Mol. Reprod. Dev.*, **60** (4), 491–497.

Brooks, D.E. (1990) Biochemistry of the male accessory glands, in *Marshall's Physiology of Reproduction* (ed. G.E. Lamming), vol. 2, Churchill Livingstone, Edinburgh, pp. 569–690.

Bucci, D., Isani, G., Spinaci, M., Tamanini, C., Mari, G., Zambelli, D., and Galeati, G. (2010) Comparative immunolocalization of GLUTs 1, 2, 3 and 5 in boar, stallion and dog spermatozoa. *Reprod. Domest. Anim.*, **45** (2), 315–322.

Bucci, D., Rodriguez-Gil, J.E., Vallorani, C., Spinaci, M., Galeati, G., and Tamanini, C. (2011) GLUTs and mammalian sperm metabolism. *J. Androl.*, **32** (4), 348–355.

Budras, K.-D. (2007) *Anatomy of the Dog: With Aaron Horowitz and Rolf Berg*, 5th revised edn, Schlütersche Verlagsgesellschaft mbH and Co. KG, Hanover, Germany, p. 224.

Buffone, M.G., Wertheimer, E.V., Visconti, P.E., and Krapf, D. (2014) Central role of soluble adenylyl cyclase and cAMP in sperm physiology. *Biochim. Biophys. Acta*, **1842** (12 Part B), 2610–2620.

Burgess, C.M., Bredl, J.C., Plummer, J.M., and England, G.C. (2001) Vital and ultrastructural changes in dog spermatozoa during cryopreservation. *J. Reprod. Fertil. Suppl.*, **57**, 357–363.

Cai, X. and Clapham, D.E. (2008) Evolutionary genomics reveals lineage-specific gene loss and rapid evolution of a sperm-specific ion channel complex: CatSpers and CatSperβ. *PLoS One*, **3** (10), e3569.

Cakmak, H., Franciosi, F., Zamah, A.M., Cedars, M.I., and Conti, M. (2016) Dynamic secretion during meiotic reentry integrates the function of the oocyte and cumulus cells. *Proc. Natl. Acad. Sci. USA*, **113** (9), 2424–2429.

Carr, D.W., Usselman, M.C., and Acott, T.S. (1985) Effects of pH, lactate, and viscoelastic drag on sperm motility: a species comparison. *Biol. Reprod.*, **33** (3), 588–595.

Downloaded From Vet-eBooks.com

Case, L. (2005) *The Dog: Its Behavior, Nutrition, & Health*, 2nd edn, Blackwell Publishing, Ames, IA, 479 pp.

Cassani, P., Beconi, M.T., and O'Flaherty, C. (2005) Relationship between total superoxide dismutase activity with lipid peroxidation, dynamics and morphological parameters in canine semen. *Anim. Reprod. Sci.*, **86** (1–2), 163–173.

Cassatella, D., Martino, N.A., Valentini, L., Guaricci, A.C., Cardone, M.F., Pizzi, F., Dell'Aquila, M.E., and Ventura, M. (2013) Male infertility and copy number variants (CNVs) in the dog: a two-pronged approach using Computer Assisted Sperm Analysis (CASA) and Fluorescent *In Situ* Hybridization (FISH). *BMC Genomics*, **14**, 921.

Chandler, J.A., Sinowatz, F., and Pierrepoint, C.G. (1981) The ultrastructure of dog epididymis. *Urol. Res.*, **9** (1), 33–44.

Chang, M.C. (1951) Fertilizing capacity of spermatozoa deposited into the fallopian tubes. *Nature*, **168**, 997–998.

Chastant-Maillard, S., Chebrout, M., Thoumire, S., Saint-Dizier, M., Chodkiewicz, M., and Reynaud, K. (2010) Embryo biotechnology in the dog: a review. *Reprod. Fertil. Dev.*, **22** (7), 1049–1056.

Chastant-Maillard, S., Viaris de Lesegno, C., Chebrout, M., Thoumire, S., Meylheuc, T., Fontbonne, A., Chodkiewicz, M., Saint-Dizier, M., and Reynaud, K. (2011) The canine oocyte: uncommon features of *in vivo* and *in vitro* maturation. *Reprod. Fertil. Dev.*, **23** (3), 391–402.

Chatdarong, K., Chaivechakarn, A., Thuwanut, P., and Ponglowhapan, S. (2012) Effects of cold storage prior to freezing on superoxide dismutase, glutathione peroxidase activities, level of total reactive oxygen species and sperm quality in dogs. *Reprod. Domest. Anim.*, **47** (Suppl. 6), 274–277.

Chen, Y., Cann, M.J., Litvin, T.N., Iourgenko, V., Sinclair, M.L., Levin, L.R., and Buck, J. (2000) Soluble adenylyl cyclase as an evolutionarily conserved bicarbonate sensor. *Science*, **289** (5479), 625–628.

Cheon, K.W., Choi, Y.J., Byun, H.K., Hong, J.Y., Choi, H.K., and Seo, J.T. (2004) Expression of sperm-specific cation channel CatSper in human spermatozoa. *Korean J. Urol.*, **45** (4), 365–372.

Chung, J.J., Navarro, B., Krapivinsky, G., Krapivinsky, L., and Clapham, D.E. (2011) A novel gene required for male fertility and functional CATSPER channel formation in spermatozoa. *Nat. Commun.*, **2**, 153.

Chung, J.J., Shim, S.H., Everley, R.A., Gygi, S.P., Zhuang, X., and Clapham, D.E. (2014) Structurally distinct Ca(2+) signaling domains of sperm flagella orchestrate tyrosine phosphorylation and motility. *Cell*, **157** (4), 808–822.

Clarke, G.N. and Yanagimachi, R. (1978) Actin in mammalian sperm heads. *J. Exp. Zool.*, **205** (1), 125–132.

Clement, P.B. (1987) Anatomy and histology of the ovary, in *Blaustein's Pathology of the Female Genital Tract*, 3rd edn (ed. R.J. Kurman), Springer, New York, pp. 438–470.

Clermont, Y. (1963) The cycle of the seminiferous epithelium in man. *Am. J. Anat.*, **112**, 35–51.

Cochran, P.E. (2011) *Laboratory Manual for Comparative Veterinary Anatomy & Physiology*, 2nd edn, Cengage Learning, Clifton Park, NY, p. 416.

Concannon, P.W. (2009) Endocrinologic control of normal canine ovarian function. *Reprod. Domest. Anim.*, **44** (Suppl. 2), 3–15.

Concannon, P.W. (2011) Reproductive cycles of the domestic bitch. *Anim. Reprod. Sci.*, **124**, 200–210.

Concannon, P., Hansel, W., and McEntee, K. (1977) Changes in LH, progesterone and sexual behavior associated with preovulatory luteinization in the bitch. *Biol. Reprod.*, **17** (4), 604–613.

Concannon, P., Tsutsui, T., and Shille, V. (2001) Embryo development, hormonal requirements and maternal responses during canine pregnancy. *J. Reprod. Fertil. Suppl.*, **57**, 169–179.

Downloaded From Vet-eBooks.com

Concannon, P.W., Castracane, V.D., Temple, M., and Montanez, A. (2009) Endocrine control of ovarian function in dogs and other carnivores. *Anim. Reprod.*, **6**, 172–193.

Conquer, J.A., Martin, J.B., Tummon, I., Watson, L., and Tekpetey, F. (1999) Fatty acid analysis of blood serum, seminal plasma, and spermatozoa of normozoospermic vs. asthenozoospermic males. *Lipids*, **34** (8), 793–799.

Constantinescu, G.M. (2007) Anatomy of reproductive organs, in *Comparative Reproductive Biology* (eds H. Schatten and G.M. Constantinescu), Blackwell Publishing, Ames, IA, pp. 5–59.

Cooper, T.G. (2011) The epididymis, cytoplasmic droplets and male fertility. *Asian J. Androl.*, **13** (1), 130–138.

Cooper, T.G. and Yeung, C.H. (2003) Acquisition of volume regulatory response of sperm upon maturation in the epididymis and the role of the cytoplasmic droplet. *Microsc. Res. Tech.*, **61** (1), 28–38.

Cortes, C.J., Codelia, V.A., Manosalva, I., de Lange, J., De Los Reyes, M., and Moreno, R.D. (2006) Proacrosin/acrosin quantification as an indicator of acrosomal integrity in fresh and frozen dog spermatozoa. *Anim. Reprod. Sci.*, **93** (1–2), 165–175.

Courcier, E.A., Thomson, R.M., Mellor, D.J., and Yam, P.S. (2010) An epidemiological study of environmental factors associated with canine obesity. *J. Small Anim. Pract.*, **51** (7), 362–367.

Coy, P., Garcia-Vazquez, F.A., Visconti, P.E., and Aviles, M. (2012) Roles of the oviduct in mammalian fertilization. *Reproduction*, **144** (6), 649–660.

Cummins, J.M. and Woodall, P.F. (1985) On mammalian sperm dimensions. *J. Reprod. Fertil.*, **75**, 153–175.

Dahlbom, M., Andersson, M., Vierula, M., and Alanko, M. (1997) Morphometry of normal and teratozoospermic canine sperm heads using an image analyzer: work in progress. *Theriogenology*, **48** (4), 687–698.

Dale, B., Menezo, Y., Cohen, J., DiMatteo, L., and Wilding, M. (1998) Intracellular pH regulation in the human oocyte. *Hum. Reprod.*, **13** (4), 964–970.

Darin-Bennett, A., Poulos, A., and White, I.G. (1974) The phospholipids and phospholipid-bound fatty acids and aldehydes of dog and fowl spermatozoa. *J. Reprod. Fertil.*, **41** (2), 471–474.

De Lesegno, C.V., Reynaud, K., Pechoux, C., Thoumire, S., and Chastant-Maillard, S. (2008) Ultrastructure of canine oocytes during *in vivo* maturation. *Mol. Reprod. Dev.*, **75** (1), 115–125.

De los Reyes, M., Palomino, J., de Lange, J., Anguita, C., and Barros, C. (2009) *In vitro* sperm penetration through the zona pellucida of immature and *in vitro* matured oocytes using fresh, chilled and frozen canine semen. *Anim. Reprod. Sci.*, **110** (1–2), 37–45.

De los Reyes, M., Palomino, J., Martínez, V., Aretio, C., and Gutiérrez, M. (2011) Acrosin release and acrosin activity during incubation in capacitating media using fresh and frozen-thawed dog sperm. *Biol. Res.*, **44** (2), 139–144.

De los Reyes, M., Palomino, J., Jofre, S., Villarroel, A., and Moreno, R. (2012) Golgi apparatus and endoplasmic reticulum dynamic during meiotic development in canine oocytes. *Reprod. Domest. Anim.*, **47** (Suppl. 6), 93–97.

de Vries, K.J., Wiedmer, T., Sims, P.J., and Gadella, B.M. (2003) Caspase-independent exposure of aminophospholipids and tyrosine phosphorylation in bicarbonate responsive human sperm cells. *Biol. Reprod.*, **68** (6), 2122–2134.

Del Carro, A.P., Rosset, E., Josson-Schramme, A., Lambert, V., and Buff, S. (2014) First description of scrotal testicles in a dog affected by 78, XX testicular disorder of sex development. *Reprod. Domest. Anim.*, **49** (5), E48–E52.

Deng, W. and Lin, H. (2002) *miwi*, a murine homolog of *piwi*, encodes a cytoplasmic protein essential for spermatogenesis. *Dev. Cell*, **2** (6), 819–830.

Doak, R.L., Hall, A., and Dale, H.E. (1967) Longevity of spermatozoa in the reproductive tract of the bitch. *J. Reprod. Fertil.*, **13**, 51–58.

Downloaded From Vet-eBooks.com

Drake, A.G., Coquerelle, M., and Colombeau, G. (2015) 3D morphometric analysis of fossil canid skulls contradicts the suggested domestication of dogs during the late Paleolithic. *Sci. Rep.*, **5**, 8299.

Drier, H.K. (1998) Canine infertility, in *Canine Medicine and Therapeutics*, 4th edn (ed. N.T. Gorman), Blackwell Science, Ltd., Osney Mead, Oxford, pp. 734–752.

du Plessis, S.S., Agarwal, A., Mohanty, G., and van der Linde, M. (2015) Oxidative phosphorylation versus glycolysis: what fuel do spermatozoa use? *Asian J. Androl.*, **17** (2), 230–235.

Duleba, A., Skonieczna, K., Bogdanowicz, W., Malyarchuk, B., and Grzybowski, T. (2015) Complete mitochondrial genome database and standardized classification system for *Canis lupus familiaris*. *Forensic Sci. Int. Genet.*, **19**, 123–129.

Edashige, K., Yamaji, Y., Kleinhans, F.W., and Kasai, M. (2003) Artificial expression of aquaporin-3 improves the survival of mouse oocytes after cryopreservation. *Biol. Reprod.*, **68** (1), 87–94.

Eddy, E.M. and O'Brien, D.A. (1994) The spermatozoon, in *The Physiology of Reproduction*, 2nd edn (eds E. Knobil and J.D. Neill), Raven Press Ltd., New York, NY, pp. 189–317.

Ellinwood, N.M., Casal, M.L., and Haskins, M.E. (2006) Gene therapy for metabolic inherited diseases in dogs, in *The Dog and Its Genome* (eds E.A. Ostrander, U. Giger, and K. Lindblad-Toh), Cold Spring Harbor Press, Cold Spring Harbor, NY, pp. 473–495.

England, G.C.W. (1993) Cryopreservation of dog semen: a review. *J. Reprod. Fertil. Suppl.*, **47**, 243–255.

England, G.C.W. (2013) *Dog Breeding, Whelping and Puppy Care*, John Wiley & Sons, Ltd., Chichester, 340 pp.

England, G.C.W. and Allen, W.E. (1989) Seminal characteristics and fertility in dogs. *Vet. Rec.*, **125**, 399.

England, G.C., Russo, M., and Freeman, S.L. (2009) Follicular dynamics, ovulation and conception rates in bitches. *Reprod. Domest. Anim.*, **44** (Suppl. 2), 53–58.

England, G.C., Burgess, C.M., Clutterbuck, A.L., and Freeman, S.L. (2013) Epithelial surface changes and spermatozoa storage in the reproductive tract of the bitch. *Vet. J.*, **195** (2), 185–191.

Evans, E.I. (1933) The transport of sperm in the dog. *Am. J. Physiol.*, **105**, 287–293.

Evans, H.M. and Cole, H.H. (1931) *An Introduction to the Study of the Oestrous Cycle in the Dog*. Memoirs of the University of California, vol. 9, pp. 65–118.

Evans, H.E. and De Lahunta, A. (2013) *Miller's Anatomy of the Dog*, 4th edn, Elsevier, St. Louis, MO, 850 pp.

Ezashi, T., Yuan, Y., and Roberts, R.M. (2016) Pluripotent stem cells from domesticated mammals. *Annu. Rev. Anim. Biosci.*, **4**, 223–253.

Fahiminiya, S., Reynaud, K., Labas, V., Batard, S., Chastant-Maillard, S., and Gerard, N. (2010) Steroid hormones content and proteomic analysis of canine follicular fluid during the preovulatory period. *Reprod. Biol. Endocrinol.*, **8**, 132.

Falzone, N., Huyser, C., Becker, P., Leszczynski, D., and Franken, D.R. (2011) The effect of pulsed 900-MHz GSM mobile phone radiation on the acrosome reaction, head morphometry and zona binding of human spermatozoa. *Int. J. Androl.*, **34**, 20–26.

Farstad, W. (2000) Assisted reproductive technology in canid species. *Theriogenology*, **53**, 175–186.

Fawcett, D.W. (1975) The mammalian spermatozoon. *Dev. Biol.*, **44**, 394–436.

FCI (2015) Federation Cynologique Internationale also called World Canine Organization. Retrieved from www.fci.be (July 2, 2015).

Federici, F., Mulugeta, E., Schoenmakers, S., Wassenaar, E., Hoogerbrugge, J.W., van der Heijden, G.W., van Cappellen, W.A., Slotman, J.A., van IJcken, W.F., Laven, J.S., Grootegoed, J.A., and Baarends, W.M. (2015) Incomplete meiotic sex chromosome inactivation in the domestic dog. *BMC Genomics*, **16**, 291.

Downloaded From Vet-eBooks.com

Fehr, J., Meyer, D., Widmayer, P., Borth, H.C., Ackermann, F., Wilhelm, B., Gudermann, T., and Boekhoff, I. (2007) Expression of the G-protein alpha-subunit gustducin in mammalian spermatozoa. *J. Comp. Physiol. A Neuroethol. Sens. Neural. Behav. Physiol.*, **193** (1), 21–34.

Feldman, E.C. and Nelson, R.W. (2004) *Canine and Feline Endocrinology and Reproduction*, 3rd edn, Saunders, St. Louis, MO, 1091 pp.

Fernández-Novell, J.M., Ballester, J., Altirriba, J., Ramió-Lluch, L., Barberà, A., Gomis, R., Guinovart, J.J., and Rodríguez-Gil, J.E. (2011) Glucose and fructose as functional modulators of overall dog, but not boar sperm function. *Reprod. Fertil. Dev.*, **23** (3), 468–480.

Ferreira, C.R., Saraiva, S.H., Catharino, R.R., Garcia, J.S., Gozzo, F.C., Sanvido, G.B., Santos, L.F.A., Lo Turco, E.G., Pontes, J.H.F., Basso, A.C., Bertolla, R.P., Sartori, R., Guardieiro, M.M., Perecin, F., Meirelles, F.V., Sangalli, J.R., and Eberlin, M.N. (2010) Single embryo and oocyte lipid fingerprinting by mass spectrometry. *J. Lipid Res.*, **51** (5): 1218–1227.

Ferrer, M., Rodriguez, H., Zara, L., Yu, Y., Xu, W., and Oko, R. (2012) MMP2 and acrosin are major proteinases associated with the inner acrosomal membrane and may cooperate in sperm penetration of the zona pellucida during fertilization. *Cell Tissue Res.*, **349** (3), 881–895.

Flesch, F.M. and Gadella, B.M. (2000) Dynamics of the mammalian sperm plasma membrane in the process of fertilization. *Biochim. Biophys. Acta*, **1469** (3), 197–235.

Florman, H.M. and Fissore, R.A. (2015) Fertilization in mammals, in *Knobil and Neill's Physiology of Reproduction*, 4th edn (eds T.M. Plant and A.J. Zeleznik), vol. 1, Academic Press, Waltham, MA, pp. 149–196.

Foote, R.H., Swierstra, E.E., and Hunt, W.L. (1972) Spermatogenesis in the dog. *Anat. Rec.*, **173** (3), 341–351.

Ford, W.C. (2006) Glycolysis and sperm motility: does a spoonful of sugar help the flagellum go round? *Hum. Reprod. Update*, **12** (3), 269–274.

Forsberg, C.L. and Reynaud, K. (2012) Biology of reproduction and modern reproductive technology, in *The Genetics of the Dog*, 2nd edn (eds E.A. Ostrander and A. Ruvinsky), CABI Publishing, Oxford, pp. 295–320.

Fransson, B.A. (2012) Ovaries and uterus, in *Veterinary Surgery: Small Animal*, 1st edn (eds K.M. Tobias and S.A. Johnston), vol. 1, Elsevier, St. Louis, MO, pp. 1871–1890.

Freedman, A.H., Gronau, I., Schweizer, R.M., Ortega-Del Vecchyo, D., Han, E. et al. (2014) Genome sequencing highlights the dynamic early history of dogs. *PLoS Genet.*, **10** (1), e1004016.

Freeman, S.L. and England, G.C. (2013) Storage and release of spermatozoa from the pre-uterine tube reservoir. *PLoS One*, **8** (2), e57006.

Fukuda, N., Yomogida, K., Okabe, M., and Touhara, K. (2004) Functional characterization of a mouse testicular olfactory receptor and its role in chemosensing and in regulation of sperm motility. *J. Cell Sci.*, **117** (Part 24), 5835–5845.

Fulton, R.M., Keskintepe, L., Durrant, B.S., and Fayrer-Hosken, R.A. (1998) Intracytoplasmic sperm injection (ICSI) for the treatment of canine infertility. *Theriogenology*, **49**, 366 (Abstract).

Gadelha, C.R.F., Vicente, W.R.R., Ribeiro, A.P.C., Apparicio, M., Covizzi, G.J., and Campos, A.C.N. (2013) Prostatic acid phosphatase in serum and semen of dogs. *Arch. Med. Vet.*, **45**, 321–325.

Gadella, B.M. and Boerke, A. (2016) An update on post-ejaculatory remodeling of the sperm surface before mammalian fertilization. *Theriogenology*, **85** (1), 113–124.

Gardner, D.K., Lane, M., Calderon, I., and Leeton, J. (1996) Environment of the preimplantation human embryo *in vivo*: metabolite analysis of oviduct and uterine fluids and metabolism of cumulus cells. *Fertil. Steril.*, **65** (2), 349–353.

Garner, D.L., Evans, K.M., and Seidel, G.E. (2013) Sex-sorting sperm using flow cytometry/cell sorting. *Methods Mol. Biol.*, **927**, 279–295.

Gelberg, H.B. and McEntee, K. (1986) Pathology of the canine and feline uterine tube. *Vet. Pathol.*, **23** (6), 770–775.

Downloaded From Vet-eBooks.com

Gergely, A., Kovanci, E., Senturk, L., Cosmi, E., Vigue, L., and Huszar, G. (1999) Morphometric assessment of mature and diminished-maturity human spermatozoa: sperm regions that reflect differences in maturity. *Hum. Reprod.*, **14** (8), 2007–2014.

Giger, U., Sargan, D.R., and McNiel, E.A. (2006) Breed-specific hereditary diseases and genetic screening, in *The Dog and Its Genome* (eds E.A. Ostrander, U. Giger, and K. Lindblad-Toh), Cold Spring Harbor Press, Cold Spring Harbor, NY, pp. 249–289.

Gobello, C., Castex, G., and Corrada, Y. (2002) Serum and seminal markers in the diagnosis of disorders of the genital tract of the dog: a mini-review. *Theriogenology*, **57** (4), 1285–1291.

Gomez, P.N., Alvarez, J.G., Risopatron, J., Romero, F., and Sanchez, R. (2012) Effect of tubal explants and their secretions on bovine spermatozoa: modulation of ROS production and DNA damage. *Reprod. Fertil. Dev.*, **24** (6), 871–876.

González, R. and Dobrinski, I. (2015) Beyond the mouse monopoly: studying the male germ line in domestic animal models. *ILAR J.*, **56** (1), 83–98.

González-Fernández, L., Ortega-Ferrusola, C., Macias-Garcia, B., Salido, G.M., Peña, F.J., and Tapia, J.A. (2009) Identification of protein tyrosine phosphatases and dual-specificity phosphatases in mammalian spermatozoa and their role in sperm motility and protein tyrosine phosphorylation. *Biol. Reprod.*, **80** (6), 1239–1252.

Gordeeva, E.G., Shileiko, L.V., Pankratova, O.S., and Kurilo, L.F. (2011) Aneuploidy frequency in sperm of fertile men. *Russ. J. Genet.*, **47** (6), 732–738.

Goudet, G., Mugnier, S., Callebaut, I., and Monget, P. (2008) Phylogenetic analysis and identification of pseudogenes reveal a progressive loss of zona pellucida genes during evolution of vertebrates. *Biol. Reprod.*, **78**, 796–806.

Grimm, D. (2015a) Dawn of the dog. *Science*, **348** (6232), 274–279.

Grimm, D. (2015b) Why we outlive our pets. *Science*, **350** (6265), 1182–1185.

Groppetti, D., Aralla, M., Bronzo, V., Bosi, G., Pecile, A., and Arrighi, S. (2015) Periovulatory time in the bitch: what's new to know? Comparison between ovarian histology and clinical features. *Anim. Reprod. Sci.*, **152**, 108–116.

Gulaya, N.M., Margitich, V.M., Govseeva, N.M., Klimashevsky, V.M., Gorpynchenko, I.I., and Boyko, M.I. (2001) Phospholipid composition of human sperm and seminal plasma in relation to sperm fertility. *Arch. Androl.*, **46** (3), 169–175.

Gustavsson, I. (1963) The chromosomes of the dog. *Hereditas*, **51** (1), 187–189.

Gwatkin, R.B.L. (1977) *Fertilization Mechanisms in Man and Mammals*, Plenum Press, New York.

Haenisch-Woehl, A., Kölle, S., Neumüller, C., Sinowatz, F., and Braun, J. (2003) Morphology of canine cumulus-oocyte complexes in pre-pubertal bitches. *Anat. Histol. Embryol.*, **32** (6), 373–377.

Haifler, M., Girshovitz, P., Band, G., Dardikman, G., Madjar, I., and Shaked, N.T. (2015) Interferometric phase microscopy for label-free morphological evaluation of sperm cells. *Fertil. Steril.*, **104** (1), 43–47.

Hall, V., Hinrichs, K., Lazzari, G., Betts, D.H., and Hyttel, P. (2013) Early embryonic development, assisted reproductive technologies, and pluripotent stem cell biology in domestic mammals. *Vet. J.*, **197** (2), 128–142.

Hallap, T., Nagy, S., Jaakma, U., Johannisson, A., and Rodriguez-Martinez, H. (2006) Usefulness of a triple fluorochrome combination Merocyanine 540/Yo-Pro 1/Hoechst 33342 in assessing membrane stability of viable frozen-thawed spermatozoa from Estonian Holstein AI bulls. *Theriogenology*, **65** (6), 1122–1136.

Harris, S.E., Gopichandran, N., Picton, H.M., Leese, H.J., and Orsi, N.M. (2005) Nutrient concentrations in murine follicular fluid and the female reproductive tract. *Theriogenology*, **64** (4), 992–1006.

Downloaded From Vet-eBooks.com

Harrison, R.A., Ashworth, P.J., and Miller, N.G. (1996) Bicarbonate/CO_2, an effector of capacitation, induces a rapid and reversible change in the lipid architecture of boar sperm plasma membranes. *Mol. Reprod. Dev.*, **45** (3), 378–391.

Hassold, T. and Hunt, P. (2001) To err (meiotically) is human: the genesis of human aneuploidy. *Nat. Rev. Genet.*, **2** (4), 280–291.

Hatoya, S., Sugiyama, Y., Torii, R., Wijewardana, V., Kumagai, D., Sugiura, K., Kida, K., Kawate, N., Tamada, H., Sawada, T., and Inaba, T. (2006) Effect of co-culturing with embryonic fibroblasts on IVM, IVF and IVC of canine oocytes. *Theriogenology*, **66** (5), 1083–1090.

Hayes, H.M., Tarone, R.E., Casey, H.W., and Huxsoll, D.L. (1990) Excess of seminomas observed in Vietnam service U.S. military working dogs. *J. Natl. Cancer Inst.*, **82** (12), 1042–1046.

Hayes, B., Fagerlie, S.R., Ramakrishnan, A., Baran, S., Harkey, M., Graf, L., Bar, M., Bendoraite, A., Tewari, M., and Torok-Storb, B. (2008) Derivation, characterization, and *in vitro* differentiation of canine embryonic stem cells. *Stem Cells*, **26** (2), 465–473.

Hereng, T.H., Elgstoen, K.B., Cederkvist, F.H., Eide, L., Jahnsen, T., Skalhegg, B.S., and Rosendal, K.R. (2011) Exogenous pyruvate accelerates glycolysis and promotes capacitation in human spermatozoa. *Hum. Reprod.*, **26** (12), 3249–3263.

Hess, R.A. and Renato de Franca, L. (2008) Spermatogenesis and cycle of the seminiferous epithelium. *Adv. Exp. Med. Biol.*, **636**, 1–15.

Hewitt, D.A. and England, G.C.W. (2001) Manipulation of canine fertility using *in vitro* culture techniques. *J. Reprod. Fertil. Suppl.*, **57**, 111–125.

Heyn, H., Ferreira, H.J., Bassas, L., Bonache, S., Sayols, S., Sandoval, J., Esteller, M., and Larriba, S. (2012) Epigenetic disruption of the PIWI pathway in human spermatogenic disorders. *PLoS One*, **7** (10), e47892.

Hoeppner, M.P., Lundquist, A., Pirun, M., Meadows, J.R.S., Zamani, N. et al. (2014) An improved canine genome and a comprehensive catalogue of coding genes and non-coding transcripts. *PLoS One*, **9** (3), e91172.

Hohšteter, M., Artuković, B., Severin, K., Kurilj, A.G., Beck, A., Šoštarić-Zuckermann, I.C., and Grabarević, Ž. (2014) Canine testicular tumors: two types of seminomas can be differentiated by immunohistochemistry. *BMC Vet. Res.*, **10**, 169.

Holst, P.A. and Phemister, R.D. (1971) The prenatal development of the dog: pre-implantation events. *Biol. Reprod.*, **5**, 194–206.

Hong, S.G. Kim, M.K. Jang, G. Oh, H.J. Park, J.E. Kang, J.T. Koo, O.J. Kim, T. Kwon, M.S. Koo, B.C. Ra, J.C. Kim, D.Y. Ko, C. and Lee, B.C. (2009) Generation of red fluorescent protein transgenic dogs. *Genesis*, **47** (5), 314–322.

Hook, S.J. and Hafez, E.S.E. (1969) A comparative anatomical study of the mammalian uterotubal junction. *J. Morphol.*, **125** (2), 159–184.

Hori, T., Matsuda, Y., Kobayashi, M., Kawakami, E., and Tsutsui, T. (2011) Comparison of fertility on intrauterine insemination between cryopreserved ejaculated and cauda epididymal sperm in dogs. *J. Vet. Med. Sci.*, **73** (12), 1685–1688.

Hossain, M.S., Johannisson, A., Wallgren, M., Nagy, S., Siqueira, A.P., and Rodriguez-Martinez, H. (2011) Flow cytometry for the assessment of animal sperm integrity and functionality: state of the art. *Asian J. Androl.*, **13** (3), 406–419.

HSUS (2015) Humane Society of the United States. Retrieved from http://www.humanesociety.org/issues/pet_overpopulation/facts/pet_ownership_statistics.html (July 2, 2015).

Huang, S.Y., Kuo, Y.H., Tsou, H.L., Lee, Y.P., King, Y.T., Huang, H.C., Yang, P.C., and Lee, W.C. (2000) The decline of porcine sperm motility by geldanamycin, a specific inhibitor of heat-shock protein 90 (HSP90). *Theriogenology*, **53** (5), 1177–1184.

Huson, H.J. (2012) Genetic aspects of performance in working dogs, in *The Genetics of the Dog*, 2nd edn (eds E.A. Ostrander and A. Ruvinsky), CABI Publishing, Oxford, pp. 477–495.

Downloaded From Vet-eBooks.com

Ibach, B., Weissbach, L., and Hilscher, B. (1976) Stages of the cycle of the seminiferous epithelium in the dog. *Andrologia*, **8** (4), 297–307.

Inaba, K. (2011) Sperm flagella: comparative and phylogenetic perspectives of protein components. *Mol. Hum. Reprod.*, **17** (8), 524–538.

Inoue, N., Hagihara, Y., Wright, D., Suzuki, T., and Wada, I. (2015) Oocyte-triggered dimerization of sperm IZUMO1 promotes sperm–egg fusion in mice. *Nat. Commun.*, **6**, 8858.

Itach, S.B., Finklestein, M., Etkovitz, N., and Breitbart, H. (2012) Hyper-activated motility in sperm capacitation is mediated by phospholipase D-dependent actin polymerization. *Dev. Biol.*, **362** (2), 154–161.

Ito, J., Kawabe, M., Ochiai, H., Suzukamo, C., Harada, M., Mitsugi, Y., Seita, Y., and Kashiwazaki, N. (2008) Expression and immunodetection of aquaporin 1 (AQP1) in canine spermatozoa. *Cryobiology*, **57** (3), 312–314.

Jang, G., Kim, M.K., Oh, H.J., Hossein, M.S., Fibrianto, Y.H., Hong, S.G., Park, J.E., Kim, J.J., Kim, H.J., Kang, S.K., Kim, D.Y., and Lee, B.C. (2007) Birth of viable female dogs produced by somatic cell nuclear transfer. *Theriogenology*, **67** (5), 941–947.

Jin, Y.X., Lee, H.S., Yin, X.J., Cui, X.S., Kong, I.K., and Kim, N.H. (2006) Chromatin, microtubule and microfilament configurations in the canine oocyte. *Reprod. Fertil. Dev.*, **18** (8), 849–856.

Jodar, M. and Oliva, R. (2014) Protamine alterations in human spermatozoa. *Adv. Exp. Med. Biol.*, **791**, 83–102.

Johnson, P.A., Yelick, P.C., Liem, H., and Hecht, N.B. (1988) Differential distribution of the P1 and P2 protamine gene sequences in eutherian and marsupial mammals and a monotreme. *Gamete Res.*, **19** (2), 169–175.

Jones, D.E. and Joshua, J.O. (1988) *Reproductive Clinical Problems in the Dog*, 2nd edn, Wright, London, Chapter 4, pp. 33–54.

Karger, S., Arlt, S., Haimerl, P., and Heuwieser, W. (2014) A systematic review of studies performing the hypo-osmotic swelling test to evaluate the quality of canine spermatozoa. *Reprod. Domest. Anim.*, **49** (1), 1–6.

Karre, I., Meyer-Lindenberg, A., Urhausen, C., Beineke, A., Meinecke, B., Piechotta, M., Beyerbach, M., and Günzel-Apel, A.R. (2012) Distribution and viability of spermatozoa in the canine female genital tract during post-ovulatory oocyte maturation. *Acta Vet. Scand.*, **54**, 49.

Kasimanickam, V.R. and Kasimanickam, R.K. (2015) Differential expression of microRNAs in sexually immature and mature canine testes. *Theriogenology*, **83** (3), 394–398.

Kasimanickam, V.R., Kasimanickam, R.K., and Dernell, W.S. (2014) Dysregulated microRNA clusters in response to retinoic acid and CYP26B1 inhibitor induced testicular function in dogs. *PLoS One*, **9** (6), e99433.

Kawakami, E., Naitoh, H., Ogasawara, M., Tamura, M., Hasegawa, J., Tsutsui, T., and Ogasa, A. (1991) Hyperactivation and acrosome reaction *in vitro* in spermatozoa ejaculated by cryptorchid dogs after orchiopexy. *J. Vet. Med. Sci.*, **53** (3), 447–450.

Kawakami, E., Vandevoort, C.A., Mahi-Brown, C.A., Tollner, T.L., and Overstreet, J.W. (1993a) Comparison of a fluoresceinated lectin stain with triple staining for evaluating acrosome reactions of dog sperm. *J. Exp. Zool.*, **265** (5), 599–603.

Kawakami, E., Vandevoort, C.A., Mahi-Brown, C.A., and Overstreet, J.W. (1993b) Induction of acrosome reactions of canine sperm by homologous zona pellucida. *Biol. Reprod.*, **48** (4), 841–845.

Kawakami, E., Arai, T., and Oishi, I. (1999a) Changes in hyaluronidase, acrosin, and *N*-acetylhexosaminidase activities of dog sperm after incubation. *J. Vet. Med. Sci.*, **61** (2), 183–184.

Kawakami, E., Arai, T., and Nakamura, U. (1999b) Effects of medium containing heparin and theophylline on capacitation and metabolic enzyme activities of ejaculated spermatozoa from dogs with asthenozoospermia. *Anim. Reprod. Sci.*, **54** (4), 251–259.

Downloaded From Vet-eBooks.com

Kawakami, E., Sato, T., Hirano, T., Hori, T., and Tsutsui, T. (2004a) Disappearance of the PHA-E lectin binding site on the surface of ejaculated sperm and sperm capacitation in the dog. *J. Vet. Med. Sci.*, **66** (5), 495–500.

Kawakami, E., Hirano, T., Hori, T., and Tsutsui, T. (2004b) Protease-induced hyperactivation of canine spermatozoa associated with disappearance of lectin-binding glycoproteins on their surface. *J. Vet. Med. Sci.*, **66** (9), 1027–1031.

Kawakami, E., Ozawa, T., Hirano, T., Hori, T., and Tsutsui, T. (2005) Formation of detached tail and coiled tail of sperm in a beagle dog. *J. Vet. Med. Sci.*, **67** (1), 83–85.

Kawakami, E., Nishizono, Y., Miyata, C., Hirano, T., Hori, T., and Tsutsui, T. (2006) Effects of hyaluronic acid on Ca^{2+} influx, lactate dehydrogenase activity, and cyclic AMP synthesis in canine ejaculated sperm during *in vitro* capacitation. *J. Vet. Med. Sci.*, **68** (2), 119–123.

Kawakami, E., Takemura, A., Sakuma, M., Takano, M., Hirano, T., Hori, T., and Tsutsui, T. (2007) Superoxide dismutase and catalase activities in the seminal plasma of normozoospermic and asthenozoospermic Beagles. *J. Vet. Med. Sci.*, **69** (2), 133–136.

Kawakami, E., Kobayashi, M., Hori, T., and Kaneda, T. (2015) Therapeutic effects of vitamin E supplementation in 4 dogs with poor semen quality and low superoxide dismutase activity in seminal plasma. *J. Vet. Med. Sci.*, **77** (12), 1711–1714.

Kay, V.J. and Robertson, L. (1998) Hyperactivated motility of human spermatozoa: a review of physiological function and application in assisted reproduction. *Hum. Reprod. Update*, **4** (6), 776–786.

KC (2015) The Kennel Club of the United Kingdom. Retrieved from www.thekennelclub.org.uk (July 2, 2015).

Kempisty, B., Piotrowska, H., Bukowska, D., Wozna, M., Ciesiolka, S., Wojtanowicz-Markiewicz, K., Włodarczyk, R., Jopek, K., Jeseta, M., Bruska, M., Nowicki, M., Jaśkowski, J.M., Brüssow, K.P., and Zabel, M. (2015) Expression and cellular distribution of zona pellucida glycoproteins in canine oocytes before and after *in vitro* maturation. *Zygote*, **23** (6), 863–873.

Kim, K.S., Lee, S.E., Jeong, H.W., and Ha, J.H. (1998) The complete nucleotide sequence of the domestic dog (*Canis familiaris*) mitochondrial genome. *Mol. Phylogenet. Evol.*, **10** (2), 210–220.

Kim, M.J., Oh, H.J., Park, J.E., Kim, G.A., Hong, S.G., Jang, G. et al. (2011) Generation of transgenic dogs that conditionally express green fluorescent protein. *Genesis*, **49** (6), 472–478.

Kim, M.J., Oh, H.J., Kim, G.A., Park, J.E., Park, E.J., Jang, G., Ra, J.C., Kang, S.K., and Lee, B.C. (2012) Lessons learned from cloning dogs. *Reprod. Domest. Anim.*, **47** (Suppl. 4), 115–119.

Kirchhoff, C. (2002) The dog as a model to study human epididymal function at a molecular level. *Mol. Hum. Reprod.*, **8** (8), 695–701.

Kleene, K.C. and Bagarova, J. (2008) Comparative genomics reveals gene-specific and shared regulatory sequences in the spermatid-expressed mammalian *Odf1*, *Prm1*, *Prm2*, *Tnp1*, and *Tnp2* genes. *Genomics*, **92** (2), 101–106.

Kobayashi, M., Wada, M., Hori, T., and Kawakami, E. (2014) Superoxide dismutase activity in the oviductal and uterine fluid of the bitch and the effects of the enzyme on viability, motility and hyperactivation of canine sperm *in vitro*. *J. Vet. Med. Sci.*, **76** (5), 741–743.

Koehler, J.K. (1981) Lectins as probes of the spermatozoon surface. *Arch. Androl.*, **6** (3), 197–217.

Komaki, H., Oi, M., and Suzuki, H. (2014) Detection of sex chromosome aneuploidy in dog spermatozoa by triple color fluorescence *in situ* hybridization. *Theriogenology*, **82** (4), 652–656.

Kotaja, N. (2014) MicroRNAs and spermatogenesis. *Fertil. Steril.*, **101** (6), 1552–1562.

Kowalewski, M.P. (2014) Luteal regression vs. prepartum luteolysis: regulatory mechanisms governing canine corpus luteum function. *Reprod. Biol.*, **14** (2), 89–102.

Kowalewski, M.P., Gram, A., Kautz, E., and Graubner, F.R. (2015) The dog: nonconformist, not only in maternal recognition signaling. *Adv. Anat. Embryol. Cell Biol.*, **216**, 215–237.

Downloaded From Vet-eBooks.com

Kozono, D., Yasui, M., King, L.S., and Agre, P. (2002) Aquaporin water channels: atomic structure molecular dynamics meet clinical medicine. *J. Clin. Invest.*, **109** (11), 1395–1399.

Kuijk, E.W., de Gier, J., Lopes, S.M., Chambers, I., van Pelt, A.M., Colenbrander, B., and Roelen, B.A. (2010) A distinct expression pattern in mammalian testes indicates a conserved role for NANOG in spermatogenesis. *PLoS One*, **5** (6), e10987.

La Spina, F.A., Puga Molina, L.C., Romarowski, A., Vitale, A.M., Falzone, T.L., Krapf, D., Hirohashi, N., and Buffone, M.G. (2016) Mouse sperm begin to undergo acrosomal exocytosis in the upper isthmus of the oviduct. *Dev. Biol.*, **411** (2), 172–182.

Larson, G., Karlsson, E.K., Perri, A., Webster, M.T., Ho, S.Y., Peters, J., Stahl, P.W., Piper, P.J., Lingaas, F., Fredholm, M., Comstock, K.E., Modiano, J.F., Schelling, C., Agoulnik, A.I., Leegwater, P.A., Dobney, K., Vigne, J.D., Vilà, C., Andersson, L., and Lindblad-Toh, K. (2012) Rethinking dog domestication by integrating genetics, archeology, and biogeography. *Proc. Natl. Acad. Sci. USA*, **109** (23): 8878–8883.

Leahy, T. and Gadella, B.M. (2015) New insights into the regulation of cholesterol efflux from the sperm membrane. *Asian J. Androl.*, **17** (4), 561–567.

LeBlanc, A.K., Mazcko, C., Brown, D.E., Koehler, J.W., Miller, A.D., Miller, C.R., Bentley, R.T., Packer, R.A., Breen, M., Boudreau, C.E., Levine, J.M., Simpson, R.M., Halsey, C., Kisseberth, W., Rossmeisl, J.H., Jr., Dickinson, P.J., Fan, T.M., Corps, K., Aldape, K., Puduvalli, V., Pluhar, G.E., and Gilbert, M.R. (2016) Creation of an NCI comparative brain tumor consortium: informing the translation of new knowledge from canine to human brain tumor patients. *Neuro Oncol.*, pii: now051. doi: 10.1093/neuonc/now051.

Leblond, C.P. and Clermont, Y. (1952) Definition of the stages of the cycle of the seminiferous epithelium in the rat. *Ann. N. Y. Acad. Sci.*, **55** (4), 548–573.

Lee, C.H. and Cho, Y.H. (1999) Aspects of mammalian spermatogenesis: electrophoretical analysis of protamines in mammalian species. *Mol. Cells*, **9** (5), 556–559.

Lee, B.C., Kim, M.K., Jang, G., Oh, H.J., Yuda, F., Kim, H.J., Shamim, M.H., Kim, J.J., Kang, S.K., Schatten, G., and Hwang, W.S. (2005) Dogs cloned from adult somatic cells. *Nature*, **436**, 641.

Lee, S.R., Kim, B.S., Kim, J.W., Kim, M.O., Kim, S.H., Yoo, D.H., Shin, M.J., Park, Y.S., Lee, S., Park, Y.B., Ha, J.H., and Ryoo, Z.Y. (2007) *In vitro* maturation, *in vitro* fertilization and embryonic development of canine oocytes. *Zygote*, **15** (4): 347–353.

Lee, H.S., Yin, X.J., Jin, Y.X., Kim, N.H., Cho, S.G., Bae, I.H., and Kong, I.K. (2008) Germinal vesicle chromatin configuration and meiotic competence is related to the oocyte source in canine. *Anim. Reprod. Sci.*, **103** (3–4), 336–347.

Leonard, J.A., Vilà, C., and Wayne, R.K. (2006) From wild wolf to domestic dog, in *The Dog and Its Genome* (eds E.A. Ostrander, U. Giger, and K. Lindblad-Toh), Cold Spring Harbor Press, Cold Spring Harbor, NY, pp. 95–117.

Li, X., Staszewski, L., Xu, H., Durick, K., Zoller, M., and Adler, E. (2002) Human receptors for sweet and umami taste. *Proc. Natl. Acad. Sci. USA*, **99** (7), 4692–4696.

Li, K., Xue, Y., Chen, A., Jiang, Y., Xie, H., Shi, Q., Zhang, S., and Ni, Y. (2014) Heat shock protein 90 has roles in intracellular calcium homeostasis, protein tyrosine phosphorylation regulation, and progesterone-responsive sperm function in human sperm. *PLoS One*, **9** (12), e115841.

Li, W., Tang, W., Teves, M.E., Zhang, Z., Zhang, L., Li, H., Archer, K.J., Peterson, D.L., Williams, D.C., Jr., Strauss, J.F., 3rd, and Zhang, Z. (2015) A MEIG1/PACRG complex in the manchette is essential for building the sperm flagella. *Development*, **142** (5), 921–923.

Liang, P., Xu, Y., Zhang, X., Ding, C., Huang, R., Zhang, Z., Lv, J., Xie, X., Chen, Y., Li, Y., Sun, Y., Bai, Y., Songyang, Z., Ma, W., Zhou, C., and Huang, J. (2015) CRISPR/Cas9-mediated gene editing in human tripronuclear zygotes. *Protein Cell*, **6** (5), 363–372.

Downloaded From Vet-eBooks.com

Lindblad-Toh, K., Wade, C.M., Mikkelsen, T.S. et al. (2005) Genome sequence, comparative analysis and haplotype structure of the domestic dog. *Nature*, **438** (7069), 803–819.

Lishko, P.V., Botchkina, I.L., and Kirichok, Y. (2011) Progesterone activates the principal Ca^{2+} channel of human sperm. *Nature*, **471** (7338), 387–391.

Lishko, P.V., Kirichok, Y., Ren, D., Navarro, B., Chung, J.J., and Clapham, D.E. (2012) The control of male fertility by spermatozoan ion channels. *Annu. Rev. Physiol.*, **74**, 453–475.

Long, S. (2006) *Veterinary Genetics and Reproductive Physiology*, 1st edn, Butterworth-Heinemann, Oxford, UK, 132 pp.

Loos, R.J. (2012) Genetic determinants of common obesity and their value in prediction. *Best. Pract. Res. Clin. Endocrinol. Metab.*, **26** (2), 211–226.

Lopes, G., Rocha, A., and Sousa, M. (2010) Comparative ultrastructural analysis of diestrous and anestrous canine Grade 1 cumulus–oocyte complexes. *Anim. Reprod. Sci.*, **122** (3–4), 244–252.

López-Torres, A.S. and Chirinos, M. (2016) Modulation of human sperm capacitation by progesterone, estradiol, and luteinizing hormone. *Reprod. Sci.*, pii: 1933719116641766.

Lunardon, N.T., Silva-Santos, K.C., Justino, R.C., Dessunti, G.T., Seneda, M.M., and Martins, M.I. (2015) Population estimate of the preantral follicles and frequency of multioocyte follicles in prepubertal and adult bitches. *Theriogenology*, **83** (6), 1015–1020.

Lunn, M.O. and Wright, S.J. (2009) Imaging the zona pellucida of canine and feline oocytes using scanning electron microscopy. *Microsc. Microanal.*, **15** (1), 2–14.

Lunn, M.O. and Wright, S.J. (2013) Distinct subtypes of zona pellucida morphology reflect canine oocyte viability and cumulus–oocyte complex quality. *Theriogenology*, **80** (5), 498–506.

Luvoni, G.C., Chigioni, S., Allievi, E., and Macis, D. (2005) Factors involved *in vivo* and *in vitro* maturation of canine oocytes. *Theriogenology*, **63** (1), 41–59.

Magerkurth, C., Töpfer-Petersen, E., Schwartz, P., and Michelmann, H.W. (1999) Scanning electron microscopy analysis of the human zona pellucida: influence of maturity and fertilization on morphology and sperm binding pattern. *Hum. Reprod.*, **14** (4), 1057–1066.

Mahi, C.A. and Yanagimachi, R. (1976) Maturation and sperm penetration of canine ovarian oocytes *in vitro*. *J. Exp. Zool.*, **196** (2), 189–196.

Mainigi, M.A., Sapienza, C., Butts, S., and Coutifaris, C. (2016) A molecular perspective on procedures and outcomes with assisted reproductive technologies. *Cold Spring Harb. Perspect. Med.*, **6** (4), a023416.

Marcinkowska-Swojak, M., Szczerbal, I., Pausch, H., Nowacka-Woszuk, J., Flisikowski, K., Dzimira, S., Nizanski, W., Payan-Carreira, R., Fries, R., Kozlowski, P., and Switonski, M. (2015) Copy number variation in the region harboring SOX9 gene in dogs with testicular/ovotesticular disorder of sex development (78,XX; SRY-negative). *Sci. Rep.*, **5**, 14696.

Martin-Coello, J., Gomendio, M., and Roldan, E.R. (2011) Protamine 3 shows evidence of weak, positive selection in mouse species (genus *Mus*): but it is not a protamine. *Biol. Reprod.*, **84** (2), 320–326.

Martinez-Soto, J.C., Landeras, J., and Gadea, J. (2013) Spermatozoa and seminal plasma fatty acids as predictors of cryopreservation success. *Andrology*, **1** (3), 365–375.

Merlo, B., Zambelli, D., Cunto, M., Iacono, E., Nasi, L., Giaretta, E., Galeati, G., Bucci, D., and Spinaci, M. (2015) Sex-sorted canine sperm cryopreservation: limits and procedural considerations. *Theriogenology*, **83** (7), 1121–1127.

Meyer, D., Voigt, A., Widmayer, P., Borth, H., Huebner, S., Breit, A., Marschall, S., de Angelis, M.H., Boehm, U., Meyerhof, W., Gudermann, T., and Boekhoff, I. (2012) Expression of Tas1 taste receptors in mammalian spermatozoa: functional role of Tas1r1 in regulating basal Ca^{2+} and cAMP concentrations in spermatozoa. *PLoS One*, **7** (2), e32354.

Meyers, M.A., Burns, G., Arn, D., and Schenk, J.L. (2008) Birth of canine offspring following insemination of a bitch with flow-sorted spermatozoa. *Reprod. Fertil. Dev.*, **20**, 213 (Abstract).

Downloaded From Vet-eBooks.com

Meyers-Wallen, V.N. (2006) Sex chromosomes, sexual development and sex reversal in the dog, in *The Dog and Its Genome* (eds E.A. Ostrander, U. Giger, and K. Lindblad-Toh), Cold Spring Harbor Press, Cold Spring Harbor, NY, pp. 383–405.

Meyers-Wallen, V.N. (2012) Gonadal and sex differentiation abnormalities of dogs and cats. *Sex. Dev.*, **6** (1–3), 46–60.

Michael, A.J., Alexopoulos, C., Pontiki, E.A., Hadjipavlou-Litina, D.J., Saratsis, P., Ververidis, H.N., and Boscos, C.M. (2009) Effect of antioxidant supplementation in semen extenders on semen quality and reactive oxygen species of chilled canine spermatozoa. *Anim. Reprod. Sci.*, **112** (1–2), 119–135.

Miki, K. and Clapham, D.E. (2013) Rheotaxis guides mammalian sperm. *Curr. Biol.*, **23** (6), 443–452.

Miki, K., Qu, W., Goulding, E.H., Willis, W.D., Bunch, D.O., Strader, L.F., Perreault, S.D., Eddy, E.M., and O'Brien, D.A. (2004) Glyceraldehyde 3-phosphate dehydrogenase-S, a sperm-specific glycolytic enzyme, is required for sperm motility and male fertility. *Proc. Natl. Acad. Sci. USA*, **101** (47), 16501–16506.

Miyata, H., Satouh, Y., Mashiko, D., Muto, M., Nozawa, K., Shiba, K., Fujihara, Y., Isotani, A., Inaba, K., and Ikawa, M. (2015) Sperm calcineurin inhibition prevents mouse fertility with implications for male contraceptive. *Science*, **350** (6259), 442–445.

Mogas, M.T., Alamo, M.R., and Rodriguez-Gil, J.E. (2011) Roles of Na^+/K^+-dependent ATPase, Na^+/H^+ antiporter and GLUT hexose transporters in the cryosurvival of dog spermatozoa: effects on viability, acrosome state and motile sperm subpopulation structure. *Theriogenology*, **75** (9), 1669–1681.

Mogielnicka-Brzozowska, M., Strzeżek, R., Wasilewska, K., and Kordan, W. (2015) Prostasomes of canine seminal plasma: zinc-binding ability and effects on motility characteristics and plasma membrane integrity of spermatozoa. *Reprod. Domest. Anim.*, **50** (3), 484–491.

Moody, J.A., Clark, L.A., and Murphy, K.E. (2006) Canine history and breed clubs, in *The Dog and Its Genome* (eds E.A. Ostrander, U. Giger, and K. Lindblad-Toh), Cold Spring Harbor Press, Cold Spring Harbor, NY, pp. 1–18.

Moore, W. and Lambert, P.D. (1963) The chromosomes of the Beagle dog. *J. Hered.*, **54**, 273–276.

Morales, C.R., Ni, X., Smith, C.E., Inagaki, N., and Hermo, L. (2012) ABCA17 mediates sterol efflux from mouse spermatozoa plasma membranes. *Histol. Histopathol.*, **27** (3), 317–328.

Mosinger, B., Redding, K.M., Parker, M.R., Yevshayeva, V., Yee, K.K., Dyomina, K., Li, Y., and Margolskee, R.F. (2013) Genetic loss or pharmacological blockade of testes-expressed taste genes causes male sterility. *Proc. Natl. Acad. Sci. USA*, **110** (30), 12319–12324.

Mossman J.A., Pearson J.T., Moore H.D., and Pacey A.A. (2013) Variation in mean human sperm length is linked with semen characteristics. *Hum. Reprod.*, **28** (1), 22–32.

Muciaccia, B., Boitani, C., Berloco, B.P., Nudo, F., Spadetta, G., Stefanini, M., de Rooij, D.G., and Vicini, E. (2013) Novel stage classification of human spermatogenesis based on acrosome development. *Biol. Reprod.*, **89** (3), 60.

Mukai, C. and Okuno, M. (2004) Glycolysis plays a major role for adenosine triphosphate supplementation in mouse sperm flagellar movement. *Biol. Reprod.*, **71** (2), 540–547.

Mukai, C. and Travis, A.J. (2012) What sperm can teach us about energy production. *Reprod. Domest. Anim.*, **47** (Suppl. 4), 164–169.

Nagaoka, S.I., Hassold, T.J., and Hunt, P.A. (2012) Human aneuploidy: mechanisms and new insights into an age-old problem. *Nat. Rev. Genet.*, **13** (7), 493–504.

Nagashima, J.B., Sylvester, S.R., Nelson, J.L., Cheong, S.H., Mukai, C., Lambo, C., Flanders, J.A., Meyers-Wallen, V.N., Songsasen, N., and Travis, A.J. (2015) Live births from domestic dog (*Canis familiaris*) embryos produced by *in vitro* fertilization. *PLoS One*, **10** (12), e0143930.

Downloaded From Vet-eBooks.com

Nagy, A., Gertsenstein, M., Vintersten, K., and Behringer, R. (2003) *Manipulating the Mouse Embryo: A Laboratory Manual*, 3rd edn, Cold Spring Harbor Press, Cold Spring Harbor, NY, p. 200.

Nakanishi, T., Isotani, A., Yamaguchi, R., Ikawa, M., Baba, T., Suarez, S.S., and Okabe, M. (2004) Selective passage through the uterotubal junction of sperm from a mixed population produced by chimeras of calmegin-knockout and wild-type male mice. *Biol. Reprod.*, **71** (3), 959–965.

Nascimento, J.M., Shi, L.Z., Tam, J., Chandsawangbhuwana, C., Durrant, B., Botvinick, E.L., and Berns, M.W. (2008) Comparison of glycolysis and oxidative phosphorylation as energy sources for mammalian sperm motility, using the combination of fluorescence imaging, laser tweezers, and real-time automated tracking and trapping. *J. Cell. Physiol.*, **217** (3), 745–751.

Neagu, V.R., García, B.M., Rodr íguez, A.M., Ferrusola, C.O., Bolaños, J.M., Fernández, L.G., Tapia, J.A., and Peña, F.J. (2011) Determination of glutation peroxidase and superoxide dismutase activities in canine seminal plasma and its relation with sperm quality and lipid peroxidation post thaw. *Theriogenology*, **75** (1), 10–16.

Niakan, K.K., Han, J., Pedersen, R.A., Simon, C., and Pera, R.A. (2012) Human pre-implantation embryo development. *Development*, **139** (5), 829–841.

Nickson, D.A., Boyd, J.S., Eckersall, P.D., Ferguson, J.M., Harvey, M.J., and Renton, J.P. (1993) Molecular biological methods for monitoring oocyte maturation and *in vitro* fertilization in bitches. *J. Reprod. Fertil. Suppl.*, **47**, 231–240.

Nie, W., Wang, J., Su, W., Wang, D., Tanomtong, A., Perelman, P.L., Graphodatsky, A.S., and Yang, F. (2012) Chromosomal rearrangements and karyotype evolution in carnivores revealed by chromosome painting. *Heredity (Edinb.)*, **108** (1), 17–27.

Nishigaki, T., Jose, O., Gonzalez-Cota, A.L., Romero, F., Trevino, C.L., and Darszon, A. (2014) Intracellular pH in sperm physiology. *Biochem. Biophys. Res. Commun.*, **450** (3), 1149–1158.

Noakes, D.E. (1998) Conditions of the male external genital system, in *Canine Medicine and Therapeutics*, 4th edn (ed. N.T. Gorman), Blackwell Science, Ltd., Osney Mead, Oxford, pp. 753–759.

Nolan, C.M., O'Sullivan, F.M., Brabazon, D.C., and Callanan, J.J. (2009) Genomic imprinting in *Canis familiaris*. *Reprod. Domest. Anim.*, **44** (Suppl. 2), 16–21.

Nomura, N., Verdon, G., Kang, H.J., Shimamura, T., Nomura, Y., Sonoda, Y., Hussien, S.A., Qureshi, A.A., Coincon, M., Sato, Y., Abe, H., Nakada-Nakura, Y., Hino, T., Arakawa, T., Kusano-Arai, O., Iwanari, H., Murata, T., Kobayashi, T., Hamakubo, T., Kasahara, M., Iwata, S., and Drew, D. (2015) Structure and mechanism of the mammalian fructose transporter GLUT5. *Nature*, **526** (7573), 397–401.

Núñez-Martínez, I., Morán, J.M., and Peña, F.J. (2005) Do computer-assisted, morphometric-derived sperm characteristics reflect DNA status in canine spermatozoa? *Reprod. Domest. Anim.*, **40**, 537–543.

Oettlé, E.E. (1993) Sperm morphology and fertility in the dog. *J. Reprod. Fertil. Suppl.*, **47**, 257–260.

Oettlé, E.E. and Soley J.T. (1985) Infertility in a Maltese poodle as a result of a sperm midpiece defect. *J. S. Afr. Vet. Assoc.*, **56** (2), 103–106.

O'Flaherty, C. (2015) Redox regulation of mammalian sperm capacitation. *Asian J. Androl.*, **17** (4), 583–590.

Oh, H.J., Park, J.E., Kim, M.J., Hong, S.G., Ra, J.C., Jo, J.Y., Kang, S.K., Jang, G., and Lee, B.C. (2011) Recloned dogs derived from adipose stem cells of a transgenic cloned beagle. *Theriogenology*, **75** (7), 1221–1231.

Oi, M., Yamada, K., Hayakawa, H., and Suzuki, H. (2013) Sexing of dog sperm by fluorescence *in situ* hybridization. *J. Reprod. Dev.*, **59** (1), 92–96.

Okabe, M. (2015) Mechanisms of fertilization elucidated by gene-manipulated animals. *Asian J. Androl.*, **17** (4), 646–652.

Downloaded From Vet-eBooks.com

Okamura, N., Tajima, Y., Soejima, A., Masuda, H., and Sugita, Y. (1985) Sodium bicarbonate in seminal plasma stimulates the motility of mammalian spermatozoa through direct activation of adenylate cyclase. *J. Biol. Chem.*, **260** (17), 9699–9705.

Olar, T.T., Amann, R.P., and Pickett, B.W. (1983) Relationships among testicular size, daily production and output of spermatozoa, and extragonadal spermatozoal reserves of the dog. *Biol. Reprod.*, **29** (5), 1114–1120.

Oliva, R. (2006) Protamines and male infertility. *Hum. Reprod. Update*, **12** (4), 417–435.

O'Rahilly, R. and Müller, F. (2001) *Human Embryology and Teratology*, 3rd edn, Wiley-Liss, New York, 505 pp.

Ostrander, E.A. and Wayne, R.K. (2005) The canine genome. *Genome Res.*, **15**, 1706–1716.

Ostrander, E.A., Giger, U., and Lindblad-Toh, K. (2006) *The Dog and Its Genome* (eds E.A. Ostrander, U. Giger, and K. Lindblad-Toh), Cold Spring Harbor Press, Cold Spring Harbor, NY, 585 pp.

Otoi, T., Murakami, M., Fujii, M., Tanaka, M., Ooka, A., Une, S., and Suzuki, T. (2000) Development of canine oocytes matured and fertilised *in vitro*. *Vet. Rec.*, **146** (2), 52–53.

Pacey, A.A., Freeman, S.L., and England, G.C. (2000) Contact of dog spermatozoa with homologous uterine tube epithelium prolongs flagellar activity in relation to the stage of the estrous cycle. *Theriogenology*, **54** (1), 109–118.

Palme, N., Becher, A.C., Merkl, M., Glosmann, M., Aurich, C., and Schafer-Somi, S. (2014) Immunolocalization of the cholesterol transporters ABCA1 and ABCG1 in canine reproductive tract tissues and spermatozoa. *Reprod. Domest. Anim.*, **49** (3), 441–447.

Palmerini, M.G., Antinori, M., Maione, M., Cerusico, F., Versaci, C., Nottola, S.A., Macchiarelli, G., Khalili, M.A., and Antinori, S. (2014) Ultrastructure of immature and mature human oocytes after cryotop vitrification. *J. Reprod. Dev.*, **60** (6), 411–420.

Palomino, J. and De los Reyes, M. (2009) A scanning electron microscopy study of frozen/thawed dog sperm during *in vitro* gamete interaction. *Reprod. Domest. Anim.*, **44** (2), 278–283.

Palomo, M.J., FernAndez-Novell, J.M., Peña, A., Guinovart, J.J., Rigau, T., and Rodríguez-Gil, J.E. (2003) Glucose- and fructose-induced dog-sperm glycogen synthesis shows specific changes in the location of the sperm glycogen deposition. *Mol. Reprod. Dev.*, **64** (3), 349–359.

Parmentier, M., Libert, F., Schurmans, S., Schiffmann, S., Lefort, A., Eggerickx, D., Ledent, C., Mollereau, C., Gérard, C., Perret, J. et al. (1992) Expression of members of the putative olfactory receptor gene family in mammalian germ cells. *Nature*, **355** (6359), 453–455.

Payan-Carreira, R. and Pires, M.A. (2008) Multioocyte follicles in domestic dogs: a survey of frequency of occurrence. *Theriogenology*, **69** (8), 977–982.

Peña, A.I., Johannisson, A., and Linde-Forsberg, C. (2001) Validation of flow cytometry for assessment of viability and acrosomal integrity of dog spermatozoa and for evaluation of different methods of cryopreservation. *J. Reprod. Fertil. Suppl.*, **57**, 371–376.

Peña, F.J., Nunez-Martinez, I., and Moran, J.M. (2006) Semen technologies in dog breeding: an update. *Reprod. Domest. Anim.*, **41** (Suppl. 2), 21–29.

Peña, A.I., Barrio, M., Becerra, J.J., Quintela, L.A., and Herradón, P.G. (2007) Infertility in a dog due to proximal cytoplasmic droplets in the ejaculate: investigation of the significance for sperm functionality *in vitro*. *Reprod. Domest. Anim.*, **42** (5), 471–478.

Peña, L., Gama, A., Goldschmidt, M.H., Abadie, J., Benazzi, C., Castagnaro, M., Díez, L., Gärtner, F., Hellmén, E., Kiupel, M., Millán, Y., Miller, M.A., Nguyen, F., Poli, A., Sarli, G., Zappulli, V., and de las Mulas, J.M. (2014) Canine mammary tumors: a review and consensus of standard guidelines on epithelial and myoepithelial phenotype markers, HER2, and hormone receptor assessment using immunohistochemistry. *Vet. Pathol.*, **51** (1), 127–145.

Pesch, S. and Bergmann, M. (2006) Structure of mammalian spermatozoa in respect to viability, fertility and cryopreservation. *Micron*, **37** (7), 597–612.

Downloaded From Vet-eBooks.com

Peters, M.A., de Rooij, D.G., Teerds, K.J., van der Gaag, I., and van Sluijs, F.J. (2000) Spermatogenesis and testicular tumours in ageing dogs. *J. Reprod. Fertil.*, **120** (2), 443–452.

Petrunkina, A.M., Simon, K., Günzel-Apel, A.R., and Töpfer-Petersen, E. (2003) Specific order in the appearance of protein tyrosine phosphorylation patterns is functionally coordinated with dog sperm hyperactivation and capacitation. *J. Androl.*, **24** (3), 423–437.

PFMA (2015) Pet Food Manufacturers Association. Retrieved from http://www.pfma.org.uk/pet-population-2014/ (July 2, 2015).

Phillips, T.C. (2010) Canine spermatozoa: purification, assessment, and preservation. Doctoral dissertation, University of Florida, Gainesville, FL.

Pieri, N., Souza, A.F., Casals, J.B., Roballo, K., Ambrosio, C.E., and Martins, D.S. (2015) Comparative development of embryonic age by organogenesis in domestic dogs and cats. *Reprod. Domest. Anim.*, **50** (4), 625–631.

Pineda, M.H., Kainer, R.A., and Faulkner, L.C. (1973) Dorsal median postcervical fold in the canine vagina. *Am. J. Vet. Res.*, **34** (12), 1487–1491.

Plewes, J.L. and Jennings, D.B. (1973) Varying the temperature around the scrotum of a conscious dog between 15 degrees C and 31 degrees C does not affect respiration or metabolism. *Can. J. Physiol. Pharmacol.*, **51** (3), 197–204.

Poth, T., Breuer, W., Walter, B., Hecht, W., and Hermanns, W. (2010) Disorders of sex development in the dog: adoption of a new nomenclature and reclassification of reported cases. *Anim. Reprod. Sci.*, **121** (3–4), 197–207.

Poulos, A. and White, I.G. (1973) The phospholipid composition of human spermatozoa and seminal plasma. *J. Reprod. Fertil.*, **35** (2), 265–272.

Pretzer, S.D. (2008) Canine embryonic and fetal development: a review. *Theriogenology*, **70** (3), 300–303.

Provost, M.P., Acharya, K.S., Acharya, C.R., Yeh, J.S., Steward, R.G., Eaton, J.L., Goldfarb, J.M., and Muasher, S.J. (2016) Pregnancy outcomes decline with increasing recipient body mass index: an analysis of 22,317 fresh donor/recipient cycles from the 2008–2010 Society for Assisted Reproductive Technology Clinic Outcome Reporting System registry. *Fertil. Steril.*, **105** (2), 364–368.

Qi, H., Moran, M.M., Navarro, B., Chong, J.A., Krapivinsky, G., Krapivinsky, L., Kirichok, Y., Ramsey, I.S., Quill, T.A., and Clapham, D.E. (2007) All four CatSper ion channel proteins are required for male fertility and sperm cell hyperactivated motility. *Proc. Natl. Acad. Sci. USA*, **104** (4), 1219–1223.

Quill, T.A., Sugden, S.A., Rossi, K.L., Doolittle, L.K., Hammer, R.E., and Garbers, D.L. (2003) Hyperactivated sperm motility driven by CatSper2 is required for fertilization. *Proc. Natl. Acad. Sci. USA*, **100** (25), 14869–14874.

Quinn, P. (2003) Media used in the assisted reproductive technologies laboratory, in *A Color Atlas for Human Assisted Reproduction: Laboratory & Clinical Insights* (eds P. Patrizio, M.J. Tucker, and V. Guelman), Lippincott Williams and Wilkins, Philadelphia, PA, pp. 241–256.

Rankin, T.L., Coleman, J.S., Epifano, O., Hoodbhoy, T., Turner, S.G., Castle, P.E. et al. (2003) Fertility and taxon-specific sperm binding persist after replacement of mouse sperm receptors with human homologs. *Dev. Cell*, **5**, 33–43.

Rathi, R., Colenbrander, B., Bevers, M.M., and Gadella, B.M. (2001) Evaluation of *in vitro* capacitation of stallion spermatozoa. *Biol. Reprod.*, **65** (2), 462–470.

Ren, D., Navarro, B., Perez, G., Jackson, A.C., Hsu, S., Shi, Q., Tilly, J.L., and Clapham, D.E. (2001) A sperm ion channel required for sperm motility and male fertility. *Nature*, **413** (6856), 603–609.

Rengan, A.K., Agarwal, A., van der Linde, M., and du Plessis, S.S. (2012) An investigation of excess residual cytoplasm in human spermatozoa and its distinction from the cytoplasmic droplet. *Reprod. Biol. Endocrinol.*, **10**, 92.

Downloaded From Vet-eBooks.com

Renton, J.P., Boyd, J.S., Eckersall, P.D., Ferguson, J.M., Harvey, M.J., Mullaney, J., and Perry, B. (1991) Ovulation, fertilization and early embryonic development in the bitch (*Canis familiaris*). *J. Reprod. Fertil.*, **93** (1), 221–231.

Reynaud, K., Saint-Dizier, M., and Chastant-Maillard, S. (2004) *In vitro* maturation and fertilization of canine oocytes. *Methods Mol. Biol.*, **253**, 255–272.

Reynaud, K., Fontbonne, A., Marseloo, N., Thoumire, S., Chebrout, M., de Lesegno, C.V., and Chastant-Maillard, S. (2005) *In vivo* meiotic resumption, fertilization and early embryonic development in the bitch. *Reproduction*, **130** (2), 193–201.

Reynaud, K., Fontbonne, A., Marseloo, N., Viaris de Lesegno, C., Saint-Dizier, M., and Chastant-Maillard, S. (2006) *In vivo* canine oocyte maturation, fertilization and early embryogenesis: a review. *Theriogenology*, **66** (6–7), 1685–1693.

Reynaud, K., de Lesegno, C.V., Chebrout, M., Thoumire, S., and Chastant-Maillard, S. (2009) Follicle population, cumulus mucification, and oocyte chromatin configuration during the periovulatory period in the female dog. *Theriogenology*, **72** (8), 1120–1131.

Reynaud, K., Fontbonne, A., Saint-Dizier, M., Thoumire, S., Marnier, C., Tahir, M.Z., Meylheuc, T., and Chastant-Maillard, S. (2012a) Folliculogenesis, ovulation and endocrine control of oocytes and embryos in the dog. *Reprod. Domest. Anim.*, **47** (Suppl. 6), 66–69.

Reynaud, K., Chebrout, M., Tanguy-Dezaux, C., de la Villeon, G., and Chastant-Maillard, S. (2012b) Chromatin patterns of immature canine oocytes after *in vitro* maturation. *Reprod. Domest. Anim.*, **47** (Suppl. 6), 70–73.

Reynaud, K., Saint-Dizier, M., Tahir, M.Z., Havard, T., Harichaux, G., Labas, V., Thoumire, S., Fontbonne, A., Grimard, B., and Chastant-Maillard, S. (2015) Progesterone plays a critical role in canine oocyte maturation and fertilization. *Biol. Reprod.*, **93** (4), 87.

Rhodes, L. (2016) New approaches to non-surgical sterilization for dogs and cats: opportunities and challenges. *Reprod. Domest. Anim.* doi: 10.1111/rda.12862.

Rigau, T., Farré, M., Ballester, J., Mogas, T., Peña, A., and Rodríguez-Gil, J.E. (2001) Effects of glucose and fructose on motility patterns of dog spermatozoa from fresh ejaculates. *Theriogenology*, **56** (5), 801–815.

Rigau, T., Rivera, M., Palomo, M.J., Fernández-Novell, J.M., Mogas, T., Ballester, J., Peña, A., Otaegui, P.J., Guinovart, J.J., and Rodríguez-Gil, J.E. (2002) Differential effects of glucose and fructose on hexose metabolism in dog spermatozoa. *Reproduction*, **123** (4), 579–591.

Rijsselaere, T., Van Soom, A., Van Cruchten, S., Coryn, M., Görtz, K., Maes, D., and de Kruif, A. (2004) Sperm distribution in the genital tract of the bitch following artificial insemination in relation to the time of ovulation. *Reproduction*, **128** (6), 801–811.

Rijsselaere, T., England, G., Freeman, S., Maes, D., and Van Soom, A. (2014) Current knowledge on the transport and fate of spermatozoa in the reproductive tract of the bitch. *Reprod. Domest. Anim.*, **49** (Suppl. 2), 2–7.

Rimbault, M., Beale, H.C., Schoenebeck, J.J., Hoopes, B.C., Allen, J.J., Kilroy-Glynn, P., Wayne, R.K., Sutter, N.B., and Ostrander, E.A. (2013) Derived variants at six genes explain nearly half of size reduction in dog breeds. *Genome Res.*, **23** (12), 1985–1995.

Rodenas, C., Lucas, X., Tarantini, T., Del Olmo, D., Roca, J., Vazquez, J.M., Martinez, E.A., and Parrilla, I. (2014) The effects of Hoechst 33342 staining and the male sample donor on the sorting efficiency of canine spermatozoa. *Reprod. Domest. Anim.*, **49**, 115–121.

Rodríguez-Gil, J.E. (2013) in *Energy Management of Mature Mammalian Spermatozoa, Success in Artificial Insemination: Quality of Semen and Diagnostics Employed* (ed. A. Lemma), InTech., doi: 10.5772/51711.

Rodgers, R.J. and Irving-Rodgers, H.F. (2010) Formation of the ovarian follicular antrum and follicular fluid. *Biol. Reprod.*, **82** (6), 1021–1029.

Downloaded From Vet-eBooks.com

Rogers, N. (2015) Canine clues: dog genomes explored in effort to bring human cancer to heel. *Nat. Med.*, **21** (12), 1374–1375.

Rogers, B.J. and Perreault, S.D. (1990) Importance of glycolysable substrates for *in vitro* capacitation of human spermatozoa. *Biol. Reprod.*, **43** (6), 1064–1069.

Romagnoli, S. and Lopate, C. (2014) Transcervical artificial insemination in dogs and cats: review of the technique and practical aspects. *Reprod. Domest. Anim.*, **49** (Suppl. 4), 56–63.

Romano, J. and Brinsko, S.P. (2013) Reproductive physiology of the male, in *Cunningham's Textbook of Veterinary Physiology* (ed. B.G. Klein), Elsevier Saunders, St. Louis, MO, pp. 451–459.

Romar, R., Funahashi, H., and Coy, P. (2016) *In vitro* fertilization in pigs: new molecules and protocols to consider in the forthcoming years. *Theriogenology*, **85** (1), 125–134.

Ronquist, K.G., Ek, B., Morrell, J., Stavreus-Evers, A., Ström-Holst, B., Humblot, P., Ronquist, G., and Larsson, A. (2013) Prostasomes from four different species are able to produce extracellular adenosine triphosphate (ATP). *Biochim. Biophys. Acta*, **1830** (10), 4604–4610.

Root Kustritz, M.V. (2014) Applied small animal andrology, in *Animal Andrology: Theories and Applications* (eds P.J. Chenoweth and S.P. Lorton), CABI International, Oxfordshire, UK, pp. 177–196.

Rosenfeld, C.S. and Schatten, H. (2007) Overview of female reproductive organs, in *Comparative Reproductive Biology* (eds H. Schatten and G.M. Constantinescu), Blackwell Publishing, Ames, IA, pp. 99–109.

Rosenkrantz, H., Langille, J., and Mason, M.M. (1961) The chemical analysis of normal canine prostatic fluid. *Am. J. Vet. Res.*, **22**, 1057–1065.

Ross, M.T., Grafham, D.V., Coffey, A.J., Scherer, S., McLay, K., Muzny, D. et al. (2005) The DNA sequence of the human X chromosome. *Nature*, **434**, 325–337.

Rossi, E., Radi, O., De Lorenzi, L., Vetro, A., Groppetti, D., Bigliardi, E., Luvoni, G.C., Rota, A., Camerino, G., Zuffardi, O., and Parma, P. (2014) Sox9 duplications are a relevant cause of Sry-negative XX sex reversal dogs. *PLoS One*, **9** (7), e101244.

Rota, A., Manuali, E., Caire, S., and Appino, S. (2008) Severe tail defects in the spermatozoa ejaculated by an English bulldog. *J. Vet. Med. Sci.*, **70** (1), 123–125.

Ruiz-Pesini, E., Díez-Sánchez, C., López-Pérez, M.J., and Enríquez, J.A. (2007) The role of the mitochondrion in sperm function: is there a place for oxidative phosphorylation or is this a purely glycolytic process? *Curr. Top. Dev. Biol.*, **77**, 3–19.

Russell, L.D. and Malone, J.P. (1980) A study of Sertoli-spermatid tubulobulbar complexes in selected mammals. *Tissue Cell*, **12** (2), 263–285.

Russell, L.D., Ettlin, R.A., Hikim, A.P.S., and Clegg, E.D. (1990) *Histological and Histopathological Evaluation of the Testis*, Cache River Press, Clearwater, FL, 286 pp.

Russell, S.J., Stalker, L., Gilchrist, G., Backx, A., Molledo, G., Foster, R.A., and LaMarre, J. (2016) Identification of PIWIL1 isoforms and their expression in bovine testes, oocytes, and early embryos. *Biol. Reprod.*, **94** (4) 75, 1–11.

Ruvinsky, A. and Hill, M. (2012) Developmental genetics, in *The Genetics of the Dog*, 2nd edn (eds E.A. Ostrander and A. Ruvinsky), CABI Publishing, Oxford, pp. 321–358.

Sabeur, K., Vo, A.T., and Ball, B.A. (2001) Characterization of angiotensin-converting enzyme in canine testis. *Reproduction*, **122** (1), 139–146.

Sabeur, K., Foristall, K., and Ball, B.A. (2002) Characterization of PH-20 in canine spermatozoa and testis. *Theriogenology*, **57** (2), 977–987.

Sadeu, J.C. and Nogueira, D. (2011) Folliculogenesis and oogenesis *in vivo* and *in vitro*, in human females, in *Physiologie, pathologie et thérapie de la reproduction chez l'humain* (eds C. Poncelet and C. Sifer), Springer, Paris, France, pp. 3–24.

Saint-Dizier, M., Reynaud, K., and Chastant-Maillard, S. (2004) Chromatin, microtubules, and kinases activities during meiotic resumption in bitch oocytes. *Mol. Reprod. Dev.*, **68** (2), 205–212.

Downloaded From Vet-eBooks.com

Saladin, K.S. (2008) *Human Anatomy*, 2nd edn, McGraw-Hill, New York, NY, p. 817.
Sánchez, F. and Smitz, J. (2012) Molecular control of oogenesis. *Biochim. Biophys. Acta*, **1822** (12), 1896–1912.
Satouh, Y., Inoue, N., Ikawa, M., and Okabe, M. (2012) Visualization of the moment of mouse sperm–egg fusion and dynamic localization of IZUMO1. *J. Cell Sci.*, **125** (Part 21), 4985–4990.
Schäfer-Somi, S., Beceriklisoy, H.B., Budik, S., Kanca, H., Aksoy, O.A., Polat, B., Cetin, Y., Ay, S.S., and Aslan, S. (2008) Expression of genes in the canine pre-implantation uterus and embryo: implications for an active role of the embryo before and during invasion. *Reprod. Domest. Anim.*, **43** (6), 656–663.
Schneider, M.R., Wolf, E., Braun, J., Kolb, H.J., and Adler, H. (2008) Canine embryo-derived stem cells and models for human diseases. *Hum. Mol. Genet.*, **17** (R1), R42–R47.
Schoenebeck, J.J. and Ostrander, E.A. (2014) Insights into morphology and disease from the dog genome project. *Annu. Rev. Cell Dev. Biol.*, **30**, 535–560.
Schoonees, R., Reynoso, G., and Murphy, G.P. (1972) The effect of androgen on canine prostatic secretion. *J. Surg. Oncol.*, **4** (3), 169–179.
Seidel, G.E., Jr. (2015) Lessons from reproductive technology research. *Annu. Rev. Anim. Biosci.*, **3**, 467–487.
Setchell, B.P. (1982) Spermatogenesis and spermatozoa, in *Reproduction in Mammals: Book 1: Germ Cells and Fertilization*, 2nd edn (eds C.R. Austin and R.V. Short), Cambridge University Press, Cambridge, pp. 63–101.
Setchell, B.P., Maddocks, S., and Brooks, D.E. (1994) Anatomy, vasculature, innervation, and fluids of the male reproductive tract, in *The Physiology of Reproduction*, 2nd edn (eds E. Knobil and J.D. Neill), Raven Press Ltd., New York, NY, pp. 1063–1175.
Shannonhouse, J.L., Urbanski, H.F., Woo, S.L., Fong, L.A., Goddard, S.D., Lucas, W.F., Jones, E.R., Wu, C., and Morgan, C. (2014) Aquaporin-11 control of testicular fertility markers in Syrian hamsters. *Mol. Cell. Endocrinol.*, **391** (1–2), 1–9.
Shearin, A.L. and Ostrander, E.A. (2010) Leading the way: canine models of genomics and disease. *Dis. Model. Mech.*, **3** (1–2), 27–34.
Shimizu, T., Tsutsui, T., Murao, I., and Orima, H. (1990) Incidence for transuterine migration of embryos in the dog. *Nihon Juigaku Zasshi*, **52** (6), 1273–1275.
Shirazi, A., Khadivi, A., and Shams-Esfandabadi, N. (2014) Male pronuclear formation using dog sperm derived from ectopic testicular xenografts, testis, and epididymis. *Avicenna J. Med. Biotechnol.*, **6** (3), 140–146.
Shrestha, A., Wadhwa, N., and Gupta, S.K. (2014) Evaluation of recombinant fusion protein comprising dog zona pellucida glycoprotein-3 and Izumo and individual fragments as immunogens for contraception. *Vaccine*, **32** (5), 564–571.
Shrestha, A., Srichandan, S., Minhas, V., Panda, A.K., and Gupta, S.K. (2015) Canine zona pellucida glycoprotein-3: up-scaled production, immunization strategy and its outcome on fertility. *Vaccine*, **33** (1), 133–140.
Simerly, C., Wu, G.J., Zoran, S., Ord, T., Rawlins, R., Jones, J., Navara, C., Gerrity, M., Rinehart, J., Binor, Z., Asch, R., and Schatten, G. (1995) The paternal inheritance of the centrosome, the cell's microtubule-organizing center, in humans, and the implications for infertility. *Nat. Med.*, **1** (1), 47–52.
Simpson, J. and Binns, M.M. (2006) The Kennel Club and the early history of dog shows and breed clubs, in *The Dog and Its Genome*, 1st edn (eds E.A. Ostrander, U. Giger, and K. Lindblad-Toh), Cold Spring Harbor Press, Cold Spring Harbor, NY, pp. 19–30.
Sirivaidyapong, S., Bevers, M.M., and Colenbrander, B. (1999) Acrosome reaction in dog sperm is induced by a membrane-localized progesterone receptor. *J. Androl.*, **20** (4), 537–544.

Downloaded From Vet-eBooks.com

Sirivaidyapong, S., Bevers, M.M., Gadella, B.M., and Colenbrander, B. (2001) Induction of the acrosome reaction in dog sperm cells is dependent on epididymal maturation: the generation of a functional progesterone receptor is involved. *Mol. Reprod. Dev.*, **58** (4), 451–459.

Smith, J.F., Syritsyna, O., Fellous, M., Serres, C., Mannowetz, N., Kirichok, Y., and Lishko, P.V. (2013) Disruption of the principal, progesterone-activated sperm Ca2+channel in a CatSper2-deficient infertile patient. *Proc. Natl. Acad. Sci. USA*, **110**, 6823–6828.

Soares, J.M., Avelar, G.F., and França, L.R. (2009) The seminiferous epithelium cycle and its duration in different breeds of dog (*Canis familiaris*). *J. Anat.*, **215** (4), 462–471.

Solano-Gallego, L. and Masserdotti, C. (2016) Reproductive system, in *Canine and Feline Cytology: A Color Atlas and Interpretation Guide*, 3rd edn (eds R.E. Raskin and D. Meyer), Elsevier Health Sciences, St. Louis, MO, pp. 313–352.

Soler, C., De Monserrat, J.J., Gutierrez, R., Nunez, J., Nunez, M., Sancho, M., Perez-Sanchez, F., and Cooper, T.G. (2003) Use of the sperm-class Analyser® for objective assessment of human sperm morphology. *Int. J. Androl.*, **26**, 262–270.

Songsasen, N. and Wildt, D.E. (2005) Size of the donor follicle, but not stage of reproductive cycle or seasonality, influences meiotic competency of selected domestic dog oocytes. *Mol. Reprod. Dev.*, **72** (1), 113–119.

Spehr, M., Schwane, K., Riffell, J.A., Zimmer, R.K., and Hatt, H. (2006) Odorant receptors and olfactory-like signaling mechanisms in mammalian sperm. *Mol. Cell. Endocrinol.*, **250** (1–2), 128–136.

Spinaci, M., Bucci, D., Mazzoni, M., Giaretta, E., Bernardini, C., Vallorani, C., Tamanini, C., Clavenzani, P., and Galeati, G. (2014) Expression of α-gustducin and α-transducin, G proteins coupled with taste receptors, in boar sperm. *Theriogenology*, **82** (1), 144–151.

Stalker, L., Russell, S.J., Co, C., Foster, R.A., and LaMarre, J. (2016) PIWIL1 is expressed in the canine testis, increases with sexual maturity, and binds small RNAs. *Biol. Reprod.*, **94** (1), 17.

Starkey, M.P., Scase, T.J., Mellersh, C.S., and Murphy, S. (2005) Dogs really are man's best friend: canine genomics has applications in veterinary and human medicine! *Brief. Funct. Genomic. Proteomic.*, **4** (2), 112–128.

Steckler, D., Stout, T.A., Durandt, C., and Nöthling, J.O. (2015) Validation of merocyanine 540 staining as a technique for assessing capacitation-related membrane destabilization of fresh dog sperm. *Theriogenology*, **83** (9), 1451–1460.

Ström-Holst, B., Larsson, B., Linde-Forsberg, C., and Rodriguez-Martinez, H. (2000) Sperm binding capacity and ultrastructure of the zona pellucida of stored canine oocytes. *J. Reprod. Fertil.*, **119** (1), 77–83.

Strünker, T., Goodwin, N., Brenker, C., Kashikar, N.D., Weyand, I., Seifert, R., and Kaupp, U.B. (2011) The CatSper channel mediates progesterone-induced Ca2+ influx in human sperm. *Nature*, **471**, 382–386.

Strzeżek, R., Koziorowska-Gilun, M., and Filipowicz, K. (2010) Acrosin system of dog spermatozoa and reproductive tract secretions. *Pol. J. Vet. Sci.*, **13** (1), 69–73.

Strzeżek, R., Szemplińska, K., Filipowicz, K., and Kordan, W. (2015) Semen characteristics and selected biochemical markers of canine seminal plasma in various seasons of the year. *Pol. J. Vet. Sci.*, **18** (1), 13–18.

Suarez, S.S. (2015) Gamete and zygote transport, in *Knobil and Neill's Physiology of Reproduction*, 4th edn (eds T.M. Plant and A.J. Zeleznik), vol. 1, Academic Press, Waltham, MA, pp. 197–232.

Suarez, S.S. (2016) Mammalian sperm interactions with the female reproductive tract. *Cell Tissue Res.*, **363** (1), 185–194.

Sullivan, R. (2015) Epididymosomes: a heterogeneous population of microvesicles with multiple functions in sperm maturation and storage. *Asian J. Androl.*, **17** (5), 726–729.

Downloaded From Vet-eBooks.com

Sullivan, R., Saez, F., Girouard, J., and Frenette, G. (2005) Role of exosomes in sperm maturation during the transit along the male reproductive tract. *Blood Cells Mol. Dis.*, **35** (1), 1–10.

Sullivan, R., Frenette, G., and Girouard, J. (2007) Epididymosomes are involved in the acquisition of new sperm proteins during epididymal transit. *Asian J. Androl.*, **9** (4), 483–491.

Switonski, M. (2014) Dog as a model in studies on human hereditary diseases and their gene therapy. *Reprod. Biol.*, **14** (1), 44–50.

Szabo, C., Ischiropoulos, H., and Radi, R. (2007) Peroxynitrite: biochemistry, pathophysiology and development of therapeutics. *Nat. Rev. Drug Discov.*, **6** (8), 662–680.

Szász, F., Sirivaidyapong, S., Cheng, F.P., Voorhout, W.F., Marks, A., Colenbrander, B., Solti And, L., and Gadella, B.M. (2000) Detection of calcium ionophore induced membrane changes in dog sperm as a simple method to predict the cryopreservability of dog semen. *Mol. Reprod. Dev.*, **55** (3), 289–298.

Tamburrino, L., Marchiani, S., Vicini, E., Muciaccia, B., Cambi, M., Pellegrini, S., Forti, G., Muratori, M., and Baldi, E. (2015) Quantification of CatSper1 expression in human spermatozoa and relation to functional parameters. *Hum. Reprod.*, **30** (7), 1532–1544.

Tan, J.H., Wang, H.L., Sun, X.S., Liu, Y., Sui, H.S., and Zhang, J. (2009) Chromatin configurations in the germinal vesicle of mammalian oocytes. *Mol. Hum. Reprod.*, **15** (1), 1–9.

Tash, J.S. and Means, A.R. (1982) Regulation of protein phosphorylation and motility of sperm by cyclic adenosine monophosphate and calcium. *Biol. Reprod.*, **26** (4), 745–763.

Tash, J.S. and Means, A.R. (1983) Cyclic adenosine 3′,5′ monophosphate, calcium and protein phosphorylation in flagellar motility. *Biol. Reprod.*, **28** (1), 75–104.

Tash, J.S., Kakar, S.S., and Means, A.R. (1984) Flagellar motility requires the cAMP-dependent phosphorylation of a heat-stable NP-40-soluble 56kd protein, axokinin. *Cell*, **38** (2), 551–559.

Tash, J.S., Hidaka, H., and Means, A.R. (1986) Axokinin phosphorylation by cAMP-dependent protein kinase is sufficient for activation of sperm flagellar motility. *J. Cell Biol.*, **103** (2), 649–655.

Tash, J.S., Krinks, M., Patel, J., Means, R.L., Klee, C.B., and Means, A.R. (1988) Identification, characterization, and functional correlation of calmodulin-dependent protein phosphatase in sperm. *J. Cell Biol.*, **106** (5), 1625–1633.

Tecle, E. and Gagneux, P. (2015) Sugar-coated sperm: unraveling the functions of the mammalian sperm glycocalyx. *Mol. Reprod. Dev.*, **82**, 635–650.

Tesoriero, J.V. (1981) Early ultrastructural changes of developing oocytes in the dog. *J. Morphol.*, **168** (2), 171–179.

Thirumala, S., Ferrer, M.S., Al-Jarrah, A., Eilts, B.E., Paccamonti, D.L., and Devireddy, R.V. (2003) Cryopreservation of canine spermatozoa: theoretical prediction of optimal cooling rates in the presence and absence of cryoprotective agents. *Cryobiology*, **47** (2), 109–124.

Thomas, R., Smith, K.C., Ostrander, E.A., Galibert, F., and Breen, M. (2003) Chromosome aberrations in canine multicentric lymphomas detected with comparative genomic hybridisation and a panel of single locus probes. *Br. J. Cancer*, **89** (8), 1530–1537.

Thomas, R., Borst, L., Rotroff, D., Motsinger-Reif, A., Lindblad-Toh, K., Modiano, J.F., and Breen, M. (2014) Genomic profiling reveals extensive heterogeneity in somatic DNA copy number aberrations of canine hemangiosarcoma. *Chromosome Res.*, **22** (3), 305–319.

Tomes, C.N., Roggero, C.M., De Blas, G., Saling, P.M., and Mayorga, L.S. (2004) Requirement of protein tyrosine kinase and phosphatase activities for human sperm exocytosis. *Dev. Biol.*, **265** (2), 399–415.

Toshimori, K. and Eddy, E.M. (2015) The spermatozoon, in *Knobil and Neill's Physiology of Reproduction*, 4th edn (eds T.M. Plant and A.J. Zeleznik), vol. 1, Academic Press, Waltham, MA, pp. 99–148.

Tsai, K.L., Clark, L.A., and Murphy, K.E. (2007) Understanding hereditary diseases using the dog and human as companion model systems. *Mamm. Genome*, **18** (6–7), 444–451.

Downloaded From Vet-eBooks.com

Tsutsui, T., Shimizu, T., Hori, T., and Kawakami, E. (2002) Factors affecting transuterine migration of canine embryos. *J. Vet. Med. Sci.*, **64** (12), 1117–1121.

Tsutsui, T., Hori, T., Endo, S., Hayama, A., and Kawakami, E. (2006) Intrauterine transfer of early canine embryos. *Theriogenology*, **66** (6–7), 1703–1705.

Tsutsui, T., Takahashi, F., Hori, T., Kawakami, E., and Concannon, P.W. (2009) Prolonged duration of fertility of dog ova. *Reprod. Domest. Anim.*, **44** (Suppl. 2), 230–233.

Tsutsui, T., Hori, T., Takahashi, F., and Concannon, P.W. (2012) Ovulation compensatory function after unilateral ovariectomy in dogs. *Reprod. Domest. Anim.*, **47** (Suppl. 6), 43–46.

Turathum, B., Saikhun, K., Sangsuwan, P., and Kitiyanant, Y. (2010) Effects of vitrification on nuclear maturation, ultrastructural changes and gene expression of canine oocytes. *Reprod. Biol. Endocrinol.*, **8**, 70.

Turner, R.M. (2006) Moving to the beat: a review of mammalian sperm motility regulation. *Reprod. Fertil. Dev.*, **18** (1–2), 25–38.

Upadhyay, R.D., Kumar, A.V., Ganeshan, M., and Balasinor, N.H. (2012) Tubulobulbar complex: cytoskeletal remodeling to release spermatozoa. *Reprod. Biol. Endocrinol.*, **10**, 27.

Valentini, L., Iorga, A.I., De Santis, T., Ambruosi, B., Reynaud, K., Chastant-Maillard, S., Guaricci, A.C., Caira, M., and Dell'Aquila, M.E. (2010) Mitochondrial distribution patterns in canine oocytes as related to the reproductive cycle stage. *Anim. Reprod. Sci.*, **117** (1–2), 166–177.

Valeri, C., Pappalardo, S., De Felici, M., and Manna, C. (2011) Correlation of oocyte morphometry parameters with woman's age. *J. Assist. Reprod. Genet.*, **28** (6), 545–552.

Van Soom, A., Rijsselaere, T., and Filliers, M. (2014) Cats and dogs: two neglected species in this era of embryo production *in vitro*? *Reprod. Domest. Anim.*, **49** (Suppl. 2), 87–91.

Vanderhaeghen, P., Schurmans, S., Vassart, G., and Parmentier, M. (1993) Olfactory receptors are displayed on dog mature sperm cells. *J. Cell Biol.*, **123** (6 Part 1), 1441–1452.

Vanderhaeghen, P., Schurmans, S., Vassart, G., and Parmentier, M. (1997) Specific repertoire of olfactory receptor genes in the male germ cells of several mammalian species. *Genomics*, **39** (3), 239–246.

Varesi, S., Vernocchi, V., Faustini, M., and Luvoni, G.C. (2013) Morphological and acrosomal changes of canine spermatozoa during epididymal transit. *Acta Vet. Scand.*, **55**, 17.

Verstegen-Onclin, K. and Verstegen, J. (2008) Endocrinology of pregnancy in the dog: a review. *Theriogenology*, **70** (3), 291–299.

Vigil, P., Salgado, A.M., and Cortés, M.E. (2012) Ultrastructural interaction between spermatozoon and human oviductal cells *in vitro*. *J. Electron Microsc. (Tokyo)*, **61** (2), 123–126.

Vilà, C. and Leonard, J.A. (2012) Canid phylogeny and origin of the domestic dog, in *The Genetics of the Dog* (eds E.A. Ostrander and A. Ruvinsky), CABI Publishing, Oxford, pp. 1–11.

Vilà, C., Savolainen, P., Maldonado, J.E., Amorim, I.R., Rice, J.E., Honeycutt, R.L. et al. (1997) Multiple and ancient origins of the domestic dog. *Science*, **276**, 1687–1689.

Volpe, S., Galeati, G., Bernardini, C., Tamanini, C., Mari, G., Zambelli, D., Seren, E., and Spinaci, M. (2008) Comparative immunolocalization of heat shock proteins (Hsp)-60, -70, -90 in boar, stallion, dog and cat spermatozoa. *Reprod. Domest. Anim.*, **43** (4), 385–392.

Volpe, S., Leoci, R., Aiudi, G., and Lacalandra, G.M. (2009) Relationship between motility and mitochondrial functional status in canine spermatozoa. *Reprod. Domest. Anim.*, **44** (Suppl. 2), 275–278.

Wade, C.M., Karlsson, E.K., Mikkelsen, T.S., Zody, M.C., and Lindblad-Toh, K. (2006) The dog genome: sequence, evolution and haplotype structure, in *The Dog and Its Genome* (eds E.A. Ostrander, U. Giger, and K. Lindblad-Toh), Cold Spring Harbor Press, Cold Spring Harbor, NY, pp. 179–207.

Walsh, P.C. and Wilson, J.D. (1976) The induction of prostatic hypertrophy in the dog with androstanediol. *J. Clin. Invest.*, **57** (4), 1093–1097.

Downloaded From Vet-eBooks.com

Warinrak, C. Wu, J.T. Hsu, W.L. Liao, J.W. Chang, S.C. and Cheng, F.P. (2015) Expression of matrix metalloproteinases (MMP-2, MMP-9) and their inhibitors (TIMP-1, TIMP-2) in canine testis, epididymis and semen. *Reprod. Domest. Anim.*, **50** (1), 48–57.

Westhoff, D. and Kamp, G. (1997) Glyceraldehyde 3-phosphate dehydrogenase is bound to the fibrous sheath of mammalian spermatozoa. *J. Cell Sci.*, **110** (Part 15), 1821–1829.

Whitfield, M., Pollet-Villard, X., Levy, R., Drevet, J.R., and Saez, F. (2015) Posttesticular sperm maturation, infertility, and hypercholesterolemia. *Asian J. Androl.*, **17** (5), 742–748.

Wilcox, J.T. Semple, E. Gartley, C. Brisson, B.A. Perrault, S.D. Villagómez, D.A. Tayade, C. Becker, S. Lanza, R. and Betts, D.H. (2009) Characterization of canine embryonic stem cell lines derived from different niche microenvironments. *Stem. Cells Dev.*, **18** (8), 1167–1178.

Williams, A.C. and Ford, W.C. (2001) The role of glucose in supporting motility and capacitation in human spermatozoa. *J. Androl.*, **22** (4), 680–695.

Williams, H.L., Mansell, S., Alasmari, W., Brown, S.G., Wilson, S.M., Sutton, K.A., Miller, M.R., Lishko, P.V., Barratt, C.L., Publicover, S.J., and Martins da Silva, S. (2015) Specific loss of CatSper function is sufficient to compromise fertilizing capacity of human spermatozoa. *Hum. Reprod.*, **30** (12), 2737–2746.

Wilton, A.N. and Henthorn, P.S. (2012) The canine model in medical genetics, in *The Genetics of the Dog*, 2nd edn (eds E.A. Ostrander and A. Ruvinsky), CABI Publishing, Oxford, pp. 458–476.

Wolf, D.P., Mitalipov, N., and Mitalipov, S. (2015) Mitochondrial replacement therapy in reproductive medicine. *Trends Mol. Med.*, **21** (2), 68–76.

Woodall, P.F. and Johnstone, I.P. (1988) Dimensions and allometry of testes, epididymides and spermatozoa in the domestic dog (*Canis familiaris*). *J. Reprod. Fertil.*, **82** (2), 603–609.

Wozencraft, W.C. (2005) *Mammal Species of the World: A Taxonomic and Geographic Reference*, 3rd edn (eds D.E. Wilson and D.M. Reeder), vol. 1, Johns Hopkins University Press, Baltimore, MD, p. 2142.

Wu, J.T. Tsai, P.S. Lee, S.L. and Cheng, F.P. (2005) Characterisation of the progesterone receptor on canine spermatozoa. *Reprod. Fertil. Dev.*, **17** (7), 733–741.

Wu, X., Wan, S., Pujar, S., Haskins, M.E., Schlafer, D.H., Lee, M.M., and Meyers-Wallen, V.N. (2009) A single base pair mutation encoding a premature stop codon in the MIS type II receptor is responsible for canine persistent Müllerian duct syndrome. *J. Androl.*, **30** (1), 46–56.

Yamada, S., Shimazu, Y., Kawaji, H., Nakazawa, M., Naito, K., and Toyoda, Y. (1992) Maturation, fertilization, and development of dog oocytes *in vitro*. *Biol. Reprod.*, **46** (5), 853–858.

Yamada, S., Shimazu, Y., Kawano, Y., Nakazawa, M., Naito, K., and Toyoda, Y. (1993) *In vitro* maturation and fertilization of preovulatory dog oocytes. *J. Reprod. Fertil. Suppl.*, **47**, 227–229.

Yanagimachi, R. (1994) Mammalian fertilization, in *The Physiology of Reproduction*, 2nd edn (eds E. Knobil and J.D. Neill), Raven Press Ltd., New York, NY, pp. 189–317.

Yániz, J.L., Soler, C., and Santolaria, P. (2015) Computer assisted sperm morphometry in mammals: a review. *Anim. Reprod. Sci.*, **156**, 1–12.

Yao, M.W.M. and Batchu, K. (2007) Oogenesis, in *Clinical Reproductive Medicine and Surgery*, 1st edn (eds T. Falcone and W. Hurd), Mosby-Elsevier, Philadelphia, PA, pp. 51–72.

Yeung, C.H. (2010) Aquaporins in spermatozoa and testicular germ cells: identification and potential role. *Asian J. Androl.*, **12** (4), 490–499.

Young, A. and Bannasch, D. (2006) Morphological variations in the dog, in *The Dog and Its Genome* (eds E.A. Ostrander, U. Giger, and K. Lindblad-Toh), Cold Spring Harbor Press, Cold Spring Harbor, NY, pp. 47–65.

Young, S.A., Aitken, J., and Baker, M.A. (2015) Phosphorylation of Izumo1 and its role in male infertility. *Asian J. Androl.*, **17** (5), 708–710.

Downloaded From Vet-eBooks.com

Yuan, S., Tang, C., Zhang, Y., Wu, J., Bao, J., Zheng, H., Xu, C., and Yan, W. (2015) mir-34b/c and mir-449a/b/c are required for spermatogenesis, but not for the first cleavage division in mice. *Biol. Open*, **4** (2), 212–223.

Zelli, R., Bellezza, I., Rambotti, M.G., Minelli, A., and Polisca, A. (2013) Ultrastructural and enzymatic activity of membranous vesicles isolated from canine seminal plasma. *Reprod. Domest. Anim.*, **48** (2), 252–257.

Zhao, F.Q. and Keating, A.F. (2007) Functional properties and genomics of glucose transporters. *Curr. Genomics*, **8** (2), 113–128.

Zinaman, M.J., Clegg, E.D., Brown, C.C., O'Connor, J., and Selevan, S.G. (1996) Estimates of human fertility and pregnancy loss. *Fertil. Steril.*, **65** (3), 503–509.

Zou, Q., Wang, X., Liu, Y., Ouyang, Z., Long, H., Wei, S., Xin, J., Zhao, B., Lai, S., Shen, J., Ni, Q., Yang, H., Zhong, H., Li, L., Hu, M., Zhang, Q., Zhou, Z., He, J., Yan, O., Fan, N., Zhao, Y., Liu, Z., Guo, L., Huang, J., Zhang, G., Ying, J., Lai, L., and Gao, X. (2015) Generation of gene-target dogs using CRISPR/Cas9 system. *J. Mol. Cell Biol.*, **7** (6), 580–583.

Downloaded From Vet-eBooks.com

12

Animal Models of Inflammation During Pregnancy

Karen E. Racicot[1] *and Keith E. Latham*[2]

[1]*Department of Obstetrics, Gynecology and Reproductive Biology, Reproductive and Development Science Program, Van Andel Institute, Michigan State University, MI, USA*
[2]*Department of Animal Science, Reproductive and Developmental Science Program, Michigan State University, MI, USA*

12.1 Introduction

Mammalian embryo implantation, pregnancy, placenta formation, and gestation to term require a continuous dialog between embryonic/fetal cells and the mother. A long-standing view of pregnancy has been that local immunosuppression is required to prevent maternal rejection of the fetus, which is a genetic semiallograft and thus potentially subject to attack by the immune system (Billington, 2003). More recently, the essential contributions of the maternal immune system to successful embryo implantation, placental health, and pregnancy have become apparent (Zenclussen *et al*., 2007; Dekel *et al*., 2014; Racicot *et al*., 2014). Indeed, the maternal immune system is essential for preventing and controlling harmful bacterial and viral infections in the placenta, thereby also protecting the fetus. Immune cells release cytokines, chemokines, and other regulatory factors that promote embryo adhesion and implantation, stimulate angiogenesis, and support normal intrauterine fetal growth (Racicot *et al*., 2014; Zenclussen, 2006). Unfortunately, environmental and maternal factors can dysregulate the maternal immune system, leading to reduced/lost fertility, embryo resorption, spontaneous abortion (SA), preterm birth (PTB), fetal growth restriction (FGR), preeclampsia (PE), and gestational hypertension (Racicot *et al*., 2014; Romero *et al*., 2014). These observations reveal that a delicate balance must be maintained wherein the placenta, endometrium, and maternal immune system must manifest an optimum amount of inflammation, and well-controlled stress responses in order to ensure successful pregnancy.

Rodent, sheep, and nonhuman primate models of pregnancy have been developed to investigate the role of inflammation in poor pregnancy outcomes. Models include injection of microbial products or inflammatory cytokines directly into the uterus or vagina to study local ascending infections, or i.p./i.v. injections of infectious agents to study the role of systemic infection on pregnancy. In addition, obesity and chronic stress models address questions about chronic, low-grade noninfectious inflammation during pregnancy. Finally, the use of transgenic rodent models and cell grafting has helped identify specific genes and pathways involved in the inflammatory response during healthy and adverse pregnancies.

This chapter focuses on the value of these different animal models in understanding the complex process of inflammation during pregnancy. We review maternal and environmental factors that can result in inflammatory responses during pregnancy, and how this affects pregnancy outcome, fetal development, and health of progeny.

Animal Models and Human Reproduction, First Edition. Edited by Heide Schatten and Gheorghe M. Constantinescu.
© 2017 John Wiley & Sons, Inc. Published 2017 by John Wiley & Sons, Inc.

Downloaded From Vet-eBooks.com

12.2 Local Inflammation of the Pregnant Female Reproductive Tract

12.2.1 Introduction

Inflammation in response to microbial infections of the female reproductive tract (FRT) can cause adverse pregnancy outcomes such as spontaneous abortion or preterm labor (PTL) (Romero *et al*., 1989). Microbes can ascend from the lower reproductive tract invading the amnionic cavity, fetal membranes, placental disk, or decidua, and trigger an inflammatory response detrimental to pregnancy and/or fetal development (Romero *et al*., 2007, 2014). Here we review rodent and nonhuman primate models of local inflammation within the FRT, in the context of adverse pregnancy outcomes.

12.2.2 *In Utero* Inflammation and Adverse Pregnancy Outcomes

Local *in utero* inflammation (IUI) can result from microbial invasion from the vagina, invasion from the oral cavity, or from microbes being introduced during amniocentesis. Using rodent, sheep, and nonhuman primate models, IUI can be studied by administration of microbial products or inflammatory factors directly into the uterus. To do this, animals are usually anesthetized and laparotomy is performed in the lower abdomen exposing the uterus. Treatment may be applied between fetal compartments, by careful injection between individual fetuses self-contained within their own membranes (rodents) (Elovitz *et al*., 2003; Bennett *et al*., 2000), into the amniotic cavity (sheep and monkeys) (Grigsby *et al*., 2003; Gravett *et al*., 1996), or into the space between the decidua and chorionic membrane (monkeys) (Figure 12.1) (Gravett *et al*., 1996; Elovitz, 2004). These techniques are typically used to model infection-induced inflammation resulting in SA (injections in mice typically E7.5 resulting in abortion at approximately 50% gestation) or PTL (injections typically E14.5–15.5 in mice; 70–79% gestation = late-onset chorioamnionitis in women), depending on the time of treatment.

In most studies modeling PTL or SA, purified toll-like receptor (TLR) ligands or whole pathogens are injected into one of these compartments to trigger inflammatory responses. The TLRs are innate receptors directly responsible for initiation of inflammation upon binding of their individual pathogen-associated molecular patterns (PAMPs) (Medzhitov, 2001). Examples of purified PAMPs or whole organisms that have been used to induce *in utero* inflammation to study preterm labor are bacterial lipopolysaccharide (LPS) (TLR4 ligand) (Elovitz *et al*., 2003; Bennett *et al*., 2000; Grigsby *et al*., 2003), lipoteichoic acid (TLR2/6 ligand) (Kajikawa *et al*., 1998), poly(I:C) (viral mimic: TLR3 ligand) (Lin *et al*., 2005, 2006; Zhang *et al*., 2007), *Escherichia coli* (Mussalli *et al*., 1999), and group B streptococcus (Gravett *et al*., 1996).

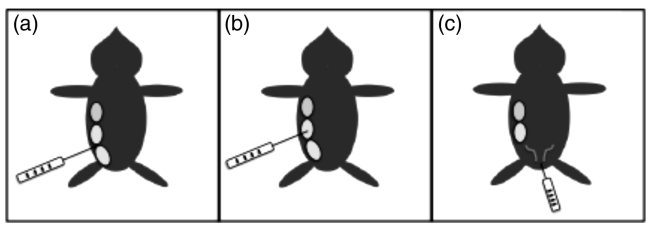

Figure 12.1 Schematic representation of potential injection sites in a rodent model of local reproductive tract inflammation. (a) Between fetal compartments that are encapsulated by the fetal membranes. (b) Intra-amniotic, or through the fetal membranes into the amnion. (c) Transvaginal, into the vagina but not past the cervix or transcervical, when the instrument is passed through the cervix with treatment directly into the uterus.

Downloaded From Vet-eBooks.com

Inflammatory cytokines such as IL-1 and TNF-α have also been infused directly into the uterus to induce preterm birth (Bagga *et al*., 1996) (Table 12.1). It is important to consider the advantages and disadvantages of these different sources of inflammation.

While TLR ligands are extremely helpful when testing specific molecular pathways that result in inflammation, they are not the strongest models of the typical physiological response to pathogens. Heat-killed or living bacteria, or viruses more closely mimic the clinical condition, but can be dangerous to work with and difficult to grow and maintain.

The use of these pathogens in animal IUI models gives researchers firm control over local concentration and point of treatment, reducing experimental variation. On the other hand, injections directly into the reproductive tract are typically done surgically, adding surgery as a potentially confounding factor. To avoid this, intracervical inoculation has been performed in mice and rabbits, using LPS (Reznikov *et al*., 1999), whole *E. coli* (Reznikov *et al*., 1999), *Prevotella bivia* (Gibbs *et al*., 2004), or *Fusobacterium necrophorum* (McDuffie, 1994), allowing for direct infection of the uterine compartment late in gestation, and removing the need for laparotomy. Of note, this technique must be used with exceptional care as a needle can easily be passed into the peritoneum resulting in systemic infection (Table 12.1).

12.2.3 Ascending Infections and Adverse Pregnancy Outcomes

Injecting microbial products into the vagina (Figure 12.1) is another way to study microbe-induced PTL. These experiments are typically designed for the study of ascending infections and the effect of microbial populations on cervical capacity in relation to pregnancy outcome. For example, to better understand why some women suffer from ascending bacterial infections, mice have received intravaginal *Ureaplasma urealyticum*, with and without cervical viral infection, to determine if viral infection reduces cervical capacity to protect the fetus from bacterial infection (Racicot *et al*., 2013). Another study used intravaginal LPS to study the differences in cervices of mice with infection-induced preterm labor verses normal term labor (Gonzalez *et al*., 2011).

Others have used intravaginal infection with *Trichomonas vaginalis*, a parasite that can cause local inflammation, affect the local microflora, and can be a carrier of endosymbiotic viruses also capable of infecting the host (Fichorova *et al*., 2012). *Trichomonas* infections are also associated with preterm labor in women, and murine models have been used to test the underlying mechanism of induction of preterm birth and potential intravaginal treatments (Table 12.1) (Fichorova *et al*., 2012). These models of intrauterine and intravaginal infection require more skill and often more invasive procedures but they are valuable in that they produce a localized infection with inflammation primarily within the reproductive tract. Therefore, they are useful for studying conditions that are initiated at the genital tract. At other times, systemic infection or other chronic conditions may cause inflammation at the maternal–fetal interphase, affecting pregnancy outcome and the developing fetus. These models are reviewed in the next section.

12.3 Systemic Inflammation During Pregnancy

12.3.1 Introduction

While local infection can induce acute or chronic inflammation within the FRT, inflammation can also stem from maternal systemic conditions such as chronic stress and clinical/subclinical infections of distant tissues. Systemic immune responses directed against the placenta or in association with placental dysfunction can also affect pregnancy outcome. These systemic and

Downloaded From Vet-eBooks.com

Table 12.1 Animal models of reproductive tract inflammation during pregnancy.

Animal models	Reagent	Modes of delivery	Clinical condition	References
Mouse, rat, rabbit, sheep	Lipopolysaccharide (LPS)	Between fetal compartments Intra-amniotic Intracervical Intravaginal	Preterm birth Spontaneous abortion	Elovitz *et al.*, 2003; Bennett *et al.*, 2000; Grigsby *et al.*, 2003; Kajikawa *et al.*, 1998; Reznikov *et al.*, 1999; Gibbs *et al.*, 2004; Gonzalez *et al.*, 2011; Celik, 2002; Kaga *et al.*, 1995; Schlafer *et al.*, 1994; Ilievski *et al.*, 2007
Mouse, rat, sheep, rabbit	*E. coli*	Intracervical Between fetal compartments, Intra-amniotic	Preterm birth	Mussalli *et al.*, 1999; Reznikov *et al.*, 1999; McDuffie, 1994; Racicot *et al.*, 2013
Monkey	Group B streptococcus	Intra-amniotic Between decidua and chorion	Preterm birth	Gravett *et al.*, 1996
Rabbit	*P. bivia*	Intracervical	Preterm birth	Gibbs *et al.*, 2004
Mouse	*F. necrophorum*	Intracervical	Preterm birth	McDuffie and Gibbs, 1994
Mouse	*U. urealyticum*	Intravaginal	Preterm birth	Racicot *et al.*, 2013
Mouse, monkey	TNF, IL1	Intra-amniotic Between fetal compartments	Preterm birth	Mussalli *et al.*, 1999; Bagga *et al.*, 1996; Reznikov *et al.*, 1999; Romero, 1992
Mouse	MHV68	IP but targets cervix	Preterm birth	Racicot *et al.*, 2013
Mouse	*T. vaginalis*	Intravaginal	Preterm birth	Fichorova *et al.*, 2012
Mouse	Herpes simplex virus-2	Intravaginal	Preterm birth Spontaneous abortion	Elovitz and Mrinalini, 2004; McDuffie and Gibbs, 1994

Downloaded From Vet-eBooks.com

environmental factors have been associated with multiple pregnancy complications including spontaneous abortion, preeclampsia, preterm birth, and even maternal death. This section reviews animal models used to study the effect of systemic infection, systemic immune activation, or chronic sterile inflammation on pregnancy outcomes.

12.3.2 Systemic Viral or Bacterial Infection

12.3.2.1 Influenza During Pregnancy

Pandemic influenza A (IA) infection has been associated with PTB and maternal mortality, usually in the context of an overwhelming inflammatory response to secondary bacterial infection (Jamieson *et al*., 2009, 2010; Small *et al*., 2010; Creanga *et al*., 2010). Despite confirmation of maternal risks associated with pandemic influenza (2009), there are still limited animal models for studying the role of influenza in PTB and maternal health. Mice given intranasal inoculations with influenza B demonstrated an increased risk of death in pregnant females compared to their infected nonpregnant counterparts, providing a model of maternal mortality (Kim *et al*., 2014). Inbred mouse strains (C3H, BALB/c) and outbred strains (Prince Henry) have been used as models of the increased maternal mortality associated with pandemic influenza A. Intranasal infection with two mouse-adapted H1N1 strains in the third week of murine pregnancy resulted in higher mortality compared to nonpregnant females (Williams, 1977). Similar models also demonstrated fetal loss and high concentrations of proinflammatory cytokines in lungs and the periphery, demonstrating influenza-associated inflammation and PTB (Chan *et al*., 2010; Kim *et al*., 2012).

While these mouse models have improved our understanding of the virus–host relationship during pregnancy, they are quite removed from the human condition. This is partially due to the difficulty in adapting flu virus to animal models. These viruses generally have species-specific tropism and must be passaged in the model species to produce infectious virus. These species-adpated viruses are inherently different from the clinical virus (Sidwell, 2004). Also, influenza affects the respiratory system of rodents differently than it affects humans, making some comparisons difficult (Sidwell, 2004). The cost associated with using nonhuman primates is probably a reason for the lack of studies using these models to study the effects of influenza A during pregnancy, but macaques are susceptible to influenza A and therefore research with monkeys may help determine the mechanism of influenza-associated PTB and maternal mortality.

12.3.2.2 Periodontal Disease During Pregnancy

Periodontal diseases (PD), including gingivitis and periodontitis, are characterized by bacterial overgrowth in subgingival sites of the mouth, and associated with chronic inflammation. These bacteria can spread through the body during pregnancy and colonize the amniotic fluid of women (Han *et al*., 2006, 2009; Han, 2011). The presence of bacteria from amniotic fluid, but originating from the mouth, has been associated with PTB (Jeffcoat *et al*., 2001), SA, and preeclampsia (Han, 2011; Xiong *et al*., 2006). CF-1 mice have been used to model PD during pregnancy. After receiving tail vain injections with *Fusobacterium nucleatum*, the injected bacteria can be found in the uterus, but not systemically. This treatment resulted in preterm delivery and stillbirths (Han *et al*., 2004). In another study mice were fitted with subcutaneous steel chambers to establish a localized infection with *Porphyromonas gingivalis* on gestation day 7.5. While some fetuses appeared normal, several from each litter suffered growth restriction, and those pups were associated with placental infection with *P. gingivalis* (Lin *et al*., 2003).

These murine models are robust, as they closely mimic the human condition, but they require the ability to grow and maintain the bacteria, and they are specific to PD. More general models of

Downloaded From Vet-eBooks.com

systemic bacterial infection and/or inflammation include i.p. injection of LPS (20–800 μg/kg) (Celik, 2002; Kaga *et al*., 1995; Schlafer *et al*., 1994), LTA and peptidoglycan (Kajikawa *et al*., 1998; Ilievski *et al*., 2007), or systemic administration of proinflammatory cytokines such as interleukin-1 (Romero and Tartakovsky, 1992). These techniques are less specific to one particular clinical condition, but are reproducible and useful for studying the role of systemic inflammation in pregnancy complications such as SA, PE, and PTB. They have demonstrated that the inflammation associated with toll-like receptor ligation is sufficient to cause aberrant pregnancy outcomes.

12.3.3 Maternal Stress: Chronic Sterile Inflammation

Noninfectious conditions, such as psychosocial stress, can cause low-grade chronic inflammation systemically and/or in the placenta characterized by enhanced circulating inflammatory markers such as C-reactive protein (Goldenberg *et al*., 2008; Sheldon *et al*., 1993), Il-1 (Ruiz *et al*., 2007), and IL-6 and TNF-α (Coussons-Read *et al*., 2007; Christian, 2012). Although there is heterogeneity in the measures of stress in clinical studies, several have demonstrated that maternal psychosocial stress is associated with PTB (Christian, 2012; Copper *et al*., 1996; Wadhwa *et al*., 2001) and several animal models support these findings. Treating sheep with dexamethasone will cause preterm delivery (Grigsby *et al*., 2000), but this treatment does not result in PTD in nonhuman primate models (Elovitz, 2004). Stress can be induced in pregnant rats using multiple techniques, including physical restraint, forced swimming, noise, or combination treatments, but is not typically reported to induce PTB in the F0 generation. Interestingly, the F1 and F2 generations experience reduced gestation lengths, suggesting a possible heritable, transgenerational epigenetic change affecting gestation length (Yao *et al*., 2014). Murine models of stress during pregnancy have also been developed; while mice generally do not experience PTB or other obvious adverse pregnancy outcomes following maternal stress, development of the fetus and future offspring can be affected (Lim *et al*., 2014; Pincus-Knackstedt *et al*., 2006). Therefore, rodent models are not ideal to study stress-induced PTB. Despite the expense, further development of nonhuman primate models could prove helpful. Although previous studies show no effect of stress on PTB, there is a lot of diversity in the effect of stress in human populations. It would be interesting to determine if specific types of stressors affect pregnancy outcome in animals with enhanced intelligence and emotional responsiveness. These studies could explain the heterogeneity in human studies of stress and PTB.

12.3.4 Preeclampsia-Related Inflammation Models

Preeclampsia is characterized by hypertension and proteinuria after gestation week 20 in women who were not previously hypertensive (Young *et al*., 2010). The condition is often associated with inflammation, although it is not known if this is the cause or a result of the disorder (Rustveld *et al*., 2008). Interestingly, the condition has been linked to urinary tract infections (Banhidy *et al*., 2007; Villar *et al*., 2006; Schieve *et al*., 1994) and periodontal disease (Canakci *et al*., 2004; Ruma *et al*., 2008), suggesting infection and the resulting systemic or placental inflammation enhance risk (Conde-Agudelo *et al*., 2008). Both rats and baboons have been used to determine the role of inflammatory mediators on preeclampsia symptoms. Pregnant baboons have received i.v. administration of antibodies directed against IL-10, an immune modulator, and tested for effects on mean arterial pressure and heart rate (Orange *et al*., 2005). They have also been treated with i.v. infusions of TNF-α at 170 ng/kg/day using an osmotic mini pump to determine effect on blood pressure and soluble markers of preeclampsia such as sFLT-1 and

Downloaded From Vet-eBooks.com

sEng (Sunderland *et al*., 2011). Similarly, pregnant Sprague Dawley rats have received TNF-α infusions from d14-19 of pregnancy to determine the effect on arterial pressure and nitric oxide, another potential mediator of preeclampsia (Alexander *et al*., 2002).

These models are valuable for identifying the role of specific factors in the context of the disease, but inflammation likely enhances the negative effects of preeclampsia, while not being the initiating event. Therefore, studying inflammation in conjunction with animal models of preeclampsia that have vascular defects and hypoxic phenotypes provides a better option that more closely mimics the clinical condition (McCarthy *et al*., 2011).

12.3.5 Models of Antiphospholipid Antibody Syndrome (APS)

Antiphospholipid antibody syndrome is caused by a maternal B-cell (antibody) response against placental tissue that can result in an inflammatory immune "attack" on the developing fetus often resulting in SA (Holers *et al*., 2002). The inflammation associated with APS is mediated by the activation of complement and this has been demonstrated using murine models of APS (Holers *et al*., 2002). Mice that received injections of human antiphospholipid (aPL) antibodies display similar symptoms as seen in humans with APS, including complement activation, inflammation, and fetal loss (Branch *et al*., 1990; Blank *et al*., 1991; Piona *et al*., 1995). Furthermore, pregnant mice treated with inhibitors of indoleamine 2,-3-dioxygenase (IDO) experience extensive complement deposition in the placenta and fetal loss, and can also be used to study APS (Mellor *et al*., 2001; Munn *et al*., 1998).

These models are quite robust as they mimic the clinical condition in many ways. Transgenic mice lacking key elements of the complement system have also been powerful tools and further support a role for complement in APS.

12.4 Genetic Models and Cellular Manipulation to Study Inflammation During Pregnancy

12.4.1 Introduction

Due to the complexity of the immune system and the multiple factors involved in the induction of inflammation, it is important to identify key factors and pathways that are upstream of pathologies such as preterm birth, abortion, or preeclampsia. The use of abortion-prone breeding crosses, transgenic mouse models, and immune cell manipulation has helped to identify integral components of the inflammatory milieu. These models display pathologies that can be manipulated by adding or removing a gene or a cell type. This section reviews some of the murine models and methodologies used to determine master regulators of pregnancy loss and help to identify therapeutic targets.

12.4.2 Breeding Cross Models of Induced Inflammation

Murine models of spontaneous abortion can be developed by taking advantage of the genetic predispositions of some mouse strains to exhibit enhanced inflammatory responses to the semiallogeneic fetus and placenta. The most established model is the female CBA/J X male DBA/2 (Clark *et al*., 1980; Chaouat *et al*., 1983) (Figure 12.2). This cross results in pregnancies characterized by an infiltration of activated natural killer cells and macrophages (Clark *et al*., 1980; Chaouat *et al*., 1990) into the implantation sites at gestational day 6.5 and initiation of

Downloaded From Vet-eBooks.com

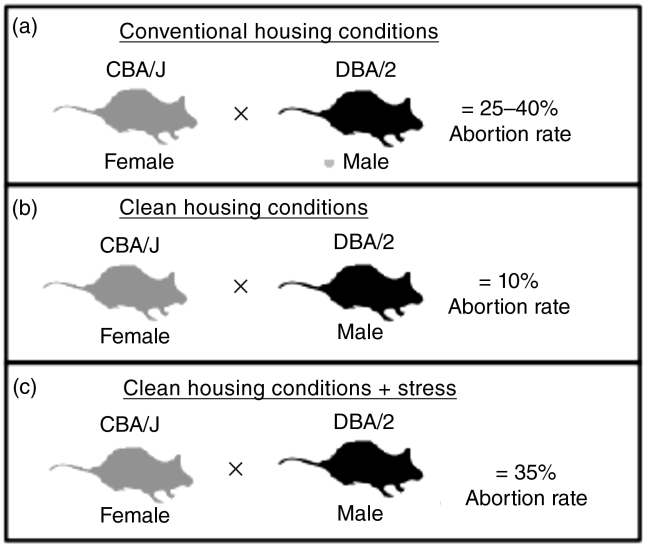

Figure 12.2 Abortion rates of CBA/J females bred to DBA/2 males. (a) Pregnant mice maintained in nonsterile housing experience 25–40% abortion rate. (b) Pregnant mice maintained in clean, high-barrier facilities have lower abortion rates, approximately 10%. (c) Pregnant mice in clean facilities can be induced to suffer up to 35% abortion rates if they are subjected to treatments inducing stress (Arck *et al.*, 1995a, 1995b; Clark *et al.*, 1998; Hamilton, 1987; Dokras *et al.*, 2006; Davisson *et al.*, 2001; Poltorak *et al.*, 1998; Hirsch *et al.*, 2006).

abortions at day 8.5 at a rate of ~25–40% in conventional housing conditions (Arck *et al.*, 1995a, 1995b, 1997; Clark *et al.*, 1998; Hamilton and Hamilton 1987). These abortions are associated with tissue necrosis and inflammation, specifically the proinflammatory cytokines TNF-α, IL-2, and IFN-γ (Arck *et al.*, 1997; Clark *et al.*, 1998). The same cross can be used in clean cage conditions and the SA rate can be reduced to ~10% (Arck *et al.*, 1995a, 1995b, 1997).

Interestingly, female CBA/J mice mated to DBA/2 males can be further induced to experience ~35% SA by ultrasonic sound stress at day 5–6 of pregnancy (Arck *et al.*, 1997). This model provides a valuable "inducible" phenotype that can be used to study the role of specific inflammatory factors in the process of abortion (Figure 12.2). For example, treatment with neutralizing receptors of TNF-α and IL-1 reduced abortions (Arck *et al.*, 1997), demonstrating the role of inflammation in stress-associated abortion. These models are valuable tools for dissecting the roles of stress, infection, and inflammation in SA and will be important for finding clinical interventions.

Another inbred mouse strain, the borderline hypertensive BPH/5, has been used as a model for preeclampsia. These mice were developed by BPH/2 brother–sister matings over several generations resulting in animals with elevated blood pressure and a PE phenotype during pregnancy (McCarthy *et al.*, 2011). Specifically, during pregnancy, the BPH/5 suffers from proteinuria, gestational hypertension, vascular abnormalities, and inadequate development of the placenta (Dokras *et al.*, 2006; Davisson *et al.*, 2001). Similar to the CBA/J X DBA/2 mice, these animals exhibit many characteristics of gestational disease in women making them a reasonable model for the disease.

A shortcoming of the CBA/J X DBA/2 and the BPH/5 models is that the mechanisms linking genotype to phenotype are not completely understood. Also, there are cases of abortion that may not be immune-mediated, so that the CBA/J X DBA/2 model would not be appropriate. Similarly, BPH/5 mice are hypertensive before pregnancy. Although this is sometimes the case in women, PE often occurs in women who were previously normotensive (McCarthy *et al.*,

Downloaded From Vet-eBooks.com

2011). Therefore, these animal models mimic several important clinical phenotypes and are valuable for studying the effect of stress, microorganisms, and some hypertensive phenotypes on pregnancy outcomes. To begin understanding the role of specific inflammatory factors on these conditions, we utilize genetically modified animals.

12.4.3 Genetically Modified Models of Inflammation and Pregnancy

The use of genetically modified mice lacking individual immune factors has helped delineate the mechanisms of inflammation-mediated pregnancy loss. Infection-associated pregnancy loss does not occur in mice lacking some TLRs (Poltorak *et al*., 1998), proinflammatory cytokines/receptors (Hirsch *et al*., 2006), or associated immunomodulatory factors (Agrawal *et al*., 2014; Blank *et al*., 2008; Filipovich *et al*., 2009). For example, C3H/HeJ mice lacking functional TLR4 are resistant to endotoxin-induced PTB (Poltorak *et al*., 1998). Similarly, TLR3 knockout mice are resistant to preterm birth induced by polyinosinic:polycytidylic acid (poly(I:C)) (Koga *et al*., 2009), a synthetic mimic of viral dsRNA. Furthermore, mice lacking the pro-inflammatory cytokine receptors, IL-1 receptor and TNF receptor (Hirsch *et al*., 2006), or the cytokine IFN-γ (Ashkar, 2001), are less sensitive to bacteria-induced PTB. Conversely, IL-10 knockout mice are affected at much lower doses of endotoxin and other TLR ligands compared to controls, demonstrating the importance of the immunomodulatory properties of that cytokine (Robertson *et al*., 2006).

There are also several transgenic models that have improved our understanding of the underlying factors resulting in preeclampsia. For example, mice lacking catechol-*O*-methyltransferase (COMT−/−) have a preeclampsia phenotype characterized by enhanced HIF-1α and soluble vascular endothelial growth factor receptor (sFLT-1), placental atherosis, and hypertension between gestation days 10–17 (Kanasaki *et al*., 2008). There is a loss of an estrogen metabolite in this model, and this study demonstrated the importance of that factor in the third trimester of pregnancy (Kanasaki *et al*., 2008). The loss of heme oxygenase is also associated with PE in women (Zenclussen *et al*., 2003; Barber *et al*., 2001). While homozygous null ($HO\text{-}1^{-/-}$) mice are infertile (Poss, 1997), heterozygotes ($HO^{+/-}$) have increased blood pressure, abnormal placental morphology, and increased sFLT-1 and soluble endoglin (Cudmore *et al*., 2007; Zhao *et al*., 2009, 2011). Therefore, while these models do not necessarily directly mimic human conditions, much has been learned with them about the underlying factors responsible for inflammation-associated pregnancy disorders.

12.4.4 Immune Cell Manipulation to Study Inflammation

Inflammation resulting in loss or complication of pregnancy can be caused by the activation and/or recruitment of specific immune cell populations to the maternal–fetal interface or other parts of the reproductive tract. While gene knockout studies can help characterize factors involved in recruitment and activation, cell ablation or reconstitution are stronger models for understanding the multifaceted nature of immune cell populations. Studies using rodents include whole animal or targeted ablation of macrophages, dendritic cells, neutrophils, lymphocytes, and natural killer cells, while the role of regulatory T cells have been defined in cell reconstitution studies (Table 12.2).

12.4.4.1 Macrophages

Macrophages in the reproductive tract produce numerous factors implicated with term and preterm birth including matrix metalloproteinases (MMPs) proinflammatory cytokines, and nitric oxide (Gomez-Lopez *et al*., 2014). Macrophages can be depleted in a murine model by injecting

Downloaded From Vet-eBooks.com

Table 12.2 Animal models of immune cell manipulation during pregnancy.

Immune cell type	Clinical condition	Experimental treatment	Treatment effect	References
Macrophage	Preterm birth	Ablation: antibodies, F4/80, i.p. CD11b-diphtheria toxin receptor mouse	Protection from PTB	Turner *et al.*, 2011; Cailhier *et al.*, 2005; Hamilton *et al.*, 2012
Neutrophil	Preterm birth	Ablation: antibodies, GR-1, i.p.	Does not reverse PTB but reduces inflammation	Rinaldi *et al.*, 2014
Natural killer and NKT cells	Preterm birth Preeclampsia	Ablation: antibodies, Asialo GM1, NK1.1 Genetic ablation, $J\alpha18^{-/-/-}$, tgε26, $p56^{lck-/-/-}$/IL-2Rβ$^{-/-/-}$, RAG2$^{-/-/-}$/γc$^{-/-/-}$	Ablation protects from PTB; Ablation results in PE phenotype	Li *et al.*, 2012; Murphy *et al.*, 2009; Miko *et al.*, 2008; Wang *et al.*, 1994; Greenwood *et al.*, 2000; Guimond *et al.*, 1997; Mazurier *et al.*, 1999
T lymphocytes: CD4+ TH1	Abortion Preeclampsia	Ablation with antibodies, P-selectin (abortion model); cell transfer with activated TH1 (preeclampsia model)	Depletion protects from abortion; transfer of activated TH1 cause PE symptoms	Wang *et al.*, 1994; Bertoja *et al.*, 2005; Zenclussen *et al.*, 2004; Austrup *et al.*, 1997
T lymphocytes: CD4+ CD25+ T-regs	Abortion	Ablation with antibodies, CD25; cell transfer into abortion-prone mice	Required for normal pregnancy; transfer protects mice from abortion	Aluvihare *et al.*, 2004; Zenclussen *et al.*, 2005

Downloaded From Vet-eBooks.com

antibodies directed against the macrophage protein F4/80, i.p., which protects mice from PTB induced by treatment with LPS (Gonzalez *et al.*, 2011) and CpG oligodeoxynucleotide (Thaxton *et al.*, 2009). Macrophages can also be ablated genetically. A conditional ablation mouse has been developed allowing for transient loss of CD11b+ macrophages (Turner *et al.*, 2011; Cailhier *et al.*, 2005). This model has the human diphtheria toxin receptor (DTR) under the control of a macrophage promoter sequence, CD11b. Since mouse cells are not sensitive to the toxin, when mice are treated with diphtheria, only macrophages are eliminated. The strength of this model is the complete, transient loss of macrophages, more so than antibody ablation, but because CD11b is expressed in other cell types, these results should be evaluated carefully.

12.4.4.2 Neutrophils

Neutrophils are short-lived scavenging cells thought to play a role in infection-associated PTB (Hamilton *et al.*, 2012). These cells can be depleted using antibodies directed against the surface marker GR-1, i.p. on day 16, preceding treatment with the TLR ligand LPS on gestation day 17, directly into the uterine horn (Rinaldi *et al.*, 2014). Depletion of GR-1 positive neutrophils does not reverse LPS-induced PTB or cervical ripening but reduces proinflammation at the maternal–fetal interface (Rinaldi *et al.*, 2014).

12.4.4.3 Natural Killer Cells

Uterine natural killer (NK) cells are innate cytotoxic cells, and natural killer T (NKT) cells are unique in having an invariant T-cell receptor and cytotoxic capabilities. Both cell types are found in the uterus and play a role in the inflammatory response during PTB (Li *et al.*, 2012; Murphy *et al.*, 2009) and PE (Miko *et al.*, 2008). The NK cells can be ablated in mice using i.p. injections of antiasialo GM1 or NK1.1 antibodies (Murphy *et al.*, 2009). There is also a genetic ablation model, the $J\alpha18^{-/-}$ mouse, which has lymphocytes and NK, but not NKT cells (Li *et al.*, 2012). This mouse has been used to show a role for NKT in infection-induced PTB (Li *et al.*, 2012). Other genetic models that lack NK cells include tgε26, $p56^{lck-/-}$/IL-$2R\beta^{-/-}$, and $RAG2^{-/-}/\gamma c^{-/-}$ mice (Ashkar, 2001; Wang *et al.*, 1994; Greenwood *et al.*, 2000; Guimond *et al.*, 1997; Mazurier *et al.*, 1999). All models have abnormal uterine arteries and endothelial anomalies, demonstrating that NK cells regulate vascular function and play a role in the development and pathophysiology of PE.

12.4.4.4 T-Lymphocytes (T Cells)

CD4+ helper T cells direct inflammatory responses by differentiating into proinflammatory, or TH1 cells and have been implicated in miscarriage and preeclampsia (Bertoja *et al.*, 2005; Zenclussen *et al.*, 2004). TH1 cells express P-selectin, unlike other T-cell populations (Austrup *et al.*, 1997). Treating mice with an antibody against P-selectin inhibits TH1 cells from exiting blood vessels and invading the maternal–fetal interface (Bertoja *et al.*, 2005). The contribution of local TH1 cells to SA can thus be measured by using this technique in conjunction with the CBA/J × DBA/2 abortion-prone mice. Preeclampsia can also be recreated in pregnant mice by transferring activated TH1 cells into pregnant recipients (Zenclussen *et al.*, 2004). Spleens from donor animals are collected and lymphocytes are incubated with IL-2 and IL-12 to stimulate differentiation into TH1 cells. These activated cells (10^7) can be injected into pregnant recipients, i.v., on gestational days 12 and 14 (Zenclussen *et al.*, 2004). The recipients of these treatments suffer PE symptoms including increased blood pressure and proteinuria (Zenclussen *et al.*, 2004). Finally, another subset of T cells, regulatory T (T-reg) cells are important for the regulation of inflammation during pregnancy (Zenclussen, 2006). T-regs can be depleted from mice using an antibody against CD25 and these experiments indicate they are important and necessary for healthy pregnancy (Aluvihare *et al.*, 2004). Furthermore, transferring T-regs into the CBA/J × DBA/2 abortion-prone mice prevents spontaneous abortion (Zenclussen *et al.*, 2005).

Downloaded From Vet-eBooks.com

These models have been invaluable for deciphering the contribution of different immune cell populations to healthy and abnormal pregnancy. While genetic ablation indicates what specific factors are important, the immune cell reconstitution studies indicate which cell types are responsible for producing these factors. These specific populations could serve as therapeutic targets and will help identify immune-mediated pregnancy complications.

12.5 Inflammation During Pregnancy and Offspring Disease

12.5.1 Introduction

"The stage is set before the play COMMENCES" is a quote from Sir Joseph Barcroft (1934) perfectly describing the necessity of proper placental development preceding normal fetal development. Maternal and fetal inflammation can be a result of acute infections, chronic subclinical infections, or even maternal obesity causing inflammation that can affect development of the placental or placental function later in pregnancy. These maternal and environmental factors can then result in fetal growth restriction and have been associated with the development of numerous offspring pathologies, including behavioral, cardiovascular, metabolic, neuronal, and immune disorders. This section reviews rodent, sheep, and nonhuman primate models that have been used to study the underlying mechanisms of the fetal origins of disease (Table 12.3).

Table 12.3 Animal models of the fetal origins of disease.

Animal model	Maternal treatment	Fetal/offpring outcome	References
Sheep	Fed 150% NRC recommended diet	Placental inflammation Fetal hyperinsulinemia Fetal hyperglycemia Offspring increased adiposity Offspring glucose tolerance	Zhu *et al.*, 2010; Li *et al.*, 2011
Rodent	High-fat diet Cafeteria diet	Placental inflammation Offspring abnormal eating behavior, insulin resistance, liver disease	Liang *et al.*, 2010; Li *et al.*, 2011; Bayol *et al.*, 2005
Nonhuman primate	High-fat diet	Placental inflammation Fetal high liver triglycerides Changes in fetal melanocortin system Offspring early-onset weight gain independent of postnatal diet	Farley *et al.*, 2009; Frias *et al.*, 2011; Li *et al.*, 2011; McCurdy *et al.*, 2009; Grayon *et al.*, 2009
Rodent	Bacterial infection (LPS; i.p., intrauterine, s.c.)	Placental inflammation Offspring brain injury Offspring behavior disorders	Wang *et al.*, 2007; Elovitz *et al.*, 2011; Kirsten *et al.*, 2012, 2013
Rodent	Viral infection (poly (I:C), H1N1; i.v., i.p., intranasal)	Placental inflammation Offspring brain injury Offspring behavior disorders	O'Callaghan *et al.*, 1991a, 1991b; Brown, 2006; Winter *et al.*, 2008, 2009; Shi *et al.*, 2003, 2009

Downloaded From Vet-eBooks.com

12.5.2 Models of Inflammation During Pregnancy Resulting in Offspring Disease

12.5.2.1 Maternal Obesity

Maternal obesity is proposed to affect fetal development by causing a chronic low-grade inflammatory environment during pregnancy (Challier *et al*., 2008; Ramsay *et al*., 2002). There are several animal models that have been used to test this hypothesis, including sheep, rodents, and nonhuman primates. When sheep are fed 150% National Research Council (NRC) recommended dietary needs, they will become significantly heavier than controls fed 100% NRC dietary needs and will have higher free fatty acids, triglycerides, and cholesterol Zhu *et al.*, 2010. Furthermore, this model exhibits heightened placental inflammation characterized by increased expression of immune cell markers, proinflammatory cytokines, and TLRs, making it a good model for studying the effect of maternal diet-induced placental inflammation on fetal outcomes (Ramsay *et al*., 2002; Zhu *et al*., 2010). Rodents can also be used to study obesity-dependent placental inflammation. In a mouse model of gestational diabetes mellitus induced by feeding a high-fat diet of 60% fat, placentas were characterized as having high oxidative stress, mixed inflammation, and tissue necrosis (Liang *et al*., 2010). Finally, baboons can be fed *ad libitum* to achieve a significant increase in an obesity index developed for nonhuman primates, and these females experience increased placental inflammation as characterized by macrophage infiltration and CD14 expression (Farley *et al*., 2009). But maternal obesity per se may not be the only contributory factor. A study using Japanese Macaques found that a maternal high-fat diet, *independent of maternal obesity*, also induced placental inflammation and TLR4 expression (Frias *et al*., 2011). This suggests that high-fat diet with or without maternal obesity may provide a model of maternal placental immune activation.

The placental inflammation associated with maternal obesity and diet may play a role in development of liver, cardiovascular and metabolic disorders in offspring. Rodent models typically utilize a diet high in sugar or fat, or alternately, the "cafeteria diet," which is an attempt to mimic a typical Western diet (Li *et al*., 2011; Bayol *et al*., 2005). These diets can increase adiposity before or during pregnancy and offspring of these mothers can develop abnormal eating behaviors, insulin resistance, liver disease, and hypertension (Bayol *et al*., 2005; Segovia *et al*., 2014). Similarly, pregnant sheep can be overfed (150% NRC recommendations verses 100% NRC for controls) to induce increased adiposity, and associated *in utero* inflammation, at mating and throughout gestation to study the effect on the developing fetus or offspring (Ramsay *et al*., 2002). Depending on the amount of maternal adiposity and timing of the weight gain, fetuses exhibit hyperinsulinemia and hyperglycemia, and adult progeny can suffer increased adiposity and glucose tolerance (Ramsay *et al*., 2002).

There are several nonhuman primate models of high caloric diet and/or maternal obesity, which suffer obesity-associated inflammation, that have been used to study fetal origins of liver and metabolic disorders. Macaques can be fed a high-fat diet (17% protein, 56% carbohydrate, and 15% fat) that will induce obesity and insulin resistance (McCurdy *et al*., 2009). Fetuses from females consuming this diet are characterized as having high liver triglycerides and symptoms of nonalcoholic fatty liver disease (McCurdy *et al*., 2009).

In another study using macaques, high-fat diets were defined as 35% fat and included high caloric treats (Grayon *et al*., 2009). The animals sensitive to this diet double the amount of body fat and also are insulin-resistant while not becoming diabetic (Grayon *et al*., 2009). This model of obesity and obesity-associated inflammation has been used to determine that maternal high-fat diet induces changes in the fetal melanocortin system (responsible for appetite and regulation of energy use) and offspring of these mothers have early onset weight gain independent of postnatal diet (Grayon *et al*., 2009).

Downloaded From Vet-eBooks.com

12.5.2.2 Maternal Infection

Maternal bacterial infections have been associated with chorioamnionitis and development of offspring behavioral disorders and brain injury (Wang *et al*., 2007; Emond *et al*., 1989). There are numerous rodent models that have been used to study the role of these infections and associated changes in cytokines in the developing brain that are thought to be at least partially responsible for offspring phenotypes. In CD-1 or C57BL/6 mice given intrauterine infusion of LPS (50–125 μg; mimicking Gram-negative bacterial infection) on gestation day 15, offspring suffer brain injury characterized by aberrant cytokine expression, brain lesions, and nerve injury (Wang *et al*., 2007; Elovitz *et al*., 2011; Kirsten *et al*., 2013). Pregnant rats treated with 0.02–4 mg/kg LPS, i.p. on gestation days 9.5 or 15–19.5 also yield offspring with abnormal brain development and autism-like symptoms, including abnormal socialization, impaired learning and memory, and induced repetitive behaviors (Kirsten *et al*., 2012, 2013).

Maternal viral infections are strongly associated with maternal immune activation, placental inflammation, aberrant cytokine expression in fetal brain, and development of offspring brain injury (O'Callaghan *et al*., 1991a, 1991b; Brown, 2006). Pregnant mice injected with 5 mg/kg of the viral mimic and TLR3 ligand poly(I:C), i.v., on gestation day 9 yield offspring with long-term changes in neurochemicals such as serotonin and dopamine (Winter *et al*., 2008, 2009), factors involved in regulation of moods and behaviors. These factors are also changed in the brains of offspring from mothers receiving intranasal challenge with a sublethal dose of H1N1 Influenza A virus at gestation day 16 (Shi *et al*., 2003, 2009). In addition, influenza infection and poly(I:C) treatments induce histological changes in offspring brain (brain damage) and behavioral aberrations, much like LPS-treated animals, suggesting that offspring have schizophrenia and/or autism-type phenotypes (Makinodan *et al*., 2008; Nyffeler *et al*., 2006). Similar findings have been reported in pregnant rats treated with poly(I:C) at different times during gestation (Zuckerman *et al*., 2003).

These models can be used to better understand the factors driving developmental changes in offspring following inflammation during pregnancy. For example, following previous findings, one study gave mice a single injection of IL-6 at gestation day 12.5, and observed changes in offspring behavior, while an IL-6 neutralizing antibody prevented behavioral deficits in poly(I:C)-treated animals (Smith *et al*., 2007). This is one example of how powerful these models can be to identify important factors that regulate fetal development.

12.6 Perspectives and Conclusions

The pregnant immune system is specifically modulated to ensure there is appropriate inflammation during implantation and labor or during infection that puts the mother and/or fetus at risk. During the remainder of pregnancy, cytokines such as IL-10 and TGF-β are expressed and are associated with healthy pregnancy. Maternal and environmental factors that change this careful immune regulation are associated with poor pregnancy and/or fetal outcomes. Studying the effect of these factors on pregnancy is difficult because they affect multiple tissues, cells, and pathways that then culminate in adverse pregnancy outcomes and maternal morbidity. Therefore, animal models provide a robust tool for understanding what factors affect pregnancy, how they affect it, and how they may be reversed. These models have already shown us that activated immune cells and inflammatory cytokines, that is, inflammation, are associated with many adverse pregnancy outcomes. It is now time to focus on how these cells and factors are being activated and how they affect the placenta and fetus at the molecular level. Studies like these will help identify clinical targets for prevention and treatment in the future.

Downloaded From Vet-eBooks.com

One further consideration is the lessons learned from the CBA/J X DBA/2J cross in mice. Finding that the caging system employed affects reproductive performance highlights the potential impact of environment and organismal microbiome on experimental outcomes. Accounting for this variable could be crucial for proper discovery of factors affecting pregnancy, be it nutritional, genetic, or pathogenic. Failure to control for environmental sources of reproductive tract inflammation could confound efforts to replicate research findings in different laboratories, and could lead to spurious conclusions.

Acknowledgments

Work in the authors' laboratories is supported in part by grants from the National Institutes of Health, National Institute of Child Health and Development (1R01HD075903), and the Office of Research Infrastructure Programs Division of Comparative Medicine Grants (R24 OD-012221) (to K.E.L.), and MSU AgBioResearch and Michigan State University.

References

Agrawal, V., Jaiswal, M.K., Ilievski, V., Beaman, K.D., Jilling, T., and Hirsch, E. (2014) Platelet activating factor (PAF): a role in preterm delivery and an essential interaction with toll-like receptor (TLR) signaling in mice. *Biol. Reprod.*, **91** (5), 119.

Alexander, B., Cockrell, K., Massey, M., Bennett, W.A., and Granger, J.P. (2002) Tumor necrosis factor-alpha-induced hypertension in pregnant rats results in decreased renal neuronal nitric oxide synthase expression. *Am. J. Hypertens.*, **15**, 170–175.

Aluvihare, V.R., Kallikourdis, M., and Betz, A.G. (2004) Regulatory T cells mediate maternal tolerance to the fetus. *Nat. Immunol.*, **5** (3), 266–271.

Arck, P.C., Merali, F.S., Manuel, J., Chaouat, G., and Clark, D.A. (1995a) Stress-triggered abortion: inhibition of protective suppression and promotion of tumor necrosis factor-α (TNF-α) release as a mechanism triggering resorptions in mice. *Am. J. Reprod. Immunol.*, **33** (1), 74–80.

Arck, P., Merali, F.S., Stanisz, A., Stead, R., Chaouat, G., Manuel, J., and Clark, D. (1995b) Stress-induced murine abortion associated with substance P-dependent alteration in cytokines in maternal uterine decidua. *Biol. Reprod.*, **53**, 814–819.

Arck, P., Troutt, A., and Clark, D. (1997) Soluble receptors neutralizing TNF-α and IL-1 block stress-triggered murine abortion. *Am. J. Reprod. Immunol.*, **37**, 262–266.

Ashkar, A.A. and Croy, B.A. (2001) Functions of uterine natural killer cells are mediated by interferon gamma production during murine pregnancy. *Semin. Immunol.*, **13** (4), 235–241.

Austrup, F., Vestweber, D., Borges, E., Lohning, M., Brauer, R., Herz, U., Renz, H., Hallmann, R., Scheffold, A., Radbruch, A., and Hamann, A. (1997) P- and E-selectin mediate recruitment of T-helper-1 but not T-helper-2 cells into inflamed tissue. *Nature*, **385** (2), 81–83.

Bagga, S., Gravett, M., Witkin, S., Haluska, G., and Novy, M. (1996) Interleukin-1 beta intra-amniotic infusion induces tumor necrosis factor-alpha, prostaglandin production, and preterm contractions in pregnant rhesus monkeys. *J. Soc. Gynecol. Investig.*, **3** (3), 121–126.

Banhidy, F., Acs, N., Puho, E.H., and Czeizel, A.E. (2007) Pregnancy complications and birth outcomes of pregnant women with urinary tract infections and related drug treatments. *Scand. J. Infect. Dis.*, **39** (5), 390–397.

Barber, A., Robson, S., Myatt, L., Bulmer, J., and Lyall, F. (2001) Heme oxygenase expression in human placenta and placental bed: reduced expression of placenta endothelial HO-2 in preeclampsia and fetal growth restriction. *FASEB J.*, **15**, 1158–1168.

Downloaded From Vet-eBooks.com

Barcroft, J. (1934) *Features in the Architecture of Physiological Function*, Cambridge University Press, Cambridge, UK.

Bayol, S.A., Simbi, B.H., and Stickland, N.C. (2005) A maternal cafeteria diet during gestation and lactation promotes adiposity and impairs skeletal muscle development and metabolism in rat offspring at weaning. *J. Physiol.*, **567** (Part 3), 951–961.

Bennett, W.A., Terrone, D.A., Rinehart, B.K., Kassab, S., Martin, J.N., Jr., and Granger, J.P. (2000) Intrauterine endotoxin infusion in rat pregnancy induces preterm delivery and increases placental prostaglandin F2alpha metabolite levels. *Am. J. Obstet. Gynecol.*, **182** (6), 1496–501.

Bertoja, A.Z., Zenclussen, M.L., Casalis, P.A., Sollwedel, A., Schumacher, A., Woiciechowsky, C., Volk, H.D., and Zenclussen, A.C. (2005) Anti-P- and E-selectin therapy prevents abortion in the CBA/J × DBA/2J combination by blocking the migration of Th1 lymphocytes into the foetal–maternal interface. *Cell. Immunol.*, **238** (2), 97–102.

Billington, W.D. (2003) The immunological problem of pregnancy: 50 years with the hope of progress. A tribute to Peter Medawar. *J. Reprod. Immunol.*, **60** (1), 1–11.

Blank, M., Cohen, J., Toder, V., and Shoenfeld, Y. (1991) Induction of anti-phospholipid syndrome in naive mice with mouse Lupus monoclonal and human polyclonal anti-cardiolipin antibodies. *Proc. Natl. Acad. Sci. USA*, **88**, 3069–3073.

Blank, V., Hirsch, E., Challis, J.R., Romero, R., and Lye, S.J. (2008) Cytokine signaling, inflammation, innate immunity and preterm labour: a workshop report. *Placenta*, **29** (Suppl. A), S102–S104.

Branch, D.W., Dudley, D.J., Mitchell, M.D., Creighton, K.A., Abbott, T.M., Hammond, E.H., and Daynes, R.A. (1990) Immunoglobulin G fractions from patients with antiphospholipid antibodies cause fetal death in BALB/c mice: A model for autoimmune fetal loss. *Am. J. Obstet. Gynecol.*, **163** (1), 210–216.

Brown, A.S. (2006) Prenatal infection as a risk factor for schizophrenia. *Schizophr. Bull.*, **32** (2), 200–202.

Cailhier, J.F., Partolina, M., Vuthoori, S., Wu, S., Ko, K., Watson, S., Savill, J., Hughes, J., and Lang, R.A. (2005) Conditional macrophage ablation demonstrates that resident macrophages initiate acute peritoneal inflammation. *J. Immunol.*, **174** (4), 2336–2342.

Canakci, V., Canakci, C., Canakci, H., Canakci, E., Cicek, Y., Ingec, M., Ozgoz, M., Demir, T., Dilsiz, A., and Yagiz, H. (2004) Periodontal disease as a risk factor for pre-eclampsia: a case control study. *Austral. N.Z. J. Obstet. Gynecol.*, **44**, 568–573.

Celik, H. and Ayar, A. (2002) Effects of erythromycin on pregnancy duration and birth weight in lipopolysaccharide-induced preterm labor in pregnant rats. *Eur. J. Obstet. Gynecol. Reprod. Biol.*, **103**, 22–25.

Challier, J.C., Basu, S., Bintein, T., Minium, J., Hotmire, K., Catalano, P.M. and Hauguel-de Mouzon, S. (2008) Obesity in pregnancy stimulates macrophage accumulation and inflammation in the placenta. *Placenta*, **29** (3), 274–281.

Chan, K.H., Zhang, A.J., To, K.K., Chan, C.C., Poon, V.K., Guo, K., Ng, F., Zhang, Q.W., Leung, V.H., Cheung, A.N., Lau, C.C., Woo, P.C., Tse, H., Wu, W., Chen, H., Zheng, B.J., and Yuen, K.Y. (2010) Wild type and mutant 2009 pandemic influenza A (H1N1) viruses cause more severe disease and higher mortality in pregnant BALB/c mice. *PLoS One*, **5** (10), e13757.

Chaouat, G., Kiger, N., and Wegmann, T. (1983) Vaccination against spontaneous abortion in mice. *J. Reprod. Immunol.*, **5**, 389–392.

Chaouat, G., Menu, E., Clark, D., Dy, M., Minkowski, M., and Wegmann, T. (1990) Control of fetal survival in CBA × DBA/2 mice by lymphokine therapy. *J. Reprod. Fertil.*, **89**, 447–458.

Christian, L.M. (2012) Psychoneuroimmunology in pregnancy: immune pathways linking stress with maternal health, adverse birth outcomes, and fetal development. *Neurosci. Biobehav. Rev.*, **36** (1), 350–361.

Downloaded From Vet-eBooks.com

Clark, D., McDermott, M.P., and Szewczuk, M. (1980) Impairment of host-versus-graft reaction in pregnant mice. *Cell. Immunol.*, **52**, 106–118.

Clark, D., Chaouat, G., Arck, P., Mittruecker, H., and Levy, G. (1998) Cutting edge: cytokine-dependent abortion in CBA × DBA/2 mice is mediated by the procoagulant fgl2 prothrombinase. *J. Immunol.*, **160**, 545–549.

Conde-Agudelo, A., Villar, J., and Lindheimer, M. (2008) Maternal infection and risk of preeclampsia: systematic review and metaanalysis. *Am. J. Obstet. Gynecol.*, **198** (1), 7–22.

Copper, R., Goldenberg, R.L., Das, A., Elder, N., Swain, M.G., Norman, G., Ramsey, R., Cotroneo, P., Collins, B., Johnson, F., Jones, J., and Meier, A. (1996) The preterm prediction study: maternal stress is associated with spontaneous preterm birth at less than thirty-five weeks' gestation. *Am. J. Obstet. Gynecol.*, **175** (5), 1286–1292.

Coussons-Read, M.E., Okun, M.L., and Nettles, C.D. (2007) Psychosocial stress increases inflammatory markers and alters cytokine production across pregnancy. *Brain Behav. Immun.*, **21** (3), 343–350.

Creanga, A.A., Johnson, T.F., Graitcer, S.B., Hartman, L.K., Al-Samarrai, T., Schwarz, A.G., Chu, S.Y., Sackoff, J.E., Jamieson, D.J., Fine, A.D., Shapiro-Mendoza, C.K., Jones, L.E., Uyeki, T.M., Balter, S., Bish, C.L., Finelli, L., and Honein, M.A. (2010) Severity of 2009 pandemic influenza A (H1N1) virus infection in pregnant women. *Obstet. Gynecol.*, **115** (4), 717–726.

Cudmore, M., Ahmad, S., Al-Ani, B., Fujisawa, T., Coxall, H., Chudasama, K., Devey, L.R., Wigmore, S.J., Abbas, A., Hewett, P.W., and Ahmed, A. (2007) Negative regulation of soluble Flt-1 and soluble endoglin release by heme oxygenase-1. *Circulation*, **115** (13), 1789–1797.

Davisson, R.L., Hoffmann, D.S., Butz, G., Aldape, G., Schlager, G., Merrill, D., Sethi, S., Weiss, R.M., and Bates, J. (2001) Discovery of a spontaneous genetic mouse model of preeclampsia. *Hypertension*, **39** (2), 337–342.

Dekel, N., Gnainsky, Y., Granot, I., Racicot, K., and Mor, G. (2014) The role of inflammation for a successful implantation. *Am. J. Reprod. Immunol.*, **72** (2), 141–147.

Dokras, A., Hoffmann, D.S., Eastvold, J.S., Kienzle, M.F., Gruman, L.M., Kirby, P.A., Weiss, R.M., and Davisson, R.L. (2006) Severe feto-placental abnormalities precede the onset of hypertension and proteinuria in a mouse model of preeclampsia. *Biol. Reprod.*, **75** (6), 899–907.

Elovitz, M.A. and Mrinalini, C. (2004) Animal models of preterm birth. *Trends Endocrinol. Metab.*, **15** (10), 479–487.

Elovitz, M.A., Wang, Z., Chien, E.K., Rychlik, D.F., and Phillippe, M. (2003) A new model for inflammation-induced preterm birth. *Am. J. Pathol.*, **163** (5), 2103–2111.

Elovitz, M.A., Brown, A.G., Breen, K., Anton, L., Maubert, M., and Burd, I. (2011) Intrauterine inflammation, insufficient to induce parturition, still evokes fetal and neonatal brain injury. *Int. J. Dev. Neurosci.*, **29** (6), 663–671.

Emond, A., Golding, J., and Peckham, A. (1989) Cerebral palsy in two national cohort studies. *Arch. Dis. Child.*, **64**, 848–852.

Farley, D., Tejero, M.E., Comuzzie, A.G., Higgins, P.B., Cox, L., Werner, S.L., Jenkins, S.L., Li, C., Choi, J., Dick, E.J., Jr., Hubbard, G.B., Frost, P., Dudley, D.J., Ballesteros, B., Wu, G., Nathanielsz, P.W., and Schlabritz-Loutsevitch, N.E. (2009) Feto-placental adaptations to maternal obesity in the baboon. *Placenta*, **30** (9), 752–760.

Fichorova, R.N., Lee, Y., Yamamoto, H.S., Takagi, Y., Hayes, G.R., Goodman, R.P., Chepa-Lotrea, X., Buck, O.R., Murray, R., Kula, T., Beach, D.H., Singh, B.N., and Nibert, M.L. (2012) Endobiont viruses sensed by the human host: beyond conventional antiparasitic therapy. *PLoS One*, **7** (11), e48418.

Filipovich, Y., Lu, S.J., Akira, S., and Hirsch, E. (2009) The adaptor protein MyD88 is essential for *E. coli*-induced preterm delivery in mice. *Am. J. Obstet. Gynecol.*, **200** (1), 93.

Frias, A.E., Morgan, T.K., Evans, A.E., Rasanen, J., Oh, K.Y., Thornburg, K.L., and Grove, K.L. (2011) Maternal high-fat diet disturbs uteroplacental hemodynamics and increases the frequency

Downloaded From Vet-eBooks.com

of stillbirth in a nonhuman primate model of excess nutrition. *Endocrinology*, **152** (6), 2456–2464.

Gibbs, R.S., McDuffie, R.S., Jr., Kunze, M., Barr, J.M., Wolf, D.M., Sze, C.I., Shikes, R., and Sherman, M.P. (2004) Experimental intrauterine infection with *Prevotella bivia* in New Zealand white rabbits. *Am. J. Obstet. Gynecol.*, **190** (4), 1082–1086.

Goldenberg, R.L., Culhane, J.F., Iams, J.D., and Romero, R. (2008) Epidemiology and causes of preterm birth. *Lancet*, **371** (9606), 75–84.

Gomez-Lopez, N., StLouis, D., Lehr, M.A., Sanchez-Rodriguez, E.N., and Arenas-Hernandez, M. (2014) Immune cells in term and preterm labor. *Cell. Mol. Immunol.*, **11** (6), 571–81.

Gonzalez, J.M., Franzke, C.W., Yang, F., Romero, R., and Girardi, G. (2011) Complement activation triggers metalloproteinases release inducing cervical remodeling and preterm birth in mice. *Am. J. Pathol.*, **179** (2), 838–849.

Gravett, M., Haluska, G., Cook, M., and Novy, M. (1996) Fetal and maternal endocrine responses to experimental intrauterine infection in rheses monkeys. *Am. J. Obstet. Gynecol.*, **174**, 1725–1733.

Grayon, B., Levasseur, P., Williams, S., Smith, M.A., Marks, D., and Grove, K.L. (2009) Changes in melanocortin expression and inflammatory pathways in fetal offspring of nonhuman primates fed a high-fat diet. *Endocrinology*, **151** (4), 1622–1632.

Greenwood, J.D., Minhas, K., di Santo, J.P., Makita, M., Kiso, Y., and Croy, B.A. (2000) Ultrastructural studies of implantation sites from mice deficient in uterine natural killer cells. *Placenta*, **21** (7), 693–702.

Grigsby, P.L., Poore, K.R., Hirst, J.J., and Jenkin, G. (2000) Inhibition of premature labor in sheep by a combined treatment of nimesulide, a prostaglandin synthase type 2 inhibitor, and atosiban, an oxytocin receptor antagonist. *Am. J. Obstet. Gynecol.*, **183** (3), 649–657.

Grigsby, P.L., Hirst, J.J., Scheerlinck, J.P., Phillips, D.J., and Jenkin, G. (2003) Fetal responses to maternal and intra-amniotic lipopolysaccharide administration in sheep. *Biol. Reprod.*, **68** (5), 1695–702.

Guimond, M., Luross, J., Wang, B., Terhorst, C., Danial, S., and Croy, B.A. (1997) Absence of natural killer cells during murine pregnancy is associated with reproductive compromise in TgE26 mice. *Biol. Reprod.*, **56**, 169–179.

Hamilton, M. and Hamilton, B. (1987) Environmental influences on immunologically associated spontaneous abortion in CBA/J mice. *J. Reprod. Immunol.*, **11**, 237–241.

Hamilton, S., Oomomian, Y., Stephen, G., Shynlova, O., Tower, C.L., Garrod, A., Lye, S.J., and Jones, R.L. (2012) Macrophages infiltrate the human and rat decidua during term and preterm labor: evidence that decidual inflammation precedes labor. *Biol. Reprod.*, **86** (2), 39.

Han, Y.W. (2011) Oral health and adverse pregnancy outcomes: what's next? *J. Dental Res.*, **90** (3), 289–293.

Han, Y.W., Redline, R.W., Li, M., Yin, L., Hill, G.B., and McCormick, T.S. (2004) *Fusobacterium nucleatum* induces premature and term stillbirths in pregnant mice: implication of oral bacteria in preterm birth. *Infect. Immun.*, **72** (4), 2272–2279.

Han, Y.W., Ikegami, A., Bissada, N.F., Herbst, M., Redline, R.W., and Ashmead, G.G. (2006) Transmission of an uncultivated Bergeyella strain from the oral cavity to amniotic fluid in a case of preterm birth. *J. Clin. Microbiol.*, **44** (4), 1475–1483.

Han, Y.W., Shen, T., Chung, P., Buhimschi, I.A., and Buhimschi, C.S. (2009) Uncultivated bacteria as etiologic agents of intra-amniotic inflammation leading to preterm birth. *J. Clin. Microbiol.*, **47** (1), 38–47.

Hirsch, E., Filipovich, Y., and Mahendroo, M. (2006) Signaling via the type I IL-1 and TNF receptors is necessary for bacterially induced preterm labor in a murine model. *Am. J. Obstet. Gynecol.*, **194** (5), 1334–1340.

Downloaded From Vet-eBooks.com

Holers, V., Girardi, G., Mo, L., Guthridge, J., Molina, H., Pierangeli, S., Espinola, R., Xiaowei, L., Mao, D., Vialpando, C., and Salmon, J. (2002) Complement C3 activation is required for antiphospholipid antibody-induced fetal loss. *J. Exp. Med.*, **195** (2), 211–220.

Ilievski, V., Lu, S.J., and Hirsch, E. (2007) Activation of toll-like receptors 2 or 3 and preterm delivery in the mouse. *Reprod. Sci.*, **14** (4), 315–320.

Jamieson, D.J., Honein, M.A., Rasmussen, S.A., Williams, J.L., Swerdlow, D.L., Biggerstaff, M.S., Lindstrom, S., Louie, J.K., Christ, C.M., Bohm, S.R., Fonseca, V.P., Ritger, K.A., Kuhles, D.J., Eggers, P., Bruce, H., Davidson, H.A., Lutterloh, E., Harris, M.L., Burke, C., Cocoros, N., Finelli, L., MacFarlane, K.F., Shu, B., and Olsen, S.J. (2009) Novel influenza APWG: H1N1 2009 influenza virus infection during pregnancy in the USA. *Lancet*, **374** (9688), 451–458.

Jamieson, A.M., Yu, S., Annicelli, C.H., and Medzhitov, R. (2010) Influenza virus-induced glucocorticoids compromise innate host defense against a secondary bacterial infection. *Cell Host Microbe*, **7** (2), 103–114.

Jeffcoat, M.K., Geurs, N.C., Reddy, M.S., Cliver, S.P., Goldenberg, R.L., and Hauth, J.C. (2001) Periodontal infection and preterm birth: results of a prospective study. *J. Am. Dent. Assoc.*, **132** (7), 875–880.

Kaga, N., Katsuki, Y., Obata, M., and Shibutani, Y. (1995) Repeated administration of lipopolysaccharide induces preterm delivery in mice. *Am. J. Obstet. Gynecol.*, **174** (2), 755–759.

Kajikawa, S., Kaga, N., Futamura, Y., Kakinuma, C., and Shibutani, Y. (1998) Lipoteichoic acid induces preterm delivery in mice. *J. Pharmacol. Toxicol. Methods*, **39**, 147–154.

Kanasaki, K., Palmsten, K., Sugimoto, H., Ahmad, S., Hamano, Y., Xie, L., Parry, S., Augustin, H.G., Gattone, V.H., Folkman, J., Strauss, J.F., and Kalluri, R. (2008) Deficiency in catechol-*O*-methyltransferase and 2-methoxyoestradiol is associated with pre-eclampsia. *Nature*, **453** (7198), 1117–1121.

Kim, H.M., Kang, Y.M., Song, B.M., Kim, H.S., and Seo, S.H. (2012) The 2009 pandemic H1N1 influenza virus is more pathogenic in pregnant mice than seasonal H1N1 influenza virus. *Viral Immunol.*, **25** (5), 402–410.

Kim, J.C., Kim, H.M., Kang, Y.M., Ku, K.B., Park, E.H., Yum, J., Kim, J.A., Kang, Y.K., Lee, J.S., Kim, H.S., and Seo, S.H. (2014) Severe pathogenesis of influenza B virus in pregnant mice. *Virology*, **448**, 74–81.

Kirsten, T.B., Chaves-Kirsten, G.P., Chaible, L.M., Silva, A.C., Martins, D.O., Britto, L.R., Dagli, M.L., Torrao, A.S., Palermo-Neto, J., and Bernardi, M.M. (2012) Hypoactivity of the central dopaminergic system and autistic-like behavior induced by a single early prenatal exposure to lipopolysaccharide. *J. Neurosci. Res.*, **90** (10), 1903–1912.

Kirsten, T.B., Lippi, L.L., Bevilacqua, E., and Bernardi, M.M. (2013) LPS exposure increases maternal corticosterone levels, causes placental injury and increases IL-1beta levels in adult rat offspring: relevance to autism. *PLoS One*, **8** (12), e82244.

Koga, K., Cardenas, I., Aldo, P., Abrahams, V.M., Peng, B., Fill, S., Romero, R., and Mor, G. (2009) Activation of TLR3 in the trophoblast is associated with preterm delivery. *Am. J. Reprod. Immunol.*, **61** (3), 196–212.

Li, M., Sloboda, D.M., and Vickers, M.H. (2011) Maternal obesity and developmental programming of metabolic disorders in offspring: evidence from animal models. *Exp. Diabetes Res.*, **2011**, 592408.

Li, L.P., Fang, Y.C., Dong, G.F., Lin, Y., and Saito, S. (2012) Depletion of invariant NKT cells reduces inflammation-induced preterm delivery in mice. *J. Immunol.*, **188** (9), 4681–4689.

Liang, C., DeCourcy, K., and Prater, M.R. (2010) High-saturated-fat diet induces gestational diabetes and placental vasculopathy in C57BL/6 mice. *Metabolism*, **59** (7), 943–950.

Lim, R., Fedulov, A.V., and Kobzik, L. (2014) Maternal stress during pregnancy increases neonatal allergy susceptibility: role of glucocorticoids. *Am. J. Physiol. Lung Cell. Mol. Physiol.*, **307** (2), L141–L148.

Downloaded From Vet-eBooks.com

Lin, D., Smith, M.A., Elter, J., Champagne, C., Downey, C.L., Beck, J., and Offenbacher, S. (2003) *Porphyromonas gingivalis* infection in pregnant mice is associated with placental dissemination, an increase in the placental Th1/Th2 cytokine ratio, and fetal growth restriction. *Infect. Immun.*, **71** (9), 5163–5168.

Lin, Y., Zeng, Y., Di, J., and Zeng, S. (2005) Murine CD200+ CK7+ trophoblasts in a poly(I:C)-induced embryo resorption model. *Reproduction*, **130** (4), 529–537.

Lin, Y., Liang, Z., Chen, Y., and Zeng, Y. (2006) TLR3-involved modulation of pregnancy tolerance in double-stranded RNA-stimulated NOD/SCID mice. *J. Immunol.*, **176** (7), 4147–4154.

Makinodan, M., Tatsumi, K., Manabe, T., Yamauchi, T., Makinodan, E., Matsuyoshi, H., Shimoda, S., Noriyama, Y., Kishimoto, T., and Wanaka, A. (2008) Maternal immune activation in mice delays myelination and axonal development in the hippocampus of the offspring. *J. Neurosci. Res.*, **86** (10), 2190–2200.

Mazurier, F., Fontanellas, A., Salesse, S., Taine, L., Landriau, S., Moreau-Gaudry, F., Reiffers, J., Peault, B., Di Santo, J.P., and De Verneuil, H. (1999) A novel immunodeficient mouse model-RAG2 X common cytokine receptor gamma chain double mutants-requiring exogenous cytokine administration for human hematopoietic stem cell engraftment. *J. INterferon and cytokine res.*, **19**, 533–541.

McCarthy, F.P., Kingdom, J.C., Kenny, L.C., and Walsh, S.K. (2011) Animal models of preeclampsia: uses and limitations. *Placenta*, **32** (6), 413–419.

McCurdy, C., Bishop, J., Williams, S., Grayson, B., Smith, M.A., Friedman, J.E., and Grove, K.L. (2009) Maternal high-fat diet triggers lipotoxicity in the fetal livers of nonhuman primates. *J. Clin. Investig.*, **119** (2), 323–335.

McDuffie, R. and Gibbs, R.S. (1994) Animal models of ascending genital-tract infection in pregnancy. *Infect. Dis. Obstet. Gynecol.*, **2**, 60–70.

Medzhitov, R. (2001) Toll-like receptors and innate immunity. *Nat. Rev.*, **1**, 135–145.

Mellor, A.L., Sivakumar, J., Chandler, P.R., Smith, K.D., Moina, H., Mao, D., and Munn, D.H. (2001) Prevention of T cell-driven complement activation and inflammation by tryptophan catabolism during pregnancy. *Nat. Immunol.*, **2** (1), 64–68.

Miko, E., Szereday, L., Barakonyi, A., Jarkovich, A., Varga, P., and Szekeres-Bartho, J. (2008) The role of invariant NKT cells in pre-eclampsia. *Am. J. Reprod. Immunol.*, **60** (2), 118–126.

Munn, D.H., Zhou, M.X., Attwood, J., Bondarev, I., Conway, S., Marshall, B., Brown, C., and Mellor, AL. (1998) Prevention of allogeneic fetal rejection by tryptophan catabolism. *Science*, **281**, 1191–1193.

Murphy, S.P., Hanna, N.N., Fast, L.D., Shaw, S.K., Berg, G., Padbury, J.F., Romero, R., and Sharma, S. (2009) Evidence for participation of uterine natural killer cells in the mechanisms responsible for spontaneous preterm labor and delivery. *Am. J. Obstet. Gynecol.*, **200** (3), 308.

Mussalli, G., Blanchard, R., Brunnert, S., and Hirsch, E. (1999) Inflammatory cytokines in a murine model of infection-induced preterm labor: cause or effect? *J. Soc. Gynecol. Investig.*, **6**, 188–195.

Nyffeler, M., Meyer, U., Yee, B.K., Feldon, J., and Knuesel, I. (2006) Maternal immune activation during pregnancy increases limbic GABAA receptor immunoreactivity in the adult offspring: implications for schizophrenia. *Neuroscience*, **143** (1), 51–62.

O'Callaghan, E., Sham, P., Takei, N., Glover, G., and Murray, R.M. (1991a) Schizophrenia after prenatal exposure to 1957 A2 influenza epidemic. *Lancet*, **337** (8752), 1248–1250.

O'Callaghan, E., Sham, P., Takei, N., Glover, G., and Murray, R. (1991b) Schizophrenia after prenatal exposure to 1957 A2 influenza epidemic. *Lancet*, **337**, 1248–1250.

Orange, S., Rasko, J.E., Thompson, J.F., Vaughan, J., Olive, E., Pedler, M., Horvath, J.S., and Hennessy, A. (2005) Interleukin-10 regulates arterial pressure in early primate pregnancy. *Cytokine*, **29** (4), 176–185.

Downloaded From Vet-eBooks.com

Pincus-Knackstedt, M.K., Joachim, R.A., Blois, S.M., Douglas, A.J., Orsal, A.S., Klapp, B.F., Wahn, U., Hamelmann, E., and Arck, P.C. (2006) Prenatal stress enhances susceptibility of murine adult offspring toward airway inflammation. *J. Immunol.*, **177** (12), 8484–8492.

Piona, A., La Rosa, L., Tincani, A., Faden, D., Magro, G., Grasso, S., Nicoletti, F., Balestrieri, G., and Meroni, P.L. (1995) Placental thrombosis and fetal loss after passive transfer of mouse lupus monoclonal or human polyclonal anti-cardiolipin antibodies in pregnant naive BALB/c mice. *Scand. J. Immunol.*, **41** (5), 427–432.

Poltorak, A., He, X., Smirnova, I., Liu, M., Van Huffel, C., Du, X., Birdwell, D., Alejos, E., Silva, M., Galanos, C., Freudenberg, M., Ricciardi-Castagnoli, P., Layton, B., and Beutler, B. (1998) Defective LPS signaling in C3H/HeJ and C57BL/10ScCr mice: mutations in Tlr4 gene. *Science*, **282**, 2085–2088.

Poss, K. and Tonegawa, S. (1997) Reduced stress defense in heme oxygenase 1-deficient cells. *Proc. Natl. Acad. Sci. USA*, **94**, 10925–10930.

Racicot, K., Cardenas, I., Wunsche, V., Aldo, P., Guller, S., Means, R.E., Romero, R., and Mor, G. (2013) Viral infection of the pregnant cervix predisposes to ascending bacterial infection. *J. Immunol.*, **191** (2), 934–941.

Racicot, K., Kwon, J.Y., Aldo, P., Silasi, M., and Mor, G. (2014) Understanding the complexity of the immune system during pregnancy. *Am. J. Reprod. Immunol.*, **72** (2), 107–116.

Ramsay, J.E., Ferrell, W.R., Crawford, L., Wallace, A.M., Greer, I.A., and Sattar, N. (2002) Maternal obesity is associated with dysregulation of metabolic, vascular, and inflammatory pathways. *J. Clin. Endocrinol. Metab.*, **87** (9), 4231–4237.

Reznikov, L., Fantuzzi, G., Selzman, C., Shames, B., Barton, H., Bell, H., McGregor, J., and Dinarello, C. (1999) Utilization of endoscopic inoculation in a mouse model of intrauterine infection-induced preterm birth: role of interleukin 1b1. *Biol. Reprod.*, **60**, 1231–1238.

Rinaldi, S.F., Catalano, R.D., Wade, J., Rossi, A.G., and Norman, J.E. (2014) Decidual neutrophil infiltration is not required for preterm birth in a mouse model of infection-induced preterm labor. *J. Immunol.*, **192** (5), 2315–2325.

Robertson, S.A., Skinner, R.J., and Care, A.S. (2006) Essential role for IL-10 in resistance to lipopolysaccharide-induced preterm labor in mice. *J. Immunol.*, **177** (7), 4888–4896.

Romero, R. and Tartakovsky, B. (1992) The natural interleukin-1 receptor antagonist prevents interleukin-l-induced preterm delivery in mice. *Am. J. Obstet. Gynecol.*, **167** (4), 1041–1045.

Romero, R., Sirtori, M., Oyarzun, E., Avila, C., Mazor, M., Callahan, R., Sabo, V., Athanassiadis, A.P., and Hobbins, J.C. (1989) Infection and labor: V. Prevalence, microbiology, and clinical significance of intraamniotic infection in women with preterm labor and intact membranes. *Am. J. Obstet. Gynecol.*, **161** (3), 817–824.

Romero, R., Espinoza, J., Goncalves, L.F., Kusanovic, J.P., Friel, L., and Hassan, S. (2007) The role of inflammation and infection in preterm birth. *Semin. Reprod. Med.*, **25** (1), 21–39.

Romero, R., Dey, S.K., and Fisher, S.J. (2014) Preterm labor: one syndrome, many causes. *Science*, **345** (6198), 760–765.

Ruiz, R., Stowe, R., Goluszko, E., Clark, M., and Tan, A. (2007) The relationships among acculturation, body mass index, depression, and interleukin 1-receptor antagonist in hispanic pregnant women. *Ethn. Dis.*, **17**, 338–343.

Ruma, M., Boggess, K., Moss, K., Jared, H., Murtha, A., Beck, J., and Offenbacher, S. (2008) Maternal periodontal disease, systemic inflammation, and risk for preeclampsia. *Am. J. Obstet. Gynecol.*, **198** (4), 389.

Rustveld, L.O., Kelsey, S.F., and Sharma, R. (2008) Association between maternal infections and preeclampsia: a systematic review of epidemiologic studies. *Matern. Child Health J.*, **12** (2), 223–242.

Downloaded From Vet-eBooks.com

Schieve, L., Handler, A., Hershow, R., Persky, V., and Davis, F. (1994) Urinary tract infection during pregnancy: its association with maternal morbidity and perinatal outcome. *Am. J. Public Health*, **84** (3), 405–410.

Schlafer, D., Yuh, B., Goley, G., Elssaser, T., Sadowsky, D., and Nathanielsz, P.W. (1994) Effect of *Salmonella* endotoxin administered to the pregnant sheep at 133–142 days gestation on fetal oxygenation, maternal and fetal adrenocorticotropic hormone and cortisol, and maternal plasma tufnor necrosis factor a concentrations. *Biol. Reprod.*, **50**, 1297–1302.

Segovia, S.A., Vickers, M.H., Gray, C., and Reynolds, C.M. (2014) Maternal obesity, inflammation, and developmental programming. *BioMed Res. Int.*, **2014**, 418975.

Sheldon, J., Riches, P., Gooding, R., Soni, N., and Hobbs, J. (1993) C-reactive protein and its cytokine mediators in intensive-care patients. *Clin. Chem.*, **39** (1), 147–150.

Shi, L., Fatemi, S.H., Sidwell, R.W., and Patterson, P.H. (2003) Maternal influenza infection causes marked behavioral and pharmacological changes in the offspring. *J. Neurosci.*, **23** (1), 297–302.

Shi, L., Smith, S.E., Malkova, N., Tse, D., Su, Y., and Patterson, P.H. (2009) Activation of the maternal immune system alters cerebellar development in the offspring. *Brain Behav. Immun.*, **23** (1), 116–123.

Sidwell, R.W. and Smee, D.F. (2004) Experimental disease models of influenza virus infections: recent developments. *Drug Discov. Today Dis. Models*, **1** (1), 57–63.

Small, C.L., Shaler, C.R., McCormick, S., Jeyanathan, M., Damjanovic, D., Brown, E.G., Arck, P., Jordana, M., Kaushic, C., Ashkar, A.A., and Xing, Z. (2010) Influenza infection leads to increased susceptibility to subsequent bacterial superinfection by impairing NK cell responses in the lung. *J. Immunol.*, **184** (4), 2048–2056.

Smith, S.E., Li, J., Garbett, K., Mirnics, K., and Patterson, P.H. (2007) Maternal immune activation alters fetal brain development through interleukin-6. *J. Neurosci.*, **27** (40), 10695–10702.

Sunderland, N.S., Thomson, S.E., Heffernan, S.J., Lim, S., Thompson, J., Ogle, R., McKenzie, P., Kirwan, P.J., Makris, A., and Hennessy, A. (2011) Tumor necrosis factor alpha induces a model of preeclampsia in pregnant baboons (Papio hamadryas) *Cytokine*, **56** (2), 192–199.

Thaxton, J.E., Romero, R., and Sharma, S. (2009) TLR9 activation coupled to IL-10 deficiency induces adverse pregnancy outcomes. *J. Immunol.*, **183** (2), 1144–1154.

Turner, E.C., Hughes, J., Wilson, H., Clay, M., Mylonas, K.J., Kipari, T., Duncan, W.C., and Fraser, H.M. (2011) Conditional ablation of macrophages disrupts ovarian vasculature. *Reproduction*, **141** (6), 821–831.

Villar, J., Carroli, G., Wojdyla, D., Abalos, E., Giordano, D., Ba'aqeel, H., Farnot, U., Bergsjo, P., Bakketeig, L., Lumbiganon, P., Campodonico, L., Al-Mazrou, Y., Lindheimer, M., and Kramer, M., and World Health Organization Antenatal Care Trial Research Group (2006) Preeclampsia, gestational hypertension and intrauterine growth restriction, related or independent conditions? *Am. J. Obstet. Gynecol.*, **194** (4), 921–931.

Wadhwa, P.D., Culhane, J.F., Rauh, V., and Barve, S. (2001) Stress and preterm birth: neuroendocrine, immune/inflammatory, and vascular mechanisms. *Matern. Child Health J.*, **5** (2), 119–125.

Wang, B., Biron, C., She, J., Higgins, K., Sunshine, M., Lacy, E., Lonberg, N., and Terhorst, C. (1994) A block in both early T lymphocyte and natural killer cell development in transgenic mice with high-copy numbers of the human CD3E gene. *Proc. Natl. Acad. Sci. USA*, **91**, 9402–9406.

Wang, X., Hagberg, H., Zhu, C., Jacobsson, B., and Mallard, C. (2007) Effects of intrauterine inflammation on the developing mouse brain. *Brain Res.*, **1144**, 180–185.

Williams, K. and Mackenzie, J. (1977) Influenza infections during pregnancy in the mouse. *J. Hyg. Camb.*, **79**, 249–257.

Downloaded From Vet-eBooks.com

Winter, C., Reutiman, T.J., Folsom, T.D., Sohr, R., Wolf, R.J., Juckel, G., and Fatemi, S.H. (2008) Dopamine and serotonin levels following prenatal viral infection in mouse: implications for psychiatric disorders such as schizophrenia and autism. *Eur. Neuropsychopharmacol.*, **18** (10), 712–716.

Winter, C., Djodari-Irani, A., Sohr, R., Morgenstern, R., Feldon, J., Juckel, G., and Meyer, U. (2009) Prenatal immune activation leads to multiple changes in basal neurotransmitter levels in the adult brain: implications for brain disorders of neurodevelopmental origin such as schizophrenia. *Int. J. Neuropsychopharmacol.*, **12** (4), 513–524.

Xiong, X., Buekens, P., Fraser, W.D., Beck, J., and Offenbacher, S. (2006) Periodontal disease and adverse pregnancy outcomes: a systematic review. *BJOG*, **113** (2), 135–143.

Yao, Y., Robinson, A., Zucchi, F., Robbins, J., Babenko, O., Kovalchuk, O., Kovalchuk, I., Olson, D., and Metz, G. (2014) Ancestral exposure to stress epigenetically programs preterm birth risk and adverse maternal and newborn outcomes. *BMC Med.*, **13**, 121–133.

Young, B.C., Levine, R.J., and Karumanchi, S.A. (2010) Pathogenesis of preeclampsia. *Annu. Rev. Pathol.*, **5**, 173–192.

Zenclussen, A.C. (2006) Regulatory T cells in pregnancy. *Springer Semin. Immunopathol.*, **28** (1), 31–9.

Zenclussen, A.C., Lim, E., Knoeller, S., Knackstedt, M., Hertwig, K., Hagen, E., Klapp, B.F., and Arck, P.C. (2003) Heme oxygenases in pregnancy II: HO-2 is downregulated in human pathologic pregnancies. *Am. J. Reprod. Immunol.*, **50**, 66–76.

Zenclussen, A.C., Fest, S., Joachim, R., Klapp, B.F., and Arck, P.C. (2004) Introducing a mouse model for pre-eclampsia: adoptive transfer of activated Th1 cells leads to pre-eclampsia-like symptoms exclusively in pregnant mice. *Eur. J. Immunol.*, **34** (2), 377–387.

Zenclussen, A.C., Gerlof, K., Zenclussen, M.L., Sollwedel, A., Bertoja, A.Z., Ritter, T., Kotsch, K., Leber, J., and Volk H.-D. (2005) Abnormal T-cell reactivity against paternal antigens in spontaneous abortion. *Am. J. Pathol.*, **166** (3), 811–822.

Zenclussen, A.C., Schumacher, A., Zenclussen, M.L., Wafula, P., and Volk, H.D. (2007) Immunology of pregnancy: cellular mechanisms allowing fetal survival within the maternal uterus. *Expert Rev. Mol. Med.*, **9** (10), 1–14.

Zhang, J., Wei, H., Wu, D., and Tian, Z. (2007) Toll-like receptor 3 agonist induces impairment of uterine vascular remodeling and fetal losses in CBA × DBA/2 mice. *J. Reprod. Immunol.*, **74** (1–2), 61–67.

Zhao, H., Wong, R.J., Kalish, F.S., Nayak, N.R., and Stevenson, D.K. (2009) Effect of heme oxygenase-1 deficiency on placental development. *Placenta*, **30** (10), 861–868.

Zhao, H., Azuma, J., Kalish, F., Wong, R.J., and Stevenson, D.K. (2011) Maternal heme oxygenase 1 regulates placental vasculature development via angiogenic factors in mice. *Biol. Reprod.*, **85** (5), 1005–1012.

Zhu, M.J., Du, M., Nathanielsz, P.W., and Ford, S.P. (2010) Maternal obesity up-regulates inflammatory signaling pathways and enhances cytokine expression in the mid-gestation sheep placenta. *Placenta*, **31** (5), 387–391.

Zuckerman, L., Rehavi, M., Nachman, R., and Weiner, I. (2003) Immune activation during pregnancy in rats leads to a postpubertal emergence of disrupted latent inhibition, dopaminergic hyperfunction, and altered limbic morphology in the offspring: a novel neurodevelopmental model of schizophrenia. *Neuropsychopharmacology*, **28** (10), 1778–1789.

Downloaded From Vet-eBooks.com

13

Practical Approaches, Achievements, and Perspectives in the Study on Signal Transduction in Oocyte Maturation and Fertilization: Focusing on the African Clawed Frog *Xenopus laevis* as an Animal Model

Ken-ichi Sato

Laboratory of Cell Signaling and Development, Department of Molecular Biosciences, Faculty of Life Sciences, Kyoto Sangyo University, Kyoto, Japan

13.1 Introduction to Reproductive Biology of Frog Oocytes and Eggs

For the general public, frog is one of the most companionable and friendly animals that can be seen in several common places such as garden, pond, river, and their surrounding areas. The same is also true for the developmental biologists: For the past several decades, a number of researches, using frog as a model animal, have been directed by them to explore and understand a long-thought biological problem—how is "like father, like son" made possible, in other words, how is fertilized egg made and developed to adult animal as like its parents, in the species preservation (Iwao 2000a, 2000b). This chapter provides a collection of experimental approaches, including a know-how for setup of the frog laboratory, being employed by our research group to explore and understand the cellular and molecular mechanisms of fertilization in the African clawed frog *Xenopus laevis*, and discusses the outcomes of our experimental approaches as well as the problems awaiting further investigation.

13.2 Practical Approaches

13.2.1 Maintenance of Adult Frogs

We usually purchase adult female and male frogs of *X. laevis*, which are fully competent to ovulate and to supply active sperm, respectively, from local dealers. They live only in water throughout their life: In this sense, *X. laevis* is *not* really a species of amphibian that lives both on land and in water (Figure 13.1a). Therefore, living environment for *X. laevis* is quite simple and its laboratory setup is relatively easy to establish (at least much easier than mouse or fly). Transparent polycarbonate or polypropylene tank with a filling capacity of 10–20 l is suitable for maintaining 3–5 adult females or 6–10 adult males: Minimally, 1–1.5 l of water per frog is necessary. Natural mating rarely occurs; however, it is recommended to maintain females and males separately in a different tank. To prevent escaping of frogs, the rigidity of the top sealing is important. The sealing top also needs some holes for aeration. Frogs need freshwater. However, it does not mean a quality of laboratory-grade purified water; tap water is enough. In Japan, tap water contains a significant amount of chloride ion that is harmful to the mucosal layer of frog skin surface. The simplest way for dechlorination is to leave water for more than 1 day at

Animal Models and Human Reproduction, First Edition. Edited by Heide Schatten and Gheorghe M. Constantinescu.
© 2017 John Wiley & Sons, Inc. Published 2017 by John Wiley & Sons, Inc.

Downloaded From Vet-eBooks.com

ambient temperature. Dewatering is done twice a week—one day after feeding (see below). Frogs require temperature between 20 and 22 °C year-round, so air-conditioning for them is necessary. Frogs are usually fed twice a week with either commercially available floating baits or pieces of chicken liver.

13.2.2 Collection of Immature Oocytes and Unfertilized Eggs

Adult female frogs hold in their ovary more than thousands of immature oocytes at germinal vesicle stage (GV stage), the cell cycle of which is paused in the prophase of the first meiosis (Pro-I). Dissection and removal of the ovarian tissues involves, as the first step, anesthetization of frogs in a solution containing 2 mg/ml 2-aminobenzoate for about 15 min at ambient temperature. Manual cutting and breaking of the abdominal skin and muscle layers allows us to observe the ovarian tissues that consist of two lobes, spreading from the midline of the frog body (Figure 13.1b). Fragments of the ovarian tissues are removed by ophthalmic scissors and placed in a plastic dish filled with isotonic buffer solution: modified Barth's solution (MBS) or OR-2 solution (see Appendix). To maintain an effective aeration for the oocytes, fragments of the ovarian tissues are subdivided into small portions as quickly as possible: This allows the oocytes to contact directly with the buffer solution, by which prolonged viability of the oocytes is guaranteed.

13.2.2.1 Immature Oocytes

To ensure that oogenesis stage (I through VI)-specific analysis of immature oocyte is made possible, the subdivided fragments of ovarian tissues are subjected to gentle agitation treatment in the presence of 2.5 mg/ml collagenase in MBS or OR-2 solution, which removes the connective tissue surrounding the oocytes—so-called follicle cells. After the 2–3 h treatment, defolliculated oocytes are washed several times with the same buffer solution. Stereomicroscopic observation enables us to identify oocytes at six different oogenesis stages by their cell size and characteristic morphology (Figure 13.1c). Stage I oocyte is the smallest and youngest cell. Its transparency allows us to detect germinal vesicle. Stage II oocyte loses its transparency and becomes entirely white-colored cell. Stage III oocyte has randomly or entirely darkened cell

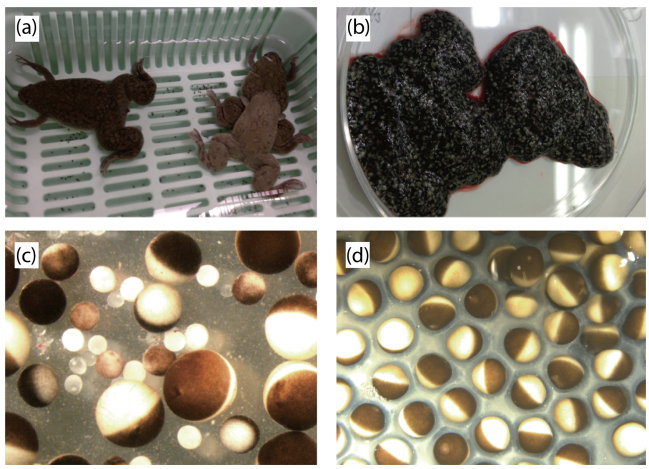

Figure 13.1 Oocytes and eggs of *X. laevis*. (a) Female and male frogs that are maintained in water-filled tanks. (b) Ovarian tissues that are dissected from a female frog. (c) Collagenase-treated and defolliculated oocytes. (d) Ovulated unfertilized egg that are surrounded by jelly coats.

Downloaded From Vet-eBooks.com

surface in response to pigmentation. Stage IV oocyte is characterized by a completion of distribution of the pigmented and nonpigmented areas on the cell surface. Oocytes up to this stage are not yet competent to hormone-induced oocyte maturation (see below). Stage V and VI oocytes have cell size with a diameter of 0.9–1.1 and 1.1–1.3 mm, respectively. The latter oocyte is called fully grown oocyte. Importantly, both stage V and VI oocytes are responsive to hormone-induced oocyte maturation. For *in vitro* hormone treatment (see below) and other manipulations including simple storage in a viable condition, oocytes should be kept at 18–22 °C in MBS or OR-2 solution supplemented with antibiotics (e.g., 50 μg/ml gentamycin).

13.2.2.2 Unfertilized Egg

Unfertilized egg (*in situ*-matured and ovulated oocyte, the cell cycle of which repaused at metaphase of second meiosis: Meta-II or MII) can be obtained by administration of human chorionic gonadotropin (200–500 international units per frog) into female frogs. The hormonal administration is made by a dorsal subcutaneous injection with a 24 gauge needle. Ovulation usually starts in 8 h after hormonal administration, during which ovarian fully grown oocytes are subjected to oocyte maturation (see below) and passage through oviduct where the cell surface of maturing oocytes are decorated with pars rectal substances and jelly components (Figure 13.1d). The pars rectal substances contain acrosome reaction-inducing substance in *Xenopus* (ARISX). It attaches to the oocyte vitelline envelope, which is the glycoprotein-based structure surrounding the entire oocyte surface. It has been shown that ARISX on the vitelline envelope of unfertilized egg interacts with fertilizing sperm, so that the sperm become "acrosome-reacted," in other words, fully competent to fertilize. On the other hand, further decoration of maturing oocytes with jelly components results in a formation of three jelly layers that surround the oocyte. The jelly layers of oocyte contribute to physical as well as antibacterial barrier. In addition, the jelly layers are the reservoir for allurin, a protein component that acts as chemoattractant for fertilizing sperm. Thus, matured oocyte, which completes the meiotic cell cycle progression from Pro-I to MII, acquires pars recta-derived ARISX on its vitelline envelope and three jelly layers and is subjected to spawning into freshwater environment. In the laboratory, the spawned eggs are immersed in DeBoer solution (see Appendix) at 18–22 °C, in which eggs maintain their ability to be fertilized for 2–3 h.

13.2.3 Preparation of Sperm

Adult male frogs hold a pair of testis that each contains about 10^8 sperm cells. Manual dissection of anesthetized male frogs and removal of testes are performed as similarly as those performed in collection of immature oocytes (see above). Testes removed are placed in a sterile microtube (one testis per tube) and kept on ice as "dry sperm." For a longer storage (up to about 1 week), the tube is filled with DeBoer solution supplemented with 1 mg/ml bovine serum albumin and kept at 4 °C. The following manipulations should be done at 4 °C or on ice. For an immediate use, dry sperm specimen in a microtube is cut several times by ophthalmic scissors, by which testis becomes macerated and sperm cells become accessible to outside of the tissues. The macerated sample is added with 1 ml of DeBoer solution and mixed vigorously by repeated pipetting, so that sperm cells are effectively released into the solution. The resulting sperm suspension is subjected to centrifugation at 50 *g* for 5 min, after which the debris can be removed as the pellet materials. The supernatant is centrifuged again at 1000 *g* for 5 min, so that the sperm cells are concentrated into the pellet materials. The resulting preparation of "debris-free and concentrated" sperm is ready for *in vitro* fertilization experiment. Until use, the concentrated sperm samples should be kept on ice (the maximum time for storage is 1 day). When necessary, the sperm samples are resuspended with DeBoer solution to give a sperm concentration of 10^6–10^8 per ml.

Downloaded From Vet-eBooks.com

13.2.4 In Vitro Oocyte Maturation and Fertilization

13.2.4.1 Oocyte Maturation

For *in vitro* oocyte maturation, the defolliculated GV oocytes at oogenesis stage VI are used. Maturation is induced by addition of progesterone (PG) at 0.5–2 μM and is determined by the appearance of a white spot on the top of the animal hemisphere, directly under where germinal vesicle breakdown (GVBD) takes place at the same time. GVBD can be confirmed by microscopic observation of oocyte that is cut into halves. In most cases, oocyte maturation begins to occur in some oocytes from 2 to 3 h and complete within 6–8 h after the PG treatment. The mature oocytes are regarded as MII oocytes and can be further used for some experiments.

Fertilization

For *in vitro* fertilization, jelly layers of unfertilized eggs are removed by gentle swirling in excess volume of DeBoer solution containing 2% (w/v) L-cysteine and 0.06 N NaOH, pH 7.8, for 3–8 min. After the dejelly layer treatment, eggs are washed more than five times with 0.5× Steinberg solution (see Appendix). Egg jelly water for sperm activation is prepared by gentle rocking (25–50 rpm) of jelly-intact unfertilized eggs (5–8 *g*) in a 60 mm plastic culture dish filled with 10 ml of 0.33× modified Ringer's solution (see Appendix). After 60 min of the treatment, the soluble material containing solubilized egg jelly components is collected and mixed with Ficoll (MW 400,000; Sigma) with its final concentration of 10% (w/v). The Ficoll-mixed egg jelly water is stored in aliquots at −30 °C and used within 2 months after the preparation. For insemination, groups of 20–100 dejellied eggs are placed in monolayer in a plastic culture dish (35 mm diameter) that is filled with 0.1–0.25× Steinberg solution. The sperm suspension and egg jelly water (100 μl) is dropped on the top surface of the egg layer. Our initial characterization of *Xenopus* Src tyrosine kinase, as an egg-associated enzyme that activates in response to insemination, was done by *in vitro* kinase assay using the solubilized membrane fractions that were prepared from unfertilized and fertilized egg samples (Figure 13.2a).

13.2.4.2 Parthenogenetic Egg Activation

Oocytes and eggs of *X. laevis* are also actively employed to evaluate the effect of a variety of natural and nonnatural compounds on oocyte maturation and fertilization. For parthenogenetic egg activation with either calcium ionophore, hydrogen peroxide, or purified preparation of cathepsin B protease, dejellied unfertilized eggs maintained in 0.5× SB solution are transferred to new dish filled with fresh 0.5× SB solution supplemented with the aforementioned substances at the appropriate concentrations. The successful egg activation rate is determined by monitoring the occurrence of cortical contraction of the pigmented area in the animal half of the eggs—a hallmark of successful egg activation—in another group of the same batch of eggs. At the specified time after activation treatments, eggs are quickly washed more than three times with excess volume of 0.5× SB solution, removed of the buffer solution, and frozen by liquid nitrogen. The frozen samples can be kept for months at −80 °C. Experimental groups of egg samples that showed successful egg activation rate of more than 80% within 20 min of the activation treatment were used for evaluation of signal transduction events.

13.2.5 Microinjection and Other Pharmacological Treatments

Because of their large size, oocytes (in particular, those at stage VI) and eggs of *X. laevis* are suitable for microinjection experiment, for which laboratory equipment is relatively simple, economical, not space consuming, and easy to set up. For example, in order to determine a requirement of enzymatic activity of some signaling molecules for activation of eggs by either sperm or other

Downloaded From Vet-eBooks.com

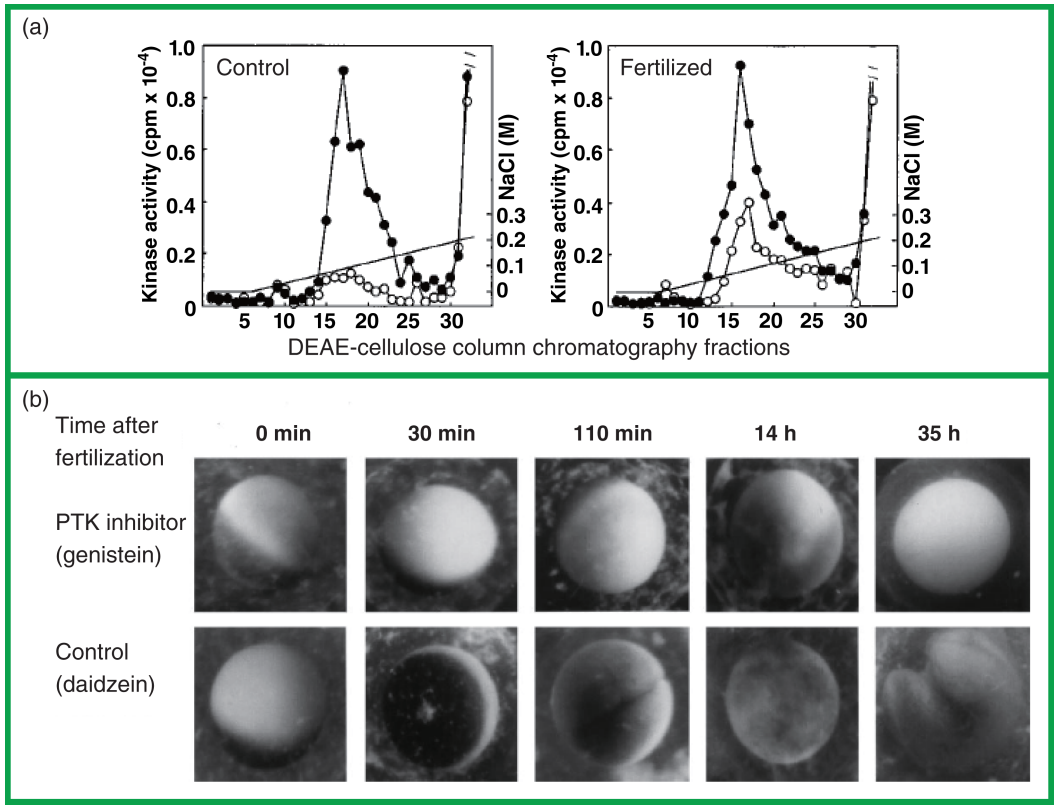

Figure 13.2 Src (p57/Xyk)-mediated signal transduction and fertilization in *X. laevis*. (a) Activation of p57/Xyk at fertilization: peptide kinase assay in the absence or presence of a kinase-activating antibody (Sato *et al*. 1996). (b) Genistein, but not daidzein, inhibits sperm-induced egg activation and embryogenesis (Sato *et al*. 1998). (c) Peptide A7, a synthetic peptide inhibitor for Src, attenuates the sperm entry (closed arrow) and meiotic resumption of the egg chromosomes (opened arrow) (Sato *et al*. 1999). (d) PP1 and U-73122, but neither PP3 nor U-73343, inhibit the sperm-induced Ca^{2+} transient (Sato *et al*. 2000). (e) Phosphotyrosine signal becomes evident in a limited area of the plasma membrane in fertilized egg, as assessed by indirect immunofluorescent studies (Sato *et al*. 2002b). (f) Immunodepletion of PLC© from the cytostatic factor-arrested egg extract (Sato *et al*. 2003). (g) Triton X-100 extraction and sucrose density gradient ultracentrifugation of egg samples allow us to isolate low-density, detergent-insoluble membrane (LD-DIM or membrane microdomain) (Sato *et al*. 2002a, 2002b). Red circles in a schematic drawing (left) and a photograph (right) indicate the positions of the MD fractions. (h) The isolated MD fractions can be used as an experimental platform, in which sperm-induced tyrosine kinase signaling events are reconstituted *in vitro* (Mahbub Hasan *et al*. 2014; Sato *et al*. 2002a, 2002b, 2003). (i) Phosphoproteome analysis of the MD fractions that are prepared from unfertilized, fertilized, and parthenogenetically activated (H_2O_2-treated) eggs demonstrates that a 30 kDa protein is predominantly tyrosine-phosphorylated in the activated eggs, the molecular identity of which is determined to be uroplakin III (UPIII), a single transmembrane protein (Sakakibara *et al*. 2005). UPIII has an extracellular domain containing a target sequence for sperm tryptic protease and a carboxyl-terminal region containing a tyrosine residue for Src phosphorylation (Mahbub Hasan *et al*. 2005, 2007, 2011, 2014). (j) Current model for fertilization signaling at the gamete plasma membrane level in *X. laevis* (Mahbub Hasan *et al*. 2014).

substances, we performed microinjection of unfertilized eggs. Inhibitors used are genistein, peptide A7, PP1, and PP2, all of which are potent inhibitors for the Src family proteins (SFK or Src PTK) (Figure 13.2b and c), U-73122, a potent phospholipase C (PLC)-specific inhibitor with broad specificity toward all PLCs (Smith *et al.*, 1990), LY294002, a potent inhibitor of phosphatidylinositol 3-kinase (PI3K), and guanosine 5′-*O*-(2-thiodiphosphate (GDP*S), an inhibitor for GTP-binding

Downloaded From Vet-eBooks.com

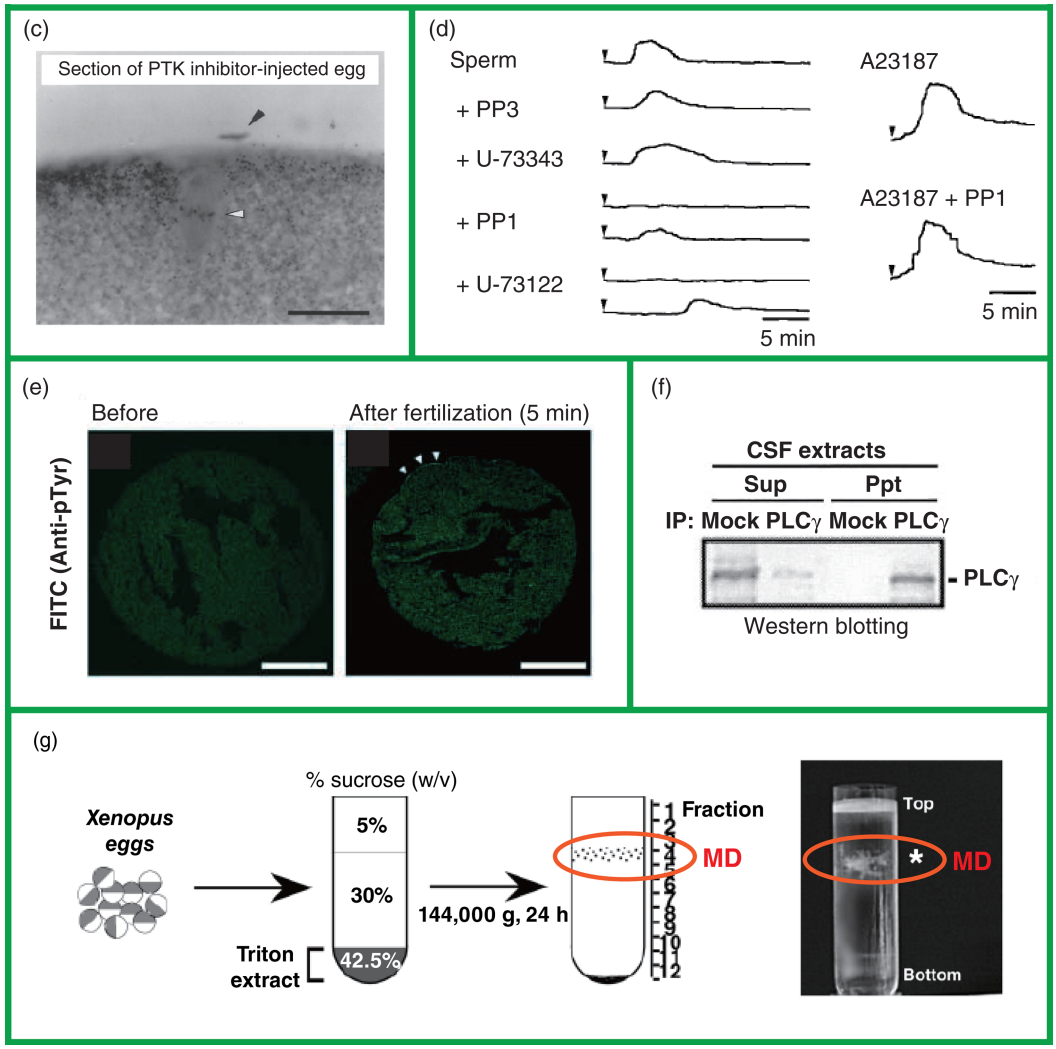

Figure 13.2 (*Continued*)

protein such as monomeric as well as trimeric G-proteins (Mahbub Hasan *et al.* 2014; Mammadova *et al.* 2009; Sato *et al.* 1998, 1999, 2000, 2004). As a negative control experiment, we have also employed inactive analogue substances of the inhibitors as already described: PP3 (for PP1 and PP2) and U-73343 (for U-73122) (Sato *et al.* 2000). When required, the stock solutions of inhibitors at 1–10 mM, dissolved in dimethylsulfoxide (DMSO) or ethanol, are thawed and diluted with an inhibitor dilution buffer (see Appendix) containing an appropriate amount of DMSO so that the final concentration of DMSO in all the diluted solutions was 5%. The inhibitor solutions are then loaded into a glass capillary (e.g., those provided by Drummond), with a tip diameter of 10–30 nm, which is filled with silicon oil and is connected to a pulse-directed injector system (e.g., Nanoject system of Drummond). Prior to microinjection, dejellied unfertilized eggs are washed and incubated with an injection buffer (see Appendix). Quantitative injection of the inhibitor solution, the maximal volume of which should be 50 nl per egg, is made under microscopic observation. The cytoplasmic volume of the *Xenopus* egg is estimated to be about 1 µl, that is, 20 times larger than the

Downloaded From Vet-eBooks.com

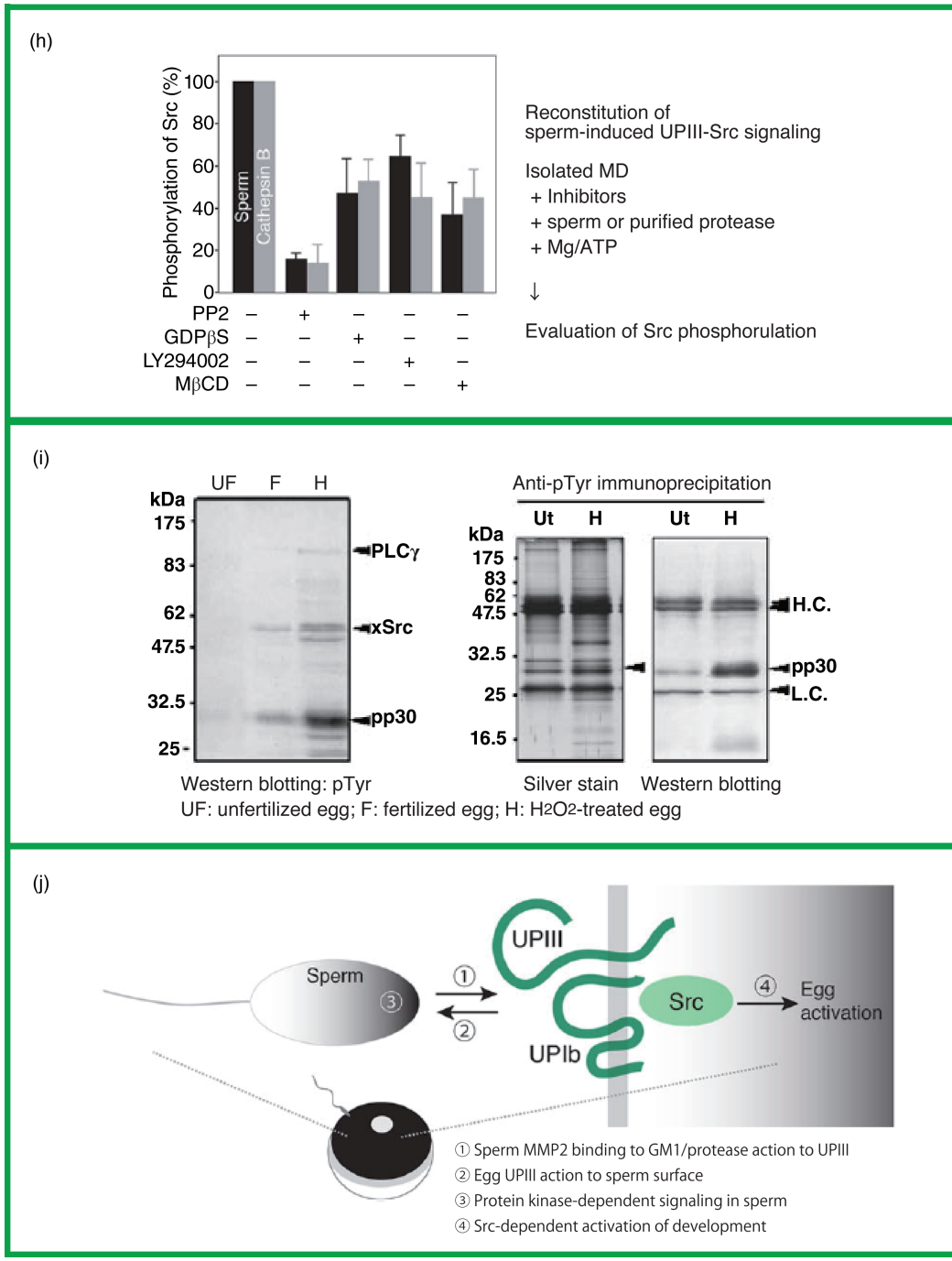

Figure 13.2 (*Continued*)

Downloaded From Vet-e-Books.com

maximally injected volume. Therefore, the final concentration of the inhibitor in the egg is estimated to be 0.1, 0.3, 1, 3, and 10 μM, when microinjection of the inhibitor solutions is done with 50 nl of the 2, 6, 20, 60, and 200 μM stock solutions, respectively. After the injection, eggs are recovered and healed in DoBear solution for 10–15 min, during which any prick-activated or dead eggs, showing cortical contraction or abnormal discoloring, will be removed. Then, eggs are washed three times with 0.5× SB solution and subjected to egg activation treatment (see below).

13.2.6 Biochemical Fractionations of Oocytes and Eggs

13.2.6.1 Whole-Egg Lysate

For evaluating major series of signal transduction events associated with oocyte maturation and fertilization (e.g., phosphorylation and dephosphorylation of MAPK, protein synthesis and breakdown of Mos protein kinase and cyclin B), frozen egg samples prepared as above are mixed with 20 μl per egg of ice-cold whole-cell extraction buffer (see Appendix). The mixture is mixed vigorously and treated with sonication for 1–3 min with an ultrasonic disrupter. The sample is then centrifuged at 15,000 rpm for 10 min. The resultant supernatant is collected and used as Triton X-100-solubilized whole egg lysate (WE lysate) within 2 h of extraction. In general, 50–80 μg of protein, as determined by a spectrophotometer, is recovered from one egg. Calibration of the protein determination is made with bovine serum albumin (Calbiochem). When amount of IP3 is evaluated, an alternative method to obtain WE lysate is applied (see Section 13.2.7).

Egg Membrane Microdomain (MD)

For more complicated and/or minor arrays of signal transduction events that occur in plasma membrane or cytoplasm (e.g., modification of egg surface molecules, protein–tyrosine phosphorylation), subcellular fractionation techniques as described below are employed and are also applied to *in vitro* reconstitution of the events and several kinds of protein function assays (see Section 13.2.7). For preparation of membrane microdomain (MD) of stage VI immature oocytes (GV oocytes), progesterone-treated mature oocytes (MII oocytes), or unfertilized eggs (UF eggs), these cell samples are mixed with fivefold volume of ice-cold extraction buffer A (see Appendix) and homogenized with a Dounce tissue grinder. The homogenates are centrifuged at 500 *g* for 10 min, and the supernatants are collected and centrifuged at 150,000 *g* for 20 min. Triton X-100 is then added to the fluffy layer of the membranous pellet, which is devoid of mitochondrial heavier components, to yield the final concentration of 1%. The mixtures are homogenized again, incubated on ice for 10 min, and mixed with equal volumes of extraction buffer B (see Appendix). The resulting mixtures (5 ml) are layered first with 30% sucrose and then with 5% sucrose in the same buffer. The samples are centrifuged at 144,000–200,000 *g* for 18–24 h in a swing rotor (e.g., Beckman SW28 rotor) (Figure 13.2g). After the centrifugation, aliquots of 12 fractions are collected from the top to the bottom of the tubes. Fractions containing the interface between 5 and 30% sucrose layers are pooled as MD samples (low-density, detergent-insoluble membranes), whereas 2–3 fractions at the bottom are pooled as detergent-soluble non-MD samples (Figure 13.2g). In some experiments, the MD samples are diluted with water more than fourfold and centrifuged again at 150,000 *g* for 30 min. The resulting concentrated MD materials are resuspended with 200 μl extraction buffer A containing 150 mM NaCl and used for further experiments.

13.2.6.2 CSF Extract

For preparation of cytostatic factor-arrested cytoplasmic extract, or CSF extract, unfertilized eggs are washed extensively with CSF extraction buffer (see Appendix). Then, the eggs are transferred to the centrifuge tubes containing CSF extraction buffer plus 100 μg/ml cytochalasin

Downloaded From Vet-eBooks.com

B and 10 μg/ml each of leupeptin, pepstatin, and chymostatin, and are then centrifuged for 30 s at 500 *g*, then for 30 s at l000 *g*. Remove buffer as much as possible from the top of the tubes and crush the packed eggs by centrifugation for 15 min at 15,000 *g*. After the centrifugation, the cytoplasmic fractions are collected as the supernatant and centrifuged again under the same conditions as the first centrifugation. Add 10% volume of cytochalasin B, protease inhibitors, and energy mix to the resulting extracts. The extracts are kept on ice until use.

13.2.7 Biochemical and Cell Biological Assays

13.2.7.1 In Vitro Protein-Tyrosine Kinase Assay Using Isolated MD Fraction

MD fractions (10 μl, an equivalent of 30–60 eggs/oocytes) are preincubated with or without activators such as 10^6/ml sperm, 1 mM GTP©S, 1 mM cAMP, 1 mM RGDS peptide, or 1 mM $CaCl_2$ at a final volume of 12.5–25 μl for 10 min at 30 °C. The mixtures were further incubated at 30 °C for 10 min in the presence of kinase reaction mixture (see Appendix) of 5 mM $MgCl_2$, 20 mM tris-HCl, 1 mM DTT, 2 μM [©-^{32}P]ATP (10 μCi), and 1 mM synthetic substrate peptide (e.g., cdc2 peptide: residues 7–26 of human CDK1) at a final volume of 50 μl. The reaction was stopped by the addition of 50 μl of Laemmli's SDS sample buffer followed by heat treatment at 98 °C for 5 min. Phosphorylated samples were separated by SDS polyacrylamide gel electrophoresis (PAGE) on 16% gels. ^{32}P-labeled synthetic substrate peptide is visualized and quantified by a phospho-imaging analyzer (e.g., Fuji Film BAS2000 imager).

13.2.7.2 Tyrosine Phosphorylation and/or Partial Proteolysis of UPIII and Src

MD fraction alone (3 μl: 10–20 egg/oocyte equivalent), CSF extracts alone (27 μl: 30 egg equivalent), or a mixture of the both are incubated in the absence or presence of 1.5 μl of the activators (e.g., sperm) or 1.5 μl of various inhibitors (e.g., PP2, GDPbS, LY294002, methyl-®-cyclodextrin) for 10 min at 30 °C (Figure 13.2h). The mixtures are then incubated with 5 mM $MgCl_2$ and 1 mM ATP for 10 min at 30 °C. The kinase reaction was terminated by the addition of 30 μl of 10 mM EDTA on ice. Proteins are solubilized by incubation in the presence of 0.1% SDS and 1 mM sodium orthovanadate at 37 °C for 10 min and collected as the supernatant fractions after centrifugation at 150,000 *g* for 10 min at 4 °C. To assess tyrosine phosphorylation of 12 Src and MAPK, protein samples (10–30 μg) are separated by SDS-PAGE on 8% gels and analyzed by immunoblotting (see below) with either antiphospho Src Y418 antibody (1 μg/ml) or antiphospho-MAPK antibody (0.5 μg/ml). For tyrosine phosphorylation of uroplakin III (UPIII) and PLC©, protein samples (50–500 μg protein) are subjected to immunoprecipitation with either anti-UPIII extracellular domain antibody or anti-PLC© antibody (1 μg/ml) followed by immunoblotting with anti-phosphotyrosine antibody PY99 (1 μg/ml). Partial proteolysis of UPIII is assessed by immunoblotting of the MD fractions with anti-UPIII extracellular domain antibody, by which fragments of the UPIII bands are demonstrated.

13.2.7.3 Immunoprecipitation, SDS-PAGE, and Immunoblotting

Protein samples (50–500 μg at 1 μg/ml) are immunoprecipitated with 1–5 μl appropriate antibody (e.g., anti-PLC© antibody, as described below) for 3–6 h at 4 °C. After centrifugation at 2000 *g* for 2 min at 4 °C, the immune complexes are adsorbed onto 10 μl protein A-Sepharose beads by gentle agitation for 30 min at 4 °C. The beads are washed three times with 500 μl radioimmunoprecipitation buffer (see Appendix), washed once with extraction buffer containing 1% Triton X-100, and used as immunoprecipitated samples. The immunoprecipitates prepared as above are treated with Laemmli's SDS sample buffer (see Appendix) at 98 °C for 5 min. SDS-PAGE and immunoblotting of the SDS-denatured proteins are done as described previously using an apparatus (e.g., Atto, Tokyo, and Japan) and semidry blotting apparatus, respectively.

Downloaded From Vet-eBooks.com

13.2.7.4 Enzyme Assay for PLC© and Its Immunochemical Depletion

Anti-PLC© immunoprecipitated protein samples (10 µl of beads) are washed two times with PLC assay buffer (see Appendix). The PLC reaction is initiated by adding 40 µl of PLC assay buffer supplemented with mixed micelles of phosphatidylethanolamine and [^{3}H]phosphatidylinositol 4,5-bisphosphate (PI 4,5-P_2) (148 Bq/nmol) at final concentrations of 100 and 200 µM, respectively. After 15 min incubation at 30 °C, the reaction mixture is separated from beads by a brief centrifugation (2000 rpm, 1 min) and added to 100 µl of water containing 10 µg of bovine serum albumin and 100 nmol of unlabeled PI 4,5-P_2. The mixture is then immediately combined with 250 µl of ice-cold 10% trichloroacetic acid. It is then centrifuged at 15,000 rpm for 10 min at 4 °C. The resultant supernatant is collected and centrifuged again in the same condition. The finally obtained supernatant (ca. 400 µl) is mixed with 5 ml of a scintillation cocktail and subjected to °-particle counting with the use of a liquid scintillation counter. The same anti-PLC© antibody for enzyme assay can also be used for the immunochemical depletion of PLC© from egg extracts (Figure 13.2f).

IP_3 Assay

All manipulations are carried out on ice or at 4 °C. Samples in groups of 10 eggs were homogenized with a glass pestle in 120 µl of 15% (v/v) trichloroacetic acid. The insoluble materials are collected by centrifugation at 5000 rpm for 15 min, extracted three times with 10 volumes of water-saturated diethyl ether, and subjected to neutralization with 1 M $NaHCO_3$ (10 µl per 100 µl extract). The amount of IP_3 in the neutralized extracts is determined by the use of a D-myo-IP_3 [^{3}H] assay system (Amersham Pharmacia). This assay is based on the competition between unlabeled IP3 in the sample and a fixed quantity of a tracer, [^{3}H]IP_3, for a limited number of binding sites on IP_3-binding protein supplied by the kit. In our experimental system, the neutralized extracts of 100 µl (about 80% of the total; 10 eggs) are subjected to the aforementioned assay conditions. Therefore, the evaluation of the data for the amount of IP_3 per egg requires calculation involving a dilution factor of $100/80 \times 1/10$ (total egg number tested in one trial). Calibration of fixed amounts of IP_3 (0.19–25 pmol) is also done on the same day of experiment.

13.2.7.5 Calcium Release Assay

Ultraviolet excitable ratiometric fluorescent calcium indicator Fura-2 is added to the CSF extracts in a final concentration of 2 µM, at several minutes in advance the initiation of reconstitution of signaling events. The level of free calcium in the extracts is continuously monitored by ratio imaging microscopy using the high-frame digital CCD imaging ARGUS/HISCA system from Hamamatsu Photonics. Excitation wavelengths are set at 340 and 380 nm; monitoring of the emission is made at 510 nm. The basal level of fluorescent signal is monitored over several minutes at 21–23 °C prior to the initiation of the reactions. Then the reaction is initiated by administration of the effectors (e.g., MD fraction) that have been preincubated in the absence or the presence of various inhibitors or activators. Further monitoring of the fluorescent signal is made at intervals of 8–20 s. Initial time of the calcium rise, the peak amplitude, and duration of the rise over the control level are successively recorded. Calcium rise is defined for the fluorescent signal that gives more than 0.04 unit of the ratio of 340/380 values, which persists for more than 30 s (Figure 13.2d).

13.2.7.6 Cell Cycle Transition Assay

Nuclei of lysolecithin-treated sperm (1 µl: final concentration of 106/ml equivalent) are added to the CSF extracts (27 µl) on ice prior to the initiation of reconstitution experiments. Reaction is initiated by the addition of MD fractions as described above. Nuclear morphology of the added

Downloaded From Vet-eBooks.com

sperm nuclei is observed and scored by fluorescent microscopy after withdrawing 1 µl of extract at appropriate time intervals and adding 4 µl of 0.33× modified Ringer's solution containing 1 µg/ml Hoechst 33342, 10% (w/v) formaldehyde, and 50% (v/v) glycerol.

13.2.8 Indirect Immunofluorescent Study

To analyze subcellular localization of signaling proteins such as the tyrosine kinase Src in eggs, dejellied unfertilized eggs prepared as above are subjected to immunocytochemical experiments. Dejellied eggs were fixed in a fixation buffer (see Appendix) for 3 h at 18 °C. Fixed specimens are further treated with absolute methanol for 12–18 h at −30 °C. Then the specimens are rehydrated with phosphate-buffered saline supplemented with 20% (w/v) sucrose, embedded in a medium containing polyvinyl alcohol and polyethylene glycol (e.g., O.C.T. compound, Tissue-Tek), and frozen at −80 °C. Serial sections of 5–10 µm thickness are prepared in a planar direction of the animal–vegetal axis, placed on poly-L-lysine-coated slide glasses at −20 °C, and then washed with phosphate-buffered saline for 20–30 min at ambient temperature. All following manipulations are carried out at ambient temperature unless otherwise indicated. The washed specimens are treated for 15 min with phosphate-buffered saline supplemented with 3% (v/v) hydrogen peroxide to quench enzymatic activity of peroxidase. After washing with phosphate-buffered saline for five times, nonspecific binding sites of the specimens are blocked for 1 h with a buffer supplied by a kit (e.g., TSA-Direct, Daiichikagaku, Tokyo, Japan). After the treatments, the specimens are treated with an antibody of interest or its control antibody at 4 °C for 12–18 h. The specimens are then washed with phosphate-buffered saline and blocked again for 30 min. The specimens are further treated with horseradish peroxidase-conjugated secondary antibody for 1 h. After washing with phosphate-buffered saline, the specimens are treated for 30 min with fluorescein isothiocyanate (FITC)-conjugated tyramide supplied by the kit. After washing with phosphate-buffered saline for five times, the specimens are mounted with mounting medium (see Appendix) and are kept under dark conditions. Fluorescent signal of the specimens is observed with a confocal laser-scanning microscope at 488 nm argon excitation using a 515 nm long-pass barrier filter (Figure 13.2e). The same sample is also observed using a microscope equipped with Nomarski interference to record the cellular structure. Alternatively, dejellied unfertilized eggs and fertilized embryos are analyzed by whole-mount immunocytochemical experiment. Fertilized embryos were collected at 60 min post insemination: The successful fertilization of the same batch of eggs is verified by observing the first embryonic cleavage at 90 min post insemination. The egg/embryo specimens are fixed in methanol at −20 °C overnight and are rehydrated in a series of excess volume of methanol versus phosphate-buffered saline containing 0.025% (v/v) Tween 20 (PBS-T) (9 : 1, 8 : 2, 7 : 3, 5 : 5, 2.5 : 7.5, 1 : 9, and 0 : 10), reach rehydration series of which takes for 20–25 min at ambient temperature. The rehydrated samples are further washed two times with PBS-T for 20 min, and then incubated overnight at 4 °C in a solution containing a primary antibody of interest, PBS-T, and 1% (v/v) fetal bovine serum. After the treatment, the specimens are washed with PBS-T (60 min×__2) and are incubated overnight at 4 °C in a solution containing fluorescein FITC-conjugated secondary antibody, PBS-T and 1% (v/v) fetal bovine serum. After wash treatment with PBS-T (60 min × 2), the specimens are incubated in methanol (40 min × 4) and are then cleared for optical sectioning by two rounds of 10 min incubation in Murray's clear solution containing 1 : 2 volume of benzyl alcohol and benzyl benzoate. The resulting whole-mount specimens are mounted in Murray's clear solution and are maintained in dark conditions until use. Fluorescent signal of the specimens is analyzed with a confocal laser-scanning microscope as described above. The same specimens are simultaneously analyzed using a microscope equipped with Nomarski interference to demonstrate their cellular structures.

Downloaded From Vet-eBooks.com

13.2.9 Protein Identification by Mass Spectrometry Analysis

To identify unknown oocyte/egg protein that is, for example, tyrosine-phosphorylated in response to fertilization, we perform concentration of the protein of interest and its mass spectrometry analysis. Concentration of protein and its evaluation are usually done by immunoprecipitation and SDS-PAGE of proteins of interest as described above (e.g., phosphotyrosine-containing protein) (Figure 13.2i). Protein bands that are visualized by staining with Coomassie Brilliant Blue or silver in SDS polyacrylamide gels are excised and are subjected to a destaining treatment in 0.1–0.5 ml of the destaining solution provided by the commercial kit for 15 min. After the treatment, the destaining solution is removed and the remaining gels are incubated in 0.2 ml of solution containing 20 mM EDTA/100 mM NH_4HCO_3 at ambient temperature for more than 15 min. The gels are then washed three to five times with 1 ml of water at ambient temperature for 3 min. After the wash treatments, the gels are removed of all water by centrifugal concentrator-connected vacuum pump system. The resulting dried gels are mixed with 50–100 µl of protein-reducing solution (see Appendix) and allowed to swell again at ambient temperature. Reduction-treated proteins in gels are further heated at 50 °C for 1 h. After the treatment, all solution is removed, the remaining gel pieces are added with 50–100 µl of protein alkylation solution (see Appendix), and are incubated for 30–60 min under dark condition at ambient temperature. After the treatment, all solution is removed and the remaining gel pieces are washed three to five times with 1 ml of water at ambient temperature. For in-gel proteolytic digestion of proteins, dry gel pieces are added with a solution containing 100 mM Tris-HCl, pH 8.9, and *Achromobacter* protease I (lysyl endopeptidase) (0.05 amidase unit) and are incubated at 37 °C for 15–24 h. For peptide purification and its mass spectrometry analysis, the proteolysis-treated gel samples are added with appropriate volume (30–60 µl), which is enough to cover gel pieces, of 5% (v/v) formic acid and are incubated at ambient temperature for 10 min. The gel pieces are briefly centrifuged, the supernatant is collected (sup 1), and stored on ice. The remaining gel samples are then added with appropriate volume (30–60 µl) of 50% (v/v) acetonitrile/5% (v/v) formic acid and are incubated at ambient temperature for 10 min. The gel pieces are briefly centrifuged. The supernatant, sup 2, is collected and combined with sup 1. The remaining gel samples are added with appropriate volume (30–60 µl) of 95% (v/v) acetonitrile/5% formic acid (v/v) and are incubated at ambient temperature for 10 min. The gel pieces are briefly centrifuged. The supernatant is collected and transferred into a tube in which the supernatants 1 and 2 have been combined. Organic solvent in the supernatants is fully evaporated and reduced of its volume by a centrifugal concentrator for desalting treatments. Finally, the peptide fragments contained in the desalted samples are subjected to mass spectrometry analysis and the annotation of the results with peptide/protein database.

13.2.10 Emerging Approaches: Live-Cell Imaging and Genome Manipulations

Live-cell imaging of oocytes and eggs of *X. laevis* has been a matter of difficulty for long because of the yolk materials and cell surface pigmentation in oocytes and eggs interfere with the transparency of the cell samples. However, our recent study has shown that it is possible to examine the live cell dynamics of intracellular ATP in oocytes of *X. laevis*, by employing ATeam, a newly developed ATP sensor polypeptide that involves the fluorescent energy transfer as a base mechanism. For this purpose, we use translucent oocyte/egg, whose cytoplasm and other cellular compartments (e.g., yolk platelets, pigmented granules) are separated noninvasively by centrifugation, or albino oocyte/egg, whose pigmented granules lose their authentic colors. We are now in the process of investigating the ATP dynamics during PG-induced oocyte maturation and its biochemical details

Downloaded From Vet-eBooks.com

(Ijiri *et al*. 2014). Study of frog fertilization at the genetic level (e.g., gene knockout) has also been a matter of great concern for many investigators. Newly emerging genome-editing technologies, for example, TALE nuclease or CRISPR/Cas9, have become available very recently to the developmental studies using *X. laevis* and its related species, *Xenopus tropicalis*. A particular benefit in this experimental technology is that the first generation of genome-edited animals, that is, F_0 animals, is expected to have an alteration in their genome including those in their germ cells, so that their gametogenesis would produce oocyte or sperm, in which a targeted gene by genome editing has already been knocked out. This is an especially important point for the study using frog, whose life cycle is much longer than other model animals, in which conventional gene knockout approaches (e.g., irradiation-mediated gene disruption, embryonic stem cell-mediated production of chimera animals) are actively employed. Under this circumstance, it will be interesting to examine whether the mammalian components that have been shown to be essential for gamete interaction and signaling (i.e., IZUMO1 in sperm, CD9 and Juno in egg) are also essential for fertilization in *X. laevis*. We are now in the process of producing *X. tropicalis* that is defected in the expression of UPIII.

13.3 Achievements and Perspectives

In 1996, we published our first paper on a possible involvement of the egg-associated Src family protein-tyrosine kinase at fertilization in *X. laevis* (Sato *et al*. 1996). In this study, we fractionated unfertilized and fertilized eggs (10 min post insemination) into two parts: cytoplasmic and nonionic detergent-solubilized membrane/particulate fractions. Both fractions were independently chromatographed on a DEAE-cellulose column and the column fractions obtained were analyzed for the presence of a peptide substrate kinase activity in the absence or presence of a kinase-activating antibody that recognizes Src family protein-tyrosine kinase (Figure 13.2a). The results demonstrated that the membrane/particulate fractions of unfertilized eggs contain the peptide kinase activity that could be seen only when the kinase-activating antibody is present, suggesting the presence of an "inactive" enzyme. On the other hand, the same fractions of fertilized eggs were shown to contain the kinase activity that could be seen irrespective of the antibody, suggesting the presence of an "active" enzyme. Thus, it was hypothesized that fertilization of *X. laevis* eggs is accompanied by the activation of an egg-associated Src family protein-tyrosine kinase. We named the kinase as p57 kinase or Xyk (*Xenopus* tyrosine kinase), and performed further investigation aiming to evaluate physiological importance of the sperm-induced activation of p57/Xyk.

Pharmacological studies using inhibitors specific to Src family protein-tyrosine kinase demonstrated that these compounds block the normal fertilization processes such as cortical contraction (Figure 13.2b), sperm entry and resumption of meiotic cell cycle (Figure 13.2c), and first cell division (Figure 13.2b) (Sato *et al*. 1998, 1999, 2004). Importantly, PP1, a potent Src-specific inhibitor, was shown to inhibit sperm-induced Ca_{2+} transient, but not A23187-induced Ca_{2+} transient (Figure 13.3d) (Sato *et al*. 2000, 2004), indicating that the sperm-induced activation of p57/Xyk may act as an intermediate system between gamete interaction and Ca_{2+} transient. Consistently, we later found that the activated p57/Xyk physically associates, phosphorylates, and activates PLC© and that the sperm-induced production of IP_3, a second messenger for sperm-induced Ca_{2+} transient, could be blocked by PP1 and U73122, a potent PLC inhibitor (Sato *et al*. 2000, 2004).

Our studies were also designed to analyze the mechanism by which sperm–egg interaction promotes the activation of p57/Xyk. Indirect immunofluorescent studies of the egg sections demonstrated that sperm-induced tyrosine phosphorylation of egg proteins occurs in a limited

Downloaded From Vet-eBooks.com

area on the egg plasma membrane, which could be at and/or near the sperm–egg interaction site (Figure 13.2e). Isolation and characterization of low-density, detergent-insoluble membranes (LD-DIM or MD, membrane microdomain) from unfertilized and fertilized eggs demonstrated that the egg MD is enriched in p57/Xyk and that sperm-induced tyrosine phosphorylation of egg proteins, which includes that of a 30 kDa protein, occurs predominantly in this membrane fraction (Figure 13.2g and i). Interestingly, addition of sperm to the isolated MD samples promotes the activation of p57/Xyk (Figure 13.2h). In addition, the isolated MD fractions were shown to functionally interact with the cytostatic factor-arrested egg extract, by which they exert a series of biochemical and cell biological processes that are seen in fertilized egg. These results suggest that the sperm-interacting and p57/Xyk-activating machinery is also present in this membrane fraction (Figure 13.2f) (Sato *et al*. 2003, 2006a). Further characterization of the 30 kDa tyrosine-phosphorylated protein by mass spectrometry, preparation of the specific antibody, and biochemical experiments examining its signaling function demonstrated that it is a single-transmembrane protein UPIII, whose amino-terminal, extracellular part contains a target site for sperm protease essential for sperm-induced egg activation, and cytoplasmic sequence contains a tyrosine phosphorylation site (Mahbub Hasan *et al*. 2005, 2007, 2011; Sakakibara *et al*. 2005). Thus, UPIII represents a strong candidate for long-thought sperm-interacting machinery, whose activation by sperm triggers the intracellular activation of p57/Xyk (Figure 13.2j) (Sato *et al*. 2006b; Sato, 2014; Mahbub Hasan *et al*. 2014). Study using *X. laevis* oocyte and egg is advantageous for biochemical and cell biological experiments to elucidate protein functions. By employing this excellent animal model, a number of pioneering findings have been made in the field of oocyte maturation at the oocyte cytoplasm and egg/oocyte coat levels. On the other hand, *X. laevis* oocyte and egg have not been effectively employed as an experimental platform to characterize plasma membrane-associated components that act in gamete interaction and signaling. Our current fertilization study using *X. laevis* eggs aim to understand how structure and function of egg MDs are developed and how egg MDs and MD-associated molecules contribute to successful fertilization and subsequent embryogenesis. We believe that the knowledge obtained with this project in itself would contribute to general understanding of the fertilization system. In addition, fertilization system involves, with no exception, membrane interaction and fusion between female and male gametes, in spite of a countless variety of species-specific differences in the fertilization system such as molecules of fertilization (e.g., requirement of Src PTK signaling), systems for egg activation (e.g., physiological monospermy and polyspermy), extracellular environment for fertilization (e.g., internal and external fertilization), and even animal and nonanimal fertilization. Therefore, our approach would be useful for fertilization studies on a wide range of other organisms.

Acknowledgments

This work was supported by a Grant-in-Aid for Scientific Research (C) from Japan Society for the Promotion of Science, Grant Number 15K07083.

Appendix

CSF extraction buffer
100 mM KCl
0.1 mM $CaCl_2$
1 mM Mg Cl_2

Downloaded From Vet-eBooks.com

5 mM EGTA
50 mM sucrose
50 mM HEPES-NaOH, pH 7.8
100 µg/ml cytochalasin B
10 µg/ml leupeptin
10 µg/ml pepstatin
10 µg/ml chymostatin

DeBoer solution
100 mM NaCl
1.3 mM KCl
0.44 mM $CaCl_2$
pH 7.2 by addition of $NaHCO_3$

Extraction buffer A
20 mM tris-HCl, pH 7.5
150 mM NaCl
1 mM EDTA
1 mM EGTA
10 mM β-mercaptoethanol
1 mM sodium orthovanadate
10 µg/ml leupeptin
20 µM APMSF

Extraction buffer B
20 mM tris-HCl, pH 7.5
1% (v/v) Triton X-100
150 mM NaCl
1 mM EDTA
1 mM EGTA
10 mM β-mercaptoethanol
1 mM sodium orthovanadate
10 µg/ml leupeptin
20 µM APMSF

Fixation buffer
10 mM NaH_2PO_4/Na_2HPO_4, pH 7.2
145 mM NaCl
4% (w/v) paraformaldehyde

Inhibitor dilution buffer
20 mM sodium phosphate, pH 7.4
100 mM NaCl

Injection buffer
110 mM NaCl
1.3 mM KCl
20 mM $MgSO_4$
0.1 mM EGTA
10 mM chlorobutanol

Kinase reaction mixture
5 mM $MgCl_2$
20 mM tris-HCl, pH 7.5
1 mM DTT
2 µM [©-^{32}P]ATP (10 µCi)
1 mM synthetic substrate peptide

Laemmli's SDS sample buffer
200 mM tris-phosphate, pH 6.7
5% (w/v) SDS

Downloaded From Vet-eBooks.com

100 mM dithiothreitol
50% (w/v) sucrose
0.025% (w/v) bromophenol blue

Modified Barth's solution
7.5 mM tris-HCl, pH 7.5
88 mM NaCl
1 mM KCl
2.5 mM $NaHCO_3$
0.82 mM MgSO4
0.33 mM $Ca(NO_3)_2$
0.41 mM $CaCl_2$

0.33 × Modified Ringer's solution
33.3 mM NaCl
0.6 mM KCl
0.33 mM $MgCl_2$
0.66 mM $CaCl_2$
1.67 mM Hepes–NaOH, pH 7.8

Mounting medium
10 mM NaH_2PO_4/Na_2HPO_4, pH 7.2
145 mM NaCl
50 mg/ml 1,4-diazabicyclo[2]octane
90% (v/v) glycerol

OR-2 solution
82.5 mM NaCl
2.5 mM KCl
1 mM $CaCl_2$
1 mM $MgCl_2$
1 mM Na_2HPO_4
5 mM HEPES, pH 7.8

PLC assay buffer
50 mM tris-HCl, pH 7.5
70 mM KCl
1 mM $CaCl_2$
1 mM EGTA
0.2% °-octylglucoside

Protein alkylation solution
40 mM iodoactamide
10 mM EDTA
100 mM NH_4HCO_3

Protein-reducing solution
10 mM DTT
10 mM EDTA
100 mM NH_4HCO_3

Radioimmunoprecipitation buffer
50 mM tris-HCl, pH 7.5
150 mM NaCl
1% Triton X-100
1% Nonidet P-40
0.5% SDS

0.5 × Steinberg solution
29 mM NaCl
0.34 mM KCl
0.17 mM$CaCl_2$

Downloaded From Vet-eBooks.com

0.43 mM Mg_2SO_4
2.3 mM tris-HCl, pH 7.4

Whole-cell extraction buffer
20 mM tris-HCl, pH 7.5
1% Triton X-100
1 mM EDTA
1 mM EGTA
10 mM®-mercaptoethanol
1 mM Na_3VO_4
10 μg/ml leupeptin
20 μM APMSF

References

Ijiri, T.W., Kishikawa, J., Imamura, H., Iwao, Y., Yokoyama, K., and Sato, K. (2014) ATP imaging in *Xenopus laevis* oocytes, in *Sexual Reproduction in Animals and Plants* (eds H. Sawada *et al.*), Springer, Berlin, pp. 181–186.

Iwao Y. (2000a) Fertilization in amphibians, in *Fertilization in Protozoa and Metazoan Animal* (eds J.J. Tarín and A. Cano,), Springer, Berlin, pp. 147–191.

Iwao Y. (2000b) Mechanisms of egg activation and polyspermy block in amphibians and comparative aspects with fertilization in other vertebrates. *Zoolog. Sci.*, **17**, 699–709.

Mahbub Hasan, A.K., Sato, K., Sakakibara, K., Ou, Z., Iwasaki, T., Ueda, Y., and Fukami, Y. (2005) Uroplakin III, a novel Src substrate in *Xenopus* egg rafts, is a target for sperm protease essential for fertilization. *Dev. Biol.*, **286**, 483–492.

Mahbub Hasan, A.K., Ou, Z., Sakakibara, K., Hirahara, S., Iwasaki, T., Sato, K., and Fukami, Y. (2007) Characterization of *Xenopus* egg membrane microdomains containing uroplakin Ib/III complex: roles of their molecular interactions for subcellular localization and signal transduction. *Genes Cells*, **12**, 251–267.

Mahbub Hasan, A.K., Fukami, Y., and Sato, K. (2011) Gamete membrane microdomains and their associated molecules in fertilization signaling. *Mol. Reprod. Dev.*, **78**, 814–830.

Mahbub Hasan, A.K., Hashimoto, A., Maekawa, Y., Matsumoto, T., Kushima, S., Ijiri, T.W., Fukami, Y., and Sato, K. (2014) Egg membrane microdomain-associated uroplakin III-Src 25 system becomes functional during oocyte maturation and is required for bidirectional gamete signaling at fertilization in *Xenopus laevis*. *Development*, **141**, 1705–1714.

Mammadova, G., Iwasaki, T., Tokmakov, A.A., Fukami, Y., and Sato, K. (2009) Evidence that phosphatidylinositol 3-kinase is involved in sperm-induced tyrosine kinase signaling in *Xenopus* egg fertilization. *BMC Dev. Biol.*, **9**, 68.

Sakakibara, K., Sato, K., Yoshino, K., Oshiro, N., Hirahara, S., Mahbub Hasan, A.K., Iwasaki, T., Ueda, Y., Iwao, Y., Yonezawa, K., and Fukami, Y. (2005) Molecular identification and characterization of *Xenopus* egg uroplakin III, an egg raft-associated transmembrane protein that is tyrosine-phosphorylated upon fertilization. *J. Biol. Chem.*, **280**, 15029–15037.

Sato, K. (2014) Transmembrane signal transduction in oocyte maturation and fertilization: focusing on *Xenopus laevis* as a model animal. *Int. J. Mol. Sci.*, **16**, 114–134.

Sato, K., Aoto, M., Mori, K., Akasofu, S., Tokmakov, A.A., Sahara, S., and Fukami, Y. (1996) Purification and characterization of a Src-related p57 protein-tyrosine kinase from *Xenopus* oocytes: isolation of an inactive form of the enzyme and its activation and translocation upon fertilization. *J. Biol. Chem.*, **271**, 13250–13257.

Downloaded From Vet-eBooks.com

Sato, K., Iwasaki, T., Tamaki, I., Aoto, M., Tokmakov, A.A., and Fukami, Y. (1998) Involvement of protein-tyrosine phosphorylation and dephosphorylation in sperm-induced *Xenopus* egg activation. *FEBS Lett.*, **424**, 113–118.

Sato, K., Iwao, Y., Fujimura, T., Tamaki, I., Ogawa, K., Iwasaki, T., Tokmakov, A.A., Hatano, O., and Fukami, Y. (1999) Evidence for the involvement of a Src-related tyrosine kinase in *Xenopus* egg activation. *Dev. Biol.*, **209**, 308–320.

Sato, K., Tokmakov, A.A., Iwasaki, T., and Fukami,, Y. (2000) Tyrosine kinase-dependent activation of phospholipase C© is required for calcium transient in *Xenopus* egg fertilization. *Dev. Biol.*, **224**, 453–469.

Sato, K., Iwasaki, T., Sakakibara, K., Itakura, S., and Fukami, Y. (2002a) Towards the molecular dissection of fertilization signaling: our functional genomic/proteomic strategies. *Proteomics*, **2**, 1079–1089.

Sato, K., Iwasaki, T., Ogawa, K., Konishi, M., Tokmakov, A.A., and Fukami, Y. (2002b) Low density detergent-insoluble membrane of *Xenopus* eggs: subcellular microdomain for tyrosine kinase signaling in fertilization. *Development*, **129**, 885–896.

Sato, K., Tokmakov, A.A., He, C.L., Kurokawa, M., Iwasaki, T., Shirouzu, M., Fissore, R.A., Yokoyama, S., and Fukami, Y. (2003) Reconstitution of Src-dependent phospholipase C© phosphorylation and transient calcium release by using membrane rafts and cell-free extracts from *Xenopus* eggs. *J. Biol. Chem.*, **278**, 38413–38420.

Sato, K., Iwasaki, T., Hirahara, S., Nishihira, Y., and Fukami, Y. (2004) Molecular dissection of egg fertilization signaling with the aid of tyrosine kinase-specific inhibitor and activator strategies. *Biochim. Biophys. Acta*, **1697**, 103–121.

Sato, K., Yoshino, K., Tokmakov, A.A., Iwasaki, T., Yonezawa, K., and Fukami, Y. (2006a) Studying fertilization in cell-free extracts: focusing on membrane/lipid raft functions and proteomics. *Methods Mol. Biol.*, **322**, 395–411.

Sato, K., Fukami, Y., and Stith, B.J. (2006b) Signal transduction pathways leading to Ca^{2+} release in a vertebrate model system: lessons from *Xenopus* eggs. *Semin. Cell Dev. Biol.*, **17**, 285–292.

Smith, J.C., Price, B.M.J., Van Nimmen, K., and Huylebroek, D. (1990) Identification of a potent *Xenopus mesoderm* inducing factor as homologue of activing A. *Nature*, **345**, 729–731.

Downloaded From Vet-eBooks.com

14

Prezygotic Chromosomal Examination of Mouse Spermatozoa

Hiroyuki Watanabe and Hiroyuki Tateno

Department of Biological Sciences, Asahikawa Medical University, Asahikawa, Japan

14.1 Introduction

Since Steptoe and Edwards (1978) first reported the live birth of a baby from *in vitro* fertilized (IVF) oocytes, assisted reproductive technologies (ARTs) have rapidly advanced and prevailed worldwide. One of the most important advances in ARTs is the use of intracytoplasmic sperm injection (ICSI) in which a single spermatozoon is injected into an oocyte to ensure fertilization, which is often opted for by male patients with severe infertility (Palermo *et al.*, 1992). Currently, ARTs such as IVF and ICSI have become a requisite technology for infertile couples that desire to have children of their own.

However, there is concern about spontaneous abortion of embryos and fetuses after ART. Products of aborted conception following ART have been reported to have chromosome aberrations, including autosome trisomy, polyploidy, X monosomy, and structural anomalies (Bettio *et al.*, 2008). Furthermore, chromosome aberrations were detected in approximately 3% of live fetuses following ICSI (Bonduelle *et al.*, 2002). A major cause of pregnancy loss is embryonic chromosome aberrations that originated in spermatozoa and oocytes. Growth of most embryos with chromosome aberrations is terminated during the first trimester, which leads to pregnancy loss (Plachot *et al.*, 1988). Spermatozoa collected from patients with abnormal semen quality have a relatively high incidence of sex chromosome aneuploidy (Storeng *et al.*, 1998). An abnormal karyotype, especially a translocation, in either patient is also involved in pregnancy loss due to the generation of chromosomally unbalanced gametes during meiotic divisions (Suzumori and Sugiura-Ogasawara, 2010).

Significant efforts have been made to select normal embryos during ARTs. Intracytoplasmic morphologically selected sperm injection (IMSI) is a unique approach to the reduction of pregnancy loss (Bartoov *et al.*, 2003). However, the incidence of structural chromosome aberrations was not always reduced in embryos fertilized by IMSI (Watanabe *et al.*, 2011). Preimplantation genetic diagnosis (PGD) is believed to be the most reliable method of detecting defective embryos after ARTs. In this technique, transferrable embryos are screened by genetic analyses of polar bodies or blastomeres surgically taken from the embryos (for details, see Harper and SenGupta (2012)). Once the embryos are identified to be genetically abnormal, they are never rescued. If sperm and oocyte chromosomes could be analyzed prior to embryo production, the production of defective embryos would be minimized.

Recently, we developed a new technique using the mouse model (sperm chromosome screening (SCS)) to screen sperm chromosomes prior to fertilization (for detailed information,

Animal Models and Human Reproduction, First Edition. Edited by Heide Schatten and Gheorghe M. Constantinescu.
© 2017 John Wiley & Sons, Inc. Published 2017 by John Wiley & Sons, Inc.

Downloaded From Vet-eBooks.com

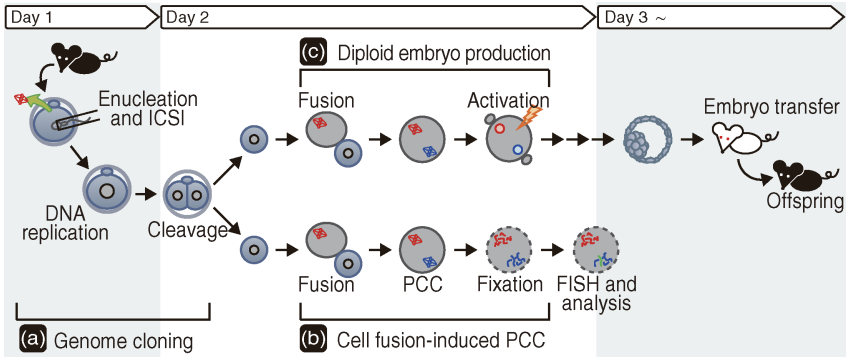

Figure 14.1 A flowchart of sperm chromosome screening (SCS) before fertilization. Some modifications were made to the original figure by Watanabe *et al.* (2013). (See color plate section.)

see Watanabe *et al.* (2013)). In this chapter, we showed the outline and practical use of the SCS. This method may be a powerful tool to reduce the production of genetically abnormal embryos for those seeking infertility treatment.

14.2 Procedure of Sperm Chromosome Screening

SCS involves the following three steps: (i) cloning of a sperm genome by using an androgenic embryo, (ii) induction of premature chromosome condensation (PCC) for paternal (sperm) chromosome analysis, and (iii) production of a diploid embryo by using an androgenic haploid blastomere (Figure 14.1).

14.2.1 Sperm Genome Cloning Using an Androgenic Embryo (Step (a))

At least two identical copies of a sperm genome are essential to concurrently execute sperm chromosome analysis and embryo production. A haploid cell line was developed from a sperm genome by androgenesis (Barra and Renard, 1988; Kuznyetsov *et al.*, 2007; Takeuchi *et al.*, 2007, 2008; Vichera *et al.*, 2011). The sperm head was injected into an enucleated oocyte by using a micromanipulator. In the androgenic haploid 1-cell embryo, sperm DNA replicated normally; the replicated sperm genomes were divided into two sister blastomeres during the first cleavage.

Technical Note

To induce superovulation, mature B6D2F1 female mice were hormonally stimulated by administering 10 IU equine chorionic gonadotropin (eCG) followed by the same dose of human chorionic gonadotropin (hCG) 48 h later. Fresh metaphase II (MII) oocytes with cumulus cells were released from the oviducts into HEPES-buffered CZB medium (Chatot *et al.*, 1989) containing 0.1% hyaluronidase to remove cumulus cells. The cumulus-free MII oocytes were enucleated as previously described (Wakayama *et al.*, 1998). Spermatozoa were collected from the epididymis of B6D2F1 males. Sperm heads were microsurgically injected into the enucleated oocytes by using a micromanipulator installed with piezomicropipette-driving unit according to Kimura and Yanagimachi (1995). The haploid androgenic 1-cell embryos were cultured in modified CZB medium supplemented with 5.55 mM D-glucose.

Downloaded From Vet-eBooks.com

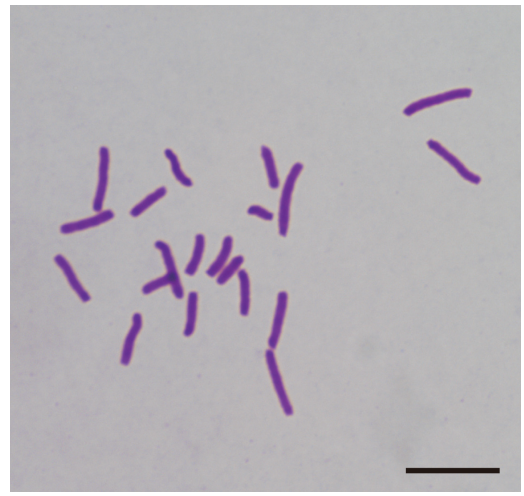

Figure 14.2 A haploid set ($n = 20$) of PCC-chromosomes in a sister blastomere from an androgenic 2-cell embryo. Chromosomes were conventionally stained with Giemsa solution. Bar: 10 μm.

14.2.2 Induction of PCC for Rapid Chromosome Visualization (Step (b))

PCC was adopted to accelerate the chromosome analysis of blastomeres (Willadsen *et al.*, 1999). At 24 h after ICSI when two sister blastomeres of androgenic 2-cell embryos were synchronously in G_2 phase of the cell cycle, blastomeres were individually fused with a fresh zona-free-MII oocyte. The fused oocytes were incubated for 2 h to induce PCC, and then processed for chromosome visualization (Figure 14.2).

Approximately 90% of androgenic 2-cell embryos had chromosomal homology between two sister blastomeres, indicating that the chromosome constitution of one blastomere represents that of another blastomere.

Technical Note

Fresh MII oocytes were appropriately treated with 0.1% hyaluronidase and 0.5% protease to remove cumulus cells and the zona pellucida. The zona-free MII oocytes were fused with blastomeres of androgenic 2-cell embryos by using the envelope of hemagglutinating virus of Japan. Before incubation to induce PCC, the fused oocytes were exposed to a Ca^{2+} chelating agent BAPTA-AM (10 μM) to inhibit accidental activation of the recipient oocytes. Because the fused oocytes were vulnerable to osmotic change, hypotonic treatment with a twofold dilution of modified CZB medium was performed for 10 min. Chromosome slides of oocytes were prepared by the gradual-fixation/air-drying method (Mikamo and Kamiguchi, 1983).

14.2.3 Production of Diploid Embryos by Fusion of Blastomere with MII Oocytes (Step (c))

Blastomeres of the androgenic 2-cell embryo were fused with fresh zona-free MII oocyte, as described above. The fused oocytes were incubated for 1.5–2.0 h to allow them to construct a spindle with PCC-chromosomes of blastomere origin. The oocytes were artificially activated to produce diploid embryos. In association with extrusion of a second polar body of the recipient oocytes, a haploid set of paternal chromosomes of blastomere origin was also extruded as an additional polar body, resulting in the generation of normal diploid embryos with parental genomes.

Downloaded From Vet-eBooks.com

Technical Note

Strontium chloride (10 mM, 30 min) was used to activate the reconstructed oocytes. Because the embryos lacked a zona pellucida, they were cultured in a small depression on the surface of a culture dish (Vajta *et al.*, 2000) to prevent dissociation of blastomeres during development. Blastocysts were transferred into the oviducts on the first day of pseudopregnancy in CD1 females.

14.3 Practical Use of SCS Before Fertilization

To validate our SCS, we used a mouse carrier heterozygous for a Robertsonian translocation between chromosomes 6 and 15, abbreviated Rb(6.15). As described earlier, haploid androgenic 2-cell embryos were produced and two sister blastomeres were individually fused with MII oocytes, one for analysis of PCC-chromosomes and another for production of diploid embryos. Based on the results of PCC-chromosome analysis (Figure 14.3), diploid embryos derived from blastomeres with a normal chromosome complement and those derived from blastomeres with a balanced chromosome complement were separately transferred to the surrogate mothers. The karyotypes of the offspring grown from the respective embryos were predicted by PCC-chromosome analysis of the blastomeres (Table 14.1). Thus, SCS prevented a transmission of chromosomal aberrations from spermatozoa to embryos and/or offspring. The PCC-chromosome analysis could also detect chromosomal mutations of spermatozoa irradiated with 2 Gy gamma-rays (Figure 14.4), conversely suggesting that SCS could be applicable to determination

Table 14.1 Chromosome analysis of offspring delivered from embryos after SCS.

Karyotype of blastomeres used for embryo production	No. of offspring karyotyped	Normal	Rb(6.15)
Normal	16	16	0
Rb(6.15)	5	0	5

Adapted from Watanabe *et al.* (2013).

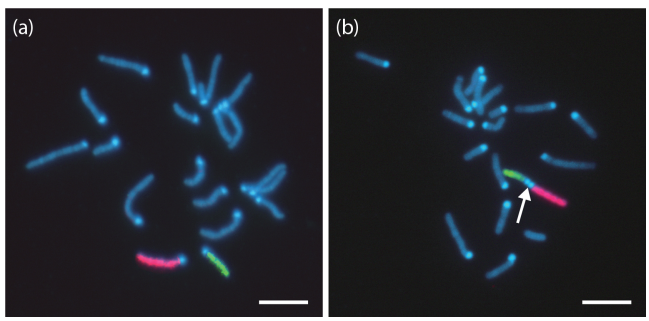

Figure 14.3 Fluorescence *in situ* hybridization (FISH) analysis of blastomere chromosomes in androgenic 2-cell embryos derived from spermatozoa in a carrier with a Robertsonian translocation between chromosomes 6 and 15, Rb(6.15). Chromosomes 6 and 15 can be seen in red and green, respectively. (a) Normal chromosome complement. (b) Balanced chromosome complement with Rb(6.15) (arrow). Bar: 10 μm. (See color plate section.)

Downloaded From Vet-eBooks.com

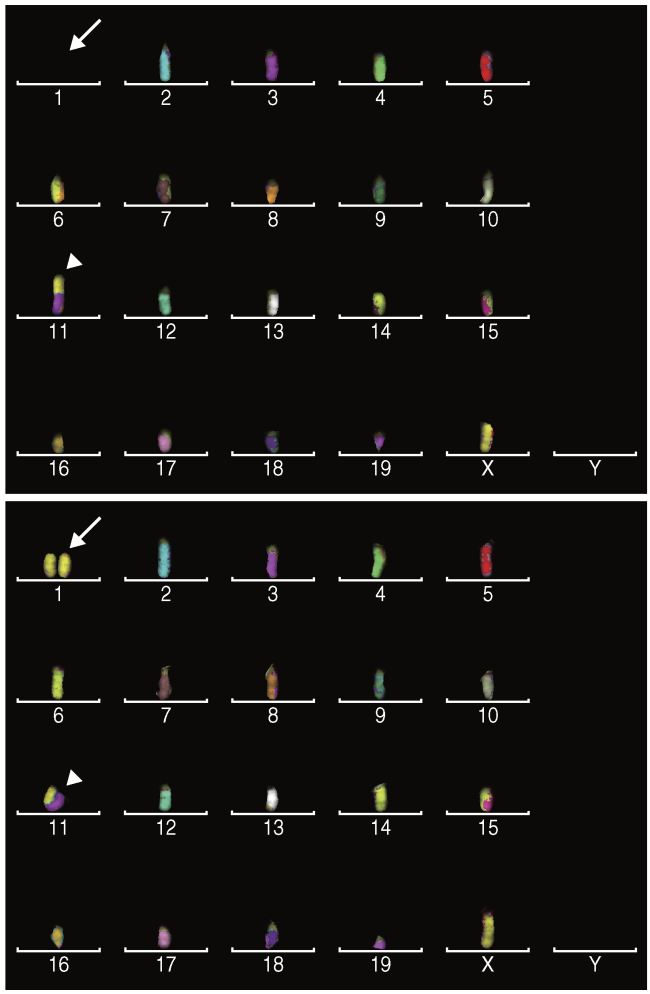

Figure 14.4 Multicolor fluorescence *in situ* hybridization (multicolor FISH) analysis of blastomere chromosomes in an androgenic 2-cell embryo derived from irradiated spermatozoon. *Top*: Absence of chromosome 1 (arrow), and a dicentric chromosome by exchange between chromosomes 1 and 11 (arrowhead). *Bottom*: Two acentric fragments of chromosome 1 (arrow), and a dicentric chromosome by exchange between chromosomes 1 and 11 (arrowhead).

of chromosomal integrity in spermatozoa collected from father accidentally exposed to radiation and environmental chemical mutagens.

In addition, blastomeres of androgenic haploid 2-cell embryos were used to identify X or Y chromosome-bearing androgenic blastomeres before fertilization (Figure 14.5), as X- and

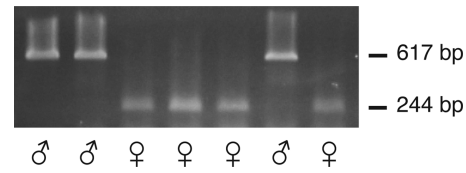

Figure 14.5 Electrophoretogram of DNA amplified by PCR from a single androgenic haploid blastomere. X- and Y-chromosomes-specific gene sequences were visible as a primary band of 244 and 617 base pairs (bp), respectively.

Downloaded From Vet-eBooks.com

Y-specific gene sequences in DNA retrieved from a single haploid blastomere were amplified using PCR (Vichera *et al.*, 2011).

14.4 Conclusion

The current SCS has many advantages, including the fact that sperm genome cloning can be efficiently achieved using androgenic embryos and that chromosomes can be rapidly visualized by cell-fusion-induced PCC. Thus, we are able to produce mouse zygotes without any chromosome aberrations of sperm origin.

Cryopreservation of androgenic haploid blastomeres before embryo production has been demonstrated (Watanabe *et al.*, 2013). This allows sufficient time for detailed analysis of PCC-chromosomes with molecular cytogenetic techniques, including multicolor FISH. Moreover, DNA diagnosis of androgenic haploid blastomeres may provide detailed information on genetic disorders of paternal origin.

In the current SCS, at least three oocytes are needed, that is, one for preparing androgenic haploid embryos, one for analyzing PCC-chromosomes, and the other for producing diploid embryos. Technical improvements such as PCC induction by calyculin A, a specific inhibitor of protein phosphatases, may provide an alternative to the use of extra oocytes. Our goal is to establish the best method of prezygotic gamete chromosome examination by using a single pair of spermatozoon and oocyte.

Acknowledgments

The authors thank Dr. A. Kohda (Institute for Environmental Sciences) for his technical assistance. This work was supported by a Grants-in-Aid for Scientific Research (22·8495 and 23890013 to H.W.) from the Japan Society for the Promotion of Sciences. There are no conflicts of interest to be declared.

Addendum

To reduce the extra oocytes used for the SCS procedure, substantial improvements had been made in our recent work (Watanabe *et al.*, 2015). Briefly, genome cloning of spermatozoa was achieved using a small cytoplast derived from MII oocyte, and PCC of the duplicated nuclei was induced by the cultivation with calyculin A. The remaining karyoplast of MII oocyte (the counterpart of small cytoplast) was used for the embryo production. Although these procedures for SCS remain to be brushed up further, SCS is capable of prezygotic selection of spermatozoa with normal chromosomes and a desirable haplotype during ARTs.

References

Barra, J. and Renard, J.P. (1988) Diploid mouse embryos constructed at the late 2-cell stage from haploid parthenotes and androgenotes can develop to term. *Development*, **102** (4), 773–779.

Bartoov, B., Berkovitz, A., Eltes, F., Kogosovsky, A., Yagoda, A., Lederman, H., Artzi, S., Gross, M., and Barak, Y. (2003) Pregnancy rates are higher with intracytoplasmic morphologically selected

Downloaded From Vet-eBooks.com

sperm injection than with conventional intracytoplasmic injection. *Fertil. Steril.*, **80** (6), 1413–1419.

Bettio, D., Venci, A., and Levi Setti, P. (2008) Chromosomal abnormalities in miscarriages after different assisted reproduction procedures. *Placenta*, **29** (Suppl. 2), 126–128.

Bonduelle, M., Van Assche, E., Joris, H., Keymolen, K., Devroey, P., Van Steirteghem, A., and Liebaers, I. (2002) Prenatal testing in ICSI pregnancies: incidence of chromosomal anomalies in 1586 karyotypes and relation to sperm parameters. *Hum. Reprod.*, **17** (10), 2600–2614.

Chatot, C.L., Ziomek, C.A., Bavister, B.D., Lewis, J.L., and Torres, I. (1989) An improved culture medium supports development of random-bred 1-cell mouse embryos *in vitro*. *J. Reprod. Fertil.*, **86** (2), 679–688.

Harper, J.C. and SenGupta, S.B. (2012) Preimplantation genetic diagnosis: state of the art 2011. *Hum. Genet.*, **131** (2), 175–186.

Kimura, Y. and Yanagimachi, R. (1995) Intracytoplasmic sperm injection in the mouse. *Biol. Reprod.*, **52** (4), 709–720.

Kuznyetsov, V., Kuznyetsova, I., Chmura, M., and Verlinsky, Y. (2007) Duplication of the sperm genome by human androgenetic embryo production: towards testing the paternal genome prior to fertilization. *Reprod. BioMed. Online*, **14** (4), 504–514.

Mikamo, K. and Kamiguchi, Y. (1983) A new assessment system for chromosomal mutagenicity using oocytes and early zygotes of the Chinese hamster, in *Radiation-Induced Chromosome Damage in Man*, (eds T. Ishihara and M.S. Sasaki), A.R. Liss, pp. 411–432.

Palermo G., Joris, H., Devroey, P., and Van Steirtegham, A.C. (1992) Pregnancies after intracytoplasmic injection of single spermatozoon into an oocyte. *Lancet*, **340** (8810), 17–18.

Plachot, M., de Grouchy, J., Junca, A.M., Mandelbaum, J., Salat-Baroux, J., and Cohen, J. (1988) Chromosomal analysis of human oocytes and embryos in an *in vitro* fertilization program. *Ann. N. Y. Acad. Sci.*, **541**, 384–397.

Steptoe, P.C. and Edwards, R.G. (1978) Birth after the reimplantation of a human embryo. *Lancet*, **2** (8085), 366.

Storeng, R.T., Plachot, M., Theophile, D., Mandelbaum, J., Belaisch-Allart, J., and Vekemans, M. (1998) Incidence of sex chromosome abnormalities in spermatozoa from patients entering an IVF or ICSI protocol. *Acta Obstet. Gynecol. Scand.*, **77** (2), 191–197.

Suzumori, N. and Sugiura-Ogasawara, M. (2010) Genetic factors as a cause of miscarriage. *Curr. Med. Chem.*, **17** (29), 3431–3437.

Takeuchi, T., Neri, Q.V., Cheng, M., and Palermo, G.D. (2007) Cloning the male genome. *Hum. Reprod.*, **22** (Suppl. 1), i62.

Takeuchi, T., Neri, Q.V., Rosenwaks, Z., and Palermo, G.D. (2008) Offspring generated from androgenic "octets." *Hum. Reprod.*, **23** (Suppl. 1), i103.

Vajta, G., Peura, T.T., Holm, P., Páldi, A., Greve, T., Trounson, A.O., and Callesen, H. (2000) New method for culture of zona-included or zona-free embryos: the Well of the Well (WOW) system. *Mol. Reprod. Dev.*, **55** (3), 256–264.

Vichera, G., Olivera, R., Sipowicz, P., Radrizzani, M., and Salamone, D. (2011) Sperm genome cloning used in biparental bovine embryo reconstruction. *Reprod. Fertil. Dev.*, **23** (6), 769–779.

Wakayama, T., Perry, A., Zuccotti, M., and Johnson, K.R. (1998) Full-term development of mice from enucleated oocytes injected with cumulus cell nuclei. *Nature*, **394** (6691), 369–374.

Watanabe, S., Tanaka, A., Fujii, S., Mizunuma, H., Fukui, A., Fukuhara, R., Nakamura, R., Yamada, K., Tanaka, I., Awata, S. *et al.* (2011) An investigation of the potential effect of vacuoles in human sperm on DNA damage using a chromosome assay and the TUNEL assay. *Hum. Reprod.*, **26** (5), 978–986.

Downloaded From Vet-eBooks.com

Watanabe, H., Kusakabe, H., Mori, H., Yanagimachi, R., and Tateno, H. (2013) Production of offspring after sperm chromosome screening: an experiment using the mouse model. *Hum. Reprod.*, **28** (2), 531–537.

Watanabe, H., Kohda, A., and Tateno, H. (2015) Experimental approach to prezygotic chromosome screening using only a single pair of gametes in mice. *J. Reprod. Dev.*, **61** (6), 511–518.

Willadsen, S., Levron, J., Munné, S., Schimmel, T., Márquez, C., Scott, R., and Cohen, J. (1999) Rapid visualization of metaphase chromosomes in single human blastomeres after fusion with *in-vitro* matured bovine eggs. *Hum. Reprod.*, **14** (2), 470–475.

Downloaded From Vet-eBooks.com

15

Molecular and Cellular Aspects of Mammalian Sperm Acrosomal Exocytosis

Florenza A. La Spina,[1] Cintia Stival,[2] Dario Krapf,[2] and Mariano G. Buffone[1]

[1]*Instituto de Biología y Medicina Experimental (IBYME), National Research Council of Argentina (CONICET), Buenos Aires, Argentina*
[2]*Institute of Molecular and Cell Biology of Rosario (CONICET-UNR) and Área Biología, Facultad de Ciencias Biológicas y Farmacéuticas, UNR, Rosario, Argentina*

15.1 Introduction

After ejaculation, mammalian sperm perform a maturational process called capacitation. During capacitation, sperm activate a complex cascade of signaling pathways leading to acquire two essential features: the development of hyperactivated motility and the ability to undergo acrosomal exocytosis upon stimulation with the proper stimuli. Mammalian sperm must undergo acrosomal exocytosis to penetrate the extracellular matrix surrounding the egg, named zona pellucida (ZP). Following exocytosis, the posterior region of the acrosome, known as the equatorial segment, engages in membrane fusion with the oocyte (Moore and Bedford, 1978; Oura and Toshimori, 1990; Wassarman, 1987). A critical protein for sperm–egg fusion is IZUMO1, which is localized on the acrosomal membrane. As a consequence of acrosomal exocytosis, this protein relocalizes to the surface of the equatorial region, and sperm become fusion competent (Satouh *et al.*, 2012; Sosnik *et al.*, 2009, 2010).

Acrosomal exocytosis shares many molecular mechanisms in common with other cellular secretory processes. However, there are some features that make this process a special type of regulated secretion: (i) a single exocytotic granule per cell is involved; (ii) there is no membrane recycling; and (iii) rather than a single vesicle–plasma membrane union point, fusion between the outer acrosomal and the plasma membranes occurs at multiple sites to destabilize the structure of the acrosome (Mayorga *et al.*, 2007).

15.2 Structure of the Acrosome

The acrosome is essential for fertilization in mammals. Sperm must possess properly formed acrosomes in order to be functional in the fertilization process; men or animal models carrying mutations that affect the formation or function of the sperm acrosome are infertile or display severe subfertility (Dam *et al.*, 2007; Kang-Decker *et al.*, 2001; Lin *et al.*, 2007; Sotomayor and Handel, 1986).

Acrosomal biogenesis commences in the late pachytene spermatocyte phase of meiosis and continues throughout the first half of spermiogenesis, the haploid phase of spermatogenic differentiation in the seminiferous tubules of the testis (Anakwe and Gerton, 1990; Escalier

Animal Models and Human Reproduction, First Edition. Edited by Heide Schatten and Gheorghe M. Constantinescu.
© 2017 John Wiley & Sons, Inc. Published 2017 by John Wiley & Sons, Inc.

Downloaded From Vet-eBooks.com

et al., 1991; Kashiwabara *et al.*, 1990). First, proacrosomal vesicles are formed in close contact to the perinuclear region near the Golgi apparatus of pachytene spermatocytes. These vesicles are then distributed to the four resulting spermatids during the following meiotic cell divisions. Later on, in early spermiogenesis, these vesicles coalesce into a single granule that attaches to the round spermatid nucleus and continues to enlarge as Golgi-derived material is added to the developing acrosome. By the time the elongating spermatids are developing, the acrosome–nucleus complex undergoes extensive morphological changes to acquire the shape that is characteristic for mature sperm. Additional maturation of the acrosome might occur while spermatozoa are transiting through the different regions of the epididymis, as in the case of guinea pig sperm. In these species, the heads of testicular sperm entering the rete testis from the seminiferous tubules are planar (Fawcett and Hollenberg, 1963). As sperm travel through the epididymis to the vas deferens, the acrosome transforms such that it resembles a cupped hand, where the fingers represent the apical segment of the acrosome and the remainder of the hand, the sperm nucleus. The acrosome forms a convex (dorsal) face with a bulge, a concave (ventral) surface, and a leading edge that tapers to a pronounced tip.

The acrosome of a mature mammalian sperm contains several structural compartments. This was shown more clearly in species with large acrosomes such as guinea pig or hamster but also seen in small acrosomes, like mouse and human. Enclosing the lumen of the acrosomal vesicle is a continuous membrane called the outer acrosomal membrane (OAM) and the inner acrosomal membrane (IAM). The OAM closely associates with the plasma membrane overlying the acrosome and the IAM is laminated to the nuclear membrane (Eddy, 2006).

The acrosomal lumen contains both soluble and particulate components called the acrosomal matrix (Buffone *et al.*, 2008; Foster *et al.*, 1997; Kim *et al.*, 2001; Olson and Winfrey, 1994a; Westbrook-Case *et al.*, 1995). Morphological subcompartments within this matrix can be distinguished as regions of differing density by electron microscopy or areas containing different acrosomal antigens as detected by immunoelectron microscopy (Foster *et al.*, 1997; Olson and Winfrey, 1994a; Westbrook-Case *et al.*, 1994a). A protein located in the acrosomal lumen can be considered either as a soluble constituent or an acrosomal matrix component according to its Triton X-100 solubility (Huang *et al.*, 1985). In addition, some components have been localized to defined domains within the acrosome (Olson and Winfrey, 1994b; Olson *et al.*, 1988; Tanii *et al.*, 1994; Westbrook-Case *et al.*, 1994b). This discrete localization suggests that the position and/or solubility of a given acrosomal protein may govern its function, being released or relocated during the course of acrosomal exocytosis. In this scenario, a protein of the acrosomal matrix is predicted to remain associated with the sperm for a longer period of time than a soluble protein. Compartmentalization of the acrosome into "soluble" or "nonsoluble or particulate" fraction is thought to control the differential release of different components during the process of exocytosis (Green, 1978; Green and Hockaday, 1978; Hardy *et al.*, 1991; Noland *et al.*, 1989; Nuzzo *et al.*, 1990; Talbot and Franklin, 1974). As an example, autoantigen 1, hyaluronidase, and dipeptidyl peptidase 1 freely diffuse upon membrane fusion during exocytosis, while acrosin and ZP3R require proteolysis of the acrosomal matrix, thus remaining associated with the sperm for a longer period of time (Buffone *et al.*, 2009a). Most of our knowledge on compartmentalization of acrosomal components originates on studies with guinea pig sperm. The guinea pig acrosome consists of a large apical segment that extends past the nucleus, the principal segment (a thin, perinuclear, posterior acrosomal region), and the equatorial segment that delimits the posterior boundaries of the acrosome and encircles the nucleus (Fawcett and Hollenberg, 1963). Three different electron density zones can be differentiated in epididymal sperm: the electron-lucent dorsal bulge (Ml), a zone of intermediate electron density (M2), and the most electron-dense area (M3) (Olson *et al.*, 1987). The enzyme dipeptidyl peptidase 1 and AM67 have been localized in the M1 zone (Foster *et al.*, 1997; Talbot and Dicarlantonio, 1985). The autoantigen 1 was

Downloaded From Vet-e-Books.com

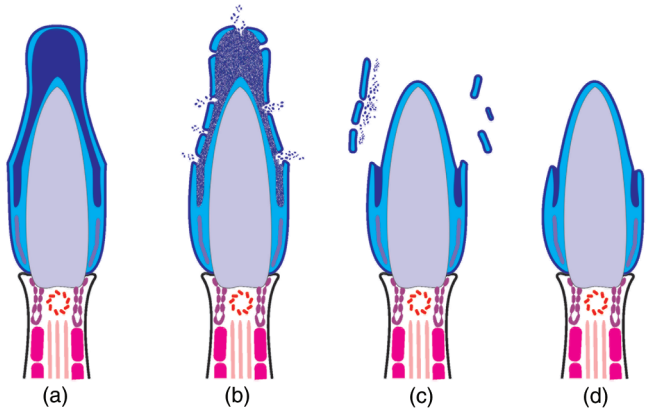

Figure 15.1 Schematic diagram of the process of acrosomal exocytosis in mammals. (a) Acrosome-intact sperm. (b) Fusion of the plasma membrane and the outer acrosomal membrane with the resulting formation of hybrid vesicles and exposure of the acrosomal matrix. (c) Release of the acrosomal matrix and exposure of the inner acrosomal membrane. (d) Acrosome-reacted sperm. (See color plate section.)

found to be distributed throughout the whole acrosome, while proacrosin was localized exclusively in the most electron-dense regions (M2 and M3) of the acrosome (Hardy *et al.*, 1991). Westbrook-Case *et al.* (1994) published the initial characterization of AM50, a protein of the apical segment of guinea pig sperm. This protein is restricted to the ventral domain (M3) of the acrosomal matrix and is proteolytically processed during the acrosomal exocytosis.

During acrosomal exocytosis, the OAM and plasma membrane (PM) fuse to form hybrid vesicles that are shed from the sperm, revealing the IAM as a newly exposed area of the plasma membrane. Upon fusion of the OAM with the PM, the soluble components of the acrosome may diffuse away while the Triton X100-unsoluble acrosomal matrix remains on the sperm surface until it breaks down, releasing most of its components (Buffone *et al.*, 2009a; Foster *et al.*, 1997; Kim and Gerton, 2003; Kim *et al.*, 2001, 2011; Noland *et al.*, 1994) (Figure 15.1). As a consequence of the disassembly of the acrosomal matrix, some of its components undergo posttranslational modifications. Although the acrosomal lumen contains several proteases, processing of acrosomal matrix proteins could result mainly from proteolytic cleavage by acrosin as judged from the studies of proacrosin-null mutant mice. Although these transgenic mice are fertile, penetration through the egg zona pellucida is delayed. This phenotype may be related to the delayed dissipation of certain acrosomal proteins (Baba *et al.*, 1994), suggesting that processing of specific acrosomal proteins may alter their association with the matrix. Additional work is needed in order to establish the biological relevance of the delayed disassemble of the acrosomal matrix.

Several proteins are cleaved during the process of disassembly of the acrosomal matrix. Representative examples are the proteins AM50 in guinea pig, and AM67/ZP3R in the guinea pig and mouse, respectively. AM50 is proteolytically processed to AM50ar as a consequence of its release from the sperm (Westbrook-Case *et al.*, 1994b). This cleavage pattern is attributed with proteolysis by acrosin, suggesting that this protease may function in the dispersion of the acrosomal matrix during acrosomal exocytosis. AM50 might be a structural component of the acrosomal matrix of zone M3. Similar to guinea pig AM50, mouse ZP3R is converted to a lower molecular weight form coincident with its release from the sperm into the supernatant during the course of spontaneous acrosomal exocytosis (Buffone *et al.*, 2009a). Proteolysis takes place in the C-terminal region of the protein in the short consensus repeat number 6 (SCR6), a region that is not present in guinea pig AM67, which consistently is not processed as a consequence of

Downloaded From Vet-eBooks.com

acrosomal exocytosis. Proacrosin is also proteolytically modified during acrosomal exocytosis. Proacrosin was detected in immunoblots of mature sperm, but was not detected in either the pellet or supernatant of A23187-treated sperm, suggesting that the protein had been modified during acrosomal exocytosis. Consistently, protease activity involved in the activation of proacrosin, generating a lower molecular weight form of acrosin, was detected in the soluble acrosomal components released from A23187-stimulated sperm (Moos *et al.*, 1993).

Acrosomal matrix can be isolated by spermatozoa treatment with nonionic detergent until most of acrosomes have detached from the sperm heads (Guyonnet *et al.*, 2012). In electron-microscopic views, the AM appeared as a bilaminate structure, the shape and integrity of which was not a function of a delimiting membrane. Previous reports showed that AM disassembly can be induced in isolated acrosomal matrices by changing the buffer conditions from acidic (pH 5.2) to physiological (pH 7.4) or by washing out the proteases inhibitors (Hardy *et al.*, 1991; Noland *et al.*, 1994). Proteomic analysis of the isolated AM in the presence of a diverse group of proteins included proteases, chaperones, hydrolases, transporters, enzyme modulators, transferases, cytoskeletal proteins, and others (Guyonnet *et al.*, 2012).

15.3 Intermediate Stages of Exocytosis

Acrosomal exocytosis is far from being an all or none event where the acrosome could be classified as "intact" or "reacted." As determined by transmission electron microscopy of human sperm undergoing acrosomal exocytosis, six stages can be identified, with the intermediate ones involving loss of acrosomal matrix material, while outer membranes appear to retain their integrity (Stock and Fraser, 1987; Yudin *et al.*, 1988). There is a temporal relationship among four stages of acrosomal exocytosis in the mouse: plasma membrane intact over the acrosome (class 1), plasma membrane initiating fusion with outer acrosomal membrane with soluble components retained within the acrosome (class 2), soluble acrosomal proteins lost but acrosomal matrix materials still present (class 3), and most acrosomal components lost (class 4) (Figure 15.2). It is thought that these patterns may represent successive transitional stages leading to the complete release of acrosomal components (Kim and Gerton, 2003). The exposure and release of soluble and matrix acrosomal proteins during spontaneous acrosomal exocytosis is not synchronous but is regulated as the sperm are incubated under capacitating conditions (DiCarlantonio and Talbot, 1988; Hardy *et al.*, 1991). In this differential time-released event, the AM components of sperm undergoing acrosomal exocytosis remain associated with sperm longer than soluble acrosomal proteins. Solubilization of the acrosomal matrix proteins may be associated, at least in part, with posttranslational modifications as they are released from the acrosome.

15.4 Sperm Capacitation Prepare the Sperm to Undergo Acrosomal Exocytosis

Recently ejaculated mammalian spermatozoa are incapable to fertilize. These cells should reside in the female genital tract for certain periods of time, depending on the species, before gaining the ability to fertilize the egg. This process, known as sperm capacitation, was mimicked in the laboratory, thanks to the independent work by Austin, 1951; Chang (1951), nearly six decades ago. During capacitation, multiple physiological and biochemical modifications take place (Yanagimachi, 1994), including efflux of cholesterol from the plasma membrane,

Downloaded From Vet-eBooks.com

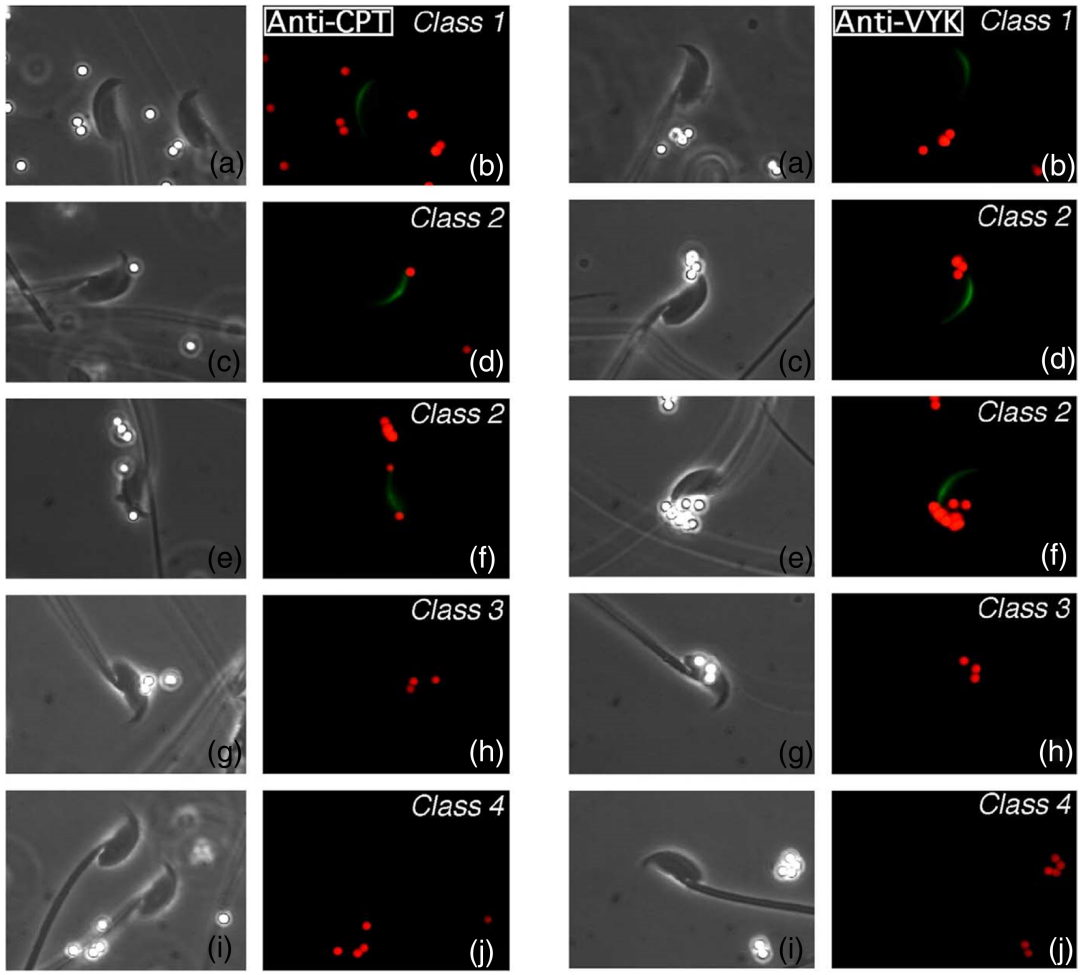

Figure 15.2 Simultaneous detection of acrosomal GFP in transgenic mouse sperm and the binding of anti-sp56 antibody-coated FluoSpheres. GFP expression, driven by the proacrosin promoter, was targeted to the mouse sperm acrosome using the signal sequence and part of the N-terminus of proacrosin. Some sperm bound antibody-coated FluoSpheres, demonstrating the exposure of the acrosomal matrix in those sperm. Four classes of sperm were identified by this assay. Anti-CPT and anti-VYK are two peptide-specific antibodies to mouse sp56. (a) Anti-CPT-coated FluoSpheres. (b) Anti-VYK-coated FluoSpheres. Paired phase-contrast (A, C,E,G,I) and fluorescence (B,D,F,H,J) (GFP, green; FluoSpheres, red) images of sperm. (Reproduced from Kim and Gerton (2003).) (See color plate section.)

hyperpolarization of the plasma membrane (Hernández-González *et al.*, 2006), increase of bicarbonate (HCO_3^-) and Ca^{2+} concentrations, increase of intracellular pH and cyclic adenosine monophosphate (cAMP) levels, and changes in protein phosphorylation due to altered protein kinase activity (Arcelay *et al.*, 2008; Baldi *et al.*, 2000; Visconti, 2009). The capacitation period ranges from 1 h in mouse to more than 6 h in human. However, during capacitation, some events are quickly triggered, while others require longer periods (Visconti, 2009). Fast events include immediate rise of intracellular cAMP due to fast activation of HCO_3^- sensitive-adenylyl cyclase (SAC aka SACY10), with the consequent activation of PKA. The slow events include hyperpolarization of the sperm plasma membrane and the development of protein

Downloaded From Vet-eBooks.com

tyrosine phosphorylation of many sperm proteins, which is a hallmark of capacitation. All these changes occur with the final aim of achieving changes in the sperm motility pattern (i.e., hyperactivation) with chemotactic ability, and preparing the sperm to carry out the acrosome reaction induced by a physiological agonist as progesterone; overall, the sperm are capable of fertilizing an egg.

Interestingly, PKA plays a pivotal role in almost all known aspects of sperm capacitation, not only restricted to fast events. The mechanisms by which PKA triggers pathways that ultimately endow the sperm with fertilizing capacity are not fully understood. In mouse sperm, PKA co-immunoprecipitates with the tyrosine kinase Src (Baker *et al.*, 2006). Recently, it has been shown that PKA is necessary for Src activation in mouse sperm as well as in bovine sperm (Etkovitz *et al.*, 2009). In turn, Src activation is required for hyperpolarization of sperm plasma membrane, which in turn is necessary for the AR (Stival *et al.*, 2015). In the same context, Src has been associated with gelsolin regulation (Finkelstein *et al.*, 2010), in a direct role on actin remodeling (see below).

Although poorly understood, the molecular mechanisms that take place during capacitation assemble all the fusion machinery needed for AR to occur. During these events, the cytoskeleton assists in tethering of the plasma membrane and the outer acrosomal membrane, endowing SNAREs to bring the two membranes close enough for the AR to take place. SNAREs are membrane-associated proteins that, in collaboration with proteins as Rab3A, α-SNAP, NSF, complexin, the calcium-binding protein synaptotagmin (Hutt *et al.*, 2005; Michaut *et al.*, 2001), and calmodulin (Yunes *et al.*, 2002), participate in the acrosomal exocytosis. An important body of literature explores the role of members of the SNARE family both in the preparation to undergo the AR and in the AR itself (see below).

15.5 Physiological Site for the Occurrence of Acrosomal Exocytosis

Over the last 30 years and largely based upon laboratory experiments using *in vitro* fertilization of mouse oocytes, denuded of their cumulus cells, one of the central dogmas of the fertilization process in mammals has been that capacitated, acrosome-intact sperm bind to the ZP to undergo acrosomal exocytosis (Saling *et al.*, 1979a). Following what is called "primary binding," the OAM and PM fuse, releasing the contents of the acrosome (Yanagimachi, 1994). After the acrosomal contents are released, a second kind of interaction called "secondary binding" of the sperm to the ZP is mediated by proteins on the inner acrosomal membrane. Penetration of the ZP would then occur following acrosomal exocytosis and the release of zona-hydrolyzing enzymes (Gaddum and Blandau, 1970). The concept has been that, following the acquisition of hyperactivated motility and the liberation of acrosomal contents, the fertilizing sperm gains the ability to penetrate the ZP and reach the perivitelline space between the ZP and the oolemma. The concept that the OAM and PM are intact when the sperm encounters the ZP arose over 25 years ago from studies in the mouse (Florman and Storey, 1982; Saling and Storey, 1979; Saling *et al.*, 1979b). However, there is evidence that guinea pig and human sperm in the process of undergoing acrosomal exocytosis may be competent to bind to the ZP (Huang *et al.*, 1981; Morales *et al.*, 1989). Furthermore, rabbit sperm isolated from the perivitelline space of fertilized eggs and, therefore, presumed to have undergone acrosomal exocytosis, are capable of fertilization in a second insemination (Valdivia *et al.*, 1999). Thus, although the current perspective is that sperm must be "acrosome-intact" to bind to the ZP, one must consider these other findings and realize that the story might be more complex in other species.

Downloaded From Vet-eBooks.com

Experimental evidence, using transgenic mouse sperm carrying green fluorescent protein (GFP) in their acrosomes, indicated that binding the ZP of unfertilized WT mouse eggs, an event to transgenic eggs expressing human ZP2 instead of the murine orthologue, was not sufficient to induce acrosomal exocytosis (Baibakov *et al.*, 2007; Nakanishi *et al.*, 1999). In this scenario, Baibakov *et al.* (2007) also challenged the prevalent model of sperm binding to a carbohydrate ligand of the ZP from an unfertilized eggs that is claimed by other laboratories, in which, following fertilization, a ZP carbohydrate ligand for sperm is removed by an egg glycosidase released upon cortical granules exocytosis, thereby precluding other sperm from binding to zona of fertilized eggs (Shur *et al.*, 2006; Wassarman, 2005). Instead, Baibakov *et al.* (2007) proposed a mechanosensory mechanism that involves (i) the binding of acrosome-intact sperm to the zona surface followed by (ii) the loss of the acrosome as the sperm penetrate the ZP.

Other lines of evidence also challenged the need for sperm to be acrosome intact when binding to the zona. As mentioned previously, rabbit sperm isolated from the perivitelline space of fertilized eggs were still capable of fertilization in a second insemination (Valdivia *et al.*, 1999). As expected, the acrosomes were lost from these sperm recovered from the perivitelline space, but still, they proved to be capable of penetrating the ZP of other unfertilized eggs (Kuzan *et al.*, 1984). In the mouse, Jin *et al.* (2011) made a remarkable observation with imaging studies of spermatozoa fertilizing cumulus-enclosed oocytes. By observing the loss of GFP from transgenic sperm acrosomes, they claimed that fertilizing mouse spermatozoa initiate acrosome exocytosis prior to contacting the ZP of cumulus-enclosed oocytes (Figure 15.3). Others have claimed that cumulus cell mass may be the site of acrosomal exocytosis, a concept later substantiated by recent studies showing that syndecan-1 is present on cumulus cells and possess the ability to induce exocytosis *in vivo* (Joshi *et al.*, 2014). Inoue *et al.* (2011) had supported these results using sperm from mice with a targeted mutation in the gene encoding IZUMO1, a protein required for sperm binding and fusion with the oolemma (Inoue *et al.*, 2005). These mutant sperm can penetrate the ZP but accumulate in the perivitelline space from where they can be recovered following *in vitro* fertilization (IVF). The retrieved sperm had all undergone acrosomal

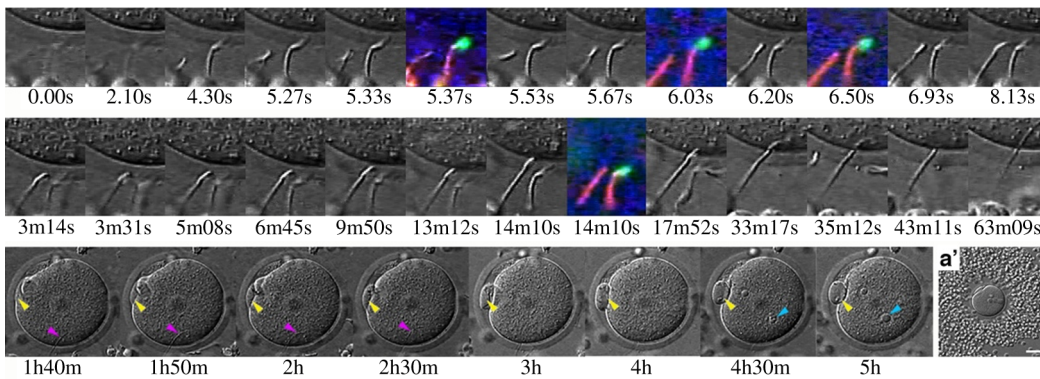

Figure 15.3 Visualization of a fertilizing spermatozoon. Photographs showing sperm penetration into the ZP and the cytoplasm of a single oocyte. Whether it was the actual fertilizing spermatozoon was determined retrospectively after video recording. Times are shown in seconds (s), minutes (min), and hours (h) after the fertilizing spermatozoon entered the field of view (0 s). Successive stages of sperm attachment to the ZP. The fertilizing spermatozoon (left sperm at 4.30 s) had no EGPF fluorescence (i.e., was acrosome reacted) before reaching the ZP surface at 6.20 s. The head of this fertilizing spermatozoon passed through the ZP and reached the egg surface at 13 min 12 s. Note that an acrosome-intact spermatozoon (at 14 min 10 s) with EGFP fluorescence remained on the ZP surface. The oocyte under low magnification, showing formation of a second polar body (yellow arrowheads), sperm tail (red arrowheads), and sperm pronucleus (blue arrowhead). (á) The cumulus-enclosed oocyte before insemination under low magnification. (Scale bar: 100 μm.) (Reproduced from Jin *et. al.* (2011).)

Downloaded From Vet-eBooks.com

exocytosis (as is evident by the loss of the acrosomal GFP marker). When used to inseminate a second set of unfertilized eggs, the recovered, acrosome-reacted perivitelline sperm were again able to bind and penetrate the ZP of these eggs. Under these circumstances, if sperm do not initiate acrosomal exocytosis upon contact with the ZP, it is unknown where and when does this event take place under physiologically normal situations. Similarly, it is uncertain whether acrosomal exocytosis occurs in response to ligand binding of a receptor or if there is another mechanism.

As sperm travel up the oviduct, they become closer to the ovary and ovulated oocytes with their associated cumulus cells, which actively secrete progesterone. This steroid hormone has gained attention for its role as both a possible physiological inducer of exocytosis and a sperm chemoattractant (Jaiswal *et al.*, 1999; Meizel *et al.*, 1997a; Teves *et al.*, 2006). Progesterone interacts and activates CatSper channels in the tail of human sperm (Lishko *et al.*, 2011; Strunker *et al.*, 2011), opening the possibility that progesterone modulates calcium levels in the sperm and, thus, may indirectly stimulate exocytosis via these channels. However, this seems not to be the case, because null mice for any of the reported CatSper channels undergo acrosomal exocytosis in a similar way as wild-type sperm do. Ren and Xia (2010) reported that mouse sperm treated with solubilized ZP proteins exhibit an influx of CatSper-dependent calcium that progresses from the distal regions of the sperm tail toward the head. In a similar manner, mouse sperm containing GFP in their acrosomes lose the fluorescent probe when the sperm are treated with solubilized ZP proteins in an anterograde manner from the posterior margin of the acrosome toward the anterior limit (Buffone *et al.*, 2009b), raising the possibility that a calcium wave originating in the sperm tail may move forward through the sperm to elicit acrosomal exocytosis. In the case of humans, another possibility is that progesterone induces acrosomal exocytosis via its interaction with progesterone receptors located in the flagellar midpiece-neck region of the sperm (Thomas *et al.*, 2009). Interestingly, progesterone has been recently shown to inhibit the K^+ channel Slo1 in human sperm, which would depolarize the sperm plasma membrane and trigger the AR (see below) (Mannowetz *et al.*, 2013). This effect is not present in mouse sperm, due to the existence of the K^+ channel Slo3 instead of Slo1. The detailed spatiotemporal relationship between calcium changes in the flagellum and progesterone and/or other agonist effects on acrosomal exocytosis is still completely unknown.

Without knowing the exact location where acrosomal exocytosis occurs during the course of normal fertilization, a role for the ZP in stimulating or inducing exocytosis may not be ruled out. During the formation of the ZP within the ovarian follicle, it is likely that ZP proteins diffuse into the extracellular matrix (ECM) of the cumulus cells surrounding the oocyte, either by not being incorporated into the ZP during assembly or by the slight degradation of ZP proteins after insertion into the zona. However, this possibility has not been demonstrated yet.

15.6 SNARES and Other Proteins from the Fusion Machinery

The SNARE superfamily is composed by Syntaxin1, SNAP-25, and synaptobrevin2. During tethering, SNAREs bring the two bilayers in proximity by their assembly in highly stable hetero-oligomeric complexes, of R or Q subunits, based on the identity of a highly conserved residue. An accepted model indicates that SNARE proteins zipper progressively from the N-terminal portion of the molecules toward the membranes. This zippering-like movement drives the required energy for bilayer mixing (Hong, 2005; Jahn and Scheller, 2006). Current evidence indicates that SANREs need an organizing platform to operate. A multi-PDZ domain protein, named MUPP1, containing 13 potential protein-binding motifs, has been identified in the

Downloaded From Vet-eBooks.com

acrosomal region of spermatozoa of different mammalian species (Heydecke *et al.*, 2006). This protein has been proposed as a molecule that controls the initial tethering and/or docking of the acrosomal vesicle at specific sites of the plasma membrane (Ackermann *et al.*, 2009). In this regard, MUPP1 has been shown to interact *in vitro* with Ca^{2+}-calmodulin kinase II (CaMKII) (Ackermann *et al.*, 2009), which acts freezing the AR machinery at a stand by point ready for exocytosis, waiting for a rise of Ca^{2+} that displaces CaMKII from MUPP1 (Ackermann *et al.*, 2009). This type of control deserves special attention in the case of regulated exocytosis, as sperm unveils, where that the cell requires stimulation to take place. This kind of secretion, in contrast to constitutive exocytosis, needs an arresting step until the right stimulus triggers the system. A second checkpoint operates at the phosphorylation status of the soluble *N*-ethylmaleimide-sensitive factor. This factor provides the metabolic energy required for unraveling of trans-SNARE complexes to promote membrane fusion. Interestingly, the dissociating activity of NSF is repressed by tyrosine phosphorylation (Zarelli *et al.*, 2009), whereas, on sperm activation, protein tyrosine phosphatase 1B (PTP1B) dephosphorylates NSF, thus derepressing its activity.

15.7 Hyperpolarization

Capacitation involves many molecular and physiological events, as the activation of a cAMP signaling cascade (Buffone *et al.*, 2014), increases of intracellular pH (Zeng *et al.*, 1996), tyrosine phosphorylation of sperm proteins (Visconti *et al.*, 1995) and of the intracellular Ca^{2+} concentration ($[Ca^{2+}]i$) (DasGupta *et al.*, 1993), and the decrease in $[Na^+]_I$ (Escoffier *et al.*, 2012) and the activation of SLO1/3 K^+ channels that together cause a hyperpolarization of the sperm plasma membrane potential (Em) (Santi *et al.*, 2010). The sequence of events is unfortunately not clear yet, and whether they are interrelated or take place independently is not fully understood. However, it has been established that hyperpolarization is necessary for the acquisition of acrosomal responsiveness, at least in mouse sperm (De La Vega-Beltran *et al.*, 2012). Moreover, sperm hyperpolarization has been recently shown also in human sperm, although its physiological relevance awaits to be demonstrated. Despite the existence of several transporters in mammalian sperm, that might also participate in the establishment of resting potential, hyperpolarization appears to be driven by Slo3 in mouse sperm (Chávez *et al.*, 2014) and possibly by Slo1 also in human sperm (Mannowetz *et al.*, 2013). Despite the importance of Em hyperpolarization, less is known about the downstream effectors of this phenomenon. Membrane hyperpolarization accentuates the Ca^{2+} driving force, promoting the uptake through Ca^{2+} permeable channels as TRPs and specially CatSper (Ren and Xia, 2010). Additionally, Em hyperpolarization would remove inactivation of voltage-dependent CaVs, provided their functional availability that awaits demonstration in mature capacitated sperm. Interestingly, mouse sperm flagellum contains a sperm-specific Na^+/H^+ exchanger (sNHE). This channel exhibits a cAMP-binding motif and a voltage sensor promoting activation upon hyperpolarization and cAMP presence, which can contribute, in addition to HCO_3^-, to an internal alkalinization of the sperm. Internal alkalinization could in turn activate CatSper channels. Noteworthy, Ca^{2+} entry through CatSper channels is deficient in Slo3 mutant sperm, which lack hyperpolarization.

15.8 Actin Cytoskeleton

The actin cytoskeleton plays an important role in controlling the process of exocytosis in many cell types, including sperm. Depending on the species, actin is located in the sperm tail as well as

Downloaded From Vet-eBooks.com

in the sperm head. For example, in hamster sperm, it was observed between the plasma membrane and outer acrosomal membrane; in the perinuclear space underlying the post-acrosomal sheath of bull and rabbit sperm; around the connecting piece in the neck region of sperm from all four species; and on the external surface of the fibrous sheath of human sperm (Flaherty *et al.*, 1988). As in other somatic cells, actin is present in its monomeric, globular form (G-actin) as well as filamentous actin (F-actin). Remarkably, during the course of capacitation, many authors demonstrated that G-actin is polymerized to F-actin (Brener *et al.*, 2003; Cabello-Agüeros *et al.*, 2003; Finkelstein *et al.*, 2010).

In somatic systems, the cortical filamentous actin network acts as a dominant negative clamp that blocks constitutive exocytosis (Muallem *et al.*, 1995). Using a two-photon excitation imaging system, Nemoto *et al.* (2004) revealed that priming of zymogen granules for fusion in pancreatic acinar cells is accompanied by the rapid coating with F-actin, which serves to slow the rate of granule fusion without reducing the overall extent of exocytosis, whereas latrunculin A, an inhibitor of actin polymerization, reduced the latency to exocytosis. When actin depolymerization is inhibited by phalloidin in a permeabilized sperm model, there is a marked reduction in the percentage of sperm that undergo acrosomal exocytosis, indicating that the dispersion of F-actin may be necessary for acrosomal exocytosis to occur (Hernández-González *et al.*, 2000). Thus, F-actin stabilizes the exocytotic machinery to restrict secretory granules from fusing with the plasma membrane. On the other hand, when capacitated sperm are stimulated to undergo acrosomal exocytosis, rapid F-actin depolymerization occurs (Spungin *et al.*, 1995). Inhibition of actin polymerization blocks ZP-induced acrosomal exocytosis and sperm penetration into zona-free eggs, thus interfering with the ability of boar and mouse sperm to become competent for *in vitro* fertilization (Brener *et al.*, 2003; Castellani-Ceresa *et al.*, 1993; Liu *et al.*, 1999; Rogers *et al.*, 1989). Activation of both PKA and PKC significantly enhances actin polymerization in bovine sperm (Brener *et al.*, 2003). A rise in intracellular calcium appears to be a key event in the depolymerization of actin, resulting in acrosomal exocytosis (Spungin *et al.*, 1995). This appears to function, in part, through the activation of the actin severing protein, gelsolin (Finkelstein *et al.*, 2010).

Members of the GTPase Rho family such as Rho, Rac, and CDC42 have important roles in calcium-regulated exocytosis and actin dynamics (Sadok and Marshall, 2014). Although their participation in sperm capacitation and acrosome reaction are not well understood, they may participate in these processes through actin polymerization. For example, the association between CDC42 and caveolin-1 is involved in the regulation of capacitation and acrosome reaction of guinea pig and mouse sperm (Baltiérrez-Hoyos *et al.*, 2012).

15.9 Calcium

The cation calcium is necessary for acrosomal exocytosis to occur as is the general case in other exocytic systems. The rise in intracellular calcium that triggers the acrosomal exocytosis is postulated to come from both extracellular and intracellular sources (Florman and Ducibella, 2006). On one hand, a theory postulates that the acrosome is a calcium store and that depletion of Ca^{2+} from the acrosome activates store-operated channels that allow sustained entry of Ca^{2+} from the medium (Herrick *et al.*, 2005). On the other hand, others have demonstrated that the Ca^{2+} rise induced by exposure to ZP or progesterone started at different sites within the sperm head, indicating that these agonists may stimulate acrosomal exocytosis via different mechanisms (Fukami *et al.*, 2003; Meizel *et al.*, 1997b). Another report identified the redundant nuclear envelope at the posterior end of the sperm head as a calcium store (Ho *et al.*, 2009),

Downloaded From Vet-eBooks.com

however, its participation in the process of exocytosis is not clear. Along these lines, Xia and Ren (2009) have recently captured intriguing video images with Fluo-4, which indicate that the ZP-induced Ca^{2+} increase starts in the sperm tail and propagates toward the head (anterograde direction). Using calcium-imaging studies, the anterograde wave of calcium in response to soluble ZP suggests that a calcium store near the head–tail junction may be associated with ZP-stimulated acrosomal exocytosis (Costello *et al.*, 2009; Ho *et al.*, 2009). The direction of a Ca^{2+} wave progressing from the base of the head toward the apical tip is reminiscent of our studies demonstrating the anterograde loss of acrosomal GFP from transgenic mouse sperm exposed to soluble zona proteins (Buffone *et al.*, 2009b). Determining the acrosome reaction and its associated intracellular calcium change continuously in time is fundamental to fully understand this fundamental process, as many questions remain regarding the kinetic and location correlations between these two physiological parameters (Darszon *et al.*, 2011).

Triggering of the sperm acrosomal exocytosis involves complex signaling pathways that regulate G-protein activation, cAMP, and changes in intracellular pH. Identification of ion channels involved in this process has been long studied by several groups using different experimental approaches (Darszon *et al.*, 2011). It is also well accepted that the rise in intracellular calcium, which is important for exocytosis, occurs in two steps: an initial transient calcium rise, which is then followed by a sustained calcium rise. Regarding the initial transient calcium rise, the nature of the channels involved in the increase in calcium is not clear, although it may involve a combination of CaVs, SOCs, and intracellular channels in a complex network of signaling cascades (Guzmán-Grenfell and González-Martínez, 2004; Linares-Hernández *et al.*, 1998; Publicover *et al.*, 2007; Thomas *et al.*, 2009; Torres-Flores *et al.*, 2008).

The initial and transient Ca^{2+} elevation triggered by solubilized ZP or progesterone is followed by a slow and prolonged Ca^{2+} elevation that can last several minutes depending on the specie involved. It is currently accepted that the initial and transient Ca^{2+} rise activates a Ca^{2+}-sensitive PLC-δ (Fukami *et al.*, 2003) that hydrolyzes PIP2 to produce DAG and IP3 (Walensky and Snyder, 1995), which is supported by the observation that PLC- δ4 null mice are infertile and unable to undergo acrosomal exocytosis (Fukami *et al.*, 2003). In addition, it was demonstrated that ZP induces IP_3 increases in mouse spermatozoa (Tomes *et al.*, 2004) and its binding to its specific receptor results in depletion of calcium stores located in the acrosome and the redundant nuclear envelope (De Blas *et al.*, 2002; Herrick *et al.*, 2005; Ho and Suarez, 2003). The release of calcium for the intracellular stores would in turn induce the opening of Ca^{2+} channels at the plasma membrane (SOC activity).

References

Ackermann, F., Zitranski, N., Borth, H., Buech, T., Gudermann, T., and Boekhoff, I. (2009) CaMKIIalpha interacts with multi-PDZ domain protein MUPP1 in spermatozoa and prevents spontaneous acrosomal exocytosis. *J. Cell Sci.*, **122**, 4547–4557.

Anakwe, O.O. and Gerton, G.L. (1990) Acrosome biogenesis begins during meiosis: evidence from the synthesis and distribution of an acrosomal glycoprotein, acrogranin, during guinea pig spermatogenesis. *Biol. Reprod.*, **42**, 317–328.

Arcelay, E., Salicioni, A.M., Wertheimer, E., and Visconti, P.E. (2008) Identification of proteins undergoing tyrosine phosphorylation during mouse sperm capacitation. *Int. J. Dev. Biol.*, **52**, 463–472.

Austin, C.R. (1951) Observations on the penetration of the sperm in the mammalian egg. *Aust. J. Sci. Res. B Biol. Sci.*, **4**, 581–596.

Downloaded From Vet-eBooks.com

Baba, T., Azuma, S., Kashiwabara, S., and Toyoda, Y. (1994) Sperm from mice carrying a targeted mutation of the acrosin gene can penetrate the oocyte zona pellucida and effect fertilization. *J. Biol. Chem.*, **269**, 31845–31849.

Baibakov, B., Gauthier, L., Talbot, P., Rankin, T.L., and Dean, J. (2007) Sperm binding to the zona pellucida is not sufficient to induce acrosome exocytosis. *Development*, **134**, 933–943.

Baker, M.A., Hetherington, L., and Aitken, R.J. (2006) Identification of SRC as a key PKA-stimulated tyrosine kinase involved in the capacitation-associated hyperactivation of murine spermatozoa. *J. Cell Sci.*, **119**, 3182–3192.

Baldi, E., Luconi, M., Bonaccorsi, L., Muratori, M., and Forti, G. (2000) Intracellular events and signaling pathways involved in sperm acquisition of fertilizing capacity and acrosome reaction. *Front. Biosci.*, **5**, E110–E123.

Baltiérrez-Hoyos, R., Roa-Espitia, A.L., and Hernández-González, E.O. (2012) The association between CDC42 and caveolin-1 is involved in the regulation of capacitation and acrosome reaction of guinea pig and mouse sperm. *Reproduction*, **144**, 123–134.

Brener, E., Rubinstein, S., Cohen, G., Shternall, K., Rivlin, J., and Breitbart, H. (2003) Remodeling of the actin cytoskeleton during mammalian sperm capacitation and acrosome reaction. *Biol. Reprod.*, **68**, 837–845.

Buffone, M.G., Foster, J.A., and Gerton, G.L. (2008) The role of the acrosomal matrix in fertilization. *Int. J. Dev. Biol.*, **52**, 511–522.

Buffone, M.G., Kim, K.-S., Doak, B.J., Rodriguez-Miranda, E., and Gerton, G.L. (2009a). Functional consequences of cleavage, dissociation and exocytotic release of ZP3R, a C4BP-related protein, from the mouse sperm acrosomal matrix. *J. Cell Sci.*, **122**, 3153–3160.

Buffone, M.G., Rodriguez-Miranda, E., Storey, B.T., and Gerton, G.L. (2009b). Acrosomal exocytosis of mouse sperm progresses in a consistent direction in response to zona pellucida. *J. Cell. Physiol.*, **220**, 611–620.

Buffone, M.G., Wertheimer, E.V., Visconti, P.E., and Krapf, D. (2014) Central role of soluble adenylyl cyclase and cAMP in sperm physiology. *Biochim. Biophys. Acta.* **1842** (12 Part B), 2610-L 2620.

Cabello-Agüeros, J.F., Hernández-González, E.O., and Mújica, A. (2003) The role of F-actin cytoskeleton-associated gelsolin in the guinea pig capacitation and acrosome reaction. *Cell Motil. Cytoskeleton*, **56**, 94–108.

Castellani-Ceresa, L., Mattioli, M., Radaelli, G., Barboni, B., and Brivio, M.F. (1993) Actin polymerization in boar spermatozoa: fertilization is reduced with use of cytochalasin D. *Mol. Reprod. Dev.*, **36**, 203–211.

Chang, M.C. (1951) Fertilizing capacity of spermatozoa deposited into the fallopian tubes. *Nature*, **168**, 697–698.

Chávez, J.C., Ferreira, J.J., Butler, A., De La Vega Beltrán, J.L., Treviño, C.L., Darszon, A., Salkoff, L., and Santi, C.M. (2014) SLO3 K+ channels control calcium entry through CatSper channels in sperm. *J. Biol. Chem.*, **289**, 32266–32275.

Costello, S., Michelangeli, F., Nash, K., Lefievre, L., Morris, J., Machado-Oliveira, G., Barratt, C., Kirkman-Brown, J., and Publicover, S. (2009) Ca2+-stores in sperm: their identities and functions. *Reproduction*, **138**, 425–437.

Dam, A.H., Feenstra, I., Westphal, J.R., Ramos, L., van Golde, R.J, and Kremer, J.A. (2007) Globozoospermia revisited. *Hum. Reprod. Update*, **13**, 63–75.

Darszon, A., Nishigaki, T., Beltran, C., and Treviño, C.L. (2011) Calcium channels in the development, maturation, and function of spermatozoa. *Physiol. Rev.*, **91**, 1305–1355.

DasGupta, S., Mills, C.L., and Fraser, L.R. (1993) Ca(2+)-related changes in the capacitation state of human spermatozoa assessed by a chlortetracycline fluorescence assay. *J. Reprod. Fertil.*, **99**, 135–143.

Downloaded From Vet-eBooks.com

De Blas, G., Michaut, M., Treviño, C.L., Tomes, C.N., Yunes, R., Darszon, A., and Mayorga, L.S. (2002) The intraacrosomal calcium pool plays a direct role in acrosomal exocytosis. *J. Biol. Chem.*, **277**, 49326–49331.

De La Vega-Beltran, J.L., Sánchez-Cárdenas, C., Krapf, D., Hernandez-González, E.O., Wertheimer, E., Treviño, C.L., Visconti, P.E., and Darszon, A. (2012) Mouse sperm membrane potential hyperpolarization is necessary and sufficient to prepare sperm for the acrosome reaction. *J. Biol. Chem.*, **287**, 44384–44393.

DiCarlantonio, G. and Talbot, P. (1988) Evidence for sequential deployment of secretory enzymes during the normal acrosome reaction of guinea pig sperm *in vitro*. *Gamete Res.*, **21**, 425–438.

Eddy, E.M. (2006) The Spermatozoon, in *Knobil and Neill's Physiology of Reproduction* (ed E. Knobil), Elsevier, Amsterdam, pp. 3–54.

Escalier, D., Gallo, J.M., Albert, M., Meduri, G., Bermudez, D., David, G., and Schrevel, J. (1991) Human acrosome biogenesis: immunodetection of proacrosin in primary spermatocytes and of its partitioning pattern during meiosis. *Development*, **113**, 779–788.

Escoffier, J., Krapf, D., Navarrete, F., Darszon, A., and Visconti, P.E. (2012) Flow cytometry analysis reveals a decrease in intracellular sodium during sperm capacitation. *J. Cell Sci.*, **125**, 473–485.

Etkovitz, N., Tirosh, Y., Chazan, R., Jaldety, Y., Daniel, L., Rubinstein, S., and Breitbart, H. (2009) Bovine sperm acrosome reaction induced by G-protein-coupled receptor agonists is mediated by epidermal growth factor receptor transactivation. *Dev. Biol.*, **334**, 447–457.

Fawcett, D.W. and Hollenberg, R.D. (1963) Changes in the acrosome of the guinea pig spermatozoa during passage through the epididymis. *Z. Zellforsch. Mikrosk. Anat.*, **60**, 276–292.

Finkelstein, M., Etkovitz, N., and Breitbart, H. (2010) Role and regulation of sperm gelsolin prior to fertilization. *J. Biol. Chem.*, **285**, 39702–39709.

Flaherty, S.P., Winfrey, V.P., and Olson, G.E. (1988) Localization of actin in human, bull, rabbit, and hamster sperm by immunoelectron microscopy. *Anat. Rec.*, **221**, 599–610.

Florman, H.M. and Ducibella, T. (2006) Fertilization in mammals, in *Knobil and Neill's Physiology of Reproduction* (eds T.M. Plant and A.J. Zeleznik), Academic Press, pp. 55–112.

Florman, H.M. and Storey, B.T. (1982) Mouse gamete interactions: the zona pellucida is the site of the acrosome reaction leading to fertilization *in vitro*. *Dev. Biol.*, **91**, 121–130.

Foster, J.A., Friday, B.B., Maulit, M.T., Blobel, C., Winfrey, V.P., Olson, G.E., Kim, K.S., and Gerton, G.L. (1997) AM67, a secretory component of the guinea pig sperm acrosomal matrix, is related to mouse sperm protein sp56 and the complement component 4-binding proteins. *J. Biol. Chem.*, **272**, 12714–12722.

Fukami, K., Yoshida, M., Inoue, T., Kurokawa, M., Fissore, R.A., Yoshida, N., Mikoshiba, K., and Takenawa, T. (2003) Phospholipase Cdelta4 is required for Ca2+ mobilization essential for acrosome reaction in sperm. *J. Cell Biol.*, **161**, 79–88.

Gaddum, P. and Blandau, R.J. (1970) Proteolytic reaction of mammalian spermatozoa on gelatin membranes. *Science*, **170**, 749–751.

Green, D.P. (1978) The activation of proteolysis in the acrosome reaction of guinea-pig sperm. *J. Cell Sci.*, **32**, 153–164.

Green, D.P. and Hockaday, A.R. (1978) The histochemical localization of acrosin in guinea-pig sperm after the acrosome reaction. *J. Cell Sci.*, **32**, 177–184.

Guyonnet, B., Zabet-Moghaddam, M., SanFrancisco, S., and Cornwall, G.A. (2012) Isolation and proteomic characterization of the mouse sperm acrosomal matrix. *Mol. Cell. Proteomics*, **11**, 758–774.

Guzmán-Grenfell, A.M. and González-Martínez, M.T. (2004) Lack of voltage-dependent calcium channel opening during the calcium influx induced by progesterone in human sperm: effect of calcium channel deactivation and inactivation. *J. Androl.*, **25**, 117–122.

Downloaded From Vet-eBooks.com

Hardy, D.M., Oda, M.N., Friend, D.S., and Huang, T.T. (1991) A mechanism for differential release of acrosomal enzymes during the acrosome reaction. *Biochem. J.*, **275** (Part 3), 759–766.

Hernández-González, E.O., Lecona-Valera, A.N., Escobar-Herrera, J., and Mújica, A. (2000) Involvement of an F-actin skeleton on the acrosome reaction in guinea pig spermatozoa. *Cell Motil. Cytoskeleton*, **46**, 43–58.

Hernández-González, E.O., Sosnik, J., Edwards, J., Acevedo, J.J., Mendoza-Lujambio, I., López-González, I., Demarco, I., Wertheimer, E., Darszon, A., and Visconti, P.E. (2006) Sodium and epithelial sodium channels participate in the regulation of the capacitation-associated hyperpolarization in mouse sperm. *J. Biol. Chem.*, **281**, 5623–5633.

Herrick, S.B., Schweissinger, D.L., Kim, S.-W., Bayan, K.R., Mann, S., and Cardullo, R.A. (2005) The acrosomal vesicle of mouse sperm is a calcium store. *J. Cell. Physiol.*, **202**, 663–671.

Heydecke, D., Meyer, D., Ackermann, F., Wilhelm, B., Gudermann, T., and Boekhoff, I. (2006) The multi PDZ domain protein MUPP1 as a putative scaffolding protein for organizing signaling complexes in the acrosome of mammalian spermatozoa. *J. Androl.*, **27**, 390–404.

Ho, H.-C. and Suarez, S.S. (2003) Characterization of the intracellular calcium store at the base of the sperm flagellum that regulates hyperactivated motility. *Biol. Reprod.*, **68**, 1590–1596.

Ho, K., Wolff, C.A., and Suarez, S.S. (2009) CatSper-null mutant spermatozoa are unable to ascend beyond the oviductal reservoir. *Reprod. Fertil. Dev.*, **21**, 345–350.

Hong, W. (2005) SNAREs and traffic. *Biochim. Biophys. Acta*, **1744**, 493–517.

Huang, T.T., Fleming, A.D., and Yanagimachi, R. (1981) Only acrosome-reacted spermatozoa can bind to and penetrate zona pellucida: a study using the guinea pig. *J. Exp. Zool.*, **217**, 287–290.

Huang, T.T., Hardy, D., Yanagimachi, H., Teuscher, C., Tung, K., Wild, G., and Yanagimachi, R. (1985) pH and protease control of acrosomal content stasis and release during the guinea pig sperm acrosome reaction. *Biol. Reprod.*, **32**, 451–462.

Hutt, D.M., Baltz, J.M., and Ngsee, J.K. (2005) Synaptotagmin VI and VIII and syntaxin 2 are essential for the mouse sperm acrosome reaction. *J. Biol. Chem.*, **280**, 20197–20203.

Inoue, N., Ikawa, M., Isotani, A., and Okabe, M. (2005) The immunoglobulin superfamily protein Izumo is required for sperm to fuse with eggs. *Nature*, **434**, 234–238.

Inoue, N., Satouh, Y., Ikawa, M., Okabe, M., and Yanagimachi, R. (2011) Acrosome-reacted mouse spermatozoa recovered from the perivitelline space can fertilize other eggs. *Proc. Natl. Acad. Sci. USA*, **108**, 20008–20011.

Jahn, R. and Scheller, R.H. (2006) SNAREs: engines for membrane fusion. *Nat. Rev. Mol. Cell Biol.*, **7**, 631–643.

Jaiswal, B.S., Tur-Kaspa, I., Dor, J., Mashiach, S., and Eisenbach, M. (1999) Human sperm chemotaxis: is progesterone a chemoattractant? *Biol. Reprod.*, **60**, 1314–1319.

Jin, M., Fujiwara, E., Kakiuchi, Y., Okabe, M., Satouh, Y., Baba, S.A., Chiba, K., and Hirohashi, N. (2011) Most fertilizing mouse spermatozoa begin their acrosome reaction before contact with the zona pellucida during *in vitro* fertilization. *Proc. Natl. Acad. Sci. USA*, **108**, 4892–4896.

Joshi, C.S., Khan, S.A., and Khole, V.V. (2014) Regulation of acrosome reaction by Liprin α3, LAR and its ligands in mouse spermatozoa. *Andrology*, **2**, 165–174.

Kang-Decker, N., Mantchev, G.T., Juneja, S.C., McNiven, M.A., and van Deursen, J.M.A. (2001) Lack of acrosome formation in Hrb-deficient mice. *Science*, **294**, 1531–1533.

Kashiwabara, S., Arai, Y., Kodaira, K., and Baba, T. (1990) Acrosin biosynthesis in meiotic and postmeiotic spermatogenic cells. *Biochem. Biophys. Res. Commun.*, **173**, 240–245.

Kim, K.-S. and Gerton, G.L. (2003) Differential release of soluble and matrix components: evidence for intermediate states of secretion during spontaneous acrosomal exocytosis in mouse sperm. *Dev. Biol.*, **264**, 141–152.

Kim, K.S., Cha, M.C., and Gerton, G.L. (2001) Mouse sperm protein sp56 is a component of the acrosomal matrix. *Biol. Reprod.*, **64**, 36–43.

Downloaded From Vet-eBooks.com

Kim, K.-S., Foster, J.A., Kvasnicka, K.W., and Gerton, G.L. (2011) Transitional states of acrosomal exocytosis and proteolytic processing of the acrosomal matrix in guinea pig sperm. *Mol. Reprod. Dev.*, **78**, 930–941.

Kuzan, F.B., Fleming, A.D., and Seidel, G.E., Jr. (1984) Successful fertilization *in vitro* of fresh intact oocytes by perivitelline (acrosome-reacted) spermatozoa of the rabbit. *Fertil. Steril.*, **41**, 766–770.

Lin, Y.-N., Roy, A., Yan, W., Burns, K.H., and Matzuk, M.M. (2007) Loss of zona pellucida binding proteins in the acrosomal matrix disrupts acrosome biogenesis and sperm morphogenesis. *Mol. Cell. Biol.*, **27**, 6794–6805.

Linares-Hernández, L., Guzmán-Grenfell, A.M., Hicks-Gomez, J.J., and González-Martínez, M.T. (1998) Voltage-dependent calcium influx in human sperm assessed by simultaneous optical detection of intracellular calcium and membrane potential. *Biochim. Biophys. Acta*, **1372**, 1–12.

Lishko, P.V., Botchkina, I.L., and Kirichok, Y. (2011) Progesterone activates the principal Ca2+ channel of human sperm. *Nature*, **471**, 387–391.

Liu, D.Y., Martic, M., Clarke, G.N., Dunlop, M.E., and Baker, H.W. (1999) An important role of actin polymerization in the human zona pellucida-induced acrosome reaction. *Mol. Hum. Reprod.*, **5**, 941–949.

Mannowetz, N., Naidoo, N.M., Choo, S.-A.S., Smith, J.F., and Lishko, P.V. (2013) Slo1 is the principal potassium channel of human spermatozoa. *eLife*, **2**, e01009.

Mayorga, L.S., Tomes, C.N., and Belmonte, S.A. (2007) Acrosomal exocytosis, a special type of regulated secretion. *IUBMB Life*, **59**, 286–292.

Meizel, S., Turner, K.O., and Nuccitelli, R. (1997a). Progesterone triggers a wave of increased free calcium during the human sperm acrosome reaction. *Dev. Biol.*, **182**, 67–75.

Meizel, S., Turner, K.O., and Nuccitelli, R. (1997b). Progesterone triggers a wave of increased free calcium during the human sperm acrosome reaction. *Dev. Biol.*, **182**, 67–75.

Michaut, M., De Blas, G., Tomes, C.N., Yunes, R., Fukuda, M., and Mayorga, L.S. (2001) Synaptotagmin VI participates in the acrosome reaction of human spermatozoa. *Dev. Biol.*, **235**, 521–529.

Moore, H.D. and Bedford, J.M. (1978) Ultrastructure of the equatorial segment of hamster spermatozoa during penetration of oocytes. *J. Ultrastruct. Res.*, **62**, 110–117.

Moos, J., Peknicova, J., and Tesarik, J. (1993) Relationship between molecular conversions of acrosin and the progression of exocytosis in the calcium ionophore-induced acrosome reaction. *Biochim. Biophys. Acta*, **1176**, 199–207.

Morales, P., Cross, N.L., Overstreet, J.W., and Hanson, F.W. (1989) Acrosome intact and acrosome-reacted human sperm can initiate binding to the zona pellucida. *Dev. Biol.*, **133**, 385–392.

Muallem, S., Kwiatkowska, K., Xu, X., and Yin, H.L. (1995) Actin filament disassembly is a sufficient final trigger for exocytosis in nonexcitable cells. *J. Cell Biol.*, **128**, 589–598.

Nakanishi, T., Ikawa, M., Yamada, S., Parvinen, M., Baba, T., Nishimune, Y., and Okabe, M. (1999) Real-time observation of acrosomal dispersal from mouse sperm using GFP as a marker protein. *FEBS Lett.*, **449**, 277–283.

Nemoto, T., Kojima, T., Oshima, A., Bito, H., and Kasai, H. (2004) Stabilization of exocytosis by dynamic F-actin coating of zymogen granules in pancreatic acini. *J. Biol. Chem.*, **279**, 37544–37550.

Noland, T.D., Davis, L.S., and Olson, G.E. (1989) Regulation of proacrosin conversion in isolated guinea pig sperm acrosomal apical segments. *J. Biol. Chem.*, **264**, 13586–13590.

Noland, T.D., Friday, B.B., Maulit, M.T., and Gerton, G.L. (1994) The sperm acrosomal matrix contains a novel member of the pentaxin family of calcium-dependent binding proteins. *J. Biol. Chem.*, **269**, 32607–32614.

Downloaded From Vet-eBooks.com

Nuzzo, N.A., Anderson, R.A., and Zaneveld, L.J. (1990) Proacrosin activation and acrosin release during the guinea pig acrosome reaction. *Mol. Reprod. Dev.*, **25**, 52–60.

Olson, G.E. and Winfrey, V.P. (1994a) Structure of acrosomal matrix domains of rabbit sperm. *J. Struct. Biol.*, **112**, 41–48.

Olson, G.E. and Winfrey, V.P. (1994b) Structure of acrosomal matrix domains of rabbit sperm. *J. Struct. Biol.*, **112**, 41–48.

Olson, G.E., Winfrey, V.P., and Flaherty, S.P. (1987) Cytoskeletal assemblies of mammalian spermatozoa. *Ann. N.Y. Acad. Sci.*, **513**, 222–246.

Olson, G.E., Winfrey, V.P., and Davenport, G.R. (1988) Characterization of matrix domains of the hamster acrosome. *Biol. Reprod.*, **39**, 1145–1158.

Oura, C. and Toshimori, K. (1990) Ultrastructural studies on the fertilization of mammalian gametes. *Int. Rev. Cytol.*, **122**, 105–151.

Publicover, S., Harper, C.V., and Barratt, C. (2007) [Ca2+]i signalling in sperm: making the most of what you've got. *Nat. Cell Biol.*, **9**, 235–242.

Ren, D. and Xia, J. (2010) Calcium signaling through CatSper channels in mammalian fertilization. *Physiology (Bethesda)*, **25**, 165–175.

Rogers, B.J., Bastias, C., Coulson, R.L., and Russell, L.D. (1989) Cytochalasin D inhibits penetration of hamster eggs by guinea pig and human spermatozoa. *J. Androl.*, **10**, 275–282.

Sadok, A. and Marshall, C.J. (2014) Rho GTPases: masters of cell migration. *Small GTPases*, **5**, e29710.

Saling, P.M. and Storey, B.T. (1979) Mouse gamete interactions during fertilization *in vitro*. Chlortetracycline as a fluorescent probe for the mouse sperm acrosome reaction. *J. Cell Biol.*, **83**, 544–555.

Saling, P.M., Sowinski, J., and Storey, B.T. (1979a) An ultrastructural study of epididymal mouse spermatozoa binding to zonae pellucidae *in vitro*: sequential relationship to the acrosome reaction. *J. Exp. Zool.*, **209**, 229–238.

Saling, P.M., Sowinski, J., and Storey, B.T. (1979b) An ultrastructural study of epididymal mouse spermatozoa binding to zonae pellucidae *in vitro*: sequential relationship to the acrosome reaction. *J. Exp. Zool.*, **209**, 229–238.

Santi, C.M., Martínez-López, P., de la Vega-Beltrán, J.L., Butler, A., Alisio, A., Darszon, A., and Salkoff, L. (2010) The SLO3 sperm-specific potassium channel plays a vital role in male fertility. *FEBS Lett.*, **584**, 1041–1046.

Satouh, Y., Inoue, N., Ikawa, M., and Okabe, M. (2012) Visualization of the moment of mouse sperm–egg fusion and dynamic localization of IZUMO1. *J. Cell Sci.*, **125**, 4985–4990.

Shur, B.D., Rodeheffer, C., Ensslin, M.A., Lyng, R., and Raymond, A. (2006) Identification of novel gamete receptors that mediate sperm adhesion to the egg coat. *Mol. Cell. Endocrinol.*, **250**, 137–148.

Sosnik, J., Miranda, P.V., Spiridonov, N.A., Yoon, S.-Y., Fissore, R.A., Johnson, G.R., and Visconti, P.E. (2009) Tssk6 is required for Izumo relocalization and gamete fusion in the mouse. *J. Cell Sci.*, **122**, 2741–2749.

Sosnik, J., Buffone, M., and Visconti, P.E. (2010) Analysis of CAPZA3 localization reveals temporally discrete events during the acrosome reaction. *J. Cell. Physiol.*, **224** (3), 575–580.

Sotomayor, R.E. and Handel, M.A. (1986) Failure of acrosome assembly in a male sterile mouse mutant. *Biol. Reprod.*, **34**, 171–182.

Spungin, B., Margalit, I., and Breitbart, H. (1995) Sperm exocytosis reconstructed in a cell-free system: evidence for the involvement of phospholipase C and actin filaments in membrane fusion. *J. Cell Sci.*, **108** (Part 6), 2525–2535.

Downloaded From Vet-eBooks.com

Stival, C., La Spina, F.A., Baró Graf, C., Arcelay, E., Arranz, S.E., Ferreira, J.J., Le Grand, S., Dzikunu, V.A., Santi, C.M., Visconti, P.E., Buffone, M.G., and Krapf, D. (2015) Src kinase is the connecting player between protein kinase A (PKA) activation and hyperpolarization through SLO3 potassium channel regulation in mouse sperm. *J. Biol. Chem.*, **290**(30), 18855–18864.

Stock, C.E. and Fraser, L.R. (1987) The acrosome reaction in human sperm from men of proven fertility. *Hum. Reprod.*, **2**, 109–119.

Strunker, T., Goodwin, N., Brenker, C., Kashikar, N.D., Weyand, I., Seifert, R., and Kaupp, U.B. (2011) The CatSper channel mediates progesterone-induced Ca2+ influx in human sperm. *Nature*, **471**, 382–386.

Talbot, P. and Dicarlantonio, G. (1985) Cytochemical localization of dipeptidyl peptidase II (DPP-II) in mature guinea pig sperm. *J. Histochem. Cytochem.*, **33**, 1169–1172.

Talbot, P. and Franklin, L.E. (1974) The release of hyaluronidase from guinea-pig spermatozoa during the course of the normal acrosome reaction *in vitro*. *J. Reprod. Fertil.*, **39**, 429–432.

Tanii, I., Araki, S., and Toshimori, K. (1994) Intra-acrosomal organization of a 90-kilodalton antigen during spermiogenesis in the rat. *Cell Tissue Res.*, **277**, 61–67.

Teves, M.E., Barbano, F., Guidobaldi, H.A., Sanchez, R., Miska, W., and Giojalas, L.C. (2006) Progesterone at the picomolar range is a chemoattractant for mammalian spermatozoa. *Fertil. Steril.*, **86**, 745–749.

Thomas, P., Tubbs, C., and Garry, V.F. (2009) Progestin functions in vertebrate gametes mediated by membrane progestin receptors (mPRs): identification of mPRalpha on human sperm and its association with sperm motility. *Steroids*, **74**, 614–621.

Tomes, C.N., Roggero, C.M., De Blas, G., Saling, P.M., and Mayorga, L.S. (2004) Requirement of protein tyrosine kinase and phosphatase activities for human sperm exocytosis. *Dev. Biol.*, **265**, 399–415.

Torres-Flores, V., Hernández-Rueda, Y.L., Neri-Vidaurri, P. del C., Jiménez-Trejo, F., Calderón-Salinas, V., Molina-Guarneros, J.A., and González-Martínez, M.T. (2008) Activation of protein kinase A stimulates the progesterone-induced calcium influx in human sperm exposed to the phosphodiesterase inhibitor papaverine. *J. Androl.*, **29**, 549–557.

Valdivia, M., Sillerico, T., De Ioannes, A., and Barros, C. (1999) Proteolytic activity of rabbit perivitelline spermatozoa. *Zygote*, **7**, 143–149.

Visconti, P.E. (2009) Understanding the molecular basis of sperm capacitation through kinase design. *Proc. Natl. Acad. Sci. USA*, **106**, 667–668.

Visconti, P.E., Bailey, J.L., Moore, G.D., Pan, D., Olds-Clarke, P., and Kopf, G.S. (1995) Capacitation of mouse spermatozoa: I. Correlation between the capacitation state and protein tyrosine phosphorylation. *Development*, **121**, 1129–1137.

Walensky, L.D. and Snyder, S.H. (1995) Inositol 1,4,5-trisphosphate receptors selectively localized to the acrosomes of mammalian sperm. *J. Cell Biol.*, **130**, 857–869.

Wassarman, P.M. (1987) The biology and chemistry of fertilization. *Science*, **235**, 553–560.

Wassarman, P.M. (2005) Contribution of mouse egg zona pellucida glycoproteins to gamete recognition during fertilization. *J. Cell. Physiol.*, **204**, 388–391.

Westbrook-Case, V.A., Winfrey, V.P., and Olson, G.E. (1994a) A domain-specific 50-kilodalton structural protein of the acrosomal matrix is processed and released during the acrosome reaction in the guinea pig. *Biol. Reprod.*, **51**, 1–13.

Westbrook-Case, V.A., Winfrey, V.P., and Olson, G.E. (1994b) A domain-specific 50-kilodalton structural protein of the acrosomal matrix is processed and released during the acrosome reaction in the guinea pig. *Biol. Reprod.*, **51**, 1–13.

Downloaded From Vet-eBooks.com

Westbrook-Case, V.A., Winfrey, V.P., and Olson, G.E. (1995) Sorting of the domain-specific acrosomal matrix protein AM50 during spermiogenesis in the guinea pig. *Dev. Biol.*, **167**, 338–349.

Xia, J. and Ren, D (2009) The BSA-induced Ca^{2+} influx during sperm capacitation is CatSper channel-dependent. *Reprod. Biol. Endocrinol.*, **7**, 119.

Yanagimachi, R. (1994) Fertility of mammalian spermatozoa: its development and relativity. *Zygote*, **2**, 371–372.

Yudin, A.I., Gottlieb, W., and Meizel, S. (1988) Ultrastructural studies of the early events of the human sperm acrosome reaction as initiated by human follicular fluid. *Gamete Res.*, **20**, 11–24.

Yunes, R., Tomes, C., Michaut, M., De Blas, G., Rodriguez, F., Regazzi, R., and Mayorga, L.S. (2002) Rab3A and calmodulin regulate acrosomal exocytosis by mechanisms that do not require a direct interaction. *FEBS Lett.*, **525**, 126–130.

Zarelli, V.E.P., Ruete, M.C., Roggero, C.M., Mayorga, L.S., and Tomes, C.N. (2009) PTP1B dephosphorylates *N*-ethylmaleimide-sensitive factor and elicits SNARE complex disassembly during human sperm exocytosis. *J. Biol. Chem.*, **284**, 10491–10503.

Zeng, Y., Oberdorf, J.A., and Florman, H.M. (1996) pH regulation in mouse sperm: identification of Na(+)-, Cl(−)-, and HCO_3(−)-dependent and arylaminobenzoate-dependent regulatory mechanisms and characterization of their roles in sperm capacitation. *Dev. Biol.*, **173**, 510–520.

Downloaded From Vet-eBooks.com

16

Sperm Chromatin Dynamics Associated with Male Fertility in Mammals

Naseer A. Kutchy,[1] Sule Dogan,[2] Abdullah Kaya,[3] Arlindo Moura,[4] and Erdogan Memili[1]

[1]*Department of Animal and Dairy Sciences, Mississippi State University, MS, USA*
[2]*IVF Michigan P.C., MI, USA*
[3]*Department of Animal Reproduction and Artificial Insemination, Selcuk University, Konya, Turkey*
[4]*Department of Animal Sciences, Federal University of Ceara, Fortaleza, Brazil*

16.1 Introduction

Spermatogenesis is a sequential, developmental process with continuous cell proliferation and differentiation of primordial germ cells into functional spermatozoa within the testis (Govindaraju *et al.*, 2012). Primordial germ cells differentiate to spermatogonia via mitosis to form primary spermatocytes that undergo meiosis to produce haploid secondary spermatocytes, which then terminally differentiate into spermatozoa (Oliva, 2006). During spermatogenesis, the chromatin of sperm is tightly packed mostly with protamines (85–98%), forming DNA toroids. During the beginning of this concise compaction process called chromatin packaging, sperm histones with globular structure are first replaced by transition proteins and then by protamines, arginine-rich oligopeptides (Lewis *et al.*, 2003) having α-helical structure with β-rings (Vilfan *et al.*, 2004), or β-pleated structure (Biegeleisen, 2006). At this transition that occurs during spermatogenesis, DNA is packed 10 times more tightly than in somatic cells and it results in the arrest of DNA replication or RNA transcription in sperm (Shaman *et al.*, 2007; Miller *et al.*, 2010). However, the transition is not complete as some histones are still retained in mouse (4%) and human sperm (15–30%). The histone-bound DNA loci can encode transcription factors and indeed play important roles during postfertilization events and early embryonic development (Hammoud *et al.*, 2009). Errors in histone to protamine replacement and abnormal protamine ratios have been associated with sperm abnormalities, causing male infertility (Balhorn *et al.*, 1988; de Yebra *et al.*, 1993). Instead of two protamines (PRM1 and PRM2) as in human and mouse sperms (Balhorn, 1989), presence of only PRM1 in bull sperm raises an interesting question about the mechanism(s) regulating sperm chromatin structure.

Fertilization is a well-regulated process that occurs by the union of two gametes containing only one half of the diploid complement in order to ensure restoration of diploidy and subsequent embryonic development (Palermo *et al.*, 1997). During spermatogenesis, spermatozoa that are present in syncytium share mRNA and proteins through cytoplasmic

Animal Models and Human Reproduction, First Edition. Edited by Heide Schatten and Gheorghe M. Constantinescu.
© 2017 John Wiley & Sons, Inc. Published 2017 by John Wiley & Sons, Inc.

Downloaded From Vet-eBooks.com

bridges and are phenotypically diploid (Cho *et al.*, 2003; Braun *et al.*, 1989; Caldwell and Handel, 1991). In theory, out of the syncytium, one spermatozoon becomes dominant and is recruited above other spermatozoa for successful maturation. Packing its DNA into a volume less than 5% gives profound advantage to sperm, improves the hydrodynamics of sperm, and helps protect the sperm from endonucleases of female reproductive tract (Wyrobek *et al.*, 1976). Spermatozoa with efficiently packaged chromatin due to replacement of histones with protamines are the ones most likely to fertilize the oocyte and regulate egg activation and subsequent embryo development (Balhorn *et al.*, 1988). During fertilization, sperm not only provide the protomines but also inherits retained histones and sperm nuclear matrix attachment regions (MARs) to zygote, forming the paternal pronucleus (Ward, 2010). Epigenetic regulations involving posttranslational modifications (PTMs) of chromatin remodeling proteins, such as histones, are thought to influence fertilization and early embryonic development (de Oliveira *et al.*, 2013). Regions of sperm chromatin bound to methylated histones are mainly present in heterochromatin regions where the genes are occasionally silenced (Fischle *et al.*, 2003). Acetylated histones, on the other hand, are associated with the euchromatin architecture, reducing histone–DNA links and facilitating both replacement of protamines and activation of transcription during spermatogenesis (Struhl, 1998). Researchers have recently demonstrated the presence of PTM in protamines (Brunner *et al.*, 2014), and that PTM in histones may modulate protamine–DNA interactions (Balhorn, 2007).

Chromatin remodeling occurs during spermatogenesis where linker histones are gradually replaced by testis-specific variants, followed by the replacement of histones with transition proteins and then with protamines (Kimmins and Sassone-Corsi, 2005). Testis-specific histone (TH2B) is the most commonly retained (Gatewood *et al.*, 1990) and its increased levels in sperm lead to lower levels of protamines (Zhang *et al.*, 2006). A decreased level of protamines in sperm due to abnormality in retained histones is one of the major factors associated with infertility in humans (Blanchard *et al.*, 1990). In eutherians, the sperm chromatin has two different arginine- and cysteine-rich protamines (PRM1 and PRM2) (Balhorn *et al.*, 1977; Bélaïche *et al.*, 1987; Bellvé *et al.*, 1988). The PRM1 contains 50 amino acids with a highly conserved amino-terminal hexapeptide sequence and a central DNA binding region containing several arginine-rich anchoring domains (Bélaïche *et al.*, 1987; Balhorn, 1989; Pirhonen *et al.*, 1989). However, PRM2 is synthesized from a precursor protein that is shortened by 40% and yields an arginine- and histidine-rich protein that is 63 amino acids long (Yelick *et al.*, 1987; Carré-Eusèbe *et al.*, 1991; Debarle *et al.*, 1995). Humans, some species of hamsters (Campbell, Syrian, Siberian, and Turkish), and stallions contain two protamines (PRM1 and PRM2) in the sperm chromatin (Balhorn, 1989; Pirhonen *et al.*, 1989; Corzett *et al.*, 1999), whereas bulls (Coelingh *et al.*, 1972; Mazrimas *et al.*, 1986), rams (Loir and Lanneau, 1980; Sautiere *et al.*, 1984), and boars (Tobita *et al.*, 1983) contain a single protamine (PRM1). A recent study revealed that, like histones, protamines are also subjected to PTM. Due to their positive charges, protamines are responsible for tight packaging of the sperm DNA, which is believed to contribute to transcriptional silencing in the mature cells (Brunner *et al.*, 2014). Following fertilization, protamines of the paternal genome are replaced by maternal histones; therefore, the retained sperm histones with PTM could play a role in egg activation and embryo development. Functional significance of PTM of the protamine is unknown. Abnormal protamine replacement is associated with increased histone retention (Zini *et al.*, 2008), but the mechanisms regulating sperm viability in one versus two PRM are unknown. Furthermore, roles of protamine in protecting the sperm from damaging agents are yet to be determined.

Downloaded From Vet-eBooks.com

16.2 Sperm Chromatin Structure Modulates Sperm Nuclear Shape and Function

Increased percentage of histone retention is expected to cause infertility in males. Abnormal histone retention compromises the protamine replacement and causes inefficient chromatin condensation (Kazerooni *et al.*, 2009). Abnormalities in chromatin condensation affect size of the sperm head (Kazerooni *et al.*, 2009), and this may cause failure of egg activation by such spermatozoa. Histone to protamine replacement occurs in two steps: (i) The modified histones are replaced with the transition proteins 1 and 2. (ii) Transition proteins 1 and 2 are replaced with protamines (Aoki *et al.*, 2006). Species variation occurs in the presence of protamine types, as humans and mice contain PRM1 and PRM2, whereas bulls contain only PRM1. Changes in the size of sperm head and elongation are associated with increased divergence of *prm1* sequence in most mammals (Lüke *et al.*, 2014). Replacement of histones with protamines plays an important role in crucial cellular processes such as changes in the sperm head and temporary arrest of transcription in the haploid male genomes, which protects and stabilizes sperm DNA. For example, Lüke *et al.* (2014) demonstrated that abnormalities in replacement of histones with protamines can cause major defects in sperm morphology and physiology. Cho *et al.* (2003) demonstrated that defective histone replacement results in flagellum tightly wrapped around the head or elongated heads having reduced ventral flexure. As such, proper nuclear architecture facilitating sperm hydrodynamics is a big advantage for sperm to reach, fertilize, and activate the egg. Protamines form a toroiodal structure that helps maintain sperm nuclear shape and efficient compaction of DNA.

The association of protamines with DNA brings about a unique chromatin remodeling in spermatozoa and appears to facilitate the hydrodynamic shape of the sperm head (Brunner *et al.*, 2014). Swimming velocity of spermatozoa depends on sperm head shape and size, which in turn affects hydrodynamic efficiency of the sperm (Tourmente *et al.*, 2011; Roldan *et al.*, 1992). Smaller and more elongated heads with proper compaction have less resistive drag during swimming and allow higher sperm velocity (Humphries *et al.*, 2008), enabling the journey to reach and fertilize the egg. Hydrodynamic spermatozoa are highly motile, and help protect the paternal genome from physical and chemical change and damage in the female reproductive tract (Rathke *et al.*, 2014).

Although protamines are involved in sperm chromatin condensation and function, there is restrictive positive selection on only a few functional sites (Lüke *et al.*, 2014). Abnormalities in associations between protamines and DNA lead to low sperm counts, loss of hydrodynamicity in spermatozoa, and increased damage to sperm chromatin and morphology. These abnormalities negatively affect ability of sperm to travel in the female reproductive tract and to fertilize the egg (Carrell *et al.*, 2007; Aoki *et al.*, 2005). Increased incorporation of protamines into sperm chromatin has been found to block transcription of genes (Lee *et al.*, 1995; Kleene, 2003). Deficiencies in protamine levels are related to infertility in men (Balhorn *et al.*, 1988; de Yebra *et al.*, 1993; Belokopytova *et al.*, 1993). Errors in sperm DNA compaction due to improper protamine replacement is a major cause of sperm DNA damage. This is strongly correlated with failure of embryonic development (Morris *et al.*, 2002).

Efficient protamination is essential for chromatin integrity, function of sperm, and development of embryos (de Oliveira *et al.*, 2013; Franken *et al.*, 1999; Esterhuizen *et al.*, 2000, 2002; Sakkas *et al.*, 1996; Lolis *et al.*, 1996; Nasr-Esfahani *et al.*, 2001; Razavi *et al.*, 2003). Improper retention of histones is a result of improper protamination that affects preferential activation of genes during early embryogenesis (Hammoud *et al.*, 2009). Genes such as *igf1* and *globin* that are highly expressed during embryogenesis are enriched in histone binding (Gardiner-Garden

Downloaded From Vet-eBooks.com

et al., 1998; Wykes and Krawetz, 2003). The PTM such as methylation, acetylation, and phosphorylation of sperm histones are important epigenetic control mechanisms regulating expression of the paternal genome by the maternal transcriptional factors during early embryonic development (Hammoud *et al.*, 2009; Miller *et al.*, 2010). Although the PTM on protamines have been demonstrated, precise mechanisms and specific causes and effects of these modifications on embryogenesis are still unclear (Brunner *et al.*, 2014).

Chromatin integrity of sperm is important in successful fertilization, proper egg activation, and embryo development as well as survival of a species (Morris *et al.*, 2002; Gawecka *et al.*, 2013). Because quality of sperm chromatin has such an important impact on the reproductive performance of the male, advanced methods are needed in the study of sperm chromatin health. These methods include sperm chromatin structure assays (SCSA), sperm chromatin dispersion (SCD), terminal deoxynucleotidyl transferase dUTP nick-end labeling (TUNEL) or the Comet assay, immunocytochemistry, and flow cytometry (de Oliveira *et al.*, 2013; Noblanc *et al.*, 2014; Dogan *et al.*, 2015). Although these methods provide valuable insights into molecular integrity of the sperm chromatin, there is still lacking a technique to analyze (noninvasively) the chromatin integrity of a single spermatozoon that can then be used to fertilize the egg.

16.3 The Bull Is a Suitable Model for the Study of Male Fertility in Humans

There have been 3799 studies reported worldwide over the past 5 years concerning male infertility. While 2740 of these aimed to reveal male infertility in humans, the rest were animal-based studies. Filters found only 57 of these to be sperm chromatin-related male infertility studies. Sperm deficiency, including chromatin and DNA damage, is still considered to be the main cause of male infertility. As new and sophisticated technologies are discovered to analyze sperm DNA, it is not surprising to see that there has been a gradual increase in studies of sperm chromatin in both humans and livestock. Although tools are now available to analyze sperm DNA, for the case of humans, there is not sufficient progeny data concerning human male fertility. The only way to measure this is to test hormone levels such as follicle-stimulating hormone (FSH), and testosterone (T), and to perform semen analysis measuring the sperm concentration, motility, and morphology.

There are significant similarities between the human and bovine genome (Elsik *et al.*, 2009) as well as the embryonic development. Contrary to human fertility research relying on anecdotal records of one or a few infertility treatment cycles per couple, there is an abundance of field fertility data available in the agricultural sector, focused on improving livestock reproduction. Sperm samples from bulls with detailed breeding records for thousands of AI services exist. In addition, well-documented fertility phenotype records enhance the background of knowledge from animal research data (Feugang *et al.*, 2009). Furthermore, bulls produce such vast numbers of spermatozoa that semen can be repeatedly collected from the same donor in large quantities, allowing IVF and embryo culture to be well developed, accurate, and reliable.

16.4 Conclusions and Prospects

Among the Western populations of the world, male infertility is a rising trend affecting one in 20 men (Zamudio *et al.*, 2008). Improper packaging of sperm DNA caused partly by reduced protamination predisposes sperm DNA to damage, which then interferes with fertilization and

Downloaded From Vet-eBooks.com

early embryonic development. Although the paternal genome is believed to be reprogrammed between generations (Oswald *et al.*, 2000), inheritance of epigenetic marks is also possible (Zamudio *et al.*, 2008). Abnormal chromatin condensation in sperm during spermatogenesis (prefertilization event) and abnormal chromatin decondensation during pronucleus formation (postfertilization) can result in reproductive problems (Ward, 2010). Despite the advances in the knowledge base and technologies, reproductive success influenced by paternal effects is still in urgent need of further research for successful application. Newly developed molecular technologies, including precise measurements of genomic and epigenomic landscapes within single cells, are expected to enhance the production of new knowledge and to result in new and significant applications.

Acknowledgments

This study was funded in part by Mississippi Agriculture Forestry and Experiment Station (E. Memili and N. Kutchy), Selcuk University and Merit Scholarship from Islamic Development Bank (A. Kaya), Special Program of International Cooperation and Scholarship for Visiting Professors from Brazilian Research Council (CNPq) (A. Moura and E. Memili), and by Indian Council for Agricultural Research (N. Kutchy).

References

Aoki, V.W., Moskovtsev, S.I., Willis, J., Liu, L., Mullen, J.B., and Carrell, D.T. (2005) DNA integrity is compromised in protamine-deficient human sperm. *J. Androl.*, **26** (6), 741–748.

Aoki, V.W., Christensen, G.L., Atkins, J.F., and Carrell, D.T. (2006a) Identification of novel polymorphisms in the nuclear protein genes and their relationship with human sperm protamine deficiency and severe male infertility. *Fertil. Steril.*, **86** (5), 1416–1422.

Balhorn, R. (1989) Mammalian protamines: structure and molecular interactions, in *Molecular Biology of Chromosome Function* (ed. K.W. Adolph), Springer, New York, pp. 365–399.

Balhorn, R. (2007) The protamine family of sperm nuclear proteins. *Genome Biol.*, **8** (9), 227.

Balhorn, R., Gledhill, B.L., and Wyrobek, A.J. (1977) Mouse sperm chromatin proteins: quantitative isolation and partial characterization. *Biochemistry*, **16** (18), 4074–4080.

Balhorn, R., Reed, S., and Tanphaichitr, N. (1988) Aberrant protamine 1/protamine 2 ratios in sperm of infertile human males. *Experientia*, **44** (1), 52–55.

Bélaïche, D., Loir, M., Kruggle, W., and Sautière, P. (1987) Isolation and characterization of two protamines St1 and St2 from stallion spermatozoa, and amino-acid sequence of the major protamine St1. *Biochim. Biophys. Acta*, **913** (2), 145–149.

Bellvé, A.R., McKay, D.J., Renaux, B.S., and Dixon, G.H. (1988) Purification and characterization of mouse protamines P1 and P2: amino acid sequence of P2. *Biochemistry*, **27** (8), 2890–2897.

Belokopytova, I.A., Kostyleva, E.I., Tomilin, A.N., and Vorob'ev, V.I. (1993) Human male infertility may be due to a decrease of the protamine P2 content in sperm chromatin. *Mol. Reprod. Dev.*, **34** (1), 53–57.

Biegeleisen, K. (2006) The probable structure of the protamine–DNA complex. *J. Theor. Biol.*, **241** (3), 533–540.

Blanchard, Y., Lescoat, D., and Le Lannou, D. (1990) Anomalous distribution of nuclear basic proteins in round-headed human spermatozoa. *Andrologia*, **22** (6), 549–555.

Braun, R.E., Behringer, R.R., Peschon, J.J., Brinster, R.L., and Palmiter, R.D. (1989) Genetically haploid spermatids are phenotypically diploid. *Nature*, **337** (6205), 373–376.

Downloaded From Vet-eBooks.com

Brunner, A.M., Nanni, P., and Mansuy, I.M. (2014) Epigenetic marking of sperm by post-translational modification of histones and protamines. *Epigenetics Chromatin*, **7** (1), 2.

Caldwell, K.A. and Handel, M.A. (1991) Protamine transcript sharing among postmeiotic spermatids. *Proc. Natl. Acad. Sci. USA*, **88** (6), 2407–2411.

Carré-Eusèbe, D., Lederer, F., Lê, K.H., and Elsevier, S.M. (1991) Processing of the precursor of protamine P2 in mouse: peptide mapping and N-terminal sequence analysis of intermediates. *Biochem. J.*, **277** (Part 1), 39–45.

Carrell, D.T., Emery, B.R., and Hammoud, S. (2007) Altered protamine expression and diminished spermatogenesis: what is the link? *Hum. Reprod. Update*, **13** (3), 313–327.

Cho, C., Jung-Ha, H., Willis, W.D., Goulding, E.H., Stein, P., Xu, Z., Schultz, R.M., Hecht, N.B., and Eddy, E.M. (2003) Protamine 2 deficiency leads to sperm DNA damage and embryo death in mice. *Biol. Reprod.*, **69** (1), 211–217.

Coelingh, J.P., Monfoort, C.H., Rozijn, T.H., Leuven, J.A., Schiphof, R., Steyn-Parvé, E.P., Braunitzer, G., Schrank, B., and Ruhfus, A. (1972) The complete amino acid sequence of the basic nuclear protein of bull spermatozoa. *Biochim. Biophys. Acta*, **285** (1), 1–14.

Corzett, M., Kramer, C., Blacher, R., Mazrimas, J., and Balhorn, R. (1999) Analysis of hamster protamines: primary sequence and species distribution. *Mol. Reprod. Dev.*, **54** (3), 273–282.

de Oliveira, R.V., Dogan, S., Belser, L.E., Kaya, A., Topper, E., Moura, A., Thibaudeau, G., and Memili, E. (2013) Molecular morphology and function of bull spermatozoa linked to histones and associated with fertility. *Reproduction*, **146** (3), 263–272.

de Yebra, L., Ballescà, J.L., Vanrell, J.A., Bassas, L., and Oliva, R. (1993) Complete selective absence of protamine P2 in humans. *J. Biol. Chem.*, **268** (14), 10553–10557.

Debarle, M., Martinage, A., Sautiere, P., and Chevaillier, P. (1995) Persistence of protamine precursors in mature sperm nuclei of the mouse. *Mol. Reprod. Dev.*, **40** (1), 84–90.

Dogan, S., Vargovic, P., Oliveira, R., Belser, L.E., Kaya, A., Moura, A., Sutovsky, P., Parrish, J., Topper, E., and Memili, E. (2015) Sperm protamine-status correlates to the fertility of breeding bulls. *Biol. Reprod.*, **92** (4), 92.

Elsik, C.G., Tellam, R.L., and Worley, K.C. (2009) The genome sequence of taurine cattle: a window to ruminant biology and evolution. *Science*, **324** (5926), 522–528.

Esterhuizen, A.D., Franken, D.R., Lourens, J.G., Prinsloo, E., and van Rooyen, L.H. (2000) Sperm chromatin packaging as an indicator of *in-vitro* fertilization rates. *Hum. Reprod.*, **15** (3), 657–661.

Esterhuizen, A.D., Franken, D.R., Becker, P.J., Lourens, J.G., Muller, I.I., and van Rooyen, L.H. (2002) Defective sperm decondensation: a cause for fertilization failure. *Andrologia*, **34** (1), 1–7.

Feugang, J., Kaya, A., Page, G., Chen, L., Mehta, T., Hirani, K., Nazareth, L., Gibbs, R., and Memili, E. (2009) Two-stage genome-wide association study identifies integrin beta 5 as having potential role in bull fertility. *BMC Genomics*, **10**, 176.

Fischle, W., Wang, Y., and Allis, C.D. (2003) Histone and chromatin cross-talk. *Curr. Opin. Cell Biol.*, **15**, 172–183.

Franken, D.R., Franken, C.J., de la Guerre, H., and de Villiers, A. (1999) Normal sperm morphology and chromatin packaging: comparison between aniline blue and chromomycin A3 staining. *Andrologia*, **31** (6), 361–366.

Gardiner-Garden, M., Ballesteros, M., Gordon, M., and Tam, P.P. (1998) Histone and protamine–DNA association: conservation of different patterns within the beta-globin domain in human sperm. *Mol. Cell Biol.*, **18** (6), 3350–3356.

Gatewood, J.M., Schroth, G.P., Schmid, C.W., and Bradbury, E.M. (1990) Zinc induced secondary structure transitions in human sperm protamines. *J. Biol. Chem.*, **265** (33), 20667–20672.

Downloaded From Vet-eBooks.com

Gawecka, J.E., Marh, J., Ortega, M., Yamauchi, Y., Ward, M.A., and Ward, W.S. (2013) Mouse zygotes respond to severe sperm DNA damage by delaying paternal DNA replication and embryonic development. *PLoS One*, **8** (2), e56385.

Govindaraju, A., Uzun, A., Robertson, L., Atli, M.O., Kaya, A., Topper, E., Crate, E.A., Padbury, J., Perkins, A., and Memili, E. (2012) Dynamics of microRNAs in bull spermatozoa. *Reprod. Biol. Endocrinol.*, **10**, 82.

Hammoud, S.S., Nix, D.A., Zhang, H., Purwar, J., Carrell, D.T., and Cairns, B.R. (2009) Distinctive chromatin in human sperm packages genes for embryo development. *Nature*, **460** (7254), 473–478.

Humphries, S., Evans, J.P., and Simmons, L.W. (2008) Sperm competition: linking form to function. *BMC Evol. Biol.*, **8**, 319.

Kazerooni, T., Asadi, N., Jadid, L., Kazerooni, M., Ghanadi, A., Ghaffarpasand, F., Kazerooni, Y., and Zolghadr, J. (2009) Evaluation of sperm's chromatin quality with acridine orange test, chromomycin A3 and aniline blue staining in couples with unexplained recurrent abortion. *J. Assist. Reprod. Genet.*, **26** (11–12), 591–596.

Kimmins, S. and Sassone-Corsi, P. (2005) Chromatin remodelling and epigenetic features of germ cells. *Nature*, **434** (7033), 583–589.

Kleene, K.C. (2003) Patterns, mechanisms, and functions of translation regulation in mammalian spermatogenic cells. *Cytogenet. Genome Res.*, **103** (3–4), 217–224.

Lee, K., Haugen, H.S., Clegg, C.H., and Braun, R.E. (1995) Premature translation of protamine 1 mRNA causes precocious nuclear condensation and arrests spermatid differentiation in mice. *Proc. Natl. Acad. Sci. USA*, **92** (26), 12451–12455.

Lewis, J.D., Song, Y., de Jong, M.E., Bagha, S.M., and Ausió, J. (2003) A walk though vertebrate and invertebrate protamines. *Chromosoma*, **111** (8), 473–482.

Loir, M. and Lanneau, M. (1980) Partial characterization of ram spermatidal basic nuclear proteins. *Biochem. Biophys. Res. Commun.*, **80** (4), 975–982.

Lolis, D., Georgiou, I., Syrrou, M., Zikopoulos, K., Konstantelli, M., and Messinis, I. (1996) Chromomycin A3-staining as an indicator of protamine deficiency and fertilization. *Int. J. Androl.*, **19** (1) 23–27.

Lüke, L., Vicens, A., Tourmente, M., and Roldan, E.R. (2014) Evolution of protamine genes and changes in sperm head phenotype in rodents. *Biol. Reprod.*, **90** (3), 67.

Mazrimas, J.A., Corzett, M., Campos, C., and Balhorn, R. (1986) A corrected primary sequence for bull protamine. *Biochim. Biophys. Acta*, **872** (1–2), 11–15.

Miller, D., Brinkworth, M., and Iles, D. (2010) Paternal DNA packaging in spermatozoa: more than the sum of its parts? DNA, histones, protamines and epigenetics. *Reproduction*, **139** (2), 287–301.

Morris, I.D., Ilott, S., Dixon, L., and Brison, D.R. (2002) The spectrum of DNA damage inhuman sperm assessed by single cell gel electrophoresis (Comet assay) and its relationship to fertilization and embryo development. *Hum. Reprod.*, **17** (4), 990–998.

Nasr-Esfahani, M.H., Razavi, S., and Mardani, M. (2001) Relation between different human sperm nuclear maturity tests and *in vitro* fertilization. *J. Assist. Reprod. Genet.*, **18** (4), 199–205.

Noblanc, A., Kocer, A., and Drevet, J.R. (2014) Recent knowledge concerning mammalian sperm chromatin organization and its potential weaknesses when facing oxidative challenge. *Basic Clin. Androl.*, **24**, 6.

Oliva, R. (2006) Protamines and male infertility. *Hum. Reprod. Update*, **12** (4), 417–435.

Oswald, J. Engemann, S. Lane, N. Mayer, W. Olek, A. Fundele, R. Dean, W. Reik, W. and Walter, J. (2000) Active demethylation of the paternal genome in the mouse zygote. *Curr. Biol.*, **10** (8), 475–478.

Downloaded From Vet-eBooks.com

Palermo, G.D., Avrech, O.M., Colombero, L.T., Wu, H., Wolny, Y.M., Fissore, R.A., and Rosenwaks, Z. (1997) Human sperm cytosolic factor triggers Ca2+ oscillations and overcomes activation failure of mammalian oocytes. *Mol. Hum. Reprod.*, **3** (4), 367–374.

Pirhonen, A., Linnala-Kankkunen, A., and Mäenpää, P.H. (1989) Comparison of partial amino acid sequences of two protamine 2 variants from stallion: structural evidence that the variants are products of different genes. *FEBS Lett.*, **1244** (1), 199–202.

Rathke, C., Baarends, W.M., Awe, S., and Renkawitz-Pohl, R. (2014) Chromatin dynamics during spermiogenesis. *Biochim. Biophys. Acta*, **1839** (3), 155–168.

Razavi, S., Nasr-Esfahani, M.H., Mardani, H., Mafi, A., and Moghadam, A. (2003) Effect of human sperm chromatin anomalies on fertilization outcome post ICSI. *Andrologia*, **35** (4), 238–243.

Roldan, E.R., Gomendio, M., and Vitullo, A.D. (1992) The evolution of eutherian spermatozoa and underlying selective forces: female selection and sperm competition. *Biol. Rev.*, **67** (4), 551–593.

Sakkas, D., Urner, F., Bianchi, P.G., Bizzaro, D., Wagnar, I., Jaquenoud, N., Manicardi, G., and Campana, A. (1996) Sperm chromatin anomalies can influence decondensation after intracytoplasmic sperm injection. *Hum. Reprod.*, **11** (4), 837–843.

Sautiere, P., Belaiche, D., Martinage, A., and Loir, M. (1984) Primary structure of the ram (Ovis aries) protamine. *Eur. J. Biochem.*, **144** (1), 121–125.

Shaman, J.A., Yamauchi, Y., and Ward, W.S. (2007) Function of the sperm nuclear matrix. *Syst. Biol. Reprod. Med.*, **53** (3), 135–140.

Struhl, K. (1998) Histone acetylation and transcriptional regulatory mechanisms. *Genes Dev.*, **12** (5), 599–606.

Tobita, T., Tsutsumi, H., Kato, A., Suzuki, H., Nomoto, M., Nakano, M., and Ando, T. (1983) Complete amino acid sequence of boar protamine. *Biochim. Biophys. Acta*, **744** (2), 141–146.

Tourmente, M., Gomendio, M., and Roldan, E.R. (2011) Mass-specific metabolic rate and sperm competition determine sperm size in marsupial mammals. *PLoS One*, **6** (6), e21244.

Vilfan, I.D., Conwell, C.C., and Hud, N.V. (2004) Formation of native-like mammalian sperm cell chromatin with folded bull protamine. *J. Biol. Chem.*, **279** (19), 20088–20095.

Ward, W.S. (2010) Function of sperm chromatin structural elements in fertilization and development. *Mol. Hum. Reprod.*, **16** (1), 30–36.

Wykes, S.M. and Krawetz, S.A. (2003) The structural organization of sperm chromatin. *J. Biol. Chem.*, **278** (32), 29471–29477.

Wyrobek, A.J., Meistrich, M.L., Furrer, R., and Bruce, W.R. (1976) Physical characteristics of mouse sperm nuclei. *Biophys. J.*, **16** (7), 811–825.

Yelick, P.C., Balhorn, R., Johnson, P.A., Corzett, M., Mazrimas, J.A., Kleene, K.C., and Hecht, N.B. (1987) Mouse protamine is synthesized as a precursor whereas mouse protamine 1 is not. *Mol. Cell Biol.*, **7** (6), 2173–2179.

Zamudio, N.M., Chong, S., and O'Bryan, M.K. (2008) Epigenetic regulation in male germ cells. *Reproduction*, **136** (2), 131–146.

Zhang, X., Yazaki, J., Sundaresan, A., Cokus, S., Chan, S.W., Chen, H., Henderson, I.R., Shinn, P., Pellegrini, M., Jacobsen, S.E., and Ecker, J.R. (2006) Genome-wide high-resolution mapping and functional analysis of DNA methylation in arabidopsis. *Cell*, **126** (6), 1189–1201.

Zini, A., Boman, J.M., Belzile, E., and Ciampi, A. (2008) Sperm DNA damage is associated with an increased risk of pregnancy loss after IVF and ICSI: systematic review and meta-analysis. *Hum. Reprod.*, **23** (12), 2663–2668.

Downloaded From Vet-eBooks.com

17

Epigenome Modification and Ubiquitin-Dependent Proteolysis During Pronuclear Development of the Mammalian Zygote: Animal Models to Study Pronuclear Development

Jan Nevoral[1,2] *and Peter Sutovsky*[2,3]

[1]*Department of Veterinary Sciences, Czech University of Life Sciences, Prague, Czech Republic*
[2]*Division of Animal Science, University of Missouri-Columbia, Columbia, USA*
[3]*Department of Obstetrics, Gynecology and Women's Health, University of Missouri-Columbia, Columbia, USA*

17.1 Introduction

The oocyte, a terminally differentiated female germ cell, is transformed into a totipotent zygote by fusing with the fertilizing spermatozoon. Once the transcriptionally quiescent gametes unite, the resultant embryo becomes a source of many specialized cell types with distinct transcriptional profiles. However, during very early embryo development immediately after fertilization, the respective maternal and paternal genomes are mostly transcriptionally silent and the zygote relies on an oocyte-stored pool of RNAs and proteins. After one or several rounds of embryo cleavage, the embryonic genome becomes reactivated in a species-specific manner. Epigenetic changes modulate transcriptional activity through genome reprogramming, setting the stage for ensuing cellular differentiation. Unique expression patterns of various cell types during organogenesis are determined by epigenetic memory, the so-called epigenetic inheritance regulated by epigenetic modifiers. The DNA methylation and core histone posttranslational modifications are responsible for crucial epigenetic changes (reviewed by Rivera and Ross (2013)). A number of enzymes with specific activity toward DNA and histones regulate these genome changes, thus predetermining gene expression and developmental success of an embryo.

Frequent blastomere disintegration and embryo fragmentation are problems associated with human-assisted reproductive therapy (ART) and animal *in vitro* embryo production. Embryo fragmentation has been accompanied by the presence of apoptotic markers and altered gene expression (Han *et al.*, 2010; Monk and Salpekar, 2001). However, the regulatory mechanisms of normal and aberrant embryonic development are yet to be defined and improving embryo quality *in vitro* remains difficult. Appropriate sequence of epigenetic changes during early embryogenesis, corresponding to early embryonic development *in vivo* and including the particularly stress-sensitive phase of pronucleus formation, may hold the key to producing high-quality embryos *in vitro*. Recent studies suggest the involvement of ubiquitin proteasome system (UPS), the default cellular protein recycling mechanism, in the regulation of early embryonic development from the onset of pronuclear formation to blastocyst development and implantation. This chapter will discuss the zygotic epigenome modifications and UPS-dependent aspects of zygotic development by reviewing evidence generated in rodent and large animal models, and making connections to human development.

Animal Models and Human Reproduction, First Edition. Edited by Heide Schatten and Gheorghe M. Constantinescu.
© 2017 John Wiley & Sons, Inc. Published 2017 by John Wiley & Sons, Inc.

Downloaded From Vet-eBooks.com

17.2 Milestones of Pronuclear Development

Formation of the paternal and maternal pronuclei is the starting point of a global process called maternal-to-zygotic transition (MZT). The physiological course of MZT starts with sperm-induced oocyte activation. Subsequent to sperm-zona pellucida (ZP) binding, acrosomal exocytosis, and sperm-zona penetration, the sperm plasma membrane fuses with the oolemma and introduces the soon to be demembranated sperm nucleus in the ooplasm with the help of oocyte's cortical cytoskeleton (Sutovsky, 2009). Exposure to ooplasmic environment modifies sperm nuclear structure and protein composition in a series of changes referred to as the sperm chromatin remodeling. First, sperm head decondensation takes place in ooplasm simultaneously with the completion of oocyte's second meiotic division (Yanagimachi, 1988). Sperm-nuclear decondensation is associated with the disassembly of the poreless sperm nuclear envelope and nuclear lamina directed by the ooplasmic protein kinase C-mediated lamin phosphorylation (Collas and Poccia, 1998a; Poccia and Collas, 1997). Thereafter, histone–protamine exchange during sperm nuclear remodeling takes place; it is facilitated by the oocyte-produced disulfide bond reducing peptide glutathione (GSH) (Perreault *et al.*, 1984; Sutovsky and Schatten, 1997), and proteasomal activities or nuclear factors that will be discussed later. Once the female chromosomes reach second meiotic telophase, transient male pronucleus recondensation is observed in the murine zygote, followed by *de novo* formation of the nuclear envelope (Adenot *et al.*, 1991). While the chromosomes within the sperm nucleus lack kinetochores that are necessary for chromosome attachment to mitotic spindle, kinetochore components of ooplasmic origin infiltrate the nascent male pronucleus prior to pronuclear DNA replication (McLay and Clarke, 2003; Palermo *et al.*, 1997; Schatten *et al.*, 1988). Together with male chromatin changes, female genome is reshaped immediately after meiosis completion, and the still haploid genomes of both gametes become surrounded by pronuclear envelopes. Pronucleus formation depends on rapid decrease of the activity of key kinases controlling oocyte meiosis, the M-phase promoting factor (MPF) and the mitogen-activated protein kinase (MAPK), responsible for the maintenance of second-meiotic arrest (Ducibella *et al.*, 2002). Despite the asymmetry due to maternal versus paternal origin of chromosomes, and unique requirements of paternal pronucleus formation, nuclear envelope assembly around both pronuclei occurs at approximately the same time (Florman and Ducibella, 2006). Nuclear pore complexes (NPC) form *de novo* on both pronuclei envelopes; the pool of pronuclear NPCs may be derived from annulate lamellae preassembled in the oocyte cytoplasm, as shown in bovine oocytes and zygotes (Sutovsky *et al.*, 1998).

Maternal pronucleus formation follows the exit from metaphase II (MII) block and the completion of second meiosis is marked by second polar body extrusion. Exit from MII stage depends on decrease of MPF activity and subsequently also MAPK inactivation driven by repetitive oscillatory release of intracellular Ca^{2+} ions (Ducibella *et al.*, 2002; Moos *et al.*, 1995, 1996). Hence, nuclear envelope and chromatin are capable of being reconstituted and decondensed, respectively (Mtango *et al.*, 2008). Restoration of the MPF/MAPK activity, which is a key factor for nuclear envelope disassembly and chromatin condensation prior to entry to first mitosis, follows the apposition of male and female pronuclei and pronuclear DNA replication. High activity of the aforementioned protein kinases heralds the end of pronuclear stage in zygotes, ushering in the MZT phase of development (Florman and Ducibella, 2006).

Parental DNA in zygotes undergoes dramatic changes encompassing the modification of DNA's cytosine bases with methyl group ligation, referred to as DNA methylation. Methylation of DNA by the addition of 5-methylcytosine (5mC) is responsible for epigenetic inheritance (Bird and Wolffe, 1999; Sharif *et al.*, 2007; Wigler, 1981). After fertilization, two waves of demethylation occur followed by *de novo* DNA methylation and reshaping of heterochromatin

Downloaded From Vet-eBooks.com

(reviewed by Hajkova *et al.* (2010)). The process of DNA methylation is catalyzed by DNA methyl transferases DNMT1, 2, and 3. The DNMT1 binds to a hemimethylated double stranded DNA during replication and methylates daughter DNA strand (Bestor, 2000; Giraldo *et al.*, 2013). This process is responsible for the maintenance of specific methylation patterns during preimplantation development (Hirasawa *et al.*, 2008). On the other hand, DNMT3A and DNMT3B are able to methylate existing double-stranded DNA *de novo* (Okano *et al.*, 1999). These DNMT3 isoforms are involved in *de novo* gene imprinting during gametogenesis (Kato *et al.*, 2007) as well as embryonic cell differentiation (Smallwood *et al.*, 2011).

The DNA demethylation process is most intense immediately after fertilization. Demethylation leads to genome-wide reprogramming after the union of male and female gametes that contain highly methylated DNA, and the formation of totipotent embryonic cells with broad developmental potential. Despite demethylation during MZT, basal methylation pattern determined by maternal versus paternal origin of DNA is still evident. This basal level of DNA methylation causes origin-specific monoallelic expression during early embryonic development (Reik *et al.*, 2001a; Reik and Walter, 2001). Such changes of DNA methylation are necessary for following tissue-specific DNA methylation program (reviewed by Reik *et al.* (2001b)).

Asymmetric dynamics and DNA demethylation patterning of maternal and paternal pronuclei have been described. The DNA demethylation is faster in the paternal than in the maternal pronucleus, wherein the paternal pronucleus of most mammals is demethylated within 4 h after fertilization, while the maternal pronucleus methylation persists from 1-cell until blastocyst stage (Dean and Ferguson-Smith, 2001; Guo *et al.*, 2014; Mayer *et al.*, 2000; Reik and Walter, 2001). During MZT in human embryo, the major wave of genome-wide demethylation occurs at the 2-cell stage (Guo *et al.*, 2014). However, the exact time course of DNA demethylation in maternal and paternal pronuclei varies by species (Jeong *et al.*, 2007) and the significance of methylation pattern loss for early embryogenesis remains unclear. Therefore, paternal DNA demethylation appears to be an active process that occurs prior to first DNA replication and is independent of it (Dean and Ferguson-Smith, 2001; Mayer *et al.*, 2000).

Accordingly, paternal DNA is actively demethylated and 5mC is oxidized to 5-hydroxymethylcytosine (5hmC) (Iqbal *et al.*, 2011). This conversion is catalyzed by TET3 dioxygenase in the mammalian zygote (Gu *et al.*, 2011; Wossidlo *et al.*, 2011). Together with 5hmC, 5-formylcytosine and 5-carboxylcytosine are among the oxidized forms of 5mC (Auclair and Weber, 2012; Inoue and Zhang, 2014). Oxidized forms are subsequently excised from DNA double strand by thymine DNA glycosylase (TDG) (Auclair and Weber, 2012; He *et al.*, 2011; Kohli and Zhang, 2013; Ma *et al.*, 2014). However, the demethylation process can also occur in the absence of TDG (TGD depletion), suggesting that an alternative demethylation mechanism exists. Evidently, this hypothetical active demethylation machinery still depends on aforementioned TET3 dioxygenase (Guo *et al.*, 2014).

Maternal DNA demethylation occurs passively over consecutive embryo cleavages until late morula stage due to DNA replication. Originally, it was thought that the maternal pronucleus did not contain significant amounts of 5hmC (Hajkova *et al.*, 2010; Rougier *et al.*, 1998). However, recent studies (Guo *et al.*, 2014; Shen *et al.*, 2014) have identified a basal active demethylation process also in the maternal DNA and detected 5hmC and others oxidized 5mC forms in both parental pronuclei (Wang *et al.*, 2012). Interestingly, both paternal and maternal DNA demethylation is mediated by TET3, at certain loci; demethylated forms of cytosine are diminished by DNA replication-mediated dilution during subsequent cell cycles. Therefore, this DNA demethylation mode is TDG-independent and mediated by still unknown regulators (Gkountela and Clark, 2014; Guo *et al.*, 2014; Shen *et al.*, 2014).

Based on previously discussed, already known demethylation mechanisms, at least three different pathways participate in DNA demethylation in early zygotes: (i) active enzymatically

Downloaded From Vet-eBooks.com

catalyzed demethylation through 5mC conversion to oxidized forms; (ii) *de novo* 5hmC synthesis combined with further replication-dependent dilution; and (iii) replication-mediated dilution of 5mC in the absence of *de novo* synthesis (Gkountela and Clark, 2014; Guo *et al.*, 2014; Shen *et al.*, 2014; Wang *et al.*, 2012). Exact representation and possible synergy of all putative demethylation pathways in the pronuclei and their alterations during early development remain to be explored.

In addition to DNA methylation, posttranslational modifications of DNA-associated histones, collectively termed the histone code, coregulate epigenetic inheritance. The histone code compensates for absent or rare DNA methylation and insufficient DNA methylation-induced epigenetic regulation in lower animals such as the yeast and fruit flies (Lyko, 2001; Strahl and Allis, 2000). Either way, the result of histone and DNA modifications is a parent-of-origin specific, properly dosed gene expression in the early embryo (Aoki *et al.*, 1997; Bouniol *et al.*, 1995; Cho *et al.*, 2002; Majumder *et al.*, 1997; Wiekowski *et al.*, 1993).

Observations of unique, parent-of-origin-specific pronucleus features in the shared cytoplasmic environment of a zygote point to diverse cytoplasmic factors discriminating between the respective parental pronuclei. The result of such pronuclear specialization is an asymmetric histone code and, by inference, DNA methylation based on parent of origin (Liu *et al.*, 2004; Yeo *et al.*, 2005). Many of the ooplasmic factors regulating DNA and histone modifications remain to be identified, while relevant factors of paternal origin are intensively studied. Sperm-borne noncoding RNAs (ncRNAs) have been implicated in the epigenetic regulation of early embryonic development (Rassoulzadegan *et al.*, 2006), with presumed ability to modify DNA methylation and histone code (Yan, 2014).

Once the specific genome remodeling is completed, both pronuclei enter S-phase; upon completion, their pronuclear envelopes are disassembled and the chromosomes become condensed. Syngamy of maternal and paternal chromosomes and first mitotic division take place in zygote, followed by cytokinesis, a process termed embryo cleavage. Ooplasmic signaling thus determines correct progression of pronuclear development and assembly of mitotic apparatus.

17.3 Nuclear Envelope, Nuclear Pore Complexes, and Nuclear Lamina Changes During Pronuclear Development

Post fertilization, the progression of MZT starts with paternal and maternal chromatin remodeling and nuclear envelope (NE) assembly, resulting in paternal and maternal pronucleus formation. The NE is composed of outer and inner membranes creating a lumen contiguous with endoplasmic reticulum. The inner membrane contains a set of specific proteins interacting with other structures including cytoskeleton and chromatin (Gerace and Burke, 1988; Newport and Forbes, 1987). Based on study of a cell-free system of *Xenopus laevis* egg extract, the NE assembly is stepwise, starting with membrane vesicles assembly followed by nuclear pore complex (NPC) incorporation and finally nuclear lamina scaffold establishment (Baur *et al.*, 2007; Bernis and Forbes, 2014; Leno *et al.*, 1992; Lohka, 1998; Lohka and Masui, 1984; Sutovsky *et al.*, 1998).

The assembly of pronuclear NE following fertilization starts with the membrane vesicle gathering around maternal and paternal chromatin and their fusion into a continuous NE membrane (Newport and Dunphy, 1992; Pfaller *et al.*, 1991). First, the primary tubules and small cisternae of membrane vesicles bind to chromatin; subsequently, flattening of these cisternae occurs (Dreier and Rapoport, 2000; Hetzer *et al.*, 2001, 2005). Such a membrane vesicle reshaping requires cytosolic Ca^{2+}, adenosine triphosphate (ATP), and guanosine triphosphate

Downloaded From Vet-eBooks.com

(GTP) (Boman *et al*., 1992; Macaulay and Forbes, 1996). Experiments using the sea urchin egg extract revealed the ATP- and GTP-dependent binding of membrane vesicles to chromatin and membrane fusion, respectively (Collas and Poccia, 1998b). Subsequent hydrolysis of these nucleotides by AAA-ATPase (Holaska *et al*., 2002), Ran GTPase, and its upstream factors, including regulator of chromosome condensation 1 (RCC1) and phosphoinositide 3-kinase beta (PI3Kβ), are necessary for correct NE assembly and preservation of membrane integrity (Hetzer *et al*., 2000; Redondo-Munoz *et al*., 2015). Moreover, nuclear envelope fusion and sealing is mediated by soluble NSF attachment protein receptors – SNAREs (Jahn *et al*., 2003). After the sealing of nuclear envelope, its surface area increases concomitantly with nucleus growth (Baur *et al*., 2007). The membrane vesicles contain specific receptors for nuclear lamina proteins (Collas *et al*., 1996).

Similar to somatic cell NE, the pronuclear NE communicates with ooplasm by the way of nuclear pore complexes (NPC) composed of a family of O-glycosylated glycoproteins called nucleoporins. Nucleoporins form a three-dimensional scaffold for the channel structure of the NPCs (Davis and Blobel, 1986; Hanover *et al*., 1987). Due to extensive O-linked glycosylation of nucleoporins (Hanover *et al*., 1987), lectins with specificity affinity to O-linked glycans, such as the wheat germ agglutinin (WGA), block pronuclear development and insertion of NPC in pronuclear NE in the mammalian zygote and in a cell free system composed of demembranated mammalian spermatozoa and *Xenopus* egg extracts (Sutovsky *et al*., 1998). The NPCs assembly depends on morphological changes of nuclear vesicles resulting in the formation of intermediary NE precursor structures such as the flattened cisternae (Goldberg *et al*., 1997; Macaulay and Forbes, 1996). Time-course experiments revealed that NPC assembly occurs relatively late in the process of NE assembly, that is, around the time of sealing of the NE membrane (Franz *et al*., 2005). The NPC anchoring is guided by an evolutionarily conserved mechanism including AAA-ATPase pathway (Shi *et al*., 2014; Webster *et al*., 2014). In mammalian embryos, the NE association with chromatin is necessary for NPC integration (Inoue and Zhang, 2014; Popken *et al*., 2014). Incorporation of NPC into NE promotes nucleo-cytoplasmic transport by bi-directional exchange of proteins and other large molecules (Pante and Aebi, 1993). These processes are essential for pronuclear formation during early zygote development (Sutovsky *et al*., 1998). Maternal extra-nuclear clusters of nucleoporins are mobilized to increase NPC assembly during embryonic genome reprogramming. These changes in the density of NPCs on the NE presumably satisfy an increased need for nucleo-cytoplasmic transport during this developmental phase (Popken *et al*., 2014). Annulate lamellae (AL), cytoplasmic stacks of preassembled NPCs (Dabauvalle *et al*., 1991), are also important for correct NPC-NE insertion and thus for nucleo-cytoplasmic transport. After sperm incorporation in the ooplasm, AL assembly is triggered in the peripronuclear region of fertilized bovine oocytes (Sutovsky *et al*., 1998). A coincident assembly of AL and formation of NPC on the NE has been described in the fertilized human oocytes wherein the deviation from such a spatial and temporal pattern is among presumed reasons for early developmental failure after assisted reproductive therapy (ART) (Rawe *et al*., 2003).

The last step in NE-biogenesis is the incorporation of nuclear lamins that form a scaffold underneath the NE (Newport *et al*., 1990). Two types of lamins, type A and type B, create a stable yet dynamic structure (Stuurman *et al*., 1998). Trafficking of lamins is regulated by sorting nexin 6 (SNX6), a component of retromer complex, via NPCs and Ran-GTP-dependent mechanism (Gonzalez-Granado *et al*., 2014). Together with lamin-binding proteins, both types of lamins form a structure called nuclear lamina. The A-kinase anchoring proteins (AKAPs) are associated with lamin B and play a role in its recruitment during NE assembly (Holaska *et al*., 2002). These lamin–protein complexes mediate the adhesion of nuclear lamina to membrane vesicles (Hutchison *et al*., 1994) promoted by the

Downloaded From Vet-eBooks.com

aforementioned lamina receptors' incorporation into membrane vesicle (Buendia and Courvalin, 1997). Interestingly, lamin B receptor is capable of recognizing certain histone modifications during heterochromatin formation (Hirano *et al*., 2012), from which finding the involvement of nuclear skeleton in the regulation of epigenetic changes during early embryogenesis could be inferred.

17.4 Molecular Mechanism of Paternal and Maternal Pronucleus Biogenesis

Following the removal and proteasomal degradation of spermatid histones during spermiogenesis (Chen *et al*., 1998), a majority of sperm DNA becomes packaged by protamines, leaving only a small amount of DNA bound to residual histones and nuclear matrix (Fuentes-Mascorro *et al*., 2000; Hud *et al*., 1993; Martins *et al*., 2004). Early after fertilization, the nonprotaminated portion of sperm DNA is responsible for basal paternal genome transcription observed within the paternal pronucleus, which could play a regulatory role during pronucleus formation (Ostermeier *et al*., 2004). On the contrary, protamine-bound sperm chromatin within the ooplasm is subject to protamine removal and replacement by oocyte-derived histones (Gao *et al*., 2004), and this step is important for subsequent embryonic development (reviewed by Ward (2010)). Protamine–histone exchange occurs soon after sperm incorporation, for example, ~2–4 h after fertilization in mice (Ajduk *et al*., 2006). Because of a small amount of intrinsic sperm histones, the pool of ooplasmic histones is recruited to the nascent paternal pronucleus to replace protamines and convey a transcription-permissive state onto paternal genome (reviewed by Mtango *et al*. (2008)). During paternal pronucleus formation, the volume of paternal genome multiplies compared to intact sperm head (McLay and Clarke, 2003). Protamine removal and protamine–histone exchange during sperm head decondensation are responsible for these dramatic changes (Ward and Coffey, 1991). Reduction of protamine disulfide bonds by ooplasmic agents promotes protamine replacement (Florman and Ducibella, 2006; Perreault *et al*., 1984; Sutovsky and Schatten, 1997). Besides oocyte-produced tripeptide glutathione (GSH), the ooplasmic nuclear proteins, nucleoplasmins NPM1, NPM2, and NPM3 facilitate sperm head decondensation and protamine–histone exchange (Arnan *et al*., 2003; Burns *et al*., 2003; Inoue *et al*., 2011; Maeda *et al*., 1998; Ohsumi and Katagiri, 1991). Following the histone–protamine swap, nucleoplasmins are important for correct maternal and paternal pronucleus formation, development to 2-cell stage and nucleolar organization (Burns *et al*., 2003; Okuwaki *et al*., 2012). Nucleoplasmin sequences are among the early expressed maternal effect genes transcribed before major zygotic genome activation (Burns and Matzuk, 2006). In addition to already present oocyte cytoplasmic factors, certain chromosomal loci within maternal genome modify the incoming paternal genome during early embryogenesis until embryonic genome is activated. The effect of parental specific gene imprinting and moderate expression of maternal genes, known as maternal effect, is consistent with identification of several candidate gene loci (Latham and Sapienza, 1998).

Prior to zygotic genome activation, the zygote metabolism is regulated by maternally inherited mRNAs and proteins (Yanagimachi, 1988). Subsequently, most maternal RNAs are eliminated during the zygotic/embryonic genome activation (Walser and Lipshitz, 2011) by microRNAs and through their adenylation (Lee *et al*., 2014). Thereafter, the zygotic genome activation occurs in a stepwise manner and its timing is species-specific (Latham, 1999; Latham and Schultz, 2001). Reflecting *de novo* embryonic mRNA production, protein synthesis increases during zygotic genome reactivation (Latham *et al*., 1991).

Downloaded From Vet-eBooks.com

For successful embryonic genome activation, previous correct development of zygotic pronuclei and blastomere nuclei including nucleoli are essential. Timely biogenesis and functional activation of the nucleolus, the rRNA producing nuclear organelle is a crucial part of embryonic cell nucleus formation and embryonic genome function. In early embryos, the oocyte-derived precursors of the embryonic nucleoli, referred to as nucleolus precursor bodies (NPBs), shows spherical structure with densely packed fibrils. The NPBs are specifically associated with the chromosomal nucleolus organizer regions (NORs) of the genome, the transcriptional activity of which is indispensable for the assembly of ribosomal subunits. Therefore, NPBs are the key precursor structures for future embryo nucleoli, essential for early embryogenesis (Laurincik *et al*., 2004; Ogushi *et al*., 2008; Ogushi and Saitou, 2010). Zygotic nucleoli inside the paternal and maternal pronuclei, still considered NPBs at 1-cell stage of development, are exclusively of maternal origin until embryonic RNA polymerase I responsible for ribosomal gene transcription is fully activated. Upon activation, zygotic NPBs are transformed into somatic cell-like reticulate nucleoli (Ogushi *et al*., 2008; Zatsepina *et al*., 2003). Reticulated nucleolus transformation into fibrillo-granular organelle is a marker of ribosomal RNA gene activation and embryonic genome reactivation of 4-cell porcine embryos obtained *in vivo* (Hyttel *et al*., 2000; Kopecny *et al*., 1989; Laurincik *et al*., 2004; Viuff *et al*., 2002). This spike in rRNA synthesis coincides with the completion of S-phase or the onset of G2-phase beginning during the third mitotic cell cycle in porcine embryos *in vivo* (Viuff *et al*., 2002). In the *in vitro*-produced porcine embryos, these changes associated with transcriptional activation of NORs are delayed until the fifth mitotic cell cycle (16-cell stage), while extra-nucleolar transcription precedes rDNA transcription and occurs in 4-cell embryos after the completion of third mitotic cell cycle, as also observed in porcine embryos *in vivo* (Laurincik *et al*., 2004). Differences between *in vivo* and *in vitro* embryogenesis indicate possible deficiency and the inability of current *in vitro* culture systems to replicate development *in vivo*.

Proteins involved in nucleolus formation and rRNA gene transcription include RNA polymerase I, topoisomerase I, fibrillarin, nucleolin, and nucleophosmin (Hyttel *et al*., 2000). The number and distribution of NPBs and nucleolar morphology reflects oocyte quality *in vitro*, and has a bearing on correct chromosome segregation and developmental potential of embryos, important especially for ART in human medicine (Coskun *et al*., 2003; Younis *et al*., 2008). However, early embryo is capable of the *de novo* formation of nucleoli NPBs removal from zygote by micromanipulation. Recent study indicates that mouse zygote NPBs are not utilized in early embryogenesis, and the rRNA synthesis-competent embryonic nucleoli can be assembled from *de novo*-synthesized embryonic precursors (Kyogoku *et al*., 2014). In addition, the transient loss of the nucleolus granular component was observed around 8-cell stage in the SCNT-derived bovine embryos. The observation of subsequent nucleolus full reconstitution suggests that transcriptional silencing of early embryo nucleoli is overridden and establishment of final embryo nucleoli is associated with general genome reprogramming (Camous *et al*., 1986; Kanka *et al*., 1991; King *et al*., 1996; Lavoir *et al*., 1997). Nucleolar activity ceases during embryo cleavage when karyokinesis-cytokinesis evenly partitions nucleolar components between the daughter cells. Such transformations are regulated by small nuclear ribonucleoproteins (snRNPs) originating from oocyte (Dean and Schultz, 1990; Kanka *et al*., 1996). In addition to NPBs importance for early embryonic development, their removal alters euchromatin and heterochromatin establishment. Differential distribution of certain histone variants was observed in enucleolated zygotes (Fulka and Langerova, 2014), indicating a requirement for NBPs in embryonic genome activity, and by inference in epigenome regulation (Hamdane *et al*., 2014).

Downloaded From Vet-eBooks.com

17.5 Role of UPS in Pronuclear Biogenesis

The UPS is the universal, versatile cellular protein recycling mechanism, considered as a crucial oocyte-derived system that affects both pronuclear biogenesis and genome modifications during early embryogenesis. In the canonical protein degradation pathway, covalently linked multi-ubiquitin isopeptide chains form on one or more internal Lys-residues of the substrate protein (Glickman and Ciechanover, 2002). This process is catalyzed by ubiquitin-activating enzyme E1/UBA1, a small group of ubiquitin-conjugating enzymes (E2 type/UBE2 enzymes), and a variety of E3-type ubiquitin ligases belonging to several distinct families, together counting hundreds of members (Heride *et al*., 2014; Neutzner and Neutzner, 2012). Multiubiquitin chains on target proteins are recognized and engaged by the 26S proteasome, a proteolytic holoenzyme that removes the multiubiquitin chain and degrades the substrate protein (Jung and Grune, 2013; Jung *et al*., 2013). Alternative to polyubiquitin-dependent proteasomal degradation, protein di-ubiquitination can lead to lysosomal degradation, or can be reversed by deubiquitinases to act as a protein activity switch (Komander and Rape, 2012; Neutzner and Neutzner, 2012).

The UPS can contribute to the regulation of pronuclear development directly by controlling the removal of sperm-derived proteins from nuclear matrix early after fertilization and the turnover of ooplasmic proteins imported in the nascent pronuclei. Such a function of UPS is suggested by the observation that proteasomes are present in both paternal and maternal pronuclei, and PN development can be stunned by reversible proteasomal inhibitors (Huo *et al*., 2004; Rawe *et al*., 2008; Sutovsky *et al*., 2004). In addition to blocking PN development, the proteasomal inhibitor treatment also seemed to prevent pronuclear apposition by inhibiting the formation of sperm aster in bovine and human zygotes, two species in which this important zygotic function depends on the exposure of the sperm-borne proximal centriole to zygotic cytoplasm (Rawe *et al*., 2008). Such functions of UPS have implications for human ART as well as for somatic cell nuclear transfer technology in animals, as will be discussed below.

Indirectly, UPS may influence pronuclear development by regulating the life span, turnover, and/or activity of proteins involved in the regulation of zygotic cell cycle and pronuclear development.

The role of UPS in the regulation of both mitotic and meiotic cell cycle is well established (Glotzer *et al*., 1991). During oocyte meiosis, metaphase–anaphase transition depends upon ubiquitination and proteasomal degradation of the cyclin component of the M-phase promoting factor (MPF) (reviewed by Karabinova *et al*. (2011)). This activity is guided by the activity of anaphase-promoting complex/cyclosome (APC/C) within which the SKP1-cullin-F-box protein (SCF) complex has an E3 ubiquitin-ligase activity (Skowyra *et al*., 1997; Zhou *et al*., 2013). Prior to fertilization, meiotically mature oocytes are arrested at metaphase II by the cytostatic factor (CSF) activity, dependent on the activity of early mitotic inhibitor protein 1 (EMI1 (Reimann and Jackson, 2002)). At fertilization, the exit from metaphase-II arrest is triggered by ubiquitin-proteasome-dependent degradation of EMI1, catalyzed by the SCF complex (Tung *et al*., 2005).

Ubiquitination of histones plays a role in the establishment of epigenetic marks including X-chromosome silencing during spermatogenesis (Mulugeta Achame *et al*., 2010). While most spermatid histones are replaced with protamines during spermiogenesis, the protamination of sperm DNA is not complete. Varied amounts of DNA-associated histones are observed in mammalian spermatozoa, preferentially associated with genes activated early during pronuclear/embryonic development (Gardiner-Garden *et al*., 1998). Consequently, deubiquitination and/or degradation of ubiquitinated histones associated with paternal epigenome could occur after fertilization and aid in the erasing of those epigenetic marks. Although little is known about zygotic proteasome activities in mammals, oocyte activation by the spermatozoon appears to coincide with a transient rise in proteasomal proteolytic activity in echinoderms and ascidians

Downloaded From Vet-eBooks.com

(reviewed by Imschenetzky *et al*. (1999)). Besides direct ubiquitination of histones, specific ubiquitin-ligase activities regulate the activity of enzymes involved in histone acetylation, as will be discussed for sirtuin family of histone deacethylases.

17.6 Posttranslational Modifications of Pronuclear Histones

Nucleosome, the functional unit of eukaryotic chromatin, consists of ~147 base pairs (bp) of DNA wrapped around histone core formed by an octamer of four different core histone variants (H2A, H2B, H3, and H4), cross-linked by linker histone H1. A number of core histone splicing variants are known in somatic cells as well as in gametes, zygotes, and embryonic cells. While the functions and dynamics of some histone variants in embryogenesis are subjects of intensive study, others such as H2B and H4 remain to be explored. In addition to alternative splicing, histones' posttranslational modifications affect structure and function of chromatin. Common histone modifications include acetylation, methylation, phosphorylation, sumoylation, and ubiquitination (reviewed by Yuan and Zhu (2014)).

Histone H2A variants, including H2A.Z, MacroH2A, H2A-Bbd, and H2A.X (Kamakaka and Biggins, 2005) are involved in genome reprogramming after fertilization (Wu *et al*., 2014). The H2A.Z is present at transcriptional start sites and thus involved in genomic transcriptional activation (Bonisch and Hake, 2012). Conversely, MacroH2A is a hallmark of X chromosome inactivation due to its role in gene silencing and inhibition of transcription factor binding (Angelov *et al*., 2003; Mietton *et al*., 2009). The time course of embryonic gene expression of H2A variants is consistent with their role during early development (Kafer *et al*., 2010). The H2A.Bbd variant is usually colocalized with general histone acetylation sites in mouse oocytes (Kim *et al*., 2003) and also involved in histone-protamine replacement during late spermatogenesis (Ishibashi *et al*., 2010). Phosphorylation of H2A.X, abbreviated as γH2A.X, has been detected as an early step in response to DNA strand breaks (Kuo and Yang, 2008) and thus important for genome stability as predicted earlier (Celeste *et al*., 2002).

Histone H3 variants comprise H3.1, H3.2, and H3.3 in differentiated somatic as well as embryonic stem cells (Yuan and Zhu, 2014; Zhou and Dean, 2014). It has been reported that H3.1 and H3.2 variants are absent from paternal pronucleus of early mouse zygotes, while the H3.3 is the predominant H3 variant inside paternal chromatin (Torres-Padilla *et al*., 2006; van der Heijden *et al*., 2005). In murine embryos reconstructed by somatic cell nuclear transfer (SCNT), maternally derived H3.3 replaces somatic H3 in donor cell nucleus shortly after transfer, and its replacement in specific loci plays a role in embryonic genome reprogramming (Wen *et al*., 2014a, 2014b). In addition to aforementioned H2A.X phosphorylation, phosphorylation of H3 has been described. Surprisingly, this H3 modification is presumed to help in preserving pericentric heterochromatin compaction and thus faithful segregation of chromosomes during cell cycle (Hendzel *et al*., 1997; Wei *et al*., 1999).

Histone acetylation is one of the most common posttranslational histone modifications, denoted as a marker of transcriptional activity (Hebbes *et al*., 1988, 1994) and a facilitator of the binding of transcription factors to nucleosomal DNA (Lee *et al*., 1993; Vettese-Dadey *et al*., 1996). In the mouse zygote, hyperacetylation of histone H4 is associated with paternal chromatin during histone–protamine exchange at fertilization; consequently, paternal pronucleus exhibits higher transcriptional activity than the maternal one. Next, the hyperacetylation of maternal pronucleus occurs to equalized histone acetylation pattern of both pronuclei in spite of their differential transcriptional activity. Core histone acetylation has been described as a phenomenon associated with embryonic genome activation (Adenot *et al*., 1997). On the

Downloaded From Vet-eBooks.com

other hand, underacetylation of histones in the centromeric heterochromatin is involved in correct chromosome segregation (Ekwall *et al*., 1997; Jeppesen *et al*., 1992). Histone acetylation is specifically catalyzed by histone acetyltransferase enzymes (HATs) (Brownell and Allis, 1996). The HAT1 enzyme is responsible for acetylation of newly synthesized H4 and involved in H3 acetylation maintenance during mammalian embryo development (Nagarajan *et al*., 2013). Other, non-HATs enzymes with histone acetyltransferase activity have been described (Mizzen *et al*., 1996; Wittschieben *et al*., 1999).

From the point of view of transcriptional activity, histone methylation is considered an opposite, gene silencing form of core histone modification to histone acetylation. Histone methylation is crucial for epigenetic inheritance, cellular memory maintenance, and genome stabilization (Grewal and Jia, 2007; Grunstein, 1997; Muramatsu *et al*., 2013; Zhang and Reinberg, 2001), all of which are required for early embryonic development. Specifically, methylation of histone H3 on Lys-9 (H3K9 modification) (Figure 17.1) is fundamental for epigenetic changes resulting in gene silencing, heterochromatin establishment and stabilization,

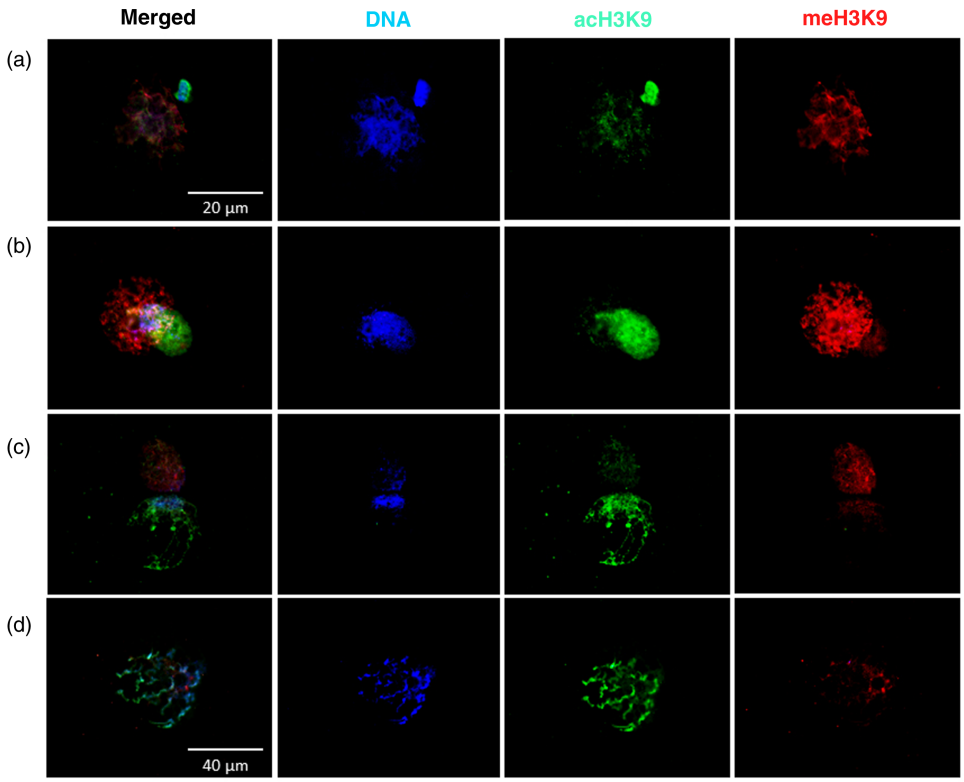

Figure 17.1 Dynamics of histone acetylation and methylation during pronucleus formation in the *in vitro*-produced porcine zygotes. First, histone hyperacetylation (green color indicates H3K9 acetylation) occurs during sperm protamine–histone exchange (a) and early male pronucleus development (b). Conversely, methylated H3K9 (indicated by red color), a marker of heterochromatin formation is abundant in the female pronucleus. The histone code asymmetry of both pronuclei counterstained by DAPI (blue channel) is apparent during early (b) and advanced (c) pronucleus formation. Following pronuclear apposition and entry into the first mitotic cell cycle (d), histone methylation retreats while histone acetylation persists (demonstrated by H3K9 methylation and H3K9 acetylation, respectively). These modifications of histone code are essential for subsequent embryonic gene reprogramming. Hence, embryonic genome is sensitive to DNA damage and early embryonic developmental failure. (See color plate section.)

Downloaded from Vet-e-Books.com

and subsequent X-chromosome inactivation during inner cell mass (ICM) formation (Bannister and Miska, 2000; Cao *et al*., 2002; Plath *et al*., 2004; Rea *et al*., 2000). Biological effect of H3K9 di-/trimethylation is mediated by specific factors, often transcription and cell cycle regulators with binding ability to a specific H3K9 methylation pattern. Among them, ICBP90 plays an important role in heterochromatin formation and genome stabilization (Karagianni *et al*., 2008). Heterochromatin formation involves the linkage of multiple proteins. The α- and β-isoforms of heterochromatin protein 1 (HP1) are factors recognizing H3K9 di-/trimethylation and genome stabilization (Bannister *et al*., 2001; Jacobs and Khorasanizadeh, 2002; Lachner *et al*., 2001; Maison and Almouzni, 2004; Nakayama *et al*., 2001).

Further to the above modifications, ubiquitination of H2A and H2B modulates heterochromatin formation and maintenance. The polycomb repressive complex 1 (PRC1)-dependent ubH2A facilitates H3 methylation and further heterochromatin formation (Blackledge *et al*., 2014; Kalb *et al*., 2014). The ubH2B modification is mediated by specific histone H2B-ubiquitinating complex (HULC) and the ubH2B-derived heterochromatin formation is independent of histone methylation (Zofall and Grewal, 2007).

Male and female pronuclei show an asymmetric pattern of histone modification. While the maternal pronucleus is typically di- and tri methylated on lysine (K) 4, K9, and K27 of histone H3, and K20 of H4, the paternal pronucleus displays lesser histone methylation, restricted to monomethylation of H3 on K4, K9, and K27. This H3 monomethylation pattern is symmetric for both pronuclei (Lepikhov and Walter, 2004; Santos *et al*., 2005; van der Heijden *et al*., 2005). Interestingly, the Lys-20 residue of histone H4 is rapidly monomethylated in the fully formed paternal pronucleus. Consequently, paternal chromatin is not divided into euchromatin and heterochromatin, as suggested by the absence of trimethylated H3 and extensive H4 monomethylation (van der Heijden *et al*., 2005).

Some histone modifications, such as trimethylation of H3K9, are well conserved evolutionarily from mouse to humans (van der Heijden *et al*., 2009). Absent from paternal chromatin, the H3K9 methylation mark is distinct in the maternal chromatin after fertilization (Liu *et al*., 2004). However, the presence of parent-of-origin specific H3K9 dimethylation in porcine embryos remains controversial (Sega *et al*., 2007), pointing to evolutionary divergence of histone methylation patterns in mammals. Moreover, K9 trimethylation pattern of residual exiguous sperm-borne H3 permeates into the oocyte and directs paternal H3K9/heterochromatin protein HP1 and heterochromatin formation in human embryos (van de Werken *et al*., 2014). Though not completely understood, the H3K9 methylation is a well-established epigenetic marker of heterochromatin inherited during cell division (Peters and Schubeler, 2005).

Although histone methylation is usually associated with gene silencing, the methylation of H3 on Lys-4 appears to colocalize with active transcription sites (Eissenberg and Shilatifard, 2010; Heintzman *et al*., 2007) and appears essential for genome reprogramming (Shao *et al*., 2014). Accordingly, the H3K4 methylation increases around the time of embryonic genome activation in the mouse (Shao *et al*., 2014). The pattern of H3K4 methylation in the *in vitro* fertilized embryos is similar to *in vivo*-produced embryos; however, its total methylation level is higher *in vivo* (Wu *et al*., 2012). The H3K4 trimethylation together with acetylation of other lysine residues on euchromatin are associated with increased transcriptional activity (Nightingale *et al*., 2007).

Although active demethylation by histone demethylases occurs naturally, histone methylation appears to be more stable than other modifications, such as acetylation (Burns *et al*., 2003). This phenomenon is reflected in a wide spectrum of methyltransferases known in mammals. Factors with methyltransferase activity, such as SUV39H1/2, G9A, ESET, and EHMT1, are responsible for H3K9 methylation. Sharing the same methylated target, these enzymes show differing chemical structures and distribution patterns (O'Carroll *et al*., 2000; Ogawa *et al*., 2002; Schultz

Downloaded From Vet-eBooks.com

et al., 2002; Peters and Schubeler, 2005; Rea *et al*., 2000; Tachibana *et al*., 2001; Yang *et al*., 2002). In addition, many isoforms of H3K4 methyltransferases catalyzing mono-, di-, and trimethylation are present in mammalian embryos (Flanagan *et al*., 2005; Shi *et al*., 2006; Wysocka *et al*., 2006). Among them, the SET proteins (also known as SET/mixed lineage leukemia family – MLL) and lysine/K-specific methyltransferases (KMTs) have been described (Black *et al*., 2012; Dou *et al*., 2006). Counterbalancing active demethylation of H3K4 by lysine/K-specific demethylases (KDMs) has also been described (Fang *et al*., 2010; Klose *et al*., 2006; Shi *et al*., 2004). Dynamics and levels of H3K4 trimethylation correlate with the expression of KMT2B and KDM5A, its key methyltransferase and demethylase, respectively (Shao *et al*., 2014). In addition to histone methyltransferases, short recruiter genome sequences are capable of attracting methylated histones as is the case of trimethylated H3K27 (Jermann *et al*., 2014).

Among histone methyltransferases, SUV39H1 is a well-known key factor for facultative heterochromatin establishment, maintenance and genome stability, gene repression, and its regulation through transcription factors during cell cycle (Firestein *et al*., 2000; Nielsen *et al*., 2001; Peters *et al*., 2001; Vaquero *et al*., 2004). The activity of enzymes with methyltransferase activity and subsequent H3K9 methylation has an essential role in embryogenesis and embryonic cell lineage commitment (Cheedipudi *et al*., 2014; Park *et al*., 2011).

The HP1 recognition factor already discussed is associated with SUV39H1, thus recognizing centromeric regions and constituting an SUV39H1-HP1 methylation system important for chromosome segregation (Aagaard *et al*., 2000). On centromeric heterochromatin, SUV39H1 acts in an H3K9 methylation-specific manner to maintain genome stability (Peters *et al*., 2003). Furthermore, interplay between SUV39H1-HP1-H3K9 and other DNA methylation marks has been described (Johnson *et al*., 2002; Lehnertz *et al*., 2003; Peters and Schubeler, 2005; Yeo *et al*., 2005). Surprisingly, the induction of active DNA demethylation by DNA glycosylase TDG is accompanied by an increase of H3K9 di-/trimethylation levels (Ma *et al*., 2014). On the contrary, DNMT1 and DNMT3B seem to be strictly downstream factors of SUV39H1 on pericentromeric chromosome loci in embryonic stem cells where DNMTs form complexes with HP1 isoforms (Lehnertz *et al*., 2003). Moreover, DNMT1 directly interacts with histone H3 methyl transferase G9A at the replication fork, resulting in H3K9 methylation (Cheedipudi *et al*., 2014; Esteve *et al*., 2005). On the other hand, methylated H3K9 recruits cofactors of other DNA methyltransferases (Karagianni *et al*., 2008).

17.7 Sirtuin Family Histone Deacetylases in Gametogenesis and Development

Methyltransferase activity increases after the exposure of binding sites for methyl group, usually occupied by acetyl group. The histone deacetylase enzymes (HDACs) are responsible for removing the acetyl group and thus enact underacetylation in their substrate histones. The HDACs have been isolated for the first time from *Saccharomyces cerevisiae* (Dangond *et al*., 2001). Based on original description, they are divided into three classes: Rpd3p (class I), Hda1p (class II), and Sir2p (class III). An important group within this family is the NAD^+-dependent class III HDACs named sirtuins (Imai *et al*., 2000; Landry *et al*., 2000).

Sirtuin family has seven members (SIRT1 – 7) collectively identified as key regulators of life span/longevity in various organisms. Moreover, sirtuin activity has been linked to protection against DNA damage and response to DNA strand breaks (Canto and Auwerx, 2009; Haigis and Guarente, 2006; Herranz *et al*., 2010; Kim and Um, 2008; Milner, 2009). Beneficial effects of sirtuins during gametogenesis and early embryo development have been described (Bell *et al*.,

Downloaded From Vet-eBooks.com

2014; Coussens *et al*., 2008; Di Emidio *et al*., 2014; Kawamura *et al*., 2010; Kwak *et al*., 2012; Zhang *et al*., 2014). One possible explanation of sirtuins' protective role is their ability to deacetylate H1 on K26, H3 on K9, K26, and K56, and H4 on K16 (Chen *et al*., 2010; Oberdoerffer *et al*., 2008; Vaquero *et al*., 2004; Vaquero *et al*., 2007b). These deacetylations lead to higher abundance of heterochromatin marks such as the methylation of H2, H3, and H4. Multiepitope histone methylation requires lysine residue release and activation of multiple methyltransferases (Vaquero *et al*., 2004; Yuan and Zhu, 2014). Moreover, the SUV39H1 enzyme with methyltransferase activity has to be activated by deacetylation of K266 within its catalytic SET domain by SIRT1 (Rea *et al*., 2000; Vaquero *et al*., 2007a). Further, SIRT1 may protect and prolong the half-life of SUV39H1 by suppressing its degradation-promoting polyubiquitination by E3-type ubiquitin-ligase MDM2 (Bosch-Presegue *et al*., 2011). Therefore, higher H3K9 trimethylation and HP1 and heterochromatin formation occur in the presence of increased SIRT1 activity (Peters *et al*., 2003; Vaquero *et al*., 2004, 2007a). The H3K9 di-/trimethylations are subsequently recognized by HP1α, to facilitate their interaction with H3K9-methyl group binding protein ICBP90. The ICBP90 protects histone H3 from E3 ubiquitin-ligase activity and is required for heterochromatin establishment and maintenance (Karagianni *et al*., 2008). These changes originating from H3K9 methylation are responsible for epigenetic regulation of mammalian development (Matoba *et al*., 2014; Peters *et al*., 2003). Pertinent to genome integrity preservation, SIRT1 also supports the maintenance of telomere length (Palacios *et al*., 2010).

Sirtuins positively influence early embryogenesis through proteasomal degradation of essential transcriptional factors such as p53 and Forkhead box O-class (FOXO) proteins by way of modulating MDM2 ubiquitin-ligase activity (Chao, 2014; Chen *et al*., 2010; Kawamura *et al*., 2010; Sparks *et al*., 2014). Expression levels of p53 determine the size of pluripotent stem cell population/cell number in the inner cell mass of a blastocyst (O'Neill *et al*., 2012). Moreover, MDM2-regulated p53 turnover is important for response to DNA strand breaks/DNA repair during embryogenesis (Tollini *et al*., 2014). On the other hand, the p53-induced, MDM2-mediated proteasomal degradation of FOXO acts as a downstream factor in the p53-regulated signaling cascade of transcriptional control (Fu *et al*., 2009). In addition to influencing MDM2 signaling pathway, p53, p65 (a subunit of transcription factor NF-κB), and FOXO proteins are known nonhistone substrates of sirtuins, and the sirtuin-catalyzed deacetylation increases their activity (Wang *et al*., 2012; Shinozaki *et al*., 2014). Deacetylation makes lysine residues of FOXO available for ubiquitination (Tseng *et al*., 2014; Wang *et al*., 2012). Simultaneously, NF-κB signaling is attenuated by SIRT6 via H3K9 deacetylation and prevention of NF-κB binding to gene promoters, resulting in an extended organismal life span (Kawahara *et al*., 2009). Thus, the components of ubiquitin proteasome system are required for sirtuin-mediated signaling that promotes epigenetic changes and regulates transcriptional activity during embryo development.

17.8 Clinical and Technological Considerations

At molecular and cellular levels, early embryos obtained by assisted reproductive therapies (ART) in humans or by *in vitro* embryo culture and micromanipulations in animals differ from the *in vivo* grown embryos. Furthermore, individual ART techniques may affect embryo development differentially. For example, the time course of zygotic development and pronucleus formation is slightly delayed in the IVF-derived human embryos compared to those fertilized by intracytoplasmic sperm injection (ICSI) (Nagy *et al*., 1998; Papale *et al*., 2012).

During somatic cell nuclear transfer, various genome-regulating factors are replaced during the process of donor cell-nuclear remodeling. Some of somatic nucleus components are

Downloaded From Vet-eBooks.com

replaced by orthologous oocyte-derived proteins, including histones, heterochromatin-specific proteins, and silencing polycomb-group proteins (Jullien *et al*., 2011; Nashun *et al*., 2011; Wen *et al*., 2014a). Other donor cell-derived nuclear proteins must be replaced for gene reactivation to occur in SCNT-derived embryos (Jullien *et al*., 2010, 2012; Wen *et al*., 2014a). Histone modifications in reconstructed embryos after SCNT recapitulate modification patterns observed in naturally fertilized embryos (Brero *et al*., 2009; Wu *et al*., 2014). However, inaccurate histone replacement might be related to persistent epigenetic memory of donor cell and thus embryonic development failure (Ng and Gurdon, 2008). Failure of pluripotency gene (i.e., *Oct4, Nanog*) reactivation has been ascribed to the lack of maternal H3.3 in SCNT-derived embryos; thus, H3.3 is considered essential for pluripotent gene reactivation (Wen *et al*., 2014b). Concurrently, reduction of H3K27 trimethylation, a marker of genome stability and gene silencing, takes place in donor cell nucleus during remodeling after SCNT (Bogliotti and Ross, 2012; Wen *et al*., 2014b). Developmental stage-specific gene expression is essential for successful development to blastocyst and incorrect expression pattern is responsible for embryogenesis failure after genome reprogramming (Han *et al*., 2010).

As already discussed, PN development and function is directly and indirectly regulated by proteasomal proteolysis and by other mechanisms controlled by ubiquitin proteasome system. This is obvious from experiments in which the inhibition of proteasomal chymotrypsin-like activity with MG-132 prevented PN development in bovine zygotes (Rawe *et al*., 2008) and even more pronouncedly from SCNT experiments where proteasomal inhibitors efficiently blocked the remodeling of donor cell nucleus in the reconstructed zygotes (Sutovsky and Prather, 2004; Whitworth *et al*., 2009). Porcine SCNT experiments with proteasomal inhibitors were inspired by the first successful SCNT/cloning of rats, a species previously refractory to SCNT procedure, in which MG132 was used to prevent spontaneous oocyte activation during oocyte collection from hormonally stimulated rats (Zhou *et al*., 2003). Based on these results, we speculated that a transient oocyte exposure to a reversible proteasomal inhibitor may be beneficial beyond preventing spontaneous activation, for example, by protecting ooplasmic pro-survival proteins from proteasomal degradation or by stimulating the assembly of functional proteasomes through a negative feedback loop (Sutovsky and Prather, 2004). This observation inspired the development of SCNT protocols aimed at improving reconstituted embryo development to term. Improved pregnancy rates and higher numbers of live births were observed after embryo transfer (ET) of porcine SCNT zygotes transiently exposed to a low concentration of MG-132 (Whitworth *et al*., 2009). Improvements of various aspects of donor cell nuclear remodeling, genomic reprogramming, and embryo development were subsequently reported in porcine/bovine embryos cloned with MG-132 (Le Bourhis *et al.*, 2010; You *et al.*, 2010.). Further studies confirmed the benefit of proteasomal inhibitors in rat cloning (Mizumoto *et al*., 2009; Nakajima *et al*., 2008; Sterthaus *et al*., 2009), and mice were cloned using a similar procedure from cell lines previously thought to be refractory to cloning (Yu *et al*., 2005), although one study reported limited success (Gao *et al*., 2005). More recently, embryos from naturally fertilized bovine oocytes were shown to develop better if treated with MG-132 late in oocyte maturation period (Xiao *et al*., 2014; You *et al*., 2012a, 2012b), an approach that could be useful clinically for human oocyte maturation, if properly safeguarded.

The benefit of transiently blocking proteasomal proteolysis during early stages of SCNT/remodeling/reprogramming could be explained by the retention as in *protection from proteasomal degradation* of maternal proteins that may promote embryo survival and development. The major vault particle protein MVP/LRP is known to have a pro-proliferative and cell-protectant action, and accumulates in zygotes treated with MG-132 (Sutovsky *et al*., 2005). It is possible that this and other maternally stored proteins would be degraded by proteasome shortly after fertilization/nuclear transfer in the absence of proteasomal inhibitors. Similarly, transient

Downloaded From Vet-eBooks.com

proteasome inhibition could increase the life span and delay the degradation of maternally stored ooplasmic factors involved in reprogramming and resetting of epigenetic marks, thus giving the donor cell nucleus more resting time in the ooplasmic environment. To this end, SCNT outcomes may be improved by combining proteasomal inhibition with the modulation of factors affecting donor cell epigenome/histone modification, though first attempts with combination of MG-132 and histone-deacetylase inhibitor Scriptaid did not show further improvement of porcine SCNT (Mao *et al*., 2012). Similar to genome-wide sweep of maternal, oocyte stored ribonucleic acids after fertilization, a substantial portion of the ooplasmic proteins accumulated during oocyte growth and meiotic maturation is removed after fertilization (DeRenzo and Seydoux, 2004). Given the early proteasomal infiltration of donor cell nucleus after SCNT (Figure 17.2) (Sutovsky and Prather, 2004; Whitworth *et al*., 2009) and both male and female pronuclei in naturally fertilized zygotes (Rawe *et al*., 2008; Sutovsky *et al*., 2004), it should also be considered that proteasomal biogenesis and activity at the onset of zygotic genome reprogramming could be stimulated by transient proteasomal inhibition. First, a transient block of oocyte activation/proteasome-dependent metaphase II exit during donor cell remodeling (SCNT) or male pronuclear histone-protamine exchange (IVF) could give the "stranger" nucleus (Latham *et al*., 2007) more time to acclimatize in the oocyte cytoplasm. Second, the activity of ooplasmic UPS enzymes and/or the translation of maternally stored mRNAs encoding for proteasomal subunits and UPS enzymes (Lundgren *et al*., 2005), and/or the assembly of enzymatically active proteasomes could be hyper-stimulated through a feedback mechanism sensing the inhibition of proteasomal proteolysis resulting in the accumulation of undegraded ubiquitinated proteins. Proteasomal inhibition at this stage could also induce

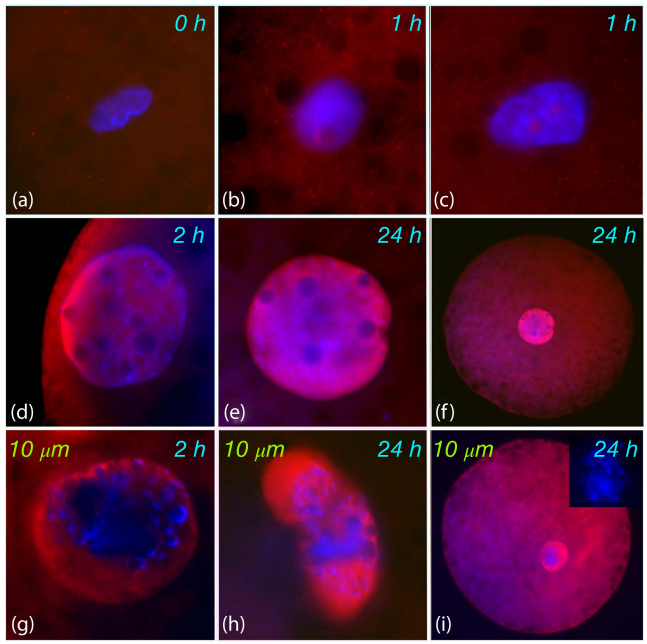

Figure 17.2 Visualization of proteasomes (red) and DNA (blue) in control SCNT zygotes and zygotes treated with 10 μM MG132. (a–d): Control, NT1 zygotes at the indicated time points after SCNT. (e): The MG132-pulsed NT2 zygote has a normal pronucleus at 24 h post SCNT (i.e., 22 h after removal of MG132). (g–i): Nuclei of zygotes exposed to MG132 continually for 24 h after SCNT. Note abnormal chromatin structure in parts (g) and (h), and failed remodeling in panel (i) (chromatin shown in insert). (Reproduced from Whitworth *et al*. (2009) with permission from Wiley.) (See color plate section.)

Downloaded From Vet-eBooks.com

beneficial compensatory effects by intersecting with other pro-proliferative pathways essential for pre-implantation development, such as the autophagic pathway (Lee *et al*., 2011; Tsukamoto *et al*., 2008).

17.9 Conclusions

Pronuclear biogenesis marks the onset of embryonic development, the success of which depends upon proper remodeling of paternal and maternal chromatin and proper reprogramming of their respective genomes. Animal model studies will continue to be useful for further exploration of how proteolytic and epigenome-regulating pathways intersect during normal pronuclear development, and how these pathway components' expression patterns and functions deviate in human diseases of embryonic origin. There are practical benefits to be derived from deeper knowledge of pronuclear biogenesis. In livestock species, modulation of proteasomal activities during late oocyte maturation period and early pronuclear stages could improve developmental potential of bovine and porcine embryos in commercial embryo transfer programs. Both livestock and rodent cloning/nuclear transfer procedures used to create transgenic animal models of human disease can be improved by the manipulation of donor cell nuclear remodeling and reprogramming with small molecule inhibitors targeting cytoplast/donor cell proteasomes and epigenome-regulating enzymes. If properly safeguarded, such pharmacological interventions could be incorporated into oocyte maturation and embryo culture protocols for human-assisted reproduction. Furthermore, the ever-expanding assisted reproductive therapy in humans will benefit from a better understanding of pronuclear development afforded by animal model studies. Learning more about human/animal zygote may allow clinicians to mitigate birth defects and adult onset diseases arising from altered pronuclear epigenomes brought about by inherently suboptimal IVF and embryo-culture conditions.

Acknowledgments

Some of the original work discussed in this chapter was supported by grant awards #2011-67015-20025, 2013-67015-20961, and 2015-67015-23231 from USDA National Institute of Food and Agriculture, and by the Food for the 21st Century Program funding from University of Missouri. We thank our long-time collaborators who have been working with us on various aspects of zygote/embryo development, including Drs. Randall Prather, Jaroslav Petr, Billy N. Day, Richard Oko, Kathy L. Sharpe-Timms, and Keith Latham, as well as our past and present graduate students, associates, and coworkers. Editorial assistance by Ms. Kathryn Craighead is sincerely appreciated.

References

Aagaard, L., Schmid, M., Warburton, P., and Jenuwein, T. (2000) Mitotic phosphorylation of SUV39H1, a novel component of active centromeres, coincides with transient accumulation at mammalian centromeres. *J. Cell Sci.*, **113** (Part 5), 817–829.

Adenot, P.G., Szollosi, M.S., Geze, M., Renard, J.P., and Debey, P. (1991) Dynamics of paternal chromatin changes in live one-cell mouse embryo after natural fertilization. *Mol. Reprod. Dev.*, **28**, 23–34.

Downloaded From Vet-eBooks.com

Adenot, P.G., Mercier, Y., Renard, J.P., and Thompson, E.M. (1997) Differential H4 acetylation of paternal and maternal chromatin precedes DNA replication and differential transcriptional activity in pronuclei of 1-cell mouse embryos. *Development*, **124**, 4615–4625.

Ajduk, A., Yamauchi, Y., and Ward, M.A. (2006) Sperm chromatin remodeling after intracytoplasmic sperm injection differs from that of *in vitro* fertilization. *Biol. Reprod.*, **75**, 442–451.

Angelov, D., Molla, A., Perche, P.Y., Hans, F., Cote, J., Khochbin, S., Bouvet, P., and Dimitrov, S. (2003) The histone variant macroH2A interferes with transcription factor binding and SWI/SNF nucleosome remodeling. *Mol. Cell*, **11**, 1033–1041.

Aoki, F., Worrad, D.M., and Schultz, R.M. (1997) Regulation of transcriptional activity during the first and second cell cycles in the preimplantation mouse embryo. *Dev. Biol.*, **181**, 296–307.

Arnan, C., Saperas, N., Prieto, C., Chiva, M., and Ausio, J. (2003) Interaction of nucleoplasmin with core histones. *J. Biol. Chem.*, **278**, 31319–31324.

Auclair, G. and Weber, M. (2012) Mechanisms of DNA methylation and demethylation in mammals. *Biochimie*, **94**, 2202–2211.

Bannister, A.J. and Miska, E.A. (2000) Regulation of gene expression by transcription factor acetylation. *Cell. Mol. Life Sci.*, **57**, 1184–1192.

Bannister, A.J., Zegerman, P., Partridge, J.F., Miska, E.A., Thomas, J.O., Allshire, R.C., and Kouzarides, T. (2001) Selective recognition of methylated lysine 9 on histone H3 by the HP1 chromo domain. *Nature*, **410**, 120–124.

Baur, T., Ramadan, K., Schlundt, A., Kartenbeck, J., and Meyer, H.H. (2007) NSF- and SNARE-mediated membrane fusion is required for nuclear envelope formation and completion of nuclear pore complex assembly in *Xenopus laevis* egg extracts. *J. Cell Sci.*, **120**, 2895–2903.

Bell, E.L., Nagamori, I., Williams, E.O., Del Rosario, A.M., Bryson, B.D., Watson, N., White, F.M., Sassone-Corsi, P., and Guarente, L. (2014) SirT1 is required in the male germ cell for differentiation and fecundity in mice. *Development*, **141**, 3495–3504.

Bernis, C. and Forbes, D.J. (2014) Analysis of nuclear reconstitution, nuclear envelope assembly, and nuclear pore assembly using *Xenopus in vitro* assays. *Methods Cell Biol.*, **122**, 165–191.

Bestor, T.H. (2000) The DNA methyltransferases of mammals. *Hum. Mol. Genet.*, **9**, 2395–2402.

Bird, A.P. and Wolffe, A.P. (1999) Methylation-induced repression: belts, braces, and chromatin. *Cell*, **99**, 451–454.

Black, J.C., Van Rechem, C., and Whetstine, J.R. (2012) Histone lysine methylation dynamics: establishment, regulation, and biological impact. *Mol. Cell*, **48**, 491–507.

Blackledge, N.P., Farcas, A.M., Kondo, T., King, H.W., McGouran, J.F., Hanssen, L.L., Ito, S., Cooper, S., Kondo, K., Koseki, Y. *et al.* (2014) Variant PRC1 complex-dependent H2A ubiquitylation drives PRC2 recruitment and polycomb domain formation. *Cell*, **157**, 1445–1459.

Bogliotti, Y.S. and Ross, P.J. (2012) Mechanisms of histone H3 lysine 27 trimethylation remodeling during early mammalian development. *Epigenetics*, **7**, 976–981.

Boman, A.L., Delannoy, M.R., and Wilson, K.L. (1992) GTP hydrolysis is required for vesicle fusion during nuclear envelope assembly *in vitro*. *J. Cell Biol.*, **116**, 281–294.

Bonisch, C. and Hake, S.B. (2012) Histone H2A variants in nucleosomes and chromatin: more or less stable? *Nucleic Acids Res.*, **40**, 10719–10741.

Bosch-Presegue, L., Raurell-Vila, H., Marazuela-Duque, A., Kane-Goldsmith, N., Valle, A., Oliver, J., Serrano, L., and Vaquero, A. (2011) Stabilization of Suv39H1 by SirT1 is part of oxidative stress response and ensures genome protection. *Mol. Cell*, **42**, 210–223.

Bouniol, C., Nguyen, E., and Debey, P. (1995) Endogenous transcription occurs at the 1-cell stage in the mouse embryo. *Exp. Cell Res.*, **218**, 57–62.

Downloaded From Vet-eBooks.com

Brero, A., Hao, R., Schieker, M., Wierer, M., Wolf, E., Cremer, T., and Zakhartchenko, V. (2009) Reprogramming of active and repressive histone modifications following nuclear transfer with rabbit mesenchymal stem cells and adult fibroblasts. *Cloning Stem Cells*, **11**, 319–329.

Brownell, J.E. and Allis, C.D. (1996) Special HATs for special occasions: linking histone acetylation to chromatin assembly and gene activation. *Curr.Opin. Genet. Dev.*, **6**, 176–184.

Buendia, B. and Courvalin, J.C. (1997) Domain-specific disassembly and reassembly of nuclear membranes during mitosis. *Exp. Cell Res.*, **230**, 133–144.

Burns, K.H. and Matzuk, M.M. (2006) Preimplantation embryogenesis, in *Knobil and Neill's Physiology of Reproduction*, 3rd edn (ed. J.D. Neill), Elsevier Inc., pp. 261–310.

Burns, K.H., Viveiros, M.M., Ren, Y., Wang, P., DeMayo, F.J., Frail, D.E., Eppig, J.J., and Matzuk, M.M. (2003) Roles of NPM2 in chromatin and nucleolar organization in oocytes and embryos. *Science*, **300**, 633–636.

Camous, S., Kopecny, V., and Flechon, J.E. (1986) Autoradiographic detection of the earliest stage of [3*H*]-uridine incorporation into the cow embryo. *Biol. Cell*, **58**, 195–200.

Canto, C. and Auwerx, J. (2009) Caloric restriction, SIRT1 and longevity. *Trends Endocrinol. Metab.*, **20**, 325–331.

Cao, R., Wang, L., Wang, H., Xia, L., Erdjument-Bromage, H., Tempst, P., Jones, R.S., and Zhang, Y. (2002) Role of histone H3 lysine 27 methylation in Polycomb-group silencing. *Science*, **298**, 1039–1043.

Celeste, A., Petersen, S., Romanienko, P.J., Fernandez-Capetillo, O., Chen, H.T., Sedelnikova, O.A., Reina-San-Martin, B., Coppola, V., Meffre, E., Difilippantonio, M.J. *et al*. (2002) Genomic instability in mice lacking histone H2AX. *Science*, **296**, 922–927.

Chao, C.C. (2014) Mechanisms of p53 degradation. *Clin. Chim. Acta*, **438**, 139–147.

Cheedipudi, S., Genolet, O., and Dobreva, G. (2014) Epigenetic inheritance of cell fates during embryonic development. *Front. Genet.*, **5**, 19.

Chen, H.Y., Sun, J.M., Zhang, Y., Davie, J.R., and Meistrich, M.L. (1998) Ubiquitination of histone H3 in elongating spermatids of rat testes. *J. Biol. Chem.*, **273**, 13165–13169.

Chen, L., Li, Z., Zwolinska, A.K., Smith, M.A., Cross, B., Koomen, J., Yuan, Z.M., Jenuwein, T., Marine, J.C., Wright, K.L. *et al*. (2010) MDM2 recruitment of lysine methyltransferases regulates p53 transcriptional output. *EMBO J.*, **29**, 2538–2552.

Cho, T., Sakai, S., Nagata, M., and Aoki, K. (2002) Involvement of chromatin structure in the regulation of mouse zygotic gene activation. *Anim. Sci. J.*, **73**, 113–122.

Collas, P. and Poccia, D. (1998a) Methods for studying *in vitro* assembly of male pronuclei using oocyte extracts from marine invertebrates: sea urchins and surf clams. *Methods Cell Biol.*, **53**, 417–452.

Collas, P. and Poccia, D. (1998b) Remodeling the sperm nucleus into a male pronucleus at fertilization. *Theriogenology*, **49**, 67–81.

Collas, P., Courvalin, J.C., and Poccia, D. (1996) Targeting of membranes to sea urchin sperm chromatin is mediated by a lamin B receptor-like integral membrane protein. *J. Cell Biol.*, **135**, 1715–1725.

Coskun, S., Hellani, A., Jaroudi, K., Al-Mayman, H., Al-Kabra, M., and Qeba, M. (2003) Nucleolar precursor body distribution in pronuclei is correlated to chromosomal abnormalities in embryos. *Reprod. Biomed. Online*, **7**, 86–90.

Coussens, M., Maresh, J.G., Yanagimachi, R., Maeda, G., and Allsopp, R. (2008) Sirt1 deficiency attenuates spermatogenesis and germ cell function. *PLoS One*, **3**, e1571.

Dabauvalle, M.C., Loos, K., Merkert, H., and Scheer, U. (1991) Spontaneous assembly of pore complex-containing membranes ("annulate lamellae") in *Xenopus* egg extract in the absence of chromatin. *J. Cell Biol.*, **112**, 1073–1082.

Downloaded From Vet-eBooks.com

Dangond, F., Henriksson, M., Zardo, G., Caiafa, P., Ekstrom, T.J., and Gray, S.G. (2001) Differential expression of class I HDACs: roles of cell density and cell cycle. *Int. J. Oncol.*, **19**, 773–777.

Davis, L.I. and Blobel, G. (1986) Identification and characterization of a nuclear pore complex protein. *Cell*, **45**, 699–709.

Dean, W. and Ferguson-Smith, A. (2001) Genomic imprinting: mother maintains methylation marks. *Curr. Biol.*, **11**, R527–R530.

Dean, W.L. and Schultz, G.A. (1990) Relocalization of small ribonucleoprotein particles (snRNPs) during the first cell cycle of mouse embryo development is independent of RNA synthesis, DNA synthesis and cytokinesis. *Cell Differ. Dev.*, **31**, 43–51.

DeRenzo, C. and Seydoux, G. (2004) A clean start: degradation of maternal proteins at the oocyte-to-embryo transition. *Trends Cell Biol.*, **14**, 420–426.

Di Emidio, G., Falone, S., Vitti, M., D'Alessandro, A.M., Vento, M., Di Pietro, C., Amicarelli, F., and Tatone, C. (2014) SIRT1 signalling protects mouse oocytes against oxidative stress and is deregulated during aging. *Hum. Reprod.*, **29**, 2006–2017.

Dou, Y., Milne, T.A., Ruthenburg, A.J., Lee, S., Lee, J.W., Verdine, G.L., Allis, C.D., and Roeder, R.G. (2006) Regulation of MLL1 H3K4 methyltransferase activity by its core components. *Nat. Struct. Mol. Biol.*, **13**, 713–719.

Dreier, L. and Rapoport, T.A. (2000) *In vitro* formation of the endoplasmic reticulum occurs independently of microtubules by a controlled fusion reaction. *J. Cell Biol.*, **148**, 883–898.

Ducibella, T., Huneau, D., Angelichio, E., Xu, Z., Schultz, R.M., Kopf, G.S., Fissore, R., Madoux, S., and Ozil, J.P. (2002) Egg-to-embryo transition is driven by differential responses to Ca(2+) oscillation number. *Dev. Biol.*, **250**, 280–291.

Eissenberg, J.C. and Shilatifard, A. (2010) Histone H3 lysine 4 (H3K4) methylation in development and differentiation. *Dev. Biol.*, **339**, 240–249.

Ekwall, K., Olsson, T., Turner, B.M., Cranston, G., and Allshire, R.C. (1997) Transient inhibition of histone deacetylation alters the structural and functional imprint at fission yeast centromeres. *Cell*, **91**, 1021–1032.

Esteve, P.O., Patnaik, D., Chin, H.G., Benner, J., Teitell, M.A., and Pradhan, S. (2005) Functional analysis of the N- and C-terminus of mammalian G9a histone H3 methyltransferase. *Nucleic Acids Res.*, **33**, 3211–3223.

Fang, R., Barbera, A.J., Xu, Y., Rutenberg, M., Leonor, T., Bi, Q., Lan, F., Mei, P., Yuan, G.C., Lian, C. *et al.* (2010) Human LSD2/KDM1b/AOF1 regulates gene transcription by modulating intragenic H3K4me2 methylation. *Mol. Cell*, **39**, 222–233.

Firestein, R., Cui, X., Huie, P., and Cleary, M.L. (2000) Set domain-dependent regulation of transcriptional silencing and growth control by SUV39H1, a mammalian ortholog of *Drosophila* Su(var)3-9. *Mol. Cell. Biol.*, **20**, 4900–4909.

Flanagan, J.F., Mi, L.Z., Chruszcz, M., Cymborowski, M., Clines, K.L., Kim, Y., Minor, W., Rastinejad, F., and Khorasanizadeh, S. (2005) Double chromodomains cooperate to recognize the methylated histone H3 tail. *Nature*, **438**, 1181–1185.

Florman, H.M. and Ducibella, T. (2006) Fertilization in mammals, in *Knobil and Neill's Physiology of Reproduction* (ed. J.D. Neill), Elsevier Inc., pp. 55–112.

Franz, C., Askjaer, P., Antonin, W., Iglesias, C.L., Haselmann, U., Schelder, M., de Marco, A., Wilm, M., Antony, C., and Mattaj, I.W. (2005) Nup155 regulates nuclear envelope and nuclear pore complex formation in nematodes and vertebrates. *EMBO J.*, **24**, 3519–3531.

Fu, W., Ma, Q., Chen, L., Li, P., Zhang, M., Ramamoorthy, S., Nawaz, Z., Shimojima, T., Wang, H., Yang, Y. *et al.* (2009) MDM2 acts downstream of p53 as an E3 ligase to promote FOXO ubiquitination and degradation. *J. Biol. Chem.*, **284**, 13987–14000.

Fuentes-Mascorro, G., Serrano, H., and Rosado, A. (2000) Sperm chromatin. *Arch. Androl.*, **45**, 215–225.

Downloaded From Vet-eBooks.com

Fulka, H. and Langerova, A. (2014) The maternal nucleolus plays a key role in centromere satellite maintenance during the oocyte to embryo transition. *Development*, **141**, 1694–1704.

Gao, S., Chung, Y.G., Parseghian, M.H., King, G.J., Adashi, E.Y., and Latham, K.E. (2004) Rapid H1 linker histone transitions following fertilization or somatic cell nuclear transfer: evidence for a uniform developmental program in mice. *Dev. Biol.*, **266**, 62–75.

Gao, S., Han, Z., Kihara, M., Adashi, E., and Latham, K.E. (2005) Protease inhibitor MG132 in cloning: no end to the nightmare. *Trends Biotechnol.*, **23**, 66–68.

Gardiner-Garden, M., Ballesteros, M., Gordon, M., and Tam, P.P. (1998) Histone- and protamine-DNA association: conservation of different patterns within the beta-globin domain in human sperm. *Mol. Cell. Biol.*, **18**, 3350–3356.

Gerace, L. and Burke, B. (1988) Functional organization of the nuclear envelope. *Annu. Rev. Cell. Biol.*, **4**, 335–374.

Giraldo, A.M., DeCourcy, K., Ball, S.F., Hylan, D., and Ayares, D.L. (2013) Gene expression of Dnmt1 isoforms in porcine oocytes, embryos, and somatic cells. *Cell Reprogram.*, **15**, 309–321.

Gkountela, S. and Clark, A.T. (2014) A big surprise in the little zygote: the curious business of losing methylated cytosines. *Cell Stem Cell*, **15**, 393–394.

Glickman, M.H. and Ciechanover, A. (2002) The ubiquitin-proteasome proteolytic pathway: destruction for the sake of construction. *Physiol. Rev.*, **82**, 373–428.

Glotzer, M., Murray, A.W., and Kirschner, M.W. (1991) Cyclin is degraded by the ubiquitin pathway. *Nature*, **349**, 132–138.

Goldberg, M.W., Wiese, C., Allen, T.D., and Wilson, K.L. (1997) Dimples, pores, star-rings, and thin rings on growing nuclear envelopes: evidence for structural intermediates in nuclear pore complex assembly. *J. Cell Sci.*, **110** (Pt 4), 409–420.

Gonzalez-Granado, J.M., Navarro-Puche, A., Molina-Sanchez, P., Blanco-Berrocal, M., Viana, R., Font de Mora, J., and Andres, V. (2014) Sorting nexin 6 enhances lamin a synthesis and incorporation into the nuclear envelope. *PLoS One*, **9**, e115571.

Grewal, S.I. and Jia, S. (2007) Heterochromatin revisited. *Nat. Rev. Genet.*, **8**, 35–46.

Grunstein, M. (1997) Molecular model for telomeric heterochromatin in yeast. *Curr. Opin. Cell Biol.*, **9**, 383–387.

Gu, T.P., Guo, F., Yang, H., Wu, H.P., Xu, G.F., Liu, W., Xie, Z.G., Shi, L., He, X., Jin, S.G. *et al.* (2011) The role of Tet3 DNA dioxygenase in epigenetic reprogramming by oocytes. *Nature*, **477**, 606–610.

Guo, H., Zhu, P., Yan, L., Li, R., Hu, B., Lian, Y., Yan, J., Ren, X., Lin, S., Li, J. *et al.* (2014) The DNA methylation landscape of human early embryos. *Nature*, **511**, 606–610.

Haigis, M.C. and Guarente, L.P. (2006) Mammalian sirtuins--emerging roles in physiology, aging, and calorie restriction. *Genes Dev.*, **20**, 2913–2921.

Hajkova, P., Jeffries, S.J., Lee, C., Miller, N., Jackson, S.P., and Surani, M.A. (2010) Genome-wide reprogramming in the mouse germ line entails the base excision repair pathway. *Science*, **329**, 78–82.

Hamdane, N., Stefanovsky, V.Y., Tremblay, M.G., Nemeth, A., Paquet, E., Lessard, F., Sanij, E., Hannan, R., and Moss, T. (2014) Conditional inactivation of upstream binding factor reveals its epigenetic functions and the existence of a somatic nucleolar precursor body. *PLoS Genet.*, **10**, e1004505.

Han, Z., Mtango, N.R., Zhong, Z., Vassena, R., and Latham, K.E. (2010) Early transcription from the maternal genome controlling blastomere integrity in mouse two-cell-stage embryos. *Am. J. Physiol. Cell Physiol.*, **298**, C1235–C1244.

Hanover, J.A., Cohen, C.K., Willingham, M.C., and Park, M.K. (1987) *O*-Linked *N*-acetylglucosamine is attached to proteins of the nuclear pore: evidence for cytoplasmic and nucleoplasmic glycoproteins. *J. Biol. Chem.*, **262**, 9887–9894.

Downloaded From Vet-eBooks.com

He, Y.F., Li, B.Z., Li, Z., Liu, P., Wang, Y., Tang, Q., Ding, J., Jia, Y., Chen, Z., Li, L. *et al*. (2011) Tet-mediated formation of 5-carboxylcytosine and its excision by TDG in mammalian DNA. *Science*, **333**, 1303–1307.

Hebbes, T.R., Thorne, A.W., and Crane-Robinson, C. (1988) A direct link between core histone acetylation and transcriptionally active chromatin. *EMBO J.*, **7**, 1395–1402.

Hebbes, T.R., Clayton, A.L., Thorne, A.W., and Crane-Robinson, C. (1994) Core histone hyperacetylation co-maps with generalized DNase I sensitivity in the chicken beta-globin chromosomal domain. *EMBO J.*, **13**, 1823–1830.

Heintzman, N.D., Stuart, R.K., Hon, G., Fu, Y., Ching, C.W., Hawkins, R.D., Barrera, L.O., Van Calcar, S., Qu, C., Ching, K.A. *et al*. (2007) Distinct and predictive chromatin signatures of transcriptional promoters and enhancers in the human genome. *Nat. Genet.*, **39**, 311–318.

Hendzel, M.J., Wei, Y., Mancini, M.A., Van Hooser, A., Ranalli, T., Brinkley, B.R., Bazett-Jones, D.P., and Allis, C.D. (1997) Mitosis-specific phosphorylation of histone H3 initiates primarily within pericentromeric heterochromatin during G2 and spreads in an ordered fashion coincident with mitotic chromosome condensation. *Chromosoma*, **106**, 348–360.

Heride, C., Urbe, S., and Clague, M.J. (2014) Ubiquitin code assembly and disassembly. *Curr. Biol.*, **24**, R215–R220.

Herranz, D., Munoz-Martin, M., Canamero, M., Mulero, F., Martinez-Pastor, B., Fernandez-Capetillo, O., and Serrano, M. (2010) Sirt1 improves healthy ageing and protects from metabolic syndrome-associated cancer. *Nat. Commun.*, **1**, 3.

Hetzer, M., Bilbao-Cortes, D., Walther, T.C., Gruss, O.J., and Mattaj, I.W. (2000) GTP hydrolysis by Ran is required for nuclear envelope assembly. *Mol. Cell*, **5**, 1013–1024.

Hetzer, M., Meyer, H.H., Walther, T.C., Bilbao-Cortes, D., Warren, G., and Mattaj, I.W. (2001) Distinct AAA-ATPase p97 complexes function in discrete steps of nuclear assembly. *Nat. Cell Biol.*, **3**, 1086–1091.

Hetzer, M.W., Walther, T.C., and Mattaj, I.W. (2005) Pushing the envelope: structure, function, and dynamics of the nuclear periphery. *Annu. Rev. Cell. Dev. Biol.*, **21**, 347–380.

Hirano, Y., Hizume, K., Kimura, H., Takeyasu, K., Haraguchi, T., and Hiraoka, Y. (2012) Lamin B receptor recognizes specific modifications of histone H4 in heterochromatin formation. *J. Biol. Chem.*, **287**, 42654–42663.

Hirasawa, R., Chiba, H., Kaneda, M., Tajima, S., Li, E., Jaenisch, R., and Sasaki, H. (2008) Maternal and zygotic Dnmt1 are necessary and sufficient for the maintenance of DNA methylation imprints during preimplantation development. *Genes Dev.*, **22**, 1607–1616.

Holaska, J.M., Wilson, K.L., and Mansharamani, M. (2002) The nuclear envelope, lamins and nuclear assembly. *Curr. Opin. Cell Biol.*, **14**, 357–364.

Hud, N.V., Allen, M.J., Downing, K.H., Lee, J., and Balhorn, R. (1993) Identification of the elemental packing unit of DNA in mammalian sperm cells by atomic force microscopy. *Biochem. Biophys. Res. Commun.*, **193**, 1347–1354.

Huo, L.J., Fan, H.Y., Liang, C.G., Yu, L.Z., Zhong, Z.S., Chen, D.Y., and Sun, Q.Y. (2004) Regulation of ubiquitin-proteasome pathway on pig oocyte meiotic maturation and fertilization. *Biol. Reprod.*, **71**, 853–862.

Hutchison, C.J., Bridger, J.M., Cox, L.S., and Kill, I.R. (1994) Weaving a pattern from disparate threads: lamin function in nuclear assembly and DNA replication. *J. Cell Sci.*, **107** (Pt 12), 3259–3269.

Hyttel, P., Laurincik, J., Rosenkranz, C., Rath, D., Niemann, H., Ochs, R.L., and Schellander, K. (2000) Nucleolar proteins and ultrastructure in preimplantation porcine embryos developed *in vivo*. *Biol. Reprod.*, **63**, 1848–1856.

Imai, S., Armstrong, C.M., Kaeberlein, M., and Guarente, L. (2000) Transcriptional silencing and longevity protein Sir2 is an NAD-dependent histone deacetylase. *Nature*, **403**, 795–800.

Downloaded From Vet-eBooks.com

Imschenetzky, M., Puchi, M., Morin, V., Diaz, F., Oliver, M.I., and Montecino, M. (1999) Potential involvement of post-translational modifications as a mechanism modulating selective proteolysis after fertilization. *J. Cell. Biochem.*, **(Suppl. 32–33)**, 149–157.

Inoue, A. and Zhang, Y. (2014) Nucleosome assembly is required for nuclear pore complex assembly in mouse zygotes. *Nat. Struct. Mol. Biol.*, **21**, 609–616.

Inoue, A., Ogushi, S., Saitou, M., Suzuki, M.G., and Aoki, F. (2011) Involvement of mouse nucleoplasmin 2 in the decondensation of sperm chromatin after fertilization. *Biol. Reprod.*, **85**, 70–77.

Iqbal, K., Jin, S.G., Pfeifer, G.P., and Szabo, P.E. (2011) Reprogramming of the paternal genome upon fertilization involves genome-wide oxidation of 5-methylcytosine. *Proc. Natl. Acad. Sci. USA*, **108**, 3642–3647.

Ishibashi, T., Li, A., Eirin-Lopez, J.M., Zhao, M., Missiaen, K., Abbott, D.W., Meistrich, M., Hendzel, M.J., and Ausio, J. (2010) H2A.Bbd: an X-chromosome-encoded histone involved in mammalian spermiogenesis. *Nucleic Acids Res.*, **38**, 1780–1789.

Jacobs, S.A. and Khorasanizadeh, S. (2002) Structure of HP1 chromodomain bound to a lysine 9-methylated histone H3 tail. *Science*, **295**, 2080–2083.

Jahn, R., Lang, T., and Sudhof, T.C. (2003) Membrane fusion. *Cell*, **112**, 519–533.

Jeong, Y.S., Yeo, S., Park, J.S., Koo, D.B., Chang, W.K., Lee, K.K., and Kang, Y.K. (2007) DNA methylation state is preserved in the sperm-derived pronucleus of the pig zygote. *Int. J. Dev. Biol.*, **51**, 707–714.

Jeppesen, P., Mitchell, A., Turner, B., and Perry, P. (1992) Antibodies to defined histone epitopes reveal variations in chromatin conformation and underacetylation of centric heterochromatin in human metaphase chromosomes. *Chromosoma*, **101**, 322–332.

Jermann, P., Hoerner, L., Burger, L., and Schubeler, D. (2014) Short sequences can efficiently recruit histone H3 lysine 27 trimethylation in the absence of enhancer activity and DNA methylation. *Proc. Natl. Acad. Sci. USA*, **111**, E3415–E3421.

Johnson, L., Cao, X., and Jacobsen, S. (2002) Interplay between two epigenetic marks: DNA methylation and histone H3 lysine 9 methylation. *Curr. Biol.*, **12**, 1360–1367.

Jullien, J., Astrand, C., Halley-Stott, R.P., Garrett, N., and Gurdon, J.B. (2010) Characterization of somatic cell nuclear reprogramming by oocytes in which a linker histone is required for pluripotency gene reactivation. *Proc. Natl. Acad. Sci. USA*, **107**, 5483–5488.

Jullien, J., Pasque, V., Halley-Stott, R.P., Miyamoto, K., and Gurdon, J.B. (2011) Mechanisms of nuclear reprogramming by eggs and oocytes: a deterministic process? *Nat. Rev. Mol. Cell. Biol.*, **12**, 453–459.

Jullien, J., Astrand, C., Szenker, E., Garrett, N., Almouzni, G., and Gurdon, J.B. (2012) HIRA dependent H3.3 deposition is required for transcriptional reprogramming following nuclear transfer to *Xenopus* oocytes. *Epigenetics Chromatin*, **5**, 17.

Jung, T. and Grune, T. (2013) The proteasome and the degradation of oxidized proteins. Part I: structure of proteasomes. *Redox Biol.*, **1**, 178–182.

Jung, T., Hohn, A., and Grune, T. (2013) The proteasome and the degradation of oxidized proteins. Part II: protein oxidation and proteasomal degradation. *Redox Biol.*, **2C**, 99–104.

Kafer, G.R., Lehnert, S.A., Pantaleon, M., Kaye, P.L., and Moser, R.J. (2010) Expression of genes coding for histone variants and histone-associated proteins in pluripotent stem cells and mouse preimplantation embryos. *Gene Exp. Patterns*, **10**, 299–305.

Kalb, R., Latwiel, S., Baymaz, H.I., Jansen, P.W., Muller, C.W., Vermeulen, M., and Muller, J. (2014) Histone H2A monoubiquitination promotes histone H3 methylation in polycomb repression. *Nat. Struct. Mol. Biol.*, **21**, 569–571.

Kamakaka, R.T. and Biggins, S. (2005) Histone variants: deviants? *Genes Dev.*, **19**, 295–310.

Downloaded From Vet-eBooks.com

Kanka, J., Fulka, J., Jr., Fulka, J., and Petr, J. (1991) Nuclear transplantation in bovine embryo: fine structural and autoradiographic studies. *Mol. Reprod. Dev.*, **29**, 110–116.

Kanka, J., Hozak, P., Heyman, Y., Chesne, P., Degrolard, J., Renard, J.P., and Flechon, J.E. (1996) Transcriptional activity and nucleolar ultrastructure of embryonic rabbit nuclei after transplantation to enucleated oocytes. *Mol. Reprod. Dev.*, **43**, 135–144.

Karabinova, P., Kubelka, M., and Susor, A. (2011) Proteasomal degradation of ubiquitinated proteins in oocyte meiosis and fertilization in mammals. *Cell Tissue Res.*, **346**, 1–9.

Karagianni, P., Amazit, L., Qin, J., and Wong, J. (2008) ICBP90, a novel methyl K9 H3 binding protein linking protein ubiquitination with heterochromatin formation. *Mol. Cell Biol.*, **28**, 705–717.

Kato, Y., Kaneda, M., Hata, K., Kumaki, K., Hisano, M., Kohara, Y., Okano, M., Li, E., Nozaki, M., and Sasaki, H. (2007) Role of the Dnmt3 family in *de novo* methylation of imprinted and repetitive sequences during male germ cell development in the mouse. *Hum. Mol. Genet.*, **16**, 2272–2280.

Kawahara, T.L., Michishita, E., Adler, A.S., Damian, M., Berber, E., Lin, M., McCord, R.A., Ongaigui, K.C., Boxer, L.D., Chang, H.Y. *et al.* (2009) SIRT6 links histone H3 lysine 9 deacetylation to NF-kappaB-dependent gene expression and organismal life span. *Cell*, **136**, 62–74.

Kawamura, Y., Uchijima, Y., Horike, N., Tonami, K., Nishiyama, K., Amano, T., Asano, T., Kurihara, Y., and Kurihara, H. (2010) Sirt3 protects *in vitro*-fertilized mouse preimplantation embryos against oxidative stress-induced p53-mediated developmental arrest. *J. Clin. Invest.*, **120**, 2817–2828.

Kim, E.J. and Um, S.J. (2008) SIRT1: roles in aging and cancer. *BMB Rep.*, **41**, 751–756.

Kim, J.M., Liu, H., Tazaki, M., Nagata, M., and Aoki, F. (2003) Changes in histone acetylation during mouse oocyte meiosis. *J. Cell Biol.*, **162**, 37–46.

King, W.A., Shepherd, D.L., Plante, L., Lavoir, M.C., Looney, C.R., and Barnes, F.L. (1996) Nucleolar and mitochondrial morphology in bovine embryos reconstructed by nuclear transfer. *Mol. Reprod. Dev.*, **44**, 499–506.

Klose, R.J., Kallin, E.M., and Zhang, Y. (2006) JmjC-domain-containing proteins and histone demethylation. *Nat. Rev. Genet.*, **7**, 715–727.

Kohli, R.M. and Zhang, Y. (2013) TET enzymes, TDG and the dynamics of DNA demethylation. *Nature*, **502**, 472–479.

Komander, D. and Rape, M. (2012) The ubiquitin code. *Annu. Rev. Biochem.*, **81**, 203–229.

Kopecny, V., Flechon, J.E., Camous, S., and Fulka, J., Jr. (1989) Nucleologenesis and the onset of transcription in the eight-cell bovine embryo: fine-structural autoradiographic study. *Mol. Reprod. Dev.*, **1**, 79–90.

Kuo, L.J. and Yang, L.X. (2008) Gamma-H2AX: a novel biomarker for DNA double-strand breaks. *In Vivo*, **22**, 305–309.

Kwak, S.S., Cheong, S.A., Yoon, J.D., Jeon, Y., and Hyun, S.H. (2012) Expression patterns of sirtuin genes in porcine preimplantation embryos and effects of sirtuin inhibitors on *in vitro* embryonic development after parthenogenetic activation and *in vitro* fertilization. *Theriogenology*, **78**, 1597–1610.

Kyogoku, H., Fulka, J., Jr., Wakayama, T., and Miyano, T. (2014) *De novo* formation of nucleoli in developing mouse embryos originating from enucleolated zygotes. *Development*, **141**, 2255–2259.

Lachner, M., O'Carroll, D., Rea, S., Mechtler, K., and Jenuwein, T. (2001) Methylation of histone H3 lysine 9 creates a binding site for HP1 proteins. *Nature*, **410**, 116–120.

Landry, J., Sutton, A., Tafrov, S.T., Heller, R.C., Stebbins, J., Pillus, L., and Sternglanz, R. (2000) The silencing protein SIR2 and its homologs are NAD-dependent protein deacetylases. *Proc. Natl. Acad. Sci. USA*, **97**, 5807–5811.

Downloaded From Vet-eBooks.com

Latham, K.E. (1999) Mechanisms and control of embryonic genome activation in mammalian embryos. *Int. Rev. Cytol.*, **193**, 71–124.

Latham, K.E. and Sapienza, C. (1998) Localization of genes encoding egg modifiers of paternal genome function to mouse chromosomes one and two. *Development*, **125**, 929–935.

Latham, K.E. and Schultz, R.M. (2001) Embryonic genome activation. *Front Biosci.*, **6**, D748–D759.

Latham, K.E., Garrels, J.I., Chang, C., and Solter, D. (1991) Quantitative analysis of protein synthesis in mouse embryos. I: extensive reprogramming at the one- and two-cell stages. *Development*, **112**, 921–932.

Latham, K.E., Gao, S., and Han, Z. (2007) Somatic cell nuclei in cloning: strangers traveling in a foreign land. *Adv. Exp. Med. Biol.*, **591**, 14–29.

Laurincik, J., Bjerregaard, B., Strejcek, F., Rath, D., Niemann, H., Rosenkranz, C., Ochs, R.L., and Maddox-Hyttel, P. (2004) Nucleolar ultrastructure and protein allocation in *in vitro* produced porcine embryos. *Mol. Reprod. Dev.*, **68**, 327–334.

Lavoir, M.C., Kelk, D., Rumph, N., Barnes, F., Betteridge, K.J., and King, W.A. (1997) Transcription and translation in bovine nuclear transfer embryos. *Biol. Reprod.*, **57**, 204–213.

Le Bourhis, D., Beaujean, N., Ruffini, S., Vignon, X., and Gall, L. (2010) Nuclear remodeling in bovine somatic cell nuclear transfer embryos using MG132-treated recipient oocytes. *Cell Reprogram.*, **12**, 729–738.

Lee, D.Y., Hayes, J.J., Pruss, D., and Wolffe, A.P. (1993) A positive role for histone acetylation in transcription factor access to nucleosomal DNA. *Cell*, **72**, 73–84.

Lee, S.E., Hwang, K.C., Sun, S.C., Xu, Y.N., and Kim, N.H. (2011) Modulation of autophagy influences development and apoptosis in mouse embryos developing *in vitro*. *Mol. Reprod. Dev.*, **78**, 498–509.

Lee, M., Choi, Y., Kim, K., Jin, H., Lim, J., Nguyen, T.A., Yang, J., Jeong, M., Giraldez, A.J., Yang, H. *et al.* (2014) Adenylation of maternally inherited microRNAs by Wispy. *Mol. Cell*, **56**, 696–707.

Lehnertz, B., Ueda, Y., Derijck, A.A., Braunschweig, U., Perez-Burgos, L., Kubicek, S., Chen, T., Li, E., Jenuwein, T., and Peters, A.H. (2003) Suv39h-mediated histone H3 lysine 9 methylation directs DNA methylation to major satellite repeats at pericentric heterochromatin. *Curr. Biol.*, **13**, 1192–1200.

Leno, G.H., Downes, C.S., and Laskey, R.A. (1992) The nuclear membrane prevents replication of human G2 nuclei but not G1 nuclei in *Xenopus* egg extract. *Cell*, **69**, 151–158.

Lepikhov, K. and Walter, J. (2004) Differential dynamics of histone H3 methylation at positions K4 and K9 in the mouse zygote. *BMC Dev. Biol.*, **4**, 12.

Liu, H., Kim, J.M., and Aoki, F. (2004) Regulation of histone H3 lysine 9 methylation in oocytes and early pre-implantation embryos. *Development*, **131**, 2269–2280.

Lohka, M.J. (1998) Analysis of nuclear envelope assembly using extracts of *Xenopus* eggs. *Methods Cell Biol.*, **53**, 367–395.

Lohka, M.J. and Masui, Y. (1984) Roles of cytosol and cytoplasmic particles in nuclear envelope assembly and sperm pronuclear formation in cell-free preparations from amphibian eggs. *J. Cell Biol.*, **98**, 1222–1230.

Lundgren, J., Masson, P., Mirzaei, Z., and Young, P. (2005) Identification and characterization of a *Drosophila* proteasome regulatory network. *Mol. Cell Biol.*, **25**, 4662–4675.

Lyko, F. (2001) DNA methylation learns to fly. *Trends Genet.*, **17**, 169–172.

Ma, J.Y., Zhao, K., OuYang, Y.C., Wang, Z.B., Luo, Y.B., Hou, Y., Schatten, H., Shen, W., and Sun, Q.Y. (2014) Exogenous thymine DNA glycosylase regulates epigenetic modifications and meiotic cell cycle progression of mouse oocytes. *Mol. Hum. Reprod.*, **21**, 186–194.

Macaulay, C. and Forbes, D.J. (1996) Assembly of the nuclear pore: biochemically distinct steps revealed with NEM, GTP gamma S, and BAPTA. *J. Cell Biol.*, **132**, 5–20.

Downloaded From Vet-eBooks.com

Maeda, Y., Yanagimachi, H., Tateno, H., Usui, N., and Yanagimachi, R. (1998) Decondensation of the mouse sperm nucleus within the interphase nucleus. *Zygote*, **6**, 39–45.

Maison, C. and Almouzni, G. (2004) HP1 and the dynamics of heterochromatin maintenance. *Nat. Rev. Mol. Cell. Biol.*, **5**, 296–304.

Majumder, S., Zhao, Z., Kaneko, K., and DePamphilis, M.L. (1997) Developmental acquisition of enhancer function requires a unique coactivator activity. *EMBO J.*, **16**, 1721–1731.

Mao, J., Tessanne, K., Whitworth, K.M., Spate, L.D., Walters, E.M., Samuel, M.S., Murphy, C.N., Tracy, L., Zhao, J., and Prather, R.S. (2012) Effects of combined treatment of MG132 and scriptaid on early and term development of porcine somatic cell nuclear transfer embryos. *Cell Reprogram.*, **14**, 385–389.

Martins, R.P., Ostermeier, G.C., and Krawetz, S.A. (2004) Nuclear matrix interactions at the human protamine domain: a working model of potentiation. *J. Biol. Chem.*, **279**, 51862–51868.

Matoba, S., Liu, Y., Lu, F., Iwabuchi, K.A., Shen, L., Inoue, A., and Zhang, Y. (2014) Embryonic development following somatic cell nuclear transfer impeded by persisting histone methylation. *Cell*, **159**, 884–895.

Mayer, W., Niveleau, A., Walter, J., Fundele, R., and Haaf, T. (2000) Demethylation of the zygotic paternal genome. *Nature*, **403**, 501–502.

McLay, D.W. and Clarke, H.J. (2003) Remodelling the paternal chromatin at fertilization in mammals. *Reproduction*, **125**, 625–633.

Mietton, F., Sengupta, A.K., Molla, A., Picchi, G., Barral, S., Heliot, L., Grange, T., Wutz, A., and Dimitrov, S. (2009) Weak but uniform enrichment of the histone variant macroH2A1 along the inactive X chromosome. *Mol. Cell Biol.*, **29**, 150–156.

Milner, J. (2009) Cellular regulation of SIRT1. *Curr. Pharm. Des.*, **15**, 39–44.

Mizumoto, S., Kato, Y., and Tsunoda, Y. (2009) The effect of the time interval between injection and parthenogenetic activation on the spindle formation and the *in vitro* developmental potential of somatic cell nuclear-transferred rat oocytes. *Zygote*, **18**, 9–15.

Mizzen, C.A., Yang, X.J., Kokubo, T., Brownell, J.E., Bannister, A.J., Owen-Hughes, T., Workman, J., Wang, L., Berger, S.L., Kouzarides, T. *et al.* (1996) The TAF(II)250 subunit of TFIID has histone acetyltransferase activity. *Cell*, **87**, 1261–1270.

Monk, M. and Salpekar, A. (2001) Expression of imprinted genes in human preimplantation development. *Mol. Cell Endocrinol.*, **183** (Suppl. 1), S35–S40.

Moos, J., Visconti, P.E., Moore, G.D., Schultz, R.M., and Kopf, G.S. (1995) Potential role of mitogen-activated protein kinase in pronuclear envelope assembly and disassembly following fertilization of mouse eggs. *Biol. Reprod.*, **53**, 692–699.

Moos, J., Xu, Z., Schultz, R.M., and Kopf, G.S. (1996) Regulation of nuclear envelope assembly/disassembly by MAP kinase. *Dev. Biol.*, **175**, 358–361.

Mtango, N.R., Potireddy, S., and Latham, K.E. (2008) Oocyte quality and maternal control of development. *Int. Rev. Cell. Mol. Biol.*, **268**, 223–290.

Mulugeta Achame, E., Wassenaar, E., Hoogerbrugge, J.W., Sleddens-Linkels, E., Ooms, M., Sun, Z.W., van IJcken, W.F., Grootegoed, J.A., and Baarends, W.M. (2010) The ubiquitin-conjugating enzyme HR6B is required for maintenance of X chromosome silencing in mouse spermatocytes and spermatids. *BMC Genomics*, **11**, 367.

Muramatsu, D., Singh, P.B., Kimura, H., Tachibana, M., and Shinkai, Y. (2013) Pericentric heterochromatin generated by HP1 protein interaction-defective histone methyltransferase Suv39h1. *J. Biol. Chem.*, **288**, 25285–25296.

Nagarajan, P., Ge, Z., Sirbu, B., Doughty, C., Agudelo Garcia, P.A., Schlederer, M., Annunziato, A.T., Cortez, D., Kenner, L., and Parthun, M.R. (2013) Histone acetyl transferase 1 is essential for mammalian development, genome stability, and the processing of newly synthesized histones H3 and H4. *PLoS Genet.*, **9**, e1003518.

Downloaded From Vet-eBooks.com

Nagy, Z.P., Janssenswillen, C., Janssens, R., De Vos, A., Staessen, C., van de Velde, H., and van Steirteghem, A.C. (1998) Timing of oocyte activation, pronucleus formation and cleavage in humans after intracytoplasmic sperm injection (ICSI) with testicular spermatozoa and after ICSI or *in-vitro* fertilization on sibling oocytes with ejaculated spermatozoa. *Hum. Reprod.*, **13**, 1606–1612.

Nakajima, N., Inomata, T., Ito, J., and Kashiwazaki, N. (2008) Treatment with proteasome inhibitor MG132 during cloning improves survival and pronuclear number of reconstructed rat embryos. *Cloning Stem Cells*, **10**, 461–468.

Nakayama, J., Rice, J.C., Strahl, B.D., Allis, C.D., and Grewal, S.I. (2001) Role of histone H3 lysine 9 methylation in epigenetic control of heterochromatin assembly. *Science*, **292**, 110–113.

Nashun, B., Akiyama, T., Suzuki, M.G., and Aoki, F. (2011) Dramatic replacement of histone variants during genome remodeling in nuclear-transferred embryos. *Epigenetics*, **6**, 1489–1497.

Neutzner, M. and Neutzner, A. (2012) Enzymes of ubiquitination and deubiquitination. *Essays Biochem.*, **52**, 37–50.

Newport, J. and Dunphy, W. (1992) Characterization of the membrane binding and fusion events during nuclear envelope assembly using purified components. *J. Cell Biol.*, **116**, 295–306.

Newport, J.W. and Forbes, D.J. (1987) The nucleus: structure, function, and dynamics. *Annu. Rev. Biochem.*, **56**, 535–565.

Newport, J.W., Wilson, K.L., and Dunphy, W.G. (1990) A lamin-independent pathway for nuclear envelope assembly. *J. Cell Biol.*, **111**, 2247–2259.

Ng, R.K. and Gurdon, J.B. (2008) Epigenetic memory of an active gene state depends on histone H3.3 incorporation into chromatin in the absence of transcription. *Nat. Cell Biol.*, **10**, 102–109.

Nielsen, S.J., Schneider, R., Bauer, U.M., Bannister, A.J., Morrison, A., O'Carroll, D., Firestein, R., Cleary, M., Jenuwein, T., Herrera, R.E. *et al.* (2001) Rb targets histone H3 methylation and HP1 to promoters. *Nature*, **412**, 561–565.

Nightingale, K.P., Gendreizig, S., White, D.A., Bradbury, C., Hollfelder, F., and Turner, B.M. (2007) Cross-talk between histone modifications in response to histone deacetylase inhibitors: MLL4 links histone H3 acetylation and histone H3K4 methylation. *J. Biol. Chem.*, **282**, 4408–4416.

O'Carroll, D., Scherthan, H., Peters, A.H., Opravil, S., Haynes, A.R., Laible, G., Rea, S., Schmid, M., Lebersorger, A., Jerratsch, M. *et al.* (2000) Isolation and characterization of Suv39h2, a second histone H3 methyltransferase gene that displays testis-specific expression. *Mol. Cell. Biol.*, **20**, 9423–9433.

O'Neill, C., Li, Y., and Jin, X.L. (2012) Survival signaling in the preimplantation embryo. *Theriogenology*, **77**, 773–784.

Oberdoerffer, P., Michan, S., McVay, M., Mostoslavsky, R., Vann, J., Park, S.K., Hartlerode, A., Stegmuller, J., Hafner, A., Loerch, P. *et al.* (2008) SIRT1 redistribution on chromatin promotes genomic stability but alters gene expression during aging. *Cell*, **135**, 907–918.

Ogawa, H., Ishiguro, K., Gaubatz, S., Livingston, D.M., and Nakatani, Y. (2002) A complex with chromatin modifiers that occupies E2F- and Myc-responsive genes in G0 cells. *Science*, **296**, 1132–1136.

Ogushi, S. and Saitou, M. (2010) The nucleolus in the mouse oocyte is required for the early step of both female and male pronucleus organization. *J. Reprod. Dev.*, **56**, 495–501.

Ogushi, S., Palmieri, C., Fulka, H., Saitou, M., Miyano, T., and Fulka, J., Jr. (2008) The maternal nucleolus is essential for early embryonic development in mammals. *Science*, **319**, 613–616.

Ohsumi, K. and Katagiri, C. (1991) Characterization of the ooplasmic factor inducing decondensation of and protamine removal from toad sperm nuclei: involvement of nucleoplasmin. *Dev. Biol.*, **148**, 295–305.

Downloaded From Vet-eBooks.com

Okano, M., Bell, D.W., Haber, D.A., and Li, E. (1999) DNA methyltransferases Dnmt3a and Dnmt3b are essential for *de novo* methylation and mammalian development. *Cell*, **99**, 247–257.

Okuwaki, M., Sumi, A., Hisaoka, M., Saotome-Nakamura, A., Akashi, S., Nishimura, Y., and Nagata, K. (2012) Function of homo- and hetero-oligomers of human nucleoplasmin/nucleophosmin family proteins NPM1, NPM2 and NPM3 during sperm chromatin remodeling. *Nucleic Acids Res.*, **40**, 4861–4878.

Ostermeier, G.C., Miller, D., Huntriss, J.D., Diamond, M.P., and Krawetz, S.A. (2004) Reproductive biology: delivering spermatozoan RNA to the oocyte. *Nature*, **429**, 154.

Palacios, J.A., Herranz, D., De Bonis, M.L., Velasco, S., Serrano, M., and Blasco, M.A. (2010) SIRT1 contributes to telomere maintenance and augments global homologous recombination. *J. Cell Biol.*, **191**, 1299–1313.

Palermo, G.D., Colombero, L.T., and Rosenwaks, Z. (1997) The human sperm centrosome is responsible for normal syngamy and early embryonic development. *Rev. Reprod.*, **2**, 19–27.

Pante, N. and Aebi, U. (1993) The nuclear pore complex. *J. Cell Biol.*, **122**, 977–984.

Papale, L., Fiorentino, A., Montag, M., and Tomasi, G. (2012) The zygote. *Hum. Reprod.*, **27** (Suppl. 1), i22–i49.

Park, K.E., Johnson, C.M., Wang, X., and Cabot, R.A. (2011) Differential developmental requirements for individual histone H3K9 methyltransferases in cleavage-stage porcine embryos. *Reprod. Fertil. Dev.*, **23**, 551–560.

Perreault, S.D., Wolff, R.A., and Zirkin, B.R. (1984) The role of disulfide bond reduction during mammalian sperm nuclear decondensation *in vivo*. *Dev. Biol.*, **101**, 160–167.

Peters, A.H. and Schubeler, D. (2005) Methylation of histones: playing memory with DNA. *Curr. Opin. Cell Biol.*, **17**, 230–238.

Peters, A.H., O'Carroll, D., Scherthan, H., Mechtler, K., Sauer, S., Schofer, C., Weipoltshammer, K., Pagani, M., Lachner, M., Kohlmaier, A. *et al.* (2001) Loss of the Suv39h histone methyltransferases impairs mammalian heterochromatin and genome stability. *Cell*, **107**, 323–337.

Peters, A.H., Kubicek, S., Mechtler, K., O'Sullivan, R.J., Derijck, A.A., Perez-Burgos, L., Kohlmaier, A., Opravil, S., Tachibana, M., Shinkai, Y. *et al.* (2003) Partitioning and plasticity of repressive histone methylation states in mammalian chromatin. *Mol. Cell*, **12**, 1577–1589.

Pfaller, R., Smythe, C., and Newport, J.W. (1991) Assembly/disassembly of the nuclear envelope membrane: cell cycle-dependent binding of nuclear membrane vesicles to chromatin *in vitro*. *Cell*, **65**, 209–217.

Plath, K., Talbot, D., Hamer, K.M., Otte, A.P., Yang, T.P., Jaenisch, R., and Panning, B. (2004) Developmentally regulated alterations in polycomb repressive complex 1 proteins on the inactive X chromosome. *J. Cell Biol.*, **167**, 1025–1035.

Poccia, D. and Collas, P. (1997) Nuclear envelope dynamics during male pronuclear development. *Dev. Growth Differ.*, **39**, 541–550.

Popken, J., Graf, A., Krebs, S., Blum, H., Guengoer, T., Zakhartchenko, V., Wolf, E., and Cremer, T. (2014) 82 structural remodelling of the nuclear envelope in bovine pre-implantation embryos. *Reprod. Fertil. Dev.*, **27**, 134.

Rassoulzadegan, M., Grandjean, V., Gounon, P., Vincent, S., Gillot, I., and Cuzin, F. (2006) RNA-mediated non-mendelian inheritance of an epigenetic change in the mouse. *Nature*, **441**, 469–474.

Rawe, V.Y., Olmedo, S.B., Nodar, F.N., Ponzio, R., and Sutovsky, P. (2003) Abnormal assembly of annulate lamellae and nuclear pore complexes coincides with fertilization arrest at the pronuclear stage of human zygotic development. *Hum. Reprod.*, **18**, 576–582.

Rawe, V.Y., Diaz, E.S., Abdelmassih, R., Wojcik, C., Morales, P., Sutovsky, P., and Chemes, H.E. (2008) The role of sperm proteasomes during sperm aster formation and early zygote development: implications for fertilization failure in humans. *Hum. Reprod.*, **23**, 573–580.

Downloaded From Vet-eBooks.com

Rea, S., Eisenhaber, F., O'Carroll, D., Strahl, B.D., Sun, Z.W., Schmid, M., Opravil, S., Mechtler, K., Ponting, C.P., Allis, C.D. *et al.* (2000) Regulation of chromatin structure by site-specific histone H3 methyltransferases. *Nature*, **406**, 593–599.

Redondo-Munoz, J., Perez-Garcia, V., Rodriguez, M.J., Valpuesta, J.M., and Carrera, A.C. (2015) Phosphoinositide 3-kinase beta protects nuclear envelope integrity by controlling RCC1 localization and Ran activity. *Mol. Cell. Biol.*, **35**, 249–263.

Reik, W. and Walter, J. (2001) Evolution of imprinting mechanisms: the battle of the sexes begins in the zygote. *Nat. Genet.*, **27**, 255–256.

Reik, W., Davies, K., Dean, W., Kelsey, G., and Constância, M. (2001a) Imprinted genes and the coordination of fetal and postnatal growth in mammals. *Novartis Found. Symp.*, **237**, 19–31.

Reik, W., Dean, W., and Walter, J. (2001b) Epigenetic reprogramming in mammalian development. *Science*, **293**, 1089–1093.

Reimann, J.D. and Jackson, P.K. (2002) Emi1 is required for cytostatic factor arrest in vertebrate eggs. *Nature*, **416**, 850–854.

Rivera, R.M. and Ross, J.W. (2013) Epigenetics in fertilization and preimplantation embryo development. *Prog. Biophys. Mol. Biol.*, **113**, 423–432.

Rougier, N., Bourc'his, D., Gomes, D.M., Niveleau, A., Plachot, M., Paldi, A., and Viegas-Pequignot, E. (1998) Chromosome methylation patterns during mammalian preimplantation development. *Genes Dev.*, **12**, 2108–2113.

Santos, F., Peters, A.H., Otte, A.P., Reik, W., and Dean, W. (2005) Dynamic chromatin modifications characterise the first cell cycle in mouse embryos. *Dev. Biol.*, **280**, 225–236.

Schatten, G., Simerly, C., Palmer, D.K., Margolis, R.L., Maul, G., Andrews, B.S., and Schatten, H. (1988) Kinetochore appearance during meiosis, fertilization and mitosis in mouse oocytes and zygotes. *Chromosoma*, **96**, 341–352.

Schultz, D.C., Ayyanathan, K., Negorev, D., Maul, G.G., and Rauscher, F.J., 3rd. (2002) SETDB1: a novel KAP-1-associated histone H3, lysine 9-specific methyltransferase that contributes to HP1-mediated silencing of euchromatic genes by KRAB zinc-finger proteins. *Genes Dev.*, **16**, 919–932.

Sega, M.F., Lee, K., Machaty, Z., and Cabot, R. (2007) Pronuclear stage porcine embryos do not possess a strict asymmetric distribution of lysine 9 dimethylation of histone H3 based solely on parental origin. *Mol. Reprod. Dev.*, **74**, 2–7.

Shao, G.B., Chen, J.C., Zhang, L.P., Huang, P., Lu, H.Y., Jin, J., Gong, A.H., and Sang, J.R. (2014) Dynamic patterns of histone H3 lysine 4 methyltransferases and demethylases during mouse preimplantation development. *In Vitro Cell. Dev. Biol. Anim.*, **50**, 603–613.

Sharif, J., Muto, M., Takebayashi, S., Suetake, I., Iwamatsu, A., Endo, T.A., Shinga, J., Mizutani-Koseki, Y., Toyoda, T., Okamura, K. *et al.* (2007) The SRA protein Np95 mediates epigenetic inheritance by recruiting Dnmt1 to methylated DNA. *Nature*, **450**, 908–912.

Shen, L., Inoue, A., He, J., Liu, Y., Lu, F., and Zhang, Y. (2014) Tet3 and DNA replication mediate demethylation of both the maternal and paternal genomes in mouse zygotes. *Cell Stem Cell*, **15**, 459–470.

Shi, Y., Lan, F., Matson, C., Mulligan, P., Whetstine, J.R., Cole, P.A., and Casero, R.A. (2004) Histone demethylation mediated by the nuclear amine oxidase homolog LSD1. *Cell*, **119**, 941–953.

Shi, X., Hong, T., Walter, K.L., Ewalt, M., Michishita, E., Hung, T., Carney, D., Pena, P., Lan, F., Kaadige, M.R. *et al.* (2006) ING2 PHD domain links histone H3 lysine 4 methylation to active gene repression. *Nature*, **442**, 96–99.

Shi, Y., Fernandez-Martinez, J., Tjioe, E., Pellarin, R., Kim, S.J., Williams, R., Schneidman-Duhovny, D., Sali, A., Rout, M.P., and Chait, B.T. (2014) Structural characterization by cross-linking reveals the detailed architecture of a coatomer-related heptameric module from the nuclear pore complex. *Mol. Cell. Proteomics*, **13**, 2927–2943.

Downloaded From Vet-eBooks.com

Shinozaki, S., Chang, K., Sakai, M., Shimizu, N., Yamada, M., Tanaka, T., Nakazawa, H., Ichinose, F., Yamada, Y., Ishigami, A. *et al.* (2014) Inflammatory stimuli induce inhibitory *S*-nitrosylation of the deacetylase SIRT1 to increase acetylation and activation of p53 and p65. *Sci. Signal.*, **7**, 106.

Skowyra, D., Craig, K.L., Tyers, M., Elledge, S.J., and Harper, J.W. (1997) F-box proteins are receptors that recruit phosphorylated substrates to the SCF ubiquitin-ligase complex. *Cell*, **91**, 209–219.

Smallwood, S.A., Tomizawa, S., Krueger, F., Ruf, N., Carli, N., Segonds-Pichon, A., Sato, S., Hata, K., Andrews, S.R., and Kelsey, G. (2011) Dynamic CpG island methylation landscape in oocytes and preimplantation embryos. *Nat. Genet.*, **43**, 811–814.

Sparks, A., Dayal, S., Das, J., Robertson, P., Menendez, S., and Saville, M.K. (2014) The degradation of p53 and its major E3 ligase Mdm2 is differentially dependent on the proteasomal ubiquitin receptor S5a. *Oncogene*, **33**, 4685–4696.

Sterthaus, O., Skoczylas, E., De Geyter, C., Burki, K., and Ledermann, B. (2009) Evaluation of *in vitro* cultured rat oocytes, from different strains, by spindle morphology and maturation-promoting-factor activity combined with nuclear-transfer experiments. *Cloning Stem Cells*, **11**, 463–472.

Strahl, B.D. and Allis, C.D. (2000) The language of covalent histone modifications. *Nature*, **403**, 41–45.

Stuurman, N., Heins, S., and Aebi, U. (1998) Nuclear lamins: their structure, assembly, and interactions. *J. Struct. Biol.*, **122**, 42–66.

Sutovsky, P. (2009) Sperm-egg adhesion and fusion in mammals. *Expert Rev. Mol. Med.*, **11**, e11.

Sutovsky, P. and Prather, R.S. (2004) Nuclear remodeling after SCNT: a contractor's nightmare. *Trends Biotechnol.*, **22**, 205–208.

Sutovsky, P. and Schatten, G. (1997) Depletion of glutathione during bovine oocyte maturation reversibly blocks the decondensation of the male pronucleus and pronuclear apposition during fertilization. *Biol. Reprod.*, **56**, 1503–1512.

Sutovsky, P., Simerly, C., Hewitson, L., and Schatten, G. (1998) Assembly of nuclear pore complexes and annulate lamellae promotes normal pronuclear development in fertilized mammalian oocytes. *J. Cell Sci.*, **111** (Part 19), 2841–2854.

Sutovsky, P., Manandhar, G., McCauley, T.C., Caamano, J.N., Sutovsky, M., Thompson, W.E., and Day, B.N. (2004) Proteasomal interference prevents zona pellucida penetration and fertilization in mammals. *Biol. Reprod.*, **71**, 1625–1637.

Sutovsky, P., Manandhar, G., Laurincik, J., Letko, J., Caamano, J.N., Day, B.N., Lai, L., Prather, R.S., Sharpe-Timms, K.L., Zimmer, R. *et al.* (2005) Expression and proteasomal degradation of the major vault protein (MVP) in mammalian oocytes and zygotes. *Reproduction*, **129**, 269–282.

Tachibana, M., Sugimoto, K., Fukushima, T., and Shinkai, Y. (2001) Set domain-containing protein, G9a, is a novel lysine-preferring mammalian histone methyltransferase with hyperactivity and specific selectivity to lysines 9 and 27 of histone H3. *J. Biol. Chem.*, **276**, 25309–25317.

Tollini, L.A., Jin, A., Park, J., and Zhang, Y. (2014) Regulation of p53 by Mdm2 E3 ligase function is dispensable in embryogenesis and development, but essential in response to DNA damage. *Cancer Cell*, **26**, 235–247.

Torres-Padilla, M.E., Bannister, A.J., Hurd, P.J., Kouzarides, T., and Zernicka-Goetz, M. (2006) Dynamic distribution of the replacement histone variant H3.3 in the mouse oocyte and preimplantation embryos. *Int. J. Dev. Biol.*, **50**, 455–461.

Tseng, A.H., Wu, L.H., Shieh, S.S., and Wang, D.L. (2014) SIRT3 interactions with FOXO3 acetylation, phosphorylation and ubiquitinylation mediate endothelial cell responses to hypoxia. *Biochem. J*, **464**, 157–168.

Tsukamoto, S., Kuma, A., Murakami, M., Kishi, C., Yamamoto, A., and Mizushima, N. (2008) Autophagy is essential for preimplantation development of mouse embryos. *Science*, **321**, 117–120.

Downloaded From Vet-eBooks.com

Tung, J.J., Hansen, D.V., Ban, K.H., Loktev, A.V., Summers, M.K., Adler, J.R., 3rd, and Jackson, P.K. (2005) A role for the anaphase-promoting complex inhibitor Emi2/XErp1, a homolog of early mitotic inhibitor 1, in cytostatic factor arrest of *Xenopus* eggs. *Proc. Natl. Acad. Sci. USA*, **102**, 4318–4323.

van de Werken, C., van der Heijden, G.W., Eleveld, C., Teeuwssen, M., Albert, M., Baarends, W.M., Laven, J.S., Peters, A.H., and Baart, E.B. (2014) Paternal heterochromatin formation in human embryos is H3K9/HP1 directed and primed by sperm-derived histone modifications. *Nat. Commun.*, **5**, 5868.

van der Heijden, G.W., Dieker, J.W., Derijck, A.A., Muller, S., Berden, J.H., Braat, D.D., van der Vlag, J., and de Boer, P. (2005) Asymmetry in histone H3 variants and lysine methylation between paternal and maternal chromatin of the early mouse zygote. *Mech. Dev.*, **122**, 1008–1022.

van der Heijden, G.W., van den Berg, I.M., Baart, E.B., Derijck, A.A., Martini, E., and de Boer, P. (2009) Parental origin of chromatin in human monopronuclear zygotes revealed by asymmetric histone methylation patterns, differs between IVF and ICSI. *Mol. Reprod. Dev.*, **76**, 101–108.

Vaquero, A., Scher, M., Lee, D., Erdjument-Bromage, H., Tempst, P., and Reinberg, D. (2004) Human SirT1 interacts with histone H1 and promotes formation of facultative heterochromatin. *Mol. Cell*, **16**, 93–105.

Vaquero, A., Scher, M., Erdjument-Bromage, H., Tempst, P., Serrano, L., and Reinberg, D. (2007a) SIRT1 regulates the histone methyl-transferase SUV39H1 during heterochromatin formation. *Nature*, **450**, 440–444.

Vaquero, A., Sternglanz, R., and Reinberg, D. (2007b) NAD+-dependent deacetylation of H4 lysine 16 by class III HDACs. *Oncogene*, **26**, 5505–5520.

Vettese-Dadey, M., Grant, P.A., Hebbes, T.R., Crane-Robinson, C., Allis, C.D., and Workman, J.L. (1996) Acetylation of histone H4 plays a primary role in enhancing transcription factor binding to nucleosomal DNA *in vitro*. *EMBO J.*, **15**, 2508–2518.

Viuff, D., Greve, T., Holm, P., Callesen, H., Hyttel, P., and Thomsen, P.D. (2002) Activation of the ribosomal RNA genes late in the third cell cycle of porcine embryos. *Biol. Reprod.*, **66**, 629–634.

Walser, C.B. and Lipshitz, H.D. (2011) Transcript clearance during the maternal-to-zygotic transition. *Curr. Opin. Genet. Dev.*, **21**, 431–443.

Wang, F., Chan, C.H., Chen, K., Guan, X., Lin, H.K., and Tong, Q. (2012) Deacetylation of FOXO3 by SIRT1 or SIRT2 leads to Skp2-mediated FOXO3 ubiquitination and degradation. *Oncogene*, **31**, 1546–1557.

Ward, W.S. (2010) Function of sperm chromatin structural elements in fertilization and development. *Mol. Hum. Reprod.*, **16**, 30–36.

Ward, W.S. and Coffey, D.S. (1991) DNA packaging and organization in mammalian spermatozoa: comparison with somatic cells. *Biol. Reprod.*, **44**, 569–574.

Webster, B.M., Colombi, P., Jager, J., and Lusk, C.P. (2014) Surveillance of nuclear pore complex assembly by ESCRT-III/Vps4. *Cell*, **159**, 388–401.

Wei, Y., Yu, L., Bowen, J., Gorovsky, M.A., and Allis, C.D. (1999) Phosphorylation of histone H3 is required for proper chromosome condensation and segregation. *Cell*, **97**, 99–109.

Wen, D., Banaszynski, L.A., Liu, Y., Geng, F., Noh, K.M., Xiang, J., Elemento, O., Rosenwaks, Z., Allis, C.D., and Rafii, S. (2014a) Histone variant H3.3 is an essential maternal factor for oocyte reprogramming. *Proc. Natl. Acad. Sci. USA*, **111**, 7325–7330.

Wen, D., Banaszynski, L.A., Rosenwaks, Z., Allis, C.D., and Rafii, S. (2014b) H3.3 replacement facilitates epigenetic reprogramming of donor nuclei in somatic cell nuclear transfer embryos. *Nucleus*, **5**. 369–375.

Whitworth, K.M., Li, R., Spate, L.D., Wax, D.M., Rieke, A., Whyte, J.J., Manandhar, G., Sutovsky, M., Green, J.A., Sutovsky, P. *et al.* (2009) Method of oocyte activation affects cloning efficiency in pigs. *Mol. Reprod. Dev.*, **76**, 490–500.

Downloaded From Vet-eBooks.com

Wiekowski, M., Miranda, M., and DePamphilis, M.L. (1993) Requirements for promoter activity in mouse oocytes and embryos distinguish paternal pronuclei from maternal and zygotic nuclei. *Dev. Biol.*, **159**, 366–378.

Wigler, M.H. (1981) The inheritance of methylation patterns in vertebrates. *Cell*, **24**, 285–286.

Wittschieben, B.O., Otero, G., de Bizemont, T., Fellows, J., Erdjument-Bromage, H., Ohba, R., Li, Y., Allis, C.D., Tempst, P., and Svejstrup, J.Q. (1999) A novel histone acetyltransferase is an integral subunit of elongating RNA polymerase II holoenzyme. *Mol. Cell*, **4**, 123–128.

Wossidlo, M., Nakamura, T., Lepikhov, K., Marques, C.J., Zakhartchenko, V., Boiani, M., Arand, J., Nakano, T., Reik, W., and Walter, J. (2011) 5-Hydroxymethylcytosine in the mammalian zygote is linked with epigenetic reprogramming. *Nat. Commun.*, **2**, 241.

Wu, F.R., Liu, Y., Shang, M.B., Yang, X.X., Ding, B., Gao, J.G., Wang, R., and Li, W.Y. (2012) Differences in H3K4 trimethylation in *in vivo* and *in vitro* fertilization mouse preimplantation embryos. *Genet. Mol. Res.*, **11**, 1099–1108.

Wu, B.J., Dong, F.L., Ma, X.S., Wang, X.G., Lin, F., and Liu, H.L. (2014) Localization and expression of histone H2A variants during mouse oogenesis and preimplantation embryo development. *Genet. Mol. Res.*, **13**, 5929–5939.

Wysocka, J., Swigut, T., Xiao, H., Milne, T.A., Kwon, S.Y., Landry, J., Kauer, M., Tackett, A.J., Chait, B.T., Badenhorst, P. *et al*. (2006) A PHD finger of NURF couples histone H3 lysine 4 trimethylation with chromatin remodelling. *Nature*, **442**, 86–90.

Xiao, X., Zi, X.D., Niu, H.R., Xiong, X.R., Zhong, J.C., Li, J., Wang, L., and Wang, Y. (2014) Effect of addition of FSH, LH and proteasome inhibitor MG132 to *in vitro* maturation medium on the developmental competence of yak (Bos grunniens) oocytes. *Reprod. Biol. Endocrinol.*, **12**, 30.

Yan, W. (2014) Potential roles of noncoding RNAs in environmental epigenetic transgenerational inheritance. *Mol. Cell. Endocrinol.*, **398**, 24–30.

Yanagimachi, R. (1988) Mammalian fertilization, in *The Physiology of Reproduction* (eds E. Knobil and J. Neill), *Raven Press*, New York, pp. 230–278.

Yang, L., Xia, L., Wu, D.Y., Wang, H., Chansky, H.A., Schubach, W.H., Hickstein, D.D., and Zhang, Y. (2002) Molecular cloning of ESET, a novel histone H3-specific methyltransferase that interacts with ERG transcription factor. *Oncogene*, **21**, 148–152.

Yeo, S., Lee, K.K., Han, Y.M., and Kang, Y.K. (2005) Methylation changes of lysine 9 of histone H3 during preimplantation mouse development. *Mol. Cell*, **20**, 423–428.

You, J., Lee, J., Kim, J., Park, J., and Lee, E. (2010) Post-fusion treatment with MG132 increases transcription factor expression in somatic cell nuclear transfer embryos in pigs. *Mol. Reprod. Dev.*, 77, 149–157.

You, J., Kim, J., Lee, H., Hyun, S.H., Hansen, P.J., and Lee, E. (2012a) MG132 treatment during oocyte maturation improves embryonic development after somatic cell nuclear transfer and alters oocyte and embryo transcript abundance in pigs. *Mol. Reprod. Dev.*, **79**, 41–50.

You, J., Lee, E., Bonilla, L., Francis, J., Koh, J., Block, J., Chen, S., and Hansen, P.J. (2012b) Treatment with the proteasome inhibitor MG132 during the end of oocyte maturation improves oocyte competence for development after fertilization in cattle. *PLoS One*, **7**, e48613.

Younis, J.S., Radin, O., Mirsky, N., Izhaki, I., Majara, T., Bar-ami, S., and Ben-ami, M. (2008) First polar body and nucleolar precursor body morphology is related to the ovarian reserve of infertile women. *Reprod. Biomed. Online*, **16**, 851–858.

Yu, Y., Yong, J., Li, X., Qing, T., Qin, H., Xiong, X., You, J., Ding, M., and Deng, H. (2005) The proteasomal inhibitor MG132 increases the efficiency of mouse embryo production after cloning by electrofusion. *Reproduction*, **130**, 553–558.

Yuan, G. and Zhu, B. (2014) Histone variants and epigenetic inheritance. *Biochim. Biophys. Acta*, **1819**, 222–229.

Downloaded From Vet-eBooks.com

Zatsepina, O., Baly, C., Chebrout, M., and Debey, P. (2003) The step-wise assembly of a functional nucleolus in preimplantation mouse embryos involves the cajal (coiled) body. *Dev. Biol.*, **253**, 66–83.

Zhang, Y. and Reinberg, D. (2001) Transcription regulation by histone methylation: interplay between different covalent modifications of the core histone tails. *Genes Dev.*, **15**, 2343–2360.

Zhang, L., Hou, X., Ma, R., Moley, K., Schedl, T., and Wang, Q. (2014) Sirt2 functions in spindle organization and chromosome alignment in mouse oocyte meiosis. *FASEB J.*, **28**, 1435–1445.

Zhou, L.Q. and Dean, J. (2014) Reprogramming the genome to totipotency in mouse embryos. *Trends Cell Biol.*, **25**, 82–91.

Zhou, Q., Renard, J.P., Le Friec, G., Brochard, V., Beaujean, N., Cherifi, Y., Fraichard, A., and Cozzi, J. (2003) Generation of fertile cloned rats by regulating oocyte activation. *Science*, **302**, 1179.

Zhou, L., Yang, Y., Zhang, J., Guo, X., Bi, Y., Li, X., Zhang, P., Lin, M., Zhou, Z., Shen, R. *et al.* (2013) The role of RING box protein 1 in mouse oocyte meiotic maturation. *PLoS One*, **8**, e68964.

Zofall, M. and Grewal, S.I. (2007) HULC, a histone H2B ubiquitinating complex, modulates heterochromatin independent of histone methylation in fission yeast. *J. Biol. Chem.*, **282**, 14065–14072.

Downloaded From Vet-eBooks.com

18

Alterations of the Epigenome Induced by the Environment in Reproduction

Zhao-Jia Ge,[1] Shen Yin,[2] and Heide Schatten[3]

[1]*College of Animal Science and Veterinary Medicine, Qingdao Agricultural University, Qingdao, China*
[2]*Key Laboratory of Animal Reproduction and Germplasm Enhancement in Universities of Shandong, College of Animal Science and Technology, Institute of Reproductive Sciences, Qingdao Agricultural University, Qingdao, China*
[3]*Department of Veterinary Pathobiology, University of Missouri-Columbia, Columbia, USA*

18.1 Introduction

The word "epigenetics" was first suggested to describe "the study of the processes by which genotype gives rise to phenotype" in 1942. With the ever-expanding knowledge, epigenetics is explained as "a study of the changes in gene expression that are mitotically and/or meiotically heritable and do not involve a change in the DNA sequence" (Wu and Morris, 2001). In essence, this definition indicates that epigenetic modifications can regulate gene expression, and epimutations will be transmitted to generations. Epigenetic mechanisms regulate gene expression mainly through DNA methylation, histone modification, chromatin modifications, and noncoding RNA (Panning and Jaenisch, 1998; Callinan and Feinberg, 2006; Peaston and Whitelaw, 2006). However, epigenetic modifications are prone to being affected by external and internal factors (Flanagan *et al*., 2006; Bird, 2007), and epimutations may be inherited by the next generations by germ cells (Figure 18.1) (Holliday, 1987; Aiken and Ozanne, 2014).

Establishing proper epigenetic modifications in gametes and embryos is crucial for fetal development and health of generations. The Barker hypothesis proposes that diseases initiate in the fetus (Barker, 1995). The study of Dutch Hunger Winter also shows that if women are exposed to famine during gestation, the health of their offspring may be affected (Stein *et al*., 2007; Heijmans *et al*., 2008). Recent studies indicate that the disease of offspring may start in gametes (Carone *et al*., 2010; Zeybel *et al*., 2012; Ge *et al*., 2014d). This means that epigenetic modifications of gametes and/or early embryos may be affected by internal and/or external factors (Figure 18.1). It is proved that epigenomes in germ cells and embryos are changed by nutrition, noncommunicable diseases, artificial manipulation, and other factors. In this chapter, we will mainly discuss animal models used to investigate alterations of epigenome induced by the environment in reproduction. Epigenetic changes are also reviewed, caused by environmental factors and artificial manipulations, such as assisted reproductive technology (ART) in humans.

18.2 Epigenetic Reprogramming

For mammalian adults, cells share the same genetic information, while each cell type has its own expression pattern. Epigenetic modifications, including those that alter chromatin structure,

Animal Models and Human Reproduction, First Edition. Edited by Heide Schatten and Gheorghe M. Constantinescu.
© 2017 John Wiley & Sons, Inc. Published 2017 by John Wiley & Sons, Inc.

Downloaded From Vet-eBooks.com

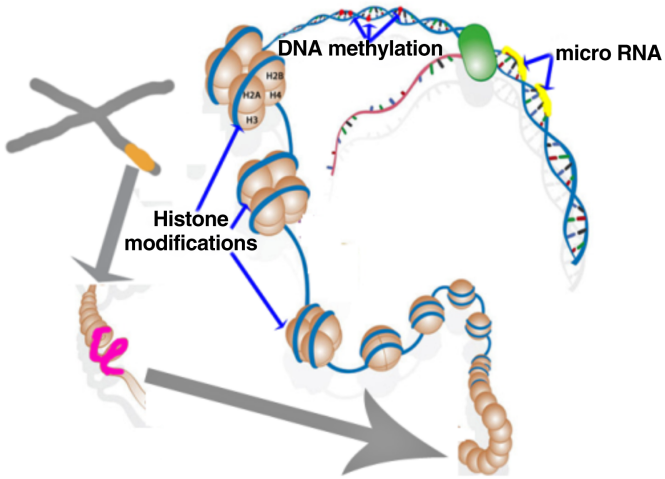

Figure 18.1 Epigenetic modifications including DNA methylation, histone modifications, and microRNA. (See color plate section.)

modify DNA and histones, remodel nucleosomes, incorporate variant histones, and play a key role in ensuring the specific cell types. Therefore, these epigenetic modifications have to be erased and reprogrammed for sexual reproduction. Epigenetic reprogramming is one of the most remarkable features during gametogenesis and embryonic development. Somatic epigenetic marks are erased in primordial germ cells (PGCs) and sex-specific epigenetic patterns are established in mature gametes to produce the next generation. After fertilization, these epigenetic marks in gametes are erased again and epigenetic patterns for embryonic development are reestablished. The epigenetic reprogramming is commonly considered to occur in these two processes (Figure 18.2).

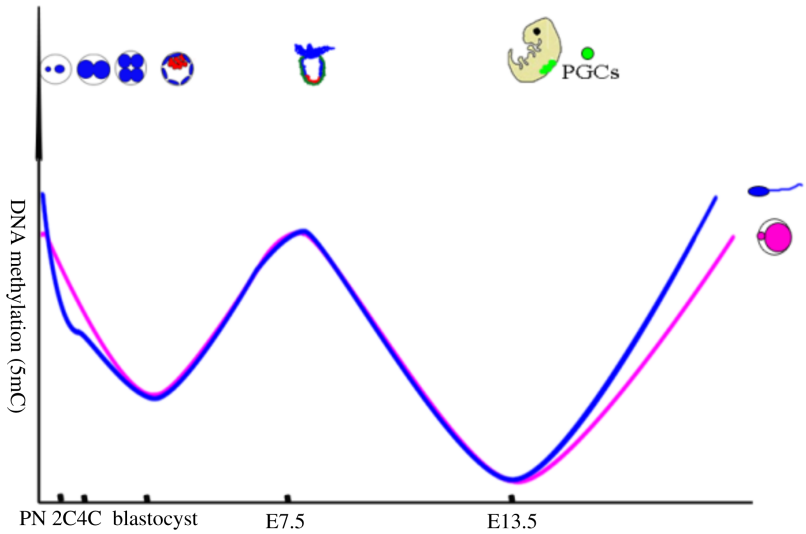

Figure 18.2 Reprogramming of 5 mC in germ cells and embryos. PN, pronucleus; PGCs, primordial germ cells. (See color plate section.)

Downloaded From Vet-eBooks.com

18.2.1 The Epigenetic Reprogramming in Germ Lines

PGCs originate from epiblast cells of the postimplantation embryo at E7.5 (embryonic day) and migrate to the genital ridge between E8.0 and E8.5 (McLaren, 2003; Hajkova *et al*., 2008). At this stage, a number of epigenetic changes have been documented to occur immediately. The earliest global chromatin events during E7.5–E9.5 are a reciprocal loss of histone 3 lysine 9 dimethylation (H3K9me2) and increase of histone 3 lysine 27 trimethylation (Seki *et al*., 2007). The reduction in GLP, a SET domain protein forming a heterometric complex with G9a, may be the main reason for the decrease in H3K9me2 because both G9a and GLP are required for the H3K9 methyltransferase (HMT) activity of the complex. From E7.25, the transcription of *Glp* is reduced in PGCs. Changes in H3K9me2 and H3K27me3 suggest that germ cells may need more flexible silencing mechanisms at this stage for the derivation of embryonic germ cells (Margueron and Reinberg, 2011; Mansour *et al*., 2012).

With the accumulation of *Prmt5*, an arginine-specific HMT mediating dimethylation of arginine 3 on histone H2A and/or H4 tails (H2A/H4R3me2s), the level of H2A/H4R3me2s is higher in PGCs than that in soma at E10.5 (Ancelin *et al*., 2006). At an early stage of PGC development, the inactive X chromosome in females is reactivated (Chuva de Sousa Lopes *et al*., 2008). From E7.0 to E10.5, there is a progressive loss of the *Xist* signal in PGCs (Sugimoto and Abe, 2007). During migration to the genital ridges, the H3K27me3 is also gradually lost (Chuva de Sousa Lopes *et al*., 2008).

With changes of histone modification, DNA methylation level is also reduced during germ cells migrating to genital ridges. Approximately at E8.0, 5 mC levels are reduced coincident with the loss of H3K9me2, which is triggered by the decrease of *Glp* (Tachibana *et al*., 2005). The expression of DNA methyltransferase 3a and 3b decreases at E7.25 and E8.0 (Seki *et al*., 2005). At E11.5 and E12.5, DNA methylation is erased rapidly in PGCs (Guibert *et al*., 2012).

Once PGCs migrate to the genital ridge, there is a genome-wide DNA demethylation process at around E11, including the erasure of genomic imprinting, the reactivation of the inactivated X chromosome in females, and the demethylation of the transposable/repetitive elements (Monk *et al*., 1987; Kafri *et al*., 1992), resulting in changes of chromatin structure, and loss of numerous histone modifications brought about by genome-wide histone replacement (Hajkova *et al*., 2002, 2008). PGCs are at hypomethylated states at E13.5 (Popp *et al*., 2010), which suggests that the DNA demethylation in PGCs is rapid and active. However, mechanisms underlying this active demethylation in PGCs are still unclear, although studies show some enzymes may be included (Kriaucionis and Heintz, 2009; Tahiliani *et al*., 2009; Hajkova *et al*., 2010).

In mammals, DNA methylation patterns are reestablished gradually in germ cells after sex determination initiation. In the mouse, this occurs at E12.5 (McLaren, 1984). The process is different for male and female germ cells. For male germ cells, the remethylation initiates at E14.5, and PGCs have already attained 50% global DNA methylation at E16.5 (Kota and Feil, 2010). The DNA methylation is fully established in male PGCs at birth (days 19–21) and maintained before cells enter meiosis (Davis *et al*., 2000). The remethylation in female PGCs initiates only at birth during oogenesis and DNA methylation is almost accomplished at meiosis II (Kota and Feil, 2010). DNA *de novo* methylation is mainly catalyzed by DNA methyltransferases (DNMTs), including DNMT1o, 3a, 3b, and 3l (Bourc'his *et al*., 2001; Howell *et al*., 2001; Bourc'his and Bestor, 2004; Ko *et al*., 2005).

During meiosis, histone posttranslational modifications are also changed. For example, levels of H3 lysine 4 me1, 2, and 3 and H3K9me2 are altered globally at meiotic prophase I, and during chromosome pairing and DSBs (double strand breaks) formation and progression (Sasaki and Matsui, 2008). The role of changes of histone modifications is still not fully understood.

Downloaded From Vet-eBooks.com

18.2.2 The Epigenetic Reprogramming in the Early Embryo

Another genome-wide epigenetic reprogramming wave occurs in the preimplantation embryos. After fertilization, protamines in sperm chromatin are rapidly replaced by maternally inherited histones, (Adenot *et al*., 1997; Arney *et al*., 2002). Meanwhile, histone modifications are also changed in paternal chromatin, for example, high acetylation and methylation levels in the male pronucleus (Adenot *et al*., 1997; Santos *et al*., 2002). With changes of histone modifications in the male pronucleus, global DNA demethylation also occurs rapidly after fertilization (Figure 18.2) (Mayer *et al*., 2000). The DNA demethylation of male chromatin is completed before the onset of DNA replication at the pronucleus 3 phase (Mayer *et al*., 2000; Oswald *et al*., 2000). This indicates that it is an active demethylation process that is catalyzed by TET3 (10–11 translocation) (Gu *et al*., 2011).

Conversely, histone modifications established during oogenesis are mainly maintained in the maternal pronucleus (Santos *et al*., 2005). Female chromatin displays a passive DNA demethylation, which is replication-dependent (Mayer *et al*., 2000; Santos *et al*., 2002).

There are further changes in global DNA methylation and histone modifications during early embryonic development. By the blastocyst stage, the inner cell mass (ICM) and the trophectoderm (TE) are set up (Morgan *et al*., 2005). At this time, DNA methylation change is progressive with cleavage divisions and DNA replication-dependent, resulting in unequally methylated sister chromatin (Monk *et al*., 1987; Howlett and Reik, 1991; Rougier *et al*., 1998). This gradual demethylation is probably caused by excluding DNMT1o from the nucleus before the 8-cell stage (Howell *et al*., 2001). However, DNA methylation patterns of imprinted genes are retained as their germline imprints, which may be guided by histone modifications. Although transient histone marks are changed, at present it is not yet clear how histone modifications are reprogrammed during passive DNA demethylation.

In ICM, there is an extensive *de novo* methylation process, which is not observed in TE (Watanabe *et al*., 2002).

18.3 Environment and Epigenetic Alterations

With ontogenic development and aging, proper changes of epigenomes are necessary (Reik, 2007). Meanwhile, both intrinsic and extrinsic factors can cause apparently random variations with no natural biological function (Feil and Fraga, 2011). These negative epigenetic modifications, such as alterations in DNA methylation or histone modifications, may induce abnormal gene expression, which in turn can be associated with some diseases, including various reproductive disorders (Cortessis *et al*., 2012). The earlier these changes happen, the longer its long-term effects can be (Figure 18.3) (Lindstrom, 1999).

Changes of epigenome can occur throughout the life, but it has more significance to understand the impact of the environment at two different periods: embryogenesis and adult life (Aguilera *et al*., 2010). The most important key period is during embryonic development, because a high level of cell differentiation and numerous epigenetic marks are established at this stage. Moreover, changes in the epigenome can be transmitted to daughter cells, kept in the adult during postnatal development, and can even be inherited to the next generations (Frias and Grove, 2012). Numerous pregnancy problems, such as early pregnancy loss, preterm birth, intrauterine growth restriction (IUGR), congenital syndromes, and preeclampsia, are associated with environmental and epigenetic alterations (Robins *et al*., 2011). Epimutations, induced by an adverse uterine environment during embryogenesis, could also be a reason for later adult diseases. This

Downloaded From Vet-eBooks.com

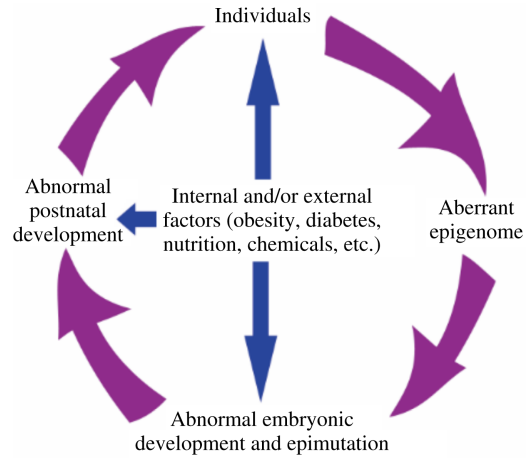

Figure 18.3 Schedule of effects induced by internal and/or external factors on epigenome in individuals and the next generations.

phenomenon could be explained by the hypothesis "Development Origin of Health and Diseases" (Hales and Barker, 2001).

Maternal nutrients may affect epigenetics of the offspring. For example, studies of the offspring from pregnant mothers experiencing the Dutch Hunger Winter (1944–1945, a famine that took place in the Netherlands during World War II) show an association between maternal nutrition and epigenetics (Heijmans *et al.*, 2008). Individuals prenatally exposed to the famine during this period presented less DNA methylation of the imprinted insulin-like growth factor 2 (IGF2) gene compared with their unexposed siblings. IGF2 may play a role in certain diseases associated with food deprivation during gestation (Heijmans *et al.*, 2008). Another famous example is the Agouti viable yellow (A^{vy}) mice. The Agouti gene, which is regulated by DNA methylation status of an intra-cisteral A particle (IAP), controls the mouse's coat color. Supplemented methyl diet during gestation affects epigenetic patterns of fetal germ cells and the coat color of the offspring (Cropley *et al.*, 2006).

Maintaining normal endocrine function is a crucial event during pregnancy because there are adverse effects on embryos exposed to abnormal endocrine systems. Although endocrine disruptors, such as chemical products, pharmaceuticals, personal care products, and nutraceuticals, cannot actually change the DNA sequence, they may influence changes in the epigenome, which can affect normal reproductive physiological development. Once females are exposed to an excess of androgens during gestation, the adults are more susceptible to developing polycystic ovaries (Abbott *et al.*, 2005). Noncommunicable diseases also could disrupt normal endocrine function. This may affect embryogenesis during pregnancy. For untreated preexisting maternal diabetes mellitus, DNA methylation patterns of imprinted genes are affected in mice (Ge *et al.*, 2013b). Epigenetics may be involved, at least in part, in the mechanisms inducing diseases in adults when affected by a disrupted endocrine system during embryonic development.

Another important environmental factor is pollution. Pollutants in the environment adversely affect the prenatal fetus by changing the epigenome. For example, if fetuses are exposed to tobacco prenatally, children show abnormal epigenetic modifications (Lee and Pausova, 2013). In addition, the global DNA methylation in cord blood cells of newborns is altered if fetuses were exposed to atmospheric pollutants (polycyclic aromatic hydrocarbons, PAHs) during embryogenesis.

Besides effects of the environment on the epigenome prenatally, the epigenetic modification can be affected by the environment during postnatal development. Not only the epigenetic modification would be altered by the environment in organs at the adult stage, there would also

Downloaded From Vet-eBooks.com

be changes in germ cells. The typical example is alterations of epigenome in germ cells of the A^{vy} model as described earlier (Cropley *et al*., 2006). In the high-fat-diet-induced mouse model, the DNA methylation pattern of *Leptin* is altered in metaphase II oocytes (Ge *et al*., 2014b).

Concerning the effects of the environment or environmental conditions on the epigenome is the transmission of epigenetic changes from one generation to the next generation (Figure 18.3). Therefore, it is crucial to produce proper animal models to investigate epimutations in reproduction.

18.4 Animal Models Used in Reproduction to Research Epigenetic Alterations Induced by the Environment

In the past decades, many animal models have been developed to investigate the relationship between the environment and reproduction. These models provide a valuable resource in the field of environmental epigenetics. Epigenetic modifications during gametogenesis and embryogenesis can be altered by intrinsic and/or extrinsic factors, such as diet, endocrine disruptors, environmental toxicants, artificial manipulation, and pollutants. In this section, we will review animal models used to research alterations of the epigenome induced by the environment in reproduction.

18.4.1 Viable Yellow (A^{vy}) Mouse Model

The coat color of mice is controlled by expression of the agouti gene (A). Once a single IAP inserts into the upstream of A, its expression is regulated by DNA methylation patterns in IAP (Duhl *et al*., 1994). The coat color ranges from yellow, through continuum of mottled agouti yellow, to a pseudoagouti phenotype due to variations of the DNA methylation status in IAP. When A^{vy} mice are given a diet supplemented with methyl during pregnancy, the coat color and health of the offspring can change. These epimutations can be transmitted to the offspring by germ cells (Wolff *et al*., 1998).

18.4.2 Axin 1 Mouse (Fu) Model

The mouse axin 1 fused ($axin1^{Fu}$) allele, the expression of which associates with its DNA methylation status, is a metastable epiallele that has a 5.1-kb IAP inserted in an antisense direction in intron 6 of Axin 1, which regulates embryonic axis formation in vertebrates (Vasicek *et al*., 1997). The $axin1^{Fu}$ phenotype consists of kinks in the tail (Zeng *et al*., 1997). When maternal diet is supplemented with methyl before and during pregnancy, the DNA methylation level of $Axin1^{Fu}$ increases and thereby reduces the incidence of kinking tail in $Axin1^{Fu/+}$ offspring by half (Waterland *et al*., 2006).

18.4.3 Micronutrient Animal Models

When female mice are fed low or control/high-folate diets during mating, and through pregnancy and lactation, global DNA methylation patterns in the offspring are altered (McKay *et al*., 2011). The global DNA methylation in sperm of male mice fed with folate-deficient diet through life is altered compared to that in sperm of male mice fed a folate-sufficient diet. H3K4 and H3K9 monomethylation is also reduced by folate-deficient diet in sperm (Lambrot *et al*., 2013).

When mice and/rats are fed a choline-deficient diet during pregnancy, epigenetic modifications including DNA methylation and histone modification could be changed compared with those animals fed with normal diets (Kovacheva *et al*., 2007; Mehedint *et al*., 2010).

Downloaded From Vet-eBooks.com

When rats are fed with supplemented vitamin B12 or no diets, global DNA methylation levels in placentas are lower for rats fed with deficient B12 diets compared with those fed with supplemented B12 diets (Kulkarni *et al*., 2011).

18.4.4 The Protein-Restricted Diet Model

Feeding a protein-restricted diet to pregnant rats causes alterations of DNA methylation in promoters of specific genes in the offspring compared to those fed with normal diet. Reduced expression of DNMT1 may play a role. Meanwhile, histone modifications in offspring are changed in this model (Lillycrop *et al*., 2007; Zheng *et al*., 2011).

18.4.5 The Caloric Restriction Model

When restricting calories by 50% in C57BL6 pregnant mice from gestational days 10–19, the expression of glucose transporter 3 decreases in the placenta and this may be caused by changes of DNA methylation in the promoter region (Ganguly *et al*., 2014). The whole DNA methylation in the placenta is also altered by the calories-restricted diet during pregnancy (Chen *et al*., 2013).

18.4.6 The Animal Model of Zinc Deficiency

Weaned 18-day-old female CD1 mice, fed with a control diet (zinc, 29 mg/kg) or a zinc-deficient diet for 3 or 5 days before ovulation and analyzed for epigenetic modifications in oocytes, showed that histone H3K4 trimethylation and the global DNA methylation have a dramatic decrease in zinc-deficient oocytes compared to control oocytes (Tian and Diaz, 2013).

18.4.7 Undernutrition Models

When pregnant female ICR mice aged 6–8 weeks are fed with control (21% of calories from protein, 21% from fat, and 56% from carbohydrate (wheat/corn)) or undernutritional (50% food restricted) diets from E12.5 to E18.5, sperm DNA methylomes of F1 adults are affected in a locus-specific manner (Radford *et al*., 2014).

At day 18 or 19 gestational age, while the bilateral and unilateral uterine arteries are ligated in the gestational rat, epigenetic modifications in tissues of offspring are altered (Seki *et al*., 2012).

For undernutritioned female sheep, when are supplemented during the periconceptional period (70% of control intake from 60 days before until 6 days after conception) and early preimplantation period (70% of control intake for 6 days after conception), the expression of IGF2R and the DNA methylation in DMR of IGF2/H19 and IGF2R are altered in adrenal components. This may be caused in oocytes and embryos by the undernutritional environment (Williams-Wyss *et al*., 2014).

18.4.8 The Obese Model

Obesity is a common noncommunicable disease in our current society. Reproduction may be affected by obesity including epigenetic modifications. The high-fat-diet-induced animal model is widely used. Weaned 21-day- old female CD1 mice are fed with high-fat-diet (60% of fat) or control diet for 12 weeks before collecting oocytes or mating with male mice fed with control diet. The DNA methylation level in promoter of *Leptin* is altered in obese oocytes compared with control oocytes (Ge *et al*., 2014b). The DNA methylation of imprinted genes in sperm of offspring of obese female mice is also changed (Ge *et al*., 2014a). Histone modifications in E8.5

Downloaded From Vet-eBooks.com

embryos are also altered in the high-fat-induced mouse model (Salbaum and Kappen, 2012). When C57BL6 male mice (5 weeks old) are fed with control diet (6% fat) or high-fat-diet (21% fat) for 10 weeks the expression of 11 microRNA and global DNA methylation in sperm of obese mice are altered compared with that in sperm of control mice (Fullston *et al*., 2013).

18.4.9 The Diabetes Mellitus Model

Female CD1 mice (6–7 weeks old) receive a single intraperitoneal injection of streptozotocin at a dose of 230 mg/kg to mimic type 1 diabetes mellitus. If the glucose level is ≥17.0 mmol/l 4 days after the injection of streptozotocin, then the mice are recognized as diabetic mice. The DNA methylation in DMRs of imprinted genes is altered in metaphase II (MII) oocytes. Non-obese diabetic mice present a spontaneous diabetic model. The DNA methylation of imprinted genes is also changed in MII oocytes (Ge *et al*., 2013b). Epigenetic modifications are changed in embryos of diabetic mice (Shao *et al*., 2008; Salbaum and Kappen, 2012; Ge *et al*., 2013a). The DNA methylation of imprinted genes in sperm of the offspring of diabetic mothers is also observed (Ge *et al*., 2014a). If male CD1 mice (3 weeks old) are fed with high-fat diet for 9 weeks with an intraperitoneal injection of streptozotocin at a dose of 100 mg/kg, the methylome is changed in sperm of prediabetic mice compared with that in sperm of control mice (Wei *et al*., 2014). If fetuses are exposed to a diabetic uterus during gestation, epigenetic modifications in offspring are also affected (Lehnen *et al*., 2013).

18.4.10 Polycystic Ovary Syndrome (PCOS)

At gestational days 40–44, female monkeys are injected with 10–15 mg testosterone propionate for 15–40 consecutive days. The genome-wide DNA methylation in visceral adipose tissue of the offspring of testosterone-treated mothers is significantly changed compared with controls (Xu *et al*., 2011). When embryos of zebrafish are exposed to androgens at 26–56 h post fertilization, the global DNA methylation in ovaries of F0 and F1 is altered compared to that of controls (Xu *et al*., 2014). For the rat model, the genome-wide DNA methylation analysis in ovaries shows that 528 genes are hypermethylated in ovaries of adults exposed to high-androgens during gestation (Zhang *et al*., 2014). BALB/c mice (25-days old) are injected dehydroepiandrosterone at a dose of 6 mg/100 g body weight for 20 consecutive days and then ovaries are collected. The DNA methylation in LHR is lost in ovaries of PCOS compared with controls (Zhu *et al*., 2010).

18.4.11 The Aging Model

With aging, epigenetic modifications in oocytes and embryos are altered and the health of offspring from aged parents is also affected. In aged female murine models, the DNA methylation and histone modifications are altered in post- and preovulated oocytes (Ge *et al*., 2014c). The DNA methylation is also altered in sperm of aged male mice and it may be transmitted to the offspring (Jenkins *et al*., 2013, 2014; Niederberger, 2014).

18.4.12 Other Models

Environmental factors such as estrogens, diethylstilbestrol, and BPA (bisphenol A) have adverse effects on reproduction (Cruz *et al*., 2014). Exposure of oocytes to BPA during follicle development alter epigenetic modifications in germinal vesicles and MII oocytes in mice (Trapphoff *et al*., 2013). Epigenetic modifications are also affected by exposure to BPA during embryonic development (Susiarjo *et al*., 2013). Neonatal exposure of male rats to BPA produced

Downloaded From Vet-eBooks.com

an alteration of DNA methylation in sperm that can be inherited by the embryo and leads to postimplantation loss (Doshi *et al*., 2013).

Superovulation alters epigenetic modifications in germ cells and during embryonic development in murine species (Sato *et al*., 2007; Stouder *et al*., 2009; Market-Velker *et al*., 2010; Liang *et al*., 2013).

18.5 Effects of Environment on Epigenetic Modifications in Humans

In the previous section we reviewed animal models used to research environmental effects on the epigenome in reproduction. This section will discuss alterations of epigenetic modifications in humans.

In theory, epigenetic modifications of both male and female gametes are susceptible to being affected, but most studies focus on male gametes due to the low number of female gametes produced. Previous studies that have analyzed gametes of male individuals with fertility problems identified aberrant DNA methylation in imprinted genes on a genome-wide level. For example, the defective H19 methylation associates with poor quality sperm in oligozoospermic patients (Marques *et al*., 2004). The abnormal DNA methylation status in DMRs of *GTL2, Peg1, Lit1*, and *Peg3* is also observed in oligospermic individuals (Kobayashi *et al*., 2007). Testicular samples of patients with spermatogenic disorders present aberrant DNA methylation levels in the global genome (Heyn *et al*., 2012). Besides DNA methylation, histone modifications are also affected in human infertile patients (Okada *et al*., 2007; Hammoud *et al*., 2011).

Environmental factors have significant effects on human reproduction, but there are a few direct evidences indicating that the affected human reproduction associates with alterations of the epigenome. For example, the DNA methylation of *H19* is abnormal in sperm of patients exposed to chemotherapy treatment with temozolomide which is accompanied by the risk of impaired fertility (Berthaut *et al*., 2013). The aberrant DNA methylation of imprinted genes is also observed in human oocytes after long agonist stimulation (Shi *et al*., 2013). With aging, abnormal epigenetic modifications may also play a role for the decrease of human reproduction.

18.6 Epigenetics and Assisted Reproductive Technology (ART)

Assisted reproductive technology is a crucially potential risk associated with epigenetic modifications in human reproduction. Manipulations carried out for ARTs mainly include the use of hormones to stimulate the ovary to obtain supernumerary oocytes, *in vitro* maturation of oocytes, intrauterine insemination, *in vitro* fertilization (IVF), intracytoplasmic sperm injection (ICSI), *in vitro* culture of preimplantation embryos or cryopreservation of embryos, oocytes, or sperm (Figure 18.4). These manipulations are performed during germ cell development and preimplantation stage when major epigenetic events occur. Therefore, any of these steps may induce epigenetic alterations.

Animal studies suggest that ART manipulations induced aberrant epigenetic modifications in germ cells, embryos, and placentas (Laprise, 2009). In humans, similar results are reported in different studies (Nelissen *et al*., 2013; Tee *et al*., 2013). ART may also be associated with the increase in frequency of congenital malformation syndrome caused by aberrant genomic imprinting in children, such as Beckwith–Wiedemann syndrome (BWS), Angelman syndrome (AS), Silver–Russell syndrome (SRS), and retinoblastoma. However, opposite points are

Downloaded From Vet-eBooks.com

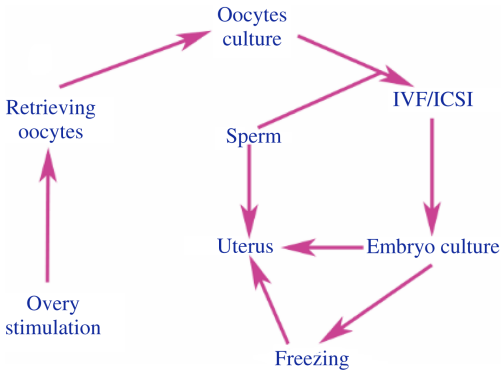

Figure 18.4 Schedule of artificial manipulations performed during assisted reproductive technology. IVF, *in vitro* fertilization; ICSI, intracytoplasm sperm injection.

supported by other studies (Laprise, 2009). This contradiction may be caused by the limitation of samples used in the studies, absence of the correlative infertile information, and the use of different statistical assumptions. But increased risks of disorders with ART births are apparent (Laprise, 2009; Fernandez *et al.*, 2014).

18.7 Priorities for the Future

It is well known that epimutation plays a crucial role in inherited diseases because only part of it can be explained by genetics. Different studies have suggested that the environment is a major factor inducing epimutations in somatic cells and germ cells. However, uncertainty still exists concerning detailed mechanisms on how environmental factors cause the alterations of the epigenome and transmit those to the next generations by germ cells. Therefore, it is useful for human reproduction to establish proper animal models to research the role of epigenetics in reproduction and avoid adverse effects induced by environmental factors on reproduction.

Another priority for the future is to monitor and discover potential risks caused by ART births in humans. Since the first ART child was born in 1978, more than 5 million children have been produced until 2013. Thus, potential risks of ART in children are hot research topics today and will remain in the future as well. To find the association between epimutation induced by ART and the health of children and how to produce a healthy child in humans are critical tasks for the future.

Acknowledgments

The lead author, Zhao-Jia Ge, thanks all people in the Reproductive Medicine Center, People's Hospital of Zhengzhou University, for their kind cooperation. Thanks is extended to Wei Shen, Shi-Ming Luo, and Jun-Yu Ma for their suggestions for this work. This work was funded by the National Natural Science Foundation of China (81401198).

References

Abbott, D.H., Barnett, D.K., Bruns, C.M., and Dumesic, D.A. (2005) Androgen excess fetal programming of female reproduction: a developmental aetiology for polycystic ovary syndrome? *Hum. Reprod. Update*, **11**, 357–374.

Downloaded From Vet-eBooks.com

Adenot, P.G., Mercier, Y., Renard, J.P., and Thompson, E.M. (1997) Differential H4 acetylation of paternal and maternal chromatin precedes DNA replication and differential transcriptional activity in pronuclei of 1-cell mouse embryos. *Development*, **124**, 4615–4625.

Aguilera, O., Fernandez, A.F., Munoz, A., and Fraga, M.F. (2010) Epigenetics and environment: a complex relationship. *J. Appl. Physiol.* **109**, 243–251.

Aiken, C.E. and Ozanne, S.E. (2014) Transgenerational developmental programming. *Hum. Reprod. Update*, **20**, 63–75.

Ancelin, K., Lange, U.C., Hajkova, P., Schneider, R., Bannister, A.J., Kouzarides, T., and Surani, M.A. (2006) Blimp1 associates with Prmt5 and directs histone arginine methylation in mouse germ cells. *Nat. Cell Biol.*, **8**, 623–630.

Arney, K.L., Bao, S., Bannister, A.J., Kouzarides, T., and Surani, M.A. (2002) Histone methylation defines epigenetic asymmetry in the mouse zygote. *Int. J. Dev. Biol.*, **46**, 317–320.

Barker, D.J. (1995) Fetal origins of coronary heart disease. *BMJ*, **311**, 171–174.

Berthaut, I., Montjean, D., Dessolle, L., Morcel, K., Deluen, F., Poirot, C., Bashamboo, A., McElreavey, K., and Ravel, C. (2013) Effect of temozolomide on male gametes: an epigenetic risk to the offspring? *J. Assist. Reprod. Genet.*, **30**, 827–833.

Bird, A. (2007) Perceptions of epigenetics. *Nature*, **447**, 396–398.

Bourc'his, D. and Bestor, T.H. (2004) Meiotic catastrophe and retrotransposon reactivation in male germ cells lacking Dnmt3L. *Nature*, **431**, 96–99.

Bourc'his, D., Xu, G.L., Lin, C.S., Bollman, B., and Bestor, T.H. (2001) Dnmt3L and the establishment of maternal genomic imprints. *Science*, **294**, 2536–2539.

Callinan, P.A. and Feinberg, A.P. (2006) The emerging science of epigenomics. *Hum. Mol. Genet.*, **15** (1), R95–R101.

Carone, B.R., Fauquier, L., Habib, N., Shea, J.M., Hart, C.E., Li, R., Bock, C., Li, C., Gu, H., Zamore, P.D., Meissner, A., Weng, Z., Hofmann, H.A., Friedman, N., and Rando, O.J. (2010) Paternally induced transgenerational environmental reprogramming of metabolic gene expression in mammals. *Cell*, **143**, 1084–1096.

Chen, P.Y., Ganguly, A., Rubbi, L., Orozco, L.D., Morselli, M., Ashraf, D., Jaroszewicz, A., Feng, S., Jacobsen, S.E., Nakano, A., Devaskar, S.U., and Pellegrini, M. (2013) Intrauterine calorie restriction affects placental DNA methylation and gene expression. *Physiol. Genomics*, **45**, 565–576.

Chuva de Sousa Lopes, S.M., Hayashi, K., Shovlin, T.C., Mifsud, W., Surani, M.A., and McLaren, A. (2008) X chromosome activity in mouse XX primordial germ cells. *PLoS Genet.*, **4**, e30.

Cortessis, V.K., Thomas, D.C., Levine, A.J., Breton, C.V., Mack, T.M., Siegmund, K.D., Haile, R.W., and Laird, P.W. (2012) Environmental epigenetics: prospects for studying epigenetic mediation of exposure–response relationships. *Hum. Genet.*, **131**, 1565–1589.

Cropley, J.E., Suter, C.M., Beckman, K.B., and Martin, D.I. (2006) Germ-line epigenetic modification of the murine A vy allele by nutritional supplementation. *Proc. Natl. Acad. Sci. USA*, **103**, 17308–17312.

Cruz, G., Foster, W., Paredes, A., Yi, K.D., and Uzumcu, M. (2014) Long-term effects of early-life exposure to environmental oestrogens on ovarian function: role of epigenetics. *J. Neuroendocrinol.*, **26**, 613–624.

Davis, T.L., Yang, G.J., McCarrey, J.R., and Bartolomei, M.S. (2000) The H19 methylation imprint is erased and re-established differentially on the parental alleles during male germ cell development. *Hum. Mol. Genet.*, **9**, 2885–2894.

Doshi, T., D'Souza, C., and Vanage, G. (2013) Aberrant DNA methylation at Igf2-H19 imprinting control region in spermatozoa upon neonatal exposure to bisphenol A and its association with post implantation loss. *Mol. Biol. Rep.*, **40**, 4747–4757.

Duhl, D.M., Vrieling, H., Miller, K.A., Wolff, G.L., and Barsh, G.S. (1994) Neomorphic agouti mutations in obese yellow mice. *Nat. Genet.*, **8**, 59–65.

Downloaded From Vet-eBooks.com

Feil, R. and Fraga, M.F. (2011) Epigenetics and the environment: emerging patterns and implications. *Nat. Rev. Genet.*, **13**, 97–109.

Fernandez, A.F., Torano, E.G., Urdinguio, R.G., Lana, A.G., Fernandez, I.A., and Fraga, M.F. (2014) The epigenetic basis of adaptation and responses to environmental change: perspective on human reproduction. *Adv. Exp. Med. Biol.*, **753**, 97–117.

Flanagan, J.M., Popendikyte, V., Pozdniakovaite, N., Sobolev, M., Assadzadeh, A., Schumacher, A., Zangeneh, M., Lau, L., Virtanen, C., Wang, S.C., and Petronis, A. (2006) Intra- and interindividual epigenetic variation in human germ cells. *Am. J. Hum. Genet.*, **79**, 67–84.

Frias, A.E. and Grove, K.L. (2012) Obesity: a transgenerational problem linked to nutrition during pregnancy. *Semin. Reprod. Med.*, **30**, 472–478.

Fullston, T., Ohlsson Teague, E.M., Palmer, N.O., DeBlasio, M.J., Mitchell, M., Corbett, M., Print, C.G., Owens, J.A., and Lane, M. (2013) Paternal obesity initiates metabolic disturbances in two generations of mice with incomplete penetrance to the F2 generation and alters the transcriptional profile of testis and sperm microRNA content. *FASEB J.*, **27**, 4226–4243.

Ganguly, A., Chen, Y., Shin, B.C., and Devaskar, S.U. (2014) Prenatal caloric restriction enhances DNA methylation and MeCP2 recruitment with reduced murine placental glucose transporter isoform 3 expression. *J. Nutr. Biochem.*, **25**, 259–266.

Ge, Z.J., Liang, Q.X., Luo, S.M., Wei, Y.C., Han, Z.M., Schatten, H., Sun, Q.Y., and Zhang, C.L. (2013a) Diabetic uterus environment may play a key role in alterations of DNA methylation of several imprinted genes at mid-gestation in mice. *Reprod. Biol. Endocrinol.*, **11**, 119.

Ge, Z.J., Liang, X.W., Guo, L., Liang, Q.X., Luo, S.M., Wang, Y.P., Wei, Y.C., Han, Z.M., Schatten, H., and Sun, Q.Y. (2013b) Maternal diabetes causes alterations of DNA methylation statuses of some imprinted genes in murine oocytes. *Biol. Reprod.*, **88**, 117.

Ge, Z.J., Liang, Q.X., Hou, Y., Han, Z.M., Schatten, H., Sun, Q.Y., and Zhang, C.L. (2014a) Maternal obesity and diabetes may cause DNA methylation alteration in the spermatozoa of offspring in mice. *Reprod. Biol. Endocrinol.*, **12**, 29.

Ge, Z.J., Luo, S.M., Lin, F., Liang, Q.X., Huang, L., Wei, Y.C., Hou, Y., Han, Z.M., Schatten, H., and Sun, Q.Y. (2014b) DNA methylation in oocytes and liver of female mice and their offspring: effects of high-fat-diet-induced obesity. *Environ. Health Perspect.*, **122**, 159–164.

Ge, Z.J., Schatten, H., Zhang, C.L., and Sun, Q.Y. (2014c) Oocyte ageing and epigenetics. *Reproduction*, **149**, R103–R114.

Ge, Z.J., Zhang, C.L., Schatten, H., and Sun, Q.Y. (2014d) Maternal diabetes mellitus and the origin of non-communicable diseases in offspring: the role of epigenetics. *Biol. Reprod.*, **90**, 139.

Gu, T.P., Guo, F., Yang, H., Wu, H.P., Xu, G.F., Liu, W., Xie, Z.G., Shi, L., He, X., Jin, S.G., Iqbal, K., Shi, Y.G., Deng, Z., Szabo, P.E., Pfeifer, G.P., Li, J., and Xu, G.L. (2011) The role of Tet3 DNA dioxygenase in epigenetic reprogramming by oocytes. *Nature*, **477**, 606–610.

Guibert, S., Forne, T., and Weber, M. (2012) Global profiling of DNA methylation erasure in mouse primordial germ cells. *Genome Res.*, **22**, 633–641.

Hajkova, P., Erhardt, S., Lane, N., Haaf, T., El-Maarri, O., Reik, W., Walter, J., and Surani, M.A. (2002) Epigenetic reprogramming in mouse primordial germ cells. *Mech. Dev.*, **117**, 15–23.

Hajkova, P., Ancelin, K., Waldmann, T., Lacoste, N., Lange, U.C., Cesari, F., Lee, C., Almouzni, G., Schneider, R., and Surani, M.A. (2008) Chromatin dynamics during epigenetic reprogramming in the mouse germ line. *Nature*, **452**, 877–881.

Hajkova, P., Jeffries, S.J., Lee, C., Miller, N., Jackson, S.P., and Surani, M.A. (2010) Genome-wide reprogramming in the mouse germ line entails the base excision repair pathway. *Science*, **329**, 78–82.

Hales, C.N. and Barker, D.J. (2001) The thrifty phenotype hypothesis. *Br. Med. Bull.*, **60**, 5–20.

Hammoud, S.S., Nix, D.A., Hammoud, A.O., Gibson, M., Cairns, B.R., and Carrell, D.T. (2011) Genome-wide analysis identifies changes in histone retention and epigenetic modifications at

Downloaded From Vet-eBooks.com

developmental and imprinted gene loci in the sperm of infertile men. *Hum. Reprod.*, **26**, 2558–2569.
Heijmans, B.T., Tobi, E.W., Stein, A.D., Putter, H., Blauw, G.J., Susser, E.S., Slagboom, P.E., and Lumey, L.H. (2008) Persistent epigenetic differences associated with prenatal exposure to famine in humans. *Proc. Natl. Acad. Sci. USA*, **105**, 17046–17049.
Heyn, H., Ferreira, H.J., Bassas, L., Bonache, S., Sayols, S., Sandoval, J., Esteller, M., and Larriba, S. (2012) Epigenetic disruption of the PIWI pathway in human spermatogenic disorders. *PLoS One*, **7**, e47892.
Holliday, R. (1987) The inheritance of epigenetic defects. *Science*, **238**, 163–170.
Howell, C.Y., Bestor, T.H., Ding, F., Latham, K.E., Mertineit, C., Trasler, J.M., and Chaillet, J.R. (2001) Genomic imprinting disrupted by a maternal effect mutation in the Dnmt1 gene. *Cell*, **104**, 829–838.
Howlett, S.K. and Reik, W. (1991) Methylation levels of maternal and paternal genomes during preimplantation development. *Development*, **113**, 119–127.
Jenkins, T.G., Aston, K.I., Cairns, B.R., and Carrell, D.T. (2013) Paternal aging and associated intraindividual alterations of global sperm 5-methylcytosine and 5-hydroxymethylcytosine levels. *Fertil. Steril.*, **100**, 945–951.
Jenkins, T.G., Aston, K.I., Pflueger, C., Cairns, B.R., and Carrell, D.T. (2014) Age-associated sperm DNA methylation alterations: possible implications in offspring disease susceptibility. *PLoS Genet.*, **10**, e1004458.
Kafri, T., Ariel, M., Brandeis, M., Shemer, R., Urven, L., McCarrey, J., Cedar, H., and Razin, A. (1992) Developmental pattern of gene-specific DNA methylation in the mouse embryo and germ line. *Genes Dev.*, **6**, 705–714.
Ko, Y.G., Nishino, K., Hattori, N., Arai, Y., Tanaka, S., and Shiota, K. (2005) Stage-by-stage change in DNA methylation status of Dnmt1 locus during mouse early development. *J. Biol. Chem.*, **280**, 9627–9634.
Kobayashi, H., Sato, A., Otsu, E., Hiura, H., Tomatsu, C., Utsunomiya, T., Sasaki, H., Yaegashi, N., and Arima, T. (2007) Aberrant DNA methylation of imprinted loci in sperm from oligospermic patients. *Hum. Mol. Genet.*, **16**, 2542–2551.
Kota, S.K. and Feil, R. (2010) Epigenetic transitions in germ cell development and meiosis. *Dev. Cell*, **19**, 675–686.
Kovacheva, V.P., Mellott, T.J., Davison, J.M., Wagner, N., Lopez-Coviella, I., Schnitzler, A.C., and Blusztajn, J.K. (2007) Gestational choline deficiency causes global and Igf2 gene DNA hypermethylation by up-regulation of Dnmt1 expression. *J. Biol. Chem.*, **282**, 31777–31788.
Kriaucionis, S. and Heintz, N. (2009) The nuclear DNA base 5-hydroxymethylcytosine is present in Purkinje neurons and the brain. *Science*, **324**, 929–930.
Kulkarni, A., Dangat, K., Kale, A., Sable, P., Chavan-Gautam, P., and Joshi, S. (2011) Effects of altered maternal folic acid, vitamin B12 and docosahexaenoic acid on placental global DNA methylation patterns in Wistar rats. *PLoS One*, **6**, e17706.
Lambrot, R., Xu, C., Saint-Phar, S., Chountalos, G., Cohen, T., Paquet, M., Suderman, M., Hallett, M., and Kimmins, S. (2013) Low paternal dietary folate alters the mouse sperm epigenome and is associated with negative pregnancy outcomes. *Nat. Commun.*, **4**, 2889.
Laprise, S.L. (2009) Implications of epigenetics and genomic imprinting in assisted reproductive technologies. *Mol. Reprod. Dev.*, **76**, 1006–1018.
Lee, K.W. and Pausova, Z. (2013) Cigarette smoking and DNA methylation. *Front. Genet.*, **4**, 132.
Lehnen, H., Zechner, U., and Haaf, T. (2013) Epigenetics of gestational diabetes mellitus and offspring health: the time for action is in early stages of life. *Mol. Hum. Reprod.*, **19**, 415–422.
Liang, X.W., Cui, X.S., Sun, S.C., Jin, Y.X., Heo, Y.T., Namgoong, S., and Kim, N.H. (2013) Superovulation induces defective methylation in line-1 retrotransposon elements in blastocyst. *Reprod. Biol. Endocrinol.*, **11**, 69.

Downloaded From Vet-eBooks.com

Lillycrop, K.A., Slater-Jefferies, J.L., Hanson, M.A., Godfrey, K.M., Jackson, A.A., and Burdge, G.C. (2007) Induction of altered epigenetic regulation of the hepatic glucocorticoid receptor in the offspring of rats fed a protein-restricted diet during pregnancy suggests that reduced DNA methyltransferase-1 expression is involved in impaired DNA methylation and changes in histone modifications. *Br. J. Nutr.*, **97**, 1064–1073.

Lindstrom, J. (1999) Early development and fitness in birds and mammals. *Trends Ecol. Evol.*, **14**, 343–348.

Mansour, A.A., Gafni, O., Weinberger, L., Zviran, A., Ayyash, M., Rais, Y., Krupalnik, V., Zerbib, M., Amann-Zalcenstein, D., Maza, I., Geula, S., Viukov, S., Holtzman, L., Pribluda, A., Canaani, E., Horn-Saban, S., Amit, I., Novershtern, N., and Hanna, J.H. (2012) The H3K27 demethylase Utx regulates somatic and germ cell epigenetic reprogramming. *Nature*, **488**, 409–413.

Margueron, R. and Reinberg, D. (2011) The polycomb complex PRC2 and its mark in life. *Nature*, **469**, 343–349.

Market-Velker, B.A., Zhang, L., Magri, L.S., Bonvissuto, A.C., and Mann, M.R. (2010) Dual effects of superovulation: loss of maternal and paternal imprinted methylation in a dose-dependent manner. *Hum. Mol. Genet.*, **19**, 36–51.

Marques, C.J., Carvalho, F., Sousa, M., and Barros, A. (2004) Genomic imprinting in disruptive spermatogenesis. *Lancet*, **363**, 1700–1702.

Mayer, W., Niveleau, A., Walter, J., Fundele, R., and Haaf, T. (2000) Demethylation of the zygotic paternal genome. *Nature*, **403**, 501–502.

McKay, J.A., Waltham, K.J., Williams, E.A., and Mathers, J.C. (2011) Folate depletion during pregnancy and lactation reduces genomic DNA methylation in murine adult offspring. *Genes Nutr*, **6**, 189–196.

McLaren, A. (1984) Meiosis and differentiation of mouse germ cells. *Symp. Soc. Exp. Biol.*, **38**, 7–23.

McLaren, A. (2003) Primordial germ cells in the mouse. *Dev. Biol.*, **262**, 1–15.

Mehedint, M.G., Craciunescu, C.N., and Zeisel, S.H. (2010) Maternal dietary choline deficiency alters angiogenesis in fetal mouse hippocampus. *Proc. Natl. Acad. Sci. USA*, **107**, 12834–12839.

Monk, M., Boubelik, M., and Lehnert, S. (1987) Temporal and regional changes in DNA methylation in the embryonic, extraembryonic and germ cell lineages during mouse embryo development. *Development*, **99**, 371–382.

Morgan, H.D., Santos, F., Green, K., Dean, W., and Reik, W. (2005) Epigenetic reprogramming in mammals. *Hum. Mol. Genet.*, **14** (1), R47–R58.

Nelissen, E.C., Dumoulin, J.C., Daunay, A., Evers, J.L., Tost, J., and van Montfoort, A.P. (2013) Placentas from pregnancies conceived by IVF/ICSI have a reduced DNA methylation level at the H19 and MEST differentially methylated regions. *Hum. Reprod.*, **28**, 1117–1126.

Niederberger, C. (2014) Paternal aging and associated intraindividual alterations of global sperm 5-methylcytosine and 5-hydroxymethylcytosine levels. *J. Urol.*, **191**, 1356.

Okada, Y., Scott, G., Ray, M.K., Mishina, Y., and Zhang, Y. (2007) Histone demethylase JHDM2A is critical for Tnp1 and Prm1 transcription and spermatogenesis. *Nature*, **450**, 119–123.

Oswald, J., Engemann, S., Lane, N., Mayer, W., Olek, A., Fundele, R., Dean, W., Reik, W., and Walter, J. (2000) Active demethylation of the paternal genome in the mouse zygote. *Curr. Biol.*, **10**, 475–478.

Panning, B. and Jaenisch, R. (1998) RNA and the epigenetic regulation of X chromosome inactivation. *Cell*, **93**, 305–308.

Peaston, A.E. and Whitelaw, E. (2006) Epigenetics and phenotypic variation in mammals. *Mamm Genome*, **17**, 365–374.

Popp, C., Dean, W., Feng, S., Cokus, S.J., Andrews, S., Pellegrini, M., Jacobsen, S.E., and Reik, W. (2010) Genome-wide erasure of DNA methylation in mouse primordial germ cells is affected by AID deficiency. *Nature*, **463**, 1101–1105.

Downloaded From Vet-eBooks.com

Radford, E.J., Ito, M., Shi, H., Corish, J.A., Yamazawa, K., Isganaitis, E., Seisenberger, S., Hore, T.A., Reik, W., Erkek, S., Peters, A.H., Patti, M.E., and Ferguson-Smith, A.C. (2014) *In utero* effects. *In utero* undernourishment perturbs the adult sperm methylome and intergenerational metabolism. *Science*, **345**, 1255903.

Reik, W. (2007) Stability and flexibility of epigenetic gene regulation in mammalian development. *Nature*, **447**, 425–432.

Robins, J.C., Marsit, C.J., Padbury, J.F., and Sharma, S.S. (2011) Endocrine disruptors, environmental oxygen, epigenetics and pregnancy. *Front. Biosci.*, **3**, 690–700.

Rougier, N., Bourc'his, D., Gomes, D.M., Niveleau, A., Plachot, M., Paldi, A., and Viegas-Pequignot, E. (1998) Chromosome methylation patterns during mammalian preimplantation development. *Genes Dev.*, **12**, 2108–2113.

Salbaum, J.M. and Kappen, C. (2012) Responses of the embryonic epigenome to maternal diabetes. *Birth Defects Res. A Clin. Mol. Teratol.*, **94**, 770–781.

Santos, F., Hendrich, B., Reik, W., and Dean, W. (2002) Dynamic reprogramming of DNA methylation in the early mouse embryo. *Dev. Biol.*, **241**, 172–182.

Santos, F., Peters, A.H., Otte, A.P., Reik, W., and Dean, W. (2005) Dynamic chromatin modifications characterise the first cell cycle in mouse embryos. *Dev. Biol.*, **280**, 225–236.

Sasaki, H. and Matsui, Y. (2008) Epigenetic events in mammalian germ-cell development: reprogramming and beyond. *Nat. Rev. Genet.*, **9**, 129–140.

Sato, A., Otsu, E., Negishi, H., Utsunomiya, T., and Arima, T. (2007) Aberrant DNA methylation of imprinted loci in superovulated oocytes. *Hum. Reprod.*, **22**, 26–35.

Seki, Y., Hayashi, K., Itoh, K., Mizugaki, M., Saitou, M., and Matsui, Y. (2005) Extensive and orderly reprogramming of genome-wide chromatin modifications associated with specification and early development of germ cells in mice. *Dev. Biol.*, **278**, 440–458.

Seki, Y., Yamaji, M., Yabuta, Y., Sano, M., Shigeta, M., Matsui, Y., Saga, Y., Tachibana, M., Shinkai, Y., and Saitou, M. (2007) Cellular dynamics associated with the genome-wide epigenetic reprogramming in migrating primordial germ cells in mice. *Development*, **134**, 2627–2638.

Seki, Y., Williams, L., Vuguin, P.M., and Charron, M.J. (2012) Minireview: epigenetic programming of diabetes and obesity: animal models. *Endocrinology*, **153**, 1031–1038.

Shao, W.J., Tao, L.Y., Gao, C., Xie, J.Y., and Zhao, R.Q. (2008) Alterations in methylation and expression levels of imprinted genes H19 and Igf2 in the fetuses of diabetic mice. *Comp. Med.*, **58**, 341–346.

Shi, X., Chen, S., Zheng, H., Wang, L., and Wu, Y. (2013) Aberrant DNA methylation of imprinted loci in human *in vitro* matured oocytes after long agonist stimulation. *Eur. J. Obstet. Gynecol. Reprod. Biol.*, **167**, 64–68.

Stein, A.D., Kahn, H.S., Rundle, A., Zybert, P.A., van der Pal-de Bruin, K., and Lumey, L.H. (2007) Anthropometric measures in middle age after exposure to famine during gestation: evidence from the Dutch famine. *Am. J. Clin. Nutr.*, **85**, 869–876.

Stouder, C., Deutsch, S., and Paoloni-Giacobino, A. (2009) Superovulation in mice alters the methylation pattern of imprinted genes in the sperm of the offspring. *Reprod. Toxicol.*, **28**, 536–541.

Sugimoto, M. and Abe, K. (2007) X chromosome reactivation initiates in nascent primordial germ cells in mice. *PLoS Genet.*, **3**, e116.

Susiarjo, M., Sasson, I., Mesaros, C., and Bartolomei, M.S. (2013) Bisphenol a exposure disrupts genomic imprinting in the mouse. *PLoS Genet.*, **9**, e1003401.

Tachibana, M., Ueda, J., Fukuda, M., Takeda, N., Ohta, T., Iwanari, H., Sakihama, T., Kodama, T., Hamakubo, T., and Shinkai, Y. (2005) Histone methyltransferases G9a and GLP form heteromeric complexes and are both crucial for methylation of euchromatin at H3-K9. *Genes Dev.*, **19**, 815–826.

Downloaded From Vet-eBooks.com

Tahiliani, M., Koh, K.P., Shen, Y., Pastor, W.A., Bandukwala, H., Brudno, Y., Agarwal, S., Iyer, L.M., Liu, D.R., Aravind, L., and Rao, A. (2009) Conversion of 5-methylcytosine to 5-hydroxymethylcytosine in mammalian DNA by MLL partner TET1. *Science*, **324**, 930–935.

Tee, L., Lim, D.H., Dias, R.P., Baudement, M.O., Slater, A.A., Kirby, G., Hancocks, T., Stewart, H., Hardy, C., Macdonald, F., and Maher, E.R. (2013) Epimutation profiling in Beckwith–Wiedemann syndrome: relationship with assisted reproductive technology. *Clin. Epigenetics*, **5**, 23.

Tian, X. and Diaz, F.J. (2013) Acute dietary zinc deficiency before conception compromises oocyte epigenetic programming and disrupts embryonic development. *Dev. Biol.*, **376**, 51–61.

Trapphoff, T., Heiligentag, M., El Hajj, N., Haaf, T., and Eichenlaub-Ritter, U. (2013) Chronic exposure to a low concentration of bisphenol A during follicle culture affects the epigenetic status of germinal vesicles and metaphase II oocytes. *Fertil. Steril.*, **100**, 1758–1767.

Vasicek, T.J., Zeng, L., Guan, X.J., Zhang, T., Costantini, F., and Tilghman, S.M. (1997) Two dominant mutations in the mouse fused gene are the result of transposon insertions. *Genetics*, **147**, 777–786.

Watanabe, D., Suetake, I., Tada, T., and Tajima, S. (2002) Stage- and cell-specific expression of Dnmt3a and Dnmt3b during embryogenesis. *Mech. Dev.*, **118**, 187–190.

Waterland, R.A., Dolinoy, D.C., Lin, J.R., Smith, C.A., Shi, X., and Tahiliani, K.G. (2006) Maternal methyl supplements increase offspring DNA methylation at Axin Fused. *Genesis*, **44**, 401–406.

Wei, Y., Yang, C.R., Wei, Y.P., Zhao, Z.A., Hou, Y., Schatten, H., and Sun, Q.Y. (2014) Paternally induced transgenerational inheritance of susceptibility to diabetes in mammals. *Proc. Natl. Acad. Sci. USA*, **111**, 1873–1878.

Williams-Wyss, O., Zhang, S., MacLaughlin, S.M., Kleemann, D., Walker, S.K., Suter, C.M., Cropley, J.E., Morrison, J.L., Roberts, C.T., and McMillen, I.C. (2014) Embryo number and periconceptional undernutrition in the sheep have differential effects on adrenal epigenotype, growth, and development. *Am. J. Physiol. Endocrinol. Metab.*, **307**, E141–E150.

Wolff, G.L., Kodell, R.L., Moore, S.R., and Cooney, C.A. (1998) Maternal epigenetics and methyl supplements affect agouti gene expression in Avy/a mice. *FASEB J.*, **12**, 949–957.

Wu, C. and Morris, J.R. (2001) Genes, genetics, and epigenetics: a correspondence. *Science*, **293**, 1103–1105.

Xu, N., Kwon, S., Abbott, D.H., Geller, D.H., Dumesic, D.A., Azziz, R., Guo, X., and Goodarzi, M.O. (2011) Epigenetic mechanism underlying the development of polycystic ovary syndrome (PCOS)-like phenotypes in prenatally androgenized rhesus monkeys. *PLoS One*, **6**, e27286.

Xu, N., Chua, A.K., Jiang, H., Liu, N.A., and Goodarzi, M.O. (2014) Early embryonic androgen exposure induces transgenerational epigenetic and metabolic changes. *Mol. Endocrinol.*, **28**, 1329–1336.

Zeng, L., Fagotto, F., Zhang, T., Hsu, W., Vasicek, T.J., Perry, W.L.,3rd., Lee, J.J., Tilghman, S.M., Gumbiner, B.M., and Costantini, F. (1997) The mouse fused locus encodes Axin, an inhibitor of the Wnt signaling pathway that regulates embryonic axis formation. *Cell*, **90**, 181–192.

Zeybel, M., Hardy, T., Wong, Y.K., Mathers, J.C., Fox, C.R., Gackowska, A., Oakley, F., Burt, A.D., Wilson, C.L., Anstee, Q.M., Barter, M.J., Masson, S., Elsharkawy, A.M., Mann, D.A., and Mann, J. (2012) Multigenerational epigenetic adaptation of the hepatic wound-healing response. *Nat. Med.*, **18**, 1369–1377.

Zhang, D., Cong, J., Shen, H., Wu, Q., and Wu, X. (2014) Genome-wide identification of aberrantly methylated promoters in ovarian tissue of prenatally androgenized rats. *Fertil. Steril.*, **102**, 1458–1467.

Downloaded From Vet-eBooks.com

Zheng, S., Rollet, M., and Pan, Y.X. (2011) Maternal protein restriction during pregnancy induces CCAAT/enhancer-binding protein (C/EBPbeta) expression through the regulation of histone modification at its promoter region in female offspring rat skeletal muscle. *Epigenetics*, **6**, 161–170.

Zhu, J.Q., Zhu, L., Liang, X.W., Xing, F.Q., Schatten, H., and Sun, Q.Y. (2010) Demethylation of LHR in dehydroepiandrosterone-induced mouse model of polycystic ovary syndrome. *Mol. Hum. Reprod.*, **16**, 260–266.

Downloaded From Vet-eBooks.com

19

Toward Development of Pluripotent Porcine Stem Cells by Road Mapping Early Embryonic Development

Stoyan Petkov,[1] Kristine Freude,[2] Kaveh Mashayekhi,[2,3,4] Poul Hyttel,[2] and Vanessa Hall[2]

[1]*Institute for Farm Animal Genetics, , Friedrich-Loeffler-Institute, Neustadt, Germany*
[2]*Faculty of Health and Medical Sciences, Department of Veterinary Clinical and Animal Sciences, University of Copenhagen, Denmark*
[3]*BioTalentum Ltd., Aulich Lajos str. 26. 2100 Gödöllő, Hungary*
[4]*Sandor Life Sciences, Sandor Medicaids Group Pvt. Ltd., Hyderabad, 500043 India.*

19.1 Introduction

Embryonic development in mammals is the extraordinary transition of a single-celled fertilized zygote into a complex fetus, which occurs in the uterus of the maternal adult during the early stages of gestation. This takes about 8 weeks to occur in humans and varies somewhat in time in the different mammalian species. In the very first days of early development, the embryo succeeds to divide by mitosis to form a cluster of cells known as blastomeres, which are alike transcriptionally and which all have equal developmental potential to form identical organisms including the extraembryonic tissues if they are artificially separated and cultured from each other. These cells are described as being totipotent. At a specified time point in early development (occurring after only a few days after fertilization), the totipotent blastomeres become altered transcriptionally and are morphologically split in their embryonic fate. Some become specified to form only extraembryonic tissues (known as trophectoderm cells), while others become specified to form only embryonic tissues (known as inner cell mass (ICM) cells), which also contribute to extraembryonic tissues through formation of some of the fetal membranes and part of the placenta as, for example, its vascularization. The cellular arrangement of these two different cell populations differs. The trophectoderm cells are restricted to an outer layer of the embryo surrounding a blastocyst cavity or fluid-filled cavity and the ICM cells form a tight cluster on one part of the inner part of the trophectoderm. Together, these cells form the early blastocyst. When these morphological and transcriptional changes occur, cellular fate becomes restricted, which is also known as the first differentiation event. The ICM cells have acquired a unique ability to form every specialized cell of the fetus, and if isolated at this stage, the cells may retain this ability as embryonic stem cells (ESCs). This differentiation ability is therefore slightly more restricted than the totipotent blastomeres, and these cells are termed pluripotent. In contrast, the trophectoderm cells only give rise to the external layer of the extraembryonic tissues forming the epithelium of the chorion and the trophoblast of the placenta. The ICM cells undergo further rounds of cell division and then segregate into two further cell types known as the epiblast cells and the hypoblast cells. The epiblast cells (also known as the primitive ectoderm) are also able to differentiate into three crucial embryonic tissues or germ lineages: the ectoderm, endoderm, and mesoderm, as well as the primordial

Animal Models and Human Reproduction, First Edition. Edited by Heide Schatten and Gheorghe M. Constantinescu.
© 2017 John Wiley & Sons, Inc. Published 2017 by John Wiley & Sons, Inc.

Downloaded From Vet-eBooks.com

germ cells, which together form the developing embryo. Hence, they are as pluripotent as the ICM. This slightly more restricted differentiation is today well recognized as the ground state of pluripotency (Hackett and Surani, 2014; Wray *et al*., 2010). In contrast, the hypoblast cells continue to differentiate into both the extraembryonic endoderm and visceral endoderm, which aid as supportive tissues for the developing embryo. The blastocyst expands and undergoes further mitotic divisions to form the postimplantation embryo (in some species such as the mouse) and the early epiblast cells differentiate into the late epiblast cells, which express more lineage-restricted markers than their earlier cell counterparts and begin to form the primitive streak, which is the primary mark for the beginning of gastrulation. These cells are considered to mark a later stage of pluripotency, which is termed "primed" pluripotency (Nichols and Smith, 2009) since transcriptional changes, including an alteration in the self-renewal signaling pathways, an upregulation of more lineage-restrictive genes, and inactivation of the female X chromosome, occur (Hackett and Surani, 2014). Despite these changes, these cells may still form all cells of the developing embryo and are therefore also considered pluripotent.

Researchers have been able to isolate pluripotent ICM cells from embryos in several species (Evans and Kaufman, 1981; Martin, 1981; Thomson *et al*., 1998; Thomson *et al*., 1995) and culture them *in vitro* where they can be maintained and self-renew without further differentiating using specific culture conditions. In addition, they can be induced to differentiate by changing culture conditions so that they form specialized cells of the embryonic or adult organism.

Cultured ICM cells are better known as ESC and reflect in many ways their embryonic ICM predecessors. However, recent evidence shows that depending on the culture conditions used, these ESCs become unique in several ways compared to the ICM cells of the embryo. First, ESCs can be cultured in a self-renewing state indefinitely, differing from the transient state of the embryonic ICM. Second, in the case of the mouse, ESCs appear to modulate the ground state of pluripotency seen in the early epiblast cells, as opposed to the ICM cells that they are generally isolated from, indicating some modification in their stem cell state, due to their altered *in vitro* environment. Recent evidence also shows that the self-renewal state of ESCs is only acquired following epiblast specification (Boroviak *et al*., 2014). These cells retain the ability to form all embryonic germ lineages when directed to differentiate *in vitro* and may contribute to all tissues of the body when injected into tetraploid noncompetent blastocysts, which undeniably indicates that they retain pluripotent characteristics. Other features that suggest these cells modulate the early epiblast include the expression of unique markers, including Oct4, Nanog, Sox2, Klf2 and Klf4, Rex1, NrOb1, and Fgf4 (Nichols and Smith, 2009). In addition, like the early epiblast of the embryo, these cells self-renew in response to activation of the LIF/STAT pathway and, in addition, in female lines, both X chromosomes are active (Nichols and Smith, 2009), as observed in the early epiblast. Such ESCs are termed "naïve," which is to reflect their status in mimicking the ground state of pluripotency. In the human, it has been shown that isolated and cultured ICM transiently form ESCs that share more characteristics similar to the later epiblast-like stem cells instead of the early epiblast cells. These cells share many characteristics with the late epiblast, such as the ability to form cells of the embryonic germ lineages upon directed or spontaneous differentiation, both *in vitro* and *in vivo* when injected into immunodeficient mice. These cells self-renew in response to activation of the FGF and ACTIVIN/NODAL pathways, as opposed to the JAK/STAT pathway (Nichols and Smith, 2009). These cells do not express the markers observed in naïve ESCs, including, KLF2, KLF4, REX1, NROB1, or FGF4 (Nichols and Smith, 2009), and interestingly, expression of the transcription factor *OCT4* (a regulatory gene of pluripotency) differs compared to mouse ESC, as expression is driven by the proximal rather than the distal enhancer (Gafni *et al*., 2013). Moreover, X chromosome inactivation of one of the two female X chromosomes is common in most human ESCs (hESCs), an upregulation of global

Downloaded From Vet-eBooks.com

DNA hypermethylation has occurred and the cells express more lineage-restrictive genes such as *LEFTY* and *FGF5* (Hackett and Surani, 2014) similar to the late epiblast cells in the developing primitive streak. These differences have led to a common recognition that hESC reflect the primed state of the late epiblast cells. Similarly, cells isolated from the epiblast of the post-implantation mouse embryo and maintained in culture media that activate the FGF and ACTIVIN/NODAL pathways reflect a very similar profile to hESC (Brons *et al*., 2007), conferring that they share a similar primed pluripotent state *in vitro*.

While there are at least two clearly identifiable pluripotent stem cell states that can be recapitulated *in vitro*, recent research has shown that a spectrum of pluripotent states can actually be observed in the cultured pluripotent stem cells simply by modulating cell culture conditions. Pluripotent states can be altered *in vitro* and revert a primed state ESC line into a naïve stem cell line or *vice versa*, in either the mouse, rat, or human. There are also apparent distinctions between cultured mESCs in 2i/LIF culture (a serum-free medium including small molecules that block members of the FGF and WNT signaling pathways) and conventional mESCs grown in serum, as the former cells display fewer mesoderm and ectoderm lineage-specific genes and are considered to reflect the ground state of pluripotency (Marks *et al*., 2012). Furthermore, there appears to exist heterogeneity of pluripotent stem cell states within individual cell lines adding to the complexity in defining pluripotency of stem cells, which has potentially been linked to the presence of serum in culture (Marks *et al*., 2012).

The pluripotent state has also been artificially modulated in recent years, thanks to discovering specific transcription factors that, when activated or introduced into adult or somatic cells, will reset the cellular fate to an early pluripotent stem cell state (Takahashi and Yamanaka, 2006). Cells that are reset to pluripotency are termed induced pluripotent stem cells (iPSC) and maintain most characteristics of *bona fide* ESC, although there are several reports that there may be a greater variation in their ability to differentiate into all three embryonic germ layers compared to ESC. In addition, their reprogramming is not always complete at the epigenetic level, particularly in early passage cells, since they may retain an epigenetic profile identical to the donor cell used in the reprogramming (Sullivan *et al*., 2010; Kim *et al*., 2010; Polo *et al*., 2010).

In the porcine species, it has proven particularly difficult to maintain isolated ICM cells *in vitro* and preserve their self-renewing pluripotent state long term (Hall, 2012; Gandolfi *et al*., 2012). Research pertaining to the isolation and establishment of porcine ESC (pESC) has continued for over two decades with no significant advancement toward this goal. Despite this lack of progress, there does remain hope that pESC can be established, since we have seen in recent years the successful establishment of true ESCs from rat embryos, which have previously resisted efforts from the scientific community. Rat ESCs are relatively comparable to naïve ESCs and fulfill most of the criteria related to pluripotency (Chen *et al*., 2013; Blair *et al*., 2012). There would be many advantages in the development of such cells also in other species for many areas of research. For an overview see Figure 19.1. Pigs remain a very appealing alternative model for modulating human disease since they share many anatomical and physiological characteristics with man (Lelovas *et al*., 2014). Biomedical pig models could serve as genetic backgrounds for establishment of ESC or other pluripotent stem cells (such as iPSC), which may be used to model and study diseases *in vitro* (Bassols *et al*., 2014; Vodicka *et al*., 2005). Pluripotent stem cells from healthy or immunodeficient pigs could be used for differentiation into specific cell types for advancing cell transplantation methodologies and technologies. Finally, development of pluripotent stem cells and differentiation into female and male gametes could pave the way for advancing infertility treatments. There have been some advances in this field in other species, including human and mouse (Medrano *et al*., 2014); however the pig could be an alternative model for improving differentiation protocols and for testing how well these gametes may

Downloaded From Vet-eBooks.com

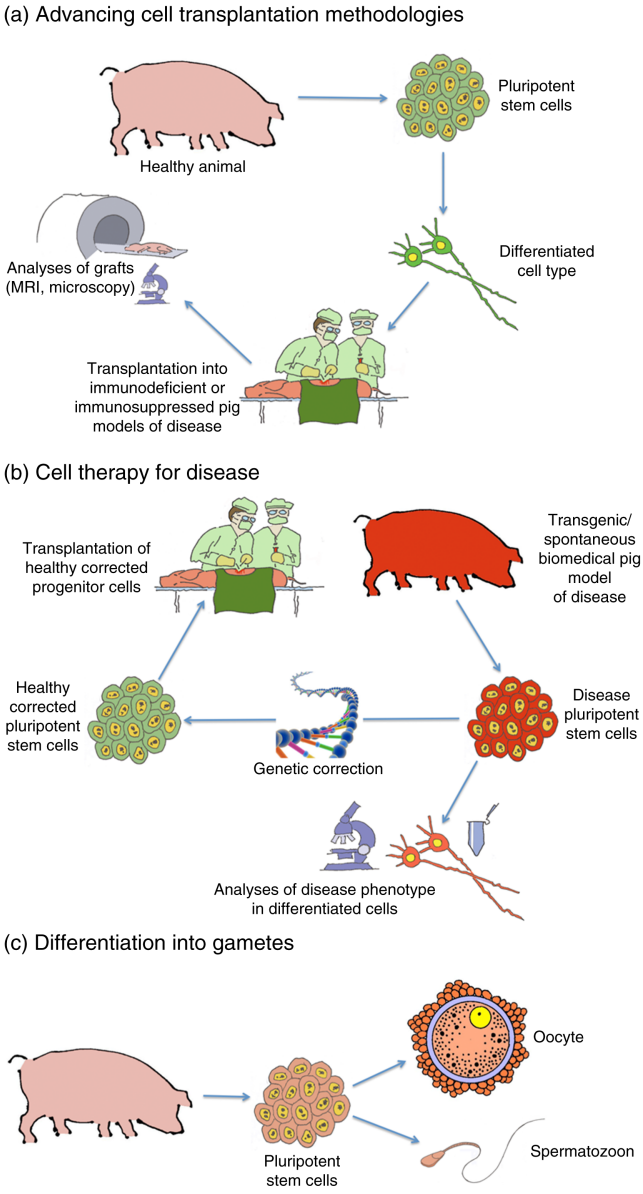

Figure 19.1 The establishment of *bona fide* porcine pluripotent stem cells would help to advance cell transplantation methodologies (a), provide an alternative model for testing and developing cell therapies (b), and may even advance alternative infertility treatments (c). (See color plate section.)

develop following transplantation *in vivo*. In this chapter, we provide insight into the current knowledge of pluripotent states in the developing pig embryo and the current status in establishment of *bona fide* pESC and piPSCs. This chapter reflects the potential causes underlying the difficulty in establishing pluripotent stem cells and reviews recent data on global profiling of the pluripotent states in this species. Future perspectives toward achievement in establishment of *bona fide* pESC are also outlined in this chapter.

Downloaded from Vet-eBooks.com

19.2 Current Status on the Pluripotent State in the Pig Embryo

A clear understanding of the molecular profile of the pluripotent states in the pig are still being developed, although recent research suggests that there are unique gene signatures in this species compared to both mouse and human cells. The pluripotent states in mouse and human embryos are separately defined according to their molecular and epigenetic characteristics. In the case of the naïve state, a commonality between both these species is the expression of *OCT4* under control of the distal enhancer (Theunissen *et al*., 2014) and ability to contribute to allogenic chimeras or interspecies chimeras (Gafni *et al*., 2013). However, the naïve states differ as mESCs display two active X chromosomes in female lines (representative of the ground state of pluripotency in the early epiblast cells), whereas induced human naïve ESCs appear to retain an inactive X chromosome, seen typically in primed epiblast cells (Theunissen *et al*., 2014), which may suggest that complete acquisition of the naïve state is not obtained. Characterization of the molecular signatures of the porcine ICM, the early and late epiblasts, would help to define how similar the ground state of pluripotency and primed states are in this species, compared to mouse and man. A better understanding of the embryonic cells and in particular which cell pathways are crucial for cell renewal could also help to improve media for maintenance and culture of porcine ESC and iPSC.

One important point to clarify is when the ground state of pluripotency and primed state exist in the developing pig embryo. Porcine embryonic development has been previously well summarized (Hall *et al*., 2013; Oestrup *et al*., 2009). This distinction can be made by morphology alone, that is, the early epiblast, which is encapsulated partly by the hypoblast, is observed in embryos at around D9 of development. This is at a significantly later time point than in mouse and human embryos, primarily due to delayed placentation events in the pig. Similarly, the primed state may be classified in the pig to be around D11, when the embryonic disc has fully formed and the late epiblast has acquired epithelial characteristics (Hall *et al*., 2010). This coincides with the epithelial characteristics acquired in the late epiblast of the mouse, which has formed into a cup-shaped epithelium (Nichols and Smith, 2009), and the epithelial characteristics of the human late epiblast (Sheng, 2014). However, there are morphological differences in the pig compared to the other two species at the later primed state, as the epiblast cells protrude through the trophectoderm and become exposed to the outer environment and the epithelium is thicker with up to three layers observed (Hall *et al*., 2010). In a recent paper we defined two earlier stages to describe the developing inner cell mass of the pig embryo, that is, the early premature ICM, which is encapsulated in the D5–D6 blastocyst and the reticent ICM, which is encapsulated in the D7–D8 nonhatched blastocyst (Hall and Hyttel, 2014), and although these stages are also interesting, they don't recapitulate the two states of pluripotency that are observed *in vitro*. By reflecting on this time development differences in the pig, we may be able to better assess and compare the pluripotent states across species.

Some research has been performed on varying cell populations of either *in vivo*- or *in vitro*-produced porcine embryos to gain some insight into the expression of different genes associated with mouse and human pluripotency. However, this has often been performed on the ICM of the pig embryos, which do not reflect the two states of pluripotency. Here we concentrate on the research that has been performed on *in vivo*-produced embryos that are specific to the early epiblast (D9 embryos) and late epiblast (D11 embryos) in the pig and focus on how it compares to the other species. In the case of pluripotent markers, OCT4 is observed in the early epiblast and late epiblast as well as NANOG and SOX2, however, NANOG and SOX2 expression is weaker in the early epiblast (Hall *et al*., 2009). Some of the considered naïve markers have also been analyzed, including REX1, NrOB1, KLF4, and *KLF2* (Hall and Hyttel, 2014). Interestingly, only two of these appear to be expressed in the naïve state in the pig, that is, NrOB1 and REX1,

Downloaded From Vet-eBooks.com

and although transcripts of the genes can be detected, protein expression was very weak (Hall and Hyttel, 2014). Moreover, justification that REX1 might be a good marker of the naïve state is difficult, since *REX1* expression was higher in the late epiblast than in the early epiblast. Thus, NrOB1 may be the only marker from the list that truly reflects the naïve state in the pig. In contrast KLF4 and *KLF2* were more highly expressed in the primed state, although KLF4 was observed only to be expressed in a small subset of cells in the late epiblast (Hall and Hyttel, 2014). The best marker expression pattern for the naïve state in the pig appears to be the expression of SSEA1 and lack of expression of SSEA3, SSEA4, TRA1-60, and TRA-1-81 (Hall *et al*., 2010; Hall and Hyttel, 2014). This cell surface marker profile compares well to the ground state of pluripotency in mouse embryos (Henderson *et al*., 2002). In contrast, in the case of the primed state, a strong hallmark feature is the loss of SSEA1 and NrOB1 in the pig late epiblast. The gene, *KLF2*, is a candidate marker of primed pluripotency in the pig and cMYC may be another promising marker, although the latter marks only a subset population in the late epiblast. The lineage-specific markers, FGF5 and LEFTY, as well as several cell surface markers (SSEA3, SSEA4, TRA-1-60, and TRA-1-81), have not yet been analyzed in the porcine late epiblast. Taken together, the pluripotent-associated genes for both the porcine naïve state and the primed state are summarized in Table 19.1. It is evident that the considered naïve markers are not comparative across species (with the exception of NrOB1) and should not be used to help define pluripotent states in *in vitro*-produced porcine pluripotent cells. The pluripotent markers OCT4, NANOG, and SOX2 are well conserved between the species but are expressed in both pluripotent states. Therefore, further research may help to strengthen the molecular signatures of the naïve versus the primed state in the pig.

A defining difference between the naïve and primed state of pluripotency is also the different cell pathways that govern cell renewal. Understanding which cell pathway is active that regulates cell renewal in the porcine naïve state versus the primed state could also help in future establishment of *bona fide* pluripotent stem cells *in vitro*. Only limited research has been performed to elucidate the active cell signaling pathways in the early epiblast and late epiblast in

Table 19.1 Known molecular signature of the ground state of pluripotency versus the primed state in the pig embryo based on current literature.

Gene/protein categories	Ground state (D9–D10 embryo)	Primed state (D11–D12 embryo)
Pluripotent genes	OCT4, NANOG,[a] SOX2[a]	OCT4, NANOG, SOX2
Cell surface markers	SSEA1 (negative for SSEA3, SSEA4, TRA1-60, TRA1-81)	(Negative for SSEA1)
Considered naïve markers in mouse and human	REX1,[a] NrOB1[a]	REX1, KLF4[b], cMYC[b] *KLF2*
FGF cell signaling	–	*FGFr1*, *FGFr2*, *cFOS*
JAK/STAT cell signaling	–	LIFr[b], *STAT3*
BMP cell signaling	–	BMPr, *SMAD1*, *SMAD5*, *SMAD4*, *BMP4*
WNT cell signaling	*β-catenin*	*SFRP1*, *GSK3β*, *β-catenin*
CRIPTO/NODAL cell signaling	*CRIPTO*	CRIPTO, SMAD2, *SMAD4*
MEK/ERK cell signaling	p-p38/MAPK	*cFOS*

D: day.
a) Weak protein expression.
b) Only small subpopulation shows expression.

Downloaded From Vet-eBooks.com

the pig. An overview of the current knowledge of different genes expressed within different cell signaling pathways associated with pluripotency is provided in Table 19.1. What is striking in this species is how little remains known about the cell signaling pathways that regulate the ground state of pluripotency. As already mentioned, JAK/STAT and the ACTIVIN/NODAL pathways are important in regulating the naïve state. So far, only genes involved in regulation of the JAK/STAT pathway have been investigated at these two stages, and interestingly there is no evidence to suggest that this pathway is active or functioning, since the LIFr is clearly not expressed in the early epiblast (Hall *et al*., 2009). Activin has only been analyzed in the porcine ICM (van de Pavert *et al*., 2001), therefore its expression in the early epiblast and late epiblast remains unknown. However, it is has been indirectly implicated in playing a role in regulation of the primed state, as ESCs isolated from the epiblast that have been treated with an inhibitor of Activin differentiate into the neural lineage *in vitro* (Alberio *et al*., 2010). In addition, several genes associated with FGF and BMP cell signaling are not expressed at this stage and only a limited number of genes associated with well-defined pathways of pluripotency, for example, WNT, NODAL, and MEK/ERK signaling, are expressed (Hall and Hyttel, 2014). Therefore, the pathway/s important for regulating the naïve state in the pig have not yet been uncovered. In contrast, investigation of genes expressed for cell pathways during the primed state of pluripotency in the pig has revealed that many genes important in the FGF, JAK/STAT, BMP, WNT, and CRIPTO/NODAL signaling are expressed (see Table 19.1) (Hall and Hyttel, 2014; Hall *et al*., 2009). Whether all these pathways are responsible for regulating cell renewal is, however, still not yet defined. Testing of inhibitors that block FGF, JAK/STAT, and BMP signaling on cultured ESCs isolated from both D5 and D10 embryos suggest that these pathways are relatively important for maintenance of cell renewal *in vitro*, as the cells differentiated or stopped proliferating earlier than nontreated cultures (Hall and Hyttel, 2014). Further research is therefore required to determine which pathway/s are important for regulating the primed state in the pig.

19.3 Current Status of the Establishment of Porcine Embryonic Stem Cells (pESCs)

Attempts to produce porcine embryonic stem cells (pESCs) have been pursued by isolation of either the ICM from porcine blastocysts or the epiblast from the later hatched embryo (see overview of pESC derivation Table 19.2). However, all attempts to date have failed to result in the generation of long-term pluripotent stem cell lines. The first reports of derivation of pluripotent cell lines from porcine blastocysts date back 25 years (Evans *et al*., 1990; Notarianni *et al*., 1990). Cultured pESC-like cells are unstable as they differentiate shortly after a few passages and cannot be proliferated long term in culture. Despite the advances in defining pluripotency in this species, pESCs, for unknown reasons, rapidly lose their pluripotent features over time and passage. The pluripotency of pESCs, like all species, is defined partly by their ability to differentiate into all three germ layers, namely, endo-, ecto-, and mesoderm. Interestingly, in earlier reported publications, differentiation of pESCs *in vitro* could only occur toward the ectoderm lineage (Evans *et al*., 1990; Talbot *et al*., 2002). Some improvement has been observed in later publications, as the number of passages in which pESCs could remain pluripotent increased, but also the ability of these cells to differentiate into all three germ layers (Son *et al*., 2009). Many of the remaining challenges in generating and maintaining *bona fide* pESCs are caused by several major hurdles that still need to be overcome in order to successfully culture pESCs.

Downloaded From Vet-eBooks.com

Table 19.2 Methods for isolation of porcine embryonic stem cells.

Pluripotent cell stage	ES culture media	References
EPI	Stem cell culture medium (SCM) with bFGF	Alberio *et al.*, 2010
ICM	DMEM, 5% FCS, 10% CS, 0.1 mM βME	Anderson *et al.*, 1994
EPI	DMEM, 10% FBS, 0.1 mM βME, L-glutamine mixed 1:1 with Medium 199, 10% FBS	Blomberg *et al.*, 2008
ICM	DMEM low glucose (50%), Hams F10 (50%), 2 mM glutamine, 0.1 mM βME, NUCLEOSIDE, NEAA, 1000 IU/ml LIF, 5 ng/ml human bFGF 10% KO serum, 5% FBS	Brevini *et al.*, 2010
ICM	ESC culture media	Chen *et al.*, 1999
ICM	DMEM, 5% FCS, 10% CS, 0.1 mM βME	Evans *et al.*, 1990
ICM	DMEM, 10% FCS	Gerfen and Wheeler, 1995
ICM + EPI	DMEM, 10% FCS, 0.1 mM βME, 1000 U/ml hLIF, 10 mg/ml hSCF, 10 ng/ml EGF, 4–25 ng/ml PDGF, 0,3 ng/ml TGFβ	Hochereau de Reviers *et al.*, 1993
ICM	DMEM, 2 mM Glutamax, 1% NEAA, 15% FBS, 20 ng/ml hLIF, 0.1 mM βME	Haraguchi *et al.*, 2012
ICM	DMEM, 0.1 mM βME, NEAA, 40 ng/ml human LIF, 20 ng/ml bFGF, nucleosides, 16% FCS	Li *et al.*, 2004
ICM	DMEM, 0.1 mM βME, NEAA, 40 ng/ml human LIF, 20 ng/ml bFGF, nucleosides, 16% FCS	Li *et al.*, 2003
ICM	DMEM low glucose (50%), Hams F10 (50%), 15% FBS, 2 mM glutamax, 0.1 mM βME, NEAA, 40 ng/ml human SCF, 20 ng/ml bFGF	Park *et al.*, 2013
EBI	DMEM, 10% FCS, 10% CS, 0.1 βME, LIF	Piedrahita *et al.*, 1990
EPI	DMEM, high glucose, 10% FCS, 10% CS, 0.1 mM βME, NEAA, nucleosides	Strojek *et al.*, 1990
EPI	DMEM, 15% FCS, 5% CS, 10–20 ng/ml human LIF	Talbot *et al.*, 1993
ICM	DMEM (50%) and Hams F10 (50%), 0.1 mM βME, NEAA, 2 mM L-glutamine, 10 μM/ml bFGF, 20% KSR	Tan *et al.*, 2012
ICM	GS2-M media with LIF	Telugu *et al.*, 2011
ICM	DMEM, 10% FBS, NEAA, PSF, α-MEM, 10% SR, ITS, sodium pyruvate, 0.1 mM βME, 10 ng/ml bFGF, 10 ng/ml human EGF, 10 ng/ml human LIF, 10 ng/ml Activin A	Vassiliev and Nottle, 2013

bFGF: basic fibroblast growth factor; CS: calf serum; DMEM: Dulbecco's modified eagle medium; EGF: epidermal growth factor; ESC: embryonic stem cell; EPI: epiblast; FBS: fetal bovine serum; FCS: fetal calf serum; ICM: inner cell mass; ITS: insulin-transferrin-selenium; KO: knockout; KSR: knockout serum replacement; LIF: leukemia inhibitory factor; NEAA: nonessential amino acids; SCF: stem cell factor βME: beta-mercaptoethanol.

The first obstacle to overcome is in knowing at which stage embryos should be harvested and cultured. This is due to the differences in early embryonic development as previously mentioned. While implantation of the blastocyst in mice occurs at embryonic day 4–5 (Paria *et al.*, 1993) and in humans at day 7–11 (Bergh and Navot, 1992), the implantation phase in

Downloaded From Vet-eBooks.com

ungulates is much longer and occurs in the pig between embryonic day 12–14 (Oestrup *et al.*, 2009). This leads to a very different environment for the early blastocyst and epiblast prior to attachment compared with other species, such as humans, where attachment occurs at an earlier time point. The embryo is completely dependent on factors secreted into the uterine cavity, which include iron, fat-soluble vitamins, steroids, and also adhesion molecules, which are important for the subsequent adhesion to the uterine wall. After attachment, the embryo receives oxygen and nutrients from the mother. The process of placentation is also very divergent in ungulates versus mice and humans. While in humans and mice the blastocyst penetrates the endometrium and becomes covered by it, ungulates develop inside the uterine cavity and the placentation process can be described as the development of a firm contact between the chorion and the endometrium (Sjaastad *et al.*, 2010). This indicates that ungulate embryos, including porcine embryos, have a prolonged exposure to a hypoxic environment and are dependent on secreted factors for longer, of which only a few are known. It has thus been more challenging to identify the right time point when the ICM or epiblast should be isolated and grown into ESCs.

The second hurdle on the path to culture *bona fide* pESCs is the lack of knowledge regarding the culture media. Even though there has been significant progress in the analyses of molecular pathways, which are active at different stages of early embryo development (Hall and Hyttel, 2014), there is no common agreement or protocol regarding the required growth factors, cytokines, or chemical compounds needed to sustain pESC culture (see overview of culture methods in Table 19.2). To date, several groups have successfully isolated putative pESCs at different time points, including either at the blastocyst stage (Notarianni *et al.*, 1990, 1991; Gerfen and Wheeler, 1995) or at the hatched later embryo containing the epiblast (Alberio *et al.*, 2010; Talbot *et al.*, 1993; Brevini *et al.*, 2007; Blomberg *et al.*, 2008; Vassiliev and Nottle, 2013), but all have encountered difficulties in the long-term maintenance of these isolated ESCs. Interestingly, a lot of studies have found that isolation of the porcine ICM at d8 results in a transient epiblast stage followed by differentiation of the ESC culture. Isolation and culture of these cells in the presence of bFGF and Activin resulted in putative pESCs that shared characteristics with EpiSCs, and were thus termed pEpiSCs. These pEpiSCs could be cultured for an extended amount of time. The pEpiSCs expressed NANOG, OCT4, SOX2, the epiblast specific marker NODAL, as well as weak expression of the cell surface markers SSEA1 and SSEA4 and were capable of differentiating into all three germ layers (Alberio *et al.*, 2010). These results imply that when cultured in these conditions, the preferable time point for the isolation of pESCs is later than in mice and humans. In addition, it provides some evidence to suggest that pESCs, which share characteristics of primed pluripotency, might also be dependent on Activin and Nodal signaling, as previously also observed in mEpiSC and hESC (Alberio *et al.*, 2010). Despite this advance, there has been little progress in establishing pESCs that mimic the naïve state of pluripotency. This is likely due to the lack of complete knowledge on genes that regulate this earlier pluripotent state and that signaling pathways may be active. Putative pESCs have been generated using a combination of both LIF and FGF2 (Brevini *et al.*, 2012), as well as FGF and LIF combined with high levels of Activin and EGF (Vassiliev *et al.*, 2010). The uncertainty of the exact roles of FGF and LIF in pESCs have led to investigations into the role of these, and current results suggest that FGF plays a more important role in maintaining pluripotency than LIF (Miyoshi *et al.*, 2000; Li *et al.*, 2003). This is consistent with the findings of constant expression of the FGF receptor in the porcine ICM and an absence in the expression of the LIF and GP-130 receptor complex (Hall and Hyttel, 2014; Hall *et al.*, 2009; Brevini *et al.*, 2010). Conversely, the addition of LIF to putative pESCs prevented EB formation and helped to maintain pESCs in an undifferentiated stage (Gandolfi *et al.*, 2012). An explanation to this contradiction could be an alternative role for LIF facilitated via signaling through the PI3K/AKT

Downloaded From Vet-eBooks.com

pathway, which may induce NANOG expression (Welham *et al*., 2007). It is also difficult to rule out a potential benefit of LIF in the culture media, as no research groups have succeeded in growing putative pESCs in the absence of feeder cells such as MEF or STO cells, which secrete low levels of LIF. Despite this research, neither of these growth factors, either added separately or together, can sustain pluripotent pESCs long term in culture. As a result, researchers have derived putative pESCs using either FGF (Li *et al*., 2004; Park *et al*., 2013) or LIF (Li *et al*., 2004; Telugu *et al*., 2011) or both bFGF and LIF simultaneously (Vassiliev *et al*., 2010; Brevini *et al*., 2010) (summarized in Table 19.2).

Finally, in addition to the issues regarding the correct timing of pluripotent stem cell isolation and lack of suitable culture media, another obstacle remains in establishing pESC, and that is the lack of known markers of pluripotency for cultured pESC, as previously mentioned. Clearly, more emphasis needs to be placed on deciphering the underlying genes that are expressed in the ground state of pluripotency and primed state in order to recapitulate these states *in vitro* by including the relevant and necessary cytokines and growth factors. Even though much has been achieved over the past 25 years, this species remains on the backbench with regard to establishment of pluripotent ESCs.

19.4 Current Status in Establishment of Porcine-Induced Pluripotent Stem Cells

The efforts to establish *bona fide* porcine pluripotent cells by culture of embryo-derived cells have clearly been unsuccessful. However, in 2006–2007, a research group led by Shinya Yamanaka successfully reprogrammed mouse somatic cells to pluripotency by ectopic over-expression of pluripotency transcription factors (Takahashi and Yamanaka, 2006; Takahashi *et al*., 2007). These so-called induced pluripotent stem cells (iPSC) presented a new alternative to the embryo-derived stem cells in all species, including the porcine.

The first reports detailing work on the derivation of piPSC (Esteban *et al*., 2009; Ezashi *et al*., 2009; Wu *et al*., 2009) showed that it was possible to reverse the differentiation of porcine fibroblasts back to a pluripotent-like state with the same reprogramming transcription factors (OCT4, SOX2, c-MYC, and KLF4) used by Yamanaka. Since then many research groups have reported the establishment of piPSC using similar methods. Typically, the four Yamanaka reprogramming factors are introduced into the starting cell populations alone or in combination with additional genes (such as NANOG, LIN28, TERT, or T-antigen) using a variety of vectors such as retroviral, lentiviral, episomal, or transposons (Table 19.3). The transduced cells are then cultured in conditions closely resembling those used for human or mouse stem cells (Table 19.3). As a result, stable piPSC-like lines with stem cell characteristics have been derived and maintained in culture for extended periods of time (Table 19.4), which represents a significant progress compared to the attempts to derive pESC. One major achievement is the generation of chimeras with demonstrated germline transmission from piPSC (West *et al*., 2010, 2011), which is the first report to date that shows germline contribution from cultured porcine stem cells. A big step forward in the use of porcine pluripotent cells as models for stem cell therapies has been the directed *in vitro* differentiation of piPSC into hepatocytes (Ao *et al*., 2014; Aravalli *et al*., 2012) and neurons (Yang *et al*., 2013). Additionally, piPSC showed an ability to differentiate into rod photoreceptors with demonstrated integration into retinas of a porcine model (Zhou *et al*., 2011) and also to differentiate into endothelial cells, which could improve myocardial function in mouse models (Gu *et al*., 2012).

Downloaded From Vet-eBooks.com

Table 19.3 Methods for establishment of porcine-induced pluripotent stem cells.

Cell source	Expression vectors	Reprogramming factors	piPSC culture medium	References
EF	Lentiviral	Human O, S, M, K	Human + mouse ESC medium mix	Ao *et al.*, 2014
FF	Episomal	Human O, S, K	KO-DMEM + 20% KSR (no growth factors)	Aravalli *et al.*, 2012
FF	Retroviral	Mouse O, S, M, K	Human ESC medium	Cheng *et al.*, 2012
FF	Retroviral	Mouse or human O, S, M, K	Human or mouse ESC medium	Esteban *et al.*, 2009
FF	Lentiviral	Human O, S, M, K	Human ESC medium	Ezashi *et al.*, 2009
FF	Retroviral	Mouse O, S, M, K	Mouse ESC medium + FK; 2i (PD,CH)	Fujishiro *et al.*, 2013
FF	Retroviral	Human O, S, M, K, T	Human + mouse ESC medium mix; 2i(PD,CH)	Gao *et al.*, 2014
ASC	Lentiviral	Mouse O, S, M, K	Human ESC medium	Gu *et al.*, 2012
FF	Lentiviral	Human O, S, M, K, N	Human ESC medium + DOX	Hall *et al.*, 2012
EF, FF, MBC	Lentiviral	Human, mouse, porcine, monkey O, S, M, K	Human ESC medium + DOX	Ji *et al.*, 2013
FF	Transposon	Mouse O, S, M, K	Human ESC medium	Kues *et al.*, 2013
MSC	Retroviral	Porcine O, K	5i (PD, CH, FK, SB, and NaB)	Liu *et al.*, 2012
Gal-F	Lentiviral	Human O, S, M, K, N, L	Human ESC medium	Liu *et al.*, 2013
EF	Retroviral	Mouse O, S, M, K	Human or mouse ESC medium	Montserrat *et al.*, 2010
FF	Transposon	Porcine O, S, M, K, N, L	Human + mouse ESC medium mix; 2i(PD,CH)	Petkov *et al.*, 2014
FF	Lentiviral	Human O, S, M, K	Human + mouse ESC medium mix; 3i(PD,CH, PD173074)	Rodrigues *et al.*, 2012
ASC, BMC	Retroviral	Mouse O, S, M, K	Mouse ESC medium	Tang *et al.*, 2012
FF	Episomal	Human O, S, M, K, N, L, large T-antigen	Mouse ESC medium + PD, CH, KP, A83-01	Telugu *et al.*, 2011
FF	Retroviral	Mouse O, S, M, K	Mouse ESC medium	Thompson *et al.*, 2012
FF	Retroviral	Mouse O, S, M, K, Nr5α2, Tbx3	Human or mouse ESC medium	Wang *et al.*, 2013
MSC	Lentiviral	Human O, S, M, K, N, L	Human ESC medium	West *et al.*, 2010
EF, BMC	Lentiviral	Human O, S, M, K, N, L	DMEM/F12 + 20% KSR (no growth factors) + DOX	Wu *et al.*, 2009
ASC, EF	Lentiviral	Mouse O, S, M, K	Mouse ESC medium + N2, B27, PD, CH	Zhang *et al.*, 2014
DF	Lentiviral	Human O, S, M, K, N	Human ESC medium	Yang *et al.*, 2013

ASC: adipose stem cells; BMC: bone marrow cells; CH: CHIR99021; DF: dermal fibroblasts; DOX: doxycycline; EF: ear fibroblasts; FF: fetal fibroblasts; FK: forskolin; Gal⁻F: xGal-knockout fibroblasts; K: Klf4; KP: kenpaullone; L: Lin28; M: c-Myc; MSC: mesenchymal stem cells; N: Nanog; NaB: sodium butyrate; O: Oct4; PD: PD0325901; S: Sox2; T: telomerase reverse transcriptase (TERT).

Downloaded From Vet-eBooks.com

Table 19.4 Characterization of putative porcine-induced pluripotent stem cells.

Morphology		Pluripotency gene expression													Differentiation			References
hES-like	mES-like	AP	SSEA-1	SSEA-3	SSEA-4	TRA-1-61/80	OCT4	SOX2	NANOG	LIN28	REX1	TERT	UTF1	CDH1	*In vitro*	Teratoma	Chimera	
+	−	+	+	−	+	+	+	+	+	ND	ND	ND	ND	ND	+	ND	ND	Ao *et al.*, 2014
+	−	+	−	−	−	−	ND	ND	+	+	ND	ND	ND	ND	+	ND	ND	Aravalli *et al.*, 2012
−	+	+	−	+	+	+	+	+	ND	ND	ND	ND	ND	ND	+	+	[a]	Cheng *et al.*, 2012
+	−	+	−	−	+	−	ND	+	+	+	+	ND	ND	ND	ND	+	ND	Esteban *et al.*, 2009
+	−	+	+	−	−	−	+	+	+	+	+	+	+	+	ND	+	ND	Ezashi *et al.*, 2009
−	+	+	+	+	+	+	+	+	+	+	ND	ND	ND	ND	ND	ND	[b]	Fujishiro *et al.*, 2013
−	+	+	−	−	+	−	+	+	+	ND	ND	+	ND	ND	+	ND	[a]	Gao *et al.*, 2014
+	−	+	+	−	−	+	+	+	+	ND	ND	ND	ND	ND	+	+	ND	Gu *et al.*, 2012
+	−	−	+	−	−	−	+	+	+	ND	+	ND	ND	ND	+	ND	ND	Hall *et al.*, 2012
+	+	+	+	+	+	+	+	ND	+	ND	ND	ND	ND	ND	+	+	[c]	Ji *et al.*, 2013
+	−	+	+	−	−	−	+	+	+	+	+	+	+	+	+	+	ND	Kues *et al.*, 2013

Downloaded From Vet-eBooks.com

−	+	+	+	−	+	+	+	+	+	ND	ND	ND	ND	ND	+	+	ND	Liu *et al.*, 2012
+	−	+	+	−	+	+	+	+	ND	ND	ND	+	ND	+	+	ND	ND	Liu *et al.*, 2013
+	−	+	−	−	+	+	ND	ND	+	ND	ND	ND	ND	ND	+	+	ND	Montserrat *et al.*, 2010
+	−	+	+	−	+	−	+	+	+	ND	+	ND	+	+	+	−	ND	Petkov *et al.*, 2014
−	+	ND	−	−	−	−	+	+	+	ND	+	ND	ND	ND	+	ND	ND	Rodrigues *et al.*, 2012
+	−	+	−	−	+	−	+	+	+	ND	+	ND	ND	ND	+	ND	ND	Tang *et al.*, 2012
−	+	+	+	−	+	−	+	+	+	ND	ND	+	ND	ND	ND	+	ND	Telugu *et al.*, 2011
−	+	+	+	−	+	−	+	+	+	ND	ND	ND	ND	+	+	ND	ND	Thompson *et al.*, 2012
+	+	+	−	−	−	−	+	+	+	ND	+	ND	ND	ND	ND	+	ND	Wang *et al.*, 2013
+	−	+	−	−	−	−	+	+	ND	ND	ND	ND	ND	ND	ND	ND	[d]	West *et al.*, 2010
+	−	+	−	+	+	+	+	+	+	ND	+	ND	ND	+	+	+	ND	Wu *et al.*, 2009
+	−	+	−	+	+	−	+	+	+	+	ND	+	ND	ND	+	+	ND	Zhang *et al.*, 2014
+	−	+	−	−	+	+	+	+	+	ND	ND	ND	ND	ND	+	ND	ND	Yang *et al.*, 2012

+: positive; −: negative; ND: not determined.

a) Chimeric blastocysts.

b) Chimeric blastocysts and fetal contribution to three germ layer derivatives up to day 23 of gestation.

c) Chimeric fetuses with piPSC contribution up to day 90 of gestation.

d) Live-born chimeric piglets with confirmed germline contribution.

Downloaded From Vet-eBooks.com

Despite these significant achievements, some problems remain that prevent the reproducible generation and application of piPSC. The derived piPSC lines reported by different research groups show a rather wide variability in their stem cell characteristics, mainly in their morphology, pluripotency gene expression, and demonstrated abilities to differentiate into defined cell types *in vitro* and *in vivo* (Table 19.4). This is in striking contrast with mouse or human iPSC, which vary very little from the criteria already established for their respective ESC. For example, while some reports describe piPSC with human ESC-like morphology, others show phenotype more characteristic of mESC (Table 19.4). The expression of some genes that are hallmarks for pluripotency in human or mouse cells, such as SSEA-1, SSEA-3, SSEA-4, TRA-1-61, and TRA-1-80, vary considerably in the piPSC lines derived by different groups (Table 19.4).

The discrepancies between the published reports also reflect the inconsistent methodology used for generation and characterization of the piPSC. Due to the lack of established *bona fide* porcine pluripotent stem cell lines, it is not known which culture conditions would be most optimal for *in vitro* maintenance of these cells, as well as which characteristics can be used to reliably identify them. To date, all piPSC lines have been derived using culture conditions adapted from human or mouse stem cell protocols, which have not been effective in the establishment of pESC. While some research groups have determined that bFGF is necessary for maintaining the pluripotency characteristics of their piPSC (Yang *et al*., 2013; Gu *et al*., 2012; Cheng *et al*., 2012; Kues *et al*., 2013), others have shown that piPSC possess a functional LIF signaling pathways and need this growth factor for their proliferation (Cheng *et al*., 2012; Thomson *et al*., 2012). In some cases, both factors were used (Ao *et al*., 2014; Gao *et al*., 2014; Rodriguez *et al*., 2012), or the cells were generated and maintained without any cytokines (Wu *et al*., 2009). The use of small molecule inhibitors, such as PD032591 (a mitogen-activated protein kinase kinase (MEK) inhibitor) and CHIR99021 (a glycogen synthesis kinase 3 (Gsk3) inhibitor) has been also reported (Table 19.4), albeit with contradictory results. While in some studies the use of these inhibitors led to the establishment of piPSC with some characteristics typical of the naïve stem cell state (Telugu *et al*., 2010), others found them to be less effective (Gao *et al*., 2014), or even detrimental for the establishment of piPSC due to the reduction of pluripotency gene expression levels in the established cell lines (Petkov *et al*., 2014). Naïve pluripotency in the piPSC has been suggested solely by the presence of naïve ESC-like morphology and LIF-dependency (Telugu *et al*., 2010) or by the expression of some pluripotency genes typical of mouse ESC, such as ERas, STELLA, and FGF5 (Fujishiro *et al*., 2013), and not by empirical evidence, such as the formation of germline chimeras by blastocyst injection or tetraploid complementation. The production of live-born chimeras, which is the ultimate proof of pluripotency, has unfortunately been demonstrated by only one research group, which used piPSC with nonnaïve stem cell characteristics (West *et al*., 2010, 2011), while others have shown that their naïve-like piPSC were not able to persist in porcine fetuses up to day 65 of gestation (Fujishiro *et al*., 2013).

One important fact that needs to be considered in the interpretation of the results from the different studies is the continuous expression of the exogenous reprogramming transcription factors in all of the piPSC lines reported to date. In contrast to miPSC and most hiPSC, the transgenes have never been completely silenced in piPSC, although some reports suggest that some downregulation takes place (Cheng *et al*., 2012; Hall *et al*., 2012). The importance of the continuous transgene expression for the maintenance of the piPSC was demonstrated in experiments where their silencing was induced by withdrawal of the transcription-activating antibiotic doxycycline, which promptly resulted in the differentiation and/or proliferation arrest of the cells (Wu *et al*., 2009; Hall *et al*., 2012; Ji *et al*., 2013). These results call into question the role that the different growth factors and small molecule supplements in the culture media really play in the maintenance of the piPSC *in vitro*. The nonsilenced reprogramming transcription

Downloaded From Vet-eBooks.com

factors also present a problem for the use of the piPSC as a model for regenerative therapies in humans. Due to their potential interference with the differentiation processes or because of the increased risks of tumor formation in the recipient patients, it is not acceptable to use iPSC expressing pluripotency genes or oncogenes such as c-MYC for therapies. Therefore, despite the initial success in the use of piPSC in some animal disease models, more improvements need to be made in the culture of piPSC before these cells find real applications in the field of the regenerative medicine.

19.5 Future Perspectives: Use of Global Profiling on Pluripotent Cells from Pig Embryo and Pluripotent Stem Cells

Gene expression profiling could be one way to uncover the unique genetic characteristics that porcine pluripotent stem cells have compared to other species. Gene or protein expression profiling of isolated cells taken from the varying pluripotent cell populations from the *in vivo* embryo could give a holistic insight into both unique pluripotent signatures and signaling pathways, which are critical for the regulation of these cells. These data could help to improve culture conditions and provide a more optimal system for the growth of porcine pluripotent stem cells.

Work in this area has already been initiated for two stages of porcine pluripotent cells, including RNA sequencing of pooled isolated porcine late ICM (isolated from expanded D7 blastocysts and D8 blastocysts) and isolated from the late epiblast (isolated from D10–D11 elongating embryos) (unpublished data). The RNA sequencing data are readily available from the gene expression omnibus (GEO), an international public repository that archives and freely distributes microarray, next-generation sequencing, and other forms of high-throughput functional genomic data sets with the accession number, GSE53387. The RNA sequencing was verified by performing both qPCR and immunostaining for a number of genes (unpublished data). From analyses of the raw data, we were able to identify a number of genes highly upregulated in the porcine late ICM and a number of genes highly upregulated in the porcine early epiblast (Tables 19.5 and 19.6), which related to a number of relevant biological processes. We selected the most highly upregulated genes with the most stringent *p*-values between the

Table 19.5 Gene expression profiling revealed a number of upregulated genes in the porcine late inner cell mass compared to the late epiblast.

Biological processes	Gene nomenclature
Cell differentiation	*TRIM10, PN-1, ZFP36L1, LGALS1, IFRD1*
Regulation of biological processes	*SPIC, LPAR1, ESRRG, TFCP2L1, EDG7, ELF3, EGR-1, STAT2, PDE7B, TFAP2C, FBXO8, RND3, SELS, CDA*
Development	*GJB5, ACSL6, LRRC4C, TFCP2L1, NPT2B, TRIM10, ESRRB, KLF5, PSAP, PPT2*
Nucleus	*SPIC, PNCK, LMO1, ESRRG, TFCP2L1, SYCP2, ELF3, NDRG1, ESRRB, STAT2, TFAP2C, PIF1*
Cell surface	*CD86, SDC4, HMMR*
Transcription regulator activity	*SPIC, ESRRG, ELF3, EGR1, ESRRB, STAT2, TFAP2C, KLF5, DDIT3, TOB1, NFE2L2*
Receptor activity	*CD86, LPAR1, ESRRG, EDG7, ESRRB, SCARB2, NPC1, PPT, LREAP1, PTPRA*

Downloaded From Vet-eBooks.com

Table 19.6 Gene expression profiling revealed a number of upregulated genes in the porcine late epiblast compared to the late inner cell mass.

Gene function/role	*Genes*
Regulation of biological processes	*RCAN2, CDX4, TESC, FAM129A, ETS1, PRNP, CREB3L4, CHRNA3, MEIS3, LIN28B, PBX2, RFX7*
Development	*CAV1, NOX4, TNFSF11, FOXO1A, SFRP1, ETV4, VSX2, RARG, FGFR1IIIC, SALL1*
Nucleus	*CDX4, TESC, ETS1, MYOZ1, PRKAA2, CREB3L4, MEIS3, FOXO1A, LIN28V, ETV4*
Transcription regulator activity	*ETS1, CREB3L4, MEIS3, FOXO1A, ETV4, VSX2, PBX2, TCF4, RCOR2, SMAD1, ARNTL2, RARG, FOXH1*

three biological replicates for both stages using the parametric statistical test, multiple testing correction. The Benjamini and Hochberg false discovery rate (FDR) was determined that indicates which genes were differentially expressed, defined by fold difference more than twofold and a *P*-value cutoff of at least 0.05. The selected genes were enriched by gene ontology (GO).

In the case of the late ICM, *KLF5* was found to be highly upregulated. Interestingly, this gene has been shown to be able to replace LIF for maintaining mESC cell renewal and plays an important role in mouse embryonic development (Parisi and Russo, 2011). High expression of *TFCP2L1* may indicate that JAK/STAT signaling is important in this earlier stage of pluripotency, which is a factor that has recently been shown to be a primary downstream target of LIF/STAT3 (Martello *et al*., 2013; Ye *et al*., 2013). In addition, the high expression of *ESRRB*, which is involved in AKT signaling, indicates that this may also be an important pathway for earlier states of pluripotency. Some novel genes of interest include *LPAR1*, of which *LPA* is known to play a role in cell renewal in cancer (Mills and Moolenaar, 2003). The addition of relevant growth factors that trigger these particular pathways could be of interest to pursue in the future attempts at establishment of porcine pluripotent stem cells. Although this state of pluripotency is earlier than the ground state, it could still help in establishing which genes are more important for regulating the ground state of pluripotency (i.e., those that are upregulated in comparison).

The RNA sequencing data also revealed some interesting clues as to what genes may play a role in governing the primed state of pluripotency. Although there were some genes expressed that may be more lineage-restrictive genes, such as *TESC*, *MYOZ1*, and *TCF4*, there were also some genes that could be directly linked to maintenance of pluripotency, including *LIN28b* and *ETS-1* (which the latter has been shown to target and activate c-MYC (Roussel *et al*., 1994)). There was also further evidence of a role of WNT signaling at this stage, as *SALL1* was highly upregulated, which has shown to initiate WNT patterning (Kiefer *et al*., 2010), and *SFRP1* is expressed, which is a well-known member of the WNT signaling pathway (Xu *et al*., 1998). There was also the high expression of *FGFrIIIC*, which is an important receptor in FGF signaling. Finally, two genes important for anteroposterior patterning were found to be upregulated: *CDX4* and *FOXH1*. Of particular interest was the latter gene, *FOXH1*, which has recently been shown to improve reprogramming in induction of iPSCs from fibroblasts (Takahashi *et al*., 2014). Together, this simplistic evaluation of the data generated from the global profiling of these two pluripotent states give some indication as to which genes may be important in regulation of pluripotency in the pig and may help researchers to apply these

Downloaded From Vet-eBooks.com

results to either improve porcine pluripotent stem cell culture or assess their roles further in these cell populations. It is anticipated that future research may help to reveal more on the other pluripotent stem cell states and also more insight into both the important pluripotency networks and cell signaling pathways that are active in these different states.

19.6 Discussion and Conclusions

The lack in production of *bona fide* porcine pluripotent stem cells has definitely been hampered by a lack of research into porcine embryo development. More in-depth research is needed into understanding the molecular signatures of the porcine ground state of pluripotency compared to the primed state. Much of the embryonic research has focused on earlier stages of pluripotent stem cells, that is, the ICM, largely because porcine *in vitro* culture is restricted to only about 7 days, and obtaining later stage *in vivo* material is more expensive and laborious. Clear delineation of the correct embryo staging has helped researchers better define both the genes and proteins that might be important in regulating pluripotency, although as yet it has not led to improvements in culture of pluripotent stem cells *in vitro*.

The lack of established *bona fide* pluripotent stem cells in the pig has also presented a number of issues for the development of human medicine as well as for farm animal research. Without these pluripotent cells it has been difficult to compare such cells to equivalent human pluripotent cell models, which would be important for understanding whether they recapitulate human stem cells and whether they can be used as a viable alternative for clinical testing and potential transplantation. If this was the case, they could at least replace human ESC models, which are ethically challenging for many in society. Without these alternative models, the risks associated with the grafting of cells or tissues derived from ESC or autologous iPSC into human patients cannot be fully assessed without conducting similar experiments in animals that bear physiological, metabolic, and genetic similarities to humans, such as the pig. Another area of research these cells could benefit would be to test how well these cells, or their differentiated progeny, survive transplantation into porcine tissues and/or organs. These data would be meaningful for improving transplantation procedures and protocols in humans. Furthermore, intensive work is being conducted in the area of xenotransplantation, in order to prevent the immune rejection of porcine xenografts by the human immune system and to eliminate the potential risks of porcine endogenous retroviral (PERV) transmission. It is clear that the generation of porcine pluripotent stem cells could also benefit this research considerably. Currently, the work on the creation of organ donor "xenopigs" involves an array of genetic modifications to the porcine organism, which requires multiple rounds of labor- and time-consuming nuclear transfers with genetically modified somatic cells. If porcine pluripotent stem cell cultures were available, the process would become much faster and more efficient due to the possibility of engineering these cells through multiple rounds of genetic modification and selection *in vitro* before using them to produce germline chimeras harboring the desired properties. Similarly, *in vitro* production of gametes from porcine pluripotent cells lags behind the research in human and mouse, which has limited our knowledge in gamete biology as well as the development of animal models for alternative infertility treatments.

To conclude, there are several factors that may contribute to the difficulties in being able to establish *bona fide* porcine pluripotent stem cells that are likely due to species-specific differences, developmental timing differences, and a lagging interest in the pig as an alternative model compared to the mouse. Despite this, new research in the field is continuing to move the

Downloaded From Vet-eBooks.com

field forward, especially in the use and application of global profiling technologies, which give more unbiased and holistic insights into the pluripotent hallmarks of the pig pluripotent populations. This technology may likely provide some important steps toward the development of *bona fide* pluripotent stem cells in the future.

Acknowledgments

We thank several financing bodies for their contribution toward our current research into the establishment and characterization of both pluripotent cells derived from the pig embryo and pESC lines, including the EU FP7 consortium, PluriSyS (HEALTH-2007-B-223485), the Danish Council for Independent Research, Natural Sciences (11-106627), the U.S. Department of Agriculture, Prime Award Number (2011-67015-30688), and a grant by the German Scientific Foundation (Ni 256/32-1).

References

Alberio, R., Croxall, N., and Allegrucci, C. (2010) Pig epiblast stem cells depend on activin/nodal signaling for pluripotency and self-renewal. *Stem Cells Dev.*, **19**, 1627–1636.

Ao, Y., Mich-Basso, J.D., Lin, B., and Yang, L. (2014) High efficient differentiation of functional hepatocytes from porcine induced pluripotent stem cells. *PLoS One*, **9**, e100417.

Aravalli, R.N., Cressman, E.N., and Steer, C.J. (2012) Hepatic differentiation of porcine induced pluripotent stem cells *in vitro*. *Vet. J.*, **194**, 369–374.

Bassols, A., Costa, C., Eckersall, P.D., Osada, J., Sabria, J., and Tibau, J. (2014) The pig as an animal model for human pathologies: a proteomics perspective. *Proteomics Clin. Appl.*, **8**, 715–731.

Bergh, P.A. and Navot, D. (1992) The impact of embryonic development and endometrial maturity on the timing of implantation. *Fertil. Steril.*, **58**, 537–542.

Blair, K., Leitch, H.G., Mansfield, W., Dumeau, C.E., Humphreys, P., and Smith, A.G. (2012) Culture parameters for stable expansion, genetic modification and germline transmission of rat pluripotent stem cells. *Biol. Open*, **1**, 58–65.

Blomberg, L., Hashizume, K., and Viebahn, C. (2008) Blastocyst elongation, trophoblastic differentiation, and embryonic pattern formation. *Reproduction*, **135**, 181–195.

Boroviak, T., Loos, R., Bertone, P., Smith, A., and Nichols, J. (2014) The ability of inner-cell-mass cells to self-renew as embryonic stem cells is acquired following epiblast specification. *Nat. Cell Biol.*, **16**, 516–528.

Brevini, T.A., Tosetti, V., Crestan, M., Antonini, S., and Gandolfi, F. (2007) Derivation and characterization of pluripotent cell lines from pig embryos of different origins. *Theriogenology*, **67**, 54–63.

Brevini, T.A., Pennarossa, G., Attanasio, L., Vanelli, A., Gasparrini, B., and Gandolfi, F. (2010) Culture conditions and signalling networks promoting the establishment of cell lines from parthenogenetic and biparental pig embryos. *Stem Cell Rev.*, **6**, 484–495.

Brevini, T., Pennarossa, G., Maffei, S., and Gandolfi, F. (2012) Pluripotency network in porcine embryos and derived cell lines. *Reprod. Domest. Anim.*, **47** (Suppl. 4), 86–91.

Brons, I.G., Smithers, L.E., Trotter, M.W., Rugg-Gunn, P., Sun, B., Chuva de Sousa Lopes, S.M., Howlett, S.K., Clarkson, A., Ahrlund-Richter, L., Pedersen, R.A., and Vallier, L. (2007) Derivation of pluripotent epiblast stem cells from mammalian embryos. *Nature*, **448**, 191–195.

Chen, Y., Blair, K., and Smith, A. (2013) Robust self-renewal of rat embryonic stem cells requires fine-tuning of glycogen synthase kinase-3 inhibition. *Stem Cell Rep.*, **1**, 209–217.

Downloaded From Vet-eBooks.com

Cheng, D., Guo, Y., Li, Z., Liu, Y., Gao, X., Gao, Y., Cheng, X., Hu, J., and Wang, H. (2012) Porcine induced pluripotent stem cells require LIF and maintain their developmental potential in early stage of embryos. *PLoS One*, **7**, e51778.

Esteban, M.A., Xu, J., Yang, J., Peng, M., Qin, D., Li, W., Jiang, Z., Chen, J., Deng, K., Zhong, M., Cai, J., Lai, L., and Pei, D. (2009) Generation of induced pluripotent stem cell lines from Tibetan miniature pig. *J. Biol. Chem.*, **284**, 17634–17640.

Evans, M.J. and Kaufman, M.H. (1981) Establishment in culture of pluripotential cells from mouse embryos. *Nature*, **292**, 154–156.

Evans, M.J., Notarianni, E., Laurie, S., and Moor, R.M. (1990) Derivation and preliminary characterization of pluripotent cell lines from porcine and bovine blastocysts. *Theriogenology*, **33**, 125–128.

Ezashi, T., Telugu, B.P., Alexenko, A.P., Sachdev, S., Sinha, S., and Roberts, R.M. (2009) Derivation of induced pluripotent stem cells from pig somatic cells. *Proc. Natl. Acad. Sci. USA*, **106**, 10993–10998.

Fujishiro, S.H., Nakano, K., Mizukami, Y., Azami, T., Arai, Y., Matsunari, H., Ishino, R., Nishimura, T., Watanabe, M., Abe, T., Furukawa, Y., Umeyama, K., Yamanaka, S., Ema, M., Nagashima, H., and Hanazono, Y. (2013) Generation of naive-like porcine-induced pluripotent stem cells capable of contributing to embryonic and fetal development. *Stem Cells Dev.*, **22**, 473–482.

Gafni, O., Weinberger, L., Mansour, A.A., Manor, Y.S., Chomsky, E., Ben-Yosef, D., Kalma, Y., Viukov, S., Maza, I., Zviran, A., Rais, Y., Shipony, Z., Mukamel, Z., Krupalnik, V., Zerbib, M., Geula, S., Caspi, I., Schneir, D., Shwartz, T., Gilad, S., Amann-Zalcenstein, D., Benjamin, S., Amit, I., Tanay, A., Massarwa, R., Novershtern, N., and Hanna, J.H. (2013) Derivation of novel human ground state naive pluripotent stem cells. *Nature*, **504**, 282–286.

Gandolfi, F., Pennarossa, G., Maffei, S., and Brevini, T. (2012) Why is it so difficult to derive pluripotent stem cells in domestic ungulates? *Reprod. Domest. Anim.*, **47** (Suppl. 5), 11–17.

Gao, Y., Guo, Y., Duan, A., Cheng, D., Zhang, S., and Wang, H. (2014) Optimization of culture conditions for maintaining porcine induced pluripotent stem cells. *DNA Cell Biol.*, **33**, 1–11.

Gerfen, R.W. and Wheeler, M.B. (1995) Isolation of embryonic cell-lines from porcine blastocysts. *Anim. Biotechnol.*, **6**, 1–14.

Gu, M., Nguyen, P.K., Lee, A.S., Xu, D., Hu, S., Plews, J.R., Han, L., Huber, B.C., Lee, W.H., Gong, Y., de Almeida, P.E., Lyons, J., Ikeno, F., Pacharinsak, C., Connolly, A.J., Gambhir, S.S., Robbins, R.C., Longaker, M.T., and Wu, J.C. (2012) Microfluidic single-cell analysis shows that porcine induced pluripotent stem cell-derived endothelial cells improve myocardial function by paracrine activation. *Circ. Res.*, **111**, 882–893.

Hackett, J.A. and Surani, M.A. (2014) Regulatory principles of pluripotency: from the ground state up. *Cell Stem Cell*, **15**, 416–430.

Hall, V.J. (2012) Early development of the porcine embryo: the importance of cell signalling in development of pluripotent cell lines. *Reprod. Fertil. Dev.*, **25**, 94–102.

Hall, V.J. and Hyttel, P. (2014) Breaking down pluripotency in the porcine embryo reveals both a premature and reticent stem cell state in the inner cell mass and unique expression profiles of the naive and primed stem cell states. *Stem Cells Dev.*, **23**, 2030–2045.

Hall, V.J., Christensen, J., Gao, Y., Schmidt, M.H., and Hyttel, P. (2009) Porcine pluripotency cell signaling develops from the inner cell mass to the epiblast during early development. *Dev. Dyn.*, **238**, 2014–2024.

Hall, V.J., Jacobsen, J.V., Rasmussen, M.A., and Hyttel, P. (2010) Ultrastructural and molecular distinctions between the porcine inner cell mass and epiblast reveal unique pluripotent cell states. *Dev. Dyn.*, **239**, 2911–2920.

Downloaded From Vet-eBooks.com

Hall, V.J., Kristensen, M., Rasmussen, M.A., Ujhelly, O., Dinnyes, A., and Hyttel, P. (2012) Temporal repression of endogenous pluripotency genes during reprogramming of porcine induced pluripotent stem cells. *Cell Reprogram.*, **14**, 204–216.

Hall, V., Hinrichs, K., Lazzari, G., Betts, D.H., and Hyttel, P. (2013) Early embryonic development, assisted reproductive technologies, and pluripotent stem cell biology in domestic mammals. *Vet. J.*, **197**, 128–142.

Henderson, J.K., Draper, J.S., Baillie, H.S., Fishel, S., Thomson, J.A., Moore, H., and Andrews, P.W. (2002) Preimplantation human embryos and embryonic stem cells show comparable expression of stage-specific embryonic antigens. *Stem Cells*, **20**, 329–337.

Ji, G., Ruan, W., Liu, K., Wang, F., Sakellariou, D., Chen, J., Yang, Y., Okuka, M., Han, J., Liu, Z., Lai, L., Gagos, S., Xiao, L., Deng, H., Li, N., and Liu, L. (2013) Telomere reprogramming and maintenance in porcine iPS cells. *PLoS One*, **8**, e74202.

Kiefer, S.M., Robbins, L., Stumpff, K.M., Lin, C., Ma, L., and Rauchman, M. (2010) Sall1-dependent signals affect Wnt signaling and ureter tip fate to initiate kidney development. *Development*, **137**, 3099–3106.

Kim, K., Doi, A., Wen, B., Ng, K., Zhao, R., Cahan, P., Kim, J., Aryee, M.J., Ji, H., Ehrlich, L.I., Yabuuchi, A., Takeuchi, A., Cunniff, K.C., Hongguang, H., McKinney-Freeman, S., Naveiras, O., Yoon, T.J., Irizarry, R.A., Jung, N., Seita, J., Hanna, J., Murakami, P., Jaenisch, R., Weissleder, R., Orkin, S.H., Weissman, I.L., Feinberg, A.P., and Daley, G.Q. (2010) Epigenetic memory in induced pluripotent stem cells. *Nature*, **467**, 285–290.

Kues, W.A., Herrmann, D., Barg-Kues, B., Haridoss, S., Nowak-Imialek, M., Buchholz, T., Streeck, M., Grebe, A., Grabundzija, I., Merkert, S., Martin, U., Hall, V.J., Rasmussen, M.A., Ivics, Z., Hyttel, P., and Niemann, H. (2013) Derivation and characterization of sleeping beauty transposon-mediated porcine induced pluripotent stem cells. *Stem Cells Dev.*, **22**, 124–135.

Lelovas, P.P., Kostomitsopoulos, N.G., and Xanthos, T.T. (2014) A comparative anatomic and physiologic overview of the porcine heart. *J. Am. Assoc. Lab. Anim. Sci.*, **53**, 432–438.

Li, M., Zhang, D., Hou, Y., Jiao, L., Zheng, X., and Wang, W.H. (2003) Isolation and culture of embryonic stem cells from porcine blastocysts. *Mol. Reprod. Dev.*, **65**, 429–434.

Li, M., Ma, W., Hou, Y., Sun, X.F., Sun, Q.Y., and Wang, W.H. (2004) Improved isolation and culture of embryonic stem cells from Chinese miniature pig. *J. Reprod. Dev.*, **50**, 237–244.

Marks, H., Kalkan, T., Menafra, R., Denissov, S., Jones, K., Hofemeister, H., Nichols, J., Kranz, A., Stewart, A.F., Smith, A., and Stunnenberg, H.G. (2012) The transcriptional and epigenomic foundations of ground state pluripotency. *Cell*, **149**, 590–604.

Martello, G., Bertone, P., and Smith, A. (2013) Identification of the missing pluripotency mediator downstream of leukaemia inhibitory factor. *EMBO J.*, **32**, 2561–2574.

Martin, G.R. (1981) Isolation of a pluripotent cell line from early mouse embryos cultured in medium conditioned by teratocarcinoma stem cells. *Proc. Natl. Acad. Sci. USA*, **78**, 7634–7638.

Medrano, J.V., Simon, C., and Pera, R.R. (2014) Human germ cell differentiation from pluripotent embryonic stem cells and induced pluripotent stem cells. *Methods Mol. Biol.*, **1154**, 563–578.

Mills, G.B. and Moolenaar, W.H. (2003) The emerging role of lysophosphatidic acid in cancer. *Nat. Rev. Cancer*, **3**, 582–591.

Miyoshi, K., Taguchi, Y., Sendai, Y., Hoshi, H., and Sato, E. (2000) Establishment of a porcine cell line from *in vitro*-produced blastocysts and transfer of the cells into enucleated oocytes. *Biol. Reprod.*, **62**, 1640–1646.

Nichols, J. and Smith, A. (2009) Naive and primed pluripotent states. *Cell Stem Cell*, **4**, 487–492.

Notarianni, E., Laurie, S., Moor, R.M., and Evans, M.J. (1990) Maintenance and differentiation in culture of pluripotential embryonic cell lines from pig blastocysts. *J. Reprod. Fertil. Suppl.*, **41**, 51–56.

Downloaded From Vet-eBooks.com

Notarianni, E., Galli, C., Laurie, S., Moor, R.M., and Evans, M.J. (1991) Derivation of pluripotent, embryonic cell lines from the pig and sheep. *J. Reprod. Fertil. Suppl.*, **43**, 255–260.

Oestrup, O., Hall, V., Petkov, S.G., Wolf, X.A., Hyldig, S., and Hyttel, P. (2009) From zygote to implantation: morphological and molecular dynamics during embryo development in the pig. *Reprod. Domest. Anim.*, **44** (Suppl. 3), 39–49.

Paria, B.C., Huet-Hudson, Y.M., and Dey, S.K. (1993) Blastocyst's state of activity determines the "window" of implantation in the receptive mouse uterus. *Proc. Natl. Acad. Sci. USA*, **90**, 10159–10162.

Parisi, S. and Russo, T. (2011) Regulatory role of Klf5 in early mouse development and in embryonic stem cells. *Vitam Horm*, **87**, 381–397.

Park, J.K., Kim, H.S., Uh, K.J., Choi, K.H., Kim, H.M., Lee, T., Yang, B.C., Kim, H.J., Ka, H.H., Kim, H., and Lee, C.K. (2013) Primed pluripotent cell lines derived from various embryonic origins and somatic cells in pig. *PLoS One*, **8**, e52481.

Petkov, S., Hyttel, P., and Niemann, H. (2014) The small molecule inhibitors PD0325091 and CHIR99021 reduce expression of pluripotency-related genes in putative porcine induced pluripotent stem cells. *Cell Reprogram.*, **16**, 235–240.

Polo, J.M., Liu, S., Figueroa, M.E., Kulalert, W., Eminli, S., Tan, K.Y., Apostolou, E., Stadtfeld, M., Li, Y., Shioda, T., Natesan, S., Wagers, A.J., Melnick, A., Evans, T., and Hochedlinger, K. (2010) Cell type of origin influences the molecular and functional properties of mouse induced pluripotent stem cells. *Nat. Biotechnol.*, **28**, 848–855.

Rodriguez, A., Allegrucci, C., and Alberio, R. (2012) Modulation of pluripotency in the porcine embryo and iPS cells. *PLoS One*, **7**, e49079.

Roussel, M.F., Davis, J.N., Cleveland, J.L., Ghysdael, J., and Hiebert, S.W. (1994) Dual control of myc expression through a single DNA binding site targeted by ets family proteins and E2F-1. *Oncogene*, **9**, 405–415.

Sheng, G. (2014) Epiblast morphogenesis before gastrulation. *Dev. Biol.*, **401**, 17–24.

Sjaastad, O.V., Hove, K., and Sand, O. (2010) *Physiology of Domestic Animals*, Scandinavian Veterinary Press, p. 804.

Son, H.-Y., Kim, J.-E., Lee, S.-G., Kim, H.-S., Lee, E., Park, J.-K., Ka, H., Kim, H.-J., and Lee, C.-K. (2009) Efficient derivation and long term maintenance of pluripotent porcine embryonic stem-like cells. *Asian Australas. J. Anim. Sci.*, **22**, 26–34.

Sullivan, G.J., Bai, Y., Fletcher, J., and Wilmut, I. (2010) Induced pluripotent stem cells: epigenetic memories and practical implications. *Mol. Hum. Reprod.*, **16**, 880–885.

Takahashi, K. and Yamanaka, S. (2006) Induction of pluripotent stem cells from mouse embryonic and adult fibroblast cultures by defined factors. *Cell*, **126**, 663–676.

Takahashi, K., Tanabe, K., Ohnuki, M., Narita, M., Ichisaka, T., Tomoda, K., and Yamanaka, S. (2007) Induction of pluripotent stem cells from adult human fibroblasts by defined factors. *Cell*, **131**, 861–872.

Takahashi, K., Tanabe, K., Ohnuki, M., Narita, M., Sasaki, A., Yamamoto, M., Nakamura, M., Sutou, K., Osafune, K., and Yamanaka, S. (2014) Induction of pluripotency in human somatic cells via a transient state resembling primitive streak-like mesendoderm. *Nat. Commun.*, **5**, 3678.

Talbot, N.C., Rexroad, C.E. Jr., Pursel, V.G., Powell, A.M., and Nel, N.D. (1993) Culturing the epiblast cells of the pig blastocyst. *In Vitro Cell Dev. Biol. Anim.*, **29A**, 543–554.

Talbot, N.C., Powell, A.M., and Garrett, W.M. (2002) Spontaneous differentiation of porcine and bovine embryonic stem cells (epiblast) into astrocytes or neurons. *In Vitro Cell Dev. Biol. Anim.*, **38**, 191–197.

Telugu, B.P., Ezashi, T., and Roberts, R.M. (2010) Porcine induced pluripotent stem cells analogous to naive and primed embryonic stem cells of the mouse. *Int. J. Dev. Biol.*, **54**, 1703–1711.

Downloaded From Vet-eBooks.com

Telugu, B.P., Ezashi, T., Sinha, S., Alexenko, A.P., Spate, L., Prather, R.S., and Roberts, R.M. (2011) Leukemia inhibitory factor (LIF)-dependent, pluripotent stem cells established from inner cell mass of porcine embryos. *J. Biol. Chem.*, **286**, 28948–28953.

Theunissen, T.W., Powell, B.E., Wang, H., Mitalipova, M., Faddah, D.A., Reddy, J., Fan, Z.P., Maetzel, D., Ganz, K., Shi, L., Lungjangwa, T., Imsoonthornruksa, S., Stelzer, Y., Rangarajan, S., D'Alessio, A., Zhang, J., Gao, Q., Dawlaty, M.M., Young, R.A., Gray, N.S., and Jaenisch, R. (2014) Systematic identification of culture conditions for induction and maintenance of naive human pluripotency. *Cell Stem Cell*, **15**, 471–487.

Thomson, J.A., Kalishman, J., Golos, T.G., Durning, M., Harris, C.P., Becker, R.A., and Hearn, J.P. (1995) Isolation of a primate embryonic stem cell line. *Proc. Natl. Acad. Sci. USA*, **92**, 7844–7848.

Thomson, J.A., Itskovitz-Eldor, J., Shapiro, S.S., Waknitz, M.A., Swiergiel, J.J., Marshall, V.S., and Jones, J.M. (1998) Embryonic stem cell lines derived from human blastocysts. *Science*, **282**, 1145–1147.

Thomson, A.J., Pierart, H., Meek, S., Bogerman, A., Sutherland, L., Murray, H., Mountjoy, E., Downing, A., Talbot, R., Sartori, C., Whitelaw, C.B., Freeman, T.C., Archibald, A.L., and Burdon, T. (2012) Reprogramming pig fetal fibroblasts reveals a functional LIF signaling pathway. *Cell Reprogram.*, **14**, 112–122.

van de Pavert, S.A., Boerjan, M.L., Stroband, H.W., Taverne, M.A., and van den Hurk, R. (2001) Uterine-embryonic interaction in pig: activin, follistatin, and activin receptor II in uterus and embryo during early gestation. *Mol. Reprod. Dev.*, **59**, 390–399.

Vassiliev, I. and Nottle, M.B. (2013) Isolation and culture of porcine embryonic stem cells. *Methods Mol. Biol.*, **1074**, 85–95.

Vassiliev, I., Vassilieva, S., Beebe, L.F., McIlfatrick, S.M., Harrison, S.J., and Nottle, M.B. (2010) Development of culture conditions for the isolation of pluripotent porcine embryonal outgrowths from *in vitro* produced and *in vivo* derived embryos. *J. Reprod. Dev.*, **56**, 546–551.

Vodicka, P., Smetana, K. Jr., Dvorankova, B., Emerick, T., Xu, Y.Z., Ourednik, J., Ourednik, V., and Motlik, J. (2005) The miniature pig as an animal model in biomedical research. *Ann. N. Y. Acad. Sci.*, **1049**, 161–171.

Welham, M.J., Storm, M.P., Kingham, E., and Bone, H.K. (2007) Phosphoinositide 3-kinases and regulation of embryonic stem cell fate. *Biochem. Soc. Trans.*, **35**, 225–228.

West, F.D., Terlouw, S.L., Kwon, D.J., Mumaw, J.L., Dhara, S.K., Hasneen, K., Dobrinsky, J.R., and Stice, S.L. (2010) Porcine induced pluripotent stem cells produce chimeric offspring. *Stem Cells Dev.*, **19**, 1211–1220.

West, F.D., Uhl, E.W., Liu, Y., Stowe, H., Lu, Y., Yu, P., Gallegos-Cardenas, A., Pratt, S.L., and Stice, S.L. (2011) Brief report: chimeric pigs produced from induced pluripotent stem cells demonstrate germline transmission and no evidence of tumor formation in young pigs. *Stem Cells*, **29**, 1640–1643.

Wray, J., Kalkan, T., and Smith, A.G. (2010) The ground state of pluripotency. *Biochem. Soc. Trans.*, **38**, 1027–1032.

Wu, Z., Chen, J., Ren, J., Bao, L., Liao, J., Cui, C., Rao, L., Li, H., Gu, Y., Dai, H., Zhu, H., Teng, X., Cheng, L., and Xiao, L. (2009) Generation of pig induced pluripotent stem cells with a drug-inducible system. *J. Mol. Cell. Biol.*, **1**, 46–54.

Xu, Q., D'Amore, P.A., and Sokol, S.Y. (1998) Functional and biochemical interactions of Wnts with FrzA, a secreted Wnt antagonist. *Development*, **125**, 4767–4776.

Yang, J.R., Liao, C.H., Pang, C.Y., Huang, L.L., Chen, Y.L., Shiue, Y.L., and Chen, L.R. (2013) Transplantation of porcine embryonic stem cells and their derived neuronal progenitors in a spinal cord injury rat model. *Cytotherapy*, **15**, 201–208.

Downloaded From Vet-eBooks.com

Ye, S., Li, P., Tong, C., and Ying, Q.L. (2013) Embryonic stem cell self-renewal pathways converge on the transcription factor Tfcp2l1. *EMBO J.*, **32**, 2548–2560.

Zhou, L., Wang, W., Liu, Y., Fernandez de Castro, J., Ezashi, T., Telugu, B.P., Roberts, R.M., Kaplan, H.J., and Dean, D.C. (2011) Differentiation of induced pluripotent stem cells of swine into rod photoreceptors and their integration into the retina. *Stem Cells*, **29**, 972–980.

Downloaded From Vet-eBooks.com

20

Applications of Metabolomics in Reproductive Biology

Ana Luiza Cazaux Velho,[1,2] Rodrigo Oliveira,[3] Thu Dinh,[1] Arlindo Moura,[2] Abdullah Kaya,[4] and Erdogan Memili[1]

[1]*Department of Animal and Dairy Sciences, Mississippi State University, MS, USA*
[2]*Department of Animal Science, Federal University of Ceara, Fortaleza, Brazil*
[3]*Department of Animal Production, Federal Rural University of Rio de Janeiro, Rio de Janeiro, Brazil*
[4]*Department of Animal Reproduction and Artificial Insemination, Selcuk University, Konya, Turkey*

20.1 Introduction

Metabolites are small molecules that are products of metabolic reactions associated with various biochemical pathways (Dunn *et al*., 2011). These molecules play important roles in biological processes and represent potential biomarkers for predicting or detecting developmental states, physiological events, diseases, or specific phenotypes. In order to assess the endogenous metabolites, several research groups have focused on understanding the networks of metabolites using metabolomics. Such explorations have yielded comprehensive identification and quantification of these small molecules, including amino acids, peptides, vitamins, minerals, lipids, and carbohydrates in diverse cells, tissues, fluids, organs, and organisms (Oliver *et al*., 1998; Fiehn, 2001 2002; Dunn *et al*., 2005). Although the term "metabolome" was first introduced in 1998 by Oliver *et al*. (1998), metabolomics studies were conducted prior to the 1960s and 1970s. As an example, Pauling *et al*. (1971) performed gas–liquid chromatography to separate and quantify substances in the vapor of human urine.

More recently, however, significant progress has been made in the study and development of a number of methodological strategies for research such as metabolomics, metabonomics, metabolics fingerprinting, metabolite targeting, and metabolic profiling. Metabonomics is used to measure differences in levels of metabolites resulting from such factors as pathological or genetic changes, toxins, or use of drugs. Metabolic fingerprinting is a rapid method to evaluate and classify biologic samples or biopsies. Metabolite target analysis in turn is used to identify specific metabolic pathways of a limited number of metabolites, while metabolic profiling evaluates a cluster of metabolites that participate in a specific metabolic pathway (Dunn and Ellis, 2005; Hollywood *et al*., 2006; Holmes *et al*., 2008; Dunn *et al*., 2011; Patti *et al*., 2012).

Metabolomics can be performed associated with other *omics* approaches such as genomics, transcriptomics, and proteomics. For example, a recent study showed interesting results using an Integrative Personal Omics Profile (iPOP) to identify markers for possible diseases affecting an individual. The authors suggested that such a method leads to an early diagnosis and facilitates prevention of certain diseases, such as type 2 diabetes, aplastic anemia, human

Animal Models and Human Reproduction, First Edition. Edited by Heide Schatten and Gheorghe M. Constantinescu.
© 2017 John Wiley & Sons, Inc. Published 2017 by John Wiley & Sons, Inc.

Downloaded From Vet-eBooks.com

rhinovirus infection, and respiratory syncytial virus infection (Chen *et al*., 2012). Although supplementary to other *omics*, metabolomics provides identification and quantification of products from metabolism and its pathways, analyses of modifications in metabolic reactions, and characterization of phenotypes and identification of potential biomarkers for such phenotypes (Fiehn, 2001, 2002; Dunn *et al*., 2005; Goodacre *et al*., 2004; Hollywood *et al*., 2006; Patti *et al*., 2012).

20.2 Metabolomics and Reproductive Biology

Along with innovative studies, advanced and more sensitive methods are vital for addressing major questions in biology and biotechnology, including those related to assisted reproductive technologies (ART). For example, using proteomic techniques, researchers have shown that seminal plasma proteins can improve the ability of sperm to fertilize the oocyte and improve the subsequent embryonic development in the bovine species (Moura *et al*., 2006, 2007; Gonçalves *et al*., 2007; Monaco *et al*., 2009). It is well known how metabolites and their roles in specific pathways are essential for reproductive success, for example, fertilization, implantation, and embryonic development. Some techniques currently used in metabolome analysis for comprehensive studies of reproductive biology include proton nuclear magnetic resonance (^{1}H NMR), mass spectrometry (MS), Fourier transform infrared spectroscopy (FTIR), near-infrared (NIR), and Raman spectroscopy (Table 20.1) (Singh and Sinclair, 2007; Seli *et al*., 2010a; Kovac *et al*., 2013; Muñoz *et al*., 2014a, 2014b).

Table 20.1 Key metabolomics approaches in reproductive biology.

Method	Advantages	Limitations	Applications and reference
Proton nuclear magnetic resonance (^{1}H NMR)	Sample preparation is simple Analyzes several molecules simultaneously Provides structural information, which can help identify metabolites Highly reproducible Noninvasive	Low sensitivity Can require a larger number of samples Expensive instrument	Analysis of metabolites in seminal plasma from men with spermatogenic failure and azoospermia (Hamamah *et al*., 1998) Metabolomics profiling of human embryo culture media (Seli *et al*., 2008) Metabolomics analysis of urine (Diaz *et al*., 2011; Maitre *et al*., 2014), plasma (Diaz *et al*., 2011), and amniotic fluid from pregnant women (Graça *et al*., 2010) Metabolomics profiling of human follicular fluid (Wallace *et al*., 2012; O'Gorman *et al*., 2013) Metabolomes of sow follicular fluid (Bertoldo *et al*., 2013)

Downloaded From Vet-eBooks.com

Table 20.1 (*Continued*)

Method	Advantages	Limitations	Applications and reference
Mass spectrometry (MS)	High sensitivity Rapid Can be used with more complex samples Can be performed isolated or coupled with other techniques (i.e., chromatography) that improve molecule identification and quantification	Requires a large sample preparation, which can result in loss of metabolites and in destruction of samples High cost	Metabolomics profiling of plasma from women with preeclampsia (Kenny *et al.*, 2010; Odibo *et al.*, 2011) Metabolomics of plasma and urine from women with gestational diabetes mellitus (Dudzik *et al.*, 2014) Metabolomics profiling of urine from normozoospermic infertile men (Zhang *et al.*, 2014a) and oligozoospermic infertile men (Zhang *et al.*, 2014b)
Fourier transform infrared spectroscopy (FTIR)	Little sample preparation Identifies functional groups High throughput Noninvasive technique	Requires dehydration of samples Gives limited structural information	Metabolomics of cow embryo culture media (Muñoz *et al.*, 2014a, 2014b) and recipient blood plasma (Muñoz *et al.*, 2014b).
Raman	Sample preparation is not necessary Noninvasive Several metabolites can be analyzed concurrently Low cost Measures mainly nonpolar bonds Not sensitive to water, which facilitates biofluids analysis	Does not identify specific metabolites Can produce a low spectral intensity	Metabolomes of human embryo culture media (Seli *et al.*, 2007) Metabolomics of seminal plasma from asthenozoospermic men (Gilany *et al.*, 2014)
Near-infrared (NIR)	Does not require sample preparation Noninvasive Can analyze numerous molecules simultaneously Cost-effective Fast	Sensitive to water Cannot identify specific metabolites	Metabolomes of human embryo culture media (Seli *et al.*, 2007, 2010b)

Reproduced from Velho *et al.* (2005) with permission from Elsevier.

For ART, metabolomics methods have been chosen as noninvasive approaches to improve the assessment of embryo quality (Singh and Sinclair, 2007; Bromer and Seli, 2008; Nagy *et al.*, 2008; Seli *et al.*, 2010a; Montag *et al.*, 2013). In this regard, ^{1}H NMR scans were performed to compare metabolomes in the culture media for implanted and not-implanted human embryos. Such

Downloaded From Vet-eBooks.com

analyses showed that the glutamate was associated with the reproductive potential of those embryos leading to successful pregnancies (Seli *et al*., 2008). NIR, Raman spectroscopy, and ^{1}H NMR used for metabolome analysis of human embryo culture media proved to be valuable methods for determining successful implantation and pregnancy after *in vitro* fertilization (IVF) (Seli *et al*., 2007, 2008, 2010b). Recently, the FTIR metabolomics approach was applied to determine gender of bovine embryos (Muñoz *et al*., 2014a, 2014b). This is also an effective and noninvasive method to determine embryo viability and metabolic profile of blood plasma from recipient cows. Further, FTIR can be used to indicate superior embryos and recipient females for optimum pregnancy outcome (Muñoz *et al*., 2014b).

Metabolic profiling analysis of follicular fluids (FF) from lactating cows and heifers by gas chromatography–mass spectrometry (GC–MS) identified the presence of greater concentrations of saturated fatty acids in follicles from cows than those from heifers (Bender *et al*., 2010). These interesting results suggested that high concentrations of fatty acids in the follicular fluid may have *negative* effects on *cow fertility*. In order to study the developmental competence of oocytes when compared with the size of their follicles, ^{1}H NMR was used to assess the metabolome of sow FF. The concentrations of various metabolites, for example, acetate, lactate, hypoxanthine, inositol, trimethylamine, and amino acids, were greater in the FF from small follicles than those from large follicles. Conversely, only one metabolite, namely glucose, was found at greater concentration in the fluid from large follicles. These reported data suggested that these metabolites could be related to oocyte quality (Bertoldo *et al*., 2013). In ovaries with and without corpus luteum (CL) and blood from dairy cows, there was a strong correlation between glucose concentrations in the blood serum and in the FF from follicles of different sizes, which might be indicative of the relationship between blood and FF metabolites. Additionally, in these ovaries, greater concentrations of glucose were observed in FF from large follicles (Shabankareh *et al*., 2013).

Methods of conventional semen evaluation most often give only descriptive information and still have limitations toward infertility diagnosis. To overcome these limitations, the molecular approaches, such as metabolomics, have been more powerful and have provided more in-depth understanding of the underlying mechanism of male infertility (Aitken, 2010; Rodríguez-Martínez, 2013; Deepinder *et al*., 2007). Metabolomics has shown promise in identifying potential male fertility and infertility biomarkers (Gilany *et al*., 2014; Goodacre *et al*., 2004; Deepinder *et al*., 2007; Kovac *et al*., 2013). The presence or changes in specific metabolite could potentially be related to functions of the male gamete, and such information could lead to rational techniques for infertility treatment or its possible intervention (Aitken, 2010). Gilany *et al.* (2014) reported that metabolomics approach using Raman spectroscopy by analyzing human seminal plasma has enabled the diagnosis of normospermic and asthenozoospermics men.

Metabolomics is also a promising technique to identify potential male fertility and infertility biomarkers (Deepinder *et al*., 2007; Kovac *et al*., 2013). Fertility-associated biomarkers from high- and low-fertility bulls were found in seminal plasma and serum after analysis by ^{1}H NMR. Metabolites such as citrate, tryptamine, taurine, and leucine were identified in seminal plasma, and others such as asparagine, glycogen, citrulline, and isoleucine were found in serum (Kumar *et al*., 2015). Using ^{1}H NMR, Hamamah *et al*. (1998) demonstrated an increase in choline/citrate, choline/lactate, and glycerophosphorylcholine/choline ratios in seminal plasma of men afflicted with spermatogenic failure versus those with obstructive azoospermia. Several small molecular markers were identified in the urine of men with normozoospermic infertility using liquid chromatography–mass spectrometry (LC–MS) in combination with bio-informatics and multivariate analyses. In this research, leukotriene E_4, 3-hydroxypalmitoyl-carnitine, aspartate, xanthosine, and methoxytryptophan were discovered as biomarkers for diagnosis of infertility (Zhang *et al*., 2014a). Gilany *et al*. (2014) also proposed a model for classification of patients with asthenozoospermia by analyzing seminal plasma by Raman

Downloaded From Vet-eBooks.com

spectroscopy. Therefore, it is evident that tools of metabolomics can be used to determine molecular markers of fertility in male.

The metabolomics approach has also been used to predict reproductive disorders in women and to monitor maternal and fetal health during pregnancy (Horgan *et al*., 2008; Diaz *et al*., 2011; Fanos *et al*., 2013; Murri *et al*., 2014). Sun *et al.* (2012), using metabolomics based on ^{1}H NMR spectroscopy, showed differences in the plasma metabolome between women with polycystic ovary syndrome (PCOS) and healthy women. The authors observed low concentrations of creatinine, choline, glycerophosphocholine/phosphocholine, citrate, and some amino acids. Greater concentrations of dimethylamine, lactate, creatine, and *N*-acetyl in plasma of patients with PCOS were reported. ^{1}H NMR was also demonstrated to be an excellent *tool* to determine small molecule markers of fetal malformations. Significant changes in metabolites such as ascorbate, isoleucine, serine, threonine, *N*-methylnicotinamide, hypoxanthine, 3-hydroxybutyric acid, and acetone in blood plasma, urine, and amniotic fluid of pregnant women were associated with fetal malformations (Graça *et al*., 2010; Diaz *et al*., 2011). Moreover, metabolomics analyses of maternal biofluids have been used to develop methods for earlier diagnostics and to elucidate mechanisms involved in disorders such as gestational diabetes mellitus (Graça *et al*., 2010; Diaz *et al*., 2011; Dudzik *et al*., 2014), preeclampsia (Kenny *et al*., 2010; Odibo *et al*., 2011), fetal growth restriction (Maitre *et al*., 2014), and preterm delivery (Graça *et al*., 2010; Diaz *et al*., 2011; Maitre *et al*., 2014).

20.3 Metabolomics Studies in Large Animals as Models for Humans

Large animals have been used as models for research of human disease and physiology due to their specific physiological characteristics, sometimes similar to the human. Moreover, some experimental observations may require a longer period, which is usually not possible when using only laboratory animals, such as mice and rats. Such laboratory animals have a high percentage of inbreeding and, therefore, lack the genetic diversity commonly seen in large animals and human populations. Thus, large animals, for example, pigs, goats, sheep, and cattle, serve as more appropriate models in several aspects of human health research, such as production of xenografts, recombinant proteins, medicine and foods, and reproductive technologies, including transgenesis, cloning, IVF, and *in vitro* embryo production (Kues and Niemann, 2004; Bahr and Wolf, 2012).

In the field of reproductive biology, the use of large animals as models for human studies is a powerful tool as research with these animals has enabled remarkable progress in the application of molecular approaches to advance knowledge base in reproduction and reproductive biotechnology (Bender *et al*., 2010; Bertoldo *et al*., 2013; Shabankareh *et al*., 2013; Muñoz *et al*., 2014a, 2014b; Kumar *et al*., 2015). Moreover, in large animals, fertilization rates have been well controlled and researched to improve the production. Therefore, they are excellent models to study human fertility (Sutovsky *et al*., 1996 Kues and Niemann, 2004). Although reproduction studies in humans using metabolomics strategies have been advancing, these methods require large and homogenous samples, which are complicated and often not feasible. Therefore, metabolomics studies using large animals are useful because of the availability of large quantities of samples, which can be acquired in farms, slaughterhouses, and artificial insemination as well as phenotypic data (Dunn *et al*., 2011).

20.4 Conclusions and Future Prospects

Recent advances in molecular biology have paved the way for the discovery of biomarkers associated with either pathological or physiological conditions. Moreover, these advances

Downloaded From Vet-eBooks.com

provide important progress in studies of drugs or their toxic effects, noninvasive diagnostic techniques in tissue, biofluids (blood, urine, feces, seminal plasma, saliva, bile, and follicular fluid), and cell culture. Despite the encouraging application of metabolomics in biology, the current state of this approach still has several limitations, particularly for the analyses of large data sets using appropriate statistical methods and bioinformatics programs. Additionally, metabolomics experiments help identify numerous classes of substances associated with different metabolic pathways, leading to challenges in interpretation of the results (Goodacre *et al*., 2004; Singh and Sinclair, 2007; Noack and Wiechert, 2014). Thus, continued innovative research is needed to enhance the sensitivity and versatility of the methods employed to advance of biology and biotechnology research. Metabolomics has been applied to studies in human reproductive biology more than that of livestock. Considering the urgent need for proteins from food animals, in the face of increasing world population, metabolomics offers a major opportunity to develop science-based solutions to increase efficiency of animal production and product quality. In addition, large animals are suitable models for metabolomics studies in humans because of the availability of samples and phenotypic data as well as *in vitro* technologies in the large animals. Integrated into a systems biology approach, metabolomics can be combined with other methods to provide better understanding of mammalian physiology, development, and diseases. Thus, genomic, transcriptomic, and proteomic approaches can be complementary to metabolomics. Identifying specific classes of molecules can lead to personalized molecular diagnosis and treatments (Singh and Sinclair, 2007; Wang *et al*., 2010). In conclusion, metabolomics will be an essential tool to understand the developmental potentials of preimplantation embryos, predict male and female fertility, and further diagnose male and female reproductive disorders early in both livestock and humans.

Acknowledgments

This study was funded in part by Mississippi Agricultural Forestry and Experiment Station and by the Brazilian Research Council – CNPq (Project # 484674/2011-0). Ana Luiza Cazaux Velho was supported by a scholarship from the Council for the Improvement of High Level Education (CAPES).

Conflict of Interest

The authors declare that there is no conflict of interest that could be perceived as prejudicing the impartiality of the research reported.

References

Aitken, R.J. (2010) Whither must spermatozoa wander? The future of laboratory seminology. *Asian J. Androl.*, **12** (1), 99–103.

Bahr, A. and Wolf, E. (2012) Domestic animal models for biomedical research. *Reprod. Domes. Anim.*, **47** (Suppl. 4), 59–71.

Bender, K., Walsh, S., Evans, A.C., Fair, T., and Brennan, L. (2010) Metabolite concentrations in follicular fluid may explain differences in fertility between heifers and lactating cows. *Reproduction*, **139** (6), 1047–1055.

Downloaded From Vet-eBooks.com

Bertoldo, M.J., Nadal-Desbarats, L., Gerard, N., Dubois, A., Holyoake, P.K., and Grupen, C.G. (2013) Differences in the metabolomic signatures of porcine follicular fluid collected from environments associated with good and poor oocyte quality. *Reproduction*, **146** (3), 221–231.

Bromer, J.G. and Seli, E. (2008) Assessment of embryo viability in assisted reproductive technology: shortcomings of current approaches and the emerging role of metabolomics. *Curr. Opin. Obstet. Gynecol.*, **20** (3), 234–241.

Chen, R., Mias, G.I., Li-Pook-Than, J., Jiang, L.H., Lam, H.Y.K., Chen, R., Miriami, E., Karczewski, K.J., Hariharan, M., Dewey, F.E., Cheng, Y., Clark, M.J., Im, H., Habegger, L., Balasubramanian, S., O'Huallachain, M., Dudley, J.T., Hillenmeyer, S., Haraksingh, R., Sharon, D., Euskirchen, G., Lacroute, P., Bettinger, K., Boyle, A.P., Kasowski, M., Grubert, F., Seki, S., Garcia, M., Whirl-Carrillo, M., Gallardo, M., Blasco, M.A., Greenberg, P.L., Snyder, P., Klein, T.E., Altman, R.B., Butte, A.J., Ashley, E.A., Gerstein, M., Nadeau, K.C., Tang, H., and Snyder, M. (2012) Personal omics profiling reveals dynamic molecular and medical phenotypes. *Cell* **148** (6), 1293–1307.

Deepinder, F., Chowdary, H.T., and Agarwal, A. (2007) Role of metabolomic analysis of biomarkers in the management of male infertility. *Expert Rev. Mol. Diagn.*, **7** (4), 351–358.

Diaz, S.O., Pinto, J., Graca, G., Duarte, I.F., Barros, A.S., Galhano, E., Pita, C., Almeida, M.D., Goodfellow, B.J., Carreira, I.M., and Gil, A.M. (2011) Metabolic biomarkers of prenatal disorders: an exploratory NMR metabonomics study of second trimester maternal urine and blood plasma. *J. Proteome Res.*, **10** (8), 3732–3742.

Dudzik, D., Zorawski, M., Skotnicki, M., Zarzycki, W., Kozlowska, G., Bibik-Malinowska, K., Vallejo, M., Garcia, A., Barbas, C., and Ramos, M. (2014) Metabolic fingerprint of gestational diabetes mellitus. *J. Proteom.*, **103**, 57–71.

Dunn, W.B. and Ellis, D.I. (2005) Metabolomics: current analytical platforms and methodologies. *Trends Analyt. Chem.*, **24** (4), 285–294.

Dunn, W.B., Bailey, N.J.C., and Johnson, H.E. (2005) Measuring the metabolome: current analytical technologies. *Analyst*, **130** (5), 606–625.

Dunn, W.B., Broadhurst, D.I., Atherton, H.J., Goodacre, R., and Griffin, J.L. (2011) Systems level studies of mammalian metabolomes: the roles of mass spectrometry and nuclear magnetic resonance spectroscopy. *Chem. Soc. Rev.*, **40** (1), 387–426.

Fanos, V., Atzori, L., Makarenko, K., Melis, G.B., and Ferrazzi, E. (2013) Metabolomics application in maternal–fetal medicine. *BioMed Res. Int.*, **2013**, 720514.

Fiehn, O. (2001) Combining genomics, metabolome analysis, and biochemical modelling to understand metabolic networks. *Comp. Funct. Genomics*, **2** (3), 155–168.

Fiehn, O. (2002) Metabolomics: the link between genotypes and phenotypes. *Plant Mol. Biol.*, **48** (1–2), 155–171.

Gilany, K., Moazeni-Pourasil, R.S., Jafarzadeh, N. and Savadi-Shiraz, E. (2014) Metabolomics fingerprinting of the human seminal plasma of asthenozoospermic patients. *Mol. Reprod. Dev.*, **81** (1), 84–86.

Gonçalves, R.F., Wolinetz, C.D., and Killian, G.J. (2007) Influence of arginine-glycine-aspartic acid (RGD), integrins (alphaV and alpha5) and osteopontin on bovine sperm-egg binding, and fertilization *in vitro*. *Theriogenology*, **67** (3), 468–474.

Goodacre, R., Vaidyanathan, S., Dunn, W.B., Harrigan, G.G., and Kell, D.B. (2004) Metabolomics by numbers: acquiring and understanding global metabolite data. *Trends Biotechnol.*, **22** (5), 245–252.

Graça, G., Duarte, I.F., Barros, A.S., Goodfellow, B.J., Diaz, S.O., Pinto, J., Carreira, I.M., Galhano, E., Pita, C., and Gil, A.M. (2010) Impact of prenatal disorders on the metabolic profile of second trimester amniotic fluid: a nuclear magnetic resonance metabonomic study. *J. Proteome Res.*, **9** (11), 6016–6024.

Downloaded From Vet-eBooks.com

Hamamah, S., Seguin, F., Bujan, L., Barthelemy, C., Mieusset, R., and Lansac, J. (1998) Quantification by magnetic resonance spectroscopy of metabolites in seminal plasma able to differentiate different forms of azoospermia. *Hum. Reprod.*, **13** (1), 132–135.

Hollywood, K., Brison, D.R., and Goodacre, R. (2006) Metabolomics: current technologies and future trends. *Proteomics*, **6** (17), 4716–4723.

Holmes, E., Wilson, I.D., and Nicholson, J.K. (2008) Metabolic phenotyping in health and disease. *Cell*, **134** (5), 714–717.

Horgan, R.P., Clancy, C.H., Myers, J.E., and Baker, P.N. (2008) An overview of proteomic and metabolomic technologies and their application to pregnancy research. *BJOG*, **116** (2), 173–181.

Kenny, L.C., Broadhurst, D.I., Dunn, W., Brown, M., North, R.A., McCowan, L., Roberts, C., Cooper, G.J., Kell, D.B., Baker, P.N. and Screening for Pregnancy Endpoints Consortium . (2010) Robust early pregnancy prediction of later preeclampsia using metabolomic biomarkers. *Hypertension*, **56** (4), 741–749.

Kovac, J.R., Pastuszak, A.W., and Lamb, D.J. (2013) The use of genomics, proteomics, and metabolomics in identifying biomarkers of male infertility. *Fertil. Steril.*, **99** (4), 998–1007.

Kues, W.A. and Niemann., H. (2004) The contribution of farm animals to human health. *Trends Biotechnol.*, **22** (6), 286–294.

Kumar, A., Kroetsch, T., Blondin, P., and Anzar, M. (2015) Fertility-associated metabolites in bull seminal plasma and blood serum: ^{1}H nuclear magnetic resonance analysis. *Mol. Reprod. Dev.*, **82** (2), 123–131.

Maitre, L., Fthenou, E., Athersuch, T., Coen, M., Toledano, M.B., Holmes, E., Kogevinas, M., Chatzi, L., and Keun, H.C. (2014) Urinary metabolic profiles in early pregnancy are associated with preterm birth and fetal growth restriction in the Rhea mother–child cohort study. *BMC Med.*, **12**, 110.

Monaco, E., Gasparrini, B., Boccia, L., De Rosa, A., Attanasio, L., Zicarelli, L., and Killian, G. (2009) Effect of osteopontin (OPN) on *in vitro* embryo development in cattle. *Theriogenology*, **71** (3), 450–457.

Montag, M., Toth, B., and Strowitzki, T. (2013) New approaches to embryo selection. *Reprod. BioMed. Online*, **27** (5), 539–546.

Moura, A.A., Chapman, D.A., Koc, H., and Killian, G.J. (2006) Proteins of the cauda epididymal fluid associated with fertility of mature dairy bulls. *J. Androl.*, **27** (4), 534–541.

Moura, A.A., Chapman, D.A., and Killian, G.J. (2007) Proteins of the accessory sex glands associated with the oocyte-penetrating capacity of cauda epididymal sperm from Holstein bulls of documented fertility. *Mol. Reprod. Dev.*, **74** (2), 214–222.

Muñoz, M., Uyar, A., Correia, E., Ponsart, C., Guyader-Joly, C., Martinez-Bello, D., Marquant-Le Guienne, B., Fernandez-Gonzalez, A., Diez, C., Caamano, J.N., Trigal, B., Humblot, P., Carrocera, S., Martin, D., Seli, E., and Gomez, E. (2014b) Metabolomic prediction of pregnancy viability in superovulated cattle embryos and recipients with Fourier transform infrared spectroscopy. *BioMed Res. Int.*, **2014**, 608579.

Muñoz, M., Uyar, A., Correia, E., Diez, C., Fernandez-Gonzalez, C.A., Caamano, A.J.N., Trigal, B., Carrocera, S., Seli, E., and Gomez, E. (2014a) Non-invasive assessment of embryonic sex in cattle by metabolic fingerprinting of *in vitro* culture medium. *Metabolomics*, **10** (3), 443–451.

Murri, M., Insenser, M., and Escobar-Morreale, H.F. (2014) Metabolomics in polycystic ovary syndrome. *Clin. Chim. Acta*, **429**, 181–188.

Nagy, Z.P., Sakkas, D., and Behr, B. (2008) Symposium: innovative techniques in human embryo viability assessment. Non-invasive assessment of embryo viability by metabolomic profiling of culture media ('metabolomics'). *Reprod. BioMed. Online*, **17** (4), 502–507.

Noack, S. and Wiechert, W. (2014) Quantitative metabolomics: a phantom? *Trends Biotechnol.*, **32** (5), 238–244.

Downloaded From Vet-eBooks.com

Odibo, A.O., Goetzinger, K.R., Odibo, L., Cahill, A.G., Macones, G.A., Nelson, D.M., and Dietzen, D.J. (2011) First-trimester prediction of preeclampsia using metabolomic biomarkers: a discovery phase study. *Prenatal Diagn.*, **31** (10), 990–994.

O'Gorman, A., Wallace, M., Cottell, E., Gibney, M.J., McAuliffe, F.M., Wingfield, M., and Brennan, L. (2013) Metabolic profiling of human follicular fluid identifies potential biomarkers of oocyte developmental competence. *Reproduction*, **146** (4), 389–395.

Oliver, S.G., Winson, M.K., Kell, D.B., and Baganz, F. (1998) Systematic functional analysis of the yeast genome. *Trends Biotechnol.*, **16** (9), 373–378.

Patti, G.J., Yanes, O., and Siuzdak, G. (2012) Innovation: metabolomics: the apogee of the omics trilogy. *Nat. Rev. Mol. Cell Biol.*, **13** (4), 263–269.

Pauling, L., Robinson, A.B., Teranishi, R., and Cary, P. (1971) Quantitative analysis of urine vapor and breath by gas–liquid partition chromatography. *Proc. Natl. Acad. Sci. USA*, **68** (10), 2374–2376.

Rodríguez-Martínez, H. (2013) Semen evaluation techniques and their relationship with fertility. *Anim. Reprod.*, **10** (3), 148–159.

Seli, E., Sakkas, D., Scott, R., Kwok, S.C., Rosendahl, S.M., and Burns, D.H. (2007) Noninvasive metabolomic profiling of embryo culture media using Raman and near-infrared spectroscopy correlates with reproductive potential of embryos in women undergoing *in vitro* fertilization. *Fertil. Steril.*, **88** (5), 1350–1357.

Seli, E., Botros, L., Sakkas, D., and Burns, D.H. (2008) Noninvasive metabolomic profiling of embryo culture media using proton nuclear magnetic resonance correlates with reproductive potential of embryos in women undergoing *in vitro* fertilization. *Fertil. Steril.*, **90** (6), 2183–2189.

Seli, E., Robert, C., and Sirard, M.A. (2010a) OMICS in assisted reproduction: possibilities and pitfalls. *Mol. Hum. Reprod.*, **16** (8), 513–530.

Seli, E., Vergouw, C.G., Morita, H., Botros, L., Roos, P., Lambalk, C.B., Yamashita, N., Kato, O., and Sakkas, D. (2010b) Noninvasive metabolomic profiling as an adjunct to morphology for noninvasive embryo assessment in women undergoing single embryo transfer. *Fertil. Steril.*, **94** (2), 535–542.

Shabankareh, H.K., Kor, N.M., and Hajarian, H. (2013) The influence of the corpus luteum on metabolites composition of follicular fluid from different sized follicles and their relationship to serum concentrations in dairy cows. *Anim. Reprod. Sci.*, **140** (3–4), 109–114.

Singh, R. and Sinclair, K.D. (2007) Metabolomics: approaches to assessing oocyte and embryo quality. *Theriogenology*, **68** (Suppl. 1), S56–S62.

Sun, L., Hu, W., Liu, Q., Hao, Q., Sun, B., Zhang, Q., Mao, S., Qiao, J., and Yan, X. (2012) Metabonomics reveals plasma metabolic changes and inflammatory marker in polycystic ovary syndrome patients. *J. Proteome Res.*, **11** (5), 2937–2946.

Sutovsky, P., Hewitson, L., Simerly, C., and Schatten, G. (1996) Molecular medical approaches for alleviating infertility and understanding assisted reproductive technologies. *Proc. Assoc. Am. Phys.*, **108** (6), 432–443.

Wallace, M., Cottell, E., Gibney, M.J., McAuliffe, F.M., Wingfield, M., and Brennan, L. (2012) An investigation into the relationship between the metabolic profile of follicular fluid, oocyte developmental potential, and implantation outcome. *Fertil. Steril.*, **97** (5), 1078–1084.

Wang, J.H., Byun, J., and Pennathur, S. (2010) Analytical approaches to metabolomics and applications to systems biology. *Semin. Nephrol.*, **30** (5), 500–511.

Zhang, J., Mu, X., Xia, Y., Martin, F.L., Hang, W., Liu, L., Tian, M., Huang, Q., and Shen, H. (2014a) Metabolomic analysis reveals a unique urinary pattern in normozoospermic infertile men. *J. Proteome Res.*, **13** (6), 3088–3099.

Zhang, J., Huang, Z., Chen, M., Xia, Y., Martin, F.L., Hang, W., and Shen, H. (2014b) Urinary metabolome identifies signatures of oligozoospermic infertile men. *Fertil. Steril.*, **102** (1), 44–53.

Downloaded From Vet-eBooks.com

21

Cryopreservation of Mammalian Oocytes

Muhammad Anzar

Agriculture and Agri-Food Canada, Saskatoon Research and Development Centre, Saskatoon, Canada

Cryo-, a Greek word used in combination, means "very low temperature or freezing." Cryopreservation is a technique in which cells or tissues are preserved for a long time in liquid nitrogen (LN_2; −196 °C). At such a low temperature, the metabolic activity of cells or tissues is nearly zero due to nonavailability of water, a requirement of cell metabolism. Only background ionizing radiations continue causing photophysical effect, which can take thousands of years to express its harmful effects on the cryopreserved cells or tissues (Mazur, 1984).

Loss of genetic diversity in farm animals is a global issue. According to FAO, several livestock breeds have already faced off from the world and approximately 20% of world's livestock breeds have a threat of extinction (Buerkle, 2007). In the modern world, the livestock industry has been focusing on few high-producing breeds for several decades to meet the market demand. In developing countries, the low-producing local livestock breeds are losing their indigenous genetics due to crossbreeding with high-producing exotic breeds. Therefore, there is a need to conserve animal genetic resources. *In situ* conservation of animal population is an ideal approach but it requires huge infrastructure, management, and money. Alternatively, *ex situ* conservation programs allow to cryopreserve animal genetics in the form of semen, oocytes, embryos, and gonadal tissues in the genebank (Prentice and Anzar, 2011). In conservation program, the cryopreserved (frozen) mammalian semen is abundantly available but it represents only half of the genetics. The cryobanking of ovarian tissue or oocytes is suitable approach to conserve the remaining half of female genetics for breed regeneration in emergency situation. Oocyte cryopreservation has clinical and social applications in human also. It is an important tool of fertility preservation in young women undergoing chemo- or radiotherapy for cancer treatment and those who plan to delay their child-bearing due to social reasons.

21.1 Principles of Cryopreservation

21.1.1 Water and Cell Cryopreservation

Water, a critical compound for cell metabolism, plays a key role in cryopreservation. Living cells have up to 85% water content depending upon cell type. Both, extra- and intracellular ice crystals are detrimental for cell survival. The extracellular ice formation leads to cell dehydration, whereas the intracellular ice formation during freezing and recrystallization during thawing/warming damage the cell organelles (Mazur, 1970, 1996). Therefore, a balance between

Animal Models and Human Reproduction, First Edition. Edited by Heide Schatten and Gheorghe M. Constantinescu.
© 2017 John Wiley & Sons, Inc. Published 2017 by John Wiley & Sons, Inc.

Downloaded From Vet-eBooks.com

Table 21.1 Cryoprotectants (CPs) used in cell/tissue cryopreservation.

Permeating CPs, low molecular weight (M_w)	Nonpermeating CPs, high molecular weight (M_w)	
$M_w < 100$ Da	$M_W \geq 100$ to ≤ 600 Da	$M_W > 1000$ Da (kDa)
Methanol (32.0)	Glucose (180)	Hydroxyethyl starch (HES) (1.35)
Ethylene glycol, EG (62.07)	Fructose (180.16)	Polyethylene glycol (PEG) (1.45)
Propylene glycol/1,2-propanediol (76.09)	Lactose (342.30)	Polyvinylpyrrolidone (PVP) (10–40)
1,3-Propanediol (76.09)	Sucrose (342.30)	Polyvinyl alcohol (PVA) (30–70)
Dimethyl sulfoxide (DMSO) (78.13)	Trehalose (378.33)	Ficoll®70 (60–80)
Glycerol or 1,2,3-propanetriol (92.09)	Raffinose (594.51)	Dextran (>500)
Butylene glycol (2,3-butanediol) (92.12)		
Acetamide (59.07), (most toxic CP)		
Formamid (45.04), (most toxic CP)		

Modified from Kuleshova *et al*. (2007).

cell dehydration and intracellular ice formation is required. The cryobiologists aim to control the intracellular water content for minimum and innocuous ice crystal formation.

21.1.2 Cryoprotectants

Cryoprotectants (CPs) are chemicals that protect cells at ultra-low temperature. They are classified as permeating and nonpermeating depending upon their ability to permeate through cell plasma membrane. The common cryoprotectants used for cells/tissues cryopreservation are presented in Table 21.1.

21.1.2.1 Permeating Cryoprotectants

The permeating cryoprotectants permeate the plasma membrane of cells and are generally considered cytotoxic. Once inside the cells, being hygroscopic, the permeating cryoprotectants bind with the intracellular free water minimizing water-to-water hydrogen bonds, a source of lethal intracellular ice formation, and simultaneously depress the freezing point of intracellular fluid (Fahy *et al.*, 1987; Kuleshova and Hutmacher, 2008; Shaw and Jones, 2003). Since the historical discovery of glycerol as a cryoprotectant, it is widely used for cryopreservation of mammalian cells (Polge *et al.*, 1949). It reduces the osmotic stress through "salt-buffering" mechanism (Kuleshova and Hutmacher, 2008; Lovelock, 1953), binds with the metallic ions (Lohmann *et al.*, 1965), dehydrates cells (Bredderman and Foote, 1969), reduces the ice expansion during water solidification, and prevents fractures in the frozen solutions (Gao *et al.*, 1995). Other common permeating cryoprotectants are dimethyl sulfoxide (DMSO) (Lovelock and Bishop, 1959), ethylene glycol (EG) (Voelkel and Hu, 1992), polyethylene glycol (PEG), and 1,2-propanediol (PROH) also called propylene glycol (PG) (Kuleshova and Hutmacher, 2008; Shaw and Jones, 2003).

The cytotoxicity of permeating cryoprotectant is one of the fundamental limitations in cryopreservation of the living cells or tissues (Fahy, 2010). It varies due to cryoprotectants and cell types (Arav *et al.*, 1993; Jomha *et al.*, 2010; Kuleshova and Hutmacher, 2008; Plachinta

Downloaded From Vet-eBooks.com

et al., 2004; Roux *et al.* 2008; Tsai *et al.*, 2008). The exact mechanism of cytotoxicity associated with the cryoprotectants is not exactly known (Fahy *et al.*, 1990). The cytotoxicity of permeating cryoprotectant is directly proportional to cryoprotectants' concentration, temperature of its addition, exposure time, and gradient across membrane (Schneider and Mazur, 1984). The addition of cryoprotectants at room temperature is preferable for cell cryopreservation but it extends the time required to permeate the cells unnecessarily. An ideal cryoprotectant should have maximum cryoprotection ability with minimum osmotic and toxic shocks to the cells. So far, there is no universal toxic-free permeating cryoprotectant for cell cryopreservation.

21.1.2.2 Nonpermeating Cryoprotectants

The nonpermeating cryoprotectants cannot cross the cell membrane due to their large size (Table 21.1). The addition of nonpermeating cryoprotectants in the medium counterbalances the osmotic shock and reduces the required concentration of permeating cryoprotectants ultimately decreasing their cytotoxic effect especially in vitrification method of cryopreservation (Abdelhafez *et al.*, 2010; Han and Critser, 2009; Kuleshova *et al.*, 1999; Leibo, 1984, 1986). The nonpermeating cryoprotectants include polymers/macromolecules (bovine serum albumin or fetal calf serum) or saccharides (sucrose, trehalose, raffinose, lactose, glucose, and fructose). The saccharides act as cell dehydrants at room temperature (Figure 21.1). The contributions of different saccharides in cell cryopreservation depend upon their type and mass (Koshimoto and Mazur, 2002; Kuleshova *et al.*, 1999). Sucrose is the most common saccharide used in slow equilibrium cooling (Renard *et al.*, 1984), rapid nonequilibrium cooling (Szell and Shelton, 1986, 1987), and vitrification (Hamano *et al.*, 1992) methods of cryopreservation. Sucrose is also used in thawing/warming solution to balance the osmolality between the extra- and intracellular fluids and to avoid cells' swelling due to influx of water following efflux of intracellular permeating cryoprotectants (Agca *et al.*, 1998; Leibo, 1984). Monosaccharides are more miscible in the concentrated solutions of cryoprotectants than disaccharides. They have better osmotic buffering capacity than disaccharides to dilute the effect of concentrated permeating cryoprotectants during warming of frozen-thawed human oocytes (McWilliams *et al.*, 1995).

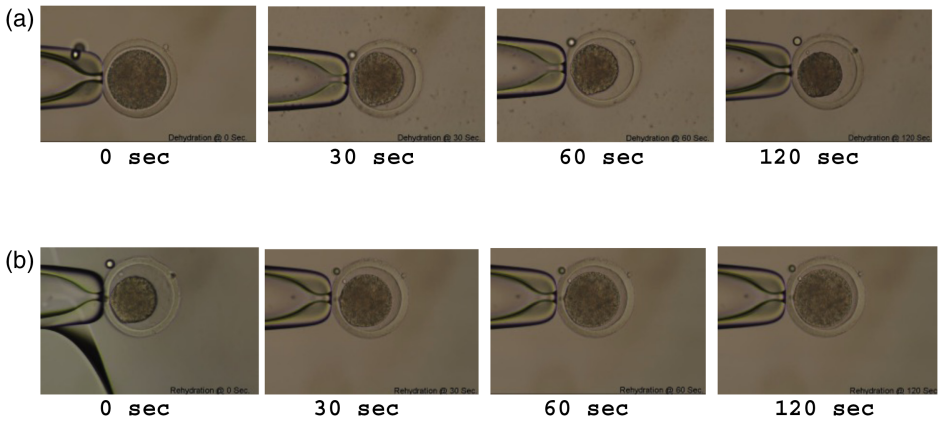

Figure 21.1 Dehydration of denuded bovine oocyte after exposure to TCM-199 containing 0.5 M sucrose (a) followed by rehydration of same oocyte in TCM alone (b), within 2 min (Alfoteisy, 2012).

Downloaded From Vet-eBooks.com

21.1.3 Cooling Rate

Optimum cooling rate is important for successful cryopreservation of mammalian cells. The sub- and supraoptimal cooling rates lead to cell dehydration (solution effect) and intracellular ice formation, respectively. There are three levels of intracellular ice formation: primary, secondary, and higher crystals (Han and Critser, 2009). The size of intracellular ice crystals ranges from <0.1 nm to several nanometers in mammalian oocytes depending upon the cooling rate. The theoretical model revealed few large ice crystals by slow cooling rate and many small ice crystals by rapid cooling rate in mouse oocytes (Zhao *et al.*, 2006). The intracellular ice crystals harm cell organelles, including cytoplasmic lipid droplets and meiotic spindle of oocytes (Yavin and Arav, 2007). Once ice crystals are formed, the growth of ice crystals is an inverse function of temperature. Generally, an "inverted U" relationship exists between cooling rate and cell survival.

21.2 Cryopreservation of Mammalian Oocytes

Oocyte cryopreservation is a promising option for long-term preservation of female genetics and fertility. It expands the usage of assisted reproductive technologies (ART) by producing embryo *in vitro*, exploits the genetic potential of superior females even after death, and avoids the ethical and legal controversies surrounding the preservation of human embryos (Checura and Seidel, 2007; Fabbri, 2006; Ledda *et al.*, 2001). Like semen, oocyte cryopreservation is beneficial for global exchange of germplasm, since it avoids the injury and potential risks of disease transmission associated with transportation of live animals (Massip, 2003). Live calves have been born from cryopreserved bovine oocytes following *in vitro* fertilization and somatic cell nuclear transfer (Vieira *et al.* 2002, 2008; Yang *et al.*, 2008). Similarly, cryopreservation of oocytes is an integral part of biobanks throughout the industrialized world. Thousands of babies have been born after use of cryopreserved oocytes without any adverse obstetric or perinatal outcomes (Cobo *et al.*, 2014).

21.2.1 History

Cryopreservation of mammalian oocytes was first reported in the late 1950s (Sherman and Lin, 1958). In the 1970s, the slow freezing method was developed for cryopreservation of mouse, sheep, and bovine embryos (Whittingham, 1971; Whittingham *et al.*, 1972; Willadsen *et al.*, 1976, 1978). Later, the first live birth of mouse pups from cryopreserved mouse oocytes was reported (Whittingham, 1977). The first pregnancy from cryopreserved human oocytes was reported in the mid-1980s (Chen, 1986). Cryopreservation of mammalian oocytes is more recent but less successful than sperm and embryos. Following the understanding of fundamental principles involved in cryobiology, the live offspring were born after *in vitro* fertilization of cryopreserved mouse oocytes (Leibo *et al.*, 1978; Parkening *et al.*, 1976; Whittingham, 1977). Vitrification, another cryopreservation technique, was developed during the early 1930s (Stiles, 1930). After more than 50 years, vitrification was used for cryopreservation of mouse embryos (Rall and Fahy, 1985) and later for oocytes. Although offspring have been born from cryopreserved oocytes in human and livestock species, the overall success rate is low (Table 21.2). This is generally attributed to the oocytes' susceptibility to damages during freezing and thawing procedures because of their own complex structure.

Downloaded From Vet-eBooks.com

Table 21.2 Cryopreservation of oocytes and its effect on fertilization and early embryonic development in different species (year 2000 onward).

Species	Stage	Permeating cryoprotectant	Nonpermeating cryoprotectant	Additive	Cryomethod	Warming method/ fertilization method	Endpoint	Reference
Human	MII	PROH	Sucrose		SF	One-step/ ICSI	FR 77%, BR 6% (SF) FR 91%, BR 6% (Control)	Cobo *et al.*, 2001
Human	MII	PROH	Sucrose	Choline chloride	SF	One-step/ ICSI	FR 59%, IR 25%, LB 2	Quintans *et al.*, 2002
Human	MII	EG	Sucrose		Vit (EMG)	Four-step/ IVF	FR 72%, PR 21%, IR 6%	Yoon *et al.*, 2003
Human	MII	PROH	Sucrose		SF	One-step/ ICSI	FR 67%, CR 91%, PR 33%, LB 5	Chen *et al.*, 2005
Human	MII	EG	Sucrose		Vit (cryotop)	Two-step/ ICSI	FR 81%, BR 50%	Kuwayama *et al.*, 2005a, 2005b
Human	MII	PROH	Sucrose	Sodium-depleted media	SF	One-step/ ICSI	PR 26%, IR 11% (PBS) PR 38%, IR 16% (mHTF)	Boldt *et al.*, 2006
Human	MII	PROH	Sucrose		SF	One-step/ ICSI	CR 54%, PR 12%, LB 13	Levi Setti *et al.*, 2006
Human	MII	EG + DMSO	Sucrose		Vit (cryotop)	Two-step/ ICSI	FR 87%, CR 94%, PR 57%	Lucena *et al.*, 2006
Human	MII	PROH	Sucrose		SF	One-step/ IVF or ICSI	FR 54%, IR 12%, PR 17%	De Santis *et al.*, 2007
Human	MII	PROH/ EG + PROH	Sucrose		SF versus Vit (cryoleaf)	One- and three-step/ ICSI	FR 61%, CR 54%, BR 12% (SF) FR 68%, CR 78%, BR 33% (Vit)	Cao *et al.*, 2009
Human	MII *in vivo* versus *in vitro*	EG + PROH	Sucrose		Vit (cryoleaf)	Three-step/ ICSI	FR 76%, IR 19%, PR 45%, LB 15 (*in vivo*) FR 64%, IR 10%, PR 20%, LB 4 (*in vitro*)	Chian *et al.*, 2009

(*continued*)

Downloaded From Vet-eBooks.com

Table 21.2 (*Continued*)

Species	Stage	Permeating cryoprotectant	Nonpermeating cryoprotectant	Additive	Cryomethod	Warming method/ fertilization method	Endpoint	Reference
Human	MII	EG + DMSO	Sucrose		Vit (cryotop)	Two-step/ ICSI	FR 72%, CR 95%, BR 54%, IR 34%, PR 47%	Cobo *et al.*, 2010
Human	MII	EG	Sucrose		Vit (EMG)	Four-step/ ICSI	FR 72%, IR 45%, PR 80%, LB 19	Kim *et al.*, 2010
Human	MII	PROH	Sucrose	Plasmanate	SF	One-step/ IVF	FR 73%, BR 88%	Magli *et al.*, 2010
Human	MII	PROH or EG + DMSO	Sucrose		SF versus Vit (cryotip)	One- and two-step/ ICSI	FR 67%, CR 71%, PR 13% (SF) FR 77%, CR 84%, PR 38% (Vit)	Smith *et al.*, 2010
Bovine	MII	EG	Sucrose		Vit (Microdrop)	One-step/ IVF	CR 52–70%, BR 6–30%	Papis *et al.*, 2000
Bovine	MII	PROH (SF)/ EG + DMSO + PEG (Vit)	Sucrose	Ficoll	SF versus Vit (cryoloop)	One- and four-step/ IVF and ICSI	CR 9% SF, 16% Vit (ICSI) CR 15% SF, 26% Vit (IVF)	Mavrides and Morroll, 2002
Bovine	GV	EG + DMSO	Sucrose	Cytochalasin D	Vit (OPS)	Two-step/	CR 46%, BR 4% (+CytD) CR 49%, BR 6.1% (-CytD)	Vieira *et al.*, 2002
Bovine	MII	EG + PROH or EG + DMSO	Sucrose		Vit (cryotop)	Two-step/ IVF	CR 70%, BR 7% (EG + PROH) CR 69%, BR 2% (EG + DMSO)	Chian *et al.*, 2004
Bovine	GV	EG	Sucrose or trehalose	Ficoll	Vit (nylon-mesh)	Three-step/ IVF	CR 21%, BR 0% (one-step Suc) CR 0%, BR 0% (one-step Tre) CR 38%, BR 8% (three-step Suc) CR 22%, BR 0% (three-step Tre)	Abe *et al.*, 2005

Downloaded From Vet-eBooks.com

Bovine	MII	EG + DMSO	Galactose	PVP, PVA, BSA, Ficoll,	Vit (OPS versus cryoloop)	Three-step/ IVF	CR 54%, BR 11% (Cryoloop) CR 49%, 5% (OPS) CR 63–76%, BR 10–23% (+MM) CR 66–80%, 9–17% (-MM)	Checura and Seidel, 2007
Bovine	GV	EG + DMSO	Sucrose		Vit (microdrop)	Three-step/ IVF	FR 66%, CR 56%, BR 2%	Kim *et al.*, 2007
Bovine	MII	EG + DMSO	Galactose	Fetuin, PVP	Vit (cryotop)	Four-step/ IVF	CR 64%, BR 11% (FCS) CR 60%, BR 5% (BAS) CR 61%, BR 6% (BSA + Fetuin)	Horvath and Seidel, 2008
Bovine	MII	EG + DMSO	Sucrose	Taxol	Vit (FDP versus OPS)	Two-step/ IVF	NSR 30%, CR 16%, BR 0% (FDP) NSR 46%, CR 43%, BR 2% (OPS)	Morato *et al.*, 2008d
Bovine	MII	EG + DMSO	Sucrose	Taxol	Vit (OPS)	Two-step/ IVF	NSR 63%, CR 42%, BR 3% (+Taxol) NSR 50%, CR 34%, BR 0% (-Taxol)	Morato *et al.*, 2008a
Bovine	MII	EG + DMSO	Sucrose	Taxol	Vit (OPS versus cryotop)	One-step/ IVF	CR 32%, BR 0% (OPS) CR 46%, BR 2% (Cryotop)	Morato *et al.*, 2008b
Bovine	GV	EG	Trehalose	Ice blocker (X1000 and/or Z1000)	Vit (cryotop)	Two-step/	CR 38%, BR 2% (BM) CR 37%, BR 2% (BM + X1000) CR 40%, BR 3% (BM + Z1000) CR 41%, BR 2% (BM + X1000 + Z1000)	Zhou *et al.*, 2010
Bovine	GV	EG + DMSO	Sucrose		Vit (cryotop)	One-step/ IVF	CR 41%, BR 2% (Vit) CR 92%, BR 34% (Control)	Prentice-Biensch *et al.*, 2012a

(*continued*)

Downloaded From Vet-eBooks.com

Table 21.2 (*Continued*)

Species	Stage	Permeating cryoprotectant	Nonpermeating cryoprotectant	Additive	Cryomethod	Warming method/ fertilization method	Endpoint	Reference
Bovine	MII	EG	Trehalose	PVP, docetaxel	SSV	Four-step/ IVF	CR 65%, BR 23% (+Dt) CR 57%, BR 17% (-Dt)	Chasombat *et al.*, 2015
Buffalo	MII	EG	Trehalose	PVP	SSV	One-step/ IVF	CR 15%, BR 2% (CC) CR 26%, BR 7% (No CC)	Gasparrini *et al.*, 2007
Porcine	GV	EG/EG + DMSO	Sucrose	Cytochalasin B	Vit (cryotop)	Three-step/ ICSI	CR 38%, BR 14% (EG) CR 39%, BR 14% (EG + DMSO)	Fujihira *et al.*, 2004
Porcine	MII	EG	Sucrose	Taxol	Vit (cryotop)	Three-step/ ICSI	CR 49%, BR 6% (+Taxol) CR 52%, BR 9% (-Taxol)	Fujihira *et al.*, 2005
Porcine	MII	EG + DMSO	Sucrose	Taxol	Vit (OPS)	Four-step/ PA	NSR 10%, CR 24%, BR 0% (+Taxol) NSR 4%, CR 6%, BR 0% (-Taxol)	Shi *et al.*, 2006
Porcine	MII	EG	Trehalose, PVP	Cytochalasin B	SSV	Four-step/ PA	CR 62%, BR 5% (+CytB) CR 26%, BR 3% (-CytB)	Somfai *et al.*, 2006
Porcine	GV versus MII	EG	Sucrose		Vit (OPS)	Two-step/ IVF	NSR 10%, CR 8% (GV) NSR 13%, CR 0% (MII)	Wu *et al.*, 2006
Porcine	GV versus MII	EG + DMSO	Sucrose	Cytochalasin B	SSV	Two-step/ IVF	CR 20%, BR 9% (GV) CR 27%, BR 3% (MII)	Gupta *et al.*, 2007
Porcine	MII	EG + DMSO	Sucrose		Vit (0.25 ml straws)	Four-step/ ICSI	NSR 43%, CR 38%, BR 2%	Shi *et al.*, 2007
Porcine	GV	EG + DMSO	Sucrose	Ruthenium red	Vit (micropipet tip)	Three-step/ IVF	CR 9%, BR 3% (+RR) CR 9%, BR 0% (-RR)	Nakagawa *et al.*, 2008

Downloaded From Vet-eBooks.com

Porcine	MII	EG + DMSO	Sucrose	HHP	Vit (cryotop)	Two-step/ PA	CR 16–42%, BR 5–13% (HHP) CR 15%, BR 0% (No HHP)	Du *et al.*, 2008
Porcine	MII	EG + DMSO	Sucrose	HHP	Vit (cryotop)	Two-step/ PA	CR 8–27%, BR 0–4%	Pribenszky *et al.*, 2008
Ovine	MII	EG + DMSO	Sucrose		Vit (cryoloops)	Three-step/ IVF	NSR 48%, CR 21%, BR 0% (Vit) NSR 83%, CR 83%, BR 23% (Control)	Succu *et al.*, 2007b
Ovine	MII	EG + DMSO	Sucrose	Cytochalasin B, Taxol	SSV	Two-step/ IVF	CR 47–52%, BR 1–8% (CytB) CR 47–51%, BR 1–10% (Taxol) CR 48%, BR 2% (Control)	Zhang *et al.*, 2009
Equine	GV and MII	EG + DMSO	Sucrose		SF versus Vit (OPS)	One-step/ ICSI	NSR 43%, MR 1% (SF) NSR 48%, MR 28% (Vit)	Tharasanit *et al.*, 2006
Equine	GV	EG + DMSO	Sucrose		Vit (OPS)	One-step/ IVM	NSR 38%, MR 36%	Tharasanit *et al.*, 2009
Murine	MII	EG + DMSO	Sucrose	Calcium-free media	Vit (cryoloop)	Two-step/ IVF	BR 37% (−Ca) BR 39% (+Ca)	Larman *et al.*, 2006
Murine	GV	DMSO	Sucrose		SF	One-step/ IVF	FR 64%, BR 33% (SF) FR 94%, BR 77% (Control)	Ruppert-Lingham *et al.*, 2006
Murine	MII	EG + DMSO	Trehalose		Vit (MC)	One-step/ IVF	CR 56%, BR 17% (Vit) CR 68%, BR 29% (Control)	Choi *et al.*, 2015
Caprine	MII	EG + DMSO	Sucrose, Trehaslose, PVP, Ficoll		SSV versus Vit (Cryoloop)	One- and two-step/ PA	CR 57%, BR 0% (SSV) CR 58%, BR 0% (CLV) CR 87%, BR 9% (Control)	Begin *et al.*, 2003
Feline	MII	EG	Sucrose, Ficoll		Vit (cryoloop)	One-step/ IVF	CR 32%, BR 12% (Vit) CR 51%, BR 28% (Control)	Merlo *et al.*, 2008

(*continued*)

Downloaded From Vet-eBooks.com

Table 21.2 (*Continued*)

Species	Stage	Permeating cryoprotectant	Nonpermeating cryoprotectant	Additive	Cryomethod	Warming method/ fertilization method	Endpoint	Reference
Feline	GV	EG + DMSO	Sucrose		Vit (OPS)	One-step/ IVF	CR 19%, BR 4% (Vit) CR 48%, BR 21% (Control)	Cocchia *et al.*, 2010
Feline	GV	EG + DMSO	Sucrose		Vit (OPS)	One-step/ IVF	CR 25%, BR 7% (Vit) CR 63%, BR 31% (Control)	Tharasanit *et al.*, 2011
Feline	MII	EG + DMSO	Sucrose		Vit (cryotop)	Two-step/ IVF versus ICSI	CR 35%, BR 0% (Vit-IVF) CR 50%, BR 0% (Vit-ICSI) CR 55%, BR 28% (Control-IVF) CR 80%, BR 0% (Control-ICSI)	Pope *et al.*, 2012
Rabbit	MII	EG + DMSO	Sucrose	CLC	SF (0.25 ml straw) versus Vit (0.25 ml straw)	Three-step (SF) One-step (Vit)/ ICSI	CR 24%, BR 3% (SF) CR 26%, BR 2% (CLC-SF) CR 28%, BR 0% (Vit) CR 27%, BR 0% (CLC-Vit) CR 51%, BR 50% (Control)	Jiménez-Trigos *et al.*, 2013

Downloaded From Vet-eBooks.com

21.2.2 Mammalian Oocyte

Cryotolerance of mammalian oocytes is different from sperm and embryos due to their unique morphological features. Mammalian oocyte ranges from 75 to 140 μm in diameter depending upon species (Griffin *et al.*, 2006). Low surface-to-volume ratio of oocytes makes them susceptible to chilling and intracellular ice formation (Arav *et al.*, 1996; Toner *et al.*, 1990; Zeron *et al.*, 1999). The main pool of female germ cells exists in the immature form, called germinal vesicles (GV), which undergo germinal vesicle breakdown (GVBD), metaphase I (MI), and metaphase II (MII) stages during maturation. After reaching puberty, a cohort of oocyte-containing primary follicles is selected in each estrus or menstrual cycle that continues to develop to a single dominant follicle in cow, mare, woman, and so on or multiple dominant follicles in sow, bitch, and so on. At the time of ovulation, the mature oocytes are at MII stage. The remaining follicles regress and undergo apoptosis. During maturation from GV to MII stage, mammalian oocytes synthesize and store large quantities of lipids, mRNA, and proteins to undergo fertilization and to support early embryonic development. Any deficiency during *in vivo* or *in vitro* culture ultimately results in suboptimal quality of oocytes (Krisher, 2004).

The different structural characteristics of GV and MII oocytes play an important role in their cryopreservation. The GV (immature) oocytes, present in small antral follicles (<5 mm), are arrested at prophase stage of first meiotic division. They are characterized by the large condensed nuclei enclosed within nuclear membrane. The GV oocytes are surrounded by compact cumulus cells (Figure 21.2), collectively known as "cumulus–oocyte complexes (COCs)". They are fully loaded with metabolic machinery, for example, Golgi apparatus, endoplasmic reticulum, and mitochondria. The MII (mature) oocytes are characterized by the expanded cumulus cells in the extracellular matrix (Figure 21.2) and large meiotic spindle apparatus with microtubules, a fundamental structure for completion of meiosis, formation of second polar body, movement of pronuclei, and arrangement of first meiotic spindle (Chen *et al.*, 2003; Eroglu *et al.*, 1998; Navara *et al.*, 1994). The chromosomes align at the equatorial plane of the meiotic spindles. Spindle abnormalities result into the loss of fertilization and embryonic development (Schatten *et al.*, 1985). Mammalian oocytes are surrounded by a special matrix of glycoproteins called "zonal pellucida," important for sperm binding and penetration. Mammalian oocytes have large number of cortical granules, derivative of Golgi apparatus, located just inside the plasma membrane (oolemma). Following oocyte fertilization by a single sperm, the secretions from cortical granules

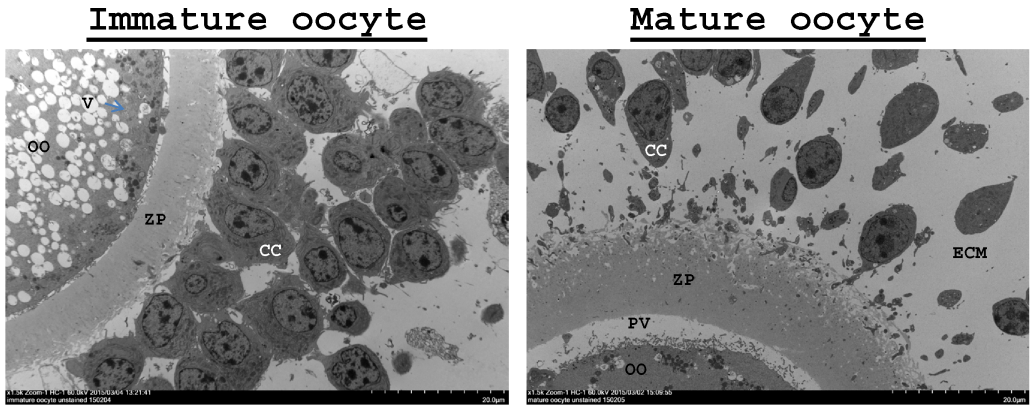

Figure 21.2 Ultrastructure of immature (GV stage) and *in vitro* matured (MII stage) bovine oocytes (magnification × 1500). The distribution of surrounding cumulus cells and extracellular matrix differ between oocytes. CC: cumulus cells; ECM: extracellular matrix; OO: ooplasm; PV: perivitelline space; V: vesicles; ZP: zona pellucida.

Downloaded From Vet-eBooks.com

block further penetration of sperm (polyspermy). The gap junctions (connexin) establish important communications between oocyte and cumulus cells and between cumulus cells for oocyte development and fertility (Juneja *et al.*, 1999; Simon and Goodenough, 1998). These gap junctions permit the exchange of substances <1 kDa, including sugars, amino acids, lipid precursors, and nucleotides by diffusion process. This is the most important route for the nutritive substances to enter the oocyte (Simon *et al.*, 1997). Cumulus cells attract, trap, and select proven sperm, and facilitate sperm capacitation, acrosome reaction, penetration, and fertilization. The denuded oocytes are depleted in maturation-promoting factor (MPF) and mitogen-activated protein kinase (MAPK) enzymes leading to poor early embryonic development (Attanasio *et al.*, 2010; Cox *et al.*, 1993; Tanghe *et al.*, 2003).

Mammalian oocytes are commonly cryopreserved at GV (immature) or MII (mature) stage. Cryopreservation of GV oocytes is ideal due to confined genetic material (chromatin and nucleolus) within nuclear envelope and absence of meiotic spindle. However, GV oocytes are more sensitive to anisosmotic stress and have lower cell membrane permeability than mature MII oocytes (Agca *et al.*, 2000; Bogliolo *et al.*, 2007; Ledda *et al.*, 2001; Men *et al.*, 2002). The plasma membrane permeability coefficients to water (*L*p), cryoprotectants (*P*s), and their interactions (σ) in different species have been reviewed in detail earlier (Critser *et al.*, 1997).

21.2.3 Cryopreservation Methods

Oocyte cryopreservation is conducted mostly following methods developed for embryo cryopreservation. It is generally believed that cryopreservation of mammalian oocytes is difficult compared with embryo mainly due to their large size, low surface-to-volume ratio, high lipid content, low permeability, low conductivity, and sensitivity to chilling (Bogliolo *et al.*, 2007; Leibo, 1980; Massip, 2003; Rojas *et al.*, 2004; Saragusty and Arav, 2011; Succu *et al.*, 2007a). Slow freezing and vitrification are common oocyte cryopreservation methods. These methods differ in the concentration of cryoprotectants used and cooling rate; otherwise, they are similar in storage, warming, and rehydration (Vajta and Kuwayama, 2006). Recent studies showed that regardless of species, stage (GV or MII), cryopreservation method (conventional slow freezing or vitrification), the permeating and nonpermeating cryoprotectants, and thawing/warming methods, oocyte cryopreservation is not as successful as embryo cryopreservation in domestic animals (Table 21.2). However, the cryopreserved human oocytes yielded promising outcomes after intracytoplasmic sperm injection (ICSI). However, ICSI is difficult in domestic animals, due to high lipid content in oocytes. Rather, *in vitro* fertilization is still a popular method to fertilize animal oocytes. In this chapter, vitrification of mammalian oocytes will be emphasized due to its emerging popularity over conventional slow freezing and lack of serious repercussions associated with embryo vitrification.

21.2.3.1 Slow Freezing

Slow freezing is an old and conventional method of mammalian oocyte and embryo cryopreservation. In this procedure, cells or tissues are frozen by initiating extracellular ice nucleation called "seeding." The seeding causes withdrawal of intracellular free water and cell dehydration before intracellular freezing takes place, called nonequilibrium freezing (Mazur, 1963). In this method, mammalian oocytes are suspended in the freezing medium containing permeating cryoprotectants, for example, ethylene glycol (EG), glycerol, dimethyl sulfoxide (DMSO), and/or 1,2-propanediol, in combination with nonpermeating cryoprotectant (sucrose, trehalose, glucose, or fructose). The oocytes are loaded into 0.25 ml straws and placed in a programmable cell freezer at −5 to −8 °C for 5–10 min for equilibration. The extracellular solution is seeded manually around −6 °C by touching outer surface of straw with ice or very

Downloaded From Vet-eBooks.com

cold metal. Seeding initiates ice nucleation in the extracellular solution, which causes intracellular dehydration prior to freezing. After ice nucleation, oocytes in straws are slowly cooled to temperature anywhere between −30 and −65 °C (depending upon the protocol) at the rate of 0.3–0.8 °C/min in a programmable cell freezer. Then, straws are quickly plunged in LN_2 for long-term storage (Cutting *et al.*, 2009; Jain and Paulson, 2006).

During slow freezing, cells undergo osmotic and phase changes, solution effect, and extra- and intracellular ice formation associated with dilution, initial cooling/freezing, and thawing processes. The success of cryopreservation largely depends upon the severity of these changes and cells' ability to tolerate them.

Osmotic Changes

Generally, the base media commonly used for cryopreservation of cells are isoosmotic but they become hyperosmotic with the addition of cryoprotectants. The osmotic response of cells after exposure to the cryoprotectant medium is represented in Figure 21.3. Immediately after an exposure to the hyperosmotic cryoprotectant medium, water diffuses out (exosmosis) and cells shrink momentarily leading to increased intracellular osmolality. Meanwhile, the permeating cryoprotectants cross the plasma membrane and intracellular osmolality further increases. In response, water diffuses inside and cells undergo swelling until the equilibrium is established between water and the permeating cryoprotectants, across the cell membrane. These osmotic events are reversed upon thawing of frozen cells. During warming, the permeating cryoprotectants must be removed from the cells due to their toxic nature. Some protocols recommend three-step removal of cryoprotectants by adding nonpermeating cryoprotectant (e.g., sucrose) in the solution, to minimize the sudden osmotic change upon warming. Cells must tolerate these osmotic fluctuations for successful cryopreservation. Otherwise, cells possessing weak plasma membrane swell and rupture under hypoosmotic conditions. Mammalian MII oocytes survive well and maintain their morphology in wider range of osmolality, that is, 200–2000 milliosmolal (mOsm) in bovine and porcine, and 150–1200 mOsm in human (Mullen *et al.*, 2004, 2007, 2008). However, the porcine oocytes exposed to slight hypo- or hyperosmotic conditions from isosmotic (290 mOsm) lead to poor blastocyst development (Figure 21.4) (Mullen *et al.*, 2007). It seems the osmotic stress affects the mammalian oocyte at molecular level which is expressed later during early embryonic development, not immediately after thawing.

Phase Changes

The fluid mosaic model represents the structure and dynamics of the plasma membrane of mammalian cells. The plasma membrane is a lipid bilayer consisting of heterogeneous phospholipids (phosphatidylcholine, phosphatidylserine, phosphatidylethanolamine, phosphatidylinositol,

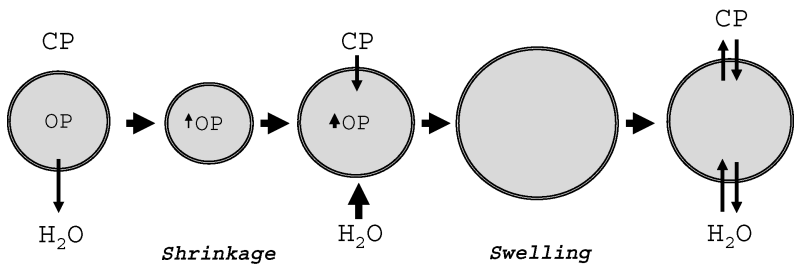

Figure 21.3 Osmotic changes in a cell after dilution in cryoprotectant medium. These events are reversed during thawing or warming.

Downloaded From Vet-eBooks.com

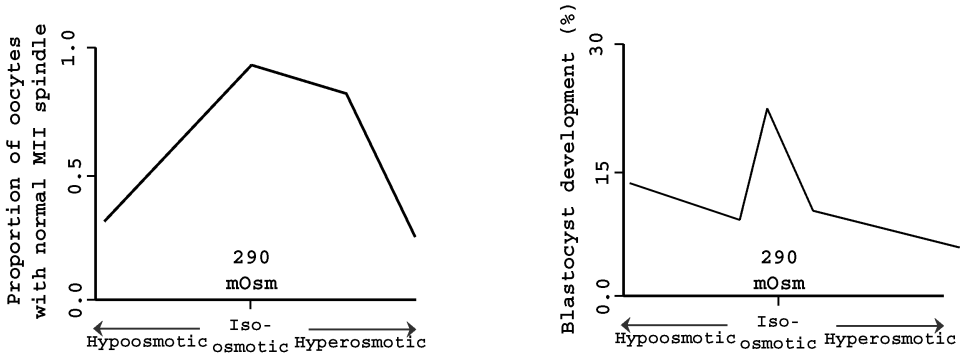

Figure 21.4 Normal spindle configuration and *in vitro* blastocyst development of porcine MII oocytes after exposure to hypo- and hyperosmotic conditions. Reproduced from Mullen *et al.* (2007) with permission from SAGE Publications.

and sphingomyelin), glycolipids, cholesterol, and proteins. It is characterized by the membrane asymmetry between inner and outer leaflets, and the lateral mobility within matrix (Nicolson, 2014; Singer and Nicolson, 1972). Lipid bilayer is mainly responsible for anchoring and orientation of different peripheral (extrinsic) and integral (intrinsic) proteins to perform cell functions. The majority of phospholipids form a bilayer in aqueous conditions. However, some phospholipids (e.g., phosphatidylethanolamine) and glycolipids (monogalactosyldiglyceride) prefer a nonbilayer formation, characterized by hexagonal II morphology while remaining within bilayer configuration. During initial cooling from room temperature to 0°C, phospholipids of plasma membrane undergo thermotropic transition from liquid crystalline (L_α) to solid-like gel (L_β) phase. In liquid crystalline phase at physiological temperature, the phospholipids are in disorder state and express lateral mobility and rotation. At lower temperatures, the rotation of hydrocarbon chains in phospholipids is reduced and the disorder state is lost. The hydrocarbon chains express parallel array due to their packing, which leads to relatively rigid (gel phase) membrane structure and limited lateral mobility (Parks, 1997). Quinn's model explains a possible mechanism of plasma membrane damage during cooling process (Quinn, 1985). According to this model, upon cooling, the high-melting-point nonbilayer preferring phospholipids turn into a gel phase and protein–lipid orientation changes. Upon further cooling, these nonbilayer preferring phospholipids experience lateral phase separation within bilayer, and form separate gel phase domains. After warming, these domains still express membrane asymmetry and disorientation of proteins (Figure 21.5). Thermotropic phase transition of plasma membrane from liquid to gel phase clusters the integral proteins, reduces enzymes' activities, and increases the cations and water permeabilities (Hazel, 1995). Both GV and MII stage oocytes are sensitive to direct chilling injury (DCI) during initial cooling. The lipid-phase transition of plasma membrane occurs at higher temperature in GV than MII stage oocytes (Arav *et al.*, 1996; Ghetler *et al.*, 2005). It indicates the higher sensitivity of GV oocytes to chilling than MII oocytes, which demands the stage-specific protocols for oocyte slow freezing. An inverse relationship exists between the length of exposure of oocytes at lower temperature and their survival. Cooling of bovine GV and MII oocytes to 10°C for only 30 s reduced their cleavage and blastocyst rates by >40% (Martino *et al.*, 1996a). Similarly, cooling of bovine GV oocytes to 4°C for as little as 10 min reduced the number of MII oocytes with normal spindle formation upon *in vitro* maturation, and cleavage rate following *in vitro* fertilization (Wu *et al.*, 1999).

Downloaded From Vet-eBooks.com

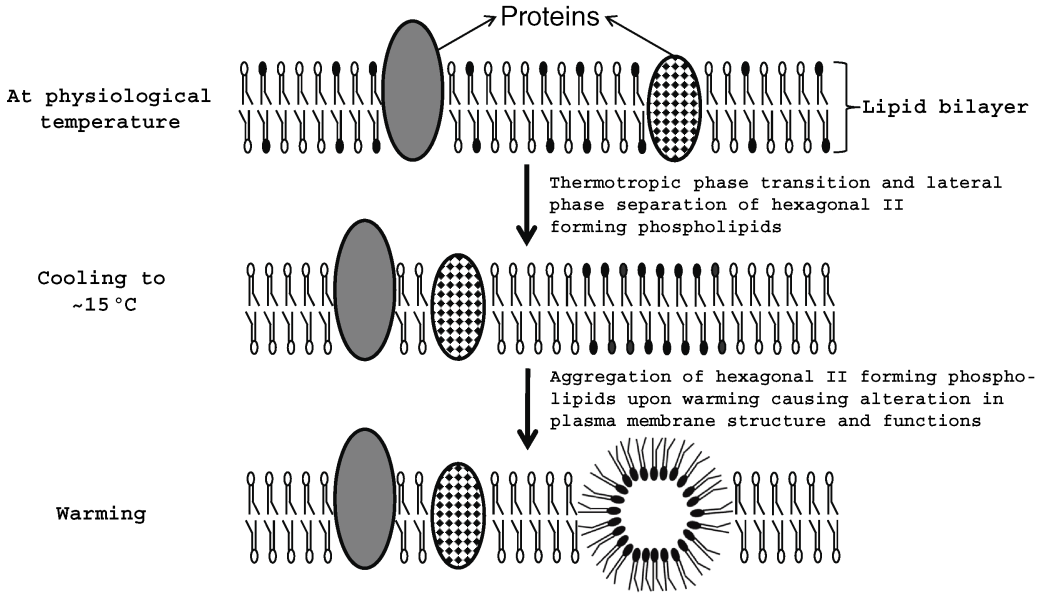

Figure 21.5 Phase separation in biological membranes during initial cooling from the normal temperature to a temperature below the gel to liquid-crystalline phase-transition temperature (~15 °C) and then rewarming to the normal temperature. Clear- and solid-head phospholipids represent bilayer forming and hexagonal II forming phospholipids, respectively. Modified from Parks (1997) and Quinn (1985).

Solution Effect and Intracellular Ice Formation

Solution effect and intracellular ice formation are interlinked biophysical changes that cells face below 0 °C (Figure 21.6). The extracellular ice formation starts between −5 and −15 °C while intracellular contents are still unfrozen. As the extracellular osmolality increases due to ice formation, the intracellular water diffuses out causing cell dehydration. The extracellular ice formation and subsequent cell dehydration depend upon cooling rate (Mazur, 1977). If cooling rate is lower than optimum, the extracellular ice crystals (large but innocuous) continue to form and cells keep dehydrating to maintain the equilibrium between extra- and intracellular compartments. The phenomenon of cell dehydration and subsequent high intracellular osmolality is collectively called "solution effect." If the cooling rate is faster than optimum, cells do not have enough time to lose water, eventually leading to intracellular ice formation upon freezing. The intracellular ice crystals are detrimental to cell organelles depending upon their size and number. Both, the intracellular ice formation and solution effect are lethal consequences in cells or tissue cryopreservation. An optimum cooling rate should be slow enough to prevent the intracellular ice formation and fast enough to minimize the solution effect (Mazur, 1970, 1984). Keeping in view the complex structure of mammalian oocyte, the slow cooling rate (0.5–1 °C/min) ensured less intracellular ice formation and reasonable survival rate (Figure 21.7). At cooling rate >1 °C/min, the number of mouse oocytes possessing intracellular ice increased and the survival rate decreased proportionately (Leibo *et al.*, 1978). During cryopreservation, cells undergo different stresses, for example, low temperature (chilling), increased extracellular solute concentration, increased ion concentration, dehydration, high viscosity and pH change leading to membrane lipid phase changes, osmotic shrinkage, membrane protein solubilization, lipid bilayer destabilization, limited osmosis, and protein denaturation, respectively.

Downloaded From Vet-eBooks.com

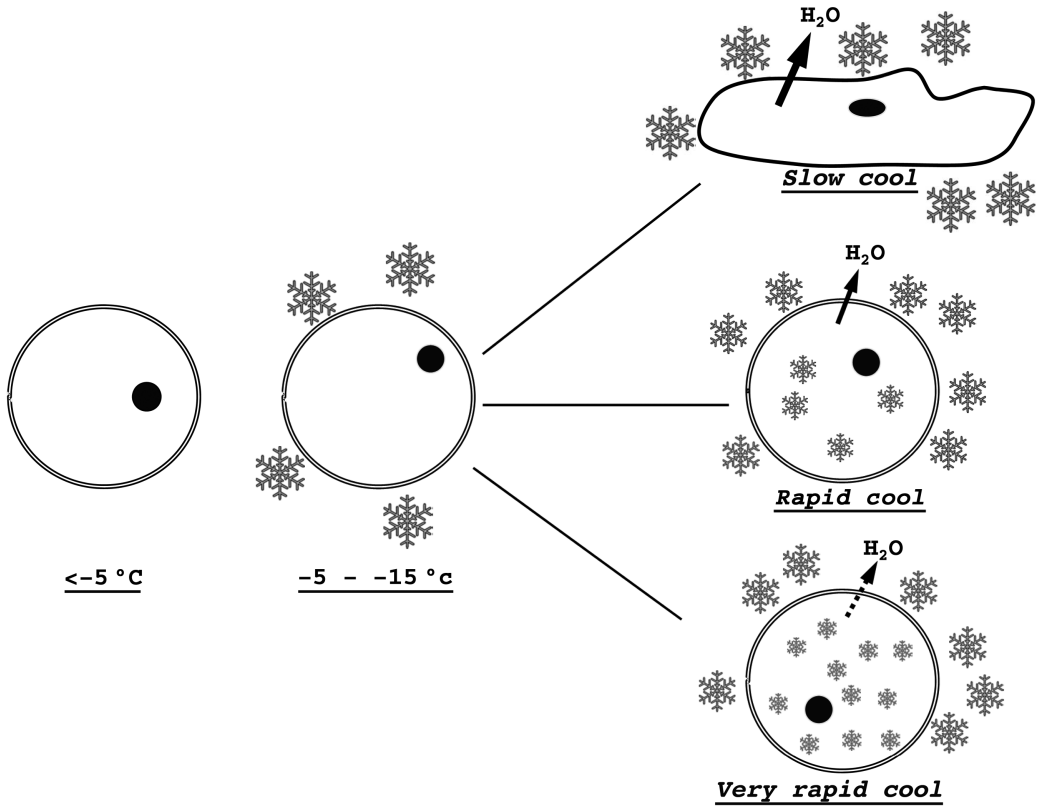

Figure 21.6 Physical events in cells at different cooling (freezing) rates. Modified from Mazur (1977).

21.2.3.2 Vitrification

Vitrification is derived from a Latin word "vitreous" meaning "glass," which prevents the ice formation. Vitrification of oocytes has been reported in mouse (Nakagata, 1989), bovine (Hamano *et al.*, 1992), buffalo (Dhali *et al.*, 2000), rabbit (Hochi *et al.*, 2004), human

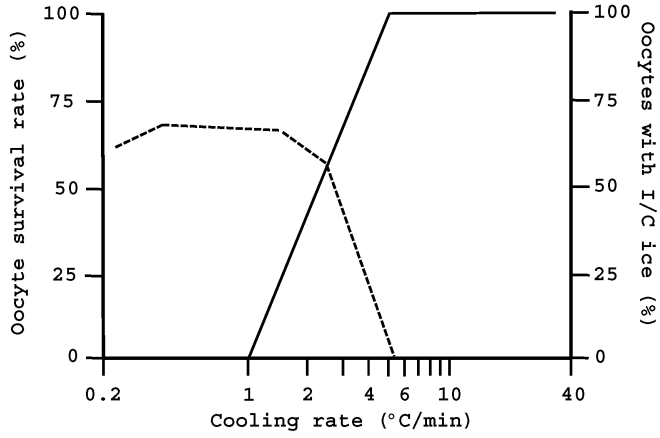

Figure 21.7 Intracellular (I/C) ice formation (solid line) and survival of unfertilized mouse oocytes (dotted line) as a function of cooling rate. Modified from Leibo *et al.* (1978).

Downloaded From Vet-eBooks.com

(Kuwayama, 2007), and other livestock species. In spite of the encouraging results following vitrification of bovine oocytes (Papis *et al.*, 2000; Vajta *et al.*, 1998; Vieira *et al.*, 2002), numerous studies reported low blastocyst rate (Table 21.2). The inconsistent results demand the optimization of vitrification method for mammalian oocytes. The blastocysts produced from the vitrified oocytes are healthy and competent to develop into full-term calves after transfer in recipient cows (Vieira *et al.*, 2002). In general, human and bovine oocytes have better cryosurvival than equine and porcine oocytes (Hurtt *et al.*, 2000; Rojas *et al.*, 2004).

Vitrification, compared with slow freezing, is a simple, quick and cheaper option. It does not require an expensive programmable cell freezer and can be performed in an insulated container. Vitrification is a better choice for cryopreservation of oocytes in wildlife and livestock species residing in zoos and remote areas (Saragusty and Arav, 2011), and in human being as well (Cao *et al.*, 2009; Ciotti *et al.*, 2009).

Vitrification avoids the chilling injury (between 15 and 0 °C) to mammalian oocytes associated with slow freezing method. It causes lesser morphological and DNA damages to oocytes than slow freezing (Men *et al.*, 2002). In vitrification, cells are exposed to high concentration of permeating cryoprotectants (~6 M), loaded on to open or closed device, and directly plunged into liquid nitrogen (−196 °C) with ultrarapid velocity resulting in glass-like solidification of the extra- and intracellular compartments of cells (Fahy *et al.*, 1984). The permeating cryoprotectants enter the cells, bind with water, increase the intracellular viscosity, and depress the freezing point below glass transition temperature (T_g, −120 °C). Ideally, vitrification should solidify the viscous extra- and intracellular contents to a glass phase avoiding ice formation in both compartments (Fahy *et al.*, 1984; Rall, 1987; Rall and Fahy, 1985). The success of vitrification is directly proportional to viscosity, cooling rate, and warming rate and inversely proportional to sample volume (Fahy *et al.*, 1984; Saragusty and Arav, 2011; Seki and Mazur, 2012). Recently, the importance of warming rate in vitrification has emerged. Regardless of the concentration of permeating cryoprotectants and cooling velocity, there are chances of small intracellular ice formation (recrystallization) in mouse oocytes if the warming rate is slow (Seki and Mazur, 2008, 2009). More than 80% mouse oocytes can survive vitrification if warming rate is $>10^7$ °C/min with laser pulse, in spite of using low cooling velocity (10,000 °C/min) and one-third standard concentration of permeating cryoprotectants (Jin *et al.*, 2014; Seki and Mazur, 2012).

The intracellular ice can be formed from the residual free water high during oocyte vitrification procedure (Mazur *et al.*, 2005; Papis *et al.*, 2000; Saragusty and Arav, 2011). Instead of glass formation, the ice crystal formation was detected in the vitrified bovine cumulus–oocyte complexes with synchrotron X-ray diffraction method (Figure 21.8) (Anzar *et al.*, 2014). The compact cumulus cells surrounding the oocytes and tight gap junctions between cells might retard the permeating cryoprotectants to reach zona pellucida and plasma membrane of oocytes. Earlier, the lack of significant cytotoxic effect of cryoprotectants on bovine GV stage oocytes indicated the insufficient penetration of permeating cryoprotectants in oocytes to manifest their toxic effects and to increase the intracellular viscosity required for typical vitrification (Prentice-Biensch *et al.*, 2012a).

During vitrification, the oocytes face cytotoxicity associated with high concentration of permeating cryoprotectants and also undergo osmotic shock due to the osmotic gradient between extra- and intracellular solutions (Massip, 2003). Both osmotic shock and cytotoxicity associated with permeating cryoprotectants are critical for oocytes' cryosurvival. The damage due to intracellular ice formation cannot be completely prevented, but can be minimized depending upon the degree of cellular dehydration and penetration of cryoprotectants while avoiding toxic and osmotic injuries (Mazur, 1990).

Downloaded From Vet-eBooks.com

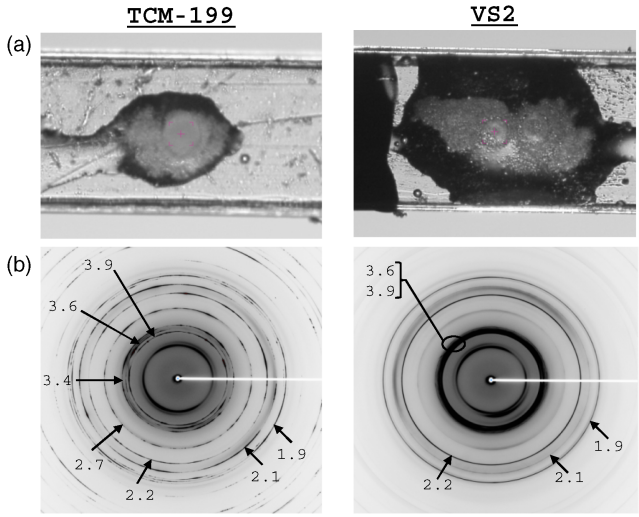

Figure 21.8 Synchrotron X-ray diffraction (SXRD) analysis of bovine GV oocytes (cumulus enclosed) in TCM-199 and vitrification solution 2 (VS2), on modified cryotop, at 102K: (a) Physical appearance of cumulus-oocyte complexes through sample camera. (b) Representative 2D SXRD with display of d-spacing (Debye's rings, Å). All Debye's rings correspond to hexagonal ice crystals, except one ring at 2.1 Å which corresponds to $NaH_2PO_4 \cdot H_2O$ (Anzar *et al.*, 2014).

Cryoprotectants' Cytotoxicity

In vitrification solution, high concentration of permeating cryoprotectants is a major concern for cryobiologists. The intensity of cytotoxicity is dependent upon the chemical nature and concentration of permeating cryoprotectants, temperature of their addition, and exposure time (Lawson *et al.*, 2011). Different strategies have been attempted to reduce the cytotoxic effects of permeating cryoprotectants without reducing their cryoprotection ability. In mouse oocytes, dimethyl sulfoxide, a common permeating cryoprotectant, caused zona pellucida hardening and asymmetric cell division, and disruption of cytokinesis by inhibiting cortical reorganization and polarization (Vincent *et al.*, 1990; Zhou *et al.*, 2014). Two or more cryoprotectants in a vitrification solution have synergistic interactions and reduce the cytotoxic effects of individual cryoprotectant in a vitrification solution (Fahy *et al.*, 2004; Vajta and Nagy, 2006; Wusteman *et al.*, 2004). Together, ethylene glycol and dimethyl sulfoxide are the most common permeating cryoprotectants used for vitrification of mammalian oocytes (Table 21.2). A mere exposure of bovine oocytes to vitrification solution 1 containing only 7.5% (v/v) ethylene glycol and dimethyl sulfoxide each reduced the blastocyst rate from 34 to 25% (Prentice-Biensch *et al.*, 2012a). The cytotoxicity of permeating cryoprotectants is species and oocyte-stage dependent. The porcine oocytes are more sensitive to permeating cryoprotectants than human and bovine oocytes. The exposure of porcine GV oocytes to ethylene glycol alone affected the spindle morphology, chromosome alignment, and actin filament distribution with no cleavage, whereas MII oocytes exhibited better cryoresistance (Rojas *et al.*, 2004).

The vitrifiability of vitrification solution is important to formulate the least toxic concentration of permeating cryoprotectants but viscous enough to induce glass phase in the oocytes. The vitrifiability of vitrification solutions used for mammalian oocytes and embryo are either based on empirical or theoretical analyses (Leibo, 2008) or direct visual assessment under liquid nitrogen environment (Liebermann *et al.*, 2003; Weiss *et al.*, 2010). Recently, the vitrifiability of a vitrification solution (ethylene glycol and DMSO, 15% v/v each), commonly used for

Downloaded From Vet-eBooks.com

vitrification of bovine embryos and oocytes, was confirmed with synchrotron X-ray diffraction method. The vitrification solution induced glass phase in bovine embryos but not in oocytes. It was mainly due to lack of sufficient penetration of permeating cryoprotectant in oocytes compared to embryos. It also indicated that the vitrifiability of a solution is not a dependable criterion to ensure the success of vitrification as it varies from cell to cell (Anzar *et al.*, 2014).

Osmotic Shock

During vitrification, a brief exposure of cells to high concentration of permeating cryoprotectants brings extreme volumetric change known as "osmotic shock," which is critical for cell survival and viability. Bovine GV oocytes are more susceptible to osmotic stress compared to MII stage (Agca *et al.*, 2000). During warming process, there is a danger of cell volume excursion due to the efflux of permeating cryoprotectants from intracellular compartment and cells undergo excessive swelling. The cell volume excursion directly affects the plasma membrane integrity and cytoskeleton of oocytes. The osmotic shock during warming can be controlled by adding nonpermeating cryoprotectant (mainly saccharide) in the warming solution to reduce the osmotic gradient between the intracellular and extracellular solutions.

The high concentration (0.5–1 M) of saccharide in vitrification solution reduces the intracellular ice formation, osmotic shock, and cytotoxicity of permeating cryoprotectants in cryopreserved mammalian oocytes and embryos (Han and Critser, 2009; Leibo, 1984; McWilliams *et al.*, 1995). An ideal vitrification solution should have a proper saccharide concentration to cause cell dehydration and to minimize the concentration of permeating cryoprotectants, while not exceeding the hyperosmotic tolerance limits of oocytes (Han and Critser, 2009). In this way, saccharide alleviates the risk of cytotoxicity associated with permeating cryoprotectants in vitrification solution (Newton *et al.*, 1999; Shaw and Jones, 2003). Sucrose, trehalose, and lactose are the common nonpermeating cryoprotectants used for vitrification of mammalian oocytes and embryos (Mazni *et al.*, 1990; Saha *et al.*, 1996; Saito *et al.*, 1994; Toth *et al.*, 1994). Among these, sucrose is the most popular disaccharide for vitrification and warming of oocytes and embryos (Kuleshova *et al.*, 1999). Vitrification of porcine GV oocytes using sucrose-containing vitrification solution yielded higher maturation rates than simple glucose (Huang *et al.*, 2008). Trehalose and lactose have also been used for vitrification of mouse (Nakagata, 1989), bovine (Hamano *et al.*, 1992), buffalo (Dhali *et al.*, 2000), and human oocytes (Kuwayama, 2007; Wright *et al.*, 2004).

Factors Affecting Oocyte Vitrification

Oocyte Stage The GV and MII oocytes vary in their structural differences, membrane permeability, presence or absence of meiotic spindle and chilling sensitivity. The nuclear maturation stage of oocytes influences their postwarming viability and developmental competence. Bovine oocyte oolemma permeability characteristics, that is, hydraulic conductivity (*Lp*) and cryoprotectant permeability, are different between GV and MII oocytes (Agca *et al.*, 1998; Ruffing *et al.*, 1993; Wang *et al.*, 2010). The GV stage oocytes are more suitable for cryopreservation as they do not have the meiotic spindle that is sensitive to low temperature. The MII oocytes are characterized by the expanded cumulus cells and microtubules that form spindle apparatus, which is sensitive to chilling (Massip, 2003). Any cryodamage to spindle apparatus in MII oocytes potentially results in chromosomal dispersion, incomplete fertilization, and developmental failure (Chen *et al.*, 2003; Massip, 2003). Following vitrification, the blastocyst rate was better in bovine GV than MII oocytes (Magnusson *et al.*, 2008; Zhou *et al.*, 2010). Regardless of the GV or MII oocytes, the overall survival rate and developmental competence following cryopreservation are low (Table 21.2).

Downloaded From Vet-eBooks.com

Cumulus Cells The success of GV oocyte cryopreservation largely depends upon the ability to preserve the structural and functional integrity of entire COCs, including the cumulus cells. The communications between oocytes and cumulus cells is important for providing nutritive substances during maturation process (Massip, 2003). Mammalian oocytes with stripped cumulus cells exhibit deficient nuclear and cytoplasmic maturation (Bogliolo *et al.*, 2007; Combelles *et al.*, 2002; Hochi *et al.*, 1996). However, the role of cumulus cells during oocyte cryopreservation is controversial. Cumulus cells are considered essential for the postwarming viability of the vitrified GV oocytes (Zhou *et al.*, 2010). On the other hand, it is assumed the cumulus cells and extracellular matrix interfere the permeating cryoprotectants to penetrate the mammalian oocytes resulting in insufficient intracellular viscosity required for glass formation (Anzar *et al.*, 2014; Checura and Seidel, 2007; Minasi *et al.*, 2012). The presence of cumulus cells surrounding oocytes hinders or at least slows down the penetration of permeating cryoprotectants and heat transfer during cryopreservation process. Therefore, different exposure times of permeating cryoprotectants are required for vitrification of cumulus-enclosed and cumulus-free human and porcine MII oocytes (Fujihira *et al.*, 2005; Minasi *et al.*, 2012). Vitrification causes death of the peripheral cumulus cells, whereas the cumulus cells adjacent to oocytes are still viable and maintain the gap junctions communication with oocytes (Tharasanit *et al.*, 2009). Vitrification of ovine GV oocytes with cumulus cells reduced the maturation-promoting factor (MPF) and mitogen-activated protein kinase (MAPK) activities (Bogliolo *et al.*, 2007). The cumulus-enclosed mouse MII oocytes yielded better blastocyst rate than cumulus-free oocytes (Park *et al.*, 2001). However, the cumulus cells in ovine MII oocytes did not improve the blastocyst formation rate following solid-surface vitrification (Zhang *et al.*, 2009). Attempts have been made to improve the postwarm viability of vitrified mammalian oocytes by completely or partially removing the cumulus cells from oocytes. The vitrification of bovine MII oocytes without cumulus cells showed higher survival rate and better embryo development than cumulus-enclosed oocytes (Chian *et al.*, 2004).

The vitrified mammalian oocytes do not express marked morphological changes upon warming. However, the changes at molecular level are reflected during subsequent *in vitro* maturation or early embryonic development. Mammalian oocytes, during culture, display apoptosis-associated changes, for example, cytoplasmic condensation and fragmentation, formation of apoptotic bodies, DNA fragmentation, and activation of caspases (Men *et al.*, 2003), and poor embryonic development (Bogliolo *et al.*, 2007; Chian *et al.*, 2004). Therefore, suitable *in vitro* maturation culture systems are important for development of the postwarm vitrified oocytes.

Vitrification Device and Cooling Velocity Cells or tissues loading device and cooling velocity are interlinked factors in vitrification method of cryopreservation. Initially, a conventional 0.25 ml straw was used to vitrify mouse embryos, which provided the cooling rate 2500 °C/min and the warming rate 1300 °C/min (Rall and Fahy, 1985). The vitrification devices available on the market are categorized as closed system or open system depending upon the contact between biological sample and liquid nitrogen. The closed system devices, for example, cryotip (Kuwayama *et al.*, 2005a, 2005b), sealed pulled straw (Yavin *et al.*, 2009), and hemi-straw (Vanderzwalmen *et al.*, 2003), provide sterile vitrification but the cooling and warming rates are low, due to physical barrier between sample and liquid nitrogen. In contrast, the open system devices, for example, electron microscope grid (Hong *et al.*, 1999; Martino *et al.*, 1996b; Steponkus *et al.*, 1990), thin glass surface (Dinnyes *et al.*, 2000), microdrop (Papis *et al.*, 2000), open pulled straw (Vajta *et al.*, 1998), cryoloop (Lane *et al.*, 1999), and cryotop (Hamawaki *et al.*, 1999; Kuwayama, 2007), provide ultrafast cooling and warming velocities but the oocytes and embryos are exposed to possible pathogens present in liquid nitrogen. Moreover, in open

Downloaded From Vet-eBooks.com

system, the volume of vitrification solution surrounding an oocyte or embryo can be reduced to ≤1 µl for ultrafast cooling and warming velocities (Arav *et al.*, 2002; Yavin and Arav, 2007). Cryotop and open pulled straw are two common devices for vitrification of oocytes and embryos. However, cryotop, an open system with a minimum sample volume, is a convenient vitrification device for mammalian oocytes (Hamawaki *et al.*, 1999; Liu *et al.*, 2008; Morato *et al.*, 2008b; Vajta and Kuwayama, 2006). It can yield ultrafast cooling rate (23,000 °C/min) and warming rate (42,000 °C/min), as demonstrated in human embryos (Kuwayama *et al.*, 2005a, 2005b).

Sterility Liquid nitrogen can be a good source of pathogens. The majority of tested microorganisms, including bacteria and viruses, can survive liquid nitrogen temperature (−196 °C), and some microorganisms can tolerate high concentrations (up to 45%) of cryoprotectants (Bielanski and Vajta, 2009). Open vitrification system brings the biosecurity risks of bacteria or viruses from LN_2 to the vitrified oocytes and embryos (Bielanski *et al.*, 2003; Bielanski and Vajta, 2009; Givens *et al.*, 2001). The viruses, such as BHV-1 and BVDV, have been found in follicular fluid, COCs, and in the fertilized embryos (Bielanski and Vajta, 2009; Stringfellow and Givens, 2000). The biosecurity concerns associated with open system is a matter of great concern in the vitrified embryos as as pathogens can transfer from LN_2 to recipient animals after warming. However, the postwarm vitrified oocytes undergo several washings during *in vitro* maturation, fertilization, and cumulus cells removal before embryo culture. Hence, there are less likelihood of carrying over microbial pathogens from oocytes to blastocyst stage and onward.

To avoid the possible microbial cross-contamination from LN_2, the closed system devices have been developed. However, the pregnancy rate from vitrified human oocytes was better in open system (cryotop) than closed system (cryotip) (Paffoni *et al.*, 2011). The open system is preferred in the majority of laboratories to achieve the required cooling and warming velocities for very sensitive samples such as oocytes (Bielanski and Vajta, 2009). A combination of closed system and supercooled slush nitrogen (SN_2; −210 °C) may be a good combination for sterile vitrification of mammalian oocytes.

Efforts to Improve Oocyte Vitrification

Additives Cryopreservation alters the distribution of cortical granules, and promotes premature cortical reaction and zona hardening, which hinder sperm entry and oocyte fertilization (Bianchi *et al.*, 2014; Morato *et al.*, 2008a; Rojas *et al.*, 2004; Succu *et al.*, 2007b). The strategies to overcome these problems involve the use of small container volume, increased thermal gradient, alterations in the surface-to-volume ratio, and the addition of chemicals to increase oocyte cryotolerance (Pereira and Marques, 2008). The addition of antifreeze proteins, sugars, cholesterol-loaded cyclodextrins, and antioxidants have been attempted to improve the cryosurvival of mammalian oocytes without any tangible success (Ledda *et al.*, 2001). Too little (0.3%) and too much (6%) bovine serum albumin, and 0.3% polyvinyl pyrrolidone for vitrification of mature bovine oocytes showed adverse effect on blastocyst formation (Checura and Seidel, 2007).

The majority of mammalian MII oocytes express broken microtubules. Taxol, a cytoskeleton stabilizer, tightens the bond between α and β tubulin dimers and binds microtubule-associated proteins with microtubule surface (Albertini *et al.*, 1984). Prior to vitrification, the treatment of bovine MII oocytes with taxol improved the spindle morphology, distribution of cortical granules, and cleavage and blastocyst rates (Morato *et al.*, 2008a, 2008c). Taxol in cryoprotectant solution improved the blastocyst rate by 34% in the vitrified cumulus-enclosed mouse MII oocytes (Park *et al.*, 2001), but it did not demonstrate the beneficial effect in the

Downloaded From Vet-eBooks.com

vitrified cumulus-enclosed porcine MII oocytes (Fujihira *et al.*, 2005). Likewise, cytochalasin B (an actin polymerization inhibitor) stabilized the microtubules in vitrified bovine oocytes (Rho *et al.*, 2002), and improved the postwarming maturation rate in porcine GV oocytes (Isachenko *et al.*, 1998) and blastocyst rate in ovine MII oocytes (Zhang *et al.*, 2009). During cryopreservation, like other cells, the plasma membrane of oocyte is the main target site of chilling injury (Zeron *et al.*, 1999). Lipid composition of plasma membrane plays a key role in cell's sensitivity to chilling. Plasma membranes possessing higher cholesterol content are more fluid at lower temperatures, making cells less sensitive to chilling. The loading of bovine COCs with exogenous cholesterol, using methyl-β-cyclodextrin as a carrier, improved the cleavage rate only without any beneficial effect on blastocyst development (Horvath and Seidel, 2006). Cycloheximide is a reversible protein synthesis inhibitor. It inhibited the meiosis resumption in bovine GV oocytes and >80% oocytes reached MII stage after the removal of cycloheximide's inhibitory effect (Lonergan *et al.*, 1997). However, cycloheximide did not improve the quality of vitrified bovine oocytes (Le Gal and Massip, 1999).

Cooling Velocity Slush nitrogen (−210 °C) is prepared by applying a negative pressure to liquid nitrogen (LN_2) using vacuum pump. It solidifies the liquid nitrogen in few minutes. Upon return to atmospheric pressure, the nitrogen collapses and the supercooled nitrogen becomes "slush." Slush nitrogen also reduces the vapors above LN_2. Low temperature and lack of nitrogen vapors above SN_2 help in achieving ultrafast cooling rate (250,000 °C/min), called "ultravitrification" for mammalian oocytes (Minasi *et al.*, 2012; Risco *et al.*, 2007). The SN_2 reduces the cytotoxicity of permeating cryoprotectants by reducing their concentrations required in routine vitrification procedure. Mouse and human oocytes vitrified in SN_2 demonstrated better cryosurvival, and cleavage and blastocyst rates than in LN_2 (Cha *et al.*, 2011; Criado *et al.*, 2011). However, vitrification of bovine MII oocytes in slush nitrogen did not improve the cleavage and blastocyst rates (Martino *et al.*, 1996b).

Helium (He) exists on earth in fixed amount. To achieve the ultrafast cooling velocity, the liquid helium (−269 °C) has been used for vitrification of bovine GV oocytes that yielded only 10% blastocyst rate compared to 5% in liquid nitrogen (Chen *et al.*, 2014). Moreover, the use of liquid helium for vitrification of oocytes and embryos at commercial level is not feasible, due to its high cost.

Reducing Cryoprotectants' Cytotoxicity As already mentioned, the permeating cryoprotectants are known for their cytotoxicity, one of the limiting factors for the successful vitrification. The suppression of cytotoxicity of cryoprotectants is a goal of cryobiologists working on vitrification of germplasm and tissues. To minimize the cytotoxicity of permeating cryoprotectants used in vitrification solution, the stepwise exposure of cryoprotectants to mammalian oocytes improved the cleavage rate of bovine GV stage oocytes from 21% (single step) to 38%; however, the blastocyst formation rate still remained low, that is, 8% (Abe *et al.*, 2005). Cryoprotectant toxicity neutralization (CTN) approach is based on the development of minimum toxic solutions by adding more permeating cryoprotectants. The vitrification of cumulus-free mouse oocytes in a solution containing permeating cryoprotectants, that is, ethylene glycol, dimethyl sulfoxide, and formamide along with nonpermeating cryoprotectant (polyvinylpyrrolidone), improved the blastocyst rate to 80% of the absolute control rate (Fahy *et al.*, 2004). The toxic effect of formamide is blocked by dimethyl sulfoxide, whereas the neutralization of toxicities of glycerol, propylene glycol, ethylene glycol, and dimethyl sulfoxide is still to be discovered (Fahy, 2010).

Stress-Induced Cryotolerance A controlled sublethal stress is relatively a new approach to improve cells' cryotolerance. It does not focus on the improvement of procedure or *in vitro*

Downloaded From Vet-eBooks.com

conditions. Rather, cells' performance is improved after exposure to osmotic or mechanical stresses. So far, osmotic and mechanical stresses have been attempted to improve the cryotolerance of mammalian oocytes. Hyperosmotic stress to porcine GV oocytes (~600 mOsm) before vitrification improved their chromosomal configuration and cleavage rate, but blastocyst formation rate remained <10% (Lin *et al.*, 2009). Prior to vitrification, a pretreatment of oocytes with high hydrostatic pressure (HHP) improved their cryosurvival. Porcine oocytes, known for their sensitivity to cryopreservation, with hydrostatic pressure (20–40 MPa) at 37 °C improved their blastocyst rate up to 14% (Du *et al.*, 2008; Pribenszky *et al.*, 2008). The exact mechanism of hydrostatic pressure on porcine oocytes' cryotolerance is not known yet.

21.2.3.3 Cryoinjuries to Mammalian Oocytes

Like other cells, oocytes also suffer considerable morphological and functional damages during cryopreservation. During cryopreservation, cells undergo first chilling phase during initial cooling from body/room temperature to the freezing point and then freezing phase below freezing point to −196 °C. Mammalian oocytes undergo both chilling and freezing phases in slow freezing and only freezing phase in vitrification method. However, the extent of cryoinjury varies depending upon species, sensitivity of the cell structures to cooling, meiotic stage, lipid content, and origin (*in vitro* and *in vivo*) (Pereira and Marques, 2008; Vajta and Kuwayama, 2006). The mechanism of cryoinjuries in mammalian oocyte is not fully understood.

During initial cooling, the disassembly of meiotic spindles in MII oocytes is the most pronounced change in mouse (Magistrini and Szollosi, 1980; Pickering and Johnson, 1987), human (Pickering *et al.*, 1990), and bovine (Aman and Parks, 1994) MII oocytes. The disassembly of meiotic spindle due to cooling leads to abnormal chromosome alignment and chromatid segregation (Vincent and Johnson, 1992). However, the chilling effect on meiotic spindle is reversible in mouse oocytes (Pickering and Johnson, 1987) and irreversible in human and bovine oocytes (Aman and Parks, 1994; Pickering *et al.*, 1990).

Many ultrastructural characteristics, critical for oocyte's homeostasis, are damaged during vitrification (Tharasanit *et al.*, 2009). Vitrification damages zona pellucida, cytoplasmic membrane, intracellular organelles, cytoskeleton, chromosomes, and cell-to-cell communications (Fuku *et al.*, 1995; Vajta, 2000). Vitrification of human GV oocyte influences DNA replication, transcription, and cell function; however, the cytoplasmic and nuclear perturbations return to normal state following warming (Van Blerkom, 1989). Immediately after warming of the vitrified bovine GV oocytes, a large number of cumulus cells showed necrosis, swollen mitochondria, abnormal endoplasmic reticulum, and cell lysis, and cortical granules expressed irregular distribution, clustering, and misalignment along the oolemma (Diez *et al.*, 2005).

During maturation, the redistribution of organelles (mitochondria, cytoskeleton, and cortical granules) in cytoplasm, and reorganization of nuclear material affect the outcome of a cryopreservation technique (Critser *et al.*, 1997). As oocytes develop to MII stage, changes in plasma membrane affect the permeability of water and cryoprotectants. Exposing MII oocytes to cryoprotectants and low temperatures damages the meiotic spindle, actin filaments, and chromosomal dispersal and microtubule depolymerization (Massip, 2003; Ogawa *et al.*, 2010). Ultrastructural examination of the vitrified bovine MII oocytes showed clusters of cortical granules with some degree of degeneration and vacuoles containing the contents from presumptive degenerated cortical granules. After *in vitro* fertilization, the vitrified oocytes exhibited either lack of cleavage or degeneration of blastomeres (Hyttel *et al.*, 2000). After fertilization, the vitrified bovine MII oocytes have multiple aster formation, which results in delayed cleavage and abnormal embryo development (Hara *et al.*, 2012).

Downloaded From Vet-eBooks.com

Surprisingly, the mammalian oocytes have the ability to fully or partially repair the cryodamage (Massip, 2003; Vajta and Kuwayama, 2006). Vitrification of bovine MII oocyte markedly reduced the mitochondrial function and endogenous antioxidant system of bovine MII oocytes. However, an additional postwarm incubation (8 h) partially restored their mitochondrial function and antioxidant system but remained lower than nonvitrified (control) oocytes (Zhao *et al.*, 2011). After IVM of the vitrified-warmed bovine GV oocytes, the nuclei and organelles looked morphologically normal (Diez *et al.*, 2005).

21.2.3.4 Oocyte's Quality Assessment Following Cryopreservation

Regardless of the source of oocytes, that is, *in vivo* pickup or *in vitro* aspirated from ovaries, the common criteria for selection of good quality GV oocyte include normal shape and size, uniform cytoplasm, and at least three layers of compacted cumulus cells (Massip, 2003). The gene expression of cumulus cells could be used as a marker for oocyte quality before freezing, in selecting the suitable oocytes for cryopreservation (Kumamoto *et al.*, 2005).

Postwarm evaluation of oocyte quality helps in developing efficient cryopreservation protocol. There are several different methods to test the oocytes' viability and the extent of cryoinjuries following cryopreservation. Routinely, the postwarm oocytes are examined under stereomicroscope for cytoplasmic degeneration or abnormalities (vacuolization), and/or fractures of zona pellucida (Ledda *et al.*, 2007). Meiotic spindle in human MII oocytes can be visualized using a polarized light microscope or Polscope (Keefe *et al.*, 2003; Wang and Keefe, 2002). However, this technique is difficult in oocytes from domestic animals due to high cytoplasmic lipid content, which hinders their spindle examination. Therefore, the oocytes of domestic animals are typically examined through biochemical or molecular markers. Aceto-orcein is a common method to study the nuclear maturation kinetics in mammalian oocytes. But this technique is laborious and a significant number of oocytes are lost during the staining process. In contrast, lamin/DAPI staining of oocytes is a method with higher throughput, minimum loss, and clarity to differentiate various stages of oocytes (Prentice-Biensch *et al.*, 2012b). But this technique is expensive and laborious. The volumetric response of oocytes to high concentrations of permeating cryoprotectants helps in developing a suitable timing and concentration of cryoprotectants exposure (Ledda *et al.*, 2007).

In the majority of animal ART laboratories, the cleavage and blastocyst formation rates, following *in vitro* fertilization, are the most common methods to assess the developmental competence of cryopreserved oocytes. However, the ultimate criteria should be the production of viable offspring from cryopreserved oocytes.

In conclusion, oocyte cryopreservation is useful for fertility preservation in human, and conservation and exploitation of female genetics in livestock species. It is more challenging in farm animals than human. For successful oocyte cryopreservation using slow freezing, the main approach should be to minimize the lethal intracellular ice formation during cooling and warming, the solution effect due to cell dehydration, as well as the toxicity of permeating cryoprotectants. An ideal vitrification procedure should minimize the osmotic shock, cytotoxicity of permeating cryoprotectants, and intracellular ice formation. Unlike embryos, the mammalian oocytes do not undergo true vitrification. There is a dire need of oocyte-specific cryopreservation protocol for successful animal genetic conservation and human fertility preservation.

Acknowledgments

The help from Dr. Jaswant Singh, Dr. Kosala Rajapaksha, LaRhonda Sobchishin, Sarah Caldwell, and Núria Arcarons in the preparation of this chapter is highly appreciated.

Downloaded From Vet-eBooks.com

Abbreviations

BR: blastocyst rate; CC cumulus cells; CLV: cryoloop vitrification; CLC: cholesterol-loaded cyclodextrin; CM: cryopreservation method; CP: cryoprotectant; CR: cleavage rate; Cyt: cytochalasin; DMSO: dimethyl sulfoxide; Dt: docetaxel; EG: ethylene glycol; EMG: electron microscope grid; FDP: flexipet denuding pipette; FR: fertilization rate; GV: germinal vesicle stage; HHP: high hydrostatic pressure; ICSI: intracytoplasmic sperm injection; IR: implantation rate; IVF: *in vitro* fertilization; LB: live births; MC: microcapillary; mHTF: modified human tubal fluid; MII: metaphase II stage; MM: macromolecule; MR: maturation rate; NSR: normal spindle rate; OPS: open pulled straw; PA: parthenogenetic activation; PE: polyethylene glycol; PR: pregnancy rate; PROH: 1,2-propanediol; PVA: polyvinyl alcohol; PVP: polyvinyl pyrrolidone; RR: ruthenium red (mitochondrial Ca^{2+} uniporter inhibitor); Suc: sucrose; SF: slow freezing; SSV: solid surface vitrification; Tre: trehalose; Vit: vitrification

References

Abe, Y., Hara, K., Matsumoto, H., Kobayashi, J., Sasada, H., Ekwall, H., Rodriguez-Martinez, H., and Sato, E. (2005) Feasibility of a nylon-mesh holder for vitrification of bovine germinal vesicle oocytes in subsequent production of viable blastocysts. *Biol. Reprod.*, **72** (6), 1416–1420.

Abdelhafez, F.F., Desai, N., Abou-Setta, A.M., Falcone, T., and Goldfarb, J. (2010) Slow freezing, vitrification and ultra-rapid freezing of human embryos: a systematic review and meta-analysis. *Reprod. Biomed. Online*, **20** (2), 209–222.

Agca, Y., Liu, J., Peter, A.T., Critser, E.S., and Critser, J.K. (1998) Effect of developmental stage on bovine oocyte plasma membrane water and cryoprotectant permeability characteristics. *Mol. Reprod. Dev.*, **49** (4), 408–415.

Agca, Y., Liu, J., Rutledge, J.J., Critser, E.S., and Critser, J.K. (2000) Effect of osmotic stress on the developmental competence of germinal vesicle and metaphase II stage bovine cumulus oocyte complexes and its relevance to cryopreservation. *Mol. Reprod. Dev.*, **55** (2), 212–219.

Albertini, D.F., Herman, B., and Sherline, P. (1984) *In vivo* and *in vitro* studies on the role of HMW-MAPs in taxol™-induced microtubule bundling. *Eur. J. Cell Biol.*, **33** (1), 134–143.

Alfoteisy, B. (2012) Natural honey as a cryoprotectant to improve viability of vitrified bovine oocytes. M.Sc. dissertation, University of Saskatchewan, Saskatoon, Canada.

Aman, R.R. and Parks, J.E. (1994) Effects of cooling and rewarming on the meiotic spindle and chromosomes of *in vitro*-matured bovine oocytes. *Biol. Reprod.*, **50** (1), 103–110.

Anzar, M., Grochulski, P., and Bonnet, B. (2014) Synchrotron X-ray diffraction to detect glass or ice formation in the vitrified bovine cumulus–oocyte complexes and morulae. *PLoS One*, **9** (12), e114801.

Arav, A., Shehu, D., and Mattioli, M. (1993) Osmotic and cytotoxic study of vitrification of immature bovine oocytes. *J. Reprod. Fertil.*, **99** (2), 353–358.

Arav, A., Zeron, Y., Leslie, S.B., Behboodi, E., Anderson, G.B., and Crowe, J.H. (1996) Phase transition temperature and chilling sensitivity of bovine oocytes. *Cryobiology*, **33** (6), 589–599.

Arav, A., Yavin, S., Zeron, Y., Natan, D., Dekel, I., and Gacitua, H. (2002) New trends in gamete's cryopreservation. *Mol. Cell. Endocrinol.*, **187** (1–2), 77–81.

Attanasio, L., De Rosa, A., De Blasi, M., Neglia, G., Zicarelli, L., Campanile, G., and Gasparrini, B. (2010) The influence of cumulus cells during *in vitro* fertilization of buffalo (*Bubalus bubalis*) denuded oocytes that have undergone vitrification. *Theriogenology*, **74** (8), 1504–1508.

Begin, I., Bhatia, B., Baldassarre, H., Dinnyes, A., and Keefer, C.L. (2003) Cryopreservation of goat oocytes and *in vivo* derived 2- to 4-cell embryos using the cryoloop (CLV) and solid-surface vitrification (SSV) methods. *Theriogenology*, **59** (8), 1839–1850.

Downloaded From Vet-eBooks.com

Bianchi, V., Macchiarelli, G., Borini, A., Lappi, M., Cecconi, S., Miglietta, S., Familiari, G., and Nottola, S. (2014) Fine morphological assessment of quality of human mature oocytes after slow freezing or vitrification with a closed device: a comparative analysis. *Reprod. Biol. Endocrinol.*, **12** (1), 110.

Bielanski, A. and Vajta, G. (2009) Risk of contamination of germplasm during cryopreservation and cryobanking in IVF units. *Hum. Reprod.*, **24** (10), 2457–2467.

Bielanski, A., Bergeron, H., Lau, P.C.K., and Devenish, J. (2003) Microbial contamination of embryos and semen during long term banking in liquid nitrogen. *Cryobiology*, **46** (2), 146–152.

Bogliolo, L., Ariu, F., Fois, S., Rosati, I., Zedda, M.T., Leoni, G., Succu, S., Pau, S., and Ledda, S. (2007) Morphological and biochemical analysis of immature ovine oocytes vitrified with or without cumulus cells. *Theriogenology*, **68** (8), 1138–1149.

Boldt, J., Tidswell, N., Sayers, A., Kilani, R., and Cline, D. (2006) Human oocyte cryopreservation: 5-year experience with a sodium-depleted slow freezing method. *Reprod. Biomed. Online*, **13** (1), 96–100.

Bredderman, P.J. and Foote, R.H. (1969) Volume of stressed bull spermatozoa and protoplasmic droplets, and the relationship of cell size to motility and fertility. *J. Anim. Sci.*, **28** (4), 496–501.

Buerkle, T. (2007) FAO sounds alarm on loss of livestock breeds. Food and Agriculture Organization of the United Nations.

Cao, Y.-X., Xing, Q., Li, L., Cong, L., Zhang, Z.-G., Wei, Z.-L., and Zhou, P. (2009) Comparison of survival and embryonic development in human oocytes cryopreserved by slow-freezing and vitrification. *Fertil. Steril.*, **92** (4), 1306–1311.

Cha, S.K., Kim, B.Y., Kim, M.K., Kim, Y.S., Lee, W.S., Yoon, T.K., and Lee, D.R. (2011) Effects of various combinations of cryoprotectants and cooling speed on the survival and further development of mouse oocytes after vitrification. *Clin. Exp. Reprod. Med.*, **38** (1), 24–30.

Chasombat, J., Nagai, T., Parnpai, R., and Vongpralub, T. (2015) Pretreatment of *in vitro* matured bovine oocytes with docetaxel before vitrification: effects on cytoskeleton integrity and developmental ability after warming. *Cryobiology*, **71** (2), 216–223.

Checura, C.M. and Seidel, G.E., Jr. (2007) Effect of macromolecules in solutions for vitrification of mature bovine oocytes. *Theriogenology*, **67** (5), 919–930.

Chen, C. (1986) Pregnancy after human oocyte cryopreservation. *Lancet*, **327** (8486), 884–886.

Chen, S.U., Lien, Y.R., Chao, K.H., Ho, H.N., Yang, Y.S., and Lee, T.Y. (2003) Effects of cryopreservation on meiotic spindles of oocytes and its dynamics after thawing: clinical implications in oocyte freezing—a review article. *Mol. Cell. Endocrinol.*, **202** (1–2), 101–107.

Chen, S.U., Lien, Y.R., Chen, H.F., Chang, L.J., Tsai, Y.Y., and Yang, Y.S. (2005) Observational clinical follow-up of oocyte cryopreservation using a slow-freezing method with 1,2-propanediol plus sucrose followed by ICSI. *Hum. Reprod.*, **20** (7), 1975–1980.

Chen, J.-Y., Li, X.-X., Xu, Y.-K., Wu, H., Zheng, J.-J., and Yu, X.-L. (2014) Developmental competence and gene expression of immature oocytes following liquid helium vitrification in bovine. *Cryobiology*, **69** (3), 428–433.

Chian, R., Kuwayama, M., Tan, L., Tan, J., Kato, O., and Nagai, T. (2004) High survival rate of bovine oocytes matured *in vitro* following vitrification. *J. Reprod. Dev.*, **50** (6), 685–696.

Chian, R.-C., Huang, J.Y.J., Gilbert, L., Son, W.-Y., Holzer, H., Cui, S.J., Buckett, W.M., Tulandi, T., and Tan, S.L. (2009) Obstetric outcomes following vitrification of *in vitro* and *in vivo* matured oocytes. *Fertil. Steril.*, **91** (6), 2391–2398.

Choi, J.K., Huang, H., and He, X. (2015) Improved low-CPA vitrification of mouse oocytes using quartz microcapillary. *Cryobiology*, **70** (3), 269–272.

Ciotti, P.M., Porcu, E., Notarangelo, L., Magrini, O., Bazzocchi, A., and Venturoli, S. (2009) Meiotic spindle recovery is faster in vitrification of human oocytes compared to slow freezing. *Fertil. Steril.*, **91** (6), 2399–2407.

Downloaded From Vet-eBooks.com

Cobo, A., Rubio, C., Gerli, S., Ruiz, A., Pellicer, A., and Remohı́, J. (2001) Use of fluorescence *in situ* hybridization to assess the chromosomal status of embryos obtained from cryopreserved oocytes. *Fertil. Steril.*, **75** (2), 354–360.

Cobo, A., Romero, J.L., Pérez, S., de los Santos, M.J., Meseguer, M., and Remohí, J. (2010) Storage of human oocytes in the vapor phase of nitrogen. *Fertil. Steril.*, **94** (5), 1903–1907.

Cobo, A., Serra, V., Garrido, N., Olmo, I., Pellicer, A., and Remohí, J. (2014) Obstetric and perinatal outcome of babies born from vitrified oocytes. *Fertil. Steril.*, **102** (4), 1006–1015.

Cocchia, N., Ciani, F., Russo, M., El Rass, R., Rosapane, I., Avallone, L., Tortora, G., and Lorizio, R. (2010) Immature cat oocyte vitrification in open pulled straws (OPSs) using a cryoprotectant mixture. *Cryobiology*, **60** (2), 229–234.

Combelles, C.M., Cekleniak, N.A., Racowsky, C., and Albertini, D.F. (2002) Assessment of nuclear and cytoplasmic maturation in in-vitro matured human oocytes. *Hum. Reprod.*, **17** (4), 1006–1016.

Cox, J.F., Hormazabal, J., and Santa Maria, A. (1993) Effect of the cumulus on *in vitro* fertilization of bovine matured oocytes. *Theriogenology*, **40** (6), 1259–1267.

Criado, E., Albani, E., Novara, P.V., Smeraldi, A., Cesana, A., Parini, V., and Levi-Setti, P.E. (2011) Human oocyte ultravitrification with a low concentration of cryoprotectants by ultrafast cooling: a new protocol. *Fertil. Steril.*, **95** (3), 1101–1103.

Critser J.K., Agca, Y. and Gunasena, K.T. (1997) The cryobiology of mammalian oocytes, in *Reproductive Tissue Banking*, (eds A.M. Karrow and J.K. Critser), Academic Press, San Diego, CA, pp. 329–357.

Cutting R., Barlow, S., and Anderson, R. (2009) Human oocyte cryopreservation: evidence for practice. *Hum. Fertil.*, **12** (3), 125–136.

De Santis, L., Cino, I., Rabellotti, E., Papaleo, E., Calzi, F., Fusi, F.M., Brigante, C., and Ferrari, A. (2007) Oocyte cryopreservation: clinical outcome of slow-cooling protocols differing in sucrose concentration. *Reprod. Biomed. Online*, **14** (1), 57–63.

Dhali, A., Manik, R.S., Das, S.K., Singla, S.K., and Palta, P. (2000) Verification of buffalo (*Bubalus bubalisi*) oocytes. *Theriogenology*, **53** (6), 1295–1303.

Diez, C., Duque, P., Gomez, E., Hidalgo, C.O., Tamargo, C., Rodriguez, A., Fernandez, L., de la Varga, S., Fernandez, A., Facal, N. *et al.* (2005) Bovine oocyte vitrification before or after meiotic arrest: effects on ultrastructure and developmental ability. *Theriogenology*, **64**, 317–333.

Dinnyes, A., Dai, Y., Jiang, S., and Yang, X. (2000) High developmental rates of vitrified bovine oocytes following parthenogenetic activation, *in vitro* fertilization, and somatic cell nuclear transfer. *Biol. Reprod.*, **63** (2), 513–518.

Du, Y., Pribenszky, C.S., Molnár, M., Zhang, X., Yang, H., Kuwayama, M., Pedersen, A.M., Villemoes, K., Bolund, L., and Vajta, G. (2008) High hydrostatic pressure: a new way to improve *in vitro* developmental competence of porcine matured oocytes after vitrification. *Reproduction*, **135** (1), 13–17.

Eroglu, A., Toth, T.L., and Toner, M. (1998) Alterations of the cytoskeleton and polyploidy induced by cryopreservation of metaphase II mouse oocytes. *Fertil. Steril.*, **69** (5), 944–957.

Fabbri, R. (2006) Cryopreservation of human oocytes and ovarian tissue. *Cell Tissue Bank.*, **7** (2), 113–122.

Fahy, G.M. (2010) Cryoprotectant toxicity neutralization. *Cryobiology*, **60** 3 (Suppl.), S45–S53.

Fahy, G.M., MacFarlane, D.R., Angell, C.A., and Meryman, H.T. (1984) Vitrification as an approach to cryopreservation. *Cryobiology*, **21** (4), 407–426.

Fahy, G.M., Levy, D.I., and Ali, S.E. (1987) Some emerging principles underlying the physical properties, biological actions, and utility of vitrification solutions. *Cryobiology*, **24** (3), 196–213.

Fahy, G.M., Lilley, T.H., Linsdell, H., Douglas, M.S.J., and Meryman, H.T. (1990) Cryoprotectant toxicity and cryoprotectant toxicity reduction: in search of molecular mechanisms. *Cryobiology*, **27** (3), 247–268.

Downloaded From Vet-eBooks.com

Fahy, G.M., Wowk, B., Wu, J., and Paynter, S. (2004) Improved vitrification solutions based on the predictability of vitrification solution toxicity. *Cryobiology*, **48** (1), 22–35.

Fujihira, T., Kishida, R., and Fukui, Y. (2004) Developmental capacity of vitrified immature porcine oocytes following ICSI: effects of cytochalasin B and cryoprotectants. *Cryobiology*, **49** (3), 286–290.

Fujihira, T., Nagai, H., and Fukui, Y. (2005) Relationship between equilibration times and the presence of cumulus cells, and effect of taxol treatment for vitrification of *in vitro* matured porcine oocytes. *Cryobiology*, **51** (3), 339–343.

Fuku, E., Xia, L., and Downey, B.R. (1995) Ultrastructural changes in bovine oocytes cryopreserved by vitrification. *Cryobiology*, **32** (2), 139–156.

Gao, D.Y., Lin, S., Watson, P.F., and Critser, J.K. (1995) Fracture phenomena in an isotonic salt solution during freezing and their elimination using glycerol. *Cryobiology*, **32** (3), 270–284.

Gasparrini, B., Attanasio, L., De Rosa, A., Monaco, E., Di Palo, R., and Campanile, G. (2007) Cryopreservation of *in vitro* matured buffalo (*Bubalus bubalis*) oocytes by minimum volumes vitrification methods. *Anim. Reprod. Sci.*, **98** (3–4), 335–342.

Ghetler, Y., Yavin, S., Shalgi, R., and Arav, A. (2005) The effect of chilling on membrane lipid phase transition in human oocytes and zygotes. *Hum. Reprod.*, **20** (12), 3385–3389.

Givens, M.D., Galik, P.K., Riddell, K.P., Stringfellow, D.A., Brock, K.V., Bishop, M.D., Eilertsen, K.J., and Loskutoff, N.M. (2001) Validation of a reverse transcription nested polymerase chain reaction (RT-nPCR) to detect bovine viral diarrhea virus (BVDV) associated with *in vitro*-derived bovine embryos and co-cultured cells. *Theriogenology*, **56** (5), 787–799.

Griffin, J., Emery, B.R., Huang, I., Peterson, C.M., and Carrell, D.T. (2006) Comparative analysis of follicle morphology and oocyte diameter in four mammalian species (mouse, hamster, pig, and human). *J. Exp. Clin. Assist. Reprod.*, **3**, 2.

Gupta, M.K., Uhm, S.J., and Lee, H.T. (2007) Cryopreservation of immature and *in vitro* matured porcine oocytes by solid surface vitrification. *Theriogenology*, **67** (2), 238–248.

Hamano, S., Koikeda, A., Kuwayama, M., and Nagai, T. (1992) Full-term development of *in vitro*-matured, vitrified and fertilized bovine oocytes. *Theriogenology*, **38** (6), 1085–1090.

Hamawaki, A., Kuwayama, M., and Hamano, S. (1999) Minimum volume cooling method for bovine blastocyst vitrification. *Theriogenology*, **51** (1), 165.

Han, X. and Critser, J.K. (2009) Measurement of the size of intracellular ice crystals in mouse oocytes using a melting point depression method and the influence of intracellular solute concentrations. *Cryobiology*, **59** (3), 302–307.

Hara, H., Hwang, I.S., Kagawa, N., Kuwayama, M., Hirabayashi, M., and Hochi, S. (2012) High incidence of multiple aster formation in vitrified-warmed bovine oocytes after *in vitro* fertilization. *Theriogenology*, **77** (5), 908–915.

Hazel, J.R. (1995) Thermal adaptation in biological membranes: is homeoviscous adaptation the explanation? *Annu. Rev. Physiol.*, **57** (1), 19–42.

Hochi, S., Kozawa, M., Fujimoto, T., Hondo, E., Yamada, J., and Oguri, N. (1996) *In vitro* maturation and transmission electron microscopic observation of horse oocytes after vitrification. *Cryobiology*, **33** (3), 300–310.

Hochi, S., Terao, T., Kamei, M., Kato, M., Hirabayashi, M., and Hirao, M. (2004) Successful vitrification of pronuclear-stage rabbit zygotes by minimum volume cooling procedure. *Theriogenology*, **61** (2–3), 267–275.

Hong, S.W., Chung, H.M., Lim, J.M., Ko, J.J., Yoon, T.K., Yee, B., and Cha, K.Y. (1999) Improved human oocyte development after vitrification: a comparison of thawing methods. *Fertil. Steril.*, **72** (1), 142–146.

Horvath, G. and Seidel, G.E., Jr. (2006) Vitrification of bovine oocytes after treatment with cholesterol loaded methyl-B-cyclodextrin. *Theriogenology*, **66** (4), 1026–1033.

Downloaded From Vet-eBooks.com

Horvath, G. and Seidel, G.E., Jr. (2008) Use of fetuin before and during vitrification of bovine oocytes. *Reprod. Domes. Anim.*, **43** (3), 333–338.

Huang, J., Li, Q., Zhao, R., Li, W., Han, Z., Chen, X., Xiao, B., Wu, S., Jiang, Z., Hu, J. *et al.* (2008) Effect of sugars on maturation rate of vitrified-thawed immature porcine oocytes. *Anim. Reprod. Sci.*, **106** (1–2), 25–35.

Hurtt, A.E., Landim-Alvarenga, F., Seidel, G.E., Jr., and Squires, E.L. (2000) Vitrification of immature and mature equine and bovine oocytes in an ethylene glycol, ficoll and sucrose solution using open-pulled straws. *Theriogenology*, **54** (1), 119–128.

Hyttel, P., Vajta, G., and Callesen, H. (2000) Vitrification of bovine oocytes with the open pulled straw method: ultrastructural consequences. *Mol. Reprod. Dev.*, **56** (1), 80–88.

Isachenko, V., Soler, C., Isachenko, E., Perez-Sanchez, F., and Grishchenko, V. (1998) Vitrification of immature porcine oocytes: effects of lipid droplets, temperature, cytoskeleton, and addition and removal of cryoprotectant. *Cryobiology*, **36** (3), 250–253.

Jain, J.K. and Paulson, R.J. (2006) Oocyte cryopreservation. *Fertil. Steril.*, **86** 4 (Suppl.), 1037–1046.

Jiménez-Trigos, E., Vicente, J.S., Mocé, E., Naturil-Alfonso, C., Fernandez-Gonzalez, R., Gutierrez-Adan, A., and Marco-Jiménez, F. (2013) Treatment with cholesterol-loaded methyl-β-cyclodextrin increased the cholesterol in rabbit oocytes, but did not improve developmental competence of cryopreserved oocytes. *Cryobiology*, **67** (1), 106–108.

Jin, B., Kleinhans, F.W., and Mazur, P. (2014) Survivals of mouse oocytes approach 100% after vitrification in 3-fold diluted media and ultra-rapid warming by an IR laser pulse. *Cryobiology*, **68** (3), 419–430.

Jomha, N.M., Weiss, A.D.H., Fraser Forbes, J., Law, G.K., Elliott, J.A.W., and McGann, L.E. (2010) Cryoprotectant agent toxicity in porcine articular chondrocytes. *Cryobiology*, **61** (3), 297–302.

Juneja, S.C., Barr, K.J., Enders, G.C., and Kidder, G.M. (1999) Defects in the germ line and gonads of mice lacking connexin43. *Biol. Reprod.*, **60** (5), 1263–1270.

Keefe, D., Liu, L., Wang, W., and Silva, C. (2003) Imaging meiotic spindles by polarization light microscopy: principles and applications to IVF. *Reprod. Biomed. Online*, **7** (1), 24–29.

Kim, D.-H., Park, H.-S., Kim, S.-W., Hwang, I.-S., Yang, B.-C., Im, G.-S., Chung, H.-J., Seong, H.-W., Moon, S.-J., and Yang, B.-S. (2007) Vitrification of immature bovine oocytes by the microdrop method. *J. Reprod. Dev.*, **53** (4), 843–851.

Kim, T.J., Laufer, L.R., and Hong, S.W. (2010) Vitrification of oocytes produces high pregnancy rates when carried out in fertile women. *Fertil. Steril.*, **93** (2), 467–474.

Koshimoto, C. and Mazur, P. (2002) The effect of the osmolality of sugar-containing media, the type of sugar, and the mass and molar concentration of sugar on the survival of frozen-thawed mouse sperm. *Cryobiology*, **45** (1), 80–90.

Krisher, R.L. (2004) The effect of oocyte quality on development. *J. Anim. Sci.*, **82** (E-Suppl.), E14–E23.

Kuleshova, L.L., Gouk, S.S. and Hutmacher, D. (2007) Vitrification as a prospect for cryopreservation of tissue-engineered constructs. *Biomaterials*, **28** (9), 1585–1596.

Kuleshova L.L., MacFarlane, D.R., Trounson, A.O., and Shaw, J.M. (1999) Sugars exert a major influence on the vitrification properties of ethylene glycol-based solutions and have low toxicity to embryos and oocytes. *Cryobiology*, **38** (2), 119–130.

Kumamoto, K., Wang, H., Yamashiro, H., and Terada, T. (2005) Easy and rapid method for the determination of gene expression in cumulus cells incubated for oocyte maturation. *Reprod. Biol. Endocrinol.*, **3**, 59.

Kuwayama, M. (2007) Highly efficient vitrification for cryopreservation of human oocytes and embryos: the cryotop method. *Theriogenology*, **67** (1), 73–80.

Downloaded From Vet-eBooks.com

Kuwayama, M., Vajta, G., Ieda, S., and Kato, O. (2005a) Comparison of open and closed methods for vitrification of human embryos and the elimination of potential contamination. *Reprod. Biomed. Online*, **11** (5), 608–614.

Kuwayama, M., Vajta, G., Kato, O., and Leibo, S.P. (2005b) Highly efficient vitrification method for cryopreservation of human oocytes. *Reprod. Biomed. Online*, **11** (3), 300–308.

Lane, M., Schoolcraft, W.B., Gardner, D.K., and Phil, D. (1999) Vitrification of mouse and human blastocysts using a novel cryoloop container-less technique. *Fertil. Steril.*, **72** (6), 1073–1078.

Larman, M.G., Sheehan, C.B., and Gardner, D.K. (2006) Calcium-free vitrification reduces cryoprotectant-induced zona pellucida hardening and increases fertilization rates in mouse oocytes. *Reproduction*, **131** (1), 53–61.

Lawson, A., Ahmad, H., and Sambanis, A. (2011) Cytotoxicity effects of cryoprotectants as single-component and cocktail vitrification solutions. *Cryobiology*, **62** (2), 115–122.

Le Gal, F. and Massip, A. (1999) Cryopreservation of cattle oocytes: effects of meiotic stage, cycloheximide treatment, and vitrification procedure. *Cryobiology*, **38** (4), 290–300.

Ledda, S., Leoni, G., Bogliolo, L., and Naitana, S. (2001) Oocyte cryopreservation and ovarian tissue banking. *Theriogenology*, **55** (6), 1359–1371.

Ledda, S., Boglioli, L., Succu, S., Ariu, F., Bebbere, D., Leoni, G., and Naitana, S. (2007) Oocyte cryopreservation: oocyte assessment and strategies for improving survival. *Reprod. Fertil. Dev.*, **19** (1), 13–23.

Leibo, S.P. (1980) Water permeability and its activation energy of fertilized and unfertilized mouse ova. *J. Membr. Biol.*, **53** (3), 179–188.

Leibo, S.P. (1984) A one-step method for direct nonsurgical transfer of frozen-thawed bovine embryos. *Theriogenology*, **21** (5), 767–790.

Leibo, S.P. (1986) Cryobiology: preservation of mammalian embryos. *Basic Life Sci.*, **37**, 251–272.

Leibo, S.P. (2008) Cryopreservation of oocytes and embryos: optimization by theoretical versus empirical analysis. *Theriogenology*, **69** (1), 37–47.

Leibo, S.P., McGrath, J.J., and Cravalho, E.G. (1978) Microscopic observation of intracellular ice formation in unfertilized mouse ova as a function of cooling rate. *Cryobiology*, **15** (3), 257–271.

Levi Setti, P.E., Albani, E., Novara, P.V., Cesana, A., and Morreale, G. (2006) Cryopreservation of supernumerary oocytes in IVF/ICSI cycles. *Hum. Reprod.*, **21** (2), 370–375.

Liebermann, J., Dietl, J., Vanderzwalmen, P., and Tucker, M.J. (2003) Recent developments in human oocyte, embryo and blastocyst vitrification: where are we now? *Reprod. Biomed. Online*, **7** (6), 623–633.

Lin, L., Kragh, P.M., Purup, S., Kuwayama, M., Du, Y., Zhang, X., Yang, H., Bolund, L., Callesen, H., and Vajta, G. (2009) Osmotic stress induced by sodium chloride, sucrose or trehalose improves cryotolerance and developmental competence of porcine oocytes. *Reprod. Fertil. Dev.*, **21** (2), 338–344.

Liu, Y., Du, Y., Lin, L., Li, J., Kragh, P.M., Kuwayama, M., Bolund, L., Yang, H., and Vajta, G. (2008) Comparison of efficiency of open pulled straw (OPS) and cryotop vitrification for cryopreservation of *in vitro* matured pig oocytes. *Cryo Lett.*, **29** (4), 315–320.

Lohmann, W., Fowler, C.F., Moss, A.J., Jr., and Perkins, W.H. (1965) Complex formation between glycerol and metal ions as studied by means of ESR, NMR, and optical absorption spectroscopy. *Experientia*, **21** (1), 31–32.

Lonergan, P., Khatir, H., Carolan, C., and Mermillod, P. (1997) Bovine blastocyst production *in vitro* after inhibition of oocyte meiotic resumption for 24 h. *J. Reprod. Fertil.*, **109** (2), 355–365.

Lovelock, J.E. (1953) The mechanism of the protective action of glycerol against haemolysis by freezing and thawing. *Biochim. Biophys. Acta*, **11** (1), 28–36.

Downloaded From Vet-eBooks.com

Lovelock, J.E. and Bishop, M.W.H. (1959) Prevention of freezing damage to living cells by dimethyl sulphoxide. *Nature*, **183** (4672), 1394–1395.
Lucena, E., Bernal, D.P., Lucena, C., Rojas, A., Moran, A., and Lucena, A. (2006) Successful ongoing pregnancies after vitrification of oocytes. *Fertil. Steril.*, **85** (1), 108–111.
Magistrini, M. and Szollosi, D. (1980) Effects of cold and of isopropyl-*N*-phenylcarbamate on the second meiotic spindle of mouse oocytes. *Eur. J. Cell Biol.*, **22** (2), 699–707.
Magli, M.C., Lappi, M., Ferraretti, A.P., Capoti, A., Ruberti, A., and Gianaroli, L. (2010) Impact of oocyte cryopreservation on embryo development. *Fertil. Steril.*, **93** (2), 510–516.
Magnusson, V., Feitosa, W.B., Goissis, M.D., Yamada, C., Tavares, L.M.T., D'Ávila Assumpção, M.E.O., and Visintin, J.A. (2008) Bovine oocyte vitrification: effect of ethylene glycol concentrations and meiotic stages. *Anim. Reprod. Sci.*, **106** (3–4), 265–273.
Martino, A., Pollard, J.W., and Leibo, S.P. (1996a) Effect of chilling bovine oocytes on their developmental competence. *Mol. Reprod. Dev.*, **45** (4), 503–512.
Martino, A., Songsasen, N., and Leibo, S.P. (1996b) Development into blastocysts of bovine oocytes cryopreserved by ultra-rapid cooling. *Biol. Reprod.*, **54** (5), 1059–1069.
Massip, A. (2003) Cryopreservation of bovine oocytes: current status and recent developments. *Reprod. Nutr. Dev.*, **43**, 325–330.
Mavrides, A. and Morroll, D. (2002) Cryopreservation of bovine oocytes: is cryoloop vitrification the future to preserving the female gamete? *Reprod. Nutr. Dev.*, **42**, 73–80.
Mazni, O.A., Valdez, C.A., Takahashi, Y., Hishinuma, M., and Kanagawa, H. (1990) Quick freezing of mouse embryos using ethylene glycol with lactose or sucrose. *Anim. Reprod. Sci.*, **22** (2), 161–169.
Mazur, P. (1963) Kinetics of water loss from cells at subzero temperatures and the likelihood of intracellular freezing. *J. Gen. Physiol.*, **47** (2), 347–369.
Mazur, P. (1970) Cryobiology: the freezing of biological systems. *Science*, **168** (3934), 939–949.
Mazur, P. (1977) The role of intracellular freezing in the death of cells cooled at supraoptimal rates. *Cryobiology*, **14** (3), 251–272.
Mazur, P. (1984) Freezing of living cells: mechanisms and implications. *Am. J. Physiol.*, **16** (2), C125–C142.
Mazur, P. (1990) Equilibrium, quasi-equilibrium, and nonequilibrium freezing of mammalian embryos. *Cell Biophys.*, **17** (1), 53–92.
Mazur, P. (1996) Principles of medical cryobiology: the freezing of living cells, tissues and organs. *Principles Med. Biol.*, **4**, 355–384.
Mazur, P., Seki, S., Pinn, I.L., Kleinhans, F.W., and Edashige, K. (2005) Extra- and intracellular ice formation in mouse oocytes. *Cryobiology*, **51** (1), 29–53.
McWilliams, R.B., Gibbons, W.E., and Leibo, S.P. (1995) Osmotic and physiological responses of mouse zygotes and human oocytes to mono- and disaccharides. *Hum. Reprod.*, **10** (5), 1163–1171.
Men, H., Monson, R.L., and Rutledge, J.J. (2002) Effect of meiotic stages and maturation protocols on bovine oocyte's resistance to cryopreservation. *Theriogenology*, **57** (3), 1095–1103.
Men, H., Monson, R.L., Parrish, J.J., and Rutledge, J.J. (2003) Degeneration of cryopreserved bovine oocytes via apoptosis during subsequent culture. *Cryobiology*, **47** (1), 73–81.
Merlo, B., Iacono, E., Regazzini, M., and Zambelli, D. (2008) Cat blastocysts produced *in vitro* from oocytes vitrified using the cryoloop technique and cryopreserved electroejaculated semen. *Theriogenology*, **70** (1), 126–130.
Minasi, M.G., Fabozzi, G., Casciani, V., Ferrero, S., Litwicka, K., and Greco, E. (2012) Efficiency of slush nitrogen vitrification of human oocytes vitrified with or without cumulus cells in relation to survival rate and meiotic spindle competence. *Fertil. Steril.*, **97** (5), 1220–1225.

Downloaded From Vet-eBooks.com

Morato, R., Izquierdo, D., Albarracin, J.L., Anguita, B., Palomo, M.J., Macedo, R.J., Paramio, M.T., and Mogas, T. (2008a) Effects of pre-treating *in vitro* matured bovine oocytes with cytoskeleton stabilizing agent taxol prior to vitrification. *Mol. Reprod. Dev.*, **75** (1), 191–201.

Morato, R., Izquierdo, D., Paramio, M.T., and Mogas, T. (2008b) Cryotops versus open pulled straws (OPS) as carriers for cryopreservation of bovine oocytes: effects on spindle and chromosome configuration and embryo development. *Cryobiology*, **57** (2), 137–141.

Morato, R., Mogas, T., and Maddox-Hyttel, P. (2008c). Ultrastructure of bovine oocytes exposed to taxol prior to OPS vitrification. *Mol. Reprod. Dev.*, **75** (8), 1318–1326.

Morato, R., Izquierdo, D., Paramio, M.T., and Mogas, T. (2008d) Embryo development and structural analysis of *in vitro* matured bovine oocytes vitrified in flexipet denuding pipettes. *Theriogenology*, **70** (9), 1536–1543.

Mullen, S.F., Agca, Y., and Critser, J.K. (2004) Modeling the probability of MII spindle disruption in bovine oocytes as a function of total osmolality using logistic regression and its application toward improved CPA addition and removal procedures. *Cell Preserv. Technol.*, **2** (2), 145–155.

Mullen, S.F., Rosenbaum, M., and Critser, J.K. (2007) The effect of osmotic stress on the cell volume, metaphase II spindle and developmental potential of *in vitro* matured porcine oocytes. *Cryobiology*, **54** (3), 281–289.

Mullen, S.F., Li, M., Li, Y., Chen, Z.J., and Critser, J.K. (2008) Human oocyte vitrification: the permeability of metaphase II oocytes to water and ethylene glycol and the appliance toward vitrification. *Fertil. Steril.*, **89** (6), 1812–1825.

Nakagata, N. (1989) High survival rate of unfertilized mouse oocytes after vitrification. *J. Reprod. Fertil.*, **87** (2), 479–483.

Nakagawa, S., Yoneda, A., Hayakawa, K., and Watanabe, T. (2008) Improvement in the *in vitro* maturation rate of porcine oocytes vitrified at the germinal vesicle stage by treatment with a mitochondrial permeability transition inhibitor. *Cryobiology*, **57** (3), 269–275.

Navara, C.S., First, N.L., and Schatten, G. (1994) Microtubule organization in the cow during fertilization, polyspermy, parthenogenesis, and nuclear transfer: the role of the sperm aster. *Dev. Biol.*, **162** (1), 29–40.

Newton, H., Pegg, D.E., Barrass, R., and Gosden, R.G. (1999) Osmotically inactive volume, hydraulic conductivity, and permeability to dimethyl sulphoxide of human mature oocytes. *J. Reprod. Fertil.*, **117** (1), 27–33.

Nicolson, G.L. (2014) The fluid–mosaic model of membrane structure: still relevant to understanding the structure, function and dynamics of biological membranes after more than 40 years. *Biochim. Biophys. Acta*, **1838** (6), 1451–1466.

Ogawa, B., Ueno, S., Nakayama, N., Matsunari, H., Nakano, K., Fujiwara, T., Ikezawa, Y., and Nagashima, H. (2010) Developmental ability of porcine *in vitro* matured oocytes at the meiosis II stage after vitrification. *J. Reprod. Dev.*, **56** (3), 356–361.

Paffoni, A., Guarneri, C., Ferrari, S., Restelli, L., Nicolosi, A.E., Scarduelli, C., and Ragni, G. (2011) Effects of two vitrification protocols on the developmental potential of human mature oocytes. *Reprod. Biomed. Online*, **22** (3), 292–298.

Papis, K., Shimizu, M., and Izaike, Y. (2000) Factors affecting the survivability of bovine oocytes vitrified in droplets. *Theriogenology*, **54** (5), 651–658.

Park, S.E., Chung, H.M., Cha, K.Y., Hwang, W.S., Lee, E.S., and Lim, J.M. (2001) Cryopreservation of ICR mouse oocytes: improved post-thawed preimplantation development after vitrification using taxol, a cytoskeleton stabilizer. *Fertil. Steril.*, **75** (6), 1177–1184.

Parkening, T.A., Tsunoda, Y., and Chang, M.C. (1976) Effects of various low temperatures, cryoprotective agents and cooling rates on the survival, fertilizability and development of frozen-thawed mouse eggs. *J. Exp. Zool.*, **197** (3), 369–374.

Downloaded From Vet-eBooks.com

Parks, J.E. (1997) Hypothermia and mammalian gametes, in *Reproductive Tissue Banking*, (eds A.M. Karrow and J.K. Critser), Academic Press, San Diego, CA, pp. 229–261.

Pereira R.M. and Marques, C.C. (2008) Animal oocyte and embryo cryopreservation. *Cell Tissue Bank.*, **9** (4), 267–277.

Pickering, S.J. and Johnson, M.H. (1987) The influence of cooling on the organization of the meiotic spindle of the mouse oocyte. *Hum. Reprod.*, **2** (3), 207–216.

Pickering, S.J., Braude, P.R., Johnson, M.H., Cant, A., and Currie, J. (1990) Transient cooling to room temperature can cause irreversible disruption of the meiotic spindle in the human oocyte. *Fertil. Steril.*, **54** (1), 102–108.

Plachinta, M., Zhang, T., and Rawson, D.M. (2004) Studies on cryoprotectant toxicity to zebrafish (*Danio rerio*) oocytes. *Cryo Lett.*, **25** (6), 415–424.

Polge, C., Smith, A.U., and Parkes, A.S. (1949) Revival of spermatozoa after vitrification and dehydration at low temperatures. *Nature*, **164** (4172), 666.

Pope, C.E., Gómez, M.C., Kagawa, N., Kuwayama, M., Leibo, S.P., and Dresser, B.L. (2012) *In vivo* survival of domestic cat oocytes after vitrification, intracytoplasmic sperm injection and embryo transfer. *Theriogenology*, **77** (3), 531–538.

Prentice, J.R. and Anzar, M. (2011) Cryopreservation of mammalian oocyte for conservation of animal genetics. *Vet. Med. Int.*, **2011**, 146405.

Prentice-Biensch, J., Singh, J., Mapletoft, R., and Anzar, M. (2012a) Vitrification of immature bovine cumulus–oocyte complexes: effects of cryoprotectants, the vitrification procedure and warming time on cleavage and embryo development. *Reprod. Biol. Endocrinol.*, **10** (1), 73.

Prentice-Biensch, J.R., Singh, J., Alfoteisy, B., and Anzar, M. (2012b) A simple and high-throughput method to assess maturation status of bovine oocytes: comparison of anti-lamin A/C-DAPI with an aceto-orcein staining technique. *Theriogenology*, **78** (7), 1633–1638.

Pribenszky, C.S., Du, Y., Molnár, M., Harnos, A., and Vajta, G. (2008) Increased stress tolerance of matured pig oocytes after high hydrostatic pressure treatment. *Anim. Reprod. Sci.*, **106** (1–2), 200–207.

Quinn, P.J. (1985) A lipid-phase separation model of low-temperature damage to biological membranes. *Cryobiology*, **22** (2), 128–146.

Quintans, C.J., Donaldson, M.J., Bertolino, M.V., and Pasqualini, R.S. (2002) Birth of two babies using oocytes that were cryopreserved in a choline-based freezing medium. *Hum. Reprod.*, **17** (12), 3149–3152.

Rall, W.F. (1987) Factors affecting the survival of mouse embryos cryopreserved by vitrification. *Cryobiology*, **24** (5), 387–402.

Rall, W.F. and Fahy, G.M. (1985) Ice-free cryopreservation of mouse embryos at −196 °C by vitrification. *Nature*, **313** (6003), 573–575.

Renard, J.P., Bui Xuan, N., and Garnier, V. (1984) Two-step freezing of two-cell rabbit embryos after partial dehydration at room temperature. *J. Reprod. Fertil.*, **71** (2), 573–580.

Rho, G.J., Kim, S., Yoo, J.G., Balasubramanian, S., Lee, H.J., and Choe, S.Y. (2002) Microtubulin configuration and mitochondrial distribution after ultra-rapid cooling of bovine oocytes. *Mol. Reprod. Dev.*, **63** (4), 464–470.

Risco, R., Elmoazzen, H., Doughty, M., He, X., and Toner, M. (2007) Thermal performance of quartz capillaries for vitrification. *Cryobiology*, **55** (3), 222–229.

Rojas, C., Palomo, M.J., Albarracín, J.L., and Mogas, T. (2004) Vitrification of immature and *in vitro* matured pig oocytes: study of distribution of chromosomes, microtubules, and actin microfilaments. *Cryobiology*, **49** (3), 211–220.

Roux, A., Sandenbergh, L., and Roodt-Wilding, R. (2008) Preliminary investigation to determine the cytotoxicity of various cryoprotectants on southern African abalone (*Haliotis midae*) embryos. *Cryobiology*, **57** (3), 308–311.

Downloaded From Vet-eBooks.com

Ruffing, N.A., Steponkus, P.L., Pitt, R.E., and Parks, J.E. (1993) Osmometric behavior, hydraulic conductivity, and incidence of intracellular ice formation in bovine oocytes at different developmental stages. *Cryobiology*, **30** (6), 562–580.

Ruppert-Lingham, C.J., Paynter, S.J., Godfrey, J., Fuller, B.J., and Shaw, R.W. (2006) Membrane integrity and development of immature murine cumulus–oocyte complexes following slow cooling to −60 °C: the effect of immediate rewarming, plunging into LN_2 and two-controlled-rate-stage cooling. *Cryobiology*, **52** (2), 219–227.

Saha, S., Rajamahendran, R., Boediono, A., Sumantri, C., and Suzuki, T. (1996) Viability of bovine blastocysts obtained after 7, 8 or 9 days of culture *in vitro* following vitrification and one-step rehydration. *Theriogenology*, **46** (2), 331–343.

Saito, N., Imai, K., and Tomizawa, M. (1994) Effect of sugars-addition on the survival of vitrified bovine blastocysts produced *in vitro*. *Theriogenology*, **41** (5), 1053–1060.

Saragusty, J. and Arav, A. (2011) Current progress in oocyte and embryo cryopreservation by slow freezing and vitrification. *Reproduction*, **141** (1), 1–19.

Schatten, G., Simerly, C., and Schatten, H. (1985) Microtubule configurations during fertilization, mitosis, and early development in the mouse and the requirement for egg microtubule-mediated motility during mammalian fertilization. *Proc. Natl. Acad. Sci. USA*, **82** (12), 4152–4156.

Schneider, U. and Mazur, P. (1984) Osmotic consequences of cryoprotectant permeability and its relation to the survival of frozen-thawed embryos. *Theriogenology*, **21** (1), 68–79.

Seki, S. and Mazur, P. (2008) Effect of warming rate on the survival of vitrified mouse oocytes and on the recrystallization of intracellular ice. *Biol. Reprod.*, **79** (4), 727–737.

Seki, S. and Mazur, P. (2009) The dominance of warming rate over cooling rate in the survival of mouse oocytes subjected to a vitrification procedure. *Cryobiology*, **59** (1), 75–82.

Seki, S. and Mazur, P. (2012) Ultra-rapid warming yields high survival of mouse oocytes cooled to −196 °C in dilutions of a standard vitrification solution. *PLoS One*, **7** (4), e36058.

Shaw, J.M. and Jones, G.M. (2003) Terminology associated with vitrification and other cryopreservation procedures for oocytes and embryos. *Hum. Reprod. Update*, **9** (6), 583–605.

Sherman, J.K. and Lin, T.P. (1958) Survival of unfertilized mouse eggs during freezing and thawing. *Proc. Soc. Exp. Biol. Med.*, **98** (4), 902–905.

Shi, W.-Q., Zhu, S.-E., Zhang, D., Wang, W.-H., Tang, G.-L., Hou, Y.-P., and Tian, S.-J. (2006) Improved development by taxol pretreatment after vitrification of *in vitro* matured porcine oocytes. *Reproduction*, **131** (4), 795–804.

Shi, L.-Y., Jin, H.-F., Kim, J.-G., Mohana Kumar, B., Balasubramanian, S., Choe, S.-Y., and Rho, G.-J. (2007) Ultra-structural changes and developmental potential of porcine oocytes following vitrification. *Anim. Reprod. Sci.*, **100** (1–2), 128–140.

Simon, A.M. and Goodenough, D.A. (1998) Diverse functions of vertebrate gap junctions. *Trends Cell Biol.*, **8** (12), 477–482.

Simon, A.M., Goodenough, D.A., Li, E. and Paul, D.L. (1997) Female infertility in mice lacking connexin 37. *Nature*, **385** (6616), 525–529.

Singer, S.G. and Nicolson, G.L. (1972) The fluid mosaic model of the structure of cell membranes. *Science*, **175** (4023), 720–731.

Smith, G.D., Serafini, P.C., Fioravanti, J., Yadid, I., Coslovsky, M., Hassun, P., Alegretti, J.R., and Motta, E.L. (2010) Prospective randomized comparison of human oocyte cryopreservation with slow-rate freezing or vitrification. *Fertil. Steril.*, **94** (6), 2088–2095.

Somfai, T., Dinnyés, A., Sage, D., Marosán, M., Carnwath, J.W., Ozawa, M., Kikuchi, K., and Niemann, H. (2006) Development to the blastocyst stage of parthenogenetically activated

Downloaded From Vet-eBooks.com

in vitro matured porcine oocytes after solid surface vitrification (SSV). *Theriogenology*, **66** (2), 415–422.

Steponkus, P.L., Myers, S.P., Lynch, D.V., Gardner, L., Bronshteyn, V., Leibo, S.P., Rall, W.F., Pitt, R.E., Lin, T.T., and MacIntyre, R.J. (1990) Cryopreservation of *Drosophila melanogaster* embryos. *Nature*, **345** (6271), 170–172.

Stiles, W. (1930) On the cause of cold death of plants. *Protoplasma*, **9**, 459–468.

Stringfellow, D.A. and Givens, M.D. (2000) Epidemiologic concerns relative to *in vivo* and *in vitro* production of livestock embryos. *Anim. Reprod. Sci.*, **60–61**, 629–642.

Succu, S., Leoni, G.G., Bebbere, D., Berlinguer, F., Mossa, F., Bogliolo, L., Madeddu, M., Ledda, S., and Naitana, S. (2007a) Vitrification devices affect structural and molecular status of *in vitro* matured ovine oocytes. *Mol. Reprod. Dev.*, **74** (10), 1337–1344.

Succu, S., Leoni, G.G., Berlinguer, F., Madeddu, M., Bebbere, D., Mossa, F., Bogliolo, L., Ledda, S., and Naitana, S. (2007b) Effect of vitrification solutions and cooling upon *in vitro* matured prepubertal ovine oocytes. *Theriogenology*, **68** (1), 107–114.

Szell, A. and Shelton, J.N. (1986) Role of equilibration before rapid freezing of mouse embryos. *J. Reprod. Fertil.*, **78** (2), 699–703.

Szell, A. and Shelton, J.N. (1987) Osmotic and cryoprotective effects of glycerol-sucrose solutions on day-3 mouse embryos. *J. Reprod. Fertil.*, **80** (1), 309–316.

Tanghe, S., Van Soom, A., Mehrzad, J., Maes, D., Duchateau, L., and De Kruif, A. (2003) Cumulus contributions during bovine fertilization *in vitro*. *Theriogenology*, **60** (1), 135–149.

Tharasanit, T., Colenbrander, B., and Stout, T.A.E. (2006) Effect of maturation stage at cryopreservation on post-thaw cytoskeleton quality and fertilizability of equine oocytes. *Mol. Reprod. Dev.*, **73** (5), 627–637.

Tharasanit, T., Colleoni, S., Galli, C., Colenbrander, B., and Stout, T.A. (2009) Protective effects of the cumulus–corona radiata complex during vitrification of horse oocytes. *Reproduction*, **137** (3), 391–401.

Tharasanit, T., Manee-In, S., Buarpung, S., Chatdarong, K., Lohachit, C., and Techakumphu, M. (2011) Successful pregnancy following transfer of feline embryos derived from vitrified immature cat oocytes using 'stepwise' cryoprotectant exposure technique. *Theriogenology*, **76** (8), 1442–1449.

Toner, M., Cravalho, E.G., and Karel, M. (1990) Thermodynamics and kinetics of intracellular ice formation during freezing of biological cells. *J. Appl. Phys.*, **67** (3), 1582–1593.

Toth, T.L., Baka, S.G., Veeck, L.L., Jones H.W., Jr., Muasher, S., and Lanzendorf, S.E. (1994) Fertilization and *in vitro* development of cryopreserved human prophase I oocytes. *Fertil. Steril.*, **61** (5), 891–894.

Tsai, S., Rawson, D.M., and Zhang, T. (2008) Studies on cryoprotectant toxicity to early stage zebrafish (*Danio rerio*) ovarian follicles. *Cryo Lett.*, **29** (6), 477–483.

Vajta, G. (2000) Vitrification of the oocytes and embryos of domestic animals. *Anim. Reprod. Sci.*, **60–61**, 357–364.

Vajta, G. and Kuwayama, M. (2006) Improving cryopreservation systems. *Theriogenology*, **65** (1), 236–244.

Vajta, G. and Nagy, Z.P. (2006) Are programmable freezers still needed in the embryo laboratory? Review on vitrification. *Reprod. Biomed. Online*, **12** (6), 779–796.

Vajta, G., Holm, P., Kuwayama, M., Booth, P.J., Jacobsen, H., Greve, T., and Callesen, H. (1998) Open pulled straw (OPS) vitrification: a new way to reduce cryoinjuries of bovine ova and embryos. *Mol. Reprod. Dev.*, **51** (1), 53–58.

Van Blerkom, J. (1989) Maturation at high frequency of germinal-vesicle-stage mouse oocytes after cryopreservation: alterations in cytoplasmic, nuclear, nucleolar and chromosomal structure and organization associated with vitrification. *Hum. Reprod.*, **4** (8), 883–898.

Downloaded From Vet-eBooks.com

Vanderzwalmen, P., Bertin, G., Debauche, C., Standaert, V., Bollen, N., Van Roosendaal, E., Vandervorst, M., Schoysman, R., and Zech, N. (2003) Vitrification of human blastocysts with the hemi-straw carrier: application of assisted hatching after thawing. *Hum. Reprod.*, **18** (7), 1504–1511.

Vieira, A.D., Mezzalira, A., Barbieri, D.P., Lehmkuhl, R.C., Rubin, M.I.B., and Vajta, G. (2002) Calves born after open pulled straw vitrification of immature bovine oocytes. *Cryobiology*, **45** (1), 91–94.

Vieira, A.D., Forell, F., Feltrin, C., and Rodrigues, J.L. (2008) Calves born after direct transfer of vitrified bovine *in vitro* produced blastocysts derived from vitrified immature oocytes. *Reprod. Domes. Anim.*, **43** (3), 314–318.

Vincent, C. and Johnson, M.H. (1992) Cooling, cryoprotectants, and the cytoskeleton of the mammalian oocyte. *Oxf. Rev. Reprod. Biol.*, **14**, 73–100.

Vincent, C., Pickering, S.J., Johnson, M.H., and Quick, S.J. (1990) Dimethylsulphoxide affects the organisation of microfilaments in the mouse oocyte. *Mol. Reprod. Dev.*, **26** (3), 227–235.

Voelkel, S.A. and Hu, Y.X. (1992) Use of ethylene glycol as a cryoprotectant for bovine embryos allowing direct transfer of frozen-thawed embryos to recipient females. *Theriogenology*, **37** (3), 687–697.

Wang, W.-H. and Keefe, D.L. (2002) Spindle observation in living mammalian oocytes with the polarization microscope and its practical use. *Cloning Stem Cells*, **4** (3), 269–276.

Wang, X., Al Naib, A., Sun, D.W., and Lonergan, P. (2010) Membrane permeability characteristics of bovine oocytes and development of a step-wise cryoprotectant adding and diluting protocol. *Cryobiology*, **61** (1), 58–65.

Weiss, A.D.H., Fraser Forbes, J., Scheuerman, A., Law, G.K., Elliott, J.A.W., McGann, L.E., and Jomha, N.M. (2010) Statistical prediction of the vitrifiability and glass stability of multi-component cryoprotective agent solutions. *Cryobiology*, **61** (1), 123–127.

Whittingham, D.G. (1971) Survival of mouse embryos after freezing and thawing. *Nature*, **233** (5315), 125–126.

Whittingham, D.G. (1977) Fertilization *in vitro* and development to term of unfertilized mouse oocytes previously stored at −196 °C. *J. Reprod. Fertil.*, **49** (1), 89–94.

Whittingham, D.G., Leibo, S.P., and Mazur, P. (1972) Survival of mouse embryos frozen to −196° and −269 °C. *Science*, **178** (4059), 411–414.

Willadsen, S.M., Polge, C., Rowson, L.E.A., and Moor, R.M. (1976) Deep freezing of sheep embryos. *J. Reprod. Fertil.*, **46** (1), 151–154.

Willadsen, S., Polge, C., and Rowson, L.E.A. (1978) The viability of deep-frozen cow embryos. *J. Reprod. Fertil.*, **52** (2), 391–393.

Wright, D.L., Eroglu, A., Toner, M., and Toth, T.L. (2004) Use of sugars in cryopreserving human oocytes. *Reprod. Biomed. Online*, **9** (2), 179–186.

Wu, B., Tong, J., and Leibo, S.P. (1999) Effects of cooling germinal vesicle-stage bovine oocytes on meiotic spindle formation following *in vitro* maturation. *Mol. Reprod. Dev.*, **54** (4), 388–395.

Wu, C., Rui, R., Dai, J., Zhang, C., Ju, S., Xie, B., Lu, X., and Zheng, X. (2006) Effects of cryopreservation on the developmental competence, ultrastructure and cytoskeletal structure of porcine oocytes. *Mol. Reprod. Dev.*, **73** (11), 1454–1462.

Wusteman, M., Robinson, M., and Pegg, D. (2004) Vitrification of large tissues with dielectric warming: biological problems and some approaches to their solution. *Cryobiology*, **48** (2), 179–189.

Yang, B.C., Im, G.S., Kim, D.H., Yang, B.S., Oh, H.J., Park, H.S., Seong, H.H., Kim, S.W., Ka, H.H., and Lee, C.K. (2008) Development of vitrified-thawed bovine oocytes after *in vitro* fertilization and somatic cell nuclear transfer. *Anim. Reprod. Sci.*, **103** (1–2), 25–37.

Downloaded From Vet-eBooks.com

Yavin, S. and Arav, A. (2007) Measurement of essential physical properties of vitrification solutions. *Theriogenology*, **67** (1), 81–89.

Yavin, S., Aroyo, A., Roth, Z., and Arav, A. (2009) Embryo cryopreservation in the presence of low concentration of vitrification solution with sealed pulled straws in liquid nitrogen slush. *Hum. Reprod.*, **24** (4), 797–804.

Yoon, T.K., Kim, T.J., Park, S.E., Hong, S.W., Ko, J.J., Chung, H.M., and Cha, K.Y. (2003) Live births after vitrification of oocytes in a stimulated *in vitro* fertilization-embryo transfer program. *Fertil. Steril.*, **79** (6), 1323–1326.

Zeron, Y., Pearl, M., Borochov, A., and Arav, A. (1999) Kinetic and temporal factors influence chilling injury to germinal vesicle and mature bovine oocytes. *Cryobiology*, **38** (1), 35–42.

Zhang, J., Nedambale, T.L., Yang, M., and Li, J. (2009) Improved development of ovine matured oocyte following solid surface vitrification (SSV): effect of cumulus cells and cytoskeleton stabilizer. *Anim. Reprod. Sci.*, **110** (1–2), 46–55.

Zhao, G., Luo, D., and Gao, D. (2006) Universal model for intracellular ice formation and its growth. *AIChE J.*, **52** (7), 2596–2606.

Zhao, X.-M., Du, W.-H., Wang, D., Hao, H.-S., Liu, Y., Qin, T., and Zhu, H.-B. (2011) Recovery of mitochondrial function and endogenous antioxidant systems in vitrified bovine oocytes during extended *in vitro* culture. *Mol. Reprod. Dev.*, **78** (12), 942–950.

Zhou, X.L., Al Naib, A., Sun, D.W., and Lonergan, P. (2010) Bovine oocyte vitrification using the cryotop method: effect of cumulus cells and vitrification protocol on survival and subsequent development. *Cryobiology*, **61** (1), 66–72.

Zhou, D., Shen, X., Gu, Y., Zhang, N., Li, T., Wu, X., and Lei, L. (2014) Effects of dimethyl sulfoxide on asymmetric division and cytokinesis in mouse oocytes. *BMC Dev. Biol.*, **14** (1), 28.

Downloaded From Vet-eBooks.com

Index

a

ABC transporters 306
abdominal aorta *62*
abnormal chromosome alignment 541
abortion 216, 240, 359, 360, 363, 365, 366, 368, 369, 401
accessory genital glands 1, 11, 16, *17*, 22, 31, 39, *40*, 43, *44*, 48, *49*
accessory genital glands (male) 59, 63
accessory thyroid glands 62
acetylation 443, 445
acrocentric chromosome translocation 215
acrosin 410, 411
acrosomal exocytosis 409, 410, 411, 412, 414, 415, 416, 418, 419, 436
acrosomal matrix(ices) 410, 411, 412, 413
acrosomal membrane 265, 268, 275, 276, 277, 279, 316, 418
acrosomal proteins 411, 412
acrosomal region 417
acrosomal vesicle 265, 267, 273, 276, 277, 410, 417
acrosome(s) 264–267, 268, 275–277, 279, 304, 306–309, 311–313, 315, 316, 409, 410, 411, 412, 413, 414, 415, 416, 417, 418, 419
acrosome reaction (AR) 301, 304–309, 311–312, 315, 316, 317, 318, 319, 324, 326, 414, 418, 419, 530
actin (G-actin) (F-actin) cytoskeleton 241, 281, 290, 303, 309, 414, 417, 418, 536, 541
activin 5
acute infections 370
ADA, Americans with Disabilities Act 250–251
adenohypophysis 59, *60*, 61
adenosine 5′-monophosphate-activated protein kinase (AMPK) 179, 193, 194, 195, 196, 197, 198
adenosine triphosphate (ATP) (production, synthesis) 146, 149, 150, 151, 152, 153, 155, 156, 159, 160, 161, 193, 194, 438
adenylyl cyclase (AC) 180
adiposity 371
adrenal gland 51, *54, 55*, 59, 62, *62*
advanced maternal age (AMA) 158
Afghan hound 329
African clawed frog/*Xenopus laevis* 1, 51, *54, 55*
age, aging 95, 159, 160, 215, 235, 237, 470, 474, 475
Ago protein(s) 111, 112, 115
Ago subfamilies 109
Agouti gene 471, 472
AKC, American Kennel Club 251, 252
A-kinase anchoring proteins (AKAPs) 180, 188, 439
AKT 180, 182, 185
alkaline phosphatase 261, 262, 271
allantois 71, 72, 73
allogenic chimeras 489
American Kennel Club (AKC) 251, 252–253
American Pit Bull Dog 264, 268
American Veterinary Medical Association (AVMA) 249
Americans with Disabilities Act (ADA) 250–251
amniocentesis 360
amnion 72, 360
amniotic cavity 360
amniotic fluid 72, 363
amniotic sac 72
amphibian 383
amphiregulin (AREG) 180

Animal Models and Human Reproduction, First Edition. Edited by Heide Schatten and Gheorghe M. Constantinescu.
© 2017 John Wiley & Sons, Inc. Published 2017 by John Wiley & Sons, Inc.

Downloaded From Vet-eBooks.com

ampulla of ductus deferens 4, 9, 11, 15, 16, 20, *23, 24*, 31, *32*, 39, *40*, 43, 44, *44*, 47
ampulla of uterine tube 7, 41, 45
ampullary gland 44, *44*, 48, *49*, 63
anaphase-promoting complex/cyclosome (APC/C) 442
anatomy 1
anatomy, reproductive. *see also specific structures*
  female reproductive organs 282–289
    cervix 282, 286–287, 323, 331
    clitoris 288, 331
    mammary glands 282, 288–289, 332
    ovary 282–285, 289, 291
    uterine horn 282, 286, 330
    uterine tube (oviduct) 282, 285–286
    uterus 282, 287, 320, 331
    vagina 282, 287, 323
    vestibule 282, 287–282, 287, 288
  male reproductive organs 258–262
    bulbourethral glands, absent in dogs 258
    ductus deferens 258–261
    epididymis 258–261
    penis 258–259, 261
    prostate 258–259, 260–262
    seminal vesicles, absent in dogs 258
    spermatic cord 259–261
    testis 258–261
    urethra 258–259, 261–262
ancestry, dog 250–252
androgen 95
androgenesis 402
androgenic 406
androgenic embryo(s) 402, 403, 404, 405, 406
anestrus 284–286, 291, 294, 305
aneuploidy 97, 158, 215, 242, 333, 401
Angelman syndrome (AS) 475
angiogenic, angiogenesis 73, 217, 359
anisosmotic stress 530
annulate lamellae (AL) 439
antiandrogenic activity 94
antibody ablation 369
antidiabetic drugs 194
antigen presentation 65
anti-Müllerian hormone (AMH) 95, 129
antioxidant(s) 159, 160, 161, 539, 542
antiphospholipid (aPL) antibodies 365
antiphospholipid antibody syndrome (APS) 365
antral follicle count (AFC) 95
antral follicles 178, 236, 237, 289
apical ligament *25*
apoptosis 93, 96, 113, 114, 435, 529, 538
aquaporins 318
arcus inguinalis 3, *3*
argonaute (Ago) family proteins 109
arsenite 194, 196
ART. *see assisted reproductive technology*
assisted reproductive technology(ies) (therapies) (ART) 81, 127, 131, 132, 145, 158, 161, 213, 216, 219, 235, 239, 240, 241, 323–330, 401, 406, 435, 439, 441, 442, 447, 450, 467, 475, 476, 510, 511, 522, 542
  artificial insemination (AI) 127, 132, 257, 323
  embryo transfer (ET) 327
  intracytoplasmic sperm injection (ICSI) 326–327
  in vitro fertilization (IVF) 325–326
  oocyte in vitro maturation 324
  sperm sexing 328–329
  superovulation 324
asthenozoospermia 272, 327
asymmetric cell division 69, 536
atresia 95
atrium *56*
autism-like symptoms 372
autism-type phenotypes 372
autophagic pathway 450
AVMA, American Veterinary Medical Association 249
axoneme 277–278, 308, 310
azoospermia 270–271
  asthenozoospermic men 510, 511, 512

b

bacteria 539
bacterial infection(s) 361, 363, 364
Beagle 251, 324–326
Beckwith–Wiedemann syndrome 219, 475
beta-arrestins 180
bicornuate, dog uterus 287
biobanks 522
biomedicine 213, 214
biosecurity 539
biotechnology 510
bisphenol A (BPA) 92, 94, 95, 97, 99, 100, 101, 474
blastocoel cavity 71, 485
blastocoel fluid 155

Downloaded From Vet-eBooks.com

blastocyst(s) 66, 69, 71, 73, 74, 78, 133, 134, 136, 145, 147, 152, 154, 155, 156, 159, 160, 161, 186, 215, 216, 217, 219, 223, 321–322, 325, 329, 404, 435, 447, 448, 437, 470, 485, 486, 489, 491, 492, 493, 499, 531, 532, 535, 537, 538, 539, 540, 541, 542
blastomere(s) 66, 77, 325, 401, 402, 403, 404, 405, 435, 441, 485, 541
boar *16*, 17, *17*
body of epididymis 4, 10, 16, 21, 30, 32, 39, 43, *43*, 47, 48
body mass index (BMI) 158, 160
bovine 178, 524, 525, 526, 531
brain *60*
breast cancer 223
breeding season 289
brilliant cresyl blue test 215
broad ligament 7, *13*, 14, 34, 41, *41, 46*, 50, *52*, 282
buck 22, 23, *26*
buffalo 526, 537
bulboglandularis M. 12, *17*, 18, 23, *24*, 32, 44, *44*, 48, *49*
bulbospongiosus M. 11, 12, *17*, 18, *23, 32, 45, 50, 51*
bulbourethral diverticulum 44, *44*, 45, 48
bulbourethral glands 4, 11, *17*, 18, 23, *23, 24*, 32, *32*, 39, *40*, 44, *44*, 48, *49, 50*, 63
  absent in dogs 258
bulbus arteriosus *56*
bulbus glandis 262
bulbus penis 5, 11, 12, 18
bull *21*, 22, *22*, 23, *23, 24, 25*

C

Ca^{2+}-calmodulin kinase II (CaMKII) 417
caffeine 215
calcineurin 307, 314
calcium release assay (Xenopus) 392
calcium 271, 302–303, 307–308, 314
  calcium-imaging 418, 419
calmodulin 184, 414
calmodulin-dependent protein kinase kinase (CaMKK) 194
Ca^{2+} ions 436
cancer 223, 251, 254, 257, 332, 500, 519
  breast cancer 332
  prostate cancer 332
  testicular cancer 332
canids 66
canine persistent Müllerian duct syndrome (PMDS) 331
canine. *see dog*
Canis lupus familiaris. see dog
canonical miRNAs family 110, 111
capacitation 302–318, 409, 413, 414, 417, 418
caprine 527
carbohydrate metabolism 151
carnivores 4, 7, 8, 9, 11, 14, 27, 61–63
cartilage of penis 5, 11
caruncles *26, 27, 28*, 29, *29*, 41, 80
cat 1, 8, 9, 12, 14, 15, 50, *60, 61, 62*
CatSper 307–308
cattle 67, 131, 132, 135, 177, 178
caudal epigastric A. *22*
caudal epigastric V. *22*
caudal lobe of thyroid gland *61*
caudal preputial Mm. 18, 24
caudal vena cava *62*
caveolae 188, 189
cavernous tissue 12
cavity of hypophysis 59, *60*, 61
cell cycle regulation 114
cell cycle transition assay (Xenopus) 392
cell death 92
cell differentiation 499
cell division 153, 156, 157, 410, 445, 485
cell fate 109
cell therapies 488
cell-fusion-induced PCC 404, 406
cellular stress 159, 161
centrioles 216
centromeric heterochromatin 444
centrosome inheritance 214, 216
centrosome(s) 215
cerebral epiphysis/pineal gland 59, *60*, 61
cervical canal 7, *13*, 14, *26*, 29, 34, *36, 37*, 47
cervical capacity 361
cervical frenulum 34
cervical trubercle 14, 15
cervix *13*, 14, *14*, 19, 20, *26*, 29, 34, *36*, 41, 42, *42*, 50, *51*, 360
chilling, chilling injury 529, 532, 535, 537
chimeras 77, 78, 498
chimeric blastocysts. 497
chimeric fetuses 497
cholesterol 262, 271, 279, 303, 306, 327
  efflux 306
chorioallantoic membrane 72
chorioallantoic placenta 63, 71, 73, 77
chorioamnionitis 372

Downloaded From Vet-eBooks.com

choriocarcinoma 73
chorion 71, 72, 485, 493
chorionic villi 67, 71, 77
chromatin 443
chromatin condensation 113, 193, 429, 431, 436
chromatin integrity 429, 430
chromatin modifications 467
chromatin packaging 427
chromatin remodeling 112, 193, 428, 429, 438
chromatin structure assays (SCSA) 430, 449, 467, 469
chromosomal abnormality(ies) 215, 240, 242, 401, 406
chromosomal errors 159, 161
chromosomal integrity 405
chromosomal mutations 404
chromosome pairing 469
chromosome segregation 444, 446
chromosome visualization 403
classification of placenta type 68
cleavage stages 77, 154, 470, 540, 541
clitoral body/body of clitoris 9, 15
clitoral crura/crura of clitoris 9, 15, *41*
clitoral fossa/fossa of clitoris *13, 14*, 15, 20, 29, 34, *35, 38*, 42
clitoral glans/glans of clitoris 9, 15, 29, 34, *38*, 42, *42*
clitoris 5, *13, 14*, 15, 19, 20, 24, *26, 27, 28*, 29, 33, 34, *35, 38*, 41, 42, 45, 47, 48, 50
cloaca 51, *54*, 55, 56
cloning 402, 406
cloning, dogs 329
coagulating glands 44, *44*, 48, *49*, 63
coccygeus M. *23*
colliculus seminalis 2, 1, 16, 18, 39
collum glandis *25*, 33, *33*
comet assay 430
commissures of vulva 8
compaction 153
comparative genomics 81
conception 127, 216
conceptus 72, 91, 221
confocal analyses, evaluations 241, 242
congenital adrenal hyperplasia 222
congenital birth defects 215
connecting piece, spermatozoa 274, 275–277, 309, 311
connexin 192, 193
constrictor M. of bulbus vestibuli 12
constrictor M. of vulva and vestibule 42, *42*
contraception, dogs 330
cooling, cooling rate(s) 522, 532, 533, 534
corona glandis 12, *12*, 32, 33, *33*
corpora hemorrhagica 293
corpora lutea (corpus luteum sing.) 63
corpus albicans 6
corpus cavernosum of clitoris 47
corpus cavernosum penis 5, 12, 18, *33, 45, 51*
corpus luteum (corpora lutea) 6, *6*, 19, 24, 129, 131, 293, 512
corpus spongiosum glandis 5, 11, 12, 45, *45*, 48, *51*
corpus spongiosum penis 5, 12, 18, 32, *33*, 45, *45*, 48, *51*
cortex of ovary 5, *6*, 33
cortical contraction 390
cortical granules 297–298, 415, 529, 536, 539, 541
cotyledon(s) 29, 67, 76, 80
cotyledonary placenta 63
cow/large ruminants/ox 1, 4, 8, 25, *26, 28*, 29, 127, 132, 134
cranial preputial Mm. 12, 18, 24
cremaster M. *3*, 4, *16, 22*, 31, *31, 32*, 39, *40*, 43
cremaster muscle 260
cremasteric fascia *3*, 4
cricoid cartilage 61, *61*, 62
cricopharyngeus M. *61*
cricothyroideus M. *61*
CRISPR/Cas9 330
crossbreeding 519
crus/crura penis/corpus cavernosum 5, 12, 18, 32
cryobanking 519
cryobiology 522
cryodamage 537, 542
cryoinjury(ies) 541, 542
cryopreservation 327–328, 406, 475, 519, 520, 521, 522, 523, 529, 530, 531, 533, 535, 537, 538, 539, 540, 541, 542
cryoprotectants (CPs) 520, 521, 523, 524, 525, 526, 527, 528, 530, 531, 535, 536, 537, 538, 540, 541, 542
cryosurvival 535, 540, 541
cryotolerance 529, 539, 540, 541
crypt 29, *29*
cryptorchidism 15
C-type natriuretic peptide (CNP) 189
culture conditions, culture media 147, 161, 486, 487, 493, 494, 498, 499

Downloaded From Vet-eBooks.com

cumulus cell(s) 131, 135, 146, 147, 148, 149, 150, 151, 152, 157, 177, 178, 179, 180, 181, 186, 187, 189, 190, 192, 193, 197, 198, 238, 239, 241, 298–299, 301, 317–318, 324, 402, 403, 414, 416, 529, 530, 535, 537, 538, 539, 541, 542
  metabolism 151
cumulus expansion 149, 178, 179
cumulus oocyte complex(es) (COC) 134, 145, 147, 148, 149, 150, 151, 178, 185, 186, 187, 188, 189, 190, 192, 194, 196, 197, 198, 294, 301, 315, 316,318, 324, 415, 529, 535, 536, 538, 539, 540
cyclic adenosine monophosphate (cAMP) 134, 178, 179, 180, 182, 183, 184, 185, 186, 187, 188, 189, 190, 192, 193, 198, 413, 417, 419
cyclic guanosine monophosphate (cGMP) 182, 184, 187, 188, 189, 190, 191, 192, 193
cyclic nucleotide-gated channels (CNGC) 182
cyclic nucleotide signaling 180, 182, 188
cyclicity 216
cytokinesis 438, 536
cytoplasmic droplet, spermatozoa 281, 282, 314, 333
cytoplasmic transfer(s) 242
cytoskeleton 214, 217, 414, 436, 438, 537, 539, 541
cytostatic factor (CSF) 442
cytostatic factor (CSF) extract(s) (Xenopus) 390, 391
cytostatic factor-arrested cytoplasmic extract, (CSF extract) 390
cytotoxicity 521, 535, 536, 537, 540, 542
cytotrophoblast 68, 69, 70, 71, 73, 74, 76

d

daidzein 387
dartos muscle 260
decapacitation factors 306
decidua 360
decidual implants 76
deciduum (decidua) 65, 70, 72, 79, 80, 81
deep sequencing techniques 219
deer 67
dendritic cells 367
denuded oocyte(s) (DO) 148, 196, 197
descent of testicle 3, 9, 15
development 71, 79, 91, 92, 93, 94, 95, 97, 98, 99, 109, 115, 117, 129, 130, 134, 135, 136, 145, 147, 148, 150, 155, 156, 157, 152, 154, 155, 156, 159, 160, 178, 216, 217, 225, 237, 404, 427, 438, 441, 443, 446, 447, 448, 450, 467, 470, 471, 474, 475, 489, 499, 500, 530
developmental abnormalities 218
developmental competence, potential 152, 179, 181, 186, 190, 193, 197, 238, 240, 241, 242, 372, 437, 441, 450, 485, 512, 514, 537, 542
developmental failure 537
developmental milestones 321–322
developmental programming 217, 219, 222
diabetes mellitus 158, 371, 471, 474
diagnosis of infertility 512
dicer 109, 110, 112, 115, 116, 117, 118
diencephalon 59, 61
diestrus 34, 36, 293–294, 305, 320, 322
diet(s) 92, 94, 472, 473
di(2-ethylhexyl) phthalate (DEHP) 222
diethylstilbestrol 474
differentiation 91, 94, 114, 409, 435, 470, 485, 486, 487, 494, 496, 499
diffuse placenta 62
dimethyl sulfoxide (DMSO) 520, 536
diphtheria toxin receptor (DTR) 369
diplotene 265–266, 289
discoidal placenta 63
disorders of sexual development 331
distal part of adenohypophysis 59, *60*
DNA damage(s) 446, 535
DNA demethylation 437, 446, 469, 470
DNA hypermethylation 487
DNA methylation 219, 435, 436, 437, 438, 446, 467, 468, 469, 470, 471, 472, 473, 474, 475
DNA methyl transferase(s) (DNMTs) 437, 446, 469
dog 1, 4, 5, 8, 9, 10, 11, 12, *12*, 13, 14, *14*, 15, 41, 50, *60*, 61, *61, 62*
  breeds 252–253
  chromosomes 253–255
  developmental milestones 321
  fertility 258, 333
  fertilization 301–303
  genome 253–256
  infertility 333
  life expectancy 257
  lifespan 250, 257
  model for human genetic disorders 256–257
  onset of puberty 257–258

Downloaded From Vet-eBooks.com

dog (*Continued*)
origin 250
pregnancy, development, birth 320–322
reproductive anatomy 258–262, 282–289
reproductive physiology 262–282, 289–301
service to human society 250, 251
taxonomy 250, 252
dorsal frenulum of cervix *36, 37*
double-stranded RNAs (dsRNAs) 115
Drosha 109, 115, 118
ducts of Gärtner *26*, 29
ductuli efferentes 2, *2*
ductus deferens 1, *2, 3*, 9, 10, 12, 15, 16, *16*, 18, 20, *21*, 22, *22, 23, 24, 26*, 30, *30*, 31, *31, 32*, 38, 39, *39, 40*, 42, 43, *43*, 47, *47*, 4, *48, 49*, 258–259, 261

e

eclampsia 217
ectoderm 485, 491
efferent ductules 258, 260
egg(s) 132, 177, 178, 186, 386, 387, 389, 390, 409, 414, 415, 416, 418
egg activation 387, 390, 428, 429, 430
egg jelly 385, 386
egg membrane microdomain (MD) 390
ejaculation 270, 409
ejaculatory duct 22, 31, 39
electron microscopy 241
electrophoretogram 405
electrophysiological syncytium 177, 186, 192
elongating spermatid 267–268
embryo(s) 69, 72, 77, 78, 79, 97, 132, 134, 145, 146, 147, 153, 154, 155, 156, 157, 158, 159, 161, 162, 178, 191, 192, 196, 198, 285, 289, 291, 297–298, 300–301, 318, 320, 322, 325–326, 328–329, 359, 401, 404, 406, 435, 437, 438, 441, 443, 445, 446, 448, 450, 467, 468, 469, 474, 475, 485, 486, 489, 491, 492, 499, 512, 519, 522, 529, 530, 537, 539, 542
embryo culture 161, 510, 511, 512
embryo(nic) development 66, 73, 148, 153, 157, 158, 159, 160, 161, 178, 213, 240, 428, 429, 430, 431, 435, 437, 438, 440, 441, 444, 447, 448, 450, 468, 470, 474, 475, 485, 489, 492, 493, 501, 510, 523, 529, 530, 531, 538, 541
embryogenesis 136, 387, 429, 443, 435, 437, 440, 441, 442, 446, 447, 448, 470, 471, 472
embryo fragmentation 435
embryo(nic) genome activation (EGA) 136, 145, 214, 320, 439, 440, 441, 443, 445
embryo(nic) genome reprogramming 439, 441, 443, 444
embryo loss 240, 242
embryoid body(ies) (EBs) 74, 75
embryology 73
embryo(nic) metabolism 152, 153, 158, 159, 160, 161, 213
embryo quality 136, 158, 435, 512
embryonic cell differentiation 437
embryonic germ cells (EGCs) 469
embryonic germ lineages 486
embryonic growth 219
embryonic stem cells (ESCs) 73, 77, 178, 443, 446, 485, 486, 491, 493, 494
and induced pluripotent stem cells 329
embryonic tissues 485
embryo transfer (ET) 127, 128, 131, 147, 257, 326–327, 330, 402, 448, 450
embryo viability 158, 161, 512
endangered canids 249–251, 328, 334
endocrine-disrupting compounds (EDC) 91, 92, 94, 96, 97, 98, 99, 100, 101, 471, 472
endocrine disrupting signals 222
endocrine functions 1, 5
endocrine ovary 59, 63
endocrine testicle 59, 63
endocytosis 193
endoderm 485, 491
endogenous small interfering RNAs (endo-siRNAs) 109, 110, 115, 117
endometrial glands 93
endometrial tissue 217, 220
endometriosis 216
endometrium 29, *29*, 65, 66, 68, 69, 73, 77, 321, 322, 359, 493
endoplasmic reticulum (ER) 160, 273, 281, 294–296, 438, 529
endosymbiotic viruses 361
endovascular mimicry 65
environmental stress 219
environmental toxicants 472
enzyme assay for PLC and immunochemical depletion (Xenopus) 392

Downloaded From Vet-eBooks.com

epiblast, epiblast cells 469, 485, 486, 487, 489, 490, 491, 493, 499, 500
epidermal growth factor (EGF) 179, 180, 181, 182, 193
epididymal canal/duct/ductus epididymidis 9, 15, 20, 30
epididymal sperm 410
epididymis 1, *2*, 9, 15, 20, *21*, 30, 38, 42, 43, 47, *47, 48*, 258–261, 271–272, 281, 282, 303, 306, 307–313, 402, 410
epididymosomes 272
epigenetic changes 435, 447
epigenetic control mechanisms 430
epigenetic inheritance 435, 436, 438, 444
epigenetic marks 431, 442, 445, 449, 468, 470
epigenetic memory 435, 448
epigenetic modification(s) 219, 467, 468, 469, 470, 471, 472, 473, 474, 475
epigenetic programming 148, 213
epigenetic regulation(s) 428, 438, 441, 447
epigenetic reprogramming 467, 468, 470
epigenetic silencing of genes 65
epigenetics 467, 468, 471, 472, 489, 487
epigenome 435, 442, 449, 450, 467, 470, 471, 472, 475, 476
epigenomic landscapes 431
epimutation(s) 467, 472, 476
epithalamus *60*, 61
epithelial-mesenchymal transition 69
equine 235, 237, 240, 527, 535
ERK1/2 181, 182
erythropoiesis 73
esophagus 61
estradiol 5, 129, 131
estrogen 285, 291, 294
estrogenic 94
estrous cycle 129, 130, 258, 285, 287–288, 291–293, 294–297, 305, 316
estrus 34, 36, 285, 286–288, 291–292, 305, 320, 324
ethylene glycol (EG) 520, 536
euchromatin 441, 445
ewe *27*, 29, *29*
exchange protein activated by cAMP (EPAC) 180
exchange protein directly activated by cAMP (EPAC or RAPGEF) 182
exocoelom 71
exocrine functions 1, 5
exocytosis 193, 410, 417, 418, 419
exosomes 272
external carotid A. 62
external obturator M. *23*
external parathyroid gland 61, 62
external pudendal A. *22*, 47
external pudendal V. *22*, 47
external spermatic fascia 4, 16, *22, 26*
external urethral ostium/orifice 45, 46, 47, 48, 50, 52
external uterine ostium *14, 20, 26, 27, 28, 36, 37*, 47, 50, *51, 52*
extraabdominal (testicular) tunics 4, 16, 43
extracellular matrix (ECM) 74, 131, 149, 178, 179, 198, 409, 416, 529, 538
extraembryonic endoderm 486
extraembryonic membranes 66, 72
extraembryonic tissues 485

f

famine 467, 471
farm animals 95, 128, 519
fasciae of penis 4, *26*
fatty acid metabolism 152
fatty acid β-oxidation (FAO) 151, 152, 157
FCI, Federation Cynologique Internationale 252
Federation Cynologique Internationale (FCI) 252
feline 66, 527, 528
female
  anatomy of genital organs 288
  mammary gland 282, 289–288, 332
  reproductive physiology 289
    anestrus 285–286, 291, 293, 305
    diestrus 291–293, 305, 320, 322
    estrous cycle 258, 285, 287–288, 289–291, 294–297, 305, 316
    estrus 285, 286–289, 291–292, 305, 320, 324
    folliculogenesis and oogenesis 289–290, 300
    proestrus 288, 291–293, 321
female genital organs/female genitalia 5, 19, 24, 33, 41, 45, *46*, 48, *52*, 55, *55*, 56
female gonad 5
female reproductive tract (FRT) 360, 361, 429
female X chromosome 486
fertility 91, 92, 94, 95, 100, 101, 102, 114, 116, 117, 127, 129, 133, 134, 136, 159, 160, 177, 182, 190, 191, 195, 216, 235, 239, 240, 242, 258, 330, 359, 475, 512, 513, 514, 522, 530, 542

Downloaded From Vet-eBooks.com

fertility biomarkers 512
fertility decline 240
fertility markers 238
fertility preservation 519
fertilization 66, 132, 133, 145, 148, 153, 159, 177, 178, 183, 186, 191, 195, 198, 216, 223, 240, 300–301, 383, 385, 386, 387, 390, 401, 402, 404, 405, 409, 414, 415, 416, 427, 428, 430, 435, 436, 437, 438, 440, 442, 443, 445, 448, 449, 468, 470, 474, 485, 510, 513, 523, 524, 526, 528, 529, 530, 537, 539, 541
  failure 216
fetal development 63, 70, 218, 360, 370, 371, 372, 404
fetal growth 217, 221
fetal growth restriction (FGR) 359, 370, 513
fetal high liver triglycerides 370
fetal hyperglycemia 370
fetal hyperinsulinemia 370
fetal loss 242, 365
fetal malformations 513
fetal melanocortin system 370
fetal membranes 63, 71
fetal physiology 80
fetal–maternal interaction 76, 79, 81
fetus(es) 66, 67, 6991, 92, 93, 94, 95, 97, 98, 99, 101, 359, 364, 365, 371, 372, 485, 498
fibrocartilage of os penis 45, *45*, 48
fibrous isthmus of thyroid gland 61, *61*
fibrocartilaginous plate of pelvic urethra *44*, 45
fimbriae 7, 34, 41
flagellum 264, 267, 269, 273, 275, 277–278, 304, 307–314, 315–318, 429
fluorescence in situ hybridization (FISH) 255, 326, 328, 332, 334, 404
follicle(s) 5, *6*, 19, 24, 33, 41, 92, 93, 94, 95, 96, 97, 98, 99, 102, 128, 129, 130, 131, 132, 133, 134, 135, 136, 145, 147, 148, 180, 190, 192, 193, 214, 236, 237, 240, 241, 416, 474, 529
follicle competence 136
follicle loss 160, 236
follicle maturation 239
follicle selection 238
follicles, ovarian 63
  atretic 291
  multioocyte 291
  preantral 290
  primary 290
  primordial 290
  secondary 290
  tertiary 290
  types 290
follicle stimulating hormone (FSH) 95, 98, 99, 130, 131, 132, 133, 134, 150, 178, 179, 180, 181, 182, 190, 195, 196, 198, 294
follicular activity 237
follicular cells 131, 239
follicular development 177, 179, 192, 238, 239, 241
follicular dynamics 235
follicular environment 238
follicular fluid(s) (FF) 135, 147, 149, 191, 238, 239, 510, 512, 539
follicular growth 191, 238
follicular physiology 128, 135
follicular reserves 237
folliculogenesis 94, 96, 99, 127, 128, 134, 136, 187, 192, 289–290, 300
folliculome 134
fornix of vagina/vaginal fornix 8, *13*, 14, *14*, 20, *26, 27, 28*, 29, *35, 36, 37*, 42, 47, 50, 287
fossa glandis 33, *33*
fourier transform infrared spectroscopy (FTIR) 510, 511, 512
freezing 519, 530, 531, 533, 541, 542
frenulum of clitoral prepuce 9, 34, *38*
frog eggs 383
frog laboratory 383
frog oocytes 383
fructose 262, 272, 309–308, 310–311

g

gamete(s) 109, 110, 114, 177, 178, 183, 188, 198, 436, 443, 467, 468, 475, 487
gametogenesis 109, 110, 115, 117, 437, 446, 468, 472
gap junction(s) 146, 148, 149, 150, 177, 190, 192, 193, 535, 530, 538
gap junction communication (GJC) 179, 186, 190, 192, 193, 197, 198
gas chromatography–mass spectrometry (GC–MS) 512
gastrulation. 486
gender 512
gene activation 429
genebank 519

Downloaded From Vet-eBooks.com

gene expression 78, 110, 119, 179, 219, 222, 238, 241, 435, 448, 467, 470, 499, 500, 542
gene imprinting 437, 440
gene manipulation 77
generation(s) 364, 467, 468, 470, 471, 472, 476
gene reactivation 448
gene sequences 406
gene silencing 444, 445, 448
genetic disorders 406
genetic diversity 513
genetic modification 501
genetically engineered pigs 223
genetically modified dogs 329–330
  gene-edited dogs 330
  transgenic dogs 330
genetics 519
genistein 387
genital apparatus/system/tract *23, 27, 28*, 30, *32, 35*, 38, *41*, 42, 47, 51, 56
genital fold 2, 15, 31, *40*, 43, *44*, 48, *49*
genital organs. *see also individual organs*
  female. *see anatomy, female reproductive organs*
  male. *see anatomy, male reproductive organs*
genital tract 361, 412
genitofemoralis N. *22*
genome(s) 253–254, 430, 435, 436
genome cloning 406
genome integrity 117, 447
genome modifications 442
genome remodeling 438
genome reprogramming 435, 443, 445, 448
genome stability 446, 448
genome transcription 440, 441, 443
genomic hybridization 215
genomic imprinting 469
genomic landscapes 431
germ cell(s) 92, 93, 97, 112, 113, 114, 115, 117, 119, 177, 435, 467, 468, 469, 471, 472, 475, 476, 485, 529
germ cell maturation 113
germ cell populations 112
germ cell-specific miRNAs 112
germinal epithelium 284
germinal vesicle(s) (GVs) 145, 147, 177, 178, 198, 295–296, 298, 300, 324, 384, 386, 474, 525, 526, 527, 529, 530, 532, 536, 537, 538, 542
germinal vesicle breakdown (GVBD) 177, 198, 214, 215, 386, 529
germ layers 491, 493
germline 114, 470, 485
germline transmission 494
germplasm 522, 540
gestation 71, 72, 73, 79, 77, 81, 91, 92, 93, 94, 95, 96, 97, 98, 99, 100, 101, 102, 128, 220, 320–321, 359, 361, 364, 367, 371, 372, 467, 471, 473, 474, 485
gestational disease 366
gestational hypertension 359, 366
gills *55, 56*
gingivitis 363
glandular isthmus of thyroid gland 61, *61*
glans penis 4, 11, 12, *12*, 18, *18, 25, 26*, 32, *33*, 4, *40*, 45, *45*, 48, *51*
global profiling technologies 502
gluconeogenesis, sperm 312
glucose 149, 150, 151, 152, 153, 154, 155, 308, 312–311, 474, 537
  metabolism 149
  transporters 311
glutamine 151, 154, 156, 157
glutamine metabolism 151
glutathione (GSH) 440
glycerol 520
glycolysis 145, 149, 150, 151, 153, 154, 155, 194
glycoproteins, zona pellucida 299
glycosylation 149
goat 1, 4, *28*, 29, *29*, *60*, 61, *61, 62*, 67
Golgi apparatus 241, 266, 273–298, 410, 529
gonadal differentiation 93
gonadal tissues 519
gonadotropin(s) 128, 129, 134, 182, 186, 187
gonads 92
G protein-coupled receptor(s) (GPCRs) 180, 182, 183
G protein-coupled receptor kinase(s) (GRKs) 180
granulosa cells 96, 129, 131, 135, 150, 177, 179, 180, 181, 187, 189, 190, 191, 192, 193, 198, 238, 239
green fluorescent protein (GFP) 330
growth restriction 79, 363
growth-retarded fetuses 97
guanosine triphosphate (GTP) 439
gubernaculum testis 3
guinea pig 79

h

habenula of cerebral epiphysis 61
haploid embryos 406

Downloaded From Vet-eBooks.com

head of epididymis 4, 10, *16*, 20, *21*, 30, *30, 32*, 38, *39*, 42, 43, *43, 47, 48*
heart *55*
heat (season) 291
  shock proteins 304
heifers 96, 100, 130, 132
helium (He) 540
hESC-derived embryoid bodies (EB) 74, 75
heterochromatin 109, 440, 441, 444, 445, 446, 447
hexokinase activity 153
hexosamine biosynthetic pathway (HBP) 145, 149, 150, 151
high hydrostatic pressure (HHP) 541
histology
  epididymis 260
  ovary 284–285, 291
  testis 264–266, 268
  uterotubal junction 286
histone acetylation 443, 444
histone acetyltransferase enzymes (HATs) 444
histone deacetylase enzymes (HDACs) 443, 446
histone deacetylase inhibitors 219
histone methylation 444, 445, 447
histone modification(s) 438, 440, 443, 444, 445, 448, 449, 467, 468, 469, 470, 473, 474, 475
histone(s) 427, 428, 429, 435, 438, 440, 442, 444, 445, 446, 448, 468, 469, 470
hollow part of infundibulum *60*
hormonal stimulation 127
horse(s) 1, 4, 5, 7, 8, 30, 31, 32, 33, *33, 60*, 61, *61*, 62, *62*, 66, 67, 235
HSUS, The Humane Society of the United States 249–250
human chorionic somatomammotrophin (hCS) 78
human embryonic stem cells (hESCs) 74, 486, 487
human embryos 214
human reproduction 213
human reproductive medicine 235
Human society, dogs importance to 249–250
The Humane Society of the United States (HSUS) 249–250
humans 63
hyaluronic acid (HA) 146, 149
hymen 15, 20, 29, 34, 42, 47
hyperglycemia 371
hyperosmotic stress 541
hyperpolarization 417
hypertensive phenotypes 367
hypoblast 485, 486, 489
hypophyseal sac/Rathke's pouch 59, 61
hypophysis/pituitary gland 59 *60*, 61
hypothalamus 59, *60*
hypoxia 194
hysterectomies 66, 82

i

ice crystals 519, 522, 536
ice formation 519, 520, 522, 529, 533, 534, 535, 537, 542
ICSI. see intracytoplasmic sperm injection
immune cells 367, 368, 370, 372
immune function 218
immune suppression 72
immune system 129, 359, 363, 365, 367, 370, 371, 372
immunoprecipitation, SDS-PAGE, and immunoblotting (Xenopus) 391
immunosuppression 359
immununocontraceptive vaccine 216
implantation 66, 69, 80, 81, 100, 132, 153, 158, 216, 298, 321, 359, 372, 492, 510, 512
imprinted genes 470, 471, 473, 474, 475
imprinting 219
indirect immunofluorescent study (Xenopus) 393
indoleamine 2,-3-dioxygenase (IDO) 365
induced pluripotent stem cells (iPSC) 487, 494, 500
infection(s) 361, 363, 364, 372, 367
infertility 96, 110, 112, 114, 115, 127, 129, 145, 158, 161, 178, 185, 191, 192, 198, 239, 333, 367, 401, 402 409, 428, 429, 475, 487, 488, 511, 512
inflammation 359, 360, 361, 363, 363, 365, 366, 367, 369, 370, 371, 372, 373
inflammatory response system 218
influenza infection 372
infundibulum
  of neurohypophysis 59, 60
  of uterine tube 5, 13, 19, 19, 25, 26, 27, 28, 34, 41, 45
inguinal canal 3, 3, 14, 15, 41, 47
inguinal ring
  deep 3, 8, 34, 39, 52
  superficial 3, 18

Downloaded From Vet-eBooks.com

inhibin 5, 129, 131
inner acrosomal membrane (IAM) 410, 411
inner cell mass (ICM) 66, 71, 78, 154, 155, 322, 445, 447, 470, 485, 486, 487, 489, 491, 492, 493, 499, 500, 501
insemination 216, 414, 415
insemination, artificial. see artificial insemination (AI)
in situ hybridization 184, 215
insulin resistance 65, 371
insulin-like growth factor 63
integrative Personal Omics Profile (iPOP) 509
integrin(s) 65
intercornual ligament 25, 26, 27, 28, 42
intermediate part of adenohypophysis 59, 60
internal abdominal oblique M. 3, *3*
internal cremaster M. 22
internal spermatic fascia 3, 4, 10, 22, 26, 31, 32, 39
interspecies chimeras 489
interstitial (Leydig) cells 63
intestine 55, 56, 56
intraabdominal (testicular) tunics 4, 47
intraabdominal testicles 51, 56
intracytoplasmic morphologically selected sperm injection (IMSI) 401
intracytoplasmic sperm injection (ICSI) 235, 240, 241, 242, 326, 401, 402, 403, 447, 475, 476, 523, 524, 526, 527, 528, 530
intrauterine fetal growth 359
intrauterine growth restriction (IUGR) 70, 79, 96, 217, 218, 219, 222, 470
intrauterine infection 361
intrauterine infusion 372
intrauterine insemination 475
intravaginal infection 361
in utero inflammation (IUI) 360, 361, 371
in vitro fertilization (IVF) 127, 132, 133, 134, 135, 160, 186, 214, 216, 239, 240, 324–325, 401, 414, 415, 418, 430, 445, 447, 449, 450, 475, 476, 512, 513, 522, 524, 525, 526, 527, 528, 530, 532, 541, 542
  with *in vitro* matured oocytes 325
  with *in vivo* matured oocytes 325
in vitro maturation (IVM) 132, 134, 135, 149, 150, 151, 161, 178, 179, 180, 185, 186, 187, 188, 190, 191, 193, 197, 198, 214, 242, 324, 475, 532, 538, 539, 542
in vitro protein-tyrosine kinase assay 391
IP3 assay (Xenopus) 392
ischemia 194
ischiatic/ischial arch 5, 12, 29, 34, 42
ischiocavernosus M. 5, 12, 18, 23, 24, 32, 40, 41, 44, 50
isthmus of thyroid gland 61
isthmus of uterine tube 7, 41
IZUMO1 319, 330

j

journey of sperm in female reproductive tract 301–302, 306

k

karyotypes 253–255, 404
KC, Kennel Club 252
kinetochore 436
Kennel Club (KC) 252
kidneys *55*, 56, *56*, 62

l

labia major/major labium 8, 15, *41*, 42, *42*
labia minor/minor labium 8, 15, *41*, 42, *42*
labiae of vulva 20, 34
laboratory animals 50
lactate 148, 149, 150, 151, 152, 153, 154, 155, 156, 261–262, 310–312
lactate dehydrogenase (LDH) 155, 156
lactation 65, 96, 98, 472
lamin(s) 436, 439, 440
lateral recess of clitoris *38*
lateral sinus of clitoris *38*
lateral vesical ligament/of urinary bladder *23, 32, 46, 52*
lectin 278, 282, 312, 316, 329
left adrenal gland *62*
left kidney *62*
left lobe of thyroid gland *61*
lentiviral transduction 78
leptin 218, 219, 473
leptotene 267–268
levator ani M. *23*
Leydig cells 2, 187
life expectancy 257
lifespan 257
ligament of tail of epididymis 4, 15, 22, *30*, 31, 38, 39, *39*, 43, *43*, 47, *47, 48*
lipids 151, 152, 154, 156, 157, 160, 188, 189, 195, 219, 222, 522, 529, 530, 540, 541, 542
  oocyte 295–296
  sperm membranes 278–281, 303–305, 306, 318, 327

Downloaded From Vet-eBooks.com

lipopolysaccharide (LPS) 360, 361, 369
liquid nitrogen (LN2) 519, 535, 536, 538, 539, 540
litter size 221
live-cell imaging and genome manipulations (Xenopus) 394
liver *56*, 59, 63
livestock breeds 519
luteinizing hormone (LH) 99, 130, 131, 133, 135, 178, 179, 182, 190, 193, 195, 290
lymphocytes 367
lysosomal degradation 442

m

macrophage(s) 365, 367, 368, 369, 371
major vestibular glands 15, 29, *42*
male
  anatomy of genital organs 257–288
  histology of testis 264–266, 268
  reproductive physiology 262–289
    acrosome reaction 301, 304–308, 309–312, 315, 317, 319, 326
    capacitation 302–311
    spermatogenesis 262–270
male fertility 113, 427, 430
male genital organs/male genitalia 1, 9, 15, 20, 30, 38, *40*, 42, 47, 51, *54*, 55, 56, *56*
male germ cell(s) 117
male gonad 1
male infertility 430, 512
male urethra 1, 12, 19
malnutrition 92
mammalian species 61
mammary gland(s) 5, 9, 50, *53, 54*
  female 281, 287–288, 330
mammary growth 63
manchette 266
mare(s) 33, 34, 35, *35, 36*, 38, 50, 63, 128, 235, 236, 237
mass spectrometry (MS) 510, 511
maternal age(ing) 158, 235, 239, 240, 241
maternal bacterial infections 372
maternal decidua 81
maternal endometrium 66
maternal–fetal interactions. 80
maternal–fetal interface 367, 369
maternal gestational supplementation 219
maternal physiology 69
maternal stress 364
maternal viral infections 372
maternal-zygotic transition (MZT) 436, 437, 438
maturation 91, 93, 95, 114, 133, 134, 147, 148, 150, 151 157, 178, 185, 186, 187, 188, 189, 192, 193, 194, 196, 197, 198, 410, 529, 537, 538, 540, 541
maturation promoting factor (MPF) 178, 179, 436, 442, 530, 538
mechanical stresses 541
median ligament of urinary bladder *46, 52*
median sinus of clitoris *38*
mediastinum testis 2, *2*, 30
medulla of ovary 5, *6*, 33
meiosis 92, 93, 94, 97, 112, 114, 128, 129, 134, 136, 145, 149, 150, 152, 177, 178, 183, 184, 185, 186, 187, 188, 190, 191, 193, 196, 197, 198, 215, 236, 384, 385, 387, 401, 409, 410, 427, 436, 442, 449, 469, 522, 529, 530, 537, 540, 541, 542
  oogenesis 285, 289
  spermatogenesis 259, 260, 262–270
membrane remodeling 303, 305
menarche 101
menopause 100, 101, 129, 236, 238, 239
menstrual cycle(s) 127, 128, 129, 195, 236, 237, 529
mesencephalic tectum *60*
mesepididymis 7
mesoderm 485, 491
mesoductus deferens 2, 3, *3, 22, 30, 31*
mesofuniculus 3, *3*, 10, 16, *22, 31, 39*
mesometrium 8, 14, *19, 20, 26*, 27, *27, 28, 46*, 47, *52*, 282
mesorchium 2, 3, *3, 16, 21, 22, 30, 31, 39, 43, 47, 48*, 51, *54*
mesosalpinx 7, 14, 19, *19, 20, 26, 27, 28, 35*, 45, *46, 52*, 282–283, 286
mesovarium 5, 7, 14, *19, 26, 27*, 33, *35*, 45, *46, 52*, 282–283
metabolic activity 145, 147, 152, 153, 161, 195, 519
metabolic biomarker(s) 157, 158
metabolic disease(s) 158, 161
metabolic disorder(s) 222, 371
metabolic enzyme activity 148, 151
metabolic exchange 66
metabolic pathways 146, 149, 150, 155
metabolic profiling 509, 510, 511, 512
metabolic regulation 218
metabolic switch 193, 194, 197
metabolic syndrome 195, 198

Downloaded From Vet-eBooks.com

metabolism 109, 145, 147, 150, 151, 152, 154, 157, 159, 160, 161
metabolite(s) 135, 147, 148, 158, 509, 510, 512, 513
  associated proteins 539
metabolome(s) 509, 510, 511
  analysis 510, 512
metabolomics 146, 147, 157, 158, 509, 510, 512, 513, 514
metaphase I (MI) 177, 529
metaphase II (MII) 147, 148, 150, 152, 178, 185, 198, 215, 242, 390, 402, 403, 404, 406, 436, 442, 449, 471, 474, 523, 524, 525, 526, 527, 530, 531, 532, 536, 537, 539, 540, 541, 542
metestrus. *see diestrus*
methylation 443
methylome 474
methyltransferase(s) 446, 447
microbial infections 360
microbiome 373
microflora 36
microorganisms 367, 539
microRNAs (miRNAs) 109, 110, 111, 112, 113, 114, 117, 193, 468, 474
microtubules 277, 296, 529, 537, 539, 540, 541
  associated proteins 539
microvilli 217
midpiece 273, 277, 278, 304, 305–311, 314, 333
minor vestibular glands 15, 20, 29, 34
miscarriage(s) 158, 215, 240, 369
mitochondria 152, 156, 157, 159, 160, 241, 242, 529, 541, 542
  oocyte 295–296
  spermatozoon 272, 276–278, 306–307
mitochondria function 159, 160, 161, 195, 221
mitochondrial activity 160
mitochondrial disease(s) 161
mitochondrial DNA (mtDNA) 241, 250
  mutations 159
mitochondrial dynamics 217
mitochondrial dysfunction(s) 159, 218
mitochondrial genome 254
mitochondrial integrity 159
mitochondrial membrane potential 159, 160
mitochondrial morphology 217
mitochondrial oxidation 150
mitochondrial respiration 151
mitochondrial transfer(s) 242
mitogen activated protein kinase (MAPK) 193, 390, 436, 530, 538
mitosis 92, 112, 427, 436, 438, 441, 442, 444, 485, 486
monovular 128
morphokinetics 158
morphologic abnormalities 240
morphology
  follicle morphology 289–293
  oocyte morphology 293–299
  sperm morphology 272–281
morula 66, 153, 154, 155, 156, 215, 437
motility 409
mouse 1, 5, 42, 43, *43*, 44, *44*, 45, *45*, *46*, 47, 48, 50, *53*, *60*, 61, *61*, 62, *62*, 63
mRNA(s) 109, 440, 529
multicolor fluorescence in situ hybridization (multicolor FISH) 405, 406
multioocyte follicle 291
murine 527
mutagens 405
myometrial vessels 81
myometrium 77, 79

n

Na^+/K^+-ATPase protein synthesis 154
$NAD(P)^+$:NAD(P)H 145
NADPH 149, 151, 155, 156
NANOG 268–269
natriuretic peptide family 190, 191
natural killer cells 365, 367, 368, 369
natural killer T (NKT) cells 368, 369
navicular fossa *33*
near-infrared (NIR) 510, 511, 512
necrosis 541
neonates 217
neural lobe of neurohypophysis 59, *60*
neurochemicals 372
neurohypophyseal recess 59
neurohypophysis 59, *60*
neutrophil(s) 367, 368, 369
noncanonical miRNAs 11
noncoding RNAs (ncRNAs) 110, 438, 467
nonhuman primates 80
Norwegian Kennel Club 322
nuclear architecture 429
nuclear envelope (NE) 438
nuclear lamina 438
nuclear matrix 440, 442
nuclear matrix attachment regions (MARs) 428
nuclear maturation 178, 179

Downloaded From Vet-eBooks.com

nuclear pore complex(es) (NPC) 438, 436, 439
nuclear pores 110
nuclear remodeling 219, 447, 448
nuclear transfer 219, 448, 450
nucleolar organization 440
nucleoli 441
nucleolus 295
nucleolus organizer regions (NORs) 441
nucleolus precursor bodies (NPBs) 441
nucleophosmin 441
nucleoplasmins 440
nucleoporins 439
nucleosomal DNA 443
nucleosome(s) 443, 468
nucleus
  oocyte (germinal vesicle) 295, 296, 298, 300, 324
  spermatid 264–267
  spermatocyte 265–266
  spermatozoon 274–276
nutrient exchange 218
nutrient restriction 79, 218, 220, 222
nutrient(s) 65, 69
nutrition 91, 94
nutritional supplementation 219

O

obesity 91, 100, 101, 159, 161, 223, 333, 370, 371, 473, 474
offspring pathologies 370
olfactory receptor, sperm 314
oligoasthenozoospermia 272
oligozoospermic patients 475, 511
omega fatty acids 221
oncogenes 499
onset of puberty 257–258
oocyte(s) 92, 94, 95, 97, 102, 110, 127, 128, 129, 131, 132, 133, 134, 135, 136, 145, 146, 147, 148, 149, 150, 151, 152, 157, 158, 159, 160, 161, 162, 191, 177, 178, 179, 183, 184, 185, 186, 187, 189, 190, 191, 192, 193, 194, 196, 197, 198, 181, 187, 188, 198, 214, 215, 216, 217, 236, 238, 239, 240, 241, 242, 294–300, 383, 385, 386, 387, 389, 390, 401, 403, 406, 409, 416, 428, 435, 436, 439, 441, 442, 448, 449, 450, 473, 474, 475, 510, 512, 519, 521, 522, 523, 527, 529, 530, 533, 534, 535, 537, 539, 540, 541, 542
oocyte developmental competence 300, 324
oocyte donation 240
oocyte maturation 290, 297–299
  oocyte *in vitro* maturation (IVM) 297, 321–324
  oocyte *in vivo* maturation 297
oocyte meiotic competence 300, 327
oocyte morphology
  cortical granules 294–297
  cytoplasm (ooplasm) 296, 320, 326
  endoplasmic reticulum 294–296
  germinal vesicle 295, 296, 300, 324
  Golgi complex 296, 298
  microtubules 296
  mitochondria 296
  nucleus 294–295, 329
oogenesis 110, 134, 285, 289, 384, 386, 469, 470
oogonia 92, 93, 94, 102, 289
oral cavity 360
orchiectomized male 4
organogenesis 435
origin of dogs 250–252
os penis 5, 11, 45, *45*, 48, *51*, 331
osmolality 531, 533
osmotic stress 520, 531, 535, 537, 541, 542
outer acrosomal membrane (OAM) 410, 411, 414
ovarian A. *28*
ovarian activity 236, 237, 238
ovarian age(ing) 128, 132
ovarian bursa 7, 13, 19, *19, 20*, 25, *28*, 41, *41*, 283–285, 324
ovarian cancer 223
ovarian cycles 129
ovarian cysts 133
ovarian function 91, 92, 98, 99, 100, 102, 128
ovarian hilus 5, 19, 24
ovarian hyperstimulation syndrome (OHSS) 132, 133, 134
ovarian/ovulation fossa 6, *6*, 33
ovarian physiology 127, 128, 133, 136, 182, 196
ovarian reserve 91, 92, 95, 96, 97, 98, 99, 102, 128, 129, 131, 132, 236, 238
ovarian stimulation 132, 133, 158
ovarian stroma 5, *6*
ovarian tissue(s) 127, 128, 384, 519
ovary(ies) 5, 13, *13*, 19, *19*, 24, 25, *26*, 27, *28*, 33, *35*, 41, *41, 45, 46*, 48, *52*, 55, *55*, 56, *56*, 92, 128, 129, 130, 132, 134, 136, 177, 182, 187, 191, 192, 214, 215, 236, 237, 239, 384, 416, 512, 542

Downloaded From Vet-eBooks.com

anatomy 282–285, 289, 293
follicle development 289–290, 300
preovulatory follicle 290, 293, 294, 300, 324
primary follicle 290
primordial follicle 285, 290, 298
secondary follicle 290
tertiary follicle 290
follicle histology 285, 300
folliculogenesis 289–290, 300
oogenesis 289
overnutrition 91, 92, 94, 96, 97, 98, 100, 101, 160
oviduct(s) 55, *55*, 145, 152, 154, 240, 402, 404
oviduct (uterine tube) 282, 285–286
oviductal fluids 147, 153, 155
oviductal funnel *55*
ovisac 55, *55*
ovulation 98, 128, 129, 131, 132, 133, 135, 136, 153, 178, 179, 181, 186, 191, 195, 177, 185, 236, 237, 238, 240, 258, 285, 289–292, 298–301, 307, 316, 320, 324, 385, 473, 529
ovulatory failure 238, 240
ovule/oocyte/ovocyte 5
ox *6, 61, 62*
oxidation 153, 155
oxidative damage 241
oxidative phosphorylation150, 156, 159, 214, 217
oxidative stress 151, 153, 159, 160, 161, 218, 371
oxygen consumption 76, 148, 154, 155, 157
oxygen environments 74
oxygen exchange 71
oxytocin 5

p

pachytene 263, 267–268, 289
pachytene spermatocyte 254, 256, 263, 265–270
pampiniform plexus *22*
pancreas *55, 56*
pandemic influenza A (IA) 363
papillae of mammary glands 50
papilla of uterine tube 7, 14, 34
PAR, pseudoautosomal region 253
paracrine factors 181
paramesometric ducts 7
paraprostatic gland 39
parathyroid glands 62
parenchyma 2, 5
parietal peritoneum 3, 14
parthenogenetic egg activation 386
parturition, dog 287, 294, 322
paternal (sperm) chromosome analysis 402
paternal genome 431
pathogens 360, 361
peduncle of cerebral epiphysis 61
pelvic symphysis 32
penis 1, 11, 12, *12*, 18, *18, 22*, 23, 24, *24, 25, 26*, 32, *33*, 40, *44*, 45, *45, 48, 51*, 258–259, 261–262
pentose phosphate pathway (PPP) 145, 149, 150, 151, 153
pericentric heterochromatin compaction 443
pericentromeric chromosome loci 446
perineal fasciae 4
perineal glands, major and minor 41, 42, *42*
perineal region 4
perineal sinus 41, 42
periodontal diseases (PD) 363, 363, 364
peristalsis 216
perivitelline space 241
personalized molecular diagnosis and treatments 514
Pet Food Manufacturers Association (PFMA) 249
PFMA, Pet Food Manufacturers Association 249
pharyngeal part of adenohypophysis 59, 61
phosphatase
dual-specificity phosphatase (DUSP3, DUSP4) 309
protein tyrosine phosphatase, PTPN11 308–309
protein tyrosine phosphatase, PTP1B 309
phosphatidylinositol 3-kinase (PI3K) 180
phosphodiesterase (PDE) 179, 180, 181, 182, 183, 184, 185, 186, 187, 188, 189, 190
inhibitor(s) 134, 181, 182, 183, 185, 186, 187, 188, 196
physiology, reproductive. *see reproductive physiology*
female 289–294
male 262–282
pig embryo(s) 213, 214
pig(s)s, piglet(s) 1, 4, 8, 15, 18 *18*, 19, 23, 24, 44, *60*, 61, *61*, 62, *62*, 66, 96, 218, 220, 221, 489, 490, 493, 513
piRNAs 110, 117, 118, 119
Pit Bull Terrier 329

Downloaded From Vet-eBooks.com

Piwi-interacting RNAs (piRNAs) 109
PIWI proteins 268
Piwi subfamilies 109
placenta(s) 29 59 63, 65, 66, 67, 68, 69, 70, 71, 74, 76, 77, 78, 79, 80, 81, 82, 217, 219, 220, 359, 361, 365, 366, 372, 473, 475, 485
  classification 66, 67
  disorders 80
  development 66, 71, 73
  function 100
  inflammation 363, 364, 367, 370, 371, 372
  insufficiency 97
  transfer 79
placentation 77, 79, 80, 81, 92, 489 , 493
placentome 29
pluripotency 448, 486, 487, 489, 490, 491, 493, 494, 498, 499, 500, 501, 502
  gene expression 490, 496, 498, 499
pluripotent gene reactivation 448
pluripotent markers 489, 490
pluripotent porcine stem cells 485
pluripotent stem cells 447, 487, 494
pneumatic duct *55, 56*
polar body(ies) 401, 403, 415, 436, 529
polarized light microscope, polscope 542
pollutants 471, 472
polycystic ovarian syndrome (PCOS) 96, 161, 195, 198, 223, 471, 474, 513
polycystic ovaries (PCOs) 132
polyethylene glycol (PEG) 520
polyploidy 215
polyspermy 320, 325, 326, 530
polyubiquitination 447
porcine 151, 526, 527, 531, 535
  culture 214
porcine embryonic stem cells (pESCs) 218, 487, 488, 489, 491, 493, 494
porcine endogenous retroviral (PERV) transmission 501
porcine GV oocytes 537, 540, 541
porcine-induced pluripotent stem cells (piPSC) 488, 489, 494, 495, 498, 499, 500, 501
porcine inner cell mass (ICM) 489, 491
porcine in vitro fertilization (IVF) 214
porcine in vitro maturation (IVM) 214
porcine MII oocytes 538, 540
porcine xenografts 501
postimplantation embryo(s) 486
posttranslational modifications (PTMs) 428, 430, 443
preeclampsia (PE) 70, 216, 217, 359, 363, 364, 365, 366, 367, 368, 369, 470, 511, 513
pregnancy(ies) 34, 65, 66, 67, 73, 75, 77, 79, 80, 81, 82, 91, 94, 95, 97, 98, 100, 101, 127, 129, 131, 133, 134, 136, 148, 158, 159, 160, 216, 217, 220, 221, 222, 223, 239, 240, 241, 258, 282, 287–289, 291, 320–322, 323, 333–334, 359, 360, 361, 363, 364, 365, 366, 367, 368, 369, 370, 371, 372, 373, 448, 470, 471, 472, 473, 512, 513, 522, 539
  loss 242, 364, 365, 401, 404
preimplantation
  development 81, 217, 470, 475, 514
  embryo 320, 325–326, 327
preimplantation genetic diagnosis (PGD) 401
preleptotene 267
premature chromosome condensation (PCC) 402, 403, 404, 406
premature ovarian failure 191
prepuce 1, 11, 12, *12*, 18, *18*, 23, 24, *25, 26*, 32, 33, *33*, 38, 40, 41, 42, 47, 48
  of clitoris/clitoral prepuce 29, *38*, 42, *42*, 45
preputial
  cavity 12, 20, *33, 51*
  diverticulum 18, *18*
  fold 33, *33*
  fornix/fornix of prepuce 45, *45*, 48, *51*
  gland *46*, 47, 48, 50, *52*
  ostium/orifice 5, 12, *33*, 45, *45*, 48, *51*
  ring 33, *33*
preterm birth (PTB) 359, 361, 363, 364, 365, 368, 369
preterm labor (PTL) 360, 361
prezygotic chromosomal examination 401
prezygotic gamete chromosome examination 406
prezygotic selection of spermatozoa 406
primary miRNAs (pri-miRNAs) 110, 112
primary oocyte 289–290, 296, 300, 324
primate models 66
primates 7
primordial follicles 236, 238
primordial germ cells (PGCs) 109, 236, 289, 427, 468, 469
proestrus 288, 291–292, 321
progesterone 5, 131, 285–286, 290–294, 298, 301, 305–306, 308, 317, 318, 320, 322, 326
progesterone receptor 306
prolactin 316, 320

Downloaded From Vet-eBooks.com

pronuclear development 216, 435, 436, 438, 439, 440, 442, 444, 447, 448, 450
pronuclear epigenome(s) 450
pronuclear histones 443
pronucleus 320
proper ligament of ovary 7, 13, *20, 26, 27, 28*, 41
proper ligament of testicle 4, 15, *21*, 22, *30*, 31, *31*, 38, *39*, 42, *43, 48*
propylene glycol (PG) 520
prostaglandin F2α (PGF2α) 63
prostasomes 272
prostate (gland) 4, 10, 11, 12, 15, 16, 17, *17*, 18, 23 *23, 24*, 31, *32*, 39, 40, *40*, 43, 44, *44*, 48, *49*, 63, 258–259, 262, 270–272, 331–332
prostatic urethra 2
protamines 276, 427, 428, 429, 430, 440
proteasomal degradation 440, 442, 447, 448
proteasomal inhibitors 442, 448, 449
proteasome(s) 442, 448, 449, 450
protein identification by mass spectrometry analysis (Xenopus) 394
protein kinase A (PKA) 180, 180, 181, 182, 184, 185, 186, 413, 414, 418
protein kinase C (PKC) 181, 194, 418
protein tyrosine phosphatase, PTPN11 309
protein tyrosine phosphorylation 302–303, 304–309
proteolysis 435
proteomic techniques 510
proton nuclear magnetic resonance spectroscopy (^{1}H NMR) 510, 511, 512, 513
proximal centriole 216, 442
pseudoautosomal region (PAR) 254
pseudopregnancy 291, 293, 320, 404
puberty 129, 131, 177, 222, 223, 236, 529
  onset 257–258
pudendal fissure 9
pudendoepigastric trunk A. *22*
pudendoepigastric trunk V. *22*
pulvini (cervicales) 19, *20, 27*
pyramidal lobe of thyroid gland *61*, 62
pyruvate metabolism 148, 149, 150, 151, 152, 153, 154, 155, 156, 157

r

rabbit 1, 38, *39, 40, 41, 42*, 43, 50, *53, 60*, 61, *61*, 62, *62*, 79, 528
radiation 405
radiolabeled substrates 145
ram 22, 23, *25*
Raman spectroscopy 510, 511, 512, 513
Ran GTPase 439
Ran-GTP dependent mechanism 439
rap guanine nucleotide exchange factor (RAPGEF) 180
raphe penis 18, *18*
rat 1, 41, 43, 44, 47, *47, 48, 49*, 50, *50, 51, 52, 54, 60*, 61, *61*, 62, *62*, 63
rat embryonic stem cells (ESCs) 487
reactive oxygen species (ROS) 159, 160, 161, 261, 272, 304–305
reconstructed oocytes 404
reconstructed zygotes 448
red fluorescent protein328
redox balance 159, 161
regenerative therapies 499
regulator of chromosome condensation 1 (RCC1) 439
regulatory T (T-reg) cells 369
relaxin 5, 320
renal arteries *62*
reproductive aging 136, 235, 239, 241, 242
reproductive biology 509, 510, 513
reproductive biotechnology 513
reproductive capacity 97, 101
reproductive cessation 236, 237
reproductive cycles 236, 237
reproductive disease 223
reproductive disorders 470, 513, 514
reproductive failure 236
reproductive life span 239
reproductive management 127
reproductive organs 177
reproductive performance 430, 431
reproductive physiology
  female 289–294
  male 262–282
  seasonality 271
reproductive potential 95, 512
reproductive quiescence 238
reproductive senescence 237, 238
reproductive success 65
reproductive system 1
reproductive technologies 513
reproductive toxicology 136
reproductive tract 235, 361, 367, 242
residual body 266, 267, 281
rete testis 2, *2*, 258, 260
retinoblastoma 475

Downloaded From Vet-eBooks.com

retractor penis M. 18, *22, 23, 24, 33*
ribonuclease III (RNase III) 110
right adrenal gland *62*
right kidney *62*
right lobe of thyroid gland *61*
RNAi 110
RNA-induced silencing complex (RISC) 112
RNA polymerase II (RNA Pol II) 110
RNA sequencing 499, 500
RNA transcription 427
Robertsonian translocation 215, 404
rodents 63
round ligament of uterus 8, *13*, 14, 27, 34, 41, *46*, 47, 50, *52*
round spermatid 263–269, 276, 314
rumen 62
ruminants 8, 18, 19, 20, 22, 23, 24, 29, 44, 50, 61, 62, 63

S

saccharides 521
sacrosciatic lig. *23*
schizophrenia 372
scrotal/interdartoic septum *22*
scrotal ligament 4, 1, 22, 31, 39, *39*, 43
scrotal raphe 16
scrotal skin 4, *22, 26*
scrotum 4, 9, 12, 16, 38, 47, 258–261
seasonality 271
semen 258–259, 260–262, 270–272, 301, 323, 325, 327–328.519, 522
  evaluation 512
  quality 401
semiallogeneic fetus 365
seminal plasma 63, 272, 305, 306, 312
seminal vesicle 4, 31, *32*, 39, *40*, 222
  absent in dogs 258
seminiferous epithelium cycle 264, 265
seminiferous tubules 2, *2*, 63, 114, 258, 259, 260, 262, 268, 319, 409, 410
septa/septula 2, *2*
septum glandis 33
Sertoli cells 2, 113
sex chromosomes 253–256, 263, 275, 331, 334S
sexual glands 59, 63
sheep 1, 4, *60*, 61, *61, 62*, 67, 80
sigmoid flexure/flexura sigmoidea 18, *18, 22*, 23, *26*
signal transduction 383, 386, 387, 389, 390
signaling pathways 177, 185, 409
Silver–Russell syndrome (SRS) 475
simulated physiological oocyte maturation (SPOM) 134
single-stranded RNAs (ssRNAs) 110
sirtuins 159, 160, 161, 443, 446
slow freezing 530, 531, 532, 535
small interfering RNAs (endo-siRNAs) 116
small non-coding RNAs (sncRNAs) 109, 110, 117
small nuclear ribonucleoproteins (snRNPs) 441
small nuclear RNAs (snRNAs) 109
small nucleolar RNAs (snoRNAs) 109
small ruminants 23, 25, 29, 61
small silencing RNA (RNA interference or RNAi) 109
smooth endoplasmic reticulum 241
SNAREs 414, 416, 439
solid part of infundibulum *60*
somatic cell nuclear transfer (SCNT) 215, 218, 219, 329, 443, 443, 447, 448, 449, 522
sow 19, *19*, 20, *20*, 27, 29, 50, 63
sperm 110, 112, 177, 198, 216, 383, 385, 386, 389, 393, 401, 402, 404, 405, 406, 427, 428, 429, 430, 435, 436, 440, 442, 470, 472, 473, 474, 475, 510, 522, 529, 530, 539
sperm acrosome reaction. *see acrosome reaction*
sperm aster 442
spermatic cord 1, 3, 9, 10, 15, 16, 16, 20, 22, 22, 26, 30, 31, 31, 32, 38, 39, 39, 42, 43, 47, 260–261
spermatid 255, 263–269, 276
spermatocytes 113, 254, 263–263, 266–269, 409, 410, 411, 412, 413, 414, 415, 416, 417, 418, 419
spermatogenesis 110, 112, 113, 114, 115, 116, 119, 259, 260, 262–270, 427, 428, 431, 440, 442, 443, 475
  cycle of seminiferous epithelium 262–266
  protein expression 268–271
  stages 266–268
spermatogonia 109, 113, 114
spermatogonial stem cells (SSCs) 114
spermatogonium 262–270, 278
spermatozoon 1, 272–282
sperm capacitation 303–313, 412, 530
  actin polymerization 309
  bicarbonate influx 304
  calcium influx 307–308
  cholesterol efflux 306

Downloaded From Vet-eBooks.com

elevation of cAMP 308
increased energy requirements 310–313
intracellular pH increase. 306 –307
membrane remodeling 305–306
protein tyrosine phosphorylation 308–309
reactive oxygen species production 304–305
sperm chemoattraction 314–316
sperm chromosome screening (SCS) 401, 402, 404, 406
sperm–egg fusion 409
sperm fatty acids bound to phospoholipids 278–281
sperm genome 402, 406, 428, 430
spermiation 263, 267
spermiogenesis 263–265, 273–276, 314, 409, 410
sperm morphological defects 333
sperm morphology 273
acrosome 276–277
centriole 273
connecting piece (neck) 274–275, 277, 309, 311
cytoplasm 281
cytoplasmic droplet 281, 282, 314, 333
endpiece 273, 277
flagellum 264, 267, 273, 275, 277, 304, 307–315, 318
head 274–275
membranes 278–281
midpiece 273, 274, 277–278, 281, 304, 305–312, 314–315, 333
mitochondria 277–278
nuclear envelope 275
nucleus 273
organelles 273
plasma membrane 278–281
principal piece 277
shape and size 273
sperm motility 313–314
sperm-oocyte interaction 318–320
sperm phospholipids 278–281
sperm plasma membrane potential(Em) 417
sperm sexing 127, 328–329
sperm viability 281–282
spindle assembly checkpoint(s) 215
spindle(s) 159, 160, 186, 215, 403, 532, 536, 537, 539, 542
spleen *55*
spontaneous abortion (SA) 359, 364, 365
stages of estrous cycle 291–294
stages of spermatogenesis 262–269
stallion 30, *32*
stem cells
culture 492, 498
embryonic stem cells (ESCs) 329
induced pluripotent stem cells (iPSCs) 329
steroidogenesis 63
stillbirths 363
straight tubules 258, 260
stress-associated abortion 366
stress responses 359
stroma 5, *6*
subfertility 235 409
subischiocavernosus M. 40, 42
suburethral diverticulum 8, 2, 29
sucrose 521 537
sumoylation 443
superficial caudal epigastric A. *22*
superficial caudal epigastric V. *22*
superficial inguinal inn. *22, 26*
superovulation 127, 128, 132, 324, 402, 475
superoxide dismutase 305
suprarenal glands 62
surrogacy 127
suspensory ligament of ovary 7, 13, 45, *46, 51*
sustentacular (Sertoli) cells 63
swimm bladder *55*, 56, *56*
swine 66, 67, 177, 178, 213, 214, 215
synaptotagmin 414
synchrotron X-ray diffraction (SXRD) 535, 536, 537
syncytiotrophoblast 69, 71, 74, 75, 78
syngamy 438

t

tail of epididymis 2, *2*, 4, 10, *16*, 20, *21, 26*, 30, *30, 31, 39*, 42, 43, *43*, 47, *47, 48*
T cells 367
taxol 539
taxonomy, dog 250
terminal deoxynucleotidyl transferase dUTP nick-end labeling (TUNEL) 430
testicle 1, *2*, 9, 10, 15, *16*, 20, *21, 22*, 24, *26*, 30, *30, 31, 32*, 38, 39, *39, 40*, 42, *43*, 47, *47, 48, 54, 55, 56*
testicular artery(ies) *3*, 9, 10, *16*, 20, *21, 26, 30, 31, 32, 39*
testicular bursa 10, *16, 21, 30*, 31
testicular cells 112
testicular miRNA 113
testicular samples 475

Downloaded From Vet-eBooks.com

testicular sperm 410
testicular tunics 4, 9, 10, 15, 30, *31*, 38, 39, *39*, 42, 43, 47
testicular vein(s) *3*, 10, *21, 30, 31, 32*
testis 113, 116, 385, 409, 410, 427
  anatomy 258–260
  descent 259
  histology 262–270
  spermatogenesis 262–270
  spermiogenesis 263–265, 273–276, 314
testis-specific histone (TH2B) 428
testis-specific miRNAs 114
testosterone 1, 92, 94, 95, 96, 97, 98, 99, 100, 101
thalamus 61
theca cells 177, 289
thermotropic transition 532
third ventricle 59
thoracic inlet 62
thymine DNA glycosylase (TDG) 437
thyrohyoideus M. *61*
thyroid cartilage 61, *61*, 62
thyroid gland 61, *61*, 62
thyropharyngeus M. *61*
tight junctions 66
tissue necrosis 366, 371
T-lymphocytes (T cells) 368, 369
tomcat 5, 40
totipotency 485
toxicity 542
trachea 61
tracheal rings 61, *61*
transcription 180, 193, 216, 217, 427, 428, 429, 430, 435, 441, 443, 445, 446, 447, 487, 499, 500
transcriptional regulators 74
transfer RNAs (tRNAs) 109
transgene expression 78, 498
transgenerational epigenetic change 364
transgenic dogs 330
translation repression 109
transplacental transfer 221
transplantation 487, 488, 501
transrectal ultrasonography 239
transuterine migration 320
transvaginal procedures 239
transverse fascia 3, 4, 14
transzonal projections 241, 298
tricarboxylic acid (TCA) cycle 145, 149, 151, 154, 155, 156
trophectoderm (TE) 66, 69, 71, 74, 77, 78, 470
  cells 154, 155, 485, 489
trophectoderm stem cells 78
trophoblast(s) 65, 68, 69, 70, 72, 73, 74, 75, 76, 77, 78, 79, 80, 81, 217
  stem cells 69, 74, 75
tuberal part of adenohypophysis 59, *60*
tuberculum spongiosum *25*
tubouterine contractility 216
tumors 73
tunica albuginea 260, 284–285
  of epididymis 2, *2*
  of ovary 5, *6*
  of penis 18, 23, *25*
  of testicle 2, *2*
tunica dartos 4, *22, 26*
tunica vaginalis 260
tunics/testicular tunics 9, 10, 16, 20, 22, 31
two-photon excitation imaging 418
type 1 diabetes 198, 474
type 2 diabetes 194
tyrosine phosphorylation and/or partial proteolysis of UPIII and Src (Xenopus) 391

u

ubiquitin ligases 442
ubiquitin proteasome system (UPS) 435, 442, 448, 449
ubiquitination 442, 443, 445, 447
ubiquitin-conjugating enzymes 442
ultrasonic sound stress 366
ultrasound imaging 79, 128, 131, 236
ultrastructure 241, 529, 541
ultravitrification 540
umbilical A. *32*
umbilical vessels 71
undernutrition 91, 92, 93, 94, 95, 96, 97, 98, 99, 100, 101, 473
unfertilized eggs 385, 390
ungulates 4
ureter 11, 15, *23, 24*, 31, *32*, 39, *40, 41, 44, 46, 52, 62*
urethra 258, 261–262, 288–287
urethral fold *44*
urethral isthmus 4, 11, 23, *24*, 32, *50*
urethral process *25, 26, 33*
urethral recess 18, 19, 23, *24*, 44 45, 48, *50*
urethral sinus 33, *33*
urethral tubercle 8, *13, 14*, 15
urethralis M. 11, 1, *17, 23, 24, 32, 40*
urinary bladder 11, *14, 17, 23*, 39, *40, 41, 44, 46*, 48, *49, 51, 54*

Downloaded From Vet-eBooks.com

urinary tract infections 364
urogenital ducts 51, *54*
urogenital pore/anus *55*, 56, *56*
uterine A. *28*
uterine activity 216
uterine body *13*, 14, *14*, 19, *19, 20*, 25, *26*, 27, *27, 28*, 34, *35, 46*, 47, 50, *52*
uterine blood flow 221
uterine capacity 218
uterine caruncles 67
uterine cavity 63, 493
uterine contractility 216
uterine endometrium 59, 63, 80
uterine environment 470
uterine epithelium 68
uterine/fallopian tube/salpinx 5, *13*, 14, 19, *19, 20*, 24, 25, *26, 27, 28*, 33, 34, *35*, 41, *41*, 45, *46*, 48, *52*
uterine fluids 147, 153, 155
uterine fundus 34
uterine horn(s) *13*, 14, 19, *20*, 25, *26*, 27, *27, 28*, 34, *35*, 41, *41, 42, 46*, 47, 50, *52*, 283, 285–286, 301–305, 318–320, 322, 327–331, 369
uterine layers 217
uterine natural killer (NK) cells 369
uterine tissue 77
uterine tube 283, 285–286, 299–301, 305, 312, 314, 316–318, 326, 328, 330
  ampulla 283, 286
  fimbriae 286
  infundibulum 283, 286
  isthmus 283, 317
  uterotubal junction 283–286
uterine velum 8, *13*, 14, 27, 42, *42*
uterine wall 69, 81, 493
uterus 5, 14, *14*, 19, *20*, 24, 25, 26, 27, 33, 34, 41, *42*, 45, 47, 48, 66, 73, 79, 93, 132, 145, 153, 217, 218, 240, 282, 286, 331, 359, 360, 361, 363, 369, 485
uterus bicornis 25
uterus duplex 41, 50
uterus masculinus 2, 22, 31, *32*

v

vagina 5, *13, 14*, 15, 19, 20, *20*, 24, *26, 27, 28*, 29, 33, 34, *35*, 41, *41*, 42, *42*, 45, *46*, 47, 48, 50, *52*, 257, 282, 284–287, 291–293, 301, 323, 331, 359, 360, 361, 363
vaginal canal *3*, 15, 16
vaginal cavity 4, *22*
Vaginal cytology 291–293, 324
vaginal part of cervix *26, 27, 28, 35*
vaginal process 4, 14, 41
vaginal ring 3, *32*, 47
vaginal tunic, parietal lamina 3, *3*, 10, *22, 26, 31, 32*
vaginal tunic, visceral lamina 3, *3, 22, 26*
vas deferens 410
vascular endothelial growth factor (VEGF) 73, 217
vasculogenesis 73
ventral frenulum of cervix *36, 37*
ventral recess of clitoris *38*
ventral scrotal br. A. *22, 26*
ventral scrotal br. V. *22*
ventricle *56*
vesicular glands 4, 15, 16, 17, *17*, 18, 22, *23, 24*, 31, 39, *40*, 42, 43, 44, *44*, 48, *49*, 63
vestibular bulb 8, 15, 20, 34, 42, *42*
vestibule/vestibulum 5, *13, 14, 15*, 19, 20, *20*, 24, *26, 27, 28*, 29, 33, 34, *35*, 41, 42, *42*, 45, 47, 48, 50, 282, 287
viability 145, 150, 158
villi labyrinth 81
visceral endoderm 486
vitrification 521, 522, 530, 534, 535, 536, 537, 538, 539, 540, 541, 542
viviparity 65
vulva 5, 14, *14*, 15, 19, *20*, 24, *26, 27*, 33, 34, 41, *41, 42*, 45, *46*, 47, 48, 50, *52*, 282, 287

w

whelping 258, 322

x

X chromosome inactivation 443, 445, 486
X-chromosome silencing 442
xenografts 513
xenopigs 501
Xenopus laevis 383, 387
xenotransplantation 501
X chromosome 253–256, 263, 328, 331
xenographic sperm 326

y

yolk sac 71, 72
  endoderm 289
  placenta 71, 72, 77
Y-chromosome 253–256, 263, 328, 331

Downloaded From Vet-eBooks.com

Z
zona pellucida (ZP) 66, 216, 241, 403, 404, 409, 411, 414, 415, 418, 419, 436, 529, 535, 536, 541, 542
zonary placenta 63
zygote(s) 110, 147, 153, 155, 156, 156, 177, 216, 435, 439, 442, 443, 448, 449, 485
zygotic cell cycle 442
zygotic/embryonic genome activation 440
zygotic pronuclei 441
zebrafish/*Brachidanio rerio* 1, *55*, 56, *56*
zona pellucida 268, 275, 290, 294, 298–299, 314, 317–320, 322, 324, 330
zygotene 265–268
zygotic gene activation 320

Downloaded From Vet-eBooks.com

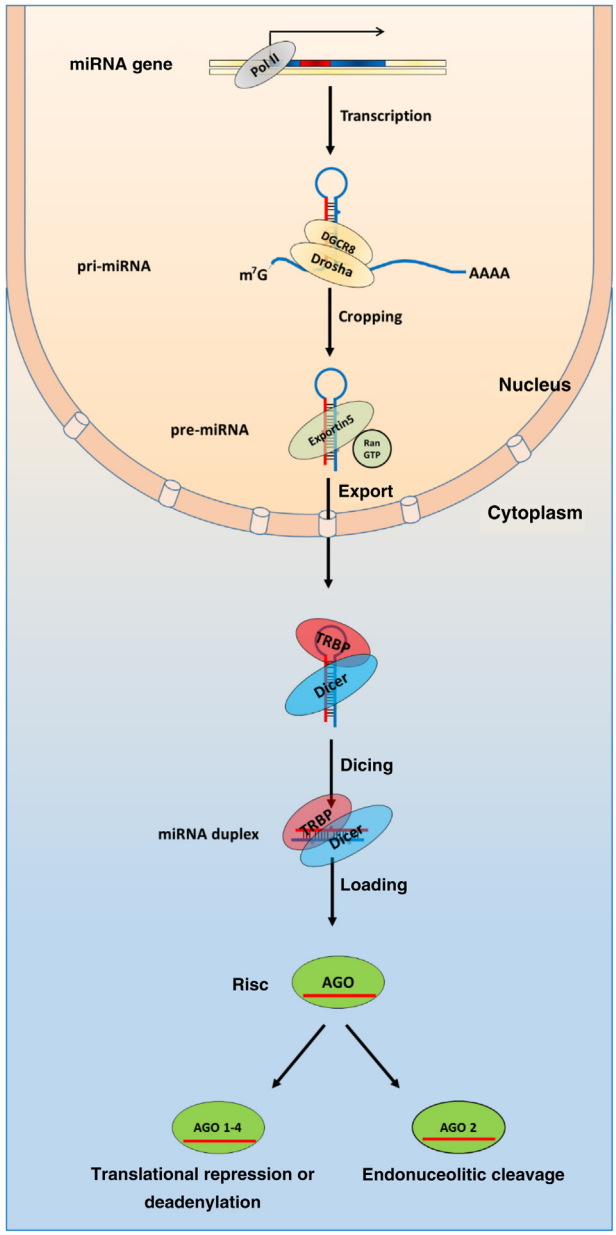

Figure 5.1 Canonical miRNA biosynthesis pathway. Canonical pathway of miRNA processing includes production of primary transcripts (pri-miRNAs) by RNA polymerase II (Pol II). Nascent pri-miRNA transcript is further processed by microprocessor complex (Drosha-Dgcr8) in the nucleus. The resulting precursor miRNAs (pre-miRNAs) are exported from the nucleus to the cytoplasm by Exportin-5-RanGTP complex. In the cytoplasm, pre-miRNAs are cropped further by Dicer to yield miRNA duplex, which is loaded into Ago protein by Dicer TRBP complex. Finally, only one strand from the duplex (termed mature or major) remains in Ago protein forming RISC and regulates the gene expression either by mRNA cleavage or translation repression. The other strand (minor) has no known function and is mostly degraded.

Animal Models and Human Reproduction, First Edition. Edited by Heide Schatten and Gheorghe M. Constantinescu.
© 2017 John Wiley & Sons, Inc. Published 2017 by John Wiley & Sons, Inc.

Downloaded From Vet-eBooks.com

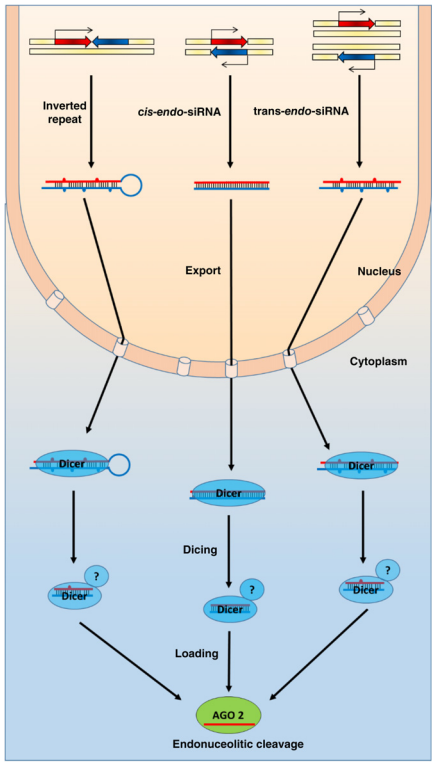

Figure 5.3 Biogenesis pathway of endogenous small interfering RNAs (*endo*-siRNAs). Precursors of *endo*-siRNAs are derived from double-stranded precursors, including long stem-loop structures (inverted repeats), bidirectional strands transcription (*cis-endo*-siRNAs), or repetitive sequence pairs (*trans-endo*-siRNA). Further *endo*-siRNA precursors are transported to cytoplasm and further processed by Dicer to produce double-stranded RNAs of ~21 nt, which is then loaded into Ago2 protein and forms RISC. Unlike miRNAs, the export of *endo*-siRNA precursors from the nucleus to cytoplasm as well as assembly of the effector complexes (RISC) is poorly understood.

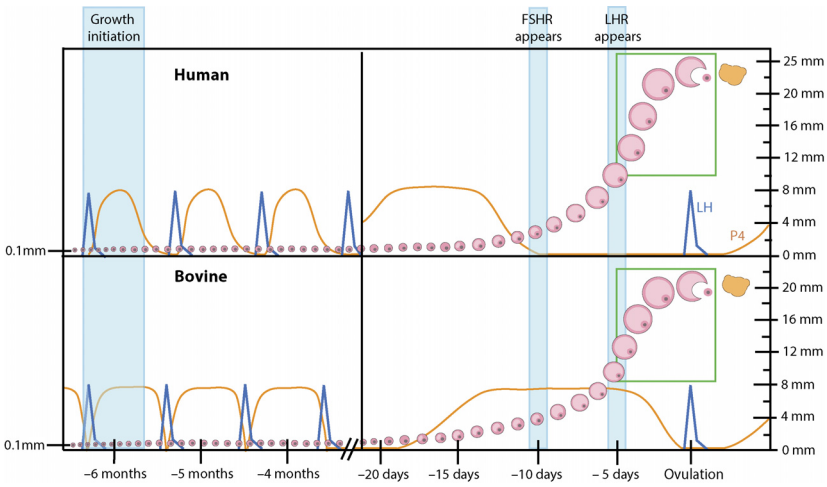

Figure 6.1 Development of the ovulatory follicle in human (top) and bovine (bottom). Progesterone profiles and LH surges are shown in orange and blue, respectively. Key elements of the dominant follicle's development are presented. The green box shows the window for competence acquisition.

Downloaded From Vet-eBooks.com

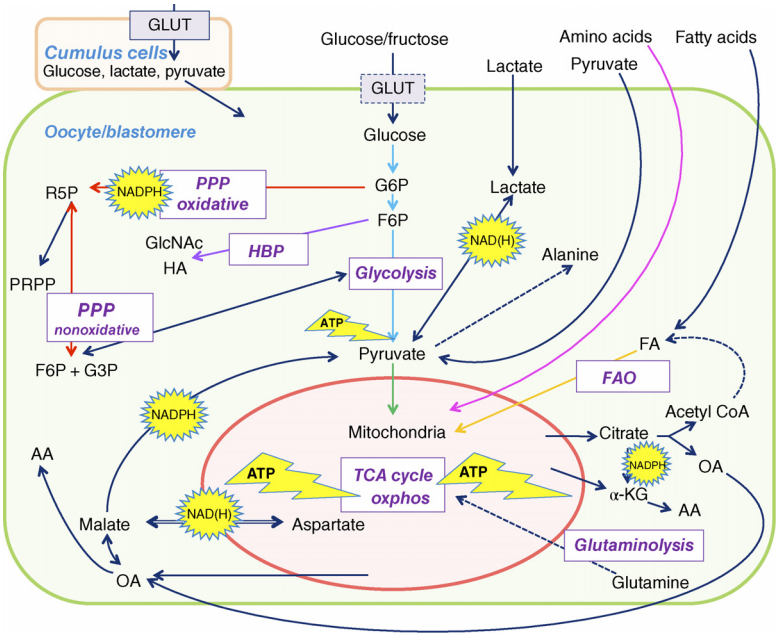

Figure 7.1 An overview of the interrelated metabolic pathways that may function in mammalian oocytes and early embryos. Multiple energy substrates can be both taken up and produced by the oocyte or embryo to meet metabolic needs via multiple pathways, maintain redox and osmotic balance, and modify the external culture environment. The oocyte receives significant metabolic substrates via gap junction communication with cumulus cells (depicted in the upper left corner), while the embryo may take up a variety of substrates directly from the culture media. Dashed lines represent pathways that have only been hypothesized. Pathways names are shown in white boxes, and important end products in yellow. *Abbreviations:* α-KG, alpha ketoglutarate; AA, amino acids; ATP; adenosine triphosphate; F6P, fructose 6 phosphate; FA, fatty acids; FAO, fatty acid β-oxidation; FAS, fatty acid synthase; G3P, glyceraldehyde 3 phosphate; G6P, glucose-6-phosphate; GlcNAc, *N*-acetylglucosamine; GLUT, glucose transporters; HA, hyaluronic acid; HBP, hexosamine biosynthetic pathway; OA, oxaloacetate; Oxphos, oxidative phosphorylation; PRPP, phosphoribosyl pyrophosphate; R5P, ribose-5-phosphate; TCA, tricarboxylic acid. (Reproduced from Krisher (2013b) with permission from Wiley.)

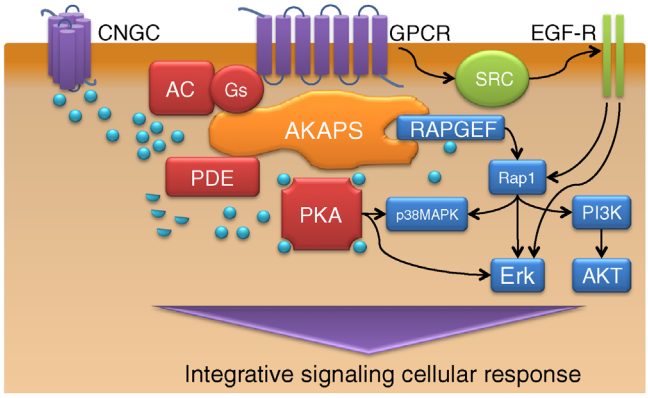

Figure 8.2 Schematic representation of the cAMP signaling cascade following the binding of a specific ligand to the specific G protein-coupled receptor (GPCR). This binding induces Gs protein translocation to activate adenylyl cyclase, which synthesizes cAMP (black dot) from ATP. Different targets are known for cAMP: cyclic nucleotide-gated channels (CNGC); protein kinase A (PKA); Rap guanine nucleotide exchange factor (RAPGEF), which activates ERK. Phosphodiesterase (PDE) hydrolyzes cAMP to inactive 5′-AMP. All of these molecules can be segregated by anchoring proteins such as A-kinase anchor proteins (AKAPs).

Downloaded From Vet-eBooks.com

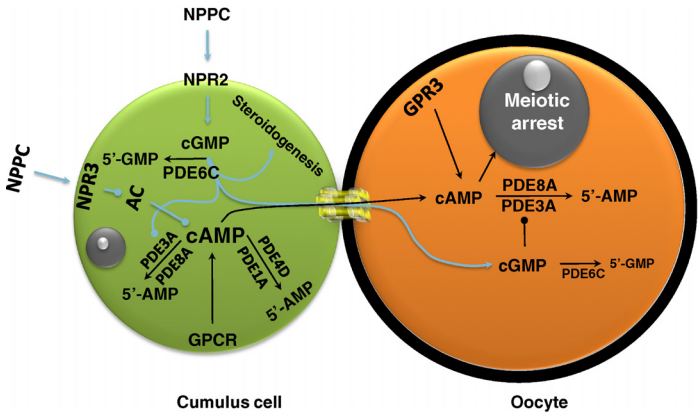

Figure 8.4 Schematic showing the signaling pathways involved during the maintenance of oocytes in meiotic arrest. See the text for details. Blue lines are the proposed NPPC signaling pathway. The white lines and characters represent the newly proposed pathways and molecules involved in the maintenance of oocyte meiotic arrest. A line ending with a dot indicates inhibition, whereas a line ending with an arrowhead represents activation.

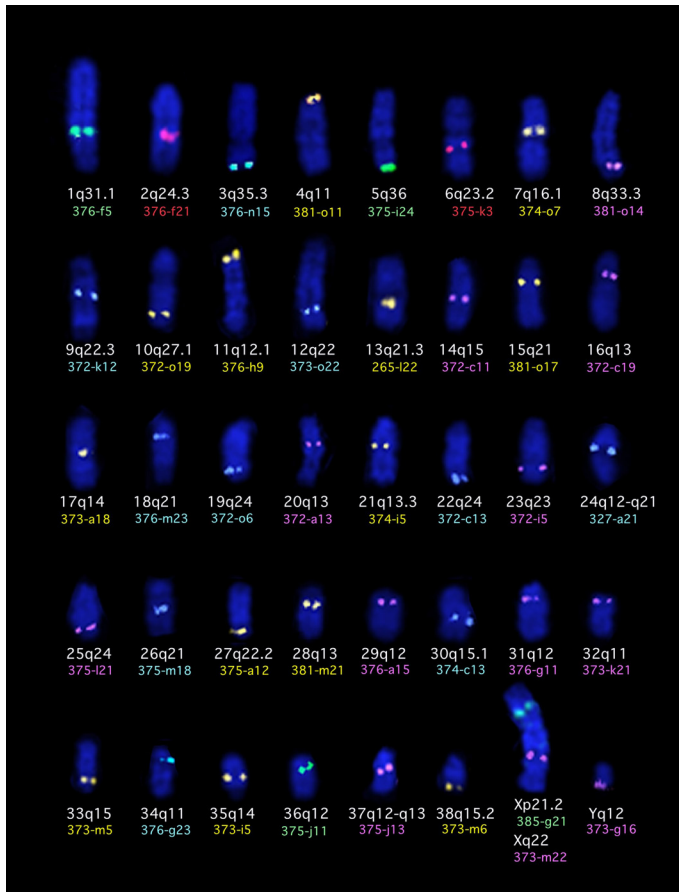

Figure 11.2 Identification of dog chromosomes. Each chromosome was identified using a panel of chromosome-specific single locus fluorescence in situ hybridization (FISH) probes from 41 BAC clones labeled with either DEAC (blue), Spectrum Green (green), Spectrum Gold (yellow), Spectrum Red (red) or biotin-Cy5 (pink), and unequivocally identified based on chromosome size, cytogenetic location of the BAC clone and its fluorochrome label. (Reproduced from Thomas (2003) with permission from Nature Publishing Group.)

Downloaded from Vet-eBooks.com

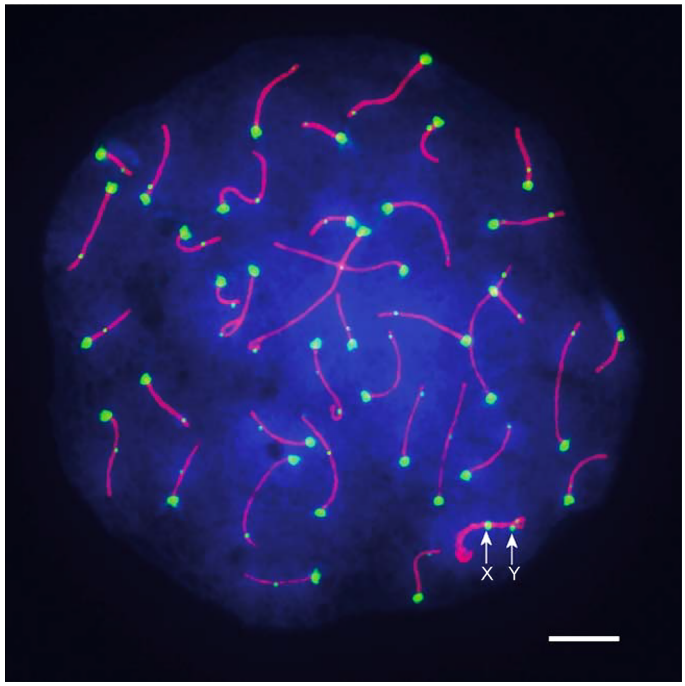

Figure 11.8 Chromosome spread from a dog spermatocyte at pachytene. MLH1 is a mismatch repair protein of mature recombination nodules, and SCP3 is synaptonemal complex protein 3. "Spread from a dog spermatocyte at pachytene, stained with DAPI (blue) and immunolabeled with antibodies to SCP3 (red), MLH1 (green) and centromere proteins (green). Centromeres differ from MLH1 foci by their brighter and more diffuse staining. Arrows indicate centromeres of X and Y chromosomes. Bar represents 5 μm." (Reproduced from *Chromosome Research*, General pattern of meiotic recombination in male dogs estimated by MLH1 and RAD51 immunolocalization, vol. 16, 2008, 709–719, Basheva EA, Bidau CJ, Borodin PM, © Springer 2008. With permission of Springer.)

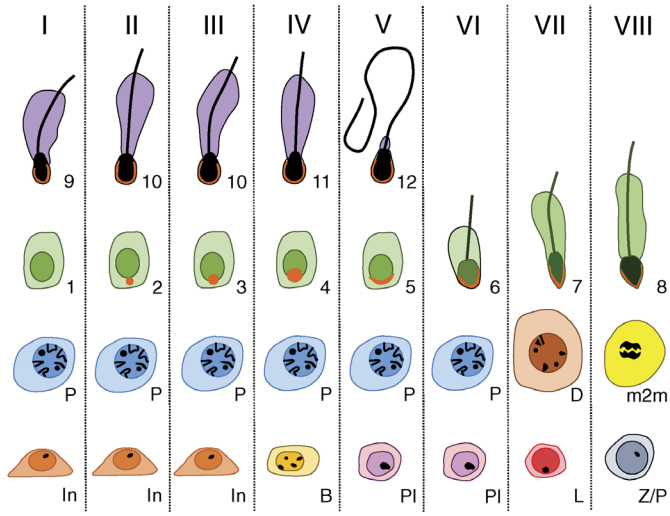

Figure 11.9 Spermatogenic cycle of the dog. Schematic representation of the stages (I to VIII) of the dog seminiferous epithelium cycle based on the acrosome system. The acrosome is shown in bright orange in step 2 to 12 spermatids. Cellular associations at each cycle stage are depicted in each vertical column. Spermatogonia type A (not shown) are present at each cycle stage. For simplicity, flagella of elongating spermatids (step 8 to 11) are drawn short. Cell types include: spermatogonia (B = type B, In = intermediate), spermatocytes (D = diplotene, L = leptotene, m2m = meiotic division, Pl = preleptotene, P = pachytene, and Z/P = zygotene-pachytene), round spermatids (1 to 5) and elongating spermatids (6 to 12). Cells at the bottom of the figure are closest to the basal lamina, and those at the top are closest to the lumen of the seminiferous tubule.

Downloaded From Vet-eBooks.com

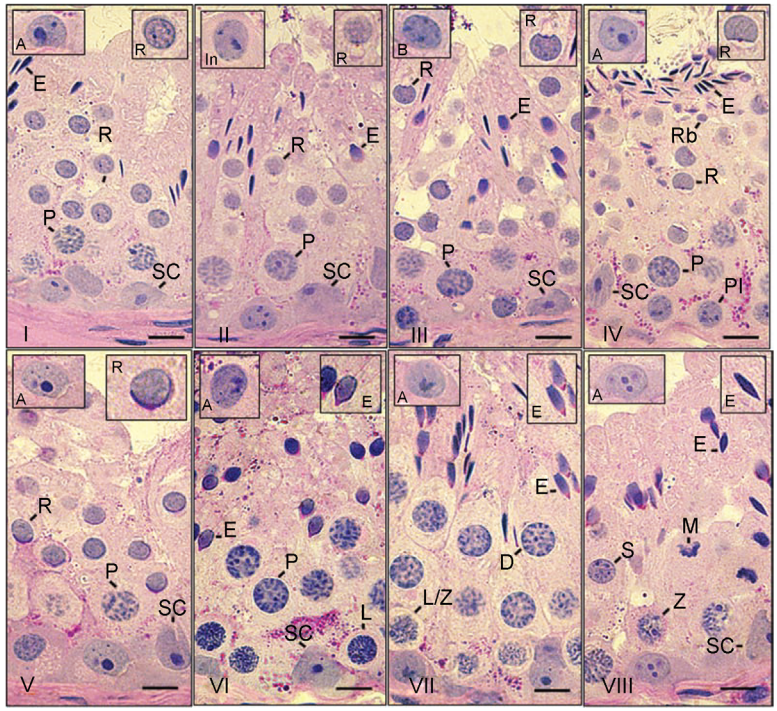

Figure 11.10 Stages of the dog seminiferous epithelium cycle. (Eight different stages based on the acrosome system were identified and the cell types included: A, Type A spermatogonia; In, intermediate spermatogonia; B, Type B spermatogonia; Pl, pre-leptotene; L, leptotene; Z, zygotene; P, pachytene; D, diplotene; M, meiotic division; R, round spermatids; E, elongated spermatids; Rb, residual bodies; SC, Sertoli cell. The figure inserts show a representative spermatogonial cell (upper left) and spermatid step (upper right) for each stage. Bar represents 10 μm. (Reproduced from Soares JM, Avelar GF, França LR, The seminiferous epithelium cycle and its duration in different breeds of dog (*Canis familiaris*), *Journal of Anatomy*, 215(4):462–471, John Wiley & Sons, Inc. © 2009 The Authors, Journal compilation © 2009 Anatomical Society of Great Britain and Ireland, with permission from Wiley)

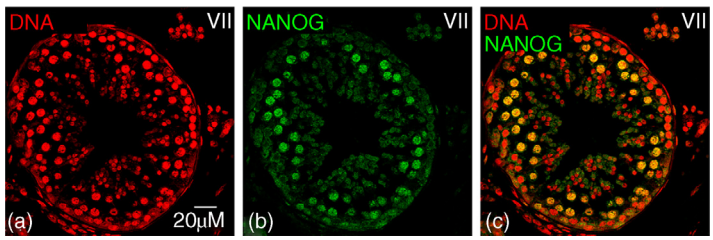

Figure 11.11 NANOG distribution in the dog testis. Confocal fluorescence micrograph of a seminiferous tubule at stage VII stained with: A) TO-PRO®-3 for DNA (red), and B) anti-NANOG antibody (green) with the merged image shown in (C). Nanog staining was present in late pachytene spermatocytes, diplotene spermatocytes and round spermatids, but not in elongating spermatids. (Reproduced from Figure 4A-C of Kuijk EW, de Gier J, Lopes SM, Chambers I, van Pelt AM, Colenbrander B, Roelen BA. (2010) A distinct expression pattern in mammalian testes indicates a conserved role for NANOG in spermatogenesis. *PLoS One* 5(6):e10987. (http://journals.plos.org/plosone/article?id=10.1371%2Fjournal.pone.0010987), © 2010 Kuijk et al. This is an open-access article distributed under the terms of the Creative Commons Attribution License, which permits unrestricted use, distribution, and reproduction in any medium, provided the original author and source are credited, with permission from PLOS.)

Downloaded From Vet-eBooks.com

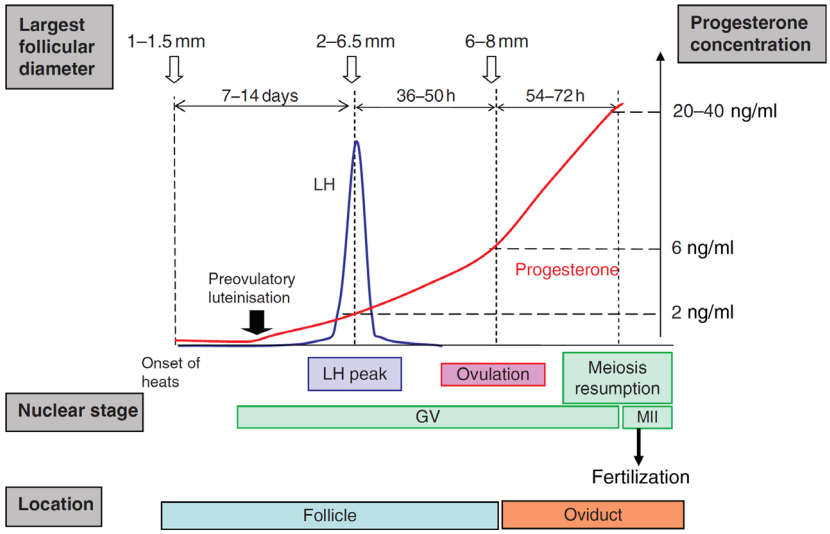

Figure 11.23 Estrous cycle events in the dog. Summary of final follicular growth, endocrine events and meiotic events in the female. (Reproduced from Chastant-Maillard S, Viaris de Lesegno C, Chebrout M, Thoumire S, Meylheuc T, Fontbonne A, Chodkiewicz M, Saint-Dizier M, Reynaud K. 2011. The canine oocyte: uncommon features of *in vivo* and *in vitro* maturation. *Reproduction, Fertility and Development* 23(3):391–402, © CSIRO 2011, reprinted by permission of CSIRO Publishing.)

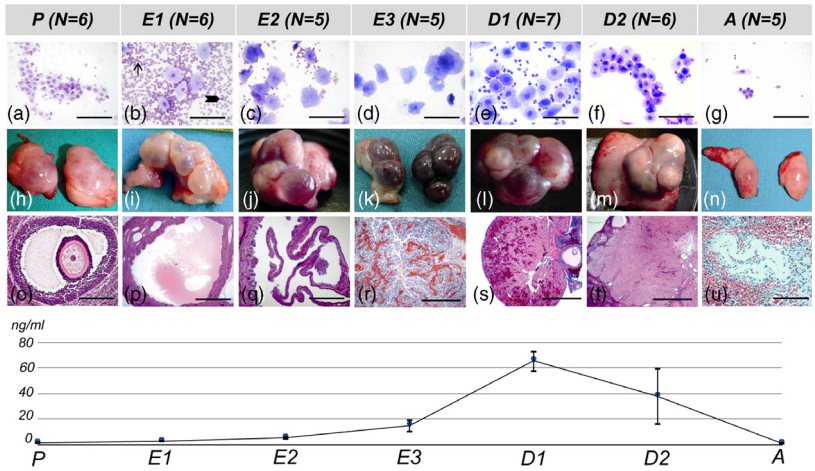

Figure 11.24 Steps of the estrous cycle of the dog. Vaginal cytology (*a*-*g*), ovarian macroscopic aspects (*h*-*n*), ovarian histology (*o*-*u*), and mean blood progesterone levels (graph) in the dog during the estrous cycle. Data were collected during several time points: one in proestrus (*P*), three in estrus (*E1-3*), two in diestrus (*D1*, *D2*) and one in anestrus (*A*). (*a*) Parabasal cells with some erythrocytes, (*b*) intermediate cells, some leukocytes (arrows) and many erythrocytes, (*c*) superficial cells with rare erythrocytes, (*d*) superficial anucleate cells, (*e*) superficial cells, intermediate cells and abundant neutrophils, (*f*) heterogeneous population of epithelial cells with some neutrophils, (*g*) few cells in sample with small groups of parabasal cells, (*h*) translucent, small vesicular structures characterize proestrus, (*i*) vesicular structures increase in diameter during preovulatory estrus, (*j*) large follicles present before ovulation, (*k*) corpora hemorrhagica present after ovulation, (*l*) both corpora hemorrhagica and corpora lutea present at beginning of diestrus, (*m*) mature corpora lutea characterize medium-late diestrus, (*n*) small, inactive ovaries characteristic of anestrus, (*o*) small tertiary follicle, (*p*) large preovulatory follicle, (*q*) ruptured, large follicle just after ovulation, (*r*) collapsed tertiary follicle transforming into a corpus hemorrhagicum, (*s*) corpus hemorrhagicum transforming into corpus luteum, (*t*) mature corpus luteum, and (*u*) involuted corpus luteum (corpus albicans). Scale bars: (*a* - *g*) = 100 µm, (*o*, *u*) = 500 µm, (*p*, *q*) = 700 µm, (*r*, *s*, *t*) = 1000 µm. (Reproduced from *Animal Reproduction Science*, volume 152, Groppetti D, Aralla M, Bronzo V, Bosi G, Pecile A, Arrighi S., Periovulatory time in the bitch: whata's new to know? Comparison between ovarian histology and clinical features, pages 108-116, Copyright 2015, with permission from Elsevier.)

Downloaded From Vet-eBooks.com

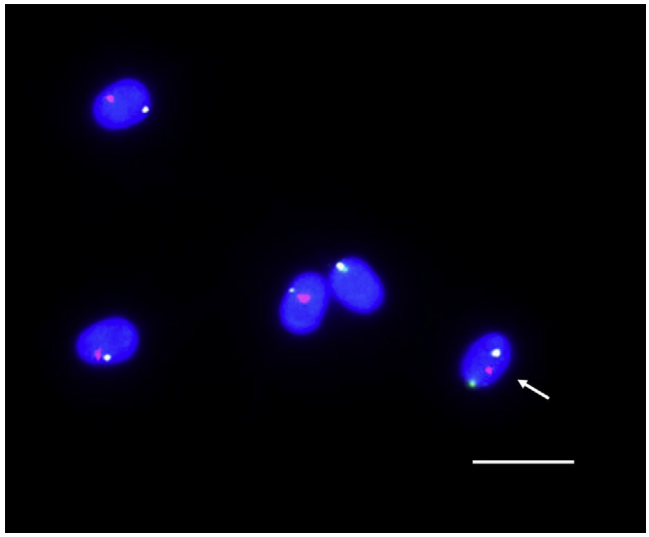

Figure 11.34 Detection of chromosomes X, Y, and 1 in dog spermatozoa by multicolor fluorescence *in situ* hybridization (FISH). Each spermatozoon has one yellow signal for chromosome 1, and either a green signal (X chromosome) or a red signal (Y chromosome). X-bearing spermatozoa have one green and one yellow signal. Y-bearing sperm have one red and one yellow signal. A spermatozoon (arrow) with all three signals (yellow, green and red) was considered to be aneuploid. Bar is 100 µm. (Reproduced from *Theriogenology*, volume 82, number 4, Komaki H, Oi M, Suzuki H., Detection of sex chromosome aneuploidy in dog spermatozoa by triple color fluorescence *in situ* hybridization, pages 652–656, Copyright 2014, with permission from Elsevier.)

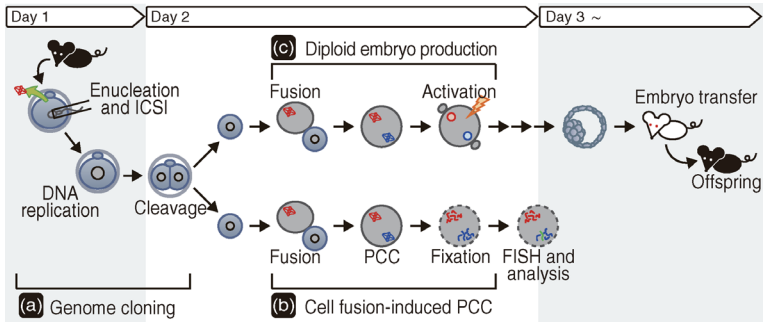

Figure 14.1 A flowchart of sperm chromosome screening (SCS) before fertilization. Some modifications were made to the original figure by Watanabe *et al.* (2013).

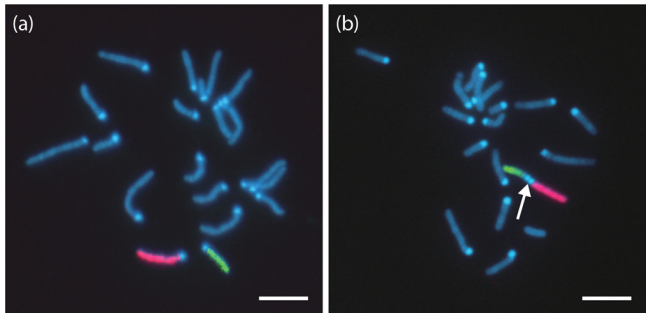

Figure 14.3 Fluorescence *in situ* hybridization (FISH) analysis of blastomere chromosomes in androgenic 2-cell embryos derived from spermatozoa in a carrier with a Robertsonian translocation between chromosomes 6 and 15, Rb(6.15). Chromosomes 6 and 15 can be seen in red and green, respectively. (a) Normal chromosome complement. (b) Balanced chromosome complement with Rb(6.15) (arrow). Bar: 10 µm.

Downloaded From Vet-eBooks.com

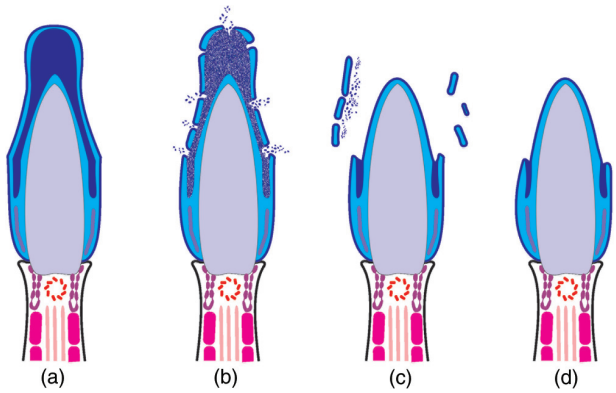

Figure 15.1 Schematic diagram of the process of acrosomal exocytosis in mammals. (a) Acrosome-intact sperm. (b) Fusion of the plasma membrane and the outer acrosomal membrane with the resulting formation of hybrid vesicles and exposure of the acrosomal matrix. (c) Release of the acrosomal matrix and exposure of the inner acrosomal membrane. (d) Acrosome-reacted sperm.

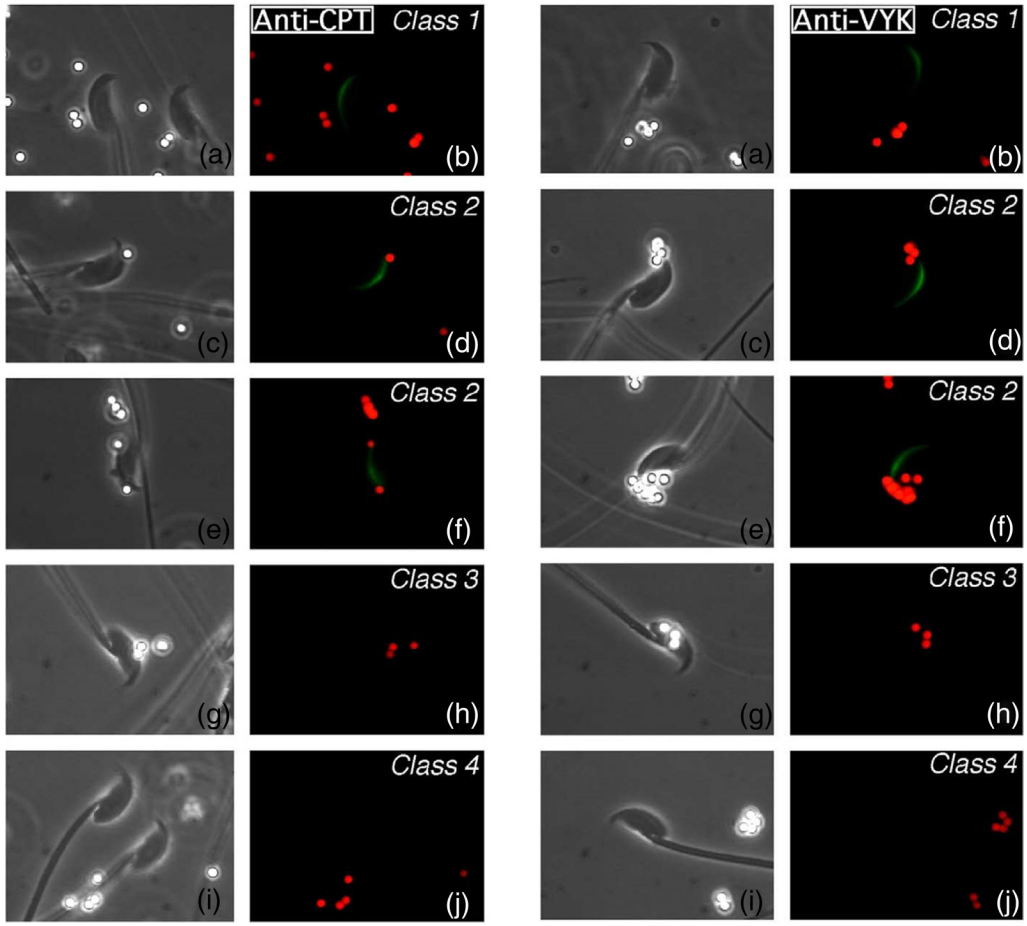

Figure 15.2 Simultaneous detection of acrosomal GFP in transgenic mouse sperm and the binding of anti-sp56 antibody-coated FluoSpheres. GFP expression, driven by the proacrosin promoter, was targeted to the mouse sperm acrosome using the signal sequence and part of the N-terminus of proacrosin. Some sperm bound antibody-coated FluoSpheres, demonstrating the exposure of the acrosomal matrix in those sperm. Four classes of sperm were identified by this assay. Anti-CPT and anti-VYK are two peptide-specific antibodies to mouse sp56. (a) Anti-CPT-coated FluoSpheres. (b) Anti-VYK-coated FluoSpheres. Paired phase-contrast (A,C,E,G,I) and fluorescence (B,D,F,H,J) (GFP, green; FluoSpheres, red) images of sperm. (Reproduced from Kim and Gerton (2003).)

Downloaded From Vet-eBooks.com

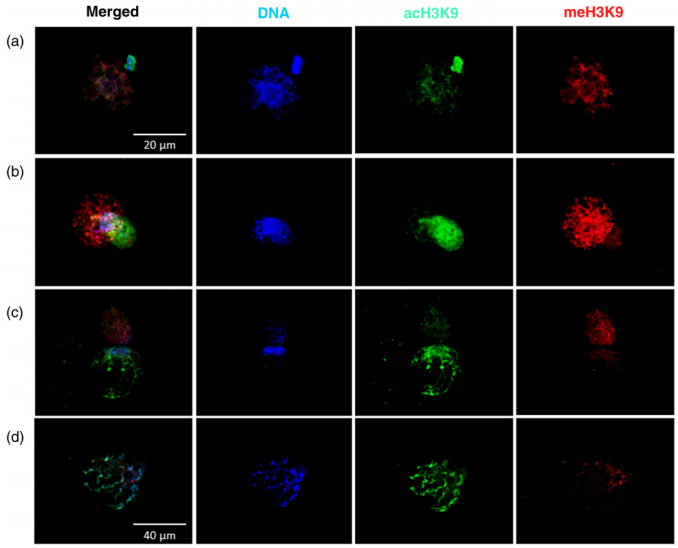

Figure 17.1 Dynamics of histone acetylation and methylation during pronucleus formation in the *in vitro*-produced porcine zygotes. First, histone hyperacetylation (green channel indicates H3K9 acetylation) occurs during sperm protamine–histone exchange (a) and early male pronucleus development (b). Conversely, methylated H3K9 (indicated by red color), a marker of heterochromatin formation is abundant in the female pronucleus. The histone code asymmetry of both pronuclei counterstained by DAPI (blue channel) is apparent during early (b) and advanced (c) pronucleus formation. Following pronuclear apposition and entry into the first mitotic cell cycle (d), histone methylation retreats while histone acetylation persists (demonstrated by H3K9 methylation and H3K9 acetylation, respectively). These modifications of histone code are essential for subsequent embryonic gene reprogramming. Hence, embryonic genome is sensitive to DNA damage and early embryonic developmental failure.

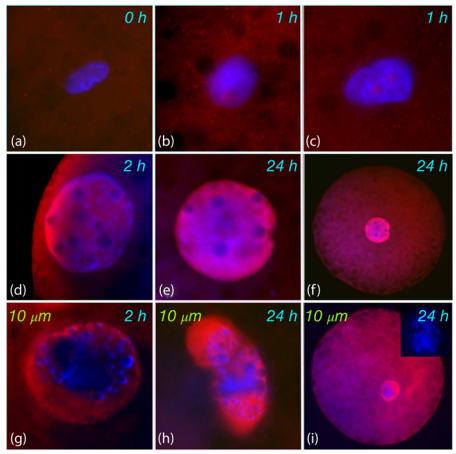

Figure 17.2 Visualization of proteasomes (red) and DNA (blue) in control SCNT zygotes and zygotes treated with 10 μM MG132. (a–d): Control, NT1 zygotes at the indicated time points after SCNT. (e): The MG132-pulsed NT2 zygote has a normal pronucleus at 24 h post SCNT (i.e., 22 h after removal of MG132). (g–i): Nuclei of zygotes exposed to MG132 continually for 24 h after SCNT. Note abnormal chromatin structure in parts (g) and (h), and failed remodeling in panel (i) (chromatin shown in insert). (Reproduced from Whitworth *et al.* (2009) with permission from Wiley.)

Downloaded From Vet-eBooks.com

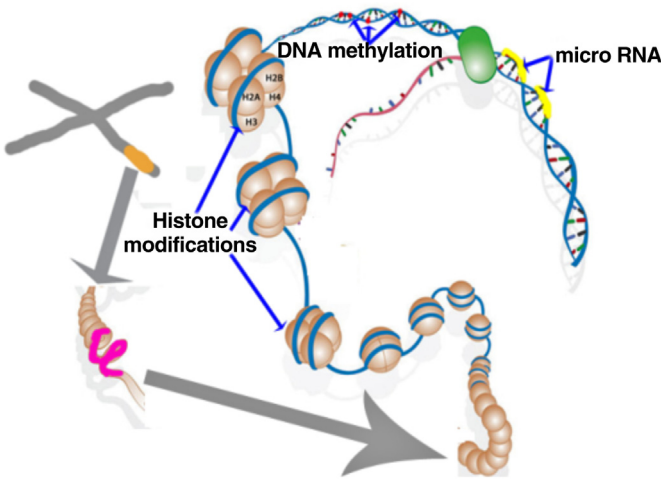

Figure 18.1 Epigenetic modifications including DNA methylation, histone modifications, and microRNA.

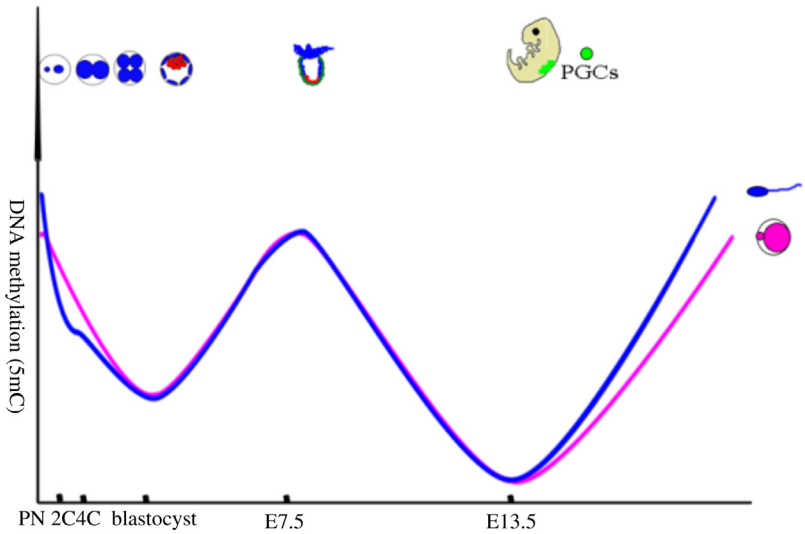

Figure 18.2 Reprogramming of 5 mC in germ cells and embryos. PN, pronucleus; PGCs, primordial germ cells.

Downloaded From Vet-eBooks.com

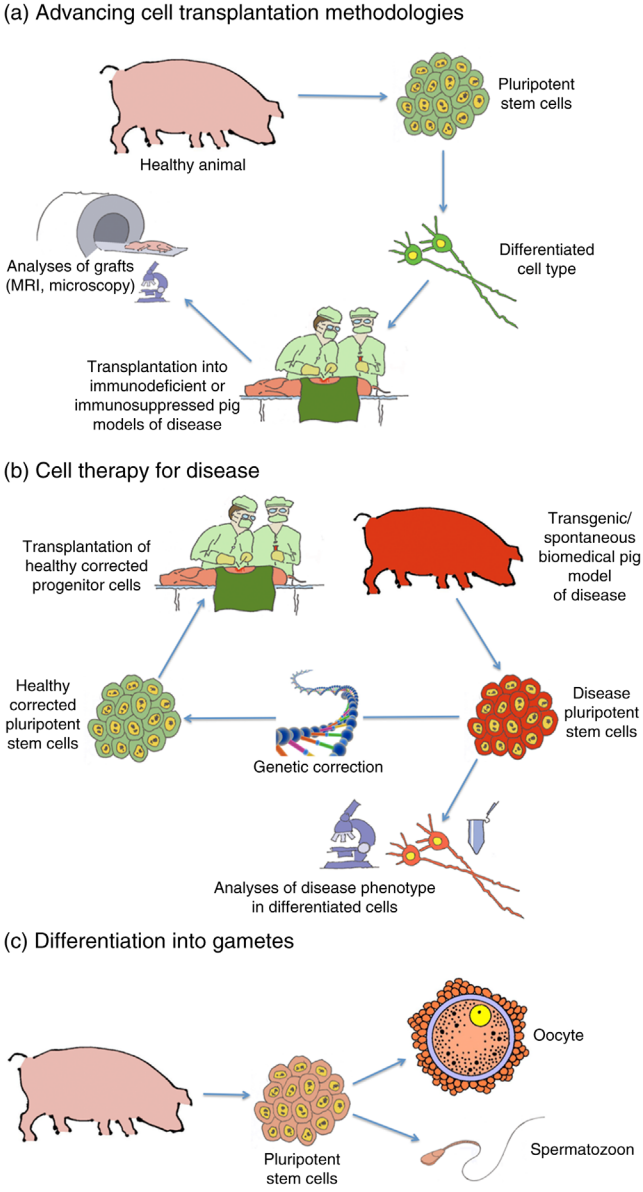

Figure 19.1 The establishment of *bona fide* porcine pluripotent stem cells would help to advance cell transplantation methodologies (a), provide an alternative model for testing and developing cell therapies (b), and may even advance alternative infertility treatments (c).

Downloaded From Vet-eBooks.com